11th Hardwood Conference

30-31 May 2024
Sopron

11TH HARDWOOD CONFERENCE PROCEEDINGS

Róbert Németh, Christian Hansmann, Holger Militz, Miklós Bak, Mátyás Báder

11TH HARDWOOD CONFERENCE PROCEEDINGS

Sopron, Hungary, 30-31 May 2024

Editors: Róbert Németh, Christian Hansmann, Holger Militz, Miklós Bak, Mátyás Báder

11TH HARDWOOD CONFERENCE PROCEEDINGS

Sopron, Hungary, 30-31 May 2024

Content

Session II - Hardwood resources, product approaches, and timber trade

Session III - Surface coating and bonding characteristics of hardwoods

Session IV - Hardwood structure and properties

Session V - Hardwoods in composites and engineered materials

Session VI - Modification & functionalization

Preface to the
11TH HARDWOOD CONFERENCE

Róbert Németh

For the 11th time we are organising our Hardwood Conference in Sopron. Over the last two decades, the European wood industry has faced many challenges, especially in the field of hardwood processing. I am confident that the achievements of our hardwood research community have helped us to meet these challenges and solve these problems.

The richness of hardwood species provides an extraordinary diversity of wood materials. Describing material properties is a major task in itself, and new properties need to be investigated as technologies and products evolve.

There is an increasing focus on plantation hardwoods. Wood production and wood use have become a joint research effort that goes hand in hand. The publication contains a number of articles on forestry and complex (biological and technical) issues. Wood chemistry is also an "evergreen" topic of our conference. It is difficult to imagine significant scientific and industrial progress without this discipline. Hardwood forests, and of course their managers, are facing major challenges. New pests and diseases have emerged, affecting the condition of the forests and, unfortunately, the quality of the wood. Dryer climates are lowering groundwater levels and stressing some trees, affecting growth and therefore the quantity and quality of wood available.

Raw material supply chains are being fundamentally damaged by the crises affecting Europe and the world. The availability of conventional raw materials is limited or non-existent and prices are subject to large fluctuations (mainly upwards), which poses a challenge to the wood processing industry. In the future, the availability of hardwood is expected to decrease and competition from the energy sector is expected to increase. Substitute, under-utilised and undervalued wood and semi-finished products will have to be used, and new, material-efficient structures will have to be designed, while maintaining the quality of the finished products. The feasibility of these steps is a major research challenge for scientists.

The conference provides an excellent forum for the exchange of ideas between young and experienced researchers. Among the authors of the papers, including the speakers, there is a welcome number of young researchers, many of whom are "only" students. We can therefore look forward to the future of wood research with confidence, as the "next generation" seems to be secured.

Thank you for your interest in our conference and the significant number of scientific papers submitted!

Sopron, May 2024
Róbert Németh

Plenary Session
Keynotes of the
11TH HARDWOOD CONFERENCE

The role of black locust (*Robinia pseudoacacia*) in Czechia

Ivan Kuneš[1*], Martin Baláš[1], Přemysl Šedivka[1], Vilém Podrázský[1]

[1]Czech University of Life Sciences Prague, Faculty of Forestry and Wood Sciences. Kamýcká 129, 165 00 Praha-Suchdol, Czech Republic.

Email: kunes@fld.czu.cz; balas@fld.czu.cz; sedivka@fld.czu.cz; podrazsky@fld.czu.cz

Keywords: black locust; *Robinia pseudoacacia*; production; invasiveness; silvicultural management

ABSTRACT

Black locust (*Robinia pseudoacacia* L.) is the most widespread non-native tree species in Europe and has had a significant impact on the Central European landscape and forestry. The black locust has many exceptional characteristics that represent considerable potential for use by man. The climate shift in recent decades in Central Europe could further strengthen the importance of this tree species. However, there are also risks arising from the invasiveness of the black locust. Like Hungary, Czechia has had many years of experience with this tree species. Still, the current approach between these two countries, particularly in conventional forestry, differs. This paper attempts to summarise how the management of *Robinia* and its stands is viewed in Czechia, where the common forestry utilization of black locust is currently not considered due to its invasiveness. The reason for a more reserved forestry attitude in Czechia can be associated with the relatively frequent stem deformities of *Robinia* stands, which are often attributed to frost. However, the frost deformities and low stem-form quality of some *Robinia* stands do not affect their vigour and potential to invade adjacent habitats. It often takes considerable effort to remove black locust, especially where the spreading of *Robinia* threatens valuable adjacent ecosystems. On the other hand, there is great potential for the use of *Robinia* in Czechia. It can be found in controlled energy crops, fast-growing plantations (lignicultures), some land reclamation projects or urban greenery. *Robinia* can also be grown in small stands or in groups of trees surrounded by arable land that does not allow the tree to spontaneously spread. Regarding the production plantations of *Robinia*, the Hungarian experience and breeding program can be very inspiring for Czechia. Generally, there is a move towards 'site-specific management', but with a strong emphasis on the precautionary principle. Finding and then consistently applying a balanced approach to black locust management that not only allows for the potential but also respects the risks of *Robinia* – it is currently a key challenge for Czech forestry, landscape and nature conservation.

INTRODUCTION

The natural distribution range of black locust is North America, specifically the Appalachian Mountains and the Ozark and Ouachita highlands. Gradually, as a result of human activity, the species has spread across much of the United States (Cierjacks et al. 2013) and parts of Canada (Huntley 1990), where it is more abundant in the eastern part of the continent.

Information about the introduction of black locust to Europe has discrepancies. However, there were probably several independent routes by which the species got to Europe. The first cultivation of *Robinia* in Europe is usually associated with Jean Robin and Vespasian Robin (father and son). That is how the generic name of black locust was established in Linné's nomenclature. Nevertheless, France is unlikely to be the first European country where black locust was imported from North America. The Hungarian polymath Ernyey (1927) questioned whether Jean or Vespasian Robin were directly involved in the introduction of the black locust to Europe from North America. According to Ernyey, it is more likely that the black locust was introduced to Europe by the Spanish, English or Portuguese, and that Vespasian Robin probably acquired the reproduction material of the black locust later (after 1640). Thus, the current population of *Robinia* in Europe presumably did not come from one place and one tree.

In Central Europe, the first record of the black locust comes from Germany, specifically from Berlin in 1672. The first introduction into Bohemia (Czechia) and Hungary was mentioned in 1710. Initially, the black locust was used as an ornamental tree. However, it was soon applied to afforestation; in Germany, it was supposedly before 1700 (Kolbek et al. 2004). Subsequently, *Robinia* was introduced into forest stands in other Central-European countries: in Hungary by 1750, Czechia sometime after 1760, Slovakia

1769, Switzerland ca. 1850, Slovenia 1858 and Poland 1860 (Vítková et al. 2017). Especially during the 19th century, *Robinia* became a popular tree species.

In terms of the stand area, black locust is now the most widespread non-native tree species in Europe, where it is most abundant in Hungary. The area of Hungarian *Robinia* stands is about 465 thousand ha. Other European countries with a significant proportion of black locust are Ukraine (423 thousand ha), Italy (377 thousand ha), Romania (250 thousand ha), France (191 thousand ha), Serbia (191 thousand ha) and Bulgaria (151 thousand ha) (Nicolescu et al. 2020).

Robinia is also a globally widespread tree species today. Apart from Europe, it is found in subtropical and temperate zones of Asia, Africa, Australia and South America (Li et al. 2014, Martin 2019).

REVIEW ON BLACK LOCUST IN CZECHIA AND CENTRAL EUROPE
Use of *Robinia*

While in Hungary, Austria and Poland, *Robinia* stands were established on flat terrain, in Czechia and also Switzerland, the black locust was often planted on steep slopes around rivers (e.g. the Vltava River), as well as on abandoned pastures and erosion-prone land to protect against erosion and regenerate shallow disturbed soil.

In Prague and its surroundings, *Robinia* plantations were also intended to increase the aesthetic value of the landscape. In the lowlands around the Labe River (surroundings of Mělník) and the České středohoří Hills, the plantations had, among other things, a honey-bearing function (Kolbek et al. 2004). Black locust was also grown near vineyards, where its durable wood was used for the production of vineyard posts. In the past, several waves of *Robinia* afforestation have taken place in various areas of Bohemia. Currently, black locust occupies approximately 14.2 thousand ha in the forests of Czechia, which corresponds to approximately 0.54% of the area of the Czech forests. However, black locust is also found outside forest land. Thus, the actual area of *Robinia* stands is higher. The mean age of *Robinia* forest stands was 67 years in 2022, and the mean growing stock was 121 $m^3 \cdot ha^{-1}$ (FMI 2022). The extent and biological parameters of *Robinia* stands growing on non-forest lands, such as on arable land, in parks and urban and mining areas are mostly unknown (Sádlo et al. 2017).

The low value of stand stock is due to the extremity of habitats where *Robinia* was preferentially planted. Presently, new *Robinia* (conventional) forestry plantations are neither conducted nor planned in Czechia. Earlier forestry cultivation of *Robinia* in Czechia did not bring the expected results. This is due to several factors, which will be briefly listed here and more extensively described in the later text. *Robinia* used to be planted in highly unfavourable sites in Czechia, often steep slopes with poor shallow soils. On such sites, the production of black locust lacks quality and volume. Low soil moisture on slopes causes scrubby forms of black locust (Figure 1) (Vítková et al. 2015).

Figure 1: The railway corridor in Prague, lined with black locust trees. The individuals in the picture demonstrate the distinctive scrubby shape of the trunks, characteristic of many Robinia stands in Czechia. (Photo: Kuneš 2018)

Black locust in Czechia often suffers from frost. Frosts, although they do not affect the vigour of black locust, negatively affect the shape of trees (stem malformations). Moreover, *Robinia* creates ruderal habitats where it grows and outcompetes some native species. Therefore, in many places (e.g. in forests of the capital city of Prague), *Robinia* stands are gradually being converted to stands more corresponding to the native species composition. However, in light of climate change and bark beetle calamity (ca between 2017 and 2021), a renewed interest in *Robinia* and its possible forestry use can be observed among the Czech foresters. Due to the significant invasiveness of the species, this interest needs to be directed towards special forestry plantations or conditions where this tree species can be controlled (in specific cases of urban greenery).

Impact on the environment

Robinia is a pioneer species with broad ecological valence for a range of environmental factors. In its natural distribution range, *Robinia* is limited by its light-demanding nature (Trimble 1975) and especially its vulnerability to certain insect pests and diseases (Huntley 1990). However, in Europe, black locust is a very competitive species, despite its light-demanding nature. In Central Europe, it often forms more continuous groups or stands from which it successively outcompetes some native woody and herbaceous species (Vítková and Kolbek 2010).

In *Robinia*-dominated stands, ground vegetation is often altered (Kolbek et al. 2004). Black locust is able to 'control' occupied habitats for several decades (Sádlo et al. 2017). It can modify the habitats by altering soil chemistry (including the availability of some nutrients) and understorey vegetation. Its stands have specific moisture and light conditions. *Robinia* often forms stands that differ substantially from the native or previous plant communities (Kowarik 1996). *Robinia* is equipped with the ability of allelopathic action. According to some observations, *Robinia* influence caused smaller leaves and shoot apex dieback in birch (*Betula* spp.) and, to a lesser extent, in beech (*Fagus* spp.). Black locust has been found to delay the growth of elm (*Ulmus* spp.). The extracts from *Robinia* roots were thought to reduce photosynthetic rates in pedunculate oak (*Quercus robur* L.) (Bartha et al. 2008).

However, rather than allelopathic activity, *Robinia* in Central-European conditions seems to modify phytocenoses mainly by soil nitrogen enrichment, acidification of topsoil and increased leaching of soil bases (Berthold et al. 2009, Vítková 2014, Vítková et al. 2015). Principle factors responsible for the shift in the plant species composition in black locust stands include increased depletion of some nutrients (because black locust is phosphorus, calcium and potassium-demanding) (Kolbek et al. 2004), specific climate and shade in *Robinia* stands (Vasilopoulos et al. 2007, Vítková 2014) and the tendency to cause aridification of the topsoil (Kolbek et al. 2004), which is likely a consequence of the very intense evapotranspiration of *Robinia* (Bartha et al. 2008). Although the understorey of *Robinia* can be relatively species-rich (approximately 20 to 45 species per 200 m^2), in terms of abundance, nitrophilous species such as *Chelidonium majus* L. (Erteld 1952), *Bromus sterilis* L., *Galium aparine* L., *Urtica dioica* L., *Hedera helix* L., *Sambucus nigra* L. (Sádlo et al. 2017) and *Rubus fruticosus* L. (Kuneš et al. 2019) generally dominate. Recently, an article comparing the black locust stands with native forest stands in hardwood flood-plain forest in western Slovakia concluded that black locust negatively altered the microclimatic conditions and species composition of forest stands. The microclimate under *Robinia* was warmer and less humid than in native forest stands. The alien and ruderal plant species in the understorey of *Robinia* were supported due to the brighter conditions and nitrogen fixation in the soil. Additionally, the other groups of organisms responded negatively to changes under *Robinia* trees in terms of microclimatic conditions, food and shelter sources (Slabejová et al. 2023).

It is worth mentioning that in the northern deciduous forests in North America, where *Robinia* is also a non-native species, no differences in ground vegetation between stands of *Robinia* and native deciduous trees have been observed, and minimal differences in soil chemistry have been noted (Deneau 2013).

Reproduction of black locust and its invasiveness

Reproduction of *Robinia* can take place both generatively and vegetatively. During an average seed year, a stand of *Robinia* produces 120 to 150 kg of seeds per hectare (Nicolescu et al. 2020). The species begin to fruit at approximately six years of age (Olson 1974). *Robinia* is capable of forming a seed bank in the soil with long-lived seeds that will germinate when conditions are favourable and seed dormancy is overcome (Bartha et al. 2008). For example, in a fully stocked 115-year-old stand in Prague (with

a proportion of *Robinia* in the species composition equalling 40%), a seed bank was found in the uppermost 10 cm of soil under the projection of black locust crowns, corresponding to values ranging from 3.3 to 23 thousand seeds per 1 m^2. Seedlings usually do not establish if there is strong competition from ground vegetation, e.g. sward of grass. However, the situation may change if the soil is mechanically disturbed or after a ground fire. In addition, *Robinia* can encroach on grassland areas or sufficiently sun-lighted habitats by root suckers.

Vegetative propagation occurs through stump (stem) and especially root suckers (Figure 2) (Cierjacks et al. 2013). In the case of black locust, the ability to form suckers is one of the most developed of all known woody species (Erteld 1952), and the tree retains it for a very long time. The rate at which *Robinia* encroaches with its sprouts into the surrounding area in dry grassland habitats can be as much as 1 m per year in Central Europe (Kowarik 1996). The spontaneous frontal expansion of black locust in abandoned agricultural land can be ca 2.0–2.2 m per year in South Europe (Crosti et al. 2016). If a parent tree is cut down or mechanically damaged, root suckers can appear up to 7 m from the stump (Trylč 2007). Based on studies of root systems and knowledge of root distribution, root sprouts can probably form even farther from the trunks. The success of *Robinia* in colonising new habitats is also given by the ability of the species to fix atmospheric nitrogen.

Figure 2: The interior of the Robinia stand, which had regrown from stumps and roots following the felling of a portion of mature trees. No chemical treatment was most likely applied. (Photo: Kuneš 2018)

In Czechia, *Robinia* is ranked among ten species of neophytes with the widest range of habitats (according to the 'EUNIS habitat classification') that the species can occupy (Chytrý et al. 2005). In Bohemia, the spread of *Robinia* into surrounding ecosystems was documented in 1874 (Pyšek et al. 2012). However, it is possible that escapes occurred earlier. On a European scale, black locust ranks among the 100 most invasive non-native species (Vilà et al. 2009), and globally the species belongs among the 38 angiosperms classified as invasive in at least six of the fifteen regions of the world (Richardson and Rejmánek 2011). *Robinia* is also considered an invasive woody species in some regions of America (mainly in the eastern part). It colonizes roadsides as well as open habitats (Kershner et al. 2008, Kurz and Hansen 2017).

Ecological limits

In Central Europe, the distribution of *Robinia* is determined by ecological limits, including a cool climate with a shorter growing season. Therefore, *Robinia* in Czechia has the most abundant distribution in the lowlands and lower elevations. Black locust does not ascend to the mountains in Central Europe. Early (autumn) frosts, frequent in Czechia, cause trunk malformations and poor shape (habitus). The vigour of the frost-malformed trees is generally unaffected, but their potential for economic use is significantly reduced. Notably, the recent climatic changes taking place in Central Europe (a shift

towards higher average temperatures) are unlikely to solve this problem, as these changes are not expected to mitigate temperature extremes and anomalies, including late and early frosts.

In contrast, black locust is quite resistant to heat. The trunk of the black locust is protected by a thick bark. On hot sunny days, *Robinia* can position its foliage in such a way as to regulate (reduce) the amount of light falling on it (Erteld 1952). *Robinia* does not tolerate heavy, poorly aerated and also waterlogged soil and shading. Black locust is also sensitive to regular grazing and browsing (Vítková et al. 2017), which does occur, although it is considered poisonous to many wild and domestic animals. On the contrary, it establishes itself in unmaintained areas ('brownfields' and 'urban jungles' in the municipalities, unused agricultural land, etc.).

Use in forestry and outside the forest

The potential of *Robinia* in Central Europe can be summarised as follows: rapid growth when young and the ability to establish itself against beech, ability to fix atmospheric nitrogen, high density, durability, flexibility and calorific value of the wood and its good suitability for processing into fibre/wood pulp, resistance to diseases and pests, ability to grow in poor habitats, resistance to air pollution, drought and high temperatures, a very adaptive root system consisting of both skeletal roots and a dense network of fine roots, flowering from a young age (of importance for beekeeping), frequent and abundant seed years, easy seed processing, good emergence and easy seed storage, rapid seed germination, high genetic variability and ease of in vitro cultivation (Greene 2015, Rédei et al. 2011; Wojda et al. 2015).

Robinia is a very tolerant woody plant well suited to urban greenery. It is often used in urban alleys and as a solitary park tree. It shows exceptional adaptability to drought (Moser et al. 2016) and a range of stresses that the urban environment brings (Figure 3). Despite the generally lower crown volume (compared to, for example, lindens), *Robinia* can display more crown projection area and likely more shade efficient crown shapes (Bayer et al. 2018). Although some dispersal vectors (wind, especially in combination with snow cover, fast-moving vehicles, etc.) can facilitate the distribution of *Robinia* pods and seeds (Cierjacks et al. 2013), dispersal of black locust seeds can be generally viewed as limited. Therefore, plantations of black locust along streets in urban centres (with car speed limitation) or in parks surrounded by buildings can be considered safe (Sjöman et al. 2016).

Figure 3: Black locust is a tree that is highly resilient and can thrive in challenging environments. These traits exemplify the remarkable potential of Robinia, yet they also present a potential risk in terms of the invasive nature of the species. The image depicts a young black locust tree growing in a gap between pavement and asphalt in a street in Prague where black locust trees serve as urban greenery. The planting of Robinia as urban tree greenery is generally not risky, as the presence of buildings and other obstacles effectively prevents the uncontrolled spread of this tree. (Photo: Kuneš 2023)

Under certain circumstances, *Robinia* can be used in the reclamation and revitalisation of anthropogenically disturbed (or destroyed) habitats in industrial or urban environments (Kowarik 2011) or in abandoned open-cast mining areas (Mantovani et al. 2015). The targeted use of *Robinia* in reclamation schemes (usually in combination with agricultural plants in alley cropping systems) may require lower use of herbicides and fertilizers and can lead to a more efficient remediation effect than using purely agricultural techniques (Böhm et al. 2011).

Robinia can complement native species in fulfilling a range of ecological functions (Kowarik 2011; Kowarik et al. 2013), even in specific (extreme) urban environments (Kowarik 2005), where the cultivation of many geographically native tree species encounters their limits. By accepting and judiciously using the existing *Robinia* stands in specific harsh habitats out of contact with valuable native communities, the desired greening of such specific habitats can be achieved and the biodiversity promoted.

The spontaneously established stands of *Robinia* and *Betula* in the industrial area near the former Tempelhof airport in Berlin can serve as an example. The Natur-Park Südgelände in Tempelhof is now a valuable and protected patch of urban and industrial nature (Kowarik and Langer 2005). Elsewhere, birds can benefit from the presence of *Robinia* in mixed forests up to approximately equal proportions of black locust and native trees, although a higher share of *Robinia* (above 50%) causes shifts in bird community compositions toward a dominance of generalist species at the expense of specialists (Kroftová and Reif 2017).

Robinia is a beneficial honey tree that contributes significantly to the production and export of high-quality honey in some countries (Farkas and Zajácz 2007, Keresztesi 1977, Samsonova et al. 2018), as well as for medicinal use.

Although *Robinia* is not considered for common forestry use in Czechia, there are situations where this tree species may find application, whether it is for energy crops, fast-growing (short-rotation) plantations, reclamation or urban greenery. Black locust can also be grown in small stands or groups of trees surrounded by cultivated farmland (regular ploughing, mowing) that does not allow this species to spread spontaneously.

Damage caused by abiotic factors, pests and diseases

As mentioned earlier, *Robinia* is well-adapted to heat, though frost can be a stress factor for this tree. Of the three different types of frost events (early frost at the end of the growing season, winter frost and late frost before or after the growing season), early (autumn) frost has the most frequent effect on *Robinia* in Germany (Liese 1952) and Czechia as well. Black locust does not break its buds until late spring. Leaf expansion in Central Europe occurs from the end of April to early May (Gams in Cierjacks et al. 2013). However, *Robinia* often does not complete the development of shoots until late summer or early autumn. Therefore, early (autumn) frosts can cause damage or death to shoot leaders that have not yet hardened off. If the main shoot leader is damaged, further development the following year continues through the lower situated buds on the shoot as they grow and take over the leading role. The known crooked-grown (Figure 1 and 4) shape of trees in Czechia is often associated with such early frost damage. In addition, young damaged or dead shoots or branchlets provide opportunities for opportunistic fungal parasites (*Nectria cinabarina*) to infect the tree, which can cause further damage (Liese 1952).

Black locust in Central Europe is considered to be a very resilient species due to the absence of many pests and diseases or a lighter course of infestation compared to America, but some organisms can adversely affect the vigour of the species. Seeds of *Robinia* collected in Prague and the Podyjí region have become parasitised by *Eurytoma caraganae* Nikolskaya, (Kuneš et al. 2019). *Robinia* seeds are also susceptible to damage by the *Etiella zinckenella* Treitschke (Georgevits 1981, Kulfan 2012).

Black locust seedlings can be infected by *Alternaria alternata* (Fr.) Keissl. or fungi of the genera *Phytophthora* and *Fusarium* (Cierjacks et al. 2013; Rédei et al. 2011).

The shoots and leaves of *Robinia* may be damaged by the *Parthenoclanium corni* Bouché (Rédei et al. 2011). The leaves can be invaded by introduced species such as *Phyllonorycter* or, more recently, *Macrosaccus robiniella* Clemens or *Parectopa robiniella* Clemens (Šefrová 2006). Leaves are also attacked by the introduced *Obolodiplosis robiniae* Haldeman (Skuhravá and Skuhravý 2004), which spreads rapidly in Europe (Mally et al. 2021), *Euura tibialis* Newman (Medzihorský et al. 2023) or some aphids (*Aphis* spp.) (Rédei et al. 2011).

Young *Robinia* stands can be damaged by hares (*Lepus europaeus* L.), rabbits (*Oryctolagus cuniculus* L.) and also roe (*Capreolus capreolus* L.) and red deer (*Cervus elaphus* L.) (Rédei et al. 2011).

A short discussion on the wood-decaying fungi that sometimes infect *Robinia* should be given because some of them can affect the safety of trees in built-up areas, where black locust is often found and cultivated. The representatives of such fungi reported on black locust are e.g. *Laetiporus sulphureus* (Bull.) Murrill, *Polliota squarrosa* (Batsch) P. Kumm., *Phellinus torulosus* (Pers.) Bourdot et Galzin. Perhaps the most important of these species is *Laetiporus sulphureus,* a cellulose-degrading fungus causing brown rot. The fungus infects its host at wounded parts of a tree (branch stubs, spots of damaged bark, frost cracks). The fungus initially develops in sapwood, which can decompose relatively easily. Later, *Laetiporus* spreads to the adjacent heartwood. Since the bark usually remains over the decaying wood, the existing internal rot cannot be visually detected from the outside. This is only possible when the fruiting bodies of the fungus appear. *Laetiporus* can gradually decompose the heartwood of living trees to the extent that branches break off, and the trees themselves may even collapse. This is particularly noticeable in older *Robinia* trees (Liese 1952).

Old monumental black locust trees may be placed under state (nature) protection due to their advanced age, dimensions and cultural or aesthetic value. These trees should be carefully monitored for *Laetiporus sulphureus* (or other wood-decaying fungi) to avoid accidents due to sudden breakage of heavy branches due to extensive rot. In rot-affected trees, in addition to wind, rainwater also increases the risk of branch fall or tree collapse if it has the opportunity to infiltrate the decayed parts of the tree (Liese 1952).

Wood properties

Black locust has a ring-porous wood structure. Its wood contains about 46% cellulose, 29% lignin and 22% pentosan. The remainder consists of other organic compounds and unburnable ash. Black locust has a distinctive brown heartwood and usually a relatively thin layer of lighter yellow-brown sapwood. A slight greenish tinge can often be perceived in the colour of *Robinia* wood, but this disappears on hot drying and changes to chocolate brown (Göhre 1952).

Klisz et al. (2015) found that the heartwood diameter in *Robinia* stands (aged 31 to 46 years) ranged between 90% and 96% of the total trunk diameter. *Robinia* wood has extraordinary properties. It is very strong, flexible and durable. It is hard, does not shrink much and is easy to work, bend and polish. However, it is difficult to impregnate and is harder to nail in construction work (Göhre 1952).

The wood of the black locust is highly durable. The heartwood can last up to 1500 years in a dry environment, up to 500 years when submerged in water and up to 80 years when exposed to the outside environment (Pacyniak in Wojda et al. 2015).

In Czechia, *Robinia* is often used for outdoor construction, especially where shape irregularity may not be a problem (e.g. outdoor playgrounds) and whole debarked logs of lesser dimensions can be utilised. It is also used for handles, posts, poles (vineyards) and planks. Quality assortments of black locust timber can be used to produce exterior structural components, such as planks and prisms for terraces and pergolas. Sawn timber of black locust is used for flooring or wainscotting. Currently, processes are being tested for glueing laths made from thinner *Robinia* wood assortments into beams, which would allow the use of small-dimension timber from intensive crops managed under the low forest or thinner logs from *Robinia* stands.

Robinia wood is regarded as a good energy source, and the bark increases its heating value. The calorific value of 3.3 m^3 of well-dried *Robinia* wood is comparable to 1 tonne of fuel oil (Molnár and Németh 1983).

Site-specific to management approach of *Robinia pseudoacacia*

The conflicts between positive and negative effects on ecosystem services, which result from the use or presence of non-native shrub and tree species with invasive potential (Figure 4), are generally known and were well-described, e.g. by Dickie (2014). These conflicts of interest among different groups of stakeholders (e.g. general public, foresters, nature conservationists, urban and landscape designers, etc.), are certainly not only related to the issue of black locust in Europe. Black locust, however, represents a vivid example of a tree species where not only the attitude of particular groups differs, but also the general attitude of individual countries and their legal treatment (Vítková et al. 2017).
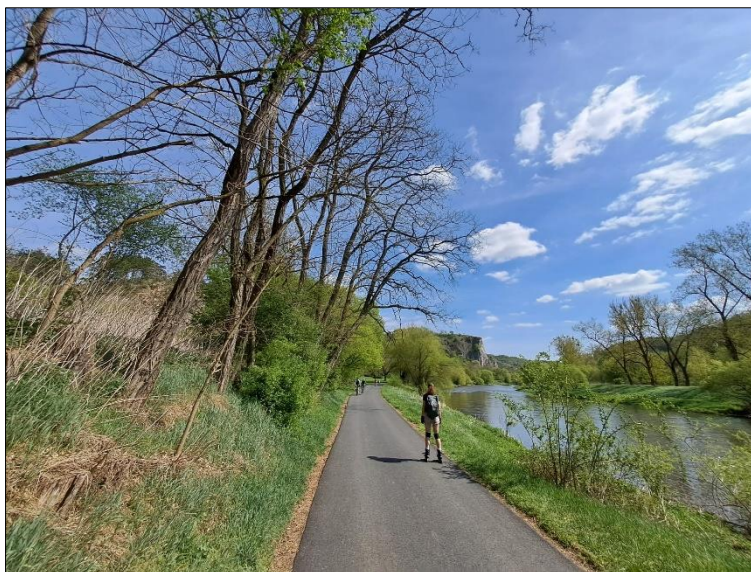
Figure 4: Non-native black locust is a common tree species found along roads and communication routes. Its presence may enhance the aesthetic appeal of the surrounding landscape. However, the black locust trees depicted are located in the Český Ráj Protected Landscape Area (Central Bohemia), where valuable habitats are also found that are threatened by the Robinia invasion. (Photo: Kuneš 2024)

Therefore, Sádlo et al. (2017) suggested a decision framework for sustainable management of black locust based on cost-benefit analysis. Their approach rests in searching for potential threats associated with the presence of *Robinia*, including hazards resulting from the existing management of its stands (pure stands or mixed ones). If no hazards are found, the applied management (including purposeful cultivation of black locust for various reasons) can continue. Where conflict is identified, new altered management approaches are proposed to eliminate or mitigate the hazards. These proposed new approaches range from slow conversion to prompt eradication. To define the 'stratified' management approach, Sádlo et al. (2017) identified eight types of *Robinia* stands: (1) regularly managed *Robinia* forests (pure or with a significant proportion of black locust); (2) regularly managed mixed *Robinia* forests; (3) unmanaged old *Robinia* forests; (4) stands in human-made habitats; (5) dwarf *Robinia* stands growing in natural grasslands; (6) young *Robinia* stands spreading into vulnerable habitats; (7) intensive short rotation plantations, and (8) cultivated single trees and rows. For each type, the ecological conditions, economic benefits and environmental risks were described, and sustainable management practices were proposed.

Some level of risk is related to many of these eight types of *Robinia* stands. However, according to the authors mentioned, only the *Robinia* stand type (6) – the young *Robinia* stands spreading into vulnerable habitats – urgently needs prompt eradication of all black locust individuals (and their sprouts). According to Vítková (2017), species-rich dry and semi-dry grasslands are particularly endangered by *Robinia* invasion resulting from expansion of *Robinia* stand type 6. Among forest habitats, expanding *Robinia* poses a threat chiefly to thermophilous dwarfed oak stands and boreo-continental pine forests Chytrý et al. (2010).

As for some other types of *Robinia* stands, for example, (3) the unmanaged old *Robinia* forests are also generally environmentally risky. Nonetheless, these are frequently recommended to be left to natural succession, when they do not pose a hazard to human safety or infrastructure (traffic, buildings). According to Vítková (2014), slowly decaying old black locust trees growing on slopes along rivers in central Bohemia (belonging to the *Robinia* stand type 3) often can successively be replaced by naturally regenerating European ash (*Fraxinus excelsior* L.), Norway maple (*Acer platanoides* L.), field maple (*Acer campestre* L.) and various shrub species such as European spindle (*Euonymus europaeus* L.), blackthorn (*Prunus spinosa* L.) or buckthorn (*Rhamnus catartica* L.). Recently, the situation has become more complex because *Chalara* disease (Bakys et al. 2009) seriously endangers the population of European ash. European ash was considered a suitable native tree for the natural or artificial conversion of black locust stands. However, there are still enough woody species that can be utilised in the conversions of *Robinia* forests.

On the other hand, the spontaneously or artificially established *Robinia* stands in human-made habitats (*Robinia* stand type 4) and cultivated single trees and avenues (i.e. *Robinia* stand type 8) can often be viewed as sustainable (Sádlo et al. 2017) and can contribute to aesthetical and biological value of their sites. This is not only the Czech approach but the method applied elsewhere in Europe and the world (DeGomez and Wagner 2001, Kowarik and Langer 2005). We would add that a natural or artificial barrier to prevent them from spreading into the surrounding environment is strongly advised.

The (5) dwarf *Robinia* stands growing in natural grasslands, which do not tend to spread, are viewed as more or less stable. The status of the regularly managed *Robinia* forests and regularly managed mixed *Robinia* forests (*Robinia* forest types 1 and 2) may range from risky to more or less sustainable stands. The (7) intensive short-rotation plantations are usually profitable, yet they are unstable and highly risky when abandoned (Sádlo et al. 2017). Unfortunately, for these last three referred types, we can suggest that the higher the environmental risk, the more difficult, costly and time-consuming it is to bring the habitat to a sustainable state. Finally, it should be stressed that the classification of *Robinia* forest types proposed by Sádlo et al. (2017) provides initial information. A particular decision should always be made in a contextual and site-dependant manner.

In the Czech setting, a good example of the need to proceed on a case-by-case basis can be the intensive short-rotation plantations. These can be risky if they are established on sites and areas in contact with vulnerable habitats. However, these crops can also be installed in places where the spreading of black locust to surrounding area can be efficiently prevented (e.g. arable land surrounding the *Robinia* plantations), and the cultivation of these short-rotation productive plantations can be strictly controlled. Regarding such productive plantations of *Robinia*, the Hungarian experience and breeding program can be an inspiration for Czechia.

CONCLUSIONS

Black locust cannot be viewed only unilaterally. It is a tree species with ecological, economic and aesthetic properties that may become more important in light of the current climate development. In Czechia, these characteristics predestine black locust for urban and industrial landscapes or special-production plantations where spontaneous spreading can be prevented. On the other hand, black locust is a highly invasive species that reproduces both generatively and vegetatively, and can threaten valuable forests – and in particular, non-forest communities. Black locust can modify the habitats by altering soil chemistry (ruderalisation) and understorey vegetation and 'control' the occupied habitats for a long time. Black locust management must, therefore, involve a high degree of caution in the first instance. In Czechia, species-rich dry and semi-dry grasslands, thermophilous dwarfed oak stands and boreo-continental pine forests are most vulnerable to *Robinia* invasion.

ACKNOWLEDGEMENTS

REFERENCES

Bakys R, Vasaitis R, Barklund P, Ihrmark K, Stenlid J (2009) Investigations concerning the role of *Chalara fraxinea* in declining *Fraxinus excelsior*. Plant Pathol 58:284–292. https://doi.org/10.1111/j.1365-3059.2008.01977.x

Bartha D, Csiszár Á, Zsigmond V (2008) Black locust (*Robinia pseudoacacia* L.) In: Botta-Dukát Z, Balogh L (eds) The Most Invasive Plants in Hungary. Institute of Ecology and Botany, Hungarian Academy of Sciences, Vácrátót, Hungary, pp 63–76

Bayer D, Reischl A, Rötzer T, Pretzsch H (2018) Structural response of black locust (*Robinia pseudoacacia* L.) and small-leaved lime (*Tilia cordata* Mill.) to varying urban environments analyzed by terrestrial laser scanning: Implications for ecological functions and services. Urban For Urban Gree 35:129–138. https://doi.org/10.1016/j.ufug.2018.08.011

Berthold D, Vor T, Beser F (2009) Effect of cultivating black locust (*Robinia pseudoacacia* L.) on soil chemical properties in Hungary. Forstarchiv 80:307–313. https://doi.org/10.237603004112-80-307

Böhm C, Quinkenstein A, Freese D, Hüttl RF (2011) Assessing the short rotation woody biomass production on marginal post-mining areas. J For Sci 57:303–311. doi: 10.17221/94/2010-JFS

Cierjacks A, Kowarik I, Joshi J, Hempel S, Ristow M, Lippe M, Weber E (2013) Biological Flora of the British Isles: *Robinia pseudoacacia*. J Ecol 101:1623–1640. https://doi.org/10.1111/1365-2745.12162

Crosti R, Agrillo E, Ciccarese L, Guarino R, Paris P, Testi A (2016) Assessing escapes from short rotation plantations of the invasive tree species *Robinia pseudoacacia* L. in Mediterranean ecosystems: a study in central Italy. iForest 9:822–828. https://doi.org/10.3832/ifor1526-009

DeGomez T, Wagner MR (2001) Culture and Use of Black Locust. HortTechnology 11:279–288. https://doi.org/10.21273/horttech.11.2.279

Deneau KA (2013) The Effects of Black Locust (*Robinia pseudoacacia* L.) on Understory Vegetation and Soils in a Northern Hardwood Forest. Master thesis. Swedish University of Agricultural Sciences, Alnarp, Sweden.

Dickie IA, Bennett BM, Burrows LE., Nuñez MA, Peltzer DA, Porté A, Richardson DM, Rejmánek M, Rundel PW, van Wilgen BW (2014) Conflicting values: ecosystem services and invasive tree management. Biological Invasions. 16:705–719. https://doi.org/10.1007/s10530-013-0609-6

Ernyey J (1927) Die Wanderwege de Robinie und ihre Ansiedlung in Ungarn. Magy Botan Lapok 25:161–191 (in Hungarian with German Summary)

Erteld W (1952) Wachstum un Ertrag der Robinie im Gebiet der Deutschen Demokratischen Republik. In: Göhre K (ed) Die Robinie und Ihr Holz. Deutscher Bauerverlag, Berlin, Germany, pp 15–146

Farkas Á, Zajácz E (2007) Nectar Production for the Hungarian Honey Industry. Eur J Plant Sci Biotechnol 1:125–151

FMI (2022) Information about forest and hunting (Informace o lese a myslivosti). Forest Management Institute, Brandýs nad Labem, Czech Republic. Available at: https://www.uhul.cz/wp-content/uploads/2022.zip Accessed 17 Apr 2024

Georgevits RP (1981) Seed insects of *Robinia pseudoacacia*. Dasikon Ereunon 2:223–255

Göhre K (1952) Technologische Eigenschaften und Verwertung des Holzes der Robinie. In: Göhre K (ed) Die Robinie und Ihr Holz. Deutscher Bauerverlag, Berlin, Germany, pp 175–268

Greene W (2015) Black Locust: The Tree on Which the US Was Built. In: Live Science. https://www.livescience.com/50732-black-locust-tree-shaped-the-united-states.html Accessed 4 Apr 2024

Huntley JC (1990) *Robinia pseudoacacia* L. Black Locust. In: Burns RM, Honkala BH (eds) Silvics of North America: 2. Hardwoods. Agriculture Handbook 654:2. USDA, Forest Service, Washington DC, USA, pp 755–761

Chytrý M, Kučera T, Kočí M, Grulich V, Lustyk P (eds) (2010) Habitat Catalogue of the Czech Republic (Katalog biotopů České republiky), 2nd ed. Agentura ochrany přírody a krajiny ČR, Praha, Czech Republic.

Chytrý M, Pyšek P, Tichý L, Knollová I, Danihelka J (2005) Invasions by alien plants in the Czech Republic: a quantitative assessment across habitats. Preslia 77:339–354

Keresztesi B (1977) *Robinia Pseudoacacia*: The Basis of Commercial Honey Production in Hungary. Bee World 58:144–150. https://doi.org/10.1080/0005772X.1977.11097669

Kershner B et al. (2008) Field guide to trees of North America. Sterling Publishing, New York, USA and London, UK

Klisz M, Wojda T, Jastrzębowski S, Ukalska J (2015) Circumferential variation of heartwood in tree stands of black locust. Drewno 58:31–44. https://doi.org/10.12841/wood.1644-3985.116.03

Kolbek J, Vítková M, Větvička V (2004) From history of Central European *Robinia* growths and its communities (Z historie středoevropských akátin a jejich společenstev). Zprávy Čes Bot Společ Praha 39:287–298 (in Czech with English abstract)

Kowarik I (1996) Functions of clonal growth in trees during wasteland succession with special reference to *Robinia pseudoacacia* (Funktionen klonalen Wachstums von Bäumen bei der Brachflächen-Sukzession unter besonderer Beachtung von *Robinia pseudoacacia*). Verhandlungen der Gesellschaft für Ökologie 26:173–181 (in German)

Kowarik I (2005) Wild urban woodlands: Towards a conceptual framework. In: Kowarik, I., Körner, S. (eds) Wild Urban Woodlands: New Perspectives for Urban Forestry. Springer Berlin and Heidelberg, Germany, pp 1–32. https://doi.org/10.1007/3-540-26859-6_1

Kowarik I (2011) Novel urban ecosystems, biodiversity, and conservation. Environ Pollut 159:1974–1983. https://doi.org/10.1016/j.envpol.2011.02.022

Kowarik I, Langer A (2005) Natur-Park Sudgelande: Linking conservation and recreation in an abandoned railyard in Berlin. In: Kowarik, I., Körner, S. (eds) Wild Urban Woodlands: New Perspectives for Urban Forestry. Springer Berlin and Heidelberg, Germany, pp 287–299. https://doi.org/10.1007/3-540-26859-6_18

Kowarik I, von der Lippe M, Cierjacks A (2013) Prevalence of alien versus native species of woody plants in Berlin differs between habitats and at different scales. Preslia 85:113–132

Kroftová M, Reif J (2017) Management implications of bird responses to variation in non-native/native tree ratios within central European forest stands. Forest Ecol Manag 391:330–337. https://doi.org/10.1016/j.foreco.2017.02.034

Kulfan M (2012) Lepidoptera on the introduced *Robinia pseudoacacia* in Slovakia, Central Europe. Check List 8:709–711. https://doi.org/10.15560/8.4.709

Kuneš I, Baláš M, Gallo J, Šulitka M, Suraweera C (2019) Black locust (*Robinia pseudoacacia*) and its role in Central Europe and Czech Republic: review (Trnovník akát (*Robinia pseudoacacia*) a jeho role ve středoevropském a českém prostoru: review). Zprávy lesnického výzkumu 64:181–190. (in Czech with English summary)

Kurtz CM, Hansen MH (2017) An Assessment of Black Locust in Northern U.S. Forests. Res. Note NRS-248. USDA, Forest Service, Northern Research Station, Newtown Square, PA, USA. https://doi.org/10.2737/NRS-RN-248

Li G, Xu G, Guo K, Du S (2014) Mapping the Global Potential Geographical Distribution of Black Locust (*Robinia Pseudoacacia* L.) Using Herbarium Data and a Maximum Entropy Model. Forests 5:2773–2792. https://doi.org/10.3390/f5112773

Liese J (1952) Krankenheiten der Robinie. In: Göhre K (ed) Die Robinie und ind ihr Holz. Deutscher Bauernverlag, Berlin, Germany, pp 271–279

Mally R, Ward SF, Trombik J, Buszko J, Medzihorský V, Liebhold AM (2021) Non-native plant drives the spatial dynamics of its herbivores: the case of black locust (*Robinia pseudoacacia*) in Europe. NeoBiota 69:155–175. https://doi.org/10.3897/neobiota.69.71949

Mantovani D, Veste M, Bohm C, Vignudelli M, Freese D (2015) Spatial and temporal variation of drought impact on black locust (*Robinia pseudoacacia* L.) water status and growth. iForest 8:743–747. https://doi.org/10.3832/ifor1299-008

Martin GD (2019) Addressing geographical bias: A review of *Robinia pseudoacacia* (black locust) in the Southern Hemisphere. S Afr J Bot 125:481–492. https://doi.org/10.1016/j.sajb.2019.08.014

Medzihorský V, Trombik J, Mally R, Turčáni M, Liebhold AM (2023) Insect invasions track a tree invasion: Global distribution of black locust herbivores. J Biogeogr 50: 1285–1298. https://doi.org/10.1111/jbi.14625

Molnár S, Németh K (1983) Investigations into the heat of combustion and heating value of black locust. Faipar 33:78–79

Moser A, Rötzer T, Pauleit S, Pretzsch H (2016) The Urban Environment Can Modify Drought Stress of Small-Leaved Lime (*Tilia cordata* Mill.) and Black Locust (*Robinia pseudoacacia* L.). Forests 7:71. https://doi.org/10.3390/f7030071

Nicolescu V-N, Rédei K, Mason WL, Vor T, Pöetzelsberger E, Bastien J-C, Brus R, Benčať T, Đodan M, Cvjetkovic B, Andrašev S, La Porta N, Lavnyy V, Mandžukovski D, Petkova K, Roženbergar D, Wąsik R, Mohren GMJ, Monteverdi MC, Musch B, Klisz M, Perić S, Keça L, Bartlett D, Hernea C, Pástor M (2020) Ecology, growth and management of black locust (*Robinia pseudoacacia* L.), a non-native species integrated into European forests. Journal of Forestry Research 31:1081–1101. https://doi.org/10.1007/s11676-020-01116-8

Olson DF (1974) *Robinia* L.: Locust. In: Schopmeyer CS (ed) Seeds of woody plants in the United States. Agriculture handbook 450. USDA, Forest Service, Washington DC, USA, pp 728–731

Pyšek P et al. (2012) Catalogue of alien plants of the Czech Republic (2ⁿᵈ edition): Checklist update, taxonomic diversity and invasion patterns Preslia 84:155–255

Rédei K, Csiha I, Keserű Z, Végh Á, Győri J (2011) The Silviculture of Black Locust (*Robinia pseudoacacia* L.) in Hungary: a Review. South-east Eur For 2:101–107. https://doi.org/10.15177/seefor.11-11

Richardson DM, Rejmánek M (2011) Trees and shrubs as invasive alien species – a global review. Divers Distrib 17:788–809. https://doi.org/10.1111/j.1472-4642.2011.00782.x

Sádlo J, Vítková M, Pergl J, Pyšek P (2017) Towards site-specific management of invasive alien trees based on the assessment of their impacts: the case of *Robinia pseudoacacia*. NeoBiota 35:1–34 https://doi.org/10.3897/neobiota.35.11909

Samsonova I, Gryazkin A, Belyaeva N, Belyaev V, Petrik V, Bespalova V, Lyubimov A (2018) Nature-oriented potential resource and melliferous value of forest belts in steppe agro-forest landscapes. Folia Forestalia Polonica 60:99–107. https://doi.org/10.2478/ffp-2018-0010

Sjöman H, Morgenroth J, Sjöman JD, Sæbø A, Kowarik I (2016) Diversification of the urban forest— Can we afford to exclude exotic tree species? Urban For Urban Gree 18:237–241. https://doi.org/10.1016/j.ufug.2016.06.011

Skuhravá M, Skuhravý V (2004) Bejlomorka akátová – nový invazní druh hmyzu na trnovníku akátu. Lesnická práce 83: 520 (in Czech)

Slabejová D, Čejka T, Hegedüšová K, Májeková J, Medvecká J, Mikulová K, Šibíková M, Škodová I, Šustek Z, Jarolímek I (2023) Comparison of alien *Robinia pseudoacacia* stands with native forest stands across different taxonomic groups. Forest Ecol Manag 548:15. https://doi.org/10.1016/j.foreco.2023.121413

Šefrová H (2006) Invazní druhy motýlů. Veronica – časopis pro ochranu přírody a krajiny 20:4–6 (in Czech)

Trimble GR (1975) Summaries of Some Silvical Characteristics of Several Appalachian Hardwood Trees. Gen. Tech. Rep. NE-16. USDA Forest Service, Upper Darby, PA, USA

Trylč L (2007) Sukcesní změny po odstranění akátu a zhodnocení managementu na vybraných lokalitách v Praze. Diploma thesis. Univerzita Karlova v Praze, Přírodovědecká fakulta, Ústav pro životní prostředí, Praha, Czech Republic (in Czech)

Vasilopoulos G, Tsiripidis I, Karagiannakidou V (2007) Do abandoned tree plantations resemble natural riparian forests? A case study from northeast Greece. Bot Helv 117:125–142. https://doi.org/10.1007/s00035-007-0796-9

Vilà M, Basnou C, Gollasch S, Josefsson M, Pergl J, Scalera R (2009) One Hundred of the Most Invasive Alien Species in Europe. In: Handbook of Alien Species in Europe. Springer, Dordrecht, Netherlands, pp 265–268. https://doi.org/10.1007/978-1-4020-8280-1_12

Vítková M (2014) Management of Black Locust Stands (Management akátových porostů). Životné Prostredie 48:81–87 (in Czech with English abstract)

Vítková M, Kolbek J (2010) Vegetation classification and synecology of Bohemian *Robinia pseudacacia* stands in a Central European context. Phytocoenologia 40:205–241. https://doi.org/10.1127/0340-269X/2010/0040-0425

Vítková M, Müllerová J, Sádlo J, Pergl J, Pyšek P (2017) Black locust (*Robinia pseudoacacia*) beloved and despised: A story of an invasive tree in Central Europe. Forest Ecol Manag 384:287–302. https://doi.org/10.1016/j.foreco.2016.10.057

Vítková M, Tonika J, Müllerová J (2015) Black locust–Successful invader of a wide range of soil conditions. Sci Total Environ 505:315–328. https://doi.org/10.1016/j.scitotenv.2014.09.104

Wojda T, Klisz M, Jastrzębowski S, Mionskowski M, Szyp-Borowska I, Szczygieł K (2015) The Geographical Distribution of The Black Locust (*Robinia pseudoacacia* L.) in Poland and Its Role on Non-Forest Land. Papers on Global Change 22:101–113. doi:10.1515/igbp-2015-0018

Engineered wood products for construction based on beech and poplar resources in Europe

Joris Van Acker[1*], Liselotte De Ligne[1], Tobi Hallez[1], Jan Van den Bulcke[1]

[1] Ghent University, UGent-Woodlab - Laboratory of Wood Technology, Coupure Links 653, 9000 Ghent, Belgium

E-mail: Joris.VanAcker@UGent.be; Liselotte.DeLigne@UGent.be; Tobi.Hallez@UGent.be; Jan.VandenBulcke@UGent.be

Keywords: Engineered wood products, beech, poplar, hybrid

ABSTRACT

Beech is a major tree species in Europe, offering significant potential as a resource for building products. Also, hybrid poplar has a high potential for the construction sector, given its availability from both plantations and trees outside forests. Both hardwood species can be used complementary in construction products, as the high density of beech can complement the lower density of poplar. Density is related to a wide range of properties related to building with wood: strength and stiffness, duration of load, creep, hardness, fire resistance and dimensional stability.

The historical use of poplar timber in construction demonstrates its potential as an alternative material to softwoods, such as spruce. Specific properties like the presence of tension wood impacting drying and surface quality might hinder the current use of timber products. Beech has not been considered for timber constructions as such, but is to some extent similar to oak which was the eminent wood species for construction in the past. The higher density of beech and the related low dimensional stability are also influencing the potential for building with wood. Both wood species can be used for engineered wood products and as such some of the properties can be designed to fit for purpose. Combining both in this respect might lead to major advantages in providing commodities suitable to complement the current volumes of wood products for green building.

Beech and poplar exhibit a low natural durability against fungi, similar to many types of softwood timber that are commonly used. Enhancing the durability of engineered wood products based on these species can be based on a range of technological solutions, such as thermal or chemical modification. The durability against insects is also low, but the biological agents involved might be less critical for these hardwood species. Furthermore, wood protection options can be positively integrated in a fit-for-purpose context.

Enhancing performance by combined engineered wood products, so-called hybrid EWPs should provide extra potential. For solid timber-based products like glulam (GLT) and cross laminated timber (CLT) this was already tested for both species and has been underpinned by research projects. Also veneer based products like plywood and laminated veneer lumber (LVL) are very suitable for combining wood species and rheological performance can further be improved by using natural fibres as extra embedded component. Current trends in strand-based panel and beam products like OSB and LSL demonstrate a tendency to incorporate multiple wood species as resources, with an increased interest in hardwoods. Here also properties can be defined through careful combination of wood species creating as such a fit for purpose mix of beech and poplar.

INTRODUCTION

Although hardwoods have been part of historical use in timber construction currently mainly softwood species are used. The trend to focus more on broadleaved and mixed forests as well as initiatives related to increased building with wood leads to a logic relationship between both.

In this paper both beech (*Fagus sylvatica*) and poplar (*Populus* spp.) are discussed in relationship to extra opportunities when focussing on engineered wood products (EWP). As complementary options to the common softwood based product there is not only potential to use wood species specific products but also hybrid or mixed wood species products are relevant.

Beech is a major tree species in Europe, offering significant potential as a resource for building products. Also, hybrid poplar has a high potential for the construction sector, given its availability from both plantations and trees outside forests. Both hardwood species can be used complementary in construction products, as the high density of beech can complement the lower density of poplar. Density is related to a wide range of properties related to building with wood: strength and stiffness, duration of load, creep, hardness, fire resistance and dimensional stability.

Tree species

The distribution and available volumes in Europe for both beech and (hybrid) poplar show the major potential of these hardwood materials as complementary resource for some of the softwood uses today. Poplar trees are among the fastest growing trees in Europe as they can be harvested after 10 to 20 years. Nowadays poplar is the main species used in the production of plywood in several European countries like Spain, France, Italy and Hungary. Poplar plywood has applications in decoration and furniture, and a soaring demand in high-end industries like campervans, trains or yachts and boats where it is used for interiors and furnishing. Poplar wood is also used for matches, cheese boxes, medical tools, chopsticks, among others, and the fact that it is colourless, odourless and tasteless makes it an ideal material for the manufacturing of packaging for the agri-food industry.

Currently, in the EU there are approximately 450.000 hectares of production-oriented hybrid poplar forests and plantations, mainly concentrated in the Mediterranean countries, that are also the main producers of poplar plywood. France is the first country in poplar production in Europe followed by Spain and Italy (PROPOPULUS). Some other countries are also important, e.g. Turkey with some 130.000 hectares of poplar plantations, half *Populus nigra* clones and half *Populus x euramericana + Populus deltoides* clones (Zoralioglu 2003). European aspen (*Populus tremula*) is present European wide but mainly of interest in Northern Europe. Poplars in Europe are beside *Populus tremula* mainly focussing on hybrid poplar often based on planted forest, mainly plantations. These hybrid poplars are still today part of selection and breeding programs based on cultivars based on European and American species (*Populus x euramericana* mainly based on *P. nigra* and *P. deltoides*), only American species (*Populus x interamericana* mainly based on *P. deltoides* and *P. trichocarpa*), and also Asian species (*Populus x asiamericana* mainly involving also *P. maximowiczii*). Hybrid poplars can be designed to desired properties (Defoirdt et al. 2017) and easily vegetatively propagated as clones (Zsuffa et al. 1993). The International Commission on Poplars and Other Fast-Growing Trees Sustaining People and the Environment (IPC) is providing an eminent network as treaty-based statutory body placed within the framework of the FAO (Food and Agriculture Organization of the United Nations).

Figure 1: Main EU-regions with hybrid poplar plantations (PROPOPULUS).

European beech, *Fagus sylvatica* L. (Fagales: Fagaceae), is an Atlantic tree species growing on a broad range of site conditions over a substantial elevational range. The wood is appreciated for indoor use and musical instruments, as well as for plywood, veneering and pulp. Due to its high energetic potential, beech is coppiced for firewood, and charcoal and is expected to increase its role as a construction material (Pramreiter and Grabner 2023).

A change in tree species composition in Central Europe to increase the resilience of forests when coping with climate change effects is imminent. The present and expected future role of the European beech,

(*Fagus sylvatica* L.) is considered with respect to the expansion of its habitat. Stands of highly productive tree species such as spruce are gradually being replaced mixed-species forests. Beech is considered an important species in relation to this transition. However, the vulnerability to drought and pathogens are limiting factors for beech forests (Jandl et al. 2023). Martinez del Castillo et al. (2022) raised serious concern related to the climate-change-driven growth decline of European beech forests.

The European beech is the most prevalent deciduous tree species in Central Europe. In Croatia, Romania, and Slovenia it is economically the most important tree species, representing 36%, 31.5%, and 31% of the tree species composition, respectively. Also, in Slovakia it is of great economic significance, accounting for 30% of forest area. In Germany it constitutes 15% of the tree species composition, being the most widespread hardwood tree. In Austria, Czechia, and Poland, the percentage share of that tree species is much lower (10%, 7%, and 5.5%, respectively). In 2000, the growing stock of beech in Germany amounted to 583 million m^3 (352 m^3/ha); it has now increased to more than 635 million m^3. The beech stocks amount to more than 166 million m^3 in Poland, 139 million m^3 in Slovakia, 105 million m^3 in Slovenia, 100 million m^3 in Austria, and 41 million m^3 in Czechia. In the years 2001-2018, the total exports and imports of beech roundwood in Europe remained at similar levels, amounting to 56.8 million m^3 and 54.0 million m^3, respectively. Beech roundwood was exported mainly from Germany 665.1 thousand m^3 $year^{-1}$, as well as France and Slovakia approx. 444 thousand m^3 $year^{-1}$ (14%). At the same time, the greatest volumes of beech roundwood were imported by Austria 892.7 thousand m^3 $year^{-1}$, Italy (572.9 thousand m^3 $year^{-1}$), and Belgium (475 thousand m^3 $year^{-1}$). It should be noted that in 2013-2017 France and Germany were the largest exporters, jointly responsible for 44% of hardwood log exports. A substantial portion of those exports went to Asia, with 23% of beech roundwood being shipped to China, which is the largest timber importer in the world, accounting for as much as 32% of total industrial roundwood imports. Export prices of German beechwood to China without freight costs in 2004 was 226 € m^{-3} for beech lumber and 52 € m^{-3} beech logs, but more recent prices were often closer to 100 € m^{-3} (Kożuch and Banaś 2020).
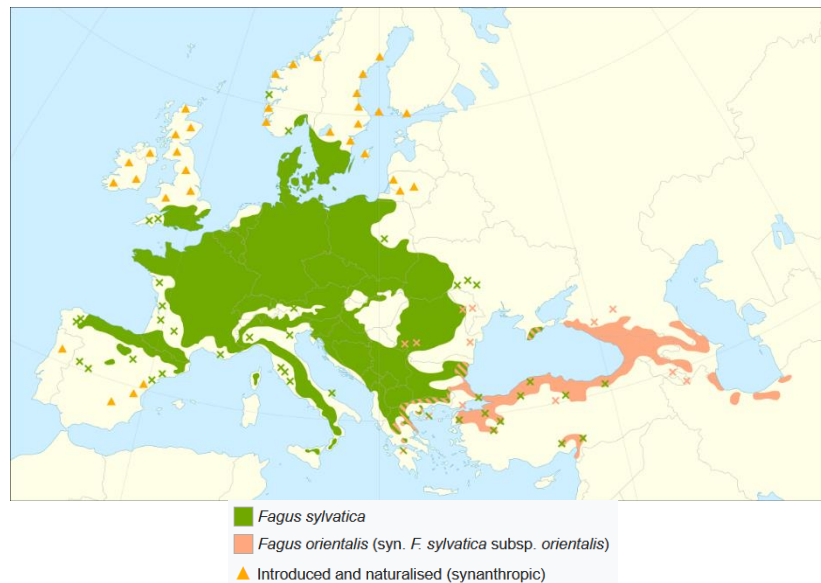
Figure 2: Distribution map of Fagus sylvatica (European beech) and Fagus orientalis (Oriental beech) (EUFORGEN)

Wood species

The historical use of poplar timber in construction demonstrates its potential as an alternative material to softwoods, such as spruce. Specific properties like the presence of tension wood impacting drying and surface quality might hinder the current use of timber products. Beech has not been considered for timber constructions as such, but is to some extent similar to oak which was the eminent wood species for construction in the past. The higher density of beech and the related low dimensional stability are also influencing the potential for building with wood. Both wood species can be used for engineered wood products and as such some of the properties can be designed to fit for purpose. Combining both

in this respect might lead to major advantages in providing commodities suitable to complement the current volumes of wood products for green building.

Beech (*Fagus sylvatica*) and poplar (*Populus* spp.) differ considerably in basic wood properties and hence can be assessed in relation to a range of both processing and performance options. In the below overview (Table 1) details are provided in relation to the basic properties of these wood species. It is also relevant to notify that both beech and poplar are of low durability, classified as durability class DC5, meaning 'not durable' in EN 350 (2016) and corresponding to a service life in ground contact of less than 5 years. Beech and poplar do exhibit a low natural durability against fungi, though this is similar to many types of softwood timber that are commonly used. Enhancing the durability of engineered wood products based on these species can be based on a range of technological solutions, such as thermal or chemical modification. The durability against insects is also low, but the biological agents involved might be less critical for these hardwood species as critical beetles like the house longhorn beetle (*Hylotrupes bajulus*) are not relevant.

Table 1: Main physical and mechanical properties of beech, poplar and softwood references
(density and mechanical values at 12% MC)

Tree species	Density [kg/m³]	Shrinkage (green to 0%) [%]	MOR [MPa]	MOE [GPa]	Janka hardness [N]
European beech (*Fagus sylvatica* L.) [a]	(690-)710(-750)	R: 5.2; T: 11.2 T/R: 2.1	113	12.3	5500
European beech (*Fagus sylvatica*) [b]	710	R: 5.8; T: 11.7 T/R: 2.0	110	14.3	6460
American beech (*Fagus grandifolia*) [b]	720	R: 5.8; T: 11.7 T/R: 2.0	103	11.9	5780
Black poplar (*Populus nigra* L.), Eastern cottonwood (*Populus deltoides* Marshall), Aspen (European: *Populus tremula* L. & Canadian: *Populus tremuloides* Michx), Hybrid poplar (*Populus x canadensis* Moench) [a]	(380-)440(-530)	R: 2.9; T: 8.3 T/R: 2.9	70	9.7	2300
Black poplar (*Populus nigra*) [b]	385	R: 4.0; T: 9.3 T/R: 2.3	64	7.2	2020
Eastern cottonwood (*Populus deltoides*) [b]	450	R: 3.9; T: 9.2 T/R: 2.4	59	9.5	1910
Black cottonwood (*Populus trichocarpa*) [b]	385	R: 3.6; T: 8.6 T/R: 2.4	59	8.8	1560
European aspen (*Populus tremula*) [b]	450	R: 4.8; T: 8.3 T/R: 1.7	62	9.8	1650
Quaking aspen (*Populus tremuloides*) [b]	415	R: 3.5; T: 6.7 T/R: 1.9	58	8.1	1560
Norway spruce (*Picea abies* (L.) H.Karst.) [a]	(300-)460(-620)	R: 4.1; T: 8.9 T/R: 2.1	69	8.9	1910
Norway spruce (*Picea abies*) [b]	405	R: 3.9; T: 8.2 T/R: 2.1	63	9.7	1680
Scots Pine (*Pinus sylvestris*) [b]	550	R: 5.2; T: 8.3 T/R: 1.6	83	10.1	2420

Consulted database: [a]*Houtvademecum;* [b]*Wood Database*

Both beech and poplar are diffuse porous hardwood species with in general no real distinction between earlywood and latewood also limiting the impact of growth rate on wood properties. In Figure 3 a 3D CT image is presented of poplar wood and a growth ring analysis of a core from a beech tree including density values. The higher latewood density can contribute to differences in mechanical properties related to growth rate.

(a)

(b)
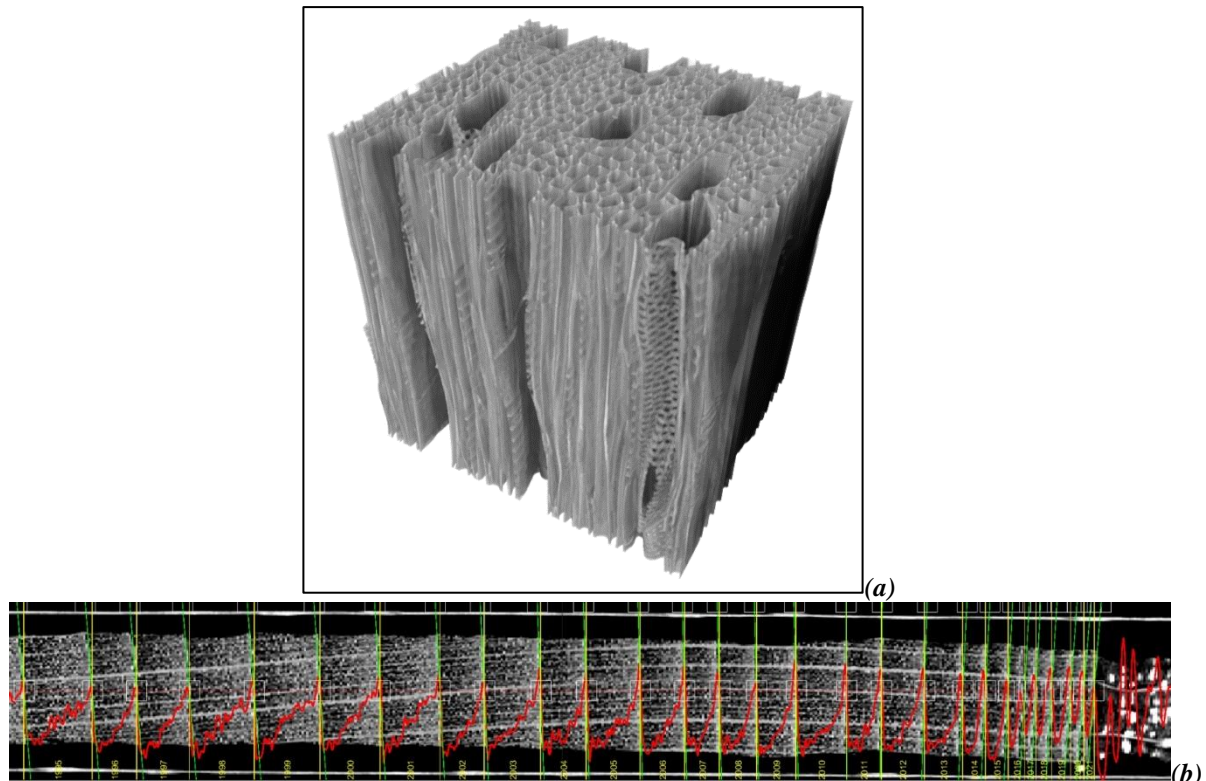
Figure 3: Diffuse porous poplar and beech (a) 3D CT image of poplar (b) CT image of growth rings of beech with wood density as red line (Verschuren et al. 2023)

Wood processing

Trees are portioned into logs of different quality based on their diameter and defects present. These logs serve different purposes, including producing veneer, sawn timber, and chips (strands). Engineered wood products for construction serve either as load-bearing beams or as panels for separation or reinforcement purposes. While bio-based materials primarily intended for structural purposes in construction, many wood species can also be used for decorative applications (such as furniture and flooring) and even as insulation products.

European beech is one of the dominating wood species in central Europe, particularly noted for its abundance in Austrian, German, and Swiss forests, where it is identified as the most prevalent hardwood. Its primary applications today revolve around energy provision and the furniture industry (Pramreiter and Graner 2023). Based on their reviewed literature, current research efforts deal with different engineered wood products like glued laminated timber, cross-laminated timber and laminated veneer lumber. Currently, the most-used raw materials for structural timber are still softwood species, which is due to the actual situation of standards. Relevant standards of the European Union (EU), for example EN 14080 (2013), only permit the use of poplar and no mixture of different wood species (Krackler et al. 2011).

The production of plywood is by far the most important and remunerative destination for the best raw material resulting from intensive poplar cultivation (Castro and Fragnelli 2006). Beyond this "noblest" portion (about 70 %), typically used for the production of plywood panels, the remaining parts are generally used for the production of packaging (pallets and fruit boxes), particleboard, pulp or biomass for energy.

ENGINEERED WOOD PRODUCTS

When considering options for using hardwood-based engineered wood products in construction, it's important to explore the state-of-the-art products related to beech and poplar. Depending on the required tree or log quality, products can be categorized based on rotary-cut veneer, sawn timber, and chip or strands. Each of these categories has separate processing methodologies, with more traditional products like plywood, glulam, and OSB (Oriented Strand Board). However, there are also more innovative

products such as LVL (Laminated Veneer Lumber), CLT (Cross Laminated Timber), and LSL (Laminated Strand Lumber). This diversity allows for differentiation in both beams and panel products. Among these options, glulam or glued laminated timber (GLT), is a well-known product complementing timber. Glulam made of hardwood is a modern construction product developed in line with the current changes in the forestry industry. In the last decade, studies on hardwoods (deciduous) such as beech, oak, chestnut and ash have been intensively conducted in Europe (Glavinić et al. 2020). The relevance of hardwoods today is exemplified by the French beech forests, which occupies about 1.4 Mha with an annual volume of harvested wood (1 million m^3) for sawn timber estimated at 400000 m^3. The goal of French industry is to extend the knowledge of mechanical properties of French beech (already initiated in Germany), thus promoting its use in construction applications (sawn timbers, glulam beams) (Lanvin et al. 2019). European hardwood species such as beech, oak and ash present a potential alternative to commonly used softwoods in glued engineered wood products. Primarily, amino- and phenoplast adhesives are used for bonding these hardwoods, but some one-component polyurethane (1C-PUR) adhesives prove to offer an alternative when combined with a primer pretreatment (Luedtke et al. 2015). Emulsion Polymer Isocyanate adhesive (EPI) could offer benefits for the production of hardwood based products as it is well suited for bonding difficult wood species and could even be used for metal-wood bonding (Grøstad and Bredesen 2014).

Pramreiter et al. (2023) provided a nice overview of the main 6 different engineered wood products discussed in this paper (Figure 4). Firstly, logs with the highest quality are selected for veneer peeling, leading to the cross oriented wood-based panel product plywood (PLY) and the equivalent parallel oriented laminated veneer lumber (LVL). Secondly, the general use of lumber (timber) lead to glulam or glued laminated timber (GLT), and more recently, the very relevant mass timber product known as cross laminated timber (CLT). Finally, the smaller and lower quality logs can be used for strand based products like oriented stand board (OSB) and the related structural composite lumber (SCL) products such as oriented and laminated strand lumber (LSL).
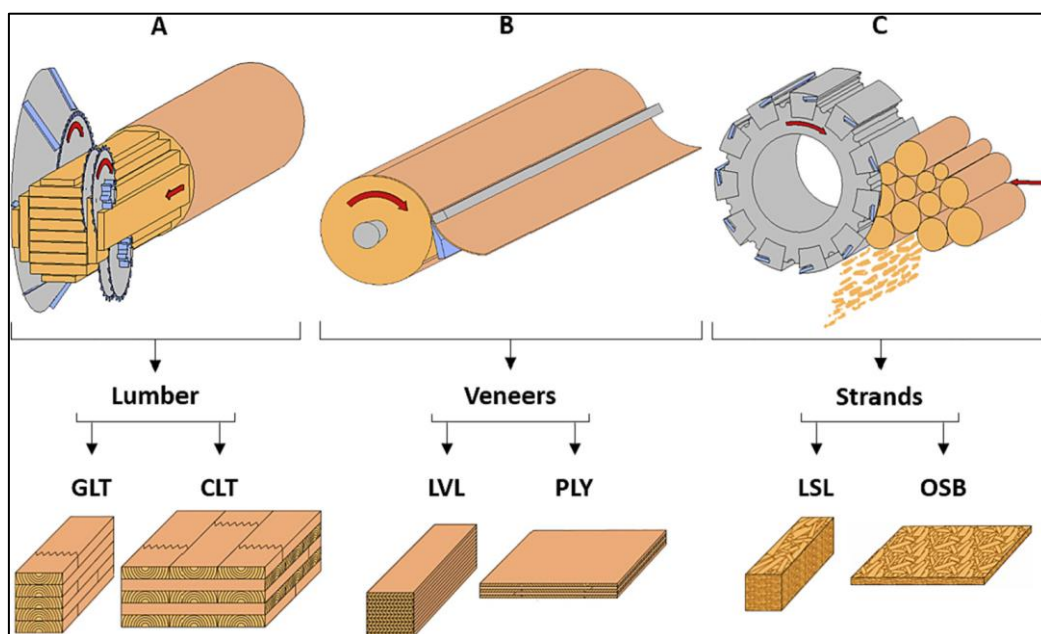
Figure 4: Schematic depiction of main disintegration processes for round wood and subsequently produced engineered wood products relevant for structural applications. A: Sawmilling to produce lumber/timber used in GLT = Glued Laminated Timber and CLT = Cross Laminated Timber. B: Veneer peeling to produce veneers used in LVL = Laminated Veneer Lumber and PLY = Plywood. C: Stranding to produce strands used in LSL = Laminated Strand Lumber and OSB = Oriented Strand Board (Pramreiter et al. 2023)

Since both wood species are of low durability, wood protection options can be positively integrated in a fit-for-purpose context. A range of methods have been proposed and depending on the type of engineered wood product their potential for use in more continuous humid environments, referred to as use classes higher than 2 in EN 335 (2013), can be implemented (Van Acker 2019).

In the following parts research output is being reviewed for veneer based, timber based and strand based engineered wood products. Those related to beech and poplar (aspen) resources are discussed separately as well as hybrid materials of both and with other wood species. Each time there is also a reflection on options to enhance the properties by treating or reinforcing the EWP.

Plywood (PLY) and Laminated Veneer Lumber (LVL)

The bottom log of high-quality trees can be used for the production of rotary cut veneer. Peeling these logs yields tangentially oriented layers, which are used in the production of cross-layered plywood panels or parallel-layered beams known as laminated veneer lumber (LVL).

Beech plywood

Beech allows for the production of high-performance plywood with excellent mechanical properties. The material properties for European beech (*Fagus sylvatica* L.) are defined as mean values: density of 690 kg/m^3 at 12% moisture content, moduli of elasticity and Poisson's coefficient $E_L=E_{11}=14000$MPa, $E_T=E_{22}=1160$MPa, $G_{12}=S_{66}=1080$MPa, (major)$\nu_{LT}=\nu_{12}=0,52$, (minor)$\nu_{TL}=\nu_{21}=0,043$. These values allow for the calculation of normal stresses in individual laminate layers of plywood (Makowski 2015). The veneer elastic constants data enables a strength analysis of structural members made of beech plywood, especially finite element analysis in the case in which orthotropic 3D elements within each ply of plywood are used (Wilczynski 2011).

Poplar and aspen plywood

Hybrid poplar plywood is a standard product produced in Europe, sourced mainly from plantations in countries such as France, Spain and Italy. Although these products have only recently been considered for use in construction with wood, experimental values obtained for poplar plywood demonstrate its structural potential, despite the wood itself not possessing particularly high-performance properties (Baldassino et al. 1998).

The density variability of 10 different poplar clones helped to predict the plywood stiffness, with no other effects showing significant impacts on the static modulus. And although it was not possible to predict the strength, this finding contributes to the development of adequate processing strategies for multicultivar poplar stands (El Haouzali et al. 2020). Additionally, research has shown that plywood bonded with a melamine-urea-formaldehyde (MUF) adhesive exhibits superior mechanical strength compared to that bonded with a polyvinyl acetate (PVAc) adhesive. Bao and Liu (2001) indicated that it is possible to satisfactorily predict the quality of veneer and plywood of Chinese plantation poplar based on a selection of key wood properties. Recent research related to high-quality birch plywood production also explored the potential of incorporating aspen into lay-up schemes (Kallakas et al. 2020). Besides standard plywood products, innovative products have also been investigated. For instance, poplar plywood produced with high-density polyethylene (HDPE) films assessed by SEM and optical microscopy showed resins penetration into the lumens of vessels, rays and wood fibers near the bondline, contributing to mechanical interlocking and filling providing plywood with excellent bonding properties (Chang et al. 2017). Furthermore, the development and testing of sound absorbing poplar plywood for the acoustic improvement of dining rooms or open space offices resulted in effective sound absorbers enabling their industrialization to become a valuable niche for poplar plywood producers (Negro et al. 2016).

The production of flexible plywood, utilizing combinations of poplar (*Populus deltoides*) and paulownia (*Paulownia fortunei*) veneers resulted in plywood capable of bending around a cylinder with a diameter of 6.5 mm, reaching the minimum bending radius with no sign of damage (Sedighizadeh et al. 2023).

Treated plywood

Both low durability and limited dimensional stability of beech often are overcome by treatment methods. Drying at higher temperature (180 °C) initiates the formation of acetic and formic acid, which lower the pH and effect the curing of acid catalyzed UF resin. This process results in improved shear strength and dimensional stability (water absorption and thickness swelling) of beech (*Fagus orientalis* L.) plywood. However, chemical surface degradation caused by UV irradiation can counteract these effects (Jamalirad et al. 2011). Beech plywood boards that have been heat-treated at 200°C for 3 hours exhibit improved

performance in very humid environments, with a reduced thickness swell of 4% and a water absorption rate reduced by more than 12% (Lunguleasa et al. 2018).

Besides thermal modification also chemical wood modification treatments can easily be used for veneer treatments. Rotary cut beech (*Fagus sylvatica* L.) veneers were treated with two formulations based on N-methylolmelamine (NMM). The study demonstrated that regardless of the production process, the modification of veneers with both types of NMM compounds caused only minor changes in MOR and MOE compared to the control plywood (Trinh et al. 2012). Furthermore, the treated plywood weathered outdoors exhibited higher dimensional or form stability, fewer cracks and delamination, and reduced surface colonization by staining fungi compared to the control plywood (Trinh et al. 2012b). Additionally, research findings indicated for acetylated plywood, ignition time increased due to raised weight percent gains and glowing decreased (Mohebby et al. 2007).

Beech veneers treated with resins produced at elevated pressure have long been used to produce specific products such as compreg and impreg (Stamm and Seborg 1960). Compreg is similar to impreg, except that it involves compressing the material before the resin is cured within the wood. The resin-forming chemicals (usually phenol-formaldehyde) act as plasticizers for the wood so that it can be compressed under modest pressure (6.9 MPa) to a density of 1.35 g/cm³. In an industrial trial, rotary-cut beech (*Fagus sylvatica* L.) veneers (2.5 mm thick) treated with low molecular weight phenol-formaldehyde (PF) in aqueous solution provided plywood with significantly higher static bending properties compared to unmodified specimens, as well as increased durability against the white rot fungus *Trametes versicolor* (Bicke et al. 2012).

Poplar plywood is especially critical when biological durability is required. MUF glued plywood panels, made of veneers of the poplar clone 'I-214', were evaluated against the attack of wood decay fungi showing all a high level of biodegradation (Zanuttini et al. 2003). Today thermal modification is considered a good option to overcome this. Poplar plywood panels were manufactured with urea-melamine-formaldehyde adhesive, both in a standard mixture and added with resorcinol and then treated by the Termovuoto® process at 170, 190 and 210°C for 2 h. The bonding quality of treated panels complied with the requirements of EN 314-1 (2004) and 2 (1993); bending strength and modulus of elasticity decreased, color darkened and durability increased (Zanuttini et al. 2019). However, the mechanical performance and the bonding quality of heat-treated poplar plywood samples showed large reductions of shear strength. Interestingly, specimens glued after treatment resulted in slightly better results compared to those glued before treatment (Goli et al. 2014). Thermal modification of poplar veneer was considered optimal at temperatures 200-210 °C. This temperature range allowed for the production of plywood boards with the best results in terms of moisture absorption and dimensional stability when using solely this material. However, when combined with other veneers, the resulting plywood exhibited better mechanical properties (Lovrić et al. 2017).

Especially for poplar, densification can be used to improve some mechanical properties. Based on evaluating veneer surface roughness/quality, the optimum range of aspen panel densification was identified with a panel compression ratio (CR) ranging from 11.3% to 18.0% and validated for plywood/LVL manufacturing. This densification process resulted in improved panel quality, increased material recovery, and dimensional stability, while also achieving superior panel bending and glue bond (shear) performance (Wang et al. 2006).

In addition to resistance against decay, fire resistance treatments are also important and can have a significant impact on mechanical performance. Plywood, manufactured with flame-retardant polyvinyl alcohol adhesive and using eucalyptus, birch, and poplar veneers respectively, showed varying static bending strengths. Specifically, the plywood made with eucalyptus veneer exhibited the highest static bending strength at 54.4 MPa, followed by birch veneer at 38.3 MPa, and poplar veneer at 31.2 MPa. (Yin et al. 2021). The layered two dimensional material α-Zirconium Phosphate (α-ZrP) was used to explore its effect on the flame-retardant properties of poplar plywood, providing a strong basis for the application of this product in flame retardancy of wood-based composites (Xu et al. 2021).

Option to enhance the properties of plywood can be very similar for beech and poplar. Beech and poplar veneers immersed in 25% solutions of monoammonium phosphate (MP) and sodium acetate (SA) showed that the fire resistance effect was better with poplar than with beech veneers. Adhesive curing might be affected during hot pressing of plywood, since impregnants changed the original pH value of veneers. The best fire resistance was realised by combination of MP and poplar veneers (Miljković et al. 2005).

Hybrid or combined plywood

To improve some properties of plywood, hybrid or combined wood species can be used. Three-layer beech plywood were overlaid with thin veneers of seven tropical species: aningré (*Aningeria robusta*), bubinga (*Guibourtia demeusei*), iroko (*Milicia* sp.), khaya (*Khaya ivorensis*), padouk (*Pterocarpus* sp.), sapelli (*Entandrophragma* sp.) and wengé (*Millettia laurentii*). Beech plywood overlaid with padouk veneers had the lowest mass loss after fungal attack. However, good antifungal effects were also accomplished using the iroko, bubinga and wengé veneers (Reinprecht et al. 2012). Improvement of fungal resistance of beech plywood can be obtained by incorporation of more durable oak (*Quercus robur*) or black locust (*Robinia pseudoacacia*) surface veneers and through usage of fungicides (Reinprecht and Kmeťová 2014). A Comparison of plywood produced from tropical species with beech revealed that densities of beech plywood are higher than those of solid wood and exceed those of common plywood based on okoumé and ozigo (Birinci 2022).

The effect of different lay-up schemes and usages of gray alder, black alder and aspen on the mechanical properties of plywood, by replacing birch veneer in the plywood core with these alternative wood species, revealed several findings. Birch and black alder plywood panels demonstrated generally the highest bending strength properties, followed by grey alder and aspen. Birch veneers exhibited the lowest glue consumption at 152 g/m2, while aspen had the highest at 179 g/m2. Low-density wood veneers exhibited higher glue consumption and greater compaction in thickness compared to birch veneers under the same pressure, leading to increased product density. With appropriate lay-up schemes, these wood species could be effectively utilized by the veneer-based products industry (Kallakas et al. 2020). Aspen and black alder, alone and in combination with birch faces and with different veneer thicknesses, were used to produce plywood. Birch plywood had the highest MOR and MOE, followed by aspen and black alder. Aspen had the highest glue consumption and birch the lowest, when applied with a spreader roll, but the common practice of using relatively thick 2.6 mm aspen veneers resulted in the lowest glue consumption per mm of product. Birch gave the best strength properties while aspen gave the best price and weight combination (Akkurt et al. 2022).

A comparison was conducted to assess the technological advantages of using alder wood over beech wood as a raw material in the manufacturing of plywood and laminated veneer lumber (LVL). While the mechanical properties of beech plywood were better, the alder plywood was still meeting the standards and with and annual increment per hectare of up to 20m^3 increment can contribute to meet the raw material demand (Toksoy et al. 2006). Five-layer Norway spruce (*Picea abies* [L.] Karst.) and European beech (*Fagus sylvatica* L.) plywoods were used to show differences in glue penetration and underpinned the limited impact in cell wall deformation for beech when applying higher pressure (Šrajer et al. 2013). Pressing temperature, pressing time, pressing pressure, and veneer glue spread were assessed as influencing the bond strength of structural plywood made from eucalyptus/poplar showing the potential to obtain superior products (Yao et al. 2012). The elastic moduli of the beech veneers surpass those of the pine veneer. The anisotropy of the elastic properties of the veneer in the veneer plane, expressed by the ratio of the modulus in the grain direction to the modulus in the direction perpendicular to the grain, is greater for pine than for beech veneer (Wilczyński and Warmbier 2012).

The flexural properties and tensile shear strength of five-ply plywood panels produced with eucalyptus (*Eucalyptus grandis*), beech (*Fagus orientalis*), and hybrid poplar (*Populus x euramericana*) using urea-formaldehyde (UF), melamine-urea-formaldehyde (MUF) and phenol-formaldehyde (PF) adhesives showed that the effects of wood species, direction of load, and type of adhesive were significant for MOR, but not for the specific MOR (Bal and Bektaþ 2014).

A finite element method (FEM) numerical model predicting the warping of Douglas fir (*Pseudotsuga menziesii*) and mixed beech (*Fagus sylvatica*) - poplar (*Populus x euramericana*) plywood panels started from a description of the intraveneer properties in response to moisture content changes with beech veneers showing the highest tangential swelling and a standard deviation of tangential swelling for Douglas fir is twice that for beech and poplar. Using the strong connections with growth models, in the future we aim to be able to assess the consequences of silvicultural practices or longer-term phenomena, such as the increase of carbon dioxide, which modify tree growth rate on wood product quality. To improve the prediction accuracy, it is obvious that efforts must be concentrated on wood properties, especially inputs like swelling coefficients or viscoelastic behaviour, with a closer relationship to heat and mass transfer phenomena (Constant et al. 2003).

The tensile-shear strengths of plywood using phenol formaldehyde resin based on wood species combinations covering Uludağ fir (*Abies nordmanniana* subsp. bornmülleriana Mattf.), alder (*Alnus glutinosa* L.), Scots pine (*Pinus sylvestris* L.) and Samsun poplar (77/51 *Populus deltoides* Bartr.) showed values for poplar, pine-poplar, fir-poplar and alder-poplar plywood types were found to be in average 1.34 N.mm^{-2}, 1.66 N.mm^{-2}, 2.18 N.mm^{-2} and 2.46 N.mm^{-2} respectively, with no significant difference between the alder-poplar and fir-poplar plywood types (Öncel et al. 2019).

Reinforced plywood
Epoxy resin is well suited for flax fiber reinforcement of beech plywood, whereas ureaformaldehyde, melamine urea-formaldehyde, and isocyanate prepolymer improved modulus of elasticity, modulus of rupture, shear strength, and screw withdrawal resistance, but lowered tensile strength (Jorda et al. 2021). Three dimensionally molded plywood formed parts showed that flax fiber reinforcement relates to the occurrence and position of cracks, delamination and maximum load capacity. Designs with cut-outs are preferred when molding complex geometries and flax fiber reinforcement is a promising way of increasing load capacity and stiffness of beech plywood formed parts by respectively 76 and 38% on average (Jorda et al. 2020). The potential of poplar plywood reinforced with short hemp fibers and bonded with ligninphenol-formaldehyde adhesives for structural applications is underpinned by an increase in strength of the composite up to 95.3 MPa compared with the control group of 78.5 MPa (Karri et al. 2022).
Plywood panels produced using poplar veneer, phenol formaldehyde adhesive and glass fiber fabric reinforcement exhibited a decreased equilibrium moisture content and an increased density. The MOR values of the samples with perpendicular reinforcement were significantly higher than those of the control group (Bal et al. 2015). Carbon-fiber fabric (CF fabric) reinforced poplar/eucalyptus composite plywood were prepared by using fast-growing poplar and eucalyptus veneer as base materials and CF fabric as reinforcement material. The resulting panels showed that the flexural performance of plywood as poplar/eucalyptus composite structure was better than pure poplar and eucalyptus. Specifically, surface reinforcement led to a significant increase in the longitudinal modulus of elasticity and modulus of rupture of the poplar/eucalyptus composite plywood, whereas core layer reinforcement resulted in a substantial increase in the transverse moduli (Liu et al. 2019). Finite element analysis (FEA) method was used to numerically simulate the composite plywood bending test verifying the failure mode predicted by FEA, which will be a very good prediction method for material failure (Guan et al. 2020).

Beech LVL
The inherent strength of beech and the homogenisation due to the production process of LVL make it a material with very high characteristic strength values. Longitudinal strength values are two to four times as high as the corresponding values for spruce glulam. A material having such strength properties provides new structural possibilities but also requires new approaches in mechanical connections in order to also reach sufficient load-carrying-capacities in joints (Blass et al. 2016). Though engineered wood products might show similarities to solid wood, some physical parameters differ such as the electrical resistance used to measure wood moisture content (MC) of beech laminated veneer lumber (LVL) (Grönquist et al. 2021).
Laminated veneer lumber (LVL) prepared from Turkish beech (*Fagus orientalis* L.), Scots pine (*Pinus sylvestris* L.), and Lombardy poplar (*Populus nigra*) veneers bonded with polyvinyl acetate and ureaformaldehyde adhesives showed that the effects of wood species on the mechanical properties were statistically significant and related to the properties of the solid wood (Erdil et al. 2009). On average, Laminated Veneer Lumber (LVL) panels experience a notable increase in density compared to solid wood, with approximately a 23% increase for beech LVL and a 31% increase for spruce LVL, both of which include steaming processes. However, it's noteworthy that steaming substantially reduced all investigated strength properties of these LVL panels (Çolak et al. 2007).
Compared to most softwoods, the hardwood species beech (*Fagus sylvatica*) exhibits higher strength and stiffness properties, but – for structural use – also a number of drawbacks. The drawbacks, however, can be overcome partly by processing beech wood to laminated veneer lumber (LVL). The characteristic compression strength values reach a level of more than 70 N/mm^2, making beech LVL glulam the strongest wood based structural component, placing it in the range of high-strength concrete (Dill-Langer and Aicher 2014). The mean value of the modulus of elasticity of LVL panels produced from

beech veneers (19.5 kN/mm^2) was twice that of the LVL panels produced from eucalyptus veneers (9.4 kN/mm^2) (Aydin et al. 2004).

The peeling process can induce lathe checks, small cracks along the length of the veneer, with various depth and spatial frequencies. The longitudinal modulus of elasticity is marginally affected by checking, while the shear rigidity of the beech LVL beam is significantly reduced in edgewise bending if checks are not glued (Pot et al. 2015). Laboratory X-ray density profile scans were performed on beech LVL to identify the part of the material cross section in which the densification took place revealing that the higher density was found to be located in the area of the adhesive joints, uniformly over the cross section, while the density in the middle of the veneers corresponded to that of solid beech wood (Engehausen et al. 2021).

Tests on full truss structures confirmed that the favourable behaviour of beech LVL are reflected in the performance of dowel-type connections and can be used to improve the behaviour of structural elements such as trusses (Kobel et al. 2016). During the initial moistening process following production, beech LVL exhibits significant swelling in the radial direction due to the irreversible spring back (approximately 2 mm at 50 mm; i.e., 4%). Once the maximum spring back is reached, beech LVL shows sorption behavior in the radial and tangential direction, which is comparable to that of solid beech wood in the radial direction, which must be taken into account when dimensioning components in order to avoid damage to building structures (Benthien et al. 2020). The decrease in mechanical characteristics of beech LVL with the increase of veneer thickness in the range 1 to 5 mm appears limited. However, an increase of veneer thickness does induce an increase of glue spread because of the degradation of veneer surface topography (Daoui et al. 2011).

Forestry management systems as can have a strong influence on the mechanical properties of beech laminated veneer lumber, with bending strength and moduli of elasticity values being 17 % and 11 % higher for beams based on wood from high forest compared to that from coppice (with standards). Also veneer defects identified by X-ray analysis had an impact (Viguier et al. 2017).

Finding an alternative use of secondary quality hardwood is essential. The valorization of this resource for the structural application requires an improvement of the mechanical properties and a better knowledge of the effect of defects on mechanical properties. The mechanical properties of laminated veneer lumber (LVL) made of secondary quality beech and oak varied with veneer thickness. Good quality products were obtained with LVL made with 3 mm thick veneer compared to veneer thicknesses of approx. 2 and 4 mm (Purba et al. 2018). Recent research has also focussed on the elastic material modelling of glulam made of beech laminated veneer lumber (beech LVL) (Töpler et al. 2023).

Poplar and aspen LVL

Aspen (*Populus tremuloides*) is emerging as an important species for laminated veneer lumber (LVL) products in North America. LVL stiffness enhancement (the ratio of LVL MOE over veneer MOE) in relation to veneer grading underpinned the potential for manufacturing of high-stiffness LVL for engineered applications (Wang and Dai 2005).

LVLs manufactured from rotary-peeled hybrid poplar clones (I-214 and I-77/51) and bonded with MUF adhesive showed that a longer press duration of 30 min could be recommended to obtain improved physical and mechanical properties (Kurt et al. 2011). Laminated veneer lumbers (LVLs) manufactured from veneers of 3 rotary peeled fast growing hybrid poplar clones, I-214 (*Populus × euramericana*), I-77/51 (*Populus deltoides*), and S.307-26 (*Populus deltoides*), with a phenol formaldehyde (PF) adhesive showed that the two *Populus deltoides* clones performed similarly and would be more suitable for structural composite lumber manufacturing than I-214 (Kurt et al 2012).

LVL boards produced from rotary-cut poplar veneer using phenol formaldehyde (PF) adhesive were tested for impact bending strength. The results indicated that the impact bending strength was affected by the span-to-depth ratio with the lowest values recorded (0.39 kgm/cm² for flatwise and 0.32 kgm/cm² for edgewise) when the ratio was set at 10 (Bal 2016).

Using veneers from mature poplar wood showed an improvement of 15 to 20 %, on average, for mechanical properties, with almost the same LVL panel weight. This indicates that, for poplar, the differentiation of materials based on veneers made from juvenile wood (corewood) and veneers made from mature wood (outerwood) is important. Five out of 10 cultivars have a real potential for structural applications, some should be used with careful sample selection and while 4 cultivars including I-214 should be excluded (Rahayu et al. 2015).

Mechanical properties of laminated veneer lumber produced from different cultivars of poplar underpinned that the use of poplar wood for structural purposes will require a radical change in the silvicultural regime practiced by adopting longer rotation or finding a way to speed up the transition from juvenile wood to mature wood (El Haouzali et al. 2020).

Some innovative approaches allow to use hybrid poplar wood also for alternative engineered wood products. A study on chemical constituent changes of fibrosis (fluffing and separation technique of thick veneer) veneers during heat treatment was helpful to expand the application areas of scrimbers. The treatment led to an increase in the contents of lignin and extractives, while a decrease in holocellulose and α-cellulose was noted (Wei et al. 2018). A novel LVL was produced with poplar fibrosis veneers and phenolic formaldehyde with products ranging in density from 0.8 to 1.2 g cm^{-3} showing improved mechanical properties and water resistance compared to traditional LVL (Wei et al. 2019). An innovative poplar LVL orthogonal rib beam floor diaphragm showed that under the service loading level of 2.5 kN/m^2, no overall damage occurred (Sun et al. 2022). The use of resonance-based acoustic technologies for sorting poplar logs for laminated veneer lumber (LVL) showed this is a promising and valuable tool in assessing log dynamic MOE for sorting of the log supply chain (Zhou et al. 2013).

The average toughness values for poplar LVL of the mode-I along-grain interlaminar fracture, mode-I cross-grain interlaminar fracture, and mode-II interlaminar fracture were underpinning the potential of this product with values 15.43, 270.15, and 39.72 MPa·mm$^{1/2}$, respectively (Xiao et al. 2023).

Mixed hardwood LVL

The production of structural LVL in North America and Asia has been based predominantly on low density hardwoods. Meanwhile in Europe, there has been a shift towards utilizing medium-density hardwoods for structural LVL, evolving from their previous use in furniture components (Ozarska 1999). The Trus Joist MacMillan Limited, one of the largest integrated timber companies in North America, has been producing structural engineered panels based on softwood for many years. The main products include Microllam^{TM} Laminated Veneer Lumber (LVL), Parallam® Parallel Strand Lumber (PSL) and Timber-Strand® Laminated Strand Lumber (LSL). Some plants have been using yellow poplar (*Liriodendron tulipifera*) and aspen as lower density hardwoods (Ozraska 1999).

LVL of silver maple (*Acer saccharinum*) veneers (to some extent the homologue wood species in North America to beech in Europe) and PVAc glue showed improved properties compared to yellow poplar (*Liriodendron tulipifera*) and aspen poplar or aspen (*Populus tremuloides*) based LVL, especially when focusing on laminated veneer flooring (Shukla and Kamden 2008).

The usage of alder wood instead of beech wood as a raw material in plywood and laminated veneer lumber (LVL) manufacturing was considered relevant because of an annual increment reaching 20 m^3 per hectare (Toksoy et al. 2006). Different types of LVL were produced combining 7-layers of beech and poplar using melamine formaldehyde adhesive showing significant effect on physical and mechanical properties. As the proportion of beech veneer in LVL increased, the strength values of the LVLs also increased (Ilkay et al. 2016). Physical characteristics of laminated veneer lumber (LVL) obtained in different compositions from cut veneers of Oriental beech (*Fagus orientalis* Lipsky) and Lombardy poplar (*Populus nigra*) with thicknesses of 4 mm and 5 mm showed that wood density is an important characteristic (Kılıç 2012).

The bending strength and modulus of elasticity of laminated poplar (P) and beech (B) combinations were increased in relation to density, and the configuration BBPBPBBA determined to be the most reasonable ply organization when the bending strength and modulus of elasticity values of laminated composite materials were examined (Burdurlu et al. 2007). The results of corner window frame double tenon glue joint strength produced from combined PF bonded poplar-beech veneer LVL showed that torque was 2 to 3 times higher than with window frames produced from spruce solid wood. This indicates that LVL composed of poplar veneers in core layers, and only outer layers of beech veneers have good potential (Zdravković et al. 2017). The impact bending strength (IBS) of laminated veneer lumber (LVL) varies depending on the wood species used. Research suggests that eucalyptus tends to yield the highest IBS values, while poplar typically produces the lowest. However, it's important to note that IBS values for LVL are generally lower compared to the corresponding solid wood counterparts across all species (Bal and Bektaş 2012).

Treated and reinforced hardwood LVL

Heat treatment at relatively high temperatures (from 150 to 260 °C) is an effective way to improve dimensional stability and bio durability. However, heat treatments usually reduce most of the mechanical properties of wood. The incorporation of carbon fiber fabric allowed to improve some mechanical and physical properties of LVL manufactured from heat-treated and untreated beech (*Fagus orientalis* Lipsky) wood (Percin and Altunok 2017).

Acetylation with acetic anhydride is well known to improve the dimensional stability and durability of wood. Veneer is appealing for acetylation because of its thin thickness, which supports a complete and even impregnation of difficult-to-treat wood species, such as beech (*Fagus sylvatica* L.). However acetylated beech veneer is considerably less compressible, most likely caused due to a decrease in moisture content (MC), but still providing a similar density as reference material due to weight gain by the acetylation process (Slabohm et al. 2022). Acetylation of beech veneers with acetic anhydride highly improves the durability of the manufactured LVL. It can be stated that acetylated beech LVL is very durable (durability class DC 1) against wood-destroying fungi (Slabohm et al. 2023). The bonding performance of acetylated solid wood was found to be quite variable, depending on the adhesive type and application, as well as the wood species and acetylation method. It appears that acetylated veneer products perform better in wet conditions, which is also beneficial for the bonding (Slabohm et al. 2022b).

Compared with untreated LVL, LVL containing veneers impregnated with a water-soluble, phenolformaldehyde resin had improved mechanical properties and dimensional stability (Chui et al. 1994). Laminated Veneer Lumber (LVL) made from rotary cut beech (*Fagus sylvatica* L.) veneers, which were treated with low molecular weight alkaline phenolic resins with the aim of cell wall modification showed that volumetric swelling can be reduced by 57% at moderate Weight-Percent-Gain (WPG) while the MOR could be preserved and MOE was significantly increased (Bicke et al. 2017). Rotary cut beech (*Fagus sylvatica* L.) veneers treated with lignin phenol formaldehyde (LPF) solutions using dimethyl sulfoxide (DMSO) as a solvent and then bonded with PF adhesive to produce laminated veneer lumber (LVL) showing the potential of substituting part of the PF resin for modification (Fleckenstein et al. 2018).

Veneer of beech wood (*Fagus orientalis* L.) that were treated with borax-boric acid, monoammonium phosphate and diammonium phosphate using a full-cell pressure process significantly increased the surface roughness of the produced LVLs (Dundar et al. 2008). Boric acid treatment of beech veneers used in producing of LVL had no effect on the average MOE, compression strength parallel to grain, Brinell hardness and pull-out of screw strength perpendicular to the surface; but it reduced average static bending strength, compression strength and splitting strength perpendicular to the grain (Colakoglu et al. 2003).

To improve the durability of poplar laminated veneer lumber (LVL), the veneers were impregnated with alkaline copper quaternary (ACQ) and copper azole (CA) at four retention levels The effects of the treatments on the LVL properties demonstrated that the treatments substantially improved the decay resistance. Additionally, no significant effects of the treatments were observed on the mechanical properties of LVLs, and the LVLs did not display any visible delamination after boil-dry treatment (Jin et al. 2016).

Before manufacturing LVL, veneers were subjected to heat treatment at varying temperatures (up to 180 °C) and for varying durations of heating inducing significant differences in physical and mechanical properties of the poplar LVLs. The improved characteristics in swelling of LVL made from heat treated plies have to be balanced against the decrease in strength values when evaluating the effectiveness of using this treatment. All values were lower than those obtained for the control that showed flat-wise and edge-wise modulus of rupture (MOR) (107.67 MPa and 102.1 MPa) and modulus of elasticity (MOE) (6190 MPa and 6017 MPa) (Nazerian and Ghalehno 2011).

Laminated wood composed solely from beech veneers densified by a simple rolling process showed 17.4% higher bending strength compared to the reference (Gaff and Gašparík 2015).

The mechanical properties of poplar laminated veneer lumber (LVL) with carbon fiber reinforced polymer (CFRP) were improved, e.g. the MOE increased with 67 % when including a double sided reinforcement (Wei et al. 2013). For the bending mechanical behavior (static and dynamic moduli, and maximum stress) of Douglas fir and poplar LVL (Laminated Veneer Lumber), beams reinforced with fiber polymer material (FRP) showed a clear improvement with the use of unidirectional carbon; up to

40% more in the elastic modulus for the flatwise layout and more than 20% of the maximum stress, for both wood species (Rescalvo et al. 2020).

Glulam or Glued Laminated Timber (GLT) and Cross Laminated Timber (CLT)

Glulam also called GLT (Glued-laminated timber) is made of (strength) graded, planed and finger-jointed spruce boards glued together under pressure on their flatwise surface where all boards run parallel to the length to create rectangular cross-sections. GLT is often used in long-span designs, where it can replace steel and concrete beams, columns, and other load-bearing structures.

Cross-laminated timber (CLT) is an engineered wood product that is made by gluing and nailing three or more layers of lumber or wood-based materials together at angles of 0° and 90° in accordance and has become one of the most popular engineered wood panels of the 21st century. Various types of CLTs have been developed to improve planar or rolling shear failure (RF), bending moments under out-of-plane load, and local lumber utilization (Wang et al. 2015).

GLT and CLT are products used for mass timber construction. Mass timber construction, in contrast to light-frame wood construction, is using a category of engineered wood products typically made of large, solid wood panels, columns or beams often manufactured off-site for load-bearing wall, floor and roof construction.

Beech glulam

An extensive numerical and experimental investigation was carried out to determine the characteristic bending strength of beech glulam. Bending tests on full size beams composed of mechanically graded boards confirm a characteristic bending strength of at least 44.5 N/mm^2 (Frese and Blaß 2007). Process conditions can be implemented to enable sufficient glue line performance for beech glulams constructed from lamellae with a maximum thickness of 30 mm (Ohnesorge et al. 2010). The shear force capacities of the investigated glulam beams of strength class GL 42c revealed no statistically significant influence of the red heartwood content in the bulk timber material and in the glued interfaces (Aicher and Ohnesorge 2010). A comparison of the block shear results with EN 386 (now EN 14080 2013) indicates that the present requirements on block shear strength in the European standard are not applicable to beech glulam (Aicher and Ohnesorge 2010).

Because of the lack of standards regulating the production process, the quality control, and specifying the mechanical properties of glued laminated timber (GLT) made from European beech wood, work was initiated to come to a standard on the production and performance requirements for GLT made from hardwood. This initiative aims to define production protocols and performance criteria for hardwood GLT, similar to the standards set by EN 14080 (2013) for GLT made from coniferous species and poplar (Ehrhart et al. 2018). The mechanical properties of GLT made from European beech wood are considerably higher than softwood GLT and show the great potential of its use for structural purposes (Ehrhart et al. 2018b). The current Eurocode 5 design rules based on the effective-length method for verifying the stability of columns subjected to axial compression do not allow to accurately predict the buckling resistance of glulam columns made of European beech (*Fagus sylvatica* L.) wood. Ehrhart et al. (2020) concluded that the determination of buckling design curves for softwood and beech glulam columns should be based on the same assumptions, especially regarding the considered imperfections. Today, results are considered relevant for the standardization of beech (and other hardwood) glulam on a European level in the future product standard prEN 14080-2 (Ehrhart et al 2021).

The MOEdyn, stiffness is a relevant property for wood quality in the construction sector showed that beech glued laminated timber of higher strength classes (≥GL 40c) was not viable when using beech from mixed stands. Furthermore, it was also shown that axial board position and cambial age impacted the on MOEdyn (Rais et al. 2020). Based on extensive experimental and numerical investigations, it was shown that it is possible to produce GLT of strength classes GL40, GL48 and GL55 with homogeneous and combined layups from European beech wood (Ehrhart et al. 2020).

The quality of the raw material can be very variable with beech. Currently, most of the attention is paid to the high quality pieces to produce very high-performing structural products. Therefore, a suitable grading system could reduce waste and increase yields in the perspective of a more sustainable and efficient use of the wood resource. Strength grading can be very effective for beech timber: machine grading, as well as visual grading, worked properly both with good quality boards and with weaker pieces and the yields reflected the quality of the raw material (Brunetti et al. 2020). More efficient

sawing techniques, higher lamella grading yields and solving of adhesion challenges may increase the competitiveness of beech glulam and promote its use (Westermayr et al. 2022).

The adhesives used to produce glued multilayered beech timber beams can be of major importance for their structural behaviour since a finger-joint can weaken the entire multi-layered beam, especially when located in the maximum tension zone (Tran et al. 2014). Beech glulam wood joints with polyurethane adhesives were earlier reported needing adequate consideration in relation to creep (George et al. 2003). Compared to most softwoods, the hardwood species beech (*Fagus sylvatica*) exhibits higher strength and stiffness properties, but – for structural use – also a number of drawbacks. The drawbacks, however, can be overcome partly by processing beech wood to laminated veneer lumber (LVL). The secondary processing of beech LVL into the innovative structural material "glued-laminated beech LVL" yields significant further enhancement of the already high strength values of beech LVL itself. This has been revealed in the paper for the example of compression strength parallel to the fibre. The characteristic compression strength values reach a level of more than 70 N/mm^2, which is in the range of high-strength concrete (Dill-Langer and Aicher 2014).

Poplar glulam
Four main groups of adhesives were considered to produce poplar glulam: PRF (3 different adhesives), MUF, EPI and PUR (without and with primer) and bond quality was evaluated using delamination and shear strength criteria according to EN 14080 (2013) showing the impact of wood species on performance (Martins et al. 2017). Glued laminated timber (GLT) beams made with poplar revealed a very promising mechanical behavior. Bending strength tests evidenced a ductile behavior on more than 70% of the beams (Monteiro et al. 2020). Martins et al. (2023) obtained a characteristic value of 22.4 MPa of tensile strength for Portuguese poplar wood and a T12 strength grade (equivalent to C20) could be assigned to the studied sample.

The bending properties of Cathay poplar glulam were compared to those of Douglas fir glulam showing that Cathay poplar glulam has a lower stiffness, but a marginally higher strength. One-component polyurethane adhesive also proved to be more effective than resorcinol formaldehyde resin adhesive highlighting the potential of Cathay poplar as a viable material for glulam in China (Gao et al. 2015). Moreover, better adhesion was observed with respect to the wettability of poplar boards, with the site of origin also influencing this aspect in glulam production. However, all poplar material manifested higher contact angle values measured with distilled water compared to Scots pine samples, suggesting that their expected adhesion does not reach that of Scots pine (Rábai et al. 2020).

Treated glulam
Glued laminated timber (glulam) beams and finger-jointed boards made out of thermally modified hardwood beech showed that such glulam could only be used for a limited range of structural elements (Widmann et al. 2014). Moisture induced stresses were studied in glulam beams made from hydrothermally treated poplar (*Populus deltoides*), showing reduced cross-sectional moisture induced stresses as well as relevant moisture gradients with related impact on bending strength as well as stiffness of the treated wood and the glulam beams (Mirzaei et al. 2017). The technological properties of glulam beams made from hydrothermally treated poplar (*Populus deltoides*) wood were investigated revealing that density, mass loss (ML), anti-swelling effect (ASE), water repellent effect (WRE) and both modulus of elasticity and modulus of rupture were increasing (Mirzaei et al. 2018).

To improve the structural applications of glued laminated timber (glulam) in high RH environment according to its relatively lower MOE, fast-growing poplar laminae with a thickness of 35 mm were thermally treated at 200 °C for 3.5 h showed that MOE of glulam beams was significantly improved with a reduction in MOR indicating glulam beams made out of thermally treated fast-growing poplar laminae can be used in construction (Yue et al. 2020). Thermal treatment in the region of 170-180 °C was a practical approach to improving wood properties in view of their structural use, providing a basis for developing a design guide for structural uses of thermally-treated poplar wood (Yue et al. 2023).

The effect of ACQ preservatives on the mechanical properties of glulam made from beech, hard maple, and red oak were examined showing that MOE values of both lumber and the glulam decreased after ACQ preservatives treatment (Yang et al. 2012). The bending properties of glulam made from fast-growing poplar barely meet requirements, however full-scale testing of preservative alkaline copper quaternary (ACQ)-treated and phenol resin reinforced poplar in different configurations greatly

enhanced Young's modulus and bending strength of modified fast growing poplar wood members and glulam compared with those of untreated groups (Han et al. 2018).

Compared with the fast-growing poplar glulam beams, the mechanical performance was considerably higher for steel reinforced fast-growing poplar glulam beams (Wang et al. 2021). The major engineering potential in combining (hard)wood species of lower (poplar) and higher (beech) densities can also be complemented by modification strategies. The one option in line with this engineering potential is densification of wood species like spruce, beech and poplar wood to come to high-strength densified wood (Jakob et al. 2022).

Glulam made from compressed poplar wood (*Populus deltoides*) through a combination of hygrothermal treatment and densification exhibited significantly improved mechanical properties, including enhanced bending strength and bending modulus of elasticity. However, a decrease in shear strength of the glue line was noted (Hajihassani et al. 2020). Poplar wood densified by hygro-thermo-mechanical technique (steam and pressurize compaction) can also be used to produce glulam by a finger joint technique and polyurethane glue. This resulted in improved physical and mechanical properties (Hajihassani et al. 2022).

Densifying of poplar wood through delignification was conducted using a commercial soda pulping process under various NaOH concentrations of 0-6% with a reduced liquor-to-wood ratio of 3, along with a novel hydrotropic fractionation process using maleic acid. The delignified wood was then pressed with or without stop bars at a low pressure of 1 MPa at 150 °C for 15 min or 100 °C for 2 or 10 h. Results indicate that wood density is the key variable dictating wood strength properties rather than extent of delignification. Modulus of rupture (MOR), modulus of elasticity (MOE), and Brinell hardness (HB) all increased linearly with wood density up to 150 MPa, 20.7 GPa, and 43.2 MPa for a density of 0.81 g/cm^3 while these values for undensified poplar were 88.5 MPa, 6.5 GPa, and 14.8 MPa at a density of 0.46 g/cm^3 (Wang et al. 2020). Further results showed that the complete wood cell collapse was observed near the surface of all the delignified wood blocks, as well as some micro-cracks in the cell walls. The chemical analysis indicated that delignification occurred mainly near the surface of the wood blocks and enhanced hydrogen bonding among the aligned cellulose fibers (Wang et al. 2021). The most suitable process parameters for bulk densification and heat treatment to modify poplar wood with a moisture content of approximately 3-5% have been determined. The optimal preheating temperature and time for the bulk densification process were found to be 180°C and 361 seconds, respectively. Similarly, the optimal heat treatment temperature and time were identified as 190°C and 3 hours, respectively. The resulting product should be suitable for solid wood flooring applications and have a long service life (Wang et al. 2021b). Fourier transform infrared (FTIR) microscopy along with X-ray diffraction (XRD) were used to explain the viscoelastic and hygroscopicity of this delignified and densified poplar wood. Hemicelluloses and lignin were selectively dissolved during alkali treatment. Wood crystallinity was increased after alkali treatment at a moderate concentration of 2%, beneficial to improving the dimensional stability and mechanical performance of delignified and densified wood. The results support mild delignification and densification as a feasible way towards extending the service life of wood products used as structural materials (Wang et al. 2023).

Poplar wood blocks were delignified with glycerol, in order to keep the hemicelluloses, as it is an important component in hydrogen and ester bond formation during densification. Afterwards, the delignified blocks were immersed in glycerol-maleic anhydride solution and compressed at 100 °C for 24 h. Removal of lignin increased hydrogen bonds formation between the adjacent fibers during pressing and reduced the set recovery of the compressed product up to 2%. The set recovery of densified samples was further significantly decreased following surface polymerization with glycerol and maleic anhydride (68% lower than the non-polymerized ones). Combined delignification/polymerization increased the specific tensile strength of densified samples by 37% as compared to non-densified ones (Yahyaee et al. 2022).

Physical and mechanical properties of wood can be significantly improved by a densification process. Prior to densification, a pre-treatment should be adopted to soften the wood cell walls. Densified wood has a tendency to recover to its original dimensions, and thus a post-treatment can be adopted to improve its dimensional stability. Suitable manufacturing of the densified wood was done by subjecting poplar samples to the alkali pre-treatment and compressing along the radial direction at 100 °C to the target thickness and then maintained at 100 °C for 24 hours, or at 150 °C to the target thickness and then maintained at 150 °C for one hour. Both densification processes strongly reduced the set recovery, but

the densification process at 150 °C for about one hour decreased the density and ductility of the densified poplar (Xu et al. 2023).

Consecutive densification and thermal modification processes were applied to address the reduced mechanical properties resulting from thermal modification. Five European wood species: poplar (*Populus nigra* L.), beech (*Fagus sylvatica* L.), Norway spruce (*Picea abies* Karst.), English oak (*Quercus robur* L.) and European ash (*Fraxinus excelsior* L.) were subjected to this treatment. Depending on the mean density of the species, a thermo-mechanical densification of 43 or 50% was imposed. Subsequently, the densified material was thermally modified in the so-called Vacu^3-process at 230 °C and 20 or 80% vacuum and at 240 °C and 20% vacuum. Test results showed that the consecutive application of thermo-mechanical densification and thermal modification leads to significantly improved durability whilst mechanical properties at least for beech, ash and poplar remained and the material is dimensionally stable (Wehsener et al. 2018). A combination of delignification (in NaOH and Na$_2$SO3 solution) and densification to enhance bending strength and ASE (anti-swelling efficiency) was applied on poplar (*Populus nigra* L.). The wood was compressed 80% perpendicular to the grain resulting in a bending strength increase of up to 450 MPa (Wehsener et al. 2023).

European aspen and silver birch sawn timber were compressed at two different moisture contents and a thermal modification at 190°C was used as a means to reduce the post-compression set recovery. Increase in Brinell hardness and MOE values was the greatest with aspen when the compression was started at the green state (Möttönen et al. 2015).

Reinforced glulam

The modulus of elasticity (MOE) of fiber-reinforced plastic (FRP) reinforced fast-growing poplar glulam showed that with increased FRP length, the dynamic and static MOE increased (Cheng and Hu 2011). Composite materials resulting from the combination of materials with low mechanical properties (poplar timber) and materials with high mechanical properties in low proportions (carbon composites) stand as a good technological solution, in that they can provide low-weight products with competitive mechanical properties. An experimental campaign involving glued laminated beams made of poplar timber and carbon composite material demonstrated that the position and the type of reinforcement along the cross-section bear a clear influence on the mechanical behavior of the whole element. In terms of stiffness and strength, respective improvements of up to 44% and 33% are achieved. Moreover, high ductility values are obtained when the reinforcement is placed at the tension area, whereas brittle behavior is observed when the reinforcement is placed only at the compression zone (Rescalvo et al. 2021).

Flexural strengthening of screwed tree-layer glulam made with poplar (*Populus alba*) using polyurethane adhesive were reinforced with galvanized steel, aluminium sheet and glass fiber reinforcement providing that failure modes of glulams changed from brittle to ductile by reinforcing resulting in flexural behavior effected by types and arrangements of reinforcing (Rostampour-Haftkhani 2020).

Various layouts of composite glulam beams, comprising poplar wood in combination with pine wood and/or carbon fiber reinforced polymer (CFRP), underwent bending tests. These tests facilitated the assessment of an extensive analytical model used to compute the relationships between elastic moduli for composite timber beams, both with and without CFRP material. The composite layouts made from pine and poplar feature high stiffness, closer to that of the pine (-14% difference) than to the poplar (54% difference) layout (Tibolmas et al. 2022).

Solid wood beams of *Populus x euramericana* cv. I-214, and duo beams of the same species, some longitudinally reinforced with flax fibres glued with wet and dry application methods, with glass fibre and with carbon fibres. A significant increase in strength and modulus of elasticity was obtained when reinforced with carbon fibre, while the other reinforced beams presented no significant increase in their mechanical properties (Bastera et al. 2012). The bending strength of the specially reinforced glued laminated timbers (glulams) with glass fiber-reinforced plastic (GFRP) was studied for glulam that was produced using 5 layers of beech (*Fagus orientalis*) and poplar (*Populus deltoides*). Glulam made with beech wood have higher strength than samples made by poplar wood and the highest strength was obtained using 4 layers of GFRP. Also, the 3 point bending test results showed that fracture place was changed from shear side to compression side by increasing of GFRP layers (Osmannezhad et al. 2014).

Combined glulam

Recent investigation into novel homogeneous and hybrid beech-Corsican pine glue-laminated timber (glulam) beams using melamine-based adhesive underpins the suitability of hardwood for the manufacturing of glulam beams, even in hybrid configuration in which the inner layers are made of low graded timber boards (Sciomenta et al. 2022).

A standard four-point bending test on a hybrid glulam beam made of beech and spruce laminations with melamine urea formaldehyde (MUF) adhesive finger jointing and lamination, revealed failure in a brittle manner. The outer beech laminations predominantly remained undamaged, whereas the critical areas were the longitudinal adhesive layers and the finger joints (Kržan et al. 2019). A qualitative comparison of the behavior of mixed glued laminated timber made of pine in their outer layers and of poplar in their inner layers, provided evidence that the use of poplar as a low-grade species in the inner layers of the laminated timber can be a promising technology to decrease the weight of the glulam while maintaining the good mechanical properties of pine (Rescalvo et al. 2020).

A feasibility study of glulam was carried out in French Guiana using local wood species underlining that gluing parameters need to be adjusted to the wood species, especially in a tropical climate. Seemingly current European standard delamination tests are too strict and may not be easy to use or adapt to validate a structural glued assembly using tropical hardwoods. The amount of glue sometimes needs to be increased and, in order to avoid high shrinkage constraints, the lamella thickness should be decreased. For the densest wood the pressure level needs to be decreased in order to prevent glue from being squeezed out of the joint (Bourreau et al. 2013).

Mixed glulam beams showed higher structural efficiency in bending than those entirely constructed from poplar or eucalyptus The lower than expected increase in mechanical performance and structural efficiency found in the mixed beams (with respect to those constructed entirely in poplar) was seemingly caused by the combination of good quality poplar and poor quality eucalyptus material (Castro and Paganini 2003).

Furthermore, glued laminated timber (GLT) from softwoods and intercalated cross-layered plates of laminated veneer lumber (LVL) made of beech is especially suited for beams with multiple, large rectangular holes, where the LVL acts as a highly efficient internal reinforcement and contributes to a damage-tolerant ultimate load behavior (Aicher and Tapia 2018).

Beech CLT

CLT elements out of beech show a great potential. Especially the determined mechanical values like the rolling shear and the compression strength perpendicular to the grain open new applications of CLT in timber structures (Franke 2016). Moreover, investigations in North America have further validated this potential. Specimens of large leaf beech (*Fagus grandifolia* Ehrh.) were subjected to gluing with various polyurethane adhesives to manufacture beech CLT. Despite the species' inherent challenges with swelling and shrinkage, testing revealed its suitability for CLT applications, paving the way for its utilization in CLT products (Essoua and Blanchet 2017).

Poplar CLT

Recent research endeavors have shed light on the suitability of aspen (*Populus tremula L*) and poplar (*Populus spp.*) woods in cross-laminated timber (CLT) manufacturing, offering promising alternatives to traditional softwood-based CLT. Studies assessing aspen CLT panels, bonded with one-component polyurethane (1C-PUR) and melamine adhesive (ME), have demonstrated comparable or superior mechanical properties to those of traditional softwoods, indicating its viability for CLT production (Das et al. 2023b). Similarly, lower grade fast-growing poplar lumber has been successfully utilized in CLT panels, showcasing its compatibility as a core layer in mixed-species maple-poplar CLT panels. Notably, both 1C-PUR and ME bonded CLT samples exhibited higher shear strength properties than spruce wood CLT (Das et al. 2023).

Poplar wood (*Populus* spp.), known for its economic significance in regions like Hungary, has also been explored for CLT applications. There are several relatively high density, high strength varieties, that may be used as alternatives to softwood based CLT, with comparable properties (Marko et al. 2016). Test results show that poplar CLT panels have potential application in CLT structures, with only an 8% difference in structural properties compared to spruce CLT. Accelerated aging reduced the mechanical properties of poplar CLT and converted its failure mode from plasticity to brittleness (Shi et al. 2023).

An effort is being made to explore the use of regionally produced CLT materials from Iran, including the testing of fast-grown, hand-planted poplar (*Populus alba*). The average values of M_{max}, MOR, and MOE_{app} of CLTs increased in both the major and minor directions with an increase of pan-to-depth ratios (SDR) from 6 to 25. (Hematabadi et al. 2020). The effect of layer arrangement on bending properties of CLT panels made from poplar (*Populus deltoides* L.) was investigated using experimental, theoretical, and numerical methods. Based on both average MOE and MOR values in both major and minor direction, the optimal CLT was constructed in 0/30/0 orientation and based on average MOE values, the optimal construction of CLT was in 0/30/0, 0/45/0, and 0/90/0 orientations, while according to average MOR, the optimal construction of CLTs was in 0/30/0, 0/90,0, and 0/45/0, respectively (Rostampour-Haftkhani and Hematabadi 2022).

Kramer et al. (2014) presented a study that demonstrates the viability of a Forest Stewardship Council (FSC) certified sustainable plantation grown low-density species, hybrid poplar (marketed as Pacific Albus), for use in performance-rated CLT panels by following the ANSI/APA PRG-320-2012 based approval. The feasibility of using poplar (*Populus euramericana* cv. I-214) as cross layer to fabricate cross-laminated timber (CLT) was examined in comparison with Douglas fir (*Pseudotsuga menziesii*) and Monterey pine (*Pinus radiata*). It was found that the mechanical properties of CLT panels containing poplar were similar to those made of softwoods with major failure modes found were joint failure, shear failure and delamination. The results underpin that is it could be feasible to use poplar as a cross layer to fabricate CLT without decreasing its strength properties (Wang et al. 2014).

Furthermore, adhesive bonds of hybrid poplar CLT made with PUR (polyurethane) and PRF (phenol resorcinol formaldehyde) adhesive have similar characteristic shear strengths. A high percentage of samples made from PUR failed in the cyclic delamination test. This research concluded that a lightweight structural CLT product made from hybrid poplar could be used as a model for other low density CLT products made from other less utilized resources (Weidman 2015).

When comparing poplar as fast-growth hardwood species with fir it could be concluded the poplar is a proper wood for manufacturing CLTs in terms of fastener withdrawal performance (Abdoli et al. 2022). The effects of fastener type, end distance, layer arrangement, and panel strength direction and their interaction on the lateral resistance of single shear plane lap joints made out of poplar CLT panels (*Populus alba*) showed that appropriate fasteners and their optimal end distances have significant impacts on the lateral resistance of CLTs. The arrangement of 0–45–0° exhibited the highest lateral resistance, although the panel direction of 90–45–90° showed the weakest (Abdoli et al. 2023).

So far, there were no European standards available for the production of GLT or CLT made from hardwood (except for poplar). The softwood (and poplar) requirements for the production of GLT are defined in EN 14080 (2013) while for CLT production requirements are in EN 16351 (2015). Target strength classes GL 40, GL 48 and GL 55 appear realistic and reachable (Ehrhart et al. 2016).

Mixed – hybrid CLT
The exploration of hybrid CLT offers promising avenues not only in terms of mechanical properties but also in incorporating layers with specific functionalities like thermal insulation. While research on hardwood CLT remains limited, existing studies suggest its technical feasibility and potential for specific applications. However, to make hardwood CLT a practical reality, the industry must address significant challenges (Espinoza and Buehlmann 2018).

When comparing the rolling shear strength and shear modulus of softwood and hardwood used to manufacture CLT, hardwood has both rolling shear strength and shear modulus values up to twice as high as those of softwood. The use of hardwoods a cross-layer material has advantages such as improvement of rolling shear properties and utilization of lesser-used species, but it is judged that it is necessary to additionally evaluate the adhesion performance between softwoods and hardwoods (Yang et al. 2021).

CLT cross-layer materials are mainly manufactured with a 90° arrangement, but adjusting the angle of the layers can lead to a 1.5 times improvement in rolling shear strength of CLT, an 8.3 times improvement in its shear modulus, and a 4.1 times improvement in its bending stiffness (Yang et al. 2021). For larch CLT, it is recommended to use lower density and lower grade material like red pine as minor axial laminate since low density wood can add high value in products with high longevity. The bending strength of this mixed larch CLTs was similar to that of larch CLT. Since in out of plane test, the bending test and the rolling shear failure occurred it is relevant to look for minor layer species with

high rolling shear resistance (Kim 2020). In comparison to Norway spruce, the outstanding rolling shear properties of beech and ash are underlined as an asset for these species to be used in CLT. Pine, poplar and birch also have a great potential as base material for CLT (Ehrhart et al. 2015). Extending the production of CLT by producing them out of beech or of beech and spruce in combination as hybrid product is relevant since CLT elements out of beech show a great potential, especially when considering mechanical values like the rolling shear and the compression strength perpendicular to the grain will open new applications of CLT in timber structures (Franke 2016).

The rolling shear properties of European beech wood (*Fagus sylvatica*) are considerably higher than those of softwood. The rolling shear strength and modulus exceed the respective characteristic values for softwoods by roughly factors of 5 and 7, indicating great potential for beech wood cross-layers in CLT (Aicher et al. 2016). Planar (rolling) shear properties in cross laminated timber (CLT) is an important factor that should be considered for CLT structural components with short span or openings. The planar shear properties of SPF (Spruce-pine-fir) dimension lumber and Douglas fir laminated veneer lumber (LVL) showed that the bending properties of generic CLT could be improved by using LVL as parallel layers (Wang et al. 2017). Bending and shear performance of hybrid cross-laminated timber (HCLT) panels made from Spruce-Pine-Fir (South) (SPFs) and laminated strand lumber (LSL). The incorporation of LSL in the core of CLT panels increased mean panel bending stress at failure by 23% through mitigation of rolling shear failure. The LSL is an engineered composite lumber that is made from approximately 300 mm long strands of fast-growing species (often aspen or poplar) that are bonded and densified during manufacture and oriented with the long axis of the structural member (Davids et al. 2017).

All the hybrid CLT (HCLT) specimens had higher shear resistance than that of regular CLT with the same number of layers. The difference of the shear resistance between the two strength directions of HCLT decreased as the number of OSB layers increased. The shear resistance and stress of CLT were improved significantly by using OSB in SPF dimension lumber based CLT (Li et al. 2020). The interlaminar shear performance of CLT using three different laminates - larch, poplar and OSB - as showed that, although larch, poplar and OSB have little difference in overall density, the interlaminar shear strength of CLT was significantly affected with the use of each as the transverse layer. The interlaminar shear failure modes of the three CLT specimens are different: in the major strength direction, when larch was used as the transverse layer, the interlaminar shear failure mode was rolling shear failure of the transverse layer. When poplar was used as the transverse layer, the interlaminar shear failure modes of CLT were transverse layer shear failure and surface layer shear failure. When OSB was used as a transverse layer, the interlaminar shear failure mode of CLT was the internal shear failure of OSB. The significant difference of larch earlywood and latewood resulted in the rolling shear failure of the transverse layer along the direction of the growth rings, while the characteristics of poplar wood with diffuse pores resulted in the rolling shear failure along the load path (Li et al. 2022).

Hybrid cross laminated timber (HCLT) fabricated using Lodgepole pine (*Pinus contorta*) lumber lumber and/or laminated strand lumber (LSL based on aspen poplar (*Populus tremuloides*) as the outer layers resulted in significant improvements in mechanical performance compared to generic CLT products. Specifically, the modulus of elasticity (MOE) and modulus of rupture (MOR) of HCLT panels with LSL as the outer layers were found to be 19% and 36% higher, respectively, than those of standard CLT products. When LSL was used as the core layer, replacing the cross lumber layer, the MOE and MOR values increased by 13% and 24%, respectively, compared to generic CLT panels (Wang et al. 2015). Given the nature of cross-laminated timber (CLT), with an orthogonal arrangement and rolling shear characteristics of transverse layers, it has a more complex duration-of-load (DOL) effect than glued-laminated timber. Construction oriented strand board (OSB) and spruce-pine-fir (SPF) dimension lumber were used to fabricate hybrid CLT (HCLT) specimens showing that the fatigue life and long-term performance of CLT can be improved by using OSB panels as CLT layers (Song et al. 2022). By using structural wood-based materials with a proven strength performance, such as LVL, LSL, and plywood, for the CLT cross layer, MOR improved by up to 1.35 times, MOE by up to 1.5 times, and the rolling shear strength 1.59 times (Yang et al. 2021).

Experimental simulation of hybrid CLT (HCLT) members in compression perpendicular to grain under the vertical load imposed by columns or walls in the platform frame structure system showed that HCLT using structural composite materials (e.g. laminated strand lumber, LSL) instead of timber leads to

different failure modes were mainly the cracks along the wood ray direction of SPF material, while no obvious damage for LSL under full surface loading (Gong et al. 2023).

Among these types, more studies have been conducted on hybrid CLTs that utilize wood-based materials as the layer material. One option is to use plywood to produce so-called ply-lam CLTs. The mechanical properties of ply-lam CLTs were compared with GLT and CLT. The bending properties of ply-lam CLTs predicted by beam theory were compared with the experimental values. The ply-lam CLTs showed higher strength than CLT, but lower than GLT (Yang et al. 2024). The flexural behavior of cross laminated bamboo and timber (CLBT) and cross laminated timber (CLT) showed the potential of using glued laminated bamboo (glubam) in hybrid poplar based CLT panels to obtain similar or even better mechanical performance and other constructional and environmental merits (Wen and Xiao 2023).

The bonding quality of CLT and glulam made from oak and mixed poplar and oak species showed that CLT or glulam made from pure oak delaminated more than the mixed specimens. However, their residual shear strength can be comparable or even superior to what was obtained with mixed poplar-oak specimens. As a result, residual shear strength after delamination test may be interesting to consider as an additional criterion to assess the glue line integrity of hardwood CLT or glulam products (Purba et al. 2022). Three adhesives (one-component polyurethane - PUR, PUR + primer and melamine-urea– formaldehyde – MUF) and two press systems (hydraulic and vacuum press) were explored in the production of pure beech and combined beech-spruce-beech cross laminated timber (CLT). None of the adhesives that were tested met the requirements for delamination tests provided by the current standard for softwood. A size effect was noticed in the delamination test: the larger the specimen, the greater the delaminations that were observed. The shear tests on dry specimens proved to be less efficient in determining the influence of the several bonding parameters, even if a 45° grain orientation seemed to reduce the rolling shear (Brunetti et al. 2020). Three-layered CLT panels made up of beech-Corsican pine timber and melamine based adhesive were checked on their mechanical performance and compared with the widely diffused market product (C24 Spruce CLT panels). The collected experimental and numerical results reveal an overall good behavior of homogeneous hardwood panels, and an excellent performance of hybrid softwood-hardwood configuration, with great opportunity on construction applications (Sciomenta et al. 2021). In the comparison of the column buckling behavior of three-layer Cross Laminated Timber (CLT) panels under compression, homogeneous CLT panels entirely made of beech were compared with hybrid specimens featuring Corsican pine inner layers. While different failure mechanisms were observed, there was little difference in the results in terms of load-bearing capacity between the two types of specimens. However, the hybrid specimens exhibited a larger difference in terms of standard deviation compared to the homogeneous specimens (Sciomenta et al. 2024).

Homogeneous beech, poplar, and spruce CLT panels, as well as their combinations, using a polyurethane adhesive were tested. Poplar CLT's modulus of elasticity (MOE) and modulus of rupture (MOR) values reached or exceeded those of high-grade commercial softwood CLT. The bending properties of beech and hybrid beech-poplar panels far exceeded the performance of commercial panels, which shows the excellent potential of high-density hardwoods for high-performance CLT production. Beech-spruce hybrid panels seriously underperformed caused due to issues related to gluing (Altaher Omer Ahmed et al. 2023).

The structural out-of-plane bending performance of three-layer hybrid cross-laminated-timber manufactured from outer layers of fast-growing poplar (*Populus alba*) and a crosslayer of Iranian beech species (*Fagus orientalis*) using polyurethane as a binder both experimental and theoretical results revealed that comparison with poplar CLT, hybrid poplar-beech CLT had more potential for structural bending performance in the construction and building sector (Hematabadi et al. 2021).

Similarly, hybrid, three-layered, softwood-hardwood cross-laminated timber build-up with outer layers of European spruce (*Picea abies*) and a center cross-layer of European beech (*Fagus sylvatica*) were tested in out-of-plane bending indicating the characteristic values of rolling shear modulus and strength of the beech cross-layer. The results from the bending tests were $G_{r,mean} = 350$ N/mm^2 and $f_{v,r,05} = 2.6$ N/mm^2, respectively. This provides a great potential of mixed softwood-hardwood CLT build-ups for structural elements in the building sector (Aicher et al. 2016).

Additionally, research on hybrid CLT specimens, combining Douglas fir and poplar, showed that while the flexural strength remained largely unchanged compared to pure poplar CLT, the stiffness increased by 8% to 22%. (Lu et al. 2019). The mechanical properties of hybrid (mixed-species) cross-laminated

timber (CLT) panels made with low-value sugar maple (*Acer saccharum*) surface layers and white spruce (*Picea glauca*) were improved significantly compared with those of the current standard layups (Ma et al. 2021).

Lum et al. (2022) provided an overview of the bending and shear properties of CLT made from different timber species with various densities including timbers such as softwood, temperate hardwood as well as tropical hardwood. Validation of relatively simple FEM models for simulation and virtual prototyping of alternative CLT combinations also revealed that for shear tests, the lack of orthotropic material properties of hybrid poplar could be sufficiently substituted by using cottonwood (*Populus delotides*) material properties (Sebera et al. 2015).

Reinforced & treated CLT
Different binding/wrapping techniques have been checked in India to utilize poplar in a laminated form, known as cross-laminated timber (CLT). Related to columns maximum improvement in the load-carrying capacity, stiffness and ductility were observed using reinforcement by double cross helix fibre reinforced polymer (FRP) wrapping (Bath 2021).

The effect of micronized copper azole type C (MCA-C) treatment on rolling shear (RS) strength and RS modulus of southern yellow pine (SYP) based cross-laminated timber (CLT) was evaluated showing that the preservative treatment reduced the mean RS strength from 2.16 MPa to 1.87 MPa, while it increased the mean RS modulus from 132.11 MPa to 147.72 MPa, though not statistically significant (Lim et al. 2020).

<u>Oriented Strand Board (OSB) and Laminated Strand Lumber (LSL)</u>
OSB (Oriented Strand Board) is a wood-based panel commonly used to stiffen timber-frame structures and mitigate shear issues. It serves as a complementary product to plywood for this application. Additionally, OSB has gained importance as the vertical web positioned between the horizontal flanges of an I-joist.

LSL (Laminated Strand Lumber) is part of a family of products called structural composite lumber (SCL). LSL is made of strands or flakes that are bonded together with a moisture-resistant adhesive, while similar products based on veneers include laminated veneer lumber (LVL) and parallel strand lumber (PSL).

Poplar – aspen OSB
Oriented strand boards (OSB) made from trembling aspen, a low-density hardwood species, and OSB made from paper birch, a medium-density hardwood species, performed equally well in IB (Internal Bond). While the MOE in flatwise bending was slightly lower for birch compared to aspen panels (11.8 GPa for aspen and 10.6 GPa for birch), the MOR values did not show significant differences. Additionally, the edgewise bending properties were also comparable between the two types of OSB. (Beck et al. 2010). OSB panels made from aspen obtained better bonding properties, while IB and TS properties were lower compared to OSB panels from black spruce (Zhuang et al. 2022).

Oriented structural boards (OSB) and random strand boards produced from wood of hybrid poplar (I-72, *Populus × euramericana* cv. San Martine [Populus 'San Martino']) grown in China, showed that the optimum density for OSB made from this fast-growing poplar was 0.65-0.70 g/cm^3 (Zhou 1990). Tamjidi et al. (2017) produced 12 mm thick laboratory OSB boards made from mixture of three clones of ten-years-old hybrid poplar showing the importance of mat moisture content and press temperature.

Mixed OSB
Various techniques have been explored to enhance the properties of oriented strand boards (OSB) made from softwood and aspen strands. Incorporating aspen strands significantly improved the thickness swelling of softwood-based OSB. Moreover, reducing the density of the surface layer could potentially mitigate thickness swelling in OSB manufactured from softwoods (Zhuang et al. 2022b).

In another study, five sets of three-layer OSB were made from aspen and/or Moso bamboo strands. Complete replacement of the aspen in the surface layers with internode Moso strands resulted in over 45 % greater MOR. Moso bamboo surface OSB were low in MOE which is consistent with unadulterated tissue being high in bending strength and fracture toughness but low in specific stiffness (Semple et al. 2015). Bamboo has been known as a good substitute of engineered wood raw material for

its naturally oriented high strength. A composite OSB made from a combination of bamboo and poplar, with varying hybrid ratios, was able to enhance the properties of the board (Yong et al. 2012).

The influence of three different content levels of fine strands in the core layers on the physical and mechanical properties of European beech and poplar OSB showed that increasing the fines content in the core layer from 10 to 50 %, based on total board weight has no significant effect on bending strength and MOE. The highest MOR and MOE were determined for panels solely made of poplar with different level of fines content. Increasing the amount of fines in the core layer raised the internal bond (IB) and both thickness swelling as well as water absorption after 24 h decreased (Akrami et al. 2014). Beech and poplar strands with three different combinations of face/core ratios at densities of 650 and 720 kg/m3 were examined, using poly methylene diphenyl diisocyanate glue at 5 % with press conditions of 180 °C and 240 s. Panels made of 60 % beech in face layers showed higher modulus of rupture and modulus of elasticity. Panels with 75 % beech strands in the core layer showed the maximum internal bond strength at 720 kg/m^3. It was also observed that increasing the amount of beech in the core layer from 40 to 75 % decreased thickness swelling at both densities (Akrami et al. 2014b). The MOR and MOE properties of OSB panels composed of mixed beech and poplar strands exhibited values twice as high as those required for compliance with EN300 standards at a density of 720 kg m^{-3}. This offers opportunities for the industry in Europe to use alternative wood species that could assist in meeting the future demands of the construction industry (Akrami et al. 2014c).

OSBs made from the following mixtures: European beech and poplar, beech and pine, poplar and pine and 100% pine (i.e. the conventional raw material for OSB in Europe) showed that panels comprising a mixture of European beech and poplar have higher mechanical properties compared to panels made with mixtures of pine-beech or pine-poplar (Akrami et al. 2015). The results on selected mechanical properties of beech and poplar OSB such as screw holding strength (SH) and Brinell hardness (BH) showed that density has a positive effect on both properties and that wood species (beech or poplar) and size of strands (normal or fine size) also had an effect on SH (Akrami and Laleicke 2018).

Developing specialty OSB with high stiffness for products such as engineered wood flooring (EWF) showed that higher values of bending MOE for panels made from aspen/birch mixture of 90% aspen (*Populus tremuloides*) and 10% of paper birch (*Betula papyrifera*), and of small diameter ponderosa pine logs (*Pinus ponderosa*), of 8190 and 9050 MPa, respectively were obtained, which are values very close to Baltic birch (*Betula pendula*) plywood, a product known for its high stiffness (Barbuta et al. 2011). OSBs made in the laboratory from a mixture of softwood species (fir, spruce, and pine) were compared to those made from hardwood species (poplar, willow, and birch), the latter showing better mechanical properties notably a MOR = 43.48 N/mm^2, MOE = 7253 N/mm^2, and IB = 1.57 N/mm^2 (Lunguleasa et al. 2020). OSB manufactured at an industrial scale with different shares of poplar and sweet chestnut wood (respectively, 50–50%, 40–60%, and 100% in weight) indicated that sweet chestnut OSB can be realized with a process similar to that currently used for manufacturing poplar OSB (Zanuttini et al. 2020).

Poplar LSL

Laminated Strand Lumber (LSL) stands out as a versatile structural material, particularly notable for its application with Hungarian hardwoods, including Turkey oak (*Quercus cerris*), European hornbeam (*Carpinus betulus*), European beech (*Fagus sylvatica*), and various domestic poplar species such as *Populus alba*, *Populus nigra*, and *Populus tremula*. Engineered from thin wood strands bonded in layers, LSL offers a range of advantages, including reliability, durability, and consistent performance (Hasan et al. 2023).

In comparative studies, oriented strand lumber (OSL), laminated veneer lumber (LVL) and plywood made out of poplar (*Populus deltoides*) were experimentally evaluated in relation to screw withdrawal resistance indicating that OSL joints were stronger than same joints constructed of LVL, plywood and poplar wood (Maleki et al. 2017). Another investigation focused on laminated strand lumber and oriented strand lumber using fast-growing poplar (*Populus deltoides*) and paulownia (*Paulownia fortunei*). Notably, panels made from poplar demonstrated excellent performance, with the addition of a small percentage (7.5%) of nanoclay into urea-formaldehyde (UF) resin leading to enhanced mechanical properties. LSL made from poplar showed values of 104.67 MPa for MOR, and 13517 MPa for MOE and an internal bonding strength of 0.98 MPa (Bayatkashkoli and Faegh 2014).

Furthermore, the determination of diffusion coefficients has proven instrumental in modeling moisture transfer within LSL, particularly when utilizing wood species like aspen. Such coefficients are valuable for accurately predicting time-dependent deflections during service, offering insights into the material's behavior over time (Cai et al. 1997).

Poplar PSL

Parallel strand lumbers (PSLs) manufactured from rotary peeled hybrid poplar I-214 veneers and glued with phenol formaldehyde (PF) and urea formaldehyde (UF) adhesives showed strength properties surpassing those of solid hybrid poplar I-214 wood. For instance, the PSLs showed MOR values comparable to those of established wood species, with reported values of 80.2 N.mm^{-2} for PSLs manufactured from southern pine and 87.5 N.mm^{-2} for PSLs from yellow poplar (Kurt and Cavus 2011). The effect of resin type and strand thickness on the applied properties of parallel strand lumber (PSL) made from poplar (*Populus deltoides* L.) showed that the mechanical properties of panels made with 2 mm thick strands employing PF and pMDI resin were better. Moradpour et al. (2019) concluded that producing parallel strand lumbers from poplar as an underutilized lightweight fast-growing species is more suitable with higher value-added in comparison to other engineered wood products such as laminated veneered lumber and laminated strand lumber.

Beyond traditional construction applications, various engineered wood products are demonstrating promise in alternative sectors. An illustrative instance is the Longitudinally-Laminated Timber (LLT) panel incorporating beech and oak, tailored for the furniture industry (Smardzewski and Łabeda 2018).

Treated OSB & PSL

The effect of thermo-vacuum treatment on the characteristics of poplar OSB as produced now in Northern Italy, has also been examined. The thermal treatment significantly changed the properties of poplar OSB. Notably, the mass, the bending strength, the modulus of elasticity and the internal bond decreased with different intensities. The swelling after immersion in water decreased indicating the potential for using this product for new applications with particular attention to non-structural uses in humid conditions (Cetera et al. 2018).

Nano-zinc oxide can be used to treat Iranian beech laminated strand lumber (LSL) composites made with PF and pMDI adhesives without having any negative effect on mechanical properties and at low concentrations, a decrease in thickness swelling and improved dimensional stability were observed (Mohammadi et al. 2018).

Hybrid poplar, known for its rapid growth in temperate regions with growth rate up to 35 m^3 ha^{-1} y^{-1} after eight to 12 year rotations, density of 300 to 375 kg m^{-3} and MOE of 7 to 8 GPa, has historically lacked the mechanical properties required for building construction applications. However, the densification process known as viscoelastic thermal compression (VTC) has opened new possibilities. By processing thin wood laminates through VTC, resulting in densities ranging from approximately 750 to 1200 kg m^{-3} and moduli of elasticity between 18 to 29 GPa, it becomes feasible to manufacture parallel-laminated composites. These composites, incorporating VTC wood in the outer layers and untreated hybrid poplar in the core, exhibit bending properties that exceed the structural design values mandated for load-bearing applications in wood frame construction (Kamke and Kutnar 2010).

Furthermore, densification of *Nothofagus pumilio* and *N. antarctica* (known as the southern beeches) wood improved the strength, stiffness, and hardness of the three-layer wood composites used in this study presenting a likely use case for densified lenga or ñire as a thin layer adhered to some core material and used in furniture, flooring, or where other high-abrasion surfaces are needed (Schwarzkopf et al 2018).

Reinforced LSL

The effect of incorporating glass fiber reinforced polymer (GFRP) on the technical properties of LSL made from poplar (*Populus deltoides* L.) using pMDI as binder, showed that properties such as MOR, MOE, IS, SS and CS were improved by 123, 114, 100, 94, and 90%, respectively (Moradpour et al. 2018).

MODELLING OF EWPS AND DESIGN FOR STRUCTURES

Starting from the 2 wood species, poplar and beech, and related differentiated levels of density and related physicochemical properties allows to design both panel and beam concepts of engineered wood products. Different modelling approaches provide input for design and predict mechanical performance starting from veneer, timber and strands. A hierarchical model was developed for the prediction of hardwood (birch) timber board stiffness and the reduction of stiffness due to knots. Suitable global and local predictions for silver birch timber are feasible, given the dynamic modulus of elasticity, median slope of grain, and knot geometries (Collins and Fink 2022). Similarly, a mechanical model was developed to accurately predict the strength of laminated veneer lumber (LVL) beams manufactured from veneers rotary, peeled from early to mid-rotation subtropical hardwood plantation logs, allowing to check for various construction strategies. The design bending strength of these hardwood LVL beams were found to be superior to commercialised softwood LVL beams, ranging between 37.0 MPa and 83.9 MPa on flat and between 38.7 MPa and 97.2 MPa on edge (Gilbert et al. 2017).

Töpler et al. (2023) performed experimental investigations of the benchmark on the elastic material behaviour of beech LVL and determined the complete elastic material stiffness matrix of beech LVL for the first time. This breakthrough facilitates the calculation of the elastic stiffness matrix, which is pivotal for finite element-based design of timber structures. To better guide the manufacturing and application of laminated veneer lumber (LVL), a theoretical model to describe the formation of the modulus of elasticity for LVL based on the laminated plate theory was proposed. The measured values corroborated well with the theoretical predictions, affirming the validity of the model and providing valuable insights to guide LVL manufacturing and application (Wei et al. 2019).

Since birch plywood is considered most promising in structural applications, due to the combined advantages of its superior mechanical properties and the cross lamination configuration, a comprehensive experimental dataset that could serve as the input in the analytical or numerical models to design birch plywood under various load conditions (Wang et al. 2022).

Several design guides are available today with some guidance on how to use engineered wood products for building with wood and bio-based materials in general but often the option to use hardwoods like beech and poplar is missing. Some of these guidelines do address lay-up options enabling hybrid combinations: LVL handbook Europe, Design Guide Structural Plywood and LVL, Glulam Design Properties and Layup Combinations, The CLT handbook…, but also the similarity with composite theory in general can be of useful as presented in more detail in 'Guide to composite' books.

CONCLUSIONS

Green building and the related building with wood has evolved over the past decades including not only timber frame construction using mainly timber and wood-based panels, but also an increased usage of engineered wood products for larger beams (glulam, LVL, I-joists) and the development of mass timber construction and hybrid building systems based on CLT with options for high rise buildings and topping up of existing ones.

Modelling and manufacturing fit-for-purpose products through prediction of mechanical performance by designing engineered wood products does not only offer a range of opportunities for hardwoods, but also provides extra positive synergies like the improved rolling shear strength when including hardwood in softwood products. These combined or hybrid products are not only based on different wood species as such, the layered structure of CLT can also be based on layer existing of other engineered wood products like LVL, plywood and OSB and can cover also functionalities beyond mechanical performance like insulation. Hardwood species provides extra option to combine different densities and balance as such better weight and mechanical performance. The positive impact on rolling shear properties can be provided in combination with low density, e.g. when incorporating hardwoods like (hybrid) poplar.

Innovative densification processing of poplar allows to mimic denser hardwoods, leading to increased mechanical properties in particular those related to surface quality like hardness. Similarly, the densification of beech, often combined with resin treatments, has been instrumental in producing exceptional engineered wood products for many decades. These products include wood dowels, connectors, as well as compreg and impreg plywood, renown for a range of niche markets such as bullet proof plywood.

Furthermore, it is important that hardwood-based EWPs for building with wood, including both structural elements and other bio-based components, are sourced from sustainably managed forests. This ensures the availability of high-quality trees from a diverse range of wood species, ideally located close to where the engineered wood products will be utilized in construction projects. This should underpin the need for a European wide approach related to resource management. Using both (hybrid) poplar and beech as complementary resources for the construction sector is enhancing the rural development aspects. This can be further improved by using modelling and design methodology to predict the mechanical performance of mixed hardwood EWP's. Starting from different wood species and primary processing technologies (veneer, timber, stands), engineers can calculate and select fit for purpose building commodities. Architects are now able to take into account opportunities and barriers related to the use of mixed hardwood EWP's.

The objective of this review-based paper was to explore potential and options to combine poplar and beech for tailored engineered wood products in view of future design-based building concepts. This fits in a wider framework on hardwood based engineered wood products as summarized by Van Acker (2021). The hybrid or combined products enhance even more the potential of poplar (Van Acker et al. 2016) and beech as complementary resources for building with wood.

Since both wood species show a low resistance against decay and beech in particular that is also prone to low dimensional stability, it's essential to explore various wood protection and improvement treating technologies. These technologies encompass both the use of biocides and wood modification techniques, including thermal or chemical treatments (Van Acker 2019). Although moisture dynamics of engineered wood products, like plywood (De Windt et al 2018), show that in many applications a better performance can be expected than based on the wood species composition, it remains an option for some applications to include wood protection options to enhance resistance against decay and also to improve fire safety of products like CLT (Van Acker et al. 2023).

Enhancing performance by combined engineered wood products, so-called hybrid EWPs should provide extra potential. For solid timber-based products like glulam (GLT) and cross laminated timber (CLT), this was already tested for both species and has been underpinned by research projects. Also veneer based products like plywood and laminated veneer lumber (LVL) are very suitable for combining wood species and rheological performance can further be improved by using natural fibres as extra embedded component. Current trends in strand-based panel and beam products like OSB and LSL demonstrate a tendency to incorporate multiple wood species as resources, with an increased interest in hardwoods. Here also properties can be defined through careful combination of wood species creating as such a fit for purpose mix of beech and poplar.

The overall conclusion is that a wide range of options are available for both beech and poplar as hardwood species as such and even more combined to participate in the building with wood framework when incorporated in fit for purpose design of engineered wood products.

ACKNOWLEDGEMENTS

REFERENCES

Abdoli F, Rashidi M, Rostampour-Haftkhani A, Layeghi M, Ebrahimi G (2023) Effects of fastener type, end distance, layer arrangement, and panel strength direction on lateral resistance of single shear lap joints in cross-laminated timber (CLT). *Case Studies in Construction Materials*, *18*, e01727.

Abdoli F, Rashidi M, Rostampour-Haftkhani A, Layeghi M, Ebrahimi G (2022) Withdrawal performance of nails and screws in cross-laminated timber (CLT) made of Poplar (*Populus alba*) and Fir (*Abies alba*). *Polymers*, 14(15), 3129.

Aicher S, Christian Z, Hirsch M (2016) Rolling shear modulus and strength of beech wood laminations. *Holzforschung*, *70*(8), 773-781.

Aicher S, Hirsch M, Christian Z (2016) Hybrid cross-laminated timber plates with beech wood cross-layers. *Construction and Building Materials*, 124, 1007-1018.

Aicher S, Ohnesorge D (2010) Shear strength of glued laminated timber made from European beech timber. *European Journal of Wood and Wood Products, 69*(1), 143-154.

Aicher S, Tapia C (2018) Novel internally LVL-reinforced glued laminated timber beams with large holes. *Construction and Building Materials*, *169*, 662-677.

Akkurt T, Kallakas H, Rohumaa A, Hunt C G, Kers J (2022) Impact of Aspen and Black Alder Substitution in Birch Plywood. *Forests*, *13*(2), 142.

Akrami A, Barbu M C, Frühwald A (2014b) Characterization of properties of oriented strand boards from beech and poplar. *European Journal of Wood and Wood Products*, *72*, 393-398.

Akrami A, Barbu M C, Frühwald A (2014c). European hardwoods for reducing dependence on pine for oriented strand board. *International Wood Products Journal, 5*(3), 133-135.

Akrami A, Fruehwald A, Barbu M C (2014) The effect of fine strands in core layer on physical and mechanical properties of oriented strand boards (OSB) made of beech (*Fagus sylvatica*) and poplar (*Populus tremula*). *European Journal of Wood and Wood Products*, *72*, 521-525.

Akrami A, Frühwald A, Barbu M C (2015) Supplementing pine with European beech and poplar in oriented strand boards. *Wood Material Science & Engineering*, *10*(4), 313-318.

Akrami A, Laleicke P F (2018) Densification, screw holding strength, and Brinell hardness of European beech and poplar oriented strand boards. *Wood Material Science & Engineering*, *13*(4), 236-240.

Altaher Omer Ahmed A, Garab J, Horváth-Szováti E, Kozelka J, Bejó L (2023) The Bending Properties of Hybrid Cross-Laminated Timber (CLT) Using Various Species Combinations. *Materials*, *16*(22), 7153.

Aydın İ, Çolak S, Çolakoğlu G, Salih E (2004) A comparative study on some physical and mechanical properties of Laminated Veneer Lumber (LVL) produced from Beech (*Fagus orientalis* Lipsky) and Eucalyptus (*Eucalyptus camaldulensis* Dehn.) veneers. *European Journal of Wood and Wood Products*, *62*(3), 218-220.

Bal B C (2016) The effect of span-to-depth ratio on the impact bending strength of poplar LVL. *Construction and Building Materials*, *112*, 355-359.

Bal B C, Bektaş İ (2012) The effects of some factors on the impact bending strength of laminated veneer lumber. *BioResources*, *7*(4).

Bal B C, Bektaþ Ý (2014) Some mechanical properties of plywood produced from eucalyptus, beech, and poplar veneer. *Maderas. Ciencia y tecnología*, *16*(1), 99-108.

Bal B, Bekta İ, Mengeloğlu F, Karakuş K, Demir H Ö (2015) Some technological properties of poplar plywood panels reinforced with glass fiber fabric. *Construction and Building Materials*, *101*, 952-957.

Baldassino N, Zanon P, Zanuttini R (1998) Determining mechanical properties and main characteristic values of Poplar plywood by medium-sized test pieces. *Materials and Structures*, *31*, 64-67.

Bao F, Liu S (2001) Modeling the relationships between wood properties and quality of veneer and plywood of Chinese plantation poplars. *Wood and fiber science*, 264-274.

Barbuta C, Cloutier A, Blanchet P, Yadama V, Lowell E (2011) Tailor made OSB for special application. *European Journal of Wood and Wood Products*, *69*(4), 511.

Basterra L A, Acuna L, Casado M, Lopez G, Bueno A (2012) Strength testing of Poplar duo beams, *Populus x euramericana* (Dode) Guinier cv. I-214, with fibre reinforcement. *Construction and Building Materials*, *36*, 90-96.

Bayatkashkoli A, Faegh M (2014) Evaluation of mechanical properties of laminated strand lumber and oriented strand lumber made from Poplar wood (*Populus deltoides*) and Paulownia (*Paulownia*

fortunei) with urea formaldehyde adhesive containing nanoclay. *International Wood Products Journal*, *5*(4), 192-195.

Beck K, Cloutier A, Alexander S, Beauregard R (2010) Comparison of mechanical properties of oriented strand board made from trembling aspen and paper birch. *European Journal of Wood and Wood Products*, *68*(1), 27-33.

Benthien T J, Riegler M, Engehausen N, Nopens M (2020) Specific dimensional change behavior of laminated beech veneer lumber (baubuche) in terms of moisture absorption and desorption. *Fibers*, *8*(7), 47.

Bhat J A (2021) Improved strength and stiffness characteristics of cross-laminated poplar timber columns. *International Journal of Engineering* 34.4: 803-810.

Bicke S, Biziks V, Militz H (2017) Dimensional stable and durable laminated veneer lumber (LVL) from European beech (*Fagus sylvatica*) by impregnation with low molecular weight phenolic resin. In *Book of Abstracts*, 39.

Bicke S, Mai C, Militz H (2012) Modification of beech veneers with low molecular weight phenol formaldehyde for the production of plywood: Durability and mechanical properties. In *European Conference on Wood Modification*.

Birinci E (2022) Determination of physical and mechanical properties of plywood produced using beech, okoume and ozigo species. *Anadolu Orman Araştırmaları Dergisi*, *8*(2), 11-15.

Blass H, Frese M, Enders-Comberg M (2016) Beech LVL-high strength material for engineered timber structures. In *Structures and Architecture: Beyond their Limits,* 102-109. CRC Press.

Bourreau D, Aimene Y, Beauchêne J, Thibaut B (2013) Feasibility of glued laminated timber beams with tropical hardwoods. *European Journal of Wood and Wood Products*, *71*(5), 653-662.

Brunetti M, Nocetti M, Pizzo B, Aminti G, Cremonini C, Negro F, Zanuttini R, Romagnoli M, Scarascia Mugnozza G (2020) Structural products made of beech wood: quality assessment of the raw material. *European Journal of Wood and Wood Products*, *78*, 961-970.

Brunetti M, Nocetti M, Pizzo B, Negro F, Aminti G, Burato P, Cremonini C, Zanuttini R (2020) Comparison of different bonding parameters in the production of beech and combined beech-spruce CLT by standard and optimized tests methods. *Construction and Building Materials*, *265*, 120168.

Burdurlu E, Kilic M, Ilce A C, Uzunkavak O (2007) The effects of ply organization and loading direction on bending strength and modulus of elasticity in laminated veneer lumber (LVL) obtained from beech (*Fagus orientalis* L.) and lombardy poplar (*Populus nigra* L.). *Construction and Building Materials*, *21*(8), 1720-1725.

Cai L, Avramidis S, Enayati A A (1997) Feuchtesorption und Feuchtebewegung in "Parallam" und "Timber Strand". *Holz als Roh-und Werkstoff*, *55*, 365-369.

Castro G L, Fragnelli G (2006) New technologies and alternative uses for poplar wood. *Boletín Informativo CIDEU*, (2), 27-36.

Castro G, Paganini F (2003) Mixed glued laminated timber of poplar and *Eucalyptus grandis* clones. *Holz als Roh-und Werkstoff*, *61*, 291-298.

Cetera P, Negro F, Cremonini C, Todaro L, Zanuttini R (2018) Physico-mechanical properties of thermally treated poplar OSB. *Forests*, *9*(6), 345.

Chang L, Guo W, Tang Q (2017) Assessing the tensile shear strength and interfacial bonding mechanism of poplar plywood with high-density polyethylene films as adhesive. *BioResources*, *12*(1), 571-585.

Cheng F, Hu Y (2011) Nondestructive test and prediction of MOE of FRP reinforced fast-growing poplar glulam. *Composites Science and Technology*, *71*(8), 1163-1170.

Chui Y H, Schneider M H, Zhang H J (1994) Effects of resin impregnation and process parameters on some properties of poplar LVL. *Forest Products Journal*, *44*(7, 8), 74.

Çolak S, Çolakoğlu G, Aydin I (2007) Effects of logs steaming, veneer drying and aging on the mechanical properties of laminated veneer lumber (LVL). *Building and Environment*, *42*(1), 93-98.

Colakoglu G, Colak S, Aydın İ, Yildiz Ü, Yildiz S (2003) Effect of boric acid treatment on mechanical properties of laminated beech veneer lumber. *Silva Fennica*, *37*(4).

Collins S, Fink G (2022) Modeling the tensile mechanical properties of silver birch timber boards. *Construction and Building Materials, 344*, 128147.

Constant T, Badia M A, Mothe F (2003) Dimensional stability of Douglas fir and mixed beech-poplar plywood: experimental measurements and simulations. *Wood science and technology*, *37*, 11-28.

Daoui A, Descamps C, Marchal R, Zerizer A (2011) Influence of veneer quality on beech LVL mechanical properties. *Maderas. Ciencia y tecnología*, *13*(1), 69-83.

Das S, Gašparík M G, Sethy A K, Niemz P, Lagaňa R, Kytka T, Sviták M, Kamboj G (2023b) Suitability of aspen (*Populus tremula* L.) for cross-laminated timber (CLT). *Wood Research, 68*, 502-520.

Das S, Gašparík M, Sethy A K, Kytka T, Kamboj G, Rezaei F (2023) Bonding performance of mixed species cross laminated timber from poplar (*Populus nigra* L.) and maple (*Acer platanoides* L.) glued with melamine and PUR adhesive. *Journal of Building Engineering*, *68*, 106159.

Davids W G, Willey N, Lopez-Anido R, Shaler S, Gardner D, Edgar R, Tajvidi M (2017) Structural performance of hybrid SPFs-LSL cross-laminated timber panels. *Construction and Building Materials*, *149*, 156-163.

De Windt I, Li W, Van den Bulcke J, Van Acker J (2018) Classification of uncoated plywood based on moisture dynamics. *Construction and Building Materials, 158*, 814-822.

Defoirdt N, Sen A, Dhaene J, De Mil T, Pereira H, Van Acker J, Van den Bulcke J (2017) A generic platform for hyperspectral mapping of wood. *Wood Science and Technology, 51*, 887-907.

Dill-Langer G, Aicher S (2014) Glulam composed of glued laminated veneer lumber made of beech wood: superior performance in compression loading. In *Materials and Joints in Timber Structures: Recent Developments of Technology,* 603-613. Springer Netherlands.

Dill-Langer G, Aicher S (2014) Glulam composed of glued laminated veneer lumber made of beech wood: superior performance in compression loading. In *Materials and Joints in Timber Structures: Recent Developments of Technology*. Springer Netherlands, 603-613.

Dundar T, Ayrilmis N, Candan Z (2008) Evaluation of surface roughness of laminated veneer lumber (LVL) made from beech veneers treated with various fire retardants and dried at different temperatures. *Forest Products Journal*, *58*(1), 71.

Ehrhart T, Brandner R, Schickhofer G, Frangi A (2015) Rolling shear properties of some European timber species with focus on cross laminated timber (CLT): test configuration and parameter study. In *International Network on Timber Engineering Research: Proceedings of Meeting 48* (Vol. 2015), 61-76. Timber Scientific Publishing, KIT Holzbau und Baukonstruktionen.

Ehrhart T, Fink G, Steiger R, Frangi A (2016) Strength grading of European beech timber for the production of GLT & CLT. In *International Network on Timber Engineering Research: Proceedings of Meeting 49* (Vol. 49), 29-44. Timber Scientific Publishing, KIT Holzbau und Baukonstruktionen.

Ehrhart T, Grönquist P, Schilling S, Steiger R, Frangi A (2021) Mechanical properties of European beech glulam after 32 years in a service class 2 environment. In *8th International Network on Timber Engineering Research Meeting 54 (INTER 2021)*.

Ehrhart T, Palma P, Steiger R, Frangi A (2018b) Numerical and experimental studies on mechanical properties of glued laminated timber beams made from European beech wood. In *Proceedings of the 2018 World Conference on Timber Engineering*. National Institute of Forest Science.

Ehrhart T, Steiger R, Lehmann M, Frangi A (2020). European beech (*Fagus sylvatica* L.) glued laminated timber: Lamination strength grading, production and mechanical properties. *European Journal of Wood and Wood Products*, *78*, 971-984.

Ehrhart T, Steiger R, Palma P, Frangi A (2018) Mechanical properties of European beech glued laminated timber. In *Proceedings of the International Network on Timber Engineering Research, INTER, Meeting* (Vol. 51).

Ehrhart T, Steiger R, Palma P, Gehri E, Frangi A (2020) Glulam columns made of European beech timber: compressive strength and stiffness parallel to the grain, buckling resistance and adaptation of the effective-length method according to Eurocode 5. *Materials and Structures*, *53*(4), 91.

El Haouzali H, Marchal R, Bléron L, Butaud J C, Kifani-Sahban F (2020) Some properties of plywood produced from 10 cultivars of poplar. *International wood products journal*, *11*(2), 101-106.

El Haouzali H, Marchal R, Bléron L, Kifani-Sahban F, Butaud J C (2020) Mechanical properties of laminated veneer lumber produced from ten cultivars of poplar. *European Journal of Wood and Wood Products*, *78*, 715-722.

EN 314-1&2 (2004&1993) Plywood - Bonding quality - Part 1: Test methods – Part 2: Requirements.

EN 335 (2013) Durability of wood and wood-based products. Use classes: definitions, application to solid wood and wood-based products.

EN 350 (2016) Durability of wood and wood-based products. Testing and classification of the durability to biological agents of wood and wood-based materials.

EN 14080 (2013) Timber structures - Glued laminated timber and glued solid timber – Requirements.

EN 16351 (2021) Timber structures - Cross laminated timber – Requirements.

Engehausen N, Benthien J T, Nopens M, Ressel J B (2021) Density profile analysis of laminated beech veneer lumber (BauBuche). *Fibers*, *9*(5), 31.

Erdil Y Z, Kasal A, Zhang J, Efe H, Dizel T (2009) Comparison of mechanical properties of solid wood and laminated veneer lumber fabricated from Turkish beech, Scots pine, and Lombardy poplar. *Forest Products Journal*, *59*(6), 55.

Espinoza O, Buehlmann U (2018) Cross-laminated timber in the USA: Opportunity for hardwoods? *Current Forestry Reports*, *4*, 1-12.

Essoua G G E, Blanchet P (2017) Cross laminated timber made from large-leaf beech: Production, characterization and testing. In *6 th International Scientific Conference on Hardwood Processing,* 208.

EUFORGEN. European Forest Genetic Resources Programme. 2023. Available online: https://www.euforgen.org/species/fagus-sylvatica/ (accessed on 20 March 2024).

Fleckenstein M, Biziks V, Mai C, Militz H (2018) Modification of beech veneers with lignin phenol formaldehyde resins in the production of laminated veneer lumber (LVL). *European journal of wood and wood products*, *76*, 843-851.

Franke S (2016) Mechanical properties of beech CLT. In *Proceedings of the WCTE 2016 World Conference on Timber Engineering, Vienna, Austria*, 22-25.

Frese M, Blaß, H J (2007) Characteristic bending strength of beech glulam. *Materials and structures, 40*, 3-13.

Gaff M, Gašparík M (2015) Influence of densification on bending strength of laminated beech wood. *BioResources*, *10*(1), 1506-1518.

Gao Y, Wu Y, Zhu X, Zhu L, Yu Z, Wu Y (2015) Numerical analysis of the bending properties of cathay poplar glulam. *Materials*, *8*(10), 7059-7073.

George B, Simon C, Properzi M, Pizzi A, Elbez G (2003) Comparative creep characteristics of structural glulam wood adhesives. *European Journal of Wood and Wood Products*, *61*(1), 79-80.

Gilbert B P, Bailleres H, Zhang H, McGavin R L (2017) Strength modelling of laminated veneer lumber (LVL) beams. *Construction and Building Materials, 149*, 763-777.

Glavinić I U, Boko I, Torić N, Vranković J L (2020) Application of hardwood for glued laminated timber in Europe. *J. Croation Assoc. Civil Eng*, *72*, 607-616.

Goli G, Cremonini C, Negro F, Zanuttini R, Fioravanti M (2014) Physical-mechanical properties and bonding quality of heat treated poplar (I-214 clone) and ceiba plywood. *iForest-Biogeosciences and Forestry*, *8*(5), 687.

Gong Y, Xiong S, Li M, Wang Y, Ren H, Wang Z (2023) Behaviour of hybrid cross laminated timber in compression perpendicular to grain in different layup structure, support conditions, and loading configurations. *Industrial Crops and Products*, 200, 116804.

Grönquist P, Weibel G, Leyder C, Frangi A (2021) Calibration of electrical resistance to moisture content for beech laminated veneer lumber "BauBuche S" and "BauBuche Q". *Forests*, *12*(5), 635.

Grøstad K, Bredesen R (2014) EPI for glued laminated timber. In *Materials and Joints in Timber Structures: Recent Developments of Technology* (pp. 355-364). Springer Netherlands.

Guan M, Liu Y, Zhang Z, Huang Z (2020) Evaluation of bending performance of carbon fiber-reinforced eucalyptus/poplar composite plywood by digital image correlation and FEA analysis. *Journal of Materials science*, *55*, 8388-8402.

Hajihassani R, Ghahri S, Zamani S M, Nourbakhsh A (2022) Performance of densified wood glulam as building bio-material. *Journal of Renewable Materials*, *10*(2), 511.

Hajihassani R, Mohebbi B, Kazemi Najafi S (2020) The effect of hygro-thermo-mechanical modification on the applied properties of glulam made from poplar. *Iranian Journal of Wood and Paper Industries*, *11*(2), 241-253.

Han Z, Zhang R, Song B (2018) Evaluation of the bending properties of modified fast-growing poplar glulam based on composite mechanics. *BioResources*, *13*(3), 7071-7085.

Hasan K F, Bak M, Ahmed A A O, Garab J, Horváth P G, Bejó L, Alpár T (2023) Laminated strand lumber (LSL) potential of Hungarian and Central European hardwoods: a review. *European Journal of Wood and Wood Products*, 1-20.

Hematabadi H, Madhoushi M, Khazaeian A, Ebrahimi G (2021) Structural performance of hybrid Poplar-Beech cross-laminated-timber (CLT). *Journal of Building Engineering*, *44*, 102959.

Hematabadi H, Madhoushi M, Khazaeyan A, Ebrahimi G, Hindman D, Loferski J (2020) Bending and shear properties of cross-laminated timber panels made of poplar (*Populus alba*). *Construction and Building Materials*, *265*, 120326.

HOUTVADEMECUM (2018) (in Dutch). RKWM Klaassen (editor-in-chief), 832 pp., Centrum Hout Almere and Vakbladen.com & Smartwave, Zwolle, The Netherlands. ISBN 978-90-828-172-94.

Ilkay A T A R, Başboğa I H, Karakuş K, Mengeloğlu F (2016) Suitability of poplar and beech laminas for laminated veneer lumber manufacturing using melamine formaldehyde adhesive. *Mugla Journal of Science and Technology*, *2*(2), 131-134.

Jakob M, Czabany I, Veigel S, Müller U, Gindl-Altmutter W (2022) Comparing the suitability of domestic spruce, beech, and poplar wood for high-strength densified wood. *European Journal of Wood and Wood Products, 80*(4), 859-876.

Jamalirad L, Doosthoseini K, Koch G, Mirshokraie S A, Hedjazi S (2011) Physical and mechanical properties of plywood manufactured from treated red-heart beech (*Fagus orientalis* L.) wood veneers. *BioResources*, *6*(4).

Jandl R, Foldal C B, Ledermann T, Kindermann G (2023) European Beech Forests in Austria—Current Distribution and Possible Future Habitat. *Forests, 14*(10), 2019.

Jin J, Wang J, Qin D, Luo N, Niu H (2016) Effects of veneer treatment with copper-based preservatives on the decay resistance and mechanical properties of poplar LVL. *Journal of Wood Chemistry and Technology*, *36*(5), 329-338.

Jorda J, Kain G, Barbu M C, Haupt M, Krišťák Ľ (2020) Investigation of 3D-Moldability of Flax Fiber Reinforced Beech Plywood. *Polymers*, *12*(12), 2852.

Jorda J, Kain G, Barbu M C, Petutschnigg A, Král P (2021) Influence of adhesive systems on the mechanical and physical properties of flax fiber reinforced beech plywood. *Polymers*, *13*(18), 3086.

Kallakas H, Rohumaa A, Vahermets H, Kers J (2020) Effect of different hardwood species and lay-up schemes on the mechanical properties of plywood. *Forests*, *11*(6), 649.

Kamke F, Kutnar A (2010) Structural Composite from FSC Certified Hybrid-Poplar. *Proceedings of the International Convention of Society of Wood Science and Technology and United Nations Economic Commission for Europe – Timber Committee*.

Karri R, Lappalainen R, Tomppo L, Yadav R (2022) Bond Quality of Poplar Plywood Reinforced with Hemp Fibers and Lignin-Phenolic Adhesives. *Composites Part C: Open Access*, 100299.

Kılıç M (2012) Some important physical properties of laminated veneer lumber (LVL) made from oriental beech and Lombardy poplar. In *AIP Conference Proceedings* (Vol. 1479, No. 1), 397-401. American Institute of Physics.

Kim K H (2020) Influence of layer arrangement on bonding and bending performances of cross-laminated timber using two different species. *BioResources*, *15*(3), 5328-5341.

Kobel P, Frangi A, Steiger R (2016) Timber trusses made of European beech LVL. In *World Conference on Timber Engineering, 22-25*.

Kożuch A, Banaś J (2020) The dynamics of beech roundwood prices in selected central European markets. *Forests*, 11(9), 902.

Krackler V, Keunecke D, Niemz P, Hurst A (2011) Possible fields of hardwood application. *Wood Res*, *56*(1), 125-136.

Kramer A, Barbosa A R, Sinha A (2014) Viability of hybrid poplar in ANSI approved cross-laminated timber applications. *Journal of Materials in Civil Engineering*, *26*(7), 06014009.

Kržan M, Azinović B, Fortuna B (2019) Hybrid glulam beam made of beech and spruce laminations– experimental and numerical investigation. *CompWood*, 89-89.

Kurt R, Cavus V (2011) Manufacturing of parallel strand lumber (PSL) from rotary peeled hybrid poplar I-214 veneers with phenol formaldehyde and urea formaldehyde adhesives. *Wood Research*, *56*(1), 137-144.

Kurt R, Cil M, Aslan K, Cavus V (2011) Effect of pressure duration on physical, mechanical, and combustibility characteristics of laminated veneer lumber (LVL) made with hybrid poplar clones. *BioResources*, *6*(4).

Kurt R, Meriç H, Aslan K, Çil M (2012) Laminated veneer lumber (LVL) manufacturing using three hybrid poplar clones. *Turkish Journal of Agriculture and Forestry*, *36*(2), 237-245.

Lanvin J D, Reuling D, Legrand G (2019) French beech - a new opportunity in wood housing. In *Proceedings of the 7th "International Scientific Conference on Hardwood Processing" (ISCHP).* Delft (Netherlands), 129-137.

Li M, Ren H (2022) Study on the interlaminar shear properties of hybrid cross-laminated timber (HCLT) prepared with larch, poplar and OSB. *Industrial Crops and Products*, *189*, 115756.

Li Q, Wang Z, Liang Z, Li L, Gong M, Zhou J (2020) Shear properties of hybrid CLT fabricated with lumber and OSB. *Construction and Building Materials*, *261*, 120504.

Lim H, Tripathi S, Li M (2020) Rolling shear modulus and strength of cross-laminated timber treated with micronized copper azole type C (MCA-C). *Construction and Building Materials*, 259, 120419.

Liu Y, Guan M, Chen X, Zhang Y, Zhou M (2019) Flexural properties evaluation of carbon-fiber fabric reinforced poplar/eucalyptus composite plywood formwork. *Composite Structures*, *224*, 111073.

Lovrić A, Zdravković V, Popadić R, Milić G (2017) Properties of plywood boards composed of thermally modified and non-modified poplar veneer. *BioResources*, *12*(4), 8581-8594.

Lu W, Gu J, Wang B (2019) Study on flexural behavior of cross-laminated timber based on different tree species. *Advances in Materials Science and Engineering*, *2019*, 1-8.

Luedtke J, Amen C, van Ofen A, Lehringer C (2015) 1C-PUR-bonded hardwoods for engineered wood products: influence of selected processing parameters. *European Journal of Wood and Wood Products*, *73*, 167-178.

Lum W C, Norshariza M B, Nordin M S, Ahmad Z (2022) Overview on Bending and Rolling Shear Properties of Cross-Laminated Timber (CLT) as Engineered Sustainable Construction Materials. In Hassan R et al.. *Green Infrastructure: Materials and Applications*, 93-111.

Lunguleasa A, Ayrilmis N, Spirchez C, Özdemir F (2018) Investigation of the effects of heat treatment applied to beech plywood. *Drvna industrija*, *69*(4), 349-355.

Lunguleasa A, Dumitrascu A E, Ciobanu V D (2020) Comparative studies on two types of OSB boards obtained from mixed resinous and fast-growing hard wood. *Applied Sciences*, *10*(19), 6634.

Ma Y, Si R, Musah M, Dai Q, Xie X, Wang X, Ross R J (2021) Mechanical property evaluation of hybrid mixed-species CLT panels with sugar maple and white spruce. *Journal of Materials in Civil Engineering*, *33*(7), 04021171.

Makowski A (2015) Analytical and experimental investigation of bending stresses in beech plywood. *Annals of Warsaw University of Life Sciences-SGGW. Forestry and Wood Technology*, *92*.

Maleki S, Najafi S K, Ebrahimi G, Ghofrani M (2017) Withdrawal resistance of screws in structural composite lumber made of poplar (*Populus deltoides*). *Construction and Building Materials*, *142*, 499-505.

Marko G, Bejó L, Takats P (2016) Cross-laminated timber made of Hungarian raw materials. In *IOP Conference Series: Materials Science and Engineering* (Vol. 123, No. 1, p. 012059). IOP Publishing.

Martinez del Castillo, E., Zang, C. S., Buras, A., Hacket-Pain, A., Esper, J., Serrano-Notivoli, R., ... & de Luis, M. (2022) Climate-change-driven growth decline of European beech forests. *Communications Biology, 5*(1), 163.

Martins C, Dias A M P G, Cruz H (2017) Glulam made by Poplar: delamination and shear strength tests. In *6th International Scientific Conference on Hardwood Processing, 222-231.*

Martins C, Ferreira C, Negrão J, Dias A M (2023) Poplar as an Alternative Species for Load Bearing Structures. In *Sustainable and Digital Building: Proceedings of the International Conference, 2022*. Cham: Springer International Publishing, 117-126.

Miljković J, Grmuša I, Điporović M, Kačarević-Popović Z (2005) The influence of fire retardants on the properties of beech and poplar veneers and plywood. *Glasnik Šumarskog fakulteta*, (92), 111-124.

Mirzaei G, Mohebby B, Ebrahimi G (2017) Glulam beam made from hydrothermally treated poplar wood with reduced moisture induced stresses. *Construction and Building Materials*, *135*, 386-393.

Mirzaei G, Mohebby B, Ebrahimi G (2018) Technological properties of glulam beams made from hydrothermally treated poplar wood. *Wood Material Science & Engineering*, *13*(1), 36-44.

Mohammadi H, Mastery Farahani M R, Yousefi H, Habibpuor B (2018) Effect of nano-zinc oxid and adhesive type on Physical and Mechanical properties of Laminated Strand Lumber. *Journal of Wood and Forest Science and Technology*, *25*(1), 39-48.

Mohebby B, Talaii A, Najafi S K (2007) Influence of acetylation on fire resistance of beech plywood. *Materials Letters*, *61*(2), 359-362.

Monteiro S R, Martins C, Dias A M, Cruz H (2020) Mechanical performance of glulam products made with Portuguese poplar. *European Journal of Wood and Wood Products*, *78*(5), 1007-1015.

Moradpour P, Behnia M, Pirayesh H, Shirmohammadli Y (2019) The effect of resin type and strand thickness on applied properties of poplar parallel strand lumber made from underutilized species. *European Journal of Wood and Wood Products*, *77*, 811-819.

Moradpour P, Pirayesh H, Gerami M, Jouybari I R (2018) Laminated strand lumber (LSL) reinforced by GFRP; mechanical and physical properties. *Construction and Building Materials*, *158*, 236-242.

Möttönen V, Bütün Y, Heräjärvi H, Marttila J, Kaksonen H (2015) Effect of combined compression and thermal modification on mechanical performance of aspen and birch wood. *Pro Ligno,11* (4), 310-317.

Nazerian M, Ghalehno M D (2011) Physical and mechanical properties of laminated veneer lumber manufactured by poplar veneer. *Journal of Agricultural Science and Technology A*, *1*(11), 1040-1045.

Negro F, Cremonini C, Zanuttini R, Fringuellino M (2016) Development of framed poplar plywood for acoustic improvement. *Wood Research*, 121-128.

Ohnesorge D, Richter K, Becker G (2010) Influence of wood properties and bonding parameters on bond durability of European Beech (*Fagus sylvatica* L.) glulams. *Annals of Forest Science*, *67*, 601-601.

Öncel M, Vurdu H, Aydoğan H, Özkan O E, Kaymakci A (2019) The tensile shear strength of outdoor type plywood produced from Fir, Alnus, Pine and Poplar wood. *Wood Research*, *64*(5), 913-920.

Osmannezhad S, Faezipour M, Ebrahimi G (2014) Effects of GFRP on bending strength of glulam made of poplar (*Populus deltoides*) and beech (*Fagus orientalis*). *Construction and Building Materials*, *51*, 34-39.

Ozarska B (1999) A review of the utilisation of hardwoods for LVL. *Wood Science and Technology*, *33*(4), 341-351.

Percin O, Altunok M (2017) Some physical and mechanical properties of laminated veneer lumber reinforced with carbon fiber using heat-treated beech veneer. *European Journal of Wood and Wood Products*, *75*, 193-201.

Pot G, Denaud L E, Collet R (2015) Numerical study of the influence of veneer lathe checks on the elastic mechanical properties of laminated veneer lumber (LVL) made of beech. *Holzforschung*, *69*(3), 337-345.

Pramreiter M, Grabner M (2023) The Utilization of European Beech Wood (*Fagus sylvatica* L.) in Europe. *Forests*, *14*(7), 1419.

Pramreiter M, Nenning T, Huber C, Müller U, Kromoser B, Mayencourt P, Konnerth J (2023) A review of the resource efficiency and mechanical performance of commercial wood-based building materials. *Sustainable Materials and Technologies*, e00728, 20pp.

prEN 14080-2 (n.d.) Timber structures - Part 2: Glued laminated timber and glued laminated solid timber made of hardwood - Requirements.

PROPOPULUS. Industrial applications of poplar wood. 2021. European poplar, a local, sustainable, efficient choice. 2023. Available online: https://www.euforgen.org/species/fagus-sylvatica/ (accessed on 20 March 2024).

Purba C Y C, Pot G, Collet R, Chaplain M, Coureau J L (2022) Assessment of bonding durability of CLT and glulam made from oak and mixed poplar-oak according to bonding pressure and glue type. *Construction and Building Materials*, 335, 127345.

Purba C Y C, Pot G, Viguier J, Ruelle J, Denaud L, Fournier M (2018) Mechanical properties of laminated veneer lumber (LVL) made of secondary quality oak and beech: The effect of veneer thickness. *Proceedings of the WCTE*.

Rábai L, Horváth N, Kánnár A, Csiha C (2020) Study on the wettability of Pannónia poplar (*P. x euramericana* Pannónia) from two Hungarian plantations: Győr and Solt. *European Journal of Wood and Wood Products*, *78*, 1057-1060.

Rahayu I, Denaud L, Marchal R, Darmawan W (2015) Ten new poplar cultivars provide laminated veneer lumber for structural application. *Annals of Forest Science*, *72*, 705-715.

Rais A, van de Kuilen J W G, Pretzsch H (2020) Impact of species mixture on the stiffness of European beech (*Fagus sylvatica* L.) sawn timber. *Forest Ecology and Management*, *461*, 117935.

Reinprecht L, Kmeťová L (2014) Fungal resistance and physical–mechanical properties of beech plywood having durable veneers or fungicides in surfaces. *European Journal of Wood and Wood Products*, *72*, 433-443.

Reinprecht L, Kmeťová L, Iždinský J (2012) Fungal decay and bending properties of beech plywood overlaid with tropical veneers. *Journal of Tropical Forest Science*, 490-497.

Rescalvo F J, Duriot R, Pot G, Gallego A, Denaud L (2020) Enhancement of bending properties of Douglas-fir and poplar laminate veneer lumber (LVL) beams with carbon and basalt fibers reinforcement. *Construction and Building Materials, 263*, 120185.

Rescalvo F J, Timbolmas C, Bravo R, Gallego A (2020) Experimental and numerical analysis of mixed I-214 poplar/*Pinus sylvestris* laminated timber subjected to bending loadings. *Materials*, *13*(14), 3134.

Rescalvo F J, Timbolmas C, Bravo R, Valverde-Palacios I, Gallego A (2021) Improving ductility and bending features of poplar glued laminated beams by means of embedded carbon material. *Construction and Building Materials*, *304*, 124469.

Rostampour-Haftkhani A (2020) Effect of reinforcement of the galvanized steel, Aluminum sheet and Glass fiber reinforcement polymer wrapped on flexural behavior of screwed glued laminated timber (glulam) made with poplar. *Forest and Wood Products*, *72*(4), 327-338.

Rostampour-Haftkhani A, Hematabadi H (2022) Effect of layer arrangement on bending strength of cross-laminated timber (CLT) manufactured from poplar (*Populus deltoides* L.). *Buildings*, *12*(5), 608.

Schwarzkopf M, Burnard M, Martinez Pastur G, Monelos L, Kutnar A (2018) Performance of three-layer composites with densified surface layers of *Nothofagus pumilio* and *N. antarctica* from Southern Patagonian forests. *Wood Material Science & Engineering*, *13*(5), 305-315.

Sciomenta M, Bedon C, Fragiacomo M (2024) Experimental and Numerical Column Buckling Analysis of Hardwood Cross-Laminated Timber Panels. *Journal of Structural Engineering*, 150(5), 04024030.

Sciomenta M, Spera L, Bedon C, Rinaldi V, Fragiacomo M, Romagnoli M (2021) Mechanical characterization of novel Homogeneous Beech and hybrid Beech-Corsican Pine thin Cross-Laminated timber panels. *Construction and Building Materials*, *271*, 121589.

Sciomenta M, Spera L, Peditto A, Ciuffetelli E, Savini F, Bedon C, Romagnoli M, Nocetti M, Brunetti M, Fragiacomo M (2022) Mechanical characterization of homogeneous and hybrid beech-Corsican pine glue-laminated timber beams. *Engineering Structures*, *264*, 114450.

Sebera V, Muszyński L, Tippner J, Noyel M, Pisaneschi T, Sundberg B (2015) FE analysis of CLT panel subjected to torsion and verified by DIC. *Materials and Structures*, *48*, 451-459.

Sedighizadeh P, Moradpour P, Hosseinabadi H Z (2023) Possibility of making flexible three-ply plywood using poplar (*Populus deltoides*) and Paulownia (*Paulownia fortunei*) veneers. *European Journal of Wood and Wood Products*, *81*(1), 209-221.

Semple K E, Zhang P K, Smith G D (2015) Hybrid oriented strand boards made from Moso bamboo (*Phyllostachys pubescens* Mazel) and Aspen (*Populus tremuloides* Michx.): species-separated three-layer boards. *European Journal of Wood and Wood Products*, *73*, 527-536.

Shi X, Yue K, Jiao X, Zhang Z, Li Z (2023) Experimental investigation into lateral performance of cross-laminated timber shear walls made from fast-growing poplar wood. *Wood Material Science & Engineering*, 18(4), 1212-1227.

Shukla S R, Kamden D P (2008) Properties of laminated veneer lumber (LVL) made with low density hardwood species: effect of the pressure duration. *European Journal of Wood and Wood Products*, *66*(2), 119-127.

Slabohm M, Brischke C, Militz H (2023) The durability of acetylated beech (*Fagus sylvatica* L.) laminated veneer lumber (LVL) against wood-destroying basidiomycetes. *European Journal of Wood and Wood Products*, 1-11.

Slabohm M, Mai C, Militz H (2022b) Bonding acetylated veneer for engineered wood products - a review. *Materials*, 15(10), 3665.

Slabohm M, Mayer A K, Militz H (2022) Compression of acetylated beech (*Fagus sylvatica* L.) laminated veneer lumber (LVL). *Forests*, *13*(7), 1122.

Smardzewski J, Łabeda K (2018) Mechanical and Hygroscopic Properties of Longitudinally-Laminated Timber (LLT) Panels for the Furniture Industry. *BioResources*, *13*(2), 2871-2886.

Song H, Wang Z, Gong Y, Li L, Zhou J, Gong M (2022) Low-cycle fatigue life and duration-of-load effect for hybrid CLT fabricated from lumber and OSB. *Journal of Building Engineering*, *46*, 103832.

Šrajer J, Král P, Čermák M, Mazal P (2013) Structure evaluation of compressing of spruce and beech plywoods. Part 1: Microscopic structure. *Wood Research*, *58*(1), 101-112.

Stamm A J, Seborg R M (1960) Forest Products Laboratory resin-treated, laminated, compressed wood (compreg). *USDA Forest Products Laboratory report N°1381*, 20pp.

Sun X, Wang C, Liu Y, Ma H, Tang S (2022) Experimental Investigation on Bending Behavior of Innovative Poplar LVL Floor Diaphragms. *Sustainability*, *14*(17), 10481.

Tamjidi A, Faezipour M M, Doosthoseini K, Ebrahimi G, Khademieslam H (2017) Investigation on the properties of oriented strand boards (OSB) made from mixture ten-years-old poplar clones. *Iranian Journal of Wood and Paper Science Research*, *31*(4).

Timbolmas C, Bravo R, Rescalvo F J, Gallego A (2022) Development of an analytical model to predict the bending behavior of composite glulam beams in tension and compression. *Journal of Building Engineering*, *45*, 103471.

Toksoy D, Çolakoğlu G, Aydin I, Çolak S, Demirkir C (2006) Technological and economic comparison of the usage of beech and alder wood in plywood and laminated veneer lumber manufacturing. *Building and Environment*, *41*(7), 872-876.

Töpler J, Buchholz L, Lukas J, Kuhlmann U (2023) Guidelines for a finite element based design of timber structures and their exemplary application on modelling of beech LVL. *Buildings*, *13*(2), 393.

Tran V D, Oudjene M, Méausoone P J, Pizzi A, Gautier M, Roy K (2014) Experimental study of multi-layered beams made of beech timber glued with different adhesives. In *World Conference on Timber Engineering (WCTE),* 10-14.

Trinh H M, Militz H, Mai C (2012) Modification of beech veneers with N-methylol-melamine compounds for the production of plywood. *European Journal of Wood and Wood Products*, *70*(4), 421-432.

Trinh H M, Militz H, Mai C (2012b) Modification of beech veneers with N-methylol melamine compounds for the production of plywood: natural weathering. *European Journal of Wood and Wood Products*, *70*(1), 279-286.

Van Acker J (2019) Towards better integration of wood protection in the forestry wood industry chain - a case study on hybrid poplar. *Proceedings IRG Annual Meeting*, IRG/WP 19-50359.

Van Acker J (2021) Opportunities and challenges for hardwood based engineered wood products. *Proceedings of the 9th Hardwood Proceedings Part II*.

Van Acker J, Defoirdt N, Van den Bulcke J (2016) Enhanced potential of poplar and willow for engineered wood products. In *Proceedings of: 2nd Conference on Engineered Wood Products based on Poplar/Willow Wood,* León, Spain, 187-210.

Van Acker J, Li W, Jiang X, Durimel M, De Ligne L, Parakhonskiy B, Skirtach A, Van den Bulcke J (2023) Combining wood protection options to enhance resistance against decay and improve fire safety of engineered wood products like CLT. In *XVI International Conference on Durability of Building Materials and Components* (DBMC). Eds. K.F. Li and D.P. Fang. 15pp.

Verschuren L, De Mil T, De Frenne P, Haneca K, Van Acker J, Vandekerkhove K, Van den Bulcke J (2023) Heading for a fall: The fate of old wind-thrown beech trees (*Fagus sylvatica*) is detectable in their growth pattern. *Science of the total environment*, 903, 166148.

Viguier J, Marcon B, Girardon S, Denaud L (2017) Effect of forestry management and veneer defects identified by X-ray analysis on mechanical properties of laminated veneer lumber beams made of beech. *BioResources*, *12*(3), 6122-6133.

Wang B J, Dai C (2005) Hot-pressing stress graded aspen veneer for laminated veneer lumber (LVL). *Holzforschung, 59*(1):10-17

Wang B J, Ellis S, Dai C (2006) Veneer surface roughness and compressibility pertaining to plywood/LVL manufacturing. Part II. Optimum panel densification. *Wood and fiber science*, 727-735.

Wang J, Chai Y, Liu J, Zhu J Y (2023) The Viscoelastic and Hygroscopicity Behavior of Delignified and Densified Poplar Wood. *Forests*, *14*(9), 1721.

Wang J, Fishwild S J, Begel M, Zhu J Y (2020) Properties of densified poplar wood through partial delignification with alkali and acid pretreatment. *Journal of Materials Science*, *55*, 14664-14676.

Wang J, Liu J, Li J, Zhu J Y (2021) Characterization of microstructure, chemical, and physical properties of delignified and densified poplar wood. *Materials, 14*(19), 5709.

Wang T, Wang Y, Crocetti R, Wålinder M (2022) In-plane mechanical properties of birch plywood. *Construction and Building Materials*, *340*, 127852.

Wang X, Tu D, Chen C, Zhou Q, Huang H, Zheng Z, Zhu Z (2021b) A thermal modification technique combining bulk densification and heat treatment for poplar wood with low moisture content. *Construction and Building Materials*, *291*, 123395.

Wang Y, Hou Q, Xu T, Qu S, Zhang B (2021) The bending-shear behaviors of steel reinforced fast-growing poplar glulam beams with different shear-span ratios. *Construction and Building Materials*, *300*, 124008.

Wang Z, Fu H, Chui Y H, Gong M (2014) Feasibility of using poplar as cross layer to fabricate cross-laminated timber. In *Proceedings of the World Conference on Timber Engineering (WCTE)*, 5 pp.

Wang Z, Fu H, Gong M, Luo J, Dong W, Wang T, Chui, Y H (2017) Planar shear and bending properties of hybrid CLT fabricated with lumber and LVL. *Construction and Building Materials*, *151*, 172-177.

Wang Z, Gong M, Chui Y H (2015) Mechanical properties of laminated strand lumber and hybrid cross-laminated timber. *Construction and Building Materials*, 101, 622-627.

Wehsener J, Bremer M, Haller P, Fischer S (2023) Bending tests of delignified and densified poplar. *Wood Material Science & Engineering, 18*(1), 42-50.

Wehsener J, Brischke C, Meyer-Veltrup L, Hartig J, Haller P (2018) Physical, mechanical and biological properties of thermo-mechanically densified and thermally modified timber using the Vacu³-process. *European Journal of Wood and Wood Products, 76*, 809-821.

Wei P, Wang B J, Wan X, Chen X (2019) Modeling and prediction of modulus of elasticity of laminated veneer lumber based on laminated plate theory. *Construction and Building Materials*, *196*, 437-442.

Wei P, Wang B J, Zhou D, Dai C, Wang Q, Huang S (2013) Mechanical properties of poplar laminated veneer lumber modified by carbon fiber reinforced polymer. *BioResources*, *8*(4), 4883-4898.

Wei Y, Huang Y, Yu Y, Gao R, Yu W (2018) The surface chemical constituent analysis of poplar fibrosis veneers during heat treatment. *Journal of Wood Science*, *64*, 485-500.

Wei Y, Rao F, Yu Y, Huang Y, Yu W (2019) Fabrication and performance evaluation of a novel laminated veneer lumber (LVL) made from hybrid poplar. *European Journal of Wood and Wood Products*, *77*, 381-391.

Weidman A (2015) Optimizing bonding conditions for cross laminated timber (CLT) panels using low density hybrid poplar. Project submitted to Oregon State University, 59 pp.

Wen J, Xiao Y (2023) The flexural behavior of cross laminated bamboo and timber (CLBT) and cross laminated timber (CLT) beams. *Construction and Building Materials*, *408*, 133739.

Westermayr M, Zeilhofer M, Rais A, Kovryga A, Van de Kuilen J W G (2022) Tensile strength grading of beech (*Fagus sylvatica* L.) lamellas from multiple origins, cross sections and qualities. *Holzforschung*, *76*(5), 397-407.

Widmann R, Beikircher W, Cabo J L, Steiger R (2014) Bending strength and stiffness of glulam beams made of thermally modified beech timber. In *Materials and Joints in Timber Structures: Recent Developments of Technology*. Springer Netherlands, 569-576.

Wilczynski M (2011) Elastic constants of veneer in beech plywood. *Folia Forestalia Polonica. Series B-Drzewnictwo*, *42*.

Wilczyński M, Warmbier K (2012) Elastic moduli of veneers in pine and beech plywood. *Drewno: prace naukowe, doniesienia, komunikaty*, *55*(188), 47-57.

Xiao Z, Li C, Shu B, Tang S, Yang X, Liu Y (2023) Experimental Study of Mode-I and Mode-II Interlaminar Fracture Characteristics of Poplar LVL. *Journal of Renewable Materials*, 11(1), 245-255.

Xu B H, Wang T T, Yu K B, Zhao Y H, Zhang B (2023) Physical and mechanical properties of densified poplar by partial delignification. *Wood Material Science & Engineering, 18*(4), 1285-1290.

Xu F, Zhang H, Wu J (2021) Synergistic catalytic flame retardant effect of zirconium phosphate on the poplar plywood. *Construction and Building Materials*, *290*, 123208.

Yahyaee S M H, Dastoorian F, Ghorbani M, Zabihzadeh S M (2022) Combined effect of organosolv delignification/polymerization on the set recovery of densified poplar wood. *European Journal of Wood and Wood Products*, 1-9.

Yang S M, Lee H H, Kang S G (2021) Research trends in hybrid cross-laminated timber (CLT) to enhance the rolling shear strength of CLT. *Journal of the Korean Wood Science and Technology*, *49*(4), 336-359.

Yang S, Lee H, Choi G, Kang S (2024) Mechanical properties of ply-lam cross-laminated timbers fabricated with lumber and plywood. *European Journal of Wood and Wood Products*, *82*(1), 189-202.

Yang T H, Lin C H, Wang S Y, Lin F C (2012) Effects of ACQ preservative treatment on the mechanical properties of hardwood glulam. *European Journal of Wood and Wood Products*, *70*(5), 557-564.

Yao L H, Wang X M, Fei B H (2012) Study on structural plywood production technology from eucalyptus/poplar. *Advanced Materials Research*, *476*, 1547-1552.

Yin C, Zhang X, Li P, Fu F (2021) Study on Properties of Flame-Retardant Plywood Made with Eucalyptus, Birch and Poplar Wood. In *Journal of Physics: Conference Series* (Vol. 1885, No. 2, p. 022053). IOP Publishing.

Yong C, Guan M J, Zhang Q S (2012) Selected physical and mechanical properties of bamboo and poplar composite OSB with different hybrid ratios. *Key Engineering Materials*, *517*, 87-95.

Yue K, Qian J, Wu P, Jiao X, Lu D, Song X (2023) Experimental analysis of thermally-treated Chinese poplar wood with focus on structural application. *Industrial Crops and Products*, *197*, 116612.

Yue K, Song X, Jiao X, Wang L, Jia C, Chen Z, Liu W (2020) An experimental study on flexural behavior of glulam beams made out of thermally treated fast-growing poplar laminae. *Wood Fiber Sci*, *52*(2), 152-164.

Zanuttini R, Bonzano E, Negro F, Oreglia G L, Cremonini C (2020) Preliminary Assessment of Sweet Chestnut and Mixed Sweet Chestnut-Poplar OSB. *Forests*, *11*(5), 496.

Zanuttini R, Castro G, Cremonini C, Negro F, Palanti S (2019) Thermo-vacuum treatment of poplar (*Populus* spp.) plywood. *Holzforschung*, *74*(1), 60-67.

Zanuttini R, Nicolotti G, Cremonini C (2003) Poplar plywood resistance to wood decay agents: efficacy of some protective treatments in the light of the standard ENV 12038. *Annals of forest science*, *60*(1), 83-89.

Zdravković V, Lovrić A, Džinčić I, Pantović N (2017) Some properties of LVL composed of poplar and beech veneer and possibilities of their application for window frames. *Glasnik Sumarskog fakulteta 115*, 167-184.

Zhou D (1990) A study of oriented structural board made from hybrid poplar. Physical and mechanical properties of OSB. *Holz als Roh-und Werkstoff*, *48*(7-8), 293-296.

Zhou Z R, Zhao M C, Wang Z, Wang B J, Guan X (2013) Acoustic testing and sorting of Chinese poplar logs for structural LVL products. *BioResources*, *8*(3), 4101-4116.

Zhuang B, Cloutier A, Koubaa A (2022) Effects of strands geometry on the physical and mechanical properties of oriented strand boards (OSBs) made from black spruce and trembling aspen. *BioResources*, *17*(3), 3929.

Zhuang B, Cloutier A, Koubaa A (2022b) Physical and mechanical properties of oriented strand board made from eastern Canadian softwood species. *Forests, 13*(4), 523.

Zoralioglu T. (2003) Some statistical information concerning poplar wood production in Turkey. In *First International Conference on The Future of Poplar Culture*, Italy, 4pp.

Zsuffa L, Sennerby-Forsse L, Weisgerber H, Hall R B (1993) Strategies for clonal forestry with poplars, aspens, and willows. In *Clonal Forestry II: conservation and application* (pp. 91-119). Berlin, Heidelberg: Springer Berlin Heidelberg.

WOOD DATABASE. Available online: https:// www.wood-database.com (accessed on 20 March 2024). Data from Wood Handbook: Kretschmann D E (2010) Mechanical properties of wood (chapter 5). *Wood Handbook - Wood as an Engineering Material (Centennial Edition). General Technical Report FPL-GTR-190.* USDA's Forest Products Laboratory, 46pp.

The situation in the hardwood sector in Europe

Maria Kiefer-Polz[1,2*], Rainer Handl[3]

[1] EHP European-Hardwood Production GmbH, Gleinzer Straße 1, 8523 Frauental, Austria
[2] EOS- European Organisation of the Sawmill Industry, Rue Montoyer 24/box 20, BE-1000 Brussels
[3] Association of the Austrian Wood Industries, Schwarzenbergplatz 4, 1030 Vienna, Austria

E-mail: Maria.kiefer-polz@ehp.at, Handl@holzindustrie.at

Keywords: hardwood industry, Europe

ABSTRACT

Hardwoods are prized for their aesthetic and functional properties. The growing stock of the main hardwoods across Europe has been growing over the last few decades – by about 25/30% in 2020 vs 2000 - and projections show that it will keep growing, particularly oak. This does not mean that the industry will have more raw materials available. For that, the right policies and decisions have to be set. And over the last few years we have mixed signals. Securing raw materials at affordable prices is indeed one of the key issues for hardwood sawmills in Europe. Over the last few years due essentially to climate change-related factors the hardwood sector has noticed that in some instance the quality of logs, especially for beech and ash, has been declining. The oak sector instead is hampered by constantly high logs exports to China which deprive European hardwood sawmillers of precious raw materials. This is regrettable as Europe loses precious raw materials without adding value. The situation somewhat improved in 2023 due to the weak economy in China but the issue remains. It has been calculated that in France only in 2022 slightly over a quarter of harvested oak logs has been exported to China. Also, logs prices remain consistently high. At the same time, as hinted above European policies are also a factor that shape supply of logs for sawmills. While we welcome the fact that many policies seem to acknowledge the decisive contribution that wood makes in countering climate change, we regret that following European legislation some members states are increasingly setting aside forests, particularly public-owned forests, to meet their decarbonization targets. The targets in the opinion of the industry would be better met if we keep using forests in a sustainable way. Also, the increasing legislative burden on forest owners might discourage some of them to getting wood out of the forests and provide wood to the industry.

On the demand side, sales prices for sawnwood instead are quite subdued. This squeezes the margins of many hardwood sawmillers across Europe: high logs prices, low sawnwood prices, high costs for personnel, energy etc. While the situation is probably not as bad as it was feared a few months ago, demand for sawnwood in Asia and in the Middle East and North Africa areas is quite slow. The current weakness of American hardwood sawmillers is providing an opportunity for European sawmillers particularly in the MENA area. Overall, demand overseas seems to be slightly more resilient than demand in Europe with the furniture sector and the parquet industry especially in a bad shape. Looking at the future with a bit more optimism there is hope that in H2 2024 markets will improve, but we are confronted with a high margin of uncertainty, not least geopolitical uncertainty. Few people expected for instance the kind of disruption that we are seeing in the Red Sea over the last few months and all the related logistic challenges.

You can find enclosed to these few lines some figures on the production, consumption and exports of the sector collected by EOS, the European Organization of the Sawmill Industry of which we are members. Croatia is not a member of EOS but was also included in the figures because of its importance as a producer in the hardwood sector. Estimations for 2024 will be available in a few months.

Having a longer-term overview, the change in the forests composition across Europe provides an opportunity for the hardwood sawmillers, but the whole sector, together with policymakers and the wider society needs to be making an effort. Research and funds are needed to:

- Find uses and markets for as of today underutilized hardwood species
- Scale up added value hardwood products, by creating standards, markets

We need to be working all together – industry, researchers, policymakers, society at large – to make sure the sector fulfils its undoubted potential.

Session I
Silvicultural aspects and forest management of hardwoods

Monitoring xylogenesis esis as tool to assess the impact of different management treatments on wood formation: A study case on *Vitis vinifera*

Angela Balzano[1*], Maks Merela[1], Meta Pivk[1], Luka Krže[1], Veronica De Micco[2]

[1] Department of Wood Science and Technology, Biotechnical Faculty, University of Ljubljana, Ljubljana, Slovenia.
[2] Department of Agricultural Sciences, University of Naples Federico II, via Università 100, 80055, Portici, Naples, Italy

E-mail: angela.balzano@bf.uni-lj.si

Keywords: cambial activity, wood production, plant management, grapevine, drought, plasticity, climate change.

ABSTRACT

In the Mediterranean region, prolonged droughts have a significant impact on the vitality of vegetation, the stages of growth, and the intricate processes involved in the formation and ripening of grapes. It is widely recognized that changes in ecological factors and cultivation practices can significantly affect vine physiology. The dynamic field of xylogenesis provides the exclusive lens through which these phenomena can be closely observed and studied.

Viticulture is adaptive, both in regions with established irrigation systems and in those that rely solely on natural rainwater. However, the cultivation and maintenance of non-irrigated vineyards, particularly for *Vitis vinifera* L., are of current and significant importance to agricultural management.

In vineyards, microclimatic variations and management techniques can strongly influence xylem traits, leading to variations in grapevine water use efficiency. To reliably assess how wood functional traits correlate with inter- and intra-annual environmental variability and cultivation management, it is important to determine the precise timing of wood ring formation through xylogenesis analysis.

The objective of this study is to examine the effects of soil management on wood production and plasticity of grapevine through monitoring xylogenesis. For this purpose, the experimental plot was divided into three sections where three different soil management methods were applied: grassed, natural and worked and microcores (Figure 1) were collected from grapevine stems biweekly.
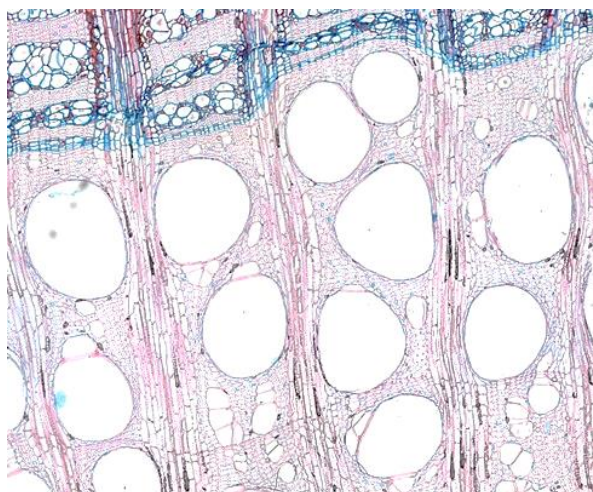
Figure 1: Thin section of microcore of Vitis vinifera; cross section

Data analysis revealed that different soil management practices have a discernible impact on the timing of wood formation in grapevines, highlighting the plant's remarkable adaptability to soil water availability. The results can help improving grapevine productivity, resource use efficiency and resilience for the sustainable management of vineyards.

The History of Forests - Climate Periods of the Middle Ages and Forestry

Emese Berzsenyi[1*], Dóra Hegyesi[2], Rita Kattein-Pornói[1], Dávid Kazai[3]

[1] Budapest University of Technology and Economics, Faculty of Economic and Social Sciences, Department of Technical Education. Magyar Tudósok Blvd. 2, Budapest, Hungary, 1117.
[2] Eötvös Loránd University, Faculty of Science, PhD School of Earth Sciences. Egyetem Pl. 1-3, Budapest, Hungary, 1053.
[3] Óbuda University, Rejtő Sándor Faculty of Light Industry and Environmental Protection Engineering, Institute of Environmental Engineering and Natural Sciences. Doberdó str. 6, Budapest, Hungary, 1034.

E-mail: berzsenyi.emese@gtk.bme.hu; hegyesi.dora@ttk.elte.hu; kattein-pornoi.rita@gtk.bme.hu; kazai.david@uni-obuda.hu

Keywords: Middle Ages, Forestery, Climate Periods, Woodworking History

ABSTRACT

The topic of climate change is of utmost importance in contemporary discussions, yet it rarely receives attention within historical research. To gain a comprehensive understanding of the culture and worldview of the three distinct historical phases of the Middle Ages – the early, developed, and declining Middle Ages – it is crucial to explore the history of forests. We must investigate the significance of forests and trees in the context of socio-cultural history and attempt to answer the following questions: What role did forests and trees play in the technological development of Europe from the 5th to the 15th century?

How did the relationship between humans and forests evolve during this millennium?

Internationally, efforts to understand the changes in past and present societal phenomena through interdisciplinary approaches, examining various external factors affecting human societies, have been in place since the mid-20th century. Researchers have started linking archaeology with explanations for uncertainties in radiocarbon dating caused by climate, geological, oceanographic, and other phenomena (C. Renfrew, 2006). Connections have been made between major famines, climatic changes, and volcanic eruptions (E. Le Roy Ladurie, 1971). *Ernst Schubert*'s 2019 work, "*Alltag im Mittelalter*," specifically examines the Middle Ages focusing on forests, water, and environmental awareness. *Wolfgang Behringer*'s 2007 publication, "*A Cultural History of Climate*," also assigns great significance to forests and forestry. This article draws on the works of these two authors and *Hansjörg Küster*'s "*Geschichte des Waldes: von der Urzeit bis zur Gegenwart*" (2013) to provide holistic answers to the questions mentioned above, applying content analysis and comparative methods. The article also benefits from *Bernhard Muigg* and *Willy Tegel*'s article "*Forest History - New Perspectives for an Old Discipline*" (2021) published in the journal "Frontiers in Ecology and Evolution" and in Hungarian, *Szabó Péter*'s study titled "*Erdőgazdálkodás s középkorban*" (2006).

This study is part of a larger research project aiming to present the history of disability in the Middle Ages in Hungarian language, based on English and German literature. The definition of disability varies across eras and cultures, depending on individual living conditions, social circumstances, technological advancements of that era, and the influence of religious teachings. Forests and trees have accompanied Europe throughout this millennium, offering a precise representation of the three major climate periods and technological development. Technically, everything was made of wood: houses, storage facilities, transportation, machinery, furniture, and even heating. While around 650 AD, early medieval Europe with its population of approximately 18 million was predominantly covered by impenetrable forests, by 1300 AD, during the flourishing Middle Ages with its population of 74 million, there were significantly fewer continuous forests left, compared to the present day.

The assessment of disabled individuals as productive force is crucial from a societal utility perspective. Therefore, our research on the history of disability in the Middle Ages must thoroughly explore the era's most vital resources and their technical possibilities.

INTRODUCTION

"By the time a tree's canopy can cast a shadow over your dwelling, it will be your sons or grandsons who reside within." (Schubert, 2019, p. 63)

In the 9th century, Europe's population began to grow gradually. As the climate warmed, famines ceased, and a sustained social upswing began. By around 1300, the continent's population had doubled, necessitating significant changes in both the conceptualization of and care for the environment. This change is symbolically represented by the transition from the small, dark, thick-walled Romanesque churches of the early Middle Ages, which barely let in light through their tiny windows, to the inability to accommodate believers. The new style, Gothic architecture, emerged in the first half of the 12th century. Its vast windows allowed the sunshine of the late Medieval warm climate period to illuminate the world, bringing light into existence. (Behringer, 2017, pp. 107-108) The construction of these monumental cathedrals required innovations: not just ladders and simple hand tools, but also massive scaffolding, formworks, counterweight and wheel lift systems, storage facilities, and transportation means. Thus, it was about overcoming previously unreachable heights, moving heavy weights, and covering large distances. This new architecture had to rediscover and invent everything anew, but only traditional materials were available, primarily stone and wood. (Aradi, 1967, p. 30) Europe gradually reached a level of cultural development that could be compared with other great civilizations. (Behringer, 2017, p. 108)

THE FOREST AND THE SURROUNDING WORLD

In this study, we focus on the history of the forest, as it reveals the specific circumstances of medieval Europe in its confrontation with nature. Nature has been subjected to continuous transformation and change over millennia due to climate change, animal migration, the expansion of flora, and human interventions. (Küster, 2001, p. 10)

Between the 5th and 10th centuries, the almost continuous forests of early medieval Europe were indeed deep and dark. After the spring leaf-out, only a little light reached the undergrowth, despite evidence from charters that thinning of the forests had begun in some areas as early as the Iron Age. Forest management and the presence of forests are an integral part of European cultural heritage. Numerous written records from the 1st century have been preserved, dealing with the processes of forest management in the Roman Empire (Agnoletti et al 2022). The primeval forest, which so impressed the Romans, was only touched on its edges by human settlements in the early Middle Ages. These small "cultural islands" could only develop in the wilderness on fields not interwoven with the massive roots of trees. It was not artificial boundaries, but forests that separated people from each other, who feared the endless and dark wilderness, the world of forests, marshes, and bogs, which was called "terra inculta," as opposed to the cultivated lands, "terra culta." (Schubert, 2019, p. 38)

When researching the historical Middle Ages, which roughly spans from the 4th to the 16th century, varying by era and culture, known as "media tempestas," our sources might not only be the imperial borders but also by the examination of the relationship between wood and people. With the tools of the time, it was only through incredibly hard work that the landscape could be altered to such an extent that the managed forests, which we read about in the documents of the late Middle Ages, could emerge from the wilderness of the early Middle Ages, and which the communities – cities, bishoprics, large estates – had to take care of preserving during the decline of the 14th and 15th centuries.

The physical environment is part of identity, which aligns with contemporary nature-centric thinking because it can retain its complex meaning over long periods of time and means the same thing to everyone within a community or culture. It represents the world that surrounds people, the familiar landscape, plants, trees, objects, as well as the warmth of the family hearth, and they are symbols of permanence. (Tomory, 2014) Forests are highly valued for numerous reasons: they are economically beneficial, provide habitats, preserve the ecological balance of an area, influence the landscape character, and are part of cultural heritage. This is especially true in Central Europe, where forests have always played a significant economic role and are considered a social value. In these regions, forests are primarily cherished not for their economic utility but for their role in forming rural identity (Elands et al., 2004).

Drawing parallels between the eras of the Middle Ages, the changes in climatic periods, the history of forests, and approximate demographic data yields significant insights:

Early Middle Ages: 476-950
- The cold climatic period with unequal territorial distribution, known as the Early Medieval Pessimum, can be dated roughly between 350-900.
- Until around 1000, Europe's forest cover was dense and in a natural state, with many uninhabited areas.
- By this time, the total population reached 35-38 million.

High Middle Ages: 950-1340
- The High Medieval Optimum, lasting from around 800/900 to 1300, brought significant warming.
- Around 1300, there was a peak in the need for wood due to the growing population, urban development, and technical progress, leading to extensive deforestation.
- The population, nearly doubled to about 74 million, was characterized by relative prosperity and an increased level of demand.

Late Middle Ages: 1340-1492
- The onset of the Little Ice Age in the early 1300s brought uneven but noticeable cooling, along with devastating plagues and famine.
- By the 14th-15th century, excessive use of wood had further reduced the area of Europe's forests compared to today.
- The population fell back to 50-52 million.

(Behringer, 2017, p. 108; Schubert, 2019, p. 36)

THE FOREST AND MAN

Europe's almost impenetrable early medieval forests were changing under the influence of warming climate, merely waiting for grazing to thin out the undergrowth and for diligent human hands to make them habitable. (Borst, 2004, p. 150) At first glance, the forest may indeed seem hostile and frightening, but human life could not exist without it. For millennia, wood was the primary raw material and source of energy. Buildings, tools, storage facilities, and both water and land transport vehicles were made of wood. Cooking and heating were done with wood. Even when working with any other material, wood was needed; it heated the furnaces for smelting metals, the workshops of blacksmiths, potters used wood to fire clay, and glass was melted in wood-fired kilns. (Küstler, 2001, p. 16; Schubert, 2019, p. 38)

However, forests were not only necessary for timber; they played a significant role in feeding the population, but it was not hunting that made the forest indispensable for survival—that was merely an amusement for the lords—but rather livestock farming. For centuries, pannage, the practice of releasing pigs into the forest to feed on acorns, formed the basis of pig breeding; pigs were driven into the forest, and when winter came, they were slaughtered to provide food. (Küstler, 2017, p. 15; 2001, p. 16)
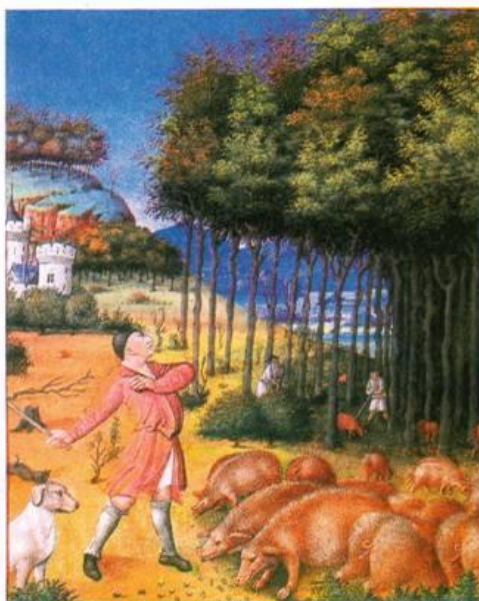
***Figure 1: Pannage (In: Rabb P. Natural conditions in the medieval Carpathian Basin.
http://arch.et.bme.hu/arch_old/korabbi_folyam/17/17rabb.html)***

In the world of the poor, there were no separate pigsties or stables. In severe cold, people shared their house or hut with their animals, which represented their wealth and supported their livelihood, or the wealthier built the animals' lodgings adjacent to their living quarters. (Schubert, 2019, p. 38; Le Roy Ladurie, 1997, pp. 50-71)

THE PRESENCE OF FORESTS AND THE QUALITY OF HARVEST

The presence of forests was closely linked to the quality of harvests, partly because the ecosystem of the forests provided organic matter to the surrounding arable and cultivated lands. Their role in local climate regulation and wind protection reduced soil erosion. Additionally, the food sources provided by the forest could offer an essential safety net in times of poor harvests; medicinal herbs and berries, which supplemented their otherwise monotonous and impoverished diet, were gathered here (Borah & Sunderland 2021).

It would be impossible to list all the forms of forest usage of the time: when necessary, foliage was carried from the forest to the fields, but pine resin was also the source of tar, the universal insulating material and adhesive of the Middle Ages.

Beekeeping could not exist without the hollow trees of the forest, from which bee wax blocks were extracted in early spring to make church candles. These couldn't use the usual smelly tallow candles or pine shavings. Rope was made from peeled bark. For a long time, honey was the only sweetener, but in the early Middle Ages, before the spread of European viticulture, honey was also the base ingredient for mead. Without forests, there is neither intoxication nor culture.

The copyist monks in scriptoriums knew all too well what they owed to the forest, as ink was made not only from soot but also from two types of oak galls. Later, charcoal burners and lime burners also worked in the forest, using specific trees for their indispensable work.

Where forest usage was so diverse and complex, the question arises: what really is a forest? For people before the 12th century, there was no independent forest as a perceivable landscape feature. There was the visible world: meadows, human settlements, rivers, and then there was "terra inculta", where a persistent squirrel could have travelled from the Black Sea to the Atlantic Ocean without ever having to descend from the treetops to the ground. (Schubert, 2019, pp. 41-42) Ernst Schubert in his book "Everyday Life in the Middle Ages" states, "the people of the early Middle Ages could not see the forest for the trees." (Schubert, 2019, p. 41)

Planned environmental intervention and territorial development also emerged and became widespread in European history during the High Middle Ages.

THE FOREST, WOOD, AND MAN

Let's briefly return to the era of cathedrals and the industrial development that began with it. Until approximately the beginning of the 13th century, deforestation made wood material virtually unlimited in supply. The construction of church roofs also required a mass of thick tree trunks. These strong oak or pine trunks were often brought from afar, and the roofs were mostly covered with wooden shingles. Where they switched to tile roofing due to fire hazard, at least as much wood was used to fire the clay. A large amount of valuable and useful timber was incorporated into the construction because scaffolding, claddings, interior design elements, and furniture still consumed a lot of wood. Indeed, the construction of a cathedral required various types of wood material and vast forests. Transportation was significantly facilitated if the city was located near a river. Logs were floated from the Alps to Venice and from the Black Forest to Holland for special constructions and shipbuilding. Log driving was a profession in its own right. As a method of transporting logwood, it had been used by humanity for a long time, but it was the demand and supply possibilities of the High Middle Ages that first created its "industrial" scale. (Küster, 2017, p. 16) A few hundred years later, in the Late Middle Ages, a good and well-documented example is the construction of Munich's "Frauenkirche," which required approximately 20,000 tree trunks, that is, an average of 1,000 per year, to be floated down the Isar River between 1468 and 1488. (Schubert, 2019, p. 54)

Two key aspects must be considered: the quantity and type of wood material, and the quality and efficiency of processing. For a long time, both wood and human labor were almost unlimitedly available. However, as the cities developed and the supply of wood slowly began to decrease, the value placed on human labor also gradually increased, coinciding with the rise of civic consciousness. Until then, work was simply perceived as a part of life, an indispensable natural basis of the believer's life. (Weber, 1995, pp. 79 and 116) It was not until the 14th century that sawmills appeared; before then, wood material – including planks – was carved and smoothed with axes. Although the saw was invented in the Bronze Age and used by the Romans as a framed tool with an iron blade, the axe, and the adze remained the fundamental tools of medieval forestry and carpentry. Especially since wood was necessary for charcoal supply, used in the smithery workshops from 1000 BCE (Muigg & Tegel 2021). The sawmill was an innovation and revolutionary invention of the advanced medieval blacksmithing industry. It introduced precision, speed, and along with it, a huge demand for "work wood" pre-sized to measurement. Additionally, sawmills operated with much less material loss, indicating a path towards more efficient and material-saving processing. (Schubert, 2019, p. 55)

While the spread of iron tools increased productivity and made work more efficient and accurate, it significantly devastated the forest. A significant improvement in iron ore processing occurred in the middle of the 13th century when open furnaces were replaced with closed smithies. The demand for wood was enormous: producing 1 ton of raw iron required 4 tons of ore and about 8 tons of charcoal (approximately 30 tons / 100m³ of wood). The forests were full of charcoal burners' heaps, but in 40 days, a single charcoal burning site could clear the trees within a 1-kilometer radius. These heaps burned for 8-12 days and could produce 80-250m³ of charcoal per heap. (Schubert, 2019, p. 59)

Salt storage as a method of meat preservation exists since the antiquity. Salt storage has been one of the fundamental methods for preserving meat since ancient times. For this purpose, each household needed at least a barrel's worth (minimum 100kg) of salt. Salt is essential for human survival and can be found in nature in various forms, but its two most basic forms are dissolved salt in water and rock salt. The former is obtained through distillation, and the latter through mining. Without the forests of Central Europe, the production of vital salt would not have been possible in the late Middle Ages. The heating of the then-common large iron pans, often more than 200 m² in size, required a huge demand for energy. It was not until the end of the 16th century that types of salt distillation works appeared that reduced the demand for fuel. (Schubert, 2019, p. 58)

MAN, AND THE FOREST

From the 13th century onward, the unstoppable development and widespread adoption of technology and industry posed increasingly urgent environmental challenges to a significant part of late medieval Europe within 100-150 years, albeit with varying levels of responsibility.

Just as it is impossible to precisely calculate how long the Earth's oil reserves will last today, people back then could not determine how long their timber supplies would last. Fearing a shortage of wood, many cities mandated their residents to plant trees, and eventually, the establishment of entire forests began. The first famous example of this was Peter Stromer of Nuremberg, who planted a pine forest in 1368. Nuremberg is mentioned in almost all literature on the subject because the city council early on recognized the importance of forest management and implemented exemplary measures. The imperial forests in front of the city gates were consistently protected from exploitation by the earliest forest management decree of 1294. (Küster, 2017, p. 16; Schubert, 2019, p. 60) In his study "Forestry in the Middle Ages," Péter Szabó notes that a significant portion of deciduous trees can sprout again from the cut stump even after multiple cuttings, while conifers do not possess this regenerative ability. (Szabó, 2006, pp. 85-86) Both he and Hansjörg Küster explain in detail the different types of forests and their use in the Middle Ages. Such are the coppice forests, which in appearance hardly differ from shrublands or thickets. From these, firewood and timber for melting and burning were taken at intervals of a few years. According to Küster, these could later evolve into middle forests, while Szabó distinguishes between coppice forests and thickets, citing that these were marked accordingly on contemporary maps for their permanence. In the middle or common forests, a few trunks, especially oaks, were allowed to grow tall and their canopies to expand. These later served as building materials and, during their life, for pannage. The rest of the trees in the common forest continued to meet the demand for firewood. The most valuable were the forests suitable for hunting, with few undergrowths and tall trunks. His research confirms that Hungarian forestry management fit well into the traditional European forestry model handed down to us. (Szabó, 2006, p. 100; Küster, 2017, pp. 15-16)

In the late Middle Ages, the common man was more concerned about securing firewood than about daily bread. For many craftsmen such as blacksmiths, brewers, bakers, and candlemakers, a regular supply of firewood or charcoal was essential. An average household consumed 4-6 m³ of firewood annually, even though in the aristocratic world, only a few rooms were heated during winter. Yet, every meal was cooked with it, and even if we cannot speak of outstanding hygiene conditions, water for washing and bathing was also heated this way. Since the 15th century, many places have restricted firewood demand, striving to preserve useful timber as much as possible. For example, only fallen trees left by wind and snowstorms, underbrush, surplus coppice shoots, and brushwood, i.e., dry, fallen branches, could be used for this purpose. The latter was mostly collected by children and poor women. Even in areas where they tried to meet the demand by cyclically clearing the undergrowth or pruning hornbeams and willows, the quality of firewood was inferior. The fire burning in medieval stoves was not as cozy as in today's fireplaces; the heated rooms had an unpleasant smell, which the wealthier tried to mitigate with spices, especially the favoured thyme. (Schubert, 2019, p. 56)

There's no doubt that the technological advancements of the Middle Ages came at the expense of trees. Although the already endangered timber stock around 1400 was made up of two-thirds deciduous trees and only one-third coniferous trees – the opposite of today's ratios – and monocultures were not yet prevalent, it was still greatly at risk. This process also reveals the interrelation between forestry and water management. The thinning of wooded areas and the clearing of different types of forests, among other things, changed the soil's water balance, groundwater levels, river floodplains, sedimentation, and accelerated soil erosion. (Schubert, 2019, p. 59)

Even the pioneer of the development of technology and science, the most famous polyhistor of his time, Leonardo da Vinci (1452-1519), could not detach himself from wood. His inventions, although containing iron components, were fundamentally made of wood, including designs for a propeller, flying machines, and water lifting devices, as well as a bicycle. (Friedenthal, 1975)

CONCLUSIONS – MAN AND WOOD

The existence, construction, maintenance, and assurance of industrial and artisanal production of a medieval city fundamentally depended on wood, that is, on the forest. Resources derived from the forest enabled not only constructions, restorations, expansions, and the direct or indirect production of goods but also met essential needs in many other areas of life. They were as important in purifying the air as they were in mitigating the forces of winds and storms or for any other reasons described previously for the world of humans. The relationship between the forest and urban development highlights that urbanization and economic growth could not have occurred without considering the forests and their sustainable use. Issues of forest scarcity and overexploitation were already present in the late Middle Ages, drawing attention to the importance of handling environmental resources and the need to promote sustainability for future generations. (Schubert, 2019, p. 55) While brown coal was known, for a very long time before the modern extraction of coal and petroleum, wood was the only energy source. (Küster, 2001, p. 16)

Observing late medieval or early modern European cityscapes, it is apparent that there are scarcely any trees in the pictures, and the spaces around the cities are empty or agricultural lands.

Figure 2: City view of Munich in the Schedel's World Chronicle of 1493 (Bavarian State Library, public domain In: https://stadtflaneurin.de/muenchen-markt-und-handel-im-mittelalter/)

This does not seem to catch the attention of historians, nor do they seek the reason for it. However, if examined with a different focus, interesting and important details unfold before us, such as the history of the forest. Wood, which for millennia was humanity's most important – or perhaps only – raw material, resource, and essentially, the element of sustenance. This wood is provided by the forest, a system of slow rhythm, complexity, and precision that cannot be replicated once it has been eradicated. We know that forest restoration after human intervention is a very lengthy process, if at all possible, because anthropogenic traces from 1000 years ago can still be found today in some forested areas of France, both in physical artifacts and in changes to the fauna (Bergès & Dupouey, 2020).

REFERENCES

Agnoletti M, Piras F, Venturi M, Santoro A (2022) Cultural values and forest dynamics: The Italian forests in the last 150 years. Forest Ecology and Management, *503*, 119655. https://doi.org/10.1016/j.foreco.2021.119655

Aradi N (1967) A katedrálistól az ipari forradalomig. Kossuth Kiadó, Budapest, Hungary

Behringer W (2017) A klíma kultúrtörténete. A jégkorszaktól a globális felmelegedésig. Corvina Kiadó, Budapest, Hungary ISBN 978-963-13-6430-9

Bergès L, Dupouey J (2020) Historical ecology and ancient forests: Progress, conservation issues and scientific prospects, with some examples from the French case. Journal of Vegetation Science, 32 (1). https://doi.org/10.1111/jvs.12846

Borst A (2004) Lebensformen im Mittelalter. Nikol Verlagsgesellschaft, Hamburg, Germany ISBN 3-933203-84-2

Borah J R, Sunderland T (2021) How do forests and trees sustain agriculture?. Open Access Government. https://www.openaccessgovernment.org/how-do-forests-and-trees-sustain-agriculture/119178/

Friedenthal R (1975) Leonardo. Gondolat Kiadó, Budapest, Hungary ISBN 963-280-297-7

Elands BHM, O'Leary TN, Boerwinkel HWJ, Freerk Wiersum K (2004) Forests as a mirror of rural conditions; local views on the role of Forests across Europe. *Forest Policy and Economics*, *6*(5), 469–482. https://doi.org/10.1016/j.forpol.2004.01.003

Küster H (2001) Auch der Wald hat seine Geschichte. In: Der deutsche Wald. Der Bürger im Saat 2001. 51/1. Landeszentrale für politische Bildung Baden-Württemberg, Germany pp.10-16. https://www.buergerundstaat.de/1_01/wald02.htm

Küster H (2013) Geschichte des Waldes: von der Urzeit bis zur Gegenwart. C. H. Beck, München, Germany ISBN 978-3406650659

Küster H (2017) Kleine Mitteleuropäische Wald- und Forstgeschichte. In: Wald. Aus Politik und Zeitgeschichte 2017. 67/49-50. Zeitschrift der Bundeszentrale für politische Bildung. Germany pp.12-18. https://www.bpb.de/shop/zeitschriften/apuz/260676/kleine-mitteleuropaeische-wald-und-forstgeschichte/

Le Roy Ladurie E (1971) Times of feast, times of famine: a history of climate since the year 1000. Doubleday and Campany Inc., Garden City - New York, USA ISBN 978-0374521226

Le Roy Ladurie E (1997) Montaillou, egy okszitán falu életrajza (1294-1324). Osiris Kiadó, Budapest, Hungary ISBN 963-379-132-4

Muigg B, Tegel W (2021) Forest history – new perspectives for an old discipline. *Frontiers in Ecology and Evolution*, *9*. https://doi.org/10.3389/fevo.2021.724775

Renfrew C (2006) A civilizáció előtt – A radiokarbon forradalom és Európa őstörténete. Osiris Kiadó, Budapest, Hungary ISBN 963-389-695-9

Schubert E (2019) Alltag im Mittelalter. WBG Theiss, Darmstadt, Germany ISBN 978-38062-3912-6

Szabó P (2006) Erdőgazdálkodás a középkorban. In: Gyöngyössy M (eds) Magyar középkori gazdaság és pénztörténet pp.81-103. Bölcsész konzorcium HEFOP Iroda, Budapest, Hungary https://gepeskonyv.btk.elte.hu/adatok/Tortenelem/83K%E1lnoki/GY%D6NGY%D6SSY%20K%D6NYV/05%20SZABO.pdf

Tomory I (2014) "Mawe Matatu" - Three Stones, or Warmth of the Family Stove: Enculturation in East-Africa. In: Láczay M, Fatula D (eds) Social Aspects of Management: Personal Development, cultural changes, economic progress Krakow, AFM Publishing House, pp. 103-115. Society for Education, Krakow, Poland https://www.researchgate.net/publication/297236789_Mave_Matau_-_Three_stones_or_Warm_of_the_Family_Stove_Enculturation_and_Social_Roles_in_East-Africa

Climate change mitigation aspects of increasing industrial wood assortments of hardwood species in Hungary

Éva Király[1*], Zoltán Börcsök[2], Attila Borovics[1]

[1] Forest Research Institute, University of Sopron, Várkerület 30/A Sárvár, Hungary, 9600.
[2] Faculty of Wood Engineering and Creative Industries, University of Sopron, Bajcsy-Zsilinszky E. Street 4 Sopron, Hungary, 9400

E-mail: kiraly.eva.ilona@uni-sopron.hu; borcsök.zoltan@uni-sopron.hu; borovics.attila@uni-sopron.hu

Keywords: HWP, CO_2, carbon storage, circular economy, sustainability, forest industry

ABSTRACT
The use of timber can foster climate change mitigation through long-term carbon storage, and through substitution of fossil products and fossil fuels. Inclusion of drought tolerant hardwood species in the production of high-quality long-lived wood products gains an increasing importance with the ongoing climate change. In our study we assessed the climate change mitigation potential of increasing industrial wood assortments of hardwood species in Hungary. For the estimation we used the harvested wood product module of the Forest Industry Carbon Model (FICM-HWP) which is based on the methodological guidance of the Intergovernmental Panel on Climate Change (IPCC). The model combines the IPCC wood product model and the IPCC waste model. Both models are used in the Hungarian Greenhouse Gas Inventory as well. The FICM-HWP model is a substantially newly developed version of the two IPCC models as it is supplemented with a waste-route selection and a recycling module. It also contains a product and energy substitution tool to evaluate the magnitude of avoided emissions through substitution effects. The model is able to estimate carbon storage of wood products, end-of-life emissions and avoided emissions, thus, contributing to informed decision making and circular economy goals. In this study we assumed increased industrial wood assortments from hardwood species, increased product half-lives and upscaled recycling. This way we could estimate the climate change mitigation aspects of a developed and intensified Hungarian wood industry which relies on hardwood species and generates long-term carbon storage, at the same time enabling emission reductions in other sectors through product substitution. According to our results increasing the industrial processing of currently underutilized hardwood species can lead to a six times higher carbon sequestration by 2050 as compared to the Business as Usual (BAU) level. While increasing product lifetime and improving waste management together with increasing industrial hardwood assortments leads to an eleven times higher carbon sequestration in the HWP pool as compared to the BAU level.

INTRODUCTION
The Paris Agreement and the European Green Deal relies on the forestry and timber sector, collectively referred to as the forest industry to achieve climate neutrality by 2050 (Verkerk et al. 2022, IPCC 2022, Borovics and Király 2022). The forest-based sector can contribute to climate change mitigation efforts through four methods: on-site carbon storage in forests, off-site carbon storage in long-lived wood products, material substitution of emission-intensive products, and energy substitution of fossil fuels (Verkerk et al. 2022, Borovics 2022). These four climate mitigation pathways define conflicting objectives of timber usage. Increasing wood harvests reduces the amount of carbon sequestered and stored in forests, at least for decades, resulting in a trade-off between carbon sequestration in forests and carbon storage in harvested wood products (HWPs) and substitution (Helin et al. 2013). To design the most suitable climate mitigation strategy for a region or country, it is crucial to evaluate the outcomes of various harvesting and wood processing scenarios and quantify the climate benefits of HWP carbon storage, as well as that of product and energy substitution. Carbon storage and greenhouse gas (GHG) emissions from the HWP pool of a country can be modelled using different tools and approaches (Brunet-Navarro et al. 2016, 2018, Király et al. 2023). The WoodCarbonMonitor model (Rüter 2016) is based on IPCC (2006, 2013) methodology, CO2FIX (Schelhaas et al. 2004), LANDCARB (Krankina

et al. 2012), and CAPSIS (Fortin et al. 2012) models also handle recycling in wood product emission modelling. The HWP-RIAL model (Király et al. 2022, 2023a,b) was created in the frame of the ForestLab project (Borovics 2022) and later it was merged with the DAS forest model (Kottek 2023, Kottek et al. 2023) to create a complex carbon accounting tool, the Forest Industry Carbon Model (Borovics et al. 2024). The HWP module of the Forest Industry Carbon Model (FICM-HWP) combines IPCC methodology for HWP emission estimation (IPCC 2006, 2019) with the IPCC Waste model (IPCC 2006) and it is also supplemented with a recycling and waste routing module and a product and energy substitution module (Király et al. 2024).

Amidst the ongoing climate change, forests encounter escalating risks of disturbance (Verkerk et al. 2022). Modelling the distribution of tree species reveals that in the forthcoming decades, nearly all major European tree species will see reductions in their suitable areas, particularly in eastern and southern Europe (Verkerk et al. 2022). These processes underline the crucial need for innovation in the wood industry, as the utilization of drought-tolerant species for industrial purposes appears inevitable in the future. Many doubts and uncertainties accompany the resource potential of hardwoods and their potential to substitute softwoods in material applications (Auer and Rauch 2020). Recently, there has been a renewed interest in heat treatment processes due to the diminishing production of high-quality timber and the growing demand for sustainable building materials (Boonstra 2008, Esteves and Pereira 2009). Numerous studies investigate methods to enhance the wood technological properties of drought-tolerant tree species, highlighting the necessity to provide additional information on the characteristics and performance of species with less industrial use and lower durability timber (Esteves and Pereira 2009, Todaro 2012). Encouraging outcomes have been reported regarding the potential enhancement of Turkey oak (*Quercus cerris*) wood properties through hydrothermal treatment, opening new possibilities for industrial applications (Todaro et al. 2012, 2013, Cetera et al. 2016). In addition to innovative hardwood products, technological advancements can also enhance wood processing efficiency, minimize waste generation (Li et al. 2022), and promote recycling (Wilson 2010, Király et al. 2023).

The aim of this study was to estimate the impact of increasing industrial utilization of hardwood species in Hungary using the FICM-HWP module. We also intended to assess the impact of possible wood industry innovations on the Hungarian HWP carbon balance.

MATERILAS AND METHODS

In order to calculate the carbon storage and emissions from the Hungarian HWP pool we used the FICM-HWP module (Király et al. 2022, 2023a,b, 2024) which is based on IPCC (2006, 2019) methodology and also handles recycling of HWPs and product and energy substitution (Figure 1).
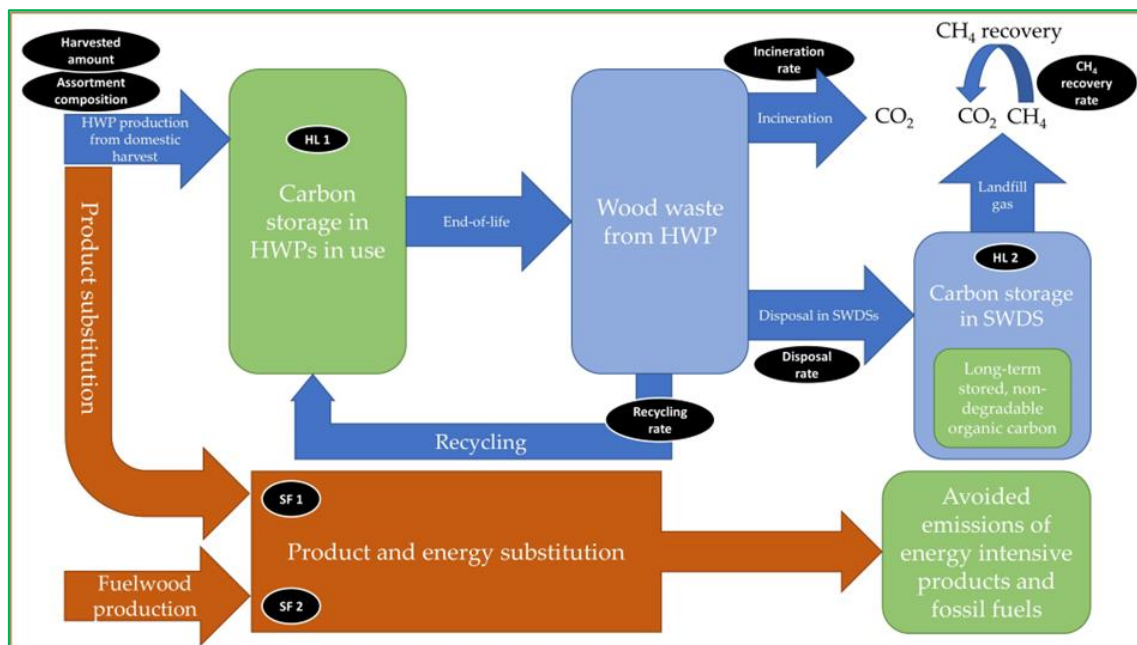
Figure 1: Flowchart of the FICM-HWP module. HL1 and HL2: half-life, SF1 and SF2: substitution factors, SWDS: solid waste disposal site. (Source: Király et al. 2024)

As input data we used the Business as Usual (BAU) harvest projection of Borovics et al. (2024) also modelled with the FICM. In this study we modelled three scenarios. In the BAU scenario the assortment composition and the wood product half-life and recycling parameters were all unchanged. In the second scenario we assumed that industrial wood assortments of hardwood species are increased, and all other parameters remain unchanged. In the third scenario we assumed that apart from increasing industrial wood assortment of hardwood species also significant wood industry innovation is carried out. This meant that half-lives of wood products, recycling, and methane-recovery on landfills were increased. In this scenario the parameters of the FICM-HWP module were set as described in Király et al. (2024). The used wood assortment data is described below (Table 1).

Table 1: BAU (2017-2021 average) and increased industrial wood assortments

	Oaks	Turkey oak	Beech	Hornbeam	Black locust	Other hard broadleaved	Hybrid poplars	Indigenous poplars	Willows	Other soft broadleaved	Pines
BAU											
Sawlog	25%	2%	23%	2%	10%	10%	55%	38%	11%	20%	26%
Pulpwood for boards	6%	4%	16%	10%	10%	8%	31%	23%	54%	14%	39%
Pulpwood for paper	0%	1%	1%	0%	0%	0%	5%	20%	2%	1%	21%
Firewood	69%	93%	59%	88%	80%	82%	8%	18%	33%	65%	14%
Increased industrial wood assortments from hardwood species											
Sawlog	50%	40%	40%	20%	40%	30%	55%	38%	11%	20%	26%
Pulpwood for boards	20%	20%	30%	30%	10%	30%	31%	23%	54%	14%	39%
Pulpwood for paper	5%	5%	5%	5%	0%	5%	5%	20%	2%	1%	21%
Firewood	25%	35%	25%	45%	50%	35%	8%	18%	33%	65%	14%

RESULTS AND DISCUSSION

According to our results the carbon stored in HWPs in use is slightly increasing under the BAU scenario, and it reaches 15,700 kt C by 2050. In the scenario characterised by increased industrial hardwood assortments the carbon stock of the HWP pool is projected to reach 27,100 kt C, while assuming increased industrial wood assortments and improved half-lives and waste management results in an increased carbon storage reaching 34,000 kt C by 2050 (Figure 2).
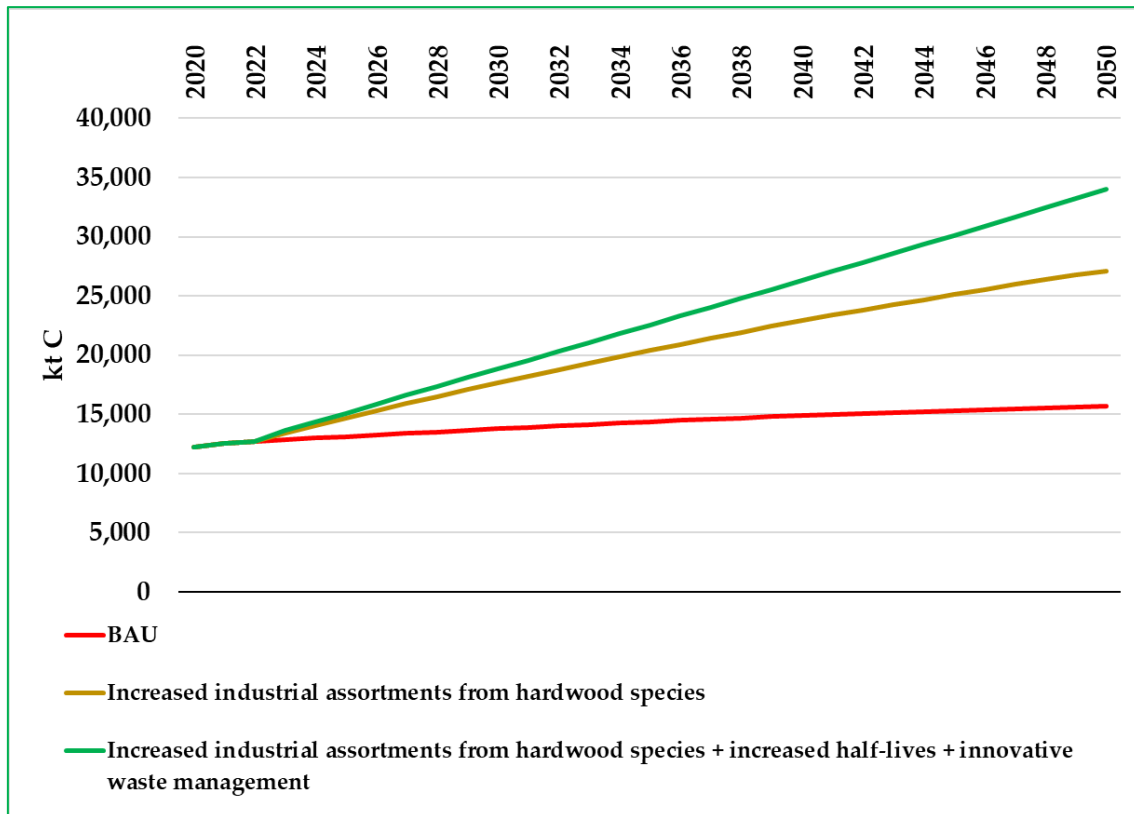
Figure 2: Carbon stored in HWPs in use under the three modelled scenarios

The modelling of the HWP net removals highlight that increasing the industrial processing of currently underutilized hardwood species can lead to a six times higher carbon sequestration by 2050 as compared to the BAU level. While increasing product lifetime, recycling, and methane recovery in landfills together with increasing industrial hardwood assortments leads to an 11 times higher carbon sequestration as compared to the BAU level (Figure 3). According to our results the more long-lived high quality HWPs are produced the better the carbon balance will be.

Product and energy substitution effects in Hungary are in the same order of magnitude as the net carbon removals of Hungarian forests (NIR 2023, Király et al. 2024). Thus, adding product and energy substitution effects to the modelling increases the net climate benefits of timber utilization up to -9,500 kt CO_2 eq in the scenario characterised with improved wood assortments, product lifetime, and waste management (Figure 4).
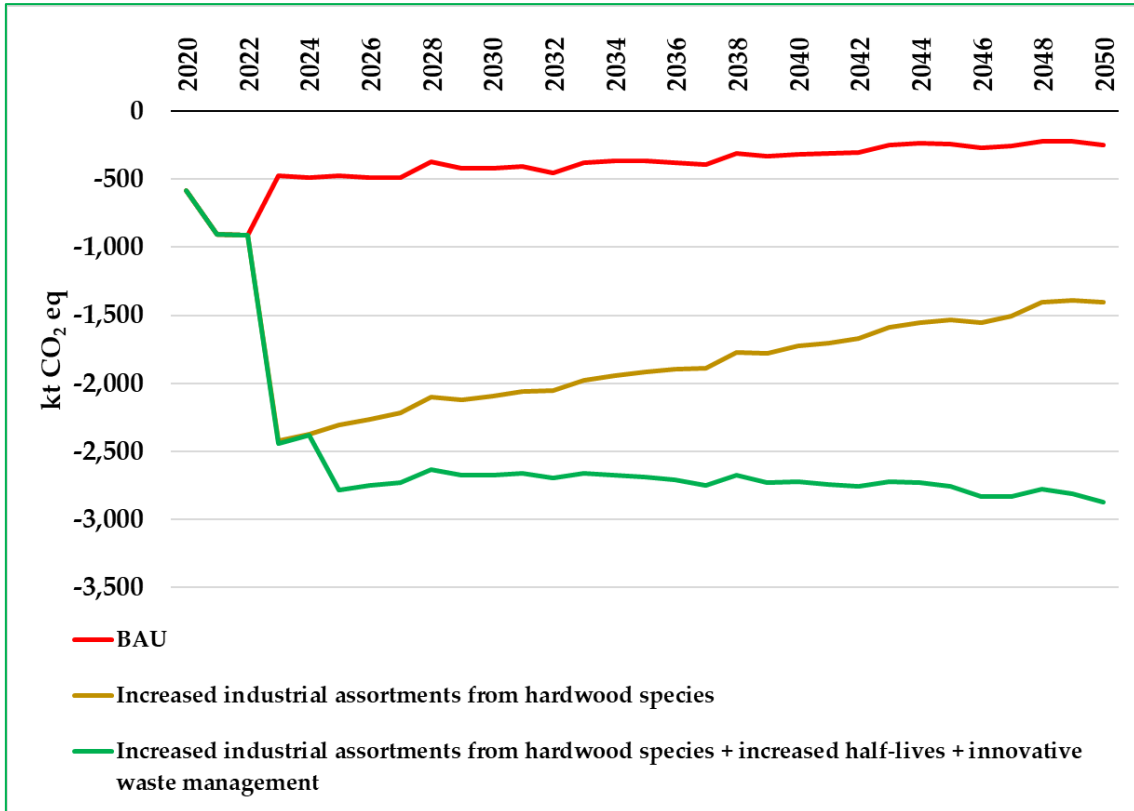
Figure 3: Projected net carbon dioxide removals of the HWP pool under the three modelled scenarios. (Negative numbers indicate carbon dioxide removals, while positive numbers indicate emissions in line with IPCC conventions)
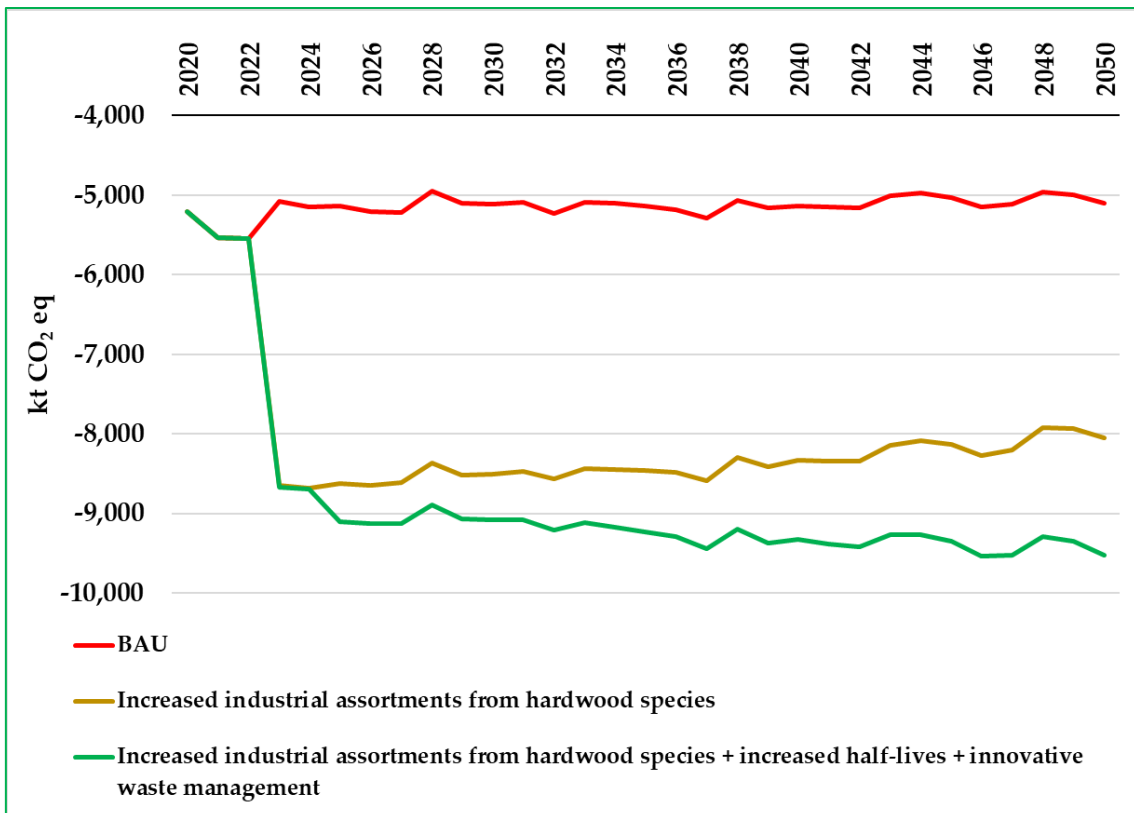
Figure 4: Projected net carbon dioxide removals of the HWP pool plus product and energy substitution effects under the three modelled scenarios. (Negative numbers indicate carbon dioxide removals, while positive numbers indicate emissions in line with IPCC conventions)

CONCLUSIONS

According to our results the increased industrial processing of hardwood species can significantly improve the HWP carbon balance of Hungary. While the modelled product and energy substitution effects are in the same order of magnitude as the annual carbon sequestration of Hungarian forests. This suggests that the Hungarian wood industry possesses significant climate change mitigation potential through well-designed measures, even without an increase in harvest rates. Consequently, it can play a crucial role in achieving the climate goals set for 2050.

ACKNOWLEDGEMENTS

REFERENCES

Auer V, Rauch P (2020) Assessing hardwood flows from resource to production through Material Flow Analysis. 9th Hardwood Proceedings, Vol 9 - pt I: An Underutilized Resource: Hardwood Oriented Research. Nemeth, R.; Rademacher, P.; Hansmann, C.; Bak, M.; Bader, M. eds. p. 13-20.

Boonstra M (2008) A two-stage thermal modification of wood. Ph.D. Thesis in Applied Biological Sciences: Soil and Forest management. Henry Poincaré University-Nancy, France.

Borovics A (2022) ErdőLab: a Soproni Egyetem erdészeti és faipari projektje: Fókuszban az éghajlatváltozás mérséklése (ErdőLab: forestry and wood industry project of the University of Sopron: Focus on mitigating climate change). Erdészeti Lapok 157: 4 pp. 114–115.

Borovics A, Király É (2022) Az erdőgazdálkodás szerepe a klímavédelemben az IPCC értékelő jelentése szerint. Erdészeti Lapok 157: 7-8 pp. 265-268., 4 p.

Borovics A, Király É, Kottek P (2024) Projection of the carbon balance of the Hungarian forestry and wood industry sector using the Forest Industry Carbon Model. Forests. (In press)

Brunet-Navarro P, Jochheim H, Kroiher F, Muys B (2018) Effect of cascade use on the carbon balance of the German and European wood sectors. Journal of Cleaner Production. 170, 137-146.

Brunet-Navarro P, Jochheim H, Muys B (2016) Modelling carbon stocks and fluxes in the wood product sector: a comparative review. Global Change Biology. 22, 2555-2569.

Cetera P, Todaro L, Lovaglio T, Moretti N, Rita A (2016) Steaming treatment decreases MOE and compression strength of Turkey oak wood. Wood Research Volume 61, Issue 2, 2016, Pages 255-264. ISSN: 13364561.

Esteves MB, Pereira HM (2009) Wood modification by heat treatment: a review. Bioresource Technology 4, 1, 370–404. https://doi.org/10.15376/biores.4.1.370-404

Fortin M, Ningre F, Robert N, Mothe F (2012) Quantifying the impact of forest management on the carbon balance of the forest-wood product chain: A case study applied to even-aged oak stands in France. Forest Ecology and Management 279, 176–188. https://doi.org/10.1016/j.foreco.2012.05.031

Helin T, Sokka L, Soimakallio S, Pingoud K, Pajula T (2013) Approaches for inclusion of forest carbon cycle in life cycle assessment–a review. GCB Bioenergy 5(5):475–486.

IPCC (2006) 2006 IPCC Guidelines for National Greenhouse Gas Inventories, Prepared by the National Greenhouse Gas Inventories Programme; Eggleston, H.S., Buendia, L., Miwa, K., Ngara, T., Tanabe, K., Eds.; IGES: Kanagawa, Japan, 2006.

IPCC (2019) 2019 Refinement to the 2006 IPCC Guidelines for National Greenhouse Gas Inventories; Calvo Buendia, E., Tanabe, K., Kranjc, A., Baasansuren, J., Fukuda, M., Ngarize, S., Osako, A., Pyrozhenko, Y., Shermanau, P., Federici, S., Eds.; IPCC: Geneva, Switzerland, 2019.

IPCC (2022) Sixth Assessment Report, Climate Change 2022: Mitigation of Climate Change, the Working Group III Contribution. Chapter 7 Agriculture, Forestry, and Other Land Uses (AFOLU); IPCC: Geneva, Switzerland, 2022.

IPCC (2013) Revised supplementary methods and good practice guidance arising from the Kyoto protocol. Hiraishi, T., Krug, T., Tanabe, K., Srivastava, N., Baasansuren, J., Fukuda, M. and Troxler, T.G. (eds). Pp. 268.

Király É, Börcsök Z, Kocsis Z, Németh G, Polgár A, Borovics A (2022) Carbon sequestration in harvested wood products in Hungary an estimation based on the IPCC 2019 refinement. Forests. 13(11):1809.

Király É, Börcsök Z, Kocsis Z, Németh G, Polgár A, Borovics A (2023b) A new model for predicting carbon storage dynamics and emissions related to the waste management of wood products: introduction of the HWP-RIAL model. Acta Agraria Debreceniensis, 1, 75-81.

Király É, Kis-Kovács G, Börcsök Z, Kocsis Z, Németh G, Polgár A, Borovics A (2023a) Modelling carbon storage dynamics of wood products with the HWP-RIAL model—projection of particleboard end-of-life emissions under different climate mitigation measures. Sustainability 15(7):6322.

Király É, Börcsök Z, Kocsis Z, Németh G, Polgár A, Borovics A (2024) Climate change mitigation through carbon storage and product substitution in the Hungarian wood industry. Wood Research. (In print.)

Kottek P (2023) Hosszútávú erdőállomány prognózisok. 142 p. Roth Gyula Erdészeti és Vadgazdálkodási Tudományok Doktori Iskola, Soproni Egyetem. Thesis.

Kottek P, Király É, Mertl T, Borovics A (2023) The Re-parametrization of the DAS Model Based on 2016-2021 Data of the National Forestry Database: New Results on Cutting Age Distributions. Acta Silvatica & Lignaria Hungarica, 19(2), 61–74. https://doi.org/10.37045/aslh-2023-0005

Krankina ON, Harmon ME, Schnekenburger F, Sierra CA (2012) Carbon balance on federal forest lands of Western Oregon and Washington: The impact of the Northwest forest plan. Forest Ecology and Management 286, 171–182. https://doi.org/10.1016/j.foreco.2012.08.028

Li L, Wei XY, Zhao JH, Hayes D, Daigneault A, Weiskittel A, Kizha AR, 'Neill SRO (2022) Technological advancement expands carbon storage in harvested wood products in Maine, USA. Biomass and Bioenergy. 161. N. 106457. https://doi.org/10.1016/j.biombioe.2022.106457

NIR (2023) National Inventory Report for 1985–2021. Hungary. Chapter: Land-Use, Land-Use Change and Forestry; Somogyi, Z., Tobisch, T., Király É., Hungarian Meteorological Service: Budapest, Hungary, 486 p.

Rüter S (2016) Der Beitrag der stofflichen Nutzung von Holz zum Klimaschutz; Das Modell WoodCarbonMonitor. Technische Universität München, Wissenschaftszentrum Weihenstephan für Ernährung, Landnutzung und Umwelt Holzforschung München, Lehrstuhl für Holzwissenschaft. München, 270 p.

Schelhaas MJ, Esch PW, Groen TA, Jong BHJ, Kanninen M, Liski J, Masera O, Mohren GMJ, Nabuurs GJ, Palosuo T, Pedroni L, Vallejo A, Vilen T (2004) CO2FIX V 3.1-A modelling framework for quantifying carbon sequestration in forest ecosystems. In: Alterra. ALTERRA, Wageningen, Netherlands, 122 p.

Todaro L, Dichicco P, Moretti N, D'Auria M (2013) Effect of combined steam and heat treatments on extractives and lignin in sapwood and heartwood of Turkey oak (Quercus cerris L.) wood. BioResources 8, 2, 1718-1730. https://doi.org/10.15376/biores.8.2.1718-1730

Todaro L, Zanuttini R, Scopa A, Moretti N (2012) Influence of combined hydrothermal treatments on selected properties of Turkey oak (Quercus cerris L.) wood. Wood Science and Technology 46, 1. 563-578. https://doi.org/10.1007/s00226-011-0430-2

Todaro L (2012) Effect of steaming treatment on resistance to footprints in Turkey oak wood for flooring. European Journal of Wood and Wood Products 70, 1-3, 209-214. https://doi.org/10.1007/s00107-011-0542-2

Verkerk PJ, Delacote P, Hurmekoski E, Kunttu J, Matthews R, Mäkipää R, Mosley F, Perugini L, Reyer CPO, Roe S, Trømborg E (2022) Forest-Based Climate Change Mitigation and Adaptation in Europe. From Science to Policy 14. European Forest Institute: Joensuu, Finland, ISBN 978-952-7426-22-7. https://doi.org/10.36333/fs14

Wilson J (2010) Life-cycle inventory of particleboard in terms of resources, emissions, energy and carbon. Wood and Fiber Science, 42 (CORRIM Special Issue), 90–106. file:///C:/Users/%C3%89va/Downloads/1349-Article%20Text-1349-1-10-20141206.pdf (accessed on 12 February 2023)

Uncovering genetic structures of natural Turkey oak populations to help develop effective climate change strategies for forestry

Botond B. Lados[1*], László Nagy[1], Attila Benke[1], Csilla É. Molnár[1], Zoltán A. Köbölkuti[1,2], Attila Borovics[1], Klára Cseke[1]

[1] University of Sopron, Forest Research Institute, Department of Forestry Breeding, Várkerület 30/A, Sárvár, Hungary, 9600
[2] Bavarian Office for Forest Genetics (AWG), Department of Applied Forest Genetics Research, Forstamtsplatz 1, Teisendorf, Germany, 83317

E-mail: lados.botond@uni-sopron.hu; nagy.laszlo@uni-sopron.hu; benke.attila@uni-sopron.hu; molnar.csilla.eva@uni-sopron.hu; zoltan.koeboelkuti@awg.bayern.de; borovics.attila@uni-sopron.hu; cseke.klara@uni-sopron.hu

Keywords: *Quercus cerris* L., ddRAD-seq, SNP, Balkan Peninsula, population genetics, reference mapping, cork oak

ABSTRACT

Turkey oak (*Quercus cerris* L.) is a widespread species of the genus *Quercus* section *Cerris*, distributed from central and southeast Europe to Asia Minor. The species has long been known for its enormous phenotypic-genotypic variability and extreme adaptability. Throughout its vast distribution range, Turkey oak occupies countless ecological niches with very different site conditions. According to the last projections, climate change is putting high pressure on the natural forest tree populations to adapt to the rapidly changing conditions. Due to their high variability and adaptability, oaks have great potential in forestry climate adaptation efforts. This is particularly true for the Turkey oak. According to recent results of climate-based modelling of species' future distribution, Turkey oak could be a winner of climate change in Central Europe, significantly increasing its distribution and abundance. As a result, its importance in forestry and the wood industry could significantly increase in the future. However, for effective adaptation strategies, it is necessary to collect detailed information on the ecological characteristics of the species, drought adaptation strategies, genic diversity and genetic structure of wild populations throughout its range. Furthermore, as this species has previously played only a marginal role in the wood industry, its growing importance would require more detailed information on its wood properties and alternative uses for its wood. In this study, we used our recently published reference-mapped genome-wide SNP dataset to investigate the genetic diversity and population structure of eight natural Turkey oak populations from Hungary and the Balkan Peninsula. Based on the diversity indices, we found that the studied population carried a relatively high amount of genetic diversity. According to various clustering approaches (fastStructure, PCA and DAPC), the studied populations were divided into four genetically distinct groups, corresponding to two Balkan, one Hungarian and one ambiguous group. The genetic isolation of these groups was found to be statistically significant and further validated by Barrier analysis, which revealed significant gene flow barriers between clusters. According to our results, Balkan populations appear to be genetically more diverse and structured, and therefore, wild populations of this biogeographical region are promising for further studies of the species' adaptation to climate change. In addition, the genetic consistency of the Hungarian populations may indicate common refugial origin. On the other hand, the outlier ambiguous group formed by one Hungarian population is probably a legacy of a historical long-distance human-assisted movement of reproductive material. In conclusion for practice, may be an important question for future studies whether strong genetic structuring of Turkey oak populations is also manifested at the phenotypic level, for instance in different stem quality and/or wood properties of genetic groups.

INTRODUCTION

Changing environmental conditions is both challenging for the forestry and wood industry sectors. For forestry, more extreme site conditions, new pests and diseases are increasing the risk of mortality in forest stands. As part of the natural adaptation of forest tree species and active forestry adaptation efforts, the composition of species in natural and planted stands could change in the future (Bolte et al. 2009). Based on climate projections for the central European region, especially for the Carpathian basin, dramatic changes are expected in site conditions and as a consequence in the species composition of natural forest stands (Buras and Menzel 2019). Thus not only the wood quality is expected to decrease, but the species of primary input material for the wood industry could also change. Accordingly, forests' economic returns may decrease both for forestry and the wood industry (Hanewinkel et al. 2013).

According to the results of climate projections, whereas some tree species are expected to decrease its distribution and abundance, a few species are expected winners of climate change in the Central European region, such as Turkey oak (*Quercus cerris* L.), pubescent oak (*Quercus pubescens* Willd.). or silver linden (*Tilia tomentosa* Moench) (Thurm et al. 2018). However, these are mainly species which had formerly only a secondary role in the wood industry or were not processed at all. Currently, it is an urgent question both in forestry and wood industry how these species are inserted into the applied technologies.

As a member of high-potential alternative forest tree species, Turkey oak may significantly increase its role in forestry in the future. Due to its relatively high drought tolerance and masting not as hectic as white oaks, Turkey oak may be a promising alternative option for forestry. Throughout its vast distribution range, from the Italian and Balkan peninsulas to Asia Minor, the species occurs in a wide variety of habitats, demonstrating its strong ecological plasticity. According to the most recent results of population genetic studies, Turkey oak carries a relatively high genetic variability and has a strong genetic structure through the distribution range (Özer 2014; Bagnoli et al. 2016). On the one hand, this high genetic diversity could be the basis of efficient adaptation but also meant that distinct populations throughout the range could have differing phenotypic behaviour as well (eg. growth, drought tolerance or wood properties).

Although it was previously processed almost exclusively for firewood, it is already the most widespread oak species in Hungary (occupying more than 200 000 ha) and may increase its area in the coming decades (Illés and Móricz 2022). Thus its wood may be available in higher and higher quantity in the future.

In our current study, we examined the genetic diversity and genetic structures in eight natural Turkey oak populations from the Balkans and the Carpathian basin. For population genetic analyses we used our recently published dataset, which is the first high-resolution genomic dataset available for this species generated by double digest restriction site-associated DNA sequencing (ddRAD-seq).

Based on the thousands of genome-wide single nucleotide polymorphisms (SNP) we found strong genetic structures among Hungarian and Balkan populations. Among Hungarian populations (except one outlier stand) we did not find any genetic structuring which may refer to their common refugial origin. Amongst the Balkan stands we found a significant genetic barrier which divides the stands into two genetic groups, which refers to different refugial origins of stands. According to our findings, the strong genetic structures and relatively high genetic diversity of this species are promising for further studies to examine the genetic background of drought adaptation and wood properties.

MATERIALS AND METHODS

For our population genetic analyses, we used our recently published dataset (Lados et al. 2024), which comprises the genomic SNP data of 88 Turkey oak individuals from eight Hungarian and Balkan populations (five from Hungary, two from Bulgaria and one from Kosovo). The dataset was generated by a reduced representation method ddRAD-seq, which allows for an effective sampling of the whole nuclear genome, obtaining thousands of genome-wide single nucleotide polymorphisms (SNP). Our published dataset consists of both *de novo* and reference-mapped SNPs. Reference mapping was carried out by using the cork oak (*Quercus suber* L.) genome (Ramos et al. 2018), as this species is the closest relative of Turkey oak which has a reference genome available. In the course of our current study we used the reference mapped SNP data (containing 26 059 genome-wide SNPs) for population genetic computations.

For basic population genetic analysis, we used the "adegenet" (Jombart and Ahmed 2011), "pegas" (Paradis 2010), "hierfstat" (Goudet and Jombart 2022) and "poppr" (Kamvar et al. 2014) packages in the statistical software R (R Core Team 2022). First, because only preliminary filtering was carried out on the raw dataset, to obtain reliable population genetic inference, we applied careful filtering by using the "missingno" function of the "poppr" package, removing any loci with missing data more than 5% and then genotypes with more than 5%. After that, we also filtered out those loci that are significantly out of Hardy-Weinberg equilibrium (HWE; $p<0.05$) using the "hw.test" function with 1000 bootstrap resampling in the package "pegas" to estimate HWE for every locus. Finally, 18 584 loci were discarded as contained missing values greater than 5%, three genotypes had more than 5% missingness (QCER-HU2-9, QCER-KO1-10, QCER-KO1-2) and 1110 loci were significantly out of HWE. After filtering, 6359 loci were kept for further analysis.

To compute basic population genetic indices we used the "basic.stat" and "allelic.richness" functions in the package hierfstat and "private_alleles" functions in "poppr". The per loci values were averaged or summed (for private alleles) over populations.

During the investigation of population structure, we applied different statistical approaches. The Bayesian clustering program fastStructure was implemented with 100 cross-validation. In addition, we also used principal component analysis (PCA) implemented in "ade4", the discriminant analysis of principal components (DAPC) implemented in "adegenet", and the analyses of molecular variance (AMOVA) also implemented in "adegenet" to further validate the results of fastStructure. Significance testing in AMOVA was carried out by using "randtest" function in "ade4" with 999 repetitions.

Finally, we also examined the existing geneflow barriers among populations under study, using Barrier v2.2 program (Taberlet et al. 1998). To obtain bootstrap values for the barriers, we implemented a custom R code to generate 1000 bootstrap F_{st} matrices. Each matrix was generated by using the "dist.genepop" function in "adegenet" to compute pairwise F_{st} between populations.

RESULTS AND DISCUSSION
Results
Based on the population genetic indices computed, the eight populations under study show relatively small differences in diversity, excluding the HU1 population (Table 1). Although the number of sampled individuals changes over populations which not favour comparisons, heterozygosity values show an interval from 0.222 to 0.250 across populations, with a gentle excess of homozygotes suggested by the positive values of the inbreeding coefficient (except BU1 and HU1 populations with negative values). In addition, the slightly higher values of the allelic richness suggest a higher number of alleles per locus in Hungarian populations than in Balkan ones.

As for the exceptions, in the case of the number of private alleles, there is an outlier among the studied populations, the HU1. Only this Hungarian population from Zselickisfalud carries private alleles, 18 in number. Another exception is that the HU1 and BU1 populations have an excess of heterozygosity based on the negative values of the inbreeding coefficient.

Table 1: Population genetic indices of the examined populations (where Pop=populations ID, n=number of sampled individuals, H_o=observed heterozygosity, H_s=gene diversity, N_p=number of private alleles, A_r=allelic richness, F_{is}=inbreeding coefficient, CI=95% confidence interval for mean F_{is})

Pop	n	H_o	H_s	N_p	A_r	F_{is}	CI	
BU1	10	0.229	0.225	0	1.676	-0.012	-0.025	-0.005
BU2	10	0.228	0.235	0	1.730	0.023	0.023	0.043
KO1	8	0.224	0.230	0	1.712	0.019	0.018	0.039
HU1	12	0.250	0.238	18	1.718	-0.034	-0.062	-0.044
HU2	12	0.230	0.238	0	1.735	0.021	0.024	0.042
HU3	8	0.235	0.239	0	1.739	0.006	0.007	0.027
HU4	12	0.236	0.240	0	1.745	0.012	0.010	0.028
HU5	13	0.236	0.241	0	1.745	0.019	0.015	0.030

The result of the analyses of principal components shows significant structuring of populations (Figure 1). The first principal component accounts for 3.87%, the second for 2.85% of the total variance, dividing the eight studied populations into four genetic clusters. As for the four clusters, five individuals of BU1 built their own group separating from the two other Balkan populations. BU2 and KO1 build a second Balkan group, and HU2, HU3, HU4, and HU5 build a consistent Hungarian group together with three individuals of HU1. Finally, nine individuals of the HU1 population build a fourth strongly differentiating group. As the separation of BU1 from the other Balkan populations is mainly along the second principal component but HU1 separating from the Hungarian populations mainly along the first principal component, it seems the differentiation of HU1 is more pronounced than BU1.
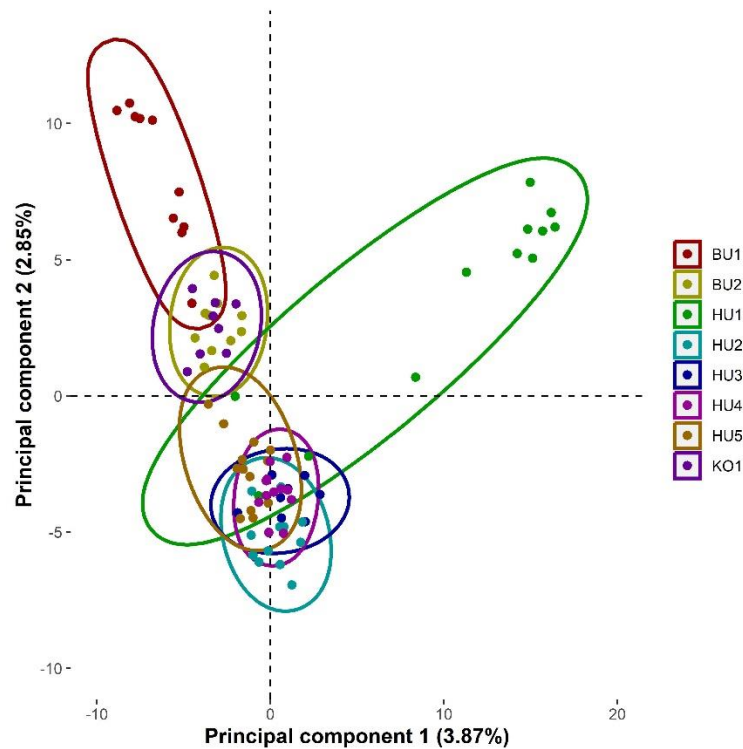
Figure 1: Principal component analyses for the 85 individuals of the eight populations

In another approach, the Bayesian clustering program fastStructure suggests only three genetic clusters (Figure 2a). However, based on the admixture pattern that appears in the BU2 and KO1 populations, these are considerable as a slightly separating group from BU1. With this consideration, similar to the results of the principal component analyses, we identified four genetically consistent groups. The first group is composed of the individuals of BU1, the second comprises BU2 and KO1, the third is all the Hungarian ones except HU1 and the fourth is a strongly separating group composed of HU1 alone.

To support the results of the latter analyses, we also carried out the discriminant analyses of the principal components (DAPC). As Figure 2b shows, it suggests a similar population structure to the latter analyses with a more pronounced separation of BU1 from the group of BU2 and KO1 populations.

The results of AMOVA (Table 2) confirm significant population and cluster level differentiation, both the clusters built by fastStructure and DAPC. Cluster level variation accounts for 2.97% of the total variance for fastStructure and 3.60% for DAPC.
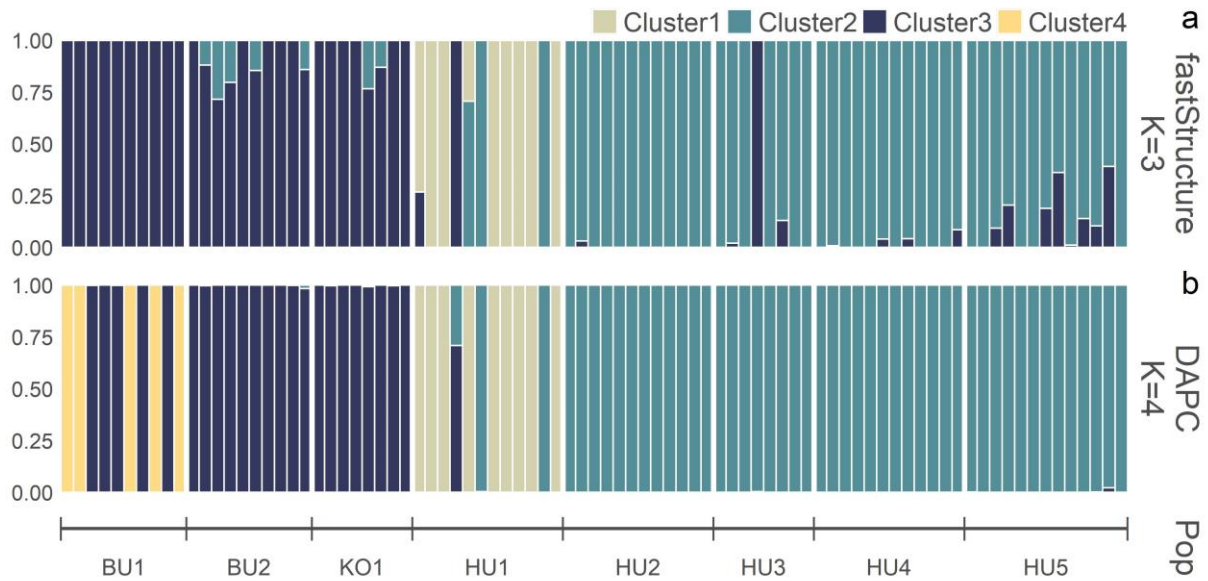
Figure 2: Results of clustering by fastStructure (a) and DAPC (b) (each bar on the plots corresponds to the probability of ancestry of a given individual)

In the final analyses, we examined the existing gene flow barriers among populations with the program Barrier. As a result, we found three significant barriers. Going from east to west, the first barrier divides Balkan populations into two groups separating BU1 from the others. The second barrier is between the Hungarian and Balkan populations, and the third separates HU1 from all the other populations.

Table 2: Analyses of molecular variance (where df=degree of freedom, SS=sum of squares, MS=mean squares, Sigma= variance, %=percentage of the total variance, Φ =phi statistics, *=significant p value on 0.05 significance level)

Source of variation	df	SS	MS	Sigma	%	Φ	p
Clustering with fastStructure							
Between clusters	2	8335.11	4167.55	46.41	2.97	0.0297	0.001*
Between populations within clusters	8	14908.88	1863.61	25.45	1.63	0.0168	0.001*
Between samples within population	74	110988.00	1499.84	7.37	0.47	0.0049	0.399
Total	169	260465.00	1541.21	1564.33	100.00		
Clustering with DAPC							
Between clusters	3	11392.84	3797.62	56.41	3.60	0.0360	0.001*
Between populations within clusters	7	13020.82	1860.12	25.36	1.62	0.0168	0.001*
Between samples within population	74	109818.30	1484.03	-0.53	-0.03	-0.0004	0.527
Total	169	260465.00	1541.21	1566.33	100.00		

Discussion

The genetic system of Turkey oak is characterized by a long lifespan, wind pollination, large, mainly gravity-distributed acorns and mass occurrence throughout its vast range. Accordingly, population genetic statistics suggest a relatively high-level extent of diversity (see observed heterozygosity), low level of inbreeding, and large effective population size (eg. clustering methods were unable to separate Hungarian populations, these considerable as a single population). However, for two populations, the number of private alleles and the excess of heterozygotes may suggest pronounced differentiation from the others. Although the number of private alleles detectable strongly depends on the filtering parameters applied to a given dataset, in our study we found such alleles only in the HU1 population from Zselickisfalud, Hungary. The appearance of private alleles only in this population may be a sign that the HU1 population is separating from the other stands. As for BU1, we did not detect any private alleles

(with the filtering parameters applied), however, the excess of heterozygosity may refer to individuals of at least two different genetic groups occur in this stand (as the results of PCA and DAPC show).

Based on the results of multiple clustering approaches the eight populations under study could be separated most likely into four genetic groups. These groups are an admixed southeast Balkan group composed of BU1 (according to PCA and DAPC), a central Balkan group composed of BU2 and KO1, a consistent Hungarian group comprising the individuals of HU2, HU3, HU4 and HU5, and finally a strongly differentiating admixed group composed of HU1. Considering the biogeographic history of the species, the detected population structures may refer to the population genetic effect of the last glacial period, as our results are consistent with the recent findings on the species' plastid diversity (Bagnoli et al. 2016). According to this, genetic groups may represent descendant populations of different glacial refugia. Thus in the case of the studied Balkan populations, our results refer to at least two separate refugia for this region. However, the populations of the Hungarian group may originate from a common refugium as we observed only a low level of differentiation between them. As for the outlier HU1 population, based on the mentioned biogeographic findings, the strong differentiation of this stand does not seem logical. The thing that each clustering approach supported admixture in this population with the members of the other Hungarian stands may refer that this population has no local origin, and this stand may be a result of a historical long-distance reproductive material movement. The reproductive materials of the individuals causing admixture may have come from the neighbouring stands in a natural way or from the original stand that inhabited that area previously.

The Barrier analyses of the gene flow between populations revealed three genetic barriers supported with high bootstrap values. Going from east to west, the first barrier divides Balkan populations into two groups, the second barrier divides Hungarian and Balkan populations, and the third barrier separates HU1 from all the other stands. Considering the locations of the statistically significant barriers, these are consistent with the results of cluster analyses.
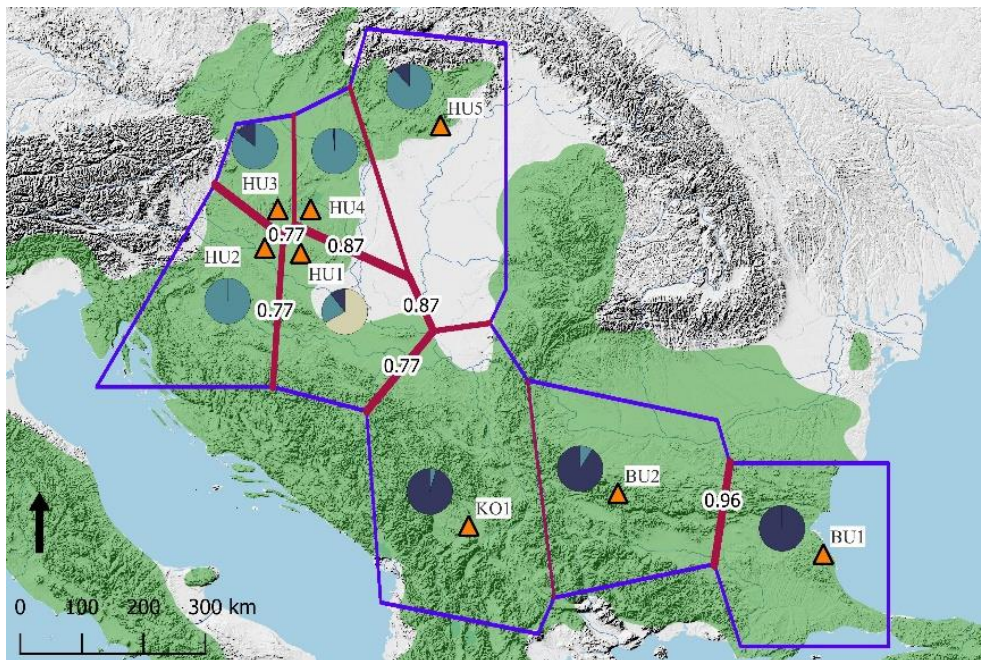
Figure 3: Results of Barrier analyses (red lines are the genetic barriers, bootstrap values on the lines show the support of the given barrier, and piecharts show the genetic structure of populations based on fastStructure clustering approach)

Our AMOVA results support statistically significant cluster and population level differentiation both for the clusters of fastStructure and DAPC. According to the higher percentage of variance on the cluster level, and the composition of Figure 2 (b), in this case, the DAPC approach was more efficient in detecting population structure. The otherwise relatively low percentage of variance on cluster and population levels seems consistent with the species' genetic system.

CONCLUSIONS

In our study, we investigated the population genetic aspects of eight central and southeast European Turkey oak populations. By using our recently published high-resolution genomic SNP dataset generated by ddRAD-seq, we provided deep insight into the species' population structure first time. Population genetic indices computed based on genome-wide data support a relatively high level of diversity of the studied populations corresponding to the species' genetic system. In addition, the occurrence of private alleles and deviation in heterozygosity may be a sign of differentiation and admixture in HU1 and BU1 populations.

According to all clustering approaches implemented, we found strong genetic structures among populations. Four genetically distinct groups were identified, strongly separating Hungarian populations from the Balkan ones. In addition, PCA and DAPC were able to separate the BU1 population from the two other Balkan populations. Interestingly the HU1 population strongly separated from the otherwise consistent Hungarian group. In our interpretation, it may be a legacy of a historical long-distance reproductive material movement. If this is the case, it would be useful to further investigate this stand as this can provide valuable information as a "historical provenance test".

In conclusion for the practice, strong genetic structuring of this species throughout its native range may be manifested not only in neutral traits but also in adaptive ones. Accordingly, in the case of Turkey oak, the geographic origin of reproductive materials may have different effects on several traits influencing the climate adaptation potential, growth traits and wood properties. As Turkey oak could be an alternative for forestry in climate adaptation, it would be important in the future to investigate the genetic background of its adaptation to harsh conditions and the options for the improvement of its wood quality. As we found relatively high genetic diversity coupled with genetic structuring, Balkan populations are promising for further studies on the genetic background of adaptation to changing environmental conditions and genetic traits influencing wood quality. However, as our current dataset has obvious limitations because of the low sample size and the few sampled populations relative to the vast distribution range, in the first step, it would be important to extend this dataset to obtain reliable data for more individuals evenly covering the distribution range.

ACKNOWLEDGEMENTS

REFERENCES

Bagnoli F. Tsuda Y. Fineschi S. Bruschi P. Magri D. Zhelev P. Paule L. Simeone M.C. González-Martínez S.C. & Vendramin G.G. 2016: Combining molecular and fossil data to infer demographic history of *Quercus cerris*: Insights on European eastern glacial refugia. Journal of Biogeography 43: 679–690. https://doi.org/10.1111/jbi.12673

Bolte A. Ammer C. Löf M. Madsen P. Nabuurs G.-J. Schall P. Spathelf P. & Rock J. 2009: Adaptive forest management in central Europe: Climate change impacts, strategies and integrative concept. Scandinavian Journal of Forest Research 24: 473–482. https://doi.org/10.1080/02827580903418224

Buras A. & Menzel A. 2019: Projecting Tree Species Composition Changes of European Forests for 2061–2090 Under RCP 4.5 and RCP 8.5 Scenarios. Frontiers in Plant Science 9 https://doi.org/10.3389/fpls.2018.01986

Goudet J. & Jombart T. 2022: hierfstat: Estimation and Tests of Hierarchical F-Statistics. https://cran.r-project.org/package=hierfstat

Hanewinkel M. Cullmann D.A. Schelhaas M.-J. Nabuurs G.-J. & Zimmermann N.E. 2013: Climate change may cause severe loss in the economic value of European forest land. Nature Climate Change 3: 203–207. https://doi.org/10.1038/nclimate1687

Illés G. & Móricz N. 2022: Climate envelope analyses suggests significant rearrangements in the distribution ranges of Central European tree species. Annals of Forest Science 79: 35. https://doi.org/10.1186/s13595-022-01154-8

Jombart T. & Ahmed I. 2011: adegenet 1.3-1: new tools for the analysis of genome-wide SNP data. Bioinformatics 27: 3070–3071. https://doi.org/10.1093/bioinformatics/btr521

Kamvar Z.N. Tabima J.F. & Grünwald N.J. 2014: Poppr: an R package for genetic analysis of populations with clonal, partially clonal, and/or sexual reproduction. PeerJ 2: e281. https://doi.org/10.7717/peerj.281

Lados B.B. Cseke K. Benke A. Köbölkuti Z.A. Molnár C.É. Nagy L. Móricz N. Németh T.M. Borovics A. Mészáros I. & Tóth E.G. 2024: ddRAD-seq generated genomic SNP dataset of Central and Southeast European Turkey oak (*Quercus cerris* L.) populations. Genet Resour Crop Evol. https://doi.org/10.1007/s10722-024-01889-5

Özer T.Y. 2014: Patterns of Genetic Diversity in Turkey Oak (*Quercus cerris* L.) Populations. Dissertation, Middle East Technical University, Ankara, Turkey. Retrieved from: https://open.metu.edu.tr/handle/11511/23662

Paradis E. 2010: pegas: an R package for population genetics with an integrated–modular approach. Bioinformatics 26: 419–420. https://doi.org/10.1093/bioinformatics/btp696

R Core Team 2022: R: A language and environment for statistical computing. R Foundation for Statistical Computing, Vienna, Austria. http//www R-project org/

Ramos A.M. Usié A. Barbosa P. Barros P.M. Capote T. Chaves I. Simões F. Abreu I. Carrasquinho I. Faro C. Guimarães J.B. Mendonça D. Nóbrega F. Rodrigues L. Saibo N.J.M. Varela M.C. Egas C. Matos J. Miguel C.M. Oliveira M.M. Ricardo C.P. & Gonçalves S. 2018: The draft genome sequence of cork oak. Scientific Data 5: 180069. https://doi.org/10.1038/sdata.2018.69

Taberlet P. Fumagalli L. Wust-Saucy A.-G. & Cosson J.-F. 1998: Comparative phylogeography and postglacial colonization routes in Europe. Molecular Ecology 7: 453–464. https://doi.org/10.1046/j.1365-294x.1998.00289.x

Thurm E.A. Hernandez L. Baltensweiler A. Ayan S. Rasztovits E. Bielak K. Zlatanov T.M. Hladnik D. Balic B. Freudenschuss A. Büchsenmeister R. & Falk W. 2018: Alternative tree species under climate warming in managed European forests. Forest Ecology and Management 430: 485–497. https://doi.org/10.1016/j.foreco.2018.08.028

Ash dieback: infection biology and management

Nina E. Nagy[1], Volkmar Timmermann[1], Isabella Børja[1], Halvor Solheim[1], Ari M. Hietala[1,2*]

[1] Norwegian Institute of Bioeconomy Research (NIBIO), Division of Biotechnology and Plant Health, Høgskoleveien 8, 1431 Ås, Norway
[2] Norwegian Institute of Bioeconomy Research (NIBIO), Division of Biotechnology and Plant Health, Skolegata 22, 7713 Steinkjer, Norway

E-mail: Nina.elisabeth.nagy@nibio.no; Volkmar.Timmermann@nibio.no; Isabella.borja@nibio.no; Halvor.Solheim@nibio.no; Ari.hietala@nibio.no;

Keywords: *Fraxinus excelsior, Hymenoscyphus fraxineus,* infection biology, biodiversity, silviculture, tree breeding

ABSTRACT

The ash dieback fungus, *Hymenoscyphus fraxineus,* considered to originate from East Asia, is threatening European ash (*Fraxinus excelsior*) on a continental scale. Trees of all ages are attacked, but young trees are particularly susceptible. It is estimated that about five percent of the ash trees in a forest have some resistance to the disease. As a result of extensive damage and high mortality throughout the natural range of European ash, the tree species is now red listed in many European countries, including Norway. Tolerance to ash dieback is also affected by environmental conditions and biotic stressors. The decline of ash and the subsequent shift in tree species has major implications for European forestry, but also for biodiversity, as many species are associated with ash.

Since the first observations of ash dieback in the early 1990s, the focus by the scientific community for the following years was to identify the cause of this disease. Once the causative pathogen was identified in 2006, the research focus shifted to understanding the mode of spread and infection by *H. fraxineus.* Along with the increasing dieback of European ash across Europe, the current research focus is on understanding how the disease and biodiversity supported by ash could be managed through silvicultural practices coupled with the use of disease resistant ash genotypes and tree breeding.

The aim of this presentation is to summarize the current understanding of the spread and mode of infection of *H. fraxineus*, the interactions of the pathogen with indigenous fungi associated with ash and environmental factors, and the possibilities of using silvicultural methods and tree breeding to control the disease and minimize the cascading effects of ash dieback on species closely associated with European ash.

INTRODUCTION

The ash dieback fungus *Hymenoscyphus fraxineus* has decimated populations of European ash (*Fraxinus excelsior*) across the continent and is also highly damaging to narrow-leaved ash (*Fraxinus angustifolia*), a tree species common in central and southern Europe (Fraxigen 2005).

Hymenoscyphus fraxineus is native to East Asia, where it is a harmless foliar associate of local ash species (Zhao et al. 2013, Drenkhan et al. 2017, Inoue et al. 2019), which are phylogenetically closely related to European ash. Symptoms of ash dieback in susceptible ash species include localized necrosis of leaf tissue, especially in areas of vascular tissue, wilting of leaves and young shoots, shoot death, premature leaf drop, and bark necrosis of varying size and color (Przybył 2002). Trees of all ages are affected and most eventually die, but saplings and young trees are particularly susceptible, while in older trees the disease progress can be comparably slow, eventually leading to gradual decline in canopy condition (Figure 1 a-g). It is estimated that only a few percent of the ash trees in a forest have some tolerance to ash dieback (McKinney et al. 2011, Kjær et al. 2012, Nielsen et al. 2017). The pathogen can also cause bark lesions and discoloration of the xylem at the base of the trunk (Figure 1 d-f, and Husson et al. 2012) and it is important to note that the genetic basis for tolerance to infection at the base

of the stem is not identical to the tolerance to infection at the shoot (Muñoz et al. 2016). Besides genetic factors, environmental conditions and other biotic perturbations may play a role in disease tolerance. According to the current life cycle model of *H. fraxineus* (Haňáčková et al. 2017)*,* the fungus spreads by wind-borne ascospores produced by ascomata that form on ash leaf debris after overwintering on the ground (Figure 1g-i). When the wind-borne ascospores become deposited on the surface of ash leaves, they germinate and establish a leaf infection (Figure 1i). The mycelia then spread through the leaf base (petiole) to shoots and twigs before the leaf drops. The necrotic bark lesions on young shoots and twigs occur during the following spring (Bengtsson et al. 2014), and once the necrosis extends around the entire circumference of the shoots and twigs, this results in gradually increasing crown dieback until the tree dies. In addition to the leaf-to-shoot pathway, lenticels (Nemesio-Gorriz et al. 2019) and direct penetration of the epidermis of young shoots (Mansfield et al. 2019) may also provide the pathogen with additional entry points into stem tissue. *H. fraxineus* has also been shown to infect the stem base of ash trees (Chandelier et al. 2016), presumably through bark cracks and lenticels (Figure 1 d-e).

In this article, we summarize the current understanding and knowledge gaps regarding the spread and infection biology of *H. fraxineus*, host-pathogen interactions, and options for management practices.

LIFE CYCLE, MODE OF INFECTION AND TISSUE COLONIZATION OF *HYMENOSCYPHUS FRAXINEUS* ON EUROPEAN ASH

The life cycle of *H. fraxineus* includes a saprotrophic phase in leaf debris, while the association with living leaves includes epiphytic, biotrophic, and necrotrophic growth stages.

Saprotrophic phase

The saprotrophic phase, i.e. decomposition and consumption, begins in the fall on dead leaves colonized by *H. fraxineus*. The first step involves the formation of a melanized layer outside of the thick-walled sclerenchyma cells that enclose the vascular cylinder in the leaf vein tissues (Baral and Bemmann 2014, Gross et al. 2014) (Figure 1 j). This so-called pseudosclerotial plate can extend over the entire petiole and rachis system, even over leaflet nerves, and together with the adjacent, highly lignified sclerenchyma cells, it protects the underlying hyphae from desiccation and UV light (Baral and Bemmann 2014). It has been shown that *H. fraxineus* can survive for months in air-dried petioles covered with a pseudosclerotial layer (Gross and Holdenrieder 2013), and that its ascomata can be formed also on older petioles, for up to five growing seasons after the leaves have been shed (Kirisits and Schwanda 2015). Fungal community profiling of overwintered ash leaf petioles showed that pseudosclerotial areas are dominated by *H. fraxineus* and possess very low fungal diversity in comparison to petiole regions that have not been secured by the pathogen pseudosclerotial plate (Kosawang et al. 2023).

After overwintering, the apothecial initials are formed from mycelium that are present in the sclerenchyma and phloem tissues (Gross et al. 2014). In some leaves, the fungus may have invaded the entire petiole/rachis region, but also the leaflet petioles and nerves - in such cases, dozens of *H. fraxineus* fruiting bodies may be formed across the vein tissues of a single compound leaf (Figure 1 g). In forests with epidemic levels of ash dieback, there may be as many as 10,000 *H. fraxineus* ascomata per m^2 of forest floor (Hietala et al. 2013). Depending on climatic conditions, the fruiting bodies of *H. fraxineus* are formed and actively sporulate between late May and September. Dry or cold summers prevent the pathogen from forming fruit bodies.

Leaf colonization by *H. fraxineus*

The formation of *H. fraxineus* fruiting bodies (Figure 1 g-h) and the production of ascospores starts a few weeks after leaf flushing, allowing the development of the parasitic phase. Under Norwegian climatic conditions, the peak of the sporulation period is usually during the hottest part of the summer, between mid-July and mid-August, and ascospores are primarily released in the early morning (Timmermann et al. 2011, Hietala et al. 2013), while leaf moisture from morning dew protects the spores from desiccation (Magarey et al. 2005, Burns et al. 2021).

During the epidemic stage of ash dieback, large numbers of pathogen ascospores become deposited on ash leaves (Figure 1i), and the number of deposited spores is likely to be greatest on small seedlings and saplings, as the concentration of *H. fraxineus* ascospores in the air decreases with distance from the ground where the fruiting bodies are located (Chandelier et al. 2014). By the time *H. fraxineus* ascospore

production begins, the leaves of European ash are already colonized by a wide range of epiphytic, endophytic, and biotrophic fungi (Cross et al. 2017). It is unknown whether the presence of specific early-arriving microbes have any impact on leaf colonization by *H. fraxineus* through factors, such as niche preemption and niche modification (Fukami 2015).

On the surface of ash leaf tissue, *H. fraxineus* ascospores can directly differentiate and form appressoria without germ tube growth (Figure 1 i), or the germ can infect leaf tissue through stomata. Mansfield et al. (2018) showed that the early phase of colonization of the leaf epidermis after direct penetration involves the formation of vesicle-like structures and bulbous and elongated intracellular hyphae in living plant cells (Figure 1 k-l), followed by a period of several days of seemingly biotrophic growth before the development of the necrotic lesions. The presence of a long asymptomatic colonization phase in European ash suggests that the fungus has co-evolved with phylogenetically related ash species in its native range and is thus "pre-adapted" to infect European ash. Under forest conditions, the necrotic leaf lesions typically appear several weeks after the onset of *H. fraxineus* ascospore discharge has started (Cross et al. 2017). The molecular interactions between pathogen and host are poorly understood but crucial. This stage is when the pathogen establishes itself without visible symptoms, highlighting the need for research into the underlying mechanisms. Identifying genes, proteins, and signaling pathways involved is essential for developing early detection and management strategies for plant diseases.

Once leaf tissue has been invaded by *H. fraxineus*, its hyphae show a high affinity for the phloem and parenchyma cells present within the vascular cylinder (Nielsen et al. 2022). Within the vascular cylinder, hyphae mostly grow axially in the parenchyma, but tangential spread between adjacent cells in the perimedullary pith parenchyma is also common (Figure 1 k-l). The parenchyma cells hosting fungal propagules generally contain little or no starch, and the hyphae are often surrounded by phenolic material, suggesting fungal assimilation of starch or conversion of these energy reserves into phenolic defense compounds (Figure 1 k-l). It appears that within ash petioles, the axial spread of the pathogen takes place within the vascular cylinder, whereas the necrotic lesions in the leaf veins originate from more basal parts of the fungal colony via lateral spread of hyphae towards the cortex. Concerning ash defense, the composition and effects of phenolics produced within the vascular cylinder of ash leaf veins of different clones during *H. fraxineus* infection remain to be determined. Ash species naturally contain constitutive foliar phenolics such as coumarins, phenolic acids, and various flavonoids (Qazi et al. 2018), with certain coumarins (fraxetin and esculetin) being associated with susceptibility to ash dieback (Nemesio-Gorriz et al. 2019, 2020). Notably, different clones of European ash with varying susceptibility to shoot dieback, consistently showed differences in constitutive twig bark phenolics, but not in constitutive leaf tissue phenolics and the former might serve as markers for selection in breeding for increased disease resistance (Villari et al. 2018).

Shoot colonization by *H. fraxineus*

Microsatellite multilocus genotyping of *H. fraxineus* isolates from leaf petioles and corresponding shoots of European ash indicate that hyphal spread via the petiole base to the shoot is a major pathway for shoot infection by this fungus (Haňáčková et al. 2017). Indirect support for this is provided by studies comparing leaf phenology between different European ash genotypes; McKinney et al. (2011) found that European ash genotypes with early leaf senescence showed less shoot dieback. The rationale for early leaf senescence preventing the leaf-to-shoot spread of the pathogen is that this pathway is only open for hyphal spread prior to the formation of the lignified and suberized abscission layer on the petiole. At present, it is not known whether different genotypes of European ash differ in the timing and extent of the physicochemical changes that occur in the petiole base in autumn, either as a natural process or as an induced response to leaf infection by *H. fraxineus*.

Within infected shoots, as within leaf veins, *H. fraxineus* hyphae appear to spread axially within the vascular cylinder, where they follow the starch-rich parenchyma cells present in radial rays and perimedullary pith (Figure 1 k-l) (Matsiakh et al. 2016). This similarity in colonization pathways would be expected, as the vascular cylinders of the leaf petiole and shoot are directly connected and form a path of least resistance for inter-tissue spread. Basal regions of an advancing colony within the shoot vascular cylinder show lateral hyphal growth towards cortex. Bengtsson et al. (2014) found that the characteristic necrotic lesions in the shoot bark typically appear in winter or spring, which would be consistent with axial spread of the pathogen within the vascular cylinder and lateral colonization of the bark from this central tissue. It is noteworthy that shoot colonization is not known to play any role in

the life cycle of *H. fraxineus*. Besides the leaf-to-shoot pathway, there is evidence that *H. fraxineus* may also be able to infect shoot tissues via lenticels (Nemesio-Gorriz et al. 2019) or directly (Mansfield et al. 2019).

Stem base colonization by *H. fraxineus*

Necrotic bark lesions at the stem base, referred to here as collar lesions, are commonly observed on ash trees with crown mortality, but can also be seen on otherwise healthy trees (Husson et al. 2012, Enderle et al. 2013, Muñoz et al. 2015). Bark cracks and lenticels are thought to serve as infection pathways for *H. fraxineus* to the stem base (Husson et al. 2012). The collar lesions typically are located less than 25 cm above the soil surface (Marçais et al. 2016) and cover 20-40% of the stem circumference (Chandelier et al. 2016, Marçais et al. 2016). In early stages, collar lesions are often found below the soil surface and can be difficult to see (Muñoz et al. 2016).

Trees as small as 8-10 cm diameter at breast height may exhibit collar lesions (Chandelier et al. 2016). *H. fraxineus* typically has a detection rate of 60-90% in collar bark lesions (Chandelier et al. 2016, Marçais et al. 2016, Enderle et al. 2017), with the underlying xylem shows wedge-shaped discoloration that taper towards the stem pith. It is evident that the discolored wood is colonized by the pathogen, as it indicated by the presence of very high *H. fraxineus* DNA (Chandelier et al. 2016). The cellular growth patterns of *H. fraxineus* in the xylem of the trunk have not yet been investigated, but the shape of the discolorations suggests that the radial rays extending from the inner bark to the pith serve as spreading pathways for the hyphae. In *H. fraxineus*-infected petioles of European ash, vessel elements show tyloses (Nielsen et al. 2022), and it is also reasonable to assume that the discolored xylem areas associated with basal bark lesions disrupt the water transport to the stem, and thus contribute to crown deterioration.

Ash trees growing in moist soils tend to have a higher frequency of collar lesions (Figure 1 e) associated with *H. fraxineus* (Marçais et al. 2016), but trees growing in moderately dry habitats can also have a relatively high frequency of collar lesions (Enderle et al. 2017), suggesting that factors other than site moisture also influence the prevalence of collar necrosis. Many studies have noted that collar necrosis appears a few years after the onset of the first crown symptoms (Husson et al. 2012, Marçais et al. 2016, Enderle et al. 2017). The concentration of *H. fraxineus* ascospores is highest near fruiting bodies at ground level (Chandelier et al. 2014), and possibly collar lesions could be initiated once a significant number of spores are deposited on the bark of the stem base - however, in the study by Marçais et al. (2016), collar lesion formation was not observed in locations with high prevalence of *H. fraxineus* fruiting bodies in the litter.

The association of other pathogens with ash dieback

Armillaria gallica and *A. cepistipes* often co-occur with *H. fraxineus* in lesions at the stem collar (e.g., Lygis et al. 2005, Bakys et al. 2009, Skovsgaard et al. 2010, Chandelier et al. 2016, Marçais et al. 2016, Enderle et al. 2017). When *Armillaria* spp. are present at the stem base, the girdling of the collar is more pronounced (Marçais et al. 2016, Enderle et al. 2017, Madsen et al. 2021). *Armillaria* spp. are opportunistic pathogens that invade hosts weakened by certain stress factors (Wargo and Harrington 1991). In the study by Lygis et al. (2005), conducted in declining ash forests before *H. fraxineus* was recognized as the causative agent of ash dieback, decay caused by *A. cepistipes* was consistently detected in 80% of the healthy-looking trees, 98.5% of declining trees, and 100% of dead trees. Currently, *Armillaria* spp. are widely recognized as secondary pathogens that benefit from the weakening of ash trees by *H. fraxineus* and that play an amplifying role in ash decline (Chandelier et al. 2016, Marçais et al. 2016, Enderle et al. 2017, Madsen et al. 2021). One hypothesis for this relation could be that crown defoliation leads to reduced photosynthesis-related translocation of energy reserves to the stem base and roots, which in turn reduces the tree's ability to resist infection by *Armillaria*.

Finally, it is noteworthy that other fungal species with pathogenic potential have also been isolated from cankers and dead shoots of European ash. These include ascomycetes such as *Alternaria alternata*, *Epicoccum nigrum* and *Phomopsis* sp. (e.g. Bakys et al. 2009) and species of *Diaporthe* and *Diplodia* (Linaldeddu et al. 2022). Whether these fungi have a similar relation to *H. fraxineus* as species of *Armillaria* have, i.e., they become pathogenic in trees weakened by the ash dieback pathogen, appears a likely scenario.
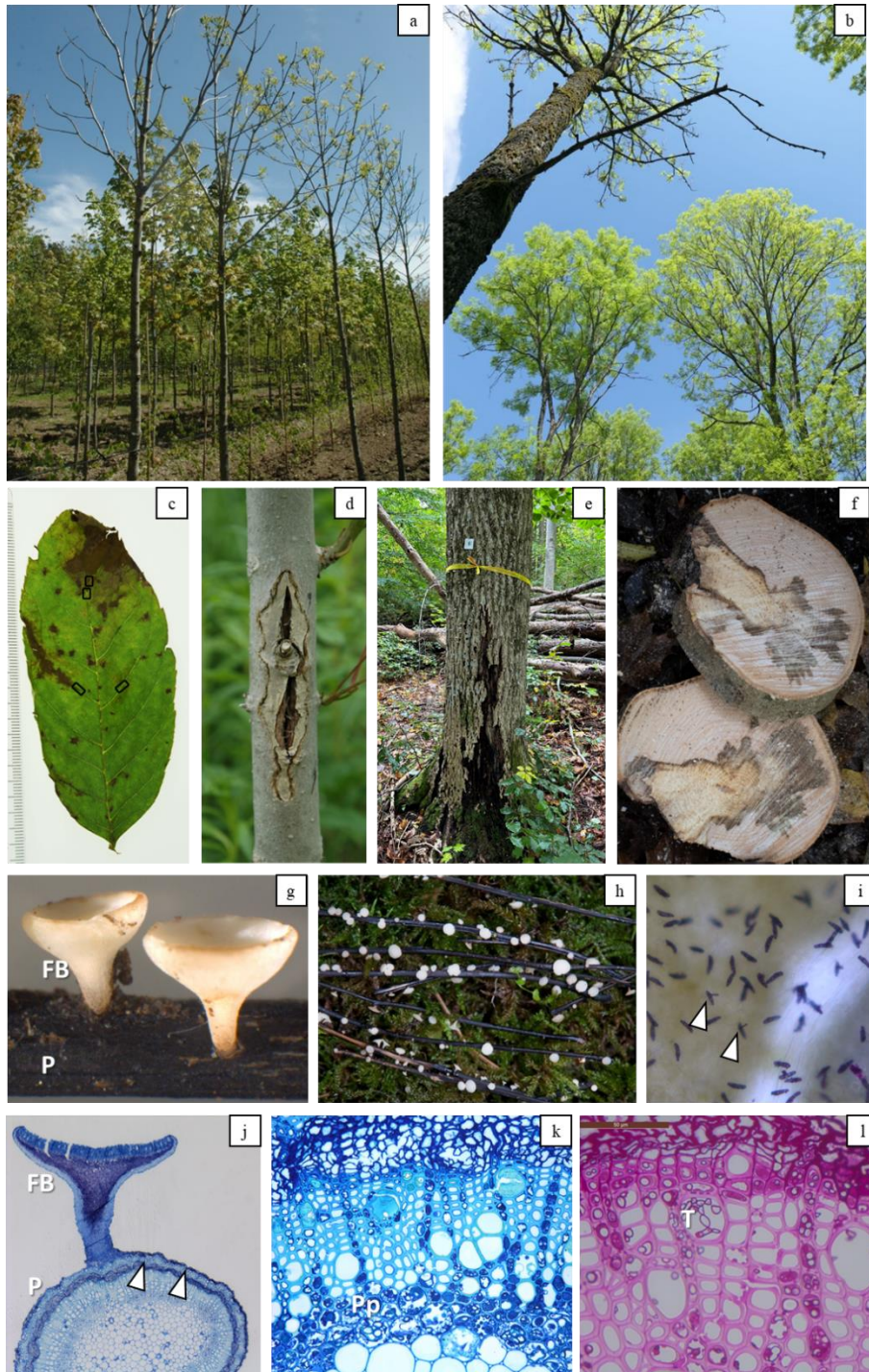
Figure 1: Sapling (a) and mature European ash trees (b) with dry, leaf-less branches that lead to crown dieback, a characteristic manifestation of the ash dieback disease caused by the pathogenic fungus Hymenoscyphus fraxineus. At a closer look, the symptoms appear as local necroses on leaflets (c), shoots (d) and trunk base (e), as well as in wood (f). Fruiting bodies (FB, ascocarp) of H. fraxineus; characteristic disc-shaped found on leaf petioles (P) (g). Large number of ascospores are produced by H. fraxineus fruiting bodies (10.000/m^2) on overwintered petioles from previous years (h). The single-celled pathogen ascospores with a cylindrical middle part and round to obtuse apex are attaching to the leaf surface (i), and form appressoria or germ tubes that enable leaf infection (arrowheads), the mycelia eventually spreading into the vascular tissue of leaf veins. A cross section of a H. fraxineus fruiting body (FB) on a leaf petiole (P), note the pseudosclerotial layer (arrow) enclosing the petiole and the neighboring sclerenchyma and phloem tissues (arrowheads) (j). Fungal hyphae show primarily axial spread in plant ray cells and vessels; were (Pp) phenolic substances (k) and (T) tylosis (l) are produced as a host response. Photos by I. Børja, A. Hietala, NE. Nagy, H. Solheim, and V. Timmermann

MANAGEMENT OF ASH DIEBACK
Breeding

A small proportion of ash trees do not develop crown damage in forests infested by *H. fraxineus* (McKinney et al. 2011, Kjær et al. 2012). Trees with early flushing and early leaf shed (McKinney et al. 2011) seem to perform best, which may reflect a mechanism of disease avoidance rather than pathogen tolerance. However, as pointed out by Muñoz et al. (2016), breeding of European ash for early flushing to achieve increased tolerance to *H. fraxineus* could come with a trade-off, as the tree species is highly sensitive to late frosts. A recent genomic study implies that tolerance of European ash to crown damage by *H. fraxineus* is a polygenic trait: 3000 Single Nucleotide Polymorphisms (SNPs, a DNA sequence variation where individuals differ at a single nucleotide for a shared sequence) were associated with crown dieback in ash stands from the UK, and a model that could predict health status with over 90% accuracy (Stocks et al. 2019) was developed.

There is a risk that the high mortality caused by *H. fraxineus* could reduce the population genetic diversity of ash to such an extent that their long-term adaptive potential to changes in environmental cues could be compromised (Evans 2019). As pointed out by this author, the selection pressure exerted by *H. fraxineus* may increase the vulnerability of European ash to other pests and diseases, such as the emerald ash borer (*Agrilus planipennis*), if tolerance to one biotic stressor is independent of that to another. This potential trade-off needs to be considered also in future breeding programs for increased tolerance to *H. fraxineus*.

Finally, it should be noted that most studies aimed at identifying traits associated with tolerance to *H. fraxineus* have focused on crown damage. The findings of Muñoz et al. (2016) indicate that susceptibility to collar infection by *H. fraxineus* is also heritable, and that there is significant genetic correlation between crown dieback severity and collar symptoms. European ash is much easier to propagate by grafting than by cuttings, and rootstock resistance to collar lesion and graft resistance to shoot infection should be considered in future breeding programs (Chandelier et al. 2016, Muñoz et al. 2016).

Silviculture

When ash dieback became epidemic throughout Europe, nursery production of European ash seedlings and planting of the tree species was practically terminated. When considering natural regeneration of European ash, management practices that reduce infection pressure by *H. fraxineus* and associated root and stem base infection by species of *Armillaria* species are meaningful. As reviewed by Skovsgaard et al. (2017), the ascomata production by *H. fraxineus* is facilitated by soil moisture, and since the frequency of collar lesions by *H. fraxineus*, but also by *Armillaria* species, tends to increase in moist habitats, avoidance of growing European ash in such sites can be recommended. Avoidance of pure ash stands and selective thinning to allow canopy expansion of vigorous ash trees is also recommended. Thinning to reduce the proportion of ash in mixed forests should both lower the infection pressure of *H. fraxineus* and allow strengthening of the canopy of pole-staged ash trees (Short and Hawe 2018 and references therein). The survival of the sapling stage of European ash is hindered by ungulate browsing in many localities, thus fencing, although expensive, may be necessary.

To combat the loss of biodiversity and to increase forest resilience towards abiotic and biotic stressors, there is currently a strong sentiment in Europe to increase the proportion of forests managed according to close-to-nature principles (Mageroy et al. 2023). This means the establishment of mixed tree species forests with several canopy layers, management involving selective loggings, including the creation of minor gaps in the forest through clear cut. European ash is shade-tolerant when young and could grow as an understory tree in seedling and sapling stages in mixed-species forests. Recently, Marçais et al. (2023) showed that foliage of ash trees without shoot dieback also supports the production of *H. fraxineus* ascomata. In moist forests, growing ash in multiple canopy layers may be particularly unfavorable for seedlings and saplings, as high foliage biomass coupled with moist soil conditions is translated into high infection pressure.

REFERENCES

Agan A, Drenkhan R, Adamson K, Tedersoo L, Solheim H, Borja I, Matsiakh I, Timmermann V, Nagy NE, Hietala AM (2020) The Relationship between fungal diversity and invasibility of a foliar niche- the case of Ash dieback. J Fungi 6:150. https://doi.org/10.3390/jof6030150

Bakys R, Vasaitis R, Barklund P, Ihrmark K, Stenlid J (2009) Investigations concerning the role of *Chalara fraxinea* in declining *Fraxinus excelsior*. Plant Pathol 58:284–292. https://doi.org/10.1111/j.1365-3059.2008.01977.x

Baral HO, Bemmann M (2014) *Hymenoscyphus fraxineus* vs. *Hymenoscyphus albidus* – A comparative light microscopic study on the causal agent of European ash dieback and related foliicolous, stroma-forming species. Mycology 5:289–290. https://doi.org/10.1080/21501203.2014.963720

Bengtsson SBK, Vasaitis R, Kirisits T, Solheim H, Stenlid J (2012) Population structure of *Hymenoscyphus pseudoalbidus* and its genetic relationship to *Hymenoscyphus albidus*. Fungal Ecol 5:147–153. https://doi.org/10.1016/j.funeco.2011.10.004

Burns P, Timmermann V, Yearsley J (2021) Meteorological factors associated with the timing and abundance of *Hymenoscyphus fraxineus* spore release. Int J Biomet. https://doi.org/10.1007/s00484-021-02211-z

Chandelier A, Gerarts F, San Martin G, Herman M, Delahaye L (2016) Temporal evolution of collar lesions associated with ash dieback and the occurrence of *Armillaria* in Belgian forest. For Pathol 46(4):289–97. https://doi.org/10.1111/efp.12258

Chandelier A, Helson M, Dvorak M, Gischer F (2014) Detection and quantification of airborne inoculum of *Hymenoscyphus pseudoalbidus* using real-time PCR assays. Plant Pathol 63:1296–1305. https://doi.org/10.1111/ppa.12218

Cross H, Sonstebo JH, Nagy NE, Timmermann V, Solheim H, Børja I, Kauserud H, Carlsen T, Rzepka B, Wasak K, Vivian-Smith A, Hietala AM (2017) Fungal diversity and seasonal succession in ash leaves infected by the invasive ascomycete *Hymenoscyphus fraxineus*. New Phytol 213:1405–1417. https://dx.doi.org/10.1111/nph.14204

Drenkhan R, Solheim H, Bogacheva A, Riit T, Adamson K, Drenkhan T, Maaten T, Hietala AM (2017) *Hymenoscyphus fraxineus* is a leaf pathogen of local Fraxinus species in the Russian Far East. Plant Pathol 66:490–5003. https://doi.org/10.111/ppa12588

Enderle R, Peters F, Nakou A, Metzler B (2013) Temporal development of ash dieback symptoms and spatial distribution of collar rots in a provenance trial of *Fraxinus excelsior*. Eur J For Res 132:865–876. https://doi.org/10.1007/s10342-013-0717-y

Enderle R, Sander F, Metzler B (2017) Temporal development of collar necroses and butt rot in association with ash dieback. iForest 10:529–536. https://doi.org/10.3832/ifor2407-010 10.3832/ifor2407-010

Evans MR (2019) Will natural resistance result in populations of ash trees remaining in British woodlands after a century of ash dieback disease? R Soc Open Sci 6:190908. http://dx.doi.org/10.1098/rsos.190908

FRAXIGEN 2005. Ash species in Europe: biological characteristics and practical guidelines for sustainable use. Oxford Forestry Institute, University of Oxford, UK, pp 128

Fukami T (2015) Historical contingency in community assembly: Integrating niches, species pools, and priority effects. Annu Rev Ecol Evol Syst 46:1–23. doi: 10.1146/annurev-ecolsys-110411-160340

Gross A, Holdenrieder O (2013) On the longevity of *Hymenoscyphus pseudoalbidus* in petioles of *Fraxinus excelsior*. For Pathol 43(2):168–170. https://doi.org/10.1111/efp.12022

Gross A, Holdenrieder O, Pautasso M, Queloz V, Sieber TN (2014) *Hymenoscyphus pseudoalbidus*, the causal agent of European ash dieback. Mol Plant Pathol 15:5–21. https://doi.org/10.1111/mpp.12073

Haňáčková Z, Koukol O, Čmoková A, Zahradník D, Havrdová L (2017) Direct evidence of *Hymenoscyphus fraxineus* infection pathway through the petiole-shoot junction. For Pathol 47(6):e12370. https://doi.org/10.1111/efp.12370

Hietala AM, Timmermann V, Børja I, Solheim H (2013) The invasive ash dieback pathogen *Hymenoscyphus pseudoalbidus* exerts maximal infection pressure prior to the onset of host leaf senescence. Fungal Ecol 6:302–308. https://doi.org/10.1016/j.funeco.2013.03.008

Husson C, Caël O, Grandjean JP, Nageleisen L, Marçais B (2012) Occurrence of *Hymenoscyphus pseudoalbidus* on infected ash logs. Plant Pathol 61:889–95. https://doi.org/10.1111/j.1365-3059.2011.02578.x

Inoue T, Okane I, Ishiga Y, Degawa Y, Hosoya T, Yamaoka Y (2019) The life cycle of *Hymenoscyphus fraxineus* on Manchurian ash, *Fraxinus mandshurica*, in Japan. Mycoscience 60:89–94. https://doi.org/10.1016/j.myc.2018.12.003

Kirisits T, Schwanda K (2015) First definite report of natural infection of *Fraxinus ornus* by *Hymenoscyphus fraxineus*. For Pathol 45(5):430–432. https://doi.org/10.1111/efp.12211

Kosawang C, Børja I, Herrero M-L, Nagy NE, Nielsen LR, Solheim H, Timmermann V, Hietala AM (2023) Fungal succession in decomposing ash leaves colonized by the ash dieback pathogen *Hymenoscyphus fraxineus* or its harmless relative *Hymenoscyphus albidus*. Front Microbiol 14:1154344. https://doi.org/10.3389/fmicb.2023.1154344

Kowalski T, Bartnik C (2010) Morphological variation in colonies of *Chalara fraxinea* isolated from ash (*Fraxinus excelsior* L.) stems with symptoms of dieback and effects of temperature on colony growth and structure. Acta Agrobotanica 63(1):99–106. https://doi.org/10.5586/aa.2010.012

Linaldeddu BT, Bregant C, Montecchio L, Brglez A, Piškur B, Ogriset N (2022) First Report of *Diplodia fraxini* and *Diplodia subglobosa* causing canker and dieback of *Fraxinus excelsior* in Slovenia. Plant Disease 106:1, short comm. https://doi.org/10.1094/PDIS-06-21-1204-SC

Lygis V, Vasiliauskas R, Stenlid J (2005) Wood-inhabiting fungi in stems of *Fraxinus excelsior* in declining ash stands of northern Lithuania, with particular reference to *Armillaria cepistipes*. Scan J For Res 20:33746. https://doi.org/10.1080/02827580510036238

Madsen CL, Kosawang C, Thomsen IM, Nørgaard Hansen L, Nielsen LR, Kjær ED (2021) Combined progress in symptoms caused by –*Hymenoscyphus fraxineus* and Armillaria species, and corresponding mortality in young and old ash trees. For Ecol Man 491:119177. https://doi.org/10.1016/j.foreco.2021.119177

Magarey RD, Sutton TB, Thayer CL (2005) A simple generic infection model for foliar fungal plant pathogens. Phytopathology 95(1):92–100. https://doi.org/10.1094/PHYTO-95-0092

Mageroy MH, Nagy NE, Steffenrem A, Krokene P, Hietala AM (2023) Conifer defences against pathogens and pests — mechanisms, breeding, and management. Curr For Rep 9:429–443. https://doi.org/10.1007/s40725-023-00201-5

Mansfield J, Brown I, Papp-Ruparet M (2019) Life at the edge – the cytology and physiology of the biotroph to necrotroph transition in *Hymenoscyphus fraxineus* during lesion formation in ash. Plant Pathol 68(5):908–920. https://doi.org/10.1111/ppa.13014

Mansfield JW, Galambos N, Saville R (2018) The use of ascospores of the dieback fungus *Hymenoscyphus fraxineus* for infection assays reveals a significant period of biotrophic interaction in penetrated ash cells. Plant Pathol 67:1354–61. https://doi.org/10.1111/ppa.12844

Marçais B, Husson C, Godart L, Caël O (2016) Influence of site and stand factors on *Hymenoscyphus fraxineus*-induced basal lesions. Plant Pathol 65(9):1452–1461. https://doi.org/10.1111/ppa.12542

Matsiakh I, Solheim H, Nagy NE, Hietala AM, Kramarets V (2016) Tissue-specific DNA levels and hyphal growth patterns of *Hymenoscyphus fraxineus* in stems of naturally infected *Fraxinus excelsior* saplings. For Pathol 46:206–214. https://doi.org/10.1111/efp.12245

McKinney LV, Nielsen LR, Hansen JK, Kjær ED (2011) Presence of natural genetic resistance in *Fraxinus excelsior* (Oleaceae) to *Chalara fraxinea* (Ascomycota): an emerging infectious disease. Heredity 106:788–97. https://doi.org/10.1038/hdy.2010.119

Muñoz F, Marçais B, Dufour J, Dowkiw A (2016) Rising out of the Ashes: Additive genetic variation for crown and collar resistance to *Hymenoscyphus fraxineus* in *Fraxinus excelsior*. Phytopathology 106(12):1444–1571. https://doi.org/10.1094/PHYTO-11-15-0284-R

Nemesio-Gorriz M, Menezes RC, Paetz C, Hammerbacher A, Steenackers M, Schamp K, Höfte M, Svatoš A, Gershenzon J, Douglas GC (2020) Candidate metabolites for ash dieback tolerance in *Fraxinus excelsior*. J Exp Bot 71:6074–6083.

Nemesio-Gorriz M, McGuinness B, Grant J, Dowd L, Douglas GC (2019) Lenticel infection in *Fraxinus excelsior* shoots in the context of ash dieback. iForest 12:160–165. https://doi.org/10.3832/ifor2897-012

Nielsen LR, McKinney LV, Hietala AM, Kjær ED (2017) The susceptibility of Asian, European and North American Fraxinus species to the ash dieback pathogen *Hymenoscyphus fraxineus* reflects their phylogenetic history. Eur J For Res 136:59–73. https://doi.org/10.1007/s10342-016-1009-0

Nielsen LR, Nagy NE, Piqueras S, Kosawang C, Thygesen LG, Hietala AM (2022). Host−pathogen interactions in leaf petioles of common Ash and Manchurian Ash infected with *Hymenoscyphus fraxineus*. Microorganisms 10:375. https://doi.org/10.3390/microorganisms10020375

Przybył K (2002) Fungi associated with necrotic apical parts of *Fraxinus excelsior* shoots. For Pathol 32(6):387–394. https://doi.org/10.1046/j.1439-0329.2002.00301.x

Qazi SS, Lombardo DA, Abou-Zaid MM (2018) A metabolomic and HPLC-MS/MS analysis of the foliar phenolics, flavonoids and coumarins of the Fraxinus species resistant and susceptible to Emerald Ash borer. Molecules 23:2734. https://doi.org/10.3390/molecules23112734

Short I, Hawe J (2018) Ash dieback in Ireland – A review of European management options and case studies in remedial silviculture. Irish Forestry 75(1&2):44-72

Skovsgaard JP, Thomsen IM, Skovgaard IM, Martinussen T (2010) Associations among symptoms of dieback in even-aged stands of ash (*Fraxinus excelsior* L.). For Pathol 40(1):7–18. https://doi.org/10.1111/j.1439-0329.2009.00599.x

Skovsgaard JP, Wilhelm GJ, Thomsen IM, Metzler B, Kirisits T, Havrdová L, Enderle R, Dobrowolska D, Cleary M, Clark J (2017) Silvicultural strategies for *Fraxinus excelsior* in response to dieback caused by *Hymenoscyphus fraxineus*. Forestry 90:455–472. https://doi.org/10.1093/FORESTRY/CPX012

Stocks JJ, Metheringham CL, Plumb WJ, Lee SJ, Kelly LJ, Nichols RA, Buggs RJA (2019) Genomic basis of European ash tree resistance to ash dieback fungus. Nat Ecol Evol 3(12):1686–1696. https://doi.org/10.1038/s41559-019-1036-6

Timmermann V, Børja I, Hietala AM, Kirisits T, Solheim H (2011) Ash dieback: pathogen spread and diurnal patterns of ascospore dispersal, with special emphasis on Norway. Bulletin OEPP/EPPO Bulletin 41:14–20. https://doi.org/10.1111/j.1365-2338.2010.02429.x

Villari C, Dowkiw A, Enderle R, Ghasemkhani M, Kirisits T, Kjær ED, Marčiulynienė D, McKinney LV, Metzler B, Muñoz F, Nielsen LR, Pliūra A, Stener L-G, Suchockas V, Rodriguez-Saona L, Bonello P, Cleary M (2018) Advanced spectroscopy-based phenotyping offers a potential solution to the ash dieback epidemic. Sci Rep 8:17448. https://doi.org/10.1038/s41598-018-35770-0

Wargo PM, Harrington TC (1991) Host Stress and Susceptibility. In: Armillaria Root Disease. Agriculture Handbook no. 691, Ed. by S HAW C. G.; KILE, G. A. Washington: USDA Forest Service, pp 88–101

Zhao YJ, Hosoya T, Baral HO, Hosaka K, Kakishima M (2013) *Hymenoscyphus pseudoalbidus*, the correct name for *Lambertella albida* reported from Japan. Mycotaxon 122:25–41. https://doi.org/10.5248/122.25

The Role of Industrial Hardwood Production Plantations and Long-Term Carbon Sequestration in a Circular Economy via the New Robinia pseudoacacia 'Turbo Obelisk' Varieties

Márton Németh[1*], Kálmán Pogrányi[2], Rezső Solymos[3]

[1]Managing Director, Silvanus Group, HU1067 Budapest, Teréz krt. 47.
[2] Forestry Researcher, Silvanus Forestry, HU1067 Budapest, Teréz krt. 47.
[3]Founder, Ökoszisztéma Kft., HU2094 Nagykovácsi, Gémeskút utca 45.
www.silvanusforestry.com

E-mail: marton.nemeth@silvanus.hu

Keywords: sustainable plantation forestry, long-term carbon sequestration, industrial hardwood production, Robinia pseudoacacia 'Turbo Obelisk', utilisation of dry marginal soils

ABSTRACT

Considering the changing climate and the tendencies which we have seen in recent years, it is ever more vital to adapt to these changing conditions. According to forecasts, an increasing amount of areas will be classified as low quality, marginal soils unsuitable for agricultural production and may even become unsuitable for several native tree species. The utilisation of these areas will most certainly prove to be of extreme importance from not only an environmental but also from an economical perspective. The demand of the hardwood market must be met in the long run and sustainable plantation-based forestry is the only solution.

At the same time, long-term carbon sequestration, forestry management and improved efficiency must be the ultimate goal, which can only be achieved through the research and development of fast, straight growing and resilient varieties, including the elimination of waste wood materials within a circular economy framework.

Building on the work of Dr. Imre Kapusi and after decades of research and development, Silvanus Group has successfully propagated the Robinia pseudoacacia 'Turbo Obelisk' variety group and developed the necessary cultivation technologies specifically for intensive industrial hardwood production plantations. Our two latest research projects, *2017-1.3.1-VKE-2017-00022* and *VEKOP-2.1.1-15-2016-00166* included consortium partners such as NYME, NYME ERTI, MATE, NÉBIH and were also heavily subsidized by the European Union, the Hungarian Government as well as the National Research, Development and Innovation Office.

In comparison to the Hungarian and traditional black locust varieties and cultivation technology, industrial hardwood production plantations established with our variety group and using our cultivation technologies can produce twice the timber yield of the traditional species in 15 years, whilst also producing a very high percentage of much higher quality, straight, defect free industrial hardwood. Our varieties and cultivation technologies can also be used in subtropical, temperate, as well as tropical climates. The outstanding yields achieved by the 'Turbo Obelisk' varieties and the extremely high industrial wood output can provide a significant contribution to the conservation and maintenance of natural ecosystems, whilst the CO2 sequestration per unit area per time is also higher than that of natural forests.

Our varieties also have an outstanding tolerance to pollution, drought and low quality, sandy, marginal soils. This can also significantly increase the advancement of less developed regions and provide economic value in areas which are currently unutilised. In addition to plantation cultivation, it also produces delicious honey and provides a cost-effective solution for the establishment of protective forest belts, road-side plantings, quicksand fixation and soil renovation.

INTRODUCTION

Climate change mitigation and adaptation to the already existing effects of climate change require rapid and highly efficient measures. Most scientists agree that we have less than 10 years to drastically reduce

greenhouse emissions before the effects will be highly detrimental and hence it is vital to introduce new technologies and to develop new solutions for climate change adaptation and mitigation.

Long-term carbon sequestration is one of the most important pillars to achieving our goals. The establishment of fast-growing hardwood plantations with high carbon content whilst producing quality industrial timber is becoming vital, especially when considering the demand of the wood industry and the preservation of natural forests. This means that, in addition to the carbon sequestered by living forests, harvested durable and high-quality industrial timber also contributes to long-term carbon storage.

THE LONG-TERM CARBON SEQUESTRATION CAPACITY OF FORESTS AND PLANTATIONS

It is noteworthy to emphasize the importance of solar energy when the industrial and energetic use of biomass produced is also among the future goals. It is commonly known that plants-including trees-convert the inorganic nutrients taken from the soil into organic matter by the means of photosynthesis with the help of the energy of the sun for the structure of their wood and their vital functions. The carbon required for this organic matter is sequestered from the carbon dioxide content of the atmosphere. This carbon sequestration serves to reduce one of the most significant greenhouse gases in the atmosphere.

The average chemical composition of wood is as follows: Carbon (C): 49,2%, Oxygen (O): 43%, Hydrogen (H): 6,2%, Nitrogen (N):0,9%, other ash components: 0,7%. The fact that forests store solar energy and reduce air pollution is researched and highly valued all over the world. Sustainable forest management is the basis for preserving the carbon storage capacity of our forests. There are two main options for the expanding the carbon storage capacity of forests:

- Expansion of forest areas
- Increasing the amount of live timber volume per hectare (selection of specific fast-growing hardwood species, utilisation of special varieties, research and utilisation of new, efficient forest and plantation maintenance technologies)

The establishment of new forests or plantations can typically take place in dry, low quality marginal soils within the forest steppe climate, which are unsuitable for agricultural production. These are mostly semi-arid, dry sandy soils with low humus content with high temperatures, under which conditions only a few species of trees can form a continuous forest population. As a result of climate change and hence the increasing temperatures, it is vital to utilise species and even more importantly special varieties of these species in these areas.

The table below should be considered when establishing new forests, plantations or when renovating existing populations with different species in forest-steppe climates with semi-arid and arid, sandy soils.

Table 1: The growth and hence the Carbon Sequestration of Various Species on Various Soils

Column1	Column2	Column3	Column4	Column5	Column6	Column7
Species	Production Capacity of Forest Land	Age	Standing Volume	Dry Matter Content	Carbon Content	Carbon Sequestration/ Year
		Years	m³/ha	t/m³	t	t
Robinia ps. 'TURBO OBELISK'	Very Good	12	288	209.66	103.15	8.60
Robinia ps. 'TURBO OBELISK'	Good	12	210	152.88	75.22	6.27
Robinia ps. 'TURBO OBELISK'	Medium	12	335	243.88	117.55	9.80
Robina ps. 'TURBO OBELISK'	Very Good	20	480	349.44	171.92	8.60
Robinia ps. 'TURBO OBELISK'	Good	20	300	218.4	107.45	5.37
Common Robinia ps.	Very Good	20	335	243.88	117.55	5.88
Common Robinia ps.	Good	20	279	203.11	99.93	5.00
Common Robinia ps.	Medium	20	169	123.03	60.53	3.03
Common Robinia ps.	Good	30	348	253.34	124.64	4.15
Common Robinia ps.	Good	40	393	286.1	140.76	3.52
Common Robinia ps.	Very Good	40	460	334.88	164.76	4.12
Common Robinia ps.	Medium	40	255	185.64	91.33	2.28
Quercus robur	Medium	40	225	141.75	61.29	1.53
Quercus robur	Poor	40	158	99.54	43.04	1.08
Quercus robur	Medium	80	388	244.44	105.7	1.32
Pinus sylvestris	Good	40	415	211.65	105.91	2.65
Pinus sylvestris	Medium	40	302	154.02	77.07	1.93
Pinus sylvestris	Good	70	513	261.66	130.93	1.87
Pinus nigra	Good	40	387	197.37	98.76	2.47
Pinus nigra	Good	70	500	255	137.6	1.97
Populus canescens	Good	40	275	110	55	1.38
Populus x euramericana	Good	15	238	95.2	47.6	3.17
Populus x euramericana	Good	20	370	148	74	3.70

Source: Silvanus Group Data

In the table above, we examined the wood-yield of Robinia pseudoacacia varieties at a given age, considering low quality, sandy soils with low humus content in a forest-steppe climate. For comparability, we analysed the wood volume and carbon content of trees and different ages. The examination in different ages allows us to determine the species and varieties to be used in plantings as well as to determine the ideal rotation periods, in accordance with the desired goals.

It is clear from the table above that Robinia pseudoacacia has not competitors when it comes to timber yield and carbon sequestration within the same timber production capacity group when considering rotation periods of 15-20-40 years. It is also clear that the 'Turbo Obelisk' variety group greatly outperforms common Robinia pseudoacacia by as much as 100%+, despite the planting density being much lower for the vegetatively propagated variety group.

RESEARCH AND DEVELOPMENT OF THE ROBINIA PSEUDOACACIA 'TURBO OBELISK' VARIETIES

The main purpose of Robinia pseudoacacia breeding is to select varieties that make better than average use of the potential wood productivity of areas with poor conditions and to adapt to changing conditions as well as to produce high quality, defect free industrial timber. In addition, stem straightness is also a vital aspect as this largely determines the percentage of the wood which can be used as industrial wood, hence greatly contributing to long-term carbon storage. Large scale vegetative propagation methods had to be developed for the practical utilisation of the selectively bred varieties and it was also necessary to determine the optimal plantation technologies and rotation periods.

The special, Robinia pseudoacacia 'Turbo Obelisk' variety group and the developed plantation technologies meets all the global development goals and thereby also serves to mitigate climate change. Building on the work of Dr. Imre Kapusi and after decades of research and development, Silvanus Group has successfully propagated the Robinia pseudoacacia 'Turbo Obelisk' variety group and developed the necessary cultivation technologies specifically for intensive industrial hardwood production plantations. Our two latest research projects, *2017-1.3.1-VKE-2017-00022* and *VEKOP-2.1.1-15-2016-00166* included consortium partners such as NYME, NYME ERTI, MATE, NÉBIH and were also heavily subsidized by the European Union, the Hungarian Government as well as the National Research, Development and Innovation Office.

In comparison to the Hungarian and traditional black locust varieties and cultivation technology, industrial hardwood production plantations established with our variety group and using our cultivation technologies can produce twice the timber yield of the traditional species in 15 years, whilst also producing a very high percentage of much higher quality, straight, defect free industrial hardwood. Our varieties and cultivation technologies can also be used in subtropical, temperate, as well as tropical climates. The outstanding yields achieved by the 'Turbo Obelisk' varieties and the extremely high industrial wood output can provide a significant contribution to the conservation and maintenance of natural ecosystems, whilst the CO2 sequestration per unit area per time is also higher than that of natural forests.

The purpose of creating woody plantations for industrial purposes is "to increase the supply of wood as a renewable resource, in addition to the tree cover, thereby reducing the pressure on indigenous forest stands caused by the increase in demand for wood. (National Forest Strategy 2016-2030.)

Our varieties also have an outstanding tolerance to pollution, drought and low quality, sandy, marginal soils. This can also significantly increase the advancement of less developed regions and provide economic value in areas which are currently unutilised. In addition to plantation cultivation, it also produces delicious honey and provides a cost-effective solution for the establishment of protective forest belts, road-side plantings, quicksand fixation and soil renovation.

We performed our calculations for the fast and straight growing Robinia pseudoacacia 'Turbo Obelisk' varieties, which tolerate a wide range of soil and weather conditions. (The carbon content of one m^3 of Robinia pseudoacacia is 1.79 times that of poplar.)

The initial data was established with the help of the measurements, calculations, and prognosis of Dr. Kálmán Pogrányi, and they cover a time interval of 20 years.

It is clear in terms of the expected wood yield and carbon sequestration that the 'Turbo Obelisk' variety group far outperforms traditional black locust as well as all the other species in its category.

THE CHARACTERISTICS OF THE ROBINIA PSEUDOACACIA 'TURBO OBELISK' VARIETY GROUP

The Robinia pseudoacacia 'Turbo Obelisk' variety group has an even better tolerance to low quality, marginal soils than the common species. This means that in areas where the common black locust's growth can be classified as weak, the growth of the 'Turbo Obelisk' varieties can be classified as good. This also means that the rotation period can be decreased due to the better growth.

The newly developed plantation maintenance technologies and the outstanding 'Turbo Obelisk' variety group also allows for high quality industrial pole wood and industrial roundwood production with a much higher output, hence decreasing the biomass or firewood output. This not only creates significantly higher value, but also allows for long-term carbon sequestration. This is due to not only its fast growth but its straight stem. This can also be extremely interesting from the perspective of the voluntary carbon credit market, as much more carbon can be sequestered with these varieties when compared to the common Robinia pseudoacacia species as well as when compared to other similar species.

As an example, when considering a 20-year-old common black locust population with excellent wood yield, approximately 36% of the timber falls within the size range of industrial pole wood or industrial roundwood. Since the stem is not straight but curved, the final industrial wood output will as low as 15-20%.

In comparison, when using the Robinia pseudoacacia 'Turbo Obelisk' variety group and the newly developed cultivation technologies, at the age of 20 years, 71% of the timber produced falls within the size range of industrial pole wood and industrial roundwood. In this situation, we can expect an approximate final industrial wood output of over 60%. This is due to the outstanding growth and form trait of the variety group as well as the plantation technologies.

Furthermore, when considering medium wood productivity, the yield of a 15-year-old common black locust forest or plantation does not allow to produce any industrial wood, whilst the 'Turbo Obelisk' variety group is already able to produce a significant amount of industrial wood at this age.

Based on the previous examples, when using the selectively bred 'Turbo Obelisk' varieties, we can expect significantly higher additional timber yield and longer sustainability due to not only the fast and straight growth of the varieties but also due to its higher tolerance to low quality soils, hence storing more carbon.

We must also consider "dead wood" as a long-term carbon storage.

The amount of harvested industrial wood plays a significant role in the storage of sequestered carbon. It makes a huge difference whether you are producing firewood/biomass or quality hardwood of which quality products can be made, resulting in true long-term carbon sequestration.

Further increasing the value of quality industrial wood is the natural durability of black locust hardwood: outdoors approx. 80 years, in constant humidity approx. 500 years, under permanently dry conditions approx. 1500 years.

DETERMINING THE MOST SUITABLE ROTATION PERIOD FOR THE 'TURBO OBELISK' VARIETY GROUP

The aim of the initial experiments was to achieve quality industrial wood in the shortest time possible, being approximately 15 years. The scientific basis for this was the selection of the clones specifically for extreme juvenile growth. After the culmination of the tree growth, the wood is harvested. Due to this, the rotation periods are much shorter, whilst the general rotation period for black locust in Hungary is around 30 years, and growth rate decreases significantly after that.

When determining the best time for harvest, it is worthwhile to examine the total standing wood yield of a plantation as well as the volume of the stump and the roots under the clear-cut level as a function of age and wood productivity.

The graph clearly shows that the annual dynamics of the increase in wood volume in stands with good wood production capacity remains significant until the age of 40. We can take advantage of this dynamic but gradually slowing growth volume if we use the 'Turbo Obelisk variety group. This offers the opportunity to create serious additional yield and hence value.

In addition to the value of the produced wood, the time content of carbon storage in the wood material above the cutting board (standing) and below the cutting board (stumps and roots) increases significantly.

It should be emphasized that after harvesting, the proportion of quality industrial wood increases dramatically, which also increases the carbon storage capacity of the "dead wood".

It should be emphasized that the tree stand established from the 'Turbo Obelisk' variety group on traditional medium-yielding sites already has good growth and wood quality.

ENVIRONMENTALLY FRIENDLY UTILISATION OF TIMBER

During the utilisation of timber, it is vital to consider and ensure the environmentally friendly and optimal utilisation. This means that the output of industrial wood should be as large as possible. During the use of industrial wood, the carbon storage capacity of the wood can be preserved for several decades (e.g. construction grade timber). As a renewable energy source, biomass can be considered carbon neutral, which can replace fossil energy.

The optimization of the environmentally friendly utilisation of wood is determined by the size and quality of the wood material produced. Sawmill raw materials play the biggest role in preserving the carbon storage capacity of the extracted wood, but other industrial uses also ensure decades of storage capacity.

The development of the standing volume of Robinia pseudoacacia taking age and growing area into account (Figure nr 1.)
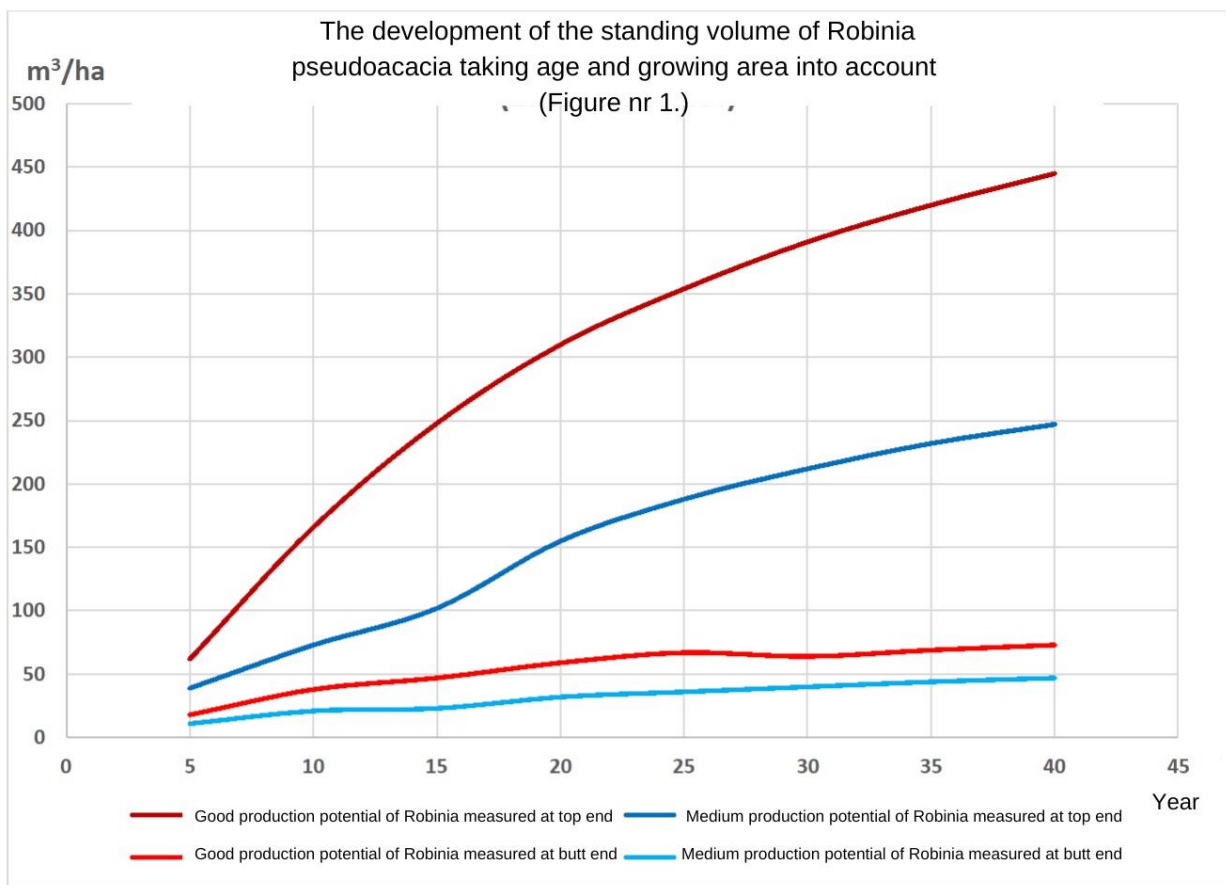
The Average Amount of Annually Sequestered CO2 per Hectare of Age Group for Robinia pseudoacacia with Good Tree Productivity, Taking into Account the Wood Volume Measured Under Butt End (Stump + Root)

Age group (year)	0-5	6-10	11-15	16-20	21-25	26-30	31-35	36-40
Average of Annually Sequestered CO_2 (t/ha/year)	21	33	24	19	14	9	9	6

It is clear from the above table that CO_2 sequestration slows after 20 years and slows even more significantly afterwards.

CONCLUSIONS

Robinia pseudoacacia is expected to become a dominant tree species for the establishment of forests and plantations on low quality, marginal, arid areas in the near future. Most of the agricultural lands are privately owned, and the owners are not always interested in creating forests or plantations, hence it is advisable to use the persuasive power of economic interest here, such as the voluntary carbon credit market.

Our findings, vegetative varieties, and cultivation technologies regarding the industrial wood production plantation utilization of the *Robinia pseuodoacacia* 'Turbo Obelisk' varieties can greatly contribute to the preservation of natural forests and other vital environmental aspects whilst also meeting the increasing demand for quality hardwood. Perhaps the most important aspect is the outstanding carbon sequestration capability of the variety group, which can greatly contribute to the mitigation of the effects of climate change whilst providing a solution for the utilisation of areas which are otherwise unsuitable for agricultural production.

Initial growth of native and introduced hardwoods at the afforested agricultural lands – preliminary results

Vilém Podrázský, Josef Gallo, Martin Baláš, Ivan Kuneš, Tama Abubakar Yahaya, Miroslav Šulitka

Czech University of Life Sciences Prague, Faculty of Forestry and Wood Sciences, Department of Silviculture, CZ 165 21, Kamýcká 129, Prague 6 - Suchdol

E-mail: podrazsky@fld.czu.cz; balas@fld.czu.cz; kunes@fld.czu.cz; gallo@fld.czu.cz; tama@fld.czu.cz; sulitka@fld.czu.cz; tama@fld.czu.cz

Keywords: noble hardwoods, afforestation, growth, prosperity, Czech Republic

ABSTRACT

Hardwoods, i.e., especially valuable broad-leaved tree species represent the increasing share of the newly established forest stands in many European countries, including the Czech Republic. On the contrary, the use of their timber is of minor extent in the country at this moment. Considering the rate of their growth and development, there is still some time for strategic and technological decisions, technology implementation and use promotion – so a great opportunity for timber processing sector. The presented study is aimed at evaluation of the plantations of wide range of tree species at a research plot with typical site conditions for a large proportion of the Czech territory. The study plot was established at the Doubek locality in the Central Bohemia, cca 20 km E of Prague, in the 2nd and 3rd vegetation altitudinal zone on the arable land of medium fertility, corresponding to natural medium rich beech-oak and oak-beech forests (*Querceto fagetum and Fageto quercetum mesotrophicum*). The plantations were established in the autumn 2019. Besides the control plot, two variants with soil improvement were established, representing the surface application and ploughing-in of ameliorative materials Humac (1,0 t.ha^{-1}) and Alginit (1,5 t.ha^{-1}).

From the hardwood tree species, the plantations were established of plane tree (*Platanus acerifolia*), sweet chestnut (*Castanea sativa*), Turkish hazel (*Corylus colurna*), wild cherry (*Prunus avium*), service tree (*Sorbus torminalis*), English oak (*Quercus robur)*, lime tree, basswood (*Tilia cordata*) and hornbeam (*Carpinus betulus*). Other tree species were studied for comparison, such as Scots pine (*Pinus silvestris*), giant sequoia (*Sequoiadendron sempervirens*), cedar (*Cedrus atlantica*) and dawn redwood (*Metasequoia glyptostroboides*). In the next years, at the end of each vegetation season, the height growth was measured and evaluated. To the year 2023, no big effects were observed of soil improving materials. The site is naturally relatively rich, as well as the former use of agricultural lands contributed to the soil fertility improvement, so the soil improving with adding soil conditioners did not show big effects. The next research of the increment and soil effects must be applied.

INTRODUCTION

Forestry in the Czech Republic, as well as in the whole Central Europe, is facing mutual challenges – climatic extremes, pest outbreaks, industry changes, environmentalist demands. One of consequences is represented by large scale disturbances, even clear-cuts (MZe 2020, Novák et al. 2020). The change of species composition of forests is considered as one of the most important contributing factors (Modlinger and Trgala 2019) and the reversion of this trend is very important mitigating treatment. The contribution of hardwoods, native as well as introduced, represents one of important options, this approach needs detailed previous analysis and considerations (Podrázský and Remeš 2008, Brundu et al. 2020, Kuneš and Baláš 2020, Podrázský et al. 2020).

The possibilities of using exotic tree species in Czech forestry are contradictory. For example, Douglas-fir (*Pseudotsuga menziesii*) is already a well-established species in the sense of its legislative anchoring in Decree No. 298/2018 Coll., and thus in Management Units and Forest Management Plans (Novák et al. 2019), despite problems made by Nature Conservation bodies. However, this is not the case with woody plants such as the Atlas cedar (*Cedrus atlantica*), giant sequoia (*Sequoiadendron giganteum*), Chinese redwood (*Metasequoia glyptostroboides*), black walnut (*Juglans nigra*) or Northern red oak (*Quercus rubra*). Other potentially promising tree species are gaining importance in the conditions of a

warming climate: *Paulownia tomentosa* or southern oaks. Some of the promising tree species have already become domesticated outside the forest stands, such as the chestnut tree (*Castanea sativa*), some of them are even becoming invasive – tree of heaven (*Ailanthus altissima*) or black locust (*Robinia pseudoacacia*) - (Kuneš et al. 2019; Kuneš, Baláš 2020, Novotný et al. 2022).

Planting of exotic tree species can only be carried out on research plots outside the forest lands without much administrative effort. To determine their suitability and potential directly in practical forestry, it is necessary to thoroughly test the possibilities of their survival and growth, as well as their invasive potential (Kuneš et al. 2019; Vacek et al. 2020). For many of these species, there is missing even basic information on their growth and prosperity potential in the Czech condition, for these reasons, the intense and complex research is necessary. Aim of the presented study is to document the initial growth and prosperity of plantations of wider set of tree species respectively native and introduced hardwoods planted on agricultural land and effect of selected soil improving materials.

MATERIAL AND METHODS

The Doubek research area was established in the autumn of 2019 on private land, on agricultural (arable) land including plantation of majority of species. The fenced area is 1.55 hectares. Climatically, the selected locality falls into an area moderately warm and moderately humid with mild winters (Quitt 1971). The nearest climatic station is located in Ondřejov, about 13 km away. The long-term mean annual temperature is 9.8 °C and the long-term mean annual precipitation is around 550 mm. The area belongs to the Natural Forest Area (PLO) 10 – Central Bohemian Uplands, while in the north it is connected to PLO 17 – Polabí (FMI 2019). The area is prone to higher average summer temperatures as well as dry periods. In the studied locality, the soils are represented by modal cambisols (KAm) and lithic cambisols (KAs), a small part of the demarcated area for afforestation is partially covered by a thin layer of Pleistocene medium-heavy loess loam. In this part of the plot there are luvic cambisols (KAl). A slight terrain depression in the vicinity of the forested part is subsequently a typical representative of soils with periodic waterlogging and corresponds to the classification of the soil type of pseudogley modal (PGm). The evaluation of soil types and species was carried out according to the classification published by Němeček et al. (2011).

Plantings were carried out in autumn 2019, additional ones in spring 2020. They are divided into two parts. In the first part (Subplot I), the area was divided into 150 plots of 6x10 m, on which trees were planted (Figure 1) in a spacing of 1x1 m, in the case of giant sequoias and cedars 2x2 m and in rows of pine in a mixture at a distance of 1x2 m. In the case of mixed variants, the mixing is in-lines. The area consists of 4 blocks, within each of which 1 t/ha of Humac material or 1.5 t/ha of Alginit material was incorporated over the entire area of a strip. One strip within each block was without the application of amelioration materials. The blocks were separated by 1 free strip, on which other material was planted in the 2019/2020 season: Chinese redwood, rowan and cedar. There are other free areas available for testing other woods. Application of soil amendment material and replication design is presented in the Fig. 1.

In the second part (Subplot II), sweet chestnut, plane tree and Turkish hazel were planted in a spacing of about 1.5x1.5 m, and the areas were also treated with amelioration materials of the same dose. Another part of the area was planted with black walnut trees (not evaluated). The overall layout of the area is documented in Figure 1, and a detailed description is provided by Gallo et al. 2022. In the fall of each year, the heights of the seedlings are measured, and their quality is described according to a simple grading scale (1 – excellent, 2 – slightly deformed, 3 – forked, twisted, 4 – dying and dead).

Figure 1: Research plot Doubek – organization of the plantation and soil improvement experiment.
Soil amendments: A – Alginite, B – Humac, C – Control, no amendments
Tree species: 1. dub letní (Quercus robur), 2. borovice lesní (Pinus silvestris), Scots pine, 3. jeřá břek (Sorbus torminalis), 4. cedr + dub letní (Cedrus antlantica+Quercus robur), 5. třešeň ptačí + lípa (Prunus avium + Tilia cordata), 6. Habr + lípa (Carpinus betulus + Tilia cordata), kaštan (Castanea sativa), líska turecká (Corylus colurna), platan (Platanus acerifolia), dub letní (Quercus robur – buffer zone), kaštan + platan (Castanea + Platanus – buffer zone), ořech (Juglans nigra – buffer zone)

The STATISTICA software was used for statistical calculations. First, the nature of the distribution of the obtained data, or their normality, was assessed. After confirming the normal distribution of the data, a single-factor analysis of variance (ANOVA) was used followed by a post-hoc test according to Tukey. The significance level was chosen at the usual significance level ($\alpha = 0.05$). The differences of individual parameters (especially height and increment) between all three variants of the experiment were assessed,

i.e. which variant had the greatest influence on the height development of the same tree species (group of tree species). Differences in individual years were assessed. Values that differed significantly from each other were marked with different letters in the result tables. At the same time, the most basic results were expressed graphically. Mortality was assessed by the number of withered and/or missing seedlings at the end of the 2023 growing season. Selected results, focusing on important broad-leaved species, are presented in this study.

RESULTS AND DISCUSSION

Development of the plantations of selected hardwoods on the Doubek locality in the Subplot I is presented in the Figure 2 and Table 1. But it has to be emphasized, that the initial heights (H_{2020}) do not represent the plantation height but reflects the growth in the vegetation season in the 2020 year. With exception of cherry, the 2020 height of the planted individuals was comparable. In the next years, the particular species on the control variant showed specific growth dynamics. The slowest growth shows the oak. Slightly higher values were documented for hornbeam, followed by basswood (both in mixture with hornbeam and cherry), service tree (*S. torminals*) and the highest values were determined for wild cherry. So, the mean heights reached 183.6-195.0 cm in 2023 for oak and particular variants, cherry exhibited me heights between 328.5-353.5 cm for particular variants. The basswood individuals planted together with cherry were showing more intense growth than those with hornbeam. For oak and service tree, the visible increment depression was detected in the year 2023, other species stagnated in the height increment in this year.
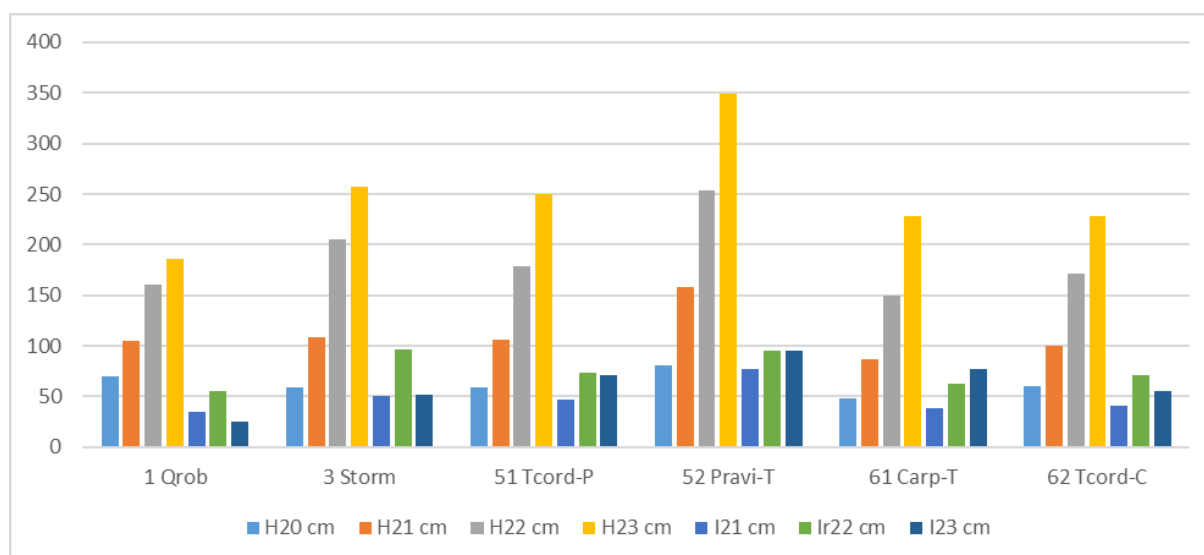
Figure 2: Mean height and mean annual height increment of different tree species in control variant on the research plot Doubek between 2020–2023 (cm). Abbreviations: Char. – characteristics, 1 Qrob – Quercus robur pure, 3 Storm – Sorbus torminalis, 51 – Tilia cordata mixture with cherry, 52 – Prunus avium in mixture with basswood, 61 – Carpinus betulus in mixture with basswood, 62 – Tilia cordata in mixture with hornbeam, H – height in respective year, I – height increment in respective year

On the plots treated by Humac, the general trend was similar, but with lower differences (Table 1). The oak presented significantly higher growth comparing to control variant (2023). Service tree expressed very similar growth dynamics between those two variants. Basswood showed significantly lower height increment for Humac variant since 2022, situation was similar for both mixtures with exception 2021 year, when the increment was higher at the amended variant. The cherry reacted with exception of the 2020 year negatively to the Humac application. Hornbeam did not show any visible trend.

As for Alhinit variant, the oak showed insignificantly lower height and higher increment, which depends on the lower initial height, determined by plantation. Service tree showed lower increment dynamics for this variant comparing to control, insignificant again, resulting in slightly lower total height in 2023. Basswood (*Tilia,* Tcord) in mixture with cherry showed significantly higher initial height, but also higher increment development. The same dynamics for this species, but insignificant, was documented for this species in the mixture with hornbeam. The cherry reacted significantly positive at the Alginit

application since beginning. Hornbeam height dynamics documented insignificantly negative effect of the Alginit. In general, the application of sol amendment materials did not affect the height increment of the studied species positively. This can be ascribed to the relative fertility of the afforested soil, where the soil improving potential of the studied materials is not visible.

Table 1: Dynamics of plantations of selected hardwoods at the Doubek locality –Subplot 1

Variant	Char.	Species					
		1 Qrob	3 Storm	51 Tcord-P	52 Pravi-T	61 Carp-T	62 Tcord-C
Alginit 1	H_{20} cm	59.9 a	59.0 a	63.4 b	88.8 c	48.5 a	60.9 a
Alginit 1	H_{21} cm	98.1 a	109.1 b	120.5 b	160.9 c	89.1 a	105.1 a
Alginit 1	H_{22} cm	153.3 a	200.7 a	193.5 c	258.0 c	143.5 a	175.5 a
Alginit 1	H_{23} cm	183.6 a	244.6 b	266.9 b	353.5 a	201.0 b	238.3 b
Alginit 1	I_{21} cm	38.2 a	50.1 c	57.1 b	72.2 b	40.6 a	44.2 b
Alginit 1	I_{22} cm	55,2 a	91.6 c	73.0 a	97.0 c	54.4 a	70.4 a
Alginit 1	I_{23} cm	30.3 b	43.9 a	73.4 a	95.5 a	57.5 a	62.8 a
Humac 2	H_{20} cm	75.5 a	57.4 a	59.2 a	81.8 b	50.6 a	62.2 a
Humac 2	H_{21} cm	110.9 a	111.6 a	102.7 a	153.1 b	88.9 a	106.2 a
Humac 2	H_{22} cm	162.5 a	206.4 a	168.9 b	240.5 b	151.1 a	173.8 a
Humac 2	H_{23} cm	195.0 b	258.9 a	231.7 a	328.5 a	222.7 a	230.2 a
Humac 2	I_{21} cm	35.4 a	54.1 b	43.5 a	71.3 b	38.3 a	43.9 b
Humac 2	I_{22} cm	51.6 a	94.8 b	66.2 b	87.4 b	62.2 a	67.6 a
Humac 2	I_{23} cm	32.5 b	52.5 b	62.8 b	88.0 a	71.6 a	56.4 a
Control 3	H_{20} cm	69.9 a	58.5 a	58.6 a	80.6 a	48.6 a	60.0 a
Control 3	H_{21} cm	105.3 a	108.8 a	105.7 a	158.1 a	87.4 a	100.5 a
Control 3	H_{22} cm	160.7 a	205.5 a	179.2 a	253.2 a	150.2 a	172.0 a
Control 3	H_{23} cm	186.4 ab	257.6 a	250.2 a	348.6 a	227.8 a	227.7 a
Control 3	I_{21} cm	35.5 a	50.3 b	47.1 a	77.5 a	38.8 a	40.6 a
Control 3	I_{22} cm	55.4 a	96.7 b	73.5 a	95.1 a	62.7 a	71.4 a
Control 3	I_{23} cm	25.7 a	52.1 a	71.0 a	95.4 a	77.6 a	55.7 a

Notes: Char. – characteristics, 1 Qrob – Quercus robur pure, 3 Storm – Sorbus torminalis, 51 – Tilia cordata mixture with cherry, 52 – Prunus avium in mixture with basswood, 61 – Carpinus betulus in mixture with basswood, 62 – Tilia cordata in mixture with hornbeam, H – height in respective year, I – height increment in respective year. The statistically significance was analysed within each species for different soil amendment variants.

The mortality of studied species at the Subplot I and their healthy state is documented in the Table 2. It was not analyzed statistically, there is only evaluated trend of: lower mortality especially for Alginit at oak, slightly higher mortality for Humac at service tee and basswood in mixture with cherry, lower mortality for Alginit at cherry, higher mortality for both amended variants at hornbeam and lower mortality for Humac at basswood in mixture with hornbeam. In general, the soil amendment did not contribute to mortality decrease and we cannot expect positive effects in the aspect.

Table 2: Total mortality and healthy state in the year 2023 for particular species and amendment variants – block I

Species	Mortality			Healthy state		
Variant	1 - Alg	2 - Hum	3 - Control	1 - Alg	2 - Hum	3 - Control
1 Qrob	10.2	12.5	16.0	1.07	1.06	1.10
3 Storm	6.5	8.5	6.2	1.03	1.02	1.04
51 Tcord-P	1.7	7.6	3.3	1.02	1.07	1.06
52 Pavi-T	6.7	10.5	10.4	1.02	1.01	1.03
61 Carp-T	37.5	32.9	23.3	1.04	1.07 a	1.02 b
62 Tcord-C	5.0	1.7	3.3	1.02	1.03	1.04

As for healthy state, the values were very favorable for all species, the very good growing individuals were totally prevailing. The only statistically proven evidence was the worse state of hornbeam individuals for Humac variant comparing to Control variant (Table 2).

The height dynamics and the height increment of species planted in the Subplot II, respectively of sweet chestnut, plane tree and Turkish hazel, is documented in the Table 3. The plane tree showed the highest growth dynamics comparing to other two species. The results did not indicate statistically significant differences, despite this fact it was visible the tendency of total heights and increment in the last year to be the biggest at the control variant.

Table 3: Average heights and final increments of chestnut, plane tree and Turkish hazel – Subplot II

Specie/Variant	Number 2023	H 2020	H 2021	H 2022	H 2023	Inc 2023
Chest – Alginit	110	44.8	71.8	109.5	150.3	40.8
Chest – Humac	107	43.1	69.7	102.2	142.6	40.4
Chest - Control	113	46.2	73.7	117.1	164.3	47.2
Plane – Alginit	110	67.4	153.1	197.0	244.1	47.1
Plane – Humc	114	57.1	112.1	148.8	182.3	**33.5 a**
Plane – Control	104	57.5	111.2	166.0	221.2	**55.2 b**
Hazel – Alginit	45	32.0	70.3	112.5	154.6	42.1
Hazel – Humac	38	32.1	57.9	98.3	132.0	**33.78 a**
Hazel - Control	22	40.4	70.1	107.2	175.7	**68.4 b**

Notes: The different indexes mark statistically significant result, their absence statistical homogeneity

The height increment was significantly lowered for Humac variant and for plane tree and Turkish hazel. Both soil amendment materials showed no effects, even negative growth effects in the studied conditions at the relatively fertile site.
The highest mortality was registered in the first year of plantation growth, no big differences were found among variants (Table 4). Only slight tendency of higher mortality for control is visible for plane tree and Humac variant mortality also shows non-significant trend.

Table 4: Mortality of chestnut, plane tree and Turkish hazel – Subplot II

Number of dead/missing individuals in particular years + Mortality 2023					
Vqariant	**2020**	**2021**	**2022**	**2023**	**Mortality 2023**
Chest – Alginit	16	0	1	1	13.8
Chest – Humac	21	0	1	1	17.7
Chest - Control	16	0	0	0	12.3
Plane – Alginit	15	0	5	0	15.4
Plane – Humac	16	0	0	0	12.3
Plane – Control	19	0	4	3	20.0
Hazel – Alginit	3	0	2	2	13.5
Hazel – Humac	10	0	2	2	26.9
Hazel - Control	3	0	0	1	16.0

The introduced hardwoods were of minor importance to the last years, despite the general rules for their use and relevance in disposable (Brundu et al. 2020, Novotný et al. 2022, Wohlgemuth et al. 2022). More attention was paid to the coniferous species (e.g., Novák et al. 2019, 2020, Podrázský, Remeš 2008). Their broader use in the future needs more detailed approach and analysis, which is at the

beginning at this moment. The comparison with other fertilization and soil improving experiments shows clear relation with the site fertility and soil treatments – at more fertile sites the effects are minor (Gallo et al. 2021). The Alginit was of a minor importance evidenced also in other research plots (Kupka et al. 2015), some minor effects were visible only in few first years since plantation establishment. This agrees with our recent knowledge. Application of similar amendment materials should be restricted, based on up-to-date experience, at sites with extreme, poor soil with low adsorption capacity.

CONCLUSIONS

The research provided at the Doubek locality shows only very preliminary results. The effects of soil improving materials are only minor, they did not improve the initial growth and vitality of plantations to significant extent. Their use is probably of higher importance at poor and extreme soils. On the contrary, service tree (*Sorbus torminalis*) and wild cherry (*Prunus avium*) exhibited growth superiority to oak (*Quercus robur*). The lime tree (*Tilia cordata*) should be planted carefully with oak, it shows more fast initial growth, suppressing potentially the oak in mixture. At similar sites, sweet chestnut (*Castanea sativa*), plane tree (*Platanus acerifolia*) and Turkish hazel (*Corylus colurna*) are also promising species. The hardwoods need more oriented research in the future I any case.

ACKNOWLEDGEMENTS

REFERENCES

Brundu G., Pauchard A., Pyšek P., Pergl J., Bindewald A.M., Brunori A., Canavan S., Campagnaro T., Celesti-Grapow L., de Sá Dechoum M., Dufour-Dror J.M., Essl F., Flory S.L., Genovesi P., Guarino F., Guangzhe L., Hulme P., Jäger H., Kettle J.C., Krumm F., Langdon B., Lapin K., Lozano V., Le Roux J.J., Novoa A., Nuñez M.A., Porté A.J., Silva J.S., Schaffner U., Sitzia T., Tanner R., Tshidada N., Vítková M., Westergren M., Wilson J.R.U., Richardson D. (2020) Global guidelines for the sustainable use of non-native trees to prevent tree invasions and mitigate their negative impacts. NeoBiota, 61: 65–116.

Gallo J., Záruba J., Baláš M., Podrázský V. (2022) Research plot Doubek – introduced tree specieas on the agricultural land (Výzkumná plocha Doubek – introdukované dřeviny na zemědělské půdě). In: Nové poznatky ve výzkumu introdukovaných dřevin. Sborník příspěvků, Česká lesnická společnost, s. 45–18. ISBN 978-80-02-02981-6 (In Czech)

Gallo J., Vacek Z., Vacek S. (2021) Quarter of century of forest fertilization and liming research at the Department of Silviculture in Prague, Czech Republic. Central European Forestry Journal, 67(2): 123-134

Kuneš I., Baláš M., Gallo J., Šulitka M., Pinidiya Arachchilage C. (2019) Black locust (*Robinia pseudoacacia*) and its role in Czech and Central European space: review (Trnovník akát (*Robinia pseudoacacia*) a jeho role ve středoevropském a českém prostoru: review). Zprávy lesnického výzkumu, 64(4): 181–190. (In Czech)

Kuneš I., Baláš M. (2020) Black locust (*Robinia pseudoacacia*) – its propagation, silviculture and eradication: review (Trnovník akát (*Robinia pseudoacacia*) – jeho množení, pěstování a likvidace: review). Zprávy lesnického výzkumu, 65: 1: 11–19. ISSN 0322-9688, eISSN 1805-9872. (In Czech)

Kupka I., Prknová H., Holubík O., Tužinský M. (2015) Algae-based materials effect on mortality and initial growth of plantations of the forest tree species (Účinek přípravku na bázi řas na ujímavost a odrůstání výsadeb lesních dřevin). Zprávy lesnického výzkumu 60(1): 24-28. (In Czech)

Modlinger R., Trgala K. (2019) Possible causes and consequences of the bark-beetle calamity in Czech Forests owing to specific calamity timber management (Možné příčiny a důsledky kůrovcové kalamity v lesích Česka s ohledem na specifika při zpracování kalamitního dříví). Praha: ČZU v Praze, 41 pp. ISBN 978-80-213-2942-3 (In Czech)

MZe (2020) Report on forests and forestry sector state in the Czech Republic in year 2019 (Zpráva o stavu lesa a lesního hospdářství v České republice v roce 2019). Praha. 128 p. ISBN: 978-80-7434-571-5 (In Czech and English)

Němeček J., Mühlhanselová M., Macků J., Vokoun J., Vavříček D., Novák P. (2011) Taxonomic classification system of soils in the Czech Republic. 2nd edition (Taxonomický klasifikační systém půd České republiky. 2. upravené vydání). Česká zemědělská univerzita Praha. 94 p. ISBN 978-80-213-2155-7. (In Czech)

Novák J., Dušek D., Kacálek D. (2019) Growth of plantations of Douglas-fir in mixture with native species at different forest sites (Růst kultur douglasky ve směsi s domácími dřevinami na různých lesních stanovištích). Zprávy lesnického výzkumu, 64: 3: 133–139. (In Czech)

Novák J., Kacálek D., Dušek D. (2020) Litterfall nutrient return in thinned young stands with Douglas fir. Central European Forestry Journal 66(2): 78–84. https://doi.org/10.2478/forj-2020-0006

Novotný P., Fulín M., Bažant V. (2022) Catalogue of introduced tree soecies taxons with potential of forestry use on sites with lower moisture availability. Certified methodic (Katalog taxonů introdukovaných dřevin s potenciálem lesnického využití na stanovištích s nižší dostupností vláhy. Certifikovaná metodika). Lesnický průvodce 1/2022. VÚLHM, 196 p. ISSN 0862-7657 (In Czech)

Podrázský V., Remeš J. (2008) Soil forming role of important introduced tree species – Douglas-fir, grand fir and Eastern white fir (Půdotvorná role významných introdukovaných jehličnanů – douglasky tisolisté, jedle obrovské a vejmutovky). Zprávy lesnického výzkumu 53(1): 27–34. ISSN 0862-7657(In Czech)

Podrázský V., Vacek Z., Vacek S., Vítámvás J., Gallo J., Prokůpková A., D'Andrea G. (2020) Production potential and structural variability of pine stands in the Czech Republic: Scots pine (*Pinus sylvestris* L.) vs. introduced pines–case study and problem review. Journal of Forest Science, 66(5): 197–207. https://doi.org/10.17221/42/2020-JFS

Quitt E. (1971) Climatic regions of the Czechoslovakia (Klimatické oblasti Československa). Praha, Academia. (In Czech)

Vacek Z., Vacek S., Eşen D., Yildiz O., Král J., Gallo J. (2020) Effect of Invasive *Rhododendron ponticum* L. on Natural Regeneration and Structure of *Fagus orientalis* Lipsky Forests in the Black Sea Region. Forests, 11(5): 603.

Wohlgemuth T., Gossner M.M., Campagnaro T., Marchante H., van Loo M., Vacchiano G., Castro-Diez P., Dobrowolska D., Gazda A., Keren S., Keseru Z., Koprowski M., La Porta N., Marozas V., Nygaard P.H., Podrázský V., Puchalka R., Reisman-Berman O., Straigyte L., Ylioja T., Potzelsberger E., Silva JS. (2022) Impact of non-native tree species in Europe on soil properties and biodiversity: a review. NeoBiota, 78: 45–69.

Poster Session

Light response curve analysis of juvenile Püspökladányi and Üllői black locust

Tamás Ábri[1], Zsolt Keserű[1*], József Csajbók[2]

[1] University of Sopron, Forest Research Institute, Department of Plantation Forestry, Farkassziget 3, Püspökladány, Hungary, 4150
[2] University of Debrecen, Faculty of Agricultural and Food Sciences and Environmental Management, Institute of Crop Sciences, Böszörményi Str. 138, Debrecen, Hungary, 4032

E-mail: abri.tamas@uni-sopron.hu; keseru.zsolt@uni-sopron.hu; csj@agr.unideb.hu

Keywords: Robinia pseudoacacia, net assimilation, intercellular CO_2 level, stomatal conductance, light response curve, carbon fixation.

ABSTRACT

Assimilation (A), intercellular CO_2 level (C_i) and stomatal conductance (total conductance of $CO_2 = g_{tc}$) light response curves (A/PPFD, C_i/PPFD, g_{tc}/PPFD curves) of 2-year-old promising black locust clone 'Püspökladányi' and the registered one, 'Üllői', were analyzed, aiming to study A, C_i and g_{tc} in function of Photosynthetic Photon Flux Density (PPFD) levels. The natural logarithmic (A/PPFD and C_i/PPFD) and quadratic (g_{tc}/PPFD) regression functions fitted well to the measured data points for both parameters. The R^2 value for the A/PPFD is 0.9745 for 'Püspökladányi' and 0.9444 for the 'Üllői' variety. The R^2 values were 0.9499 ('Püspökladányi') and 0.8629 ('Üllői') for the g_{tc}/PPFD curves and 0.8950 ('Püspökladányi') and 0.9112 ('Üllői') for the C_i/PPFD curves. The A/PPFD curves of the tested clones increased steadily with increasing illumination level, but it flattened at the 600 µmol m^{-2} s^{-1} PPFD level, which is due to the effect of photorespiration on the assimilation rate. For 'Üllői', the A/PPFD curve decreased at the 1500 µmol m^{-2} s^{-1} PPFD level. In contrast to the results for A/PPFD, the C_i/PPFD curve decreased with increasing PPFD level. In case of g_{tc}/PPFD curve, g_{tc} values peak at 900 µmol m^{-2} s^{-1} PPFD level for 'Püspökladányi' and 600 µmol m^{-2} s^{-1} PPFD level for 'Üllői'. We found significant differences between the A values, as well as the g_{tc} ones. In Europe, negative changes, e.g. increasingly frequent drought, heat, uneven distribution of precipitation, etc., in climate are predicted for the future. Under such conditions, relatively drought-tolerant tree species such as black locust will play an important role in new afforestation and uninterrupted wood supply. Consequently, the growing and improvement of black locust, included the ecophysiological studies of relatively drought tolerant, newly-bred clones is of growing importance.

INTRODUCTION

Black locust (*Robinia pseudoacacia* L.) is one of the most widespread exotic tree species in Europe (Nicolescu et al. 2020). Due to its high site plasticity, its versatile uses (wood industry, agriculture, beekeeping, environmental development) and its high quality, durable wood, it is a dominant tree species in Hungarian forestry, especially in the Nyírség region (Nicolescu et al. 2018). The ecological challenges facing forests and tree plantations, the negative effects of global and local climate change, and the various weather events (uneven rainfall, drought, frequent heat waves, etc.) have become increasingly frequent in recent years (IPCC 2023; Vacek et al. 2023). Under water stress, the rate of photosynthesis decreases, stomata close and stomatal conductance (g_{tc}) becomes low, resulting in a decrease in intercellular CO_2 concentration (C_i) depending on the intensity of photosynthesis. And thus, these parameters affect tree growth (Farquhar and Sharkey 1982, Ashraf and Harris 2013, Meng et al. 2014). Under these conditions, relatively drought-tolerant tree species such as black locust will play an important role in new afforestation. Consequently, the growing and improvement of black locust is of increasing importance. In Hungary, research projects to improve the yield and stem quality of black locust were started in the 1960s (Ábri et al. 2023a). In a recent project newly-bred black locust clones are tested. In this trial we study the growth and physiological parameters of these clones, compared to the state-approved 'Üllői' black locust cultivar (Ábri et al. 2023b).

In this study we focused on 'Püspökladányi' candidate cultivar. We studied its net assimilation (A), stomatal conductance (g_{tc}) and intercellular CO_2 level (C_i) in function of Photosynthetic Photon Flux Density (PPFD), the light response curves (A/PPFD, C_i/PPFD, g_{tc}/PPFD) compared to the registered 'Üllői' black locust genotype.

MATERIALS AND METHODS

With the new clones ('Püspökladányi' – PL251, 'Farkasszigeti' – PL040, 'Laposi' – NK1, 'Napkori' – NK2) and the 'Üllői' cultivar, a clone trial was established in 2020 in a slightly acidic, low humus sandy soil, near the settlement of Napkor in the Nyírség region, where the the annual mean temperature was 10.6 °C, and the annual mean precipitation was 537 mm. 1-year-old vegetatively propagated rooted seedlings were planted in 3 different planting spacings: 2.5×2.5 m; 3×3 m; 4×4 m (Ábri et al. 2023b). Our measurements were carried out in the planting spacing 2.5×2.5 m.

Physiological parameters for light response curves of 2-year-old candidate cultivar 'Püspökladányi' and 'Üllői' black locust were measured on 29 June 2021. Portable photosynthesis system (LI-6800, LI-COR, Lincoln, NE, USA) was used to measure net assimilation rate, stomatal conductance to CO_2 and intercellular CO_2 levels. It can be also used to analyse transpiration, leaf water vapour saturation, and air and leaf temperatures (LI-COR 2024). The light was controlled in the sample chamber of the instrument with 90% red (625 nm) and 10% blue (475 nm) light. PPFD (Photosynthetic Photon Flux Density) was decreased in 8 levels (1500, 1200, 900, 600, 300, 150, 50, 0 µmol µmol m^{-2} s^{-1}). A LI-6800-01A fluorometer head was used as light source, the measured area of the leaf was 2 cm^2. The concentration of CO_2 was also controlled (400 µmol mol^{-1}) in the sample chamber using an injector and CO_2 cartridges. Light-adapted leaves were measured four times per leaf on three plants per plot (12 measurements/clone in total). Data were recorded after the measurement results had stabilised (coefficient of variation < 1%), but after at least 120 s.

RESULTS AND DISCUSSION

Light response curves of clone 'Püspökladányi' and the state-approved 'Üllői' were analysed. There was significant difference ($p = 0.05$) in the assimilation rate between the 'Püspökladányi' and the 'Üllői' at all PPFD levels, and the difference was higher at the higher photon flux densities. The natural logarithmic regression functions fit well to the measured data points (R^2 values are 0.9444 and 0.9745), so the curves of the functions showed clearly the differences. At the low PPFD levels, from 0 to 300 µmol m^{-2} s^{-1} the 'Üllői' variety had higher assimilation rate, but as the light intensity increased, the 'Püspökladányi' clone had higher photosynthesis rate, the curve of 'Üllői' ran lower than that of the other at higher than 300 µmol m^{-2} s^{-1} photon flux density level. The assimilation rate of the clone 'Püspökladányi' increased to the 1500 µmol m^{-2} s^{-1} PPFD level. In 'Üllői' cultivar the assimilation rate decreased above 1200 µmol m^{-2} s^{-1} PPFD (Figure 1).

Figure 1: Assimilation rate (A) light response curve of black locust clones 'Püspökladányi' and 'Üllői'. Note: PPFD = Photosynthetic Photon Flux Density (Napkor, 29/6/2021)

For C_i the natural logarithmic regression functions also fit well to the measured data points (Figure 2), the R^2 values are 0.9499 ('Püspökladányi') and 0.8629 ('Üllői'). From the obtained results, the C_i of the

tested black locust clones decreased with increasing light intensity. At low PPFD levels (0-300 µmol m^{-2} s^{-1}), the clone 'Püspökladányi' produced the higher value (422.63-328.25 µmol mol^{-1}), but the differences were not significant at p = 5%. However, at higher PPFD levels (600-1500 µmol m^{-2} s^{-1}), the 'Üllői' had the highest values (301.55-280.18 µmol mol^{-1}), which were significant at 600; 1200 and 1500 µmol m^{-2} s^{-1} PPFD levels ($p < 0.05$). The C$_i$ values of clone 'Püspökladányi' varied between 271.73 µmol mol^{-1} and 236.13 µmol mol^{-1} at PPFD levels 600; 900; 1200 and 1500 µmol m^{-2} s^{-1}.
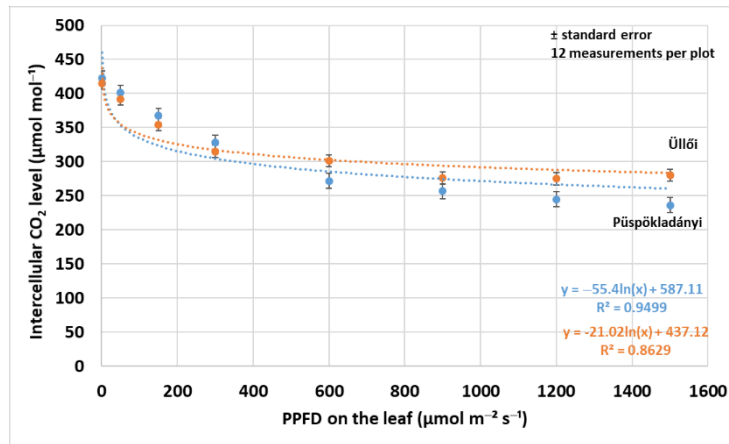
Figure 2: Intercellular CO₂ level (C_i) light response curve of black locust clones 'Püspökladányi' and 'Üllői'. Note: PPFD = Photosynthetic Photon Flux Density (Napkor, 29/6/2021)

For g$_{tc}$, the quadratic regression functions fit well to the measured data points (R^2 values are 0.8950–0.9112). When examining the g$_{tc}$ of clones 'Püspökladányi' and 'Üllői' as a function of PPFD, the present study found significant ($p < 0.05$) differences at every PPFD level. The g$_{tc}$ values peak at 900 µmol m^{-2} s^{-1} PPFD level for 'Püspökladányi' (0.1595 mol m^{-2} s^{-1}) and 600 µmol m^{-2} s^{-1} PPFD level for 'Üllői' (0.1543 mol m^{-2} s^{-1}). Furthermore, the clone 'Püspökladányi' had significantly higher g$_{tc}$ values at all the PPFD levels (Figure 3).

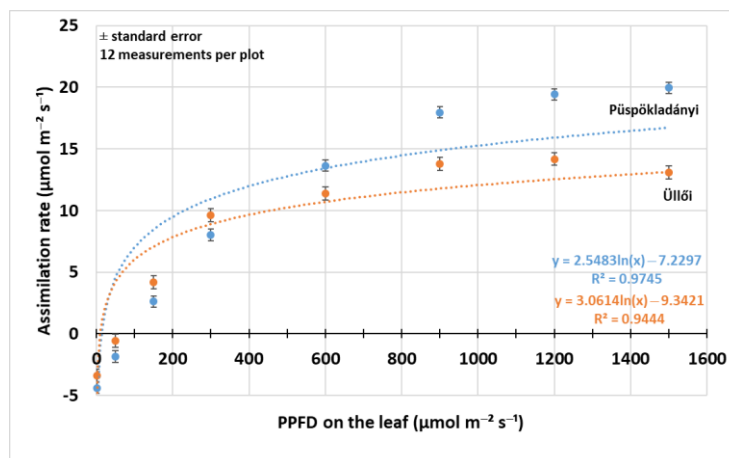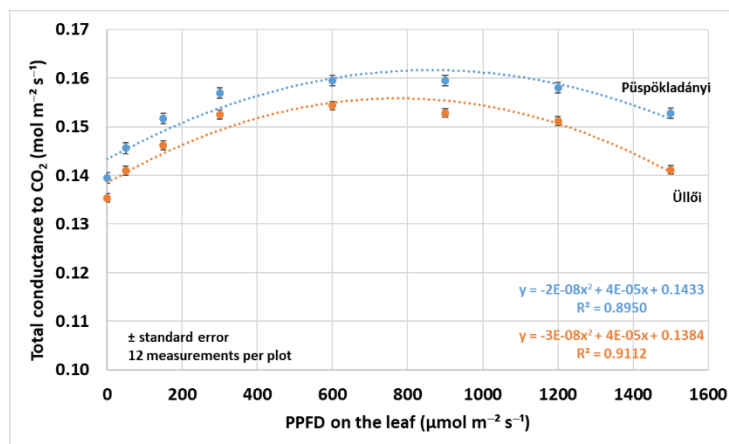***Figure 3: Total stomatal conductance (g_tc) light response curve of black locust clones 'Püspökladányi' and 'Üllői'. Note: PPFD = Photosynthetic Photon Flux Density (Napkor, 29/6/2021)***

CONCLUSIONS

Nowadays, the study of physiological parameters (photosynthesis, carbon sinking, water use management, etc.) of relatively drought tolerant tree species, such as black locust, is crucial for local and global forest managements. In this paper, we presented an early evaluation of light response curves of newly-bred black locust clone ('Püspökladányi'), compared to the state-approved cultivar ('Üllői'). We found that logarithmic (assimilation and intercellular CO_2 level) and quadtaric (stomatal conductance) regression functions fitted well to the measured data points, the R^2 values were higher than 0.85 in all cases. Furthermore, there were significant ($p < 0.05$) differences between 'Püspökladányi' and 'Üllői' for assimilation and stomatal conductance values at all photosynthetic photon flux density levels. Based on the results, it is likely that the 'Püspökladányi' clone has better shade tolerance than the 'Üllői' variety and also makes better use of more intense lighting conditions. Clone 'Püspökladányi' seems to be a promising black locust clone, which is suitable for industrial tree plantations.

ACKNOWLEDGEMENT

REFERENCES

Ábri T, Cseke K, Keserű Z, Porcsin A, Szabó FM, Rédei K (2023a) Breeding and improvement of black locust (*Robinia pseudoacacia* L.) with a special focus on Hungary: a review. iForest 16(5):290. https://doi.org/10.3832/ifor4254-016

Ábri T, Borovics A, Csajbók J, Kovács E, Koltay A, Keserű Z, Rédei K (2023b) Differences in the Growth and the Ecophysiology of Newly Bred, Drought-Tolerant Black Locust Clones. Forests 14(9):1802. https://doi.org/10.3390/f14091802

Ashraf M, Harris PJC (2013) Photosynthesis under stressful environments: An overview. Photosynthetica 51:163–190. https://doi.org/10.1007/s11099-013-0021-6

Farquhar GD, Sharkey TD (1982) Stomatal conductance and photosynthesis. Ann Rev Plant Physio 33(1):317–345. https://doi.org/10.1146/annurev.pp.33.060182.001533

IPPC (2023) AR6 Synthesis Report: Climate Change 2023. https://www.ipcc.ch/report/ar6/syr/ Accessed 19 Feb 2024

LI-COR (2024) LI-6800 (LI-COR) Portable Photosynthesis System. https://www.licor.com/env/products/photosynthesis/LI-6800/ Accessed 20 Feb 2024

Meng F, Peng M, Pang H, Huang F (2014) Comparison of photosynthesis and leaf ultrastructure on two black locust (*Robinia pseudoacacia* L.). Biochem Syst Ecol 55:170–175. https://doi.org/10.1016/j.bse.2014.03.025

Nicolescu VN, Hernea C, Bakti B, Keserű Z, Antal B, Rédei K. (2018) Black locust (*Robinia pseudoacacia* L.) as a multi-purpose tree species in Hungary and Romania: a review. J Forestry Res 29:1449–1463. https://doi.org/10.1007/s11676-018-0626-5

Nicolescu VN, Rédei K, Mason WL, Vor T, Pöetzelsberger E, Bastien JC, Brus R, Benčať T, Đodan M, Cvjetkovic B, Andrašev S, La Porta N, Lavnyy V, Mandžukovski D, Petkova K, Roženbergar D, Wąsik R, Mohren GMJ, Monteverdi MC, Musch B, Klisz M, Perić S, Keça L, Bartlett D, Hernea C, Pástor M (2020) Ecology, growth and management of black locust (*Robinia pseudoacacia* L.), a non–native species integrated into European forests. J Forestry Res 31(4):1081–1101. https://doi.org/10.1007/s11676-020-01116-8

Vacek Z, Vacek S, Cukor J (2023) European forests under global climate change: Review of tree growth processes, crises and management strategies. J Environ Manage 332:117353. https://doi.org/10.1016/j.jenvman.2023.117353

Revealing the optimum configuration of heat-treated wood dowel joints by means of Artificial Neural Networks and Response Surface Methodology

Bogdan Bedelean[1*], Cosmin Spîrchez[1]

[1] Transilvania University of Brașov, Faculty of Furniture Design and Wood Engineering, B-dul Eroilor nr.29, Brașov, Romania

E-mail: bedelean@unitbv.ro; cosmin.spirchez@unitbv.ro

Keywords: heat-treated wood joints, artificial neural networks, response surface methodology, optimization.

ABSTRACT

The most used joint in furniture construction is the dowel joint because it has a low cost and it is easy to be obtained from technological point of view. Various factors can affect the strength of dowel joints, including wood species, dowel characteristics, number of dowels, adhesive type and consumption, tightness of fit, etc. Because heat-treated wood has inferior mechanical properties compared to untreated wood, an optimization tool could be used in the designing phase of the furniture for appropriate sizing of joints. Therefore, in this work, an optimization tool is proposed. The tool consists in combining the artificial neural networks modelling technique and response surface methodology to reveal the optimum configuration of heat-treated wood dowel joints. The joints were made from heat-treated ash (*Fraxinus excelsior*). Polyvinyl acetate adhesive was uniformly dosed and applied in each hole of the joints using a syringe and a glass rod. The factors examined were dowel length, dowel diameter, and adhesive consumption. The compressive and tensile strength of the were the responses. The load was applied at a constant speed until a major separation between the two parts occurred. The ultimate failure loads were obtained during testing the joints. The joints were tested by using a universal testing machine. The obtained data set was randomly divided in two subsets. One subset was used to develop two neural networks. One is able to predict the compressive strength of joints loaded in compression and the other to predict the tensile strength of joints loaded in tension. The accuracy of the designed ANN models was checked with the other subset of data. Both ANN models have shown a reasonable predictive accuracy. These models were used to complete various experimental designs, which were used to reveal the optimal configuration of heat-treated wood dowel joints.

INTRODUCTION

The dowel joint (Figure 1) is one of the most used joint in furniture construction. This is due to the fact that has a favorable cost and production characteristics (Eckelman 2003). Factors such as dowel length, dowel diameter, distance between dowels, adhesive consumption could influence the strength of dowel joints, which could be revealed through experimental and/or various modeling techniques. In this work, two modelling techniques, namely, Artificial Neural Network (ANN) and Response Surface Methodology (RSM), have been integrated, to reveal the optimum configuration of heat-treated wood dowel joints. During the RSM four experimental designs were used, namely, face centered, rotatable, orthogonal and practical. The value of responses for each analyzed experimental design were filled by means of two ANN models that are able to predict the compression (525 N – 5370 N) and tension (1170 N – 9720 N) strength of heat-treated wood dowel joints based on dowel length (30 - 70mm), dowel diameter (6 – 10 mm) and adhesive consumption (250 – 450 g/m²). More information about the designed ANN models used in this work could be found in the literature (Răcășan et al. 2020).

Response surface methodology is a statistical technique that can be used to determine the optimal solution for a specific process. The optimization of a process consists in revealing the value factors when the analyzed response is maximized or minimized. The optimization process through RSM implies to follow the next main steps: generate an experimental design (*e.g.* central composite design (CCD)). In this design, various combinations among values of factors are generated. For each combination the value of response is reveal through experiments or simulations. The regression equation that describes the relationship between factors and response is figure out. ANOVA is applied to reveal which factors and

coefficients are significant from statistical point of view. Equations in coded form could be used to determine the influence of analyzed factors on the analyzed response or responses. The equations in real form could be used to make prediction for various scenarios. Moreover, the regression equation is solved through an optimization algorithm to reveal the optimum combination of factors that correspond to the desired response or responses of the analyzed process. More information regarding the RSM method could be found in the literature (Zu et al. 2015, Georgescu et al. 2019).
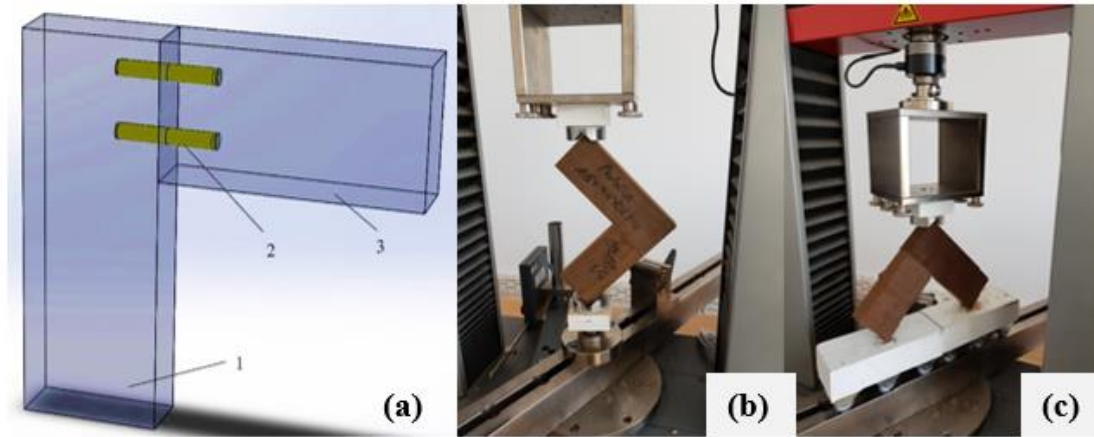
Figure 1: The L-shaped dowel joint (a) and the testing approach used for compression (b) and tension (c). 1 – leg; 2 – dowels; 3 – rail

MATERIALS AND METHODS

The parts wood joints (Figure 1) were obtained from heat-treated ash (*Fraxinus excelsior*) boards. The dowels were made of Beach (*Fagus sylvatica*) wood. A D4 polyvinyl acetate adhesive (Kleiberit 303) was used to assembly the part of the joints. To limit the possible excess of adhesive on the strength of joint, sheets of wax paper were applied between the rail and leg of joints (Dalvand et al. 2014). The joints were subjected to diagonal compressive (Figure 1b) and tensile tests (Figure 1c) by using a universal testing machine Zwick Roell Z10 (Zwick GmbH&Co. KG, Ulm, Germany). A constant speed of 3mm per minute was applied till a visible separation of leg or trail was observed with the naked eye. The value of the ultimate failure load was recorded for each dowel joint. More information regarding the testing procedure could be found in the literature (Kasal et al. 2015, Kuzman et al. 2015, Georgescu et al. 2019). The experimental designs, namely, face centered, rotatable, orthogonal quadratic and practical design (Tables 1, 2, 3 and 4) were generated through Design Expert Software (version 9, Stat-Ease Inc., Minneapolis, MN, USA). For each combination of factors, the value of tension and compression strength were revealed through ANN models, which were developed in a previous study (Răcăşan et al. 2020).

The Design-Expert software uses the desirability function approach during the multiple response optimization study. The optimization criteria were to maximize the compressive and tensile strength of heat treated wood dowels joints. The optimization study, starts by converting each response (Y_i), into an individual desirability function (d_i), which may have a value between 0 and 1. If the analyzed response fulfills the optimization goal, the $d_i = 1$. All individual desirabilities are combined by means of geometric mean that describes the overall desirability, D (Eq.1) (NIST/SEMATECH 2012):

$$D = \left(d_1(Y_1) \text{ x } d_2(Y_2) \text{ x} \ldots \text{ x } d_n(Y_n)\right)^{1/n} \tag{1}$$

where n represents the responses being optimized.

Table 1: The value of factors and responses in the case of Face Centered Design

Run	Dowel length (X_1), [mm]	Dowel diameter (X_2) [mm]	Adhesive consumption (X_3) [g/m²]	Response 1 Tension strength (Y_1), [N]	Response 2 Compressive strength (Y_2), [N]
1	70 (+1)	10 (+1)	250 (-1)	2851.96	1672.59
2	30 (-1)	8 (0)	350 (0)	3515.11	2046.89
3	50 (0)	8 (0)	350 (0)	3515.11	2046.89
4	50 (0)	8 (0)	350 (0)	3515.11	2046.89
5	30 (-1)	10 (+1)	250 (-1)	2851.96	1672.59
6	70 (+1)	6 (-1)	250 (-1)	2851.96	1672.59
7	30 (-1)	6 (-1)	250 (-1)	2851.96	1672.59
8	30 (-1)	6 (-1)	450 (+1)	4294.03	2467.97
9	50 (0)	8 (0)	350 (0)	3515.11	2046.89
10	30 (-1)	10 (+1)	450 (+1)	4294.03	2467.97
11	50 (0)	8 (0)	250 (-1)	2851.96	1672.59
12	50 (0)	8 (0)	350 (0)	3515.11	2046.89
13	70 (+1)	6 (-1)	450 (+1)	4294.03	2467.97
14	70 (+1)	8 (0)	350 (0)	3515.11	2046.89
15	50 (0)	6 (-1)	350 (0)	3515.11	2046.89
16	50 (0)	8 (0)	450 (+1)	4294.03	2467.97
17	50 (0)	8 (0)	350 (0)	3515.11	2046.89
18	50 (0)	8 (0)	350 (0)	3515.11	2046.89
19	70 (+1)	10 (+1)	450 (+1)	4294.03	2467.97
20	50 (0)	10 (+1)	350 (0)	3515.11	2046.89

Table 2: The value of factors and responses in the case of rotatable design

Run	Dowel length (X_1), [mm]	Dowel diameter (X_2) [mm]	Adhesive consumption (X_3) [g/m²]	Response 1 Tension strength (Y_1) [N]	Response 2 Compressive strength (Y_2), [N]
1	50 (0)	10 (+1.682)	350 (0)	3515.11	2046.89
2	38.10 (-1)	6.81 (-1)	290.54 (-1)	3103.06	1817.19
3	61.89 (+1)	6.81 (-1)	409.46 (+1)	3979.33	2293.26
4	50 (0)	8 (0)	350 (0)	3515.11	2046.89
5	50 (0)	8 (0)	350 (0)	3515.11	2046.89
6	50 (0)	6 (-1.682)	350 (0)	3515.11	2046.89
7	50 (0)	8 (0)	250 (-1.682)	2851.96	1672.59
8	38.10 (-1)	6.81 (-1)	409.46 (+1)	3979.33	2293.26
9	38.10 (-1)	9.18 (+1)	290.54 (-1)	3103.06	1817.19
10	70 (+1.682)	8 (0)	350 (0)	3515.11	2046.89
11	61.89 (+1)	6.81 (-1)	290.54 (-1)	3103.06	1817.19
12	50 (0)	8 (0)	350 (0)	3515.11	2046.89
13	50 (0)	8 (0)	350 (0)	3515.11	2046.89
14	38.10 (-1)	9.18 (+1)	409.46 (+1)	3979.33	2293.26
15	61.89 (+1)	9.18 (+1)	290.54 (-1)	3103.06	1817.19
16	50 (0)	8 (0)	350 (0)	3515.11	2046.89
17	50 (0)	8 (0)	350 (0)	3515.11	2046.89
18	30 (0)	8 (0)	350 (0)	3515.11	2046.89
19	50 (0)	8 (0)	450 (+1.682)	4294.03	2467.97
20	61.89 (+1)	9.18 (+1)	409.46 (+1)	3979.33	2293.26

Table 3: The value of factors and responses in the case of orthogonal quadratic design

Run	Dowel length (X₁), [mm]	Dowel diameter (X₂) [mm]	Adhesive consumption (X₃) [g/m²]	Response 1 Tension strength (Y₁), [N]	Response 2 Compressive strength (Y₂), [N]
1	63.11 (+1)	6.68 (-1)	284.41 (-1)	3063.82	1794.66
2	63.11 (+1)	9.31 (+1)	284.41 (-1)	3063.82	1794.66
3	36.88 (-1)	6.68 (-1)	284.41 (-1)	3063.82	1794.66
4	63.11 (+1)	6.68 (-1)	415.58 (+1)	4028.15	2319.39
5	63.11 (+1)	9.31 (+1)	415.58 (+1)	4028.15	2319.39
6	70 (+1.525)	8 (0)	350 (0)	3515.11	2046.89
7	50 (0)	8 (0)	350 (0)	3515.11	2046.89
8	50 (0)	8 (0)	450 (+1.525)	4294.03	2467.97
9	36.88 (-1)	6.68 (-1)	415.58 (+1)	4028.15	2319.39
10	50 (0)	10 (+1.525)	350 (0)	3515.11	2046.89
11	50 (0)	8 (0)	350 (0)	3515.11	2046.89
12	50 (0)	6 (-1.525)	350 (0)	3515.11	2046.89
13	36.88 (-1)	9.31 (+1)	284.41 (-1)	3063.82	1794.66
14	36.88 (-1)	9.31 (+1)	415.58 (+1)	4028.15	2319.39
15	50 (0)	8 (0)	350 (0)	3515.11	2046.89
16	50 (0)	8 (0)	350 (0)	3515.11	2046.89
17	50 (0)	8 (0)	350 (0)	3515.11	2046.89
18	50 (0)	8 (0)	350 (0)	3515.11	2046.89
19	50 (0)	8 (0)	250 (-1.525)	2851.96	1672.59
20	30 (-1.525)	8 (0)	350 (0)	3515.11	2046.89

Table 4: The value of factors and responses in the case of practical design

Run	Dowel length (X_1), [mm]	Dowel diameter (X_2) [mm]	Adhesive consumption (X_3) [g/m²]	Response 1 Tension Strength (Y_1), [N]	Response 2 Compressive Strength (Y_2), [N]
1	50 (0)	8 (0)	350 (0)	3515.11	2046.89
2	65.19 (+ 1)	9.51 (+1)	274.01 (-1)	2998.40	1756.98
3	50 (0)	10 (+1.316)	350 (0)	3515.11	2046.89
4	50 (0)	8 (0)	350 (0)	3515.11	2046.89
5	65.19 (+1)	9.51 (+1)	425.98 (+1)	4110.33	2363.95
6	65.19 (+1)	6.48 (-1)	274.01 (-1)	2998.40	1756.98
7	34.80 (-1)	6.48 (-1)	274.01 (-1)	2998.40	1756.98
8	50 (0)	8 (0)	350 (0)	3515.11	2046.89
9	30 (-1.316)	8 (0)	350 (0)	3515.11	2046.89
10	34.80 (-1)	9.51 (+1)	274.01 (-1)	2998.40	1756.98
11	50 (0)	8 (0)	350 (0)	3515.11	2046.89
12	50 (0)	8 (0)	350 (0)	3515.11	2046.89
13	70 (+1.316)	8 (0)	350 (0)	3515.11	2046.89
14	65.19 (+1)	6.48 (-1)	425.98 (+1)	4110.33	2363.95
15	50 (0)	8 (0)	250 (-1.316)	2851.96	1672.59
16	34.80 (1)	9.51 (+1)	425.98 (+1)	4110.33	2363.95
17	50 (0)	6 (-1.316)	350 (0)	3515.11	2046.89
18	50 (0)	8 (0)	350 (0)	3515.11	2046.89
19	34.80 (-1)	6.48 (-1)	425.98 (+1)	4110.33	2363.95
20	50 (0)	8 (0)	450 (+1.316)	4294.03	2467.97

RESULTS AND DISCUSSION

The optimal solutions that were revealed by the Design Expert software are presented in Table 5. The specified optimization criteria was to maximize both the tensile and compressive strength. The optimal solution are different for each analysed design. For each design at least two combinations could be used to obtain the same compressive or tensile strength. The face centered composite design lead both to practical technological solutions and high strength resistance. The other experimental designs required values that are not easy to obtain in special for dowel diameter. The desirability coefficient of this solutions is among the 0.77 and 0.98. The highest value was obtained for the solutions obtained through a face centered composite design. On the other hand, the lowest value of desirability coefficient was in the case of rotatable design. The practical experimental design obtained a higher desirability coefficient than orthogonal quadratic.

Table 5: Optimal solutions in the case of analyzed experimental designs

Input variable	Rotatable design				Orthogonal quadratic design				Practical design		Face cantered design		
Dowel length, [mm]	62		38		37		63		35	65	30	50	70
Dowel diameter, [mm]	9.2	6.8	6.8	9.2	6.68	9.31	6.68	9.3	6.5	9.5	6	10	8 6
Adhesive consumption, [g/m²]	409				416				426		450		
Output variable													
Compression strength, [N]	2292				2319				2364		2456		
Tensile strength, [N]	3973				4023				4107		4265		
Desirability coefficient, [-]	D=0.77				D=0.81				D=0.86		D=0.98		

CONCLUSIONS

In this work, four experimental design were analyzed to revealed the optimal configuration of wood dowel joints, which were realized from heat treated wood. The compressive and tensile strength for each analyzed configuration were established through two ANN models, which were designed in a previous work. The face centered composite design lead both to practical technological solutions and high strength resistance. In a future work, the simulation results, should be compare with experimental data.

REFERENCES

Dalvand M, Ebrahimi G, Tajvidi M, Layeghi M (2014) Bending moment resistance of dowel corner joints in case-type furniture under diagonal compression load. J Forestry Res 25: 981-984. https://doi.org/10.1007/s11676-014-0481-y

Eckelman CA (2003) Textbook of Product Engineering and Strength Design of Furniture, Purdue University Press, West Lafayette, IN, USA.

Georgescu S, Varodi AM, Răcăşan S, Bedelean B (2019) Effect of the dowel length, dowel diameter, and adhesive consumption on bending moment capacity of heat-treated wood dowel joints. Bioresources14: 6619-6632. https://doi.org/10.15376/biores.14.3.6619-6632

Kasal A, Eckelman CA, Haviarova E, Erdil YZ, Yalcin I (2015) Bending moment capacities of L-shaped mortise and tenon joints under compression and tension loadings. BioRes 10:7009 – 7020.

Kuzman MK, Kutnar A, Ayrilmis N, Kariz M (2015) Effect of heat treatment on mechanical properties of selected wood joints. Eur. J. Wood Prod. 73:689-691.

NIST/SEMATECH (2012) e-Handbook of Statistical Methods. Available online: http://www.itl.nist.gov/div898/handbook/ Aaccessed on 15 March 2024.

Racasan S, Bedelean B, Georgescu S, Varodi AM (2020) Comparison between artificial neural networks and response surface methodology to predict the bending moment capacity of heat-treated wood dowel joints. Biores 15:5764-5775.

Zhu C, Zhai X, Li L, Wu X, Li B (2015). Response surface optimization of ultrasound-assisted polysaccharides extraction from pomegranate peel. Food Chemistry 177:139-146. https://doi.org/10.1016/j.foodchem.2015.01.022

Artificial neural networks as a predictive tool for thrust force and torque during drilling of wood-based composites

Bogdan Bedelean[1*], Mihai Ispas[1], Sergiu Răcăşan[1]

[1] Transilvania University of Brașov, Faculty of Furniture Design and Wood Engineering, B-dul Eroilor nr.29, Brașov, Romania

E-mail: bedelean@unitbv.ro; ispas.m@unitbv.ro; sergiu.racasan@unitbv.ro

Keywords: drilling, wood and wood-based materials, artificial neural networks, thrust force, drilling torque.

ABSTRACT
Wood drilling represents a mandatory operation, which is used to generate holes that are needed to assure a successful connection of furniture parts. Up to now, a considerable and very diverse thematic research has been recently carried out on drilling. Many studies deal with factors that affects the drilling process such as: type of processed material, type of drill bit, drill bit diameter, drill bit tip angle, feed rate, spindle rotation speed, but a few studies address the modelling of the drilling process by means of artificial neural network, which is a machine learning technique that simulates the working mechanism of the human brain. Therefore, in this study, the artificial neural networks modelling technique was applied to predict the thrust force and torque during drilling of wood-based composites, namely, prelaminated particleboards, medium density fiberboard and plywood. The analyzed independent variables were: the drill bit tip angle, the tooth bite, the drill type (helical or flat) and the processed material type. The dependent variables were two dynamic parameters that affect both quality and the energy consumption during drilling of wood and wood-based materials, namely, the trust force and the drilling torque. The data set that was used in this study was obtained through experiments. The samples were drilled on a CNC machine centre. The obtained data set was randomly divided in two subsets. One subset was used to develop two neural networks – one that is able to predict the thrust force, and the other to predict the drilling torque. The accuracy of the designed ANN models was checked with the other subset of data. All analyzed independent variables play a significant role on the performance of models, which was quantified though coefficient of determination and graphical comparation. Based on the obtained results, it could be stated that the designed ANN models have the ability to predict the thrust force and torque during drilling of wood-based composites with a high accuracy. The models could be included in various decision support systems that are used in wood processing industry.

INTRODUCTION
Wood based composites like particleboard (PB), medium density fiberboards (MDF) and plywood are used in big quantities by the furniture industry. The furniture parts made from wood based boards must be drilled to a specific location in order to be assembled. The efficiency of drilling process is quantified through tool durability, cost and quality of holes. Many studies deal with factors that affect the drilling process of wood and wood-based boards (tip angle of the drill bit, feed rate, type of drill (flat or helical), type of material (solid wood, MDF, PB, plywood etc.), diameter of the drill and so on (Gorsky 2022). These studies were conducted through experiments and various modelling approaches like Response Surface Methodology, Taguchi optimization method, Grey Relational Analysis, Artificial Neural Network (Gaitonde et al. 2008, Prakash and Palanikumar 2010, Ispas and Răcăşan 2015, Ispas and Răcăşan 2017, Ayyildiz et al. 2021, Bedelean et al. 2023). From all these methods, the Artificial Neural Networks (ANN) was successful involved in modelling of drilling process. Zbieć (2011) developed a neural network to monitor tool wear during MDF milling based on machined surface temperature, cutting force, thrust force, and power consumption. Jegorowa et al. (2020) propose an automatic system to detect the drill bit condition by measuring various signals during machining. Bedelean et al. (2022) involved ANN to predict the drill tip angle, tooth bite, and drill type on delamination factor, thrust force, and drilling torque during drilling of prelaminated wood particle board. However, there is limited information about the modeling of wood and wood-based material drilling through ANN. Therefore, the

objective of this study consists in developing two ANN models that can predict the trust force and drilling torque based on four independent variables, namely, drill tip angle, tooth bite, drill type (helical or flat) and processed material type (wood particle board, medium density fiberboards and plywood).

MATERIALS AND METHODS
The experiments

Eight drill bits with 10mm cutting diameter were used: 4 flat drill bits (rake angle $\gamma = 0°$) and 4 twist (helical) drill bits. They had different tip angles ($2\kappa r = 30°, 60°, 90°, 120°$). The selected drills are presented in Figure 1. The clearance angle of the drills was $\alpha = 20°$. The symbols used for these drills were tip angle related: T30, T60, T90, T120.
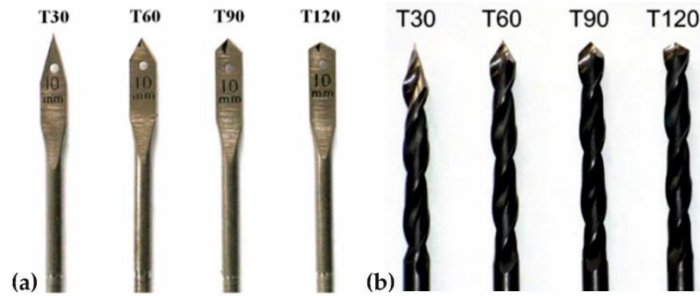
Figure 1: The drill bits used for drilling of wood-based samples. Flat drills (a) and helical drills (b)

Eighty square samples (□80mm) were cut from a single 18mm thick MDF. Another 80 samples were cut from an 18mm thick particleboard and another 80 from a similar plywood board with the same thickness (Figure 2). Each of the three groups of 80 samples were divided into 8 smaller groups of 10 samples each. Each specimen was drilled with four different drills (T30, T60, T90, T120, flat respectively helical). Each group of ten specimens was drilled with a different feed speed so that the tooth bite (f_z), was different, having the following values: 0.1, 0.3, 0.5 and 0.7mm. The rotation speed of the drills was the same, n = 3000rpm. This led to four feed speed values (v_f) = 0.6, 1.8, 3.0 and 4.2m/min.
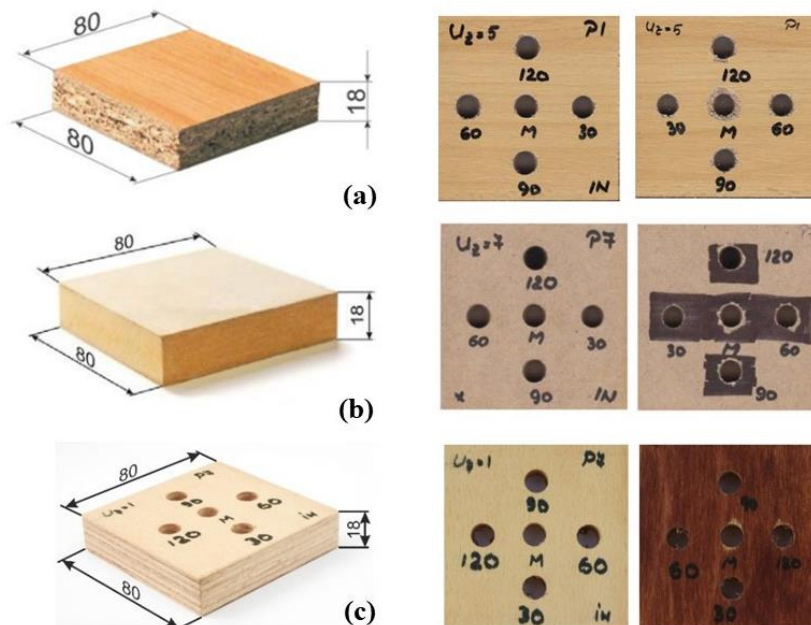
Figure 2: The wood based samples that were used during drilling experiments
(a – wood particle board, b - medium density fiberboard and c – plywood)

The drilling was done on a CNC processing center type ISEL GFV/GFY, which allowed the exact set-up of the tool rotation speed and of the feed speeds. Three HBM force transducers type S2 (nominal

force: 500N) were used to measure the thrust force. The measurement of the active power consumed by the spindle motor was performed by a Camille Bauer Sineax P530/Q531 transducer for active and reactive power. For data recording, a DAQ Board Keithley Model KUSB-3108 was used with the help of the Keithley KUSB QuickDataAcq software. Data recording was done with a frequency of 100 values/sec. simultaneously on all four channels: three for force sensors and one for the active power. More information regarding the experimental data could be found in the literature (Bedelean et al. 2023, Bedelean et al. 2022, Ispas and Răcăşan 2017, Ispas and Răcăşan 2015).

Data modeling

The ANN models were developed based on 382 experimental values (80% of available data set) by means of NeuralWorks Predict Software (NeuralWare Inc., v.3.24.1, Carnegie, PA, USA). The developed phase included the training and testing of neural networks. The other part of data set, 95 experimental values (20% of available data set), was used to validate the ANN models, namely, to check out how well the developed networks perform with data that was not used during the designing phase. According to Table 1, the independent variables were drill tip angle (X_1), tooth bite (X_2), drill type (X_3) and material type (X_4). The dependent variables were thrust force (Y_1) and drilling torque (Y_2). The data set that was used in this study contained 477 values.

Table 1: The level of independent variables that were considered in the study

| Independent variable	Values			
Drill tip angle (X_1), °	30	60	90	120
Tooth bite (X_2), mm	0.1	0.3	0.5	0.7
Drill type (X_3)	Flat		Helical	
Material type (X_4)	PB	MDF	Plywood	

The performance of ANN models, which were developed in this study, was quantified using the most applied indicators in literature, namely, coefficient of correlation (R), coefficient of determination (R^2), root mean square error (RMSE) and the mean absolute percentage error (MAPE) (Özşahin and Singer 2022). The corresponding equations are:

$$R = \frac{\sum_{i=1}^{n}(p_i - \bar{p})(a_i - \bar{a})}{\sqrt{\sum_{i=1}^{n}(p_i - \bar{p})^2}\sqrt{\sum_{i=1}^{n}(a_i - \bar{a})^2}} \tag{1}$$

$$R^2 = 1 - \frac{\sum_{i=1}^{n}(a_i - p_i)^2}{\sum_{i=1}^{n}(a_i - \bar{p}_i)^2} \tag{2}$$

$$RMSE = \sqrt{\frac{1}{n}\sum_{i=1}^{n}(a_i - p_i)^2} \tag{3}$$

$$MAPE = \frac{1}{n}\left(\sum_{i=1}^{n}\left[\left|\frac{a_i - p_i}{a_i}\right|\right]\right) \times 100 \tag{4}$$

Where: a_i is the experimental value, p_i is the predicted value of ANN model, $\bar{a}$ is the mean of experimental values; $\bar{p}$ is the mean of predicted values, n is the total number of values.
Another approach to check how well the neural network models performed with the unseen data set is to plot the predicted values against experimental data (Tiryaki et al. 2017).

RESULTS AND DISCUSSION

A typical Multi-Layer Perceptron (MLP) architecture is presented in Figure 3. This architecture contains the input layer, the hidden layer and the output layer. The input layer receives the input signals and transmits the signals to the hidden layer to be processed. The output layer receives the signals from the hidden layer(s) and shows the results of the network. A MLP architecture may contain one or more hidden layers in function to the complexity of the problem. In the case of the ANN model, which were developed to predict the thrust force, it was revealed that the optimal architecture of ANN model contains four neurons in the input layer, eight neurons for the hidden layer and one neuron in the output

layer (4 – 8 – 1). Regarding the MLP architecture that was designed to predict the drilling torque, the optimum configuration is 4-4-1. The coefficient of correlation during training and testing phase was almost 0.98 for both designed ANN models. The performance indicators of developed ANN models, which are presented in table 3, characterize the models as having a high precision. Moreover, the plots presented in Figures 4 and 5 support this statement.
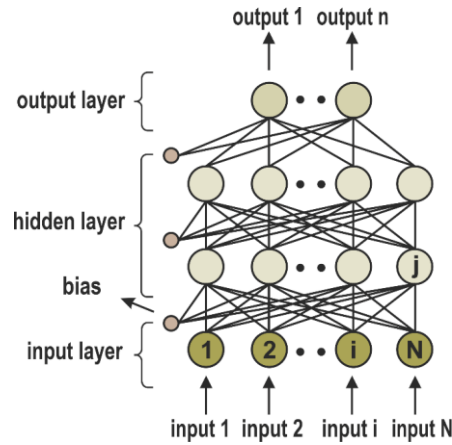
Figure 3: The Multi-Layer Perceptron Architecture

Table 3: The performance indicators obtained during the validation phase

Performance Indicator	ANN model for thrust force	ANN model for drilling torque
R	0.98	0.96
R^2	0.96	0.94
RMSE	20.57	0.129
MAPE	10.4	11.25
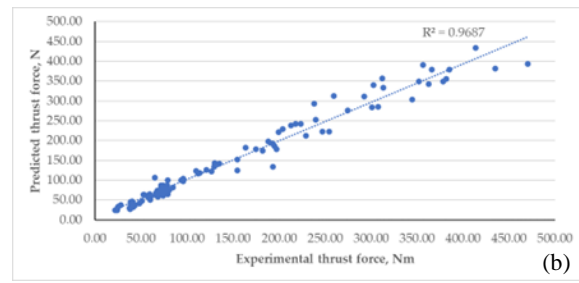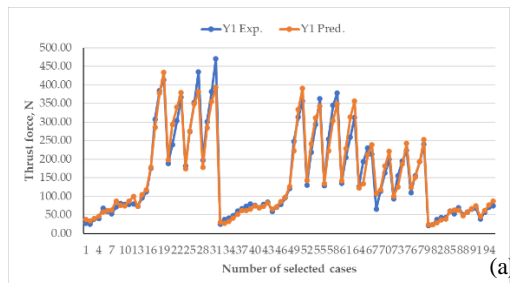
Figure 4: A graphical comparison between experimental and predicted values of thrust force using a line graph (a) and a scatter plot (b)
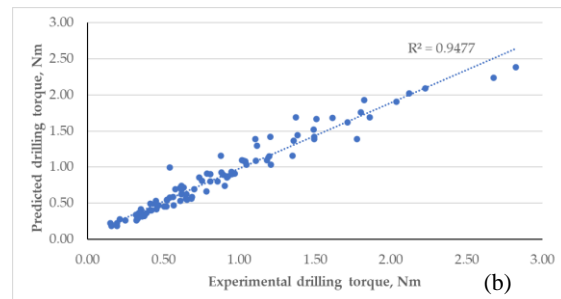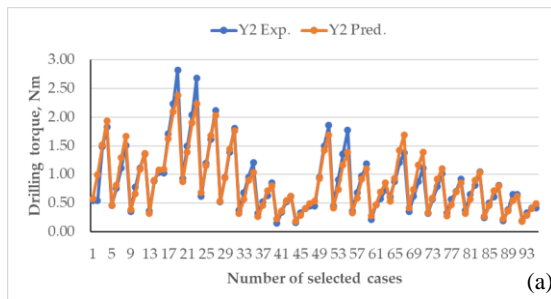
Figure 5: A graphical comparison between experimental and predicted values of drilling torque a line graph (a) and a scatter plot (b)

CONCLUSIONS

In this study, the artificial neural network modeling technique was used to predict the trust force and drilling torque during drilling of three types of wood-based materials, namely, prelaminated particleboards, medium density fiberboards and plywood. The inputs of the ANN models were drill tip

angle, tooth bite, drill type and material type. Since both models performed good during the validation phase, they can be used together with response surface methodology or other optimization techniques to reveal the optimum condition during drilling of wood and wood-based materials. Moreover, in a further study, other inputs like drill diameter, tool wear, rotation speed and including the delamination factor among the outputs of the model (thrust force and drilling torque) could be addressed.

REFERENCES

Ayyildiz EA, Ayyildiz M, Kara F (2021) Optimization of Surface Roughness in Drilling Medium-Density Fiberboard with a Parallel Robot. Adv. Mater. Sci. Eng. 2021:1-18 https://doi.org/10.1155/2021/6658968.

Bedelean B, Ispas M, Răcășan S (2023) Applying the Artificial Neural Network and Response Surface Methodology to Optimize the Drilling Process of Plywood. Appl. Sci. 13:1-16 https://doi.org/10.3390/app132011343

Bedelean B, Ispas M, Răcășan S, Baba MN (2022) Optimization of Wood Particleboard Drilling Operating Parameters by Means of the Artificial Neural Network Modeling Technique and Response Surface Methodology. Forests 13: 1-13. https://doi.org/10.3390/f13071045.

Gaitonde VN, Karnik SR, Davim JP (2008). Taguchi multiple-performance characteristics optimization in drilling of medium density fibreboard (MDF) to minimize delamination using utility concept. J Mater Process Technol *196*:73–78. https://doi.org/10.1016/j.jmatprotec.2007.05.003.

Górski J (2022) The review of new scientific developments in drilling in wood-based panels with particular emphasis on the latest research trends in drill condition monitoring. Forests 13: 1- 11 https://doi.org/10.3390/f13020242

Ispas M, Răcășan S (2015) The influence of the tool point angle and feed rate on the dynamic parameters at drilling coated particleboard. Pro Ligno 11:457–463.

Ispas M, Răcășan, S (2017) Study regarding the influence of the tool geometry and feed rate on the drilling quality of MDF panels. Pro Ligno 13:174–180.

Jegorowa A, Górski J, Kurek J, Kruk M (2020) Use of nearest neighbors (k-NN) algorithm in tool condition identification in the case of drilling in melamine faced particleboard. Maderas Cienc Tecnol 22:189-196. http://dx.doi.org/10.4067/S0718-221X2020005000205.

Özşahin S, Singer H (2022) Prediction of noise emission in the machining of wood materials by means of an artificial neural network. New Zeal J For Sci 52:1-10. https://doi.org/10.33494/nzjfs522022x92x

Prakash S, Palanikumar K (2010) Modeling for prediction of surface roughness in drilling MDF panels using response surface methodology. *J Compos Mater 45*:1639–1646. https://doi.org/10.1177/0021998310385026

Tiryaki S., Özşahin Ş, Aydin A (2017) Employing artificial neural networks for minimizing surface roughness and power consumption in abrasive machining of wood. Eur. J. Wood Prod 75: 347–358. https://doi.org/10.1007/s00107-016-1050-1

Zbieć M (2011) Application of neural network in simple tool wear monitoring and identification system in MDF milling. *Drv Ind 62*: 43–54. https://doi.org/10.5552/drind.2011.1020

Research on the value retention of hardwood products in the spirit of sustainability

Daniel Bodorkós[1*] , József Zalavári[1] , Péter György Horváth[1]

[1] University of Sopron, Institute of Creative Industries, Sopron, Hungary, 9400 Bajcsy-Zs. Str. 4.

E-mail: BodorkosDaniel@phd.uni-sopron.hu; zalavari.jozsef@uni-sopron.hu; horvath.peter.gyorgy@uni-sopron.hu

ABSTRACT
The concept of value retention is linked to a specific social stratum, which, in addition to age and various existential values, is determined by the product's styling, formal appearance, and the complexity of the product's use-related or quality-related and other added values and properties. The value and durability include everything that, due to the quality of the furniture and form, are the signs by which it becomes fashion-proof. The aim of this study is to take a new approach to these levels, in the spirit of sustainability, in the mechanism of the value of wood products, but also their definition.

INTRODUCTION
Among hardwood products, furniture is suitable for testing in several ways. Hardwood products have been chosen because the basis of the experiment is concentrated on these materials, and it is planned to extend the experiment to include non-hardwood species in the future. Furniture has become a part of our lives, according to Anthropogenesis, our closest relative is homo sapiens, which appeared approximately 200,000 years ago as a result of a long evolutionary development, simultaneously with this process, the appearance of the first primitive tools, the term or items such as "furniture", can also be dated to this time. (Kaesz, 1978) With the appearance of man came the advent of culture, which is the information that one individual of a given species passes on to another by teaching or example. Culture has changed and shaped the whole course of our development. (Attenborough, 2022) Civilizations have emerged or come into existence. (Acuna-Soto et al, 2005) Over time, the tool and material culture that surrounds people developed in parallel with mental and other endowments (Howard). In addition to these tools, there have also been developments in the various mobilities. Among these objects are the chest furniture made for storing crops, food, and later clothes, which over time expanded in function, structure, and design, and became more and more sophisticated. A simple example of the evolution of the form of objects is how, over time, mankind came from an archetype of a chair with an average sitting function, the tree trunk, to the Lounge Chair designed by Eames or the high-tech office chair of cutting-edge design. (Gy. Kaesz 1978)

RESEARCH AND METHODS
The primary objective of the research is to examine the development of value retention factors in relation to wooden furniture, which is based on the relationship between the sustainability of wooden products and the synergy of their long life cycle. Products can be assigned different subjective values, derived from emotions and experiences. According to the interpretation of literary value retention (Bárczi G. and Ország L. 1959), a material, object, or tool can be described as having a character or property that satisfies a need and is appreciated by the individual or society. In relation to quality and quality issues, relevant findings made by Szintay (Szintay et al., 2011), which, in addition to the definitions of quality, also examine ethical aspects and make statements on these issues, as Turcsányi also writes about in his thesis (Turcsányi, 2014). According to Veress (Veress, 2015), the essence of quality is to satisfy the needs of those involved in consumption and production. Products that meet quality criteria through design are recognized through various design awards. The criteria for these awards are based on compliance with the following criteria: humanity, sincerity, innovation, aesthetics, and design ethics. These are complemented by additional criteria such as attractive appearance, excellent function, and performance, high quality, user-friendly product. (G-Mark Org. 2024)

The quality thus formulated was one of the most optimal starting points for the research, and the findings related to the study of wooden toys were as follows: With regard to wooden products and toys, a company founded by a master carpenter Ole Kirk Christiansen, the company known today as LEGO, should be mentioned (Andersen, 2022). The company has a history of several decades, in whose values the production, manufacturing, and sale of wooden products of the highest quality that serve the users and that are passed down from generation to generation, have been given maximum importance. Ole has recognized learning through play as an important means of developing children's creativity. Building sets are crucial for children's development, and play has an essential role at this age, a topic that Sebestyén has described in depth in his thesis "Development opportunities with LEGO® sets in early childhood education" (Sebestyén et al. 2020). The LEGO ecosystem as we know it today can be compared to the Mercedes-Benz AG philosophy of "Best or Nothing". The popularity of wooden toys is still unbroken and they are considered eco-friendly products.

The various construction toys and models of trains, cars, and doll houses that can be found on the shelves of toy stores to this day are still a significant number of products made of wood, alongside other plastic products. The findings were based on visits to various toy stores and an examination of their product ranges.

METHODS

To support our theories, we used in-depth interviews involving 27 people. In this way, the data necessary for the research was collected and analyzed through users. In this way, we collected and analyzed data through users. The people included in the study represented different social levels, both financial and marital status, single or in a partnership. The age range chosen for the study was 25-45 years of age, with different social and value levels. This age group is the most likely to have established a home and existential values. The guided questions were freely answered by the participants in the experiment. This data was recorded and used for the research, analysis, and evaluation, and the findings were used to look for correlations. The interview questions focused on sustainability and the purchase and use of wood products, which aimed to understand users' motivations. From the subjective opinions and information of the participants in the study, which emerged from the interview responses, it was concluded that the need for sustainability is becoming increasingly important for wood products. Simultaneously with sustainability, the study also focused on the conceptual definition of value constancy in the field of individual subjectivity. For wooden furniture, the origin of the products is an increasingly important factor, with subjects considering whether the product is FSC certified as an important aspect. The average of the formulations in the interviews did not differ from the definition in the literature. It can be concluded that sustainability, recyclability, expandability, product durability, and repairability were also factors highlighted by the interviewees as important for modern society. From these responses, it can be concluded that the fate of our planet is an increasingly important factor for users. Closely related to the results of our research, and supporting our findings, is a definition already made at the 1987 UN General Assembly (Brundlandt, 1987), which states that "The Earth is one, but the world is not. The life of all of us depends on the same biosphere to sustain life." These factors are the guiding principles for the 21st century, as exemplified by the "Ecodesign for Sustainable Products Regulation", ESPR for short, and the ESG goals.

RESULTS AND DISCUSSION

In the case of products, quality can be considered a defining indicator. Which means that for a given product, a product with a higher quality attribute is better than a product with a lower quality attribute. Moreover, quality should also be guaranteed. This feature distinguishes a higher quality product from a commercial product In the interviews, it can be said that quality can also be associated with an indicator and attribute such as reliability. For a product, reliability can be associated with low maintenance and longevity. The findings on the issue of reliability, for a given product, which can be found in the literature, are based on the thesis of Szabó (Szabó és Nagy, 2009) the study of new levels of quality management provides answers. A product is considered to have a long life if it is not completely worn out by use and wear and tear during its life cycle, which is defined by the company that manufactures and markets it. In the case of wooden products, an object with such a long life can be, for example, a cabinet or a chair. During the interviews, one of the interviewed persons mentioned a wooden chest in his possession, which dates back more than 100 years. In addition, emotions are also attached to the

chest. An important object on which the family's life events were recorded, such as the birth of a child (engraved inscription on the chest): "Mariska child", which usually includes years, serves as an imprint. According to a metaphorical interpretation, an object that looks almost worthless, a wooden chest, represents value for someone or some people. It still performs its original function to this day. From this data, it can be concluded that the concept of value has an individual, subjective level. In the case of the furniture pieces, the quality in the use of materials, the accuracy of the joints, and the precise processing are the factors that were determined as a result of the interviews. The upper limit of the age range surveyed, which included an older age group in the guided interviews, is that for earlier generations, furniture was inherited, having served in a household for up to 50-60 years. In this way, it can be concluded that such pieces of furniture have a long service life. From the interviews and the study, it can be said that the furniture is replaced every 7 years on average. The following data were used to answer the question of how new furniture is chosen: replacement is influenced by many factors, most of which are fashion, changing needs, and the level of depreciation. However, it is also stated in the survey and experience that there are cases when a piece of furniture is replaced, and the worn-out, outdated piece of furniture or wooden toy is disposed of by selling or giving it away. In the past, this trend was typical for families to pass on their assets, furniture, and household items over generations. With the advent of globalization and the consumer society, which began to disappear in the 1950s, this model, fortunately, is experiencing a renaissance again today This allows the wooden product to start a new life in another place, creating a cycle. An example of this is the presence of type furniture. They play an important role, these items are still in use in some older households. They are highly valued. The late sixties was the era of the type of furniture, with mass-produced, high-precision, and made-to-measure furniture and elements appearing on the market, giving birth to the hit furniture of the seventies and eighties (Sári, 2021). These later evolved into the various flat-pack products, which incorporate the stylistic elements and material variations of the modern era, which can be observed in the product range of multinational companies in the present day (Tóth, 2001). As time has passed, it can be said that the mobility of structural solutions and flat-pack furniture is still present on the market.

CONCLUSIONS

With regard to the different hardwood products, which focus on their durability and sustainability studies, by analyzing the subjective opinions of the people interviewed through guided interviews, it can be stated that the archetype of the literary definition of durability does not differ from personal motivations and opinions. Wooden products are present in our environment almost from the beginning of our lives, whether it is a children's bed, a children's toy, and in the course of development in relation to various wood-based products, such as a cabinet, chair, or any other utility device. With the passage of time and the use of products, an attachment to the object develops, which becomes subjective values and experiences in the person of the individual. In addition, the definition of value depends not only on emotions but also on existential values developed over the years. In the course of the study, it can be established by the basic knowledge and the interview that sustainability plays an increasingly important role. The collection and incorporation of knowledge from the area and the user value system into a sustainable study of the lifespan of wooden products and furniture requires further research work, during which deeper connections and new levels of knowledge are defined.

REFERENCES

David Attenborough (2022) Egy élet a bolygónkon c. könyv [A Life On Our Planet,], Park Könyvkiadó ISBN9789633558720

György, Istvánfi (2011) Őskor Népi Építészet - Az építészet története [Prehistoric Folk Architecture - The History of Architecture]. Terc Kereskedelmi és Szolgáltató Kft. ISBN 9789639968240

Rodolfo Acuna-Soto, David W Stahle, Matthew D Therrell, Sergio Gomez Chavez, Malcolm K Cleaveland, (2005). Drought, epidemic disease, and the fall of classic period cultures in Mesoamerica (AD 750-950). Hemorrhagic fevers as a cause of massive population loss, https://doi.org/10.1016/j.mehy.2005.02.025; https://education.nationalgeographic.org/resource/key-components-civilization/

Russell Howard Tuttle (2000). Refinements in tool design, https://www.britannica.com/science/human-evolution/Refinements-in-tool-design

Furniture Design History (2016.03.03.) https://www.onlinedesignteacher.com/2016/02/furniture-design-history.html [2024.02.26.]

György, Kaesz Ismerjük meg a bútorstílusokat [Learn about furniture styles], Gondolat Kiadó, ISBN 9632806425, p4. - p. 222.

G. Bárczi, L. Ország (1959-1962) A Magyar nyelv értelmező kéziszótára I-VII. Kötet [The Explanatory Dictionary of the Hungarian Language], Szövegrögzítő: Arcanum Adatbázis Kft., XML-konverzió, Webprogramozás: Vitéz Gábor (2016), https://mek.oszk.hu/adatbazis/magyar-nyelv-ertelmezo-szotara/elolap.php

EU ESPR, 2009L0125 — EN — 04.12.2012 — 001.001 — 1, https://eur-lex.europa.eu/legal-content/EN/TXT/PDF/?uri=CELEX:02009L0125-20121204&from=EN, https://commission.europa.eu/energy-climate-change-environment/standards-tools-and-labels/products-labelling-rules-and-requirements/sustainable-products/ecodesign-sustainable-products-regulation_en

UN General Assembly Resolution nr. 70/1 2015. Transforming our world: the 2030 Agenda for Sustainable Development. 35 old. https://undocs.org/en/A/RES/70/1

LEGO History (2024) https://www.lego.com/en-us/history [2024.02.15.]

Mercedes-Benz Group, INNOVATION, A History of Making History, This Is What Makes "The Best or Nothing." https://www.mbusa.com/en/best-or-nothing/innovation [2024.02.20.]

Nobsi / Kiigesellid OÜ Harju tee 29 Aruküla, Raasiku ESTONIA 75201, Five advantages of wooden toys for children, https://mynobsi.com/five-advantages-of-wooden-toys-for-children/ [2024.02.02.]

Julianna, Bálint (2006) Minőség - Tanuljunk, tanítsunk, valósítsuk meg és fejlesszük tovább [Quality - Learn, teach, implement and improve], Terc Kereskedelmi és Szolg. Kft. ISBN 9789639535527

John Maeda (2006) The Laws of Simplicity, MIT Press, ISBN 9780262260954

Zsolt, Sári (2021) Kádárkocka és típusbútor – Vidéki életterek a szocializmusban [Kádárkocka and type furniture - Rural living spaces under socialism, https://epiteszforum.hu/kadarkocka-es-tipusbutor--videki-eletterek-a-szocializmusban [2024.02.10.]

Key Components of Civilization, National Geographic, https://education.nationalgeographic.org/resource/key-components-civilization/ [2024.02.17.]

András, Gelencsér (2023) Ábrándok bűvöletében [Under the spell of illusions – the limits of sustainable development] , Akadémiai Kiadó Zrt, EAN 9789634548997

Zoltán, Pogátsa (2023) Fenntartható gazdaság vagy társadalmi összeomlás [Sustainable economy or social collapse], Kossuth Kiadó, Bp. ISBN: 9789635449804

Geoffrey Boothroyd, Peter Dewhurst, Winston A. Knight, (2011). Product Design for Manufacture and Assembly, Third Edition, CPC Press

Matthew S. Bumgardner, David L. Nicholls, (2020) Sustainable Practices in Furniture Design: A Literature Study on Customization, Biomimicry, Competitiveness, and Product Communication, Published: 28 November 2020, https://www.mdpi.com/1999-4907/11/12/1277

KSH (2020). https://ksh.hu/s/kiadvanyok/fenntartható-fejlodes-indikatorai-2022/

William Lidwell, Gerry Manacsa, (2009) Deconstructing product design, Exploring the form, function, usability, sustainability, and commercial success of 100 amazing products, Rockport Publishers, Inc.

Yijie Li, Xingfu Xiong, Min Qu, (2023) Research on the Whole Life Cycle of a Furniture Design and Development System Based on Sustainable Design Theory, Published: 19 September 2023, https://www.mdpi.com/1999-4907/11/12/1277

J., ZalavářiZalavári J. (2008) A forma tervezése – Designökológia [Designing the form - Design ecology] . Scolar Kiadó, ISBN 9789632440446

J., Zalavári (2020). Designjátékok – A forma tervezésének játékai és játszmái [Design games - Games and games of form design]. Scolar Kiadó, ISBN 9789635092598

Mihály, Csíkszentmihályi (2018) Flow. Az áramlat. A tökéletes élmény pszichológiája [Flow. The flow. The psychology of the perfect experience]. Akadémiai Kiadó, Budapest.

Alice, Fáyné Dr. Dombi és Edit, Dr. Sztanáné Dr. Babics (2015a) Játékpedagógia [Game pedagogy]. Szegedi Tudo- mányegyetem Juhász Gyula Pedagógusképző Kar, Szeged. URL: http://www.jgypk.hu/mentorhalo/ tananyag/Jatekpedagogia/index.html

LEGO® Education (2019a) Encouraging Learning Through Play. URL: https://education.lego.com/en-us/ preschool/intro

Zosh, J. M., Hopkins, E. J., Jensen, H., Liu, C., Neale, D., Hirsh-Pasek, K., Solis, S. L. & Whitebread, D. (2017) Learning through play: A review of the evidence.

URL: https://www.legofoundation.com/ media/1063/learningthrough-play_web.pdf

Gábor, Prof. Dr. Veress (2015). Minőség és Etika [Quality and Ethics], Studia Wesperimiensia, XVI évfolyam, 2015.I-II szám, 124-167. oldal

Csaba Gábor, Szabó, Bence Jenő, Nagy (2009). Új irányok, lehetőségek és módszerek a minőségmenedzsmentben [New directions, opportunities and methods in quality management], Vezetés Tudomány XL. évf. 2009. különszám

Károly, Turcsányi (2014) Minőségelmélet és módszertan [Quality theory and methodology], Nemzeti Közszolgálati Egyetem, Budapest, ISBN 978-615-5491-08-5

G-Mark Design Award Criteria (2024). https://www.g-mark.org/en/learn/gda/overview

Abrasive Water Jet Cutting vs. Laser Jet Cutting of Oak Wood Panels

Camelia Cosereanu[1*], Gheorghe Cosmin Spirchez[1], Antonela Lungu[1], Sergiu-Valeriu Georgescu[1], Alexandru Catalin Filip [2], Sergiu Racasan[1]

[1] Transilvania University of Brasov, Department of Wood Processing and Wood Products Design, Bdul Eroilor nr.29, 500036-Brasov, Romania
[2] Transilvania University of Brasov, Department of Manufacturing Engineering, Bdul Eroilor nr.29, 500036-Brasov, Romania.

E-mail: cboieriu@unitbv.ro; cosmin.spirchez@unitbv.ro; antonela.petrascu@unitbv.ro; sergiu.georgescu@unitbv.ro; filipal@unitbv.ro; sergiu.racasan@unitbv.ro

Keywords: water jet cutting, laser jet cutting, oak wood, ImageJ, flatness

ABSTRACT
Two oak (*Quercus Robur*) wood panels were cut by abrasive water jet and laser jet respectively, using a pattern composed of circles with various diameters. The processing accuracy and the kerf widths were determined both for the holes and circles cut from the panels using the masks generated by ImageJ software, for which the area is calculated as an output data. The dimensional stability, the size of the kerf and the smoothness of the contour evaluated by microscope investigation, the visual assessment of the panel surfaces after cutting are the objects of the comparison between the abrasive water jet cutting and the laser jet cutting methods. The results show that a better processing accuracy was obtained by using the laser jet cutting method. The dimensional stability in terms of flatness was affected by the wood sensitivity to water, so deformations occurred after abrasive waterjet cutting of panels. They decreased in time, but cracks occurred along the wood grains in some areas.

INTRODUCTION
Water jet and laser jet cutting of wood are alternative methods to cut wood panels, offering thus solutions to problems like difficult-to-machine by conventional machining processes, high noise and dust exposure, contributing thus to an environment friendly production.
Water jet cutting method is based on micro erosion occurring when large volume of water is forced through a nozzle of reduced cross section at high velocity and high pressure (Babu Rao et al. 2009).
Generally, the studies on waterjet cutting of wood involve the assessment of moisture uptake, kerf width and surface roughness (Gerencsér and Bejó 2007, Kminiak and Barcik 2011, Kminiak and Gaff 2014, Kvietková 2014, Sreekesh and Govindan 2014). Among the factors that have influence on the quality of the processed wood surface, the water jet pressure is the most important one, followed by the abrasive size, wood density and feeding speed (Wang 2012). An abrasive flow of 450 g/min at a feed speed of 400 mm/min were considered to be optimum for cutting wood-based composites (Kvietkova et al. 2014), and the feed rate of 250 mm/s, cutting pressure of 310 KPa and abrasive flow rate of 35 kg/h were considered the optimum processing parameters to cut red oak wood (Xie et al. 2020). It was found (Pelit and Yaman 2020) that the roughness parameters increase with the increase of the specimen thickness and of the system feed rate during abrasive water jet cutting. An aspect that cannot be neglected in the use of this technology is the wettability of wood. Two researchers (Cioppa and Papetti 2014) have shown that the objects cut with water jet presented deformations because of the property of wood to absorb water. Still, the fields of application of this cutting method are expanding to other sectors, such as agriculture and agricultural engineering (Perotti et al. 2021, Cui et al. 2022).
The cutting process of wood products with a CO_2 laser beam is evaluated as a highly precise method having as result a narrow kerf width, and a smooth surface (Kubovský et al. 2020). The precision of cut by laser have shown that the remaining width of the material did not scatter much, the variation against the nominal width being in the range 2.5% -13.6% (Horvath 2016). It was also demonstrated that the increase of the focal point position and of the laser power decreases the roughness of the cut section, whilst the increase of the cutting speed and of the air pressure decreases the roughness of the processed surface (Eltawahni et al. 2011). One of the drawbacks of this technology is the colour changes and some chemical modifications of wood (Li et al. 2018, Gurau et al. 2022). The processing accuracy can be

assessed by various methods of measurement and calculate the deviations, such as the circularity deviation (Costa Souza et al. 2011).

The present paper deals with the investigation of the accuracy of cutting oak wood panels with two environment friendly methods, namely abrasive water jet and laser cutting. The accuracy is assessed by measuring the various diameters of the holes and of the circles cut with the two methods with the help of the masks generated by ImageJ software, and by calculating the kerf width. The influence of the water uptake by the wood during the abrasive water jet cutting upon the dimensional stability was evaluated by measuring the panel thickness before and after cutting. The microscopic investigation of the contour is also the objects of the comparison between the abrasive water jet cutting and the laser jet cutting methods.

MATERIALS AND METHODS
Materials

Two oak (*Quercus Robur*) wood panels with dimensions of 440 mm x 440 mm x 16 mm, densities of 750 kg/m³ and 760 kg/m³ respectively, and moisture content of 8.5% for the first one and 8.2% for the second one were cut by abrasive water jet and laser jet respectively, using a pattern composed of seven rows of circles with various diameters, the smallest one being of 5 mm and the biggest one of 90 mm, with an increment of 5 mm (Figure 1a).
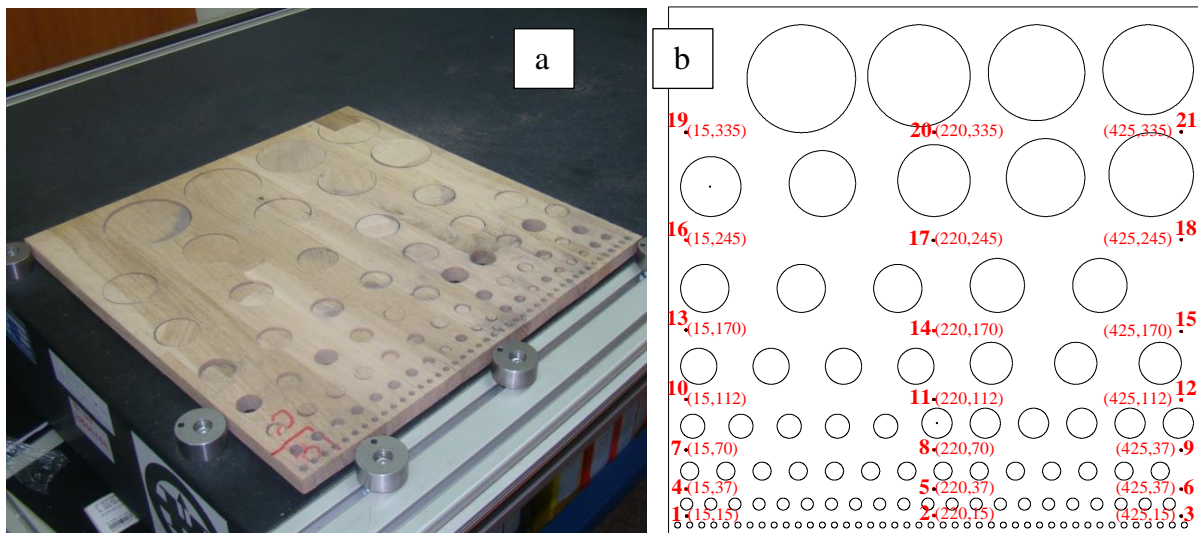
Figure 1: Oak panel after cutting (a) pattern and the measuring points for dimensional stability (b)

The 2D drawing of the pattern was drawn in AutoCAD 2012 version from Autodesk (San Francisco, California, United States) and transferred as .dxf file for processing. The twenty one points marked in the Figure 1b are the points in which the thickness was measured before and after cutting the panels with the two methods.

Equipment

The laser equipment used to cut the circles from the oak wood panel was a CO_2 laser engraver and cutting machine OmniBEAM 150 (Coherent manufacturer, Santa Clara, California, USA) with nitrogen assist gas, maximum power of 150 W, wavelength of 10.6 µm and maximum cutting speed of 50.8 m/min. The imported .dxf file drawn in AutoCAD software was used by BeamHMI software to set the cutting parameters at 100% power (150 W) and a speed of 40 m/min. The MAXIEM 1530 Abrasive Waterjet equipment (designed and manufactured at the OMAX factory in Kent, Washington, USA) was used for the abrasive waterjet cutting the second oak panel (Figure 2a). High pressure of 3448 bar, low pressure of 1379 bar, jewel diameter of 0.279 mm, abrasive flow rate of 0.340 kg/min, abrasive size of 80 mesh were used as setup. The average speed when cutting was of 498.73 mm/min.
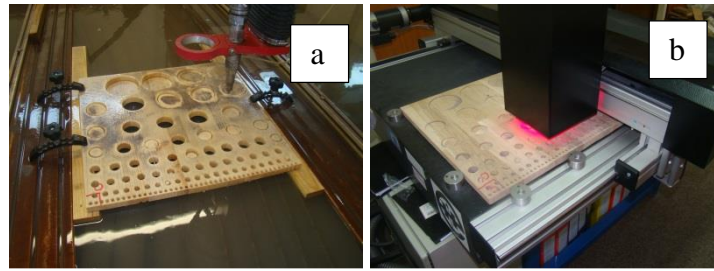
Figure 2: Abrasive waterjet cutting method with Maxiem 1530 equipment (a) OPTODesq equipment used to measure the flatness of the panels (b)

The OPTODesq equipment (Hecht manufacturer, Besigheim, Germany) presented in Figure 2b was used to measure the flatness of the panels before and after abrasive waterjet cutting, in order to assess the deformation of the panel after its immersion in water for 18 min, as long as the cutting process took place. The equipment is non-contact measurement one, having an accuracy of 0.01 mm.

Image processing software
After cutting, the panels were scanned and the traced images were processed for the holes and circles in CorelDraw X7 software. ImageJ software, an image processing program, was used to identify the shape and contour of the holes and circles cut from the panels, and to return a mask image, which transforms the traced image into grey scale with enhanced contrast (Figure 3), removing the unnecessary features. The software provided the measured area of the holes and circles masks.
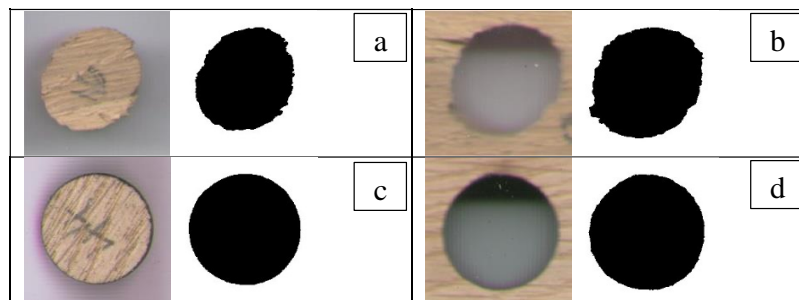
Figure 3: The mask generated by ImageJ software for circle with diameter of 15 mm circle cut by abrasive water jet method (a) and laser jet metdod (b) hole cut by abrasive waterjet method (c) and by laser jet (d)

RESULTS AND DISCUSSION
The processing accuracy
The results of the measurements obtained by ImageJ software are presented in Table 1. The ratios between the average values of the areas measured for holes and the theoretical area are higher in case of applying the laser cutting method compared with waterjet cutting one (in the range 0.32% to 32.5%), the highest differences being recorded for the smallest diameters. That means that the tolerances of the holes processed by laser cutting are higher than in the case of waterjet cutting. As regard to circles, the ratios between the theoretical area and the measured areas by ImageJ software are smaller in case of abrasive waterjet cutting compared with laser cutting (in the range 0.86% to 20.77%), which means that the tolerances of the circles are higher in this case. Based on the results in Table 1, the kerf widths were calculated from the differences between the holes areas and the circles areas. The average values of the kerf width were 1.16 mm when applying laser cutting method and 1.06 mm when applying abrasive waterjet cutting. As seen in the examples in Figure 3a and b, the deformations suffered by the holes and the circles were more pregnant in case of using abrasive waterjet method, especially for small diameters. The contours of the cuts microscopically revealed with 22.5x magnification show a smoother surface for laser cutting compared with the other method (Figure 4). The panels cut by abrasion waterjet method were deformed because of their capacity to absorb water. In order to evaluate the magnitude of the panel deformation, the measurements of the thicknesses in the 21points marked on the drawing in Figure 1 were done before cutting and after 24 hours, 1 week and 1 month. The results are shown in Table 2. The

flatness is calculated as the difference between the maximum and the minimum measured thicknesses divided by the length of the panel.

Table 1: Results of the mask measurements with ImageJ software for the circles and holes

Diameter of the circle [mm]	Theoretical area [mm²]	Average measured area by laser cutting [mm²]		Average measured area by abrasive waterjet cutting [mm²]		Ratio between measured and theoretical areas by laser cutting [%]		Ratio between measured and theoretical areas by abrasive waterjet cutting [%]	
		Holes	Circles	Holes	Circles	Holes	Circles	Holes	Circles
90	6358.5	6453.8	6280.4	6389.6	6185.4	101.50	98.77	100.49	97.28
85	5671.6	5761.5	5568.8	5743.3	5492.5	101.58	98.19	101.26	96.84
80	5024.0	5118.3	4917.3	5077.9	4852.3	101.88	97.88	101.07	96.58
75	4415.6	4531.6	4315.8	4452.6	4287.7	102.63	97.74	100.84	97.10
70	3846.5	3957.3	3751.7	3891.1	3718.0	102.88	97.53	101.16	96.66
65	3316.6	3389.9	3249.7	3345.2	3218.2	102.21	97.98	100.86	97.03
60	2826.0	2886.2	2754.9	2835.7	2732.1	102.13	97.49	100.34	96.68
55	2374.6	2426.2	2324.6	2385.2	2277.2	102.17	97.89	100.45	95.90
50	1962.5	2030.7	1906.2	1998.8	1861.9	103.47	97.13	101.85	94.87
45	1589.6	1652.3	1537.4	1624.9	1509.7	103.95	96.71	102.22	94.97
40	1256.0	1300.7	1209.2	1282.5	1169.9	103.62	96.27	102.11	93.15
35	961.6	995.9	927.4	980.4	895.3	103.56	96.44	101.95	93.10
30	706.5	735.3	674.3	728.1	646.1	104.08	95.44	103.06	91.44
25	490.6	519.9	466.1	505.6	439.9	105.97	94.99	103.05	89.65
20	314.0	328.1	293.4	326.3	274.3	106.40	93.44	103.93	87.34
15	176.6	193.6	162.6	187.9	148.3	109.62	92.06	106.42	83.95
10	78.5	92.09	71.0	83.2	58.5	117.32	90.5	105.96	74.47
5	19.6	27.4	16.3	21.0	12.2	139.64	82.96	107.14	62.19
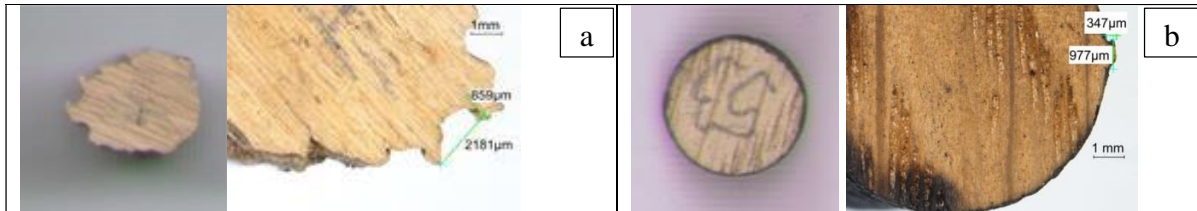
Figure 4: The circle of 10 mm diameter cut by abrasion waterjet method (left) and the contour with 22.5x magnification (right) (a) and the same by laser technology (b)

Table 2: Flatness of the oak panels measured before and after abrasive waterjet cutting

Characteristics	Before cutting	24 h after cutting	1 week after cutting	1 month after cutting
Flatness [mm/m]	0.95	5.43	4.05	2.43
Moisture content [%]	8.5	12.9	11.2	10.7

CONCLUSIONS

The calculated kerf widths based on the area measurements of the holes and circles with ImageJ software have narrow values of 1.16 mm when applying laser cutting method and 1.06 mm when applying abrasive waterjet cutting. The deformation of the oak panels increased after abrasive waterjet cutting of circles, but the deformation decreased in time, as the measurements after one week and one month show, but the decreasing of deformation had as drawbacks the occurrence of cracks in wood parallel to the grains, in some narrow areas between the holes. In case of laser jet cutting, the colour of the cut edges and of the surfaces around them became dark as the effect of the laser beam, whilst in the case of the water jet cutting, the entire surfaces of the resulted circles and of the remained panel were affected by the presence of the sand used in the combination with water, which printed a grey colour on the wood surface. The accuracy increased with the increasing of circles diameters for both methods, but the

microscopic investigation revealed an irregular contour of the circles and of the holes in case of applying the water jet cutting method.

REFERENCES

Babu Rao D, Baskey D, Rawat R.S. (2009) Water Jet Cutter: An Efficient Tool for Composite Product Development. National Conference on Scientific Achievements of SC & ST Scientists & Technologists14–16 April 2009, National Aerospace Laboratories, Bangalore-17

Cioppa G, Papetti V (2014) Application of Waterjet Technology to Wood, Course: Laboratorio di Ingegneria Meccanica, WaterJet Laboratory, Politecnico di Milano, https://www.academia.edu/9561357/Application_of_Waterjet_Technology_to_Wood Accessed 8 April 2024.

Costa Souza C, Arencibia RV, Costa HL (2011) A contribution to the measurement of circularity and cylindricity deviations. In Proceedings of COBEM 2011, 21st Brazilian Congress of Mechanical Engineering, October 24-28, 2011, Natal, RN, Brazil.

Cui D, Li H, He J, Wang Q, Lu C, Hu H, Cheng X, Wang C (2022) Applications of Water Jet Cutting Technology in Agricultural Engineering: A Review. Applied Sciences 12(18):8988. https://doi.org/10.3390/app12188988

Eltawahni HA, Olabi AG, Benyounis KY (2011) Investigating the CO_2 laser cutting parameters of MDF wood composite material. Optics & Laser Technology 43: 648–659. https://doi.org/10.1016/j.optlastec.2010.09.006

Gerencsér K, Bejó L (2007) Investigations into the waterjet cutting of solid wood. Wood Research 52(2): 57-64.

Gurău L, Coşereanu C, Timar MC, Lungu A, Condoroţeanu CD (2022) Comparative Surface Quality of Maple (Acer pseudoplatanus) Cut through by CNC Routing and by CO2 Laser at Different Angles as Related to the Wood Grain. Coatings 12(12):1982. https://doi.org/10.3390/coatings12121982

Horvath PG (2016) Determination of the Minimum Intact Dimensions Available in Practical Applications of Laser Cutting. Pro Ligno 12(2): 9-16.

Kminiak R, Barcik Š (2011) Fabrication of structural joinery items of solid wood by the mean of abrasive water jet method. Wood Research 59(3): 499-508.

Kminiak R, Gaff M (2014) Fabrication of structural joinery items of solid wood by the mean of abrasive water jet method. Wood Research 59(3): 499-508.

Kvietková M (2014) Topography of material made by the application of abrasive water jet technology. Journal of Forest Science 60(8): 318–323.

Kvietková M, Barcík Š, Gašparík M (2014) Optimization of the Cutting Process of Wood-Based Agglomerated Materials by Abrasive Water-Jet. Acta Silv. Lign. Hung. 10(1):1–47. https://doi.org/10.2478/aslh-2014-0003

Pelit H, Yaman Ö (2020) Influence of Processing Parameters on the Surface Roughness of Solid Wood Cut by Abrasive Water Jet. Bioresources 15:6135-6148. https://doi.org/10.15376/biores.15.3.6135-6148

Perotti F, Annoni M, Calcante A, Monno M, Mussi V, Oberti R (2021) Experimental Study of Abrasive Waterjet Cutting for Managing Residues in No-Tillage Techniques. Agriculture 11(5):392. https://doi.org/10.3390/agriculture11050392

Sreekesh K, Govindan P (2014) A review on abrasive water jet cutting. International Journal of Recent advances in Mechanical Engineering (IJMECH) 3(3), pp 153-158. https://doi.org/10.14810/ijmech.2014.3313

Wang Z (2012) An investigation on water jet machining for hardwood floors. Eur. J. Wood Prod. 70:55–59. https://doi.org/10.1007/s00107-010-0492-0

Xie W, Fang J, Wang ZL, Huang L (2020). Optimization of technological parameters of water jet cutting of red oak and bamboo based on three-dimensional surface topography measurement. BioResources 15(2):3270-3277. https://doi.org/10.15376/biores.15.2.3270-3277

Polyphenol content of underutilized wood species from Hungary

Tamás Hofmann [1*], Haruna Seidu [2,3], Kibet Tito Kipkoror [1]

[1] University of Sopron, Institute of Environmental Protection and Natural Conservation. Bajcsy-Zs. Str. 4, Sopron, Hungary, 9400.
[2] University of Sopron, Institute of Wood Technology and Technical Sciences. Bajcsy-Zs. Str. 4, Sopron, Hungary, 9400.
[3] CSIR – Forestry Research Institute of Ghana. P.O. Box UP 63 KNUST Kumasi, Ghana

E-mail: hofmann.tamas@uni-sopron.hu; Haruna.Seidu@phd.uni-sopron.hu; kibetit23@student.uni-sopron.hu

ABSTRACT

In the present research the radial variation of the polyphenol content was assessed from various stems of currently underutilized wood species from Hungary. The content and composition of polyphenols are closely related to various wood properties (e.g. color, durability). The sapwood, sapwood/heartwood boundary and various tissues of the heartwood were investigated. The main goal of the research was to find out if there were significant differences in the polyphenol content along the radius which may also affect utilization. Underutilized hardwood species black locust (*Robinia pseudoacacia* L.), Pannonia poplar (*Populus x euramericana cv. Pannonia*) and Turkey oak (*Quercus cerris* L.) were investigated which are interesting for future uses and afforestation in Hungary regarding the effects of changing climatic conditions. Quantification of total polyphenol content was accomplished using the Folin-Ciocalteu assay. The identification and radial variation of major polyphenolic compounds was accomplished using high-performance liquid chromatography-photodiode array detection-electrospray ionisation-multistage mass spectrometry detection.

INTRODUCTION

As a consequence of climate change the importance of domestic, drought-tolerant and underused woody species will increase in the future. Wood properties are highly influenced by the content and composition of extractives, out of which polyphenols are especially important as they determine wood color, color stability as well as wood durability. Their concentration can vary between different tissues of the same stem, moreover inside of a given tissue, too. In the present work the radial variation of the polyphenolic composition and content were assessed from various stems of black locust (*Robinia pseudoacaia* L.), Poplar (*Populus x euramericana cv. Pannonia*) and Tukey oak (*Quercus cerris* L.) originating from the forests of the Kiskunsági Erdészeti és Faipari Zrt. forestry company (KEFAG). Results contribute to the identification of compounds influencing wood material and technological properties in the future and for the selection of quality wood material.

MATERIALS AND METHODS

Sample collection was carried out in the forests of the Kiskunsági Erdészeti és Faipari Zrt. forestry company in eastern Hungary. From all species 5 representative trees were selected and discs were cut from 1 meter height. Discs were taken to the laboratory and wood chips were cut using a drill from different parts of the discs (sapwood, sapwood/heartwood boundary, middle of heartwood, growth ring 16, growth ring 12 and growth ring 4). Samples were dried at room temperature to even moisture content and extracted (0.2 g) using methanol:water 50:50 (v/v) solution (14 ml) by ultrasonication for 30 minutes. Extracts were centrifuged at 12.000 1/min for 2x10 minutes and taken to analysis.

Polyphenol content and composition was measured with two methods: the Folin-Ciocalteu's total polyphenol content (TPC) and the high-performance liquid chromatography-photodiode array detection-electrospray ionisation-multistage mass spectrometry detection (HPLC-DPA-ESI-MS/MS). The TPC was determined by the Folin-Ciocalteu assay (Singleton and Rossi 1965) and implemented using previously published methodology (Tálos-Nebehaj et al. 2019). Average was determined for each tissue

(n=5) for each species. The HPLC-PDA-ESI-MS/MS separation and identification of polyphenolic compounds was accomplished based on earlier works of the authors (Hofmann et al. 2016; Agarwal et al. 2021; Hofmann et al. 2021a).

RESULTS AND DISCUSSION
Total polyphenol content

According to previous results the significant radial variation was observed within the heartwood of sweet chestnut (*Castanea sativa* L.), where the tissues around the sapwood/heartwood boundary had the highest TPC values and the content of polyphenols decreased while moving towards the innermost tissues of the heartwood (Eichhorn et al. 2017). Comparing to the present results it was found that this tendency must be species-dependent, as different radial variations were observed for all of the three species. Figure 1 depicts the radial variation of the TPC in the three investigates species.

In general a very high standard deviation of the TPC values was reported indicating a very high natural variation of the TPC even within a given species and tissue. In black locust the lowest TPC was found in the sapwood and polyphenol content increased at the sapwood/heartwood boundary and remained very in high in the inner heartwood. Results are in accordance with earlier findings (Magel et al. 1994). Although there is a slight decreasing tendency of the TPC from sapwood/heartwood boundary towards the pith, just like in the case of sweet chestnut (Eichhorn et al. 2017), no significant differences could be evidenced between the individual heartwood tissues primarily as a result of high standard deviation values.

In poplar the highest TPC was determined in the sapwood/heartwood boundary tissue. Both sap and heartwood had significantly lower TPC levels. Interestingly the TPC of heartwood was not significantly higher compared to sapwood as opposed to general findings. The standard deviation of results is even higher compared to black locust samples.

In Tukey oak no significant differences were found between any of the tissues. According to the results there was a uniform distribution along the radius even at the sapwood/heartwood boundary no increase was determined. According to literature data the cold and hot water soluble extractive content of Turkey oak sapwood is higher compared to heartwood (Deaconu et al. 2023). The radial variation of the TPC needs further explanations as it contradicts major findings of the radial variation of polyphenols in tree stems (Magel et al. 1994; Eichhorn et al. 2017; Hofmann et al. 2021b) and can possibly accounted by the presence of other types of extractives.
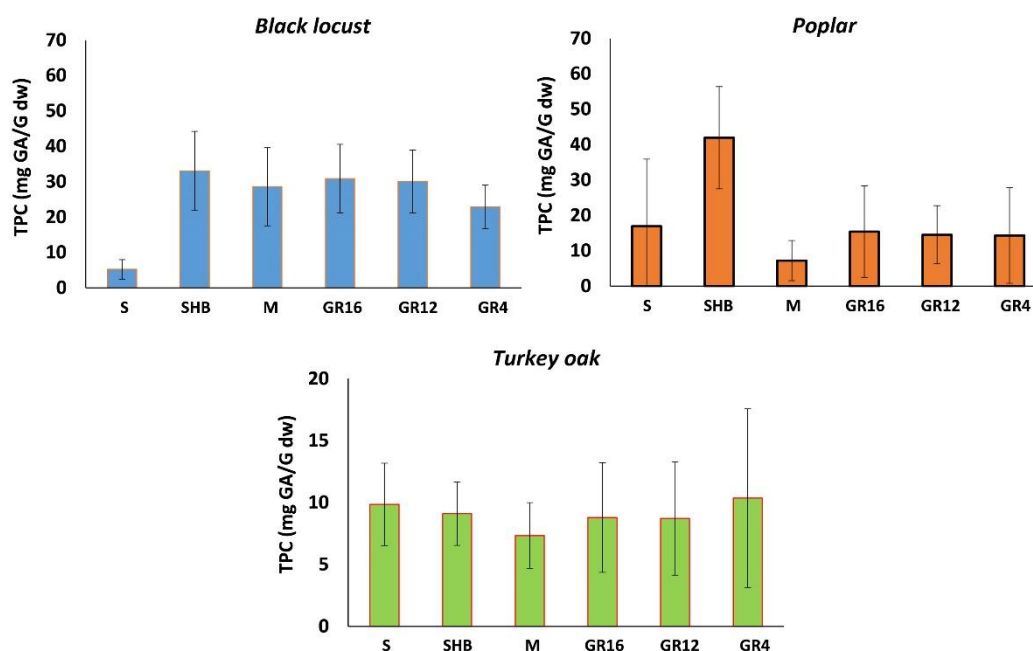

Figure 1: Radial variations of the total polyphenol content (TPC) in different species. S: sapwood, SHB: sapwood/heartwood boundary, M: middle of heartwood, GR16: growth ring 16, GR12: growth ring 12, GR4: growth ring 4

The TPC assay gives a fast quantitative evaluation of the total polyphenol content of samples, however the assay can interfere with some non-polyphenol type compounds, too (e.g. reducing sugars, organic acids, etc.) which influence results (Prior et al. 2005; Everette et al. 2010). Thus, in order to have precise knowledge on polyphenol composition and concentration the separation, identification and quantification of individual compounds has to be assessed additionally.

HPLC-PDA-ESI-MS/MS analysis of polyphenols
In the present work the HPLC-PDA-ESI-MS/MS technique was applied for the separation and identification of the individual polyphenolic compounds from the samples. The PDA (250-380 nm) chromatogram is depicted in Figure 2. Some of the compounds have been tentatively identified, yet the identification of most compounds needs to be carried out in the future.

The most abundant peaks in black locust sample correspond to tetrahydroxy-dihydroflavonol (2), dihydrorobinetin (6), fustin (7), dimeric prorobinetinidin (8) and robinetin (11). According to peak heights the highest concentrations are found in heartwood, especially at the sapwood/heartwood boundary (SHB) and the heartwood tissues next to it (GR16), while inner heartwood (GR4) has decreased concentrations, and lowest values can be measured in the sapwood. These results are in accordance with the TPC measurements.

Contrary to the TPC values, the overall highest peaks were found in the sapwood sample of poplar and not at the sapwood/heartwood boundary. Out of the highest peaks aromadendrin (9) and naringenin (14) have been identified by mass spectra, while the identification of peaks 12 and 15 and 16 require future work. According to the chromatogram concentrations decrease, while moving to inner heartwood tissues, which similarly as with TPC values. It can be assumed that other type of extractives may have been present in poplar sapwood/heartwood boundary which interfered with the TPC measurements giving very high values, which suggests that before evaluation of TPC results the presence of reducing type extractives must be considered.

The overall lowest peaks were determined in Turkey oak samples, which was found interesting also comparing with fairly high TPC values. We assume again that interfering compounds must have influenced the TPC values for Turkey oak samples. Highest peaks were determined at the sapwood/heartwood boundary, while moving toward the inner heartwood tissues peak height decrease indicating lower concentrations. Peak 4 was identified as (+)-catechin, while peak 10 has not yet been identified and requires future work.
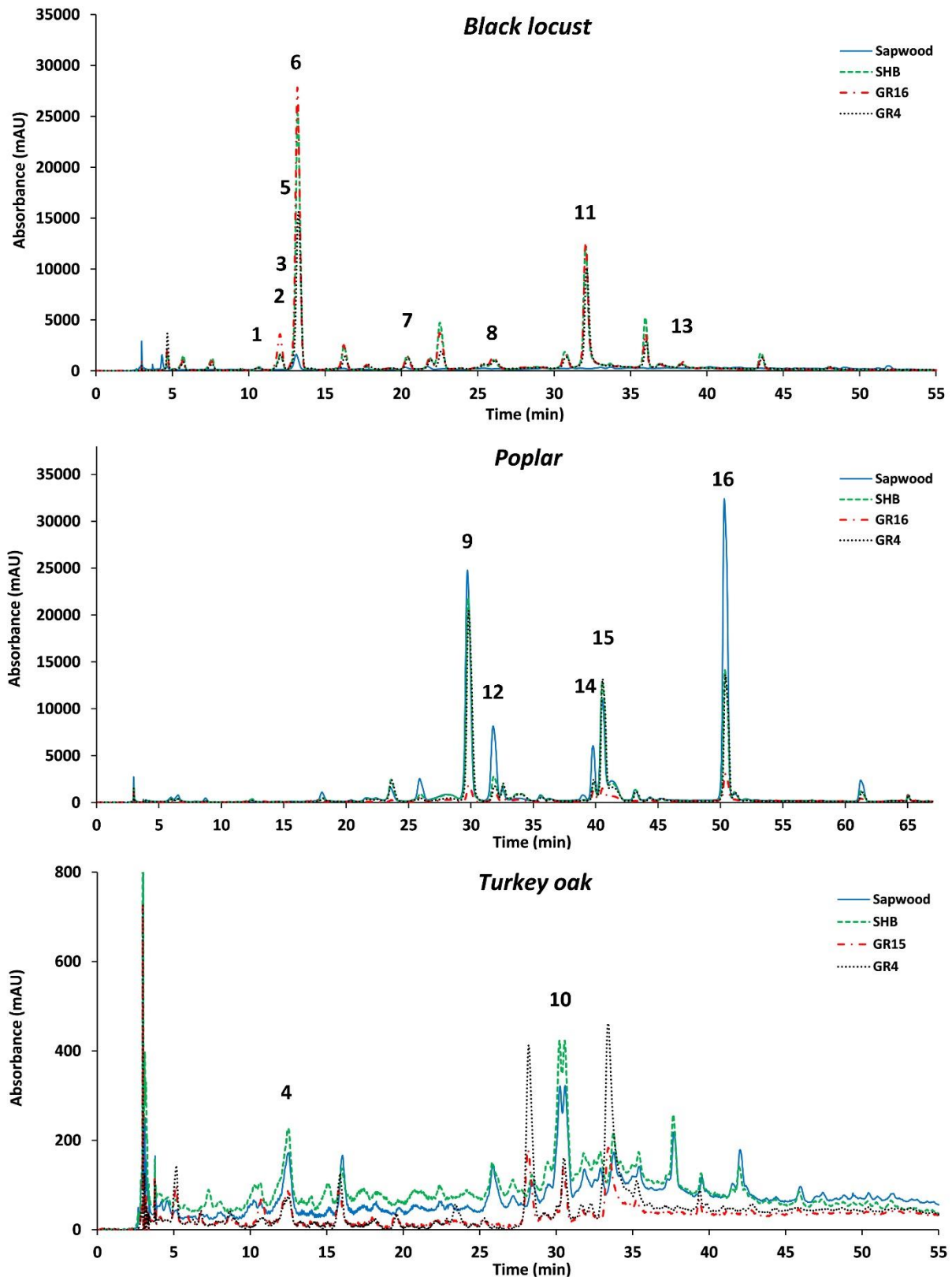
Figure 2: The HPLC-PDA (250-380 nm) chromatogram of selected wood samples (GR4: growth ring 4, RG16: growth ring 16, SHB: sapwood/heartwood boundary). 1: prorobinetinidin, 2: tetrahydroxy-dihydroflavonol, 3: fisetin, 4: (+)-catechin, 5: robtin, 6: dihydrorobinetin, 7: fustin, 8: dimeric prorobinetinidin, 9: aromadendrin, 10: unidentified (m/z 565), 11: robinetin, 12: unidentified (m/z 229), 13: robtein, 14: naringenin, 15: unidentified (m/z 561), 16: unidentified (256)

CONCLUSIONS

Climate change poses a challenge to wood industry and domestic wood resources have to be utilized in a more efficient way, which requires a more extensive use of drought tolerant and underutilized species in the future. Poplar, Tukey oak and black locust provide wood which must be better utilized in the future. Extractive content, especially polyphenols affect various wood properties. Tendencies of the radial variation of polyphenol content was found to be different in the investigated species. Folin-Ciocalteu's total phenol content assay is fast and reliable method and can give a good estimation of the total polyphenol content, yet it can interfere with reducing compounds (sugars, organic acids) thus results must be critically evaluated especially for species and tissues with high reducing sugar and organic acid content. Chromatographic/mass spectrometric determinations are more defined, yet analysis takes more time and implies higher costs.

ACKNOWLEDGEMENTS

REFERENCES

Agarwal C, Hofmann T, Vršanská M, et al (2021) In vitro antioxidant and antibacterial activities with polyphenolic profiling of wild cherry, the European larch and sweet chestnut tree bark. Eur Food Res Technol 247:2355–2370. https://doi.org/10.1007/s00217-021-03796-w

Deaconu I, Porojan M, Timar MC, et al (2023) Comparative research on the structure, chemistry, and physical properties of Turkey oak and sessile oak wood. BioResources 18(3):5724–5749. https://doi.org/10.15376/biores.18.3.5724-5749

Eichhorn S, Erfurt S, Hofmann T, et al (2017) Determination of the phenolic extractive content in sweet chestnut (*Castanea Sativa* Mill.) Wood. Wood Research 62:181–196

Everette JD, Bryant QM, Green AM, et al (2010) Thorough Study of Reactivity of Various Compound Classes toward the Folin−Ciocalteu Reagent. J Agric Food Chem 58:8139–8144. https://doi.org/10.1021/jf1005935

Hofmann T, Albert L, Németh L, et al (2021a) Antioxidant and Antibacterial Properties of Norway Spruce (*Picea abies* H. Karst.) and Eastern Hemlock (*Tsuga canadensis* (L.) Carrière) Cone Extracts. Forests 12:1189. https://doi.org/10.3390/f12091189

Hofmann T, Guran R, Zitka O, et al (2021b) Liquid Chromatographic/Mass Spectrometric Study on the Role of Beech (Fagus sylvatica L.) Wood Polyphenols in Red Heartwood Formation. Forests 13:10. https://doi.org/10.3390/f13010010

Hofmann T, Nebehaj E, Albert L (2016) Antioxidant properties and detailed polyphenol profiling of European hornbeam (*Carpinus betulus* L.) leaves by multiple antioxidant capacity assays and high-performance liquid chromatography/multistage electrospray mass spectrometry. Industrial Crops and Products 87:340–349. https://doi.org/10.1016/j.indcrop.2016.04.037

Magel E, Jay-Allemand C, Ziegler H (1994) Formation of heartwood substances in the stemwood of *Robinia pseudoacacia* L. II. Distribution of nonstructural carbohydrates and wood extractives across the trunk. Trees 8:165–171. https://doi.org/10.1007/BF00196843

Prior RL, Wu X, Schaich K (2005) Standardized Methods for the Determination of Antioxidant Capacity and Phenolics in Foods and Dietary Supplements. J Agric Food Chem 53:4290–4302. https://doi.org/10.1021/jf0502698

Singleton VL, Rossi JA (1965) Colorimetry of Total Phenolics with Phosphomolybdic-Phosphotungstic Acid Reagents. Am J Enol Vitic 16:144–158

Tálos-Nebehaj E, Albert L, Visi-Rajczi E, Hofmann T (2019) Combined multi-assay evaluation of the antioxidant properties of tree bark. Acta Silv Lign Hung 15:85–97. https://doi.org/10.2478/aslh-2019-0007

Wood quality evaluation of 32 grafted clone linages of Keyaki (*Zelkova serrata*) plus trees 12 years after planting

Kiyohiko Ikeda[1*], Shigehiro Yamamoto[2]

[1] Shizuoka Professional University of Agriculture, Japan
[2] Shizuoka Prefectural Research Institute of Agriculture and Forestry, Japan

E-mail: izx01361@nifty.ne.jp; Shigehiro1_yamamoto@pref.shizuoka.lg.jp

Keywords: *Zelkova serrata*, growth trait, wood qualities, stress-wave velocity, heartwood color

ABSTRACT
The purpose of this study was to evaluate the growth characteristics and non-destructive material properties of standing trees at the early stage of growth, 12 years after planting 32 clones of Zelkova grafted seedlings, and to understand the relationship between log material and growth characteristics. A correlation was observed between the stress wave propagation velocity of the standing wood and the dynamic Young's modulus of the standing wood, and between Pirodyn driving length and sapwood density of the standing tree, indicating that differences between linages can be evaluated non-destructively. Differences in density and dynamic Young's modulus were observed among grafted clone linages at the early growth stage of 12 years after planting. The dynamic Young's modulus (Efr) of the grafted clone linages were 8 to 12 kN/mm^2, which was almost the same as that of older matured zelkova. The relationship between the L* a*b* value of the heartwood measured by spectrophotometer, density of the heartwood, and average annual ring width suggested that about half of the grafted clone linages were like red zelkova lineage.

INTRODUCTION
Keyaki (*Zelkova serrata* Makino) is a useful hardwood that has been used as a construction material, furniture material, etc. in Japan because of its material characteristics such as processability, durability, and grain design. Many of them are sourced from natural forests, but because natural forests with superior materials and characteristics are rapidly decreasing, there has been growing interest and expectations in the cultivation and utilization of (fast-maturing, growing) hardwood resources in recent years. So far, Shizuoka Prefecture has selected 37 zelkova trees with excellent characteristics as elite trees, and has also investigated techniques for propagating their axillary bud culture clones (Yamamoto et al.2004). In this study, we aimed to evaluate the growth characteristics and wood qualities of standing trees at the early stage of growth 12 years after planting 32 grafted clone seedlings, evaluate wood quality of felled logs, and clarified the relationship with growth characteristics. Especially, we aimed to elucidate the relationship between heartwood color and wood quality, which is an excellent trait indicator for zelkova.

TEST SITE AND METHOD
Test site was a stand in which grafted seedlings clone 38 linages of Zelkova have been planted and passed 12 years. A total of 145 standing trees were used, 3 to 5 trees per clone linage, excluding clones that were dead or had extremely poor growth for standing trees, we measured the diameter at breast height, tree height, number of main trunks, stress wave propagation velocity using Fakkop, and pin driving length using Pilodyn. After that, half of the test trees were cut down in late September and the other half in late January, and logs 60 to 80 cm long were collected from the main trunk with the best growth, starting at 20 cm at the base. The dynamic Young's modulus ("Efr") of the logs was measured using the tapping method. A disk with a thickness of 3 cm was taken from the end of the log, and the L*a*b* value of the heartwood color at the end of the disk was measured using a spectrophotometer. Thereafter, sapwood and heartwood densities when greenwood and oven-dry, and the moisture content ("MC") by the oven dry method were measured for the divided specimens of sapwood and heartwood.

RESULTS AND DISCUSSION

Table 1 showed the average values of growth traits and material quality of 32 lines of grafted seedlings of Zelkova fine trees 12 years after planting. The average growth traits for all lines were diameter at breast height of 6.9 cm and tree height of 5.9 m, and a significant correlation was observed between the two. Shibakawa-1, Tenryu-4, and Mathuzaki-3 had high trunk straightness and good enlargement and elongation growth trait. Figure 1 showed the relationship between the growth traits of the Zelkova mother tree and the amount of tree height growth and thickening growth for two years, 7 to 9 years after planting, and for 5 years, 7 to 12 years, after planting. A significant correlation was observed between the two, indicating that the grafted seedlings inherited the growth traits of the mother tree. No significant correlation was observed between the growth traits of the grafted lines, stress wave propagation velocity, and Pilodyn pin driving length (Figure 2). Previously, similar results have been reported for 20-year-old zelkova in three test forests with different planting densities (Prasetyo et al.2015).

Table 1: Growth traits and wood qualities of Zelkova grafted 32 clone lineage

Grafted clone linage	DBH (cm)	Height (m)	Pilodyn pin depth (mm)	Stress wave velocity (km/sec)	Ev (kN/mm²)	Log Efr (kN/mm²)	Annual ring width (mm)	Oven-dry density Sapwood (kg/m³)	Heartwood (kg/m³)	Moisture content Sapwood (%)	Heartwood (%)
Arai1	5.3	4.1	11	3.4	10.4	10.2	2.4	816	685	52	73
Inasa 1	5.6	4.9	13	3.4	10.6	10.2	2.3	554	567	67	70
Inasa 2	5.3	5.1	13	3.5	10.7	9.7	2.4	597	657	65	76
Kawazu 2	3.7	3.7	10	3.6	11.6	10.0	2.1	742	622	60	72
Sakuma 1	7.4	6.8	14	3.9	13.7	12.6	3.1	622	603	60	105
Sakuma 4	5.7	6.3	11	3.9	13.8	11.2	2.6	747	689	62	73
Sakuma 5	5.4	5.9	12	3.8	12.9	12.4	2.7	716	701	52	61
Shibkawa 1	10.9	7.6	15	3.4	10.7	8.1	4.6	661	627	58	100
Shimizu 1	4.2	4.9	8	3.7	12.6	11.7	1.9	717	720	61	60
Shimizu 2	7.4	7.6	13	3.7	12.1	11.1	3.4	641	670	76	92
Shimizu 4	6.5	7.4	11	4.0	13.6	11.7	2.9	734	649	57	62
Shimizu 5	6.8	6.5	12	3.4	10.2	9.5	3.1	618	639	75	79
Shuzenji 2	8.2	6.4	13	3.5	11.3	11.5	3.7	699	643	67	84
Shuzenji 3	6.8	7.4	13	4.0	14.3	12.3	3.1	678	651	58	57
Shuzenji 4	8.2	5.7	13	3.7	12.4	9.4	3.7	617	622	60	84
Tathuyama 1	8.3	4.5	14	3.0	8.3	7.9	3.5	550	627	45	91
Tenryu 1	8.3	5.9	13	3.5	11.1	8.2	3.5	620	646	79	98
Tenryu 2	7.3	5.0	13	3.4	10.5	8.2	3.0	652	673	69	88
Tenryu 3	5.7	4.7	12	3.3	9.8	8.2	2.4	575	693	59	80
Tenryu 4	9.2	6.6	16	3.7	12.6	11.1	3.8	661	636	63	103
Tenryu 5	7.1	6.6	11	3.5	11.2	11.4	3.2	705	670	60	78
Tenryu 6	5.5	5.4	12	3.5	11.1	10.1	2.5	647	610	69	91
Nakaizu 1	7.6	5.0	12	3.4	10.4	8.6	3.2	674	693	68	88
Haruno 1	6.6	4.8	14	3.7	12.5	10.7	2.7	689	654	61	94
Fuji 2	9.6	6.4	15	3.6	11.8	8.7	4.0	578	551	69	119
Fujinomiya 1	4.3	4.7	14	3.7	12.4	9.5	1.8	535	545	66	68
Fujinomiya 2	5.1	5.5	11	3.5	11.3	10.2	2.1	670	702	59	85
Fujinomiya 4	8.8	7.0	10	3.9	13.6	12.7	3.7	698	660	68	70
Matuzaki 1	7.3	6.3	10	3.7	12.0	10.1	3.3	742	777	60	64
Matuzaki 2	7.9	7.1	11	3.9	13.6	12.5	3.6	800	811	60	67
Matuzaki 3	8.9	7.7	12	3.5	10.8	10.0	4.0	717	666	60	73
Minamiizu 3	6.6	6.0	11	3.6	11.9	9.5	3.0	755	717	61	72
Average	6.9	5.9	12	3.6	11.7	10.3	3.0	670	659	63	81
Max	10.9	7.7	16	4.0	14.3	12.7	4.6	816	811	79	119
Min	3.7	3.7	8	3.0	8.3	7.9	1.8	535	545	45	57
C.V. (%)	24	19	14	6	12	14	22	11	8	11	19
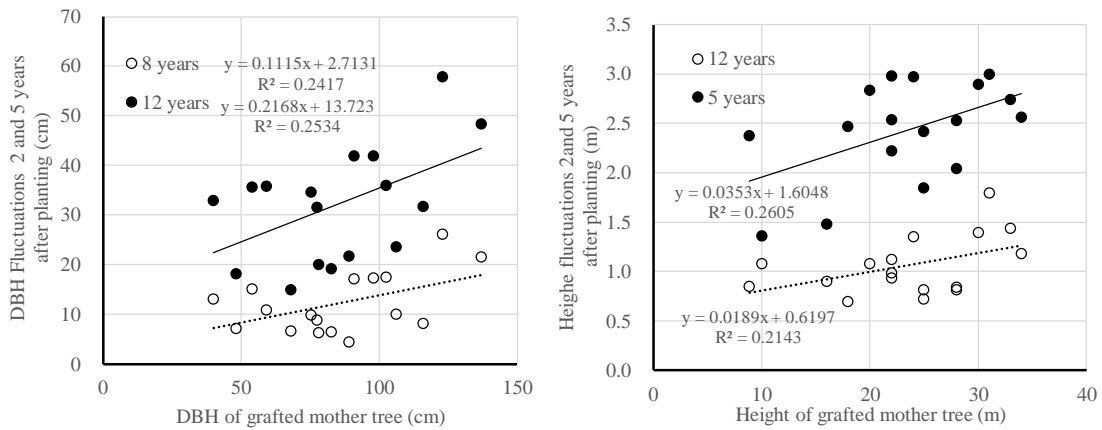
*Figure1: Comparison of mother tree growth traits of Zelkova plus trees
and growth amount 8 and 12 years after planting grafted seedlings.*
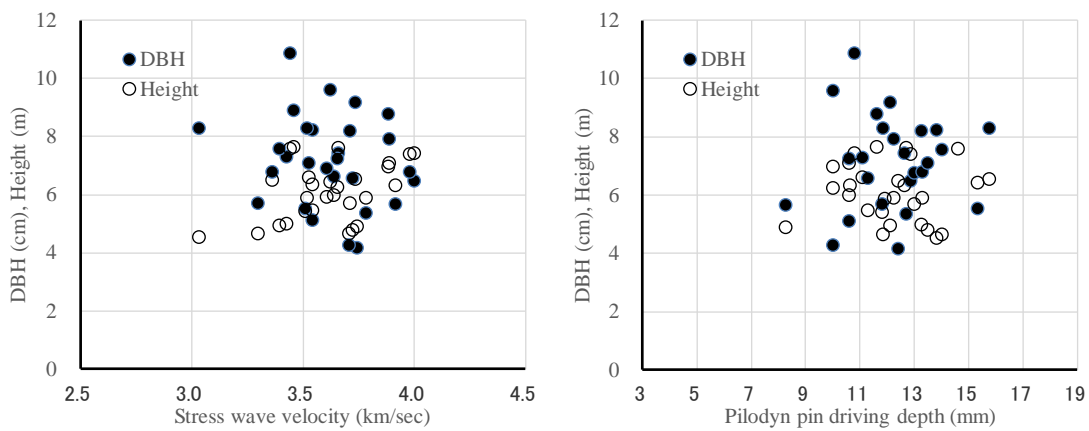
*Figure 2:   Relationship between log qualities and stress wave propagation velocity
and Pilodyn driving depth in Zelkova grafted clones*
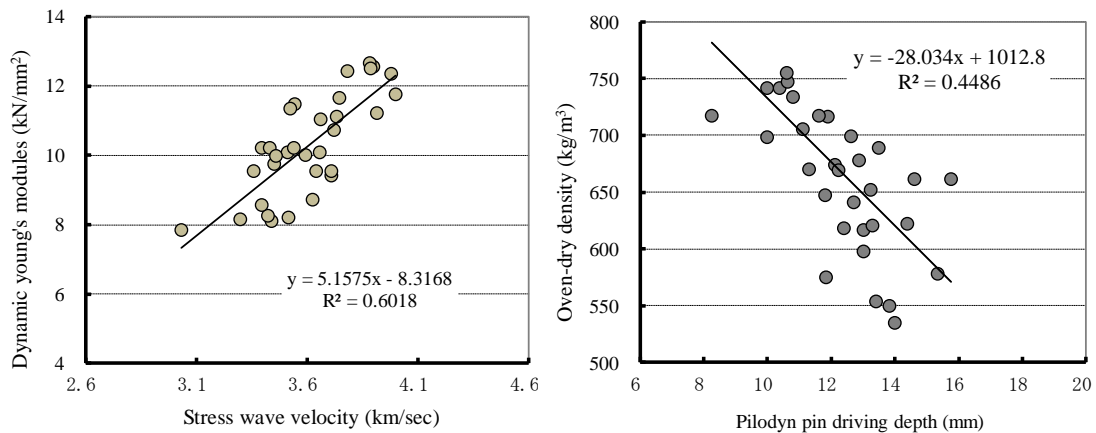
*Figure 3:   Relationship between growth traits and stress wave propagation velocity
and Pilodyn driving depth in Zelkova grafted clones.*

A significant correlation was observed between stress wave propagation velocity and Efr of logs, and between Pilodyn driving pin depth of standing trees and dry density of sapwood. It was suggested that this method could be used as a destructive method (Figure 3). The log Efr of the grafted linage was 7.9 to 12.7 kN/mm². Compared to the previously reported Young's modulus of zelkova at mature stage of 8 to 12 kN/mm² and the Efr of seasoned drying full-sized wood (cross-sectional dimensions 24 x 24 cm) of 7 to 12 kN/mm², grafted clone linage was almost the same (Forest & forest product research institute.2004, Ido et al 2012). Furthermore, Ev of the outer circumference of the tree trunk was

estimated to be 8.3 to 14.3 kN/mm^2, assuming a constant stress wave propagation velocity and green effective density (900 kg/m^3). For this reason, it was inferred that changes in Young's modulus in the radial direction of tree trunks due to the increase in forest age observed in coniferous trees were small. Oven-dry density was 535 to 816 kg/m^3 for sapwood and 545 to 811 kg/m^3 for heartwood, and differences between the lines were observed in both cases. Oven-dry density was 535 to 816 kg/m^3 for sapwood and 545 to 811 kg/m^3 for heartwood, and differences between strains were observed in both cases. The air-dry specific gravity of zelkova is 600 to 900 kg/m^3 according to the Wood Industry Handbook (Forest & forest product research institute.2004), and it has been reported that there are differences between strains, natural forests and artificial forests, and differences in planting density (Furukawa et al.1989). On the other hand, it has been reported that the density variation in the radial direction of the tree trunk decreases or remains almost constant from the pith to the outer circumference (Hashizume et al.1987). The results of this test also showed that the difference in oven dry density between sapwood and heartwood was small, and unlike coniferous trees, there was no tendency to change greatly from immature wood to mature wood. In addition, no significant correlation was observed between the average annual ring width and oven-dry density or Efr among each lineage or individual, but it was inferred that the main reason for this was the difference in vessel structure (Isamoto 2000).
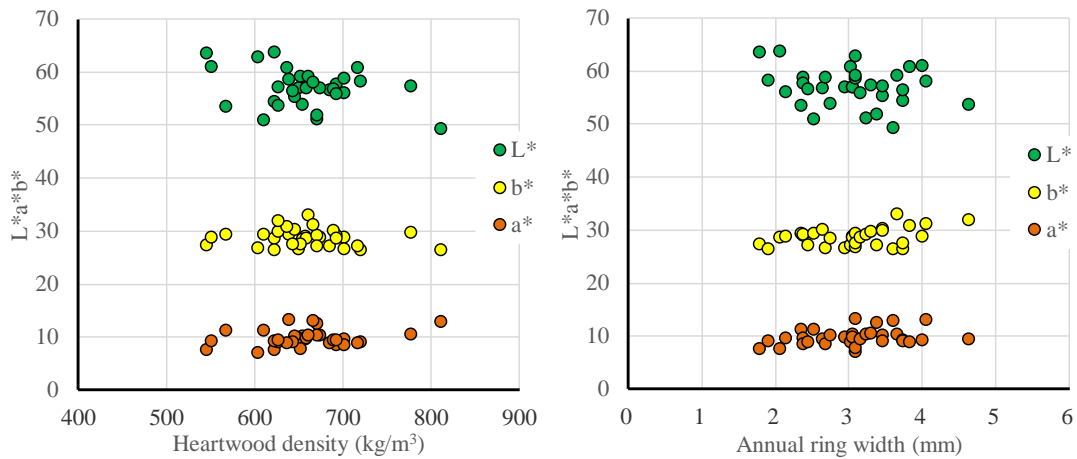
*Figure 4: Relationship between L*a*b* value and density
and average annual ring width of zelkova heartwood.*
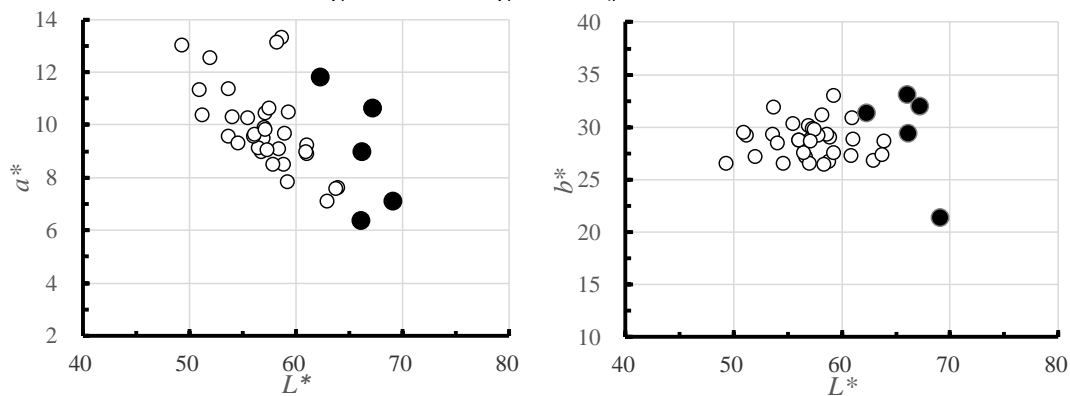
*Figure 5: Heartwood color of Zelkova clone measured by spectrophotometer.
Relationship between lightness index (L*) and chromaticness index (a*.b*).*
○: average value of 32 clones, ●: literature value (Kitamura 1987)

Average moisture content of all linages was 81% for heartwood and 63% for sapwood, which was slightly higher for heartwood, and the coefficient of variation between linages was also slightly larger for heartwood. Furthermore, no significant differences were observed in either sapwood or heartwood between the harvest periods (September and January). Green moisture content for all linages was slightly

higher in the heartwood than in the sapwood, and the coefficient of variation among the lines was also slightly larger. In the L*a*b* color system, lightness expressed as L*, hue and saturation as chromaticity of a*, b*, and in the chromaticity diagram, a* was in the red direction, -a* was in the green direction, and b * showed as yellow direction and -b* showed as blue direction (Kitamura 1987). There was no clear relationship between L*a*b* value, annual ring width, and heartwood density. In the log market, zelkova classified by heartwood color. Previous reports indicated that the red zelkova, which has a high market value, has a narrow average annual ring width of approximately 2 to 3 mm, and a density of approximately 500 to 600 kg/m^3. It has also been reported that the proportion of vessel elements and large conduits in one annual ring is high (Furukawa et al.1989). Furthermore, in a report when the density of the 12th annual ring of red zelkova is 650 to 730 kg/m^3 and the average annual ring width is 3 to 4 mm, the density after the 30th to 40th annual ring is 550 to 500 kg/m^3, and the average annual ring width is expected to stabilize at 2 mm (Furukawa et al.1989). It was compared the heartwood L*a*b* values of high-quality zelkova according to Kitamura and grafted clone linage. Hue and saturation a* and b* were in similar ranges, but there was a difference in lightness L *value, which was assumed to be a change in heartwood color with increasing tree age (Kitamura 1987). Taking these things into consideration, it was suggested that about half of the grafted linage were red zelkova lineage.

CONCLUSIONS

Differences in growth traits and material among the 32 clone lineages of Zelkova grafted trees were evaluated non-destructively 12 years after planting. It was inferred that the initial growth amount of the grafted line was inherited from the growth traits of the mother tree. No significant correlation was observed between growth traits and wood quality. At the early age of growth, there were differences in heartwood color between linages based on the L*a*b* color system, and it was inferred that half of grafted clone linages were of the red zelkova. On the other hand, no correlation was observed between heartwood color, density, and annual ring width, which are good indicators for Zelkova.

REFERENCES

Yamamoto S, Hakamata T (2004) Clone propagation by selection and tissue culture of Keyaki (Zelkova serrata Makino) elite trees grown in Shizuoka prefecture. Bulletin of Shizuoka forestry & Forest Product Institute, 32:1-13 (in Japanese).

Prasetyo A, Endo R, Takashima Y, Aiso H, Hidayati F, Tanabe J, Ishiguri F, Iizuka K, Yokota S. (2015) Variations in growth characteristics and stress-wave velocities of Zelkova serrata trees from eight half-sib families planted in three different initial spacings. Journal of Forest and Environmental Science 31: 235–240.

Forest & forest product research institute（2004）Wood industry handbook, Maruzenn 1236pp.

Ido H, Nagao H, Kato H (2012) Bending strength and compressive strength parallel to the grain of Keyaki (Zelkova serrata) timber. Mokuzai Gakkaishi 58(3) 144-152 (in Japanese).

Furukawa I, Fukutani S, Kishimoto J (1989) Characteristics of variation of wood quality within Keyaki (Zelkiva serrata Makino) trees horizontal variations of ring width, fiber length, vessel element length, specific gravity, and longitudinal compression strength. Hardwood research 5:197-206 (in Japanese).

Hashizume H, Ikuo F, Sakuno T, Oomori Y (1987) On the utilizing volume and wood quality of Zelkiva serrata. Hardwood research 4:49-59 (in Japanese).

Kitamura Y (1987) Measured color values of important domestic and imported wood, Bull. For. & For. Prod. Res. Inst. 347,203-239 (in Japanese).

Isamoto, N. (2000) Anatomical characteristics on wood quality of the three strains of keyaki (Zelkova serrata). J. Japan. For. Soc. 82(1): 87-90 (in Japanese)

Influence of the number of belts over vibrations of the cutting mechanism in woodworking shaper

Georgi Kovatchev[1*], Valentin Atanasov[1]

[1] University of Forestry, Faculty of Forest Industry, Department of Woodworking Machines, 10 Kliment Ohridski Blvd., 1797 Sofia, Bulgaria

E-mail: g_kovachev@ltu.bg; vatanasov_2000@ltu.bg

Keywords: Wood shapers, milling, vibrations, V-belts, beech wood

ABSTRACT

This study presents the influence of the belt type over vibrations of the cutting mechanism in a woodworking shaper. The cutting mechanism is driven by V-belts with a Z section. The number of belts is changed by measuring the vibration speed (V r.m.s) during operation. Measurements are made at four points in the radial direction. Two of them are located in the upper bearing housing near the cutting tooland, the other two in the lower bearing housing near the belt pulley. The details are machined on a universal milling machine with bottom location of the working shaft model FD-3.Beech testsamples were milled. The experiments were carried out with rotation frequencies of 4000 min^{-1}and6000 min^{-1}. During the research, attention was paid to some technological factors such as the feed speed of the processed material lwhich is from4m.$min^{-1}$to 16m.min^{-1}, milling width 12 mm and thickness of removed layer 12 mm. The study is aimed at improving the reliability and efficiency of a wood shaper machine as well as to ensure the accuracy and quality of products.

INTRODUCTION

The most widespread gears that are used to drive the cutting mechanisms of many woodworking machines are belt gears. Manufacturers of rubber products offer a big selection of belts with different constructions and sizes, produced from different rubber compounds in order to improve their operation.In addition, various software devised and are available on the market that help us to more easily calculate the type of belt and its section, the number of belts, their length and others. The correct assembly of the belt pulleys and the force with which the belt is stretched are only some of the factors who have a big importance for the good operation of the belt drive. In case of inaccurate installation, poorly stretched belt or incorrect calculation of the number of belts, there are prerequisites for worse operation of the belt drive, and therefore of the wholel mechanism (SOKOLOVSKI 2007, Continental-industry.com, Optibelt.com).That's why it is important to pay attention how the different types of mechanisms in woodworking machines are driven. Milling machines are widely used in furniture production field. The quality of machining has a great influence on every single detail.Each part must have accurate shape, dimensions and roughness class that meet the tolerances written in the technical documentation.All these requirements are related to the correct selection of technological cutting modes, correct selection and preparation of the cutting tools, checking the machine's serviceability and others (KORCOK *et al.*2018, KMINIAK *et al.*2018, SYDOR *et al.*2021). Woodworking milling machines work at high rotation frequencies, which necessitates constantly checking the serviceability of the cutting mechanism. Any small inaccuracy can have an impact on the processing quality of wood as well as wood-based materials. Well-processed elements and details, according to technical requirements, have a great influence on the quality and finished look of the entire product (KOVATCHEV*et al.*2022,OBRESHKOV 1997, SYDOR *et al.*2022, VITCHEV *et al.*2019).

The aim of the present work is to measure and analyze the vibration speed in the milling process of beech test samples on a universal wood shaper with bottom location of the working shaft. The object of research is the bearings load when the cutting mechanism is driven with a different number of V-belts.The study is aimed at improving the reliability and efficiency of a wood shaper machine to ensure the accuracy and quality of products.

MATERIALS AND METHODS

The whole experiment in the present work was conducted on a universal wood shaper with bottom location of the working shaft. The general view of the machine is shown in figure 1.

Figure 1: Wood shaper general view

The cutting mechanism of the selected machine has a relatively simple design. This fact helps a lot to conduct the experiments correctly.The mechanism is driven by an asynchronous electric motor with a power of 3 kW and rotation frequency of 2880 min^{-1}.The torque from the electric motor to the working shaft of the machine is transmitted using a belt drive. Two V-belts with a Z section are used. In order to also follow the influence of the number of belts, additional experiments were carried out with only one belt with a Z section.The operating frequencies of the machine are 4000 min^{-1} and 6000 min^{-1}.They provide serious technological possibilities for realizing different cutting speeds by using cutting tools with different diameters. The technical data of the cutting tool are shown in Table 1.

Table 1: Technical data of the cutting tool

Type of instrument	D mm	d mm	B mm	α °	β °	γ °	z бр	Material of the teeth
Groovecutter	125	30	12	16	55	19	6	HM

The inscriptions in the table are: *D* - diameter of the milling cutter, *d* – diameter of the bore, *B* – milling width, α – back angle of cutting, β – angle of sharpening, γ – front angle of cutting, *z* – number of teeth. During the experiment were milled beech (*Fagus sylvatica*) test samples with cross-sectional dimensions of 50 x 50 mm and length of 600 mm were milled. Table 2 shows the main technical characteristics of the experiment.

Table 2: Basic technical data

№	Rotation frequency	Diameter of the milling cutter	Cutting speed	Milling width	Thickness of removed layer
1	4000 min^{-1}	125 mm	26 m/s	12 mm	12 mm
2	6000 min^{-1}	125mm	39 m/s	12 mm	12 mm

A universal roller feeding mechanism is mounted on the milling machine figure 2. Through it we regulate the feeding speed of the test samples. The feed speeds of the treated material with which the experiments were made are respectively U1 = 4 m/min, U2 = 10 m/min, U3 = 16 m/min. The intensity of the vibrations is assessed on the basis of the root mean square value of the vibration speed (V mm/s(r.m.s.)). The measurements have been performed at four measuring points located on the bearing house. Two of them are located near the upper bearing next to the cutting tool. The other two are located near the lower bearing next to the belt pulley. The measurement points are located *mutually perpendicular,* radial to the main shaft of the machine figure 3 (БДС ISO 10816 – 2002).
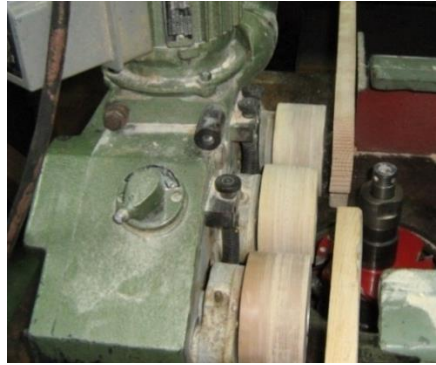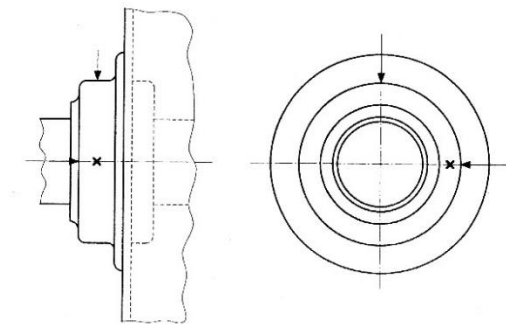
Figure 2: Roll feeder

Figure 3: Measurement points

Vibration speed V mm/s (r.m.s.) is measured using a specialized device model Bruel & Kjaer Vibrotest 60, figure 4. The sensor, which measures the intensity of the vibrations, is attached to the bearing house with a magnet, figure 5.

Figure 4: Bruel&KjaerVibrotest 60

Figure 5: Measuring sensor

RESULTS AND DISCUSSION

The experimental part includes work trials in milling of beech (*Fagus sylvatica*) test samples. The measurement points near the upper bearing are respectively: A_x – radial direction parallel to the feed direction, A_y – radial direction perpendicular to the feed direction. The measurement points near the lower bearing are respectively: B_x – radial direction parallel to the feed direction, B_y – radial direction perpendicular to the feed direction. Figure 6 and figure 7 show the variation of the vibration speed measured in the upper bearing at a rotation frequency of the working shaft 4000 min^{-1}. In order to drive the cutting mechanism V-belts one and two with Z section are used.

Figure 6. Vibration speed measured at the point A_x in the milling of beech test samples
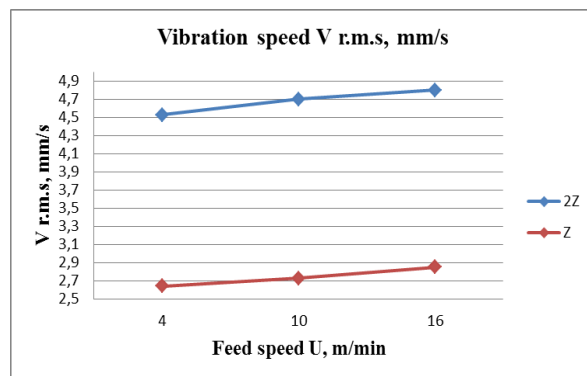
Figure 7. Vibration speed measured at the point A_y in the milling of beech test samples

From figure 6 it can be seen that at point A_x the vibration speed is not affected by how many belts are used to drive the cutting mechanism. The influence of the number of belts at point A_x on the vibration speed is slight. The measured values show small differences between 0.21 mm/s to 0.28 mm/s. From the same figure, it can be seen that the feedspeed of the test samples has a slightly more influence on the vibration. A significant increase in the vibration speed depending on the number of used belts is observed at point A_y figure 7. Here the vibration increases from 1.95 mm/s to 1.97 mm/s when two belts are used. Feed speed has minimal effect on vibration, between 0,21mm/s and 0,27 mm/s.

Figure 8 and figure 9 show the variation of the vibration speed measured in the lower bearing at a rotation frequency of the working shaft 4000 min^{-1}.

The variation of the vibration speed at point B_x shown in figure 8 is identical to that at point A_x. At point B_y shown in figure 9 the number of belts has a significant influence on the vibration speed. When the cutting mechanism is driven by two belts the vibration speed increases from 0.90 mm/s to 1 mm/s. The feed speed has little effect on the vibration speed 0.23 mm/s - 0.28 mm/s.

The variation of the vibration speed measured in the upper bearing at rotation frequency of 6000 min-1 is shown in figure 10 and figure 11.

Figure 8: Vibration speed measured at the point B_x in the milling of beech test samples

Figure 9: Vibration speed measured at the point B_y in the milling of beech test samples
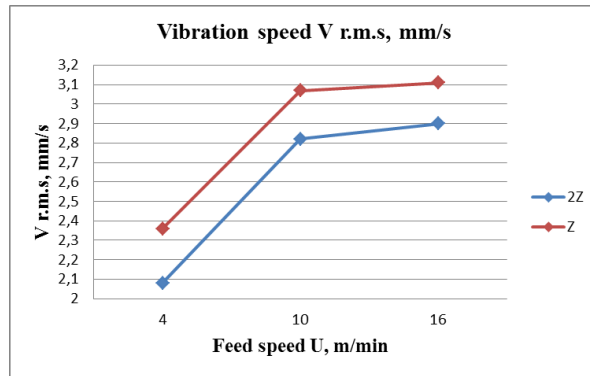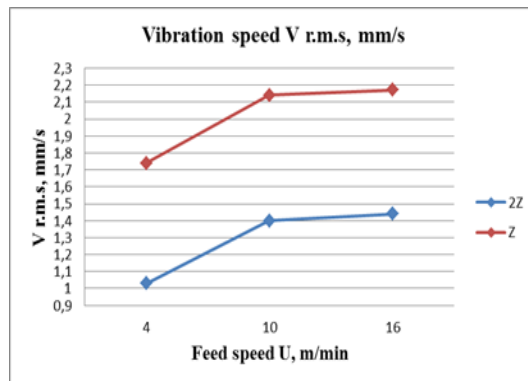

Figure 10: Vibration speed measured at the point A_x in the milling of beech test samples
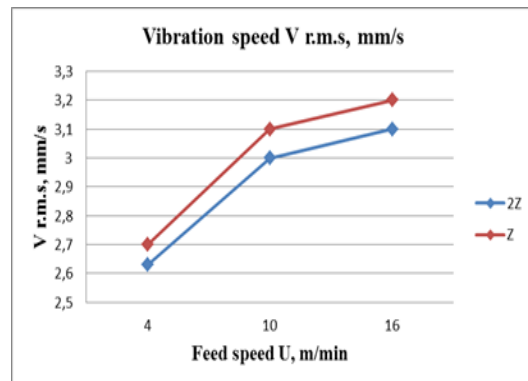
Figure 11: Vibration speed measured at the point A_y in the milling of beech test samples

When the cutting mechanism is driven only with one belt, the vibration speed measured at point A_x shown in figure 10 increases between 0.71 mm/s and 0.74 mm/s during operation. The feed rate increases the vibration between 0.41 mm/s and 0.43 mm/s. At point A_y figure 11 it can be seen that the number of belts has no effect on the vibration speed.

Figure 12 and figure 13 show the variation of the vibration speed measured in the lower bearing at a rotation frequency of the working shaft 6000 min⁻¹.The variation of the vibration speed at point B_x shown in figure 12 is identical to that at point A_y figure 11. Figure13 shows the variation of vibrations at point B_y.
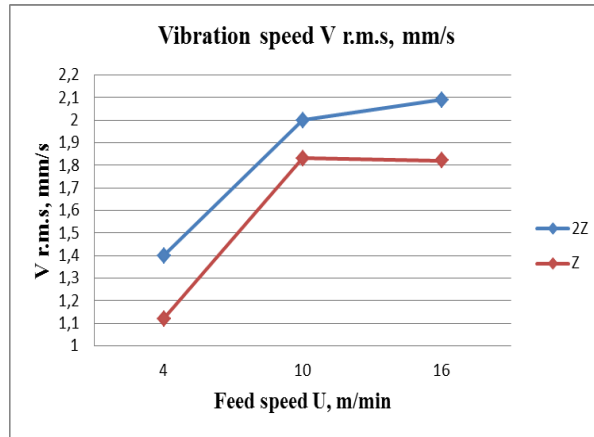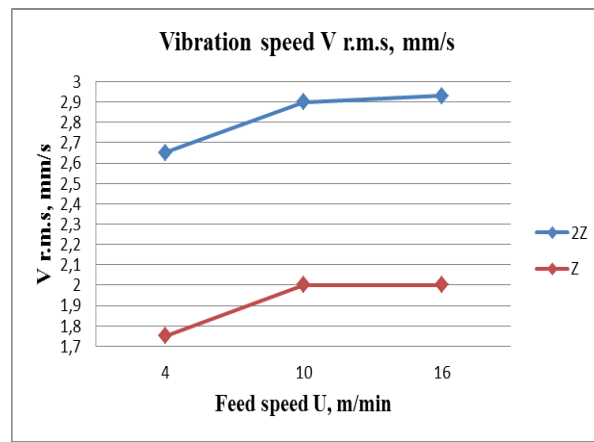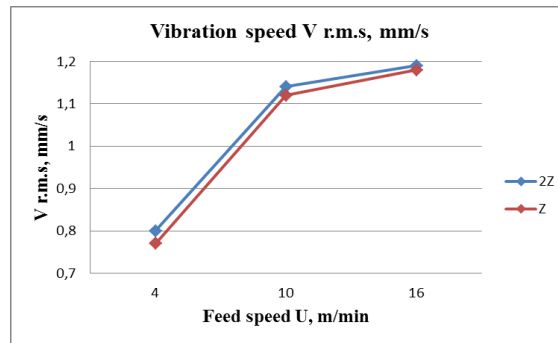

Figure 12: Vibration speed measured at the point B_x in the milling of beech test samples
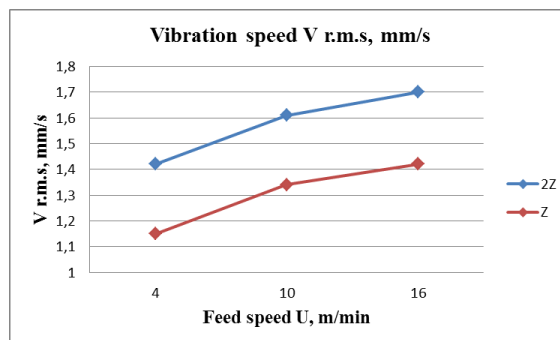
Figure 13: Vibration speed measured at the point B_y in the milling of beech test samples

When the cutting mechanism is driven with two belts the vibration speed increases during operation with 0.28 mm/s.

From the conducted experiments the following conclusions can be drawn:

- From the graphs it can be seen that at a rotation frequency of 4000 min⁻¹ in three of the measurement points (A_y, B_x and B_y) the vibration speed is lower when one belt is used to drive the cutting mechanism.
- At a rotation frequency of 6000 min⁻¹ in two of the measuring points (A_y and B_x) the reported values are almost equal. At point A_x the vibration speed increases when the cutting mechanism is driving with one belt. At point B_y the trend is opposite. This means that at different rotation frequencies, the smaller number of belts does not always lead to a reduction in the vibration speed during milling of beech specimens.

REFERENCES

KMINIAK, R., SIKLIENKA, M., SUSTEK, J.2018. Influence of the thickness of removed layer on the quality of created surface when milling oak blanks on the CNC machining center. Chip and Chipless Woodworking Processes 11 (1): 79-86, Zvolen, ISSN 2453-904X (print), ISSN 1339-8350 (online).

KORCOK, M., VANCO, M., BARCIK, S., GOGLIA, V. 2018. Influence of tool angular geometry on surface quality after milling of thermally modified oak wood. Chip and Chipless Woodworking Processes 11 (1): 87-96, Zvolen, ISSN 2453-904X (print), ISSN 1339-8350 (online).

KOVATCHEV, G., V. ATANASOV, I. RADKOVA (2022), Influence of mechanical oscillations on the accuracy of making grooves in solid wood, 13th International Science Conference "Chip and Chipless Woodworking Processes",TatranskaLomnica, TU-Zvolen, ISSN 2453-904X (print) ISSN 1339-8350 (online), pp. 65 – 71.

OBRESHKOV P. 1997. Woodworking Machines, Sofia. 182 p. (in Bulgarian)

SOKOLOVSKI, S. 2007. Machine elements, Sofia, ISBN 978-954-332-044-38, 318 p. (in Bulgarian)

SYDOR, M., R. MIRSKI, K. STUPER-SZABLEWSKA, T. ROGOZINSKI (2021), Efficiency of Machine Sanding of Wood, Applied Sciences, Volume 11 – Issue 6 /2860/ March 2 2021, ISSN 2076 – 3417, https://doi.org/10.3390/app11062860

SYDOR, M., G. PINKOWSKI, M. KUCERKA, R. KMINIAK, P.ANTOV, T. ROGOZINSKI (2022), Indentation Hardness and Elastic Recovery of Some Hardwood Species, Applied Sciences, Volume 12 – Issue 10 /5049/ May-2 2022, ISSN 2076 – 3417, https://doi.org/10.3390/app12105049

VITCHEV, P., ANGELSKI, D., MIHAILOV, V. 2019. Influence of the processed material on the sound pressure level generated by sliding table circular saw. In Acta Facultatis Xylologiae Zvolen, 61(2): 73−80, 2019, DOI: 10.17423/afx.2019.6

БДС ISO10816-1:2002, Evaluation Of Machine Vibration By Measurement On Non – Rotating Parts – Part 1: General Guidelines, 25 p.

Continental Belts and Components The Product Range – www.continental-industry.com

Optibelt Power Transmission Compact Catalogue – www.optibelt.com

The impact of litter forest fires on the internal structure of wood from stem of beech trees

Elena-Camelia Musat[1], Costin-Ovidiu Vantoiu[1], Emilia-Adela Salca[2*]

[1] Department of Forest Engineering, Forest Management Planning and Terrestrial Measurements, Faculty of Silviculture and Forest Engineering, Transilvania University of Brașov, Șirul Beethoven 1, Brasov, 500123, Romania.
[2] Faculty of Furniture Design and Wood Engineering, Transilvania University of Brașov, Universității 1, Brasov, Romania.

E-mail: elena.musat@unitbv.ro; costin.vantoiu@student.unitbv.ro; emilia.salca@unitbv.ro.

Keywords: forest fires, beech, quality of wood, tomograph, resistograph, Romania.

ABSTRACT
Forest fires represent an increasing threat to biodiversity and of course to trees, including the quality of wood inside the trees left in the forest after the fire. Due to the significant ecological and economic losses, the present research aimed to evaluate the internal quality of the wood inside the trunk of beech trees left after a litter fire. The fire occurred in 2019 and damaged many trees. Most of the affected trees were extracted from the stand, where only those that did not show external signs from the fire remained. From these were chosen the trees on which the field investigations were carried out. Both non-destructive and relative non-destructive evaluation methods were used to assess the internal quality of the wood, more precisely, analyses were carried out with the Arbotom sound tomograph and the IML Resi F-500 resistograph. After interpreting the results and comparing the tomograms with the resistograms, it was observed that, in most of the trees studied, the fire of 2019 had no negative effects, the wood inside the trunk showing no signs of internal decay or relatively low signs of decay. So, it can be appreciated that the trees existing at the moment in the burned plot can continue to exist in good conditions, not having damaged wood.

INTRODUCTION
The beech stands are ecosystems with a special weight in Romania's forest landscape. In the beech stands, higher values are recorded in terms of the average diameter at the breast height, which is why the cumulative volume of the trees, which can be extracted through harvesting, increases as the age increases (Câmpu, 2010; Câmpu and Dumitrache, 2015) and represents, for all production classes, 25% of the total volume of the stand at the age of 50 years, respectively 38% of the volume of the stand at the age of 100 years.
The quality of wood represents its ability to ensure the optimal characteristics of the products it is transformed into, through its structural, physical, mechanical, chemical, and technological properties, but taking into account that there is a variable relationship between them, the notion of quality is a relative one (Ciubotaru and David 2011). The quality of wood is influenced by defects, which represent anomalies (David and Ciubotaru 2011) regarding the shape of the trunk, the structure, the integrity of the tissues, and the chemical composition, as well as structural deformations that modify its properties, affecting, as a rule, its quality in a negative way and which, consequently, limit its processing and use possibilities (Ciubotaru 1998). One of the main defects that lead to the downgrading of wood is rotting, which means a profound change in the chemical composition of wood (Beldeanu 2008), accompanied by a change in its color, consistency, and properties. The resistance of the wood, which starts to decrease from the first stages of the attack of xylophagous fungi, is completely lost in the stage of rotting (Musat 2017, Musat 2023), rot being the advanced stage of wood degradation, as a result of rotting (Beldeanu 2008, Musat 2017). On the other hand, trees can present various injuries, which can be produced by different causes, consisting of tissue destruction and dislocations of anatomical elements from their normal connections (Bucur 2003, Beldeanu 2008). These can affect either the bark or the wood, or both the constituents of the trees (Beldeanu 2008). Forest fires could injuries to the trees, because in the forests almost all the materials are combustible and, under certain conditions, can ignite and burn,

releasing heat (Barbu 2018, Burlui and Burlui 2018). The effects of tree injury (Beldeanu 2008, David and Ciubotaru 2011) depend on the surface, depth, number of injuries, and the woody species.

The evaluation of the quality of wood in standing trees can be done by several modern methods, these being classified into three categories, respectively: destructive methods, relatively non-destructive methods, and non-destructive methods (Musat 2017, Musat 2023). The evaluation of wood quality by non-destructive methods can be defined as a process by which the physical and mechanical properties of a material can be evaluated, without damaging or changing the possibility of the final use of that material (Bucur 2003, Ciubotaru and David 2011). Among the non-destructive methods is also the visual method, which involves the external analysis of the tree to determine the defects appearing on its trunk. The methods involving the analysis of the propagation speeds of acoustic waves through the trunk of trees are based on the density of the wood. By using acoustic waves, important information is obtained regarding the location and extent of an internal defect (Bucur 2003).

Wood has the property of emitting and retaining sound energy, but everything depends on the characteristics of the propagated sound, as other factors, such as the orientation of the fibers in relation to the sound energy field, the structure of the cell walls, humidity and density, but also on the existence of some chemical substances such as tannins, gums and oleoresins (Bucur 2003, Tarasiuk et al. 2007). Once they penetrate the wood, these sounds produce in the cell walls of the anatomical elements, some complex vibrations that give rise to internal frictions, which transform the sound energy, and that is why the emitted sounds have totally changed characteristics (Beldeanu 2008).

The purpose of the research was to analyze the quality of the wood inside the trunk of the beech trees left after the litter fire occurred in October 2019, which affected the management unit 166B, which is under the administration of Local Public Authority Pădurile Şincii. Thus, to achieve the proposed goal, it was considered the determination in the field regarding the transfer speeds of sounds through wood and the evaluation of the relative resistances of wood to drilling.

EXPERIMENTAL METHODS

The fire that affected management unit 166 broke out in October 2019 in plot 165 and lasted 3 days. In extinguishing of the fire were participated foresters, firefighters, volunteers, and a helicopter. Practically, the fire started from boundaries number 78 to 80 (Figure 1), developing from the valley to the peaks, after which it descended again, affecting a total area of 15 ha in parcels 165 and 166, of which 10 ha only in the management unit number 166 (Figure 1).

Figure 1: Research location, images of the 2019 litter forest fire and the current state of the stand

Beech trees that showed signs of decay were chosen for field investigations. Their choice was not an easy one as the stand was traversed with cuttings after which a volume of approximately 1500 m$_3$ was

extracted. This fact led to the extraction of the damaged trees so that at the time of making the determination, the remaining trees did not seem to be depreciated, growing in relatively good conditions (Figure 1). Trees under study were visually analyzed and found to have either dry or cracked bark at the base, or the bark had fallen from the trunk which, in the respective regions, had dead wood (Figure 1). After choosing the trees, the north direction was marked on each of them, and three levels (at 30, 60, and 90 cm above the ground) were measured and marked to carry out the investigations. The determinations were initially made with the Arbotom Rinntech sound tomograph, after which, depending on the reconstructed tomogram, were chosen the directions and positions to carry out additional investigations with the IML Resi F-500 resistograph. The principle of operation and application of the method of assessing the quality of wood with sounds was described in the works of Musat 2017, Musat et al. 2020, and Musat 2023. It should be noted that 7 hammer blows were applied to each emitting sensor, the number of blows being chosen under the ambient noise in the area and taking into account the recommendations in the specialized literature (Rinn 2014, Tarasiuk et al. 2007).

RESULTS AND DISCUSSION
During the visual analysis of the first tree for which the results are presented, defects such as cracked bark on the trunk, dead wood, and the beginning of decay, visible from the outside, were identified at the base of the trunk, in the northwest-west-east-southeast direction. There is also a fruiting body at the height of 90 cm, in the west direction, very close to the sensor S_6 located at this level. From the analysis of the tomograms (Figure 2), it can be seen that inside the trunk, but also from the periphery to its center, a series of internal irregularities appear, which make the sound transfer speeds through the wood lower, and the tomograms to be colored in shades of yellow and yellow-green. All these irregularities appear in the direction of fire advance, i.e. north – east – southeast.

Figure 2: The field investigations carried out for a beech tree: the links between the sensors; the scale of values specific to the determination, the reconstructed tomogram and the resistogram

Compared to the expansion of this area from the level analyzed to the next level, it is found that the internal irregularities, which may indicate a possible degradation of the wood, occupy approximately two-thirds of the section at the level of 30 cm, after which the affected surface narrows to the level of 60 cm. At 90 cm, although it no longer occupies an area as large as at the 30 cm level, the tomogram shows important signs of degradation and internal irregularities of the wood, which lead to the appearance of orange shades in the area of the neighboring sensors S_{6-7}. This can be attributed to the action of xylophagous fungi, present even through the fruiting bodies, which led to the degradation of the wood (Musat, 2017).

To be able to draw pertinent conclusions regarding the state of the wood inside the trunk, additional, punctual investigations were carried out, both at the level of 30 cm from the ground, a situation in which the resistogram was made in the direction of the sensor S_8, and at the level of 90 cm, on the direction of the sensor S_6 (Figure 2). Analyzing the resistograms, it is found that the first third of the length of both resistograms shows structurally destroyed wood, in the sense that the relative resistances to drilling are either zero (S_6 – at 90 cm) or very reduced. It is also observed that after the areas with degraded or even rotten wood, the resistances begin to increase, but no significant variations appear which denotes some structural change inside the trunk, which leads to non-differentiations between latewood and earlywood in the annual rings (Musat 2017, Musat 2023).

Another beech tree shows, in the north, northeast, and east area, up to the height of 1.20 m, dry and cracked bark on the trunk. In addition, an area of dead wood appears at the base, with strong signs of decay, up to a height of 40 cm. Analyzing the results indicated by the tomograph in the case of the 30 cm section (Figure 3), it is observed that there are lower sound transfer speeds through the wood, marked in red on the image with the connecting lines between the sensors, which are highlighted on the tomogram (Figure 3) with yellow-green shades between sensors S_{7-8-9}.
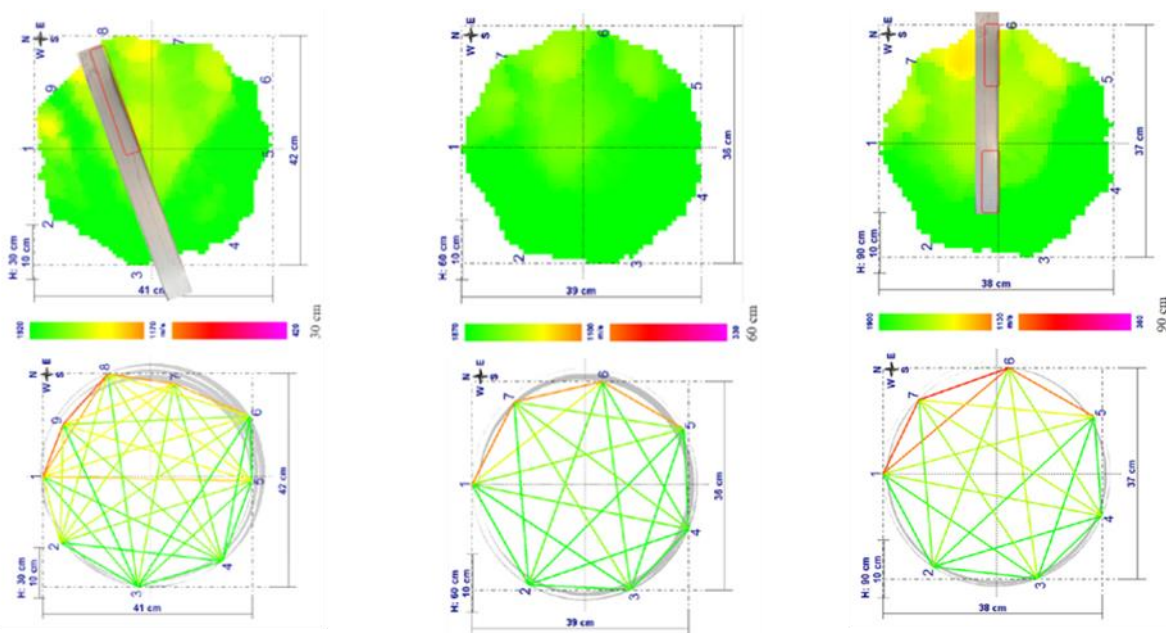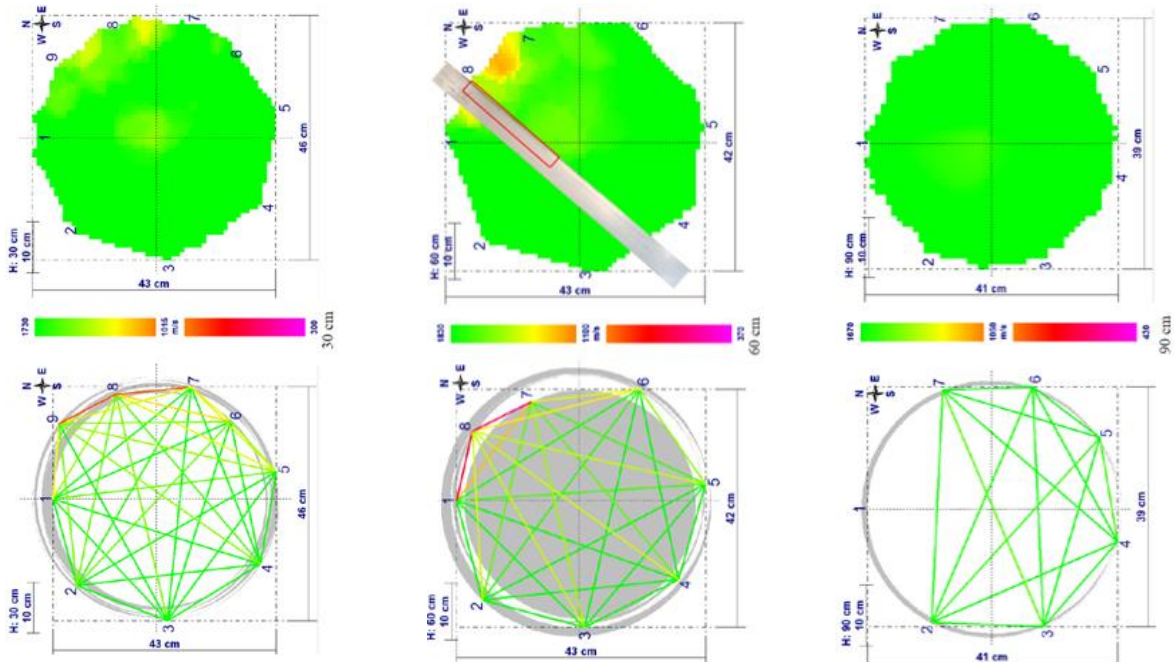

Figure 3: The field investigations carried out for another beech tree: the links between the sensors; the scale of values specific to the determination, the reconstructed tomogram, and the resistogram

At the 60 cm level, it is observed that the wood degradation is concentrated between the sensors S_{7-8-1} (Figure 3), an aspect indicated on the tomogram by shades of orange. This is also the reason why a resistogram was made in the direction of the sensor S_8, at the level of 60 cm (Figure 3). From its analysis, it can be easily seen that the entire section shows wood with low resistance to drilling. In addition, on the first third of the length of the resistogram, extremely low resistances appear, close to zero, which indicates wood with a destroyed structure. By comparing the position of the sensor S_8 on the trunk and the condition of the wood as it appears in visual analysis, it is found that the resistogram was taken just above the decayed area at the base of the trunk, which clearly shows that the rot has progressed upwards on the trunk. At the 90 cm level, both the tomogram (Figure 3) and the image with the connecting lines between the sensors indicate wood where the sound transfer speeds are high, which makes that these images to be colored in green.

Comparing the images from the three analyzed levels with the real condition of the wood, visible from the outside of the trunk, and with the resistogram made in the direction of the sensor S_8 at the 60 cm level (Figure 3), it is quite clear that the structure of the wood in the northwest area – north–north–east

is almost destroyed. The poor quality of the wood inside the trunk cannot be identified on the tomogram in the real stage, which can be attributed to the denser or less dense medium through which the sounds are transferred (Musat 2017). In this sense, the speed of sounds differs, first of all, concerning the density of the wood (Beldeanu 2008, Rinn 2014), but it can also be influenced by its humidity (Beldeanu 2008). Thus, the presence of rot in the area and the fact that the wood is in various stages of decay can lead to an increase in wood moisture as a result of the activity of xylophagous fungi (Ciubotaru 1998, Beldeanu 2008).

CONCLUSIONS

Following the investigations carried out in the field with the Arbotom Rinntech sound tomograph and the IML F-500 Resi resistograph, the following conclusions could be drawn:

- some trees show serious signs of degradation on the outside, which causes pathogenic agents to penetrate inside the trunk leading to the destruction of the integrity of the wood;
- the areas with degraded wood identified by the tomograph seem smaller in extent compared to the real condition of the wood illustrated by the resistograph or observed from the outside of the trunk;
- the resistograph provides much more accurate information about wood degradation.

REFERENCES

Barbu I (2018) Riscul de incendii în pădurile din România: cartare și metode de evaluare. Bucovina Forestieră 18(2):155–163.

Beldeanu E (2008) Produse forestiere. Transilvania University Pulishing House, Brasov, Romania.

Bucur V (2003) Nondestructive characterization and imaging of wood. Springer-Verlag Berlin Heidelberg.

Burlui I, Burlui MC (2018) Incendiile forestiere: elemente caracteristice, factori determinanți și măsuri de gestionare. Bucovina Forestieră 18(2):165–175.

Câmpu VR (2010) Research concerning the development of red heartwood and its influence on beech wood sorting. BUT – Series II 3(52):11–16.

Câmpu VR, Dumitrache R (2015) Frost crack impact on European Beech (*Fagus sylvatica* L.) wood quality. Notulae Botanicae Horti Agrobotanici Cluj-Napoca 43(1):272–277.

Ciubotaru A (1998) Exploatarea pădurilor. Transilvania University Pulishing House, Brasov, Romania.

Ciubotaru A, David EC (2011) Cercetări privind unele caracteristici ale nodurilor plopului negru (Populus nigra L.) din aliniamente. Revista Pădurilor 126(6):8–12.

David EC, Ciubotaru A (2011) Research concerning the number and the surface of the knots detected at black poplar (Populus nigra L.). BUT – Series II 4(53):13–18.

Musat EC (2017) Analyzing the sound speed through the wood of horse chestnut trees (*Aesculus hippocastanum* L.). BUT – Series II 10(59):55–66.

Musat EC (2023) The agreement in accuracy between tomograms, resistograms, and the actual condition of the wood from lime trees harvested from cities. BioResources 18(1):1757–1779.

Musat EC, Derczeni RA, Barti ME, Dumitru-Dobre C (2020) Analysis of sound velocity through the wood of spruce trees located into a burned area. Forestry Bulletin T.24(4):98–109.

Rinn F., 2014. Central basics of sonic tree tomography, 14(4):8–10. https://ictinternational.com/casestudies/central-basics-of-sonic-tree-tomography/ Accessed 04 October 2022.

Tarasiuk ST, Jednoralski G, Krajewski K (2007) Quality assessment of old-growth Scots pine stands in Poland. In: COST E53 Conference – Quality Control for Improving Competitiveness of Wood Industries, Warsaw, Poland, pp. 153–160

Analysing innovative wood joints crafted by laser cut spline curves

László Németh[1], József Garab[2*], Péter György Horváth[3]

[1] University of Sopron, Institute of Basic Sciences, Bajcsy-Zs. Str. 4, Sopron, Hungary, 9400,
[2] University of Sopron, Institute of Applied Sciences, Bajcsy-Zs. Str. 4, Sopron, Hungary, 9400 (*),
[3] University of Sopron, Institute of Creative Industries, Sopron, Hungary, 9400. Bajcsy-Zs. Str. 4.

E-mail: nemeth.laszlo@uni-sopron.hu; garab.jozsef@uni-sopron.hu;
horvath.peter.gyorgy@uni-sopron.hu

ABSTRACT

This study investigates the shape of the longitudinal joints in hardwood panels, inspired from veneer joints commonly used in the industry. The design of these joints is tailored to facilitate creative and flexible compositions. The joints adopt a mathematical description using splines, serving a good technological purpose for the wood processing. Employing laser cutting technology, the shapes are precisely crafted by a laser beam on the hardwood panels. After the process, the joints undergo a visual inspection, the material loss due to the technology is calculated, and other parameters are determined. Additionally, significant characteristics relevant to practical applications, such as joint fit, shape of accuracy, and aesthetics, are assessed. To enhance the understanding of the mechanical interactions, finite element analysis (FEA) is performed to model the mechanical contacts within the joints. A primary motivation for this research is the efficient utilization of residual wood materials. This approach aims to extend the life of the available raw materials within the value chain, contributing to sustainability goals.

INTRODUCTION

Several techniques are available for making curved cuts for decorative purposes. In order to choose the right technique the following parameters should be taken into consideration: final purpose, properties of the raw material, and the expected parameters of the processing. Options include cutting with a blade, which can be used mainly for thin wallboards and veneers. Among saws, scroll saws and bandsaws are suitable for cutting along curved lines. It is also possible to use a special cutting medium for wooden materials, such as water jet cutting. The birth of high-pressure abrasive water-jet (AWJ) cutting can be traced back to the early 1970s, when non-metallic soft materials were first cut (Jiazhong et al., 2008). With the continuously developing process, it is possible to make curved cuts, however, the watery environment and the soaking of the raw material still indicate a problem from the point of view of further processing. Laser processing is another option for curved-line cutting of wood. Certain parameters need to be considered in this procedure, including the cutting performance of the available system and the properties of the end result, such as the burnt surface obtained.

The design and analysis of the shape of joints made with different technologies were in focus of several studies, hence, the connections are vital points of any structure. Liu (2000) analysed the distribution of the stress of serpentine-end matched (SEM) joints from veneer. Sebera and Simek (2010) analysed numerically the mechanical properties of the dovetail joint made by CNC technology. Wielinga (2023) performed finite element analysis (FEA) on interlocking timber connections in order to investigate the influence of the shapes.

The main goal of our research was to determine specific curves, which can be used for joints made by laser cutting technology. This may serve as the basis for new innovative wood-based products. Therefore, our work had the following steps: curve definition for the joints with mathematical equations, laser processing with the defined curves to prepare for the joints, and finite element analysis of the joints for stress analysis.

MATERIALS AND METHODS
Definition of the curves

The base of our curves is the planar cubic Bezier curve. Let p_0, p_1, p_2, and p_3 be the control points of a Bezier curve, where p_0 and p_3 are the endpoints according to the left-hand side of Figure 1. Then the vector-scalar equation of the curve is

$$r(t) = p_0 B_0^3(t) + p_1 B_1^3(t) + p_2 B_2^3(t) + p_3 B_3^3(t), \quad t \in [0,1], \tag{1}$$

where the Bernstein polynomials are $B_i^3(t) = \binom{3}{i} t^i (1-t)^{3-i}$. Its matrix form is

$$r(t) = [t^3 \quad t^2 \quad t^1 \quad t^0] \begin{bmatrix} -1 & 3 & -3 & 1 \\ 3 & -6 & 3 & 0 \\ -3 & 3 & 0 & 0 \\ 1 & 0 & 0 & 0 \end{bmatrix} \begin{bmatrix} p_0 \\ p_1 \\ p_2 \\ p_3 \end{bmatrix}, \quad t \in in[0,1] \tag{2}$$
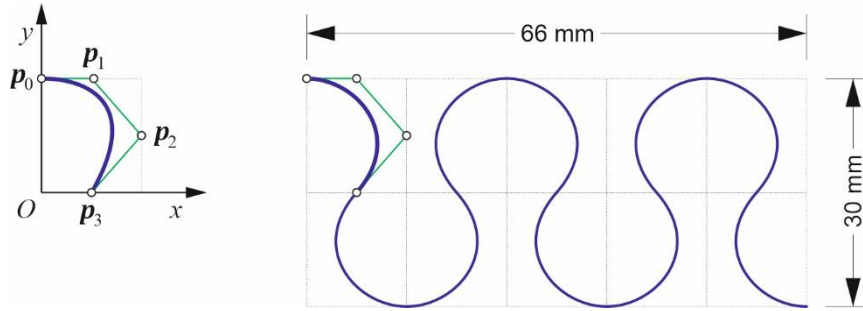
Figure 1: Definition of the joint curve no. 1

Since the width of our panel is 66 mm, we divided it into five parts, and we chose 30 mm for the joint part (see Figure 1). That way, for a symmetric joint curve, we have ten blocs, for which we define cubic Bezier arcs with four control points. Let $a = 66/5 = 13{,}2$ and $b = 30/2 = 15$. We give the coordinates of the control points of the first arc with the functions of a and b, the coordinate system can be seen in Figure 1. In all the cases, we have $p_0 = (0, b)$ and $p_3 = (a/2, 0)$, moreover, except the last case, p_1 and p_2 are on the lines $y = b$ and $x = a$, respectively. Table 1 shows their coordinates in detail.

Table 1: Coordinates of p_1 and p_2

curves serial number	p_1	p_2
1	$(a/2, b)$	$(a, b/2)$
2	$(a/2, b)$	(a, b)
3	$(a/2, b)$	$(a, -b/2)$
4	$(a/2, b)$	$(a, 3b/2)$
5	$(3a/2, b)$	$(0, b)$

Let the second arc be the central rotation image of the first arc with $180°$ around the vertex p_3. Then the mirror of the first two arcs around the line $x = a$ provides the second pair of arcs. The following pairs are also obtained by mirrors around the vertical lines $x = 2a$, $x = 3a$, and $x = 4a$. The definitions of the control points yield that not only the tangent lines, but also the curvatures are continuous in the jointing points, which means the curve provides continuous speeded laser catting. Figure 2 shows the other four curves with their control point.
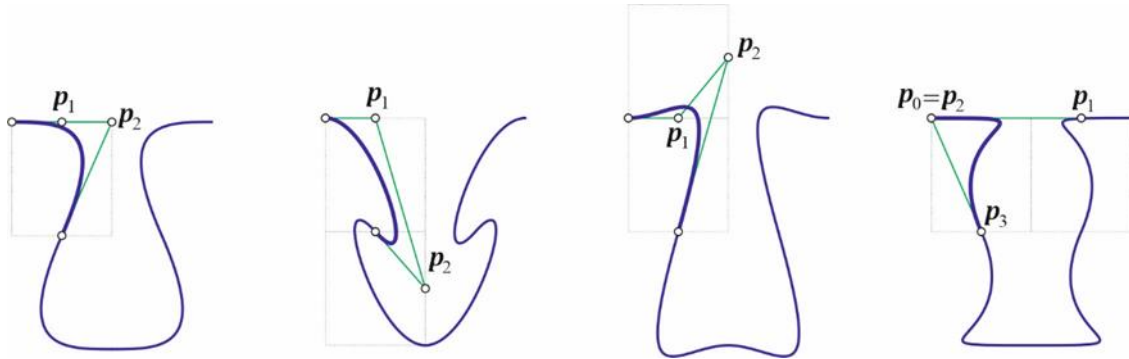
Figure 2: Definition of the joint curve no. 2 – 5

Laser processing

In our experiments involving curved cuts, we utilized European beech (*Fagus sylvatica* L.) material, which was 4 mm thick and 66 mm wide. The prepared sample bodies had a polished quality surface, the samples did not receive surface treatment. Before cutting, the curves were transformed into a form readable by the equipment (CorelDraw, cdr format). To achieve an exact fit, the cutting tool paths were perpendicular to the edge of the material at the exit, so that the cut everywhere resulted in a clean and clear exit from the material. The power of the laser beam (150 W) and the speed of the mirror head (10 mm/s) were set to optimize the cutting result (Universal Laser Systems, ILS 9.150D, Pmax=150 W, 2" focal length lens). The goal was that the beam exiting the material would cut the material, but not look for unnecessary surface burns. With this approach, our aim was to minimize material loss resulting from the cutting gap during the cutting process. Each sample was cut one by one by placing a template in the workspace, which positioned each sample, thus ensuring regular cut images. During the processing, no negative experimental effects or factors were experienced; the parameters of the cutting results coincided with the goals defined at the beginning of the experiment.

Finite Element Analysis

To conduct preliminary stress analysis, computational simulations were performed using Ansys Workbench for linear static analysis under tension (licensed product is Ansys® Academic Research Mechanical, Release 15). Pre-processing of the analysis consisted of importing the geometry definition according to the cutting samples, meshing, and defining the boundary conditions. The European beech (*Fagus sylvatica* L.) material was modelled an orthotropic one, which is described using nine material constants, namely three normal Young's moduli in longitudinal (E_L), radial (E_R), and tangential (E_T) directions; three Poisson's ratios in radial-tangential (v_{RT}), longitudinal-radial (v_{LR}) and longitudinal-tangential planes (v_{LT}); and three shear moduli in radial-tangential (G_{RT}), longitudinal-radial (G_{LR}), and tangential-longitudinal planes (G_{TL}). These constants were derived from Szalai (2001) and are presented in the Table 2. The global *X, Y, Z* axes corresponded to the anatomical coordinate system of the wood (*L, R, T*). The orientation of the samples are were in the *LT* plane. The joint was modelled as a bonded contact because the focus was on the shape of the joints. Quadratic order element was applied with the size of 3.0 mm except of the contacts, where the mesh size was 1.00 mm. The future experimental setup is not known. Therefore the grip of the samples was modelled with displacement support ($u_x = 0$) in order to prevent localized high stress from Poisson's effect. Weak springs were added in order to prevent rigid body motion during simulation. 1 mm displacement was applied to simulate the tension. The main area of interest is the peak stress locations and the stress distributions around the joints.

Table 2: Used material parameters of European beech (Fagus sylvatica L.) from Szalai (2001)

Species	Density	E_L	E_R	E_T	G_{RT}	G_{TL}	G_{LR}	v_{LR}	v_{LT}	v_{RT}
European beech	750	14000	2285	1160	467	952	1972	0.45	0.51	0.71

Density – density of the beech wood [kg/m3];EL, ER, ET – normal moduli of elasticity [MPa]; GRT, GTL, GLR – shear moduli of elasticity [MPa]; vLR, vLT, vRT – Poisson's ratios [-]

RESULTS AND DISCUSSION

In the five different cutting samples (Figure 3), it is clear that the shape of the fit is accurate, but the cutting loss arising from the technology leads to a gap between the materials. An almost identical gap can be observed on each sample (input side: 0.7-0.6 mm, output side: 0.3-0.15 mm), so it is possible to minimize them by modifying the trajectory curves.
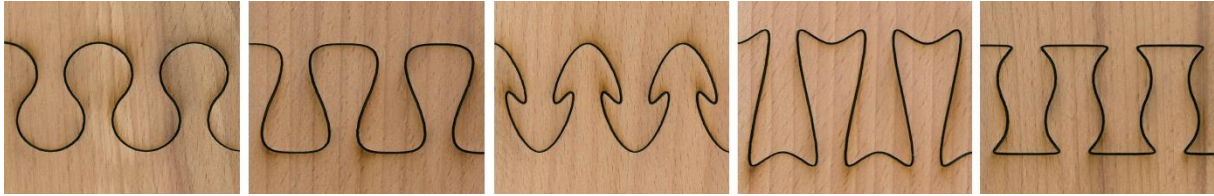
Figure 3: Cut samples 1-5

In addition to being a technical obstacle (incorrect fit during gluing), the visible gap between the elements is also a problem from an aesthetic point of view. An additional aesthetic problem can be the appearance of randomly located surface burns at the cutting gap narrowing towards the output side, as well as the burnt surface in the gap depending on the wood species. The cause-and-effect relationship between the resulting gap and the size of the surface burn is summarized in the Ishikawa diagram below (Figure 4). Surface burning and unevenness resulting from the nature of the technology cannot be eliminated, only the size can be reduced.
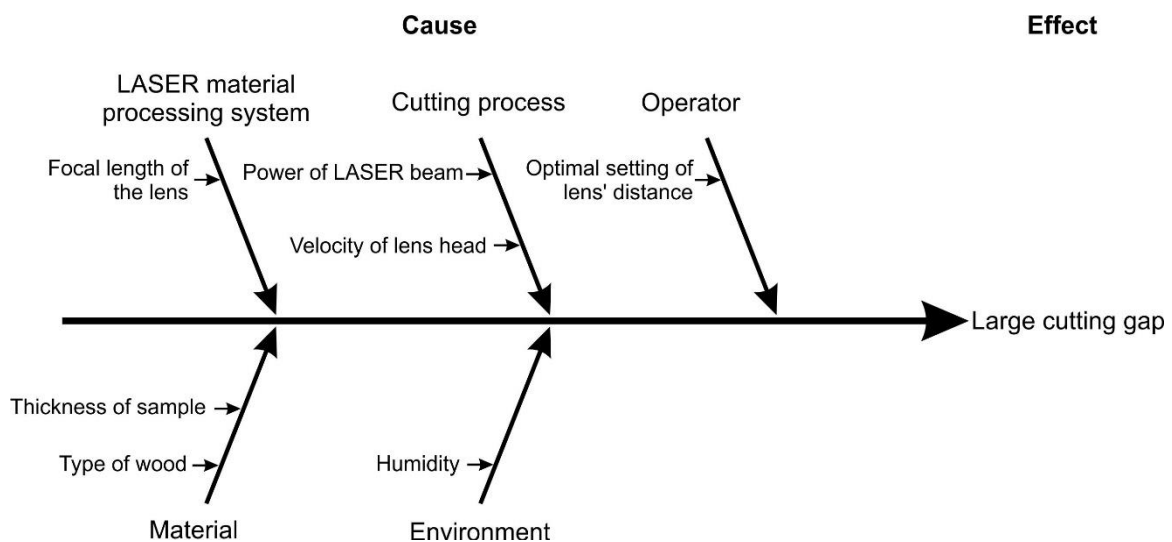
Figure 4: Ishikawa diagram of gap reduction

The curve geometry has a significant influence for the stress distribution around the joints (Figure 5 and Figure 6). Significant normal stresses occur around the wall of the joints. Although the cutting gap and the adhesive is not taken into consideration into this simulation, the differences between the joint geometries are visible. The highest peak stress occurred at joint curve 1 (112.42 MPa) but the peak stresses at the other joints have also similar peak stresses: joint curve 2 (σ_{LL} = 106.81 MPa), joint curve 3 (σ_{LL} =106.60 MPa), joint curve 4 (σ_{LL} = 101.31 MPa) and joint curve 5 (σ_{LL} = 109.84 MPa). Joint curve 1, 2 and 4 are similar to traditional joints, and joint curve 3 and 5 are more design specific. The sharp corners and arches with small radius may be not advisable.
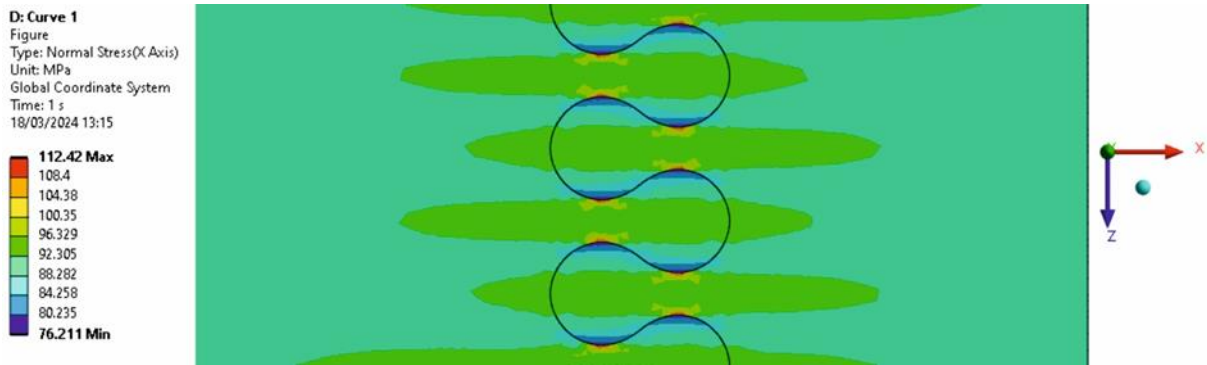
Figure 5: Normal stresses parallel to the longitudinal directions on the joint made by Curve 1

| *Curve 2* | *Curve 3* | *Curve 4* | *Curve 5* |
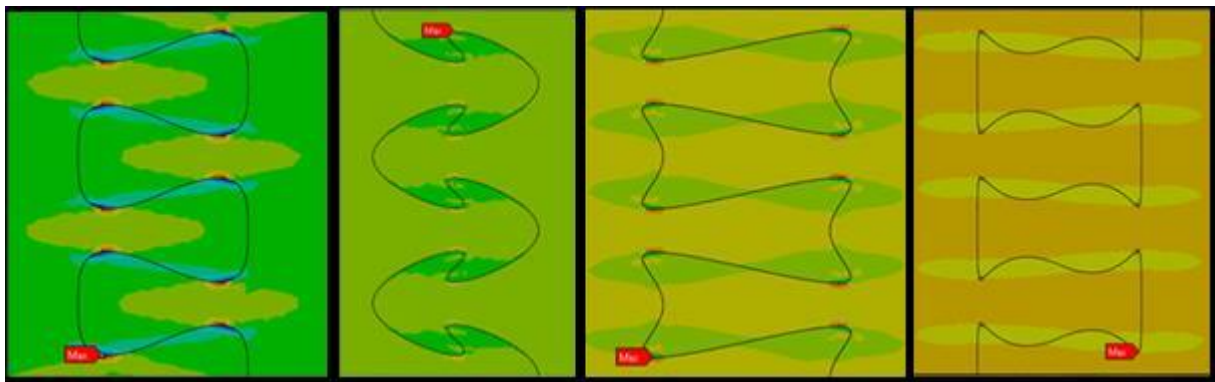
Figure 6: Normal stresses parallel to the longitudinal directions on the joints made by joint curves 2 - 5

CONCLUSIONS

Mathematical relationships can be used to select the cutting image, during which cutting lines for different purposes can be defined by changing the parameters. The formation of gaps in general cutting toolpaths can be observed here as well, and it can also be reduced by changing technological parameters. The finite element analysis was a useful preliminary analysis tool. The stress distributions are different according to the joint curve geometry. However, future investigations are needed to incorporate the adhesives and the laser cutting gap into the model. Furthermore, physical testing should be performed in order to gather experimental results for the joints.

The flexibility of the presented laser cut system is emphasized. There is no need for different cutting tools, only the laser is used. Utilizing even smaller pieces of waste wood further contributes to sustainability goals.

REFERENCES

Liu, Y. (2000). Properties of veneer sliced from serpentine-end-matched flitches. MSc thesis. Oregon State University.

Xu, J., You, B., and Kong, X. (2008). Design and Experiment Research on Abrasive Water-jet Cutting Machine Based on Phased Intensifier, IFAC Proceedings Volumes, 41(3), 14846-14851.

Sebera, V., Simek, M. (2010). Finite element analysis of dovetail joint made with the use of CNC technology. Acta universitatis agriculturae et silviculturae mendelianae brunensis, 58(3), 321-328.

Szalai, J. (2001). Faszerkezetek méretezését és gyártását befolyásoló sajátosságok. [Specific characteristics of design and production of timber structures] In: Wittmann, Gy. (ed.) Mérnöki faszerkezetek. [Engineered Wooden Structures] II. kötet. Mezőgazdasági Szaktudás kiadó. Budapest, 143-259.

Wielinga, E. (2023). Finite Element Analysis of Interlocking Timber Connections in Plywood Diaphragm Floors: Optimizing Form for Strength. MSc thesis, Eindhoven University of Technology

Dynamic fatigue tests of hardwoods

Gábor Orbán[1], Antal Kánnár[1]

[1] University of Sopron, Institute of Creative industry Bajcsy-Zs. Str. 4, Sopron, Hungary, 9400

E-mail: orbangabor@phd.uni-sopron.hu; kannar.antal@uni-sopron.hu;

Keywords: dynamic axial fatigue test of wood

ABSTRACT

Static testing of the parameters of wood as a structural material has been practised for at least 100 years. In the meantime, investigating repeated dynamic impacts and loads required significant improvements in measurement techniques. These cyclic fatigue tests became widespread for assessing metals, rubber and plastics, rather than wood.

This study aims to examine the dynamic strength characteristics of wood as an elastic material. This will provide data for designing wooden structures exposed to dynamic loads, like wooden bridges, lookout towers and possibly innovative machine parts. Based on the available literature, this appears to be an extensive, little researched topic of investigation.

The goals of the research is to create Wöhler curves for hardwoods, which shows the fatigue limits of wood as a function of the applied stresses. This involves performing cyclic tensile tests with maximum loading levels of 60, 70, 80 and 90 % of the static tensile strength. At least three specimens are tested at each load level for calculating the average fatigue limit.

Tests are currently underway. Completed tests yielded a fatigue curve for oak. Results show that oak material resists fatigue testing well, even at high stress levels. It can withstand hundreds of thousands of cycles at stress levels as high as 80 % of the static tensile strength.

INTRODUCTION

Wood is one of the most ubiquitous construction materials due to its specific strength, rigidity, and easy workability. Wooden bridges need to withstand dynamic loads from vehicular traffic, and wooden lookout towers and other wooden structures are exposed to wind loads. The fatigue characteristics of wood at different levels of loads are important when designing structures in earthquake-prone areas. Despite all of these areas of application, information and examination of wood under special circumstances like fatigue is not common. The most important reason for this is that classic dynamic fatigue tests are especially time-consuming.

Karr et al. (2022) examined birch wood using a newly developed ultrasonic resonance test at a frequency of 20 kHz, up to 109 cycles. They compared the results to those of servo-hydraulic testing at 50 Hz and 5×10^6 cycles. The number of cycles as a function of stress amplitudes measured at both frequencies show similar slopes and deviations up to failure in the system of overlapping life spans.

Myslicki et al. (2016) created a new measurement technique whereby the amplitude was increased by 2.5 MPa after each 10,000 cycle. Measurements were validated against constant amplitude measurement results. Furthermore, they compared beech samples with various grain orientations. At identical loading levels, the more the specimens deviated from 0° grain angle, the lower number of cycles were necessary to induce failure.

Bao et al. (1996) tested various composite materials like chipboard, MDF, OSB and plywood. Based on their results, each material exceeded 1 million cycles of fatigue life span at stress levels corresponding to 30% of the MOR.

Gašparík and Gaff (2015b) examined the effect of cyclic stresses on the deflection damping rates of beech solid wood and laminated wood. Solid wood results showed that the thicker the material, the higher the attenuation. The effect of cycle number on the damping ratio is negligible. They found similar trends for laminated wood too. There was no significant difference between the behaviour of solid and laminated specimens.

Bonfield and Ansell (1991) investigated the fatigue characteristics of wood laminates in tension, compression and shear. Fatigue life spans were significantly lower in compression than in tension. They

determined the existence of an inflection point in the constant life span lines at the transition of all compression and partial tensile fatigue loads.

Tsai and Ansell (1990) provided an overview of the literature on wood fatigue and emphasized the necessity of experiments performed with load control at various moisture contents. They tested two laminated harwoods Khaya ivorensis and beech, and a softwood Sitka spruce under load control, using four-point loading. They established that increasing moisture contents decreased the static strength and fatigue life span.

Watanabe et al. (2014) examined the fatigue behaviour of Japanese cedar and Selangan batu. They used irreversible triangular wave forms of 0.5 and 5 Hz in frequency for loading. The applied load level was 110-70 % of the static strength. The fatigue life of Japanese cedar was longer at 5 Hz, especially at lower stress levels. In case of Selangan batu, loading frequency did not influence the fatigue life span.

Yildirim et al. (2015) investigated the static strength and fatigue of Scots pine and oriental beech wood. Fatigue and static strength were measured using three-point bending. Specimen preparation and fatigue/static bending tests followed the protocol of ISO 3129 (1975) and ISO 3133 (1975) respectively. Fatigue tests were performed at stresses corresponding to 80, 70, 60, 50 and 40 % of the MOR. Allowable design stresses are based on a certain percentage the furniture design MOR. In this regard, beech and Scots pine allowable design stresses can be determined at 50 and 40 %, respectively.

One lesser-known aspect of modified wood is dynamic strength, and the effect of modification thereupon. Pečnik et al (2020) applied low molecular weight phenol-formaldehyd (PF) resin onto Scots pine and European beech wood. They evaluated the effect of such modification using cyclic three-point bending tests. Compared to the control sample, modified wood resulted in higher strength, but the cyclic fatigue strength decreased (by 9 % and 14 % for pine and beech, respectively. The cyclic fatigue strength of the control sample was 67 % of the static MOR for both species. The fatigue strength of PF resin-modified pine and beech decreased to 58 % and 54 % of the original, respectively.

Based on the available literature, research into the dynamic strength of wood is still ongoing. Measurement methods are diverse, because there is no standard for fatigue testing of wood.

MATERIALS AND METHODS

Dynamic strength investigation involved English oak (Quercus robur) material. For tensile tests parallel with the grain, the cross section of the 20 x 50 x 300 mm specimens was reduced in both directions over an 18 cm long section, according to DIN EN ISO 527-2:2012 (Figure 1)
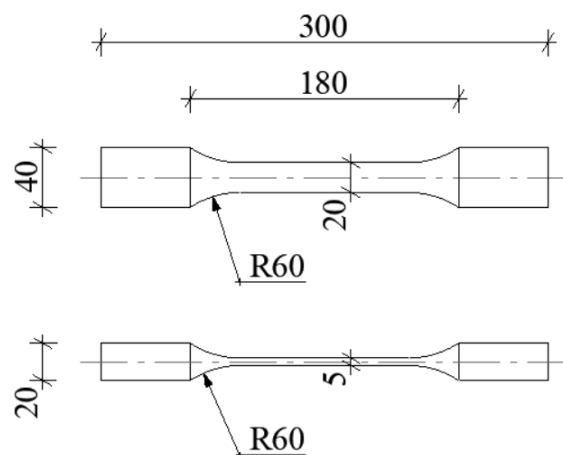
Figure 1: Dumbbell shaped specimens according to DIN EN ISO 527-2:2012 (dimensional unit in mm)

Weakening the cross section on both sides ensures that the compound stresses arising at the clamp are distributed over a larger cross section. This ensures that failure occurs in the section of the specimen subjected to pure tension.

The raw material of the specimens came from logs grown in various sites. Samples were stored in a normal climate according to ISO 554:1976 (at a temperature of 20±2 °C and Relative Humidity of 65±5 %), until reaching an equilibrium moisture content of 8 to 13 %. Dynamic loading was performed at 7

different load levels, at 60 to 90 % of the static tensile strength, with 5 % increments, and an amplitude of ±1 kN.

The amplitude of ±1 kN resulted from preliminary experimentation. This meant that frequencies higher than 20 Hz were not possible to apply, because it would have prevented regular sine waves to be induced. This lead to significantly increased measurement times.

3 specimens were tested at each load level, for a total of 21 specimens. Static tensile strength was determined from another 3 specimens, tested using linearly increasing loading. Average results at f_{mean}=95,95 Mpa (Table 1) were very close to literature data $f_{t,0,k}$=89,9 MPa (**Németh et al. 2015**). Cyclic testing occurred at a frequency of 20 Hz, using sine wave loading. Testing duration was 2 million cycles or failure, using an INSTRON 8802 servo hydraulic fatigue testing machine (Figure 2).

Figure 2: Fatigue Testing Set Up In Instron 8802

RESULTS AND DISCUSSION

Collected results yielded two Woehler curves (Figures 3 and 4).

Table 1: Results of the test (loads of 80 to 90% of static strength)

Stress level [%]		static testing	90%	85%	80%
σ [Mpa]		95,9	86,4	81,6	76,8
F [N]		12081	10873	10269	9665
Number of cycles	Mean value		4219	9292	16159
	Min.		1129	4072	4373
	Max.		9978	16469	25961
	Std. Deviation		4991	6426	10929

Table 2: Results of the test (loads of 60 to 75% of static strength)

Stress level [%]		75%	70%	65%	60%
σ [Mpa]		72	67,2	62,4	57,6
F[N]		9061	8457	7853	7249
Number of cycles	Mean value	34436	363121	1445966	2000000
	Min.	11619	142475	766978	2000000
	Max.	73249	662589	1831884	2000000
	Std. Deviation	33785	268866	589850	0
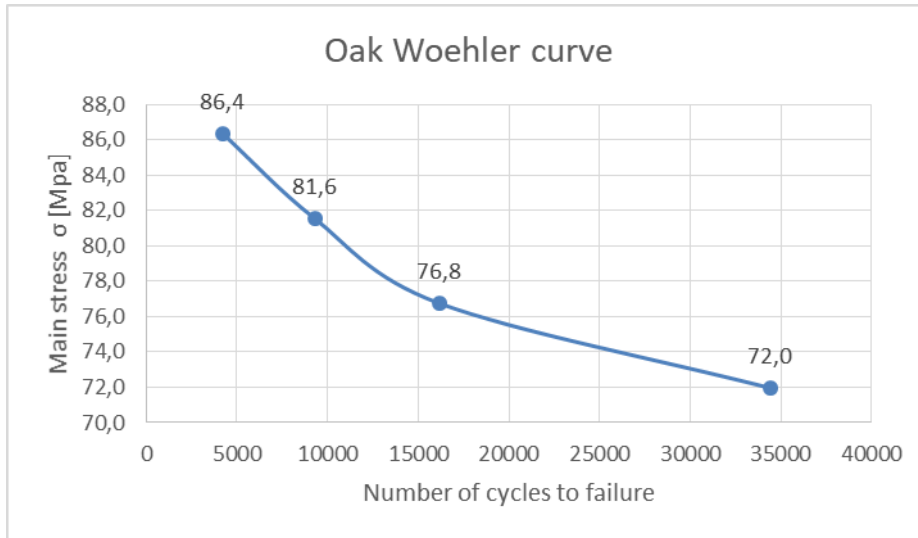
Figure 3: Woehler curve (90-75%) based on the results of the test
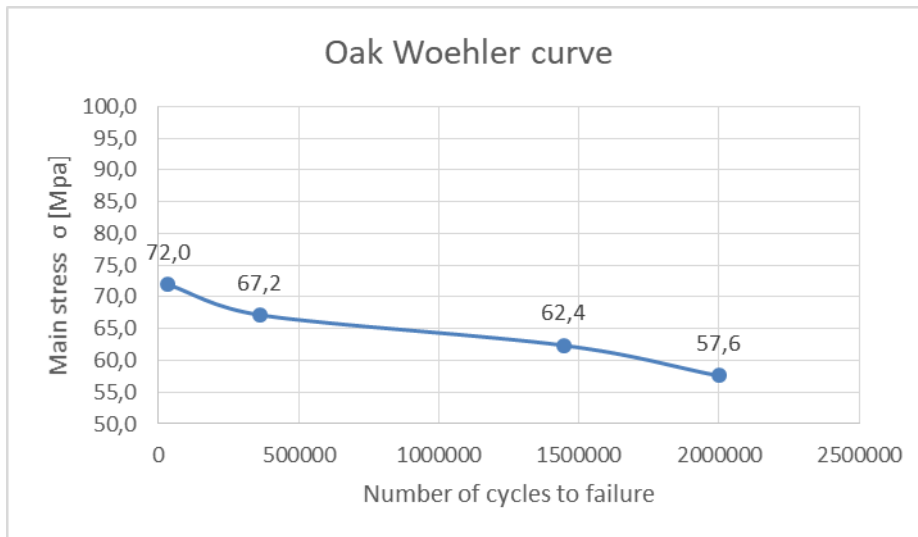
Figure 4: Woehler curve (75-60%) based on the results of the test

The current stage of our research may be regarded as a preliminary testing. We determined the order of magnitude of points of the fatigue curve based on a relatively small sample. Results show that, when loading was close to static strength (80 to 90%), failure occurred after a few thousands to 16,000 cycles (see Table 1 and Figure 3). At load levels of 70 to 75 %, failure happened at nearly identical cycle numbers, at 35,000 cycles (Table 2, Figure 4). Significant change occurred at a stress level of 65%, where approximately 1.5 million cycles were needed to reach failure, while specimens did not fail until up to 2 million cycles at a 60 % stress level. This indicates the fatigue limit of the oak material tested. This means that the wood is not expected to fail in tension at a stress level of 60 % or lower at a frequency

of 20 Hz. During its service life wood is exposed to cyclic wind loading. According to our tests, wood will not fail if stresses do not exceed 60 % of the static tensile strength in the tension zone during wind-induced cyclical bending. Cyclical bending tests, coming up next in our research agenda, may be able to confirm or disprove this statement.

CONCLUSIONS

The examination of fatigue limits of wood is an important area of research in the dynamic assessment and design process of wooden bridges and lookout towers. The presented research aims to provide a basis of investigating such characteristics. Our study established that the fatigue limit corresponds to approx. 60 % of the tensile strength, since at this load level the examined material withstood more then 2 million cycles at a frequency of 20 Hz. Further examinations are required that include compression and bending as well as the dynamic investigation of other species in addition to oak tensile tests.

REFERENCES

Bao, Z., Eckelman, C., Gibson, H. (1996). Fatigue strength and allowable design stresses for some wood composites used in furniture. Holz als Roh- und Werkstoff. 54. 377-382. https://doi.org/10.1007/s001070050204

Bonfield, P. and Ansell, M. (1991). Fatigue properties of wood in tension, compression and shear. Journal of Materials Science. 26. 4765-4773. https://doi.org/10.1007/BF00612416

Gašparík, M., and Gaff, M. (2015b). "The influence of cyclic stress on the attenuation rate of deflection of solid wood and laminated wood," Wood Research 60(3), 351-358.

Karr, U., Fitzka, M., Schönbauer, B., Krenke, T., Müller, U. & Mayer, H. (2022). Fatigue testing of wood up to one billion load cycles. Holzforschung, 76(11-12), 977-984. https://doi.org/10.1515/hf-2022-0111

Myslicki, S., Vallée, T. & Walther, F. Short-time procedure for fatigue assessment of beech wood and adhesively bonded beech wood joints. Mater Struct 49, 2161–2170 (2016). https://doi.org/10.1617/s11527-015-0640-4

Németh, R, Bak, M., Börcsök, Z. (2012): A kocsányos tölgy faanyagának jellemzői. (Characteristics of English oak material) Erdészeti Lapok 50(12), 387-388

Peˇcnik, J.G.; Kutnar, A.; Militz, H.; Schwarzkopf, M.; Schwager, H. Fatigue behavior of beech and pine wood modified with low molecular weight phenol-formaldehyde resin. Holzforschung (2020) https://doi.org/10.1515/hf-2020-0015

Tsai, K.T., Ansell, M.P. The fatigue properties of wood in flexure. J Mater Sci 25, 865–878 (1990). https://doi.org/10.1007/BF03372174

Watanabe A. and Sasaki Y. and Yamasaki M. (2014). Bending fatigue of wood: Strain energy-Based failure criterion and fatigue life prediction. Wood and Fiber Science. 46. 216-227., ISSN:0735-6161

Yildirim, M.N., Uysal, B., Ozciftci, A., Ertas, A.H., (2015). Determination o fatigue and static strength of scots pine and beech wood. Wood Research, 60(4): 679-686

Restoration of an old painted oak boardsign - A case study

Gabriel Calin Canalas[1], Emilia-Adela Salca[2,*], Elena-Camelia Musat[3]

[1]Dacia Technological High School, Libertatii 21, Caransebes, Romania.
[2] Faculty of Furniture Design and Wood Engineering, Transilvania University of Brasov Universității 1, Brasov, Romania.
[3]Department of Forest Engineering, Forest Management Planning and Terrestrial Measurements, Faculty of Silviculture and Forest Engineering, Transilvania University of Brasov, Șirul Beethoven 1, Brasov, 500123, Romania.

E-mail: calin_canalas@yahoo.com; emilia.salca@unitbv.ro; elena.musat@unitbv.ro;

ABSTRACT

The present paper refers to restoring a small dimension, but great complexity and beauty old oak board, part of a blacksmith wrought iron signboard. The object belongs to the blacksmith guild and is impressive by its shape, proportions, manufacturing, decorated wrought iron elements, and painted ornaments on wood. The object was not restored before, though there were some previous attempts to remediate defects over time. The present restoration refers to the wooden panel exclusively and it was achieved following the restoration principles and code of ethics. The materials chosen for the restoration and conservation have determined the increase in the resistance of the finish, the finishing and bio-protection agents of the wood have improved the quality of the finished surfaces, being at the same time environmentally friendly materials, giving the object a lasting resistance and thus extending its life.

INTRODUCTION

The action of restoration is assumed by generations to conserve the traditions and cultural heritage. It refers to artworks, architectural monuments, and objects including furniture (Lloyd 2001, Timar 2003). Any furniture suffers over time from frequent accidents and needs specific interventions to extend its life. Most of the damages refer to the natural degradation of wood, finishing materials, and defects that occurred on joints, along with inappropriate conditions of use and storage (Bennet 1995). The restoration of any wooden object consists of several steps that must be respected and followed based on the general technical restoration principles (Brandi 1996, Timar 2007). This way, the effort for restoration is fully justified once memories can be kept for long with no alteration of the object's original shape, message, and patina (Bromelle and Thomson 1982). The present paper refers to restoring a small dimension, but great complexity old oak board, part of a blacksmith wrought iron signboard (Figure 1a). The object belongs to the blacksmith guild and is impressive by its shape, proportions, manufacturing, decorated wrought iron elements, and painted ornaments on wood (Canalas 2020). The present restoration work intended to bring the object back to its original state by keeping also the time patina and historical information. The wrought iron metal elements were also subjected to cleaning, degreasing, and finishing through specific methods, with specific materials, under the principles of restoration (see Figure 1b), but it is not the subject of the present work (Canalas 2020). Trade signs have been used even in classical times as historical devices of identification and persuasion. The making of signboards was a collaborative art craft between joiners, painters, and ironworkers.

MATERIALS

The entire assembly was recovered from a street vendor specializing in art objects, antiques, and bargains from the Banat mountain area in Romania. The advertising ensemble probably originates from the Anina area. It is a collector's item due to its particularities and uniqueness, taking into account the fact that the piece in its entirety was made by hand and represents the guild of blacksmiths and farriers certified in our country since the 14th century. This piece is a composition suggestively representing a blacksmith striking an anvil, harmoniously framed in a mesh of wrought iron elements with a special optical effect. The panel is made of oak wood, enriched with decorative, hand-carved elements that frame the corners at the base of the panel through stylized acanthus leaves. The panel was made up of

three wooden elements bent on the edge, the joint being made at first sight with an adhesive of animal origin, probably bone glue. The panel has the following dimensions: L= 400mm, l= 320mm, g= 20mm. The panel is fixed in a wrought iron frame by nail-type fasteners on the sides of the wooden panel. Several layers of decorative and protective paint can be seen on the surface of the wooden board.
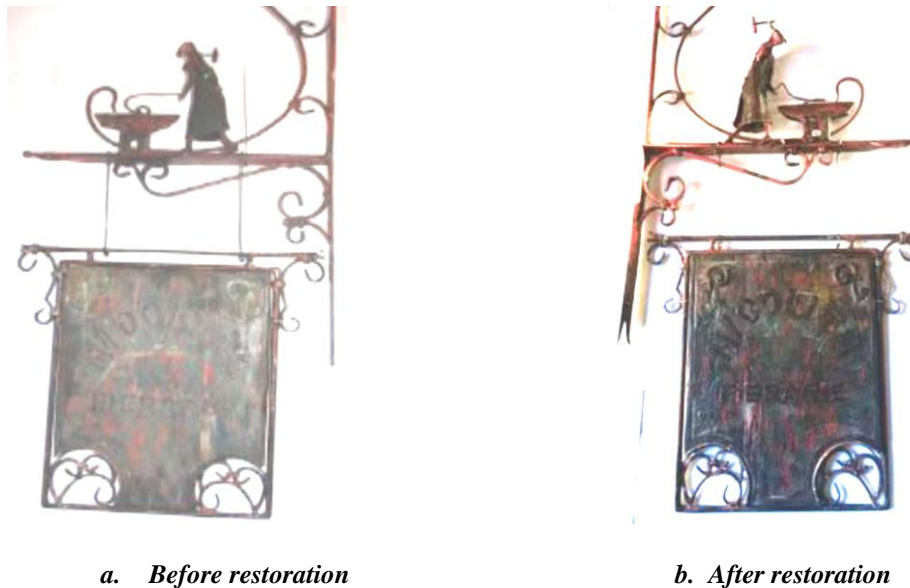
| *a.*   *Before restoration* | *b.*   *After restoration* |

Figure 1: The old painted oak boardsign (Canalas 2020)

CONSERVATION STATE BEFORE RESTORATION

The state of conservation of the assembly before conservation was conditioned by the storage environment, handling over decades, aging of materials, aging of paint layers, glue, deformation of metal parts, poor preservation, and accidents. All these factors lead to deformations, fissures, cracks, loss of component elements, and biological attack occurs when dirt is deposited and encrusted. Another factor was human intervention, easily manifested through repairs at the level of metal and wood elements. The metal elements are not in an advanced phase of decay, they mostly keep their shape, showing light hits, deformations, scratches, and layers of rust. The conservation of the piece was probably never done, only layers of paint of different colors were applied, not respecting the originality of the piece. The piece has been exposed to the weather, as evidenced by erosion on the surface of the materials, missing parts, and elements that probably do not belong to the original piece. The first evaluation concludes that the advertising set has not been exhibited or used for commercial purposes for many years, otherwise it was protected from vandalism or its commercialization as scrap metal, and it was abandoned, not finding its place in the contemporary context. The object was not restored before, though there were some previous attempts to remediate defects over time. The present restoration was achieved following the restoration principles and code of ethics (Timar 2003, 2007). The panel shows a series of cracks of different sizes (Figure 2a), between 30 and 150 mm, located in the area where the parts that make up the panel are joined, clearly visible at the ends of the panel and on the side, this area being later grouted over a layer of paint. The corner at the bottom of the semicircle shows a loss of material and embrittlement of the support. Non-adherent deposits (light atmospheric dust, cobwebs, hanging objects, light mechanical intervention) and adherent ones (hardened dust, tars, repaints, saline efflorescence) were noticed. The carved ornaments show a marked degradation and loss of volume (Figure 2c). The edges of the panel show nail marks and holes with cracks formed around them. In the lower part of the panel, in the joint area, the material is embrittled and there is a loss of material and insect attack (Figure 2b). On both sides of the panel, cracks appear along the fiber, with some mechanical wear.

Degradations of pictorial layers were also noticed, such as scaling, peeling, erasing, and blistering. Losses of painting and preparation layers were found especially in the marginal areas and at the corners (Figure 2c). In the lower part of one face, along the crack, there is a lacunar surface where the pictorial layer and the primer are missing. On the panel inscription, there are traces of grouting with an uneven texture and it shows scaly surfaces and fragments of putty. The writing and the painted frame of the

panel have been repainted. The nails that make the connection, fixing the panel in the iron frame, are of different types, which shows that they have been replaced over time. Analyzes carried out freely consisted of photographic analyses, identification of the wood and the pictorial layer on wooden support, along visual analysis. Following the macroscopic and microscopic analysis, the wood species used was established to be oak wood. With the help of the magnifying glass, in bright light, it was possible to identify the severity of the degradation of the pictorial layer, due to the shadows cast by its unevenness. In the bright light and with the help of a magnifying glass, it was found that a repainting of the inscription and the painted areas of the panel was applied over the layers of color. Chemical investigations have been carried out and the results attested that the preparation layer contained a plaster-based primer mixed with chalk.

MANNER OF RESTORATION. DISCUSSIONS
Dismantling the wooden panel
Removing the wrought iron frame was a more difficult operation because it was fixed with metal nails, and some of them were rusty. For this operation forceps, patent, and scalpels were used. In the places where the nails were rusty, and their extraction was much more difficult, a little ethyl alcohol was injected (Calalas 2020).

Mechanical cleaning of the wooden panel
A light dedusting was carried out on the entire surface of the panel, with the help of a brush with soft hair, avoiding the areas where the color layers are very fragile.

Prophylactic strengthening of the pictorial layer
It was achieved by applying the Japanese thin paper with a solution of rabbit glue in a concentration of 3%. Japanese paper was applied to the fragile surfaces of the panel (Figure 2d). After the consolidation of the pictorial layers, the Japanese paper was removed with warm water (Canalas 2020). Through this process, the paper is removed by dissolving, but also the dirt, and as a result the color is strengthened.

Strengthening the support
One of the corners of the bottom panel was impregnated with a 3% rabbit glue solution followed by a 30% glue solution. To restore the flatness of the panel and to glue the crack, after injection, the panel was pressed with the help of plates, strips of wood, three metal presses, and spangles for 24 hours (Figure 2e, f). The melinex sheet was inserted between the panel and these wooden plates, to avoid their sticking. The last stage of the panel's consolidation was the impregnation with Paraloid B72 dissolved in 10% ethyl acetate (Canalas 2020).

Consolidation of the pictorial layer
It was done both cold and hot with alternating cold and hot presses. The gaps in the pictorial layer were degreased. The putty was sanded, hydrated, and thickened with a 4:1 solution of egg yolk in water with a preservative (Canalas 2020). Thus, to ensure the cohesion of the pictorial layers on the entire surface of the wooden panel, a hot solution of 6% rabbit glue was applied and the entire surface was hot-pressed with an electric spatula at a temperature of 60ºC.

Disinsection
It was carried out with a Perxil 10 solution applied to the affected areas of the piece by injection with the syringe in all the holes, taking into account the possibility that the insect attack may still be active (Canalas 2020).

Filling in the missing parts of the panel
It was made by adding material of the same wood species, and balsit putty (Canalas 2020), prepared for the completion and reconstruction of wooden elements (Figure 2g).

Carrying out cleaning tests
Before the cleaning operation, cleaning tests were carried out to establish the solutions with good and effective responses on the pictorial layer. Thus, following the cleaning tests with different solvents, the

adherent dirt was cleaned with ammonia water (10 ml water, 10 drops of ammonia), and the encrusting dirt with a solution consisting of isopropyl alcohol, ammonia, and water in the proportions 90:10:10. The cleaning has a purely aesthetic purpose and is not necessary for the survival of the piece (Canalas 2020).

Cleaning the pictorial layers

To clean means to remove everything that disturbs the reading of the work, but it does not mean to return to the state when the work was created (Timar 2003, 2007). Among the restoration operations, cleaning is one of the most delicate. Depending on the dirt deposited on the surface of the piece and the resistance of the constituent material, certain solvents were chosen to clean the adhering and encrusted dirt. The cleaning of the pictorial layers was carried out differently, taking into account the nature of the dirt and its sensitivity to certain solvents, established after the cleaning tests (Timar 2003, 2007). The removal of adhering and encrusted dirt was carried out by methods adapted to the state of conservation and the nature of the pigments, on distinct forms and in successive stages, with time intervals between operations to control the state of the pictorial layer. The solutions were applied at different contact times, with combined cleaning methods, a condition imposed by the sensitivity of the pigments (Canalas 2020). The layer of ingrained dirt and brown areas on the bottom of the panel was removed with a solution composed of isopropyl alcohol, water, and ammonia in proportions of 90:10:10 and 50:25:25, respectively, with the help of a cotton swab, and by mechanical cleaning with a scalpel.

Gap filling

When carrying out a material addition, certain principles must be respected, such as the use of materials that are as stable as possible and resistant over time, materials that can be easily removed (reversible), the integration should not be noticeable by close, the limits of the gap should not be exceeded and the restorer should adopt a modest attitude without leaving the imprint of his personality (Timar 2007). For the superficial and deep gaps of the painting layer, a layered application of putty based on 5% rabbit glue and purified chalk dust was used (Figure 2h, i).

Chromatic integration

The chromatic integration of the grouted areas was made with oil-based colors. In the case of small gaps, point-like touch-up (rittoco) was used to establish a continuity of tone, a technique that respects the minimum intervention and the tones used are neutral grays (aqua sporca). The trattegio technique (with lines) was applied to large chromatic gaps. The chromatic integration of the putties completed the image unity of the wooden panel. Extrafine oil colors (Maimeri SPA) were used in the tratteggio technique. In the area of the inscription where the pictorial layer of the letter was missing, a shredded shoe soaked in glue was placed, recreating the volume of the letter. A paper template covered with adhesive letters, which allowed the outline of the letters to be preserved, was used (Canalas 2020).

Varnishing

The varnish used is a 10% solution of Dammar dissolved in turpentine applied by brushing (Tintoretto brush 1433). Three layers have been applied successively, with drying intervals in between. The last layer was thin and undiluted, first stretching in one direction, then changing the direction perpendicularly (Canalas 2020). This final coat gives the gloss.

CONCLUSIONS

The materials chosen for the restoration and conservation of the wooden panel have determined the increase in the resistance of the finish, the finishing and protection agents of the wood have improved the quality of the finished surfaces, being at the same time environmentally friendly materials, giving the object a lasting resistance, and thus extending its life. The restoration returned the object to a state as close as possible to the original one. The authentic elements were well-preserved and the intervention brought to light the original beauty of the restored object, its charm and patina of time.

a.Longitudinal cracks

b.Holes of insect attack

c.Carved corner ornament and the degradation of pictural layer

d.Pictural layer consolidation with japanese paper
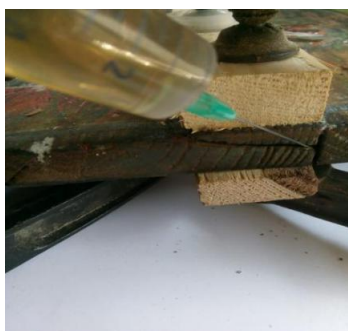
e.Wooden panel consolidation

f. Obtaining the panel flatness

g. Addition of material

h. Final cleaning by easy brushing

i. Pictural layer with putty

Figure 2: Conservation state (a-c) and steps of restoration (d-i) (Canalas 2020)

REFERENCES

Bennet M (1995) Discovering and Restoring Antique Furniture. Wellington House, London.

Brandi C (1996) Theory of Restoration. Meridiane Publishing House, Bucuresti, Romania, ISBN 973-33-0330-5.

Brommelle NS, Thomson G (1982) Science And Technology In The Service Of Conservation. Preprints of IIC Washington Congress, IIC London.

Canalas (2020) Restoration of an oak boardsign framed with wrought iron elements. Dissertation thesis, Transilvania University of Brasov, Romania.

Llyod J (2001) Furniture Restoration: A Proffesional at Work. Lewes, East Sussex, UK.

Timar MC (2003) Furniture Restoration: Theory and Practice. Transilvania University Publishing House, Braşov, Romania.

Timar MC (2007) Furniture Restoration – Science, Art and Challenge. Part 1: General Principles and Case Studies. In: PRO LIGNO 3(4): 45-54, ISSN 1841-4737

Some physical properties of native and thermo-treated *Fraxinus excelsior* timber

Cosmin Spîrchez [1*], Aurel Lunguleasa [1], Alin Olărescu [1], Camelia Coșereanu [1], Bogdan Bedelean [1]

[1] Transilvania University of Brasov, Wood Processing and Design of Wood Products Department, Str.Universitatii, Nr.1, Brașov, Brașov, Romania, 500068

E-mail: cosmin.spirchez@unitbv.ro; lunga@unitbv.ro; a.olarescu@unitbv.ro; cboieriu@unitbv.ro ; bedelean@unitbv.ro

Keywords: ash, Fraxinus excelsior L., heat treatment, thermo-wood, water absorption

ABSTRACT
In the conditions of decreasingly wood resources worldwide, the use of modern methods of high-heat treatment of wood leads to the diversification of opportunities and availabilities offered by current timber. In this sense, the thermo-wood process of treating timber with high temperature under the protection of steam, developed by Finnish researchers, gives to ash (*Fraxinus excelsior* L.) wood some new areas of use, such as in the field of sauna structures and benches, swimming pools, Olympic pools, garden furniture, etc., uses that would not have been possible a few years ago, except after laborious and expensive timber finishes. It is highlighted that the thermal process is ecological and replaces ineffective chemical processes. The material used in the work was purchased from the Holver group companies, Brasov, Romania, in the form of native and thermo-treated ash timber with dimensions of 1000x100x38 mm.

INTRODUCTION
The need for new wood resources, especially in the field of outdoor materials (gardens, bridges, etc.) or indoor materials with large variations in air humidity (kitchens and bathrooms) has led to an increasing demand for heat-treated timber (semi-finished products obtained from this kind of timber) at high temperatures of about 200 ºC. Wooden semi-finished products without significant defects are used in order to reduce the losses obtained from the timber through its dimension cutting operations (cross cutting and splitting), increasing in this way the efficiency of wood use when creating finished products. This process is known as Thermo-wood, due to the trademark obtained and registered by the Finnish Institute of Wood Processing (TWH, 2003). The main improvements have expected to be obtained through this heat treatment are the dimensional stability of the wood in relation to atmospheric humidity when temperatures of 185 ºC are used, and durability (maintenance of properties over time) when temperatures of 210 ºC are used. It is recommended to use both soft deciduous (poplar, birch), hard deciduous (beech, hornbeam) and softwood (pine, spruce) species, the heat treatment of softwoods allowing the use of temperatures 20-30 ºC higher than hardwoods.
The Thermo-wood process is characterized by the fact that wood in the form of semi-finished products is placed in a humid atmosphere at temperatures above 150 ºC, and the effective treatment duration varies between 2 and 10 hours, recording a mass loss of at least 3%. Characteristic of the Thermo-wood procedure is the fact that the treatment is carried out in an environment of saturated superheated vapors with a maximum oxygen content of 3-5% without overpressure and at an air speed of at least 10 m/s (Syrjanen and Kangas 2000). Usually, the Thermo-wood process includes three stages (Figure 1) :

- stage 1, consists in the fact that the temperature of the wood is raised in approximately 6 hours to 100 ºC and then further up to 130 ºC, thus creating the environment of superheated vapors, the temperature of 130 ºC is kept for 12 hours, until wood moisture drops to 3-4%
- stage 2, consists in the fact that the temperature in the treatment room is 185-230 ºC and maintained for 3 hours (Militz, 2002) or between 150-240 ºC for 0.5-4 hours (Syrjanen and Kangas, 2000), depending on the wood species used and the improvement expected to be obtained (stability or durability);
- stage 3, consists in the fact that the temperature in the drying chamber is reduced to 80 – 90 ºC by spraying cold water, while at the same time increasing the relative humidity of the

environment in the treatment chamber, which leads to the re-moistening of the material up to 4 -7%.
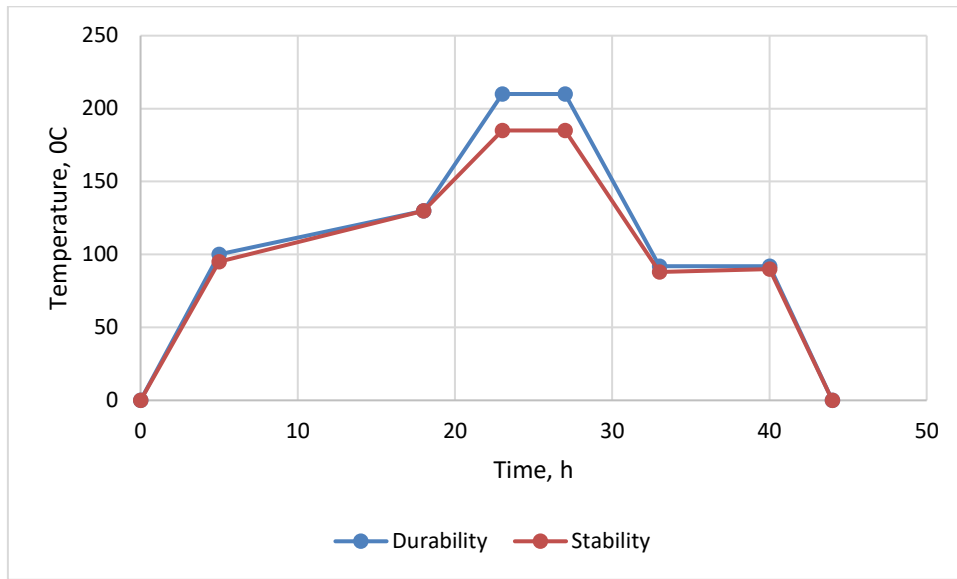
Figure 1: Diagrams of heat treatment process (for stability or durability) of wooden semi-finished products

MATERIAL AND METHODS
In the research, ash timber was used in the form of semi-finished products with dimensions of 2000 x 50 x 50 mm, both in its native-control and thermo-treated samples.

Thermo-treatment of ash wood
This operation was carried out in an industrial autoclave, with a capacity of 5 m³, in the presence of moist saturated steam in order to to reduce deformations and other defects that could appear at the treatment temperature of 185 ℃. The initial period was 22 hours, the actual treatment period was 3 hours, and the final period was 20 hours, totaling 45 hours. The semi-finished products were kept at rest after treatment for 10 days, after which they were cut into samples for specific laboratory tests.

Wood density
In order to determine the wood density, 6 planed ash samples with the dimensions of 100 x 20 x 20 mm, obtained from native and heat-treated ash, were used. The samples were conditioned for 24 hours, at a room temperature of 20 ℃ and a relative air humidity of 60%, to obtain a woody moisture content of 12%. For this test, the mass of the samples was first determined with the help of an electronic balance type Kern (Germany) with a precision of one decimal, and the dimensions with the help of an electronic vernier caliper with the precision of one decimal. Based on these values, the wood density (ρ) was determined, as a ratio between the mass and the volume of the samples, with the help of the following ratio (Eq 1):

$$\rho = \frac{m}{l \cdot b \cdot g} \cdot 10^6 \ [\frac{kg}{m^3}]$$ (1)

Where: m-mass of the wooden samples, in g; l-length of the wooden samples, in mm; b-width of wooden samples, in mm; g-thickness of the wooden samples, in mm.

Water absorption
To determine the influence of water on wood, 10 pieces of 100 X 20 X 20 mm were processed from semi-finished products. For your information, the samples were weighed with the Kern 250 balance (Germany) to obtain the mass and their thickness was measured with the electronic vernier caliper with a precision of one decimal. Then, the samples were placed in a laboratory oven (Memert, Germany) for drying at 103 ± 2 ℃, for 10 hours, to obtain the absolute dry mass of the samples. After that, to cool

down in a moisture-free environment, the samples were kept in a desiccator. Then, the cooled samples were weighed, and the thickness and mass of the samples were determined. This procedure was the basis for knowing the absolute dry mass and the thickness from which the moisture absorption process started after complete immersion in water. After obtaining the initial masses and thicknesses, the samples were inserted into a water immersion tank, at a room temperature of 20 ºC, kept 20 mm below the water level. The water used was clean and distilled. The duration of immersion in water of the two types of samples (thermally treated and native/control) was 2 hours and 24 hours, to determine the water absorption and swelling in thickness, both after 2 hours of immersion and after 24 hours of immersion (ASTM D570; EN 60811-402). After 2/24 hours, the samples were taken out of the immersion bath, swabbed with absorbent cloth to remove excess water, and weighed with the same analytical balance. The thickness of these samples was further measured in two directions (then their average was made) with the same electronic vernier caliper.

Water absorption was determined after 2 hours and 24 hours, with the following two calculation ratios (Eq. 2) :

$$A_{2h} = \frac{m_{i2}-m_0}{m_0} \cdot 100 \; [\%] \qquad A_{24h} = \frac{m_{i24}-m_0}{m_0} \cdot 100 \; [\%] \qquad\qquad (2)$$

where: A_{2h} – water absorption after 2 hours of immersion in water, in %; m_{i2} – the mass of the sample immersed for 2 hours, in g, m_0 - the initial mass of the absolute dry sample, in g; A_{24h} - water absorption after 24 hours immersion in water, in %; m_{i24}- mass of the sample immersed in water for 24 hours, in g.

RESULTS AND DISCUSSION
Wood density results
Through heat treatment, the density of the wood decreases due to the loss of some components during the heat treatment, thereby decreasing the mass of the samples. Therefore, the wood density decreased from an average of 647.3 kg/m^3 in the native state to an average of 603.3 kg/m^3 in the heat-treated state, i.e. a decrease of 6.7% (Fig. 2). A good linearity is observed between the two linear regression equations, which means a constant value of the two densities. Also, when determining the standard deviation of the density values, a value of 54 kg/m^3 in the native state and 33 kg/m^3 for heat-treated ash was found, which means that the thermo-treated ash wood has a better homogeneity than the native one.
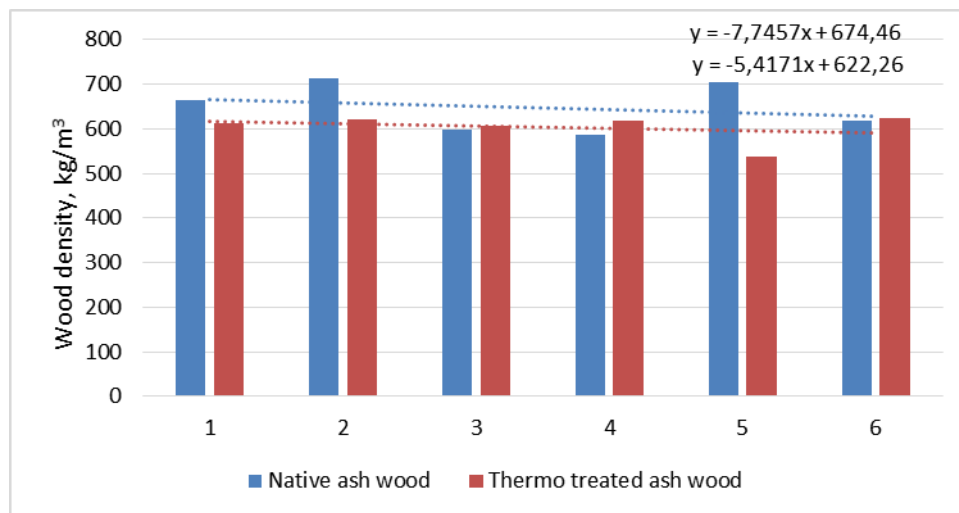
Figure 2: Density of native and thermo-treated ash wood

Water absorption results
The water absorption of the samples, i.e., the amount of water received by the two types of materials (control sample and thermo-treated ash wood sample) depended on the two types of samples and their immersion time (2 hours or 24 hours).

Water absorption at 2 hours immersion in the case of the native-control ash wood was 10.80%, while in the case of thermo-treated ash was only 6.7%. It can be seen that the water absorption at 2 hours of the

heat-treated ash was 37.9% lower compared to the native ash (Fig. 3), which means that the heat-treated ash had a weaker effect of water than the native-control ash. The linear curve, with the Pearson coefficient $R^2 = 1$, highlights this decreasing trend of water absorption at 2 hours immersion in water. Water absorption at 24 hours in the case of the control ash was 30.7%, while in the heat-treated ash it was 20.5%. It can be observed that the water absorption at 24 hours of heat-treated ash was 33.2% lower than that of native-control ash (Fig.3), which means that the trend of water absorption at 2 hours was maintained, respectively the one at which thermo-treated wood improves its performance against water, absorbing a smaller amount than native-control wood.
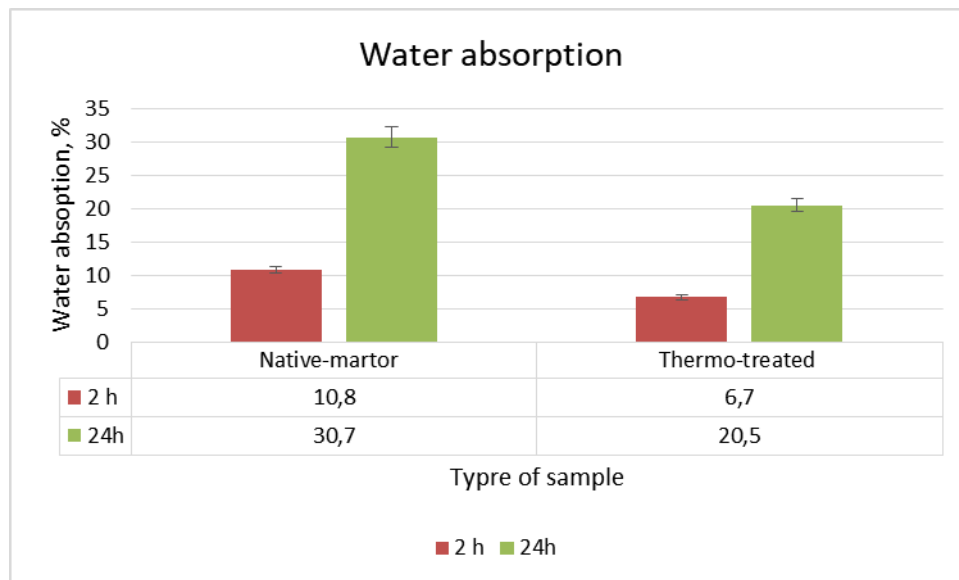
Figure 3: Water absorption at 2 and 24 hours for native-control and thermo-treated ash wood

CONCLUSIONS

Heat treatment of ash wood contributes to the reduction of water affinity (water absorption) by 28.9% at a 2-hour immersion and by 37.2% at 24%. This also proves that the intensity of absorption is high in the first 2-hour period and decreases after that.

As a general conclusion of the research, it can be said that heat treatment of ash wood not only increases its dimensional stability (this being the purpose of heat treatment at a temperature of 185 °C), but also decreases its affinity to water and increases its elasticity.

REFERENCES

Altimok M, Ozalp M, Korkut S (2010) The effect of heat treatment on some mechanical properties of laminated beech (Fagus orientalis) wood, Wood Research 55(3), 131-142

Boonstra M.J (2008) A two-stage thermal modification of wood, PhD Thesis in Applied Biological Sciences: Soil and Forest Management. Henry Poincaré University-Nancy, France

EN 60811-402 Test methods for non-metallic materials-Part 402:Miscellaneous tests-Water absorption tests

Esteves B.M., Pereira, H.M. (2009) Wood modification by heat treatment: A review, BioResources, 4(1), 370-404

Gurleyen L, Ayta, U, Esteves, B, Gurleyen T, Cakicier N (2019) Effects of thermal modification of oak wood upon selected properties of coating systems, BioResources, 14(1), 1838-1849

Hill C (2006) Wood modification: Chemical, thermal and other processes, Willey and Sons, Hoboken, NJ, USA

Kaymakci I, Akyildiz, M H (2011) Dimensional stability of heat treated Scots pine and oriental beech, Pro Ligno 7(4), 32-38

Militz H (2002) Heat treatment technologies in Europe: Scientific background and technological state-of-art, Comference on Enhancing the durability of Lumber and Engineered Wood Products. Orlando, Fl, USA

Rusche H (1973) Thermal degradation of wood at temperatures up to 200 ºC, Part I and II, Holz Roh-Werkst, 31, 273-281

Syrjanen T, Oy K (2001) Production and classification of heat treated wood in Finland, Review on heat treatments of wood, Proceedings of the special seminar held in Antibes, France

ThermoWood   Handbook   TWH   (2023)   International   Thermowood   Association. https://asiakas.kotisivukone.com/files/en.thermowood.palvelee.fi/downloads/tw_handbook_0808 13.pdf

Vybohova E, Kućerova V, Andor T, Balazova Z, Velková, V (2018) The effect of heat treatment on the chemical composition of ash wood, BioResources 13(4), 8394-8408

Windeisen, E. Strobel, C, Wegener, G (2007) Chemical changes during the production of thermo-treated beech wood, Wood Science and Technology, 41(6), 523-536, doi:10.1007/s00226-007-0146-5

Wikberg, H, Maunu, S L (2004) Characterisation of thermally modified hardwood and softwood, Carbohydrate Polymers, 58(4), 461-466

The surface morphology of sanded curly maple in comparison with straight grain maple selected for musical instruments

Mariana Domnica Stanciu[1*], Lidia Gurau[2], Florin Dinulica[3], Catalin Constantin Roibu[4], Cristian Hiciu[3], Andrei Mursa[4], Marian Stirbu[4]

[1*] Faculty of Mechanical Engineering, Transilvania University of Brașov, B-dul Eroilor 29, 500036, Brașov, Romania.
[2] Faculty of Furniture Design and Wood Engineering, Transilvania University of Brasov, B-dul Eroilor 29, 500036, Brasov, Romania.
[3] Transilvania University of Brasov, Faculty of Silviculture and Forest Engineering, Str. Sirul Beethoven, nr. 1, 500123, Brasov, Romania.
[4] Stefan cel Mare University of Suceava, Faculty of Forestry, Str. Universitatii, nr. 13, 720229, Suceava, Romania.

E-mail: mariana.stanciu@unitbv.ro; lidiagurau@unitbv.ro; dinulica@unitbv.ro; catalinroibu@usm.ro, cristian.hiciu@student.unitbv.ro. Andrei.mursa@usm.ro, marian.stirbu@unitbv.ro,

Keywords: curly maple, anatomical features, surface morphology, roughness profiles

ABSTRACT
This paper presents a study of the anatomical features in relation to surface morphology of curly maple in comparison with that of straight grain maple, in order to understand if there are major qualitative differences after preparing the surfaces "in the white" by sanding between those types of maple structures. Tree annual rings and anatomical features of microscopic specimens (porosity, cell wall thickness) were measured on the cross-section, as well as wavy grain in the radial section, using Itrax equipment, WinDENDRO, WinCELL and Roxas equipment and software. The surface metrology was performed using MarSurf XT20 instrument, on six specimens from each type of maple grain orientation - straight and curly. The results emphasize numerous relationships between measured properties and wood structure. By examining the roughness profiles, it appears at a first glance that curly maple is smoother in the core roughness, for both measuring directions (radial and longitudinal). For measurements along the grain, it can be observed a pattern difference, so that, in curly maple, rough areas seem to alternate with smooth regions, displaying a heterogeneous quality, which, can be related to the surface ripples. The fact that sanded surfaces of curly maple (Maple A) contain areas of almost crosscut pores characterized by isolated deep valleys is also confirmed by a strongly negative skewness, Rsk, in comparison with straight grain maple (Maple D).

INTRODUCTION
The analysis of maple wood in old violins revealed a preference for maple wood having a special aesthetic appearance, namely wood with wavy fibers or small grouped knots that give wood highly appreciated designs. Among the characteristics of curly maple, there can be mentioned: narrow wavy fibers; wide wavy fibers; wavy fibers arranged in wide flames; wavy fibers arranged in narrow flames (Bucur, 1992, Beldeanu 2008). In terms specific to the luthier, these wood patterns give the name of the wood variety such as curly grain maple; fiddleback figures; flame grain; partially quilted grain; bird's-eye figure, which are mentioned in various references. Curly maple represents a structural anomaly consisting in the arrangement of fibers and other anatomical elements along slightly sinuous lines, especially in the radial and tangential plane giving the appearance of a three-dimensional drawing (Dinulica et al 2023, Stanciu et al 2020, Straže et al 2020, Alkadri et al 2018). Some studies have highlighted the relationship between the anatomical and acoustic properties for maple wood with curly grain and straight grain (Krajnc et al 2015, Kúdela et al 2011, Sedlar et al 2021, Sonderegger et al 2013, Spycher et al 2008). Maple (*Acer Pseudoplatanus* L) is a deciduous species that grows in wet, dark valleys, on slopes with boulder soils with limestone content, reaching heights between 15 and 30 meters [(Bucur, 1992, Beldeanu 2008, Dinulica 2023, Stanciu 2020). The maple wood has a complex structure, with distinct annual rings of regular outline, with no pronounced difference between early and late wood.

It is white, sometimes with black-gray stripes, evident on longitudinal sections. From the point of view of microstructure, it presents uniformly scattered pores, small, invisible to the naked eye, visible with a magnifying glass, relatively rare, unitary or in radial rows, with the opening almost equal over the entire width of the annual ring, and their membranes (longitudinal walls) show helical thickenings and large intervascular pits, with a diameter of about 18 µm (Beldeanu 2008). Starting from specific anatomical features of maple wood, the question is: is this 3D effect visible in the recorded measured profiles of curly maple or not? How is this curly grain influencing the surface quality after sanding? The aim of this paper was to study the surface morphology of curly maple in comparison with that of straight grain maple, in order to understand if there are major qualitative differences after preparing the surfaces "in the white" by sanding, in order to be used in a musical instrument. This topic is part of a larger research project aiming to further investigate the effect of maple assortment and of its surface quality with or without coating upon the instrument acoustics.

MATERIALS AND METHODS
Materials
The samples of maple wood (*Acer Pseudoplatanus*) as plates with dimensions of 240 mm x 80 mm x 4 mm with the main directions of wood (length (longitudinal direction, L) x width (radial direction, R) x thickness (tangential direction, T)) were processed from semi-finished products necessary for the manufacturing of stringed musical instruments. The wood comes from the forests of the Carpathian Mountains, the log being cut in quarter sawn and the semi-finished products being naturally dried for 3 years (class D) and 10 years (class A). Before preparation, the samples were conditioned in a drying chamber up to a moisture content of 6–8%. Two quality class samples were considered, depending on their anatomical characteristics: class A and class D, selected according to the anatomical classification from previous studies (Dinulică 2023, Crețu 2022). Sycamore maple wood samples were coded Maple A (class A-with curly grain), respectively Maple D (class D- with straight grain) as can be seen in Fig. 1. In Table 1 are presented the main physical features of samples as was determined in previous studies (Dinulică 2023).
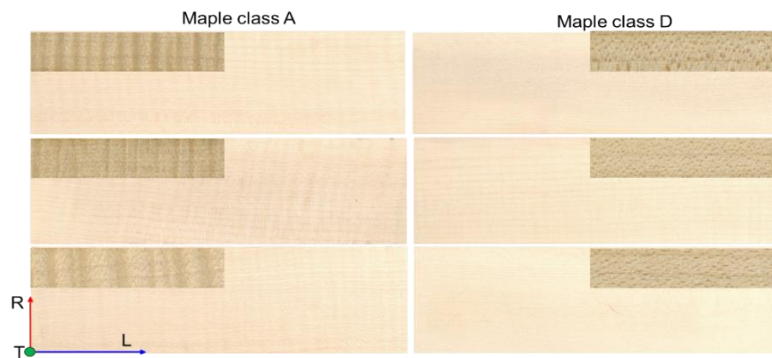
Figure 1: The maple wood samples

Table 1: Physical features of samples

Physical features/ Specimen		Maple class A	Maple class D
Annual ring width RW (mm)	Mean (STDV)	1.249 (0.167)	0.987 (0.026)
Regularity of annual ring width RRI (%)	Mean (STDV)	76.574 (5.838)	83.462 (6.650)
Fiber undulation pitch CWL (mm)	Mean (STDV)	5.448 (0.460)	NA
Wood density WD (kg/m^3)	Mean (STDV)	659 (3.022)	626 (16.308)
Moisture content (%)	Mean (STDV)	6.8 (0.5)	8.0 (0.5)

Methods
Determination of surface morphology
The equipment used for the surface metrology comprised a MarSurf XT20 instrument manufactured by MAHR Gottingen GMBH (Göttingen, Germany), fitted with a MFW 250 scanning head with a tracing arm in the range of ±750 µm and a stylus with a 2-µm tip radius and 90° tip angle (Gurau 2017). The stylus moved at a speed of 0.5 mm/s and exerted a low scanning force of 0.7 mN at a lateral resolution of 5 µm. Two measuring directions were performed per each sample: one transversal to the grain and to

the sanding direction, with a length of 30 mm and another one along the grain, with a length of 80 mm. Such long measuring lengths are recommended in case of wood, in order to cover enough anatomical variation. Three measurements per specimen and for each measuring direction were recorded according to Figure 2. The scanned profiles were processed with MARWIN XR20 software provided by the instrument supplier (Göttingen, Germany). Mean values parameters were calculated, such as: Ra (arithmetical mean deviation of the roughness profile), Rv (the largest absolute profile valley depth), Rsk (skewness of the profile), Wa (arithmetical mean deviation of the waviness profile). Other parameters were the Abbot-curve parameters: Rk (the core roughness depth), Rpk (the reduced peak height), and Rvk (the reduced valley depth) from (Gurau 2004, Gurau 2023).

a)   b)
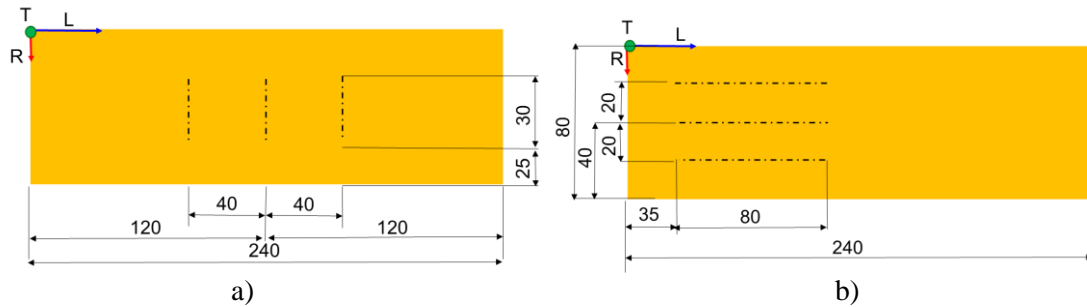
Figure 2: The principle of measuring the surface morphology of samples. Values in mm

Determination of anatomical features of maple wood

The anatomical features of microscopic specimens (porosity, cell wall thickness) were measured on the cross-section, as well as wavy grain in the radial section, using Itrax equipment, WinDENDRO, WinCELL and Roxas equipment and software.

RESULTS AND DISCUSSION

Surface morphology

An example of a roughness profile taken along and across the grain and for each category of maple grain is presented in Figure 3.

Figure 3: The roughness profile of samples measured across the grain.

By examining the profiles, it appears at a first glance that curly maple is smoother in the core roughness, for both measuring directions. For measurements along the grain, it can be observed a pattern difference, so that, in curly maple, rough areas (red color) seem to alternate with smooth regions (green color), displaying a heterogeneous quality, which, as would be seen later, can be related to the surface ripples (Figure 4). The core roughness depth denoted Rk, for the curly maple (Maple A) was smaller than for the straight grain maple (Maple D) with 36% for measurements transversal to the grain and with app.19% for measurements along the grain confirming the observations made on measured profiles. The differences in Rk were significant as tested by ANOVA (p<0.05). The differences in Rsk were

significant as tested with ANOVA; Rsk measured transversal to the grain was 37% higher and along the grain was 76.7% higher for Maple A than for Maple D.

The slightly higher density of curly maple (0.659 g/cm3) in comparison with straight grain maple (0.626 g/cm3), together with different local hardness caused by the variation in grain orientation in the curly maple, from along to almost across the grain, may have been responsible for a smoother sanded surface for the former. Similar trend was identified by the arithmetical mean deviation of the roughness profile denoted Ra, which had slightly lower values for Maple A than for Maple D. However, Rk is a more reliable parameter for characterizing the processing roughness in comparison with Ra. While Rk is a measure of the core roughness and is the least influenced by wood anatomical cavities, Ra, as an average parameter. Wa measures the arithmetic mean deviations in the waviness profile referring to the arrangement of irregularities viewed at a larger scale wavelength in comparison with roughness. The mean values of waviness parameter Wa indicate higher values with app.11% for Maple A than Maple D, for both measuring directions.
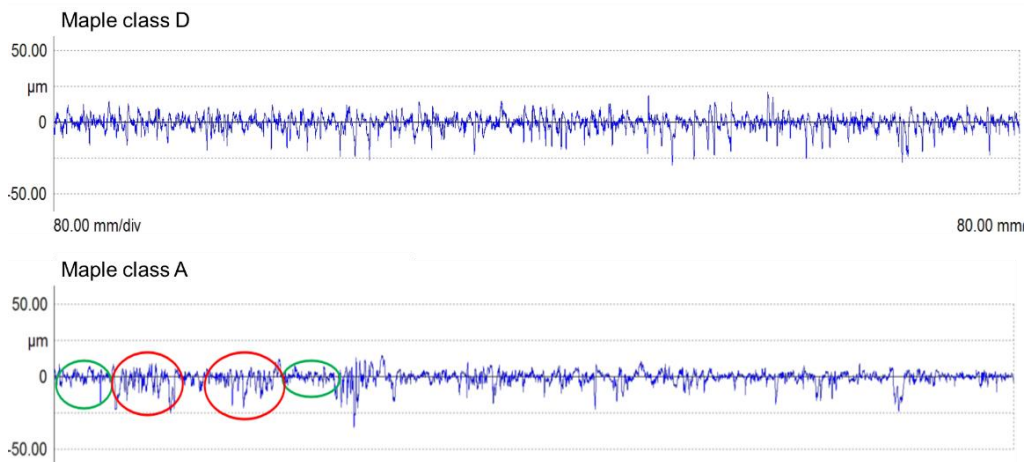
Figure 4: The roughness profile of samples measured along the grain

Anatomic properties of maple wood

The anatomical differences between the maple quality classes are due to on the one hand, the rays which are getting thicker in straight grain maple (Maple D) in comparison to curly maple (Maple A) on the other hand, the frequency of clustered vessels increases as the quality decreases, with the decrease of the quality class, the tendency of grouping in clusters was noticed as can be seen in Figure 5.
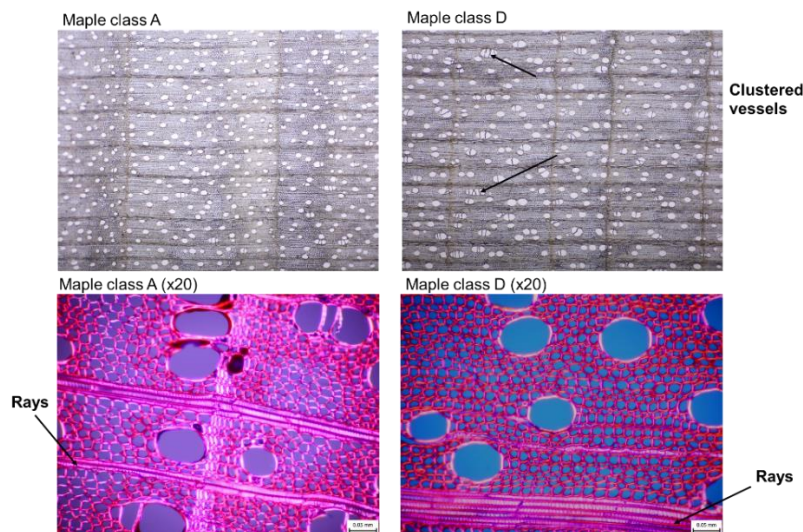
Figure 5: Microscopic images of resonance maple wood samples, 40x magnification:

CONCLUSIONS

In conclusion, the quality of both materials, straight grain maple and curly maple was similar after the surfaces were prepared by „sanding in the white" as for being used in musical instruments. The curly maple has the advantage of a more appealing aspect due to the three dimensional visual effect caused by a difference in light reflectance of the different grain exposure. The surface of curly maple after sanding was slightly smoother than that of the straight grain maple, in spite of the crosscut zones and was characterized by a high frequency anatomical waviness, which seem to follow the surface ripples. Further tests will look whether will be changes in surface morphology of the same materials or not, after finishing wood with different types of coatings appropriate for musical instruments.

ACKNOWLEDGMENTS

REFERENCES

Alkadri A, Carlier C, Wahyundi I, Grill J, Langbour P, Bremaud I (2018) Relationships between anatomical and vibrational properties of wavy sycamore maples . IAWA - Intern. Assoc. Wood Anatomists J. 39, 1: 63-86 Full-text: https://hal.archives-ouvertes.fr/hal-01667816

Beldeanu E.C. (2008) Produse forestiere (in Romanian language). Ed. Universității Transilvania din Brașov

Bucur V (1992) Anatomic structure of curly maple . Revue Forestiere Francaise XLIV, nr special : 2-8

Crețu N., Roșca I.C., Stanciu M.D., Gliga V.Gh,, Cerbu C. (2022) Evaluation of wave velocity in orthotropic media based on intrinsic transfer matrix. Exp Mech, 62, 1595–1602, https://doi.org/10.1007/s11340-022-00889-9.

Dinulica F., Savin A., Stanciu M.D. (2023) Physical and Acoustical Properties of Wavy Grain Sycamore Maple (Acer pseudoplatanus L.) Used for Musical Instruments. Forests. 14, 197. https://doi.org/10.3390/f14020197.

Gurau, L. (2004) The roughness of sanded wood surfaces, Doctoral thesis, Forest Products Research Centre, Buckinghamshire Chil-terns University College, Brunel University.

Gurau, L. (2017) Irle, M. Surface roughness evaluation methods for wood products: A review. Curr. For. Rep., 3, 119–131.

Gurău L., Timar M.C., Coșereanu C., Cosnita M., Stanciu M.D. (2023) Aging of Wood for Musical Instruments: Analysis of Changes in Color, Surface Morphology, Chemical, and Physical-Acoustical Properties during UV and Thermal Exposure. Polymers, 15, 1794. https://doi.org/10.3390/polym15071794

Krajnc L., Čufar K., Brus R. (2015) Characteristics and geographical distribution of fiddleback figure in wood of Acer pseudoplatanus L in Slovenia, Drvna Industrija, 66(3), 213–220.

Kúdela J., Kunštár M. (2011) Physical-acoustical characteristics of maple wood with wavy structure. Ann. Warsaw University of Life Sciences – SGGW, Forestry and Wood Technology, 75, 12–18.

Sedlar T., Šefc B., Stojnić S., Sinković T. (2021) Wood quality characterization of sycamore maple (Acer Pseudoplatanus l.) and its utilization in wood products industries. Croat. J. for. Eng. 42(3), 543–560, https://doi.org/10.5552/crojfe.2021.1099

Sonderegger W., Martienssen A., Nitsche C., Ozyhar T., Kaliske M., Niemz, P. (2013) Investigations on the physical and mechanical behavior of sycamore maple (Acer pseudoplatanus L.). Eur. J. Wood Prod. 71, 91–99. https://doi.org/10.1007/s00107-012-0641-8

Spycher M., Schwarze F.W.M.R., Steiger R. (2008) Assessment of resonance wood quality by comparing its physical and histological properties. Wood Sci. Technol. 42, 325–342, https://doi.org/10.1007/s00226-007-0170-5.

Stanciu M.D., Coșereanu C., Dinulică F., Bucur V. (2020) Effect of wood species on vibration modes of violins plates. Eur. J. Wood Prod. 78, 785–799. https://doi.org/10.1007/s00107-020-01538-5

Straže A., Jerman J, Brus R, Merela1 M, Gorišek Z, Krajnc L. (2020) Selected structural, physical and acoustic properties of sycamore maple wood with fiddleback figure, 9th Hardwood Conference Proceedings PI. University of Sopron Press, Sopron, Hungary, pp 261–268

Analysis of changes in the composition of beech as an important industrial raw material in Hungary

Katalin Szakálosné Mátyás[1], Attila László Horváth[1]

[1] Institute of Forestry and Natural Resource Management, Faculty of Forestry, University of Sopron, Bajcsy-Zsilinszky street 4., H-9400 Sopron, Hungary

E-mail: szakalosne.matyas.katalin@uni-sopron.hu; ahorvath@uni-sopron.hu

Keywords: beech, assortment structure change, climate change

ABSTRACT

We see and feel the impact of climate change, and global warming and weather extremes are now making their impact felt in the original ecosystem and on the health of tree stands, growth and yield rhythm.

The Beech tree species is also extremely sensitive to the place of growth, it is not without reason that the climate zone in the forestry climate classification, the coolest, most demanding of precipitation, located at the highest altitude above sea level, is characterized by the beech climate. He showed that this climate zone is moving higher and higher in our high mountains, but when the tree species is 100-150 years old, it cannot follow this so quickly. Due to the renewal, the bringing of newness, the frequent acorn harvest, it can be deceptive at first that everything is in order, but it is doubtful that our newly renovated beech trees will even be worth 100 years in their place of production.

Beech trees have had a tendency for pseudo-aging for centuries, the development of which is disputed, there are several views and no exact explanation has been established, but it is certain that healthy pseudo-aging does not actually cause any mechanical or quality problems, with the exception of star-shaped pseudo-aging, which is easily associated with gut rot, or It leads to.

The valuable industrial raw material can be selected from the extracted beech trunks and branches from the lower third part of the trunk, since there are the diameter sizes that are standard/usual for the sheet metal industry (slicing, peeling) as well as saw logs and timber. in the case of selections. In addition to quantitative requirements, there are also strict quality requirements regarding spatial curvature, skylights, false gestures, etc.). Unfortunately, we see that these are increasingly not given, so the proportions shift from valuable industrial wood to firewood, fiber wood, and chipboard.

In this research, we have tried to explore the development of the assortment structure over the past decades, to see where it is changing and moving, since it is quite possible to draw conclusions from it, and perhaps to think along the lines of trends in terms of future possibilities as well.

Of course, market expectations can also influence the selection structure (e.g. firewood program), but these effects are only temporary and not tendentious, so they can be filtered out.

INTRODUCTION

The beech is one of the most valuable native tree species in the forests of Hungary. Beech forests contribute nearly 20% of the economic value of all domestic forests, despite their "occupancy" being only close to 6.1% (in 2022: 113,759 hectares), and their standing timber volume representing 10.3% of the country's forests (in 2022: 41,8 million cubic meters). In the past, it was exclusively used as firewood since it was considered a "weed tree." Its stands were nearly wiped out in the 18th and 19th centuries due to charcoal burning. Nowadays, it is considered a tree of high-quality timber and value creation, thus one of the main goals of beech management is to produce high-quality assortments. It is important to emphasize that the significance of beech is not only due to its economic role in timber production, but also because of its properties, it serves as a foundation for further functions and purposes of the forest (such as protective, public welfare, and economic functions) and it should also play a role as an ecosystem service provider (recreation, CO_2 sequestration). Unfortunately, it should also be noted that climate change and its effects are notably and demonstrably affecting beech forests found in the beech forest climate. It is expected that the stands will not be able to adapt in the long term to the changed climatic conditions, their vitality and resistance will deteriorate, and pathogens and pests will proliferate.

In the case of beech, a long-term decline in quality will be observed, with a decrease in standing timber volume, as well as in the quantity of harvestable timber and valuable assortments (veneer logs, peeled veneer logs, saw logs).

In terms of timber, beech has numerous advantageous properties. Its valuable and beautiful timber is widely used, providing revenue similar to that of oak and pine in the timber market. It is a versatile tree species widely utilized in the timber and furniture industries. Beech is the most important timber species in European and domestic veneer and sawmill industries (~75%). It can be peeled and sliced excellently, used for veneer logs, carpentry, agricultural and household tools, making it good for furniture and popular as firewood.

In the furniture industry, beech is one of the most sought-after timber species, used in the form of veneer (decorative and plain), plywood, and solid wood. Beech-made stairs, wall coverings, and parquets are popular. Steaming makes it highly bendable, famous for bentwood chairs and furniture made from beech. It is used to make sports equipment, toys, turned wooden gifts, various household wooden items (e.g. wooden spoons), tool handles, and is also used in the production of cellulose, fiberboard, and chipboard.

MATERIALS AND METHODS

A significant portion of beech timber from forestry can be used for sawmill purposes. For the predictive modeling of assortment structure development, statistical analyses and data collection are necessary. Utilizing data from the Central Statistical Office and the National Land Administration, insightful analyses can be conducted. Data collected over the past 20-30 years have been reviewed and depicted.

RESULTS AND DISCUSSION

During the harvesting of beech forests, timber extraction ranged around 550-600 thousand cubic meters in the 1970s, showing an increasing trend. Between 1996 and 2022, the production volume fluctuated between 548-916 thousand cubic meters (Figure 1). Excluding the extremes it can be said that the annual production mostly ranged between 640-740 thousand gross cubic meters, with the usual minimal fluctuations. Considering the average of the past 27 years, it amounted to 679 thousand cubic meters per year.
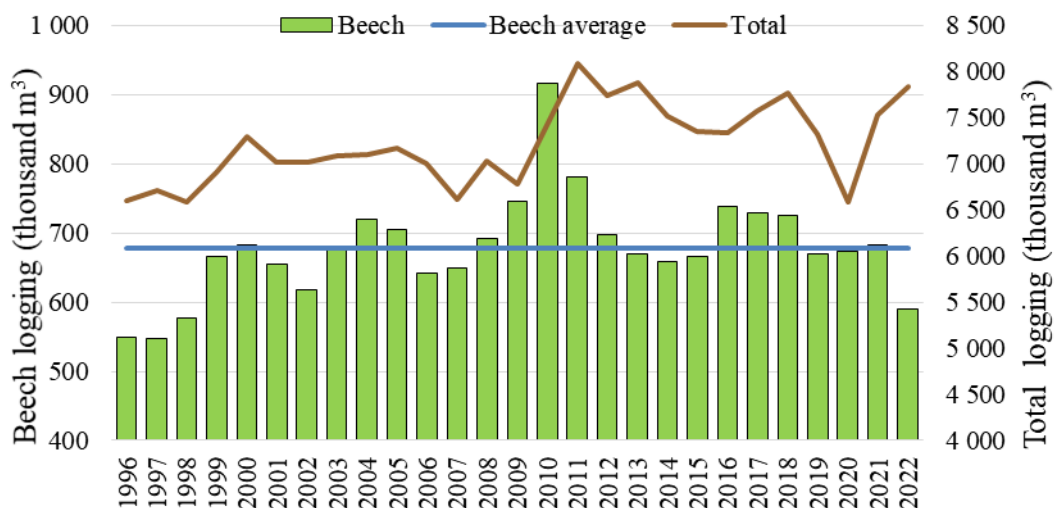
Figure 1: The trend of timber extraction quantity between 1996 and 2022 on forest management areas, specifically for beech (Edited from: Based on statistical data from the Central Statistical Office and the National Land Administration)

The deterioration in timber quality is noticeably observed in the changes in the average quantity and percentage share of harvested beech timber assortments (Table 1). Compared to the 1970s, the proportion of industrial timber decreased by nearly 13 percentage points in the post-2000 timber extractions, in favor of firewood. Within industrial timber assortments, the share of veneer logs, other sawmill raw materials, and pulpwood significantly decreased. Although the quantity of veneer logs

decreased by an average of 6 thousand cubic meters, this represents a 57% proportional decrease. The average quantity of produced pulpwood increased by 46 thousand cubic meters, which resulted in an over 7 percentage point increase in proportion.

Table 1: The average quantity and percentage share of harvested beech timber assortments in the 1970s and from 2000 to 2022 (Edited from: National Statistical Data Provider Program)

Assortments	Average in the 1970s		Average between 2000 and 2022	
Lumber logs	26 580 m³	6,20%	20 685 m³	3,46%
Sawmill logs	133 971 m³	31,40%	145829 m³	24,39%
Other sawmill materials	24 087 m³	5,60%	15 110 m³	2,53%
Mining timber	3 m³	0,00%	0 m³	0,00%
Pulpwood	81 309 m³	19,00%	57 089 m³	9,55%
Wood for fibre	4 102 m³	1,00%	50 152 m³	8,39%
All other industrial timber	3 941 m³	1,00%	18 473 m³	3,09%
Industrial wood chips	3 454 m³	0,80%	359 m³	0,06%
Energy wood chips	0 m³	0,00%	7 814 m³	1,31%
Solid cubic meters of thick firewood	133 626 m³	31,30%	262 769 m³	43,96%
Solid cubic meters of thin firewood	15 309 m³	3,50%	19 514 m³	3,26%
Total industrial timber	277 447 m³	65,10%	307 697 m³	51,47%
Total firewood	148 935 m³	34,80%	290 097 m³	48,53%
Net timber volume over cutting strip	426 382 m³	100,00%	597 799 m³	100,00%

The market demand influences the assortment structure, as it fundamentally affects marketability, as well as the opportunities considering qualitative and quantitative aspects. These trends can be tracked from the 2000s to the present day (Figures 2 and 3).

Alongside the decreasing proportion of industrial wood, which represents the most valuable type of logs, there is also a noticeable decline in the prominence of pulpwood since 2017. Regarding firewood assortments, a significant increase in the quantity of forest chips for energy purposes – 10 000 m³ – has been observed since 2010.

Figure 2: Changes in the net cubic meters of beech industrial wood assortments between 2000 and 2022 (Edited from: Based on statistical data from the Central Statistical Office and the National Land Administration)
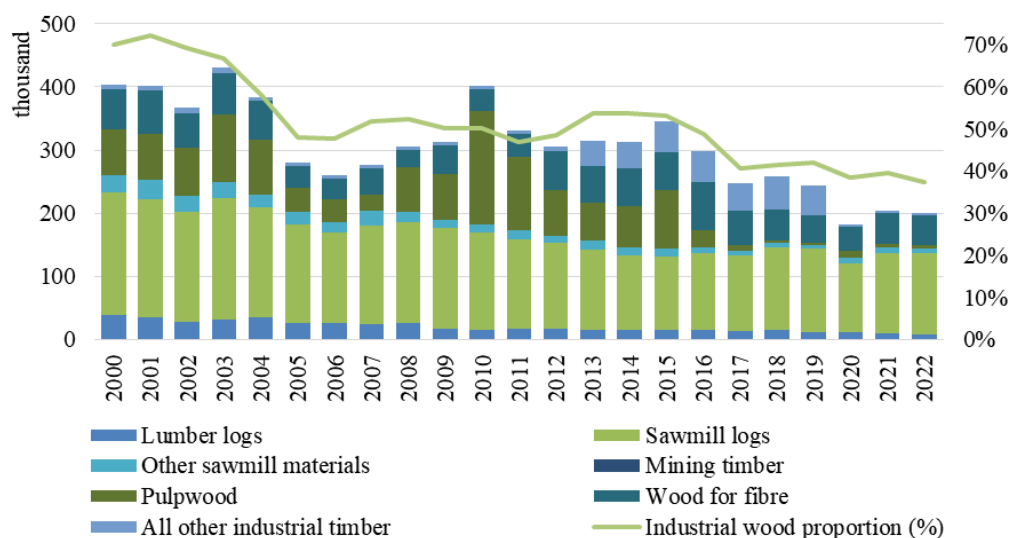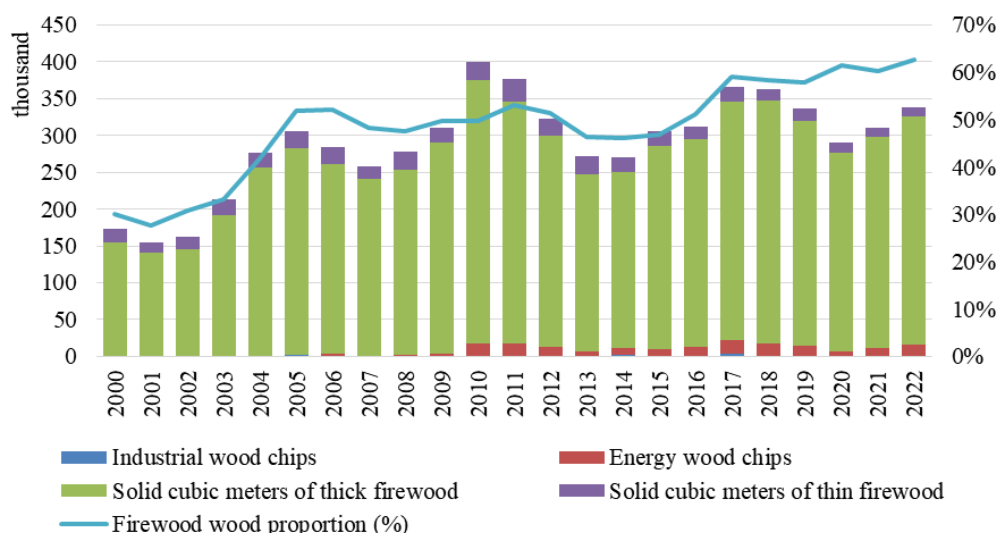
Figure 3: Changes in the net cubic meters of beech fire wood assortments between 2000 and 2022 (Edited from: Based on statistical data from the Central Statistical Office and the National Land Administration)

CONCLUSIONS

The effects of the slowly but steadily advancing climate change are currently primarily manifested in extreme conditions. Some years are characterized by prolonged droughts, while others experience exceptionally abundant rainfall or extremely cold winter periods. All of these clearly exacerbate the likelihood and magnitude of epidemics occurring in forest ecosystems. In this regard, it can be expected that in the future, our forests will face increasingly extensive and intense damages, partly due to indigenous factors and partly resulting from climate change, leading to the proliferation of new invasive pests and pathogens.

Different tree species react differently to environmental factors and their changes based on their ecological requirements. This is evidenced by the varying degrees of damage observed for different tree species. The conditions of late spring and summer water supply primarily determine the future of the beech. The beech species is extremely sensitive to summer heat and drought. Consequently, it is clear, that the overall health of Hungarian beech forests is deteriorating, exacerbated by the upward shift of climate zones, leading to a reduction in their area. It is evident, even in the short term, that the quantity of beech wood is declining, and the proportion of valuable industrial raw material is decreasing, which will paint an even more drastic picture in the long term.

Therefore, in our opinion, it can be concluded that the forestry industry must prepare and work on alternative solutions because relying on beech as a raw material in the future cannot be done with confidence.

ACKNOWLEDGMENTS

REFERENCES

Bondor A. 1986: A bükk. - Akadémiai Kiadó, Budapest, 179 pp.

Csépányi P. 2013: Az örökerdő elvek szerinti és a hagyományos bükkgazdálkodás ökonómiai elemzése és összehasonlítása. – Erdészettudományi Közlemények 3. évfolyam 1. szám: 111–124.

Czúcz Bálint, Gálhidy László és Mátyás Csaba: A bükk és a kocsánytalan tölgy elterjedésének szárazsági határa – Erdészettudományi Közlemények 3. évfolyam 1. szám: 39–53.

Gaumann, E. 1946: Über die Pilzwiderstandsfähigkeit der roten Buchenkerns. Schweizerische Zeitschrift für Forstwesen, Nr. 97, S. 24-32

Mayer-Wegelin, H. 1944: Die Verkernung des Buchenholzes. Silvae orbis, Jg. 15, S. 227-236

Mahler, G., Höwecke, B. 1991: Verkemungserscheinungen bei der Buche in Baden- Württemberg in Abhängigkeit von Alter, Standort und Durchmesser. Schwiez. Zeits. Für Forstwesen, Jg. 142, S.375-390

Molnár S. & Bariska M. 2002: Magyarország ipari fái. Szaktudás Kiadó Ház, Budapest.

Molnár, S. et al. 2001: Kísérleti technológia álgesztes bükk fűrészáru továbbfeldolgozására. K+F zárójelentés ALK 00034/2000

Investigation of old hardwood structure element

Fanni Szőke [1*], Antal Kánnár [1]

[1] University of Sopron, Creative Industry Institute, Bajcsy-Zs. Str. 4., Sopron, Hungary, 9400

Email: fanni.szoke1@gmail.com; kannar.antal@uni-sopron.hu

Keywords: Lookout tower; Solid wood; Electron microscopy; Dynamic Modulus of Elasticity; compression strength; bending strength

ABSTRACT

This paper reports on the structural testing of the dismantled Kecske hill lookout tower. The wooden structure stood in the Szárhalom forest, near Sopron, Hungary. It was erected in 1973, closed off in 2018 due to the failure of its structural elements, and finally demolished in 2021. Structural elements were tested and evaluated after 45 to 48 years of service, using, among others, electron microscopy, dynamic modulus of elasticity measurements, compression and bending tests. A literature review was conducted on the structural details of lookout towers, on the characteristics and production technology of glued-laminated wood, as well as the examined materials, including Norway spruce (*Picea abies*) and sessile oak (*Quercus petraea*). Literature values of compression and bending strength were also determined to compare them to our results. The analysis extended to describing the details of the new lookout tower, including the footing and stair installations, which were the main failure locations in the old structure. Based on the results, samples cut from the undamaged parts of the old structure had high residual strength even after 45 years of service, but the structure as a whole was no longer safe, due to the failure of certain elements.

INTRODUCTION

The old structure under investigation was made of Norway spruce (*Picea abies*) and Sessile oak (*Quercus petraea*), while the new, current edifice has a larger variety of materials. Columns are made of GL24h glulam and beams are C24 softwood. A mixture of larch and oak were used for the stairs and decking.

The structural utility of one of the examined species, Norway spruce (*Picea abies*) largely depends on knots. It is prone to warping, but its strength and elastic properties are excellent. Based on literature data, its compression strength and bending strength ranges between 35-50-79 MPa and 49-78-136 MPa (at 12% MC, Molnár 2016).

The compression strength and bending strength of Sessile oak (*Quercus petraea*) at 12% MC is 55.7 MPa and 112.4 MPa, respectively, while its density is 750 kg/m^3 (Molnár – Farkas 2016).

During an inspection in the summer of 2018, the owner TAEG Forest Enterprise realised that the ends of the structural beams and other elements have deteriorated, rendering the lookout tower unsafe to use. The tower was cordoned off, and the lower steps removed to restrict access. The old lookout tower was finally dismantled in September 24, 2021. Specimens were accrued from the owner after landfilling the debris in October. Samples were collected from various places within the structure, described in detail in the testing section.

Selected samples were transported to the Timber Structures Testing Laboratory of the Institute of Applied Mechanics and Structures of the Sopron University for testing. To protect the cutting and testing machines, nails, bolts and other pieces of hardware were removed from the material. Testing took place after this, starting with non-destructive measurements and then strength testing.

Several measurements were made on the structure. Methods, results and conclusions are discussed separately for the various tests. Second level headings will introduce these tests for electron microscopy, non-destructive testing, compression and bending, respectively.

EXPERIMENTAL METHODS
Dynamic Modulus of Elasticty Measurements

Dynamic Modulus of Elacticity (MOE) testing was done using the non-destructive PLG testing equipment, developed in Hungary, based on sound velocity measurement. This instrument measures the density, MOE and estimates the bending strength. The instrument determines the stress grade according to MSZ EN 338 for softwoods. In case of oak, we determined the grade ourselves, based on the standard.

Compression tests

Compression strength is the resistance capacity of wood against loading along or across the fibres. Investigations included both cylindrical and rectangular specimens of materials that had been loaded in compression in the original structure as well. Measurements included 5 cylindrical and 2 rectangular oak, as well as 2 sound but checked spruce specimens. Specimens were placed in a Matest Servo-Plus Evolution (3000 kN capacity) material testing machine that subjected them to a gradually increasing pressure at a rate of 0.6 MPa/s. The determination of the strength values followed values in the table "Eurocode5 stress grades of wood". Since literature values pertain to air-dry moisture content, these values were converted to 12% MC, as indicated in the tables.

Bending tests

Four-point bending tests were used to compare the bending strength of oak with literature values. The advantage of the four-point bending scheme, compared to 3-point bending is that failure occurs in clear bending. Shear failure may occur due to the shortness of the specimen. The machine loaded the specimen at a rate of 0.500 kN/s, and stopped the test after failure when the load fell back to 50% of the ultimate level. The moisture content at the time of testing was 15%, and the values were converted to 12% before assigning the stress grades.

RESULTS

Dynamic Modulus of Elasticty Measurements

8 specimens were measured as described above. The results of the dynamic MOE measurements show the mean of the spruce 11668 MPa, the oak specimen MOE 11270 MPa. The samples were also classified into the appropriate stress grade based on the results, which showed C22, C27 and D18, D30, D35, D50 categories, but in case of the Nr. 3 specimen it was out of grade. The Moisture Content of the material was 18%. The instrument converted the measured data to 12% MC as the standard MC value. (Table 1, Figure 1)

Table 1: The results of the dynamic MOE measurements

Nr.	Species	l [m]	w [mm]	h [mm]	m [kg]	ρ [kg/m^3]	MOE [MPa]	Stress grade
1	Spruce	1.36	160	160	13.62	379	11009	C22
2	Spruce	1.47	140	140	12.52	420	12326	C27
3	Oak	1.11	135	55	5.46	652	8571	out of grade
4	Oak	1.52	140	140	21.60	705	11393	D30
5	Oak	1.13	260	50	11.24	742	11762	D30
6	Oak	1.16	220	45	8.30	702	14011	D50
7	Oak	1.17	250	50	9.34	619	9682	D18
8	Oak	1.16	245	45	10.80	822	12205	D35

The Moisture Content of the material was 18%. The instrument converted the measured data to 12% MC as the standard MC value, and the values in Table 1 are these converted values.
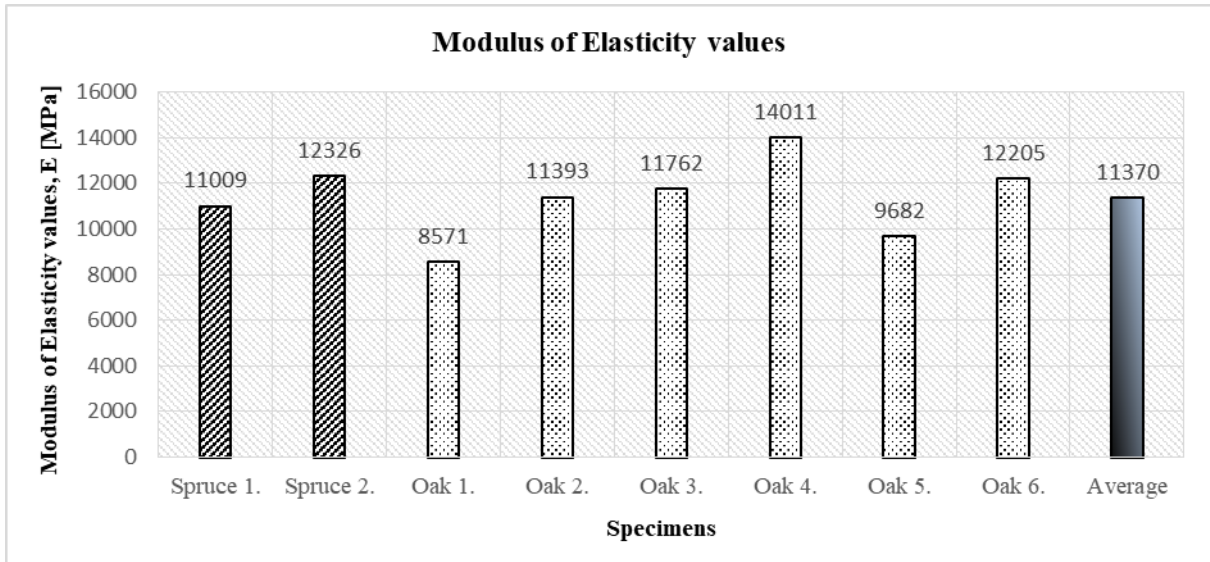
Figure 1: The measured Dynamic MOE values

Compression tests

Results of the air dry (12%) values show that the compression strength of spruce (mean: 57,5 MPa) reach and even exceed those of oak (mean: 45,8 MPa). One explanation may be that fluctuating climatic conditions induced higher stresses in oak, and thus created a larger number of drying fissures throughout the years. These fissures acted as fracture initiation locations during the failure process and manifested as a kind of cross sectional area reduction. (Figure 2)
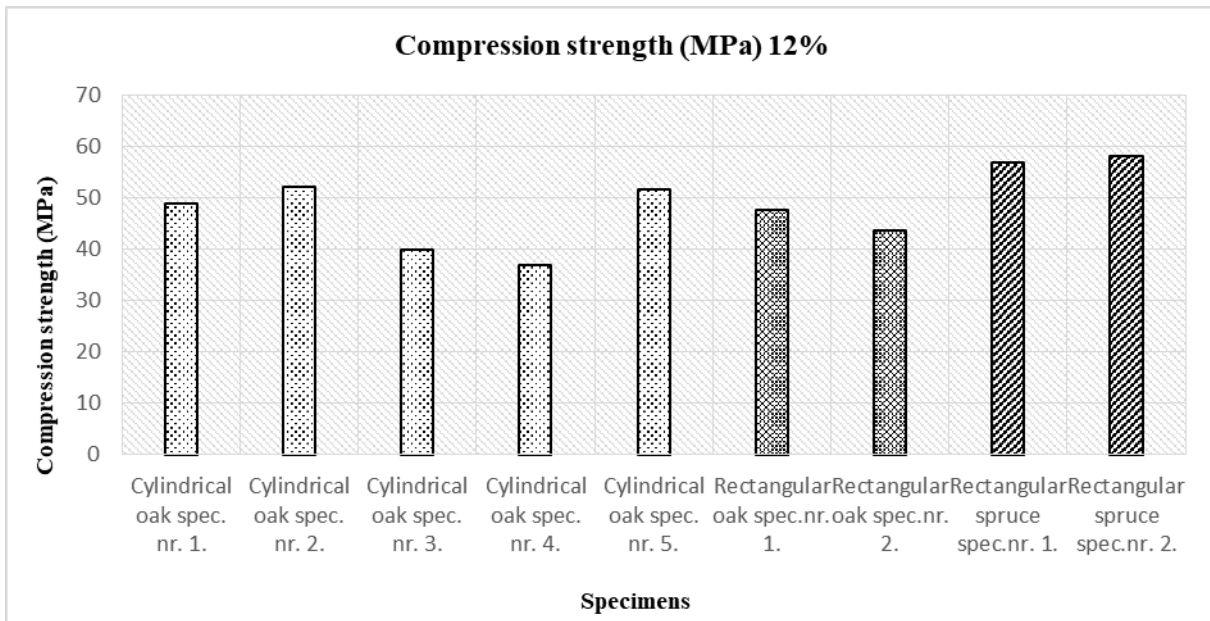
Figure 2: A comparison of compression strength values at air dried MC (u=12%)

Bending tests

The specimens show the mean of bending strength (u = 12%) 64.25 MPa. The samples were also classified into the appropriate stress grade based on the results, which showed D50, D60, D70 categories. All of them belong to one of the three highest stress grades. Specimens cut from the sound sections of the elements had high bending strength. (Table 2)

Table 2: The results of the bending tests

	a [mm]	b [mm]	u [%]	F [kN]	σ [MPa] (u=15%)	σ [MPa] (u=12%)	τ [MPa]	Stress grade
spec. nr. 1	45	90	15	21.023	51.908	58.137	7.786	D50
spec. nr. 2	45	90	15	21.210	52.370	58.654	7.856	D50
spec. nr. 3	45	90	15	29.170	75.025	84.028	10.804	D70
spec. nr. 4	45	90	15	22.074	54.504	61.045	8.176	D60
spec. nr. 5	45	90	15	19.500	48.148	53.926	7.222	D50
spec. nr. 6	45	90	15	25.202	62.227	69.694	9.334	D60
Mean	-	-	-	23.030	57.364	64.247	8.530	-
Minimum	-	-	-	19.500	48.148	53.926	7.222	-
Maximum	-	-	-	29.170	75.025	84.028	10.804	-
Std.	-	-	-	3.553	9.832	11.012	1.316	-
Var%	-	-	-	15.430	17.141	17.141	15.431	-

Table 2 shows the measurement data, where *a* is width, *b* is height, *u* is moisture content, *F* is the ultimate load in kN, which is half of the maximum force measured, due to the two-point loading, *σ* is bending strength, *τ* is the shear stress generated during bending.

DISCUSSION
Dynamic Modulus of Elasticty Measurements
MOE values are nearly identical for all specimens. Spruce and oak specimens yielded densities typical of these species. The MOE values of spruce calculated based on stress-wave velocity indicate medium quality. The measured MOE values of around 11,000 N/mm^2 correspond to medium stress grades in coniferous beams. Failure primarily occurred near the bolted connections; in farther positions, wood integrity was unaffected. The density and MOE of oak planks, in contrast, show significant variation. One of the specimens did not even reach an MOE value necessary to be classified as the lowest grade of D18. Four of the six specimens received low grades, i.e. the oak specimens showed a lowered strength after four decades.

Compression tests
Cylindrical specimens clearly show almost identical values and diagram shapes, due to the similar characteristics arising from the same species. In the diagrams of the rectangular samples, on the other hand, the differences between the two species in terms of Modulus of Elasticity, proportional to the slope of the linear portion, are clearly visible. Compared to spruce, oak specimens exhibit much steeper curves, due to the higher MOE of oak. Oak's more intensive initial checking may have caused the lower strength of these specimens. When compared to the characteristic values of 34 N/mm^2 set forth in the table for the stress grade D70 for hardwoods, these specimens exceed this value significantly, by approx. 34%. The compression strength of the columns was generally high. The failure, again, occurred at the connections, as demonstrated before.

Bending tests
Compared to values in each hardwood stress grade, the bending strength of the oak specimens proved to be outstanding. All of them belong to one of the three highest stress grades. Specimens cut from the sound sections of the elements had high bending strength. The failure of the structure was caused by fungal deterioration due to wetting, primarily in the proximity of the connections.

The new lookout tower
While inspecting the new lookout tower, which was built in 2022, we detected delamination at one of the glulam elements at the anchoring site. Vanya, Kannar and Rabb (2016) showed that „ bolted connections, which hinder shrinkage and swelling through concentrated loads at the bolts, may result in the creation of cracks", but „nailplate type connectors hold the load bearing element together, and small stress peaks generated at many locations hinder the deformation, thus no significant cracking occurs. Thus, improving nailplate type connections is recommended" (Vanya – Kánnár – Rabb 2016). In another analysis, Kánnár (2011) and Vanya (2014) identified possible reasons as follows: „Delamination in glued-laminated structures may have occured due to multiple factors, such as: restricted shrinkage and

swelling, lamella runout, moisture differences among lamellas, stresses perpendicular to the axis of the beam, adhesion problems, wood's anisotropic and inhomogeneous material properties, and the visual, rather than instrumented stress grading of the lamellas" (Kánnár 2011) (Vanya 2014). The cause of failure was stresses perpendicular to the axis of the beam, caused by the bolted connection. This may lead to wood protection problems later, since a subsequent growth of the crack may lead to wetting, and later rotting. Sealing the crack using waterproof caulking may prevent this eventuality. This is especially important in case the crack becomes wider, since wind load and occupancy load continuously change the loads in the new structure. At present, continuous monitoring of the crack during periodic inspections is sufficient. The other parts of the lookout tower are in good condition, and well-executed work.

CONCLUSIONS

There are many factors to consider in structural design. The structure should provide the intended utility value with respect to the service life and financial aspects. It should reliably resist loads arising from external loads and climate-induced stresses, which may arise during erection or use. In case of accidental actions like earthquakes fire of human errors, damage should be proportional.

During our investigation, we analysed the elements of the dismantled structure to establish the causes of failure. Based on the results, specimens cut out of the sound portion of the elements had high residual strength, and the failure of the structure was caused by the rotting of the columns, primarily in the proximity of the connections, which could thus no longer safely support the otherwise still serviceable elements. It is important to limit the extent of the damages already in the design phase, but also keep it to a minimum during construction and maintenance as well, so that the edifice can fulfil its structural purpose during the intended lifespan.

REFERENCES

Bodig J., Jayne B. A. (1982): Mechanics of Wood and Wood Composites. Van Nostrand Reinhold, 1982. Michigan, Michigan State University. pp. 291.

Kánnár A. (2011): Theoretical and experimental invistigations of damage development of glulam beams The 17th International Nondestructive Testing and Evaluation of Wood Symposium 2011. szept. 14-16. Sopron Hungary. Proceedings 367-374.

Kánnár A. (2014): A faanyag mikro- és makro-tönkremeneteli folyamatai, [Microscopuc and macroscopic failure processes in wood.] Sopron, ISBN 978-963-08-8672-7, pp. 6-7., pp. 12. (in Hungarian)

Molnár S., Farkas P. (2016): Tölgy (kocsányos és kocsánytalan tölgy) – Quercus spp., In: Földünk ipari fái, Eds.Molnár S., Farkas P., Börcsök Z., Zoltán Gy., Photog. Richter, H.G. & Szeles P., ERFARET Nonprofit Kft., Sopron, ISBN 978-963-12-5239, pp. 121-126. (in Hungarian)

Molnár S. (2016): Lucfenyő – Norway Spruce, In: Földünk ipari fái, Eds.Molnár S., Farkas P., Börcsök Z., Zoltán Gy., Photog. Richter, H.G. & Szeles P., ERFARET Nonprofit Kft., Sopron, ISBN 978-963-12-5239, pp. 89-91. (in Hungarian)

Vanya Cs., Kánnár A., Rabb, P. (2016): Javaslatok rétegelt-ragasztott fatartók tervezéséhez, gyártásához és üzemeltetéséhez, felmérési és modellezési eredmények alapján – III. rész: A tönkremeneteleket igazoló vizsgálatok és eredményei. [Design, fabrication and operation proposals for gluedlaminated timber, based on measuring and modelling results. Chapter 3: Failure examinations and their results.] Faipar, 62. évf. 1. sz. (2016), https://doi.org/10.14602/WOODSCI.2016.1.45 (in Hungarian)

An investigation of the influence of coating film thickness on the light induced colour changes of clear coated maple (*Acer pseudoplatanus*) wood surfaces with natural aspect

Mihai-Junior Torcătoru[1], Maria Cristina Timar[1,*]

[1] Transilvania University of Brașov, Faculty of Furniture Design and Wood Engineering, 29 Eroilor Boulevard, Brașov, Romania, 500036.

E-mail: mihai.totcatoru@unitbv.ro; cristinatimar@unitbv.ro

ABSTRACT

Stabilising the natural appearance of the clear coated wood surfaces for indoor applications is still a challenge for scientists and practitioners. An original laboratory method was applied in the current study to evaluate the potential influence of the coating film thickness on the initial colour and the light induced colour changes of maple (*Acer pseudoplatanus*) wood surfaces coated with a clear waterborne polyurethane lacquer (1k formulation). This was applied on two, three and four layers of about 100-110g/m^2 each on maple wood. Similar coating films were obtained on clear glass microscope slides (1 mm thick), used as ″detachable″ coating films, which were tightly fixed on uncoated wood samples to simulate wood coated surfaces. This approach offered the possibility to evaluate the colour of the wood substrate underneath the coating film and of the coating film itself. Both coated and uncoated wood samples were exposed to artificial UV-VIS radiation, simulating natural light passing through the window glass, in three cycles of 24 h light exposure at 40° C. CIELab colour parameters were determined prior and after coating, before and after light exposure, for all wood samples and coated glass slides, and the colour differences (ΔL*, Δa*, Δb*, ΔE) were calculated. The influence of the number of layers on the adherence of the coating film to the support and its resistance to cold liquids was also evaluated. The results showed only a small influence of the thickness of the coating film on the colour and light fastness of the coated surfaces. In terms of adherence to the substrate and resistance to cold liquids, application in three layers gave the best results, which is in accordance to the manufacturers' recommendations.

INTRODUCTION

Natural beauty of wood might be highlighted, enhanced and protected over time by adequate finishing technologies. Stabilising the natural appearance (colour) of the clear coated wood surfaces for both outdoor and indoor applications against light induced colour changes is still a challenge for scientists and practitioners (Yuan B. et al. 2021,) (Nikafshar S. et al. 2021). It is important to point out that the topics of light-resistant clear coatings for indoor applications has been addressed less (Kúdela J. et al. 2023) but it becomes increasingly important (Silverman C. 2016), as the market request for furniture and other wooden interior design elements with natural aspect is increasing.

The influence of wood species (Oltean L. et al. 2007), type of the clear coating materials (Aloui F. et al. 2007, Özgenç Ö. et al. 2020), time and exposure / testing conditions (Kropat M. et al. 2020), (Kanbayashi T. et al. 2024) on the light induced colour changes of wood surfaces were addressed by worldwide research. Ultraviolet (UV) radiation from the natural light or artificial sources was recognised as the most aggressive ageing factor causing both colour and surface chemistry changes, but short wavelengths components of the visible light, in the violet (403nm) and blue range (434-496) may also contribute to the overall colour changes (Kataoka Y. et al. 2007), (Živković V. et al. 2014).

The contribution of the wood substrate to the colour changes of clear coated wood surfaces was acknowledged and methods for its highlighting and quantifying by experimental approaches and calculation were developed (Chou P. L. et al. 2008). Accordingly, current approaches of stabilising the colour of clear coated surfaces are addressing pre-treatment /stabilisation of the substrate, modification of the coating film or both (Blanchet P. and Pepin S. 2021),(Yi T. and Morrell J. J. 2023).

The protective effect of a clear coating film against light induced colour changes of wood surfaces will depend on its capability to absorb, block or disperse the UV light, reducing the amount (radiation

intensity) reaching the wood surface underneath the coating film. A high transparency / transmittance of the coating film for visible light is at the same time necessary in order to highlight wood features and beauty (Evans P. et al. 2005). At the same time, colour and gloss changes of the coating film might occur by photo-degradation. It would be, therefore, logical to think that the protective effect of a coating film against light will depend on its composition, especially the content of UV protective additives, while its thickness might contribute to a better protection of the underlying substrate.

Increasing the concentration of a novel light stabilizer (NLS)) was found to have a better efficiency in improving the UV filtering capacity compared to increasing the thickness of the coating film. The calculated effect factors for reducing the degree of yellowing were 76.8% for NLS, compared to only 7.7% for the film thickness (Yung C. Y. et al. 2019).

A significant influence of the coating film thickness (resulting from 1, 2, 3 layers of three different clear finishing materials) on the gloss and light induced colour changes of beech light plywood surfaces was reported. Increased light-induced colour changes resulted for thicker polyurethane films, while a slight protective effect was obtained for thicker hard wax films (Slabejová G. and Šmidriaková M. 2022).

In terms of influence of coating film thickness on various quality aspects of coated surfaces, there are rather limited references. The influence of coating formulation (polyurethane 1k,) and film thickness (resulting from application rates of 80 g/m² and 150 g/m² on soft- and hardwood plywood) on the resistance to cold liquids was reported. It was concluded that the thickness of the coating had no statistically significant effect on the quality of the resulting film.

The current research focussed on the effect of increasing the thickness of a clear polyurethane coating film on the light induced colour changes maple wood surfaces with natural aspect and on some relevant aspects of their quality, namely adherence to the substrate and resistance to cold liquids.

MATERIALS AND METHODS
Wood material
Hardwood from the European maple species (*Acer pseudoplatanus* L) was employed in this research. Test samples of a rectangular shape, with dimensions of $120 \times 80 \times 8$ (mm × mm × mm), with radial or semi-radial faces, were prepared from air-dried wood material. All samples were sanded with abrasive paper with 120, 180 grit sizes.

Coating materials
A clear waterborne polyurethane lacquer, type YO-20-M838 (coded F3), produced by Renner Italy (https://www.renneritalia.com/en/) was purchased from Kroncolor Brasov / Romania (http://www.kroncolor.ro/contact.html). This is a matt effect coating (Gardner Gloss index 20), with 30 $\pm$ 1 % solids content, density 1.03 g/cm³ and low viscosity (flow time, 14s, ϕ 4mm, 20°C), and was employed as 1k formulation.

Preparation of test samples
Uncoated and coated wooden samples and 1mm thick glass slides were used. The coated samples were prepared in the laboratory by successively applying 2, 3, or 4 layers of lacquer, of about 100-110 g/m² each, corresponding to a liquid film of about 100 μm. Similarly, 2, 3 or 4 layers of lacquer were applied on glass slides. in 2 layers, 3 layers and 4 layers.

Similarly with previous research (Torcătoru M.-J. and Timar C. M. 2023, Torcătoru M.-J. and Timar M. 2024), coated glass slides were tightly fixed on uncoated wood samples (V1) to simulate a detachable coating film. On both uncoated (V1) and coated (V2) wood samples, there were defined areas for different exposure situations: direct exposure to light (V1/Z3; V2/Z1), exposure under clear glass (V1/Z2, V2/Z3), exposure under coated glass (V1/Z1) and covered areas as references (V1Z4, V2/Z2).

Colour measurements
Color measurements were performed in the CIELab reference system using an Ava-spec-USB2 spectrometer from Avantes (Apeldoorn, Netherlands), equipped with an integrated Ava sphere with a diameter of 80 mm, with a circular measuring opening of 8 mm in diameter, under D65 standard illuminant and measurement angle of 10 degrees, as in previous research (Torcătoru M.-J. and Timar C. M. 2023, Torcătoru M.-J. and Timar M. 2024), Statistical data processing was done in the SPSS program, using the One-Way ANOVA test.

Accelerated UV-VIS light induced ageing procedure

Feutron 400 FKS climate chamber (Feutron Klima Simulation-GmbH-Greiz, Germany), equipped with a Spot 400 T UVA lamp (Hoenle UV Technology-Olching Gilching, Germany), with an H2 glass filter was used to expose the specimens to UV-VIS light in the wavelengths range 296-600 nm, simulating natural light filtered by window glass, similarly as in previous research (Torcătoru M.-J. and Timar C. M. 2023, Torcătoru M.-J. and Timar M. 2024) . Samples were exposed for 24, 48 and 72 h to UV/VIS radiation. Samples were in triplicates for each film thickness, resulted by applying 2, 3 and 4 layers of lacquer.

Quality of the coated surfaces

The adherence of the coating film to the substrate by cross-cut method and the resistance of the surfaces to selected cold liquids were evaluated according to standard methods.(ISO-2409-(2020))

RESULTS AND DISCUSSION

Influence of coating and film thickness on the colour of coated maple wood surfaces

The colour changes brought about by coating of maple wood samples with the polyurethane lacquer F3, are shown in Table 1. The thicknesses of the clear coating films, partly impregnated into the maple wood surface, as observed under a stereomicroscope at 400x magnification, are also included (average and standard deviations for 10 measuring points).

Table 1: Colour changes of maple wood surfaces by coating with the clear waterborne polyurethane lacquer (F3) in 2, 3 and 4 layers

Coating / number of layers	Film thickness [μm]	ΔL*	Δa*	Δb*	ΔE
F3 / 2 layers	27.01±3.42	-2.10 [B] ± 0.75	0.93 [A] ± 0.37	1.16 [B] ± 0.93	2.74 [B] ± 0.80
F3 / 3 layers	38.49±9.55	-2.98 [A] ± 0.74	0.75 [A] ± 0.38	2.11 [A] ± 1.11	3.89 [A] ± 0.80
F3 / 4 layers	61.38±8.29	-2.13 [B] ± 0.59	0.29 [B] ± 0.40	1.91 [A] ± 0.81	3.00 [B] ± 0.68

Note: The data represent average values of colour changes in 12 measuring points/per coating/per number of layers; Values on columns sharing the same capital letters A, B as superscript indexes are not statistically different at a significance level α =0.05

Coating of maple wood surfaces with the clear waterborne polyurethane lacquer (F3) caused only a small colour change, expressed by ΔE values in the range 2.74-3.89 units. The differences were found statistically significant only for the application in 3 layers compared to the application in 2 and 4 layers. These small colour changes resulted from slight darkening (negative ΔL* values of about 2-3 units) and slight increase in chromaticity (positive Δa* and Δb* values of about 1 and 2 units, respectively), with small significant differences as a function of coating film thickness. It can be concluded that the lacquer succeeded very well in preserving the natural aspect of maple, which is in good accordance with visual perception.

Influence of film thickness on the light induced colour changes of coated maple surfaces

The light induced colour changes of polyurethane (F3) coated maple wood samples (with 2, 3, 4 coating layers), after exposure to UV-VIS light for 72h are shown in Table 2.

Table 2: Colour changes of coated maple wood surfaces with clear waterborne polyurethane lacquer (F3), applied in 2, 3 and 4 layers, after 72 hours exposure to light-V2Z1.

Coating / number of layers	ΔL*	Δa*	Δb*	ΔE
F3 / 2 layers	-5.6 [A] ± 0.66	1.75 [B] ± 0.29	8.86 [A] ± 0.7	10.64 [A] ± 0.78
F3 / 3 layers	-4.39 [B] ± 0.81	1.79 [B] ± 0.62	8.2 [A] ± 1.54	9.52 [B] ± 1.55
F3 / 4 layers	-4.8 [B] ± 0.41	2.19 [A] ± 0.47	8.13 [A] ± 0.89	9.72 [B] ± 0.79

Note: The data represent average values of colour changes in the 18 measuring points/per coating/per number. of layers; Values on columns sharing the same capital letters A, B as superscript indexes are not statistically different at a significance level α =0.05

Exposure to light for 72 hours, determined visible colour changes of the coated surfaces, expressed by ΔE values in the range of 9.52-10.64. A slight of increased colour difference of 10.64, statistical significantly different from the values of 9.52-9.72, was determined for the samples coated with only 2 layers. These colour changes resulted from darkening (negative ΔL* values of about 4-5 units, statistical higher for the thinnest film of 2 layer), slight increase in redness (positive Δa* values of about 2 units, statistically higher for 4 layers) and larger increases in yellowness (positive Δb* values of approximately 8-9 units, not statistically different). It can be concluded that the colour changes of the coated samples resulted mainly from yellowing and darkening, leading to a slight, but statistically significant, increased global colour difference ΔE for the thinnest film, resulting from 2 layers of lacquer.

Colour changes of the wood substrate underlying the coating film

The colour changes of wood substrate under the coating film were simulated be means of detachable coated glass slides tightly fixed on uncoated wood samples (samples V1, area Z1) during light exposure and then removed for measurements. The values after 72 h exposure are summarised in Table 3.

Table 3: Colour changes of the maple wood substrate under the clear waterborne polyurethane lacquer (F3), applied in 2,3,4 layers on glass slides, after 72 hours light exposure

Coating / number of layers	ΔL*	Δa*	Δb*	ΔE
F3 / 2 layers	-3.43 [A] ± 0.58	1.18 [A] ± 0.46	3.53 [A] ± 0.87	5.10 [A] ± 0.86
F3 / 3 layers	-3.50 [A] ± 0.84	1.38 [A] ± 0.66	3.43 [A] ± 0.90	5.14 [A] ± 1.13
F3 / 4 layers	-3.21 [A] ± 0.41	1.43 [A] ± 0.62	2.48 [A] ± 1.11	4.45 [A] ± 0.56

Note: The data represent average values of colour changes in the 9 measuring points/per coating/per number of layers; Values on columns sharing the same capital letter A as superscript indexes are not statistically different at a significance level α =0.05

Colour changes expressed by ΔE values in the range 4.45-5.14, with the lowest value for the thickest film, but statistically not different, were determined for the maple wood substrate under the detachable coating films applied on glass slides. These colour changes resulted from slight darkening (negative ΔL values of approximately 3-3.5 units), slight increase in redness (positive Δa* values of 1-1.5 units) and increase of yellowness (positive Δb* values of 2.5-3.5 units), statistically not different for different coating film thicknesses. These results highlight the significant contribution of wood substrate to the global colour changes of coated maple surfaces. These results were obtained by simulating the real situation employing a glass slide as support for a ″detachable″ coating film. The glass blocked part of the UV radiation from the source, so that even higher colour changes should be considered for the wood substrate underneath the coating films in real situations.

Colour changes of coating film

The colour changes of the coating films of different thicknesses applied on the glass slides are presented in Table 4.

Table 4: Color changes of the clear waterbased polyurethane lacquer (F3) in 2, 3, 4 layers - after 72 hours induced by light

Coating / number of layers	Film thickness [mm]	ΔL*	Δa*	Δb*	ΔE
F3 / 2 layers	0.057±0.005	-1.36 [A] ±0.26	0.09 [A] ±0.38	1.05 [A] ±0.49	1.81 [A] ±0.30
F3 / 3 layers	0.083±0.003	1.38 [A] ±0.21	0.11 [A] ±0.42	0.93 [A] ±0.77	1.82 [A] ±0.47
F3 / 4 layers	0.103±0.006	-1.42 [A] ±0.27	0.16 [A] ±0.39	0.99 [A] ±0.91	1.94 [A] ±0.48

Note: The data represent average values of colour changes in the 9 measuring points/per coating/per number of layers; Values on columns sharing the same capital letters A as superscript indexes are not statistically different at a significance level α =0.05

The clear polyurethane films applied on glass slides showed only very small colour changes, expressed by ΔE values in the range of 1.81-1.94 (statistically not different), following 72h light exposure. These resulted from slight darkening (negative values of ΔL of about 1.5 units) and (Δb* of about 1 unit).

Adherence and resistance of coated surfaces to cold liquids

In Table 5 are summarised the experimental mean results referring to the resistance of the coated surfaces to the different tested cold liquids: water, ethyl alcohol, coffee and acetone, for various periods of time (EN-12720:(2009+A1:2014) S.), alongside the adherence of the coating film to the substrate, determined by the cross-cut test. Regardless the number of lacquer layers applied, it can be noted a very good adhesion of the film to the maple wood substrate. On the other hand, it could be observed an influence of the number of layers on the resistance of the coated surfaces to cold liquids. Increasing the number of layers from two to three resulted in a better quality of the surfaces, whilst a further fourth layer reversed this trend, excepting the case of acetone. This seems rather strange and more tests are needed, but somehow similar situations could be observed when closely looking at the results reported by (Bomba J. et al. 2017) for 1k polyurethane lacquer, concluding on no significant influence of the coating film thickness in the application range recommended by the producer. For the product tested within this research, application in 2-3 layers, at application rates of 80-150 g/m² is recommended by the producer.

Table 5: Resistance to cold liquids and adhesion to the support of the clear polyurethane lacquer (F3)

Coating / Number of layers	Resistance to cold liquids								Adherence to substrate
	Water			Ethyl alcohol 50%		Coffee		Acetone	
	1 h	16 h	24 h	1 h	16 h	1 h	16 h	2 min	
F3/ 2 layers	4/5	5	5	4	4	3/4	3/4	2/3	0/1
F3/ 3 layers	5	5	5	5	5	4	4	2/3	0
F3/ 4 layers	4	4	4	4	4	2	2	4/5	0

CONCLUSIONS

The thickness of the coating film, resulting from two, three and four layers of clear waterborne polyurethane lacquer (1k) had only a very limited influence (differences of ΔE values of about 1 unit, at the limit of human eye perception) on the colour and the light induced colour changes of the coated maple wood surfaces (ΔE ~ 10 units). Based on statistical significant differences it would result a slightly better light resistance when applied in three layers of 100-110g/m². This technology resulted in adherent coating films with high resistance to water, ethyl alcohol and coffee. The limited resistance to acetone revealed limited cross-linking, which might be improved for a 2k formulation.

The coating film suffered only slight colour changes after light exposure (ΔE < 2 units), while more important colour changes were determined for the underlying maple wood (ΔE ~ 5 units), not influenced by the film thickness.

REFERENCES

Aloui, F., A. Ahajji, Y. Irmouli, B. George, B. Charrier and A. Merlin (2007). "Inorganic UV absorbers for the photostabilisation of wood-clearcoating systems: Comparison with organic UV absorbers." Applied Surface Science 253(8): 3737-3745. https://doi.org/10.1016/j.apsusc.2006.08.029

Blanchet, P. and S. Pepin (2021). "Trends in Chemical Wood Surface Improvements and Modifications: A Review of the Last Five Years." Coatings 11(12). https://doi.org/10.3390/coatings11121514

Bomba, J., J. Ježek, Š. Hýsek, A. Sikora, R. Stolariková, A. Palacká, M. Berková and T. Kolbabova (2017). "Polyurethane Coatings on Hardwood and Softwood Surfaces: Their Resistance to Household Liquids as an Educational Case Study." Bioresources 12: 5867-5877. https://doi.org/10.15376/biores.12.3.5867-5877

Chou, P. L., H. T. Chang, T. F. Yeh and S. T. Chang (2008). "Characterizing the conservation effect of clear coatings on photodegradation of wood." Bioresource Technology 99(5): 1073-1079. https://doi.org/10.1016/j.biortech.2007.02.027

EN-12720:(2009+A1:2014), S. Assessment of surface resistance to cold liquids, Slovenian Institute For Standardization, Slovenski Standard

Evans, P., M. Chowdhury, B. Mathews, K. Schmalzl, S. Ayer, M. Kiguchi and Y. Kataoka (2005). "Weathering and Surface Protection of Wood" Inc. Delmar, New York. https://doi.org/10.1016/B978-081551500-5.50016-1

http://www.kroncolor.ro/contact.html. Accessed 25 Jan 2024

https://www.renneritalia.com/en/. Accesed 7 Feb 2024

ISO-2409-(2020) -Paint and varnishes. Cross-cut test, Geneva, Switzerland.

Kanbayashi, T., M. Matsunaga, M. Kobayashi and K. Maeda (2024). "Elucidation of the degradative behavior of coated-wood surfaces exposed to artificial weathering using Raman microspectroscopy." Progress in Organic Coatings 187: 108184. https://doi.org/10.1016/j.porgcoat.2023.108184

Kataoka, Y., M. Kiguchi, R. S. Williams and P. D. Evans (2007). "Violet light causes photodegradation of wood beyond the zone affected by ultraviolet radiation." Holzforschung 61(1): 23-27. https://doi.org/10.1515/HF.2007.005

Kropat, M., M. A. Hubbe and F. Laleicke (2020). "Natural, Accelerated, and Simulated Weathering of Wodd:A Review." Bioresources 15(4): 9998-10062. http://dx.doi.org/10.15376/biores.15.4.Kropat

Kúdela, J., A. Sikora and L. Gondáš (2023). "Wood Surface Finishing with Transparent Lacquers Intended for Indoor Use, and the Colour Resistance of These Surfaces during Accelerated Aging." Polymers (Basel) 15(3). https://doi.org/10.3390/polym15030747

Nikafshar, S., J. McCracken, K. Dunne and M. Nejad (2021). "Improving UV-stability of epoxy coating using encapsulated halloysite nanotubes with organic UV-stabilizers and lignin." Progress in Organic Coatings 151. https://doi.org/10.1016/j.porgcoat.2020.106108

Oltean, L., A. Teischinger and C. Hansmann (2007). "Wood surface discolouration due to simulated indoor sunlight exposure." Holz als Roh- und Werkstoff 66(1): 51-56. https://doi.org/10.1007/s00107-007-0201-9

Özgenç, Ö., S. Durmaz, S. Şahin and İ. H. Boyaci (2020). "Evaluation of the weathering resistance of waterborne acrylic- and alkyd-based coatings containing HALS, UV absorber, and bark extracts on wood surfaces." Journal of Coatings Technology and Research 17(2): 461-475. https://doi.org/10.1007/s11998-019-00293-4

Silverman, C. (2016). "An Investigation into the Potential of Paraloid™ B-72 Modified with Zinc Oxide Nanoparticles as a UVshielding Coating for the Conservation of Wooden Furniture."

Slabejová, G. and M. Šmidriaková (2022). "The effect of coating film thickness on the quality of surface finish on lightweight plywood." https://doi.org/10.17423/afx.2022.64.1.04

Torcătoru, M.-J. and C. M. Timar (2023). "An experimental method to evaluate the contribution of the wood substrate and of the coating film in the global light in-duced colour changes of wood surfaces in indoors conditions." Bulletin of the Transilvania University of Brasov, Series II: Forestry - Wood Industry - Agricultural Wood Engineering 16(3). https://doi.org/10.31926/but.fwiafe.2023.16.65.3.15

Torcătoru, M.-J. and M. Timar (2024). "Light-Induced Colour Changes in Wood Surfaces in Indoor Conditions Determined by an Artificial Accelerated Test: Influence of Wood Species and Coating Materials." Applied Sciences 14: 1226. https://doi.org/10.3390/app14031226

Yi, T. and J. J. Morrell (2023). "Role of α/γ Fe2O3 and ZnO nano-particles in reducing photodegradation of wood components." Wood Science and Technology 57: 427–446. https://doi.org/10.1007/s00226-023-01456-8

Yuan, B., M. Guo, Z. Huang, N. Naik, Q. Hu and Z. Guo (2021). "A UV-shielding and hydrophobic graphitic carbon nitride nanosheets/cellulose nanofibril (gCNNS/CNF) transparent coating on wood surface for weathering resistance." Progress in Organic Coatings 159. https://doi.org/10.1016/j.porgcoat.2021.106440

Yung, C. Y., Y. L. Pei, H. Miles, T. L. Yin, H. L. Chung and H. H. Yao (2019). "Patel - Novel Light Stabilizers for Waterborne and Functional Coatings"

Živković, V., M. Arnold, K. Radmanović, K. Richter and H. Turkulin (2014). "Spectral sensitivity in the photodegradation of fir wood (Abies alba Mill.) surfaces: colour changes in natural weathering." Wood Science and Technology 48(2): 239-252. doi: http://dx.doi.org/10.1007/s00226-013-0601-4

Composite Material Manufacturing from Plantation Paulownia Wood with Using Microwave Technology: Technical and Cost Analyses

Grigory Torgovnikov [1*], Peter Vinden [2], Alexandra Leshchinskaia [3]

[1, 2] University of Melbourne, 4 Water St., Creswick, Victoria 3363, Australia
[3] Plekhanov Russian University of Economics. 36 Stremyannyy Pereulok, 115093 Moscow, Russia

E-mail: grigori@unimelb.edu.au; pvinden@unimelb.edu.au; alixfl@mail.ru

Keywords: composite material, microwave wood modification, Paulownia wood, specific cost, strength properties, Vintorg.

ABSTRACT

Paulownia is a very fast-growing hardwood species with low density and low strength properties. These limit the industrial use of this species. Manufacturing of composite material from Paulownia wood with applications resins can increase its density and improve mechanical properties. Paulownia is practically impermeable and therefore cannot be impregnated with industrial resins that could improve essential physical and mechanical properties. High-intensity microwave (MW) modification converts Paulownia wood to a highly porous material "Torgvin" with very high permeability for liquids and provides opportunities to impregnate it with special resins for manufacturing composite material with higher mechanical and physical properties.

In this work, the results of the experiments on developing technology for manufacturing composite material from plantation Paulownia (*Paulownia fortunei*) wood are presented. The technology of the new material "Vintorg" manufacturing includes sawn timber MW modification, kiln drying, pressure impregnation by resins, hot pressing, and finishing.

The strength tests showed that the new material has a significant increase in strength properties compared to natural wood. This provides an opportunity to use Paulownia timber as a row material for manufacturing composite materials with the required mechanical properties.

Economic analyses showed reasonable material production costs. The significant increase in material strength properties compared to Paulownia natural wood and reasonable production costs provide good opportunities for technology commercialization in small-scale mills.

INTRODUCTION

Paulownia is a fast-growing hardwood with low density and low strength properties. These limit the industrial use of this species. The Paulownia wood requires some pre-manufacturing to increase its density and improve its mechanical properties. Paulownia wood is practically impermeable and therefore cannot be impregnated with industrial resins that could improve essential physical and mechanical properties.

A high-intensity microwave (MW) wood treatment provides a significant increase in wood permeability (Torgovnikov and Vinden 2010, Vinden et.al. 2004). If wood is supplied with MW power of high intensity, the moisture in the cells starts boiling. This results in high steam pressure in the wood cells, which leads to an expansion of the cell walls resulting in the rupturing of the libriform fibers and rupturing tylosis in the vessels and in the formation of narrow checks, which extend in the radial-longitudinal planes, forming cavities in the same planes. MW modification converts wood to a material, "Torgvin", with a very high permeability that provides an opportunity for impermeable species to be impregnated with resins and preservatives (Torgovnikov and Vinden 2002).

Manufacturing of the new product from MW modified Paulownia requires the application of resins and the compression of the wood, followed by curing the resin. This new product can have the following advantages: high strength properties, natural appearance and structure, good dimensional stability, fungi protection, and fireproof properties.

The objectives of this study are: to determine the opportunities of a new product Vintorg manufacturing from Paulownia *fortunei* timber; to determine the process parameters for material manufacturing which include: MW wood modification, drying, impregnation with resin, pressing,

and curing; to study the mechanical properties of Vintorg; to estimate costs of new material manufacturing from Paulownia timber.

EXPERIMENTAL STUDY
Material and Methods

The green timber of Paulownia *fortunei* measuring 75x90x2100 mm (130 pc) was used for experiments. The samples had a wide range of moisture content (MC) from 98 to 258% with an average MC=137% and oven dry density from 242 to 344 kg/m3 with an average 280 kg/m3. The variation coefficient of moisture content was 25.7 % and oven dry density 11.2%.

Three types of commercial resins have been used for Vintorg manufacturing: Rubinate 1780 (PMDI, Diphenylmethane-4, 4'-diissosyanatex, density 1.24 g/cm3), Sylvic M550 (Melamine formaldehyde, density 1.15 g/cm3), Furfural-alcohol (FA) (with trifurfuryl borate paraformaldehyde resin, density 1.14 g/cm3).

A 60 kW MW installation was used for experiments (Figure 1). It includes a MW power supply, waveguides, tuner, MW applicator, water load, tunnel, conveyor feeding system, and air dynamic system for the removal of vapors from the applicator and the prevention of water condensation on the walls of the applicator.

Technical data of MW conveyor installation:
- MW power - 10-60 kW
- Frequency - 0.922 GHz
- Max dimensions of timber - 90x90x4500 mm
- Feed speed - 4-30 mm/sec
- Air heating power - 13 kW
- Air temperature - 20-150°.

A box applicator (Figure 1) was employed for wood modification. The timber traveled via an applicator on the belt. The following schedule for timber 75x90 mm was used: MW power 32-46 kW, average MW intensity 117-136 W/cm2, electric field strength vector E orientation parallel to the wood grain, belt speed 9.3 mm/sec, air temperature 120 –130°C.
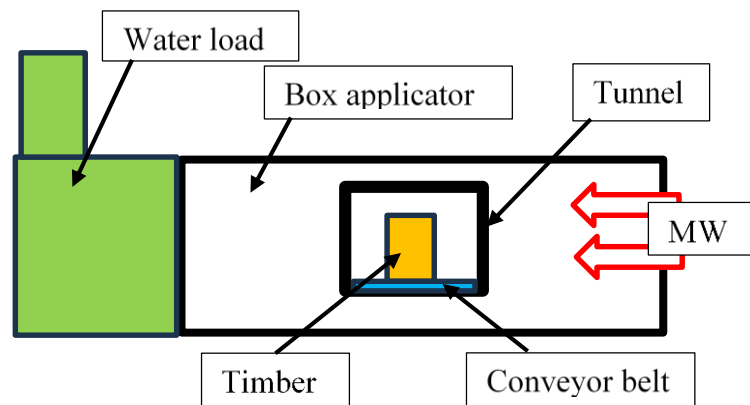

Figure 1: Microwave 60 kW (frequency 0.922GHz) experimental plant and MW applicator with cross-section 124x248 mm

MW generated, reflected, and transmitted power was measured during the experiments. The criteria for the evaluation of the degree of MW wood modification was the uniformity of the void distribution through the cross-section of the material. If more than 85% of cross-section areas have visible checks, it means the sample has an acceptable degree of modification. Paulownia wood structure was studied by analyzing microscope photos of the samples before and after MW processing.

Vintorg samples manufacturing process included: MW green timber modification (Torgvin manufacturing), drying to get the required moisture content (8-12%), impregnation with resin, pressing, and curing. Torgvin samples measuring 50x75x350 mm were used for material pressing. Special

pressure vessels were used for sample impregnation. Different regimes were used for sample impregnation of the resins: vacuum in the range of -30 to - 80 kPa, and pressure in the range of 100-500 kPa at temperature 20-25 °C. The samples after resin impregnation were pressed and curried in the press with applying pressure 3.8-5.2 MPa for 4 hours at a temperature of 120 °C.

Standard methodology was used for measuring the strength properties (MOE-modulus of elasticity, MOR-modulus of rupture, surface hardness) of the material. The tests were carried out on a Hounsfield 10K strength testing machine with a maximum variable load cell force of 10kN on the samples measured 20x20x350 mm.

RESULTS AND DISCUSSION

The MW wood processing provides the breakdown of the libriform tissue, the breakdown of tylosis in vessels, the formation of the canals in vessel walls and in surrounding vessel parenchyma cell walls, and the formation of a great number of cavities in the radial-longitudinal planes. Such kinds of destructions form a net of canals in all directions: radial, longitudinal, and tangential. The net result is a substantial improvement in wood permeability for vapors and liquids. Practically impermeable in the radial and tangential directions, Paulownia wood becomes permeable in all directions (Figure 2).

Figure 2: Samples of MW modified wood (Torgvin) from Paulownia fortunei after MW treatment and impregnation with resin

During MW treatment the timber with initial MC 195-210% loses 130-158% MC and with initial MC 155-157% loses 93-111% of MC. Depending on the conditions of MW treatment the energy consumption for timber with MC 200-210% varies in the range 237- 433 kWh/m3 and for timber with MC 120-160% - 216-282 kWh/m3.

Steam released from Paulownia timber during MW treatment was analyzed from a safety point of view. The result showed that vapors from wood do not appear to have any harmful chemicals present.

After MW modification the Paulownia MOR loses 48-68% of the initial MOR in the radial direction, and 42% in the tangential direction. The residual MOE in the radial direction is 60-86% of the initial MOE and 41-48% in the tangential direction. The residual surface hardness forms 62-74% of the initial hardness. MW Paulownia wood modification reduces strength properties significantly. Paulownia timber has a high variability of density (range of oven dry density 220-340 kg/m3). Therefore to get Vintorg of the required density from wood with different densities it is necessary to press it to a different degree. Experiments showed the pressing degree should be in the range of 20- 47% depending on the initial density and the Vintorg density desired.

All tested commercial resins Rubinate 1780; Sylvic M550 and Furfural-alcohol provide opportunities to make Vintorg from Paulownia wood with higher strength properties. Vintorg with Rubinate 1780 and Sylvic M550 at an average material density of 500 kg/m3 and resin content of 10-30% has the following strength properties:

	Vintorg (MPa)	Natural wood (MPa)	Increase
MOR	46-60	31-40	40-49%
MOE	5300-6600	3400-4100	67-92%
Surface hardness	22-30	9.5-14	122-161%

The application of Furfural-alcohol resin provides significantly lower Vintorg strength properties compared to Rubinate 1780 and Sylvic M550 resins.

Vintorg with Rubinate 1780 and Sylvic M550 has a light colour similar to natural Paulownia wood (Figure 3). Average resin consumption for Vintorg manufacturing for Rubinate1780 - 56 kg/m3 , for Sylvic M550 – 70 kg/m3.

Figure 3: Samples of new material from Paulownia wood (right image is natural Paulownia)

MATERIAL MANUFACTURING TECHNOLOGY

An outline of the process for Vintorg production from Paulownia timber is shown in Figure 4.
The manufacturing stages include:
a) Timber grading
b) Microwave timber modification – Torgvin production. MW installation is used for increasing wood permeability and reducing timber moisture content.
c) Torgvin drying up to moisture content 8-12 %
d) Impregnation with resin in pressure vessel
e) Hot pressing is used for resin curing and cross section formation
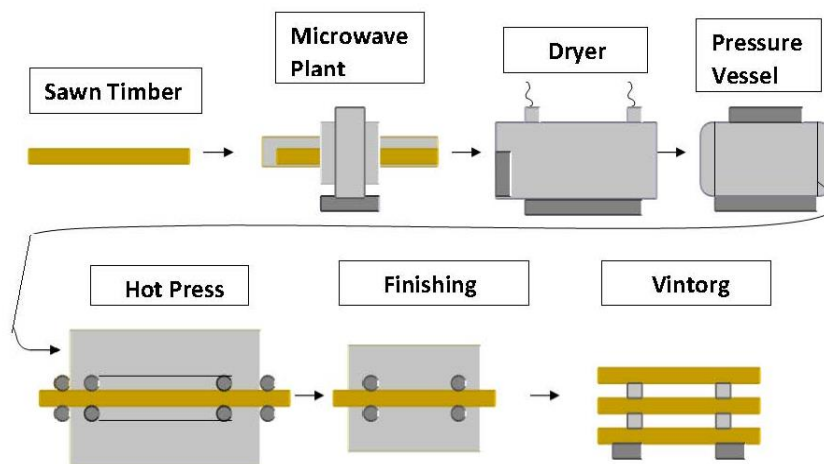f) Finishing of the material.

Figure 4: Flow diagram of composite material "Vintorg" production line

A Vintorg production plant requires designing special new equipment for MW timber modification. Standard commercial equipment can be used for timber grading, drying, impregnation, hot pressing, finishing, and material handling and transporting.

ECONOMIC ASSESSMENT OF MATERIAL MANUFACTURING

Three commercially visible plant outputs were used for the economic study: 6,300, 12,600, and 18,600 m3/year at 3 shifts per day, electricity cost US$ 0.2 kWh, labor cost U$$ 40,000/year, depreciation rate 10 -17% (depending on equipment). This cost assessment includes capital (equipment) costs, labor, electricity, fuel, consumables, and chemicals and does not include raw material costs, costs of buildings, foundations, electrical connections, and mechanical installation. Two cubic meters of green Paulownia timber are required for manufacturing 1m3 of new material.

Specific costs of Vintorg material from Paulownia wood production (including resin costs) are shown in Table 1.

Table 1: Specific production costs of Vintorg with Rubinate 1780 or Silvic M550 resins

Vintorg output in m3/y	Specific production costs (including resin costs), US $/m3					
	6300		12600		18600	
Cost items	US$/m3	%	US$/m3	%	US$/m3	%
Grading	17	3	9	2	7	1
MW treatment	207	29	181	31	178	31
Drying	111	15	93	15	88	16
Impregnation	45	**6**	23	4	17	3
Hot pressing	138	19	86	14	72	14
Finishing	9	1	7	1	6	1
Transport	19	3	18	3	17	3
Resin Rubinate or Sylvic	175	24	175	30	175	31
Total	**721**	**100**	**592**	**100**	**560**	**100**

Microwave processing costs form 29-31% of total specific costs, drying – 15-16%, and hot pressing costs – 14-19 %. Resins Rubinate 1780 and Sylvic M550 form 24-31% of total production costs.

CONCLUSIONS

The high-intensity MW processing of Paulownia wood forms a net of canals in all directions: radial, longitudinal, and tangential. Practically impermeable Paulownia wood becomes permeable and provides the required resin distribution in timber cross-section. The average MW energy consumption for Paulownia timber modification is 244-254 kW-h/m3.

Composite material Vintorg from Paulownia wood has a natural appearance and structure, and strength properties higher compared to natural wood: MOR by 40-49%, MOE by 67-92%, and surface hardness by 122-161%. These properties open up a number of new fields of industrial applications for this material.

Economic analyses of material production costs were made with taking into consideration costs of timber grading, MW treatment, drying, pressure impregnation, hot pressing, finishing, and transport for plant outputs 6,300 to 18,600 m3 per annum. Specific material production costs (including resin costs) made up for plant output 6,300 m3/y - US$721/m3, for output 12,600 m3/y - $591/m3, and for output 18,600 m3/y - $557/m3.

The significant increase in composite material strength properties compared to natural wood and reasonable production costs provide good opportunities for technology commercialization in small-scale mills.

REFERENCES

Torgovnikov G and Vinden P (2010) Microwave wood modification technology and its applications. Forest Products Journal, Vol 60, No 4, pp 173-182.

Torgovnikov G and Vinden P (2002) Modified wood product and process for the preparation thereof. Canada Patent CA 2441498.

Vinden P, Romero J, Torgovnikov G (2004) A method for increasing the permeability of wood. US Patent No 6,742,278

Thermal modification of wood as a tool for changing the colour of hardwoods

Vidholdová Zuzana[1*]

[1] Technical university in Zvolen, T.G. Masaryka 24, Zvolen, Slovak Republic, SK-962 01

E-mail: zuzana.vidholdova@tuzvo.sk

Keywords: Thermal modification; Colour measurement; CIE Lab; hardwood, tropical wood

ABSTRACT

Thermal modification is an ecological and low-cost method to improve optical properties of wood. Thermal modification processes darken the colour of wood throughout its cross section because of chemical changes in the wood. The studied hardwood species – (a) ash (*Fraxinus excelsior* L.), European beech (*Fagus sylvatica* L.), Paper birch (*Betula papyrifera* Marsh), Black locust (*Robinia pseudoacacia* L.), hornbeam (*Carpinus betulus* L.) and Pedunculate oak (*Quercus robur* L.) were thermally treated at temperature of 200°C for 3 hours, and (b) alder (*Alnus glutinosa* (L.) Gaertn), European beech (*Fagus sylvatica* L.), Paper birch (*Betula papyrifera* Marsh) and Norway maple (*Acer pseudoplatanus* L.) were hydrothermally treated with saturated water steam at the temperature of 135 ± 2.5 °C for 6 hours. Their colour coordinates L^*, a^*, and b^* were statistically compared with colour of selected eight tropical woods – ipé (*Handroanthus serratifolius*), iroko (*Milicia excelsa*), maçaranduba (*Manilkara bidentata*), makoré (*Tieghemella heckelii*), sapelli (*Entandrophragma cylindricum*) and wengé (*Millettia laurentii*). The colour similarity between thermally treated and tropical woods showed that these treatments were able to modify the coloration of the wood and its colour was similar to tropical woods. It was found that Pedunculate oak or Black locust treated at 200°C for 3 hours was similar to wengé and European beech treated at 200°C for 3 hours was similar to ipé. Other variants of heat-treated hardwoods resembled tropical woods only partially.

INTRODUCTION

The natural colour of the wood characterizes the appearance of the wood (Tolvaj et al. 2013, Slabejová et al. 2016). It is one of the most important wood features as it can be used both for identification of the wood species and indication of their appropriate use in manufacturing of furniture, musical instruments, art objects, sporting goods, and others, especially when associated with texture and design aspects. Hardwoods colour differs depending on the species. The natural colour of wood also is determined by its chemical components, i.e. cellulose, hemicelluloses and lignin. It depends more on their prominence than on their total weight or volume portion in wood. For example, cellulose has the highest percentage portion in wooden cell wall, but its white colour can be overshadowed by the colour of extractive substances, which concern only a small percentage of the weight of the wood. Hardwoods come in many shades from light to dark. The colour of the wood is evaluated according to the colouring on longitudinal surfaces, because this side of the wood is most often found on all wooden objects. On the cross section, the wood is usually darker in colour. Temperate (for example European) hardwoods without a heart (birch, hornbeam, maple, ash, lime, aspen) are light or light brown. Darker wood colouring occurs in hardwoods with high density (oak, pear, alder, walnut, cherry), and others, as well as in heart of conifers. It is caused by a denser deposition of thick-layered fibres close to each, by the settling of tannins and other extractive substances and dyes in the heart of wood. Tropical woods, on the other hand, contain higher level of extractive substances than temperate wood species, therefore their wood has a more pronounced natural colour, either light (yellow, pink) or dark (red, red-brown, purple) to black (as in the case of ebony) (Hon and Minemura 2000). Some tropical woods have so much natural dyes that would be use as a natural source of dye for textile or wood (for example bloodwood (*Haematoxylum campechianum* L.)). The reddish-brown heartwood of logwood produces a dark red solution in water and is the source of the two biological stains hematoxylin and hematein (Ortiz-Hidalgoand Pina-Oviedo, 2019).

A quantitative description of colour is often performed by using the $L^*a^*b^*$ colour space values (CIE 1976 colour system). It is nowadays the most widely used colour system within the wood industry and the majority of authors cited in the following sections refer to it (Katuščák and Kucera 2000). The colour system classifies the temperate and tropical wood species into the positive octant with the lightness (L^*) from 20 to 90, the redness index ($+ a^*$) from 0 to 20, and the yellowness index ($+ b^*$) from 10 to 30 (Janin 2001, Babiak et al. 2004,). The tropical wood species occupy a much greater portion of the colour space in comparison with temperate (for example European) species (da Silva et al. 2017, Meints et al. 2017, Vidholdová and Reinprecht 2017).

The purpose of wood modification is to improve the quality of less resistant types of wood. Modification improves the properties of wood, such as elasticity, strength or flexibility. At the same time, the modification has a positive effect on the negative properties of wood, such as wear ability and dimensional instability. The modification of wood also brings the possibility of modifying its appearance, for example its colouring. Heat-treated wood has become an established commercial product possessing a number of advantages over the natural wood. Heat-treated wood is considered an eco-friendly alternative to chemically impregnated wood materials. This treatment reduces the hydrophilic behaviour of the wood by modifying the chemical structure of its components (hemicelluloses, cellulose and lignin) which results in changes of their properties (Hill 2007, Reinprecht and Vidholdová 2011, Vidholdová et al. 2019, Sandberg et al. 2021).

The aim of the work is to analyse the colour similarity of thermally and hydrothermally modifies selected hardwoods to tropical woods using the CIE $L^*a^*b^*$ colour space.

MATERIALS AND METHODS

Hardwoods used in this study were obtained from round timber felled and further processed in Slovakia. Wood samples with dimensions of 150×15×300 mm were made by longitudinal and transverse sawing from the central lumber. The samples were without cracks, knots or other growth inhomogeneity. Eight hardwood species were: (a) heat treated under atmospheric pressure at the temperature of 200 ± 2.5 °C for 3 hours in a laboratory type heating oven (Memmert UFB 500, Germany) at Department of Wood Technology, FWST at Technical University of Zvolen or (b) hydrothermally treated with saturated water steam at the temperature of 135 ± 2.5 °C for 6 hours in a pressure autoclave AZ 240 (Himmasch AD, Haskovo, Bulgaria) installed at Sundermann s.r.o. Banská Štiavnica (Slovakia) as shown in Table 1. The heat treatment started by putting the samples at ambient temperature in oven with subsequent increasing the temperature. The period to reach treatment temperature of 200 °C was 45 minutes. Duration of heat treatment at this temperature was 3 hours. At the end of treatment, samples were cooled down in desiccators in dry environment. The other samples were hydrothermally treated with saturated water steam temperature 135 ± 2.5 °C for six hours as was described in Dudiak et al (2024).

Selected tropical woods – ipé (*Handroanthus serratifolius*), iroko (*Milicia excelsa*), maçaranduba (*Manilkara bidentata*), makoré (*Tieghemella heckelii*), sapelli (*Entandrophragma cylindricum*) and wengé (*Millettia laurentii*) in a form of naturally dried and conditioned boards in temperature 22 ± 2.5 °C and relative humidity 65% in climatic camber. It was bought from the trading company JAF Holz, Ltd., Slovakia (Table 1).

Table 1: Thermal treatment set-up

Wood species	Thermally modified (TM) 200 ± 2.5 °C for 3 hours	Hydrothermally modified (HTM) 135 ± 2.5 °C for 6 hours
Alder (*Alnus glutinosa* (L.) Gaertn),	×	×
Ash (*Fraxinus excelsior* L.)	×	
European beech (*Fagus sylvatica* L.)	×	×
Paper birch (*Betula papyrifera* Marsh)	×	×
Black locust (*Robinia pseudoacacia* L.)	×	
Hornbeam (*Carpinus betulus* L.)	×	
Norway maple (*Acer pseudoplatanus* L.)		×
Pedunculate oak (*Quercus robur* L.)	×	
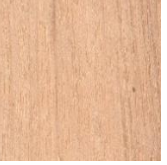
The colour measurements were performed with the Colour Reader CR-10 (Konica Minolta, Japan), having a CIE 10 standard observer, CIE standard illuminate D65, sensor head with a diameter of 8 mm. Top surface of samples were sanded with sandpaper P 180.

The MS Excel 2013 and statistical software Statistica 12 was used to analyse and present the collected data on colour parameters. Descriptive statistics deal with basic statistical characteristic (average and standard deviation), and an analysis of variance (ANOVA) - Duncan test at 0.05 significance level.

RESULTS

The colour measurements of the native surfaces of studied tropical wood species and thermally or hydrothermally treated hardwoods were summarised in Table 2. The tropical wood species differed mainly in the lightness L^*. It ranged between 34.88 (Wengé) and 64.50 (Iroko). All of the tropical wood's colour chromatic parameters a^* and b^* were in a positive sphere of distribution. The redness index $(+a^*)$ ranged from 8.00 (wengé) to 18.10 (maçaranduba), and the yellowness index $(+b^*)$ from 10.34 (wengé) to 25.32 (iroko). The results were similar to that achieved by Meints et al. (2017) or da Silva et al. (2017).

Table 2: Appearance of woods and its colour (colour coordinates - L*, a* and b*)

		Tropical wood species					
		Ipé	Iroko	Maçaranduba	Makoré	Sapelli	Wengé
L^*	Avg	42.52	64.50	45.68	49.70	53.13	34.81
	SD	0.94	5.16	1.57	1.99	1.78	1.72
a^*	Avg	8.76	8.22	18.10	11.81	13.68	8.00
	SD	0.55	0.92	1.28	0.99	0.87	0.66
b^*	Avg	16.30	25.32	14.46	18.92	18.21	10.34
	SD	1.23	2.69	0.96	0.98	0.78	1.29
		Thermally modified hardwoods					
		Ash	European beech	Paper birch	Black locust	Hornbeam	Pedunculate oak
L^*	Avg	52.62	40.74	45.99	35.05	58.88	35.19
	SD	4.83	3.86	2.23	2.66	4.96	1.37
a^*	Avg	10.39	8.78	11.15	7.47	8.56	7.47
	SD	1.87	1.17	1.46	1.87	2.19	0.82
b^*	Avg	21.87	16.59	18.45	10.23	20.54	9.94
	SD	1.65	1.85	1.58	2.56	2.08	0.86
		Hydrothermally modified hardwoods					
		Alder	European beech	Paper birch	Norway maple		
L^*	Avg	61.93	62.36	64.54	67.96		
	SD	1.94	1.79	1.86	1.61		
a^*	Avg	10.33	10.47	9.62	8.76		
	SD	0.79	0.74	0.76	0.93		
b^*	Avg	18.35	18.62	18.96	20.36		
		1.85	1.76	1.92	1.84		

Avg = Average, SD = Standard Deviation

Thermally treated selected hardwoods have the lightness L^* that ranged between 35.05 (Black locust or Pedunculate oak) and 58.88 (hornbeam). In the terms of a^* and b^* parameter, all treated hardwoods were also in the positive sphere of distribution. Their range was similar to that of tropical woods. The relationship between lightness (L^*) and the colour parameters (a^*) and (b^*) was presented in Figure 1. The distribution of thermally treated wood in the b^* - L^* space was most similar to tropical wood (Figure 1c).

However, hydrothermally treated hardwoods have lightness from 61.93 (alder) to 67.96 (Norway maple). It is clear that the variance of lightness is significantly lower. It was similarly found in the b^* - L^* or a^* - L^* space (Figures 1c, and 1d). The results were similar to that achieved by Dudiak et al. (2024).
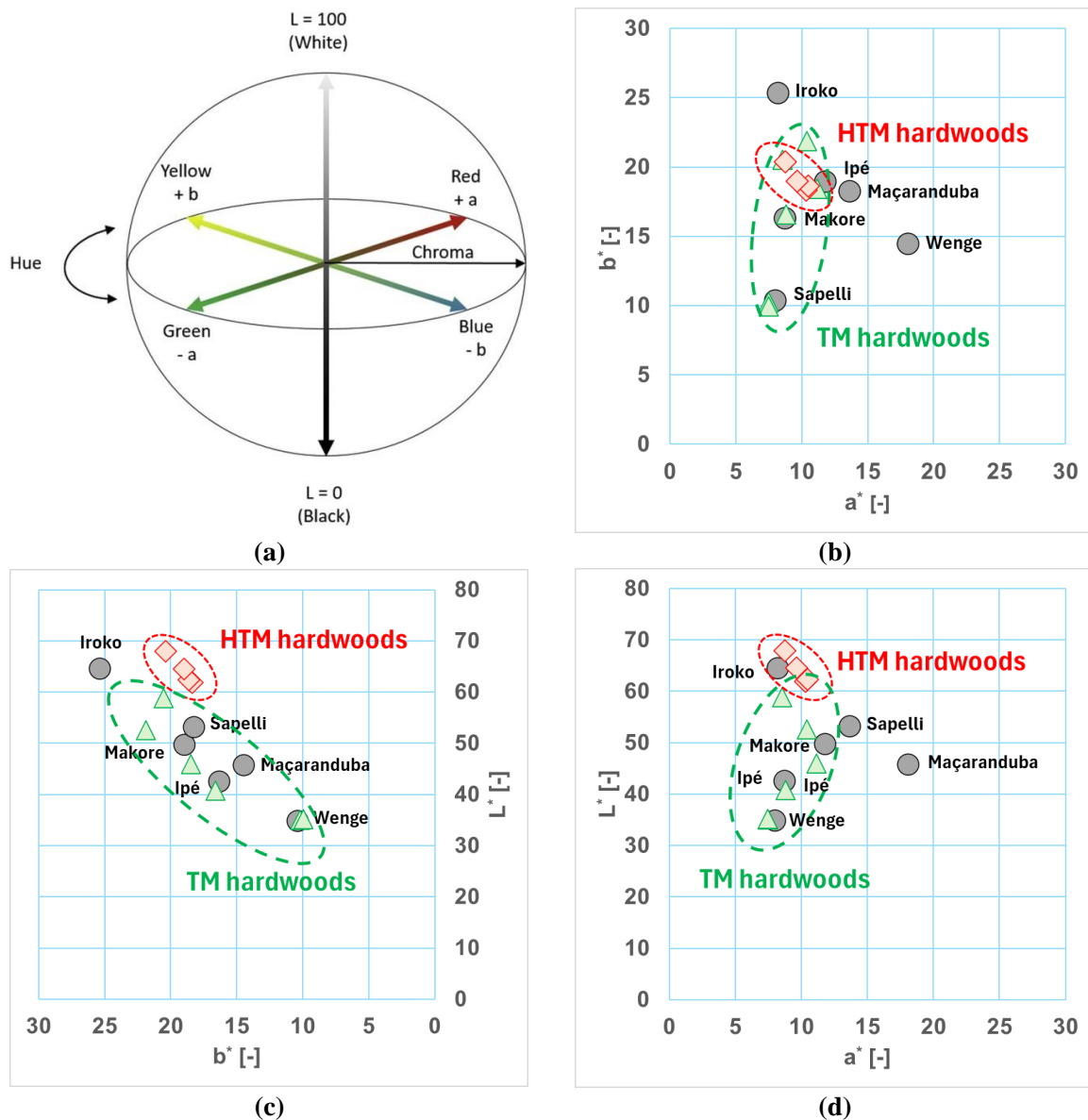
Figure 1: Colour space of selected wood species: (a) CIE Lab, (b) distribution in the colour space a^* - b^*, (c) distribution in the colour space b^* - L^*, (d) distribution in the colour space a^* - L^*. Mark: ⬤ **Tropical wood species,** △ **Thermally modified hardwoods (TM),** ◇ **Hydrothermally modified hardwoods (HTM)**

Analysis of variance and Duncan's test at the 0.05 significance level specified which colour coordinates of heat-treated woods were similar to tropical woods (Table 3). The maximum degree of colour similarity was achieved only by heat treatment at 200°C for 3 hours. Pedunculate oak or Black locust when is treated in this way; the wood will have the same colour as wengé. European beech treated also at 200°C for 3 hours has the similarity to ipé. Other variants of heat-treated hardwoods mostly provide one (or two) colour parameters similar to tropical woods.

Table 3: Results of statistical evaluations of the similarity of colour parameters between thermally treated and tropical woods

	Ipé	Iroko	Maçaranduba	Makoré	Sapelli	Wengé
TM Ash					L^*	
TM European beech	$L^*\ a^*\ b^*$	a^*				
TM Paper birch			L^*	$a^*\ b^*$	b^*	
TM Black locust						$L^*\ a^*\ b^*$
TM Hornbeam	a^*	a^*				a^*
TM Pedunculate oak						$L^*\ a^*\ b^*$
HTM Alder				b^*	b^*	
HTM European beech				b^*	b^*	
HTM Paper birch		L^*		b^*	b^*	
HTM Norway maple	a^*	a^*				

CONCLUSIONS

In recent times, a lumber import from the tropics into Slovak Republic is still high. These wood species can be also interesting for end-users by texture, colour, durability or other physical-mechanical properties. Colour is a major factor in selection of species for various engineering application, particularly in furniture, panelling, flooring material production.

The colour similarity between thermally treated and tropical woods showed that these treatments were able to modify the coloration of the wood and its colour similarity to tropical woods.

The selected two heat treatments on eight selected hardwoods showed only three similarities with tropical wood species – for European beech treated at 200°C for 3 hours - similarity to ipé and Pedunculate oak treated or Black locust treated at 200°C for 3 hours - similarity to wengé. Other variants of heat-treated hardwoods resembled tropical woods only partially. It is assumed that if the hardwoods were treated at a different temperature or duration of the process, similarity to other tropical woods would be achieved.

ACKNOWLEDGEMENTS

REFERENCES

Babiak M, Kubovský I, Mamoňová M (2004) Color space of the selected domestic species. In Interaction of Wood with Various Forms of Energy, 1st ed.; Kurjatko, S., Kúdela, J., Eds.; Technical University in Zvolen: Zvolen, Slovakia, pp 113–117.

da Silva RAF, Setter C, Mazette SS, de Melo RR, Stangerlin DM (2017) Colorimetry of wood from thirty tropical species. Ciênc. Madeira, 8, pp 36–41.

Dudiak M, Kminiak R, Banski A, Chuchala D (2024) The Effect of Steaming Beech, Birch and Maple Woods on Qualitative Indicators of the Surface. Coatings 14, 117. https://doi.org/10.3390/coatings14010117

Hill CA (2007). Wood modification: chemical, thermal and other processes. John Wiley & Sons.

Hon DN-S, Minemura N (2000) Color and discoloration. In Wood and Cellulosic Chemistry, 2nd ed.; Hon, D.N.-S., Shiraishi, N., Eds.; CRC Press: New York, USA, pp 385–442.

Janin G, Gonçalez JC, Ananías R, Charrier B, Silva GFD, Dilem A (2001) Aesthetics appreciation of wood colour and patterns by colorimetry. Part 1. Colorimetry theory for the CIE Lab system. Maderas Cienc. Tecnol. 2001, 3, 14.

Katuščák S, Kucera J (2000) CIE orthogonal and cylindrical color parameters and the color sequences of the temperate wood species. Wood Res. 45, pp 9–21.

Meints T, Teischinger A, Stingl R, Hansmann C (2017) Wood colour of central European wood species: CIE Lab characterisation and colour intensification. Eur. J. Wood Wood Prod. 75, pp 499–509.

Ortiz-Hidalgo C, Pina-Oviedo S (2019) Hematoxylin: Mesoamerica's gift to histopathology. Palo de Campeche (logwood tree), pirates' most desired treasure, and irreplaceable tissue stain. Int. J Surgical Path, 27(1), pp 4–14.

Sandberg D, Kutnar A, Karlsson O, Jones D (2021) Wood modification technologies: principles, sustainability, and the need for innovation. CRC Press.

Slabejová G, Šmidriaková M, Fekiač J (2016) Gloss of transparent coating on beech wood surface. Acta Fac. Xylologiae Zvolen, 58, pp 37–44.

Tolvaj L, Persze L, Lang E (2013) Correlation between hue angle and lightness of wood species grown in Hungary. Wood Res. 58, pp 141–145.

Vidholdová Z, Reinprecht L (2011) Thermowood Šmíra-Print, 2011.

Vidholdová Z, Reinprecht L, Iždinský J (2017) Microbial resistance of tropical woods Zvolen: Technická univerzita vo Zvolene (in Slovak)

Vidholdová Z, Sandak A, Sandak J (2019) Assessment of the chemical change in heat treated pine wood by near infrared spectroscopy. Acta Fac. Xylologiae Zvolen 61(1), pp. 31–42

High termite resistance of kempas (*Koompassia malaccensis*) hardwood protected with a novel vegetal extracts-cypermethrin wood preservative under outdoor aboveground tropical environment

Messaoudi Daouia[1*], Wong Andrew H.H.[2,3]

[1] Groupe Berkem, R&D Laboratories, 20 rue Jean Duvert, 33290 Blanquefort, France
[2] Universiti Malaysia Sarawak (UNIMAS), 94300 Kota Samarahan, Sarawak, Malaysia
[3] Presently, International Wood Culture Society (IWCS), c/- 798 Lorong Song 3C1A, Tabuan Heights, 93350 Kuching, Sarawak, Malaysia

E-mail: daouia.messaoudi@berkem.com; awong.unimas@gmail.com

Keywords: wood protection, non-biocidal additive, termite test, tropical hardwood, envelope treatment, pyrethroid, *Coptotermes curvignathus*

ABSTRACT
An environmentally-conscious society in Europe and other economically progressive regions requires that wood protecting chemicals contain lesser or lower levels of synthetic actives and be supplemented instead with bio-based ingredients to enhance the bioefficacy of the wood treatment formulations. Particular reference to the novel "Biocide 1" (proprietary Xilix7000K®) water-borne biobased formulation developed by Groupe Berkem (France), containing vegetal extracts-cypermethrin mixtures (Synerkem® Technology), was made to report the remarkable ability of such formulation to protect H3-hazard class-weathered (ie. leached and volatilized) envelope-treated tropical hardwood kempas *(Koompassia malaccensis)* against *Coptotermes curvignathus* subterranean termites representing aboveground outdoor conditions. Replicated air dried kempas test eartwood blocks brushed-on with this formulation and with the reference permethrin-based LOSP "Biocide 2", were subjected to laboratory EN84 leaching regime and then to laboratory volatilization regime (simulating long term aboveground outdoor H3-hazard class weathering exposure of treated wood) and then exposed to an innovative severe Malaysian/Australian H2-hazard class termite field test at a humid tropical test site in Sarawak, Malaysia. After 6 months exposure to termites, untreated kempas blocks were severely attacked (mean mass loss: 38.7% mean termite rating: 5.9) by termites, contrasting with those treated with the novel Synerkem® Technology (mean mass loss: 0.29%; mean termite rating: 10) and with the hazardous reference LOSP containing permethrin (mean mass loss: 0.34%; mean termite rating: 10) on an AWPA 10-point termite rating scale of 10 (sound), …, 0 (failure). These findings demonstrate the remarkable ability of such novel biobased formulation in establishing permanent protection against termites (and obviously against wood boring insects) of enveloped-treated wood structure under aboveground outdoor (and obviously indoor) conditions.

INTRODUCTION
Industrial wood protection in many developed economies of the world has evolved in accordance with regulatory requirements influenced by public perceptions seeking for cleaner environments and public health and safety issues. This has seen the decline or ban in the use of traditional wood preservatives containing heavy metals, creosote, organo-chlorines and other organo-metals as eiher water-borne or heavy oils or light organic solvent that often use pressure treatments to achieve high preservative loading into the wood (UNEP 1994, Freeman et al. 2003). Thus various novel low environmental impact wood protection strategies designed to gain acceptance for eco-friendly treated wood material involves the use of non-arsenicals, chromium-free, other non-metallics, organic-based, and bio-based, preferably water-borne wood protecting systems, chemical modification (eg. acetylation, furfurylation, DMDHEU, PF and MF resins, Sorbitol/Citric Acid) or heat treatment (Barnes 1992, Green III and Schultz 2003, Schultz and Nicholas 2003, Coggins 2008). In the use of environmentally acceptable biocides, it is desired to apply a fit-for-purpose wood treatment with low levels of biocide active which helps reduce consequent chemical wastage and environmental contamination otherwise attributed to excess use of treating solutions, and this is related to the use of envelope wood treatment technology (using simple dipping,

deluging, spray-on or brush-on) with novel water-borne formulations for long term protection of solid wood and wood composites against termites, wood boring insects and decay fungi.

A new generation water-borne bio-based wood protection system has emerged from the laboratory of Groupe Berkem (France), based in part on cypermethrin-vegetal extracts mixture (Synerkem® Technology), is developed as brushed-on envelope treatment for likely permanent wood protection in aboveground indoor (Malaysian/Australian H2-hazard class) and outdoor (Malaysian/Australian H3-hazard class) situations described by Wong (2004). This biobased formulation (Xilix® 7000K) only uses lower than usual concentration of cypermethrin found in other pyrethroid-based wood preservatives, which is offset by the enhanced bioactivity of the vegetal extracts-cypermethrin combination in the novel formulation as the polyphenolic vegetal extracts serve as booster for cypermethrin termiticidal activity. The patented Synerkem® Technology is claimed to also impart higher cypermethrin diffusion and fixation into the wood cell walls, while also providing antioxidant activity. The excellent performance of this formulation in laboratory-volatilized (representing long term H2-weathered) dip-treated tropical hardwood kempas (*Koompassia malaccensis*) against subterranean termites *Coptotermes curvignathus* in an H2-hazard class termite field test in Malaysia is recently reported (Messaoudi and Wong 2023). This paper expands on such work to report the performance of this formulation in a similar termite test on laboratory-leached-and-volatilized (representing long term H3-weathered) dip-treated wood used aboveground outdoors.

MATERIALS AND METHODS

The field trials were undertaken using an established H2-hazard class aboveground field test protocol of Wong (2005) where test treated and untreated wood block specimens were placed aboveground contact among termite-susceptible baitwood in the dark and shielded from wetting (rain, inundation) inside rectangular metal drums. These drums were sited on a peripheral humid peat swamp forest area in Kota Samarahan, Sarawak, Malaysia, where subterranean termites *Coptotermes curvignathus* are prevalent and are among the most destructive termites of wooden structures in the Southeast Asian terrestrial environment (Lee 2002, Sornnuwat et al. 1996). This H2-hazard class termite field test protocol, designed to attract termites but exclude decay fungi and wood-boring beetles, is related to the Malaysian/Australian biological hazard class selection guide (Wong 2004, Standards Australia 2005), and is also appropriate for testing H3-weathered treated wood against subterranean termites. While H3-weathered wood refers to wood exposed long term aboveground outdoors subjected to threats of termites, decay fungi and wood-boring beetles (Wong 2004, Standards Australia 2005), this test protocol involves only the termite threat. Test against other types of wood-degrading organisms require separate test protocols which are not within the scope of this study.

The popular Malaysian hardwood which is mainly the heartwood of kempas (*Koompassia malaccensis*) used as wood structures is termite-susceptible (Wong 1982, Messaoudi and Wong 2023). Replicated (n=8) air dried kempas heartwood blocks [2.5 x 4 x 5 (length) cm] were dipped for 3 minutes in nominal 0.2% permethrin-based LOSP (reference Biocide 2, Table 1) and the freshly treated wood immediately weighed in order to derive surface retention of permethrin by uptake (Table 1). Another replicate set of blocks were brushed-on with biobased Biocide 1 (candidate Xilix® 7000K, Table 1) to coat wood block surfaces, and then immediately weighed in order to derive surface retention of cypermethrin by uptake (Table 1). After air drying for at least 8 weeks, treated wood blocks were put to a 14 days leaching regime using the laboratory EN84 (1997) method, then air dried for 4 weeks before being oven dried at 40ºC for 18 days to volatilize treated wood. Untreated wood blocks were similarly leached-and-volatilized. These H3-weathered test blocks were then exposed to *Coptotermes curvignathus* using the protocol of Wong (2005) for 6 months after which the blocks were harvested, cleaned and visually rated for degree of termite attack on a 10-point AWPA scale (AWPA 2008): 10 (sound), 9.5 (trace, surface nibbles permitted), 9 (slight attack, ≤3% of cross sectional area affected), 8 (moderate attack, 3-10% of cross sectional area affected), 7 (moderately severe attack and penetration, 10-30% of cross sectional area affected), 6 (severe attack, 30-50% of cross sectional area affected), 4 (very severe attack, 50-75% of cross-sectional area affected) and 0 (failure/destroyed), and finally oven dried (105ºC) to determine percent mass loss and absolute mass loss (milligram).

Data were interrogated by One-way ANOVA using MINITAB-14 software to explore difference in termiticidal performance between wood treated with Biocide1, Biocide 2 and untreated wood, subjected

to before-test H3-weathering, for mean termite rating, mean percent mass loss and mean absolute mass loss by Least Significant Difference t-test (LSD, P<0.05).

Table 1: Partial composition of candidate biobased Biocide 1 and reference Biocide 2

Wood preservative	Nominal composition [%g/g]	Application	Mean retention of pyrethroid*		
			[%g/g]	{g/cm²}	[g/cm³]
Biocide 1 (Xilix® 7000K) - water-based	Cypermethrin [0.16%] Tebuconazole {0.08%] Polyphenolic vegetal extracts [2%]	Brush-on	0.0046 (0.0007)	0.16 (0.02)	29.48 (3.13)
Biocide 2 (Reference LOSP) - white spirit	Permethrin [0.2%] Tributyltin naphthenate [1.8%] Dichlorofluanid [0.1%]	Dipping 3 minutes	0.0051 (0.0043)	0.18 (0.13)	32.15 (23.95)

cypermethrin (Biocide 1) and permethrin (Biocide 2); ( )= std dev.

RESULTS AND DISCUSSION

Variance ratios from one-way ANOVAs for the response variables termite rating, percent mass loss and absolute mass loss (mg) comparing termiticidal performance of kempas treated with Biocide 1, Biocide 2 and untreated kempas, all H3-weathered after wood treatment or untreated, are shown in Table 2. Significant F-values (P<0.05) indicates that for each response variable, there is at least one mean value the differs significantly from among the 3 mean values (of Biocide 1, Biocide 2 and untreated wood).

Table 2: Significant variance ratios (F-values) from One-way ANOVA exploring differences between Biocide 1, Biocide 2 and untreated wood for mean values of each termite attack parameter

Termite attack parameter	F-value
Termite rating	50.48 s
Mass loss [%g/g]	17.96 s
Absolute mass loss [mg]	17.34 s

s: significant (P<0.05)

Table 3: Mean values of termite attack parameters comparing 2 treated and 1 untreated kempas heartwood blocks, all post-treated H3-weathered

Treatment	Mass loss [%g/g]	Absolute mass loss [mg]	Termite rating
Untreated, - H3-weathered	38.7 (25.7)	12054 (8119)	5.9 (1.6)
Biobased Biocide 1 - Surface-treated with cypermethrin/vegetal extracts combination, - H3-weathered	0.29 a (0.06)	92.2 a (15.2)	10 a (0)
Biocide 2 - Surface-treated with LOSP containing permethrin, - H3-weathered	0.34 a (0.09)	111.4 a (32.0)	10 a (0)
LSD values	15.39	4874.9	1.0

LSD values used for comparison within-column mean values: within-column means sharing same letter denotes that mean values do not differ at P<0.05 sig. level; n=8; ( ) denotes standard deviation

Differences in termiticidal performance between untreated and treated kempas are evident in Table 3 using LSD multiple comparison t-test statistics (P<0.05) where untreated wood was clearly attacked by C. curvignathus compared with the termite-resistant envelope-treated counterparts regardless of termite attack parameter evaluated. Untreated H3-weathered kempas was obviously termite-susceptible (mean mass loss 38.7%, mean absolute mass loss 12054 mg, mean termite rating 5.9) as reported recently (Messaoudi and Wong 2023) while both H3-weathered treated counterpart materials were completely termite resistant (Biocide 1-treated wood: mean mass loss 0.29%, mean absolute mass loss 92.2 mg,

mean termite rating 10; Biocide 2-treated wood: mean mass loss 0.34%, mean absolute mass loss 111.4 mg, mean termite rating 10).

Despite imposing a severe (EN84) leaching regime along with evaporative ageing volatilization regime (altogether representing severe wood weathering aboveground outdoors under H3-hazard class situation), imposed on treated kempas blocks before termite test, the pyrethroid actives of Biocide 1 and Biocide 2 remain in the wood to confer high termite resistance. The water-based Biocide 1 performed as well against C. curvignathus as the reference Biocide 2 LOSP product, while the latter is being discouraged in the marketplace worldwide due to the negative environmental impact of light organic solvent (white spirit) in the formulation. The former product therefore provides a safer alternative to LOSPs. The high termiticidal efficacy of Biocide 1 is perceived to be attributed to the influence of the non-biocidal additive polyphenolic vegetal extracts (2% of the product), developed as patented Synerkem® Technology from Groupe Berkem (France), which boosts the bioactivity of low concentrations of cypermethrin (0.16% of the product). Synerkem® Technology employing polyphenolic vegetal extracts apparently enhance the fixation and penetration of cypermethrin into wood cells walls (Ruel et al. 2015) despite enduring a laboratory H3-weathering regime. Furthermore, plant- or wood-based polyphenols have been found to impart antioxidant activity on wood-degrading organisms as component of biocides, hence attracting much interest and speculation about the, hitherto less understood, mechanism of biochemical action of polyphenol additive in termite protection of treated wood (Schultz et al. 2008, Joseleau et al. 2022, Joseleau et al. 2023). Since enzymic digestion of lignocellulosic wood substrate involves the activity of termite gut microbiota, it is hypothesized that antifeedant and toxic activities of polyphenolic vegetal extracts may involve their characteristic antioxidant and free radical-scavenging abilities and metal chelation properties which prevent free radical lignin attack by termites, hence would disrupt the symbiotic efficiency of termite gut microbiota to consume wood lignocellulosic substrate as a food source, essentially depriving termites from attacking wood (Joseleau et al. 2023). it is intended that the effectiveness of non-biocidal polyphenolic vegetal extracts component in Biocide 1 formulation would thus allow reduction in concentrations of synthetic active substances (cypermethrin, tebuconazole) in the formulation to yield a more environmentally-friendly wood protecting chemical, without sacrificing product bioefficacy. Thus this novel biocide, as with two new-generation biobased pyrethroid microemulsion formulations that showed equally high termite resistance of treated kempas (Messaoudi et al. 2020) are notable examples of refreshing innovations in wood protection strategies that are "kind" to the environment and consumers of treated wood.

CONCLUSIONS

Biocide 1 represents formulations that help promote a greener and healthier society. Overall it is established that the novel environmentally-friendly Biocide 1 biobased formulation provided excellent protection of H3-weathered (including H2-weathered) envelope-treated hardwood kempas against *Coptotermes* subterranean termites (and obviously wood-boring beetles too). Incorporating non-biocidal vegetal extracts in wood protecting chemicals such as Biocide 1 maintained a high termite resistance of treated kempas at reduced concentration of cypermethrin unlike the relatively higher pyrethroid (and azoles) concentrations adopted in traditional water-borne or LOSP formulations elsewhere which makes the latter formulations less environmentally desirable.

REFERENCES

AWPA (2008) American Wood Protection Association (AWPA). Standard method of evaluating wood preservatives by field test with stakes. American Wood Preservers' Association Standard E7-07, Book of Standards. Birmingham, Alabama, USA.

Barnes HM (1992) Wood protecting chemicals for the 21st century. Proceedings IRG Annual Meeting (ISSN 2000-8953), International Research Group on Wood Protection, Doc. No: IRG/WP 93-30018, 30 pp.

Coggins CR (2008) Trends in timber preservation - global perspective. Journal of Tropical Forest Science 20:264-272.

EN84 (1997) European Committee for Standardization. Wood preservatives - Accelerated ageing of treated wood prior to biological testing - Leaching procedure. European Standard EN84:1997, 4 pp.

Freeman MN, Shupe TF, Vlosky RP, Barnes HM (2003) Past, present and future of the wood preservation industry. Forest Products Journal 53:8-15.

Green-III F, Schultz TP (2003) New environmentally-benign concepts in wood protection: the combination of organic biocides and non-biocidal additives. In: Goodell B, Nicholas DD, Schultz TP (eds) "Wood deterioration and preservation: advances in our changing world", ACS Symposium Series No: 845, American Chemical Society, Washington, DC, USA, pp 378-389.

Joseleau JP, Messaoudi D, Chopinet F, Cardia JD, Ruel K (2022) Plant polyphenolic extracts as natural pesticides for wood protection treatments. American Wood Protection Association: 118th AWPA Meeting, Charleston, South Carolina, USA, June 2022, 6 pp.

Joseleau JP, Messaoudi D, Ruel K (2023) How the biochemical activities of polyphenols may be effective for the protection of wood deterioration by termites? Proceedings IRG Annual Meeting (ISSN 2000-8953), International Research Group on Wood Protection, Doc. No: IRG/WP 23-30789, 10 pp.

Lee CY (2002) Subterranean termite pests and their control in the urban environment in Malaysia. Sociobiology 40:3-10.

Messaoudi D, Wong AHH (2023) A novel wood preservative with plant extracts in a cypermethrin mixture protects envelope-treated tropical kempas hardwood against *Coptotermes* termites when exposed to an above-ground indoor situation after evaporative ageing. Bois et Forêts des Tropiques 358:7-14.

Messaoudi D, Wong AHH, Tawi CAD, Bourguiba N, Fahy O (2020) Permanent aboveground protection from termite attack on weathered envelope-treated kempas heartwood with patented cost-effective biobased pyrethroid microemulsion solutions. In; Nemeth R, Radermacher P, Hansmann C, Bak M, Bader M (eds) 9th Hardwood Conference Proceedings - Part 1 (An underutilized resource: hardwood oriented research), Online 24-25 June 2021, University of Sopron Press, Sopron, Hungary, 2020, pp 175-182.

Ruel K, Tapin-Lingua S, Messaoudi D, Fahy O, Jequel M, Petit-Conil M, Joseleau JP (2015) Probing biocide penetration and retention in wood products by immunolabelling techniques. In: Gurau L, Campean M, Ispas M (eds) Proceedings 10th International Conference on Wood Science and Engineering (ICWSE) in the third millennium, Transylvania University, Braasov, Romania, pp 211-217.

Schultz TP, Nicolas DD (2003). A brief review of non-arsenical wood preservative systems. In: Goodell B, Nicholas DD, Schultz TP (eds) "Wood deterioration and preservation: advances in our changing world", ACS Symposium Series No: 845, American Chemical Society, Washington, DC, USA, pp 420-432.

Schultz TP, Ragon K, Nicholas DD (2008). A hypothesis on a second non-biocidal property of wood extractives, in addition to toxicity, that affects termite behavior and mortality. Proceedings IRG Annual Meeting (ISSN 2000-8953), International Research Group on Wood Protection, Doc. No: IRG/WP 23-30789, 14 pp.

Sornnuwat Y, Tsunoda K, Yoshimura T, Takahashi M, Vongkaluang C (1996) Foraging populations of Coptotermes gestroi (Isoptera: Rhinotermitidae) in an urban area. Journal of Economic Entomology 89:1485-1490.

Standards Australia (2005) Specification for preservative treatment. Part 1: Sawn and round timber. AS1604.1-2005. Standards Australia, Sydney, New South Wales, Australia.

UNEP (1994) Environmental aspects of industrial wood preservation - a technical guide. United Nations Environmental Programme, Technical Report Series No:20.

Wong AHH (2004) A novel Malaysian biological hazard class selection guide. Newsletter of Malaysian Wood Preserving Association (MWPA) 8(17): pp 8-9.

Wong AHH (2005) Performance of two imidacloprid-treated Malaysian hardwoods in an accelerated aboveground termite test. Proceedings IRG Annual Meeting (ISSN 2000-8953), International Research Group on Wood Protection, Doc. No: IRG/WP 05-30389, 9 pp.

Wong TM (1982) A dictionary of Malaysian timbers. Malayan Forest Records No:30, Forest Department Peninsular Malaysia, Kuala Lumpur, Malaysia, 259 pp

Comparison of wood properties of pedunculate oak and non-native northern red oak from an anthropogenic site

Aleš Zeidler[1,*], Vlastimil Borůvka[1]

[1] Czech University of Life Sciences Prague, Faculty of Forestry and Wood Sciences, Department of Wood Processing and Biomaterials. Kamýcka 129, Prague, Czech Republic, 165 00.

E-mail: zeidler@fld.czu.cz; boruvkav@fld.czu.cz

Keywords: *Quercus rubra*, wood, density, strength

ABSTRACT
A considerable part of the north-western part of the Czech Republic is occupied by former brown coal mines. After the end of mining activities, these areas were often afforested. A wide range of species, both native and mainly introduced species from other continents, were used. It is therefore a unique habitat, allowing comparison of wood quality of such tree species that do not occur naturally together. In this study, we investigated selected wood properties of two different oak species from an afforested former mine in the Czech Republic area. The native oak species, *Quercus robur* L., was compared with the North American oak species, *Quercus rubra* L., on the basis of wood density and compressive strength. The aim of this study was to assess the extent to which this North American species is a suitable alternative to the native oak species in terms of wood replacement for applications. Higher value for wood density was achieved by the native oak species (*Q. robur*) compared to that of the non-native oak species (*Q. rubra*). In the case of compressive strength along the grain these two oak species obtained similar values. Nevertheless, the differences were not striking in terms of applications. The position in the stem, in horizontal direction, did not have significant impact on the evaluated properties and both species behaved similarly from this point of view. Compared to other studies, the reached values are higher for wood density. For compressive strength, the results are similar to those reported by other authors. The results of our research suggest that both oak species represent a suitable choice for the reclamation of anthropogenically influenced sites in terms of timber quality. Northern red oak, which is non-native to Europe, but often used for this type of site, provides timber of comparable quality to native oak species.

INTRODUCTION
Historically, northwestern part of the Czech Republic is typical for occurrence of brown coal mines. After the cessation of mining activities, mostly at the end of 20th century, those vast areas underwent extensive reclamation. One of the ways of such activities was afforestation. Wide range of tree species, both native to the Czech Republic species and species coming from other geographic areas, was used. The afforested former mines so represent an exceptional opportunity to compare tree species that are never growing together naturally. The comparison should be focused not only on a growth or production, but also on the quality of produced timber.
Quercus is one of the genera that was widely used for reclamations (Kupka and Dimitrovský 2006). It was confirmed by Bažant (2010) that oaks, namely pedunculate oak (*Quercus robur* L.) and northern red oak (*Quercus rubra* L.) are suitable species for the reclamation of such sites. Oak represents one of the most important hardwoods in the Czech Republic, occupying about 7.8% of forest area (Ministry of Agriculture 2023). It is also leading species in terms of wood quality. Thanks to its durability, high strength and hardness, and of course an attractive appearance, oak timber is used for many applications, especially flooring, furniture and constructions (Wagenführ 2007). Northern red oak is a species that is not native to the Czech Republic and it occurs naturally in North America. It is a fast growing tree species (Burns and Honkala 1990), which was introduced to Czech Republic at the end of 18ᵗʰ century. In the Czech Republic it is primarily used for land reclamations (Hejný and Slavík 1990). Currently, norther red oak occupies negligible area in the country and information on wood quality is missing.
Wood quality is something that is related to applications and can differ depending on a way of wood utilisation (Barnett and Jeronimidis 2003). Wood density is one of the frequent quality indicators as it

covers most of the criteria from industry. Wood density is influencing mechanical properties and some of physical properties. It is therefore often used as a strength predictor (Tsoumis 1991). Compressive strength is one of mechanical properties important for wood utilisation, especially in building constructions (Kollmann 1951). Although it is supposed to be correlated to density (Niemz and Sonderegger 2003), such relationship should be verified, as wood is variable in structure and consequently in properties. This variability can be revealed not only among species, individual trees, but even within one individual (Genet *et al.* 2013, Zobel and Van Buitenen 1989).

This paper deals with an issue of afforested former coal mine in the Czech Republic and its potential to produce raw material for industry. It compares two different oaks, native pedunculate oak and American northern red oak. The comparison is based on difference between the tested species in wood density and compressive strength along fibres. The variability of the tested properties within a stem, in radial directions, and an effect of wood density on compressive strength is evaluated.

MATERIALS AND METHODS

The testing material presented in this paper was obtained from research plots at afforested former brown coal mine "Větrák", northwestern part of the Czech Republic. The mine afforestation started in 1962, using various kinds of tree species, including non-native species as *Quercus rubra*. Representatives of sample trees for *Q. rubra* and *Q. robur* were felled, three for each species. According to Bažant (2010), the age of trees was about 35 years. The height of the felled trees ranged from 13.5 to 16 m, and the stem diameter varied from 21.5 to 27.5 cm at the breast heigh.

Sections, 1,2 m long, representing the stem basal area, were taken from each sample tree. Central board was cut from each section and used to produce standardised test specimens (20 x 20 x 30 mm – radial x tangential x longitudinal). The position of the specimens in the board was recorder, in order to evaluate radial variability of the tested properties in the stem. Wood density (12% MC) and compressive strength along fibres were assessed following national standards (ČSN 49 0108, ČSN 49 0110). The ANOVA and Duncan's multiple-range tests were applied to reveal differences among the evaluated factors. A significance level of 95% was used for all statistical analyses. The linear regression model was applied to evaluate the dependence of compressive strength on wood density.

RESULTS AND DISCUSSION
Wood density

Wood density is higher in *Q. robur* (771 kg.m⁻³), the native oak species, in contrast to American *Q. rubra* (733 kg.m⁻³). The difference between oak species is statistically significant, but from a view of applications is not so striking. Generally, the variability of the property is considerably low, even if the coefficient of variation is two times higher in the case of *Q. robur* compared to *Q. rubra*. More detailed statistical description is given in Table 1.

Table 1: Wood density [kg.m⁻³] comparison of the tested species

Species	Mean	Minimum	Maximum	Standard Deviation	Coefficient of Variation
Quercus robur	771	673	980	50	6.5
Quercus rubra	733	634	820	27	3.7

If the wood density distribution along stem radius is the concern, no clear trend was revealed. The property is nether growing, nor decreasing with increasing distance from the stem centre. If any differences among individual positions, there are not statistically significant. From this point of view wood density is more or less the same in the stem irrespective of position.

Comparing the results to values reported in literature for the tested oak species, obtained wood quality from such site is satisfying. Alden (1995) reported 705 kg.m⁻³ for *Q. rubra* in native areas. Similar value 700 kg.m⁻³ is presented by Wagenführ (2007). Even better result was obtained for native *Q. robur* as Wagenführ (2007) provides only 690 kg.m⁻³ for this species.

Compressive strength

Even in the case of compressive strength the value is higher for *Q. robur* (56.2 MPa), compared to *Q. rubra* (55.3 MPa). Nevertheless, the difference between oak species is less than 1 MPa. It is not only insignificant statistically, but also irrelevant from the view of wood utilisation. The variability of the property is low for both species. More detailed statistical description is given in Table 2.

Table 2: Compressive strength [MPa] comparison of the tested species

Species	Mean	Minimum	Maximum	Standard Deviation	Coefficient of Variation
Quercus robur	56.2	41.2	75.0	5.4	9.6
Quercus rubra	55.3	33.5	63.8	3.4	6.2

Compressive strength is showing mild increase with growing distance from the stem centre (Figure 1). However, when comparing individual positions, the statistical analysis did not reveal any significant differences and similarly to wood density, the within-stem position is not playing important role in terms of wood quality.
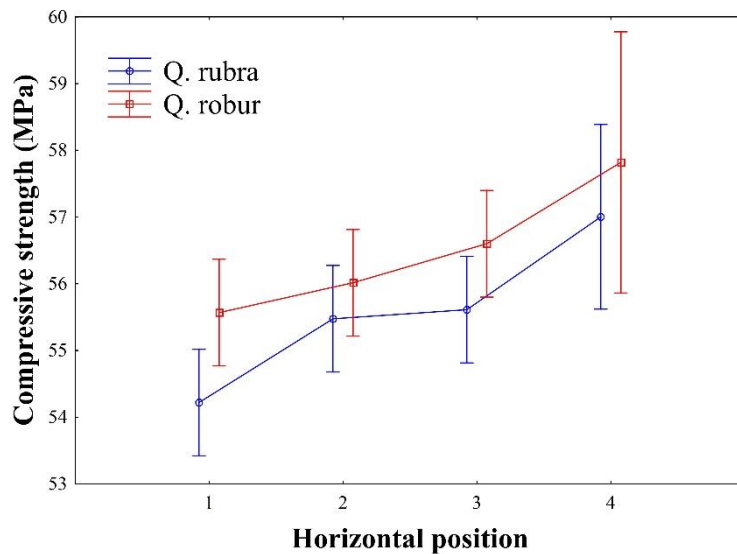
Figure 1: Compressive strength distribution within a stem (x-axis: Figures represent a relative position of the specimen, i.e., 1 is the position near the pith, 4 is the position close to the cambium)

Wood density is affecting to great extent most of mechanical properties and could be used for wood strength estimation. Figure 2 is showing linear regression model that is describing correlation between compressive strength and wood density for *Q. robur*. Although the correlation is not the strong one, it is apparent that the strength is growing with increasing wood density. In the case of *Q. rubra* the correlation was not so strong.

Figure 2: Dependence of compressive strength on wood density in Quercus robur

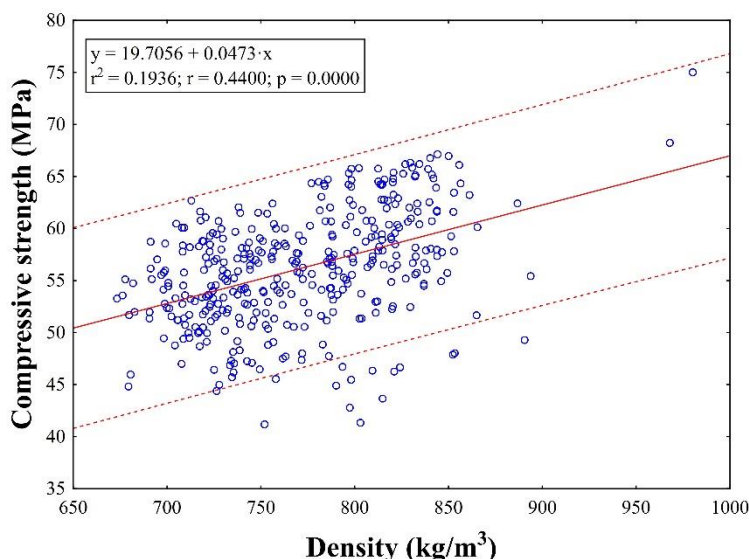Obtained results for compressive strength are similar to those mentioned in a literature, 39 – 61 MPa for *Q. rubra* and 54 – 67 MPa for *Q. robur* in Wagenführ (2007). The compressive strength for *Q. rubra* from Czech Republic is so higher than value 46.61 MPa reported for American native areas by Alden (1995).

CONCLUSIONS

Afforested former brown coal mines in the Czech Republic represent a unique manmade site. They have potential to produce timber for industry. In this study we confirmed that two different oak species, one native to the region and one species introduced from North America, can produce comparable high-quality timber. We tested wood density and compressive strength. Native *Q. robur* reached higher values for both, wood density and compressive strength. However, especially in the case of compressive strength, the results are comparable, and both species could be used for the same purposes from this point of view. Variability of the tested properties is low, only little affected by the position in a stem. The results for compressive strength are similar to those reported in another studies, in the case of wood density even higher for both oak species.

REFERENCES

Alden HA (1995) Hardwoods of North America. U.S. Department of Agriculture, Forest Products Laboratory, Madison, WI, USA

Barnett JR, Jeronimidis G (2003) Wood Quality and its Biological Basis. Blackwell Publishing, Oxford, UK

Bažant V (2010) Růstové vlastnosti dřevin na výsypkových stanovištích Mostecké pánve (Growing characteristics of tree species from reclaimed coal mines of Most basin). Ph.D. Dissertation, Czech University of Life Sciences, Prague, Czech Republic (in Czech)

Burns RM, Honkala BH (1990) Silvics of North America, Volume 2. Hardwoods. U.S. Department of Agriculture, Forest Service, Washington, DC, USA

ČSN 49 0108 (1993) Drevo. Zisťovanie hustoty (Wood. Determination of the density). Czech Normalisation Institute, Prague, Czech Republic (in Czech)

ČSN 49 0110 (1980) Drevo. Medza pevnosti v tlaku v smere vlákien (Wood. Compression strength limits parallel to the grain). Office for Standardization and Measurement, Prague, Czech Republic (in Czech)

Genet A, Auty D, Achim A, Bernier M, Pothier D, Cogliastro A (2013) Consequences of faster growth for wood density in northern red oak (*Quercus rubra* Liebl.). Forestry, 86:99–110. https://doi.org/10.1093/forestry/cps057

Hejný S, Slavík B (1990) Květena České Republiky 2 (Flora of the Czech Republic 2). Academia, Praha, Czech Republic (in Czech)

Kollmann F (1951) Technologie des Holzes und Holzverkstoffe, Volume 1. Springer-Verlag, Berlin, Germany

Kupka I, Dimitrovský K (2006) Silvicultural assessment of reforestation under specific spoil bank conditions. Journal of Forest Science 52(9):410-416

Ministry of Agriculture (2023) Zpráva o stavu lesa a lesního hospodářství ČR v roce 2022 (Report on the State of Forest and Forestry in the Czech Republic 2022). Ministry of Agriculture, Prague, Czech Republic (in Czech)

Niemz P, Sonderegger W (2003) Untersuchungen zur Korrelation ausgewählter Holzeigenschaften untereinander unt mit der Rohdichte unter Verwendung von 103 Holzarten. Schweizerische Zeitschrift fur Forstwesen 154(12):489-493. https://doi.org/10.3188/szf.2003.0489

Panshin AJ, De Zeeuw C (1980) Textbook of Wood Technology, 4th ed. McGraw Hill, New York, USA

Remeš J, Šíša R (2007) Biological activity of anthropogenic soils after spoil-bank forest reclamation. Journal of Forest Science 53(7):299-307

Tsoumis G (1991) Science and Technology of Wood – Structure, Properties, Utilization. Chapman and Hall, New York, USA

Wagenführ R (2007) Holzatlas. Fachbuchverlag, Leipzig, Germany.

Zobel BJ, Van Buitenen JP (1989) Wood Variation, its Causes and Control. Springer-Verlag, Berlin, Germany

Acoustic Parameters of Pioneer Wood Species

Petr Horák[1]*, Vlastimil Borůvka[1]

[1] Department of Wood processing and Biomaterials, Faculty of Forestry and Wood Sciences, Czech University of Life Sciences, Prague, Czechia

E-mail: horakp@fld.czu.cz

Keywords: sound, acoustic radiation, acoustic wave resistance, preparatory wood

ABSTRACT
This work deals with the analysis of the acoustic properties of pioneer wood species such as birch, rowan, alder, poplar, and willow. The acoustic properties analyzed in this paper include acoustic radiation and acoustic wave resistance. Ultrasonic method was used for these measurements. The results of method employed indicate that pioneer wood species could serve as an alternative for producing parts of musical instruments and loudspeaker enclosures, as it was the production of baffles from these wood species that was emphasized in the related research. However, the price of commonly used wood species has been rising in recent years, creating an opportunity to explore the potential of often underestimated pioneer wood species. Not only are these woods fast-growing, providing a more cost-effective manufacturing option, but they also offer unique and distinctive wood textures, sometimes thanks to their defects. Taking birch as an example, one of the most well-known pioneer wood species, it exhibits high values in acoustic constants and acoustic wave resistance. In some cases, it may outperform commonly used wood species for musical instruments, such as maple. Based on the measured values, recommendations are derived for the use of selected woods in the music industry and audio technology.

INTRODUCTION
In our daily lives, sound is everywhere, often experienced through speaker systems. For some, sound isn't just routine; it's a profession, a way of life, or a passionate pursuit. This connection with sound extends beyond electronics to musical instruments, where wood plays a crucial role, much like it does in speaker enclosures (Toumpanaki 2021). This paper delves into the acoustic qualities of pioneer wood types and discovers if they could be used in these interconnected realms.

MATERIALS AND METHODS
This methodics aims to elucidate critical acoustic parameters through the evaluation of pertinent test samples. The parameters of interest encompass the acoustic constant, which delineates the fundamental acoustic behavior and acoustic wave resistance, characterizing the medium's response to sound transmission. This meticulous examination and measurement process serves as a foundation for unraveling the intricate acoustic properties and fundamental principles governing sound propagation and resonance (Nasir et al. 2019).

<u>Measurement of physical and mechanical properties of wood</u>
The primary objective in the examination of these materials is to determine the aforementioned acoustic parameters. Simultaneously, the density of the samples will be established, as well as the speed of sound propagation and dynamic modulus of elasticity. This comprehensive analysis encompasses the critical acoustic attributes and material characteristics, enabling a holistic understanding of the acoustic behavior and structural properties within the tested materials.

<u>Measuring the time of passage of an ultrasonic wave</u>
The testing is conducted on specimens measuring 20 x 20 x 300 *mm* (height x width x length). The measurement system employed is the FAKOPP Ultrasonic Timer, comprising two piezoelectric probes along with the device itself, as illustrated in *Figure 1*. Operators manually position the probes on the surface of the specimen, initiating an ultrasonic pulse to start the timing process. The ultrasonic wave must traverse the material until it reaches the second probe, at which point the time measurement concludes.

The value of the speed of sound wave passage through wood is crucial information that can be utilized to determine many wood properties (Roohnia 2016). However, this parameter can be influenced by several factors, as described by various authors. Gerhards (1982) summarized that wave speed changes with fiber deviation, moisture, temperature, wave frequency, and amplitude. It has also been demonstrated that speed correlates with elasticity moduli and density. These relationships form the foundation for determining strength characteristics and receive significant attention (Bucur, 2006).

The speed of ultrasonic wave passage can be calculated using formula (*1*).

$$c = \frac{l}{t-k} \ [m/s] \tag{1}$$

where *l* is probe distance [*m*], *t* is time of wave passage [*s*] and *k* is correction required for the probe's zero-distance [*s*].

These parameters collectively contribute to the calculation of the dynamic modulus of elasticity (*E*) using formula (*2*).

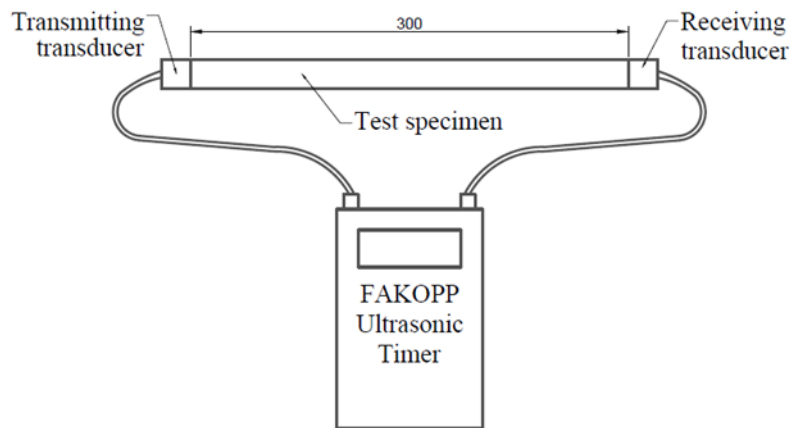$$E = c^2 \cdot \rho \ [Pa] \tag{2}$$

Figure 1: Measuring apparatus of the ultrasonic method

Determination of acoustic constant and acoustic wave resistance
The resistance of the medium to a planar sound wave is referred to as acoustic wave resistance. It involves internal friction induced by the material, which is greater in wood than in metals. This parameter is primarily influenced by the density and speed of sound propagation (Horáček 2008).
Since the value of the dynamic modulus of elasticity is already known, it is possible to determine the value of the acoustic constant K_A, which can be expressed by formula (*3*):

$$K_A = \sqrt{\frac{E}{\rho^3}} \ [m^4/kg \cdot s] \tag{3}$$

where *E* is the dynamic modulus of elasticity [*Pa*], *ρ* the density of the material [*kg/m³*].
Since we know all the necessary variables, we can determine the value of the acoustic wave resistance *Z* using the formula (*4*)

$$Z = \rho \cdot c = \rho \cdot \sqrt{\frac{E}{\rho}} \ [kg \cdot m^{-2} \cdot s^{-1}] \tag{4}$$

RESULTS AND DISCUSSION

In *Figure 2*, it is clear that birch wood achieves the highest values of acoustic wave resistance at 34.3 $(kg.m^{-2}.s^{-1}).10^{-5}$, while poplar wood shows the lowest values of 22.0 $(kg.m^{-2}.s^{-1}).10^{-5}$. Alder with values of 22.8 $(kg.m^{-2}.s^{-1}).10^{-5}$ does not exceed poplar statistically significantly, while willow and rowan stand in the middle of the spectrum at 25.6 $(kg.m^{-2}.s^{-1}).10^{-5}$ respectively 25.3 $(kg.m^{-2}.s^{-1}).10^{-5}$, they are statistically significantly higher than poplar but lower than birch.

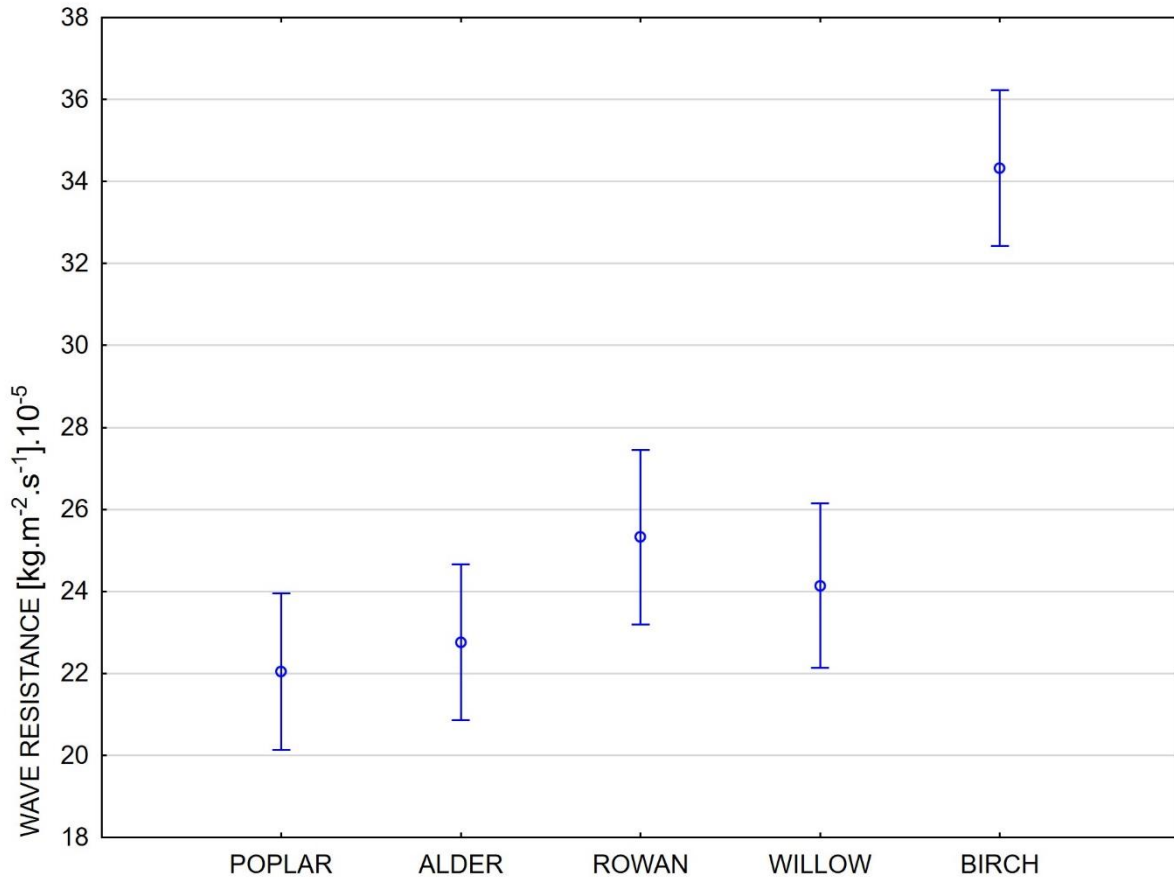*Figure 2: Acoustic wave resistance of pioneer wood species*

Table 1: Acoustic wave resistance

WOOD SPECIES	AVERAGE VALUE	MIN.	MAX.	STANDARD DEVIATION
POPLAR	22.0	19.4	26.5	2.0
ALDER	22.8	20.8	25.5	1.5
ROWAN	25.3	22.2	28.4	2.4
WILLOW	25.6	19.0	29.2	3.7
BIRCH	34.3	31.0	36.5	2.1

In *Figure 3*, it's apparent that poplar wood surprisingly exhibits the highest values of the acoustic constant (9.5 $m^4.kg^{-1}.s^{-1}$), likely owing to its relatively high measured densities. Birch wood, in comparison, demonstrates slightly lower values at 8.6 $m^4.kg^{-1}.s^{-1}$, which is for example higher than maple (Horák et al. 2023). Other preparatory woody species fall within the range of 7.3 to 8.2 $m^4.kg^{-1}.s^{-1}$ for the acoustic constant. Notably, despite this, the values achieved by these preparatory woods are considerable, significantly surpassing those of plywood or medium-density fibrous boards. Consequently, their potential applications, such as in the construction of musical instruments or speaker enclosures, cannot be dismissed, mainly for more cost-effective alternatives.
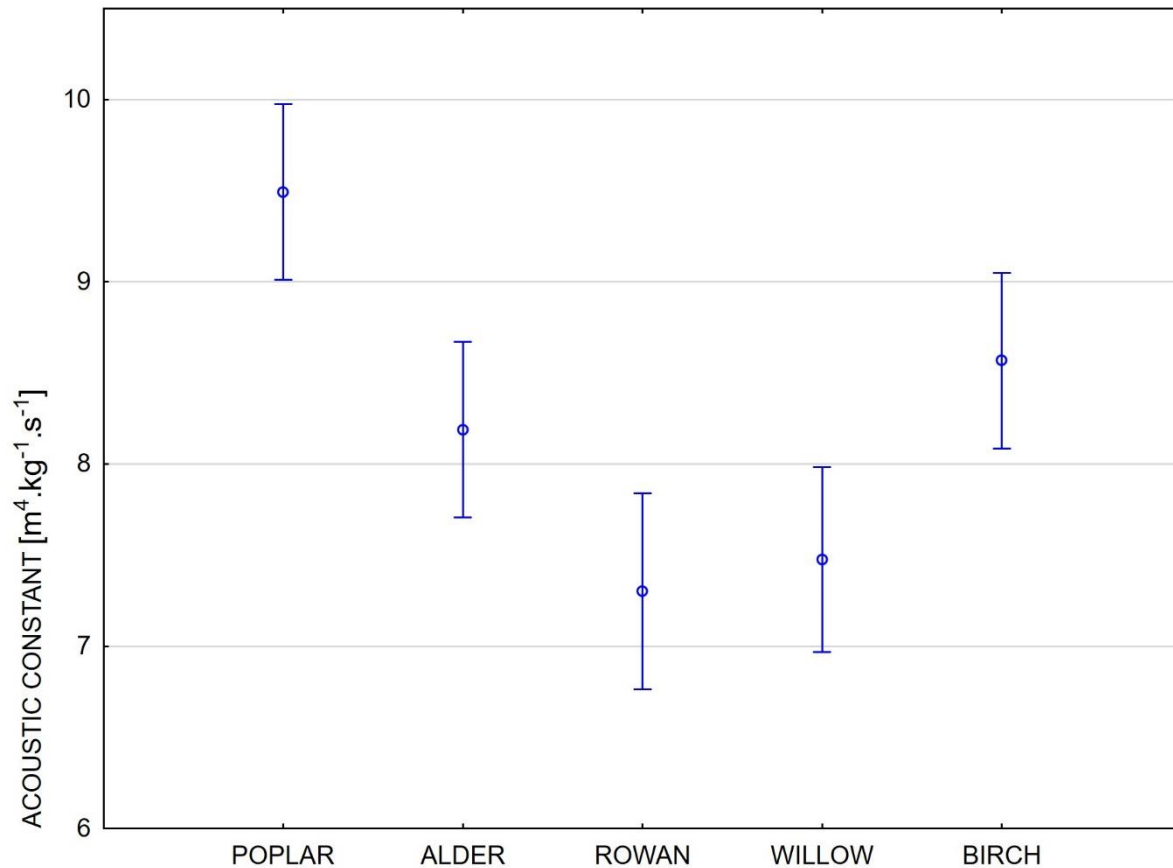
Figure 3: Acoustic radiation constant of pioneer wood species

Table 2: Acoustic radiation constant

WOOD SPECIES	AVERAGE VALUE	MIN.	MAX.	STANDARD DEVIATION
POPLAR	9.5	8.3	10.7	0.8
ALDER	8.2	7.0	8.9	0.7
ROWAN	7.5	6.4	8.7	1.0
WILLOW	7.3	5.5	8.5	0.9
BIRCH	8.6	8.3	8.9	0.2

CONCLUSIONS

The results of comparing the acoustic properties of pioneer wood species show that birch and poplar reach the highest values of acoustic radiation. Both of them achieved higher values than for example maple, which is widely used for making musical instruments (Kozel 2021). All these results are consistent with existing literature.

Poplar and birch appear to be a promising alternative not only for musical instruments but also as a suitable material for constructing speaker enclosures. The choice of enclosure shape, eventually complemented by acoustic filling to mitigate diffraction effects, plays a significant role in this context (Newell et al. 2007, Hardwood et al. 1977). The potential of pioneer woods opens avenues for further research, not only in the realm of acoustics but also from broader perspectives.

ACKNOWLEDGEMENTS

REFERENCES

Bucur, V. 2006. Acoustic of wood. Berlin: Springer- Verlag. Springer series in wood science, 2006. 393 s. ISBN 3-540-26123-0.

Fakopp Enterprise Bt. 2019. Fakopp Localization Page. Fakopp Bt - UltraSonic Timer. [Online] 2019. [Cite: 06. 11 2021.] https://fakopp.com/en/product/ultrasonic/

Gerhars, C. C. 1982. Longitudinal stress waves for lumber stress grading: factors affecting applications: state of the art. Forest Products Journal (USA). 1982, 32.

Hardwood, H. D., Mathews, R. 1977. Factors in the design of loudspeaker cabinets. BBC Research Department. Engineering Division, 1977, 3.

Horáček, P. 2008. Fyzikální a mechanické vlastnosti dřeva, (Physical and mechanical properties of wood) 2008 I. Mendelova zemědělská a lesnická univerzita v Brně.

Horák, P. Borůvka, V. Novák, D. Acoustic Parameters of Birch Wood Compared to Maple Wood and Medium Density Fibreboard. In: Unleashing The Potential of Wood-based Materials. Zagreb:Faculty of Forestry and Wood Technology, University of Zagreb, Croatia, 2023, s. 75-82, 978-953-292-083-3.

Kozel, Jan. 2021. Analýza akustických parametrů ozvučnic reproduktorů na bázi dřeva, (Analysis of the acoustic parameters of wood-based speaker enclosures) [Diploma thesis] Prague 2021, Czech University of Life Sciences, Prague, Czechia, Department of Wood processing and Biomaterials, Faculty of Forestry and Wood Sciences

Nasir, V., Nourian, S., Avramidis, S. and Cool, J., 2019. Stress wave evaluation by accelerometer and acoustic emission sensor for thermally modified wood classification using three types of neural networks. European Journal of Wood and Wood Products, 77, pp.45-55.

Newell, P., Holland, K. 2007. Loudspeakers: for music recording and reproduction. Oxford: Focal Press, 2007.

Roohnia, M. 2016. Wood: Acoustic Properties. Reference Module in Materials Science and Materials Engineering. 10. 1 2016.

Toumpanaki, E., Shah, D.U. and Eichhorn, S.J., 2021. Beyond what meets the eye: Imaging and imagining wood mechanical–structural properties. Advanced Materials, 33(28), p.2001613

Determination of Elastic Parameters of Birch and Oak Wood Using Optical Method

David Novák[1]*, Vlastimil Borůvka[1], Petr Horák[1], Tomáš Kytka[1]

[1] Department of Wood processing and Biomaterials, Faculty of Forestry and Wood Sciences, Czech University of Life Sciences, Prague, Czechia

E-mail: novakdavid@fld.czu.cz; boruvkav@fld.czu.cz; horakp@fld.czu.cz; kytkat@fld.czu.cz

Keywords: Birch, oak, anisotropy, modulus of elasticity, Poisson's ratio.

ABSTRACT

This work analyses the elasticity modulus and Poisson's ratios of birch (*Betula pendula* Roth) and oak (*Quercus robur* L.) wood. The elastic parameters of wood were determined through compression tests, and the deformations were measured using optical methods. The results were compared with those of other authors. As expected, different values of elastic moduli and Poisson's ratios were observed for oak and birch wood depending on the directions of application (L, R, T) of the loading force. Furthermore, in this work, differences were investigated depending on whether this deformation was sensed by the optical method or by contact methods that have been used in other studies. The elastic moduli for birch wood were higher when loaded in the axial direction (L). A higher modulus of elasticity was observed for oak wood in both the radial and tangential loading directions. Short-term static loading cycles in the elastic region of the material did not affect the determination of Poisson's ratios. No statistically significant difference was found between cycles. This work addresses the suitability or differences in using a particular method for strain sensing and leads to a targeted extension of the wood elastic parameter database.

INTRODUCTION

The development of new materials and technologies has also led to the development of new testing equipment and methods, both for the specification of the basic mechanical, physical, and chemical properties of various materials and for the determination of the quantitative characteristics of substances, including material constants. Testing machines and equipment of various designs are used to create external force loads on the material, which allow different types of stresses (tension, compression, bending, torsion) to be induced, and the actual test procedure (trajectory, time, force, resulting stress) to be recorded. Although these test machines allow recording of deformations, the resulting values can differ significantly from reality. This can be caused by many factors, i.e. contact between the loading head and the material, tolerances in the clamping device, indentation of the loaded material into the supports, etc. In some types of tests these nuances may be negligible, but not, when determining material constants of wood on small test samples.

Nowadays, there are many ways to determine the material constants of wood or to sense the resulting deformations under load. In the last few decades, these parameters have been measured primarily by mechanical or electrical measuring devices and systems, such as mechanical strain gauges, various types of strain gauges, and contact extensometer systems (Davis, 2004). Furthermore, methods based on the propagation of acoustic waves in the material, such as acoustic microscopy (AM), resonant ultrasound spectroscopy (RUS), resonance method (RM), and the standard ultrasound method using the direct pulse technique, are also used to detect some material constants (Dackermann et al. 2016; Gao et al., 2016). Nowadays, non-contact techniques have become more widely used to measure and acquirethe resulting deformations on the loaded sample, using optical methods such as video extensometer, laser extensometer, and a relatively new optical technology based on 3-D high-speed camera recording (Crespo et al., 2017). Increasingly, wood and wood-based materials are being tested where it is necessary to observe deformation only in a specific area of tested material, at elevated temperatures, or in multiple directions simultaneously. Some research works deal with hypotheses, of which it is necessary to know how the resulting deformations or stresses are redistributed in the investigated element when it is loaded by external forces. Based on these facts, in recent years, despite the high purchase price, optical methods

for sensing deformations on the tested material have been increasingly used. This relatively new technology for sensing emergent deformations is based on the use of cameras or combinations of cameras and lasers, i.e., video extensometer, laser extensometer, or 3D video extensometer (Požgaj et al., 1993; Bovik, 2005 Wolverton; et al., 2009; Pop et al., 2013; Gao et al., 2016; Crespo et al., 2017).

MATERIALS AND METODS

The production of the test samples was in accordance with the ČSN 49 0101 (1980) standard. The samples were made from logs of deciduous trees, whichwere obtained from the the school forestry enterprise of the Czech University of Life Sciences in Kostelec nad Černými Lesy (Czech Republic). Silver birch (*Betula pendula* Roth) was selected from the representatives with scattered porous wood structures and European oak (*Quercus robur* L.) from the representatives with ring porous wood structures. These logs were cut longitudinally into eight sections and then air-dried. Once this was achieved, the individual segments were manipulated into prisms with the requirement to maintain the orthogonal geometry of the individual basic directions in the wood *L* (longitudinal), *R* (radial), and *T* (tangential). The prisms were then cross cut into individual test samples with dimensions of $50 \times 50 \times 50$ mm. In this way, 202 test samples were made from birch wood and 180 from oak wood. Throughout the production process, the flawlessness of the samples was monitored, as well as their continuity (consecutive parallelism), which guaranteed the elimination of errors with respect to the heterogeneity of the wood. Subsequently, the moisture content of the prepared samples was adjusted using a ClimeEvent C/2000/40/3 air-conditioning chamber (Weiss Umwelttechnik GmbH, Reiskirchen, Germany). The air temperature in the air-conditioning chamber was controlled at 20 ± 2 °C with a relative humidity of 65 ± 5 %. The material constants of the wood were determined using compression tests on Instron 8802 test equipment (Instron® - Division of ITW Ltd., High Wycombe, United Kingdom). The servo-hydraulic machine was equipped with a spherical pressure plate. For deformation sensing, an Instron 2663-901 optical video extensometer (Instron® - Division of ITW Ltd., Nortwood, MA, USA) with a scanning rate of 490 Hz was used, and the signal was sensed using a strain card with a scanning rate of 10 kHz/24bit and processed using Bluehill software (Instron® - Division of ITW Ltd., Nortwood, MA, USA).

Deformation sensing

The deformations were detected by displacement of the marked points on the surface of the test sample. Points were marked at distance 10 mm to each side from the cross-field node. The node of the cross-field was in the imaginary centre of symmetry of the square surface of the sample. The loading of the samples was carried out in the *L*, *R*, and *T* directions. The deformations were monitored during loading, as shown schematically in Figure 1.
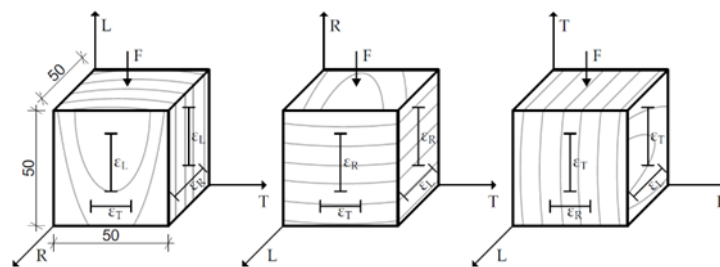
Figure 1: Schematic representation of the loading of the test samples in each direction

Determination of material constants

The method for determining the material constants of wood was partly based on the procedure given in ČSN 49 0111 (1992). When loading the samples, a proportional force (*Fp*) was applied such that the "linear" region of the stress-strain diagram, in which wood behaves to some extent as an elastic material, was not exceeded. The force was determined based on indicative tests on test samples of the same selection and the actual testing was performed since this force was determined for a particular wood species. The testing consisted of continuously loading the test sample to *Fp* for a time interval of 30 s.

Then the loading force was lowered to 800 N in the same time interval. Subsequently, the entire cycle was repeated three times, with a lower force limit of 1000 N in these subsequent cycles. Deformations were recorded at the lower and upper limits of the force of these cycles, from which the Poisson´s ratio was subsequently determined according to Equation 1:

$$\mu = \frac{\varepsilon_y}{\varepsilon_x} \ [-] \tag{1}$$

where ε_y [-] is the relative deformation in the transverse direction and ε_x [-] is the relative deformation in the loading direction. In addition, the elastic moduli EL, ET, and ER were determined on all the samples according to Equation 2:

$$E_i = \frac{\sigma_i}{\varepsilon_i} \ [MPa] \tag{2}$$

where σ_i (MPa) is the stress in the relevant direction i and ε_i (-) is the relative deformation for the relevant loading direction i. The relative deformation is expressed by Equation 3:

$$\varepsilon = \frac{\Delta l}{l_0} \ [-] \tag{3}$$

where Δ_l (mm) is the relative elongation and l_0 (mm) the original dimension of the test sample.

Data evaluation
Data and results of the investigated properties were processed in graphical and tabular form using STATISTICA Version 13.4.0.14 (TIBCO Software Inc., USA). Basic descriptive statistics, multivariate ANOVA and Tukey's test were used in this program. A uniform significance level of $\alpha = 0.05$ was used for all statistical analyses.

RESULTS AND DISCUSSION
Figure 2 shows in graphical form the individual Poisson's ratios [μ] depending on which sample plane (*LR*, *LT*, *RT*, *TL*, *RL*, *TR*) they were determined from. Next, the observed Poisson's ratios in individual cycles (cycles 1-3) are shown in the corresponding planes.
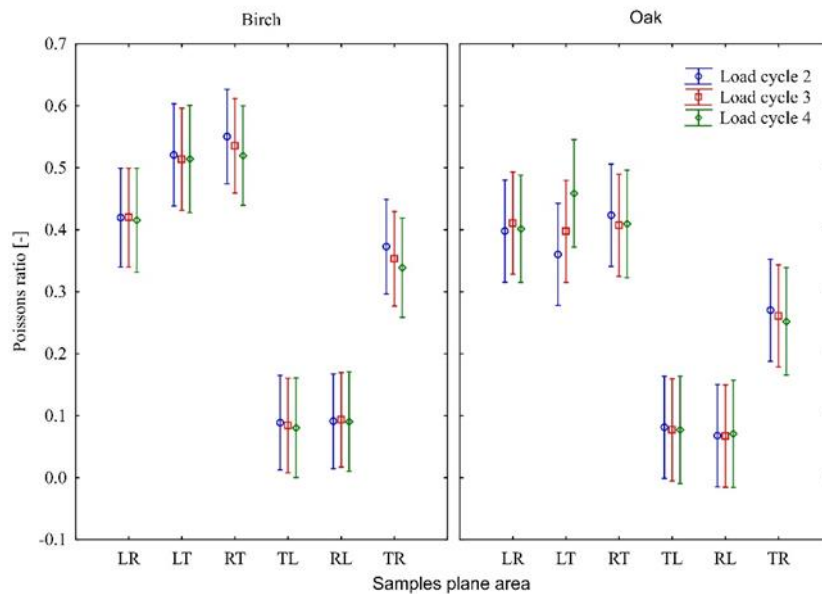

Figure 2: Graphical representation of Poisson's ratios in individual planes and cycles

The figure shows that birch wood reached the highest values in the *RT* plane in the second cycle with an average value of 0.55. Bodig and Jayne (1982) report a value for μ_{RT} of 0.697, which is higher than

the value found in this paper, but the authors do not state what method was used for the determination. In the case of μ_{LR}, an average value of 0.42 was found for birch wood across all cycles, which is identical to the value reported by Bodig and Jayne (1982). In the other planes, they report the following values for μ_{LT} (0.451), μ_{TR} (0.426), μ_{RL} (0.043), and μ_{TL} (0.024), which are slightly different values than those found in this research, but the trends of values between planes are similar. The observed average values of Poisson's ratios in individual planes and cycles are shown in Table 1.

Table 1: Basic descriptive statistics of Poisson's ratios

Samples plane area	Load cycle	Poisson´s ratios [-]									
		Birch					Oak				
		N	Average	Min.	Max.	SD	N	Average	Min.	Max.	SD
LR	2	32	0.42	0.02	1.01	0.30	30	0.40	0.02	1.03	0.29
	3	32	0.42	0.01	1.02	0.31	30	0.41	0.03	1.32	0.33
	4	32	0.42	0.01	1.05	0.30	30	0.40	0.02	1.19	0.31
LT	2	30	0.52	0.02	1.15	0.35	30	0.36	0.01	1.21	0.33
	3	30	0.51	0.03	1.16	0.33	30	0.40	0.04	1.04	0.31
	4	30	0.51	0.02	1.23	0.35	30	0.46	0.02	1.85	0.42
RL	2	35	0.09	0.00	0.68	0.13	30	0.07	0.00	0.19	0.05
	3	35	0.09	0.00	0.63	0.12	30	0.07	0.00	0.19	0.05
	4	35	0.09	0.00	0.65	0.12	30	0.07	0.00	0.19	0.05
RT	2	35	0.55	0.01	1.21	0.28	30	0.42	0.05	0.95	0.20
	3	35	0.54	0.00	1.17	0.28	30	0.41	0.08	0.94	0.21
	4	35	0.52	0.01	1.16	0.28	30	0.41	0.08	0.98	0.22
TL	2	35	0.09	0.00	0.66	0.12	30	0.08	0.00	0.75	0.13
	3	35	0.08	0.00	0.58	0.11	30	0.08	0.00	0.74	0.13
	4	35	0.08	0.00	0.44	0.09	30	0.08	0.00	0.76	0.14
TR	2	35	0.37	0.02	1.39	0.23	30	0.27	0.05	0.56	0.11
	3	35	0.35	0.01	1.37	0.22	30	0.26	0.04	0.48	0.11
	4	35	0.34	0.00	1.35	0.22	30	0.25	0.03	0.52	0.11

It can be seen from the graphical representation that the values in the individual cycles of the respective planes are almost identical. A higher difference is observed only for oak wood in the case of the *LT* plane, which could be due to a hidden defect in the sample or a slight deviation of the wood fibres. However, after conducting a post-hoc analysis of multiple comparisons via Tukey's test, no statistically significant difference was confirmed between the cycles of the respective plane in either case. Aydin and Aydin (2016) investigated material constants of Sessile oak wood (Quercus petraea Liebl.). For the determination, they used small test samples of $20 \times 20 \times 60$ mm, which were loaded in compression. A bi-axial extensometer was used for deformation sensing. In the individual planes, they determined the following Poisson's ratio values μ_{LR} (0.498), μ_{LT} (0.461), μ_{RL} (0.069), μ_{RT} (0.578), μ_{TL} (0.057), μ_{TR} (0.714). The value of the *RL* plane is almost identical to the value found in this paper; however other determined values slightly differ. The trend in the values of the respective planes is similar except for the *TR* plane, where Aydin and Aydin (2016) report a value almost 0.5 higher than that reported in this paper. This could be caused by using different sample sizes and methods for acquiring deformation. It is highly unlikely that this is due to a different oak species, as Ross et al. (2010) reports Poisson's number values in their respective planes for red and white oak wood. Their findings are almost identical and with a similar trend to that reported in this paper. The method for deformation sensing in this paper shows relatively high variability in values than those reported by Aydin and Aydin (2016) in their paper, but the average values found are similar to those of the other authors.

Figure 3 shows graphically the individual compressive elastic moduli in the respective planes (*L*, *R*, *T*). The highest average modulus of elasticity (17 797 MPa) was determined for birch wood when loaded

in the longitudinal direction, in contrast, oak wood average modulus of elasticity was 38% lower than that of birch wood. However, the opposite trend was observed in the transverse loading directions (*R*, *T*). In the radial direction of loading, the modulus of elasticity of oak wood was 60% higher compared to birch wood and 10% higher in the tangential direction. These differences are mainly due to the very different anatomical structures of oak and birch wood (thickness of wood rays, size and thickness of vessels, length of wood fibres, proportion of libriform fibres, the proportion of tracheae, etc.).
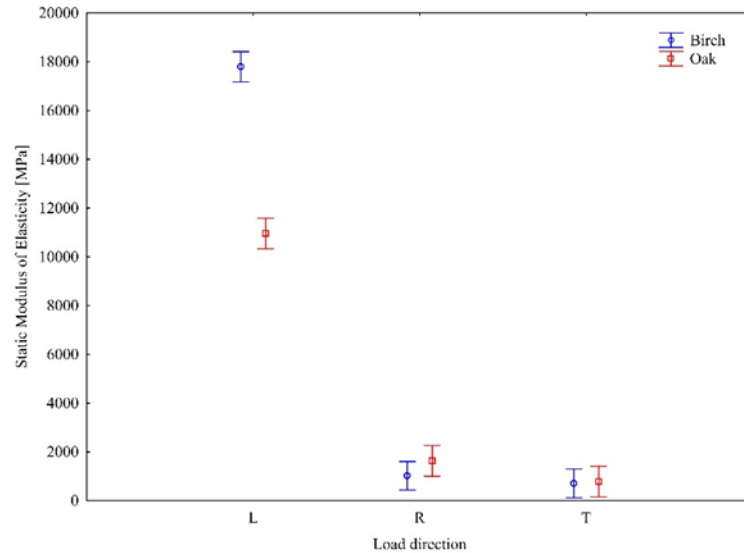

Figure 1:Graphical representation of the compressive elastic moduli in the respective loading directions

Detailed results of the compressive modulus of elasticity in each loading direction are given in Table 2.

Table 2: Basic descriptive statistics of compressive elastic moduli

| Load direction | Static Modulus of Elasticity [MPa] | | | | | | | | | |
| | Birch | | | | | Oak | | | | |
	N	Average	Min.	Max.	SD	N	Average	Min.	Max.	SD
L	62	17797	8097	33504	5227	60	10954	4991	21018	3253
R	70	1020	451	2201	373	60	1633	516	3298	557
T	70	708	286	1984	356	60	782	402	2040	294

The compressive modulus of elasticity perpendicular to the grain is rarely reported for individual wood species, and the database for some wood species is very limited. The values of elastic moduli in the different loading directions of birch and oak wood reported by Ross et al. (2010) differ considerably from the values determined in this paper. Also, Jiang et al. (2014) determined the compressive modulus of elasticity parallel to the grain for oak wood (7 830 MPa), which is considerably different from the values we found. The difference could be influenced by the different dimensions of the sample and sensing the deformation only from the piston of the machine. Also, Aydin and Aydin (2016) determined the compressive elastic moduli of oak wood in all loading directions (*L*, *R*, *T*), but their results are significantly different from the values found in this work.

CONCLUSION
In this paper, a new method for the determination of Poisson's ratios was presented. The average values determined by this method are, with slight variations, identical to those reported by other authors and show the same trend but a higher degree of variability than reported by other authors in their papers. Short-term static loading cycles in the elastic region of the material did not affect the Poisson's ratios. Using the method, the elastic modulus values determined were in almost all cases significantly different

from those reported by other authors. This will be further investigated by comparing differences and variability between the optical and contact methods on identical samples.

ACKNOWLEDGEMENTS

REFERENCES
AYDIN, T. Y., GÜNTEKIN, E., AYDIN, M. Effects of heat treatment on some orthotropic mechanic properties of oak (quercus petraea) wood. In: *1st International Mediterranean Science and Engineering Congress (IMSEC 2016)*. Çukurova University, Congress Center. 2016, 2996-3003, Paper ID:772.

BODIG, J., JAYNE, B. A. *Mechanics of wood and wood composites*. New York: Van Nostrand Reinhold Company, 1982. 712 s. ISBN 0-442-00822-8.

BOVIK, A. C. (2010). *Handbook of image and video processing*. Academic press, 2005. ISBN 978-0-12-119792-6.

CRESPO, J., AIRA, J. R., VÁZQUEZ, C., GUAITA, M. Comparative Analysis of the Elastic Constants Measured via Conventional, Ultrasound, and 3-D Digital Image Correlation Methods in Eucalyptus globulus Labill. *BioResources*. 2017, **12**(2), 3728-3743. ISSN 1930-2126.

ČSN 49 0101. Drevo. *Všeobecné Požiadavky na Fyzikálne a Mechanické Skúšky (Wood. General Requirements for Physical and Mechanical Testing);* Office for Standardization and Measurement: Prague, Czech Republic, 1 January 1980.

ČSN 49 0111 Drevo. *Metoda Zjišťovania Modulu pružnosti v Tlaku Podél Vláken (Method for determining the Modulus of Elasticity in Compression Along the Fibers);* Office for Standardization and Measurement: Prague, Czech Republic, 1 June 1992.

DACKERMANN, U., ELSENER, R., LI, J., CREWS, K. A comparative study of using static wood. *Construction and Building Materials*. 2016, 102, 963-976. DOI: 10.1016/j.conbuildmat.2015.07.195.

DAVIS, J. R. ed. *Tensile testing*. Ohio: ASM international, 2004. ISBN 9781615030958.

GAO, Z., ZHANG, X., WANG, Y., YANG, R., WANG, G., WANG, Z. Measurement of the Poisson's ratio of materials based on the bending mode of the cantilever plate. *BioResources*. 2016 **11**(3), 5703-5721. ISSN 1930-2126.

JIANG, J., LU, J., ZHOU, Y., ZHAO, Y., ZHAO, L. (2014). Compression strength and modulus of elasticity parallel to the grain of oak wood at ultra-low and high temperatures. *BioResources*. 2014, **9**(2), 3571-3579. ISSN 1930-2126.

POP, O., DUBOIS, F., ABSI, J. J-integral evaluation in cracked wood specimen using the mark tracking method. *Wood science and technology*. 2013, **47**(2), 257-267. DOI: 10.1007/s00226-012-0488-5.

POŽGAJ, A. Elastické konštanty topoľového dreva – *Populus marilandica*. *Drevársky výskum*. 1972, **17**(3), 165-173.

ROSS, R. ed. *Wood Handbook: Wood as an Engineering Material; General Technical Report FPL-GTR-190*. USA, WI, Madison: CreateSpace Independent Publishing Platform, 2010. 508 s. ISBN 9781484859704.

WOLVERTON, M., BHATTACHARYYA, A., KANNARPADY, G. K. Efficient. flexible, noncontact deformation measurements using video multi-extensometry. *Experimental Techniques*. 2009, **33**(2), 24-33. DOI: 10.1111/j.1747-1567.2008.00370.x

Preliminary study on climate change impacts on annual wood growth development in Hungary

Péter Farkas[1]*, Zsolt György Tóth[1], Huba Komán[2]

[1] Bajcsy-Zs. u. 4, 9400 Sopron, Hungary, University of Sopron
[2] Fővám tér 8, 1093 Budapest, Hungary, Corvinus University of Budapest

E-mail: farkaspeter@phd.uni-sopron.hu

Keywords: climate change in Hungary, aridity index, FAI, dendroclimatology, annual growth, latewood

ABSTRACT
The density of wood is closely related to its mechanical properties such as hardness, strength and elasticity of wood. To estimate some of these properties, one only needs to analyse the growth rings and related density data of wood. The density and growth rings have a close connection with climatic data. Based on climate change scenarios, it could be possible to prepare estimates for wood properties during the climate change period. For forestry climate simulation, the Forestry Aridity Index (FAI) was developed which can be specially applied to Hungary for estimating changes in wood species habitats under climate change scenarios. Several methods use statistical procedures to model past climatic data using the genetic properties of the tree species and annual ring data. It is also possible to simulate annual growth development based on climate data, but we do not know which wood properties will be affected by climate change in Hungary. Furthermore, research is being conducted to find the answer to this question.

INTRODUCTION
Wood anatomy overview
The xylem primarily consists of prosenchymatous, elongated and parenchymatous, brick-shaped cells. Important prosenchymatous cell types in hardwoods include tracheas (also called vessels), libriform fibers, separate fibers, fiber-tracheids, vasicentric tracheids, and vascular tracheids; in conifers, these include fiber-tracheids, vertical tracheids, strand tracheids, and ray tracheid cells. Important parenchymatous cell types in hardwoods are strand parenchyma, fusiform parenchyma, crystalliferous cells, epithelial cells, and ray cells; in conifers, they are vertical parenchyma, epithelial cells, and ray parenchyma cells (Schweingruber 1996, p. 67). The annual ring structure results from the intermittent activity of the vascular cambium in trees within the temperate zone (Molnár et al. 2007, pp. 68–69). In the spring, when the cambium activates, it produces parenchymatic cells and vessels (only in hardwoods) as well as tracheids with large lumens and thin-walled fiber cells — this forms the earlywood. Later, as summer and autumn progress, the cambium continues to produce parenchymatic cells, and the vascular area decreases with narrower-lumen vessels (only in hardwoods), along with thick-walled fiber and tracheid cells — this is the latewood. During the winter, the cambium enters dormancy. (Schweingruber 1996, p. 67; Molnár et al. 2007, pp. 68–69). The annual ring boundary is formed between the latewood and earlywood. Outside the temperate zone, in subtropical and tropical areas, the growth ring often does not correspond to the annual ring because the cambium's activity is cyclical, influenced by wet and dry periods (Molnár et al. 2007, pp. 68–69). Schultz (2005) identifies nine climatic ecozones on Earth that exhibit seasonal cambial rhythms (Schmitt et al. 2023, pp. 58–59).
Prosenchymatous cells are primarily responsible for water conduction and structural strength. In earlywood, these cells live for a few weeks, while in latewood, they can survive for a few months. This type of cell has the ability to adapt to the climate over its lifespan, reflecting the impact of environmental events. Parenchymatous cells, on the other hand, can live for several years and typically have thickened cell walls regardless of age; thus, they do not retain climatic information (Schweingruber 1996, p. 67). In the temperate zone, the earlywood and latewood can be visually distinguished in ring-porous species and some conifers. They can be separated under a microscope in semi-ring-porous or semi-diffuse-porous species and are hard to differentiate with any equipment in diffuse-porous species. Table 1 summarizes the main identification markers for earlywood and latewood in trees from the temperate zone. Earlywood

has a lower density than latewood, making the percentage of latewood within an annual ring important both technically and from the perspective of timber utilization (Molnár et al. 2007, p. 69).

Table 1: Earlywood and latewood identification marks in temperate zone trees

Tree	Earlywood identification marks	Latewood identification marks
Softwoods (conifers)	- thin-walled tracheids with shorter lengths - visibly lighter colour (in multiple species)	- thick-walled tracheids with greater lengths - Mork's criterion: in the latewood, the double tracheid cell wall thickness $\geq$ lumen[1] - visibly darker colour (in multiple species)
Ring-porous hardwoods	- the diameters of the vessels are clearly larger and arranged in a circle along the annual ring[2] - fiber cells are thin-walled	- the diameters of the vessels are clearly small and not follow the line of the annual ring[2] - fiber cells are thick-walled
Semi-ring and semi-diffuse porous hardwoods	- the transition between earlywood and latewood is continuous - the diameter of vessels decreases continuously from earlywood to latewood - the frequency of vessels decreases continuously from earlywood to latewood - there is a visible colour transition from lighter to darker between earlywood and latewood - fiber cell diameter decreases and cell wall thickness increases in a continuous transition from earlywood to latewood	
Diffuse-porous hardwoods	- the transition between earlywood and latewood is continuous - in some species, the diameter of vessels decreases slightly from earlywood to latewood (e.g., beech) - in some species, the frequency of vessels decreases from earlywood to latewood (e.g., common alder) - a visible colour transition from lighter to darker between earlywood and latewood is rare - in a continuous transition from earlywood to latewood, the diameter of fiber cells slightly decreases and cell wall thickness increases	

Own adapted table, based on sources: [1](Denne 1989), [2](Molnár et al. 2007, p. 54-55), (Schmitt et al. 2023, pp. 58–59).

Figure 1 schematically represents the relationship between tracheid cell wall thickness, radial diameters, and wood density in the annual rings of conifers (Cuny et al. 2014, p. 1232). In Figure 1, the schematic cells could also be interpreted representing the lumen area in the case of hardwood cells. For conifers, changes in annual ring width are primarily determined by the earlywood, with less variability in the latewood. In contrast, for ring-porous hardwood trees, the variability in annual ring width is determined by the latewood, because the width of the earlywood is almost constant (approximately 0.4 to 0.6 mm in Hungary). For example, the outstanding strength characteristics of black locust *(Robinia pseudoacacia)* are primarily related to the high percentage of latewood, which can reach up to 85%. The typical density$_{(MC12\%)}$ is 770 kg/m^3, porosity is 52%, fiber cell wall volume is 68%. For similar densities, the high fiber cell wall volume is responsible: 86% in the case of sessile oak *(Quercus petraea)* and Turkey oak *(Q. cerris)* which have a 60–80% latewood percentage, and also in European beech *(Fagus sylvatica)* which has an 89% fiber cell wall volume, 55% porosity, and typical density$_{(MC12\%)}$ value is 720 kg/m³. In the case of native and hybrid poplars *(Populus spp.)* the fiber cell wall is thin, with a volume of 50–60%, and the porosity can reach a high rate of 75%, resulting in a low density$_{(MC12\%)}$ that ranges from 360 to 490 kg/m³, with an typical value of 400 kg/m³ (Molnár et al. 2007).
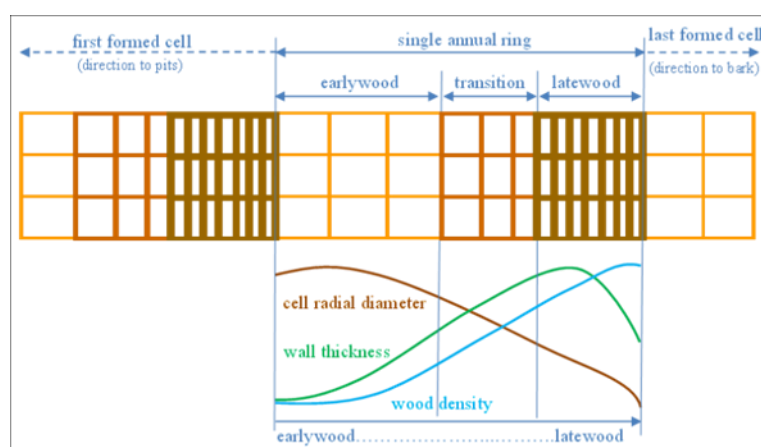

Figure 1: Relationship between tracheid cell wall thickness, radial diameters, and wood density in the annual rings of conifers. Adapted from Cuny et al. (2014).

"The density of wood is directly related to the ratio of cell wall thickness to cell diameter, meaning that the overall density depends on the proportion of thin-walled earlywood to thick-walled latewood." (Sandberg et al. 2023, p. 1839) The density of wood is closely related to mechanical properties such as hardness, strength, and elasticity. Based on this, estimating some properties may only require analysing the growth rings and related density data of the wood (Molnár et al. 2007, p. 68). The density and growth rings have a close connection with climatic data, according to Schweingruber (1996). This means that, based on climate change scenarios, it could be possible to prepare estimations of wood properties for the period affected by climate change.

Climate change and important wood species of Hungary

The current forested area in Hungary comprises 21% of the country's total land area. As of 2022, the economically most important tree species and their respective percentages of forest area are as follows: oak *(mainly: Q. robur, Q. petraea)* at 21.0 %, Turkey oak *(Q. cerris)* at 11.6%, beech *(F. sylvatica)* at 6.1%, hornbeam *(C. betulus)* at 5.2%, black locust *(R. pseudoacacia)* at 24.4%, hybrid and native poplars *(Populus spp.)* at 10.5%, softwood *(mainly: P. sylvestris, P. nigra)* at 9.4%. In 2022, the total living tree resource was 408,091,878 m³. The total annual growth and total annual timber logging amounted to 12,937,847 m³ and 7,343,656 m³, respectively (National Land Centre 2024). The forested area in Hungary is increasing. The National Forest Strategy aims to achieve a 27% forested area by 2050 (Ministry of Agriculture 2016). This goal is important both economically and ecologically. Climate change affects the forest, and monitoring this process requires the application of improved forestry climate models.

From a forest hydrology and life cycle perspective in Hungary, the period from November to April is marked by water accumulation, dormancy, and early growth. The most critical period for water consumption, vitality, and organic matter production is between May and August, when the evapotranspiration rate is high, and the forest is very sensitive to extreme weather conditions. July and August are particularly crucial, as these are arid and hot months when growth diminishes. In the concluding period, from September to October, growth gradually ceases, and the focus shifts physiologically to seed production and nutrient storage (Führer 2010; Führer et al. 2011). Based on the relationship between the girth growth of trees and meteorological parameters, and recognizing the critical period from May to August, Führer (2010) introduced the newly developed Forestry Aridity Index (FAI) for Hungarian conditions (Eq. 1):

$$FAI = 100 \cdot \frac{\bar{T}_{July-Aug}}{P_{May-July} + P_{July-Aug}} \qquad (1)$$

where $\bar{T}_{July-Aug}$ is the average temperature from July to August (℃) and $P_{May-July} + P_{July-Aug}$ is the precipitation sum (mm) in May, June, July, and again in July and August (Führer 2010), so the equation is weighted with the most critical July month.

Führer (2010), Führer et al. (2017), Gálos and Führer (2018), and Mátyás et al. (2018) identified five forestry climate categories based on the Forestry Aridity Index (FAI): beech (FAI < 4.75), hornbeam oak (FAI: 4.75–6.00), sessile oak turkey oak (FAI: 6.00–7.25), forest-steppe (FAI: 7.25–8.50), and grass steppe (FAI > 8.50). Applying the FAI, Führer et al. (2017) and Gálos and Führer (2018) projected the macroclimate classes onto the area of Hungary (Figure 2) and created simulations with climate scenario A1B for the period 2021–2050. These FAI-based aridity simulations suggest that climate change will shift Hungary's forest climate towards dry sessile oak-turkey oak and forest-steppe, and in some areas, to grass steppe. Mátyás et al. (2018) reported that the annual temperature has increased by 1.2–1.7°C over the last 30 years. Illés and Móricz (2022) conducted a climate envelope analysis for nine native wood species in Europe and Hungary under the RCP4.5 climate scenario. Their findings indicate that the applied climate model predicts an increase in the annual average temperature in Hungary (2011–2040: +1.7 °C; 2041–2070: +2.5 °C; 2071–2100: +3.1 °C). Meanwhile, the amount of annual (+5%) and summer precipitation (–10%) shows only minor changes by the end of the century compared to the period 1961–1990. Figure 3 represents the decrease in precipitation (3a) and increase in temperature (3b) over the past 120 years (World Bank Group 2024). When compared with the estimations by Illés and Móricz (2022), Figure 3 shows similar trends. Additionally, when compared with FAI-based aridity maps (Figure 2), a slight decrease in precipitation and a definite increase in temperature can be observed, which will result in a xeric shift in Hungary's forest climate. As described by Illés and Móricz (2022),

due to climate change, over the next 40-80 years, the habitats of beech *(F. sylvatica)*, Scots pine *(P. sylvestris)*, sessile oak *(Q. petraea)*, and European oak *(Q. robur)* will significantly decrease in Hungary. Conversely, the habitats of Turkey oak *(Q. cerris)*, pubescent oak *(Q. pubescent)*, and Austrian pine *(P. nigra)* are expected to increase and expand into the hilly and mid-mountain areas. Porcsin et al. (2023) investigated cultivars of black locust *(R. pseudoacacia)*. This species is frost-sensitive and tolerant of summer heat. The increasing temperatures associated with climate change in Hungary could be advantageous for this tree. It is expected that the area covered by black locust forests will increase in the forest-steppe regions. However, despite its economic importance, it is also an invasive species, necessitating well-regulated planting with high-quality cultivars. (Komán and Varga 2021; Komán and Lehoczki 2022; Komán et al. 2022). Bartha et al. (2018) estimated a significant expansion of the invasive hackberry *(Celtis occidentalis)* during the simulated period from 2021 to 2070.
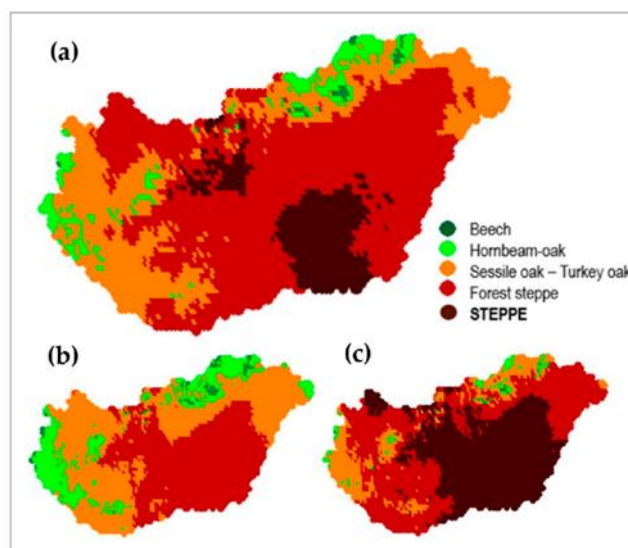

Figure 2: Simulated shift in macroclimate classes in Hungary, 2021–2050. Defined by the Forestry Aridity Index. (a) Mean of the simulation; (b) optimistic result; (c) pessimistic result of simulation (b, c: 66% range of the simulation results, emission scenario: A1B). Adapted from B. Gálos in Mátyás et al. (2018), licence CC-BY 4.0.
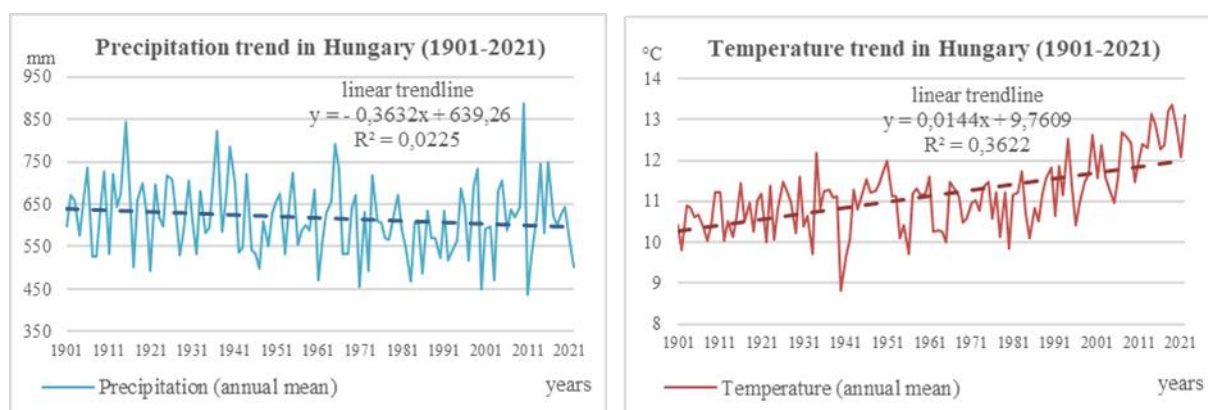

Figure 3: Precipitation (3a) and temperature (3b) change trends between 1901 and 2021 in Hungary. Own edited figure based on dataset of World Bank Group, CCKP (2024), license: (CC BY 4.0)

DISCUSSION

The international research on dendroclimatology and dendrochronology primarily focuses on softwoods or, in some cases, ring-porous analyses (Cook and Kairiukstis 1990; Schweingruber 1996; Cuny et al. 2014; Gärtner et al. 2015). In Hungary, Majer (1972) examined the relationship between annual growth and climate in beech trees. Dávid and Kern (2007) and Kern (2007) analyzed oak trees using dendroecological and dendrochronological methods. Misi (2017) conducted a comprehensive dendroclimatology analysis of Scots pine. Grynaeus (2002), Morgós (2007), and Árvai (2019) focused

their main research on dendrochronology from an archaeological perspective. Various methods employ mathematical and statistical procedures to model past climatic data using the genetic properties of tree species and annual ring data (Biondi and Waikul 2004; Jevšenak 2020). Shishov et al. (2016, 2021) developed a band model for cambium development, which simulates the seasonal cell production of cambium based on specific wood species and estimated temperature and precipitation trends. This model was tested in the semi-arid Southern-Siberian area by the authors.

Summarizing, we understand the types of climatic changes possible in Hungary and which wood species will survive in future Hungarian forests. However, we currently do not know what quality properties these woods will possess. Further research will attempt to answer this question by applying mathematical models and the aforementioned software calculation methods adapted to Hungarian climate scenarios.

ACKNOWLEDGEMENTS

REFERENCES

Árvai M (2019) Holtfaanyag évgyűrűvizsgálatával nyert információk környezettörténeti szempontú értelmezése egy hegyvidéki és egy alluviális lelőhely példáján. ELTE

Bartha D, Berki I, Lengyel A, et al (2018) Erdőtársulások és fafajaik átrendeződési lehetőségei a változó klímában. Erdészettudományi Közlemények 8:163–195

Biondi F, Waikul K (2004) DENDROCLIM2002: A C++ program for statistical calibration of climate signals in tree-ring chronologies. Comput Geosci 30:303–311. https://doi.org/10.1016/j.cageo.2003.11.004

Cook ER, Kairiukstis LA (eds) (1990) Methods of Dendrochronology. Springer Netherlands, Dordrecht

Cuny HE, Rathgeber CBK, Frank D, et al (2014) Kinetics of tracheid development explain conifer tree-ring structure. New Phytol 203:1231–1241. https://doi.org/10.1111/nph.12871

Dávid S, Kern Z (2007) Keleti-bakonyi és gerecsei tölgyek dendrokronológiai és dendroökológiai vizsgálata. In: Gömöri J (ed) AZ ERDŐ ÉS A FA RÉGÉSZETE ÉS NÉPRAJZA (Kézművesipar-történeti megközelítésben). MTA VEAB Soproni Tudós Társasága, Sopron, pp 104–122

Denne MP (1989) Definition of Latewood According to Mork (1928). IAWA J 10:59–62. https://doi.org/10.1163/22941932-90001112

Führer E (2010) A fák növekedése és a klíma. KLÍMA-21 Füzetek 61:98–107

Führer E, Gálos B, Rasztovits E, et al (2017) Erdészeti klímaosztályok területének várható változása. Erdészeti Lapok 174–177

Führer E, Horváth L, Jagodics A, et al (2011) Application of a new aridity index in Hungarian forestry practice. Idojaras (Budapest, 1905) 115:205–116

Gálos B, Führer E (2018) A klíma erdészeti célú előrevetítése. Erdészettudományi Közlemények 8:43–55

Gärtner H, Cherubini P, Fonti P, et al (2015) A Technical Perspective in Modern Tree-ring Research - How to Overcome Dendroecological and Wood Anatomical Challenges. JoVE J Vis Exp e52337. https://doi.org/10.3791/52337

Grynaeus A (2002) Dendrokronológiai kutatások és eredményei Magyarországon. Földt Közlöny 265–272

Jevšenak J (2020) New features in the *dendroTools* R package: Bootstrapped and partial correlation coefficients for monthly and daily climate data. Dendrochronologia 63:125753. https://doi.org/10.1016/j.dendro.2020.125753

Kern Z (2007) Évgyűrűvizsgálatok a Déli-Bakonyban és a Balaton-felvidéken. In: Gömöri J (ed) AZ ERDŐ ÉS A FA RÉGÉSZETE ÉS NÉPRAJZA (Kézművesipar-történeti megközelítésben). MTA VEAB Soproni Tudós Társasága, Sopron, pp 89–103

Komán S, Lehoczki M (2022) Combustion characteristics of green ash and box elder. In: Németh R, Christian Hansmann, Rademacher P, et al. (eds) 10TH HARDWOOD CONFERENCE PROCEEDINGS. University of Sopron, Sopron, p 128

Komán S, Szmorad G, Bak M (2022) Thermal modification of green ash and box elder. In: Németh R, Christian Hansmann, Rademacher P, et al. (eds) 10TH HARDWOOD CONFERENCE PROCEEDINGS. University of Sopron, Sopron, p 129

Komán S, Varga D (2021) Physical and mechanical properties of wood from invasive tree species. Maderas Cienc Tecnol 23:1–8. https://doi.org/10.4067/s0718-221x2021000100411

Majer A (1972) Évgyűrű-kronológia. Az Erdő 164–171

Mátyás C, Berki I, Bidló A, et al (2018) Sustainability of Forest Cover under Climate Change on the Temperate-Continental Xeric Limits. Forests 9:489. https://doi.org/10.3390/f9080489

Misi D (2017) Magyarországi erdeifenyő állományok komplex dendroklimatológiai elemzése az elmúlt 100 év klímaváltozásának tükrében. PhD, Szegedi Tudományegyetem

Molnár S, Peszlen I, Paukó A (2007) Faanatómia. Szaktudás Kiadó Ház, Budapest

Morgós A (2007) Faanyagok kormeghatározása – a dendrokronológia és a magyarországi helyzet. In: Gömöri J (ed) AZ ERDŐ ÉS A FA RÉGÉSZETE ÉS NÉPRAJZA (Kézművesipar-történeti megközelítésben). MTA VEAB Soproni Tudós Társasága, Sopron, pp 32–89

National Land Centre (Nemzeti Földügyi Központ - NFK) (2024) Magyarország erdeivel kapcsolatos adatok (Data related to Hungary's forests). https://nfk.gov.hu/Magyarorszag_erdeivel_kapcsolatos_adatok_news_513. Accessed 11 Apr 2024

Sandberg D, Gorbacheva G, Lichtenegger H, et al (2023) Advanced Engineered Wood-Material Concepts. In: Niemz P, Teischinger A, Sandberg D (eds) Springer Handbook of Wood Science and Technology. Springer International Publishing, Cham, pp 1835–1888

Schmitt U, Koch G, Hietz P, Tholen D (2023) Wood Biology. In: Niemz P, Teischinger A, Sandberg D (eds) Springer Handbook of Wood Science and Technology. Springer International Publishing, Cham, pp 41–138

Schultz J (2005) The ecozones of the world. The ecological division of the geosphere

Schweingruber FH (1996) Tree rings and environment dendroecology. P. Haupt, Berne

Shishov VV, Tychkov II, Anchukaitis KJ, et al (2021) A Band Model of Cambium Development: Opportunities and Prospects. Forests 12:1361. https://doi.org/10.3390/f12101361

Shishov VV, Tychkov II, Popkova MI, et al (2016) VS-oscilloscope: A new tool to parameterize tree radial growth based on climate conditions. Dendrochronologia 39:42–50. https://doi.org/10.1016/j.dendro.2015.10.001

World Bank Group (2024) World Bank Climate Change Knowledge Portal (CCKP). https://climateknowledgeportal.worldbank.org/. Accessed 11 Apr 2024

Combustion characteristics of Russian olive (*Elaeagnus angustifolia* L.)

Szabolcs Komán[1*], Krisztián Töröcsi[2]

[1] Bajcsy-Zs. u. 4., 9400 Sopron, Hungary, University of Sopron, Institute of Basic Sciences
[2] Bajcsy-Zs. u. 4., 9400 Sopron, Hungary, University of Sopron

E-mail: koman.szabolcs@uni-sopron.hu; TorocsiKF21@student.uni-sopron.hu

ABSTRACT

The majority of the timber of invasive wood species is used as fuel wood, as it is a forestry objective to control their spread. Knowledge of the higher heating value and ash content are important parameters for the use of wood for energy. In terms of these two parameters, the Russian olive does not lag behind other invasive species. The ash content of its timber is very low, only 2.7%, while its higher heating value is 19.2 MJ/kg. Its ash content is only a quarter of that of black locust, while there is no difference between their higher heating values. The use of Russian olive for energetical purposes is advisable as far as the properties examined are concerned, and it is in no respect inferior to other wood species.

INTRODUCTION

Russian olive is indigenous to the warm continental areas of Asia. It is native to the region starting from the eastern basin of the Mediterranean Sea through Asia Minor, Western and Central Asia, stretching to the Altai Mountains and the Gobi Desert. It is mostly abundant in the Caspian Depression and in the regions of the Aral Sea and Lake Balkhash, where it is a characteristic plant of the vegetation accompanying the watercourses of sandy semi-deserts. It has been cultivated for centuries in Western Asia and Europe, where it has also grown wild and became widely established (Bartha and Csiszár 2012).

In Hungary, it can primarily be found in wet areas. Its spread (Figure 1) significantly changes the subject habitat, and is of outstanding importance in certain parts of the country. It is difficult to remove from anywhere it has once become established. After cutting down, the stump begins to grow new shoots intensively; its roots are capable of binding nitrogen. Its rapid growth also contributes to its intensive propagation. It is often seen along motorways, used as a means of erosion protection and in protective forest bands of ploughfields.
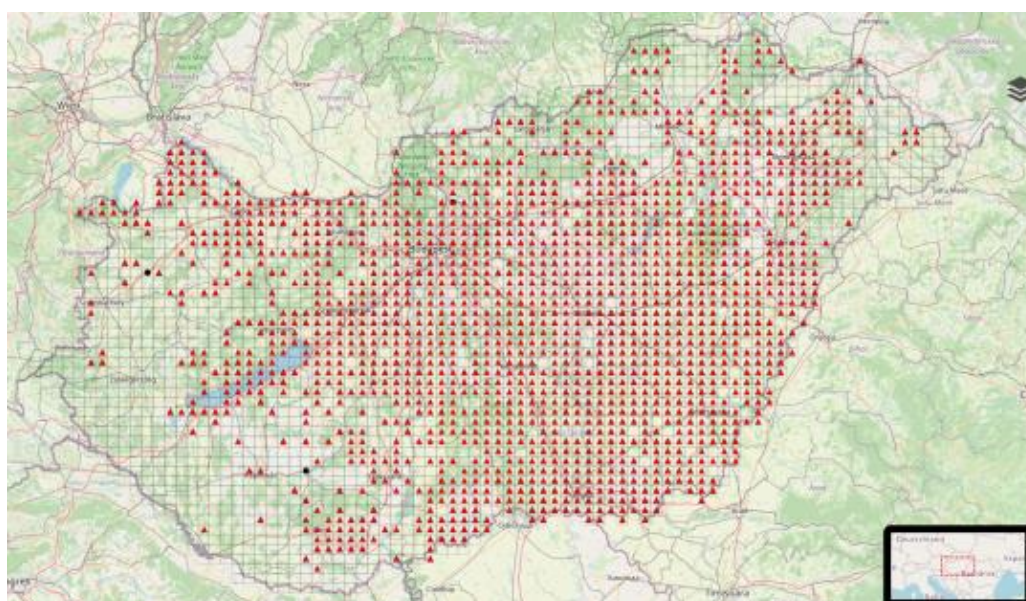

Figure 1: Spread of Russian olive in Hungary (invaziosfajok.hu 2024)

From the apiary perspective, the species gives excellent honey. Its pure monofloral honey has an intensive scent, reminiscent of flower of the tree. It is used as a flavour enhancer in mixed honeys. Its leaves, flowers and fruit rich in vitamin C are also used in folk medicine.

The use of various biomasses for energy is significantly determined by their calorific values, ash contents and other combustion parameters. The timber usually has a lower relative ash content, while that of the bark is significantly higher (Passialis et al. 2008, Nosek et al. 2016, Komán 2018). The noncombustible slag formed during the energy use of biomass raises special operational problems in larger firing plants. This is connected in part to damage caused to the firing equipment, and in part to the deposition of large volumes of ash. These problems can be primarily explained by the presence and the effect of chemical element incorporated into the biomass from the soil during its formation (Komán 2013).

During combustion of solid fuels such as wood, biomass and coal, significant volumes of non-combustible by-products are generated, including ash, slag and minerals. If these ash particles melt and get deposited in the firing equipment, they may hinder optimal heat exchange and flow. Therefore the removal of ash and the reduction of its quantity are of key importance to ensure the efficient and reliable operation of solid fuel firing equipment (Palotás 2011).

One of the key parameters of plantations is the energy yield determined based on higher heating value (Kenney et al. 1990). According to several studies, the bark's calorific value is lower than that of timber (Požgaj et al. 1997, Klašnja and Kopitovič 1999), but opposing opinions can also be found, according to which the bark's calorific value exceeds that of timber by a significant margin (Nurmi 2000).

Russian olive today has no timber industry related significance, primarily being used for firewood. The objective of the current research is to map its energetical characteristics in comparison to other wood species.

MATERIALS AND METHODS

A Russian olive trunk already having mature timber was examined, from a tree that grew in the area of the Fertő-Hanság Basin.

For the tests, 5 cm thick discs cut at the diameter at breast height were used. Ash content test took place on absolute dry samples (Figure 2). Following grinding, a 2 g quantity of the samples were analysed according to the EN ISO 18122:2026 standard, based on 3 samples.

To determine the higher heating value, 1 g pellets were pressed from the wood chips used to examine the timber's ash content (Figure 3). The samples were in absolutely dry condition of which 3 measurements were performed according to the EN ISO 1716:2019 standard.

Figure 2: Sample cross section

Figure 3: Sample of ground bark

RESULTS AND DISCUSSION

Of Russian olive's ash content, it can be said that it is very low in comparison to other wood species. Its ash content in comparison to other invasive wood species is likewise (Figure 3.) very low. Ash contents of tree of heaven, black locust and green ash are 2.5, 4 and 3 times higher than that of Russian olive, respectively.
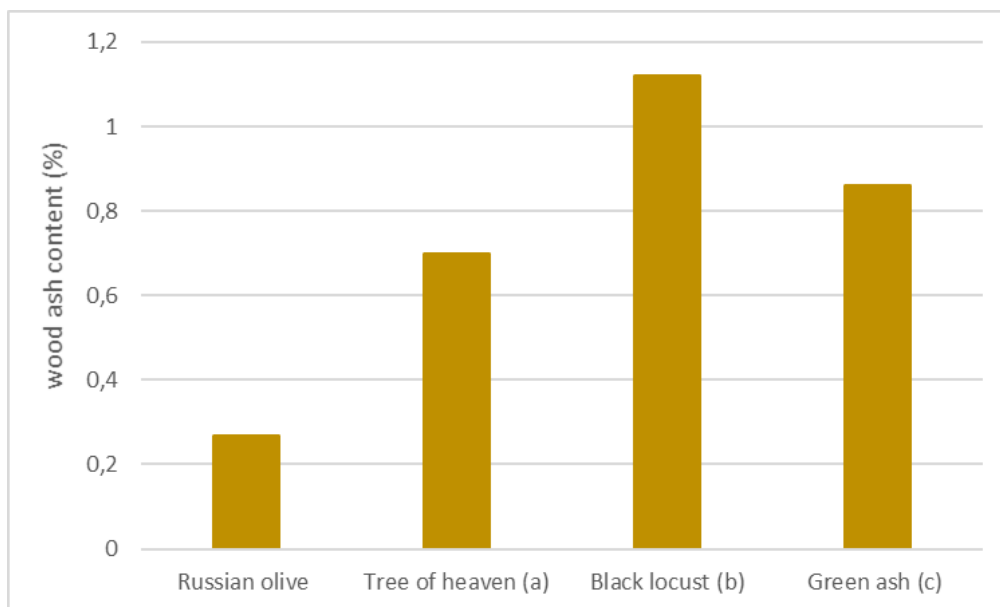

Figure 4: Ash content of Russian olive in comparison to other wood species (a – Terzopoulou and Kamperidou 2022; b – Komán 2018; c – Komán and Lehoczki 2022)

The Russian olive timber's higher heating value by weight is not inferior to the characteristic value of the majority of hardwood species. It is practically identical to the values of black locust and green ash, and is somewhat higher than that of tree of heaven. The value of its higher heating value is practically identical to that of beech and English oak (Telmo and Lousada 2011). The energetical utilisation of its timber is well advisable, considering this property.
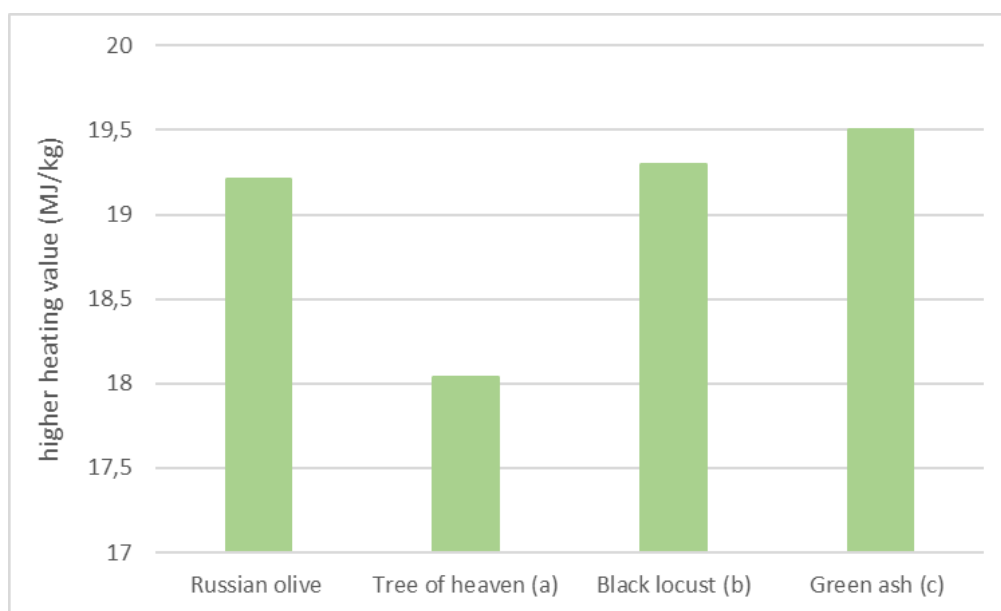
Figure 4: Higher heating value of Russian olive in comparison to other wood species (a – Kamperidou et al. 2018; b – Komán 2018; c – Komán and Lehoczki 2022)

CONCLUSIONS

The timber of Russian olive timber is of adequate quality for energetical utilisation in comparison to other invasive wood species, both in terms of ash content and higher heating value. As the volume of ash generated increases with the volume of wood burnt, its low ash content is a very favourable property. In the course of energetical utilisation, this has a positive affect on the operation of firing equipment and the deposition of the ash generated. The heat of combustion of its timber is equal to other hardwoods, therefore there is no reason not to exploit as an energy source.

ACKNOWLEDGMENTS

REFERENCES

Bartha D, Csiszár Á. (2012) Inváziós növényfajok Magyarországon. Nyugat-magyarországi Egyetem Kiadó, Sopron, pp 115-119 (in Hungarian)

EN ISO 18122 (2022) Solid Biofuels - Determination of ash content. International Organization for Standardization, Geneva, Switzerland

EN ISO 1716 (2019) Reaction to fire tests for products. Determination of the gross heat of combustion (calorific value). International Organization for Standardization, Geneva, Switzerland

Kamperidou V, Lykidis C, Barmpoutis P (2018) Utilization of wood and bark of fast-growing hardwood species in energy production. Journal of Forest Science, 64, 4:164–170 https://doi.org/10.17221/141/2017-JFS

Kenney W.A, Sennerby-Forsse L, Layton P (1990) A review of biomass quality research relevant to the use of poplar and willow for energy conversion. Biomass 21(3):163-188.

Klašnja B, Kopitovič, Š. (1999) Quality of wood of some willow and robinia clones as fuelwood. Drevársky výskum, 44, pp 9-18.

Komán Sz (2013) Anatomical and physical characteristics of hybrid poplar species influencing the modern industrial and energy utilisation (Nemesnyár-fajták korszerű ipari és energetikai hasznosítását befolyásoló faanatómiai és fizikai jellemzők). PhD dissertation, Nyugat-Magyarországi Egyetem, Sopron, Hungary (in Hungarian)

Komán Sz (2018) Energy-related characteristics of poplars and black locust. BioResources 13(2), 4323-4331. https://doi.org/10.15376/biores.13.2.4323-4331

Komán Sz, Lehoczki M (2022) Combustion characteristics of green ash and box elder. In: Németh R, Hansmann C, Rademacher P, Bak M, Báder M (eds.) 10th Hardwood Conference Proceedings, Soproni Egyetemi Kiadó, Sopron, pp 323

Nosek R, Holubcik M, Jandack, J. (2016) The impact of bark content of wood biomass on biofuel properties. BioResources 11(1):44-53. https://doi.org/10.15376/biores.11.1.44-53

Nurmi, J. (2000). Characteristics and storage of whole-tree biomass (Metsäntutkimuslaitoksen tiedonantoja), The Finnish Forest Research Institute, Kannus, Finland.

Palotás Á. B (2011) Ipari tüzeléstechnika (adaptáció). e-jegyzet, Miskolci Egyetem, 45 p. (in Hungarian)

Passialis C, Voulgaridis E, Adamopoulus S, Matsouka M (2008) Extractives, acidity, buffering capacity, ash and inorganic elements of black locust wood and bark of different clones and origin. European Journal of Wood and Wood Products 66:395-400. https://doi.org/10.1007/s00107-008-0254-4

Požgaj A, Chovanec D, Kurjatko S, Babiak M. (1997) Structure and Properties of Wood, Príroda, Bratislava, Slovak Republic. (In Slovak)

Terzopoulou P, Kamperidou V (2022) Chemical characterization of Wood and Bark biomass of the invasive species of Tree-of-heaven (*Ailanthus altissima* (Mill.) Swingle), focusing on its chemical composition horizontal variability assessment. Wood Material Science & Engineering, 17:6, 469-477. https://doi.org/10.1080/17480272.2021.1888315

Telmo C, Lousada J, (2011) Heating values of wood pellets from different species. Biomass and Bioenergy, 35(7), 2634-2639, ISSN 0961-9534. https://doi.org/10.1016/j.biombioe.2011.02.043.

http://www.invaziosfajok.hu/hu/invazios-fajok/142 Accessed 10 Apr 2024

Withdrawal capacity of Green ash (*Fraxinus pennsylvanica* Marsh.) and Box elder (*Acer negundo* L.)

Szabolcs Komán[1*], Boldizsár Déri[2]

[1] Bajcsy-Zs. u. 4., 9400 Sopron, Hungary, University of Sopron, Institute of Basic Sciences
[2] Bajcsy-Zs. u. 4., 9400 Sopron, Hungary, University of Sopron

E-mail: koman.szabolcs@uni-sopron.hu; DeriB21@student.uni-sopron.hu

Keywords: withdrawal capacity, green ash, box elder, invasive

ABSTRACT
Efforts to curb the spread of invasive species are made worldwide, but the wood mass available of these species is already significant in certain areas. The properties of these wood species are little or not at all known, such as those of green ash (*Fraxinus pennsylvanica* Marsh.) and box elder (*Acer negundo* L.). The withdrawal capacity of wood screws of the two wood species examined showed significant differences, perpendicular to the grain. The tests conducted using chipboard screws showed withdrawal capacity of green ash to be 1.5 times greater than that of box elder. For the screw and driving depth applied, the average withdrawal load of green ash and box elder were 3845 N and 2550 N respectively.

INTRODUCTION
The use of metal screws as fasteners dates back to the 15th century in Europe. The first patent was registered in the 18th century for the industrial manufacturing of wood screws. The majority of the releasable joints used in furniture production and the majority of functional fittings such as hinges, slide door hardware systems, drawer slides and mechanisms serving to store various products are connected to the structural components with the help of screws (Jivkov et al. 2017).

The resistance of the wood screw driven into timber to withdrawal characteristically shows strong correlation with the strength, density and shear modulus of the wood. Withdrawal capacity tests may be performed on various structural components, such as:

- timber structures of log cabins and off-site construction houses
- structures of viewing towers and timber bridges
- timber of roofing structures
- timber of floor structures (ÉMI 2020).

Nail and screw withdrawal capacity tests are conducted in laboratory environment on universal testing machines (UTM), but special instruments have also been developed for the on-site testing of various structures (Divós and Őry 2022).

In case of structural elements, failure is often initiated at the joints, normally at the weakest points of timber structures. It is therefore essential to examine how connections and fasteners behave under various loads. When subjected to tensile force, fasteners may be pulled out of the timber components or may snap (Abdoli et al. 2022).

Fastener pullout resistance is influenced among others by diameter, thread geometry, penetration depth of a fastener, and load-to-grain angle. In case of timber, it is usually defined parallel or perpendicular to the grain. Perpendicular to the grain may be further distinguished into radial and tangential directions. Its definition in the various anatomical directions is necessitated by the anisotropic nature of wood.

Teng et al. (2018) have come to the conclusion that the insertion angle significantly influences withdrawal capacity, while no significant difference can be observed between the cases of radial and tangential directions. A positive correlation has been found to exist between density and withdrawal strength.

According to Eckelman (1990) denser materials largely show greater withdrawal strengths, but the strength decreased with the increase of moisture content.

The spread of invasive plant species and their habitat transforming effect represent a significant environmental problem worldwide. A sizeable share of these species are woody species (Ónodi 2016). The term 'invasive species' is used by literature ambiguously. According to the most common definition,

biological invasion revers to the spread of a non-indigenous (alien) species. On the other hand IUCN defines only those alien species as 'invasive' that endanger the biodiversity of the natural areas (Csiszár 2012). There are attempts to restrict the spread of invasive species globally, and fundamental information on the use of the wood of such are less available to the related processing industry. The volume of available literature in invasiveness has seen sharp growth over the recent decades, but these do not focus on the material properties of the timber of invasive species.

Green ash, an invasive woody species, has spread very quickly in Central Europe over the past 25 years (Drescher and Prots 2016), due to certain physiological and morphological traits allowing it to survive in washlands and flooded areas as an early-to late-succession species of riparian forests, mostly observed along larger watercourses in mixed forests of *Fraxinus excelsior*, *Quercus robur* and *Ulmus spp.* (Branquart et al. 2010).

Its strong, durable, and shock-resistant timber is a valuable raw material for niche uses such as making tool handles and baseball bats. Green ash is also a popular ornamental tree and it is widely planted in urban and suburban areas throughout the US and abroad due to its suitable shape and the shade its canopy provides (Kovacs et al. 2010). The timber is of a lower grade than common ash, and is rarely a species to be found in plantations as such, but it does yield better timber than that of common ash when planted in drier areas where it can grow slower. In northwestern Turkey, where narrow-leaved ash is preferred species of fast-growing plantations in swampy lowlands, the timber of Green ash has properties similar to poplar species, making it a suitable raw material for pulp and plywood, LVL, glulam and other bonded wood products. Its leaves are suitable livestock fodder, and the tree has been traditionally cultivated in Southern Europe as such. Green ash is also a popular urban and street tree (Caudullo and Houston 2016).

Initially introduced to Europe in the 17th century as a decorative tree, box elder has by now become widespread and is considered an invasive species (Ednich et al. 2015).

Box elder has a low-grade, low-strength timber, suitable for making entry-level furniture, fences, wooden crates, etc, occasionally used as firewood, and also for park and landscape architecture. It has also been used to control wind erosion, initially in the USA and later globally, and also yields a sap used to make 'mountain molasses', similarly to other maple species. (Barstow et al. 2017)

From the perspective of industrial suitability of wood, one of the most important properties is density. The air dry density of green ash and box elder is 647 kg/m^3 and 501 kg/m^3 respectively. Green ash has been found to have greater compressive strength, modulus of rupture, modulus of elasticity and impact bending strength than box elder (Komán and Varga 2021).

The present research has examined the screw withdrawal capacity of two invasive wood species to promote the more widespread use of their timbers, not insignificantly from the perspective of fundamental research as well, as very little is known about the basic properties of the wood of these species.

MATERIALS AND METHODS

The screw withdrawal capacity test was conducted according to the provisions of the EN 1382:2016 standard. The tests were carried out on specimens stored under normal climate conditions (T=20°C; φ=65%) until equilibrium moisture was reached. During the test, chipboard screws were driven 20 mm deep into the wood, perpendicular to the grain (Figure 1).

The screw withdrawal capacity was calculated using the following formula:

$$f_{ax} = \frac{F_{max}}{d \times l_d} \tag{1}$$

where
f_{ax} – withdrawal parameter, in newtons per square millimetres
F_{max} – maximum withdrawal load, in newtons
d – is the outer thread diameter for screws
l_p – the effective depth of penetration of the fastener, in millimetres

Figure 1: Withdrawal capacity measurement

RESULTS AND DISCUSSION

The test results may be correlated to density, as the density of green ash is 30% greater than that of box elder. The difference of screw withdrawal capacity perpendicular to the grain is even greater for the two species than the difference of their densities. The screw withdrawal capacity of green ash tis 50% greater than that of box elder (Figure 2). The significant difference between the two species is also interesting from the aspect that green ash is a ring-porous species and box elder is diffuse-porous. The values obtained for the two deciduous wood species are multiples of those obtained by Gašparík et al. (2021) for larch and spruce. To pull out screws driven 20 mm deep, average forces of 3845 N and 2550 N were required for green ash and box elder respectively.
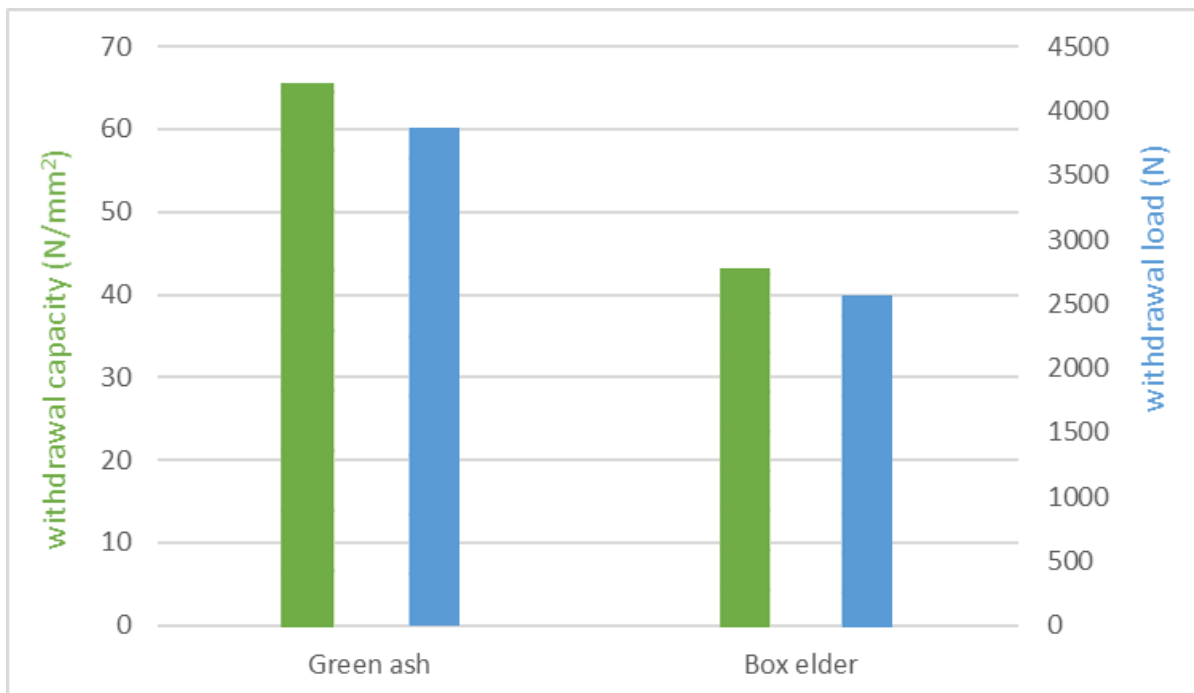

Figure 2: Withdrawal capacity and withdrawal load

CONCLUSIONS

Little information is available on the possibilities of using timbers of various invasive species, the primary objective being the restriction of their populations. From the perspective of their industrial use, besides knowing their characteristic densities – which fundamentally determines their physical and mechanical properties – knowledge of their technological parameters is no less important. Screw withdrawal capacity is also greatly influenced by anatomical structure, not only affected by the anatomical directions, but also by the ring-porous or diffuse-porous nature of hardwoods. Although the density of ring-porous green ash is 30% greater than that of box elder, and even greater difference of screw withdrawal capacity can be observed between the two species. These values, however, exceed those of softwood species by a significant margin, therefore the industrial use of both species is recommended, as far as screw withdrawal capacity is concerned.

ACKNOWLEDGMENTS

REFERENCES

Abdoli F, Rashidi M, Rostampour-Haftkhani A, Layeghi M, Ebrahimi G (2022) Withdrawal Performance of Nails and Screws in Cross-Laminated Timber (CLT) Made of Poplar (*Populus alba*) and Fir (*Abies alba*). Polymers (Basel). 14(15):3129. https://doi.org/10.3390/polym14153129
PMID: 35956645; PMCID: PMC9370617.

Barstow M, Crowley D, Rivers M.C. (2017) Acer negundo. The IUCN Red List of threatened species. 2017:e.T62940A3117065.
https://dx.doi.org/10.2305/IUCN.UK.2017-3.RLTS.T62940A3117065.en

Branquart E, Vanderhoeven S, Van Landuyt W, Van Rossum F, Verloove F (2010) Invasive species in Belgium, *Fraxinus pennsylvanica*. Harmonia version 1.2, Belgian Forum on Invasive species. https://ias.biodiversity.be/species/show/134

Eckelman CA (1990) Fasteners and their use in particleboard and medium density fiberboard. National Particleboard Association. Purdue University.

ÉMI (2020) Meglévő faszerkezetek helyszíni vizsgálata és értékelési szempontjai - faanyagvizsgálati szempontok. 8/2020. (XII.19.) ÉPMI (in Hungarian)

Caudullo G, Houston Durrant, T (2016) *Fraxinus angustifolia* in Europe: distribution, habitat, usage and threats. In Online European Atlas of Forest Tree Species. San-Miguel-Ayanz J, de Rigo D, Caudullo G, Houston Durrant T, Mauri A. (eds.). FISE Comm. Publications Office of the European Union. https://forest.jrc.ec.europa.eu/media/atlas/Fraxinus_angustifolia.pdf

Csiszár Á, Tiborcz V (2012) A növényi invázióhoz kapcsolódó fogalmak. In: Csiszár Á (ed.) Inváziós növényfajok Magyarországon. Nyugat-magyarországi Egyetem Kiadó. ISBN 978-963-334-050-9 (in Hungarian)

Divós F, Őry B.I. (2022) Műszerrel támogatott faszerkezet vizsgálatok. Anyagvizsgálók Lapja, 2022/I. (in Hungarian)

Drescher A, Prots B (2016) *Fraxinus pennsylvanica* - an invasive tree species in Middle Europe: Case studies from the Danube basin. Contributii Botanice LI: 55-69. http://contributii_botanice.reviste.ubbcluj.ro/materiale/2016/Contrib_Bot_vol_51_pp_055-069.pdf

Ednich E.M, Chernyavskaya I.V, Tolstikova T.N, Chitao S.I (2015) Biology of the invasive species *Acer negundo* L. in the conditions of the north-west caucasus foothills. Indian J. Sci. Technol. 8(30):1-3. https://dx.doi.org/10.17485/ijst/2015/v8i30/85426

Gašparík M, Karami E, Sethy A.K, Das S, Kytka T, Paukner F, Gaff M (2021) Effect of freezing and heating on the screw withdrawal capacity of Norway spruce and European larch wood. Construction and Building Materials. 303:124457. ISSN 0950-0618. https://doi.org/10.1016/j.conbuildmat.2021.124457.

Jivkov V, Kyuchukov B, Simeonova R, Marinova A (2017) Withdrawal capacity of screws and confirmat into different wood-based panels. The XXVIIIth International Conference research for furniture industry. Poznań.

Komán Sz, Varga D (2021) Physical and mechanical properties of wood from invasive tree species. Maderas-ciencia y tecnologia 23, pp 1-8. http://dx.doi.org/10.4067/s0718-221x2021000100411

Kovacs K.F, Haight R.G, McCullough D.G, Mercader R.J, Siegert N.W, Liebhold A.M (2010) Cost of potential emerald ash borer damage in U.S. communities, 2009–2019.Ecol Econ 69(3):569-578. https://doi.org/10.1016/j.ecolecon.2009.09.004

Ónodi G (2016) Az idegenhonos, illetve inváziós fafajok élőhelyformáló hatásai," Erdészettudományi Közlemények 6(2) 101-113 (in Hungarian) https://dx.doi.org/10.17164/EK.2016.008

Teng Q, Que Z, Li Z, Zhang X (2018) Effect of installed angle on the withdrawal capacity of self-tapping screws and nails. Proceedings of the World Conference of Timber Engineering, Seoul, Korea

Formaldehyde emission from wood and wood-based products

Szabolcs Komán[1*], Csilla Czók[1], Tamás Hofmann[2]

[1] Bajcsy-Zs. u. 4., 9400 Sopron, Hungary, University of Sopron, Faculty of Wood Engineering and Creative Industries, Institute of Basic Sciences, Department of Wood Science
[2] Bajcsy-Zs. u. 4., 9400 Sopron, Hungary, University of Sopron, Faculty of Forestry Engineering, Institute of Environmental Protection and Nature Conservation

E-mail: koman.szabolcs@uni-sopron.hu; czok.csilla@uni-sopron.hu; hofmann.tamas@uni-sopron.hu

Keywords: invasive wood species, formaldehyde emission, strength

ABSTRACT

Actors of timber industry are in continuous search of solutions to satisfy the industry's demand for raw materials. In addition to cross breeding of cultivars, a possibility to solve this is the use of new wood species, a raw material base of which may be the use of invasive wood species. An indispensable prerequisite of their introduction to industrial use is the knowledge of the properties of their timbers, which must nowadays also include their formaldehyde content, due to the increasingly stringent health and safety requirements. Of the invasive wood species, the use of green ash, tree of heaven, box elder, Siberian elm, black cherry in timber industry sees no restrictions related to strength properties, but their formaldehyde release must also comply with the provisions of the corresponding regulations.

INTRODUCTION

Climate change puts our indigenous wood species in a constantly changing situation. Over the recent decades, professionals were faced with increasingly aggravated challenges of drought, and these meteorological parameters have also contributed to the spread of the invasive wood species already present in Hungary. These invasive species have a significant transforming influence on indigenous flora, in addition to other, mostly negative effects. The majority of the invasive species are among woody plants, and efforts are made worldwide to restrict their spread, although little (Figure 1) or no information is available on the suitability of their timbers for industrial processing (Varga and Komán 2019).
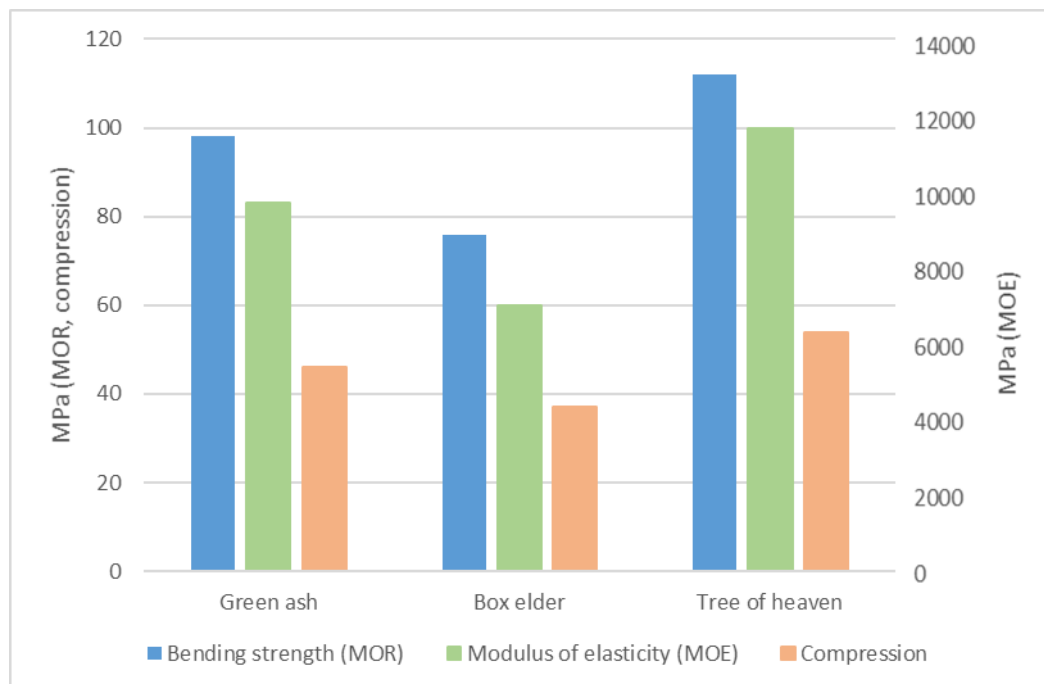

Figure 1: Strengths of the wood species (Varga and Komán 2019)

Their overwhelming propagation, outperforming that of the indigenous species in the recipient ecosystems is related among others to their growth rate, age of maturity, fertility and the spread of their speeds and pollens (Poré 2011). The most important parameter that decides the suitability of the timber of a wood species for industrial use is its density. "Denser species tend to have stronger wood than lighter ones. Knowing the value of the density is important, for example, for determining the wood chip's bulk density in cellulose or chipboard production." (Varga and Komán 2019)

In Hungary one of the most widespread (Figure 2.) invasive species is tree of heaven (*Ailanthus altissima*). Its genus has become established from Middle East to Australia, the species being originally native to central and eastern China and Korea. The tree is of medium size (-25 m), with diffuse foliage and a straight trunk, this latter covered by smooth, grey bark. As for its ecological characteristics, it tolerates warmth, has a particularly high light requirement, medium water requirement and prefers soils rich in lime, with low salt tolerance (Bartha 2012). It grows and spreads rapidly, and once it appears somewhere, it is particularly challenging to exterminate due to its aggressive suckering. The density of tree of heaven ranges between 537-617 kg/m^3, its modulus of elasticity is 10480 MPa, and has a bending strength of 81.36 MPa (Fehér and Komán 2014). International research has reported rather positively on its timber, and is considered a material of good quality based on its mechanical and physical properties (Panayotov et al. 2010). *„Test results unambiguously indicate that the technical parameters of tree of heaven wood is significantly influenced by its growth zone. Occasionally, it may yield lower grade timber in a growth zone of lower quality, where the wood's density would be around 600 kg/m^3. In contrast to this, wood from circumstances closer to optimal may exceed 700 kg/m^3."* (Fehér and Komán 2014) The durability of tree of heaven is particularly low, and is therefore not recommended for outdoor applications, but there are virtually no limits to its indoor use.

Figure 2: The presence of tree of heaven in Hungary (Fehér and Komán 2014)

In the Great Hungarian Plain, two intensive spreading invasive species are black cherry (*Padus serotina*) and Siberian elm (*Ulmus pumila*). Black cherry was primarily imported to Hungary to combat desertification in the Great Plain. It is native to the eastern part of North America and the mountainous regions of Mexico, all the way to Guatemala. As for its ecological characteristics, it requires moderate light- and heat, it is moderately drought resistant and is indifferent to the soil's acidity or basicity. It grows to medium height (-15 m) and has a good sprouting ability (Bartha 2012). Its habitat is originally a forest culture, occupying the subcanopy or shrub level in it. Its aggressive spread may cause it to compete with the wood species forming the population, endangering the renewal of indigenous wood species. Its morphological characteristics limit its industrial use to sawlogs (Nagy et al. 2016).
Siberian elm was brought to Hungary from Central and East Asia, primarily due to it immunity to Dutch elm disease (DED) caused by sac fungi. Unfortunately, it was subsequently proven that this immunity was far from being impenetrable. It prefers warmth and neutral soils, is moderately shade tolerant, and

drought and salt resistant. It grows to medium height (-15 m) and sprouts particularly well from stumps (Bartha 2012). As for its habitat, similarly to black cherry it also grows in forest cultures, and can also be found as an accompanying wood species or at the edges of populations. Resulting from the limited supply and morphology of its timber, its industrial use is marginal. When available in forestry product ranges, it may be used for sawlogs, custom sawing and strutting applications (Nagy et al. 2016).

Densities of black cherry and Siberian elm are 651 kg/m^3 and 633 kg/m^3 respectively. Modulus of elasticity of black cherry and Siberian elm are 9873 MPa and 8147 MPa. Both species are suitable for the production of interior design wood products, furniture and builders' joinery and carpentry (cabinets, seating furniture and internal doors), where aesthetic appearance is key. The two wood species are suitable for use in the timber industry (Figure 3.), but their morphological properties limit their respective yields (Nagy et al. 2016).
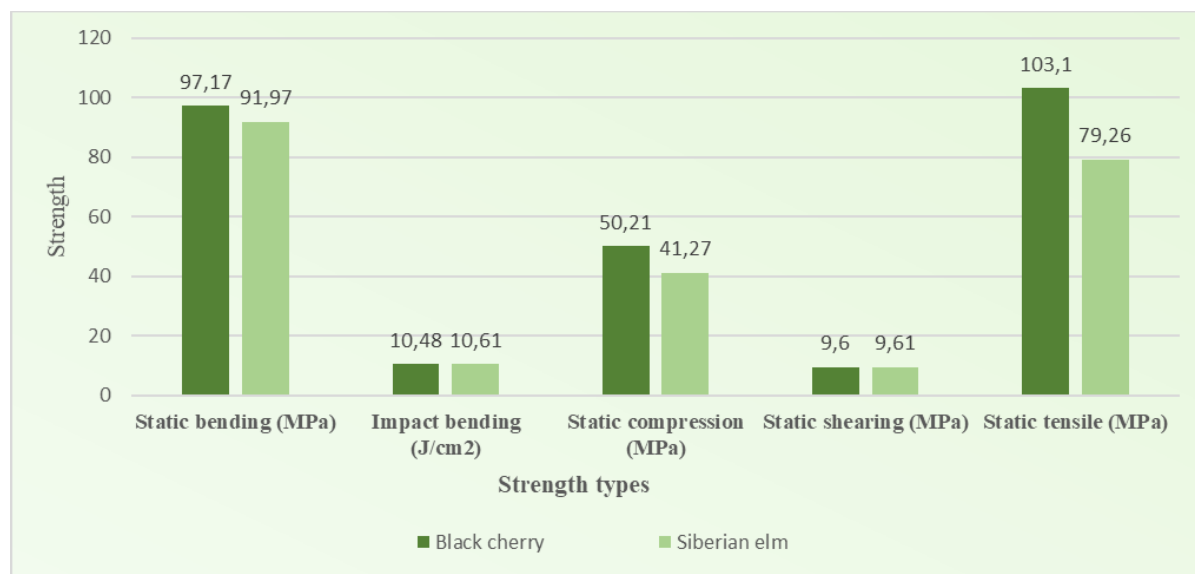

Figure 3: Strength properties of the wood species examined (Nagy et al. 2016)

Besides density, another important factor is the wood's formaldehyde content. Formaldehyde is an organic compound, in gaseous state at room temperature, it is colourless and has a pungent odour, and is quite abundant in nature. *„Formaldehyde is the most common harmful substance that evaporates from wood and wood-based construction raw materials."* (Patkó and Pásztory 2013)

Wood-based construction materials are used both indoors and outdoors, and is an adhesive (as artificial resin) for plywood, furniture and other wood-based products. To make furniture and interior design elements from wood, the material must meet several requirements, one of the most important being its formaldehyde content. At present, this may be examined in Hungary according to six standards, strictly under laboratory conditions, with predetermined apparatuses and materials. These standards are:

- MSZ EN 717-1:2005 Wood-based panels. Determination of formaldehyde release. Part 1: Formaldehyde emission by the chamber method
- MSZ EN ISO 12460-3:2021 Wood-based panels. Determination of formaldehyde release. Part 3: Gas analysis method (ISO 12460-3:2020)
- MSZ EN ISO 12460-5:2016 Wood-based panels. Determination of formaldehyde release. Part 5: Extraction method (called the perforator method) (ISO 12460-5:2015)
- MSZ EN ISO 12460-4:2016 Wood-based panels. Determination of formaldehyde release. Part 4: Desiccator method (ISO 12460-4:2016)
- ASTM D6007-14 Standard test methods for determining formaldehyde concentration in air from wood products using a small scale chamber

Commission Regulation (EU) 2023/1464 of 14 July 2023 amending Annex XVII to Regulation (EC) No 1907/2006 of the European Parliament and of the Council as regards formaldehyde and formaldehyde releasers. This regulation provides that no products may be released for commercial

circulation after 6 August 2026 whose formaldehyde concentration exceeds 0.062 mg/m^3 and 0.080 mg/m^3 in wood-based furniture and non-furniture products respectively (fatáj.hu 2024).

CONCLUSIONS

The invasive species of green ash, tree of heaven, box elder, Siberian elm and black cherry are worthy of industrial use based on their strength properties, but their aggressive spread endangers our currently dominant natural indigenous vegetation associations. When using their timber, the provisions of the EU regulations on the formaldehyde contents of the furniture and wood-based products made from them must be taken into consideration. The various timber modification procedures may change the formaldehyde content of timber, which may make it easier or harder for the end product in question to comply with the applicable limit.

ACKNOWLEDGMENTS

REFERENCES

Bartha D. (2006) Növényrendszertan I. (Dendrológia), Soproni Egyetem, Sopron, Hungary (in Hungarian)

Fehér S, Komán Sz. (2014) A bálványfa *(Ailanthus altissima)* faipari és energetikai célú alkalmazása. Alföldi Erdőkért Egyesület, Kutatói Nap, Lakitelek, pp 64-69 (in Hungarian)

Panayotov P, Kalmukov K, Panayotov M. (2011) Biological and Wood Properties of *Ailanthus altissima* (Mill.) Swingle. Forestry Ideas, 17(2), pp 122-130

Patkó Cs, Pásztory Z. (2013) Formaldehid-koncentráció egy új építésű vázszerkezetes épületben. Faipar LXI.(3) (in Hungarian)

Porté A J, Lamarque L J, Lortie, C J., Michalet R, Delzon S. (2011) Invasive *Acer negundo* outperforms native species in non-limiting resource environments due to its higher phenotypic plasticity. BMC Ecology, 11:28. https://doi.org/10.1186/1472-6785-11-28

Nagy N, Fehér S, Dufla F (2016) A kései meggy és a turkesztáni szil faanyag és felhasználhatósága. Erdészeti Lapok, CLI.(2), pp 42-45 (in Hungarian)

Varga D, Komán Sz (2019) Invazív fafajok faanyagának jellemzői. Alföldi Erdőkért Egyesület, Kutatói Nap, Lakitelek, pp 270-273. (in Hungarian)

https://fataj.hu/2024/03/limit-a-butorok-formaldehid-kibocsatasara/ Accessed 10 Apr 2024

Finite element analysis of heat transfer of Turkey oak (*Quercus cerris*)

Sándor Borza[1], Gergely Csiszár[2], József Garab[3*], Szabolcs Komán[2]

[1] University of Sopron, Institute of Basic Sciences, Department of Physics and Mechanics. Bajcsy-Zs. Str. 4, Sopron, Hungary, 9400.
[2] University of Sopron, Institute of Basic Sciences, Department of Wood Science. Bajcsy-Zs. Str. 4, Sopron, Hungary, 9400.
[3] University of Sopron, Institute of Applied Sciences, Department of Wood Technology. Bajcsy-Zs. Str. 4, Sopron, Hungary, 9400

E-mail:borza.sandor@uni-sopron.hu; csiszarg20@student.uni-sopron.hu; garab.jozsef@uni-sopron.hu; koman.szabolcs@uni-sopron.hu

Keywords: heat transfer, temperature measurement, finite element analysis, temperature distribution, Turkey oak (*Quercus cerris*)

ABSTRACT
Understanding the heat transfer in wood is essential when applying heat technological processes to it. In this study, the transient heat transfer characteristics during the heat treatment of Turkey oak (*Quercus cerris*) at 30 °C, 50 °C, and 70 °C were numerically investigated. The heat transfer model was compared to experimental results. The model aligns well with the experimental values in time, especially at the beginning and the middle phases, where the heat transfer is more dynamic than in later phase of the heat treatment process. The differences between the model and the actual temperatures varies up to 3.38 °C, indicating a maximum relative deviation of only 5.35%. This simulation of heat transfer within the hardwood samples offers valuable insights into the heat treatment processes.

INTRODUCTION
Before manufacturing wood products, special attention shall be paid to the proper preparation of the raw material. Ideally, this starts at the storage stage, where the raw material is stored at the right temperature and humidity to achieve or maintain the desired moisture content. Neglecting these parameters can cause significant problems before, during and after the technological process. The effect of changes in external temperature on the internal temperature of the wood is particularly important in certain technological processes. In the case of gluing, for example, a large temperature difference between the internal temperature of the wood and its surface causes problems because the colder layer inside can cool the adhesive below the minimum film-forming temperature. In such cases, it is important to know how long it takes for a material stored at a lower temperature than the production temperature to heat through its entire cross-section. Also important from an energy efficiency point of view is the reheating time of the wood in case of drying or heat treatment. In addition to considering the needs of manufacturing technology, knowledge of this property of wood is an important factor in the behaviour of structures and products in or in contact with the exterior environment under thermal fluctuations.

Due to the inhomogeneous, anisotropic properties, several factors influence the thermal conductivity of wood. The most important of these are the wood species, density, moisture content, anatomical orientation (longitudinal, radial, tangential), cross-sectional dimensions and the temperature. For European wood species, the coefficient of thermal conductivity perpendicular to the grain is about half that parallel to the grain. At low moisture content – between 0% and fibre saturation – wood is a good insulator. The more porous wood has a lower thermal conductivity (Rohsenow 1973), because the free water conducts more heat (Siau 1984). According to Parrot and Stuckes (1975), the heat conduction along the length of the microfibril is greater, so the thermal conductivity will be higher in the longitudinal direction than in the transverse direction. The difference between the radial and tangential anatomical directions might be affected by the rays. Since these cells are radially oriented, the conductivity will be higher in this direction. The thermal conductivity is determined by the amount of latewood for conifers (Steinhagen 1977).

Thermal properties of wood are available for the wood species in the literature. Among others Sitkei (1994) and Molnár (2004) published relevant findings, but dedicated information for Turkey oak

(*Quercus cerris*) is scarce. Therefore, the goal of this study was to create and validate a numerical model for the heat transfer process in Turkey oak when elevated temperature was applied.

MATERIALS AND METHODS
Materials and the experimental setup

The Turkey oak (*Quercus cerris*) cubic specimens had 45 mm edge length. Measurements were performed with an Ahlborn Almemo 2590 universal measuring device using NiCr-Ni thermowire with the sensor inserted in the centre of the samples through a 2 mm diameter hole (Figure 1). After conditioning the samples in normal climate (t=20°C; RH=65%), the 3 samples were put into the climate chamber with temperatures of 30°C, 50°C and 70°C. The temperature was recorded in 5 minutes incremental until 60 minutes.
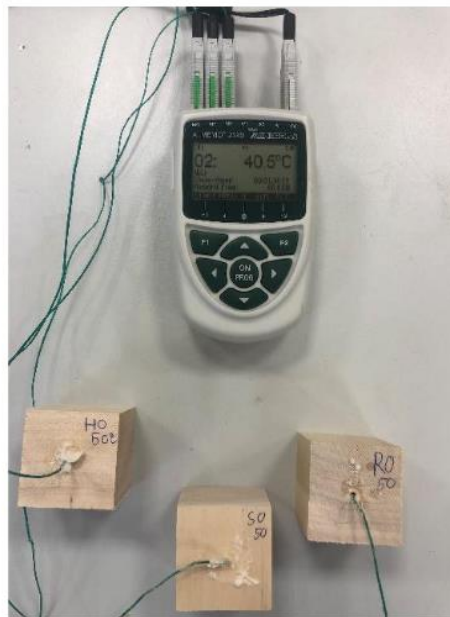

Figure 1: Measurement equipment and the positioning of the thermosensors

Numerical simulations

For the numerical simulations the followings are assumed: 1) considering the low initial moisture content of the samples and the heat treatment temperature, it can be inferred that they might be excessively dried during the treatment process, 2) The chemical reactions linked to the loss of water in the samples are not being considered, 3) the dimensional changes in the wood could be neglected, 4) no degradation of the solid material or heat generation within the wood occurred throughout the heat treatment process, 5) the sensor is represented as a node in the centre of the cube. To conduct transient thermal analysis, computational simulations were performed using Ansys Mechanical APDL (licensed product is Ansys® Academic Research Mechanical, Release 15). In all computations SOLID278 element was used. The element is applicable to a 3D transient thermal analysis. The FE model consist of 8000 elements. Orthotropic thermal conductivity was applied in the material model. The values were calculated according to Sitkei (1994). The specific heat capacity was calculated according to Molnár (2004). The thermal conductivity values and the specific heat capacity calculations were based on the density, moisture content and the temperature of the wood. Although the convective heat transfer coefficient may vary according the wind speed, the value was taken from Zhang et al. (2017).

Table 1: Material and heat treatment parameters applied in the simulation

Parameters	Value
Density ρ/(kg·m^{-3}) [a]	824.8
Moisture content (%) [a]	12
Longitudinal thermal conductivity λ/(W·m^{-1}·K^{-1})[b]	0.60

Radial thermal conductivity $\lambda/(W \cdot m^{-1} \cdot K^{-1})$[b]	0.43	
Tangential thermal conductivity $\lambda/(W \cdot m^{-1} \cdot K^{-1})$[b]	0.37	
Convective heat transfer coefficient $h/(W \cdot m^{-2} \cdot K^{-1})$[c]	15.8	
Specific heat capacity $C/(J \cdot kg^{-1} \cdot K^{-1})$[d]	from (20°C) to (70°C)	1532 1750
Initial temperature $t_0/$(°C) at 30°C treatment[e]	21.53	
Initial temperature $t_0/$(°C) at 50°C treatment[e]	21.80	
Initial temperature $t_0/$(°C) at 70°C treatment[e]	31.60	
Target temperature $t_0/$(°C) at 30°C treatment[f]	29.51	
Target temperature $t_0/$(°C) at 50°C treatment[f]	50.57	
Target temperature $t_0/$(°C) at 70°C treatment[f]	71.50	

[a]measured on the samples; [b]calculated according to Sitkei (1994); [c]adapted from Zhang et al. (2017); [d]calculated in 2°C steps according to Molnár (2004); [e] average of the temperatures measured in the samples; [f]average of temperature measured in the climate chamber

RESULTS AND DISCUSSION

The contour plot for the simulation at the time step of 600 s in case of 70°C heat treatment is presented on the Figure 2. The result of the different thermal conductivity values according to the anatomical directions are visible in the temperature distribution.

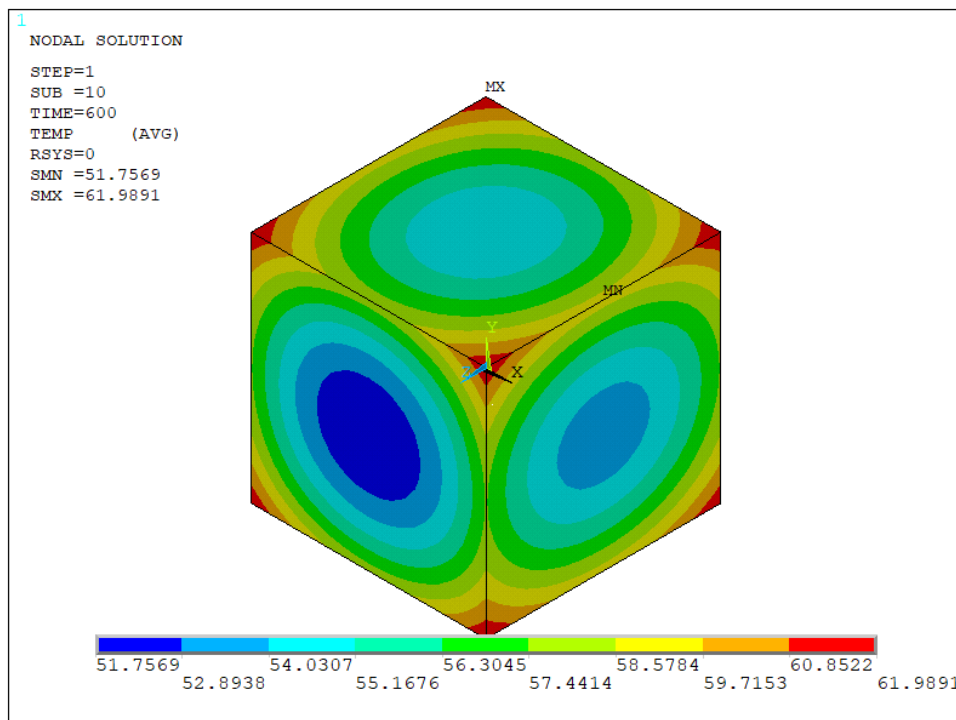*Figure 2: Temperature nephogram at 600 s at 70•C heat.*

The heat was applied to all of faces of the cube. The sensor was in the center of the cube, the temperature of the node at the center point was analysed. In case of 30°C heat treatment (Figure 3), the Sample 1 curve shows some measurement discrepancy compared to the other two samples, because the measured values up to 25th min are a bit higher.
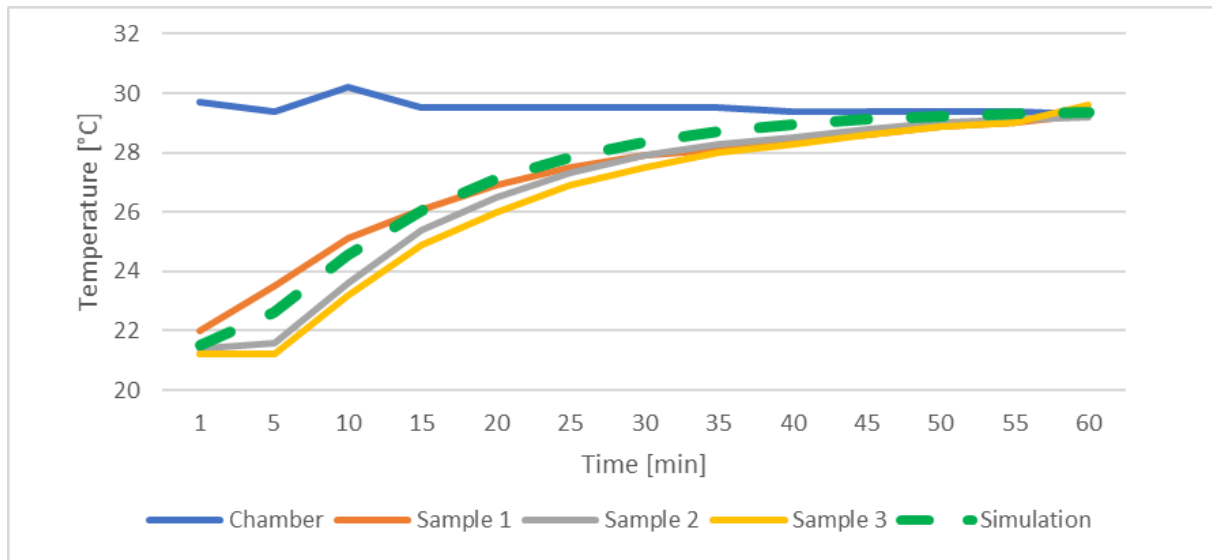
Figure 3: Comparison of experimental and simulated temperatures at 30 °C heat

In case of 50°C heat treatment (Figure 4), the misalignment is negligible. In case of 70°C treatment (Figure 5), the beginning and the middle phase of the curve is following the experimental values. However, the simulation achieved the intended final temperature, but the experimental values did not. This difference may be attributed to variations in the heat conductive coefficient and the convective heat transfer coefficient, which fluctuated with temperature. Additionally, there may thermal resistance present between the samples and their surroundings. The differences between the measurement results and the model were up to 0.6°C, 1.3°C and 3.6°C in case of 30°C, 50°C and 70°C temperatures respectively.
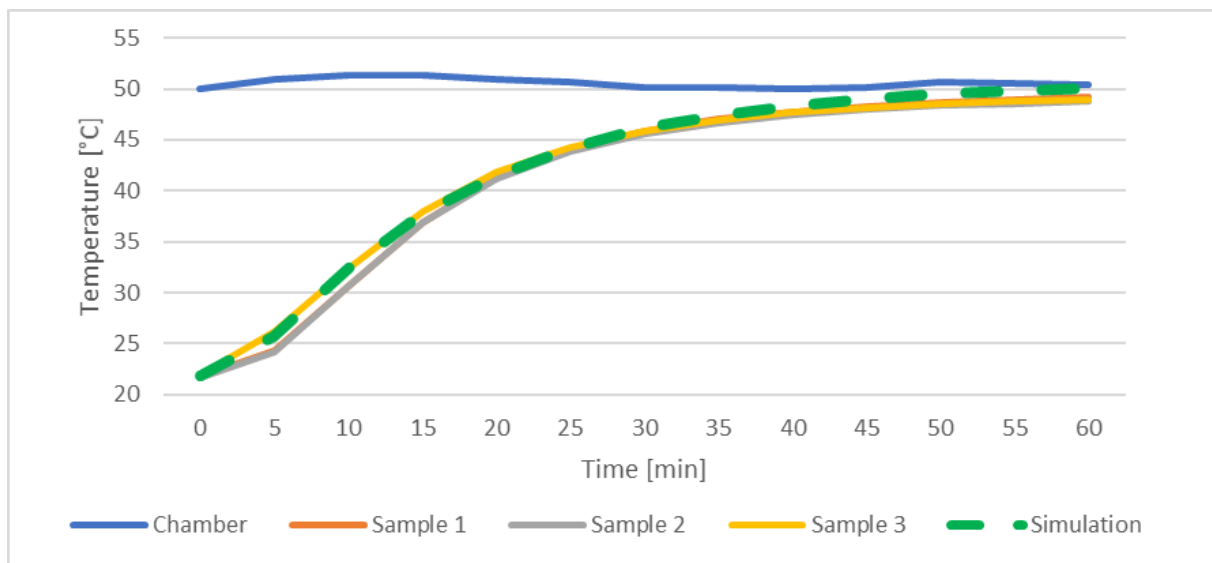

Figure 4: Comparison of experimental and simulated temperatures at 50 °C heat
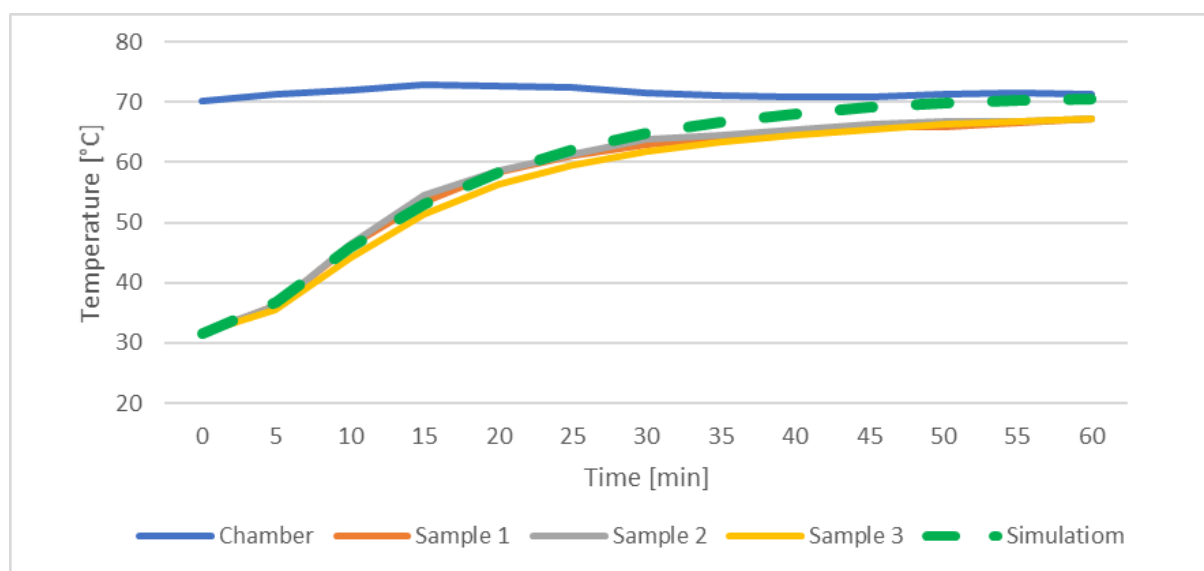
Figure 5: Comparison of experimental and simulated temperatures at 70 °C heat

CONCLUSIONS

Throughout the diverse technological processes in the wood industry, it is necessary to treat and store raw materials at given temperatures. Therefore, the heat transfer process should be carefully investigated. In order to gather more physical properties from hardwoods, the thermal conductivity of Turkey oak was modelled using the finite element method. Comparing the modelled and measured temperatures, a maximum difference of 3.38°C was observed, indicating a maximum relative deviation of only 5.35% at higher heating temperatures. At a lower heating temperature, the model is even more precise. In this case, at the vast majority of measurement points, the relative deviation was less than 3%. This accuracy can be used for planning the necessary technological time of different heat technological processes. The determination of the more accurate technological times saves time, energy and cost.

REFERENCES

Molnár, S. (2004) Faanyagismeret (Wood Science). Mezőgazdasági Szaktudás Kiadó, Budapest

Parrot, J.E., Stuckes, A.D. (1975) Thermal Conductivity of Solids, Pion, London.

Rohsenow, W., Hartnett, J., Ganic, E. (1973) Handbook of Heat Transfer Fundamentals. McGraw-Hill Book Company, New York, NY, USA

Siau, J.F. (1984) Transport processes in wood, Springer Verlag, Berlin

Sitkei, G. (1994). Faipari műveletek elmélete (Theory of wood processing). Szaktudás Kiadó Budapest

Steinhagen H.P. (1977) Thermal conductive properties of wood, green or dry, from −40° to +100 °C: a literature review. USDA Forest Service General Technical Report (FPL-9), Wisconsin.

Zhang, J., Qu, L., Wang, Z., Zhao, Z., He, Z., & Yi, S. (2017). Simulation and validation of heat transfer during wood heat treatment process. Results in physics, 7, 3806-3812

Possible alternative to creosote treated railway sleepers, Fürstenberg-System Sleeper (FSS)

Szabolcs Komán[1*], Balogh Mátyás Zalán[2], Sándor Fehér[1],

[1] Bajcsy-Zs. u. 4., 9400 Sopron, Hungary, University of Sopron, Faculty of Wood Engineering and Creative Industries, Institute of Basic Sciences, Department of Wood Science
[2] Bajcsy-Zs. u. 4., 9400 Sopron, Hungary, University of Sopron, Faculty of Wood Engineering and Creative Industries

E-mail: koman.szabolcs@uni-sopron.hu; balmaza23@student.uni-sopron.hu; feher.sandor@uni-sopron.hu;

Keywords: sleeper, bearer, creosote, Fürstenberg-System Sleepers®

ABSTRACT

High-quality railway sleepers are capable of withstanding environmental impacts such as weather conditions and the attack by wood destroying organisms, providing long service life. However, poor-quality railway sleepers, due to their shorter lifespan, can lead to early failures and jeopardize safe railway traffic. Creosote, applied to enhance durability, is harmful to the environment and human health. Research worldwide seeks alternatives, emerging not only from new preservatives but also from manufacturing technology. One possible solution is the application of Fürstenberg-System Sleeper®, offering alternatives to currently used sleepers, from machining processes that promote drying, to new wood preservatives, to species-specific impregnation processes.

INTRODUCTION

Railway sleepers continue to be used worldwide in track construction for standard tracks, switches, bridges, light railways, and tunnels. Due to favorable vibration and noise characteristics, they are suitable for train speeds below 160 km/h. They are easily machinable and can be adapted to unique track gauges. They are advantageous for sharp curves in mountain railways. Their low weight facilitates transportation and movement even without machinery in underground track construction. Environmentally friendly oak bridge sleepers can be used without preservative treatment. Compared to concrete sleepers, wooden sleepers have advantages in bending, compression, and flexibility but are susceptible to biotic damage. In extremely cold climates, the use of concrete sleepers is not possible as frozen moisture in cracks leads to deterioration of the base. The lifespan of wooden sleepers in railway tracks can be increased by 3-6 times following treatment with preservatives, with a maximum lifespan of about 30 years or more.

Generally untreated wooden sleepers undergo an itemized inspection, thus each sleeper to be treated with a wood preservative and or being installed undergoes individual examination. The quality requirements of untreated wooden sleepers are specified in the European standard EN 13145:2001+A1:2012. The standard describes various quality characteristics, permissible wood defects, wood species, manufacturing parameters, shapes, dimensions, tolerances, as well as durability and preservative treatment criteria. In Hungary, the certification is carried out by a testing organization accredited for this standard, involving approximately 15-18.000 standard sleepers and 1500-2000 m³ of switch sleepers annually.

Saturation can only be carried out on properly prepared sleepers, primarily regarding moisture content. If the wood cells are saturated with water, the preservative cannot penetrate, so the wood must be dried beforehand. The speed of drying also matters, as too rapid drying leads to various deformations and large cracks.

Prolonged natural drying, depending on weather conditions, allows for the colonization of decay fungi. Cracking is a natural consequence of drying. If this is not visible on the wood, it is likely that its moisture content is still too high. Cracks can develop for various reasons, whether as a result of drying or due to frost. Determining how these cracks formed and how they affect the strength and lifespan of the sleeper to be installed must be decided by a trained inspector for each individual piece.

In recent decades, the environmental and human health impacts of treating railway sleepers have come to the forefront. Creosote, the traditional wood preservative for railway sleepers, has been classified as a biocide in Europe, and its use was permitted for only a few years starting from 2016, with multiple extensions granted thereafter. The most recent extension occurred in 2022 (European Commission Regulation 2022/1950), permitting the use of creosote - albeit with restrictions and only in certain member states - until October 31, 2029.

Due to the importance of environmental and human health considerations, the long-term use of creosote is ruled out. Therefore, railway sleeper manufacturers are collaborating with scientific research institutes and universities to find alternatives to creosote, while retaining all the benefits it provides:

- Improving and maintaining the wood's resistance to biological attack over the long term,
- Hydrophobizing the surface of sleepers,
- Preserving the long-term flexibility of railway sleepers,
- Multiplying the service life of the wood.

Fürstenberg-System Sleeper®

The Fürstenberg-System Sleepers®, have more than a decade of application experience and have been installed in over half a million units across the European rail network (Figure 1).

The key components of the system are:

- New in Europe mechanical pre-treatment through incising perforation.
- The use of alternative oil-based wood preservatives.
- Wood species-specific impregnation process:
    - a. Single impregnation for oak.
    - b. Double impregnation for beech and pine species.

Figure 1: Advantages of Fürstenberg-System Sleepers® 1, Sleepers in their raw state: sustainable raw material, CO2-neutral, positive impact on ecological balance 2, Saturation: Tar-free, approved under the European biocide products regulation, environmental and occupational health benefits 3, After treatment, it has minimal odor and is 100% recyclable (fuerstenberg-thp.de)

Overview of Fürstenberg-System Sleeper® Technology

Mechanical pre-treatment

Mechanical pre-treatment (incising) of sleepers is carried out before drying and impregnation (Figure 2). All four longitudinal surfaces of the sleepers are machined, creating perpendicular surfaces to the grain direction, which facilitate more uniform removal of free and bound water along the entire length of the sleepers.

- Facilitates faster and more uniform drying
- Reduces drying cracks, resulting in fewer long, deep cracks

As a result of machining, the sleeper dries more uniformly and quickly, resulting in fewer large and long, quality-degrading deep cracks on the surface, thereby reducing drying losses and ensuring more uniform distribution of internal stress in the inner layers of the wood.

- Facilitates greater penetration of preservatives
- Optimizes and ensures more uniform application of preservatives for long-lasting protection

Treatment with alternative oil-based wood preservatives

- Use of alternative oils as the base for wood preservatives

SleeperProtect®, an alternative oil-based wood preservative, specifically developed for treating railway sleepers, is water-free. To ensure biological efficacy, it contains copper-based and organic

agents. This combination has been proven effective in wood protection for decades. The alternative oils serve as carriers for the active ingredients and also exhibit very effective water-repellent properties. Additionally, they provide greater flexibility to the impregnated sleepers. After treatment, the oils dry and solidify, creating a dry surface that facilitates handling.

- Water-repellent properties contribute to maintaining the flexibility of wooden sleepers for many years
- Free from tar oils and their constituents
- All active ingredients meet the requirements of the European biocide products regulation
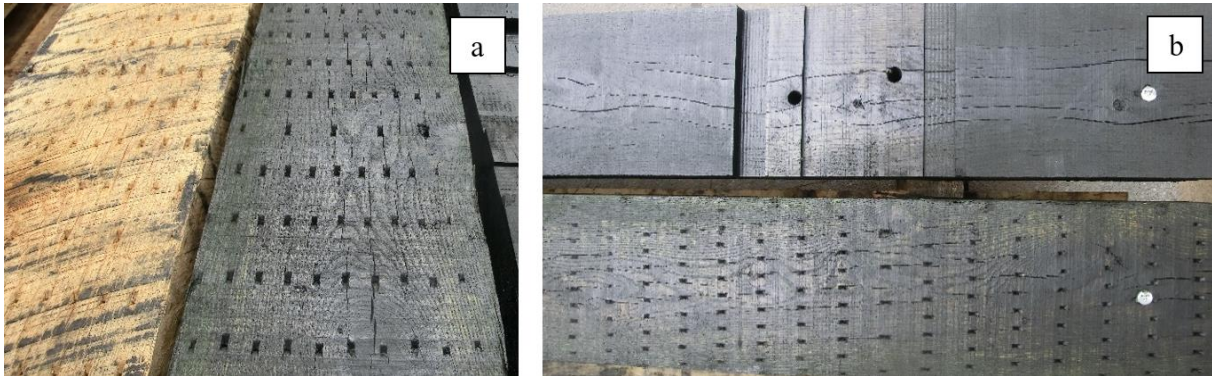- Minimal odor

Figure 2: Image of mechanical machining before and after impregnation (a), and as a result of incising, fewer deep longitudinal cracks develop on the surface of the sleepers (b)

After mechanical machining and achieving the appropriate moisture content, the sleepers undergo treatment with wood preservatives (Figure 3). The impregnation process is controlled in a computer-controlled impregnation plant, where the appropriate protection of the sleepers is achieved through an optimized impregnation process tailored to the wood species and preservative. The impregnation plant enablesempty and full cell processes , where predetermined vacuum and pressure cycles are fully controlled by the computer. This includes temperature regulation during the process, as well as control over various process parameters and preservative intake. The computer performs the setting of appropriate parameters and continuous monitoring according to pre-programmed impregnation and process protocols.

For the Fürstenberg-System Sleeper®, the impregnation technology is specialized for each wood species to achieve the most effective protection. For oak wood species, the Protect OS-320 B (SleeperProtect®) wood preservative from Koppers is used. For beech and pine wood species, a double impregnation process is used for adequate protection:

- Initially, the sleepers are impregnated with water-based wood preservatives, typically using Korazit KS or Wolmanit CX wood preservatives.
- In the second step, once the wood has reached its saturable moisture content, impregnation with Protect OS-320 B preservative is also carried out.

Figure 3: Cross-section of beech sleeper before saturation (a), Cross-section of fully saturated beech sleeper with water-based preservative (b), Image of saturated area after second saturation with SleeperProtect (beech, dark green area) (c), Image of saturated area after second saturation with SleeperProtect (Scots pine, dark green area) (d)

The possible reuse of Fürstenberg-System Sleepers® railway sleepers

The secondary use of railway sleepers impregnated with creosote is severely restricted due to the biocide agents contained within them. Any residential reuse of removed sleepers from the track has been prohibited for decades. Working with them without protective gear is prohibited, as both skin contact and inhalation of the emitted substances are highly hazardous to health. According to the latest regulations, users must ensure that no creosote or creosote-saturated residues enter bodies of water or soil, and they must also ensure that the public cannot access creosote-saturated sleepers under any circumstances. Practically, sleepers removed from the track can only be disposed of/incinerated in specially designed power plants.

In contrast, after refurbishment, the Fürstenberg-System Sleeper® can be reintegrated into lower-grade tracks (private railways, industrial sidings), and they can also be used for energy purposes and private use (e.g., garden paths, landscaping elements, agricultural posts, etc.) - of course, in accordance with other applicable regulations in the given country.

CONCLUSIONS

The elements of railway track superstructure include sleepers, crossing sleepers, and bridge beams. From safety and economic perspectives, the goal is to install suitable quality bearers and keep them on the track for as long as possible. In recent decades, the increasing emphasis on ecological, environmental, and health considerations, along with the expected complete ban on creosote use, has brought alternative solutions to the forefront. The Fürstenberg-System Sleeper® is an alternative to creosote-treated sleepers, ensuring continued use of wooden sleepers in railway construction even with the ban on creosote use. The system has been registered with the European Patent Office (EPO 17169384.9), ensuring that the quality of every sold FSS sleeper remains consistently high.

ACKNOWLEDGMENTS

REFERENCES

Commission Implementing Regulation (EU) (2022) 2022/1950 of 14 October 2022 renewing the approval of creosote as an active substance for use in biocidal products of product-type 8 in accordance with Regulation (EU) No 528/2012 of the European Parliament and of the Council

Djarwanto D., Suprapti, S., Rulliaty S (2018) Service Life of Railway Wood Sleepers in Indonesia. Wood Research Journal. 2018/6. pp. 1-7. https://doi.org/10.51850/wrj.2015.6.1.1-7

EN 13145:2001+A1(2012) Railway applications. Track. Wood sleepers and bearers. European Committee for Standardization, Brussels

Fischer Sz, Eller B, Kada, Z, Németh A (2015) Vasútépítés. Universitas-Győr Nonprofit Kft., ISBN 978-615-5298-68-4 (in Hungarian)

Fürstenberg holz® (2024) https://www.fuerstenberg-thp.de/en/products/sleepers/fss-fuerstenberg-system-sleeper/ Accessed 10 Apr 2024

Medvedev I N, Parinov D A, Shakirova O. I. (2019) Railroad ties produced from modified wood for cold climate regions. IOP Conf. Ser.: Earth Environ. Sci. 392 012064. https://doi.org/10.1088/1755-1315/392/1/012064

Investigation of bendability characteristics of wood-based polymer composites

S. Behnam Hosseini[1], Milan Gaff[1,2*]

[1] Mendel University in Brno, Department of Furniture, Design and Habitat Brno, 61300 Brno, Czech Republic.
[2] Czech Technical University in Prague, Faculty of Civil Engineering, Experimental Centre, Thakurova 7, 166 29 Prague 6, Czech Republic.

E-mail: sbh4070@gmail.com; gaffmilan@gmail.com

ABSTRACT

Bending is a widely utilized method for shaping materials, and it plays a significant role in many wood-based material processing technologies. The ratio of the thickness of material to the smallest curve radius obtained is the most common way to express the feature of bendability, which is largely dependent on the thickness of the material. In other words, the smallest possible curve radius for the bent material can be used to determine a material's bendability. Nonetheless, not enough research has been done on the theoretical definition of bendability. The main objective of this study is to determine the effect of factors such as different content and percentage of fillers, and polymer matrix on selected mechanical properties of wood-based composite based on sawdust and waste polyethylene terephthalate (PET). The bendability properties including R_{minB}, R_{minC}, K_{bendB}, K_{bendC} were measured using three-point bending test. The investigation's findings showed that the evaluated parameters have varying effects on each bending characteristic. However, filler percentage and polymer matrix showed significant effect on majority of mechanical properties.

INTRODUCTION

Wood-plastic composites (WPCs) refer to materials that, based on the composite definition, are made of two or more different materials, mainly wood particles and polymers, as well as some other additives or fillers. There are a wide range of natural fibers to produce this kind of composite, but in terms of polymer choice, the options are so limited, and the thermoset or thermoplastic polymer should have a lower melting point than the thermal degradation temperature of lignocellulosic materials. It is possible to shift from wood particles and first-hand polymers to waste natural fibers and polymers, including sawdust and waste bottles to minimize environmental and economic concerns (Hosseini et al. 2023). The combination of different materials turned WPCs into an engineered material with varied applications such as playground equipment, indoor and outdoor furniture, windows and door frames, interior and exterior design, etc. An appropriate mechanical performance is required for all the mentioned applications, but among them, the bending properties are so important because WPC products are usually faced with bending loads during service situations.

The bending diagram consisted of force-deflection results of samples under bending stress that divided into two main parts of elastic and plastic by proportionality limit (figure 1). Based on flexural results and bending diagram, many mechanical properties are calculable such as bending strength, modulus of elasticity, modulus of plasticity, plastic potential, and bendability. Most studies investigate the common flexural properties, but do not provide other bending characteristics like bendability that defines as the minimum curved radius before material's failure. There are limited sources about bendability of wood and wood based materials. However, many authors confirmed that thickness of materials is the key factor in bendability characteristic (Gaff et al. 2015; Candan et al. 2012; Colakoglu et al. 2003) and bendability coefficient. The current work investigated the effect of different compositions on the bendability properties of sawdust-rPET composites including bendability and its coefficient using three-point bending test.
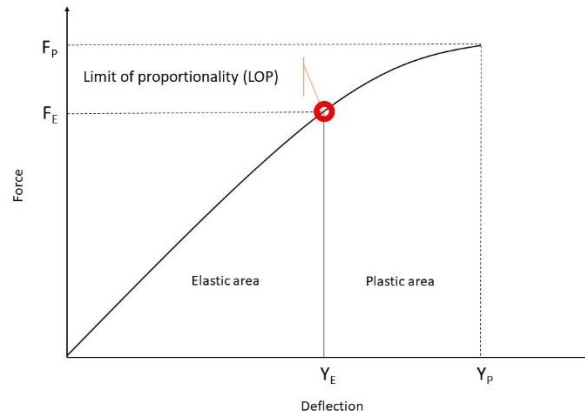
Figure 1: A typical Force-Deflection diagram

MATERIALS AND METHODS

The 0.5 mm sawdust, 0.2 mm rubber particles from waste tires, waste PET bottles and "Enmat Y1000P" biodegradable polymer were used to produce wood plastic composites according to table 1. All materials dried in an oven at $103 \pm 2°C$ for 24 hours. WPC panels ($39 \times 39 \times 0.5$ cm) were prepared by flat press method using hot press (190°C, 5 N/mm^2), then they cut and trimmed to prepare the experimental samples for three-point bending test.

Table 1: The composition of composites

Composite Code	Composition
1	Sawdust (40%), PET waste (60%)
2	Sawdust (60%), PET waste (40%)
3	Sawdust (50%), Y1000P polymer (50%)
4	Sawdust (20%), rubber (40%), PET waste (40%)

According to definition, bendability is the minimum curve radius of sample under bending load before failure. Gáborík and Dudas (2006) provided equation 1 to calculate bendability that can be taken as a first approximation of R_{minA} for test specimens of small thicknesses.

$$R_{minA} = \frac{l_0^2}{8y_{max}} + \frac{y_{max}}{2} \tag{1}$$

Gaff et al. (2006) provided more precise measurement of bendability based on geometry of samples (figure 2) for greater thicknesses (eq. 2) and also equation 3 based on the basic relationship of bending that were used in current study.

$$R_{minB} = \frac{l_0^2}{8y_{max}} + \frac{y_{max}}{2} - \frac{h}{2} \tag{2}$$

$$R_{minC} = \frac{l_0^2}{12y_{max}} \tag{3}$$

where "h" is height of samples, "l_0" is the distance between two supports, "y_{max}" is the maximum deflection, and "R" (R_{minA}, R_{minB}, R_{minC}) is the minimum bending radius.

The coefficient of bendability K_{bend} is defined a ratio of material thickness (h) to minimum curve radius which are calculate based on equations 4-6 (Gaff et al. 2006) :

$$K_{bendA} = \frac{h}{R_{minA}} \tag{4}$$

$$K_{bendB} = \frac{h}{R_{minB}} \tag{5}$$

$$K_{bendB} = \frac{h}{R_{minB}} \tag{6}$$

ANOVA analysis with 95% confidence and Duncan's grouping test were used to evaluate the effect of different variables on bendability properties of bio-composites using STATISTICA software (version 14, Statsoft Inc., USA).

RESULTS AND DISCUSSION

Figure 2 and table 2 shows the bendability (R_{minB}) of bio-composites as well as Duncan grouping results, respectively. The biodegradable polymer composite containing 50% sawdust revealed the maximum bendability (349.49) whereas rPET composite reinforced with 20% sawdust and 40% rubber revealed the minimum value of bendability (308.15). However, according to Duncan grouping test (table 2), there is no significant difference between studied composites.

Figure 2: The effect of different compositions on the bendability (R_{minB})

Table 2: The Duncan's test results of the bendability (R_{minB}) of wood plastic composites as function of different composition

Composites	(1) 332.77	(2) 327.17	(3) 349.50	(4) 308.16
1		0.781087	0.409144	0.254144
2	0.781087		0.300673	0.348681
3	0.409144	0.300673		0.065526
4	0.254144	0.348681	0.065526	

The bendability (R_{minC}) of reinforced composites based on the basic relationship of bending was indicated in figure 3. The results of bendability (R_{minC}) and Duncan grouping test (table 3) showed similar trend with bendability (R_{minB}), where biodegradable polymer composite containing 50% sawdust depicted higher bendability (R_{minC}) (233.01) compared to other studied composites. The reinforced composites containing 60% filler (mixed natural fiber and rubber particles) showed minimum bendability (R_{minC}) of 204.78 among rPET-composites. As it was obvious from the Duncan grouping test (table 3), there was no significant difference between all evaluated compositions.
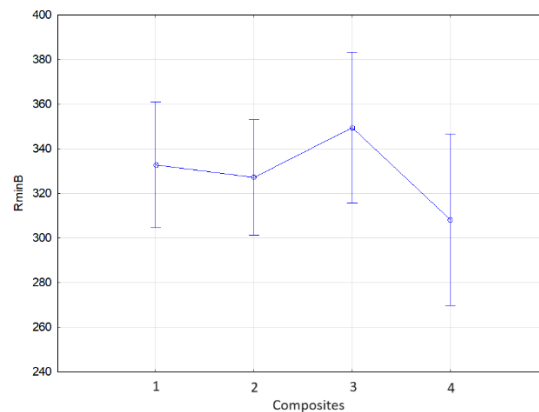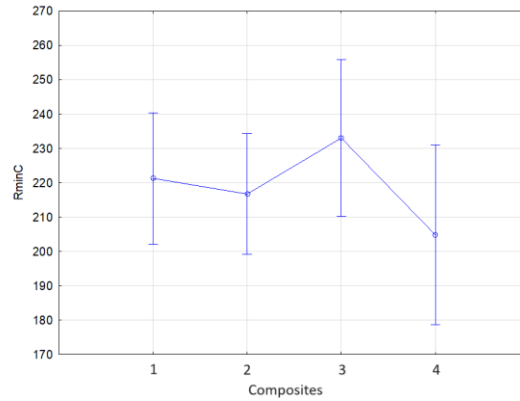
Figure 3: The effect of different compositions on the bendability (R_{minC})

Table 3: The Duncan's test results of the bendability (R_{minC}) of wood plastic composites as function of different composition

Composites	(1) 221.29	(2) 216.74	(3) 233.01	(4) 204.79
1		0.739134	0.392387	0.258717
2	0.739134		0.265114	0.383608
3	0.392387	0.265114		0.063156
4	0.258717	0.383608	0.063156	

The results of the coefficient of bendability (K_{bendB}) were depicted in figure 4, where biodegradable reinforced composite by 50% sawdust showed minimum K_{bendB} (0.019). Both 60% filled composites (60% sawdust and 60% mixed sawdust-rubber) revealed almost same values of 0.024 and 0.025, respectively. According to figure 4, the 40% sawdust-rPET composite with lower amounts of fillers reached to maximum coefficient of bendability (0.028) compared to higher filler ratio composites (50-60%). Duncan grouping test results of K_{bendB} revealed only two non-significant difference with confidence level of 95% among all investigated composites (table 4), where there is no significant difference between K_{bendB} values of 60% filled composites (composites No. 1 and 4) and also 60% mixed sawdust-rubber with 40% sawdust-rPET composite (composites No. 2 and 4).

Figure 4: The effect of different compositions on the coefficient of bendability (K_{bendB})

Table 4: The Duncan's test results of the coefficient of bendability (K_{bendB}) of wood plastic composites as function of different composition

Composites	(1) 0.02454	(2) 0.02801	(3) 0.01909	(4) 0.02503
1		0.035143	0.001047	0.749163
2	0.035143		0.000054	0.056035
3	0.001047	0.000054		0.000571
4	0.749163	0.056035	0.000571	

Regarding the obtained results, the biodegradable polymer composite containing 50% sawdust showed minimum amount of the coefficient of bendability (K_{bendC}) (0.028) among all studied composites (figure 5). By contrast, the maximum K_{bendC} (0.042) observed for 40% sawdust-rPET composite. Comparing the results of K_{bendC} with K_{bendB} demonstrates that the coefficient of bendability based on bendability relation (K_{bendC}) is noticeably higher than geometry based values (K_{bendB}) and the results of this study confirmed by Gaff et al. (2006). There was no significant deference between 40% sawdust-rPET composite with 60% mixed filler composite containing 40% rubber and 20% sawdust according to the Duncan test results (table 5). Although Duncan results showed no significant difference between 40% sawdust-rPET and 60% mix filled rPET composites, but their deference was in borderline of 95% confidence level (table 5).
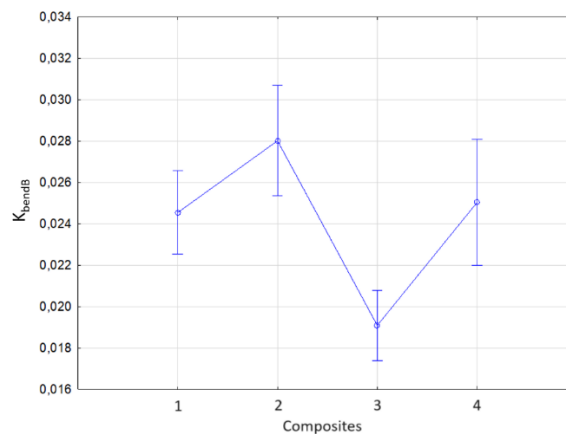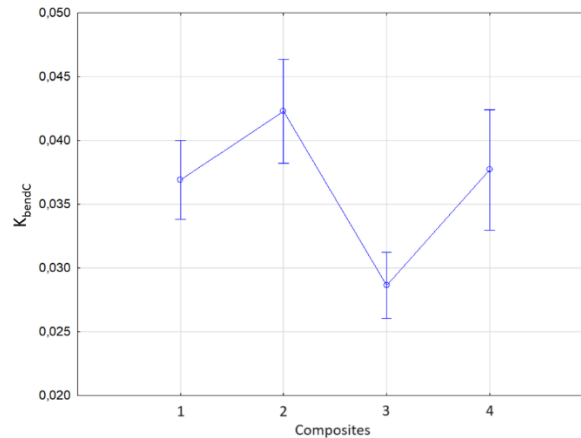

Figure 5: The effect of different compositions on the coefficient of bendability (K_{bendC})

Table 5: The Duncan's test results of the coefficient of bendability (K_{bendC}) of wood plastic composites as function of different composition.

Composites	(1) 0.03692	(2) 0.04230	(3) 0.02864	(4) 0.03771
1		0.033555	0.001169	0.735227
2	0.033555		0.000054	0.055736
3	0.001169	0.000054		0.000611
4	0.735227	0.055736	0.000611	

CONCLUSIONS

This study assessed the impact of different polymer materials and additives on the bendability properties of wood plastic composites in a three-point bending test. The findings demonstrated that bendability characteristics are influenced by both the filler and the composite matrix; however, the matrix's effect is much more significant than filler quantities. The collected results indicated that Y1000P exceeded rPET polymer in terms of bendability characteristics and the biodegradable reinforced polymer containing 50% sawdust performed best overall. According to the study's findings, mechanical properties of the rPET composite noticeably declined as the filler percentage increased from 40% to 60%. Based on the experimental data, bending coefficients derived from the geometric method are significantly lower than those derived from the basic bending equation. There was no significant difference in the bendability properties of rPET-reinforced composites filled with 60% filler (both 60% sawdust and 20% sawdust + 40% rubber), according to the Duncan grouping results.

ACKNOWLEDGEMENTS

REFERENCES

Candan Z, Ayrilmis N, Dundar T, Atar M (2012) Fire performance of LVL panels treated with fire retardant chemicals. *Wood Res*, *57*(4): 651-658.

Colakoglu G, Colak S, Aydın İSMAİL, Yildiz ÜMİT, Yildiz, S (2003) Effect of boric acid treatment on mechanical properties of laminated beech veneer lumber. *Silva Fennica*, *37*(4).

Gáborík J, Dudas J (2006) Vlastnosti lamelového dreva (The properties of laminated wood). *Proceedings of the Trieskové a Beztrieskové Obrábanie Dreva*.

Gaff M, Gašparík M, Borůvka V, Haviarová E (2015) Stress simulation in layered wood-based materials under mechanical loading. *Materials & Design*, *87*: 1065-1071.

Gaff M, Vokatý V, Babiak M, Bal BC (2016) Coefficient of wood bendability as a function of selected factors. *Construction and Building Materials*, *126*: 632-640

Hosseini SB, Gaff M, Li H, Hui D (2023) Effect of fiber treatment on physical and mechanical properties of natural fiber-reinforced composites: A review. *Reviews on Advanced Materials Science*, *62*(1): 20230131.

Comparing the blossoming and wood producing properties of selected black locust clones

Alexandra Porcsin[1*], Katalin Szakálosné Mátyás[2], Zsolt Keserű[3]

[1,2] University of Sopron, Institute of Forest and Natural Resource Management. Bajcsy-Zs. Str. 4, Sopron, Hungary, 9400.
[3] University of Sopron, Forest Research Institute, Department of Plantation Forestry, 4150, Püspökladány, Farkassziget 3.

E-mail: porcsin.alexandra@gmail.com; szakalosne.matyas.katalin@uni-sopron.hu; keseru.zsolt@uni-sopron.hu

Keywords: black locust, cultivars, blossoming, growth

ABSTRACT

Black locust (*Robinia pseudoacacia* L.) is a tree species introduced from North America, and it's well known for its positive economical and negative ecological properties, making it one of the most widely distributed tree species in European countries. Despite its rapid growth, its wood is hard and weather-resistant so it can be used, for example, as sawn wood products, barked or belted poles and vineyard posts among others and also as planting material for short rotation energy plantations. Its nectare producing ability is excellent as well, black locust honey can make up to 50% of the whole honey production of Hungary. Unfortunately, increasingly hectic weather conditions, late frosts and the rising frequency of destructive storms caused by climate change, which are nowadys more and more noticeable, have a negative impact not only on nectar production but also on the shape of stem (Jovanović 1967, Herman 1971, Vajda 1974, Rițiu et al. 1988). Consequently, fast-growing species with good stem suckers and high nectar production potential are recommended, taking into account the variable future distribution of black locust in Europe (Boer 2013, Kutnar & Kobler 2013, Guoqing et al. 2014, Giuliani et al. 2015, Dyderski et al. 2017). To decide which cultivars can be used to help the beekeepers as well as foresters, which ones are more resistant to climate change and the biotic and abiotic damages, we need to compare their growth and their blossoming properties. The height of the tree is determined firsthand by genetics, the diameter at breast height is defined by growth space according to most authors but in a recent study Ábri and Keserű (2023) found that the linkage wasn't significant in terms of juvenile black locust cultivars. There is a trade-off in most plants regarding growth and generative reproduction on the edges of distribution unrelated to whether it's the dry (South) or the cold (North) end of it (Willy and Buskirk 2022). We must therefore need to find the correlation breakers which won't show the traits of not only these trade-offs, but those regarding resistant and resilient traits and can be selected by phenotype.

INTRODUCTION

Black locust (*Robinia pseudoacacia* L.) is native to the eastern parts of North America and is imported into Europe from only a small number of populations (Bouteiller et al. 2018). Within Europe, it was mainly introduced by human activity in the 17th and 18th centuries, which led to its expansion in e.g. Germany, Hungary and the Czech Republic one century later (Hegi 1924, Nožička 1957, Böhmer et al. 2001, Bartha et al. 2008). The last boost to its spread in Europe came from the devastation of the world wars (Kohler & Sukopp 1964). In terms of its ecological requirements, black locust is highly drought tolerant in Europe and can survive with only 500-550 mm of total annual precipitation instead of the 1020-1830 mm usually required in its original distributional area (Nicolescu et al. 2020). The decline in the allelic diversity of black locust in its new habitat following its introduction into Europe was also driven by its small population size, which included only a few import activities (Uller & Leimu 2011, Bouteiller et al. 2018). This allelic decline may have implications for its future response to climate change (Enescu & Dănescu 2013).

Black locust is demanding on soil aeration, grows sluggishly on compacted clayey soils, and does not tolerate waterlogging (Rédei 2020). Future alternatives to the areas currently occupied by beech and

silver fir will include the expansion and planting of black locust, red oak, turkey oak, and fluttering elm species if the predicted northward shift occurs due to a temperature increase of 2.9°C or 4.5°C (Thurm et al. 2018). Despite its rapid growth, black locust wood is hard and weather resistant. Black locust covers up to 24% of the forested area in Hungary. It provides a livelihood for tens of thousands of people in the forestry, sawmill, and beekeeping sectors, but the native range of North American black locust populations are located 5-10° further south (Bartha et al. 2008) than the current habitat in Hungary. The increasing frequency of late frosts and destructive storms exert negative impacts on both nectar production and stem structure (Jovanovič 1967, Herman 1971, Vajda 1974, Riťiu et al. 1988). This sensitivity usually results in second flowering, drastically reducing the annual black locust honey production. Increasingly volatile, climate change-induced weather conditions are the main problem facing black locust today. Consequently, fast-growing species with good stem suckers and high nectar production potential are recommended. The economic aspects of using black locust include the widespread belief of a trade-off phenomenon between the long and abundant flowering of the species and its ability to produce quality wood for the sawmill industry. Trade-off is based on the observation that the life cycles of organisms are paired, so they can only enhance one at the expense of the other. Nevertheless, we must mention that no one has found any significant correlation in the case of tree species like pines or poplars. The hypothesis of this study is that there is no trade-off phenomenon between the intensive flowering capacity and the height growth of black locust when it's not on the dry edge of its distribution, using height as a measuring point since it is mostly determined by genetics.

MATERIALS AND METHODS

We performed the measurements in four forest subcompartments, namely Isaszeg 8/C, Isaszeg 8/E, Debrecen 17/C and Kecskemét-Méheslapos. The two subcompartments at Isaszeg are both located outside of the Gödöllő Arboretum, near the former Forest Research Institute's (hereinafter: FRI) experimental station. The plots at the Gödöllő Arboretum are at 200–220 m altitude, the subcompartment near the city of Debrecen is at an altitude of 121 m and Kecskemét-Méheslapos is at 105 m. All four subcompartments contain state-approved cultivars, candidate cultivars, clones selected for timber production, apiculture purposes, or a combination of both. Using the flowering and timber production values of the commercial black locust individuals in the plots as standard, we can measure the economic advantage of the selected clones and cultivars. The planting network is 2.5 x 1.0 m in all the subcompartments. There is a significant correlation between the average intensive flowering period (which occurs when the flowering is in its third or fourth stage and the average length of flowering (Isaszeg 8/C *p=0,879773*, Isaszeg 8/E p=*0,918902*) (Porcsin et al. 2021). The common black locust trees were planted from seedbed plants.

There are four different clones in the *Debrecen 17/C* subcompartment. We marked 30 stems altogether with the common black locust on the area. These include a clone (*R. p. 'Guth-189'*), a previously state-approved clone (*R. p. 'Szajki'*), and state-approved cultivars (*R. p. 'Appalachia' and R. p. 'Nyírségi'*). The state approved cultivars and the *R. p. 'Szajki'* clone were planted from root suckers; the clones are planted from micropropagated planting material.

There are two subcomparments in the Gödöllő Arboretum, *Isaszeg 8/C* and *Isaszeg 8/E*. We marked 78 stems in these plantations. The age difference isn't significant (3 years), so we can assume their flowering capacity is the same. Since there isn't common black locust in the Isaszeg 8/E subcomparment, we use the data from the Isaszeg 8/C one. The state-approved cultivars were planted from root suckers as well as some of the clones registered as state-approved in previous years, but not listed as them in 2024. The candidate cultivars (*R. p. Oszlopos', R. p. 'Homoki', R. p. 'Szálas', R. p. 'Vacsi'*) and the clones *(R. p. 'Nyírségi-12', R. p. 'PV-BORZ', R. p. 'PV 201 E 2/3', R. p. 'Rózsaszín-A', and R. p. 'Rózsaszín-B'*) have been planted from micropropagated planting material.

The Kecskemét-Méheslapos subcompartment was planted in 1996 and expanded by 5 clones in 2000 and added 8 more in 2002. We marked 48 stems in it. This place clearly shows the signs of the dry end of the black locust's ditribution area, since from the 45 parcels we found living plants (at least 3 to mark for study) only in 31. Besides climate change, the main reason for this was probably the damage which was caused by the locust digitate leafminer (*Parectopa robiniella*) and *Phyllonorycter robiniella*. The clones have been planted from micropropagated planting material as well as in the other experimental areas.

Methods

During the measurements, we observed the flowering stages and the extent and abundance of blossoming in May and June and recorded tree height and diameter outside of the vegetation period. Measurements of the flowering stages and the abundance should occur at the same time every day to ensure accuracy, preferably from more than one angles at least every two days. The stems were around 20 m in height, so we measured the flowering qualities with a telescope. The method follows the work of Imre Csiha.

The extent of flowering of the stems was determined based on the following criteria:

I. extent: No flower (no inflorescence is visible in the crown of the stem).

II. extent: Few flowers (flowering can be seen on 1/3 of the crown of the stem).

III. extent: Medium amount of flowers (the inflorescence can be seen on 2/3 of the crown of the stem).

IV. extent: Abundant flowers (the flowers are visible on the whole crown of the stem).

V. extent: Abundant flowering on each branch of the tree

The criteria below separate the flowering stages:

First flowering stage: Only green buds in a closed stage are visible.

Second flowering stage: The white ends of the flowers are visible at the end of the buds.

Third flowering stage: Most of the flowers are white and in an open-bud stage.

Fourth flowering stage: The flowers are fully open, and the entire inflorescence is white.

Fifth flowering stage: Wilted flowers appear in the crown; the white and brown colors are mixed and the petals beginning to fall. Scattered fallen flowers appear on the ground.

We used a Vertex height-measuring instrument with a measuring unit and an associated transponder to measure tree height. We employed a π-tape to measure the diameter at breast height (DBH) because it allowed us to read the measurement immediately.

RESULTS AND DISCUSSION

The criteria to be classified as "better" is to reach a flowering period that is at least two days longer and to have a higher height than the common black locust stems. We took common black locust stem volume to be 100% to determine the superiority of the clones and cultivars (Table 1). We used different values to determine the clones' volumes because of their straighter trunk shape and smaller crowns (Veperdi 2001).

Table 1: Performance of the clones compared to common black locust in their subcompartment

Subcomparment	Name of the clone	Average flowering period (day)	Intensive blooming period (day)	Average diameter at breast height (cm)	Average height (m)	Performance (%)	Average volume (m³)	Performance (%)
Isaszeg 8/C	Common black locust	18	7	12.9	16.3	100	0.12	100
	R. p. 'Oszlopos'	22	11	14	16.5	101	0.14	117
	R.p. 'PV-BORZ'	23	11	14.6	17.4	107	0.16	133
	R.p. 'Váti-46'	23	10	15.5	18.7	115	0.22	183
	R.p. 'PV 201 E 2/3'	21	10	16.6	18.1	111	0.21	175
Isaszeg 8/E	R.p. 'PV 201 E 2/3'	22	10	12.9	16.3	100	0.14	117

The comparing revealed that only cultivars from the two Isaszeg subcompartments showed greater values than the common black locust in the same area. There weren't any clones that would fit the criteria of greater volume and 2 days more of average and intensive blooming period length. These results show that the area of Kecskemét-Méheslapos and Debrecen aren't and won't be valuable for black locust cultivars to plant. Regarding the two still valuable plots, *R. p. 'Oszlopos', R. p. 'PV-BORZ, R. p. 'Váti-46'* and *R.p. 'PV 201 E 2/3'* is better for both wood harvesting and beekeeping reasons. These clones can also be the so-called correlation breakers. As the results show, there is no trade-off phenomenon between the intensive flowering capacity and the height growth of black locust when it's not on the dry edge of its distribution, so our hypothesis is true. The correlation between height (m),

volume (m^3), length of average flowering and blooming period (day) weren't strong to begin with, but in the drier ends of the areas (Debrecen and Kecskemét) and correlation was even smaller or slightly negative (Table 2). We can assume that this is because of the trade-off examined in other plants between growth and sexual production.

Table 2: Correlation between height, volume and flowering period lengths

p values	Kecskemét	Debrecen	Isaszeg 8/C	Isaszeg 8/E
Volume - Average flowering period	*0.22707*	*0.23085*	*0.34986*	*0.28350*
Height - Average flowering period	*0.23134*	*-0.09791*	*0.32140*	*0.38735*
Volume - Intensive flowering period	*0.64479*	*-0.01117*	*0.15220*	*0.35298*
Height - Intensive flowering period	*0.56200*	*0.07032*	*0.28363*	*0.18355*

The Kecskemét-Méheslapos subcompartment has a strong correlation between volume, height and intensive flowering period length but this occurs because all the numbers were lower regarding these qualities.

CONCLUSIONS

Several factors influence the quality of flowering and stem characteristics. Climate factors influence blossoming the most. The length of the flowering also depends on stand structure, stand age, the number and direction of the gaps and lanes, and the altitude of the population (Fritsch 2012). According to Guoqing L. et al. (2014) and Valeriu-Norocel N. et al. (2020) and an EUSTAT map (2024), it will no longer find its optimum in the southern east planes of Hungary and as our results show this is already happening. Instead, in the next 20-50 years it will spread to our northwest regions where our hills and mountains are. We can predict that since the average temperature will be higher but also the number of days with average temperature below zero will increase, the flowering period will start earlier and will be shorter than nowadays. This will have a devastating effect on our beekeeping industry. While the criteria of the site optimum of different poplar clones and cultivars have been made, no such assessment was made for black locust clones. Although the propagules are vegetatively made (via micropropagation or using root suckers), the generative reproductive capacity of the species may be an indication in future decision-making to maintain allelic diversity and adaptability (which will play a huge role in the face of climate change). We need to work on a cheaper and more effective method of growing black locust and select clones that can tolerate the effects of an even drier but more volatile climate if we want to maintain our beekeeping sector's income and microprogataion may help us in this task.

REFERENCES

Ábri T, Keserű Zs (2023): 'Farkasszigeti' és 'Laposi' akác fajtajelöltek fiatalkori növekedésének értékelése alföldi klimatikus viszonyok mellett, In.: Alföldi Erdőkért Egyesület Kutatói Nap (2023), Tudományos Eredmények a gyakorlatban, 42-52.

Bartha D, Csiszár Á, Zsigmond V (2008): Black locust (Robinia pseudoacacia L.). In: Botta-Dukát Z, Balogh L (Eds.): The Most Invasive Plants in Hungary. Institute of Ecology and Botany, Hungarian Academy of Sciences, Vácrátót, Hungary, pp. 63–76.

Boer E (2013): Risk assessment *Robinia pseudoacacia* L. Naturalis Biodiversity Center, Leiden, 18.

Böhmer HJ, Heger T, Trepl L (2001): Fallstudien Zu Gebietsfremden Arten in Deutschland. Case Studies on Allien Species in Germany, Umweltbundesamt, Berlin.

Bouteiller PX, Veru FC, Aikio E, Bloese P, Dainou K, Delcamp A, Thier De O, Guichoux E, Mengal C, MontyA, Pucheu M, Loo van M, Porté JA, Lassois L, Mariette S (2019): A few north Appalachian populations are the source of European black locust

Dyderski MK, Paź S, Frelich LE, Jagodziński AM (2017): How much does climate change threaten European forest tree species distributions? Glob Change Biol 24:1150–1163

Enescu CM, Dănescu A (2013): Black locust (*Robinia pseudoacacia* L.) – An invasive neophyte in the conventional land reclamation flora in Romania

EUSTAT map (2024): https://forest.jrc.ec.europa.eu/media/EU-Trees4F/EU-Trees4F_Robinia_pseudoacacia.html (seen: 2024.03.17.)

Fritsch O (2012): Méhlegelő, az akác. Magánkiadás (in Hungarian)

Giuliani C, Lazzaro L, Mariotti Lippi M, Calamassi R, Foggi B (2015): Temperature-related effects on the germination capacity of black locust (*Robinia pseudoacacia* L., Fabaceae) seeds. Folia Geobotanica 50:275–282

Guoqing L, Guanghua X, Ke G, Sheng D (2014): Mapping the global potential geographical distribution of black locust (Robinia pseudoacacia L.) using herbarium data and a maximum entropy model

Hegi G (1924): Illustrierte Flora von Mittel-Europa. Mit besonderer Berücksichtigung von Deutschland, Oesterreich und der Schweiz. Zum Gebrauche in den Schulen und zum Selbstunterricht. 4 (3) Dicotyledones. J. F. Lehmanns Verlag, München.

Herman J (1971): Forest dendrology. Stanbiro, Zagreb, p 470 (in Croatian)

Jovanovič B (1967): Dendrology with the basics of phytocoenology. Naučna knjiga, Beograd, p 576 (in Serbian)

Klisarič BN, Miljkovič D, Avramov S, Živkovič U, Tarasjev A (2014): Fluctuating asymmetry in *Robinia pseudoacacia* leaves – possible in situ biomarker?

Kohler A, Sukopp H (1964): Über die Gehölzentwicklung auf Berliner Trümmerstandorten. Zugleich ein Beitrag zum Studium neophytischer Holzarten. Ber. Dtsch. Bot. Ges. 76, 389–407.

Kutnar L, Kobler A (2013): The current distribution of black locust (*Robinia pseudoacacia* L.) in Slovenia and predictions for the future. Act. Silv. Lign. 102:21–30 (in Slovenian)

Nicolescu V-N, Rédei K, William LM, Torsten V, E Pöetzelsberger, Jean-Charles B, R Brus, T BenčAț, M Đodan, B Cvjetkovic, Siniša A, N La Porta, Vasyl L, D Mandžukovski, Krasimira P, D Roźenbergar, Radosław W, GMJ Mohren, MC Monteverdi, B Musch, M Klisz, S Perič, L Keça, D Bartlett, C Hernea, M Pástor (2020): Ecology, growth and management of black locust (*Robinia pseudoacacia* L.) a non-native species intergrated int o european forests

Noźička J (1957): Přehled Vy´ voje Našich Lesů. SZN, Praha

Porcsin A, Keserű Zs, Sass I, Szakálosné MK (2021): A gledícsia hatása az ERTI által szelektált fehér akác klónok virágzására (in Hungarian)

Rédei K (2020): Bevezetés az ültetvényszerű fatermesztés gyakorlatába, MED-KÖR Bt.,Kecskemét), ISBN: 978-615-00-8266-0 (in Hungarian)

Rițiu A, Nicolescu L, Nicolescu N (1988): Some considerations on windfalls and windbreaks in black locust forests in the north-west of the country. Rev pădi 3:131–133 (in Romanian)

Thurm EA, Hernandez L, Baltensweiller A, Ayan S, Rasztovits E, Bielak K, Mladenov Zlatanov T, Hladnik D, Balic B, Freudenschuss A, Büchsenmeister R, Falk W (2018): Alternative tree species under climate warming in managed European forests. For Ecol. Manag. 430:485–497

Uller L, Leimu R (2011): Founder events predict changes in genetic diversity during human-mediated range expansions In: Global Change Biology 17, 3478-3458, https://doi.org/10.1111/j.1365-2486.2011.02509.x

Vajda Z (1974): The science of forest protection. Školska knjiga, Zagreb, p 482 (in Croatian)

Valeriu-Norocel N, Rédei K, William LM, Torsten V, E Pöetzelsberger, Jean-Charles B, R Brus, T Benčaț, M Đodan, B Cvjetkovic, Siniša A, N La Porta, Vasyl L, D Mandžukovski, Krasimira P, D Roženbergar, Radosław W, GMJ Mohren, MC Monteverdi, B Musch, M Klisz, S Perić, L Keça, D Bartlett, C Hernea, M Pástor (2020): Ecology, growth and management of black locust (Robinia pseudoacacia L.) a non-native species intergrated int o european forests, https://doi.org/10.1007/s11676-020-01116-8

Veperdi G (2001): Király-féle fatérfogat függvények használata különböző kultivárok térfogatának kiszámolására, pers. comm.

Willi Y, Buskirk Van J, (2022): A review on trade-offs at the warm and cold ends of geographical distributions. Phil. Trans. R. Soc. B 377: 20210022. https://doi.org/10.1098/rstb.2021.0022

The influence of two different adhesives on structural reinforcement of oak-wood elements by carbon and glass fibres

Andrija Novosel[1], Vjekoslav Živković[1]

1 University of Zagreb, Faculty of Forestry and Wood Technology, Svetošimunska 23, HR 10000 Zagreb, Croatia

E-mail: anovosel@sumfak.unizg.hr; vzivkovic@sumfak.unizg.hr

Keywords: Laminated timber, oak – wood, four-point bending, reinforced polymer, DIC

ABSTRACT

Introducing non-wood materials into wood as reinforcements may significantly improve the mechanical properties of wood-based building elements. Various materials and product designs have been studied for this purpose. These include natural fibre materials, steel bars and profiles, glass fibres (glass fibre reinforced polymer, GFRP), carbon fibres (CFRP i.e. carbon FRP), or plates.

However, the compatibility of various non-wood materials with commercial adhesives is not yet fully understood, and the strength and durability of reinforced products are not adequately addressed.

Epoxy resin is generally recommended for glueing CFRP and GFRP, but the PUR adhesives, such as thermoplastic 1-K polyurethane adhesives, and two structural polyurethane adhesives have been used for glulam for nearly two decades. They have been standardized (according to EN 15425 and related standards), but their ability to be used in combination with GFRP or CFRP is still not fully proven.

This work presents a comparative study of two types of fibre reinforcements (carbon and glass) to improve the mechanical properties of oak wood bi-directional laminated beams.

CFRP and GFRP were glued into the laminated beams either with epoxy resin (ER) or with polyurethane adhesives (PUR) and subjected to four-point bending test according to EN 408.

Displacements and deformations were recorded using a 3D video extensometer during four-point bending tests and analysed by digital image correlation (DIC).

The average ultimate load-to-failure results for the samples glued with PUR adhesives are comparable to those glued with epoxy resin (up to 5 % lower). On the other hand, implants glued with PUR adhesives exhibit a displacement reduction of up to 5%.

Having in mind only slightly lower mechanical properties of the beams laminated with polyurethane (PUR) adhesive on one side, and very challenging utilization of epoxy adhesive in industrial conditions on the other side, PUR may be considered as an adequate alternative for bonding wood to CFRP and GFRP reinforcements.

Investigating Kerf Topology and Morphology Variation in Native Species After CO2 Laser Cutting

Lukáš Štefančin[1*], Rastislav Igaz[1], Ivan Kubovský[1], Richard Kminiak[1]

[1] Faculty of Wood Sciences and Technology, Technical University in Zvolen, T.G. Masaryka 24,96001 Zvolen, Slovakia

E-mail: xstefancin@tuzvo.sk; igaz@tuzvo.sk; kubovsky@tuzvo.sk; richard.kminiak@tuzvo.sk

Keywords: LBM, CO2 laser, kerf topology, kerf morphology,

ABSTRACT

Laser beam machining (LBM) has emerged as a promising technology for the precise cutting of various materials, including wood. This study focuses on the impact of laser beam machining using a CO2 laser on the topology and morphology of the kerf of native wood species. Experiments were conducted on beech wood boards processed at different cutting speeds and power outputs. The topology was examined at a microscopic level using a digital microscope. Statistically significant topological changes were observed in the kerf of the wood specimens, including variations in width. Direct study into the morphology of laser cut kerf was substituted by an extensive literature review, offering a comprehensive understanding of the morphology of the kerf.

INTRODUCTION

The emergence of laser cutting in the late 1970s marked its initial entrance into the realm of industry and manufacturing, with specific applications in die board cutting, inlay cutting, furniture manufacturing, marking, and speed prototyping (Hecht 1992). To ensure cost-effective production, it is crucial to consider the maximum feed rate and cut quality when using laser cutting for wood and wood composites, as the input parameters and their levels significantly impact the output quality, necessitating extensive investigations for evaluating the cut quality of representative wood species and composites (Barcikowski et al. 2004; Mushtaq et al. 2020).

Laser Beam Machining (LBM) functions based on the principle of absorbing material energy. This procedure encompasses the transformation of laser energy into thermal energy upon interaction with the target material, leading to localized melting, vaporization, and subsequent removal of material from the workpiece (Shinde and Kubade 2016). Photochemical degradation is employed for cutting thermoset plastics and wood products. In this case, the laser burns the workpiece, resulting in smoke comprising carbon and other components derived from the original material. This technique necessitates more energy compared to simple melting, and the cutting speeds and maximum thicknesses for thermosets are reduced in comparison to thermoplastics. Furthermore, the cut edge of these materials typically displays a flat and smooth surface, which is coated with a thin layer of carbon (Powell and Kaplan 2004). Additionally, laser gas cutting is well-suited for automation (Decker et al. 1984). Laser gas cutting offers a competitive alternative to mechanical cutting methods.

In the current investigation of the CO2 laser cutting of wood, several gaps and potential areas for future exploration have been identified. Mushtaq et al. underscore the necessity for additional research to optimize cutting parameters and enhance the quality of the cuts (Mushtaq et al. 2020) . Simultaneously, Decker et al. stresses the significance of comprehending the material properties and physical mechanisms of the cutting process (Decker et al. 1984). Martínez-Conde et al. furnishes a technical survey of the potential and prerequisites for the successful implementation of CO2 laser cutting in wood (Martínez-Conde et al. 2017), while Radovanovic et al. evaluates experimental inquiries on CO2 laser cutting, with a focus on process parameters and characteristics of cut quality (Radovanovic and Madić 2011).

Guo et al. and Sharma et al. both investigate the influence of processing parameters on the width of the cut in laser cutting, with Guo's study concentrating on wood and Sharma's study on a nickel-based superalloy. Guo's research discovered that a lower moisture content and slower speed produced a superior cutting effect, whereas a higher moisture content and faster speed resulted in a larger yield.

Sharma's study determined that oxygen pressure, pulse width, pulse frequency, and cutting speed were crucial parameters for optimizing the quality of the cut (Sharma et al. 2010; Guo et al. 2021). Yilbas et al. and Duan et al. contribute further insights into the laser cutting process, with Yilbas discussing the impact of laser output power and cutting speed on the width of the cut, and Duan presenting a model for predicting the geometric shape of the cut. These studies collectively emphasize the significance of processing parameters in determining the width of the cut in laser cutting, with potential applications in wood and other materials (Duan et al. 2001; Yilbas et al. 2017). Yilbas et al. found that small variations in laser power, cutting speed, and energy coupling factor significantly alter the size of the cut, and Xu et al. identified a hierarchy of factors that influence the width of the cut in laser cutting, ranking them as laser output power, nozzle height, and cutting speed. The study demonstrated that increased laser power significantly increased the width of the cut, while cutting speed had a minimal impact. Furthermore, an excessive increase in focal length resulted in both widening and shallowing of the cut (Yilbas 2001; Xu et al. 2017). These studies collectively indicate that future research in CO2 laser cutting of wood should concentrate on optimizing cutting parameters, comprehending material properties, and enhancing the quality of the cut.

The primary goal of this study is to refine our understanding of kerf characteristics, specifically focusing on beech wood. This focused approach is intended to develop more effective material utilization strategies. A key objective is to accurately measure the variations in kerf width at both the top and bottom of the cuts in beech wood. These measurements are conducted using optical methods through a digital microscope. This detailed examination is expected to enhance accuracy in material processing applications involving beech wood.

MATERIALS AND METHODS

Beech (Fagus sylvatica L.) was selected as the sample material. This species was picked as a representation of deciduous, diffuse-porous types of trees. The sample sizes were $500 \times 70 \times 6$ mm (length $\times$ width $\times$ thickness).

A thickness of 6 mm was selected as the optimal dimension for processing cultivated wood, based on the efficiency of the employed CO2 laser, which can slice through the material in a single pass. The samples were dried in an environment of $20°C$ and 60% relative humidity. Prior to laser machining, raw materials were milled on a jointer and thicknesser. Kerfs, oriented parallel to the wood fibers and measuring 35mm in length, were cut using a CO2 laser CM-1309 (Shenzhen Reliable Laser Tech, Shenzhen, China) with a peak power capacity of 135 W. Laser power settings were varied at 50%, 75%, and 100%. Feed speeds selected for the study were 5 mm/s, 10 mm/s, 15 mm/s and 20 mm/s.

The kerfs were digitized into three-dimensional models using the imaging capabilities of the Keyence VHX 7000 (Osaka, Japan) digital microscope. This process involved scanning areas measuring 30 x 2.5 mm to achieve high-resolution 3D representations. Following the digitization, we utilized the profile measurement function (Figure 1 & 2) of the Keyence VHX 7000, under a magnification level of x100, to conduct precise measurements of the kerfs' widths. For each parameter change, 30 profile traces were taken. A total of 720 kerf widths were measured.
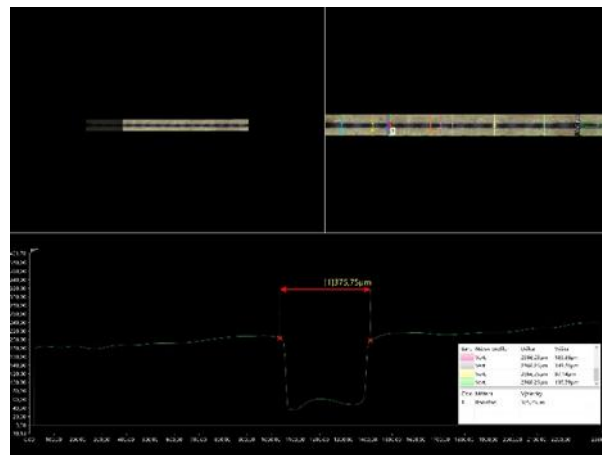

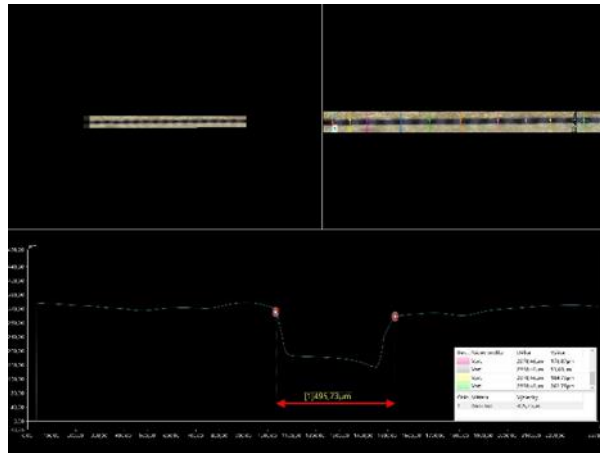*Figure 1: Kerf width measurement in Keyence VHX 7000*

Figure 2: Kerf width measurement in Keyence VHX 7000

RESULTS AND DISCUSSION

The comprehensive analysis of our experimental data examines the intricate relationship between laser cutting parameters (power, speed, and kerf position) and their combined effects on kerf width in CO_2 laser wood cutting. The data set was subjected to statistical evaluation using the STATISTICA 12 software (Tulsa, USA). Prior to this, any outliers associated with individual laser powers and feed speeds were removed from the data set. A three-factor analysis of variance with interaction (ANOVA) was conducted afterward. The dataset met the requirements of normality, equality of variance, and independence of measurements.

Table 1: Three-factor analysis of variance (ANOVA)

Effect	p-level
Side	0.000**
Power	0.000**
Speed	0.000**
Side*Power	0.001**
Side*Speed	0.000**
Power*Speed	0.000**
Side*Power*Speed	0.000**

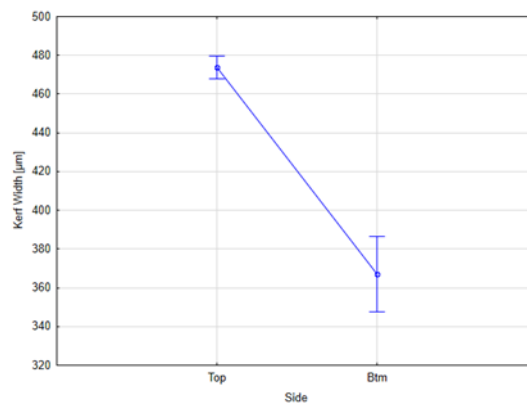*** Statistically significant effect*
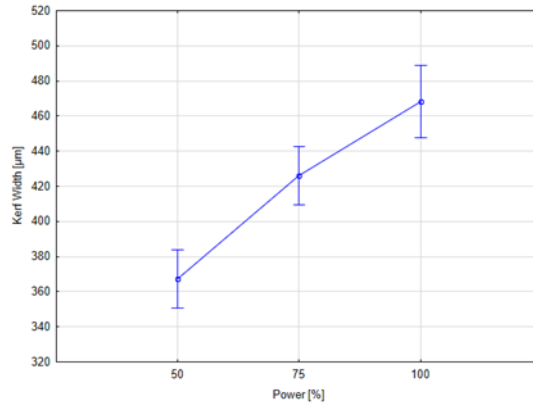

Figure 3: Kerf Width by Position
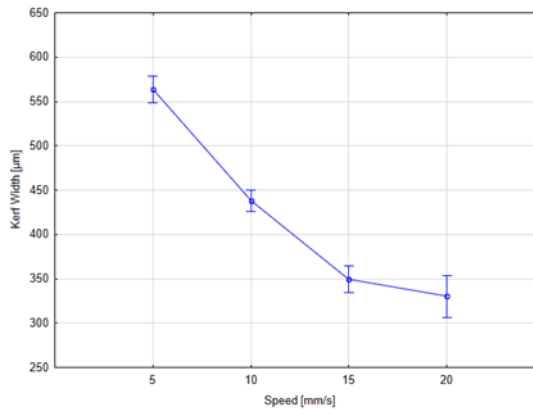
Figure 4: Kerf Width by Power

Figure 5: Kerf Width by Speed

Kerf Width by Position (Figure 3): The kerf width decreases from approximately 480 micrometers at the top to around 360 micrometers at the bottom, suggesting alterations in cutting effectiveness or beam focus over the depth of the cut.

Kerf Width by Power (Figure 4): There is a direct correlation between power percentage and kerf width, with the kerf expanding from about 360 to 500 micrometers as power increases from 50% to 100%, indicating that higher power input broadens the cut.

Kerf Width by Speed (Figure 5): As cutting speed increases from 5 mm/s to 20 mm/s, the kerf width decreases from roughly 600 to 300 micrometers, showing an inverse relationship where faster speeds yield narrower kerfs.
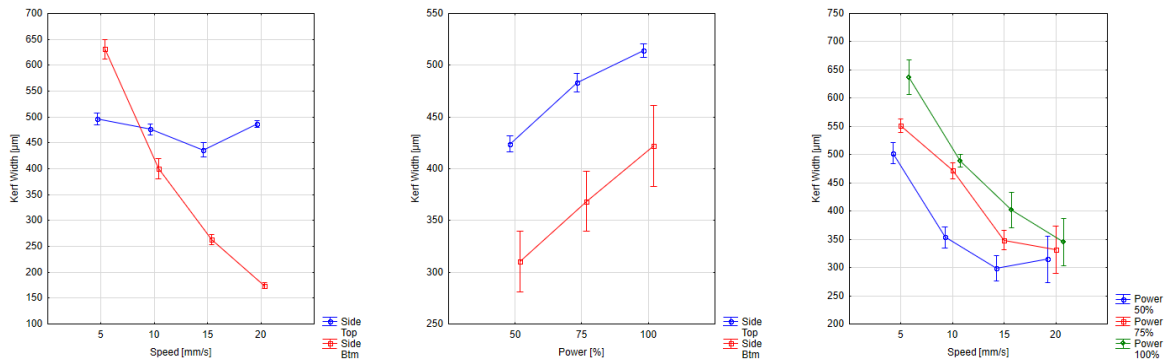

Figure 6: Interactions between cutting speed, power, and kerf width at different positions of the cut

Figure 6 presents the interactions between cutting speed, power, and kerf width at different positions of the cut (top, side, bottom).

Speed and Position Interaction (Figure 6, left): The kerf width shows a non-linear response to changes in speed, with a notable variance between the top, side, and bottom measurements. At lower speeds, kerf widths are larger, with the top position exhibiting the widest kerf which narrows significantly at the bottom. As speed increases, kerf widths decrease across all positions, but the rate of change varies, indicating that position within the material influences the cutting dynamics.

Power and Position Interaction (Figure 6, middle): The kerf width consistently increases with power at all positions, but the slope of this increase is steeper at the top than at the bottom. This suggests that higher power settings more significantly affect the upper regions of the material.

Speed and Power Interaction (Figure 6, right): When examining the combined effect of speed and power on kerf width, it is evident that at lower power settings (50%), increases in speed greatly reduce the kerf width. However, as power increases, the kerf width becomes less sensitive to changes in speed.
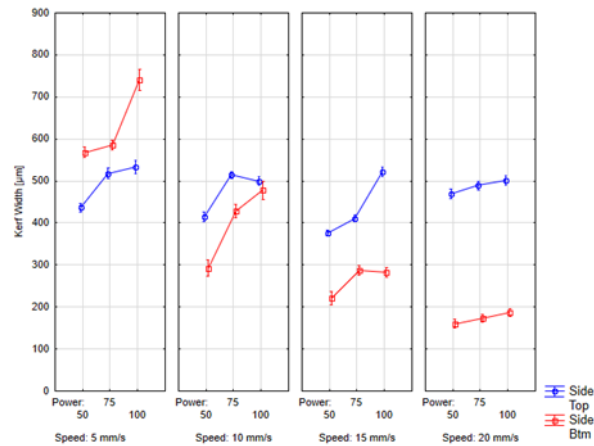

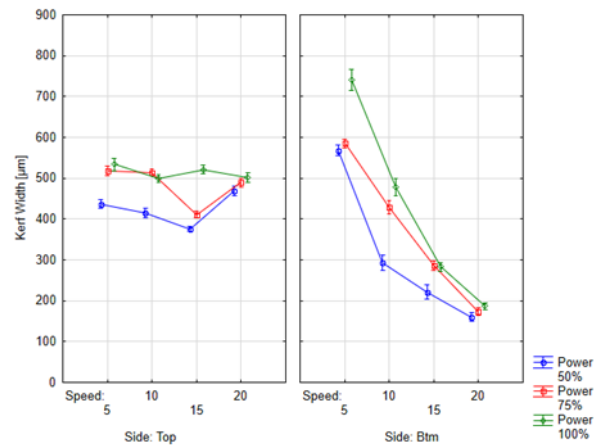*Figure 7: Kerf Width Variation with Power and Speed*

Figure 8: Position-Specific Trends

Kerf Width Variation with Power and Speed (Figure 7): Across four-speed categories (5, 10, 15, 20 mm/s), kerf width consistently increases with power at all positions (top, side, bottom). However, the extent of the increase varies with speed, suggesting a complex interaction where the kerf response to power is modulated by the cutting speed.

Position-Specific Trends (Figure 8): At the top side, the kerf width initially decreases with speed at lower power settings, then increases at higher speeds, forming a 'V' shape pattern. In contrast, at the bottom side, kerf width shows a steep decline with increased speed across all power levels, indicating a more pronounced effect of speed on kerf reduction in this region.

The process of scanning and measuring kerf widths in laser-cut wood is often complicated by the presence of anomalies and defects (Figures 9 & 10). These irregularities, such as raised burned fibers, emerge as a consequence of the intense heat generated by the laser. They create a challenging topography that can obscure the true edges of the kerf when viewed under a digital microscope. Similarly, reflections from the laser bed can introduce optical distortions creating additional cuts or scarring of samples that complicate the task of obtaining precise measurements. Recognizing and accounting for these defects is crucial in the accurate analysis of kerf widths.
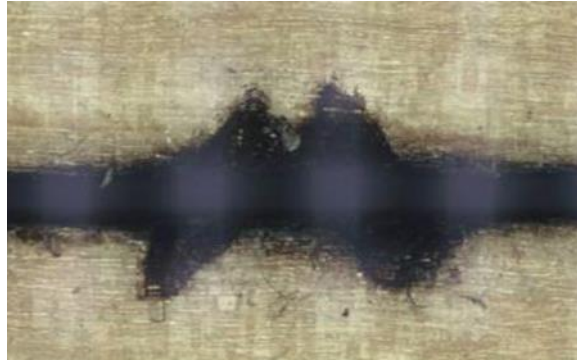
Figure 9: Additional cuts caused by reflections from the laser

Figure 10: Raised, burned fibers

The study of morphology directly was beyond the scope of this paper. Therefore, a literature review was conducted instead. In a paper by Adamcik et al. scanned topographic images have elucidated the nuanced changes in P-parameters, underscoring the potential hazards associated with evaluating the cross-section using the primary profile alone. This comprehensive understanding highlights the significant role of laser cutting in modifying wood properties, which, in turn, can influence material performance in various applications. The study's findings emphasize the need for a nuanced approach to the laser processing of wood, considering both the immediate effects on kerf morphology and the broader implications for material utilization (Adamčík et al. 2023). The studies by Rezaei et al., Guo et al., and Wust et al. provide valuable insights into the optimization of laser-cutting processes for wood. Rezaei et al. found that neither cutting speed nor focal-point position significantly impacts surface roughness, while increased gas pressure improves it, particularly in drier wood. Guo et al. highlighted that higher cutting speeds improve surface quality and reduce defects. They recommend lower speeds and moisture content for deeper cuts, and a higher speed for narrower kerfs, identifying cutting speed and moisture content as key factors. Haller et al. explored laser ablation, showing that UV and IR lasers can achieve ablation without carbonizing the wood surface, due to specific laser parameters and wood's absorption properties. These findings collectively underscore the nuanced impact of laser parameters on wood-cutting efficiency, surface quality, and show a potential gap for further research into cutting parameter optimization in laser applications in wood processing. (Wust et al. 2002; Guo et al. 2021; Rezaei et al. 2022).

CONCLUSIONS

In summary, laser power and cutting speed have complex, interdependent effects on kerf width, which are further complicated by differences between the material's top and bottom sides. Optimal cutting conditions vary notably between these sides and across different power and speed settings.

Laser cutting is a precise technique but not without shortcomings, evident in the observed wood sample defects. Raised, burned fibers (Figure 10) resulting from laser cutting can create an uneven surface, challenging accurate digital microscopic measurement and potentially leading to errors. Additionally, reflections from the laser bed (Figure 9) can distort the visual analysis.

Our results underscore the complex nature of laser-material interactions, emphasizing that both the power and speed must be carefully calibrated to achieve the desired kerf width while considering the inherent asymmetries in the cutting process. The apparent differences in kerf width between the top and

bottom sides suggest that further investigation into the laser beam profile and its impact on the cutting process may be necessary for process optimization.

In the next stage of research, we will focus on broadening the spectrum of wood species, and input parameter focal distance as well as a deeper dive into the interaction of wood morphology and its interaction in LBM.

ACKNOWLEDGEMENTS

REFERENCES

Adamčík L, Igaz R, Štefančin L, et al (2023) Evaluation of the Surface Irregularities of the Cross-Section of the Wood after CO2 Laser Cutting. Materials 16:. https://doi.org/10.3390/ma16227175

Barcikowski S, Ostendorf A, Bunte J (2004) Laser cutting of wood and wood composites - evaluation of cut quality and comparison to conventional wood cutting techniques. PICALO 2004 - 1st Pacific International Conference on Applications of Laser and Optics, Conference Proceedings 18–23. https://doi.org/10.2351/1.5056078/293031

Decker I, Ruge J, Atzert U (1984) Physical Models And Technological Aspects Of Laser Gas Cutting. https://doi.org/101117/12966211 0455:81–87. https://doi.org/10.1117/12.966211

Duan J, Man HC, Yue T (2001) Modelling the laser fusion cutting process: I. Mathematical modelling of the cut kerf geometry for laser fusion cutting of thick metal. J Phys D Appl Phys 34:2127. https://doi.org/10.1088/0022-3727/34/14/308

Guo X, Deng M, Hu Y, et al (2021) Morphology, mechanism and kerf variation during CO2 laser cutting pine wood. J Manuf Process 68:13–22. https://doi.org/https://doi.org/10.1016/j.jmapro.2021.05.036

Hecht J (1992) The Laser Guidebook. McGraw-Hill

Martínez-Conde A, Krenke T, Frybort S, Müller U (2017) Review: Comparative analysis of CO2 laser and conventional sawing for cutting of lumber and wood-based materials. Wood Sci Technol 51:943–966. https://doi.org/10.1007/s00226-017-0914-9

Mushtaq RT, Wang Y, Rehman M, et al (2020) State-Of-The-Art and Trends in CO2 Laser Cutting of Polymeric Materials—A Review. Materials 13:3839

Powell J, Kaplan A (2004) Laser cutting: From first principles to the state of the art

Radovanovic M, Madić M (2011) EXPERIMENTAL INVESTIGATIONS OF CO2 LASER CUT QUALITY: A REVIEW

Rezaei F, Wimmer R, Gaff M, et al (2022) Anatomical and morphological characteristics of beech wood after CO2-laser cutting. Wood Mater Sci Eng 17:459–468. https://doi.org/10.1080/17480272.2022.2134820

Sharma A, Yadava V, Rao R (2010) Optimization of kerf quality characteristics during Nd: YAG laser cutting of nickel based superalloy sheet for straight and curved cut profiles. Optics and Lasers in Engineering - OPT LASER ENG 48:915–925. https://doi.org/10.1016/j.optlaseng.2010.03.005

Shinde AD, Kubade PR (2016) Current Research and Development in Laser Beam Machining (LBM): A Review

Wust H, Beyer E, Wiedemann G, et al (2002) Experimental study of the effect of a laser beam on the morphology of wood surfaces

Xu Y, Wang B, Shen Y (2017) Study on laser cutting technology of bamboo. Wood Research 62:645–658

Yilbas B (2001) Effect of process parameters on the kerf width during the laser cutting process. Proceedings of The Institution of Mechanical Engineers Part B-journal of Engineering Manufacture - PROC INST MECH ENG B-J ENG MA 215:1357–1365. https://doi.org/10.1243/0954405011519132

Yilbas BS, Shaukat MM, Ashraf F (2017) Laser cutting of various materials: Kerf width size analysis and life cycle assessment of cutting process. Opt Laser Technol 93:67–73. https://doi.org/10.1016/j.optlastec.2017.02.014

Comparison of fluted-growth and cylindrical hornbeam logs from Hungarian forests

Mátyás Báder[1], Maximilián Cziczer[1*]

[1] University of Sopron, Faculty of Wood Engineering and Creative Industries. Bajcsy-Zs. Str. 4, Sopron, Hungary, 9400

E-mail: bader.matyas@uni-soporn.hu, cziczermaximilian@gmail.com

Keywords: bending strength, Brinell-Mörath hardness, density, modulus of elasticity

ABSTRACT

Hornbeam (*Carpinus betulus* L.) logs are typically noted for their fluted and twisted growth, which results in growth rings that are polygonal and faceted rather than round. This type of growth has a negative impact on their industrial use, primarily because of the low sawmill yield. Hornbeam has a high density, making it difficult to manufacture, yet it is extremely good for hard and wear-resistant wood parts. Today, however, cylindrical or almost cylindrical hornbeam logs can be found in Hungarian forests, although little information is available on their timber and overall features. Some research (drying characteristics, surface tension, chipping parameters, varnish adhesion, etc.) suggest that cylindrical hornbeams have better properties than fluted-growth hornbeams, as the density of the cylindricals are averagely 4.38% higher, and Brinell-Mörath hardness is on average 12.61% higher. By investigating some physical-mechanical properties between cylindrical and fluted hornbeams, taking into account some site influences, our research aims to improve the knowledge of wood science and wood industry. Once the results have been evaluated, we may be able to select the appropriate growing parameters using the correlations. This will enable foresters to grow high-quality logs that can be utilized much better even in the changing climate.

INTRODUCTION

The hornbeam (*Carpinus betulus* L.), typically found in European forests, holds significant importance in forestry and the wood industry (Majer 1968). Hornbeam wood grow traditionally fluted and twisted, which considerably affects the yield of timber and its workability (Molnár 2002). However, cylindrical or nearly cylindrical hornbeam logs also occur, whose wood properties are less well known but possess promising characteristics for industrial use (Solymos 1993). Previous research on hornbeam has mainly focused on the physical and mechanical properties of the wood, as well as its ecological and economic significance (Szalacsi 2015; Veres 2013). These studies, however, have not extensively examined the different trunk shapes. The aim of this study is to compare cylindrical and fluted-growth hornbeams in detail. The primary objective of the research is to investigate how the trunk shapes of hornbeam affect the physical and mechanical properties of the wood and to expand our knowledge of the significance of these two growth shapes, which could be beneficial for the industry. The long-term goal is to promote the forestry production of cylindrical hornbeam, which may support the domestic wood industry by providing higher quality timber in the distant future. We have conducted examinations of the most critical material properties, such as density, swelling, bending modulus of elasticity (*MoE*) and modulus of rupture (*MoR*). During the evaluation of the results, special attention is given to characteristics that are crucial for industrial processing. This research contributes to a better understanding of the hornbeam species and the optimization of its industrial utilization, assists in the sustainable management of hornbeam stands, and can improve the quality of wood in timber and maybe in veneer production.

MATERIALS AND METHODS

During the research, hornbeam logs were obtained from different forestry regions of Hungary. Both cylindrical and fluted-growth specimens were provided by Szombathelyi Forestry and Nyírerdő Nyírség Forestry, while only cylindrical hornbeam log was sourced from Zala County. The current sampling strategy did not distinguish between juvenile and heartwood, the exclusive aim of the research was the comparative analysis of cylindrical and fluted-growth trunk shapes, evaluated in the context of literary

data. This approach allows a focused examination of the structural and morphological differences in the wood. The various code designations for the studied samples, according to provider, origin, and growth shape, are presented in Table 1.

Table 1: Sample marking and origin

Specimen	Location	Shape of log	Code
Nyírerdő Forestry	Baktalórántháza 10/A	fluted-growth	N-H-5
Nyírerdő Forestry	Baktalórántháza 10/A	cylindrical	N-H-6
Szombathelyi Forestry.	Hegyhátszentmárton 5/a	cylindrical	S-H-14
Szombathelyi Forestry	Hegyhátszentmárton 5/a	cylindrical	S-H-16
Szombathelyi Forestry	Hegyhátszentmárton 5/a	fluted-growth	S-H-15
Zala Country	Pusztaederics 21D	cylindrical	Z-H-1

Determination of physical and mechanical properties

The examination of physical characteristics of the hornbeam samples involves two critical parameters: density and swelling. The density determination is based on the absolutely dry state, which can vary depending on the relative moisture content (*MC*) of the wood (Rónyai 2021). The measurement of swelling evaluates the dimensional changes related to the *MC* variations of wood, determined according to the ISO 13061-15 (2017) standard. For the examination, we used specimens of 20×20×30 mm (*Tangential×Radial×Longitudinal; T×R×L*) as specified in the standards.

The mechanical tests focused on determining hardness, bending strength, and impact bending strength. The hardness measurement was conducted following the widely recognized Brinell-Mörath test procedure, adhering to the Hungarian standard MSZ 6786-11 (1982). The specimen dimensions were 50×50×50 mm (*T×R×L*), conditioned to equilibrium *MC* at normal conditions (20 °C and 65% relative humidity). Hornbeam, being a very hard wood species, required a load of 1000 N, with a load duration of 30 seconds as specified in the standard. Tests were performed on the end-grain, radial, and tangential anatomical directions. Eq. 1 was used to determine hardness (*H_B*).

$$H_B = \frac{2 \cdot F}{D \cdot \pi \cdot (D - \sqrt{D^2 - d^2})} \tag{1}$$

where:
F – applied force: 1000 N,
D – diameter of the steel ball: 10 mm,
d – average diameter of the indentation.

For the measurement of bending strength, we selected the three-point bending test, ensuring easier comparability with other wood species. The ISO 13061-03 (2014) standard was applied. At the same time, the *MoE* was determined following the ISO 13061-04 (2014) standard, where the deflection as a result of gradually increasing transverse load was measured at the centre of the specimen. The load was then gradually increased until failure to determine the bending strength. Special attention was paid to the rate of the tests, as the measured mechanical properties strongly depend on the duration of the test. Strength and elasticity are factors where wood and other polymeric materials tend to behave more plastically at lower rates. At higher rates, due to the faster build-up of stress and greater load, the specimen deforms less before breaking.

Charpy impact bending tests were conducted according to the ISO 13061-10 (2017) standard. For these tests, we also used failure-free specimens of 20×20×300 mm (*T×R×L*), which were conditioned at 20 °C and 65% relative humidity. The impact bending strength tests were performed using a Charpy impact tester. The radius of curvature for the pendulum and the supports was 15 mm, and the distance between the supports was 240 mm. The specimens were symmetrically placed on the supports on the radial surface of the wood. The absorbed energy was measured with an accuracy of 1 J.

The results obtained from each testing methods were standardized to a *MC* of 12% (*σ₁₂*). For natural wood, the following conversion formula is applied (Báder and Németh 2019) (Eq. 2):

$$\sigma_{12} = \sigma_u [1 + \alpha(u - 12)] \tag{2}$$

where:

σ_u – the strength value of the tested specimen at a moisture content of u,

u – moisture content,

α – strength change per 1.0% change in moisture content within the fibre saturation point:

$\alpha_{\sigma h}$ = 0.04 (bending strength),

α_{Eh} = 0.02 (bending modulus of elasticity),

$\alpha_{\sigma \ddot{u} h}$ = 0.02 (impact bending strength),

$\alpha_{Hb\ (end-grain)}$ = 0.035 (hardness in the longitudinal direction),

$\alpha_{Hb\ (side)}$ = 0.025 (hardness in the transverse directions).

RESULTS AND DISCUSSION

During the evaluation of hardness tests, we observed that the values in different anatomical directions followed the trends reported in the literature. The fluted-growth sample from Nyírerdő exhibited 11.43% lower hardness in the radial direction compared to the tangential direction. The results of the other samples correlated in the radial and tangential directions; therefore, these directions are not detailed separately and are presented together. The results obtained during the examination are shown in Figure 1. In Figures 1-3 the different log shapes are visually distinguished by different colours. The specimens from Zala showed 3.47% higher hardness in the longitudinal direction compared to the average taken from the literature. Additionally, the fluted-growth sample from Szombathely, which also exhibited outstanding hardness, showed 8.76% higher hardness in the end-grain direction. There is no significant difference in side hardness between the cylindrical hornbeams from Zala and Szombathely. The fluted samples from Szombathely (S-H-15) differ from these samples, showing a significant difference in side hardness compared to the other samples. It is only 20.31% lower than in the longitudinal direction. The specimens from the Nyírerdő logs have an average hardness that is 45.23% lower in the end-grain direction and 38.24% lower in the side direction compared to the average of the other samples. The prominent differences can be attributed to the quality of the growing site and other growth factors.

***Figure 1: Brinell-Mörath hardness of hornbeam wood from different locations, markings are in Table 1.
Cylindrical log shape is marked by blue colour, fluted-growth logs are marked by purple***

In the bending tests, specimen failure occurred at the highest force, that means the moment of the greatest deformation. The specimens maintained a nearly constant slope from 5% to 50% of the maximum force. This phase lasted up to an average load of 1300 N, with the specimens reaching their maximum bending strength averagely at 2975 N. The obtained *MoR* and *MoE* were also compared to average values found in the literature, calculated from the values in Table 2.

Thus, the average *MoR* of the literature was determined to be 122.88 MPa, and the *MoE* was determined to be 12.99 GPa. Our test results are shown in Figure 2. The specimens exhibited no abnormalities that could affect the test results. Based on the measurements, we can state that none of the samples reached the values reported in the literature. However, wood from Zala showed somewhat higher *MoR* compared

to the other samples. The difference between the cylindrical and fluted-growth samples from Szombathely was negligible, less than 0.5%.

Table 2: Literary values of hornbeam. Abbreviations: MoR - modulus of rupture; MoE - modulus of elasticity

Author	MoR [MPa]	MoE [GPa]
Molnár (2004)	58.0–160.0–200.0	7.00-16.20–17.70
Majid (2019)	140.9–153.5	14.70–14.76
Meier (2024)	110.4–112.4	11.68–12.10

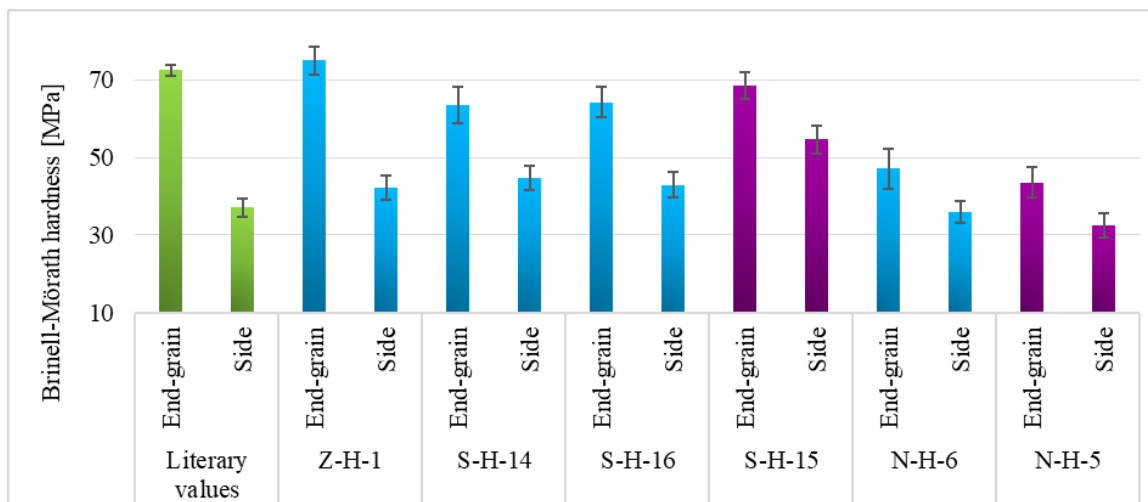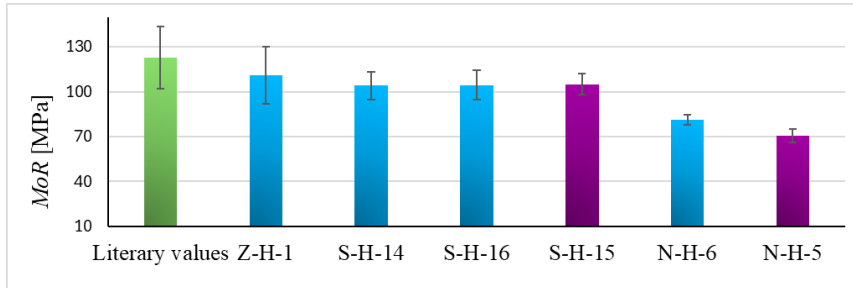*Figure 2: Modulus of rupture (MoR) of hornbeam wood from different locations, markings are in Table 1. Cylindrical log shape is marked by blue colour, fluted-growth logs are marked by purple*

In contrast, the wood from Nyírerdő exhibited drastic differences compared to the other samples. For fluted-growth logs, the *MoR* was 33.25% lower, and for cylindrical logs, it was 23.42% lower than the average *MoR* of the other samples. Even after filtering out the outliers, the overall results did not change significantly. There were no errors observed during the measurements, and the standard deviation of the final results indicates that the specimens within each sample exhibited similar values. The significantly weaker results are likely due to the specific growing conditions of the site. Further analyses will be needed to better understand why these samples differ so highly from the others. Figure 3 shows the *MoE*, where a similar trend can be observed on both Nyírerdő samples. For the cylindrical hornbeam, the *MoE* is 21.64% lower, and for fluted-growth hornbeam, it is 37.71% lower compared to the averages of the other samples. A significant difference is also noticeable for the cylindrical hornbeam from Szombathely, where the *MoE* of S-H-14 sample is statistically significantly higher. Additionally, in this case, the measured values are still below the average values reported in the literature.
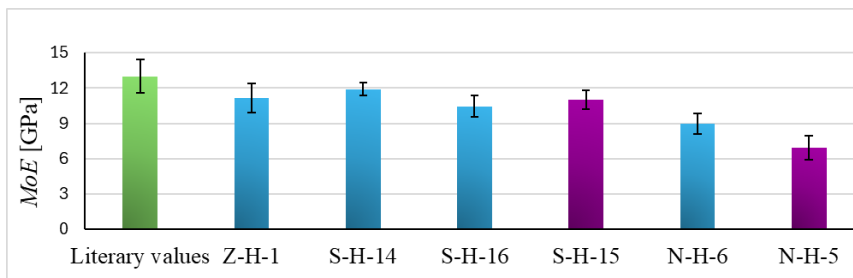
Figure 3: Modulus of elasticity (MoE) of hornbeam wood from different locations, markings are in Table 1. Cylindrical log shape is marked by blue colour, fluted-growth logs are marked by purple

The results of the impact bending strength tests are presented in Table 3. The cylindrical sample from Szombathely (S-H-14) exhibited outstanding values in the impact bending tests, showing nearly 80% higher impact bending strength than the other samples. The fluted-growth sample from Nyírerdő correlates well with the fluted-growth samples from Szombathely (S-H-15) and the literature values as well. The N-H-5 and S-H-16 samples also correlate with each other, but the Zala sample is 26.86% lower than the former and 29.29% lower than the latter. Compared to the fluted-growth samples (N-H-6 and S-H-15), Zala sample has 15.52% and 11.89% lower strength values, respectively. In the impact bending tests, the cylindrical samples showed better results than the fluted-growth samples, except for the specimens from Zala. Nonetheless, the impact bending strength results align well with the *MoE* presented in Figure 3.

Table 3: Charpy impact bending test results of hornbeam from different locations, markings are in Table 1

Sample	Impact bending strength [MPa]	Standard deviation [MPa]
Literary values	98.00	16.61
Z-H-1	84.43	7.03
S-H-14	179.52	10.74
S-H-16	116.90	11.40
S-H-15	95.82	19.28
N-H-5	119.40	16.75
N-H-6	96.51	12.02

The swelling of the different hornbeam samples is shown in Figure 4, in terms of volumetric (*V*), tangential (*T*), and radial (*R*) directions. It is evident that all six samples follow the trends obtained from the literature averages (Molnár and Bariska 2002; Meier 2024).
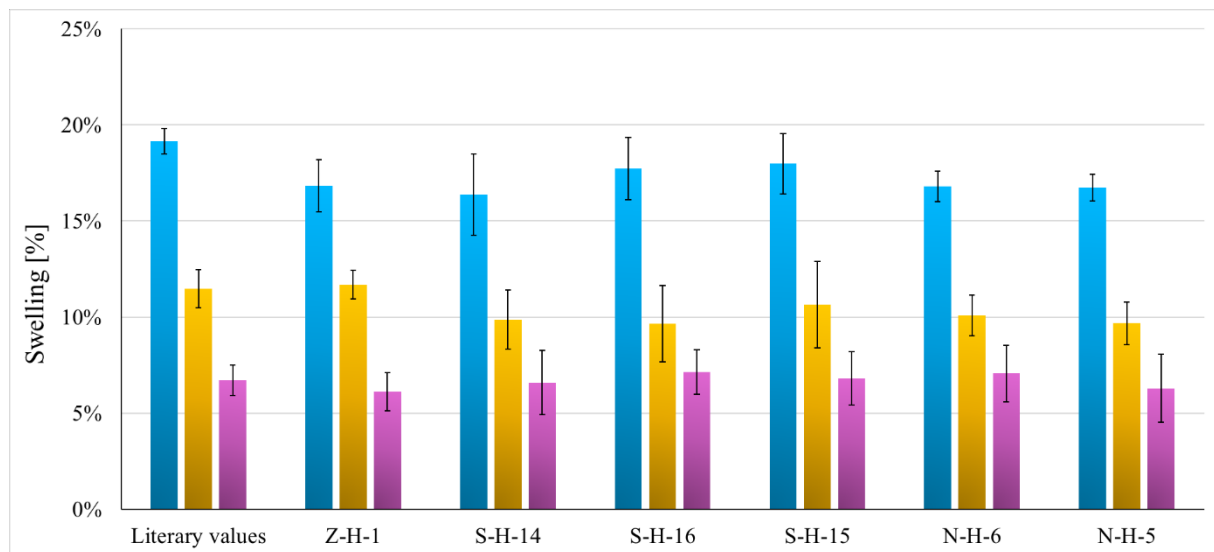

Figure 4: Swelling of hornbeam wood from different locations, markings are in Table 1. Blue columns represent volumetric, yellows tangential and purples radial swelling

In the swelling measurements, the maximum values were 17.74% for volumetric, 11.47% for tangential, and 7.13% for radial directions. The volumetric swelling values for both samples from Nyírerdő correlated with each other, similar to the Zala and Szombathely S-H-14 samples. The S-H-14 and S-H-16 samples exhibited higher volumetric swelling. In the tangential direction, the Z-H-1 sample exceeded the literature values (11.68%) and was on average 1.5% higher compared to the other samples. In the radial direction, the Z-H-1 sample stood out from the others. It has a value of 6.11%, which is lower compared to the Nyírerdő and Zala samples.

The densities for the cylindrical and fluted-growth samples are presented in Table 4. Conditioned at 20 °C and 65% relative humidity, the density values ranged between 678 and 763 kg/m³. No significant differences were found between the logs from Szombathely and Zala, but the logs from Nyírerdő had 8-10% lower density compared to the logs from West Hungary. This explains the weaker mechanical results of the Nyírerdő samples.

Table 4: Densities [kg/m³] of fluted-growth and cylindrical hornbeams, markings are in Table 1

Sample	Literary values	Z-H-1	S-H-14	S-H-16	S-H-15	N-H-5	N-H-6
Average	774	742	753	763	735	692	678
Min.	735	691	712	713	679	658	645
Max.	790	787	803	805	783	711	708
Deviance	22.47	19.61	25.64	27.05	26.92	15.93	17.04
Variance	2.90%	2.64%	3.41%	3.55%	3.66%	2.30%	2.51%

CONCLUSIONS

This study determined that the trunk shape of hornbeam (*Carpinus betulus* L.) has a significant impact on its physical and mechanical properties. The test results showed that cylindrical hornbeam possesses better average impact strength (27.91%), modulus of elasticity (18.25%) and modulus of rupture (14.01%) than the fluted-growth hornbeams, which are advantageous for industrial use. Of course, growing site is also important for quality. These observations highlight that selective breeding of cylindrical-growth hornbeam or the application of appropriate forestry practices in specific growth sites can improve the industrial applicability of hornbeam wood in the distant future. Further research is needed to gain a deeper understanding of the influencing factors. Additionally, sampling locations should be expanded, as the research results suggest that the growth sites greatly influence individual strength values, sometimes resulting in stronger or denser wood structures. For future studies, we have already started the fungal resistance tests of these samples, as well as conducted wear resistance and water permeability tests. It will be important to get to know some important anatomical, genetic, and fungal resistance differences between cylindrical and fluted hornbeams as well, to improve the knowledge of wood science and wood industry.

ACKNOWLEDGEMENT

REFERENCES

Báder M, Németh R (2019) Moisture-dependent mechanical properties of longitudinally compressed wood. Eur J Wood Prod 77:1009–1019. https://doi.org/10.1007/s00107-019-01448-1

ISO 13061-03 (2014) Physical and mechanical properties of wood - Test methods for small clear wood specimens - Part 03: Determination of ultimate strength in static bending. International Organization for Standardization, Geneva, Switzerland

ISO 13061-04 (2014) Physical and mechanical properties of wood - Test methods for small clear wood specimens - Part 04: Determination of modulus of elasticity in static bending. International Organization for Standardization, Geneva, Switzerland

ISO 13061-10 (2017) Physical and mechanical properties of wood - Test methods for small clear wood specimens - Part 10: Determination of impact bending strength. International Organization for Standardization, Geneva, Switzerland

ISO 13061-15 (2017) Physical and mechanical properties of wood - Test methods for small clear wood specimens - Part 15: Determination of radial and tangential swelling. International Organization for Standardization, Geneva, Switzerland

Kiaei M, Abadian Z (2018) Physical and Mechanical Properties of Hornbeam Wood from Dominant and Suppressed Trees. Drvna Ind 69:63–69. https://doi.org/10.5552/drind.2018.1705

Majer A (1968) Magyarország erdőtársulásai. Akadémiai Kiadó, Budapest

Meier E (2024) European Hornbeam. In: Wood Database. https://www.wood-database.com/european-hornbeam/ Accessed 22.05.2024

Molnár S (2004) Knowledge of wood (Faanyagismeret). Mezőgazdasági Szaktudás Kiadó, Budapest, Hungary

Molnár S, Bariska M (2002) Magyarország ipari fái. Szaktudás Kiadó Ház Zrt, Budapest, Hungary

MSZ 6786-11 (1982) Test methods for wood materials. Determination of hardness. Magyar Szabványügyi Hivatal, Budapest, Hungary

Rónyai B (2021) Investigation of the pleatability and certain physical-mechanical properties of elm wood (Szil faanyag rostirányú tömöríthetőségének és egyes fizikai-mechanikai tulajdonságainak vizsgálata). Bachelor's thesis, University of Sopron

Solymos R (1993) Improvement and silviculture of oaks in Hungary. Ann For Sci 50:607–614. https://doi.org/10.1051/forest:19930609

Szalacsi Á, Veres S, Király G (2015) Adatok a síkvidéki gyertyános-tölgyesek erdőműveléséhez: lékes felújítóvágás alkalmazásának gyakorlati tapasztalatai és növényzeti hatásai a Szatmár-beregi síkon. Erdészettudományi Közlemények 5:85–99. https://doi.org/10.17164/EK.2015.006

Thermal modification affects the dynamic vapor sorption of tree of heaven wood (*Ailanthus altissima, Mill.*)

Fanni Fodor[1], Lukas Emmerich[2,3], Norbert Horváth[1], Róbert Németh[1*]

[1] University of Sopron, Institute of Wood Technology and Technical Sciences. Bajcsy-Zs. Str. 4, Sopron, Hungary, 9400.
[2] Wald und Holz NRW, Centre of Forest and Wood Industry (FBV), Team Wood-Based Industries, Carlsaue Str. 91a, Olsberg, Germany, 59939.
[3] Georg-August-University Göttingen, Faculty of Wood Biology and Wood Products, Büsgenweg 4, Göttingen, Germany, 37077.

E-mail: fodor.fanni@uni-sopron.hu; lukas.emmerich@wald-und-holz.nrw.de; horvath.norbert@uni-sopron.hu; nemeth.robert@uni-sopron.hu

Keywords: thermal modification, ailanthus, tree of heaven, dynamic vapor sorption, moisture sorption, hysteresis

ABSTRACT
The utilization of tree of heaven wood is hindered by its low durability and dimensional stability. Although it has promising physical and mechanical properties similar to ash wood, it is considered as an invasive wood species, and it is rarely the base of wood property improvement research. In this study, heat treatment was carried out on this species at 180°C and 200°C to evaluate the sorption characteristics using dynamic vapor sorption tests. This way, the wood-water relationships, the rate of sorption, the reduction in moisture content could be analyzed and assumptions could be made on the change of moisture-related properties.

INTRODUCTION
Water vapor sorption is one of the most important characteristics of wood, as it affects many of its properties like dimensional stability, mechanical properties, durability, heat capacity, thermal conductivity, and corrosion (Zelinka et al. 2021).

When drawing a (water vapor) sorption isotherm, the equilibrium moisture content (EMC) of wood can be observed as a function of relative humidity (RH) at a given temperature (T). There is an absorption isotherm, where the EMC increases from oven-dry state to fiber saturation point (FSP) by increasing the humidity. There is also a desorption isotherm, where the wood is dried to 0% EMC. The sorption isotherm and the EMC depend also on the previous RH history. Scanning curves are those isotherms, which have been collected along different RH path history. Here, the desorption curves start from a fully water-saturated state with 100% RH. Those isotherms, which start from 95% RH, are scanning desorption isotherms (Fredriksson and Thybring 2018).

In dynamic vapor sorption (DVS) analyzers, small wood samples are exposed to dry and saturated streams of air, the RH of which is controlled by mass flow controllers. As the temperature and RH are tightly controlled, the mass data of the wood sample gives the sorption isotherms precisely and faster and with less labor than measuring the mass manually after equilibrating the samples at each RH level (Zelinka et al. 2021).

The base of this research was tree of heaven wood (*Ailanthus altissima* MILL. SWINGLE). It is usually used as firewood, as it is prone to fungal decay, insect damage, blue stain, cracks and warps. Although its low durability and dimensional stability hinders its usage, it has promising physical, mechanical and product-related properties (bonding, coating, manufacturing). Its colour and properties are comparable to ash wood (*Fraxinus excelsior*). Extensive literature review has been carried out on the utilization potential of this wood species recently (Terzopoulou et al. 2023).

It is considered to be an invasive species, it has a short felling time, and logs of high-quality are rare. It is fast-growing, it spreads easily and has high reproducibility. The utilization of the existing wood amount is a task to be resolved (Bartha 2020).

Using wood modification techniques, its resistance to moisture and microorganisms could be improved. In the scientific literature on the modification of this wood species, heat treatment (Barboutis and Kamperidou 2019), heat treatment in oil (Bak and Németh 2015), impregnation modification (Miao et al. 2014) were carried out with promising results like higher mechanical strength and lower hygroscopicity.

In this research, dynamic vapor sorption tests were carried out on different parts of heat-treated tree of heaven wood (*Ailanthus altissima*) to see how does thermal modification at 180° and 200° affect the wood-water relations in this underutilized wood species with low dimensional stability and durability. Based on relevant literature, heat-treatment will probably decrease the equilibrium moisture content, the hysteresis, and the rate of moisture sorption compared to untreated wood (Humar et al. 2020; Jiang et al. 2024). As the chemical components are different in annual rings closer to the pith compared to the outer part of the wood, the results may also vary in moisture-related properties (Akgul and Tozluoglu 2009).

MATERIALS AND METHODS
Material
One tree of heaven log was acquired from the Botanical Garden of Sopron (Hungary). The middle boards were taken from them, and they were cut to three pieces. These pieces were sawn to 30 by 30 mm sticks. The sticks from the middle part were marked as control, and the sticks from the sides were heat-treated (Gyuricsek 2015).

Heat-treatment
The samples were heat-treated at the University of Sopron (Hungary) in an insulated chamber, having an internal volume of 0.4 m^3. In this equipment, internal air heating is applied with two pairs of ribbed, U-shaped electric heating wires with a power of 750 W each. These are separated from the heat-treatment area by a steel plate which is located approximately 10-15 cm from the back wall. The air circulation is provided by two pieces of aluminum fans with diameter of 23cm, placed above the heater. The temperature was set by a PT100 thermometer and a Siemens control unit. The removal of decomposition products and gases was ensured by the pressure difference (Gyuricsek 2015).

The experimental thermal treatments were carried out under atmospheric conditions, in an open system, without added steam or injected water. These "dry heat treatments" were performed with schedules at 180°C and 200 °C temperatures and 10 hours duration. These temperatures indicate the temperature of the atmosphere in the chamber, not the wood itself. During the treatment, the drying chamber was heated to 100°C in the first 5 hours, then it was heated to 130°C for 7 hours. In the next phase, the temperature was set to 180 or 200°C in one hour, and it was held for 10 hours. Then, it was cooled back to 20°C in 28 hours (Gyuricsek 2015).

After heat treatment, the equilibrium moisture content (EMC) and density were determined at 20°C temperature and 65% relative humidity. The average EMC decreased from 13.6% to 7.2% for the 180°C treatment, and to 4.8% for the 200°C treatment. The average density decreased from 641kg/m^3 to 604 kg/m^3 for the 180°C treatment, and to 591 kg/m^3 for the 200°C treatment (Gyuricsek et al. 2014).

Samples of $7 \times 20 \times 30$ mm (thickness × width × length) were produced from the one control and two heat-treated pieces from each annual ring corresponding to the anatomical directions (Gyuricsek 2015).

Dynamic Vapor Sorption tests
For DVS measurements, small-sized untreated and treated wood specimens from the 5th, 9th and 13th annual rings were milled in a cutting mill (RETSCH SM 2000, Retsch GmbH, Haan, Germany) to pass through a 2 mm mesh screen. Sorption isotherms were recorded in a DVS apparatus (DVS Advantage, Surface Measurement Systems, London, UK). Approximately 20 mg of wood particles were placed on a sample holder of the DVS and sorption isotherms were recorded at a constant temperature of 25 °C and a nitrogen flow of 200 sccm (sccm = standard cubic centimeter at 0 °C). The samples were first dried at 0 % RH until the mass change of the specimen per minute (dm/dt) was < 0.002 % min^{-1} over a period of 10 min.

Afterwards, the RH was increased stepwise in the following sequence: 10, 20, 30, 40, 50, 60, 70, 80, 90, and 95 % RH (absorption curve), which was followed by a decrease to 0 % RH in the reverse order (scanning desorption curve). A window of 10 min was used to calculate the dm/dt and each RH was

maintained until the dm/dt was < 0.002 % min⁻¹ for > 10 min. The moisture content (MC, in %) was calculated by relating the mass of water to the dry mass of the wood samples, using the sample mass at the end of each RH step. The MC_R ratio was calculated by relating the MC_R of the modified sample to the corresponding reference MC at each RH step.

RESULTS AND DISCUSSION

The sorption isotherms and hysteresis can be observed in Figure 1 and Figure 2. According to our results, heat treatment did decrease the moisture sorption of tree of heaven wood.

By increasing the treatment temperature, the EMC decreased more, and the sorption isotherm became flatter. This can be associated with heat-induced degradation, where the hemicellulose fraction decreases and cellulose crystallinity increases, which reduces the amount of accessible hydroxyl groups, which lead to lower moisture content.

The peak in absolute hysteresis is usually around 75% RH (Vahtikari et al. 2017), which corresponds to our results. The highest hysteresis was found at about 70% RH, which was lower for the control samples (3.39 - 3.52%) than for the heat-treated samples (3.60 - 3.88%).

The fiber saturation point of tree of heaven was slightly higher than related literature (Kržišnik et al. 2020). It decreased on average from 28.33% to 24.57% at 180°C, and to 21.31% at 200°C treatment temperature.

As the wood with less annual rings has higher juvenile wood ratio, higher moisture content and different chemical composition, the samples with less annual rings had higher EMC in every case. For example, the fiber saturation point of samples from the 5th annual ring was 28.54%, 24.94% and 21.74% with no treatment, treatment at 180°C, and 200°C, respectively. The FSP of samples in the 9th and 13th annual rings was lower, less than 28.32%, 24.51% and 21.48% with no treatment, treatment at 180°C, and 200°C, respectively.

Consequently to the EMC reduction after heat-treatment, the moisture content ratios were below 1, and decreased with elevated temperature (Figure 3). In the case of the 5th and 9th annual ring, there is a minimum in the adsorption curve and a maximum in the desorption curve at 50-60% RH. These moisture content ratio values are lower in the 5th annual ring. The 13th annual ring did not show any peak, just continuous reduction during both adsorption and desorption, with a minimum value at 90% RH. The lowest moisture content ratio was found for treatment 200°C having the highest reduction in EMC compared to untreated wood.

Corresponding to related research on this material, there was no significant difference between the moisture content values of the annual rings, and the average airdry density was also not influenced by the annual rings. On the other hand, the anti-swelling efficiency improved, it was 19-26% for 180°C treatment and 32-44% for 200°C treatment (Gyuricsek et al. 2014; Gyuricsek 2015).
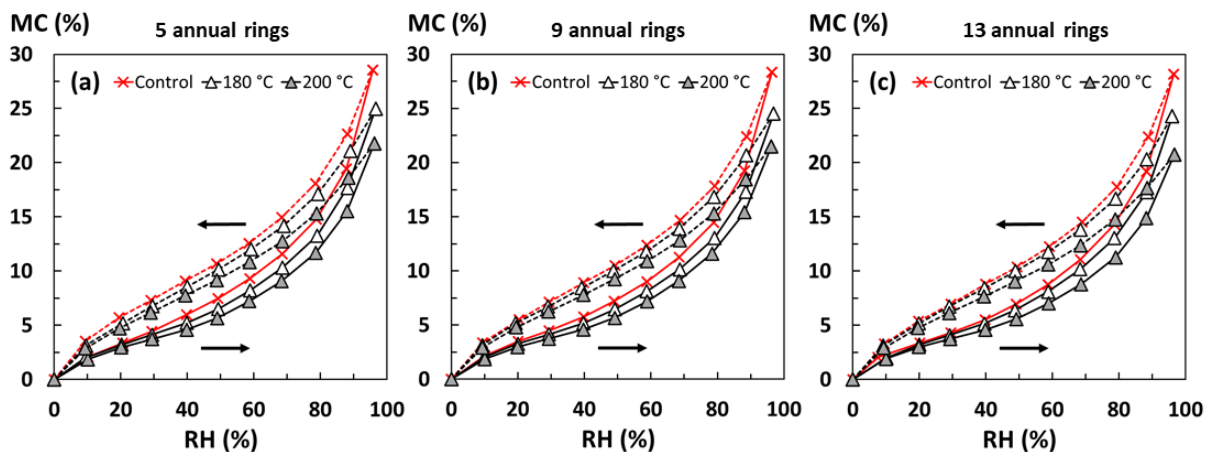
Figure 1: Sorption isotherms of untreated (Control) and heat-treated tree of heaven wood at 180•C and 200•C. Samples were taken from annual rings 5, 9 and 13. The change of moisture content (MC) is plotted in the function of relative humidity (RH).
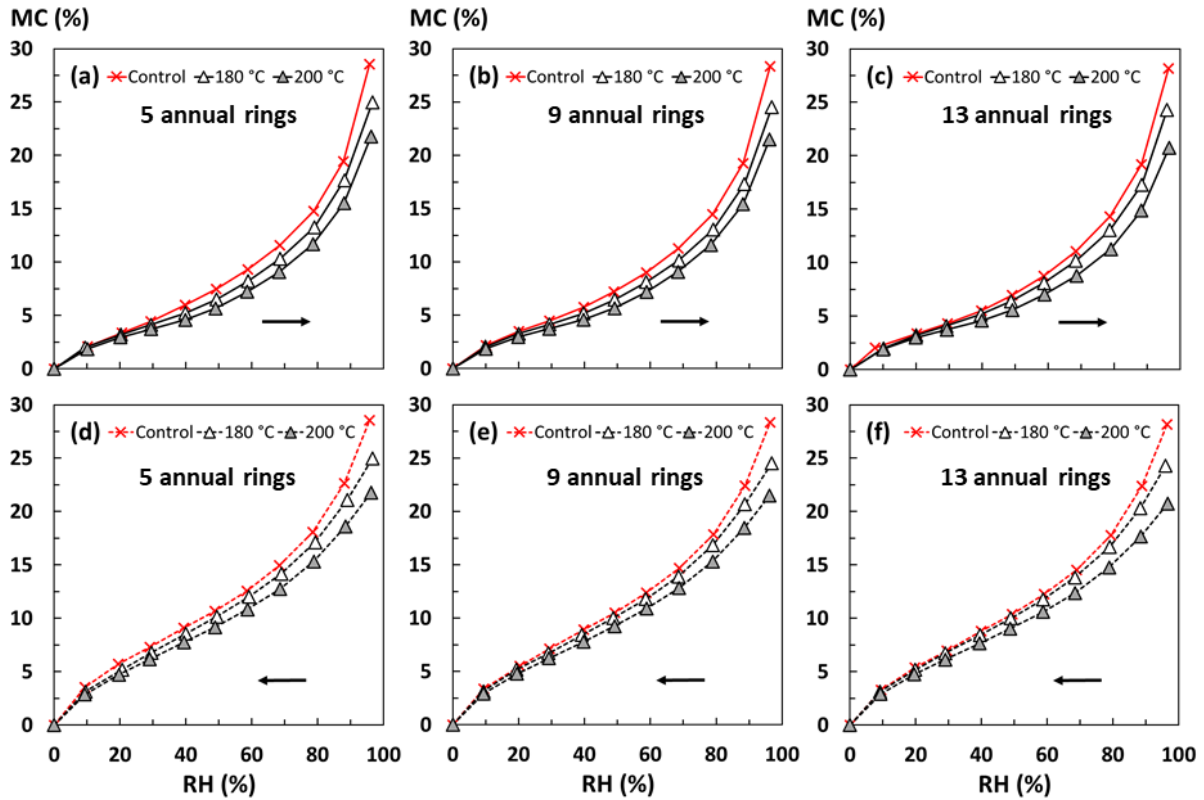
Figure 2: Adsorption and desorption curves of untreated (Control) and heat-treated tree of heaven wood at 180°C and 200°C. Samples were taken from annual rings 5, 9 and 13. The change of moisture content (MC) is plotted in the function of relative humidity (RH).
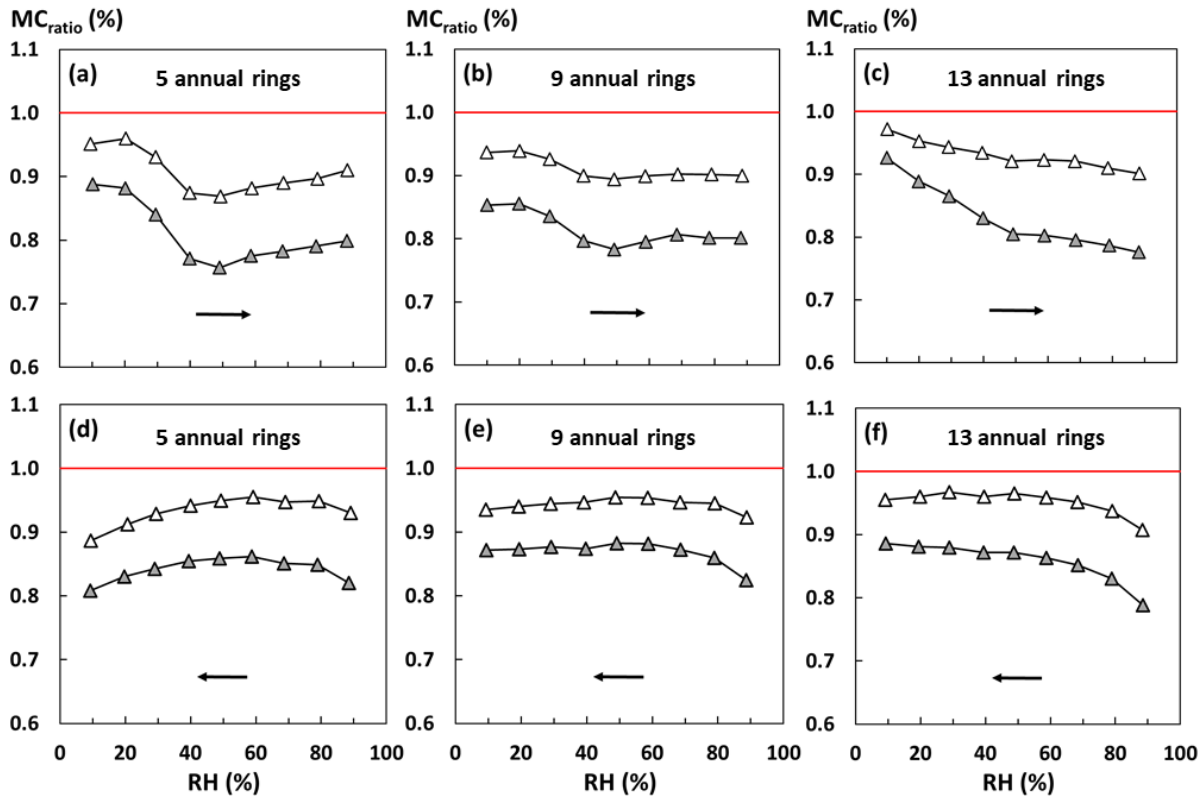
Figure 3: Moisture content ratios (MCratio) of heat-treated tree of heaven wood at 180°C (white triangles) and 200°C (grey triangles). Samples were taken from annual rings 5, 9 and 13. The arrows indicate the direction of moisture change, the upper row shows the adsorption results and the bottom row the desorption results.

CONCLUSIONS

The sorption isotherms of untreated and heat-treated tree of heaven wood were analyzed, taking into account which annual rings were they taken from. Heat-treatment resulted in the reduction of EMC, flatter sorption isotherm, and lower moisture content ratio. Samples from annual rings closer to the pith had higher EMC. Treating at 200°C had higher impact on the sorption properties than 180°C. Highest hysteresis was found at 70% RH. In the future, durability tests could be carried out to see how this species can withstand the exposure to biological organisms and weathering after heat treatment.

ACKNOWLEDGEMENTS

REFERENCES

Akgul M, Tozluoglu A (2009) Some Chemical and Morphological Properties of Juvenile Woods from Beech (Fagus orientalis L.) and Pine (Pinus nigra A.) Plantations. Trends in Applied Sciences Research 4:116–125. https://doi.org/10.17311/tasr.2009.116.125

Bak M, Németh R (2015) Crack formation during Oil-Heat-Treatment in relation with the initial moisture content. In: Proceedings of the 8th European Conference on Wood Modification. Helsinki, pp 334–337

Barboutis I, Kamperidou V (2019) Impact of Heat Treatment on the Quality of Tree-of-Heaven Wood. Drvna industrija 70:351–358. https://doi.org/10.5552/drvind.2019.1842

Bartha D (2020) Black List. Invasive tree and shrub species of Hungary. University of Sopron Press, Sopron

Fredriksson M, Thybring EE (2018) Scanning or desorption isotherms? Characterising sorption hysteresis of wood. Cellulose 25:4477–4485. https://doi.org/10.1007/s10570-018-1898-9

Gyuricsek T (2015) Bálványfa fatestének komplex faanyagtudományi vizsgálatai (Complex analysis of xylem of Tree of Heaven). Bachelor thesis, University of West Hungary

Gyuricsek T, Horváth N, Németh R (2014) Effect of heat treatments on selected properties of Tree-of-Heaven (Ailanthus altissima). In: Proceedings of the "IAWS Plenary Meeting 2014 - Sopron (Hungary) - Vienna (Austria)" - Eco-Efficient Resource Wood with Special Focus on Hardwoods. Sopron & Vienna, 2014. (14) 15-18th September. University of West Hungary Press, Sopron, pp 63–64

Humar M, Repič R, Kržišnik D, et al (2020) Quality Control of Thermally Modified Timber Using Dynamic Vapor Sorption (DVS) Analysis. Forests 11:666. https://doi.org/10.3390/f11060666

Jiang X, Van den Bulcke J, De Ligne L, Van Acker J (2024) Biological durability and moisture dynamics of untreated and thermally modified poplar. Eur J Wood Prod. https://doi.org/10.1007/s00107-023-02033-3

Kržišnik D, Humar M, Maks M (2020) The dynamic water vapour sorption behaviour of the invasive alien species in Slovenia. In: 9th Hardwood Proceedings Part I. With Special Focus on "An underutilized Resource: Hardwood Oriented Research." University of Sopron Press, Sopron, pp 149–152

Miao X, Chen H, Lang Q, et al (2014) Characterization of Ailanthus altissima Veneer Modified by Urea-formaldehyde Pre-polymer with Compression Drying. BioResources 9:5928–5939. https://doi.org/10.15376/biores.9.4.5928-5939

Terzopoulou P, Kamperidou V, Barboutis I (2023) Utilization Potential of Tree-of-Heaven Species Biomass—A Review. Applied Sciences 13:9185. https://doi.org/10.3390/app13169185

Vahtikari K, Rautkari L, Noponen T, et al (2017) The influence of extractives on the sorption characteristics of Scots pine (Pinus sylvestris L.). J Mater Sci 52:10840–10852. https://doi.org/10.1007/s10853-017-1278-0

Zelinka S, Thybring EE, Glass S (2021) Interpreting Dynamic Vapor Sorption (DVS) Measurements: Why Wood Science Needs to Hit the Reset Button. In: Proceedings of the World Conference on Timber Engineering. Santiago, p EPFT0101

How conditions after application affect the depth of penetration of gel wood preservative in oak

Jan Baar[1*], Štěpán Bartoš[1], Anna Oberle[1], Zuzana Paschová[1]

[1] Mendel University in Brno, Faculty of Forestry and Wood Technology,
Zemědělská 1665/1, 613 00, Brno.

E-mail: jan.baar@mendelu.cz; anna.oberle@mendelu.cz; zuzana.paschova@mendelu.cz

Keywords: European oak, permethrin, high performance liquid chromatography, temperature, relative humidity

ABSTRACT
Wooden constructions are often attacked during use by biotic agents such as wood-rotting fungi and wood-boring insects, and this can happen to wooden buildings in open-air museums. Chemical preservatives containing toxic active substances can provide preventive and controlling protection against wood-boring insects. Such preservatives in gel form are claimed to penetrate more deeply into wood than liquid preservatives applied to the surface.

Preservative in gel form was applied to the surface of European oak samples, which were stored for 14 days under three different conditions of air temperature and humidity that simulate climatic conditions in different seasons. The penetration depth and retention of permethrin, the active substance in the gel, was analysed at successive layers using high-performance liquid chromatography.

The permethrin penetrated to a depth of at least 10 mm, where its retention satisfied the requirements for its efficacy, but the declining concentration gradient was steep with increasing depth. Storage conditions that promoted gel drying led to less penetration of permethrin.

INTRODUCTION
Biotic agents such as wood-rotting fungi and wood-boring insects often attack wooden constructions in use and cause their gradual degradation. Historical wooden buildings and their wooden facilities in Czech open-air museums are often infested by the wood-boring beetles *Hylotrupus bajulus* and *Anobium* spp. due to favourable conditions for their development. Infested timber structures and other objects can be sterilised using various physical and chemical methods such as heating, gamma radiation and fumigation with toxic gases (Reinprecht 2016). Each of these techniques has its own advantages and limitations. For example, applying gamma radiation is restricted by its dependence on a fixed radiation source and can cause significant changes in the chemical and mechanical properties of wood if it is exposed repeatedly (Despot et al. 2012). One drawback common to all mentioned sterilisation techniques is that, as their effect fades, the wood becomes susceptible to re-infestation by biological pests. In the long-term, sterilised wood can only be protected in unfavourable conditions by using insecticides.

Chemical preservation using toxic active substances provides both controlling and preventative protection against wood-boring insects. The preservative agent can be applied in various ways; the common methods of brushing and spraying, which are suitable for wooden constructions in situ, usually achieve impregnation of only a thin surface layer, which is insufficient (Richardson 1993). The method most widely used for the curative treatment of roof trusses in housing is injecting – the wood is impregnated with liquid preservative through hollow screws in pre-bored holes by applying an external pressure. This method is unsuitable for historical buildings as it involves making permanent and destructive changes to the appearance of the wood.

For a number of years, preservatives have been available in gel form, which the manufacturers claim can penetrate as far as a few centimetres into wood without visible surface changes. Messaoudi et al. (2020) showed that the active substances in gels are able to penetrate by diffusion to a depth of 2 cm from the sprayed surface of spruce.

In this study, we analysed the depth of penetration and retention of permethrin in European oak as a function of anatomical direction and storage conditions.

MATERIALS AND METHODS

We evaluated the penetration depth and retention in the heartwood of European oak of ready-to-use gel emulsion marketed for the preventive and curative treatment of wood against wood-boring insects. The gel contained 0.5 % (w/w) of permethrin as the active substance.

Six rectangular wood prisms (three radial and three tangential; Figure 1) of dimensions $40 \times 66 \times 350$ mm (R/T $\times$ R/T $\times$ L) were prepared with planed surfaces. After 14 days of conditioning at 20 °C and 65 % humidity, each prism was cut into three samples to be stored under different conditions after preservative treatment. All samples were without visible defects such as knots or cracks. The recommended amount of preservative gel (450 g/m^2) was applied to one sample surface (40×110 mm) and spread evenly on the whole surface. Samples were stored for 14 days in three different conditions of temperature (°C) and relative humidity (%): 10/85; 20/65; 35/40 respectively. Subsequently, the samples were cut in layers (Figure 1) and treated wood was taken from different depths – 0, 10, 20 and 30 mm. The wood layers were milled into powder using an MM 400 mixer mill (Retsch GmbH); 0.3 g of wood powder from each sample and layer was extracted using a Dionex ASE 350 automatic extractor system (Thermo Scientific). The permethrin was extracted from wood with methanol under the following conditions: 40 °C, 5 min extraction time, two cycles, extraction cell volume 1 mL. The volume of extract was adjusted with methanol to 10 mL.
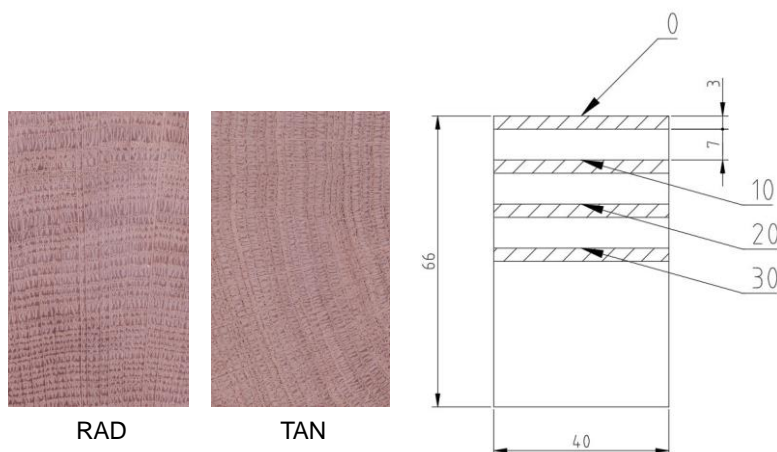
Figure 2: Wood samples orientation and sampling of individual layers for extraction

We used high-performance liquid chromatography (HPLC) to detect the presence of permethrin. The methanol extract from permethrin-treated wood was analysed using a 1260 Infinity modular chromatographic system (Agilent Technologies, Inc.) equipped with a UV/VIS diode array detector.

Chromatographic separation was carried out on a Kinetex C18 separation column, 4.6×150 mm, with a 3.5 µm particle size (Agilent Technologies, Inc.), using acetonitrile (A) and demineralised water (B) as the mobile phases. The flow rate and UV detector were set at 1 mL/min and 210 nm respectively. The column temperature was kept constant at 25 °C. The injection volume of the samples was 20 µL.

A calibration curve was obtained for the quantification of two forms of permethrin in extracts by injecting different concentrations of permethrin standard (Sigma Aldrich) dissolved in methanol. Figure 2 shows the HPLC chromatogram for a standard used for calibration and analysis of the permethrin in the extracted samples.

Permethrin retention in individual layers was expressed as the sum of trans- and cis-permethrin in µg/g of wood dust (moisture content 8 %) and also in g/m^3 based on the density of individual wood sample layers. The results are presented as the average value of three treated samples stored under the same conditions.

Figure 3: HPLC chromatogram of the permethrin standard and permethrin in treated wood extract; retention time of trans-permethrin (10.11 min) and cis-permethrin (10.66 min)

RESULTS AND DISCUSSION

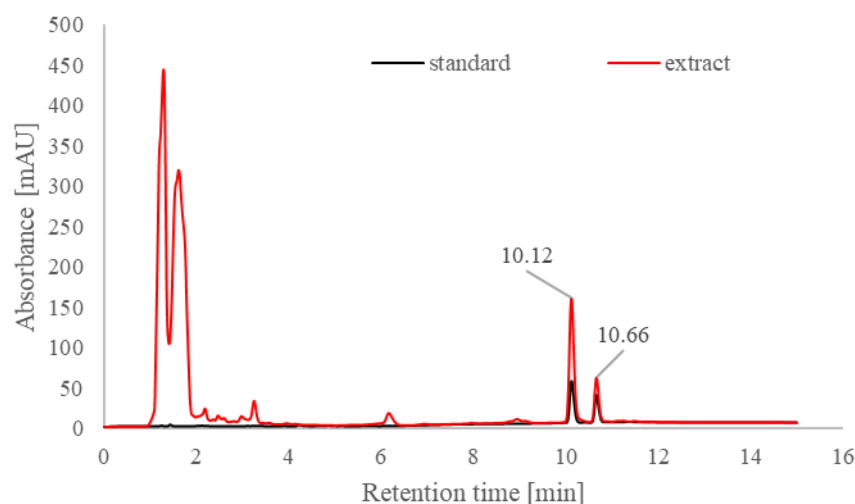We chose European oak heartwood for testing the penetration of wood preservative because of its poor impregnability associated with low permeability to liquids, despite its high natural durability that usually makes biocide treatment unnecessary.

The amount of gel applied was between 450 g/m^2 and 480 g/m^2, as determined by mass differences before and after spreading. Chemical analysis of samples taken at various depths from the surface showed the penetration depth of the active substance, permethrin. All samples, independent of anatomical direction, showed a clear negative gradient in the concentration of permethrin with the distance from the surface (Table 1). At a depth of 10 mm the concentration was around a tenth of that in the surface layer and permethrin was not detectable in most analysed samples at a depth of 20 mm. We found no significant difference between the two anatomical orientations tested, though the radial treatment was usually slightly more effective. European oak wood is characterised by large and abundant pith rays, which other research has found facilitate deeper penetration in the radial direction (Coté 1963). The technical instructions of the product tested did not state the optimal conditions for application, but it seems that the process of penetration is influenced by the conditions under which the wood is stored after treatment. Conditions leading to faster drying of the preservative gel restricted the penetration of active agent. A high temperature combined with low relative humidity, which can occur during the summer, for example in roof construction, distinctly slowed down the penetration process. Permethrin was present no deeper than in the second layer (10 mm) in most of samples and the concentration was significantly lower than in samples stored under other tested conditions (Table 1).

Table 2: Dependence of permethrin concentration at different depths on wood anatomical orientation and storing conditions (temperature/relative humidity)

	Concentration [µg/g]					
	Radial			**Tangential**		
Depth [mm]	**10/80**	**20/60**	**35/40**	**10/80**	**20/60**	**35/40**
0	990.4	723.5	1,268.1	879.2	1,065.4	1,420.4
10	141.8	76.4	14.0	102.9	73.2	6.6
20	10.1	0.0	7.3	0.0	5.2	1.2
30	6.2	5.0	0.0	0.0	4.0	0.0

The performance of chemical preservative treatments is mostly evaluated according to their penetration and retention. To ensure biosecurity, wood preservative treatments must also meet minimum retention requirements, defined as the quantity of the preservative retained in the specified assay zone. A level of 12 g/m^3 of permethrin is required to prevent development of *Hylotrupes bajulus*, while a lower retention

of 7 g/m³ is required to prevent *Anobium punctatum* in fully impregnated wood (Berry and Read 1992). In this study, the retention was due to a surface load considerably higher than the required level in the surface layer and ranged from 500 to 1,000 g/m³ depending on the storage conditions (Figure 3).

In the second layer (10 mm) the treatment reached the level of retention required to prevent infestation by both wood-boring beetles, with the exception of the condition 35/40, where the permethrin retention was below the minimum requirement in both orientations.
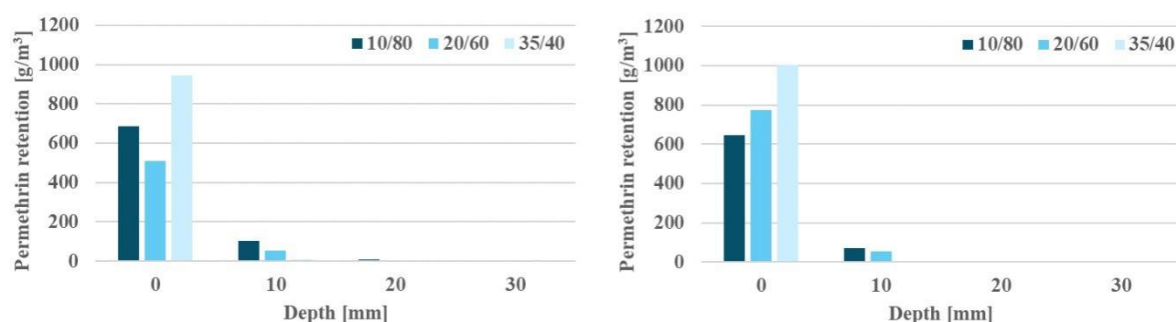

Figure 4: The effect of storage condition and wood anatomical orientation – radial (left), tangential (right) – on permethrin retention in individual layers

CONCLUSIONS

The permethrin contained in gel preservative is able to penetrate deeply into European oak heartwood. It was detectable at a depth of 10 mm from the surface and occasionally even deeper, but there was a steep negative gradient of permethrin concentration with increasing depth. The conditions under which the wood was stored after treatment influenced the depth of penetration. A higher temperature accelerated gel drying and restricted preservative penetration. The anatomy direction affected the penetration process only slightly, as pith rays facilitated penetration in the radial direction. The retention of permethrin even at a depth of 10 mm was sufficient to prevent infestation by wood-boring beetles.

ACKNOWLEDGEMENTS

REFERENCES

Berry RW, Read SJ (1992) The loss of insecticidal action from synthetic pyrethroid-treated wood samples: The effect of high temperatures and relative humidities. IRG/WP 92-1569. Int Res Group Wood Pres. IRG Secretariat, Sweden.

Côté WA (1963) Structural factors affecting the permeability of wood. Journal of Polymer Science, Part C 2: 231–242.

Despot R, Hasan M, Rapp A, Brischke C, Humar M, Welzbacher C, Ražem D (2012) Changes in Selected Properties of Wood Caused by Gamma Radiation. In: Adrovic F (ed) Gamma radiation, InTech, Rijeka, Croatia, pp 281–305

Messaoudi D, Ruel K, Joseleau PJ (2020) Uptake of insecticides and fungicides by impregnable and refractory coniferous wood species treated with commercial bio-based emulsion gel formulations. Maderas-Cienc Tecnol 22: 505–516. http://dx.doi.org/10.4067/S0718-221X2020005000409

Reinprecht L (2016) Diagnosis, sterilisation and restoration of damaged timber structures, 1st ed. Technical University in Zvolen, Zvolen, Slovakia. ISBN 978-80-2282921-2.

Richardson BA (1993) *Wood preservation, 2nd ed.* E. & F.N. Spon, London; New York. ISBN 9780419174905

The weathering of the beech wood impregnated by pigmented linseed oil

Jakub Dömény[1*], Jan Baar[1]

[1] Mendel University in Brno, Faculty of Forestry and Wood Technology, Zemědělská 3, 613 00 Brno, Czech Republic

E-mail: jakub.domeny@mendelu.cz; jan.baar@mendelu.cz

Keywords: wood coating, historic wooden conservation, natural weathering, water uptake, artificial weathering

ABSTRACT

This study was set up to investigate the impact of deep impregnation method and surface coating using linseed oil, supplemented with a small amount of brown shade pigment, on the natural and artificial weathering of wood. The treated samples, together with the reference ones, were exposed to natural weathering (4 years) and artificial weathering (1900 hours). The change in surface structure and colour during the weathering were evaluated. For specimens subjected to artificial weathering, the wettability of the treated surface was measured before and after weathering. Impregnated and painted samples lose their brown hue during weathering, and the wood turns gray. Greater disparities become evident during natural weathering, with a more significant change in the structure of the wood surface in painted samples. On the other hand, impregnated samples significantly slowed down structural changes in wood compared to the reference. Both treatments significantly reduced water uptake before weathering, however, this effect disappeared during weathering, though the wood still absorbed less water than the reference.

INTRODUCTION

Natural wood is inherently susceptible to weathering deterioration, leading to the degradation of its surface layers. Additionally, it frequently faces attacks from biotic agents such as wood-rotting fungi and wood-boring insects (Kutnar and Muthu 2016). This necessitates the application of protective coating to increase its service life during exterior use (Bansal *et al.* 2022). Coatings not only enhance protection against environmental factors, including moisture, radiation, biological decay, and potential damage from mechanical or chemical sources, but also contribute to the visual appeal of wooden materials through features like color and gloss (Meijer 2001). Currently, there is a significant emphasis on investigating ecological coatings for wood protection, taking into consideration environmental concerns and issues associated with synthetic wood coatings (Schaller and Rogez 2007). These issues may arise from factors such as their origin, toxicity, or challenges in end-of-life disposal (Meijer 2001). Historically, wood protection involved the use of coatings based on linseed oil, either in the form of covering pigment coatings or transparent linseed oil itself as a hydrophobizing agent (Eastman 1968). In the past, linseed-oil paints frequently included additives such as lead white, turpentine, Japan drier and cobalt or manganese driers, alongside earth pigments responsible for the paint's color and opacity. These supplementary components altered the paint's viscosity, longevity, drying speed, and ability to resist biological degradation (Gibbs and Wonson 2021). Growing environmental consciousness has sparked a revival of linseed oil paint as a traditional wood surface treatment spanning centuries. Linseed oil has gained popularity, finding favor in the market. However, it's essential to note that present-day products differ from their historical counterparts. Historical linseed oil paints, for instance, contained significant amounts of lead, a highly effective fungicide (Brandt and Lading 2002). Notably, there is a scarcity of comprehensive and comparable experimental data in the documentation of surface treatments using modern linseed oil products. This information gap has given rise to various myths surrounding linseed oil and its properties. Therefore, this study was set up to investigate (a) the impact of deep impregnation method and (b) surface coating using linseed oil, supplemented with a small amount of pigment, on the natural and artificial weathering of wood. The work described in this paper will be followed by tests on different wood species to produce comprehensive data.

MATERIALS AND METHODS

European beech (*Fagus sylvatica* L.) sourced from university enterprise Masaryk Forest in Křtiny, with an average density of 762 kg/m^3, served as the raw material. Flat-sawn sapwood boards were prepared to dimensions of 375 mm × 100 mm × 20 mm for natural weathering and 150 mm × 74 mm × 20 mm for artificial weathering. After storage at 65% RH and 20 °C for 20 days, the samples underwent a combination of biocide protection using a copper-based water treatment and vacuum impregnation with protective linseed oil. Firstly, a non-pressure treatment involved immersion in a 4% solution of copper-based biocide protection (Bochemit Forte Profi based on $Cu_2(OH)_2CO_3$). Following the copper treatment, the process continued with vacuum impregnation of pigmented linseed oil, featuring a brown shade (BIB), under a pressure of 50 kPa. This was followed by a simultaneous drying process for 11 hours at 80°C using the laboratory impregnation plant JHP1-0072. Another set of beech sapwood boards was exclusively painted with pigmented linseed oil (BCB). After conditioning at 65% RH and 20 °C until an equilibrium state was reached, the samples were subjected to both natural and artificial weathering. The samples designated for natural weathering were exposed to environmental conditions for a duration of 4 years, allowing for the observation of long-term effects. Additionally, accelerated artificial weathering was conducted using the xenon test chamber Q – Sun Xe –1 (Q – Lab Corp.), exposing the samples to 1900 hours of controlled environmental conditions. This included a 2-hour repeat cycle following the modified standard ASTM G155 (2013), simulating rain (18 min) and solar radiation (102 min, TUV 70 W/m^2). The surface discoloration was measured before and during the artificial weathering process at various time intervals (50, 200, 500, 1000 and 1800 h) using a Konica Minolta CM-2500 based on the CIELab color system. Water uptake during water floating was assessed following the standard EN 927-5:2006, involving different sets of samples: one exposed to artificial weathering and another comprising unweathered samples. Pre-conditioning at 65% RH and 20°C, along with end grain sealing, was followed by immersion in water, with mass measurements taken at specific intervals (0, 2, 4, 6, 8, and 10 h). Following the natural weathering exposure, an extensive visual evaluation of the samples was conducted annually, accompanied by photography. This regular inspection facilitated a detailed analysis of changes in appearance and condition over the 4-year exposure period.

RESULTS

The linseed oil treatment of the samples affected the color values as expected. Both the vacuum-impregnated linseed oil with brown pigment and the painted linseed oil with brown pigment decreased the lightness value L* (Figure 1a), as well as the a* and b* values (Figure 1b, c). Based on the visual examination (Figure 2), it's evident that the surface lightness of the reference (BR) and oil-treated wood (BCB, BIB) increased over time due to artificial weathering. The results of the visual analysis are confirmed by the values in Figure 1a. The most significant increase in the L* parameter was observed in the specimens impregnated with linseed oil (BIB) after 1900 hours of artificial weathering. Additionally, the ΔE values in Figure 1d indicate significant changes in all exposed specimens during artificial weathering. The group painted with linseed oil containing brown pigment (BCB) showing the smallest changes, possibly due to a higher pigment concentration in the surface layer, providing greater resistance to photodegradation. During weathering, both impregnated and painted samples lost their brown hue, and the wood turning gray. This observation aligns with the findings of Mallégol et al. (2000), which noted rapid degradation of linseed oil under light exposure due to photo-oxidation processes. More pronounced disparities emerged during natural weathering (Figure 3), with painted samples exhibiting more significant changes in wood surface structure compared to the impregnated samples. Conversely, impregnated samples significantly slowed down structural changes in wood compared to the reference.
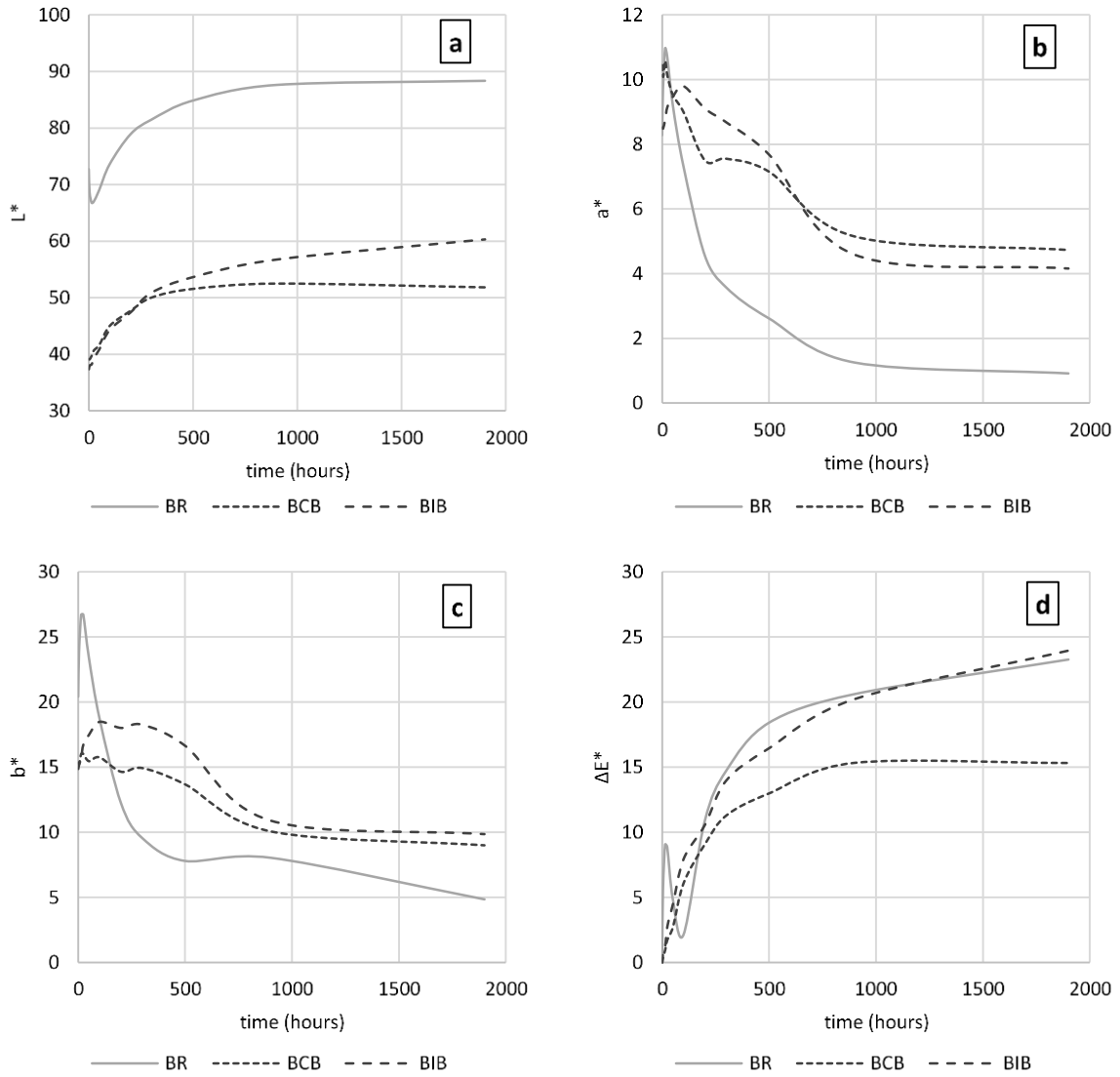
Figure 1: Effect of artificial weathering time on color values: L* (a); a* (b); b* (c). Graph (d) shows the total color change ΔE by specimens group following artificial weathering

Figure 2: Surface discoloration of artificially weathered specimens after 0, 24, 500, and 1900 hours of exposure
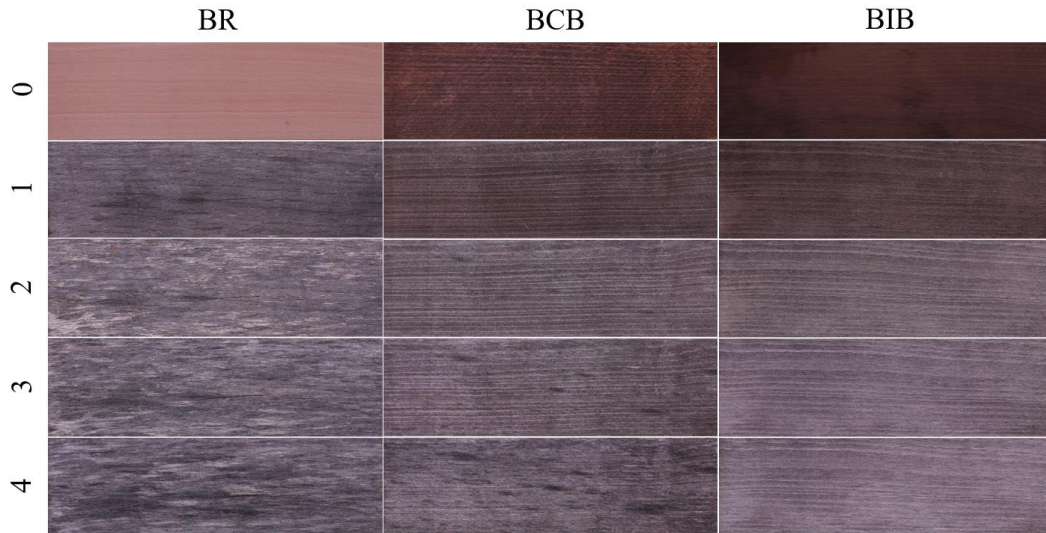
Figure 3: Surface discoloration after 1, 2, 3, and 4 years of natural weathering

The wettability of the treated surface was measured before and after weathering for all specimens subjected to artificial weathering (Figure 4). Water absorption of linseed oil-treated specimens (BCB and BIB), measured as a function of immersion time, was significantly lower than for the corresponding reference specimens (BR). Both treatments significantly reduced water uptake before weathering Figure 4a). However, this effect disappeared during weathering (Figure 4b), although the wood still absorbed less water than the reference. Linseed oil is inherently hydrophobic, but exhibits limited resistance to photodegradation, as evidenced by the water absorption results after artificial weathering. These findings align with reported surface discoloration observed during the weathering process. Furthermore, the results indicate that impregnating wood with linseed oil maintains better hydrophobicity of the surface after weathering compared to painting it.
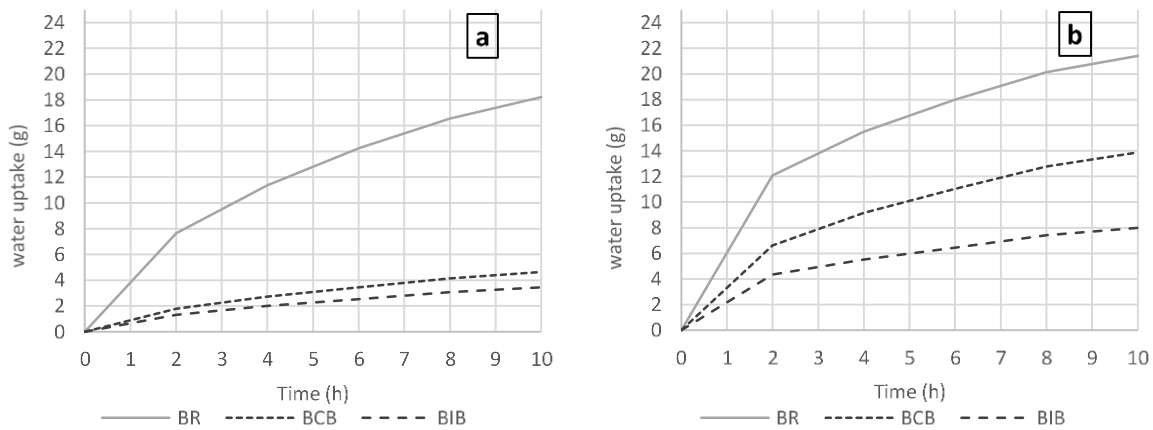
Figure 4: Water uptake of reference (BR), painted (BCB), and impregnated (BIB) specimens during liquid water floating before (a) and after artificial weathering (b)

CONCLUSIONS
Linseed oil-based treatments for protecting natural wood from weathering was studied. In conclusion, linseed oil treatment significantly influenced the color values and surface properties of wood during weathering. Both impregnated and painted linseed oil led to a transition from brown to gray, with impregnated samples showing slower structural changes. While both treatments reduced water uptake, impregnation maintained better hydrophobicity after weathering. These results suggest the potential of linseed oil-based treatments, particularly impregnation, for preserving wood properties during weathering.

REFERENCES

Bansal R, Nair S, Pandey KK (2022) UV resistant wood coating based on zinc oxide and cerium oxide dispersed linseed oil nano-emulsion, Mater. Today Commun. 30: 103177. https://doi.org/10.1016/j.mtcomm.2022.103177

Brandt E, Lading T (2002) Linseed oil paint as an alternative to wood preservatives. Paper presented at 9th International Conference on Durability of Materials and Components, Brisbane, Australia.

Eastman W (1968) History of the Linseed Oil Industry in the United States, T.S. Dension, Mineapolis, MN

Gibbs E, Wonson K (2021) Purified Linseed Oil: Considerations for Use on Historic Wood. The Journal of Preservation Technology 52(4): 25–32. https://www.jstor.org/stable/48647851

Kutnar A, Muthu SS (2016) Environmental impacts of traditional and innovative forest-based bioproducts. Springer, Berlin, p 248. https://doi.org/10.1007/978-981-10-0655-5

Mallégol J, Gardette JL, Lemaire J (2000) Long-term behavior of oil-based varnishes and paints. Fate of hydroperoxides in drying oils. Journal of the American Oil Chemists' Society. 77(3): 249-255. https://doi.org/10.1007/s11746-000-0041-5

Meijer M (2001) Review on the durability of exterior wood coatings with reduced VOC-content. Prog. Org. Coat. 43: 217–225. https://doi.org/10.1016/S0300-9440(01)00170-9

Schaller C, Rogez D (2007) New approaches in wood coating stabilization. J Coat Technol Res 4(4):401–409. https://doi:10.1007/s11998-007-9049-5

Examination of the durability of beeswax-impregnated wood

Miklós Bak[1*], Ádám Bedők[1], Róbert Németh[1]

[1] University of Sopron, Bajcsy-Zs. Str. 4, Sopron, Hungary, 9400.

E-mail: bak.miklos@uni-sopron.hu; bedoka17@student.uni-sopron.hu; nemeth.robert@uni-sopron.hu

Keywords: wood modification, beeswax, impregnation, durability

ABSTRACT
Within the framework of this research, the biological durability of two different wood species (*Pinus sylvestris* and *Fagus sylvatica*), impregnated with beeswax was investigated. The durability was tested according to the standard EN 113, and with a laboratory-scale soil contact test, based on the standard ENV 807, using modified parameters. The aim of the tests was to increase the biological durability of the samples treated with beeswax by impregnation. Test specimens modified in this way do not have any toxic effect on the environment. Unimpregnated beech and Scots pine samples showed high decomposition during both decay tests. The damage of the impregnated samples was markedly lower. Beside mass loss, this was confirmed by the visual inspection of the samples after soil exposure under laboratory conditions. Impregnated samples showed low degradation level compared to the controls.. SEM imaging showed that beeswax filled the lumens and separated most of the cell walls from the hyphae, which slowed the spreading of the fungi in the wood.

INTRODUCTION

The advantage of beeswax is its biological origin and its nontoxic nature. However, natural waxes are generally not biologically stable (Schmidt 2006). Nonetheless, they can delay the decay of wood because waxes are water repellent, and with the impregnation method, the cell lumens can be filled with wax (Bak et al. 2015). As a result of the hydrophobic properties of beeswax and the lumen filling, the decay of wood by fungi is slowed. Waxes have the effect of reducing termite damage as well, but they cannot protect wood completely (Scholz et al. 2010a). Another advantage of wax impregnation of wood is the improvement in wood's mechanical properties. For example, the hardness can be increased in beech wood up to 86 to 189% in the longitudinal and lateral directions, respectively (Scholz et al. 2010b). Different waxes, including beeswax, are often used as conservation agents for wooden artifacts (Timar et al. 2010; Timar et al. 2011). This shows that under appropriate conditions, beeswax is suitable for wood protection. Chemical composition of beeswax presents a huge diversity of components because of its lipid nature. Beeswax is mostly composed of a mixture of hydrocarbons, free fatty acids, monoesters, diesters, triesters, hydroxy monoesters, hydroxy polyesters, fatty acid polyesters, and some unidentified compounds. Each class of compounds consists of a series of homologues differing in chain length by two carbon atoms (Maia and Nunes 2013).

During the outdoor utilization of wood, the hazard class of soil contact is ranked very high among the exposure classes (use class 4, according to EN 335 (2013)). For use in soil contact, very effective protection and/or durable wood species are needed. The aim of the tests was to increase the biological durability of the samples treated with beeswax by impregnation.

MATERIALS AND METHODS

Scots pine (*Pinus sylvestris*) and beech (*Fagus sylvatica*) samples were impregnated with beeswax and exposed to fungi under laboratory conditions. Unimpregnated samples were used as the control. Wood pores were completely filled with wax, or at least their surface was coated with wax as a result of the impregnation, depending on the degree of impregnation. Beeswax was melted at 80 °C in a closed chamber, and the dry samples (moisture content: 0%) were put into the melted beeswax. After that, the pressure was decreased in the chamber to 150 mbar for 4 h. Following the vacuum period, the pressure was increased to 6 bar and the temperature of the beeswax (with the samples) was kept at 80 °C for 24 h. Weight percent gain (WPG) was calculated according to the initial dry weight of wood (m_0) and the beeswax impregnated wood (m_i) (Eq. 1):

$$WPG = \frac{m_0 - m_i}{m_0} \times 100 \ [\%] \tag{1}$$

The presence and distribution of beeswax in the structure of wood was tested with scanning electron microscopy (SEM) imaging, using a Hitachi S-3400N device.

The effect of beeswax impregnation on the durability was tested under laboratory conditions using two methods. One method was the EN113 (2020) standard method, where 15×25×50mm wooden blocks were exposed to a white rot *Trametes versicolor* and a brown rot *Coniophora puteana,* 10 pieces of each variation. The other method was based on the ENV807 standard method, but no fungi culture was added to the soil used. The fertile soil was taken from the Botanical Garden of the University of Sopron, with its original decaying organisms. Thus, the decaying organisms were unknown in this case. The moisture content of the soil in plastic containers was kept at 95% of its water holding capacity to ensure constant conditions during the test. Samples with dimensions of 5×10×150 mm were used. The incubation time was 32 weeks. Mass losses (ML) were calculated according to the initial dry weight (m_0) and the decayed dry weight of wood (m_{0d}) (Eq. 2):

$$ML = \frac{m_0 - m_{0d}}{m_0} \times 100 \ [\%] \tag{2}$$

RESULTS AND DISCUSSION

Weight percent gain

WPG of both beech and Scots pine was considered as high after the impregnation process, which indicates high efficiency of the treatment. However, wood species showed different WPGs, which is contributed to their different pore volume (Fig. 1).
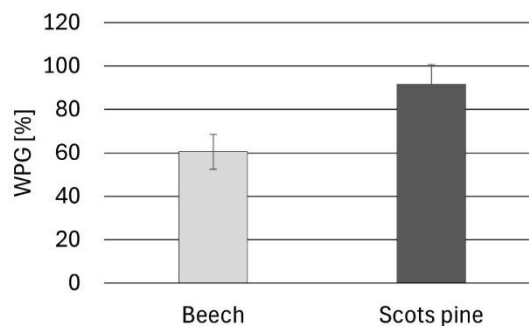
Figure 1: WPG of beech and Scots pine samples as a result of beeswax impregnation. Bars indicating standard deviation

Microscopic imaging

SEM imaging supported the results of WPG, as it showed that most of the cell lumens were entirely filled with beeswax. Only a slight amount of cell lumens was detected as empty or partly filled. Generally, the cell walls in the lumens partly filled were covered by the beeswax entirely. Besides, a low ratio of lumens without any beeswax were detected as well (Fig. 2). This is considered as a weak point of the method, as the protection mechanism of this treatment is the blocking of the lumens and excluding of the hyphae in order to slower the fungal decomposition of the wood without using fungicides. However, the impregnation efficiency could be improved by the alteration of the impregnation parameters in order to increase the amount of beeswax in the wood structure. This might further improve the protective effect of the treatment. Beside the lumen filling, it is expected that the beeswax impregnation decreases the moisture absorption of wood, which is contributing to the protection efficiency of the method.
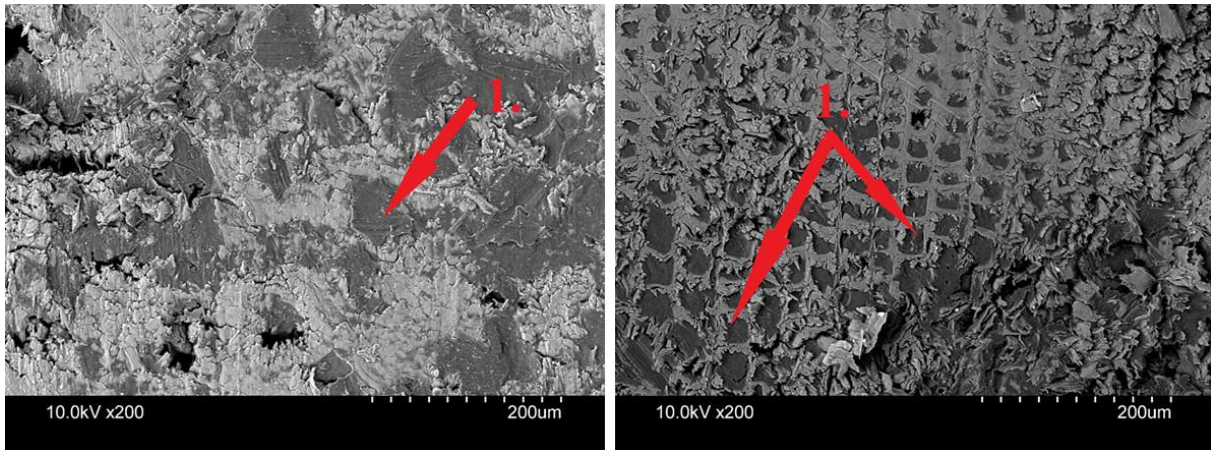
Figure 2: SEM images of beeswax impregnated beech (left) and Scots pine (right). Arrows indicating filled lumens

Durability test according to EN 113

The durability test after 16 weeks of incubation time showed a significant improvement in the durability of the impregnated wood. In *Trametes versicolor* the average ML decreased by 44.93% and 76.24% for beech and pine respectively, as a result of the beeswax impregnation (Fig. 3a). In *Coniophora puteana* the average ML decreased by 59.05% and 46.96% for beech and pine respectively, as a result of the beeswax impregnation (Fig. 3b). These results indicate that it is not possible to reach full protection to wood using beeswax, even at high impregnation levels.
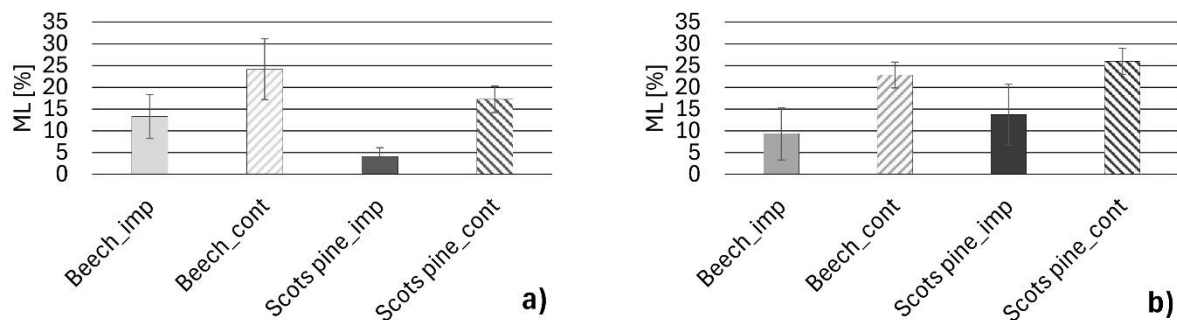
Figure 3: Mass loss of beeswax impregnated (_imp) and control (_cont) beech and Scots pine samples after EN 113 decay test, using the white rot Trametes versicolor (a) and the brown rot Coniophora puteana (b) as test fungi. Bars indicating standard deviation

Durability test according to ENV 807

The durability test after 32 weeks of incubation time showed a significant improvement in the durability of the impregnated wood in this case as well. The average ML decreased by 53.04% and 37.03% for beech and pine respectively, as a result of the beeswax impregnation (Fig. 4). These results also underline the conclusion taken according to the EN 113 test method that it is not possible to reach full protection to wood using beeswax, even at high impregnation levels. However, the results indicate that this wood modification method might be a considerable alternative solution for wood protection under less harsh conditions than soil contact.

The ML results were supported by the visual inspection. Control samples showed in some cases total decomposition (ML=100%, beech control), or at least high level of erosion with a remarkable loss in the cross section and/or the length (Scots pine control). Despite that, beeswax impregnated samples were found less affected by decay in their cross-sectional dimensions (Fig. 5). However, mass loss was high in their case as well.
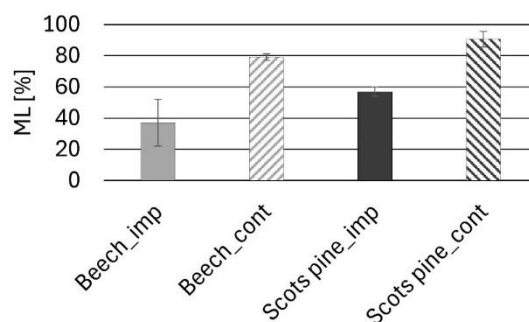
Figure 4: Mass loss of beeswax impregnated (_imp) and control (_cont) beech and Scots pine samples in soil contact after the modified ENV 807 decay test. Bars indicating standard deviation

Figure 5: Visual inspection of beeswax impregnated (_imp) and control (_cont) beech and Scots pine samples in 32 weeks of soil contact after the modified ENV 807 decay test

CONCLUSIONS

Beeswax impregnation of beech and Scots pine wood improved the decay resistance significantly. Unimpregnated beech and pine samples showed high decomposition during both decay tests compared to the beeswax impregnated ones. The damage of the impregnated samples was markedly lower. Beside mass loss, this was confirmed by the visual inspection of the samples after soil exposure under laboratory conditions. Impregnated samples showed low degradation level compared to the controls. SEM imaging showed that beeswax filled the lumens and separated most of the cell walls from the hyphae, which slowed the spreading of the fungi in the wood. However, the beeswax could not provide full protection to wood, it could only slower the decomposition. Nevertheless, the decay resistance was improved by a biomaterial, without using any biocides. Even if it is not expected to provide adequate protection in soil contact, but the results show that under certain conditions (use classes lower than 4) the beeswax impregnation might provide effective protection to wood.

ACKNOWLEDGEMENT

REFERENCES

EN 113 (2020) Durability of wood and wood-based products - Test method against wood destroying basidiomycetes. European Committee for Standardization, Brussels, Belgium.

EN 335 (2013) Durability of wood and wood-based products. Use classes: Definitions, application to solid wood and wood-based products. European Committee for Standardization, Brussels, Belgium.

ENV 807 (2001) Wood preservatives - Determination of the effectiveness against soft rotting micro-fungi and other soil inhabiting micro-organisms. European Committee for Standardization, Brussels, Belgium.

Maia M, Nunes F M (2013) Authentication of beeswax (*Apis mellifera*) by high-temperature gas chromatography and chemometric analysis. FOOD CHEM 136(2):961-968. https://doi.org/10.1016/j.foodchem.2012.09.003

Németh R, Tsalagkas D, Bak M (2015) Effect of soil contact on the modulus of elasticity of beeswax-impregnated wood. BIORESOURCES 10(1):1574-1586. https://doi.org/10.15376/biores.10.1.1574-1586

Schmidt O (2006) Damage to structural timber indoors. in: D. Czeschlik (ed) Wood and Tree Fungi, Springer, Berlin, Germany, pp. 207-237. https://doi.org/10.1007/3-540-32139-X

Scholz G, Militz H, Gascón-Garrido P, Ibiza-Palacios M S, Oliver-Villanueva J V, Peters B C, Fitzgerald C J (2010a) Improved termite resistance of wood by wax impregnation. INT BIODETER BIODEGR 64(8): 688-693. https://doi.org/10.1016/j.ibiod.2010.05.012

Scholz G, Krause A, Militz, H. (2010b) Beeinflussung der Holzfestigkeit durch Wachstränkung. Holztechnologie 51(1):30-35.

Timar M. C., Tuduce, T. A., Porojan, M., and Lidia, G. (2010). "An investigation of consolidants penetration in wood. Part 1: General methodology and microscopy," Pro Ligno 6(4), 13-27.

Timar, M C, Tuduce T A, Pałachia S, Croitoru C (2011) An investigation of consolidants penetration in wood. Part 2: FTIR spectroscopy. Pro Ligno 7(1):25-38.

Preparation of pleated oak samples and their bending tests at different moisture contents

Pál Péter Gecseg[1], Mátyás Báder[1*]

[1] University of Sopron, Faculty of Wood Engineering and Creative Industries, Bajcsy-Zs. Str. 4, Sopron, Hungary, 9400.

E-mail: gecsegpali@gmail.com; bader.matyas@uni-sopron.hu

Keywords: longitudinal compression, pleating, modulus of rupture, modulus of elasticity, moisture content, sessile oak

ABSTRACT

This study presents the steps and results of the longitudinal compression modification process (aka. pleating) and bending tests of sessile oak (*Quercus petraea* (Matt.) Liebl.) wood. Bending tests were done to determine properties under different moisture conditions. The stress values during compression of the specimens were nearly identical, attributed to proper pre-selection of the specimens. However, significant differences were observed during bending tests. The results of the three samples (pleated and conditioned to 12% moisture content (*MC*), pleated and frozen with *MC* above fibre saturation point (*FSP*), and untreated-conditioned to 12% *MC* showed significant discrepancies. Regarding modulus of rupture (*MoR*), the average values were averagely 103.20 MPa for the pleated samples conditioned to 12% *MC*, 63.26 MPa for the frozen samples, and 136.80 MPa for the untreated sample conditioned to 12% *MC*. In terms of modulus of elasticity (*MoE*), the average values were averagely 4.02 GPa, 1.42 GPa and 12.25 GPa, respectively. These results suggest that samples with higher *MC* can withstand less load but are significantly more flexible, whereas samples with lower *MC* can withstand greater load but are stiffer. We hope these findings can contribute to better decision-making regarding future wood utilization practices.

INTRODUCION

A purpose of longitudinally compression (or pleating) timber is to make it more flexible and pliable. Treating wood as an inhomogeneous fibre-reinforced composite, post-plasticization, and pleated it along the fibre axis result in compression. This process makes the timber more bendable with less force. Steam bending of wood was first utilized by Michael Thonet in the 1800s for mass production under industrial conditions. In Thonet's method, wood must be immediately shaped after steaming before it cools. In contrast, the advantage of longitudinal compression technology is that the treated timber can be stored and remains bendable at room temperature. Hardwood species with higher density (such as oak, beech, ash, maple) have been found to be compressible along the fibre direction. High-quality raw material is essential, as seemingly insignificant failures in the wood can often pose significant problems. Key factors determining the production of quality compressed timber include wood species, quality of raw material, *MC*, temperature, compression direction, and others. Most hardwood species with initial *MC* above 20% can be compressed. During the typically steam-plasticized longitudinal compression process, it's necessary to support the wood to prevent lateral deflection and reduce friction forces that inhibit uniform compression along the fibres. As a result of longitudinal pressing, changes occur in the cell structure of the wood, which has been softened by hydrothermal treatment and kept at a temperature of at least 80°C. The middle layer, mainly composed of lignin and hemicellulose, allows the high cellulose content, solidifying fibres, and other tissues to slide relative to each other, while the cell walls of these longitudinally oriented elongated elements become wrinkled (Figure 1). As a result of the process, the bending modulus of elasticity *MoE* the wood decreases, making it significantly more bendable compared to untreated wood (Báder 2015; Báder et al. 2017).
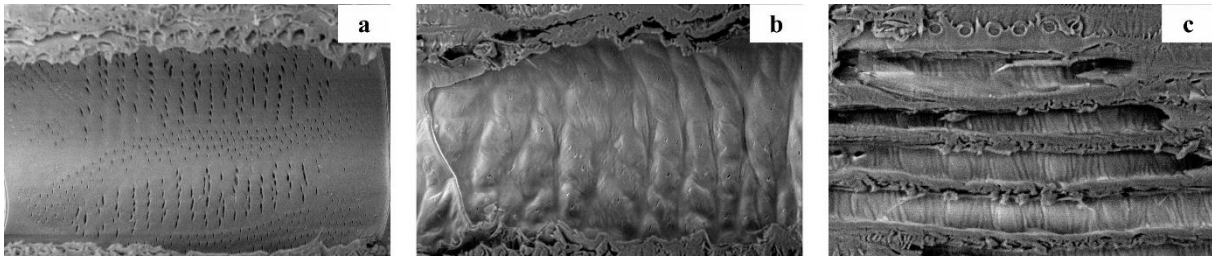
Figure 1: Changes in vessels and fibres during compression: Untreated vessels (a), pleated vessels (b) pleated fibres (c)(based on Báder and Németh 2018)

Wood contain water in two states: free water and bound water. Free water exists in the wood as liquid or vapor and has a significant impact on the wood's mass and density, particularly when the *MC* exceeds 30%. However, it does not affect the wood's shape or size changes. The removal of bound water begins only after the evaporation of free water. The point at which there is no free water left in the cell structure of the wood is called the *FSP*. While the value of the *FSP* depends on the wood species, generally, the portion of wood *MC* below 30% is considered bound water, and the *MC* threshold of 30% is referred to as the *FSP* (Fainfo.hu 2023).

Our study aims to demonstrate the changes that wood undergoes solely due to variations in *MC*. We primarily examined these changes through mechanical means. During our research, we were particularly interested in understanding the differences in load-bearing capacity and other mechanical properties of wood material in response to changes in *MC*. Moisture content in wood significantly influences the construction industry, as the load-bearing capacity of wood varies considerably with changes in *MC*.

MATERIALS AND METHODS

As a first step, we selected 10-10-10 pieces of suitable, 20×30×200 mm (thickness × width × length) dimensioned sessile oak (*Quercus petraea* (Matt.) Liebl.) specimens for each sample. Care was taken to ensure that the wood was free from failures, as these would have led to inaccuracies in the measurements. Examples of such failures include diagonal grain deviation, knots, cracks, etc. Subsequently, the specimens were numbered for tracking purposes (Figure 2), followed by the pleating of the wood. The pleating was performed using an INSTRON 4208 material testing machine (INSTRON Corp., USA). Prior to compression, the samples were steamed for 45 minutes at 100 °C. Compression was carried out by an equipment at a rate of 25%, then the specimens were kept compressed for 1 minute. After pleating, if the specimens had bent, they were manually straightened. Once pleating was complete, the specimens were cut in half, preparing them for bending test. The longitudinal dimensions of the pleated samples were on average 193.12 mm ± 0.71 mm. Thickness and width dimensions remained unchanged (20x11 mm), except for the untreated sample sample conditioned to 12% *MC*. Subsequently, the samples were conditioned. The sample with *MC* above *FSP* was stored in a freezer to maintain its green state, while the sample conditioned to 12% *MC* was stored in a climate chamber at 20 °C and 65% relative humidity until its weight stabilized. 4-point bending tests were also done on the INSTRON 4208 material testing machine. The specimens protruded at least 2-2 cm on both sides of the support span rollers. The support span was set to 140 mm, while the distance between the loading rollers was 50 mm. Bending tests were conducted at a rate of 16 mm/min for pleated specimens and at a rate of 8 mm/min for untreated specimens, with 10 specimens per sample. This was necessary to comply with the requirements of both EN 408: 2010 + A1 (2012) and ISO 13061-03 (2014) standards, which require a bending tests time between 1 and 5 minutes. Prior to each test, width and thickness parameters were measured at the centre of the sample. Upon completion of the bending tests, our subsequent task involved comparing and evaluating the collected data. Conclusions drawn from the measurements mainly involved the average results and relative deviances of the maximum compressive stress and the length of the samples after pleating.

Figure 2: Storage of the specimens in the climate room

RESULTS AND DISCUSSION

During pleating, the results of the specimens did not show significant differences. This indicated that we had performed appropriate raw material selection before pleating, ensuring that the specimens were similar anatomically and physically. With this in mind, we could state that the differences in the results obtained from the bending tests were not due to the wood itself but rather to differences in *MC* within the wood. The average *MoR* was 136.80 MPa for the sample conditioned to 12% *MC*. In comparison, the pleated sample conditioned to 12% *MC* showed 24.6% lower *MoR*, while the pleated sample frozen above *FSP* was 53.8% lower (Figure 3). We attribute the observed changes in the measurements to lignin and hemicellulose in the wood, as they behave more plastically with higher *MC* in the wood. Another reason could be that the pleated specimens were much more flexible. The average values of the *MoE* were 12.25 GPa for the untreated sample, 4.02 GPa for the pleated and conditioned sample, and only 1.42 GPa for the pleated and frozen sample. The relative deviances were under 20% in all cases. The results of these tests indicate that the higher the *MC* of the wood, the lower its *MoE*, which is in agreement with the literature. Therefore, the higher *MC* of the wood, the more pliable it becomes. Lower *MoE* of the wood exhibits more plastic properties. Our sample with high *MC* and consequently low *MoE* suffered less, or almost no damage during the bending test. During pleating, the average values of maximum compressive stress were 19.41 MPa for the pleated and conditioned sample and 21.03 MPa for the pleated and frozen sample. The relative deviations were 7.3% and 7.1%.
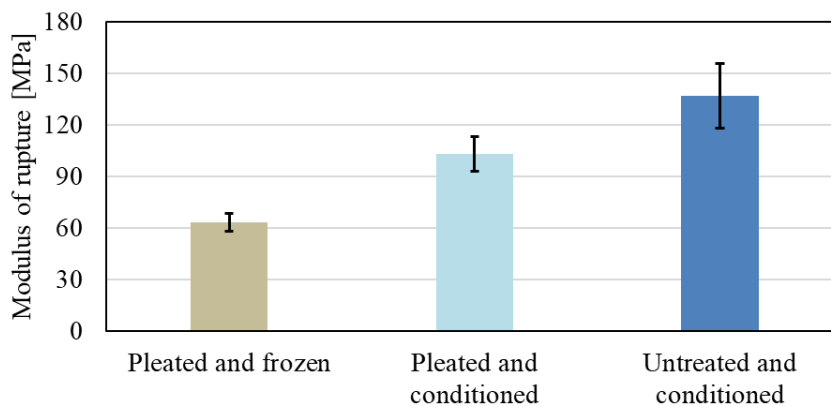
Figure 3: Modulus of rupture of the samples. The frozen sample had a moisture content above fibre saturation point, while the other two samples were conditioned to 12% moisture content

Pleating altered the cell structure of the specimens, resulting in lower *MoR* compared to untreated sample. On average, the *MoE* of sessile oak is ~10.5 GPa (Meier 2023), which may change depending on the provenance. In our case, for untreated sample, the average result was 12.25 GPa, with a relative deviance of 12.8%. However, difference was not only found in *MoE*. The bending stress measured at 4 mm deflection was 114.98 MPa for the untreated sample, 40.69 MPa for pleated and conditioned sample, and 18.60 MPa for pleated and frozen sample. The relative deviations were 12.42 MPa, 4.67 MPa and 1.46 MPa, respectively. The average deflection at maximum force was 7.51 mm, 28.45 mm and 32.54 mm with relative deviations of 11.9%, 9.5% and 7.9%, respectively. At maximum deflection, we observed that the results of the pleated samples were almost identical, with a great increase compared to the untreated sample. The maximum deflections were 7.80 mm, 35.70 mm and 35.95 mm with relative

deviances of 12.2%, 20.9% and 7.3%, respectively. The maximum deflection was averagely 25.5% higher for pleated samples than their deflection at the maximum force. Here it is also evident that the wood of the pleated samples was more flexible and could withstand less load. Thus, if we want to bend two specimens with different *MC* with the same amount of force, the specimen with the higher *MC* would be easier to bend.

CONCLUSIONS

During our research, we were able to obtain numerous data from the results of untreated sample conditioned to 12% moisture content (*MC*), pleated sample conditioned to 12% *MC*, and pleated sample frozen above *FSP*. The results obtained from pleating demonstrated that the wood of the samples was available to be the post-modification tests comparable. This means that any differences in the bending test results could be attributed to the different *MC*s. The data obtained from the bending tests showed significant differences. For the untreated sample, the average modulus of rupture was 136.80 MPa, for the pleated and conditioned samples it was 103.20 MPa, and for the pleated and frozen samples was 63.26 MPa. The higher the water content in the wood, the less load it could withstand, but its plastic properties changed inversely. These changes between the samples are caused by the lignin and hemicellulose in the wood, as they behave more plastic in the presence of water. The modulus of elasticities for the samples were 12.25 GPa, 4.02 GPa, and only 1.42 GPa, respectively. After bending test, the specimens with higher *MC* typically intended to return to their initial shape, thereby reducing the bending induced in the wood by the test. Overall, our research demonstrated that pleating can significantly reduce the modulus of elasticity of wood, thereby enhancing its plastic characteristics.

ACKNOWLEDGEMENTS

REFERENCES

Báder M (2015) Practical Issues of Longitudinally Compressed Wood. Part 1: The raw material and its preparation; the theory of compression (Faanyag rostirányú tömörítésével kapcsolatos elméleti és gyakorlati kérdések áttekintése I. rész: Az alapanyagok és előkészítésük, a tömörítés elmélete). Faipar 63(1):1-9. https://doi.org/10.14602/WOODSCI.2015.1.8 (in Hungarian)

Báder M, Németh R (2017) Research conditions of the wood's longitudinal compression – Part 1 (A faanyagok rostirányú tömörítésének kísérleti körülményei – 1. rész). GRADUS 4(2):403-411 (in Hungarian)

Báder M, Németh R (2017) Research conditions of the wood's longitudinal compression – Part 2 (Faanyagok rostirányú tömörítésének kísérleti körülményei – 2. rész). GRADUS 4(2):412-418 (in Hungarian)

Báder M (2015) Practical Issues of Longitudinally Compressed Wood. Part 3: Mechanical properties and areas of application of compressed wood (Faanyag rostirányú tömörítésével kapcsolatos elméleti és gyakorlati kérdések áttekintése III. rész: A tömörített fa mechanikai tulajdonságai, felhasználási lehetőségei). Faipar 63(2):52-63. https://doi.org/10.14602/WOODSCI.2015.2.53 (in Hungarian)

EN 408: 2010 + A1 (2012) Timber structures - Structural timber and glued laminated timber - Determination of some physical and mechanical properties, Brussels, Belgium

ISO 13061-3: 2014 + AMD1 (2017) Physical and mechanical properties of wood - Test methods for small clear wood specimens - Part 03: Determination of ultimate strength in static bending. Amendment 1, International Organization for Standardization, Geneva, Switzerland

Meier E (2023) Sessile oak. In: Wood Database. https://www.wood-database.com/sessile-oak/ Accessed 23.11.2023

Fainfo.hu (2023) Moisture content of wood II: Free water, bound water (A faanyag nedvességtartalma II.: Szabad víz, kötött víz). https://www.fainfo.hu/a-faanyag-nedvessegtartalma-ii/ Accessed 25.10.2023 (in Hungarian)

Bending test results of small-sized glued laminated oak timber consisting of 2, 3 and 5 layers

Dénes Horváth[1*], Sándor Fehér[1]

[1] University of Sopron, Institute of Basic Sciences. Bajcsy-Zs. Str. 4, Sopron, Hungary, 9400.

E-mail: horvath.denes@uni-sopron.hu; feher.sandor@uni-sopron.hu

Keywords: GLT, Modulus of Rupture, Modulus of Elasticity, non-destructive, wood failures

ABSTRACT

This paper deals with glued-laminated timber (GLT) built up of low quality oak lamellae. Two-layered (40 mm), three-layered (45 mm) and five-layered (50 mm) GLTs were assessed to dynamical and statical tests in order to get the modulus of ruptures (*MoR*) and modulus of elasticities (*MoE*). The results showed that *MoR* is more than 60 MPa for the weaker samples and 80 MPa for the five-layered samples with low variance. *MoE* showed a decrease of altogether 7.7% with the increasing of the thickness. Non-destructive and destructive tests gave similar results. It can be concluded that the quality of the outer layers is very important for a GLT. But the inner layers may contain wood failures such as dead knots, slope of grain, etc.

INTRODUCTION

There is a growing interest in using hardwoods, such as oak, in glued-laminated timber, and efforts are underway to assemble the basic knowledge that would lead to standardization for the use of hardwoods in manufacturing glued-laminated timber (Morin-Bernard et al. 2020). Glued laminated timber made from oak has been gaining importance in structural applications, with the first national and European technical approvals issued for oak glulam (Aicher and Stapf 2014). Hardwoods, including oak, have the potential for the production of glued laminated timber with favourable mechanical characteristics and provisional approvals for construction use (Glavinić et al. 2020). Oak GLT has shown particularly good mechanical performance under both monotonic and cyclic loading regimes, indicating its potential for use in construction projects. Destructive tests, such as four-point bending tests, push-out shear tests, and cyclic tensile tests, have been undertaken to evaluate the mechanical properties of oak timber for structural applications (Kytka et al. 2022).

The bending strength of oak glulam is influenced by the size of the beams, with a clear effect of size on bending strength observed (Aicher and Stapf 2014). - The size of the laminated timber beams was found to have an impact on the bending strength, with the material exhibiting a size effect associated with quasi-brittle behavior (Blank et al. 2016). The distribution of knots and finger joints in glued laminated timber plays an important role in the onset of damage evolution and the final failure pattern, highlighting the significance of considering these factors when conducting bending tests (Tran et al. 2016; Melzerová and Šmídová 2019). Melzerová and Šmídová (2019) found that the bending properties of glued laminated timber made from combinations of wood species were affected by cyclic temperature variation, with the bending strength being negatively affected by temperature, especially for hardwood species. It was observed that cyclic temperature variation negatively affected the modulus of elasticity (*MoE*) and modulus of rupture (*MoR*) of single species beams, while GLT showed an increase in bending strength, especially for hardwood species (Kytka et al. 2022).

The bending capacity and size effect of high-strength hardwood glulams, including oak, can be well predicted using a serial model that accounts for the bending stress gradient between adjacent laminations (Aicher and Stapf 2014). The type of adhesive used in the production of glued laminated timber affects its mechanical properties (Gáborík et al. 2016; Gaff et al. 2016; Gaff et al. 2017). For instance, beech wood lamellae showed the highest impact bending strength (IBS) when glued with polyvinyl acetate (PVA) adhesive (Gaff et al. 2016; Gaff et al. 2017). The method of adhesive application, including the thickness and location of the glue joint, can impact the shear strength and stiffness of glued laminated timber (Ido et al. 2022).

In conclusion, the bending strength of glued laminated oak timber is influenced by various factors including wood species, adhesive type, size effect and environmental conditions. Industry standards and best practices are being developed to optimize the use of hardwoods in glued-laminated timber, reflecting the increasing interest in utilizing hardwoods for structural applications. Our aim is to lay the foundations for the use of lower quality timber in hardwood GLTs. Accordingly, bending tests were carried out on various small-sized glued oak elements. In evaluating the results, particular emphasis was placed on wood failures.

MATERIALS AND METHODS

One of our raw materials was noble oak (*Quercus* spp.) lamella with a cross-section of 20x50 mm and a length of 500 (the latter is the direction of fibres) with planed surfaces taken from the sawmill of Zalaerdő Erdészeti Zrt, Lenti, Hungary. Our other raw material was thin oak board with dimensions of 5x100x1000 mm derived from SEFAG Erdészeti és Faipari Zrt, Barcs, Hungary. The 736 planed lamellae contained sapwood, slope of grain, sawed surfaces due to the smaller thickness, both sound and decayed knots of various sizes (Figure 1). Low quality lamellae were selected, which meet at most the appearance grade QF3 and QF4 of standard EN 975-1 (2009). All lamellae have been photographed and a detailed quality description has been obtained. The thin oak boards were free of failures.

Figure 1: Typical wood failures in the lamellae used for the specimens

The wooden raw materials were stored in a workshop after kiln drying, where they reached an average equilibrium moisture content of 11.2%. Uniform climatic conditions prevailed throughout the specimen preparation. The lamellae were finger-jointed in length and simply glued together in width with the same emulsion polymerized isocyanate glue, to produce 20x100x1000 mm elements. The finger-joints were placed side by side in the middle of the element to test the weakest assembly. The gluing of the finished elements was done similarly with PVAc glue.

Three types of small-sized GLT beams were prepared from the elements. By gluing two elements together, 2-layer GLTs of 40x100x1000 mm were produced, 20 pieces in total. The strengthened version of this one was 45x100x1000 mm with a 5 mm thick oak board in the middle. 27 pieces of them were made. The third sample is 50x100x1000 mm. The structure in thickness of the 20 specimens is 5 mm thick oak board - 16 mm lamella - 5 mm thick oak board - 16 mm lamella - 5 mm thick oak board (Figure 2). The reason for thinning the elements was to minimise the size effect, in order to be able to compare *MoR* and *MoE* of the three samples.

Figure 2: Three types of small-sized GLT beams prepared for the tests

After conditioning the samples (20 °C and 65% relative humidity), a 4-point bending test was performed with different support spans and distance between the 30 mm diameter rollers of the crosshead, as seen in Table 1. The crosshead rollers were symmetrically spaced between the supports, in accordance with EN 408: 2010 + A1 (2012).

Table 1: Test settings

Sample thickness [mm]	Sample width [mm]	Support span [mm]	Crosshead roller distance [mm]
40	90	720	240
45	90	810	270
50	90	900	300

The bending tests were performed on an Instron 4208 (Instron Corporation, USA) universal material testing machine. The load rate was 6.0 mm.min^{-1}, which meets the requirements of the standard.

Before bending tests, the specimens were first subjected to a non-destructive test. The natural longitudinal vibration frequency was used, which gives a good estimation of *MoE* (Divós et al. 1994). The measurements were performed with a Portable Lumber Grader Plus (PLG+) timber classification equipment (Fakopp Bt, Hungary). It automatically determined both ρ and MoE_{dyn} based on the Timosenko theory (Sismándy-Kiss 2012, Bejó et al. 2022). The vibration was applied with a hammer at one end of the specimen, while the signal was detected with a microphone at the other end of the specimen. The specimen was supported at two points by scales with vibration damped pads to minimize vibration distortion. The exact length of the specimens was monitored by a laser distance meter and automatically transmitted to the computer, while the cross-section had to be specified manually. After sequential decoding of the recorded vibrations, the software determined the longitudinal wave propagation velocity, the vibration spectra and frequencies of the vibration modes and automatically selected the most relevant frequency peak.

RESULTS AND DISCUSSION

The low variances of all the test results suggests that the selection of raw materials and specimen preparation was well performed, and that the tests were carried out with sufficient accuracy. In most cases, a variance of less than 10% were achieved. For wood material tests 10% variance is very good, especially considering that the highest variance among all test results was only 14.2% in this study.

In order to determine the comparability of the samples, it is worth analysing their densities first. Figure 3 shows the averages and standard deviations of the three samples as determined by the dynamic tests. It can be seen that density values increase with thickness from 729.0 to 766.7 kg/m^3. Given the otherwise low standard deviations, no significant difference between the sample groups is likely.
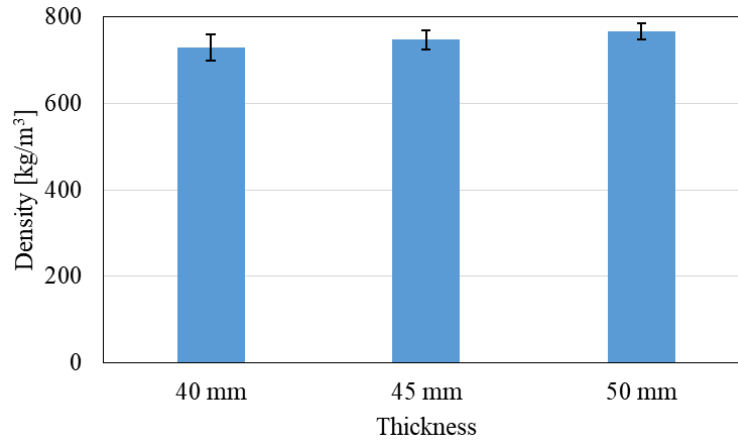
Figure 3: Densities of the small-sized GLT beam samples

Bending strength is one of the most important properties of structural elements. The diagram in Figure 4 shows that *MoR* of 40 mm and 45 mm thick specimens is almost the same. They are also statistically identical when the standard deviations are taken into account. It can be concluded that the addition of a thin oak board between the two lamellae is unnecessary and does not improve the *MoR* of the specimen. However, the 50 mm thick sample gave a 30% higher result of 80.0 MPa, i.e. the thin oak boards glued on both outer layers significantly increased the *MoR*. This is also due to the fact that the finger joints were no longer located at the outer layers of the specimens, where the highest forces located, but further inwards. They were therefore less exposed to the breaking forces and their weaker system compared to solid oak had less influence on the final result.
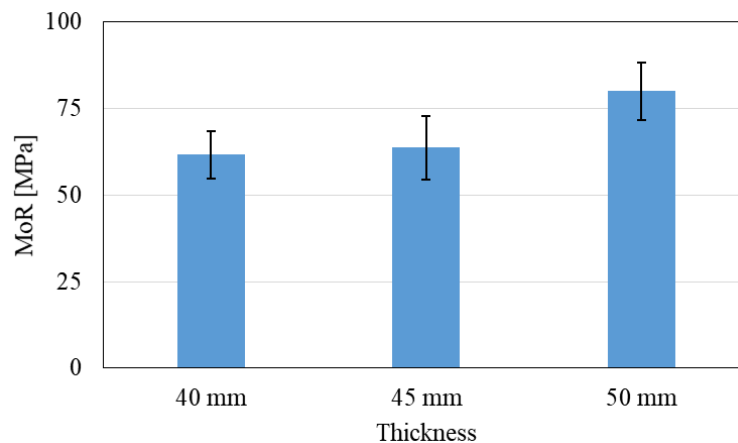
Figure 4: Modulus of Rupture (MoR) of the small-sized GLT beam samples

Regarding *MoE*, the results of two different measurement methods can be compared. The results obtained from the bending tests in the blue columns of Figure 5 are based on the requirements of the current standard EN 408: 2010 + A1 (2012). The non-destructive results obtained from the dynamic test, although not determined by direct measurement, are clearly very close to the static bending test results. Moreover, their standard deviations are similar or lower. The *MoE* of the specimens shows a slight decrease with increasing thickness. Between 40 and 50 mm thick specimens it is only 7.7%, but this is likely to be a statistically significant difference. However, the difference between 12.7 GPa and 11.7 GPa seems to be negligible in terms of strength grading.

An analysis of the fracture images shows that in most cases the failure occurred at the finger joints. A typical example is shown in Figure 6. Even for the 50 mm thick specimens, the outer layers were free of finger joints, which were subjected to the highest forces.
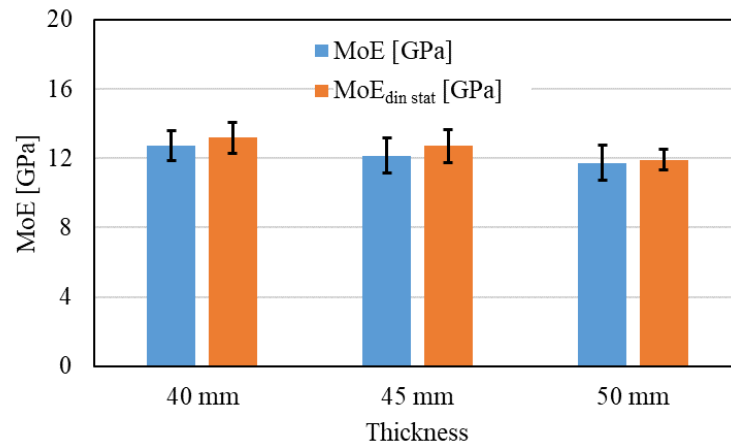
Figure 5: Modulus of Elasticity (MoE) of the small-sized GLT beam samples

Figure 6: Pictures of a typical finger joint failure in specimen 38

CONCLUSIONS

The study presents the bending tests of small-sized structural specimens of 2, 3 and 5 layers, with thicknesses of 40, 45 and 50 mm, respectively. Non-destructive testing and bending tests according to EN 408: 2010 + A1 (2012) were performed. The lamellae were not failure-free.

On the one hand, the test results showed that there was very little difference between the static bending test and the dynamic test. On the other hand, the modulus of rupture of 80 MPa for 50 mm thick sample was significantly higher than that of 40 mm thick specimens. This implies that particular attention should be paid to the quality of the most stressed, outer layers of the GLT. The modulus of elasticity decreased slightly with increasing thickness. In most cases, the bending test failures were caused by PVAc adhesive failure, not by wood defects.

In conclusion, the mechanical properties of glued laminated oak timber are influenced by factors such as adhesive type, layer structure and quality of outer layers variation. When conducting bending tests on oak GLT, it is important to consider the distribution of knots and finger joints. The advantages of using glued laminated oak timber in construction projects include its satisfactory performance under various loading conditions and its potential for structural applications. Further research specifically focusing on oak timber and different adhesive types would be beneficial to provide more direct insights into this specific query.

REFERENCES

Aicher S, Stapf G (2014) Glulam from European White Oak: Finger Joint Influence on Bending Size Effect. In: Aicher S, Reinhardt H-W, Garrecht H (eds) Materials and Joints in Timber Structures. Springer Netherlands, Dordrecht, pp 641–656

Bejó L, Sismándy-Kiss F, Divós F (2022) International practice and Hungarian research regarding structural lumber grading (A fűrészáru szilárdsági osztályozásának nemzetközi gyakorlata és hazai kutatási eredményei). Anyagvizsgálók Lapja 2022:27–37

Blank L, Jockwer R, Frangi A, Fink G (2016) Quasi-brittleness of glued laminated timber beams subjected to bending. In: Zingoni A (ed) Insights and Innovations in Structural Engineering, Mechanics and Computation. CRC Press, Taylor & Francis Group, 6000 Broken Sound Parkway NW, Suite 300, Boca Raton, FL 33487-2742, pp 1714–1719

Divós F, Daniel I, Hodasz E, Jarasi J (1994) Experimental Investigation of Thirteen Strength Predictor Parameters of Coniferous Wood. In: Proc. 1st European Symposium on Nondestructive Testing of Wood. Sopron, Hungary, pp 341–349

EN 975-1 (2009) Sawn timber. Appearance grading of hardwoods. Part 1: Oak and beech. European Committee for Standardization, Brussels, Belgium

EN 408: 2010 + A1 (2012) Timber structures - Structural timber and glued laminated timber - Determination of some physical and mechanical properties, Brussels, Belgium

Gáborík J, Gaff M, Ruman D, et al (2016) Adhesive as a Factor Affecting the Properties of Laminated Wood. BioResources 11:10565–10574. https://doi.org/10.15376/biores.11.4.10565-10574

Gaff M, Ruman D, Svoboda T, et al (2017) Impact bending strength as a function of selected factors: 2 – Layered materials from densified lamellas. BioRes 12:7311–7324. https://doi.org/10.15376/biores.12.4.7311-7324

Gaff M, Ruman D, Záborský V, Borůvka V (2016) Impact Bending Strength as a Function of Selected Factors. BioResources 11:9880–9895. https://doi.org/10.15376/biores.11.4.9880-9895

Glavinić I, Boko I, Torić N, Vranković J (2020) Application of hardwood for glued laminated timber in Europe. JCE 72:607–616. https://doi.org/10.14256/JCE.2741.2019

Ido H, Miyatake A, Hiramatsu Y, Miyamoto K (2022) Effects of the presence or absence and the position of glued edge joints in the lamina on the shear strength of glued laminated timber. J Wood Sci 68:55. https://doi.org/10.1186/s10086-022-02062-1

Kytka T, Gašparík M, Sahula L, et al (2022) Bending characteristics of glued laminated timber depending on the alternating effects of freezing and heating. Construction and Building Materials 350:128916. https://doi.org/10.1016/j.conbuildmat.2022.128916

Melzerová L, Šmídová E (2019) Different types of damages of glued laminated timber beams. In: Experimental Stress Analysis - 57th International Scientific Conference, EAN 2019 - Conference Proceedings. pp 283–285

Morin-Bernard A, Blanchet P, Dagenais C, Achim A (2020) Use of northern hardwoods in glued-laminated timber: a study of bondline shear strength and resistance to moisture. Eur J Wood Prod 78:891–903. https://doi.org/10.1007/s00107-020-01572-3

Sismándy-Kiss F (2012) Fűrészáru szilárdsága és fizikai tulajdonságainak kapcsolata. NyME Cziráki József Faanyagtudományok és Technológiák Doktori Iskola

Tran V, Oudjene M, Méausoone P (2016) Performance of oak timber in glued structural elements and joints. In: WCTE 2016 - World Conference on Timber Engineering. Vienna, Austria

Homogenized dynamic Modulus of Elasticity of structural strip-like laminations made from low-grade sawn hardwood

Simon Lux[1, 2], Johannes Konnerth[2], Andreas Neumüller[1]

[1] Holzforschung Austria, Franz Grill-Straße 7, 1030 Wien
[2] BOKU University, Institute of Wood Technology and Renewable Materials,
Konrad Lorenz Strasse 24, 3430 Tulln, Austria

E-mail: s.lux@holzforschung.at; johannes.konnerth@boku.ac.at; a.neumueller@holzforschung.at

Keywords: dynamic modulus of elasticity, structural strip-like lamination, structural use of hardwood, building products.

ABSTRACT

The changing composition of tree species, favouring hardwood species over spruce in central European forests, poses a major concern to the effort of supplying the building sector with a sufficient volume of high-quality construction material. In addition, legislature in Europe on different levels pushes for increased use of building products made from wood.

The use of hardwood species is currently uncommon in the building sector. Important factors for this are, that hardwood species are for the widest part not covered by European standards for timber structures and processing steps such as sawing and planing are more complex. The strength-grading process of hardwood species comes with some major difficulties, leading to low material yield. To realize a semi-finished product for use in glued structural building products, structural strip-like laminations made from preselected, low-grade sawn hardwood timber from Austrian *Fagus sylvatica* and *Quercus robur* / *Quercus petraea* were produced. The laminations consisted of six to eight "strips". The hypothesized homogenization of the raw material was the main focus of the study. To detect, whether this processing achieved a homogenisation effect on the mechanical properties of the material, a non-destructive testing method was chosen to collect data. Therefore, the dynamic modulus of elasticity of the sawn solid timber as well as the strip-like laminations was determined. While little change in the mean values of the dynamic modulus of elasticity was observed, the scattering of the data was reduced drastically. The reduced variation is a desirable effect, as characteristic values of building products are based on lower 5 % quantiles. Characteristic values are essential for design and planning by structural engineers. The achieved homogenization could open the door for hardwood to be used as raw material in the building sector more commonly.

INTRODUCTION

Climate change is projected to change the species composition of forests all over Europe. Spruce (*Picea abies*) and pine (*Pinus sylvestris*), the tree species most relevant for the building sector, are predicted by Dyderski et al. (2017) to lose large parts of their currently occupied ranges. The same study found the loss of the occupied ranges to be less severe for beech (*Fagus sylvatica)* and oak species and (*Quercus robur* / *Quercus petraea).* Another study by (Hanewinkel et al., 2013) made similar predictions while emphasizing the economic consequences of the conversion from productive coniferous species to hardwood species like oak and beech.

A concept to mitigate the implications of climate change is to use buildings as carbon sink by using structural timber products. A review by Tupenaite et al. (2023) found, that a large majority of the analyzed studies agree that timber construction has the potential to reduce the impact of the building sector on climate change. In Europe, climate-driven forest conversion might be a major constraint to the concept of using buildings, made from structural timber products, as carbon sink. Manufacturing of structural timber products is highly dependent on the supply of high-quality raw material. This raw material almost exclusively consists of spruce and pine wood. Most modern industrial structural timber production facilities are optimized for processing these species. The wood anatomy of hardwood species differs strongly from the anatomy of softwood. Therefore, the production facilities are not suitable for processing most hardwood species without some major changes to the process steps and the machinery.

On the one hand, the projected decrease in raw material from spruce and pine is a big challenge for the timber industry. On the other hand, implementing the use of species like beech and oak might also be beneficial. Beech was historically used for a wide variety of applications and is nowadays essential for the furniture industry, while at the same time acting as a raw material for the pulp and paper industry (Pramreiter et al., 2023). In load-bearing applications, only a small share of products made from hardwood are used in Europe. One reason for this is, that European standards for timber structures like EN 14080 (CEN, 2013) exclusively cover coniferous species except for poplar (*Populus spp*.). Pramreiter et al. (2023) also show that beech is superior to spruce and pine when it comes to strength and stiffness properties. This is also true for some other hardwood species. In a paper, analyzing the mechanical properties of beech, oak, and poplar branch-wood, Nenning et al. (2024) showed that even the branch-wood of these species has great potential for use in load-bearing applications. A comparatively higher density and stronger swelling and shrinking behaviour are common for many hardwood species.

Major challenges for the use of hardwood in structural timber products are low material yield and inhomogeneity of the material. Therefore, new ways of processing hardwood are needed, that can achieve both a good material yield and homogeneity of mechanical performance, comparable or even superior to strength-graded softwood.

Obernosterer et al. (2023) proposed such a process and produced "Strip Lamellas" from birch (*Betula pendula*). The study was able to show a good homogenization effect for tensile strength and bending strength when compared to solid birch timber boards. The approach proposed for the production of "Strip Lamellas" in this work was also the reference and inspiration for the present study.

MATERIAL AND METHODS

The total number of specimens examined in this study was 444, 375 of the specimens were ungraded sawn solid timber boards, and 69 were strip-like laminations. The sawn solid timber boards were sourced from three sawmills, two are located in Lower Austria, and one in Styria. The beech and oak trees were harvested in Austrian forests and processed in sawmills. As the aim was to manufacture laminations from low-grade sawn timber, that would otherwise have been used as fuel wood or for pulp, the sawmills selected the material accordingly. The raw material to produce the strip-like laminations did not meet certain criteria, making further processing and sale as premium products in the sawmills impossible. The criteria, that were not met were diverse. Aesthetic reasons like discolorations, strength-reducing wood characteristics, such as large knots and bark inclusions as well as cracks are among those reasons for being rejected from the standard manufacturing processes of the sawmills.
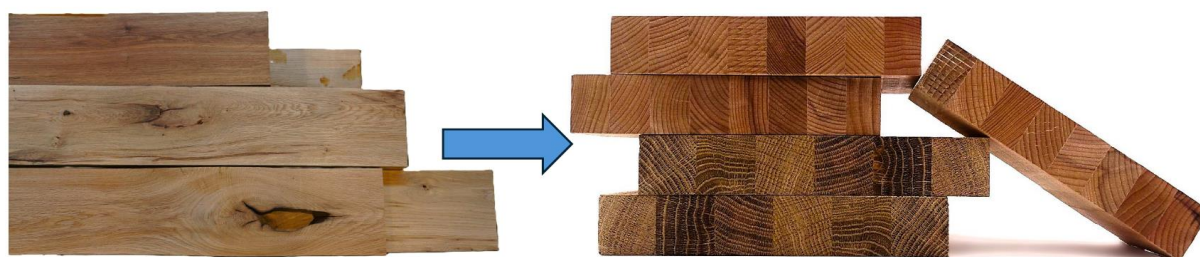
Figure 5: sawn solid oak (Quercus robur / Quercus petraea) boards (left) / Cross sections of the produced strip-like laminations from oak and beech (Fagus sylvatica) (right)

The raw material and the semi-finished product are depicted in Figure 1. Before being processed, the raw material from the sawmills was preselected. The goal of preselection was mainly to ensure proper bonding by excluding undersized material and features like large splits. Specimens, that exhibited rot were also excluded at that point. In a process similar to the production of glued laminated timber (GLT), the preselected low-grade sawn hardwood timber was finger-jointed, planed, and cut to a length of roughly 4 m, before being bonded into blocks with six to eight laminations. The sawn hardwood timber with a thickness after the final planing of 20 mm was processed into blocks of eight laminations, while the material with a thickness of 30 mm was processed into blocks of six laminations.

In contrast to the process of GLT production according to EN 14080 (CEN, 2013), in which only strength-graded material is used, the sawn solid hardwood laminations were not strength-graded before

the production process. This was done, as a highly homogeneous semi-finished product was aimed for, making a full-fledged grading process of the material before processing obsolete.

An industry-standard Melamine-Urea-Formaldehyde adhesive system was used for both, the longitudinal connection via finger joints as well as the face bonding of the laminations. At the time of production, the system was classified for bonding beech timber and not classified for use with oak timber. The processing times and other parameters were chosen according to the technical datasheet of the adhesive system.

The resulting blocks were then cut orthogonal to the plane of the face bonding in the longitudinal direction, resulting in a semi-finished product, referred to as "strip-like laminations". Obernosterer et al. (2023) already proposed this approach for his "Strip Lamellas". All strip-like laminations were cut to a final thickness of 30 mm, resulting in cross-sections of 30 mm x 160 mm with eight strips and 30 mm x 180 mm with six strips. A complete overview of the various specimens is given in Table 1.

Table 1: nominal dimensions of the specimens

Species ID	Product	Width [mm]	Thickness [mm]	Number of strips	Number of specimens
Beech I	Sawn solid timber	160	30	-	152
Beech II	Strip-like lamination	160	30	8	31
Oak III	Sawn solid timber	160	30	-	105
Oak IV	Strip-like lamination	160	30	8	19
Oak V	Sawn solid timber	160	40	-	118
Oak VI	Strip-like lamination	180	30	6	19

Determining the dynamic modulus of elasticity (E_{dyn}) was done with a "MiCROTEC Viscan" device, which measures the natural frequency of the specimens with an optical laser interferometer. In addition to the natural frequency (v), also the length of the specimens (l), and their density (ρ) are needed for the calculation of E_{dyn}. These pieces of information were gathered directly before determining the natural frequency. The following equation was used to calculate E_{dyn}:

$$E_{dyn} = \rho(2lv)^2 \tag{1}$$

The non-destructive nature of this testing method allowed for testing of the same material at two points in time. The first time, the E_{dyn} was determined before the final planing and bonding of the sawn hardwood timber. The E_{dyn} for the sawn hardwood timber was taken from boards with various lengths. After processing, sections with a length of 3.2 m, were used to determine the E_{dyn} of the strip-like laminations for the second measurement. These specimens were meant for destructive tensile testing afterward. Just a part of the material, that the data for the E_{dyn} of the sawn solid hardwood stems from, is represented in the investigated strip-like laminations. The specimens for determination of the E_{dyn} were randomly cut from the full-length (roughly 4 m) strip-like laminations. The rest of it was used to produce specimens for various mechanical tests.

The statistical analysis was conducted using R: A Language and Environment for Statistical Computing (R Core Team, 2022).

RESULTS AND DISCUSSION

The results of the E_{dyn} measurements, for each group of specimens are summarized in Table 2.

Table 2: E_{dyn} test results of the various specimens

Species ID / Product	$E_{dyn, mean}$ [N/mm²]	$E_{dyn,0.05}$ [N/mm²]	Standard deviation [N/mm²]	Coefficient of variation [%]	Number of strips	Number of specimens
Beech I / solid	15153	11777	2082	13,7	-	105
Beech II / strips	15524	14542	487	3,1	8	19
Oak III / solid	11537	7887	2283	19,8	-	118
Oak IV / strips	12315	11188	740	6	6	19
Oak V / solid	13178	8175	2708	20,5	-	152
Oak VI / strips	13934	13199	655	4,7	8	31

The $E_{dyn, mean}$ was measured to be 15153 N/mm² and 15524 N/mm² for the beech sawn solid timber and the strip-like laminations respectively. A Welch Two Sample t-test does not show a significant difference when comparing the $E_{dyn, mean}$ of the sawn solid timber and the strip-like laminations from beech at the 95 % confidence interval (p-value = 0.052). The differences between $E_{dyn, mean}$ of the sawn solid timber and the strip-like laminations for the oak with six strips (p-value = 0.006) and the oak with eight strips (p-value = 0.010) were significant, for the same kind of t-test.

The comparison of the variances between sawn solid timber and strip-like laminations resulted in highly significant F-test results for beech (p-value < 0.001), oak with six strips (p-value < 0.001), and oak with eight strips (p-value < 0.001). By processing the sawn timber into strip-like laminations, the coefficient of variation for the E_{dyn} was decreased by roughly 75 %. The strip-like laminations from oak with six strips exhibited the highest coefficient of variation with 6 %. The comparison to the strip-like laminations with eight strips (4.7 % for oak and 3.1 % for beech) supports the assumption, that homogenization increases with an increasing number of strips in the lamination.

The existence of a homogenization effect by processing the material into strip-like laminations is supported by the present study's findings. While the homogenization effect is so strong, there was no noteworthy change in $E_{dyn, mean}$, implying that the high stiffness of the material is preserved.

The tensile tests by Obernosterer et al. (2023) showed, that the coefficient of variation for tensile strength decreased from 31.4 % for solid birch boards to 20.7 % for "Strip Lamellas". At the same time, no sizeable difference between the mean values of the two groups was observed. The mean tensile strength of the solid birch was 43.9 N/mm² for solid beech boards and 43.7 N/mm² for the "Strip Lamellas". This confirms the trend that was observed for E_{dyn} in the present study.
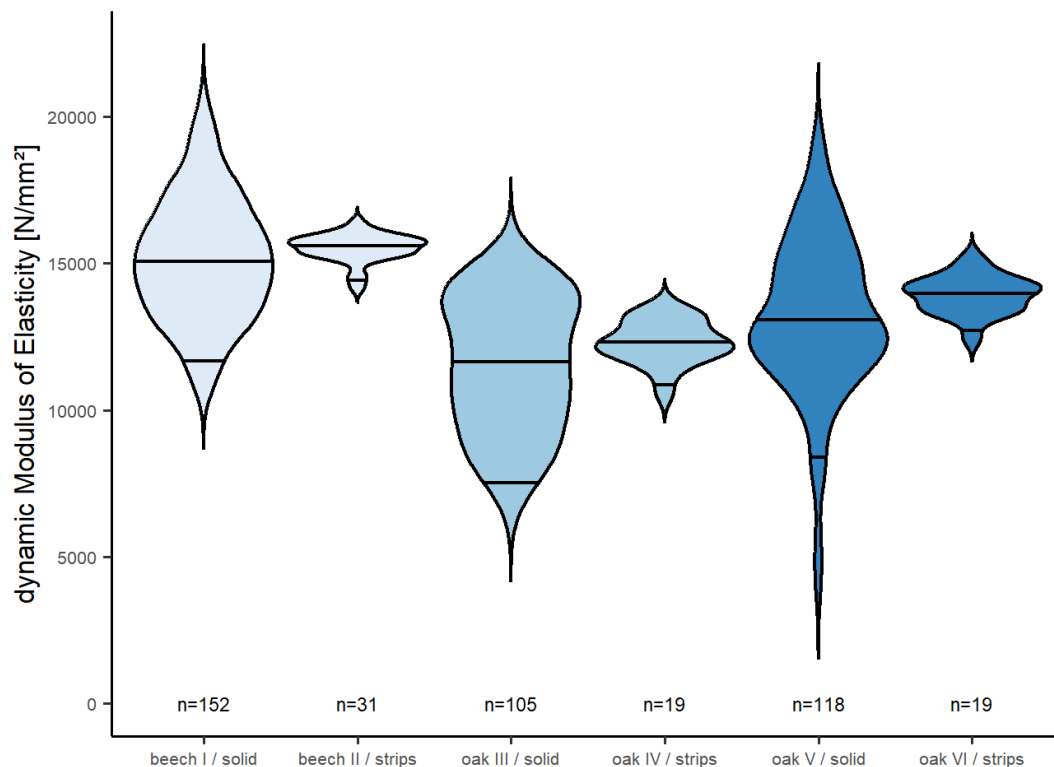
Figure 2: Violin plot of the dynamic Modulus of Elasticity for each group of specimens. The median and the lower 5 % quantile are marked with horizontal lines in the violin plots

An important indicator for the scattering within the groups is the lower 5 % quantile. In the violin plots, that are depicted in Figure 2, the median and the lower 5 % quantiles of the E_{dyn} are marked as horizontal lines. The lower 5 % quantile of the E_{dyn} improved significantly. The value increased by at least 3000 N/mm² for each of the groups. This is especially relevant, as the lower 5 % quantile is often used as "characteristic value" for various mechanical parameters in European standards for structural timber in EN 384 (CEN, 2016). These characteristic values are essential for the planning of structural systems.

CONCLUSIONS

The observed degree of homogenization might allow omitting the strength-grading process of the raw material. This would be beneficial to the material yield and through it also to the economic viability of processing hardwood into structural timber products. The superior mechanical properties of hardwood make the use in hybrid layups of structural timber products such as GLT an interesting prospect.

Further investigations into the homogenization factor based on strength and stiffness parameters from destructive testing are needed to confirm the observations in this study. The effect of the number of strips in the laminations on the extent of the homogenization effect is another interesting research topic.

ACKNOWLEDGMENTS

REFERENCES

CEN. (2013). EN 140800:2013 - Timber structures - Glued laminated timber and glued solid timber - Requirements.

CEN. (2016). EN 384:2016 Structural timber - Determination of characteristic values of mechanical properties and density.

Dyderski, M. K., Pa Z, S., Lee, |, Frelich, E., Jagodzi Nski, A. M., & Jagodzi, A. M. (2017). How much does climate change threaten European forest tree species distributions? https://doi.org/10.1111/gcb.13925

Hanewinkel, M., Cullmann, D. A., Schelhaas, M. J., Nabuurs, G. J., & Zimmermann, N. E. (2013). Climate change may cause severe loss in the economic value of European forest land. Nature Climate Change, 3(3), 203–207. https://doi.org/10.1038/NCLIMATE1687

Nenning, T., Tockner, A., Konnerth, J., Gindl-Altmutter, W., Grabner, M., Hansmann, C., Lux, S., & Pramreiter, M. (2024). Variability of mechanical properties of hardwood branches according to their position and inclination in the tree. https://doi.org/10.1016/j.conbuildmat.2024.135448

Obernosterer, D., Jeitler, G., & Schickhofer, G. (2023). BIRCH FOR ENGINEERED TIMBER PRODUCTS:: PART II. 13th World Conference on Timber Engineering, WCTE 2023, 1. https://doi.org/10.52202/069179-0084

Pramreiter, M., Jandl, R., Kirchmeir, H., & Grabner, M. (2023). The Utilization of European Beech Wood (Fagus sylvatica L.) in Europe. https://doi.org/10.3390/f14071419

R Core Team. (2022). R: A Language and Environment for Statistical Computing. R Foundation for Statistical Computing.

Tupenaite, L., Kanapeckiene, L., Naimaviciene, J., Kaklauskas, A., & Gecys, T. (2023). Timber Construction as a Solution to Climate Change: A Systematic Literature Review. https://doi.org/10.3390/buildings13040976

Impact of varnishing on the acoustic properties of sycamore maple (*Acer pseudoplatanus*) panels

Aleš Straže[1*], Jure Žigon[1], Matjaž Pavlič[1]

[1] University of Ljubljana, Biotechnical Faculty, Jamnikarjeva 101, SI 1000 Ljubljana, Slovenia

E-mail: ales.straze@bf.uni-lj.si; jure.zigon@bf.uni-lj.si; matjaz.pavlic@bf.uni-lj.si

Keywords: wood, maple, fiddleback figure, varnishing, acoustics

ABSTRACT
In this study, the effects of different varnishes on the acoustic properties of acoustic panels made of sycamore maple (*Acer pseudoplatanus* L.) suitable for use in wooden musical instruments were compared. Conditioned acoustic panels (20 °C, 65 % RH), having fiddleback figure, with nominal dimensions of 400 mm × 75 mm × 3 mm (L, R, T) were treated with 4 different varnishes: JOHA (J), Domestic (D), Nitrocellulose (N) and Polyurethane (P). The bending vibration method with direct and indirect excitation was used for the acoustic measurements. After surface treatment, curing of the varnishes and conditioning of the samples (20 °C, 65 % RH), a higher mass and thus a higher average density of the acoustic panels was observed in all samples tested, having a reduced natural frequency. The varnishes, especially the softer ones (J, D, N), significantly increased the vibration damping (tanδ) of the panels. The acoustic properties of the panels were least affected by the surface treatment with polyurethane (P) varnish, but it had a clearly negative impact on their higher weight. In contrast, the JOHA varnish led to the smallest increase in the weight of the resonance panels and the least negative impact on their relevant acoustic properties among the varnishes tested (Δtanδ = + 19.0 %, ΔACE = - 19.3 %).

INTRODUCTION
In music, wood is a traditional and irreplaceable material, valued above all for its aesthetic and acoustic qualities for the manufacture of string instruments, drums and percussion instruments, but also used for woodwind instruments and even brass instruments. A variety of wood species are used in the manufacture of musical instruments, e.g. rosewood, ebony, spruce, maple and many others (Ray et al. 2021, Straže et al. 2015). However, to ensure proper function and reduce hygroscopicity and hygromechanical instability, the wood of musical instruments must be protected so that it can withstand the ravages of time (Bucur, 2006; Rosing, 2010). For this purpose, we use coatings that form a film on the surface. These protect the wood from external influences and ensure that it comes closer to the customer's taste, but also influence its acoustic properties (Lämmlein et al. 2019).

Resonance boards are an integral part of various musical instruments where we want to achieve the best possible mechanical resistance, reduce the hygro-mechanical influences of the changing climatic conditions of the environment and at the same time preserve the acoustic and aesthetic properties of the wood. The varnishes form surface films, but also fill the cell structure of the wood beneath the surface. Compared to the solid wood used to make resonance panels, varnishes generally have a higher density and are stiffer after curing, but contribute to greater damping of mechanical vibrations once the varnish has been applied. In most cases, after surface treatment, there is a decrease in resonant frequencies and thus a decrease in the specific modulus of elasticity of wood along the grain (E_L/ρ) (Setrango et al. 2017) and, conversely, an increase in the specific modulus of elasticity in the radial direction of the grain (E_R/ρ) (Lämmlein et al. 2019). Several studies generally report an expected increase in the damping of mechanical vibrations of loudspeakers after surface treatment (Minato et al. 1995; Ono, 1993; Schleske, 1998; Sedighi-Gilani, 2016). Most authors state that surface coatings have a greater effect on damping the vibrations of wooden parts of musical instruments than on increasing their stiffness (Lämmlein et al. 2019). The anisotropic, mechanical and acoustic properties of the wood are generally also influenced by the thickness and number of coatings applied, the interaction with the wood species and the surface treatment technique.

The aim of the research was to produce acoustic panels from sycamore maple and to test on them how typical varnishes used in the manufacture of musical instruments influence their vibration behaviour and acoustic properties. We used different application techniques and change the thickness and number of varnishes.

MATERIALS AND METHODS

The sycamore maple wood (*Acer pseudoplatanus* L.), having fiddleback figure, was dried naturally and conditioned in the laboratory (20 °C, 50 % RH) for one month before the test specimens were produced. Coarse lamellae of 5 mm thickness ($n = 8$) were sawn from the conditioned, radially oriented test specimens on a circular sawing machine. The lamellae were planed on both sides to a thickness of 3 mm and cut to the final dimensions (length 400 mm, width 75 mm and thickness 3 mm) in the longitudinal and transverse directions.

Surface treatment

The types of coatings chosen in the study were (Figure 1):
- (J) Joha
- (D) Domestic
- (N) Nitrocellulose
- (P) Polyurethane

JOHA® is an oil-based coating system containing a mixture of natural and synthetic resins dissolved in turpentine and linseed oil (https://www.joha.eu/). Joha primer colourless was used for the 1st and 2nd coats, coloured varnish (brown) was used for the 3rd, 4th, 5th and 6th coats and for the 7th and 8th coats. The surfaces were dried in a UV chamber with UV-A rays, with each drying cycle in the chamber lasting 4 hours, except for the last cycle, which was exposed to UV-A rays for 12 hours. Twelve hours elapsed between each coat. After the last cycle, it was exposed to sunlight for 3 days.

The homemade paint was produced by the Demšar violin-making workshop (https://www.demsarvioline.si). First, the wood was coated with pure turpentine and left to dry for 4 hours, after which a varnish was applied to seal the surface. The mixture was boiled at around 150 °C and diluted with pure turpentine. After 24 hours, the varnish was applied, consisting of a mixture of pure resins and tannins (*Pinus pinaster*), and independently boiled linseed oil, and finally diluted with pure turpentine. It was applied three times at 48-hour intervals and dried in a UV chamber for 14 hours after each application. After the last cycle, it was exposed to sunlight for 3 days.

The nitrocellulose lacquer was applied by air spraying. For the first coat, 30 percent by weight of diluent (DF-M600) was added to the varnish (TN816); no diluent was added for the second and third coat.

The high-gloss polyurethane coating was also applied by air spraying, whereby an isocyanate hardener (FC-M640) was added to the polyurethane resin (FB-M596/NTR) in a weight ratio of 1:1 for the primer and a 20 percent of diluent (DF-M600) for the second coat. The diluent was no longer used for the third coat. Before each application, the surface of the lamellas was lightly sanded with 400 grit sandpaper.

Figure 1: Raw specimens (n = 10; left) and representative acoustic panels after varnishing (J – Joha, D – domestic, N – nitrocellulose, P – polyurethane)

Measurement of the properties of coating systems

The thickness of the surface coating was determined using an Olympus ILLC2 microscope with 120x optical magnification according to the standard methodology (EN ISO 2808, 2019).

The hardness of the coating was determined using the König method. A König pendulum (Erichsen, model 299/300) was placed on the surface of the sample. The device indicates the time required to reduce the amplitude of the oscillation from 6° to 3°. For harder surface coatings, the pendulum imprint is smaller and the oscillation time is longer (EN ISO 1522, 2007).

Determination of acoustic properties

The specimens were placed on two elastic nylon supports positioned at the first nodal points of the bending vibration (L = 22.4 % of the element length or 89.6 mm from the end of the specimen). To analyse the flexural vibration, pulsed elastic excitation was performed with a rigid steel sphere in the geometric axis at the open end of the element. A PCB 130D20 condenser microphone was placed on the opposite side of the specimen. The sound signal was recorded using the NI-9234 DAQ module (National Instruments, Ltd.) with a resolution of 24 bits and a sampling rate of 51 kHz. The measurements were carried out in a semi-anechoic room separated from the laboratory hall by a sound-absorbing wall (average ambient noise level of 11.5 dB). The signals were further processed and analysed using LabVIEW software.

The dynamic modulus of elasticity (E) at the fundamental bending frequency (f_1) was determined using the Bernoulli solution, which assumes a very high length-to-depth ratio (L/h >> 1) and disregards the shear and elastic support effect (Brancheriau and Bailléres, 2002).

$$E = 4 \cdot \pi^2 \frac{\rho \cdot A \cdot L^4}{I_x} \frac{f_n^2}{P_n} \tag{1}$$

Notation:

E – dynamic modulus of elasticity [Pa],

I_x - moment of inertia [m^4],

f_n - the bending frequency of the specimen in the n-th vibration mode (n = 1),

ρ - density [kg/m^3],

A – cross section [m^2],

P_n - parameter to solve the Bernoulli constants, depends on the vibrational mode (n = 1),

L – length.

The damping of the bending vibration (tanδ) of the tested panels was determined by measuring the logarithmic decrement of the vibration signal. The influence of wood density and structure on the mechanical stiffness was evaluated by specifying a specific modulus of elasticity (E/ρ) and the acoustic coefficient (K = $\sqrt{(E/\rho^3)}$). In addition, the acoustic conversion efficiency (ACE = K/tanδ) and the relative acoustic conversion efficiency (RACE = $\sqrt{(E/\rho)}$/tanδ) were determined. The latter represents the pure sound radiation and directly reflects the influence of the microstructure of the material on the sound radiation (Obataya et al. 2000).

In order to determine the effect of the coating on the acoustic properties of the panels, the acoustic measurements were carried out in the same way, first on the untreated panels and then, after conditioning, on the surface-treated panels.

RESULTS
Physical properties of the coating systems

When measuring the dry film thickness, we found that the thinnest coatings were achieved with the Joha (J) coating and the thickest with the polyurethane (P) coating (Figure 2a). In order to understand the penetration of the coating into the wood structure, the relationship between the dry film thickness and the coating application was also tested. It can be observed that the JOHA (J) coating penetrates the maple wood slightly better than the other coating systems (Figure 2a).
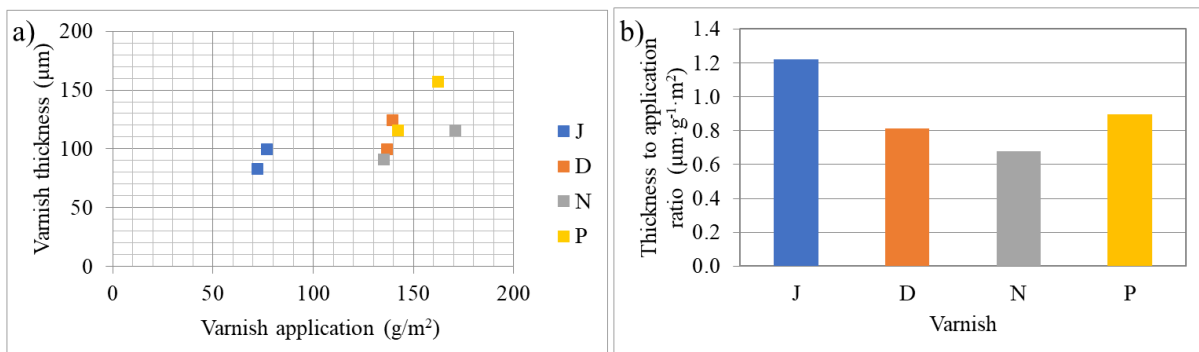
Figure 2: a) The relationship between the amount of coating applied and the thickness of the dry film, b) Ratio of thickness to amount of coating applied at individual varnish (J – Joha, D – domestic, N – nitrocellulose, P – polyurethane)

The thickness in itself does not say much about the quality of the coating, but it influences all the properties of the cured film. It is generally known that a higher film thickness means a lower hardness of the dry coating system, whereby the base material and the properties of the applied coating play an important role (Bekhta et al. 2022). In our case, we confirmed a longer oscillation time and thus probably a harder surface of the maple panels coated with nitrocellulose (N) and polyurethane (P) varnishes (Figure 3).
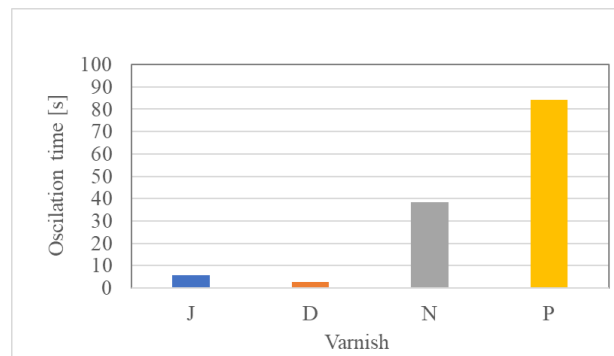
Figure 3: Determined oscillation time by König pendulum in relation to used varnish on maple wood (J – Joha, D – domestic, N – nitrocellulose, P – polyurethane)

Acoustic properties of the panels

The application of the varnish increased the mass of all maple panels and thus also their average bulk density. The greatest increase in mass was observed in the panels coated with nitrocellulose (N; +4.98 %) and polyurethane varnishes (P; +2.39 %). The application of the varnish led to a simultaneous drop in the resonant frequency for all maple panels, least for Joha (J: -1.30 %) and most for the nitrocellulose varnish (N: -2.37 %). However, the application of varnish had a clearly negative effect on the vibration damping of the panels (tanδ), which increased significantly with the exception of the panels with polyurethane varnish (Table 1).

Table 1: Acoustic properties of raw maple panels and the changes due to application of individual varnish
(J – Joha, D – domestic, N – nitrocellulose, P – polyurethane)

		Applied varnish			
	Raw maple	**Joha N (%)**	**Domestic D (%)**	**Nitrocellulose N (%)**	**Polyurethane P (%)**
Density ρ (kg/m^3)	693 (1.0)	+0.32	+0.09	+4.98	+2.39
Resonant frequency f (s^{-1})	84.8 (5.8)	-1.30	-2.54	-2.37	-1.93
Damping tan δ ( )	0.0145 (24.4)	+18.99	+32.18	+26.70	+0.47
Modulus of elasticity E (GPa)	11.6 (9.6)	-8.47	-15.79	-3.51	-9.74
Specific modulus of elasticity E/ρ (GPa)	17 (9.8)	-8.69	-15.87	-8.11	-11.85
Acoustic coefficient K (m^4 s^{-1} kg^{-1})	5.9 (5.2)	-4.66	-8.36	-8.68	-8.30
ACE (m^4 s^{-1} kg^{-1})	433.6 (32.0)	-19.33	-29.71	-27.30	-8.72
RACE (m^4 s^{-1} kg^{-1})	300.6 (32.2)	-19.16	-29.64	-23.57	-6.54

The significant decrease in the specific modulus of elasticity (E/ρ) of all tested maple panels after coating (N: -8.69 %, D: -15,87 %, N: -8.11 %; P: -11.85 %), even though they are very thin, shows that the acoustic properties of the wood are impaired by the surface treatment. As the vibration damping of the maple panels increased after surface treatment, all the acoustic indices examined (K, ACE, RACE), which depend on both stiffness (E) and damping, decreased for all maple panels.

CONCLUSIONS

The study confirms the very good acoustic properties of sycamore maple, having fiddleback figure, which deteriorate slightly after surface treatment, regardless of the type of varnish used. This is due to the fact that mass, i.e. a coating, is added to the structure of the wood, forming a varnish film that does not elastomechanically improve the structure of the wood. The use of a harder varnish such as polyurethane (P), which forms a thicker varnish film, proved to be the best in the study compared to the other coatings (J - Joha, D - Domestic, N - nitrocellulose). The damping of the mechanical vibrations of the maple panels remains unchanged after the surface treatment and the specific modulus of elasticity is only slightly reduced, which leads to a minimal reduction in the acoustic indicators.

ACKNOWLEDGEMENT

REFERENCES

Bekhta P, Krystofiak T, Lis B, Bekhta N. 2022. The Impact of Sanding and Thermal Compression of Wood, Varnish Type and Artificial Aging in Indoor Conditions on the Varnished Surface Color. Forests, 13(2):300

Brancheriau L, Bailléres H (2002) Natural vibration analysis of clear wooden beams: A theoretical review. Wood Science and Technology 36: 347-365

Bucur V. 2006. Acoustics of Wood. Berlin, Springer Verlag, 393 p.

EN ISO 1522. Paints and varnishes – Pendulum damping test. 2007: 16 p.

EN ISO 2808. Paints and varnishes - Determination of film thickness. 2019: 58 p.

Lämmlein S. L., Mannes D., Van Damme B., Schwarze F. W. M. R., Burgert I. 2019. The influence of multi-layered varnishes on moisture protection and vibrational properties of violin wood. Scientific Reports Nature research, 54: 8063-8095

Minato K., Akiyama T., Yasuda R., Yano H. 1995. Dependence of Vibrational Properties of Wood on Varnishing during Its Drying Process in Violin Manufacturing . Wood Science and Technology, 49: 222-226

Ono T. 1993. Effects of varnishing on acoustical characteristics of wood used for musical instrument soundboards. Journal of Acoustic Society of Japan, 14,6: 397-407

Obataya E, Ono T, Norimoto M (2000) Vibrational properties of wood along the grain. Journal of Materials Science 35: 2993-3001

Ray T., Kaljun J., Straže A. 2021. Comparison of the vibration damping of the wood species used for the body of an electric guitar on the vibration response of open-strings. Materials. 2021, 14 (18): 1-13

Rossing T.D. 2010. The Science of String Instruments. Berlin, Springer Verlag: 470 p.

Schleske M. 1998. On the acoustical properties of violin varnish. Catgut Acoustic Society Journal, 3,6: 27–43

Sedighi-Gilani M., Pflaum J. Hartman S., Kaufman R., Baumgartner M., Willis-Mathew-Robert-Schwarze F. 2016. Relationship of vibro-mechanical properties and microstructure of wood and varnish interface in string instruments. Applied Physics, 122: 1-11

Setragno F., Zanoni M., Antonacci F., Sarti A., Malagodi M., Rovetta T., Invernizzi C. 2017. Feature-based analysis of the impact of ground coat and varnish on violin tone qualities. Acta Acustica United Acustica, 103,1: 80-93

Straže A., Mitkovski B., Tippner J., Čufar K., Gorišek Ž. 2015. Structural and acoustic properties of African padouk (*Pterocarpus soyauxii*) wood for xylophones. European journal of wood and wood products, 73, 2: 235-243

The effect of wood and solution temperatures on the preservative uptake of Pannonia poplar and common spruce – preliminary research

Luca Buga-Kovács[1], Norbert Horváth[2]

[1,2] University of Sopron, Institute of Basic Sciences, Bajcsy-Zs. Str. 4, Sopron, Hungary, 9400

E-mail: kovacs.luca@phd.uni-sopron.hu; norbert.horvath@uni-sopron.hu

Keywords: prolonged immersion, Pannonia poplar, common spruce, temperature differences, copper-sulphate

ABSTRACT

Our research aimed to compare the effect of wood and solution temperatures on the preservative uptake of Pannonia poplar and common spruce. The choice of the wood species was motivated by the followings. Poplar trees are less used wood species in the Hungarian construction industry. Some hybrids have similar characteristics to the commonly used spruce. Among them, the properties of the hybrid Hungarian Pannonia poplar are the focus of much research nowadays, because a significant amount of Hungarian Pannonia poplar trees are maturing to cutting age. Imported spruce is a common structural timber used in the Hungarian construction industry. According to CEN EN 14734, a copper sulphate solution was used to evaluate the prolonged immersion treatment. The temperature of the wood samples was 20 °C for both tests. The temperature of the copper sulphate solution in the control test was the same as that of the wood materials at 20 °C, while in the other test the materials were soaked in a solution at 12 °C. The preservative uptake graph, the mass of the copper sulphate solution taken up and the calculated mass of copper-sulphate after 3 hours of prolonged immersion were determined. We found that Pannonia poplar can take up more solution than spruce. For both species, the uptake of preservative at the initial stage was higher for the 12 °C solution than for the room temperature solution.

INTRODUCTION

The present study focuses on Pannonia poplar, an abundant poplar hybrid in Hungary and common spruce, for several reasons. Spruce is frequently utilized as structural timber in the Hungarian construction industry. As it is found in small quantities (1%) in Hungarian forests, it is the most important imported timber (Molnár 2004). Poplar hybrids are the subject of much research nowadays among other things because of their structural potential. Additionally, the two species exhibit nearly identical physical-mechanical properties (Molnár, 2004).

Resistance to insects and decay fungi is also a major determinant of the performance of structural timber, which can be based on treatment with preservatives. According to the Hungarian building regulations, both the low-durability Pannonia poplar and the pine species used in the construction industry until now have to undergo additional chemical wood preservative treatment before installation. In Hungary, prolonged immersion treatment is the most common method of wood protection. The question arises to what extent the differences in temperature during the soaking of the two species of wood promote the absorption of the preservative. According to CEN EN 14734, a copper sulphate solution was used to evaluate the prolonged immersion.

The prolonged immersion is when the wood is immersed for a longer period of time in the liquid preservative or its solution. The liquid penetrates into the wood by means of capillary action and possibly further seepage. The effectiveness of the prolonged immersion and the depth of penetration, depends on the anatomical structure of the wood, its moisture status, the material of the preservative, the concentration of the preservative solution and the duration of the soaking (Gyarmati et al. 1964). The amount and extent of penetration of the preservative solution is influenced more by temperature than by duration (Bálint 1967).

The water in the wood freezes well below 0 ºC. In the soaking tub the protective agent can freeze, although this can and should be avoided by using a heating rod or heating blanket in modern equipment to make the technology work. The movement of the bonded water in the wood is faster the higher the temperature.

A distinction has to be made between the temperature of the wood and the outside environment, as it is often the case (in spring, after snow melt) that the daily peak temperature is already around 20 ℃, but the inside of the beam to be soaked or saturated is still frozen. In summary, the higher is the temperature of the wood, the faster is the movement of the water inside. The speed of water movement is also related to its density. Water is most dense at + 4 ℃. The higher the temperature, the lower the density and surface tension of the water. The properties of water affect the properties of the solution also. In summer, the soaking wood preservation technology can be used without any particular constraints, as both the soaking liquid and the wood are at the right temperature. If the wood or the preservative solution is cooled below +5 ℃, the effectiveness of the soaking process is severely impaired, and so the use of soaking technology is often a problem in winter. However, heating the preservative and/or the wood should be strongly considered as it is a very energy intensive operation and rarely economical (Király and Csupor 2013).

MATERIALS AND METHODS

The tested bulk samples originated from Hungarian growing areas. All the specimens had a lying annual ring position. A total of 8 spruce and 8 Pannonia poplar samples were tested. The specimens were cut from a board along the grain. Half of the test specimens served as control samples for both species. A 5% copper sulphate solution and frozen ice cubes prepared from it were used for the test to evaluate the prolonged immersion, as prescribed in CEN EN 14734. The frozen solution provided cooling and ensured that the solution did not dilute.

For the control samples, the temperature of the solution and the specimens was maintained at 20 ℃ (Figure 1, left). The initial temperature of the other group of samples was the same as the control samples, but in this case the copper sulphate solution was continuously cooled with frozen copper sulphate solution "ice cubes". The solution temperature was 12 ℃ during the test (Figure 1, right). The temperatures of the solutions and samples were determined for the reasons described above.

Figure 1: Prolonged immersion in room temperature solution (left) and with copper-sulphate "ice-cubes" cooled solution (right)

Weights were measured before adding to the solution (m_b). As the freshly immersed wood absorbs the liquid more quickly at first, the masses were measured more frequently in the initial stage. The masses were measured 7 times in both cases. The preservative uptake curves were determined from these mass measurements per sample groups.

The times of the mass measurements are summarised in the following table (Table 1).

Table 1: Times of the mass measurements

Measurement	1	2	4	4	5	6	7	8
Time (min.)	5	10	15	35	55	75	95	180

The last 8th measurement was taken 3 hours after immersion in the solution, from which the mass of the copper sulphate solution taken up was determined. The mass of the specimens was measured before (m_b) and after (m_a) the prolonged immersion. The mass of the copper sulphate solution taken up (Δm) was calculated from the difference between their weights (Eq. 1).

$$\Delta m = m_a - m_b \ [g] \tag{1}$$

Δm – the mass of the copper sulphate solution taken up
m_a– the measured mass after the treatment
m_b – the measured mass before the treatment

$$m_{CuSO_4} = \Delta m \cdot 0{,}05 \ [g] \tag{2}$$

m_{CuSO_4} – the calculated mass of copper-sulphate

RESULTS AND DISCUSSION

The curves illustrates the average preservative uptakes of the sample groups are depicted in Figure 2. The first three measurements were taken every 5 minutes. The highest uptake of preservative is observed within the first 5 minutes at the beginning of the soak for all sample groups, as indicated by the slope of the curves. During this time the Pannonia poplar samples soaked in a 12 °C solution absorbed the most protective agent on average. Spruce specimens soaked in 12 °C and 20 °C solutions did not exhibit significant differences in average preservative uptake, but more preservative was absorbed by the room temperature solution on average. Weights were measured every 20 minutes subsequently. The uptake of Pannonia poplar samples immersed in room temperature preservative surpassed that of spruce samples by the 6th measurement. After 95 minutes of prolonged immersion, the Pannonia poplar samples absorbed more preservative than the spruce samples in both cases.
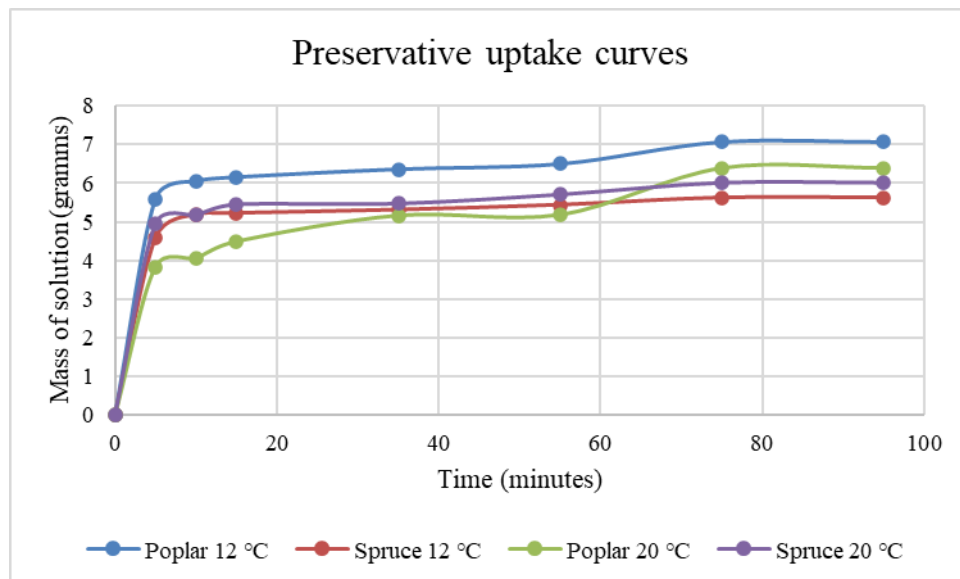
Figure 2: Preservative uptake curves during 95 minutes of prolonged immersion

Figure 3 illustrates the average preservative uptake of the sample groups after 3 hours of prolonged immersion. The Pannonia poplar specimens soaked in a cold solution at 12 °C absorbed an average of 7.11 grams of preservative, while the spruce specimens absorbed an average of 6.65 grams after three hours of prolonged immersion. The Pannonia poplar samples soaked in room temperature preservative were able to take up an average of 6.98 grams of preservative in the same time frame, while the spruce specimens absorbed an average of 6.89 grams. While in the case of Pannonia poplar, the samples soaked in the 12 °C solution exhibited a higher average uptake of preservative, in the case of spruce samples, those soaked in the 20 °C solution displayed a higher average mass of preservative. However, significant differences in preservative uptake were observed at the initial stage rather than after 3 hours of soaking.
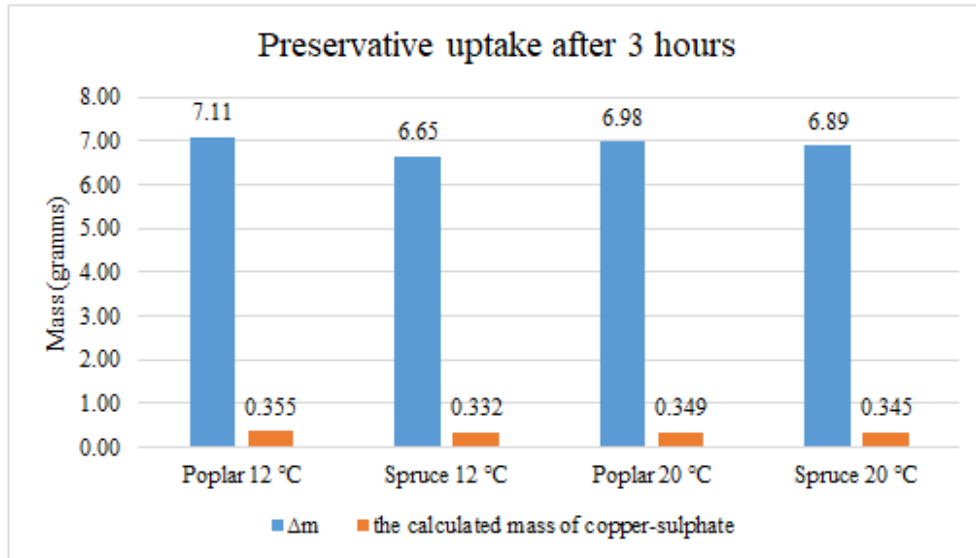
Figure 3: Preservative uptake after 3 hours of prolonged immersion

CONCLUSIONS

The prolonged immersion of Pannonia poplar has been demonstrated to be superior to that of spruce. The poplar hybrid species absorbed more of the solution at both liquid temperatures than spruce after 95 minutes of soaking. The uptake efficiency of Pannonia poplar samples is better in the 12 °C solution at the initial stage than in specimens soaked in preservative at room temperature. The Pannonia poplar samples absorbed more copper sulphate solution from both the cold and room temperature solutions after 3 hours. The differences between the groups of samples were much smaller than at the initial stage of soaking.

Overall, Pannonia poplar proved to be easier to treat with prolonged immersion than spruce, which is an important consideration for industrial protective treatment practices. Easier handling results in a higher durability class for treated wood. Pannonia Poplar can be classified in a higher durability class due to its easier prolonged immersion.

REFERENCES

Bálint, Gyula (1967): Protection of buildings. (Épületek védelme) Műszaki Könyvkiadó Budapest. (in Hungarian) p. 180

CEN EN 14734:2022 (MAIN): Durability of wood and wood-based products - Determination of treatability of timber species to be impregnated with wood preservatives - Laboratory method

Gyarmati, Béla; Igmándy, Zoltán; Pagony, Hubert (1964): Wood protection. (Faanyagvédelem) Mezőgazdasági Kiadó Budapest (in Hungarian) p. 235

Király, Béla; Csupor, Károly (2013): Materials and mixtures for chemical wood and fire protection. (A kémiai faanyag- és tűzvédelem anyagai és keverékei) Textbook. PALATIA Nyomda és Kiadó Kft. (in Hungarian) pp. 131-132

Molnár, Sándor (2004): Wood material knowledge (Faanyagismeret). Szaktudás Kiadó Ház Zrt (in Hungarian) pp. 330, 390-391

Session II
Hardwood resources, product approaches, and timber trade

Birch tar – historic material, innovative approach

Jakub Brózdowski[1*], Monika Bartkowiak[1], Grzegorz Cofta[1], Grażyna Dąbrowska[2], Ahmet Erdem Yazici[1], Zbigniew Katolik[1], Szymon Rosołowski[3], Magdalena Zborowska[1]

[1] Department of Chemical Wood Technology, Faculty of Forestry and Wood Technology, University of Life Sciences, Wojska Polskiego Street 38/42, 60-637 Poznań, Poland
[2] Department of Genetics, Faculty of Biology and Environmental Protection, Nicolaus Copernicus University in Toruń. Lwowska Street 1, 87-100 Toruń, Poland
[3] Archaeological Museum in Biskupin, Biskupin 17, 88-410 Gąsawa, Poland

E-mail: jakub.brozdowski@up.poznan.pl; monika.bartkowiak@up.poznan.pl; grzegorz.cofta@up.poznan.pl; browsk@umk.pl; aerdem.yazici2001@gmail.com; sz.rosolowski@biskupin.pl; magdalena.zborowska@up.poznan.pl

Keywords: birch tar, antioxidant properties, fractions, properties

ABSTRACT

Throughout millennia, people have mastered the art of tar production, a process which use technique of pyrolysis. This method involves thermal degradation of wood in the absence of oxygen, typically starting at temperatures of around 200°C and peaking between 450-500°C, depending on the wood species. The outcome of this thermal conversion yields three distinct products: solid charcoal, liquid wood tar —a condensate of volatile compounds—and non-condensable volatile gases.

The path from wood to tar is a nuanced one, influenced not only by the final temperature of the pyrolysis process but also by the raw material itself. For generations, tar was used as a preservative of wood, notably in the preservation of ships that were used in the discoveries of the new territories during the Middle Ages. While modern tar production is limited, its historical significance invited us to take lessons from the past and refine production methods to meet contemporary demands.

Wood tar, characterized as a complex mixture comprising several hundred chemical compounds, lacks a definitive characterization in the literature. Generally, it is composed of organic substances resulting from the thermal breakdown or gasification of any organic material, wood tar is predominantly considered a mixture of aromatic compounds.

Chemical composition of birch tar shows a great number of aromatic compounds, indicative of its considerable antioxidant properties. Research has confirmed high antioxidant activity, with variations attributed to the temperature of tar production and the specific fraction under examination. Notably, the tar fraction of birch tar exhibits significantly enhanced antioxidant properties.

INTRODUCTION

Wood tar is produced obtained by dry distillation of wooden materials without access to air . Over the years many raw materials were used for tar production, however the raw material for tar production was mostly chosen by the availability in the nearby areas of production site. For Poland most common material for tar production was pine (Pinus sp.) (Czopek 1993) while for Norway it was birch (Betula sp.) (Van Gijn and Boon 2006). Birch tar production was reported in many countries in Europe eg.: Bulgaria, Greece, Corsica (Urem-Kotsou et al. 2002; Ribechini et al. 2011; Rageot et al. 2016). Most common material for tar production from birch was birch bark, birch bark tar was produced in double-pot. In this method bark strips were heated in a top pot, and produced tar dripped to the connected bottom pot (Meijer and Pomstra 2011). Within the years this method evolved to 3 elements set of pots, with middle pot acting like a filter which allows to obtain highly pure product (Pietrzak 2010). Despite being updated within the year, pot methods of tar production were not efficient enough and production of tar slowing down and by the end of 19th century it was limited to the privet use of peasants. Beginning of 20th century gave people growing chemical industry which lead to stopping of tar production(Brzeziński and Piotrowski 1997) which was replaced by petroleum derivatives. Now with the global trend of returning to traditional products we have chance to re-evaluate the birch tar, and to update its technic of production.

The aim of this work to compare results of tar production from two raw materials: birch bark, and birch wood. Obtained in in four different temperature (450, 500, 550, and 600°C). To compare the results antioxidant assays were used.

MATERIAL AND METHODS
Raw Material
Birch bark and wood was the research material. Thin layers of birch bark and wood were sourced from trees harvested in the Gołąbki Forest District during the spring of 2022, specifically in May. Subsequently, the bark and wood underwent a drying process at room temperature before being manually chipped into irregular fragments, each measuring approximately 3×3 cm.

Pyrolysis
The pyrolysis was conducted within a laboratory system, as shown in Figure 1. The process involved placing raw material (2) into an iron, heat-resistant retort (also referred to as a reactor), which was then tightly sealed with a cover (3) and secured with screws. This retort was positioned within an electric muffle furnace (1) and connected to a vapor gas cooling system, with water as a coolant, through connector pipes (6).
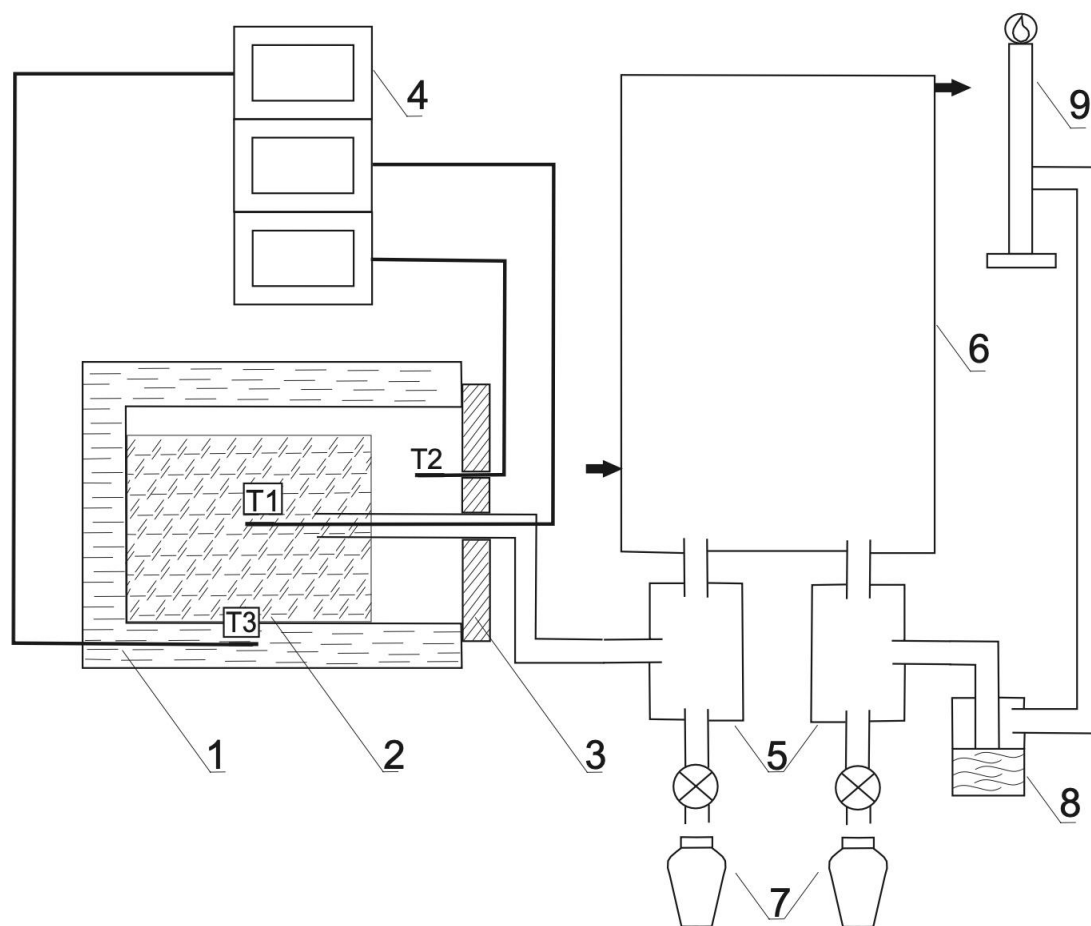
Figure 6: Scheme of pyrolysis oven

The heating of the retort, along with the feedstock material, followed a pre-set temperature program entered into the furnace heating control system (4). Thermal decomposition of the birch bark occurred under controlled conditions, with limited oxygen access, until reaching the designated final temperature. The heating rate was approximately 3°C per minute. Four final temperatures were used in the experiment: 450, 500, 550 and 600°C.

During this process, vapor gases generated from the thermal decomposition were conveyed from the retort to the cooling system. Here, some of these gases condensed, resulting in the production of birch tar (5, 7). Meanwhile, non-condensable gases were mixed with natural gas (methane) (9) and combusted. Obtained product of condensation (tar) was used for further analysis.

Tar separation
Tar was separated in the glass separatory funnel into two (bark) and three (wood) fractions. Top fraction comprises a layer of light oils. Middle fraction consists of acetic acid, methanol, and phenols. Bottom fraction forms a dense oily layer. Bark tar did not separate in the three fractions, middle fraction was dissolved partially in the top and bottom fractions. Use of four temperatures and division into two or three fraction resulted in 20 samples. These samples were used for the antioxidant analysis.

Samples description:
1 - Birch wood, top fraction 450°C | 2 -Birch wood, middle fraction 450°C | 3 - Birch wood, bottom fraction 450°C | 4 - Birch wood, top fraction, 500°C | 5 - Birch wood, middle fraction, 500°C | 6 - Birch wood, bottom fraction 500°C | 7 - Birch wood, top fraction, 550°C | 8 - Birch wood, middle fraction, 550°C | 9 - Birch wood, bottom fraction 550°C | 10 - Birch wood, top fraction, 600°C | 11 - Birch wood, middle fraction, 600°C | 12 - Birch wood, bottom fraction 600°C | 13 – Birch bark, top fraction, 450°C | 14 - Birch bark, bottom fraction, 450°C | 15 - Birch bark, top fraction, 500°C | 16 - Birch bark, bottom fraction, 500°C | 17 - Birch bark, top fraction, 550°C | 18 - Birch bark, bottom fraction, 550°C | 19 - Birch bark, top fraction, 600°C | 20 - Birch bark, bottom fraction, 600°C

Antioxidant assays
FRAP assay measures antioxidant capacity by reducing ferric ions (Fe^{3+}) to ferrous ions (Fe^{2+}), The reduction is monitored spectrophotometrically and is proportional to the total antioxidant capacity of the sample. This assay provides information about the ability of a sample to neutralize free radicals and oxidative stress. Results are compared to Trolox scale and expressed as Trolox equivalent [mM Teq].

ABTS assay is widely to evaluate the antioxidant properties of natural compounds, food products, and biological samples. The ABTS radical cation has a characteristic blue-green colour which is reduced in the presence of antioxidants. The reduction in colour intensity is then measured. The addition of tar to the ABTS caused the solution to become cloudy, preventing the analysis from being conducted.

DPPH assay measures antioxidant activity by reducing stable free radical DPPH (2,2-diphenyl-1-picrylhydrazyl) resulting in a colour change from purple to yellow. The extent of colour change is measured spectrophotometrically. Results of DPPH assay is expressed in mM Teq and were also used to calculated IC50.

FT-IR analysis
For FTIR ATR spectroscopy a Bruker Optics GmbH (Göttingen, Germany) FT-IR spectrometer with an ATR equipped with a diamond was used. The samples were scanned 32 times. The wave range used for analysis was from 3800 cm^{-1} to 800 cm^{-1} and a resolution of 4 cm^{-1}. The spectra were analysed based on the literature on FTIR studies of pitch and tar(Burger et al. 2016), organic compounds(Degen 1968; Smith 2017) and data presented at www.sigmaaldrich.com

RESULTS AND DISCUSSION
For antioxidant measurements all tar samples were used in the concentration of 0.1%. Results of antioxidant activity of birch tars are presented in the Figure 2.
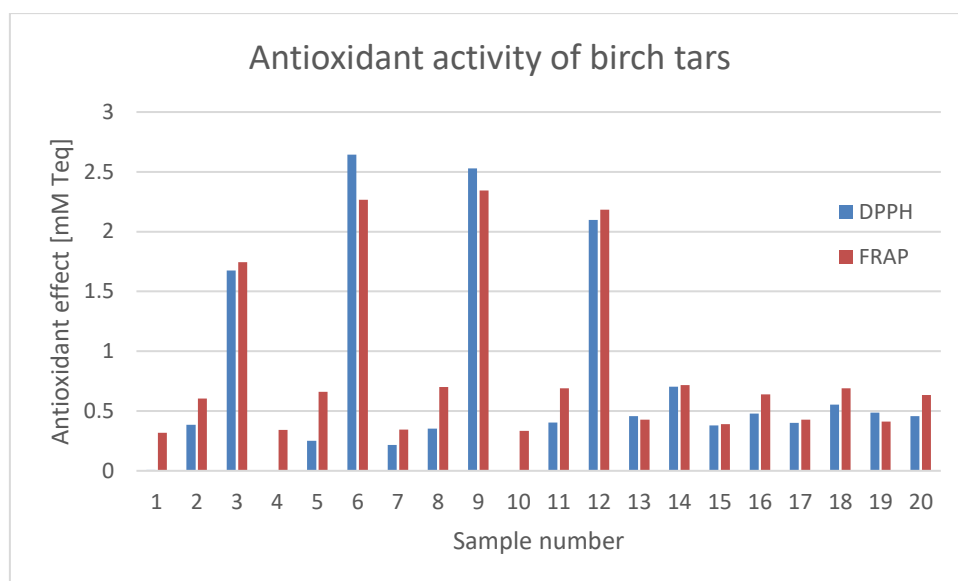
Figure 7: Results of antioxidant assays

FRAP method was more sensitive towards antioxidant activity of the samples, samples 1, 4 and 10 had no significant antioxidant effect according to DPPH assay, however FRAP assay showed results showing that these three samples had low antioxidant effect comparing to other samples. When comparing fractions, bottom fraction always had higher antioxidant effect than middle and bottom one. Bottom fraction of all the tar samples had the weaker antioxidant effect.

Results of FTIR analysis are shown on Figure 3. The results of FT-IR analyzes clearly showed that the samples of individual fractions differ from each other, but the results within the same fraction are clearly similar. Beacouse of that similarity Figure 3 shows results of analysis of one tar divided to three samples.
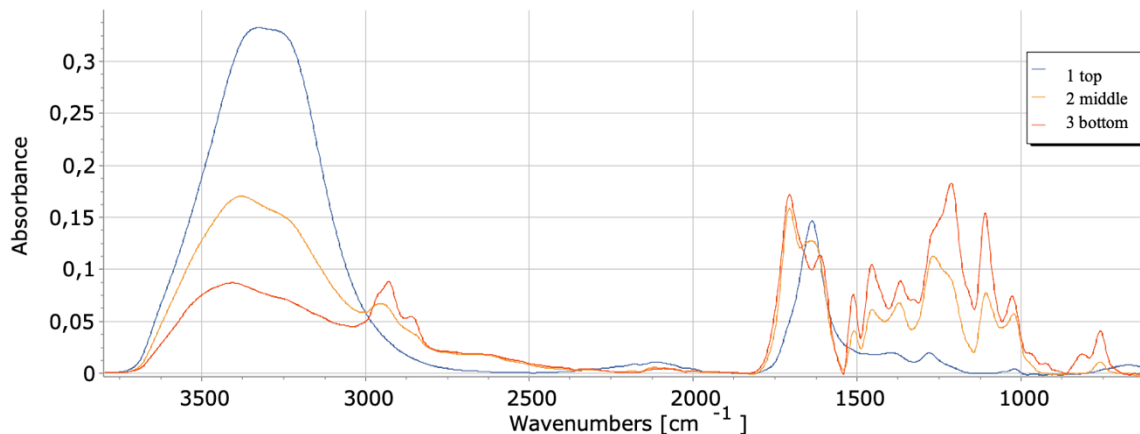
Figure 8: FTIR spectrum of samples from 3 layers of pyrolysis product

Sample 1 is the upper fraction of the obtained pyrolysis products, their FT-IR spectra are characterized by higher intensity of peaks in the band between 3500 and 3200 cm^{-1}, which indicates an increased content of phenolic compounds, aliphatic alcohols and carboxylic acids compared to the remaining samples. Analysis of the band between 2980 and 2800 cm^{-1} indicates that the content of compounds containing aliphatic hydrogens is similar in all tested samples. Samples 2, and 3 (middle and botton fraction, respectively) have a characteristic peak in their band attributed to ketones at 1709 cm^{-1}. In turn, sample 1 have a peak in their spectrum at 1642 cm^{-1}, which is assigned to the vibration of the unsaturated C=C bond. The presence of phenolic compounds is confirmed by the peak at wavelengths 1515 and 1600 cm^{-1}, present in the spectra of samples from the middle and lower fractions. The presence of hydrocarbon chains in samples 2, and 3 is confirmed by peaks at wavelengths of 1456 and 1374 cm^{-1}. Only sample from the upper fraction do not show a series of peaks in the range of 1300-1000 cm^{-1} assigned to the stretching vibrations of C-O bonds in various structures. The region between 900 and

700 cm^{-1} also contains various bands related to C-H bonds of aromatic structures, with varying degrees of substitution. Again, in this region, bands are not observed for sample 1 , while they are present for the remaining samples. The FT-IR spectrum confirms the differences in the chemical composition of the analyzed fractions, indicating the greatest differences between the upper fraction and the middle / lower fractions. Lower fraction showed less peaks assigned to antioxidant effect, compared to middle and bottom fractions. This observations were confirmed by the antioxidant assays.

Results of the calculations of IC 50, calculations were based on the results from DPPH antioxidant assay, performed for the concentrations: 10.0, 1.0, 0.1, and 0.01 %.
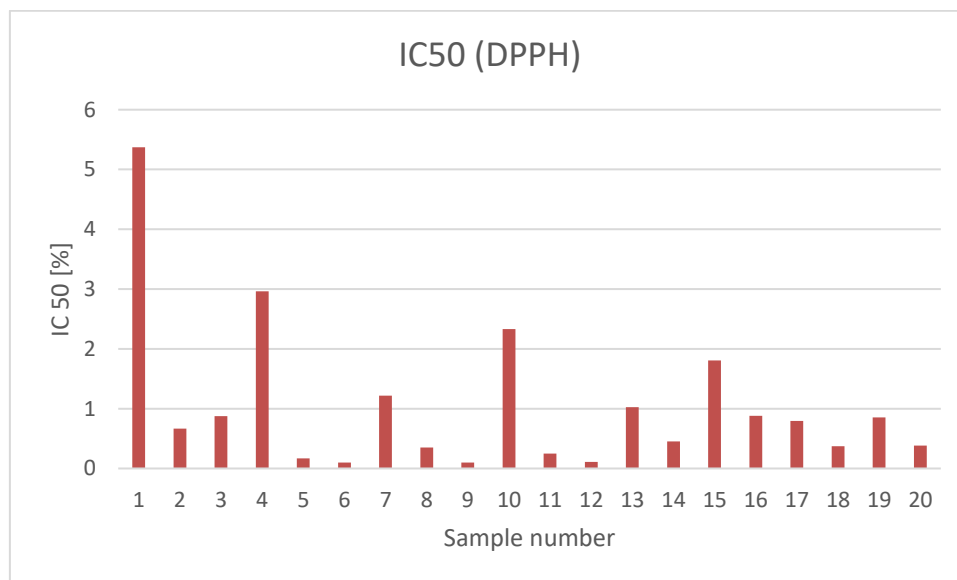
Figure 9: Results of the calculation of IC50

IC50 calculations shows that highest concertation needed to decrease DPPH free radical by 50 % was need for samples from the top fraction (Figure 4.): 1, 4, 7 and 10. The lowest concentration had to be used in the samples from the bottom fractions: 6, 9 and 12. This results are in accordance with the FTIR and FRAP results. Bark samples, 13-20 showed results which were in the middle range, and the results were similar between the fractions. This may be caused by not separation of the middle fraction, causing both fraction to contain parts of bottom fraction.

CONCLUSIONS

Pyrolysis of birch wood yielded in tar that divides in three distinct fractions: a top layer of light oils, a middle layer containing acetic acid, methanol, and phenols, and a dense, oily bottom layer. While birch bark yielded in product dividing into two fractions, top one with high content of acetic acid and methanol and bottom one with higher content of dense oils.

FRAP antioxidant assay showed that bottom tar fractions from both raw materials exhibited stronger antioxidant effects compared to other fractions.

Birch bark tar demonstrated lower antioxidant efficacy than wood tars.

DPPH assay, and based on this, calculated IC50 indicates that top fractions required higher concentrations for a 50% reduction in DPPH radical activity.

Wood bottom fractions showed IC50 values below 0.1%.

Enhanced IC50 results were observed for birch wood samples obtained at 500°C and 550°C.

ACKNOWLEDGEMENTS

REFERENCES

Brzeziński W, Piotrowski W (1997) Proceedings of the First International Symposium on Wood Tar and Pitch: Held by the Biskupin Museum (department of the State Archaeological Museum in Warsaw) and the Museumsdorf Düppel (Berlin) at Biskupin Museum, Poland, July 1st-4th 1993. Domu Wydawniczym Pawa Dabrowskiego

Burger P, Stacey RJ, Bowden SA, et al (2016) Identification, Geochemical Characterisation and Significance of Bitumen among the Grave Goods of the 7th Century Mound 1 Ship- Burial at Sutton Hoo (Suffolk, UK). PLoS One; https://doi.org/10.1371/journal.pone.0166276

Czopek S (1993) Beitrag zum Wissen über Holzteer- und Holzpechherstellung auf dem Gebiet Südpolens im 18.–19.Jh. In: Brzeziński W, Piotrowski W (eds) Proceedings of the First International Symposium on Wood Tar and Pitch Held by the Biskupin Museum (department of the State Archaeological Museum in Warsaw) and the Museumsdorf Döppel (Berlin) at Biskupin Museum. State Archaeological Museum in Warsaw, Warszawa, pp 342–342

Degen IA (1968) Detection of the Methoxyl Group by Infrared Spectroscopy. Appl Spectrosc 22:164–166. https://doi.org/10.1366/000370268774383444

Meijer R, Pomstra D (2011) The production of birch pitch with hunter-gatherer technology: a possibility. Exp Archäol Eur 10:199–204

Pietrzak S (2010) Zastosowanie i technologie wytwarzania dziegciu przez spoleczenstwa miedzyrzecza Dniepru Laby od VI do II tysiaclecia BC. Wydaw. Poznanskie

Rageot M, Pêche-Quilichini K, Py V, et al (2016) Exploitation of beehive products, plant exudates and tars in Corsica during the Early Iron Age. Archaeometry 58:315–332; https://doi.org/10.1111/arcm.12172

Ribechini E, Bacchiocchi M, Deviese T, Colombini MP (2011) Analytical pyrolysis with in situ thermally assisted derivatisation, Py (HMDS)-GC/MS, for the chemical characterization of archaeological birch bark tar. J Anal Appl Pyrolysis 91:219–223; https://doi.org/10.1016/j.jaap.2011.02.011

Smith B (2017) The CO bond III: ethers by a knockout. Spectroscopy 32:22–26

Urem-Kotsou D, Stern B, Heron C, Kotsakis K (2002) Birch-bark tar at Neolithic Makriyalos, Greece. Antiquity 76:962–967; https://doi.org/10.1017/S0003598X00091766

Van Gijn AL, Boon JJ (2006) Birch bark tar. Schipluiden: a neolithic settlement on the dutch north sea coast c 3500 cal bc 261–266

Beech Wood Steaming – Chemical Profile of Condensate for Sustainable Applications

Goran Milić[1*], Nebojša Todorović[1], Dejan Orčić[2], Nemanja Živanović[2], Nataša Simin[2]

[1] University of Belgrade – Faculty of Forestry, Department of Wood Science and Technology, Kneza Višeslava 1, 11000 Belgrade, Serbia
[2] University of Novi Sad Faculty of Sciences, Department of Chemistry, Biochemistry and Environmental Protection, Trg Dositeja Obradovića 3, 21000 Novi Sad, Serbia

E-mail: goran.milic@sfb.bg.ac.rs; nebojsa.todorovic@sfb.bg.ac.rs; natasa.simin@dh.uns.ac.rs; nemanja.zivanovic@dh.uns.ac.rs; dejan.orcic@dh.uns.ac.rs

Keywords: beech wood, steaming condensate, chemical analysis, sustainable applications

ABSTRACT

The sawn timber of beech (*Fagus sylvatica* L.), a pivotal hardwood species in Europe and of particular importance in south-eastern Europe, is traditionally steamed before the drying process. Several decades ago, this was done to equalize the color of the false heartwood and the rest of the wood, and steaming lasted 36 to 48 hours. Nowadays, in Serbia and surrounding countries, more than 90% of beech timber undergoes a process known as "light steaming" with the objective of inducing only a subtle color change. Steaming, both indirect and direct, generates vast amounts of condensate (wastewater), which poses an environmental challenge and must be chemically treated before being discharged into storm drains or watercourses. This study focused specifically on the condensate produced during the indirect steaming of beechwood timber. The process was carried out in an industrial chamber at a temperature of 95 °C and lasted 12 hours, including the heating and cooling phases. After two 12-hour steaming cycles, the condensate sample was taken from different points of the tank in the chamber's floor. The condensate underwent a comprehensive analysis, determining total phenolic content, total flavonoid content, and antioxidant activity. Moreover, qualitative and quantitative analyses were performed using HPLC coupled with UV/VIS and MS/MS. The results demonstrated high content of phenols (1885 ± 92.7 µg gallic acid equivalents per mL of condensate; including specific phenolic compounds not typical for other plants) and high flavonoid content (35.3 ± 0.86 µg quercetin equivalents per mL of condensate). Robust antioxidant activity was also observed (in DPPH assay $IC_{50}=42.9$ µg/mL), emphasizing the potential applications of condensates for direct use as biopesticides in agriculture or for isolation of biologically active phenolic compounds that can be used in diverse industries, such as the pharmaceutical and food industry. This simultaneously addresses environmental challenges in the wood industry. Further research will extend to beech wood condensate generated during different phases of the direct steaming process, but also to condensates from other wood species (walnut, oak). Furthermore, the study will investigate how changes in steaming parameters (temperature and duration) affect both the wood properties and the chemical composition of the condensate.

INTRODUCTION

European beech (*Fagus sylvatica* L.) is one of the most important and widespread broadleaved tree species in Europe, spanning from southern Scandinavia to Sicily, and from Spain in the west to northwest Turkey in the east. Nowadays, particularly in central Europe, beech is considered an essential tree species in climate-adapted forest management of the near future (Pramreiter and Grabner 2023). The importance of beech timber is significant, particularly in the southeastern regions of Europe, where it is widely utilized in various areas of the wood industry, especially for furniture production.

Traditionally, the processing of beech timber involves a steaming phase before drying, a practice that has historical roots in equalizing the color between false heartwood and the rest of the beechwood. This process typically involved exposing green wood to saturated water vapor for 36 to 48 hours, resulting in the dark red color characteristic of beech timber. However, contemporary practices, notably in Serbia and surrounding countries, have shifted towards a method known as "light steaming", where the objective is to induce only subtle color changes.

Despite its benefits, both indirect and direct steaming processes generate a significant amount of condensate. Even with shorter cycles typical for light steaming, managing the resulting condensates presents a notable challenge. Proper chemical treatment of these wastewaters before disposal into storm drains or watercourses is essential to mitigate environmental impact.

The potential application of the beech steaming condensate in other industries could be a sustainable solution. Understanding the chemical composition and properties of these condensates is crucial for devising sustainable solutions for application in other fields. Moreover, exploring innovative uses for this by-product can contribute to a circular economy, promoting resource efficiency and environmental sustainability.

MATERIALS AND METHODS

Fresh sawn beech (*Fagus sylvatica* L.) timber, 25 mm thick, was steamed in an industrial chamber with a capacity of 40 m^3. The indirect steaming was carried out at a temperature of 95 °C and lasted 12 hours, including the heating and cooling phases. After two 12-hour steaming cycles, the condensate sample was taken from different points of the tank in the chamber's floor. The condensate sample was stored in a freezer until used for testing to minimize the risk of additional bacterial or fungal contamination.

The obtained aqueous beech timber condensate (BTC) was evaporated to dryness under vacuum, followed by dissolution in DMSO:H2O = 1:1 to achieve a concentration of 100 mg/mL. This extract was used for further analysis: determination of total phenolic content, total flavonoid content, antioxidant activity and quantitative LC-MS/MS analysis of selected phenolics. The dilutions of the extract were prepared using 50% MeOH.

The determination of Total Phenolic Content (TPC) was conducted using Folin–Ciocalteu (FC) reagent, following the methodology outlined by Lesjak et al. (2011). In brief, 30 µL of the extract (ranging from 0.125 to 1.5 mg/mL) or standard (gallic acid, 0.625–80.0 µg/mL) was mixed with 150 µL 0.1 M FC reagent in 96-well microplate and incubated for 10 minutes in the dark. Subsequently, 120 µL of 0.7 M sodium carbonate was added. After 2 h of incubation in the dark at room temperature, absorbance was measured at 720 nm. All tests were performed in triplicate and the total phenolic content was expressed as mg of gallic acid equivalents per g of dry BTC (mg GAE/g dry BTC) or in µg of gallic acid equivalents per mL of BTC (mg GAE/mL of BTC).

Total flavonoid content (TFC) was determined by a colorimetric method described by Lesjak et al. (2011). In summary, 30 µL of the extract (1, 1.5 and 2 mg/mL) or standard (quercetin, ranging from 0.625 to 80.0 µg/mL) was mixed with 6 µL of 10% aluminum chloride, 6 µL of 1 M sodium acetate, 90 µL of methanol and 170 µL of distilled water in 96-well microplate. The absorbance was measured after 30 min of incubation at 415 nm. All tests were performed in triplicate and results were expressed as mg of quercetin equivalents per g of dry BTC (mg QE/g dry BTC) or in µg of quercetin equivalents per mL of BTC (mg QE/mL of BTC).

The investigation of the content of 36 selected phenolic compounds (9 phenolic acids, 22 flavonoids, 3 coumarins and 2 lignans) in BTC was carried out by liquid chromatography with tandem mass spectrometry (LC-MS/MS) as per the methodology reported in Simin et al. (2013). Standards of the compounds were purchased from SigmaeAldrich Chem (Steinheim, Germany), Fluka Chemie GmbH (Buchs, Switzerland) or ChromaDex (Santa Ana, CA, USA). Samples and standards were analyzed using Agilent Technologies 1200 Series high-performance liquid chromatograph coupled with Agilent Technologies 6410A Triple Quad tandem mass spectrometer with electrospray ion source, and controlled by Agilent Technologies MassHunter Workstation software - Data Acquisition (ver. B.06.00). The extract was diluted with 50% aqueous MeOH to the concentrations of 20 mg/mL and 2 mg/mL. A sample volume of 5 µL was injected into the system, and compounds were separated on a Zorbax Eclipse XDB-C18 (50 mm × 4.6 mm, 1.8 µm) rapid resolution column. Data were acquired in dynamic Multiple Reaction Monitoring (MRM) mode, and peak areas were determined using Agilent MassHunter Workstation Software - Qualitative Analysis (ver. B.06.00). Calibration curves, plotted using OriginLabs Origin Pro (ver. 2019b) software, were utilized for the calculation of the concentration of the investigated compounds.

Antioxidant activity was assessed by determining the ability of BTC to neutralize 2,2-diphenyl-1-picrylhydrazyl (DPPH) radicals, according to slightly modified method described by Lesjak et al. (2011). Briefly, 10 µL of the extract (concentration range 0.08–5.0 mg/mL) was mixed with 100 µL of 67.5 µM DPPH solution in methanol and 190 µL of methanol. Butylated hydroxytoluene (BHT), a

synthetic antioxidant, served as a positive control. Absorbance readings were taken after 1 hour at 515 nm. All experiments were conducted in triplicate, and the results were expressed as IC_{50} values, representing the concentration of the sample that neutralizes 50% of DPPH radicals (μg/mL).

RESULTS AND DISCUSSION
Phenolic profile of BTC was determined by evaluation of total phenolic content (TPC) and total flavonoid content (TFC) (Table 1), as well as quantitative LC-MS/MS analysis of selected compounds (Table 2).

Table 1: Total phenolic content (TPC) and total flavonoid (TFC) content in BTC

Sample	TPC [mg GAE/g de]	TPC [mg GAE/mL of BTC]	TFC [mg QE/g de]	TFC [μg QE/mL of BTC]
BTC	116 ± 5.75	1.88 ± 0.093	2.19 ± 0.053	35.3 ± 0.865

BTC – beech timber condensate; GAE – galic acid equivalents; QE – quercetin equivalents; de – dry BTC

The obtained results suggest that BTC in general is rich in phenolic compounds. In comparison to the equivalent condensate of walnut timber (Milić et al. 2024), the TPC was significantly higher in BTC (49.5 mg GAE/g de vs 116 mg GAE/g, respectively). However, the TFC values were very similar for both condensates – 2.19 mg QE/g de for BTC and 2.56 mg QE/g de for walnut condensate. It implies that BTC contains much higher amounts of phenolic compounds other than flavonoids compared to walnut condensate.

The TPC values of other effluents from the wood industry (according to the literature data) – such as log soaking water, debarking water, log boiling water – are typically much lower compared to the condensate generated during beech timber steaming. Several authors have investigated TPC and other chemical compounds in beech normal wood, knots, false heartwood and bark (e.g. Hofman et al. 2015, Vek et al. 2013) expressing TPC and TFC results per gram of dry wood. However, this expression method was not feasible for steaming condensate, making direct comparison with these studies challenging.

LC-MS/MS analysis of BTC revealed 45 analyzed compounds, among which 17 were quantified and 7 were detected but were below limit of quantitation (Table 2). The remaining 21 compounds (gentizic acid, umbelliferon, 3,4-Dimethoxycinnamic acid, sinapic acid, daidzein, apigenin, genistein, baicalein, kaemferol, catechin, epicatechin, crysoeriol, quercetin, isorhamnetin, myricetin, vitexin, baicalin, kaemferol-3-glucoside, epigallocatechin gallate, apiin and rutin) were not detected. The most predominant compounds were hydroxybenzoic acids, including protocatechuic, syringic acid, p-hydroxybenzoic and vanillic acid. Syringic acid, vanillic acid and p-hydroxybenzoic acid were also identified in beech timber steaming condensate in the study of Irmouli et al. (2002). Quinic acid, a cyclic polyhydroxy carboxylic acid, was also present in significant amounts (547 μg/g of dry BTC). Interestingly, this acid was absent in condensate generated from steaming walnut timber, suggesting species-specific variations in chemical composition of the condensate. It should be noted that longer duration of walnut steaming (usually 96 hours) allows possibility for additional chemical reactions within the condensate. The diverse chemical composition of condensates from different wood species and processes suggests different potential applications. For instance, quinic acid, found herein, is involved in the biosynthesis of certain secondary metabolites, including various quinates, chlorogenic acids, and other phenolic compounds. In foods and beverages, quinic acid contributes to taste and aroma, and it also possesses certain biological activities that may have health benefits, such as antioxidant, antidiabetic, anticancer activity, antimicrobial, antiviral, aging, protective, anti-nociceptive and analgesic effects (Benali et al. 2022). Among analysed phenylpropanoids, cinnamic acid was the most dominant (257 μg/g of dry BTC). This pattern contrasts again with the situation observed in walnut condensate. The analysed flavonoid compounds in BTC either were completely absent or were found in such small quantities that they could be considered insignificant. The total amount of identified and quantified compounds was only 2.2 mg/g of dry BTC, which is much lower than TPC (116 mg/g of dry BTC) determined by spectrophotometric method. It implies that in further research detailed qualitative analysis of individual phenolic compounds is needed.

Table 2: Content of selected phenolic compounds in BTC

	Content	
Compound	[µg/g][a]	[ng/mL][b]
Quinic acid	**547** ± 54.7	**8826** ± 883
Hydroxybenzoic acids		
p-Hydroxybenzoic acid	23.6 ± 1.42[c]	**381** ± 22.8
Protocatechuic acid	**745** ± 59.6	**12013** ± 961
Vanillic acid	71.8 ± 21.5	**1158** ± 347
Syringic acid	**535** ± 107	**8626** ± 1725
Gallic acid	<1.5[d]	<24.2
Phenylpropanoids		
Cinnamic acid	**257** ± 51.5	**4152** ± 830
p-Coumaric acid	4.63 ± 0.42	74.7 ± 6.73
o-Coumaric acid	0.61 ± 0.05	9.91 ± 0.79
Caffeic acid	1.54 ± 0.11	24.8 ± 1.73
Ferulic acid	5.69 ± 0.57	91.9 ± 9.19
5-*O*-Caffeoylquinic acid	0.38 ± 0.03	6.16 ± 0.31
Coumarins		
Esculetin	<0.08	<1.21
Scopoletin	<0.30	<4.84
Flavonoids		
Amentoflavon	<4.9	<79.0
Apigenin-7-*O*-Glc	<0.08	<1.21
Naringenin	0.08 ± 0.01	1.32 ± 0.09
Quercetin-3-*O*-Glc + Quercetin-3-*O*-Gal	0.88 ± 0.05	14.2 ± 0.85
Luteolin	<0.60	<9.68
Lueolin-7-*O*-Glc	0.11 ± 0.003	1.71 ± 0.05
Quercitrin	0.34 ± 0.02	5.54 ± 0.33
Lignans		
Secoisolariciresinol	6.47 ± 0.52	**104** ± 8.35
Matairesinol	<1.20	<19.4
Total quantified phenolics[e]	2.20 mg/g[f]	35.5 µg/mL

[a]*µg/g – µg/g of dry BTC;* [b]*ng/mL – ng/mL of BTC;* [c] *The results are given as content ± standard error of repeatability (as determined by method validation);* [d] *Concentration is below the limit of quantification; The values higher than 100 are marked with bold letters;* [e] *Sum of the contents of all detected phenolic compounds; Glc – glucose; Gal – galactose;* [f]*mg/g – mg/g of dry BTC*

Antioxidant activity was assessed by evaluating BTC's capability to neutralize DPPH radicals (Table 3). The condensate demonstrated remarkably potent antioxidant activity, with an IC_{50} value only 1.5 times higher than that of synthetic antioxidant BHT. This robust antioxidant performance correlates with the abundance of phenolic compounds present in BTC. Notably, its efficacy surpasses that of other effluents from the wood industry, including log soaking water (Barbero-Lopez et al. 2022), debarking water, and is approximately three times superior to bark press water (Peeters et al. 2023). Even when compared to walnut steaming condensate (IC_{50}= 61.4 µg/mL in DPPH assay, Milić et al. 2024), BTC exhibits a significantly lower IC_{50} value (42.9 µg/mL). The exceptional antioxidant properties of BTC cannot be attributed solely to its predominant compounds. It is likely that synergistic interactions among polyphenols or the presence of minor compounds significantly contribute to its activity (Pietarinen et al. 2006). Plant extracts with high antioxidant activity, including wood steaming condensates, have a wide range of potential applications across various industries and agriculture due to their ability to neutralize harmful free radicals and oxidative stress. They could be used in food industry as natural food preservatives to extend the shelf life of foods by inhibiting lipid oxidation (Nikmaram et al. 2018). In cosmetics industry they can be included in skincare formulations to protect against oxidative damage caused by UV radiation and environmental pollutants, thereby promoting skin health and reducing signs of aging (Hoang et al. 2021). In agriculture antioxidants could offer crop protection by enhancing the stress tolerance of crops, especially under adverse environmental conditions (Rodrigues de Queiroz et al. 2023).

Table 3: Antioxidant activity of BTC

Sample	DPPH IC$_{50}$ [µg/mL]
BTC	42.9 ± 4.14
BHT	28.4 ± 2.5

BHT - butylated hydroxytoluene, positive control

The presented results demonstrate that condensate derived from the indirect steaming of beech timber is abundant in polyphenolic compounds that express notable antioxidant properties. Prior studies have highlighted that some of these compounds also possess antimicrobial, antidiabetic, immunomodulatory, hepatoprotective and anti-inflammatory attributes (Shahidi and Yeo, 2018).

Beside previously listed potential application of BTC, it would be worthy to investigate potential utilization of BTC in three specific areas: for plant protection, in textile dyeing or as component of wood adhesive. Initial trials in plant protection have revealed that BTC significantly inhibited weed plant germination. Additionally, preliminary tests have unveiled the considerable potential of BTC in dyeing textiles, particularly wool and cotton. A very circular and sustainable solution would be to utilize the condensate extracted from the beech wood for dyeing modal, a textile obtained from fibres of the same wood species. Finnaly, the acidic nature and chemical composition of BTC render it a promising candidate for VOC scavenging and substituting deionized water in the production of UF resins for the wood panel industry.

CONCLUSIONS

The study reveals the chemical composition and biological activity of condensate obtained from beech timber steaming. This condensate showcases higher total phenolic content (TPC) and stronger antioxidant activity compared to the majority of other wood industry effluents, including walnut steaming condensate. The versatility of beech timber condensate opens doors to various practical applications in agriculture, food and cosmetic industries. Potential uses include textile dyeing and formulation of UF resins for the wood panel industry. By exploring these applications, we can contribute to sustainable practices within various areas while reducing environmental impact of the wood industry. Our findings emphasize the importance of utilizing by-products effectively to create value-added products and minimize waste in wood processing.

ACKNOWLEDGEMENTS

REFERENCES

Barbero-López A, Vek V, Poljanšek I (2022) Characterisation, Recovery and Activity of Hydrophobic Compounds in Norway Spruce Log Soaking Pit Water: Could they be Used in Wood Preservative Formulations? Waste Biomass Valor 13:2553–2564. https://doi.org/10.1007/s12649-022-01676-2

Benali B, Bakrim S, Ghchime R, Benkhaira N, El Omari N, Balahbib A, Taha D, Zengin G, Hasan MM, Bibi S, Bouyahya A (2022) Pharmacological insights into the multifaceted biological properties of quinic acid, Biotechnol Gen Engineer Rev, https://doi.org/10.1080/02648725.2022.2122303

Hofmann T, Nebehaj E, Stefanovits-Bányai E, Albert L (2015) Antioxidant capacity and total phenol content of beech (*Fagus sylvatica* L.) bark extracts, Ind Crops Prod 77:375-381. https://doi.org/10.1016/j.indcrop.2015.09.008

Hoang HT, Moon JY, Lee YC (2021) Natural antioxidants from plant extracts in skincare cosmetics: recent applications, challenges and perspectives. *Cosmetics 8:*106. https://doi.org/10.3390/cosmetics8040106

Irmouli M, Haluk JP, Kamdem P, Charrier B (2002) Chemical characterization of beech condensate, J Wood Chem Technol 22:127-136. https://doi.org/10.1081/WCT-120013357

Lesjak MM, Beara IN, Orčić DZ, Anačkov GT, Balog KJ, Francišković MM, Mimica-Dukić NM (2011) *Juniperus sibirica* Burgsdorf. as a novel source of antioxidant and anti-inflammatory agents. Food Chem 124:850–856. https://doi.org/10.1016/j.foodchem.2010.07.006

Milić G, Rančić M, Todorović N, Živanović N, Orčić D, Simin N (2024) Walnut Wood Steaming: Chemical Profile and Antioxidant Activity of the Condensate to Assess the Potential Application. Manuscript submitted for publication.

Nikmaram N, Budaraju S, Barba FJ, Lorenzo JM, Cox RB, Mallikarjunan K, Shahin Roohinejad S (2018) Application of plant extracts to improve the shelf-life, nutritional and health-related properties of ready-to-eat meat products. Meat Sci 145:245-255. https://doi.org/10.1016/j.meatsci.2018.06.031

Peeters K, Esakkimuthu ES, Tavzes Č, Kramberger K, Miklavčič Višnjevec A (2023) The potential value of debarking water as a source of polyphenolic compounds for the specialty chemicals sector. Molecules 28:542-555. https://doi.org/10.3390/molecules28020542

Pietarinen S, Willför S, Ahotupa M, Hemming J, Holmbom B (2006) Knotwood and bark extracts: strong antioxidants from waste materials. J Wood Sci, 52:436-444. http://dx.doi.org/10.1007/s10086-005-0780-1

Pramreiter M, Grabner M (2023) The Utilization of European Beech Wood (*Fagus sylvatica* L.) in Europe. Forests 14(7):1419. https://doi.org/10.3390/f14071419

Rodrigues de Queiroz A, Hines C, Brown J, Sahay S, Vijayan J, Stone JM, Bickford N, Wuellner M, Glowacka K, Buan NR, Roston RL (2023) The effects of exogenously applied antioxidants on plant growth and resilience. Phytochem Rev 22:407–447. https://doi.org/10.1007/s11101-023-09862-3

Shahidi F, Yeo J (2018) Bioactivities of phenolics by focusing on suppression of chronic diseases: a review. Int J Mol Sci 19:1573. doi: 10.3390/ijms19061573.

Simin N, Orcic D, Cetojevic-Simin D, Mimica-Dukic N, Anackov G, Beara I, Mitic-Culafic D, Bozin B (2013) Phenolic profile, antioxidant, anti-inflammatory and cytotoxic activities of small yellow onion (*Allium flavum* L. subsp. *flavum, Alliaceae*). LWT Food Sci Technol 54:139–146. https://doi.org/10.1016/j.lwt.2013.05.023

Vek V, Oven P, Humar M (2013) Phenolic extractives of wound-associated wood of beech and their fungicidal effect, Int Biodeterior Biodegrad 77:91-97. https://doi.org/10.1016/j.ibiod.2012.10.013

Towards a complete technological profile of hardwood branches for structural use: Case study on Poisson's ratio

Tobias Nenning[1*], Michael Grabner[1], Christian Hansmann[1, 2], Wolfgang Gindl-Altmutter[1], Johannes Konnerth[1], Maximilian Pramreiter[1]

[1] University of Natural Resources and Life Sciences, Vienna, Institute of Wood Technology and Renewable Materials, Austria
[2] Wood K plus – Competence Centre for Wood Composites and Wood Chemistry, Tulln an der Donau, Austria

E-mail: tobias.nenning@boku.ac.at

Keywords: Digital Image Correlation; European beech; Mechanical properties; Resource efficiency; Sessile oak; White poplar; Wood construction materials

ABSTRACT

The urgent need to build climate-friendly cities has led to a renaissance of wood as a renewable building material. However, the sustainable supply of stemwood is limited and, driven by climate change, is shifting from uniform conifers to more broadleaved trees whose morphology is more heterogeneous. To avoid an impending shortage of timber, the branches of deciduous trees, which are currently mainly burned, could serve as an untapped resource for building materials. After all, the crown wood volume of deciduous trees accounts for 20-50% of their total above-ground biomass. However, wood science has historically focused on the stem wood of conifers and its use in construction products. At the same time, the technological profile of hardwoods, and in particular branches, is less known. We are therefore working on a better technological understanding of hardwood branches to assess the potential as a building material. Extending our previous studies, we used digital image correlation (DIC) to monitor in-plane displacement on tensile specimens of beech, oak and poplar branch and stem wood and calculated the Poisson's ratio in the longitudinal-radial direction (v_{LR}). Our results showed significant differences, with stem wood having a higher Poisson's ratio on average. Surprisingly, and contrary to the literature, our results for oak show an increasing Poisson's ratio with increasing wood density. We find that the experimental setup is well suited to determine the Poisson's ratios of branch wood, although future investigations with larger numbers of samples and including other wood anatomical directions are needed to verify our preliminary findings.

INTRODUCTION

Mixed forest stands in Central Europe potentially have greater resilience to drought caused by the ever-worsening climate crisis (Pardos et al., 2021). As a result, the wood species mix available for producing engineered products for the construction sector is changing towards more deciduous trees and fewer conifers (Dyderski et al., 2018; Schier et al., 2018). This is also accompanied by a change in the share of the rather uniform stem and non-uniform crown wood volumes, as the morphology of coniferous and deciduous trees is different. The stems of deciduous trees are only moderately long compared to those of conifers, resulting in a crown wood share of 20-50% of the above-ground biomass volume, depending on the tree species, size class and location (Gschwantner et al., 2019). This crown wood, in turn, is made up of branches and stem tops, which are currently mainly used as fuel and only to a lesser extent used for wood products, depending on economic, technical and environmental constraints (Camia et al., 2021; Mantau et al., 2016; Shmulsky & Jones, 2011). In the face of growing demand for wood products and to avoid a future supply dilemma, several studies propose a strategic shift towards a resource-efficient material-first approach (Pramreiter, Nenning, Huber, et al., 2023; Pramreiter, Nenning, Malzl, et al., 2023). In the future, carbon-efficient use of wood in large-scale urban construction could also include lower-value assortments such as branches, although efficient material processing is currently seen as a major challenge (Churkina et al., 2020; Shmulsky and Jones, 2019). One reason for this may be a lack of basic knowledge about branch wood, as wood science and technology has historically focused on stem wood and its use in construction products due to practical reasons (Ramage et al., 2017). Only

recently Nenning et al. (2024) published a study that examines the mechanical properties of branch wood from beech, oak and poplar trees as a function of its morphological branch shape and growth position in the tree and compares them with those of stem wood. The study shows that branch wood has indeed a significantly different technological profile, in comparison to stem wood, most notably in density and tensile strength. The authors conducted bending, tensile and compression tests to determine the elastic and strength properties, relevant for the application as construction material.

However, to date, no study is available that investigates the Poisson's ratio of branches from deciduous trees. The Poisson's ratio is an elastic material property that indicates the relationship between transverse contraction and longitudinal elongation when a specimen is subjected to uniaxial loading (Niemz, Sonderegger, Keplinger, et al., 2023). It is an essential metric for the reliable description of materials for computational models used in civil engineering and thus also for the resource-smart material use of hardwood assortments like branches. Historically, the research on Poisson's ratio of solid wood was limited by the lack of time-efficient non-contact optical measurement techniques (G. A. Zink et al., 1997). This has been improved in recent years by methods such as Digital Image Correlation (DIC), Electronic Speckle Pattern Interferometry (ESPI) and laser and video extensometry (Keunecke et al., 2008; Kumpenza et al., 2018; Valla et al., 2011; A. G. Zink et al., 1995). In a comparison of ESPI and DIC, Valla et al. (2011) find the experimental measurements to be of similarly high quality, with DIC showing great versatility, albeit with increased effort in the application of the artificial speckle pattern. One other reason for the limited number of Poisson's ratio studies is the amount of sample preparation required due to the inhomogeneous nature of wood. From a materials science point of view, wood is an orthotropic material, i.e. it is not only directionally dependent (longitudinal, radial, tangential) but can also exhibit different properties at each point along its directions, hence it can be described as anisotropic (Niemz, Sonderegger, Gustafsson, et al., 2023). If all the necessary orthotropic Poisson's ratios are to be investigated, the following six specimen sets are required: ν_{LR}, ν_{LT}, ν_{RL}, ν_{RT}, ν_{TL}, ν_{TR}, where the first index indicates the direction of loading and the second the direction of transverse contraction. In addition to the direction of loading, the mechanical properties are also dependent on the moisture content (MC) of the wood and usually decrease with increasing MC (Niemz, Sonderegger, Gustafsson, et al., 2023). In Ozyhar et al. (2012), however, the Poisson's ratios of moisture-sensitive beech decrease slightly in the direction of ν_{RL}, but exhibit an increase in ν_{TL}, ν_{TR} and ν_{RT} direction. In contrast to most other mechanical wood properties, Bodnig & Jayne (1982) conclude that the Poisson ratio is not influenced by wood density or other anatomical properties and does not differ between softwoods and hardwoods. Qing & Mishnaevsky (2010), on the other hand, show that ν_{LR} increases for softwood with increasing microfibril angle (MFA) and decreases with increasing wood density. Overall, there are only a few studies on Poisson's Ratio of deciduous wood species and none on branch wood publicly available up to this day (Matz, 2017; Ozyhar et al., 2012; G. A. Zink et al., 1997).

Therefore, in this conference paper, we will discuss the first results of the investigation of the Poisson's ratio of branch wood compared to stem wood of the three common deciduous species, European beech *(Fagus sylvatica L.)*, Sessile oak *(Quercus petraea (Matt.) Liebl)* and White poplar *(Populus alba L.)*. For this purpose, the longitudinal-radial (ν_{LR}) direction is examined first. This case study aims to determine whether expanding research on this parameter is necessary for optimizing branch material use, or if existing stem wood values might already adequately serve modeling needs.

MATERIALS AND METHODS

The specimens used for the experimental characterization were manufactured from European beech *(Fagus sylvatica L.)*, Sessile oak *(Quercus petraea (Matt.) Liebl)* and White poplar *(Populus alba L.)* (Figure 1). The oak and beech were selected from mixed forests in the south and the poplar from the north of Lower Austria, Austria. Branches from the same trees were also used to produce the samples tested in the study by Nenning et al. (2024). Therefore, detailed information on location, laser scanning, harvesting, wood drying and sample preparation can be found in this study.

Deviating from the standard DIN 52188 (1979), a reduced sample cross section was chosen due to the small branch diameter. The final tensile specimens have a total length of 225mm and are tapered to a constant cross-section (4x8mm) of 55mm in length. Tensile specimens were mounted in a custom-built clamping system in a force-locking and form-fit steel configuration to prevent slipping (Figure 1). The configuration was fixed in a universal testing machine (ZwickRoellZ100, Ulm, Germany) equipped with a load cell capacity of 100kN. A preload of 25 N was applied and the crosshead speed was constant at

2 mm min−1 until failure. Before conducting the testing, the normal density of each specimen was determined (DIN 52182, 1976).

Digital Image Correlation (DIC) was used to monitor the in-plane displacement on the tensile specimen surface by tracking the deformation of a random spray-coated speckle pattern in an image. The pattern was applied using a commercially available permanent black spray acrylic paint. The images were taken using a two-camera (Basler ace acA4112-30um, Basler, Ahrensburg, Germany) setup from Dantec Dynamics (Q-400 3D, Dantec Dynamics, Skovlunde, Denmark). The Field of View (FOV) covered the whole specimen surface between the clamped area. The evaluated Region of Interest (ROI) measured 8x40mm and was within the constant cross-section of the sample. The reference image was taken after the preload was applied. During the tensile tests an image was taken every 0.5 seconds resulting in approximately 60 to 70 images per sample. The evaluation (longitudinal strain and lateral contraction) was performed using the ISTRA 4D software platform (version 4.9, Dantec Dynamics, Skovlunde, Denmark). Therefore, the recorded images were divided into facets of 15x15 pixels which overlapped by 50% resulting in approximately 8000 facets per image. The resulting data sets for each image were exported as HDF5 format and the Poisson´s ratio was calculated in an application module (Poisson_Ratio_Analysis) of the ISTRA 4D software. Therefore, five facets were grouped together to form a virtual strain gauge. Subsequently, the longitudinal strain and transversal contraction are calculated for each virtual strain gauge and the Poisson´s ratio is calculated based on formula 1, where the index i refers to the direction of lateral contraction and j to load-directional elongation.

$$\nu_{ij} = -\frac{\varepsilon_i}{\varepsilon_j} \ i,j = \ \epsilon \ R, L, T \ and \ i \ \neq j \tag{1}$$
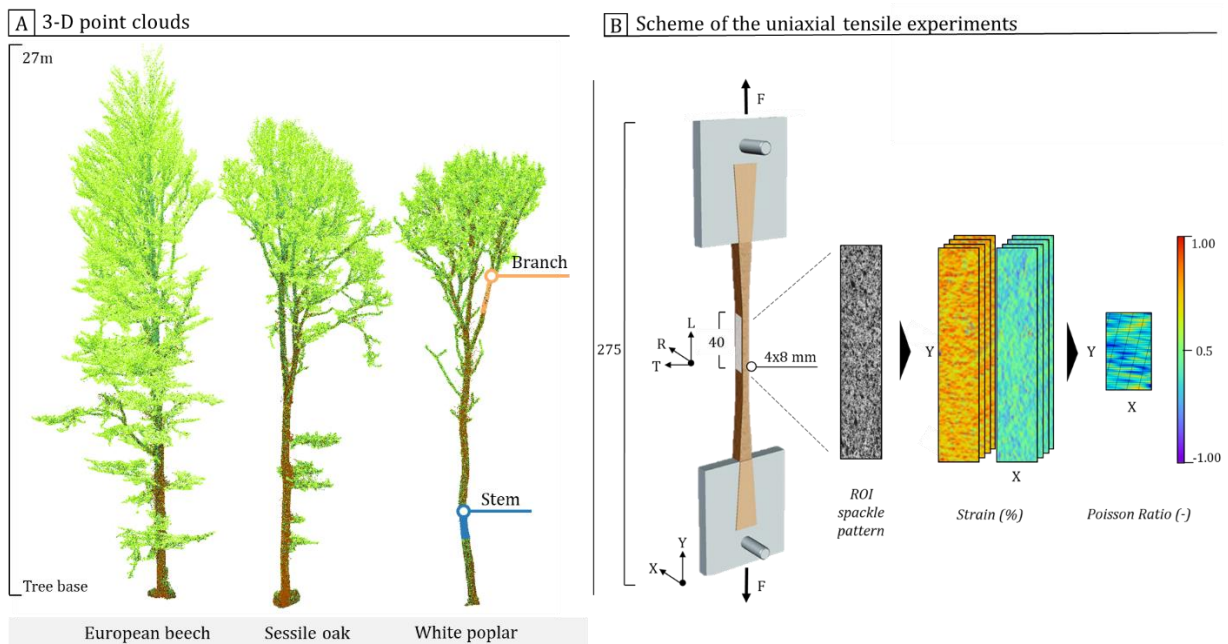
***Figure 10:** (A) depicts the full height and tree habitus of the selected trees obtained by close-range Laser Scanning. Colour differences indicate the point cloud intensity. Illustration following (Nenning et al., 2024). (B) Schematic illustration of the tensile test specimen's geometry, the digital image of a spray-coated region of interest and the spatial strain distribution in x (lateral) and y (longitudinal) coordinates for obtaining Poisson's ratio from the DIC displacement measurements*

The subsequent data analysis was conducted using RStudio software, version 2022.12.0 with R version 4.2.2. After confirming the homogeneity of variances, Welch Two Sample t-test (*p < 0.05) was performed to analyse the statistical difference between the branch and stem wood.

RESULTS AND DISCUSSION

Figure 2 displays the results for Poisson's Ratio of defect-free branch and stem wood from European beech, Sessile oak and White Poplar. A p-value of 0.018 indicates that branch and stem wood are significantly different, with the "Stem" group having a higher median value. In (B) of Figure 2, the relationship between Poisson's ratio and normal wood density is shown. Across species and wood types (stem and branch), there appears to be no trend from low-density poplar to higher-density oak and beech. This corresponds to the statement of Bodnig & Jayne (1982) that Poisson's ratio does not depend on the wood density or other anatomical properties. On the other hand, within the species, at least for beech and oak, we see an increasing Poisson ratio with increasing density. In the case of oak, there is even a strong correlation (R^2=0.8) while the relationship for poplar is only weak. Therefore, we hypothesize that anatomical traits such as annual ring width are indeed an influencing factor. The differences may be particularly marked in the case of samples prepared from oak, with its ring-porous alignments of water-conducting vessels. It is well known that the density of oak increases with wider annual rings and latewood areas, whereas samples with narrower year rings and larger earlywood areas exhibit greater porosity and lower density. In contrast, the anatomical structure of the diffuse-porous poplar and beech is much more homogeneous. From this, it can be concluded that a larger sample cross-section with a greater number of annual rings would be preferable to potentially lower variability among the results. However, larger sample cross-sections can be a challenge, especially in manufacturing defect-free samples from small-diameter branch wood. The same applies to the tree ring orientation, which should be parallel to the outer edge to be either radial or tangential, depending on the direction in focus. If, for example, specimens in the longitudinal-radial (LR) orientation contain also tangential components due to imprecise tree ring orientation, this could significantly increase the Poisson's ratio. Sample preparation is therefore a crucial step in the determination of reliable Poisson's values. In addition to the annual ring widths and orientation, radial wood rays are an anatomical peculiarity that can influence the transverse deformation of both oak and beech (Burgert, 2003). In poplar, on the other hand, which has only single-layered, narrow rays, the influence is likely to be rather small. However, it is not yet known to what extent the presence of wood rays influences the Poisson's ratio and whether they are a reason why the Poisson's ratio in the LR direction is lower than that in the LT direction for oak and beech (Matz, 2017; Ozyhar et al., 2012) and, conversely, LT is lower than LR for poplar.

At the ultrastructural level, the microfibril angle (MFA) could be an influence quantity leading to differences between branch and stem wood. Qing & Mishnaevsky (2010) have shown in their model that v_{RL} increases with increasing microfibril angle in coniferous wood. Therefore, the MFA of branch wood, influenced by tension wood areas, could also affect the Poisson's ratio, if present in a specimen. However, without an evaluation of the anatomical characteristics and the ultrastructure, this remains speculation.

These findings show that more structural parameters such as MFA, early and late wood content, wood rays etc. on the tested samples need to be recorded in future experimental tests.
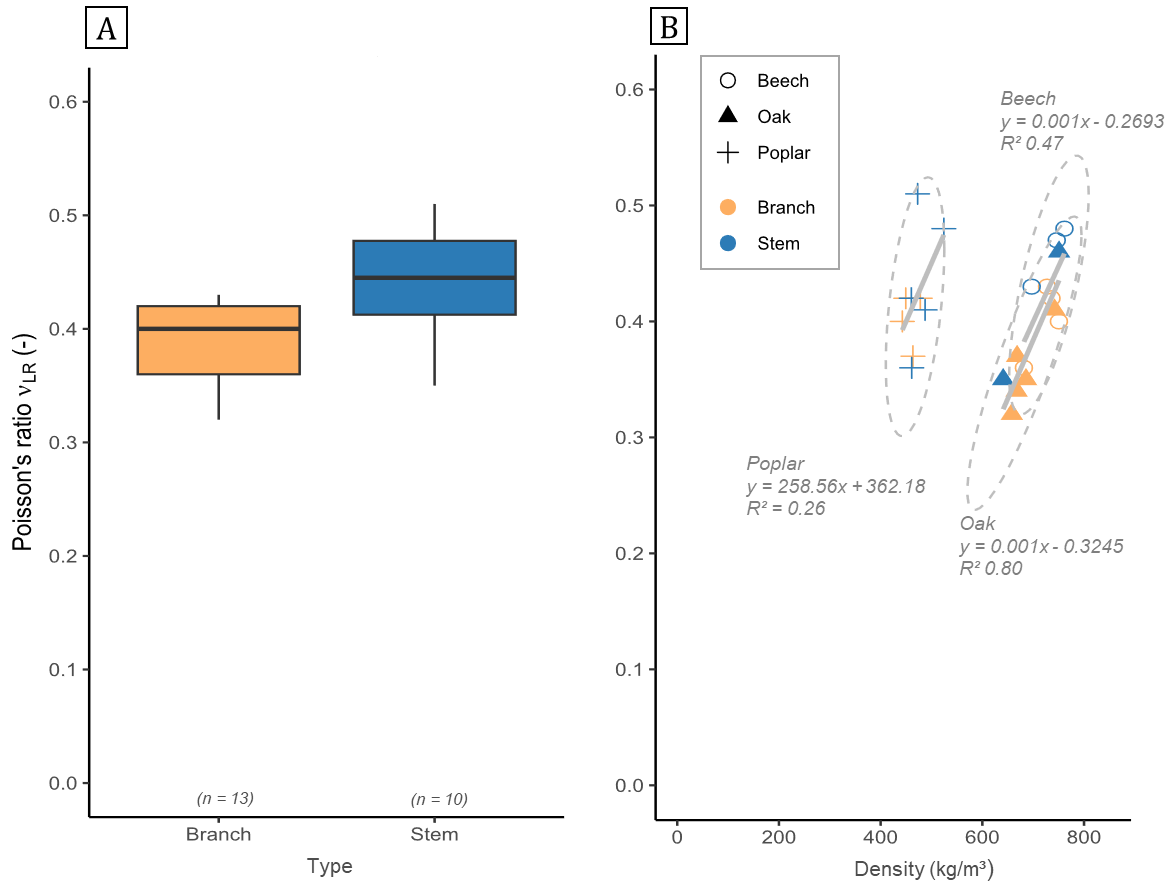
Figure 11: (A) The Poisson's Ratio test results. (A) Orange boxplots shows the results for branch wood and blue for stem wood for all species together. The number of valid samples evaluated (n) is shown in parentheses. (B) The relationship between wood density and Poisson's Ratio by wood species

Table 1 opposes Poisson's ratio and density measurements of stem and branch wood, and a comparison with the few available literature values for stem wood of beech, oak and poplar. Considering the standard deviation, our values agree well with the literature values. Even though Matz (2017) did not use DIC but ESPI and laser and video extensometers as deformation measurement methods. Further, G. A. Zink et al. (1997) did not test the Poisson values under tension but under compression. For all species, Poisson's median values range around 0.4 but tend to be lower for branch wood than for stem wood. However, given the small number of samples, one should not read too much into this difference.

Table 1: Results of Poisson's ratio determined with DIC compared with literature values

Species	Type	DIC v_{LR} [x̄ ± sd]	Density (kg/m³)	n	Literature v_{LR} [x̄]	Reference
Beech	Stem	0.46 ± 0.03	735 ± 34	3	0.43	(Ozyhar et al., 2012)
	Branch	0.40 ± 0.03	724 ± 30	4		
Oak	Stem	0.41 ± 0.08	696 ± 78	2	0.43-0.46	(Matz, 2017)
	Branch	0.36 ± 0.03	684 ± 34	5		
Poplar	Stem	0.44 ± 0.06	481 ± 27	5	0.4	(G. A. Zink et al., 1997)
	Branch	0.40 ± 0.02	458 ± 16	4		

CONCLUSIONS

- Poisson's ratios measured in this study are within the expected range of 0.4, but tend to be lower in branch wood than in stem wood.
- The newly developed experimental setup is well suited to determine the Poisson's ratios of branch wood, even though it leaves room for further development (e.g. high variability due to small sample cross-sections for ring-porous wood species).
- In terms of statistical significance, having a higher number of specimens would have been preferable. However, this was restricted in this case study due to the time-consuming preparation involved.
- The focus of our future investigations on Poisson's Ratio will be directed at the questions: Can we observe a difference between stem and branch wood in the other wood anatomical directions? What is the influence of the lower hierarchical levels (e.g. earlywood/latewood proportions, wood rays, MFA) on the Poisson's ratio?

ACKNOWLEDGEMENTS

REFERENCES

Bodnig, J., & Jayne, A. B. (1982). Mechanics of wood and wood composites. Van Nostrand Reinhold Publishing.

Burgert, I. (2003). Über die mechanische Bedeutung der Holzstrahlen. Schweizerische Zeitschrift Für Forstwesen, 153(12), 498–503.

Camia, A., Giuntoli, Jonsson, J., & Robert, R. (2021). The use of woody biomass for energy purposes in the EU. Publications Office of the European Union, Luxembourg, JRC122719. https://doi.org/10.2760/831621

Churkina, G., Organschi, A., Reyer, C. P. O., Ruff, A., Vinke, K., Liu, Z., Reck, B. K., Graedel, T. E., & Schellnhuber, H. J. (2020). Buildings as a global carbon sink. In Nature Sustainability (Vol. 3, Issue 4, pp. 269–276). Nature Research. https://doi.org/10.1038/s41893-019-0462-4

DIN 52182. (1976). Bestimmung der Rohdichte. Dtsch. Inst. für Norm.

DIN 52188. (1979). Bestimmung der Zugfestigkeit parallel zur Faser. Dtsch.Inst. für Norm.

Dyderski, M. K., Paź, S., Frelich, L. E., & Jagodziński, A. M. (2018). How much does climate change threaten European forest tree species distributions? Global Change Biology, 24(3), 1150–1163. https://doi.org/10.1111/gcb.13925

Gschwantner, T., Alberdi, I., Balázs, A., Bauwens, S., Bender, S., Borota, D., Bosela, M., Bouriaud, O., Cañellas, I., Donis, J., Har, al, Freudenschuß, A., Hervé, J.-C., Hladnik, D., Jansons, J., Kolozs, L., Korhonen, K. T., Kucera, M., Kulbokas, G., … Moore, J. (2019). Harmonisation of stem volume estimates in European National Forest Inventories. European National Forest Inventories. Annals of Forest Sci-Ence, 76(1), 24. https://doi.org/10.1007/s13595-019-0800-8ï

Keunecke, D., Hering, S., & Niemz, P. (2008). Three-dimensional elastic behaviour of common yew and Norway spruce. Wood Science and Technology, 42(8), 633–647. https://doi.org/10.1007/s00226-008-0192-7

Kumpenza, C., Matz, P., Halbauer, P., Grabner, M., Steiner, G., Feist, F., & Müller, U. (2018). Measuring Poisson's ratio: mechanical characterization of spruce wood by means of non-contact optical gauging techniques. Wood Science and Technology, 52(6), 1451–1471. https://doi.org/10.1007/s00226-018-1045-7

Mantau, U., Gschwantner, T., Paletto, A., Mayr, M. L., Blanke, C., Strukova, E., Avdagic, A., Camin, P., Thivolle-Cazat, A., Döring, P., Petrauskas, E., Englert, H., Schadauer, K., Barreiro, S., Lanz, A., & Vidal, C. (2016). From inventory to consumer biomass availability—the ITOC model. Annals of Forest Science, 73(4), 885–894. https://doi.org/10.1007/s13595-016-0582-1

Matz, P. (2017). Die Bestimmung der Poissonzahlen und anderer elastischer Konstanten von Holz und Holzwerkstoffen für die Erstellung eines FE-Modells für Massivholzprodukte [Masterthesis]. Intitut für Holztechnolgie und nachwachsende Rohstofffe.

Nenning, T., Tockner, A., Konnerth, J., Gindl-Altmutter, W., Grabner, M., Hansmann, C., Lux, S., & Pramreiter, M. (2024). Variability of mechanical properties of hardwood branches according to their position and inclination in the tree. Preprint. Construction and Building Materials. https://doi.org/10.2139/ssrn.4610716

Niemz, P., Sonderegger, W., Gustafsson, P. J., Kasal, B., & Polocoşer, T. (2023). Strength Properties of Wood and Wood-Based Materials. In Handbook of Wood Science and Technology. Springer Nature Switzerland AG 2023. https://doi.org/doi.org/10.1007/978-3-030-81315-4

Niemz, P., Sonderegger, W., Keplinger, T., Jiang, J., & Lu, J. (2023). Physical Properties of Wood and Wood-Based Materials. In Handbook of Wood Science and Technology. Springer Nature Switzerland AG 2023. https://doi.org/doi.org/10.1007/978-3-030-81315-4

Ozyhar, T. ;, Hering, S. ;, & Niemz, P. (2012). Moisture-dependent elastic and strength anisotropy of European beech wood in tension. Journal of Materials Science, 47(16), 6141–6150. https://doi.org/10.3929/ethz-b-000048871

Pardos, M., Del Río, M., Pretzsch, H., Jactel, H., Bielak, K., Bravo, F., Brazaitis, G., Defossez, E., Engel, M., Godvod, K., Jacobs, K., Jansone, L., Jansons, A., Morin, X., Nothdurft, A., Oreti, L., Ponette, Q., Pach, M., Riofrío, J., … Calama, R. (2021). The greater resilience of mixed forests to drought mainly depends on their composition: Analysis along a climate gradient across Europe To cite this version: The greater resilience of mixed forests to drought mainly depends on their composition: Analysis along a climate gradient across Europe. 481, 378–1127. https://doi.org/10.1016/j.foreco.2020.118687ï

Pramreiter, M., Nenning, T., Huber, C., Müller, U., Kromoser, B., Mayencourt, P., & Konnerth, J. (2023). A review of the resource efficiency and mechanical performance of commercial wood-based building materials. Sustainable Materials and Technologies, e00728. https://doi.org/10.1016/j.susmat.2023.e00728

Pramreiter, M., Nenning, T., Malzl, L., & Konnerth, J. (2023). A plea for the efficient use of wood in construction. Nature Reviews Materials. https://doi.org/10.1038/s41578-023-00534-4

Qing, H., & Mishnaevsky, L. (2010). 3D multiscale micromechanical model of wood: From annual rings to microfibrils. International Journal of Solids and Structures, 47(9), 1253–1267. https://doi.org/10.1016/j.ijsolstr.2010.01.014

Ramage, M. H., Burridge, H., Busse-Wicher, M., Fereday, G., Reynolds, T., Shah, D. U., Wu, G., Yu, L., Fleming, P., Densley-Tingley, D., Allwood, J., Dupree, P., Linden, P. F., & Scherman, O. (2017). The wood from the trees: The use of timber in construction. Renewable and Sustainable Energy Reviews, 68, 333–359. https://doi.org/10.1016/j.rser.2016.09.107

Schier, F., Morland, C., Janzen, N., & Weimar, H. (2018). Impacts of changing coniferous and non-coniferous wood supply on forest product markets: a German scenario case study. European Journal of Forest Research, 137(3), 279–300. https://doi.org/10.1007/s10342-018-1111-6

Shmulsky and Jones. (2019). Juvenile Wood, Reaction Wood, and Wood of Branches. Forest Products and Wood Science: An Introduction, 7, 107–133.

Shmulsky, R., & Jones, P. D. (2011). Forest Products and Wood Science: An Introduction (6th ed., Vol. 6). Wiley-Blackwell.

Valla, A., Konnerth, J., Keunecke, D., Niemz, P., Müller, U., & Gindl, W. (2011). Comparison of two optical methods for contactless, full field and highly sensitive in-plane deformation measurements using the example of plywood. Wood Science and Technology, 45(4), 755–765. https://doi.org/10.1007/s00226-010-0394-7

Zink, A. G., Davidson, R. W., & Hanna, R. B. (1995). Strain measurement in wood using a digital image correlation technique. Wood and Fiber Science, 27(4), 346–359.

Zink, G. A., Hanna, B. R., Stelmokas, & W. John. (1997). Measurement of Poisson's ratios for yellow-poplar. Forest Product Journal, 47(3), 78–80.

Low-value wood from non-native tree species as a potential source of bioactive extractives for bio-based preservation

Viljem Vek [1*], Ida Poljanšek [1], Urša Osolnik [1], Angela Balzano [1], Miha Humar [1], Primož Oven [1]

[1] University of Ljubljana, Biotechnical Faculty, Department of Wood Science and Technology, Jamnikarjeva ulica 101, 1000 Ljubljana

E-mail: viljem.vek@bf.uni-lj.si; ida.poljansek@bf.uni-lj.si; ursa.osolnik@bf.uni-lj.si; angela.balzano@bf.uni-lj.si; miha.humar@bf.uni-lj.si; primoz.oven@bf.uni-lj.si

Keywords: Black locust, heartwood, low-value biomass, extraction, polyphenols, antifungal properties, natural antioxidants

ABSTRACT
Low-value and underutilized wood species have great potential for use as a natural raw material for various bioproducts. In this context, the heartwood of black locust was analyzed in the present study as a potential feedstock for the extraction of natural bioactive compounds. With the extraction of flavonoids and the use of these polyphenols to increase the resistance of non-durable wood to wood-destroying fungi, an innovative use of black locust wood (*Robinia pseudoacacia*) is therefore presented. The preservative formulations tested in this study were prepared with the hydrophilic extractives as biocidal ingredients. These are flavonoids/robinetins, which were extracted from the heartwood of black locust using acetone. The extracts obtained were first analyzed gravimetrically, spectrophotometrically and chromatographically for their chemical composition. For the antifungal test, both hydrophilic extracts and purified robinetins were prepared. The extracts were examined colorimetrically for their antioxidant properties using the DPPH assay. The resistance of wood impregnated with black locust extractives was measured using a modified protocol according to EN 113. Wood from less durable coniferous and deciduous tree species was impregnated using aqueous solutions of the hydrophilic extracts in a vacuum pressure chamber. After impregnation, the retention of the extracts in the wood matrix was investigated gravimetrically and microscopically (CLSM and SEM). The antifungal properties of the wood extractives of black locust were determined by in vitro measurements of the inhibition of fungal growth and by measuring the resistance of the impregnated wood to fungal decay. The results of the fungal tests clearly show that the hydrophilic extractives from the low-value wood of black locust inhibit the fungal decay of the wood. It has been demonstrated that black locust extracts can be described as natural antioxidants and radical scavengers. Heartwood extractives from low-value black locust trees have potential and could be used as natural antioxidants in bio-based products. Further research is needed to confirm this.

INTRODUCTION
The side streams of the wood processing industry have great untapped potential and play an important role as independent value chains in the concept of the circular economy (Verkasalo et al. 2019). In addition to industrial residues, low-value and underutilized wood species also have great potential for use as a natural raw material for various bioproducts (Oleson and Schwartz 2016; Osolnik et al. 2024). This includes wood from non-native and invasive species that do not play an important role in existing hardwood processing chains. Black locust (Robinia pseudoacacia), also known as false acacia or simply robinia, is known as one such tree species that grows on the largest areas (2.44 million ha) in Europe (Brus et al. 2019). Black locust is considered an inferior wood species and its wood does not play a major role in the wood processing industry, but its heartwood is characterized by high natural durability (Reinprecht et al. 2010; Vítková et al. 2017). Due to its high decay resistance and good weathering behavior, black locust wood has been used for various outdoor applications. The high natural durability of black locust heartwood is scientifically explained by the presence of bioactive phenolic extractives (Rademacher 2016; Smith et al. 1989). The flavanonol dihydrorobinetin (DHR) and the flavonol robinetin (Rob) are most commonly cited as such (Bostyn et al. 2018; Magel et al. 1994). Robinetins from the heartwood of black locust (HW) have already been shown to be natural polyphenols with

antifungal, antimicrobial and antifungal properties (Hosseinihashemi et al. 2016; Sablik et al. 2016; Vek et al. 2020a). In view of the unfavorable biometric properties of the black locust trunk, the extremely low proportion of sapwood (stem cross-section, only op to 6-7 growth rings), the heartwood of the black locust represents a biorefinery raw material with high potential. Due to their bioactive properties, black locust extractives have great potential as a substitute for synthetic biocides in wood preservatives. The wood preservatives more or less commonly used to date are composed of biocidal substances, e.g. copper/chrome/boron solutions, dicloran, creosote, etc. These biocides of synthetic origin can be very dangerous for the environment and human health (Singh and Singh 2012). The question arises as to whether the extractives of black locust wood are suitable as biocidal active ingredients in green wood preservatives due to their antioxidant and antifungal properties.

The aim of the preliminary study was (a) to test various tissues of low-value black locust stems as potential raw material for the extraction of bioactive phytochemicals and to substantiate this with detailed chemical investigations, and (b) to test the black locust extracts obtained for their antifungal and antioxidant properties.

MATERIALS AND METHODS
Material
Several black locust trees that had fallen in the urban forest of Panovec near Nova Gorica in Slovenia (56046.8" N 1340005.1" E) were examined. One of the fallen black locust trees had an injured stem and was used to sample wound-associated wood tissue, which was analysed for the effects of injury on the variability of extractives content. The sampled black locust trees were on average 49 to 70 years old, 21 to 24 m tall and had a diameter of 22 to 28 cm at 1.3 m height. Several 15 cm thick stem discs were sawn out of the sampled trees. From these, blocks of bark (B), intact sapwood (SW) and heartwood (HW), wound wood (WW), reaction zone (RZ), decayed wood (DW) and knotwood (KW) as well were produced according to a comprehensive scheme. The black locust samples were then ground using a Retsch SM 2000 cutting mill with a 1 mm bottom sieve. Prior to extraction, the samples were freeze-dried at 0.040 mbar and -82°C for 24 h.

Extraction
The black locust samples were extracted using the conventional method in a Soxhlet apparatus (Vek et al. 2019). Samples of B, SW, HW, WW, RZ, DW and KW were extracted and analyzed for the content of extractives. The extractives were obtained from the samples using 90% acetone (aq, v/v), whereby the ratio of sample to solvent (w/v) was set to 1:100. Thus, 2.5 g of a freeze-dried sample was extracted with 250 ml of 90% acetone (*aq*) at 110°C for 6 h. After chemical analysis, all acetone extracts of black locust HW were combined and the mass aliquots were mixed. In this way, a homogenized hydrophilic extract of black locust heartwood (HWE) was prepared. If necessary, randomly selected HW samples were additionally selected and extracted with acetone in an accelerated solvent extractor (Thermo Dionex ASE 350) at 103.4 bar and 100°C in a 100-mL extraction cell STT (Vek et al. 2021). The HWE was freeze-dried in a lyophylizator as described above and stored in the dark until the start of the antifungal and antioxidant assays.

Chemical analysis of extractives from wood and bark of black locust
The extracts obtained were analysed for total extractives content (TEC), total phenolic content (TPC) and the content of dihydrorobinetin (DHR) and robinetin (Rob) (Vek et al. 2019). The TEC in the black locust samples was measured gravimetrically, i.e. 10 ml acetone extracts were oven-dried to constant weight. The results of the gravimetric analysis are expressed in mg TEC per gram of dried sample (mg/g, dw). The TPC in black locust wood and bark samples was measured colorimetrically using the Folin-Ciocalteu method (Singleton and Rossi 1965). An aqueous solution of the Folin-Ciocalteu phenol reagent and an aqueous solution of sodium carbonate were added to the black locust extracts and the gallic acid solutions. The semi-quantitative analysis of TPC in the samples was performed using a calibration curve prepared from differently concentrated solutions of gallic acid. The spectrophotometric method was linear in the selected mass concentration range ($R2> 0.99$). After incubation in the dark for 2 hours, the absorbances were measured at 765 nm using a Perkin-Elmer Lambda UV-Vis spectrophotometer. The TPCs are expressed as mass equivalents of gallic acid per gram of dried sample (mg GAE/g dw). The detailed analysis of dihydrorobinetin (DHR) and robinetin (Rob) and their amounts

in the black locust samples was performed using a Thermo Scientific Accela liquid chromatograph with photodiode array detector (HPLC-PDA). The separation of extractives was performed on a Thermo Accucore C18 column (4.6 ID × 150 mm, 2.6 μm) with water (A) and methanol (B) as mobile phase with 0.1% formic acid and a flow rate of 1 ml/min. The gradient used was 5–95% of solvent B. Absorbance was measured at 280 nm and UV spectra were recorded from 200 nm to 400 nm. The characteristic peaks of the HPLC traces were qualitatively evaluated by comparing the retention times and UV spectra of the compounds with those of the analytical standards. The HPLC method was linear in the selected concentration range ($R2 \geq 0.99$). The results were expressed in mg DHR and Rob per gram of dried black locust sample (mg/g dw).

Antifungal assay

The inhibition of fungal growth was measured using a modified agar well diffusion method (Vek et al. 2020b). Exactly 1 mg of dihydrorobinetin (DHR), robinetin (Rob) and hydrophilic heartwood extract (HWE) of black locust, all in 1% and 5% DMSO (dimethyl sulfoxide) solution, were added to an 8 mm diameter well in the growth medium (potato dextrose agar, PDA). The prepared Petri dishes were then inoculated with two white rot fungi (*Trametes versicolor* and *Schizophyllum commune*) and two brown rot fungi (*Gloeophyllum trabeum* and *Fibroporia vaillantii*) and incubated in a growth chamber at 25°C and 75% relative humidity. The radial growth of the fungal mycelium towards the wells containing the black locust extractives was measured in the centrifugal direction and observed every 2-3 days. The experiment was terminated when the mycelium had grown to the edge of the Petri dish in at least one direction. The final results were calculated as the percentage inhibition of fungal growth in the centrifugal direction (IN).

Antioxidant assay

The antioxidant properties of the HWE samples were measured using the radical scavenging activity of the 2,2-diphenyl-1-picrylhydrazyl (DPPH) method (Hofmann et al. 2015; Vek et al. 2021). Gallic acid (GA), ascorbic acid (AA) and butylhydroxyanisole (BHA) were used as reference. The solutions of HWE and the reference antioxidants were tested in five test concentrations. 2.25 ml of DPPH-methanol solution was mixed with 0.090 ml of the sample or reference antioxidant. The reaction mixtures were then incubated for 30 minutes in the dark at room temperature. After incubation, the reduction of the DPPH radical was monitored by measuring the absorbance at 517 nm using a Perkin Elmer Lambda UV-Vis spectrophotometer. The activity of the DPPH radical scavenger (RSA) was measured by the colour change of the DPPH solution.

Impregnation of wood blocks with black locust extractives and decay test

A decay test was carried out on sapwood samples of selected less durable coniferous and deciduous tree species, i.e. European beech (*Fagus sylvatica*) and Scots pine (*Pinus sylvestris*). The impregnation of the wood blocks with the black locust HWE was carried out in a vacuum pressure chamber as described by Vek et al. (2020a). The impregnated wood blocks were then dried in an oven at 105°C until they reached a constant weight. Distilled water was used to impregnate the wood blocks and served as a control. The decay test was performed according to the mini-block test, which is a modified protocol of the EN 113 standard (CEN, 2006). The decay test was performed to evaluate the decay inhibitory properties of black locust HWE on a wooden substrate. A petri dish with growth medium from PDA was first inoculated with wood decay fungi. All impregnated wood blocks were autoclaved before being exposed to the selected wood decay fungi. The impregnated wood samples were then carefully placed in a Petri dish containing the PDA growth medium with a thin film of fungal mycelium. The assembled Petri dishes were then incubated at 25°C and 80% relative humidity for 12 weeks. The results were expressed as mass loss of the control and impregnated wood blocks (ML) after fungal exposure.

Analysis of the efficiency of impregnation

The efficiency of the impregnation of the wood and the retention of black locust HWE in the wood matrix was analysed microscopically using a confocal laser scanning microscope (CLSM) and a scanning electron microscope (SEM). The CLSM images, obtained using the autofluorescence of the wood and with polarized light using different objectives (MPLFLN5xLEXT, MPLFLN10xLEXT, MPLAPON20xLEXT and MPLAPON50xLEXT), made it possible to observe the different appearance

of wood with and without extracts. For SEM analysis, the dried samples were mounted on stubs with conductive carbon and coated with an Au/Pd sputter coater. SEM micrographs were then taken under high and low vacuum using an FEI Quanta 250 SEM microscope at a working distance of 9 mm to 11 mm. The retention of black locust HWE in the wood blocks was also quantitatively evaluated by gravimetric analysis. The wood blocks were oven-dried to a constant weight before and after impregnation, and the amount of HWE retained in the wood was expressed by the percentage of gained weight (%) (Humar and Thaler, 2017).

RESULTS AND DISCUSSION
Extractives in black locust biomass

The detailed chemical analyses of the extractives showed that the highest amounts of extractives and phenolic compounds are characteristic for heartwood (HW) and knotwood (KW) (Figure 12). Our studies on black locust wood also showed a clear radial variability of extractives content, with the highest amounts of phenolic compounds being found in the outermost (mature) heartwood and then decreasing towards the pith (Vek et al. 2020c). High levels of extractives were also measured in the woody tissues that form as a response of the tree to mechanical wounding, i.e. wound wood (WW) and reaction zone (RZ) (Figure 12). These "traumatic" tissues protect the healthy and functional wood in an injured tree stem from the external conditions (Oven et al. 1999; Vek et al. 2014). On the other hand, bark (B), sapwood (SW) and decayed wood (DW) proved to be the poorest source of acetone-soluble extractives (Figure 12). As shown in Figure 13, dihydrorobinetin (DHR) and robinetin (Rob) are clearly the most abundant flavonoids in black locust extracts. Since black locust consists mainly of heartwood and the sapwood has only a few annual rings, it is obvious that the woody biomass of this underutilised tree species is a potential source of valuable phenolic compounds. Branchwood and wood from mechanically damaged trees can also be used as potential source material for valuable phytochemicals.

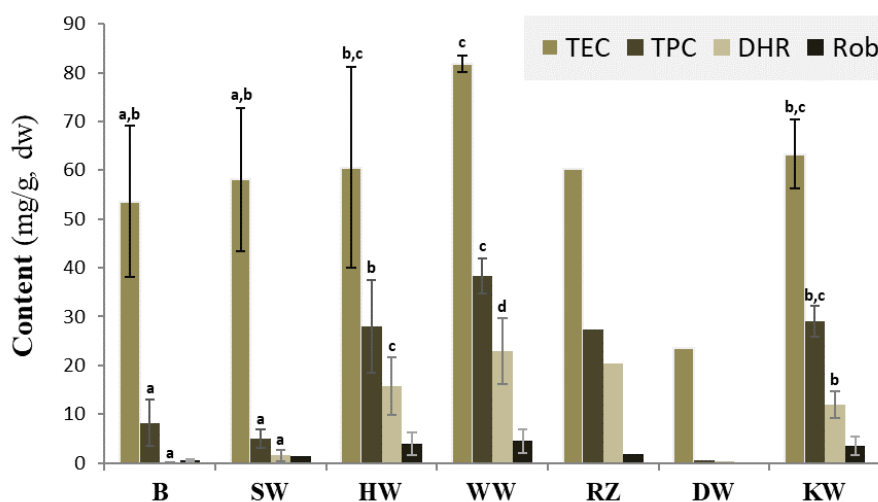*Figure 12: Content of total extractives (TEC), total phenolics (TPC), dihydrorobinetin (DHR) and robinetin (Rob) in bark and wood samples of black locust (Robinia pseudoacacia L.). B bark, SW sapwood, HW heartwood, WW wound-wood, RZ reaction zone, DW decay-wood, KW knotwood. Statistically significant differences with a confidence level of 95% were analysed using ANOVA and LSD test (Vek et al. 2020c)*
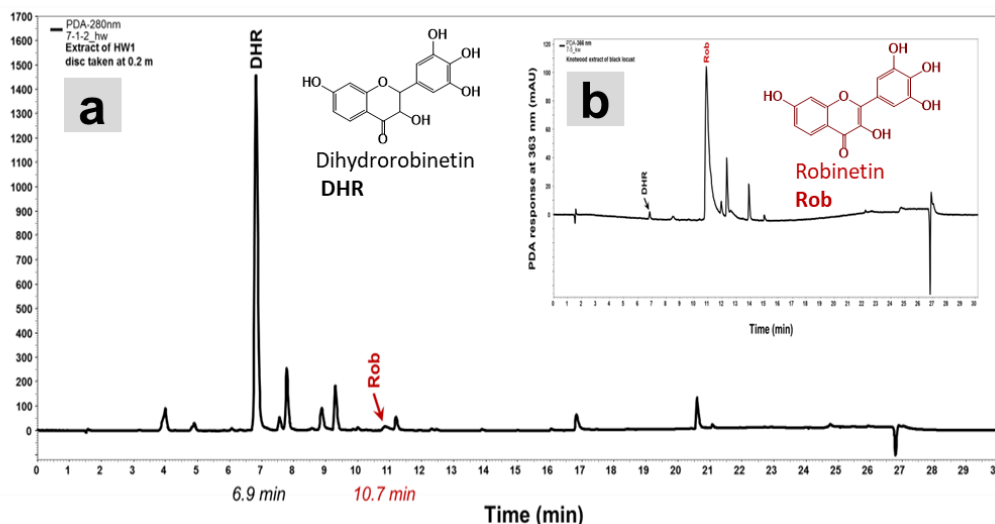
Figure 13: HPLC-PDA chromatograms of (a) heartwood and (b) knotwood extract of black locust (Robinia pseudoacacia L.). The detector response was monitored at 280 nm (a) and 366 nm (b). DHR, Dihydrorobinetin; Rob, Robinetin (Vek et al. 2020c)

Antioxidant properties of black locust extractives

The colorimetric method for measuring the radical scavenging activity of DPPH (RSA, %) showed that black locust HWE is a good radical scavenger even at lower concentrations compared to the reference antioxidants (gallic acid, ascorbic acid, BHA) (Figure 14). In all fungal and antioxidant assays of this study, the properties of black locust HWE were compared with those of the pinosylvin-rich extract of Scots pine knotwood (KWE). It has been reported that the extractives from Scots pine knotwood are bioactive compounds (Holmbom 2011; Pietarinen et al. 2006). However, the black locust HWE extract proved to be a better free radical scavenger than the KWE (Figure 14). In addition, the HWE extractives at 100 mg/l and 50 mg/l have a better RSA value then butylated hydroxyanisole (BHA) and ascorbic acid (Figure 14).
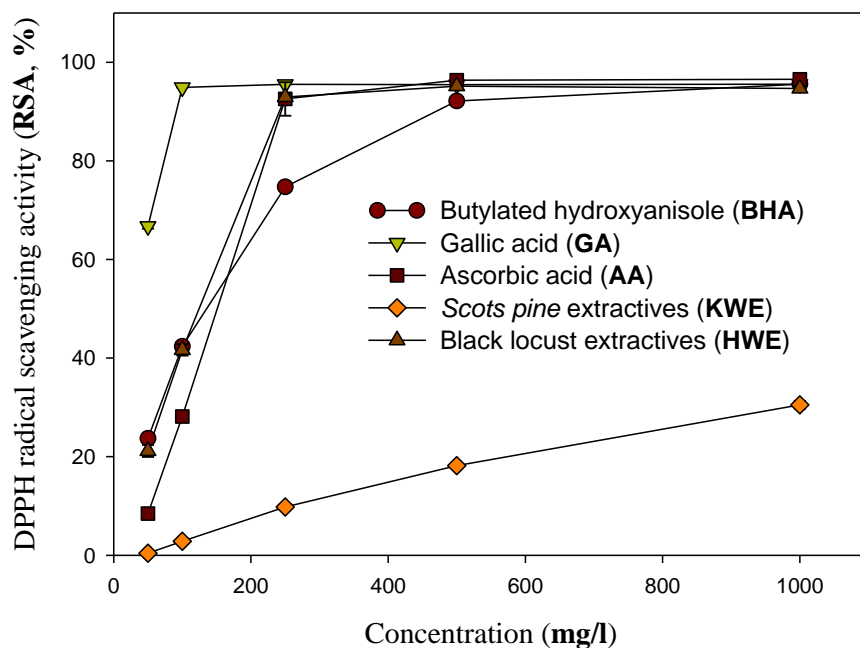
Figure 14: Radical scavenging activity DPPH (RSA, %) for black locust heartwood extract (HWE), reference antioxidants (BHA, butylated hydroxyanisole; GA, gallic acid; AA, ascorbic acid) and Scots pine knotwood extract (KWE) (Vek et al. 2020a)

Antifungal properties of black locust extractives

As already mentioned, the main objective of the study was to improve the resistance of less-durable wood species by impregnating the wood with black locust heartwood extract (HWE). The impregnation process described above was found to be efficient. The HWE was successfully introduced into the sapwood of beech and pine, as the weight gain (GW) (%, w/w) after impregnation of the wood with the HWE was significantly higher than in the control sample impregnated with water only ($p < 0.01$, LSD test). The GW is explained as a weight representing the amount of retained HWE. The CLSM and SEM results also show that we were successful in incorporating the HWE into the sapwood matrix of Scots pine and beech (Figure 15). The HWE of black locust was clearly observed as deposited material in the lumina of beech vessels, in Scots pine sapwood HWE occurred mainly in the lumina of earlywood tracheids and in the lumina of the ray parenchyma (Figure 15). The results of microscopy and gravimetry confirm to a certain extent the fact that we managed to keep HWE in the sapwood blocks before they were exposed to the tested wood fungi (Figure 15) (Vek et al. 2020a).
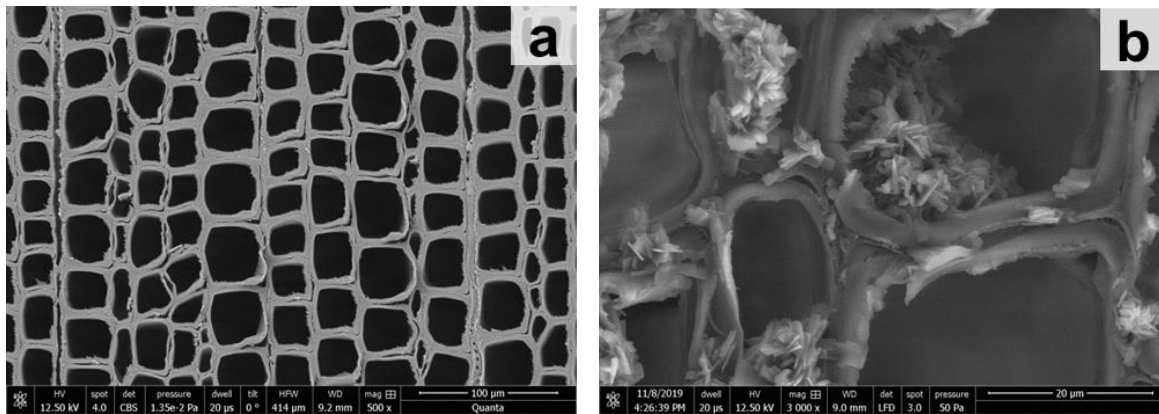
Figure 15: SEM micrographs of Scots pine sapwood (Pinus sylvestris) treated with the heartwood extract of black locust (HWE). Transverse sections: (a) Untreated Scots pine sapwood, (b) Scots pine sapwood block treated with the heartwood extract of HWE. The images were obtained at magnifications of 500× and 3000× (Vek et al. 2020a)

The *in vitro* well diffusion method on agar showed that the concentration of the extract solution has an important influence on the inhibition of fungal growth. In comparison to the extracts of Scots pine knotwood and the pinosylvins, we could not detect a significant inhibitory effect with either the purified compounds of DHR and Rob or the HWE of black locust. The black locust extractives inhibited the growth of *Fibroporia vaillantii* to some extent, but their IN was irrelevant compared to the KWE with pinosylvins.

In contrast, the decay assay with the mini block test showed a significant influence of HWE on the mass loss (ML) of beech and pine sapwood exposed to wood-decaying fungi (Table 3). The ML of HWE-impregnated wood exposed to *Trametes versicolor* was not significantly different from that of the control samples. Apart from being a good wood decomposer and a non-selective fungal species, *Trametes versicolor* is also known to decompose hardwood better and has only a limited effect on softwood (Lekounougou et al. 2008). The latter was also confirmed by the results of the decay test (Table 3).

The exact opposite was found for the impregnated wood exposed to *Gloeophyllum trabeum*. Here, a significantly smaller ML was found for HWE-impregnated beech and Scots pine wood than for the corresponding control samples (Table 3). The decay test showed a small ML, especially for Scots pine sapwood impregnated with HWE. This study clearly showed that the impregnation of less durable wood with hydrophilic extracts of pine knotwood and black locust heartwood significantly reduced the ML after exposure to *Gloeophyllum trabeum*.

Table 3: Mass loss (ML, %) of sapwood impregnated with extractives exposed to wood decaying fungi for 12 weeks (Vek et al. 2020a)

Sapwood blocks $1 \times 1.5 \times 4$ cm^3	Fungal culture	Mass loss [%, w/w] non-impregnated	Mass loss [%, w/w] KWE	Mass loss [%, w/w] HWE
Fagus sylvatica				
	Trametes versicolor	9.17 ± 1.72 [c,d]	7.75 ± 1.48 [b,c,d]	7.04 ± 1.04 [b,c]
	Gloeophyllum trabeum	10.18 ± 2.23 [d]	3.09 ± 1.61 [a]	5.23 ± 2.03 [a,b]
Pinus sylvestris				
	Trametes versicolor	7.30 ± 0.84 [b]	5.42 ± 0.87 [a,b]	4.89 ± 1.16 [a,b]
	Gloeophyllum trabeum	22.46 ± 3.87 [c]	3.36 ± 3.84 [a]	2.17 ± 2.58 [a]

[a-d] *Different letters indicate statistically significant differences at a confidence level of 95.0% (LSD). ML (%, w/w), mass loss of wood samples after exposure to the wood-decaying fungi.*

CONCLUSIONS

The results of this preliminary study confirm that the low-value biomass of black locust is a potential raw material for bioactive compounds. It was found that knotwood and heartwood of a black locust stem contains the highest amounts of polyphenols and flavonoids. In addition, the wood of mechanically damaged trees could be used not only e.g. as an energy source but also as a feedstock for biorefineries. The black locust wood extracts proved to be good free radical scavengers, while the results of the in vitro tests do not describe the black locust extractives as potential fungal inhibitors. However, the heartwood extracts reduce the fungal decay of the impregnated wood, so these compounds could be considered as natural antioxidants and free radical scavengers in the formulations rather than fungicidal compounds. Wood extracts with polyphenols have great application potential, not only as antifungal and antioxidant agents in various bio-based preservatives and bioproducts, but also as functional agents in dietary supplements.

REFERENCES

Hofmann T, Nebehaj E, Stefanovits-Bányai É, Albert L (2015) Antioxidant capacity and total phenol content of beech (Fagus sylvatica L.) bark extracts Industrial Crops and Products 77:375-381 http://dx.doi.org/10.1016/j.indcrop.2015.09.008

Holmbom B (2011) Extraction and utilisation of non-structural wood and bark components. In: Alén R (ed) Biorefining of forest resources. vol book 20. Paper Engineers' Association/Paperi ja Puu Oy, Helsinki, pp 178-224

Hosseinihashemi SK, HosseinAshrafi SK, Goldeh AJ, Salem MZM (2016) Antifungal and antioxidant activities of heartwood, bark, and leaf extracts of Robinia pseudoacacia BioResources 11:1634-1646

Lekounougou S et al. (2008) Initial stages of Fagus sylvatica wood colonization by the white-rot basidiomycete Trametes versicolor: Enzymatic characterization Int Biodeterior Biodegradation / International Biodeterioration & Biodegradation 61:287-293 http://dx.doi.org/10.1016/j.ibiod.2007.06.013

Oleson KR, Schwartz DT (2016) Extractives in Douglas-fir forestry residue and considerations for biofuel production Phytochemistry Reviews 15:985-1008 http://dx.doi.org/10.1007/s11101-015-9444-y

Osolnik U, Vek V, Korošec RC, Oven P, Poljanšek I (2024) Integration of wood-based components – Cellulose nanofibrils and tannic acid - into a poly(vinyl alcohol) matrix to improve functional properties International Journal of Biological Macromolecules 256:128495 https://doi.org/10.1016/j.ijbiomac.2023.128495

Oven P, Torelli N, Shortle WC, Zupancic M (1999) The formation of a ligno-suberised layer and necrophylactic periderm in beech bark (Fagus sylvatica L.) Flora 194:137-144

Pietarinen S, Willför S, Ahotupa M, Hemming J, Holmbom B (2006) Knotwood and bark extracts: strong antioxidants from waste materials Journal of Wood Science / J Wood Sci 52:436-444 http://dx.doi.org/10.1007/s10086-005-0780-1

Sablik P, Giagli K, Paril P, Baar J, Rademacher P (2016) Impact of extractive chemical compounds from durable wood species on fungal decay after impregnation of nondurable wood species Eur J Wood Wood Prod 74:231-236 http://dx.doi.org/10.1007/s00107-015-0984-z

Singh T, Singh AP (2012) A review on natural products as wood protectant Wood science and technology 46:851-870

Singleton VL, Rossi JA, Jr. (1965) Colorimetry of total phenolics with phosphomolybdic-phosphotungstic acid reagents American Journal of Enology and Viticulture 16:144-158

Vek V, Balzano A, Poljansek I, Humar M, Oven P (2020a) Improving Fungal Decay Resistance of Less Durable Sapwood by Impregnation with Scots Pine Knotwood and Black Locust Heartwood Hydrophilic Extractives with Antifungal or Antioxidant Properties Forests 11:23 http://dx.doi.org/10.3390/f11091024

Vek V, Keržič E, Poljanšek I, Eklund P, Humar M, Oven P (2021) Wood Extractives of Silver Fir and Their Antioxidant and Antifungal Properties Molecules 26:6412 http://dx.doi.org/10.3390/molecules26216412

Vek V, Oven P, Ters T, Poljansek I, Hinterstoisser B (2014) Extractives of mechanically wounded wood and knots in beech Holzforschung 68:529-539 http://dx.doi.org/10.1515/hf-2013-0003

Vek V, Poljansek I, Humar M, Willfor S, Oven P (2020b) In vitro inhibition of extractives from knotwood of Scots pine (Pinus sylvestris) and black pine (Pinus nigra) on growth of Schizophyllum commune, Trametes versicolor, Gloeophyllum trabeum and Fibroporia vaillantii Wood Science and Technology 54:1645-1662 http://dx.doi.org/10.1007/s00226-020-01229-7

Vek V, Poljanšek I, Oven P (2019) Efficiency of three conventional methods for extraction of dihydrorobinetin and robinetin from wood of black locust Eur J Wood Wood Prod 77:891-901 http://dx.doi.org/10.1007/s00107-019-01430-x

Vek V, Poljanšek I, Oven P (2020c) Variability in content of hydrophilic extractives and individual phenolic compounds in black locust stem Eur J Wood Wood Prod 78:501–511 http://dx.doi.org/10.1007/s00107-020-01523-y

Verkasalo E, Leppälä J, Muhonen T, Korpinen R, Möttönen V, Kurppa S (2019) Novel industrial ecosystems and value chains to utilize side-streams of wood products industries – Finnish approach Pro Ligno Journal 15:157-165 http://www.proligno.ro/ro/articles/2019/4/VERKASALO.pdf

Hardwood Processing - do we apply appropriate technologies?

Alfred Teischinger[1]

[1] BOKU University Vienna, Institute for Wood Technology and Renewable Resources
A-3430 Tulln/D, Konrad-Lorenz-Strasse 24.

E-mail: alfred.teischinger@boku.ac.at

Keywords: Hardwood processing, hardwood technology, timber production sites, change in wood industry, timber assortments, yield in volume, process efficiency

ABSTRACT

In Europe, softwood processing is predominant, but there are many regions with a destinct hardwood resource. Analysing harvest statistics, one can observe a great difference in the share of the various assortments such as saw logs, pulpwood and energy wood. Hardwoods show a much higher share of energy wood than softwoods. This rises the question about the appropriate assortment allocation to the different wood process chains and technologies applied. By the example of glued wood products and chemical processing, two destinct process chains and technologies are introduced and discussed concerning their strengths and weaknesses. Yield in volume is an important indicator in order to evaluate the resource efficiency of a technology applied. It is shown, that a typical softwood technology cannot transferred to hardwood processing without proper adaption. New and cost-efficient technologies may also contribute to resolve the trade-off about energy use and material use of wood.

INTRODUCTION

In a very holistic approach, the term technology can be described as the application of practical and scientific knowledge for solving practical problems in order to provide targeted benefits. It comprises the collection of techniques, skills, methods, and processes a society applies for providing the various goods and services needed in their civilization. Teischinger (2023) specifies technology with respect to the utilization of wood as a primary resource and the transformation of the raw material wood into the whole spectrum of wood products.

The selection of a technology for a specific task in a company may be a challenge, as any change in a production system has an impact on production costs and profits, the material resp. product performance, the product design and quality etc., and employees must be trained in the application of a new technology. The selection of an innovative and new technology may even be more challenging and can be seen as a multiple criteria decision-making challenge by considering all criteria mentioned above. Many tools, guidelines and checklists for selecting a technology are provided in the the management literature and the every-day management training services, just to give a few examples (DigitalForward 2024, Nissen et al. 2018).

Due to the main groups of wood resources, hardwoods (a general term for angiospermae) and softwoods (as a general term for gymnospermae) wood is split into hardwood processing and softwood processing. In some cases, the two groups can be mixed or combined within one or more process steps (e.g. in the particle board industry), but in general the processes are outlined as a hardwood process or softwood process. Due to the specific machines and mill equipment sawmills operate either as a softwood mill or as a hardwood mill. Pulp mills may process selectively softwood for producing a specific long-fibre pulp or a short fibre pulp from hardwoods. In most cases machines and processes are designed specifically for one or the other process and do not allow, for technical and/or economical reasons, to switch from hardwood to softwood processing or vice versa.

SOFTWOOD AND HARDWOOD PROCESSING IN EUROPE

Due to the climatic and soil conditions, Europe has typical softwood populations (e.g. nothern and alpine countries) and areas with predominat hardwoods (southern and south-eastern countries, parts of Germany etc.). There are also regions with predominant mixed species such as Finland with softwood and birch or the Baltic States with softwood and different hardwood species. But Central Europe, too, exhibits mixed forests with spruce and pine as softwoods and beech, oak, ash, mapple etc. Based on this

raw material resource, primary wood processing has devoloped historically around this specific forest areas as shown in Figure 1 by the example of the DACH-Region (DE, AT, CH).
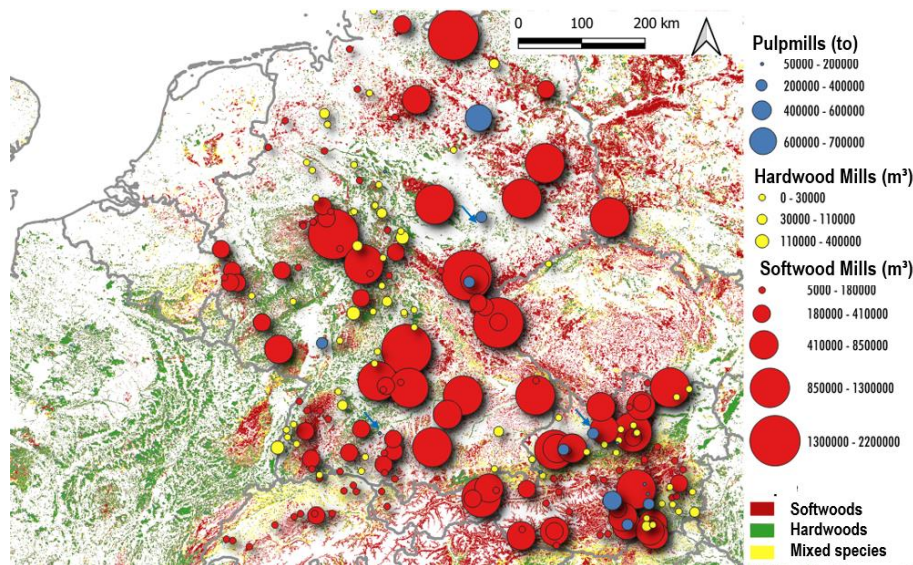

Figure 1: Current sites of hardwood, softwood and pulpmills in the DACH Region (DE, AT, CH), scaled according to their production capacity. Data retrieved from "Holzkurier" and from own inquires, Heinimann & Teischinger 2024)

According to the resource wood, most of the sawmill production capacity is related to softwood processing, and also most of the pulpmills process softwood (as industrial roundwood and wood chips from sawmills). Three pulpmills (indicated by an arrow in Figure 1) process hardwood: Lenzing AG as a special wood refinery based on beech wood with a focus on chemical pulp and Sappi Ehingen which can switch from softwood to hardwood processing on demand. The brandnew wood refinery based on beechwood in Leuna (UPM chemicals) with a new concept of a wood refinery is targeted on the huge beech wood ressources in Saxony-Anhalt in Germany.

Analysing the data of round timber processing in northern countries and the DACH-Region one can see the overwhelming importance of softwood processing. Current changes in forest management due to climate change, biodiversity reasons and societal claims, account for an increasing share of hardwoods and mixed forests, at least in Central Europe. Wood processing has to react to changing resources, but the question arises: Do we dispose of and do we apply appropriate technologies for hardwood processing?

SHARE OF ASSORTMENTS FOR HARDWOOD AND SOFTWOOD ROUND TIMBER
Within the various silvicultural regimes, hardwoods and softwoods develop different tree morphology during their growth period (Figure 2). When harvested, this tree morphology and shape of the trunk strongly influences the share of different assortments, such as crown wood, wood residues, pulpwood and round timber for sawmills. As shown in Figure 2, different wood species and softwood and hardwood in general, exhibit a different share in the main assortments such as saw logs, pulpwood, energy wood and residues. In general, for hardwoods the share of sawn timber is significantly lower than with softwoods and the share of energy wood is significantly higher.

As a resumé of this diagram in Figure 2 one can conclude, that with an expected increase in the share of hardwoods within the forest in the future, the share of sawlogs will decrease and the share of energy wood will increase, at least in central Europe. In 2016, according to a study of Kleinschmit (2017), a total of 31,7 mio m³ has been assigned to hardwood sawlogs. Hardwood sawlogs represent quite different shares within the overall industrial hardwood roundwood production in the various European countries including France, Romania, Germany, Poland, Latvia, Croatia and Slovakia as the main hardwood sawn timber producers.
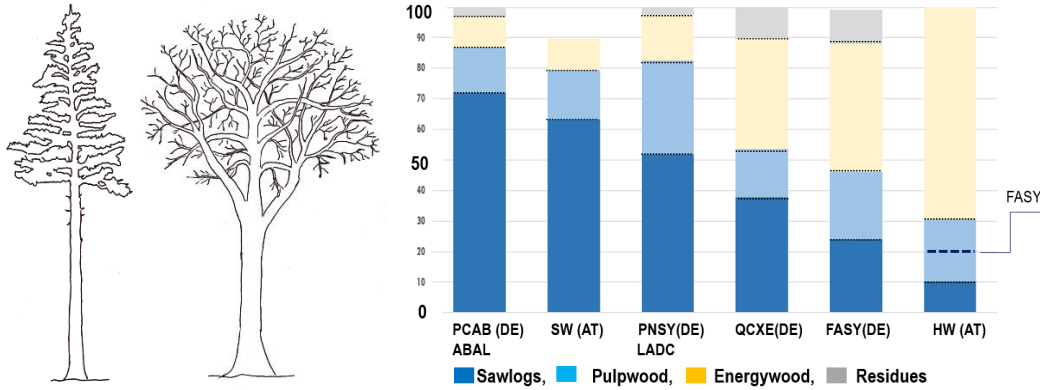
Figure 2: Typical tree shape of spruce and beech (left) and share of the different assortments (right).
Data retrieved from national forest statistics in Germany 2022 (DE) and Austria 2022 (AT), compiled by
Heinimann & Teischinger 2024)
HW … Hardwood (all species harvestet), SW … Softwood (all species harvested), 4-digit shortcuts PCAB, ABAL etc.
stand for different wood species according to EN 13556

A shift from softwoods to hardwoods will be a challenge for providing sufficient sawn timber for serving the envisaged demands of solid wood-based timber products such as timber for construction purposes including glued laminated timber (GLULAM), cross laminated timber (CLT) etc. Figure 3 depicts a data collection for Germany (FNR 2020) currently only 16.5% of the round timber harvested ends up in the final utilization (but not final products such as furniture components of parquet flooring), whereas the softwood process chain ends up with a share of 50 to 50%.

In the case of a higher share of hardwood of harvested wood, as a possible future scenario in central Europe, a resource efficient sawing technology for hardwoods (e.g. small diameter hardwood processing, Rathke et al. 2012) in order to increase the share of material use against energy use. or developments in new technologies in processing crown timber for material use. Log scanning could improve the selection of sawing pattern or optimising the peeling process (Sandberg et al. 2023). Another approach could be cutting sawlogs in short lengths in order to compensate the the crook of sawlogs. Another approach is to further develop the makro-fibre technology, which currently is described for small diameter softwood (Bliem et al. 2020) for a comminution process of crownwood from hardwoods.
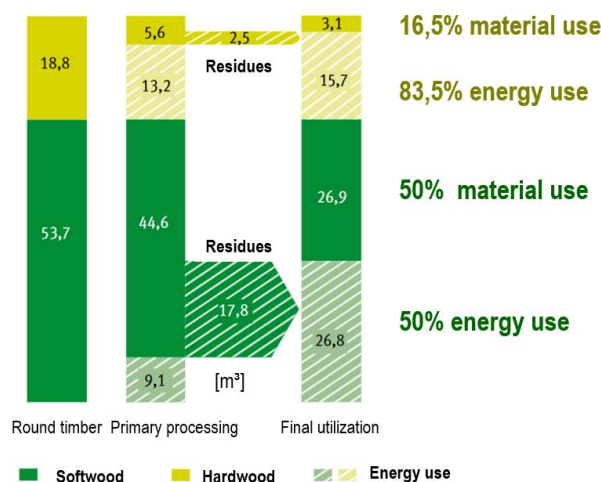
Figure 3: Utilization of "Softwoods" and "Hardwoods" in Germany, FNR 2020, based on Knauf/Frühwald
2020 and Mantau et al. 2018, Thünen Institut 2019

PROCESS EFFICIENCY – YIELD IN VOLUME

In general, the yield in Volume (Y_v) is calculated as the volume of (trimmed) sawn timber (V_B) as output devided by the total log volume (solid under bark) as input (V_L). Usually the relation is given as a percentage as shown in Eq. 1.

$$Y_V = V_B / V_L * 100\%$$ (1)

The volume yield might also be specified as main yield (for the main product) or as yield of consequence products (side boards) and by-products (sawdust, chips). When applying other processing methods such as the veneer peeling process, the yield calculation follows the same principle. Both log breakdown principles, sawing and peeling result in different yield in the main product and by-product (Fig. 4).

Figure 4: Typical beech wood log with center cracks (center), adequate sawing patterns (left) and peeling core rest (right)

By Figure 3 it becomes clear that the main yield (sawn timber in the sawmill process or veneer peeling) is strongly governened by the log geometry such as being more or less cylindrical, by the amount of crookiness, pith shakes etc. Additionally, further processing of the sawn timber or veneer sheets leads to further decline of the main yield due to cut-offs, planing the sawn timber, finger jointing etc. This may end up in only 30 to 40% of the main yield of the primary process into the final product as shown in Figure 5.
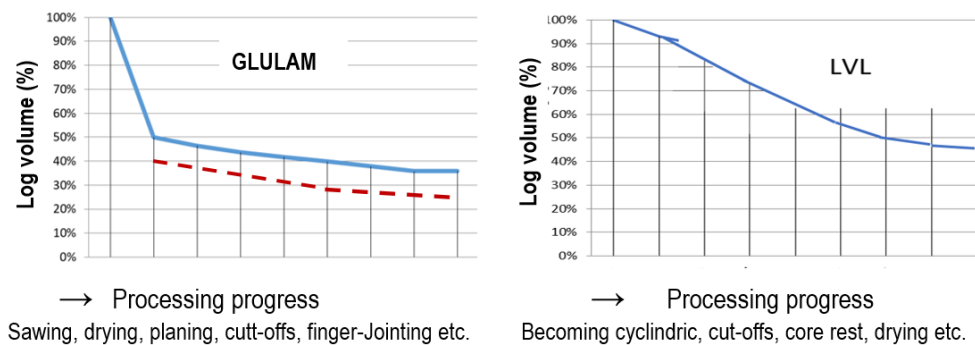
Figure 5: Decline of the main yield in volume along the production progress from sawmilling to GLULAM beams (left) and veneer peeling to LVL for softwoods (dotted line for beech wood exhibits a lower yield for GLULAM of beech), based on Knaus & Teischinger 2019 and Torno et al. 2013. GLULAM … Glued laminated timber, LVL … Laminated veneer lumber

Both yield diagrams in Figure 5, GLULAM and LVL are calculated for softwood, and GLULAM from beech clearly shows a lower yield than from softwood (Torno et al. 2013). This results from a poor volume yield in the sawmill process, more cut-offs and thinner wood laminations with more sawing and planing residues than in the softwood process. One has to emphasize that saw-dust, planer shavings and cut-offs are not production waste, but mostly used as a highly demanded energy source. This creates a trade-off in material use versus energy use and more and more becomes a burden in the pursuit of material and product efficient innovations for processes and products, as the "by-products" contribute a significant amount to the overall revenue of the production.

SELECTED APPROACHES IN HARDWOOD PROCESSING
Out of the many examples of successful and unsuccessful hardwood processing technologies two examples are discussed in the following section. By the example glued laminated timber (GLULAM) and chemical utilization of hardwood the processes and products are discussed with respect to a proper application of the technology deployed.

Example of hardwood construction elements
When becoming alert of currently barely utilized beech hardwoods in Germany and Switzerland and a prospected increase in the share of hardwoods to be harvested, several reasearch groups and selected enterprises put a focus on innovating processes and products with respect to an economically viable hardwood utilization (e.g. Frühwald 2006, Krackler et al. 2010, Wehrmann & Torno 2015).
In a first approach, some softwood GLULAM producers produced GLULAM beams with beech and other hardwood species, too (Figure 6), but not fully accounting the different material behaviour in swelling and shrinkage etc. By providing reliable material performance data and adapting adhesives adequately in research and test reports (compare Hänsel et al. 2022, Kovryga 2023), first GLULAM constructions appeared, but the higher material performance could not compensate higher costs in production and other disadvantages.
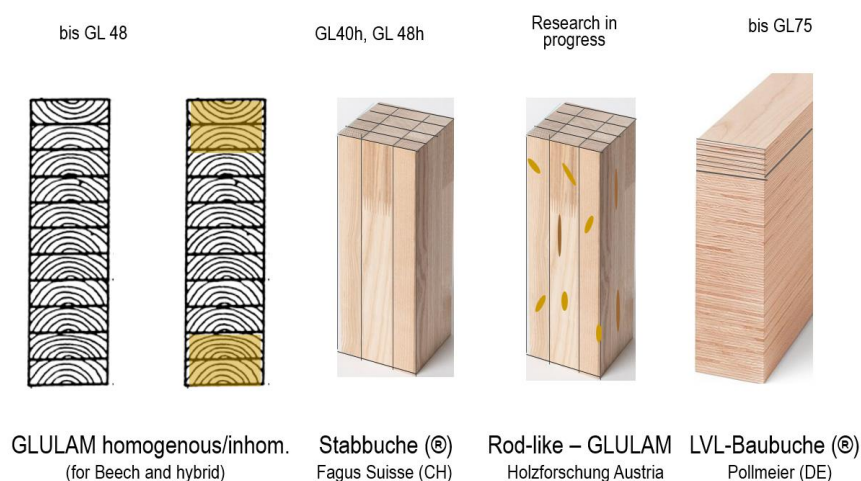
Figure 6: Different approaches in producing glued loadbearing beams from hardwood, especially from beechwood. GL xx indicates a destinct strength class of a GLULAM member

Following the first pilot constructions, hardwood GLULAM could not meet its expectations fully (Erhart 2021), and the production volume within Central Europe is still very low. The Swiss company Fagus Suisse had a new approach with preselected small beechwood rods, glued together as shown in Figure 6. This approach is more promising because of many reasons, but also limited to niche applications where the visual appearance of the clearwood surface becomes a criterion for choosing beech. A current approach under investigation is a rod-like GLULAM, where the rods are not pre-selected, but randomly glued together in order to homogenize the glued member concerning the various wood features such as knots and fibre deviation. This approach could lead to a higher yield and lower material costs. Baubuche® consists of Laminted Veneer Lumber (LVL) from beech, cut to laminations which are glued together as a GLULAM member (Figure 6). This approach leads to the highest homogenization of the material and thus the highest possible strength class. Despite of higher costs, this high-performance building component may convince architects in designing a very slim-fit construction in the appearance of a steel construction (compare examples depicted in Merz et al. 2020). But it is still open to which extent those glued hardwood members can replace softwood in construction sector to a larger extent.

Example of chemical utilization of hardwoods

Chemical wood pulping involves the extraction of cellulose from wood by dissolving the lignin that binds the cellulose fibers together. When a high purity of cellulose as dissolving pulp is targeted, the pulp yield drops dramatically to about 40% and it becomes important to add value to the byproducts such as hemicellulose and lignin. The Lenzing pulping process, by separating different chemicals from the hemicellulose (Figure 7), became a role model for a modern wood biorefinery concept (Harms 2006).

Figure 6: The concept of a wood biorefinery for beech wood pulping, targeting pure cellulose dissolving pulp as the main product and adding value to side streams (Harms 2006)

A new concept of a wood biorefinery, based on beech wood, was introduced by UPM chemicals (UPM 2023) and operation will start in Leuna, Germany, in 2024. This concept responds to the needs to replace a fossil based chemistry by converting wood into a next generation biochemicals such as bio-monoethylene glycol (BioMEG) and lignin-based renewable functional f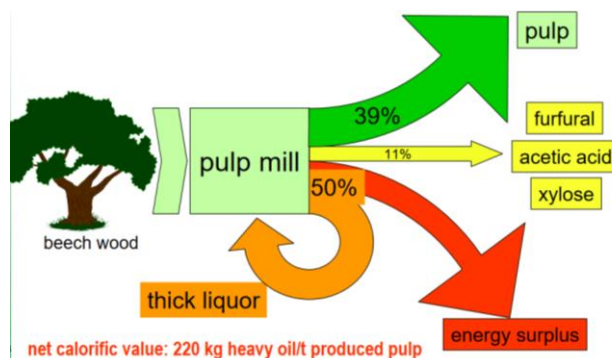illers (RFF), replacing black carbon. RFF are suitable for a broad range of rubber-like elastomers such as TPE, TPV, and plastics applications. They are suited for automotive weatherstrip, hoses, seals, interior & exterior plastics parts, and other industrial rubber applications. In addition, the biorefinery will produce bio-monopropylene glycol (BioMPG) and industrial sugars as platform chemicals. Typical end-uses of MEG are polyesters (PET) for fibers and packaging materials. This bio refinery concept is a good example of a co-production of multiple (main) products from a single raw material, wheras the Lenzing process targets a specified main product (dissolving pulp) with the endeavour to increase the added value of the side streams. Both concepts show their strengths and weaknesses.

The annual capacity of the UPM biorefinery will be 220,000 tonnes, which corresponds to a material input of more than 0.5 mio m³ beech wood a year. The Lenzing pulping process has a capacity of processing 1 mio m³ beech wood a year. As most chemical process engineering is related to the rule of economy of scale with continuous processing and large-scale process units, investment and set up costs are high and continuous wood supply is a prerequisite. A continous wood supply with beech wood, which is often harvested seasonally, is a challenge. This requires log storage with water sprinkling and a very sophisticated roundwood procurement and roundwood storage management.

CONCLUSION AND OUTLOOK

Hardwoods comprise a broader spectrum of wood properties than softwoods, which may be seen as an opportunity and weakness at the same time. Therefore, it is important to find and apply the proper technology for a targeted hardwood material and product category such as sawn timber, laminated glued products, wood based panels or chemicals from wood. In general, softwood trees are more homogenous and develop a straighter trunk than hardwoods, which drops the volume yield by applying traditional primary hardwood processing techniques. New technologies, such as log scanning, new wood comminution techniques have to be envisaged. Many processes and products do not allow a mix of different wood species, but in some cases product compounds of softwood and hardwood can be beneficial (e.g. prefabricated multilayer parquet flooring units with a thin hardwood surface layer and a softwood core layer). As currently a huge amount of hardwood is allocated to energy use, hardwood biorefineries might be a proper stragety in order to add value to low quality hardwood resources which are currently allocated to fuel wood.

REFERENCES

Ehrhart T, Steiger R, Frangi A (2021) Brettschichtholz aus Buche (GLULAM from beech wood). Bautechnik. 98(52):104-114. https://doi.org/10.1002/bate.202100016

EN 13556 Round and sawn timber. Nomenclature of timbers used in Europe. Brussels 2014

FNR (2020) Laubholz-Produktmärkte aus technischer-wirtschaftlicher und marktstruktureller Sicht (Markets for hardwoods). Fachagentur Nachwachsende Rohstoffe e.V. (FNR, Gülzow-Prüzen

Frühwald A (2006) Überblick über aktuelle Vorhaben der Laubholzforschung (Survey on hardwood research). Laubholzkongress, Hohenheim, DE, 09.03.2006. DGfH, FVA Baden-Würtemberg

Hänsel A, Sandak J, Sandak A, Mai J, Niemz P (2022). Selected previous findings on the factors influencing the gluing quality of solid wood products in timber construction and possible developments: A review. Wood Material Science & Engineering, 17(3), 230–241

Harms H (2006) Das Konzept der Holzraffinerie (The pinciple of a wood refinery). Lenzinger Berichte 86;1-8

Heinimann HR, Teischinger A (2024). Forst- und Holzwirtschaft im Wandel, Pfade für eine zukünftige Entwicklung (Forestry and wood industry in transformation), Springer, Heidelberg (in print)

Kovryga A (2023) Strength grading of hardwoods for glulam application. Mechanical properties and quality control options. PhD Thesis, University of Technology Munich (TUM), Munich

Krackler V, Keunecke D, Niemz P (2010) Verarbeitung und Verwendungsmöglichkeiten von Laubholz (Hardwood utilization). ETH Zürich, Institut für Baustoffe, Holzphysik, CH Zürich

Merz K, Nieman A, Tono S (2020) Bauen mit Laubholz (Construction with hardwoods). Detail Praxis, Munich

Nissen V, Seifert H, Blumenstein M (2018) Entwicklung einer Methode zur Unterstützung der Technologieauswahl für die Virtualisierung von Consultingleistungen (Technology selection). HMD 55, 801–828

Rathke J, Huber H, Teischinger A, Müller U, Hansmann C (2012). Verwendbarkeit von Laubschwachholz in der Sägeindustrie. Teil 1 u. Teil 2: Ausbeuteberechnung und Technologiebewertung (Small diameter hardwood processing) Holztechnologie. 53. 46-50 und 50-54

Sandberg D, Fink G, Hasener J, Kairi M, Marhenke T, Ross R J, ... & Wang X (2023). Process control and grading in primary wood processing. In: Springer Handbook of Wood Ccience and Technology (pp. 1019-1073). Cham: Springer International Publishing.

Torno S, Knorz M, Van de Kuilen JW (2013) Supply of beech lamellas for the production of glued laminatedtimber. In Proceedings of the 4th International Scientific Conference on Hardwood Processing, Florence, Italy, 7–9 October 2013; pp. 210–217

UPM (2023) Grüne Chemie mit holzbasierten Biochemikalien (Wood-based green chemicals). UPM treibt Schaffung einer Kreislaufwirtschaft durch nachwachsende Rohstoffe auf Holzbasis voran. CHEManager, 2023:(12),9

Wehrmann W, Torno S (2015) Laubholz für tragende Zwecke (Hardwood for load-bearing applications). Zusammenstellung zum Stand der Forschung und Entwicklung. Cluster-Initiative Forst und Holz in Bayern GmbH, Freising (DE)

Session III
Surface coating and bonding characteristics of hardwoods

Influence of pretreatments with essential oils on the colour and light resistance of maple (*Acer pseudoplatanus*) wood surfaces coated with shellac and beeswax

Emanuela Carmen Beldean[1], Maria Cristina Timar[1,*], Dana Mihaela Pop[1]

[1] [1] Transilvania University of Brașov, Faculty of Furniture Design and Wood Engineering, 29 Eroilor Boulevard, Brașov, Romania, 500036.

E-mail: ebeldean@unitbv.ro; cristinatimar@unitbv.ro; pop.dana.mihaela@unitbv.ro

Keywords: wood, essential oils, colour, shellac, beeswax, light exposure, colour changes, FTIR

ABSTRACT

Clove (*Eugenia carryophyllata*) and thyme (*Satureja hortensis*) essential oils (C-EO, T-EO) have demonstrated their antifungal properties and might be useful in the field of wood conservation for remedial or preventive treatments. The present research aimed at studying the effect of pre-treatments of maple (*Acer pseudoplatanus*) wood surfaces with alcoholic solutions (10%) of C-EO and T-EO on their colour, subsequent coating with shellac or beeswax and the colour stability of the finished surfaces when exposed to artificial light simulating natural light filtered by window glass.

Pre-treatments with essential oils of maple wood caused only small colour changes ($\Delta E < 3$) under the experimental conditions. Coating with shellac changed totally the colour of all wood samples ($\Delta E > 30$), slightly lower values for those pre-treated with T-EO and higher values for those pre-treated with C-EO. The corresponding values for beeswax finishing were much lower, varying in the range 4.00-7.5, with the same trend. The light induced colour changes after 96 h exposure were almost similar for the uncoated wood samples, regardless the pre-treatment with essential oils. The colour changes of the samples pre-treated with T-EO and coated with shellac or beeswax were almost similar or slightly lower compared to those measured for the controls without pre-treatment. Contrarily, pre-treatments with C-EO resulted in increased light induced colour changes of the coated surfaces, with about 3 units for shellac and 14 units for beeswax. This might be explained by the photo-induced oxidation of eugenol, the main component of C-EO, resulting in formation of new chromophores with quinoid structures, as supported by FTIR. These changes are more visible through the thinned, nearly colourless beeswax film.

INTRODUCTION

Essential oils (EOs) are environmentally friendly products, recognised for centuries as beneficial to human health, when adequately used. Their biological properties include antimicrobial, antifungal and antioxidant effects, being related to their complex organic chemical composition. A number of studies have demonstrated their potential for wood preservation (Panek et al. 2014, Bahmani and Schmidt 2018, Reiprecht et al. 2019, Simunkova et al. 2022,) by their activity against wood decay fungi and moulds. Employment of EOs as alternative to classic biocides in the field of wood / furniture conservation for remedial or preventive treatments (Pop et al. 2021, Pop et al. 2022, Tran-Ly et al. 2022) is a promising option. Conservation materials and treatments need to satisfy specific requirements. For instance, they should not change the colour of the treated materials, should be compatible with the traditional finishing material and they should not affect negatively the ageing behaviour of the artefacts. To meet these requirements, studies in the field come to demonstrate the advantages of utilisation of essential oils for wood treatments: Panek (2014) highlighted that essential oils had no negative effect on the colour stability on beech wood and Simunkova (2022) concluded that the colour of spruce wood treated with essential oils was preserved and wetting properties and adhesion of wood surfaces were improved.

The ageing of wooden artefacts is always associated with changes in colour (Kranitz 2014). Light-induced ageing of different wood species and coated surfaces is a widely studied phenomenon, but mostly for outdoor applications. Although maple wood is a common hardwood species, often employed in conservation-restoration works, quite limited research focussed on its colour investigation and behaviour when exposed to light in indoor conditions (de Moura and Hernandez 2005, Dzurenda et al. 2022, Timar et al. 2016). Considering these aspects, previous research of the authors investigated clove

(*Eugenia carryophyllata*) and thyme (*Satureja hortensis*) essential oils as modifying agents for Shellac solutions. A good compatibility with alcoholic shellac solutions was found, alongside a slight influence of modification on the colour of finished maple surfaces and their colour changes by UV-VIS light simulating indoor conditions. (Timar and Beldean 2022).

The present research aimed at studying the effect of pre-treatments of maple (*Acer pseudoplatanus*) wood surfaces with alcoholic solutions (10%) of clove and thyme essential oils on their colour, compatibility with shellac and beeswax in traditional finishing technologies and the colour stability of the coated surfaces when exposed to light in indoor conditions. An accelerated laboratory test to artificial UV-VIS radiation, simulating natural light filtered by window glass, in conjunction with colour measurements in the CIELab system and FTIR investigations, were employed for this purpose.

MATERIALS AND METHODS
Materials
Clove (*Eugenia caryophyllata)* essential oil (coded C-EO) and Thyme (*Satureja hortensis*) essential oil (coded T-EO), as a commercial products (100 %) available on Romanian market (https://www.steauadivina.ro) were employed. Solutions of EO in ethyl alcohol at volumetric ratios of 1:10 (v:v) were prepared for this purpose.

A shellac solution (coded SL) with an addition of 10% rosin was prepared by dissolving in ethyl alcohol (98%) under stirring on a warm water bath (40–50 °C). The solids content was 13.2%.

Natural beeswax sheets (coded BW) were dissolved on a warm water bath (40–50 °C) in white spirit D40-Denatured from CTS Company (https://ctsconservation.com), resulting a paste-like polish with concentration of 18-20 %.

Wood samples from European maple (*Acer pseudoplatanus*) with dimensions of (120x80x5) mm, with radial faces, were employed. The surfaces were sanded with H120, H150 grit paper and cleaned from dust. All samples were conditioned (20±2°C, 55±5% RH) before and after finishing and prior to any investigation.

Treating and finishing of wood samples
The experimental schedule for wood samples preparation (schematically presented in Figure 1) included:(*i*) pre-treatments with essential oils (C-EO, T-EO); (*ii*) coating with shellac or beeswax (SL, BW) and (*iii*) the combined pre-treatments with essential oils and subsequent coating with shellac or beeswax (C-EO-SL, T-EO-SL and C-EO-BW, T-EO-BW).
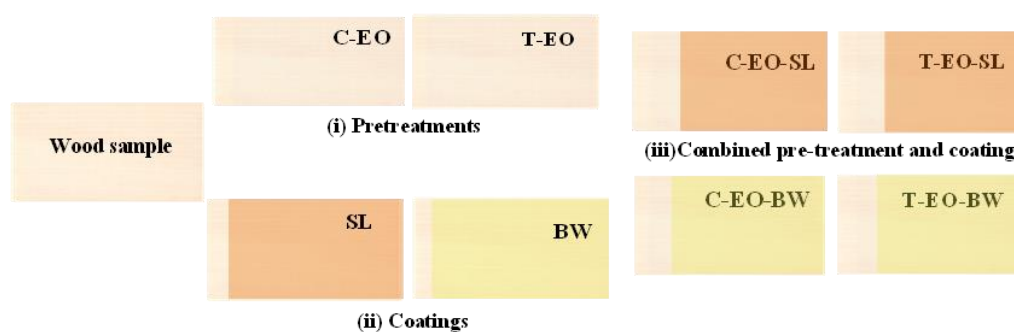
Figure 1: Experimental treating schedule and codification of the samples

The essential oils were applied by brushing until fibre saturation in two successive layers (30 min apart) at total application rates of about 160-170 g/m². This step was followed by 24h conditioning at room temperature. Control untreated samples and pre-treated samples were then finished by hand with SL and BW, following the specific traditional techniques.

Shellac base coat was applied by brushing in three layers of about 110 g/m² at intervals of 30-60 minutes drying time. Afterwards, the samples were sanded with 320 grit size paper and finishing was continued by employing a polishing rubber to apply the shellac solution in thin coats until pores filling and glossy surface were obtained.

Beeswax polish, pre-heated on water bath, was applied by brushing in three layers at a total specific consumption of 135-150 g/m². After 72 h conditioning at room temperature, the

surfaces were lustred with a polishing pad until a matt gloss was attained. Four replicates for each treating variant were prepared. Two of them were kept as control, while the other two were exposed to light

It has to be remarked that the pre-treated samples could be satisfactory finished, with no obvious incompatibility issues between pre-treatments with C-EO and T-EO and SL or BW. However, slightly longer intervals between the application of the successive layers of coatings were necessary in the case of C-EO pre-treatment.

Accelerated UV-VIS aging exposure

A Feutron 400 FKS environmental climatic chamber (Germany) equipped with a UVA Spot 400T lamp, fitted with a glass H2 filter, was employed to expose the wood samples to light in the range of 295 to 600 nm, simulating natural light filtered by window glass. Each cycle of 24 h UV exposure consisted in four steps of 6 h UV irradiation at 40°C alternated with dark periods of 0.5 h. This procedure was repeated four times, resulting 24, 48, 72 and 96 hours of exposure. More details related to procedure were previously published by the authors (Timar and Beldean 2022). Two replicates from each treating and finishing variant, alongside corresponding two uncoated controls, were tested simultaneously.

Colour measurements

An AvaSpec-USB2 spectrometer (Netherlands) equipped with an integrating AVA sphere, with a circular measuring aperture of 8 mm, were employed for colour measurements, under standard illuminant D65 and 2° standard observer. Data were processed with AVASOFT—version 7.7

The samples were measured initially, prior any treatment or finishing and after treatments, before light exposure and after each period of exposure. A special device was employed to carry out the repeated colour measurements in the same 5 points/sample. The CIELab colour coordinates L*, a*, b* were registered and averages were calculated for each sample and each treatment variant. Colour differences ΔE were calculated with Eq. 1:

$$\Delta E = \sqrt{\Delta L^{*2} + \Delta a^{*2} + \Delta b^{*2}} \tag{1}$$

Where: ΔL*, Δa* and Δb* are the differences of initial and final values (before and after treatments or ageing for different periods of time) of L*, a* and b* parameters.

FTIR Investigations

An Alpha Bruker equipment endowed with attenuated total reflection module (ATR) was used for FTIR investigation of wood surfaces prior and after pre-treatments and coating, before and after light induced ageing. All spectra were registered in the range 4000-400 cm^{-1}, at a resolution of 4 cm^{-1} and 24 scans per spectrum and were further processed for baseline correction and smoothing, employing OPUS software. Average spectra of minimum 3 recordings (on three random areas) of the investigated samples were computed for each treatment variant and exposure situation (0, 24, 48, 72, 96 hours of light exposure). The min-max normalised average spectra were compared to highlight detectable chemical changes associated with the different preparation phases and light exposure of the maple wood samples.

Statistical Data Processing

The measurements performed in duplicates were presented as mean value ±SD and were statistically analysed by One-way Anova and Post-hoc analysis in Excel. The difference between groups was considered significant at a confidence level of 95% (α=0.05) when $p<0.05$.

RESULTS AND DISSCUSION
General aspects

Pre-treatments of maple wood samples did not impede their subsequent coating with shellac and beeswax solutions by the traditional techniques. Filled grain finishes, with glossy (SL) or silky matt effect (BW), which enhanced or highlighted the natural beauty of wood were obtained. An image of the general aspect of the various samples prepared and investigated in this research is presented in Figure

2. This includes, comparatively, scanned images of the samples prior (Figure 2a) and after exposure to light induced colour ageing for 96h (Figure 2b).
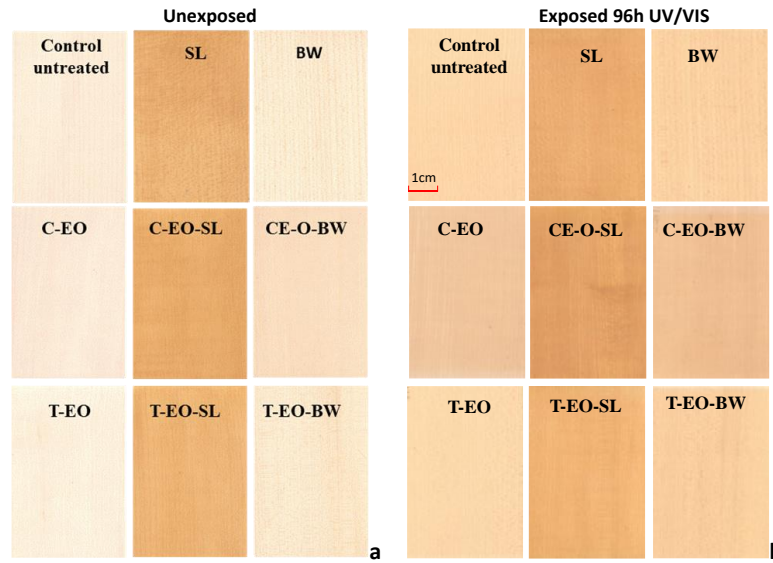
Figure: 2 General aspect of maple wood samples uncoated and coated with shellac (SL) and beeswax (BW) before (a) and after exposure to UV/VIS light, in an accelerated test, for 96 h (b). Untreated controls and samples pre-treated with clove (C-EO) and thyme (T-EO) essential oils are included in both groups

It is visible that all the samples, regardless pre-treatment or coating, suffered slight colour changes as result of exposure to light under the experimental conditions employed in this research. These colour changes were perceived as darkening and shade modifications, different samples turning more reddish or yellowing. The in-time evolution of the global colour changes (ΔE) is presented by the plots in Figure 3.
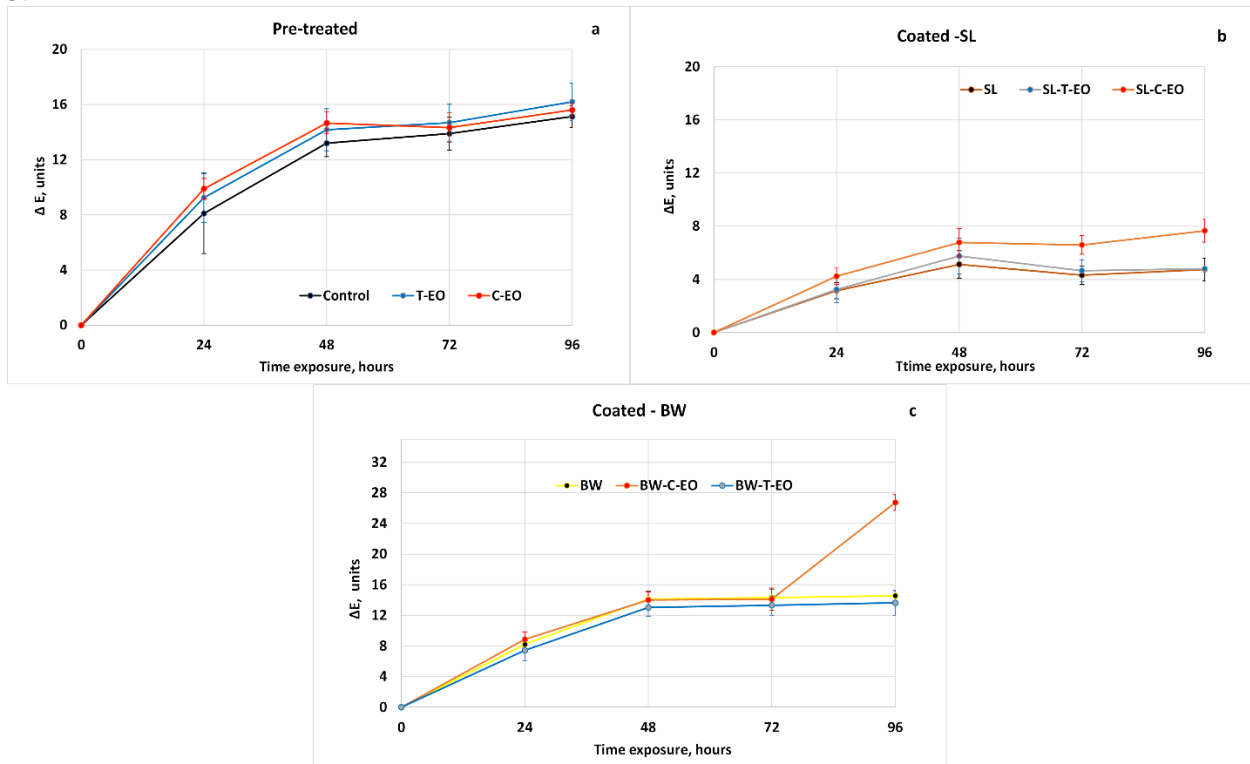
Figure 3: Evolution of colour differences (ΔE) after 24,48,72 and 96 hours of exposure to UV-VIS accelerating ageing; samples pre-treated with C-EO and T-EO(a)-, samples coated with SL(b) and BW(c)

The evolution of colour difference values ΔE indicated a rapid change at the beginning of the ageing process, and then, depending to the type of treatment, this evolution was more or less abrupt. For instance, uncoated: control and pre-treated samples (C-EO and T-EO) registered a similar increasing trend (Figure 3a). The coating with SL (Figure 3b) indicated a protective effect of shellac, reflected in smaller ΔE values (<8 units) compared with uncoated samples. Wood coated with BW recorded similar values of ΔE with uncoated samples up to 72h exposure (13-14 units) followed by a sharp increase of ΔE for C-EO-BW samples at 96h, due to increasing of redness a* and yellowness b* parameters and decreasing of lightness L*. More research and extended exposure times are necessary to explain this particular evolution.

Influence of pre-treatments on the colour of maple wood surfaces

The colour parameters (L*, a*, b*) calculated as average values and the corresponding standard deviations (*italics*) for uncoated and coated samples, without pre-treatment or pre-treated with essential oils are presented in Table 1. The colour differences ΔE resulting from pre-treatments with C-EO and T-EO and caused by coating with SL and BW are also presented.

Pre-treatments with essential oils caused only small colour changes (ΔE values of 2.46 for C-EO and 1.67 for T-EO). These values account for small colour differences (ΔE =0.2-2.0) or colour differences visible only with high quality screen (ΔE=2.0-3.0), according to Allegretti et al 2009. Statistical analysis of data indicated that pre-treatment with C-EO resulted in significant differences of parameters L* and a*(samples became more reddish and darker compared to controls) and no significant difference in yellowness b*. None of the colour parameters were found statistically different for pre-treatment with T-EO. It concludes that T-EO did not cause statistically significant colour changes of the maple wood substrate, which agreed with visual perception.

Table 1: Colour parameters for uncoated and coated samples, without pre-treatment or pre-treated with clove (C-EO) or thyme (T-EO) essential oils, before ageing test

Pre-treatment Coating		No (Control)			C-EO			T-EO			CE-O PTE index	T-EO PTE index
		L*	a*	b*	L*	a*	b*	L*	a*	b*		
Uncoated	Av	86.69	3.33	13.52	83.62	5.04	14.13	86.05	3.48	12.95	-	-
	Stdev	0.92	0.49	1.58	0.29	0.14	0.39	0.95	0.39	0.99		
	ΔE	-	-	-	2.46 (0.57)			1.67 (1.58)				
Coated-SL	Av	69.33	10.25	41.02	69.33	11.20	44.06	71.48	9.63	40.89	1.16	0.92
	Stdev	1.35	0.68	1,34	1,63	1,30	0,92	0,88	0.38	1.15		
	ΔE	33.02 (1.57)			38.54 (1.33)			30.54 (1.92)				
Coated - BW	Av	85.52	3.51	16.55	81.52	5.44	19.76	83.91	4.08	17.98	1.87	1.25
	Stdev	0.68	0.43	0.57	1.01	0.48	0.79	1.05	0.22	1.56		
	ΔE	4.00 (0.38)			7.50 (0.70)			5.00 (1.09)				
Notes	**ΔE** values represent colour changes due to the pre-treatments (grey), respectively coating with SL (pink) or BW (yellow) **PTE index** is calculated in Eq.2											

Coating with shellac changed totally the colour of all wood samples (ΔE 30.54-38.54) the values of ΔE above 12.0 corresponding to different colours in visual perception (Allegretti et al. 2009). This colour change is due to the reddish-brown colour of this natural resin, well reflected by the significant increase of the redness (Δa* values of about 6-7 units) and yellowness (Δb* values of about 27-30 units) of all the SL coated samples compared to their corresponding uncoated controls. Accordingly, a global colour difference value (ΔE) of 33.02 was obtained for the coated controls, while the values for the pre-treated substrates were slightly (by 2.5 units) lower (ΔE=30.54) for T-EO (no significant statistic) and with about 5 units higher (ΔE= 38.54) in the case of C-EO (statistically significant difference).

Coating with beeswax resulted in much lower colour changes (ΔE: 4.00-7.5 units), with the minimum change for the untreated controls and maximum value (ΔE =7.50 units) for those pre-treated with C-EO. The corresponding value for the samples pre-treated with T-EO was 5.0 units, both of them being statistically different compared to the untreated control.

In order to better highlight the influence of pre-treatments on the colour of the coated maple wood samples, a pre-treatment effect index (PTE) was calculated as the ratio between the ΔE values determined for the pre- treated samples and the control samples, according to Eq. 2

$$PTE = \frac{\Delta E \; pretretated}{\Delta E control} \tag{2}$$

The PTE indexes presented in Table 1 clearly show that influence of pre-treatment of maple wood substrates with C-EO or T-EO is dependent on both the type of essential oil and the type of finish. Clove essential oil is a slightly yellow-orange product and its influence on the colour of the uncoated substrates and final finished surfaces is higher (PTE=1.16-1.87) compared to thyme essential oil (PTE= 0.92-1.25). Also, its influence is higher for the surfaces coated with beeswax, with light beige colour (PTE=1.87), than in the case of surfaces coated with the darker, reddish-brown SL solution (PTE=1.16).

Influence of pretreatment with essential oils on the light-induced colour changes

In Table 2 are presented the final colour changes after 96 hours of exposure to accelerating UV-VIS aging, calculated as average values and their SD (*italics*) for each type of pre-treatment and coating.

The light induced colour changes after 96 h light exposure under the experimental conditions employed in this research were pretty similar for all the uncoated wood samples, regardless the pre-treatment with essential oils (ΔE: 15.13-16.20), values which were found not statistically different. Lower colour changes, varying in the range ΔE: 4.74-7.66, were registered for the shellac coated samples, with minimum values for control and T-EO pre-treated samples (4.74 vs 4.80). In all cases the protective effect of SL film on the effect of light exposure was maintained. The corresponding values for beeswax varied in a larger range ΔE: 13.64-26.74 units. Compared to the ΔE of 14.56 determined for BW coated controls without pre-treatment, the values for the T-EO pre-treated samples were slightly lower (ΔE = 13.64 – statistically not different), while that for the C-EO pre-treated samples was considerably higher (ΔE = 26.74), overpassing the value for the corresponding uncoated samples (ΔE =15.13).

Table 2: Colour changes for uncoated and coated samples, without pre-treatment or pre-treated with clove (C-EO) or thyme (T-EO) essential oils, after ageing test (96h UV/VIS)

Pre-treatment Coating		Colour changes after 96 h light exposure												Influence index	
		No (Control)				C-EO				T-EO				C-EO	T-EO
		ΔL*	Δa*	Δb*	ΔE*	ΔL*	Δa*	Δb*	ΔE*	ΔL*	Δa*	Δb*	ΔE*	PTE	PTE
Uncoated	Av	-7.38	3.70	12.68	**15.13**	-9.86	3.33	11.60	**15.60**	-6.54	2.74	14.53	**16.20**	1.03	1.07
	stdev	*0.35*	*0.30*	*0.75*	*0.80*	*0.34*	*0.39*	*0.74*	*0.48*	*1.25*	*0.66*	*1.07*	*1.34*		
Coated-SL	Av	-1.90	3.99	0.71	**4.74**	-5.16	4.76	-2.29	**7.66**	-2.33	3.87	1.11	**4.80**	1.61	1.01
	stdev	*1.03*	*0.73*	*1.39*	*0.86*	*0.89*	*0.71*	*2.15*	*1.18*	*0.71*	*0,53*	*1.30*	*0.94*		
Coated-BW	Av	-7.09	4.56	11.84	**14.56**	-12.37	8.06	22.24	**26.74**	-6.84	4.23	10.96	**13.64**	1.83	0.94
	stdev	*0.40*	*0.61*	*0.83*	*0.67*	*1.25*	*0.76*	*1.14*	*1.04*	*0.94*	*0.38*	*1.74*	*1.64*		

The calculated PTE indexes were close to 1.0 (0.94-1.07) for the T-EO pre-treated samples, showing no or very little influence on the colour changes caused by light exposure regardless the uncoated or coated state and type finish. On the contrary, in the case of C-EO, the pre-treatment had no influence on the light induced colour changes of the uncoated samples (PTE=1.03), but resulted in considerably higher colour changes for the coated samples: PTE=1.61 (SL) and PTE=1.83 (BW). This may indicate chemical changes determined by the presence of C-EO:

FTIR investigations

Both wood and the employed essential oils are organic materials with complex chemical composition, with more constituents with various chemical structures, so that complex FTIR spectra reflect these features. As infrared spectra are vibrational spectra of the different chemical bonds, functional groups and other structural moieties, it is easy to understand overlapping of most absorption bands in the spectra of wood substrates and essential oils (Figure 4a) or in the spectra of uncoated and SL coated samples (Figure 4b).
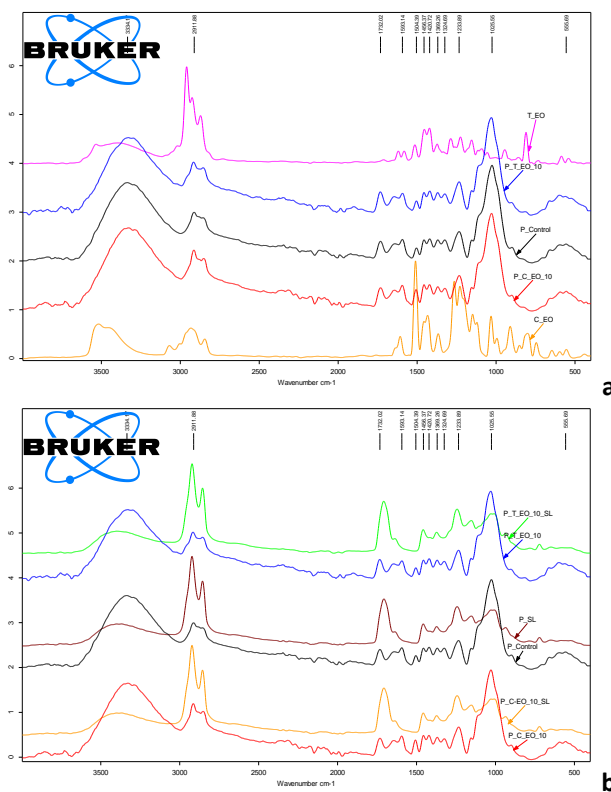
Figure 4: FTIR spectra for clove and thyme essential oils (C-EO, T-EO), control and pretreated maple wood surface (a); comparative spectra of uncoated and shellac (SL) coated maple wood surfaces with different pre-treatments, before ageing

It is worth noting that a distinct peak of C-EO at about 1514 cm^{-1}, assigned to eugenol, its main chemical component, is overlapping the absorption band at 1504 cm^{-1}, assigned to the skeletal vibration of aromatic ring in lignin, due to their common phenyl-propane skeleton. However, the increase of this peak is visible for the uncoated C-EO pre-treated samples. Coating with shellac hinders this particularity due to the fact that actually only the surface coating layer is analysed by the FTIR-ATR technique. More details on the spectra of C-EO, T-EO and shellac were previously reported (Timar and Beldean 2022).

The comparative FTIR spectra for the uncoated and coated maple samples, with or without pre-treatment, before and after 96 h light exposure are depicted in Figure 5. Only the fingerprint region was chosen for the uncoated and SL coated samples (Figure 5a, b), while the spectra on the whole registered IR range are presented for the samples coated with beeswax (Figure 5c).

The spectra of control sample (M) after 96 h light exposure (Figure 5a) clearly show the specific pattern of wood photodegradation by UV radiation: decrease of the lignin absorption at 1504 cm^{-1}, which nearly disappears due to lignin degradation, occurring in parallel with photo-oxidative processes highlighted by the increased absorptions at 1732 cm^{-1} (unconjugated carbonyl) and 1640 cm^{-1} (aromatic ketones, conjugated carbonyl bonds), while the absorption at around 1600 cm^{-1} (aromatic ring) is receded and included in the broader band at 1640 cm^{-1}. These are good accordance with previous research and literature data and explain the associated colour changes (Evans et al. 2005, Kataoka et al. 2007, Tolvaj et al. 2013, Timar et al. 2016, Timar and Beldean 2022).

For the samples pre-treated with C-EO and T-EO, similar changes occur, especially for T-EO, but the decrease of the peak at 1504 cm^{-1} is less pronounced (especially for C-EO), while the increase of the unconjugated carbonyl bond seems more important. At the same time the increase of the absorption at 1640 cm^{-1} seems smaller and the absorption at 1600 cm^{-1} remains distinct, especially in the case of C-EO pre-treatment.

These changes might suggest a possible protective effect of the two essential oils, even if the small differences in light induced colour changes were not statistically significant. C-EO and T-EO were found to absorb UV (Sharma et al. 2020) radiation and undergo photo-oxidative reaction, by a radicalic mechanism (Elgendy et al. 2008).
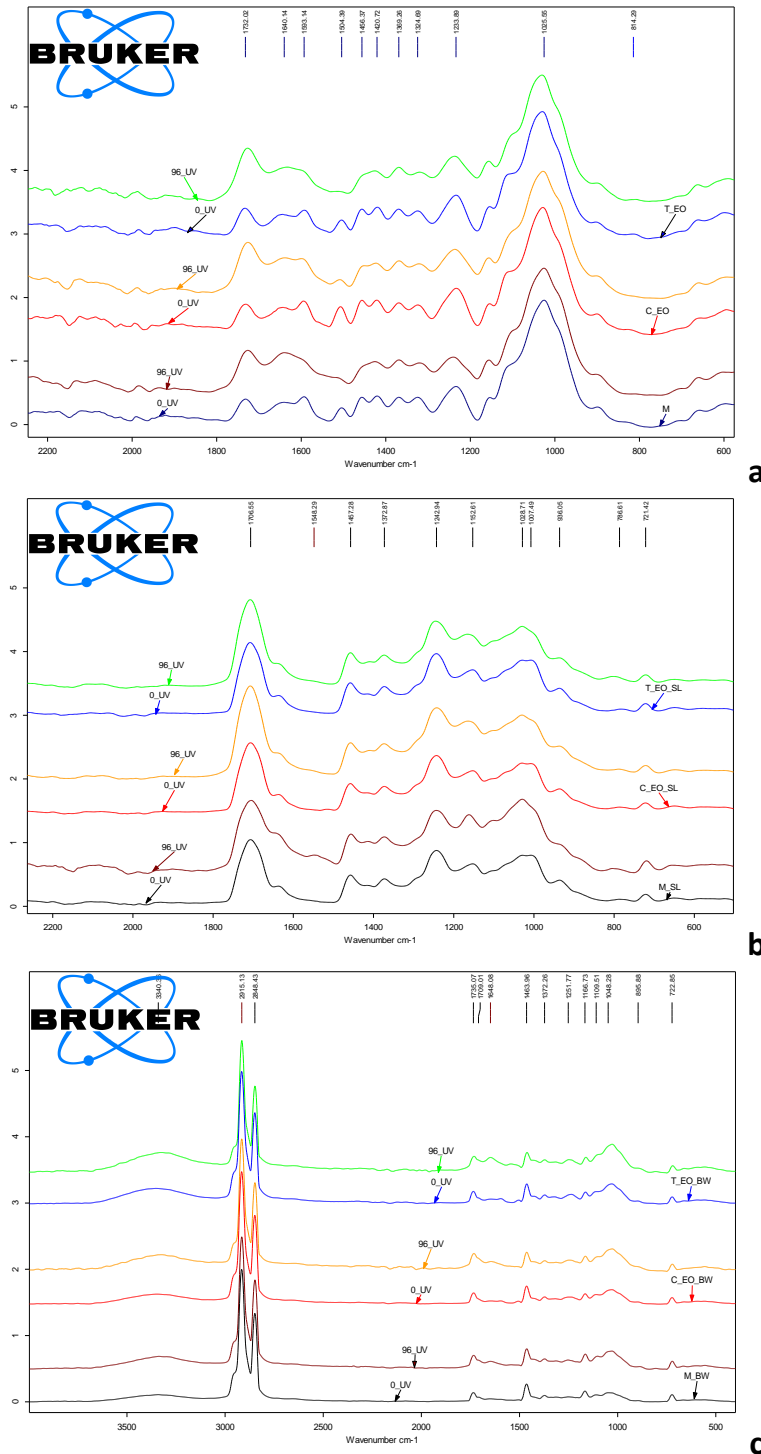
Figure 5: Comparative FTIR spectra of maple wood surface, control (M) and pretreated, before (0-UV) and after 96 h light induced accelerated ageing (96-UV) for: uncoated samples (a); shellacs (SL) coated samples (b); beeswax (BW) coated samples (c)

Essential oils with phenolic main components have been recognised as active antioxidants by their radical scavenging activity (Gulcin 2011, Fadel et al. 2020), but this may result in their own oxidation to chromophores containing products. C-EO was recognised as a very active antioxidant essential oil and its oxidation by different pathways to products containing quinoid structures (Elgendy et al. 2008, Yildiz et al. 2017), known as chromophores (Alfieri et al. 2021), was demonstrated.

The spectra of SL coated samples before and after 96h light exposure (Figure 5b) show only little differences, demonstrating a fairly good resistance. For the M_SL samples a slight increase of the small shoulder at around 1637 cm^{-1}, slight trend of broadening of absorption at 1706 cm^{-1}and a trend of a new

absorption at about 1550 cm^{-1} are observed, denoting some oxidative phenomena. For the C-EO and T-EO pre-treated samples the only detectable change is an increase of the unconjugated carbonyls absorption at 1706 cm^{-1}. An increase of this absorption band was assigned to C-EO and T-EO oxidation following sun light exposure, while their embodying in polymers matrix inhibited the degradation process of the polymers themselves (Masek et al. 2021).

The spectra of BW coated samples before and after 96h light exposure (Figure 5c) show only little differences, demonstrating a very good ageing resistance of beeswax. A slight trend of increased absorptions at around 3400 cm^{-1} (-OH groups) and around 1040 cm^{-1} (C-O, C-O-C vibrations), both of high intensity in the wood FTIR spectra, may indicate an increased transparency to FTIR of the substrate due to wax layers thinning by absorption into the wood structure, considering its thermoplastic character and the fact that light irradiation was achieved at 40°C. These results are supported by previously published research (Liu et al. 2019, Liu et al. 2022), which also concluded on the high transparency to UV light of beeswax in favour of light induced colour changes of the underneath wood substrate.

Accordingly, the higher light induced colour changes determined for the maple wood surfaces pre-treated with C-EO and T-EO and coated with beeswax should be attributed to the increased transparency of the nearly colourless and thinned coating film, making visible the colour changes of the wood substrate. These light induced colour changes were maximum for the substrate pre-treated with C-EO due to its capability of absorbing UV light and oxidation to coloured products. A similar result was reported for spruce-wood pre-treated with C-EO, which demonstrated an increased colour change under the action of UV light in a natural and an artificial weathering test (by Oberhofnerová et al. 2018).

CONCLUSIONS

Influence of pre-treatment with clove (*Eugenia carryophyllata*) and thyme (*Satureja hortensis*) essential oils on maple wood substrates is dependent on both the type of essential oil and the type of finish.

No application problems or compatibility issue were observed during the treating with clove (C-EO) and thyme (T-EO), though slightly longer intervals between the application of the successive layers of coatings were necessary in the case of C-EO pre-treatment.

Pre-treatment with T-EO had no significant influence on the colour of the uncoated or coated surfaces, neither on their resistance to light, in a simulated indoor conditions test.

Pre-treatment with C-EO resulted only in small colour changes of maple surfaces, without significant influence on the light induced colour changes of the uncoated surfaces. However, the light induced colour changes of the C-EO pre-treated coated samples were significantly higher than those of coated controls.

UV absorption and subsequent photo oxidation of C-EO, resulting in new chromophores, alongside the differences in colour and transparency to ultraviolet and visible between of shellac and beeswax, might explain these results. This hypothesis is partly sustained by FTIR, but more research is needed.

Based on the colour changes results, among the two essential oils tested, T-EO could be considered for potential application in the field of conservation, as pre-treatment in finishing technologies.

The potential recurrent benefits in terms of behaviour of the coated surfaces in conditions of biological attack risk will be investigated in future research.

REFERENCES

Alfieri ML, Panzella L, Crescenzi O, Napolitano A, d'Ischia M (2021) Nature-Inspired Functional Chromophores from Biomimetic o-Quinone Chemistry. Eur. J. Org. Chem. 2982–2989, https://doi.org/10.1002/ejoc.202100341

Allegretti O, Travan L, Cividini R (2009) Drying techniques to obtain white Beech. Wood EDG Conference, 23rd April 2009, Bled, Slovenia.

Bahmani M, Schmidt O (2018) Plant essential oils for environment-friendly protection of wood objects against fungi. Maderas, Cienc. tecnol. 2018, vol.20, n.3, pp.325-332. ISSN 0718-221X. http://dx.doi.org/10.4067/S0718-221X2018005003301.

De Moura LF, Hernandez RE (2005) Evaluation of varnish coating performance for two surfacing methods on sugar maple wood. Wood and Fiber Science 37(2) 2005 pp 355-366

Dzurenda V, Dudiak M, Výbohová E (2022) Influence of UV Radiation on the Color Change of the Surface of Steamed Maple Wood with Saturated Water Steam. Polymers 2022, 14, 217. https://doi.org/10.3390/polym14010217

Elgendy EM, Khayyat SA (2008) Oxidation reactions of some natural volatile aromatic compounds: anethole and eugenol. Russian Journal of Organic Chemistry, 44, No. 6, pp 823–829

Evans P, Chowdhury, MJ, Mathews B, Schmalzl K, Ayer S, Kiguchi M, Kataoka Y (2005) Weathering and UV Protection of Wood Surfaces (chapter 14) In*:* Handbook of Environmental Degradation of Materials, Myer Kutz Ed., 1st ed., 2005, eBook ISBN: 9780815517498, pp 277-297

Fadel HHM; El-Ghorab AH, Hussein AMS, El-Massry KF, Lotfy SN, Ahmed MYS, Soliman TN (2020) Correlation between chemical composition and radical scavenging activity of 10 commercial essential oils: Impact of microencapsulation on functional properties of essential oils. Arabian J. of Chem*,*13, 6815–6827, https://doi.org/10.1016/j.arabjc.2020.06.034

Gülçin I, (2011) Antioxidant activity of eugenol: A structure–activity relationship. Journal of Medical Food,14(9): 975-985. DOI: https://doi.org/10.1089/jmf.2010.0197

Kataoka Y, Kiguchi M, Williams R, Evans D (2007) Violet light causes photodegradation of wood beyond the zone affected by ultraviolet radiation. Holzforschung, 61: 23-27. https://doi.org/10.1515/HF.2007.005

Kranitz K (2014) Effect of natural aging on wood. PhD dissertation University of West Hungary

Liu XY, Timar MC, Varodi AM (2019) A comparative study on the artificial UV and natural ageing of beeswax and Chinese wax and influence of wax finishing on the ageing of Chinese Ash (*Fraxinus mandshurica*) wood surfaces. J. Photochem. Photobiol. B Biol. 201, 111607. https://doi.org/10.1016/j.jphotobiol.2019.111607

Liu XY, Timar MC, Varodi AM, Nedelcu R, Torcătoru, MJ (2022) Colour and Surface Chemistry Changes of Wood Surfaces Coated with Two Types of Waxes after Seven Years Exposure to Natural Light in Indoor Conditions. Coatings, 12(11), 1689. https://www.mdpi.com/2079-6412/12/11/1689

Masek A, Cichosz S, Piotrowska M (2021) Comparison of Aging Resistance and Antimicrobial Properties of Ethylene–Norbornene Copolymer and Poly(Lactic Acid) Impregnated with Phytochemicals Embodied in Thyme (Thymus vulgaris)and Clove (Syzygium aromaticum). Int. J. Mol. Sci. 22, 13025. https://doi.org/10.3390/ijms222313025

Oberhofnerová E, Pánek M, Böhm M, (2018) Effect of Surface Pretreatment with Natural Essential Oils on the Weathering Performance of Spruce Wood. BioResources 13(3), 7053-7070. https://doi.org/10.15376/biores.13.3.7053-7070

Panek M, Reinprecht L, Hulla M (2014) Ten essential oils for beech wood protection-efficacy against wood destroying fungi and moulds and effect on wood discolouration. BioResources 9(3) 5588-5603

Pop DM, Timar MC, Beldean EC, Varodi AM (2020) Combined testing approach to evaluate the antifungal efficiency of clove (*Eugenia caryophyllata*) essential oil for potential application in wood conservation. BioResources 2020, 15, 9474–9489

Pop DM, Timar MC, Varodi AM, Beldean EC (2022) An evaluation of clove (*Eugenia caryophyllata*) essential oil as a potential alternative antifungal wood protection system for cultural heritage conservation. *Maderas, Cienc. tecnol.* 2022, vol.24, 11. http://dx.doi.org/10.4067/s0718-221x2022000100411.

Reinprecht L, Pop DM, Vidholdová Z, Timar MC (2019) Anti-decay potential of five essential oils against the wood-decaying fungi Serpula lacrymans and Trametes versicolor. Acta Facultatis Xylologiae Zvolen, 61(2): 63−72, Zvolen, https://doi.org/10.17423/afx.2019.61.2.06

Sharma S, Barkauskaite S, Duffy B, Jaiswal AK, Jaiswal S (2020) Characterization and Antimicrobial Activity of Biodegradable Active Packaging Enriched with Clove and Thyme Essential Oil for Food Packaging Application Foods, 9, 1117; https://doi.org/10.3390/foods9081117

Simunkova K, Hysek S, Reinprecht L, Sobotnik J, Liskova T, Panek M (2022) Lavender oil as eco-friendly alternative to protect wood against termites without negative effect on wood propertie.Scientific Reports 12:1909 | https://doi.org/10.1038/s41598-022-05959-5

Timar MC, Beldean EC (2022). Modification of Shellac with Clove (*Eugenia caryophyllata*) and Thyme (*Satureja hortensis*) Essential Oils: Compatibility Issues and Effect on the UV Light Resistance of Wood Coated Surfaces. *Coatings, 12(*10), 1591; https://www.mdpi.com/2079-6412/12/10/1591

Timar MC, Varodi AM, Gurău L (2016) Comparative study of photodegradation of six wood species after short-time UV exposure. Wood Sci Technol, 50:135–163, https://doi.org/10.1007/s00226-015-0771-3

Tolvaj L, Molnár Z, Németh R. (2013) Photodegradation of wood at elevated temperature: Infrared spectroscopic study. J. Photochem. Photobiol. B Biol. 2013;121:32–36. https://doi.org/10.1016/j.jphotobiol.2013.02.007

Tran-Ly AN, Heeb M, Kalac T, Schwarze F (2022) Antimicrobial of fungal melanin in combination with plant oil for the treatment of wood. Front. Mater. 9:915607. https://doi.org/10.3389/fmats.2022.915607

Yildiz G, Aydogmus Z, Cinar ME, Senkal F, Ozturk T (2017) Electrochemical oxidation mechanism of eugenol on graphene modified carbon paste electrode and its analytical application to pharmaceutical analysis. Talanta, 173 ,1–8, http://dx.doi.org/10.1016/j.talanta.2017.05.056

Oak timber cross-cutting based on fiber orientation scanning and mechanical modelling to ensure finger-joints strength

Soh Mbou Delin[1*], Besseau Benoit[2], Pot Guillaume[1], Viguier Joffrey[1], Marcon Bertrand[1], Milhe Louis[1], Lanvin Jean-Denis[3], Reuling Didier[3]

[1] Arts et Metiers Institute of Technology, LaBoMaP, UBFC, HESAM Université, F-71250 Cluny, France.
[2] Ducerf Groupe, Le Bourg, 71120 Vendenesse-lès-Charolles, France.
[3] FCBA, Allée de Boutaut BP227, 33028 Bordeaux, France.

E-mail: delin.soh_mbou@ensam.eu; benoit.besseau@ducerf.com; guillaume.pot@ensam.eu; joffrey.Viguier@ensam.eu; bertrand.marcon@ensam.eu; louis.milhe@ensam.eu; jean-denis.lanvin@fcba.fr; didier.reuling@fcba.fr

Keywords: cross-cutting, finger-joint, glued laminated timber, knot, slope of grain, oak

ABSTRACT

The mechanical properties of wood depend on its characteristics at different scales, in particular its knots and the orientation of its fibers. As wood is a highly anisotropic material, its strength and elastic properties are much better in the longitudinal direction of the fibers than in the perpendicular directions, so the orientation of the fibers is an extremely important parameter. Finger-jointing is a technique for joining sawn timbers into large panels for structural use, such as finger-jointed panels (GLT) and laminated timbers (CLT). In this study, the tensile strength of oak sawn timbers was modelled by considering the local fiber orientation obtained by using laser diffusion patterns onto the timber faces. Strength thresholds were established to ensure an equivalent mechanical performance to T11 tensile strength class, with the possibility of cross-sectional splitting if required. In addition, the tensile strength of the finger-joints was determined in accordance with (NF EN 14080 2013). Lamellas were assembled, glued and subjected to tensile tests, and the method was found to be satisfactory in terms of characteristic strength of the finger joints.

INTRODUCTION

Finger-jointed lamellas are used in the manufacture of large glued laminated timber (GLT) beams or cross laminated timber (CLT) panels. The aim of finger-jointing is to produce long timber elements while removing the weakest parts of the wood by cross-cutting. According to (NF EN 14080 2013), t finger joint strength is ensured by checking it's distance to a knot relatively to its diameter, d: "the grain at the cross-cut shall be approximately parallel to the axis of the board. The distance between the edge of a knot and the cross cut shall be at least 1.5 d. The grain deviation needs not to be checked if the distance is 3 d". It is important to note that the (NF EN 14080 2013) standard applies for GLT made of coniferous species or poplar, no standard for CLT nor GLT exists yet. For GLT made of hardwood, a standard is being prepared, but an European assessment document already exists (EAD 130320-00-0304 2018), using the exact same rule to ensure finger-joint strength. However, hardwood anatomy is very different from that of coniferous and thus knot limits are much more difficult to define on hardwoods. In addition, significant fiber deviation can appear whereas no knots are really visible in the considered board. Fiber deviation is very difficult to observe visually, as an operator is reduced to guessing based on the shapes drawn by growth rings, the parenchyma orientation (for the species for which they are visible by naked eye), and so on. As a result, this rule looks very difficult to apply and can be more restrictive for hardwoods than softwoods, because knots are often larger (requiring to remove more material when it comes to produce GLT or CLT applying the existing standard restrictions).

Fiber orientation can be measured by an industrial laser scanning machine. Due to the anisotropic scattering properties of wood, the resulting image of a laser spot on the wood surface takes the form of an ellipse. The major axis of this ellipse is aligned in the direction of the fiber orientation, a phenomenon known in the literature as the "tracheid effect" . This name derives from the first observations on softwoods (Nyström 2003) (Simonaho et al. 2002) and (Simonaho and Silvennoinen 2004), which is

based on the anisotropic scattering of concentrated laser light projected onto the wood surface (Daval et al. 2015; Purba et al. 2020) . (Olsson et al. 2019) and (Besseau 2021) suggested using fiber orientation measured from such scanners to ensure the finger-joint strength rather than knot diameter (d) or distance to knot. Both authors offering promising prospects for reducing material waste and improving the reliability of finger-jointed lamellas. (Olsson et al. 2019) defined a threshold of 8° to determine quantitatively when fibers are "approximately parallel to the axis of the board" as it is stated in (NF EN 14080 2013) standard. They found out that wasted material when cross-cutting Norway spruce can be decreased from 7.4% to 4% when applying a rule based on a minimum distance of 1.5 times d from the knot and a fiber deviation below 8°. However, the results were not validated by actual mechanical tests on the finger-joint. (Besseau 2021) dealt with French oak hardwood species measuring of fiber deviation on the timbers faces with a scanner around various finger-jointed samples, and then performed bending tests on them. This approach is similar to that of machine timber strength grading (EN 14081-2+A1 2022), like a non-destructive testing of finger-jointed lamellas. Thereby, the results were similar than in timber strength grading enabling to introduce an Indicating Properties (IP) that can be used as a threshold to exclude too weak finger joints. However, the objective of an industrial process would be to define cross-cutting positions on the basis of a threshold before performing the finger jointing, and not having to exclude lamellas with weak finger-joints.

The objective of the present work is to define a method based solely on fiber orientation scanning data to perform the cross-cutting operations, ensuring the resistance of both the finger-joints and the short-length wood elements between these joints, in the case of oak timber lamellas. Eventually, this approach aims to propose a standardized machine method to ensure finger-joints strength that could be more consistent and efficient than the current visual method, especially in the case of hardwood.

For this purpose, a method to compute the averaged 3D fiber orientation across the cross-section was firstly defined. This data was used to define an IP of tensile strength based on more than 900 tensile tests of oak sawn timber. Then, cross-cutting operations were performed, relying on this IP to define the appropriate cross-cutting positions which ensure both plain wood and finger-jointed strength of a given lamella strength class. The cross-cut elements were finger-jointed together, and finally tensile tests were performed to verify the method.

MATERIALS AND METHODS
Lists of main abbreviations used in this article

Table 1: Lists of main abbreviations used

Symbol / Abbreviation	Description
MoE	Modulus of elasticity (MPa)
E_0	Modulus of elasticity in the longitudinal direction of fibers (MPa)
E_{90}	Modulus of elasticity in the transversal direction of fibers (MPa), the material being considered as transversely isotropic (no difference between the radial and tangential material directions)
G_{LTrans}	Shear modulus in transversal-longitudinal plane of fibers (MPa)
ν_{LTrans}	Poisson's ratio characterizing the transversal strains in relation to longitudinal one
γ_{xyz}	Spatial orientation angle of a fiber element (°)
$f_{t,0,k}$	Axial tensile strength for wood (MPa)
$f_{t,j,k}$	Axial tensile strength for finger joints (MPa)
d	Knot diameter (mm)

Calculation of fiber orientation in sawn timber

So far, the fiber orientation has primarily been considered in the plane, that of the surface on which elliptical light scattering of the laser dots is captured. This means that the measured angle is actually the projection of the actual fiber orientation within the wood material.

As proposed in (Besseau 2021), in the present article and parallelly in (Pot et al. 2024), a 3D angle was calculated by interpolating the planar angles measured on the orthogonal large and narrow faces of a wood plank. Figure 1 illustrates the configuration in the coordinate system $(\vec{x}, \vec{y}, \vec{z})$ of a volume element of wood with the average fiber direction represented by the vector $(\vec{u}_{Fiber})$. The projection of this vector onto the $(\vec{x}, \vec{y})$ plane is denoted by $(\vec{u}_{xy})$ while the projection onto the $(\vec{x}, \vec{z})$ plane is noted as $(\vec{v}_{xz})$. The

three-dimensional orientation of a fiber element is determined by the angle γ_{xyz} between ($\vec{u}_{Fiber}$) and the normal vector ($\vec{n}$) which coincides with the ($\vec{x}$) direction, *i.e.* the axial direction of the plank. Coordinates b and c can be expressed in terms of a using Eq. 1 and 2.

$$b = a \times \tan(\alpha_{xy}) \tag{1}$$

$$c = a \times \tan(\beta_{xz}) \tag{2}$$

The 3D angle γ_{xyz} being expressed as a combination of α_{xy} and β_{xz} angles:

$$\vec{u}_{Fibre} \cdot \vec{x} = \|\vec{u}_{Fibre}\| \times \|\vec{x}\| \times \cos(\gamma_{xyz}) \tag{3}$$

$$\cos(\gamma_{xyz}) = \frac{\vec{u}_{Fibre} \cdot \vec{x}}{\|\vec{u}_{Fibre}\| \times \|\vec{x}\|} = \frac{a}{\sqrt{a^2+b^2+c^2}} \tag{4}$$

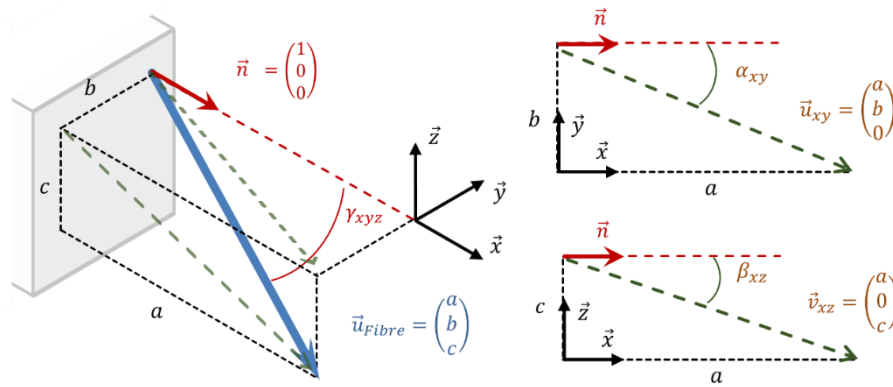$$\gamma_{xyz} = arc(\frac{1}{\sqrt{1+tan^2(\alpha_{xy})+tan^2(\beta_{xz})}}) \tag{5}$$

Figure 1: Setting a fiber element in space (Besseau 2021)

When considering a plank of rectangular cross-section, fiber orientation data on the four scanned faces provides what corresponds to the surface angles α_{xy} and β_{xz} for large and narrow faces, respectively. These planar angle measurements on the plank envelope are insufficient to calculate precisely angles γ_{xyz} within the timber volume. An interpolation method is proposed to overcome this difficulty, The missing values are located in the cross-sectional area of the plank, which is subdivided into $1 \times 1 \times 1$ mm³ cubes. For fibers beneath the two larger faces of a wood plank, the α_{xy} angles are directly derived from laser measurements, while the diving angles β_{xz} are only known at the ends. For fibers beneath the edges, the situation is reversed: the β_{xz} angles are known, but not the α_{xy} angles except at the ends. The missing components of angles α_{xy} et β_{xz} angles were respectively obtained through linear interpolation in thickness and width.

Local MoE based on fibers orientation
In practice, in the absence of an automatic and precise method for differentiating the radial direction from the tangential direction, a transverse isotropic model was preferred. The material properties were therefore defined as follows: E_0, the modulus of elasticity in the longitudinal direction of the fibers, was set at the 95ᵗʰ percentile of the experimental results of the study (Pot et al. 2024) used as a reference for the local modulus of elasticity in tension, i.e., 14620 MPa. The choice of the value of E_L is of little importance since relative comparisons were made; however, choosing such a value makes the absolute results of the modelled local moduli of elasticity consistent with the measured local moduli of elasticity, which is more practical. The value of E_0 influenced other material properties such as transverse modulus and shear modulus. Indeed, E_{90}, the modulus of elasticity in the direction orthogonal to the local fiber direction in this transverse isotropic model was calculated as the average of the orthotropic ratios E_R/E_L

and E_T/E_L from (Kretschmann 2010) and regularized by the actual 95th percentile longitudinal stiffness of the set (E_0, from (Pot et al. 2024)). G_{LTrans} the shear modulus in the transverse isotropic plane was similarly calculated as the average of the orthotropic ratios G_{LT}/E_L and G_{LR}/E_L from (Kretschmann 2010), and multiplied as before by E_0. Finally, ν_{LTrans} the Poisson's ratio in the transverse isotropic model, was taken equal to the average of the orthotropic Poisson's ratios ν_{LT} and ν_{LR} from (Kretschmann 2010), which is 0.4.

Table 2: Orthotropic mechanical properties of oak according to (Kretschmann 2010) and the corresponding simplified isotropic transverse mechanical properties introduced for the present research

E_L (MPa)	E_R (MPa)	E_T (MPa)	G_{LR} (MPa)	G_{LT} (MPa)	ν_{LR}	ν_{LT}
14000	2280	1010	1200	1100	0.37	0.43

E_0 (MPa)	E_{90} (MPa)		G_{LTrans} (MPa)		ν_{LTrans}	
14620	1718		1201		0.4	

These parameters can be arranged in the compliance matrix [S] of Eq. 1 from the local material system (L, Trans):

$$[S] = \begin{bmatrix} \frac{1}{E_0} & -\frac{\nu_{TransL}}{E_{90}} & 0 \\ -\frac{\nu_{LTrans}}{E_0} & \frac{1}{E_{90}} & 0 \\ 0 & 0 & \frac{1}{G_{LTrans}} \end{bmatrix} \tag{6}$$

For each element of the grid of interpolated angles γ_{xyz}, the material compliance matrix $[S]$ was rotated according to γ_{xyz}, by application of Eq. 7 using the basis changing transfer matrix (here being a rotation matrix $[T_\gamma]$ ⌧$\vec{x}$ to obtain the local compliance matrix in the specimen system of axes ($\vec{y}, \vec{z}, [S']$) (x, y, z) for each (x, y, z) location:

$$[S'] = [T_\gamma^{-1}] [S] [T_\gamma] = \begin{bmatrix} S'_{11} & S'_{12} & S'_{16} \\ S'_{12} & S'_{22} & S'_{26} \\ S'_{16} & S'_{26} & S'_{66} \end{bmatrix} \tag{7}$$

with $[T_\gamma] = \begin{bmatrix} Cos^2(\gamma_{xy}) & Sin^2(\gamma_{xy}) & 2 \times Cos(\gamma_{xy}) \times Sin(\gamma_{xy}) \\ Sin^2(\gamma_{xy}) & Cos^2(\gamma_{xy}) & -2 \times Cos(\gamma_{xy})Sin(\gamma_{xy}) \\ -Cos(\gamma_{xy}) \times Sin(\gamma_{xy}) & Cos(\gamma_{xy}) \times Sin(\gamma_{xy}) & Cos^2(\gamma_{xy}) - Sin^2(\gamma_{xy}) \end{bmatrix}$

the transfer matrix, from the local fiber coordinate system to the global specimen coordinate system, dependent on the fiber orientation γ_{xyz} obtained locally (abbreviated γ in the following). This gives E_x, the MoE in the main, lengthwise direction of the specimen ($\vec{x}$), as the inverse of the first coefficient of the compliance matrix $[S']$:

$$E_x(x, y, z) = \frac{1}{S'_{11}} = \frac{1}{\frac{1}{E_{90}} \sin^4(\gamma) + \frac{1}{E_0} \cos^4(\gamma) + \left(\frac{1}{G_{LTrans}} - 2\frac{\nu_{LTrans}}{E_0}\right) \sin^2(\gamma) \cos^2(\gamma)} \tag{8}$$

The average longitudinal stiffness of the plank was calculated for each position x within the volume of the plank by integrating over the surface of the cross-sectional area of the plank (Eq. 9).

$$E_{a,BT}(x) = \frac{\iint E_x dy dz}{b \times h} \tag{9}$$

The apparent axial MoE can be calculated as the harmonic mean of the localized MoE, i.e., the equivalent stiffness of series springs of individual stiffness $E_{a,BT}(x)$ (Eq. 9) averaged over a length of

90 mm (Olsson et al. 2019) (Eq. 10). This variable is the IP of the tensile strength that will be used in the present study.

$$E_{a,app,90,BT}(x) = 90/\int_{x-\frac{90}{2}}^{x+\frac{90}{2}} \frac{1}{E_{a,BT}(\xi)}\, d\xi \tag{10}$$

where app stands for apparent, BT refers to analytical beam theory and $d\xi = 1$ mm by numerical integration.

Sampling and digitalization

Two different samplings were used for the present study. The first one is constituted of 924 oak planks that were carefully selected following the guidelines of EN 14081-2 (2022), focusing on a specific quality representative of the resource that would be used in a sawmill to produce structural timber. This sampling was aimed to assess the mechanical modelling used to predict the tensile strength, which is explained in detail in (Pot et al. 2024).

The second sampling is specifically designed for this present study. It is constituted of 92 dry oak boards. They were coming from the same batch as the previous one, but with a single cross-section measuring 21×70 mm². The strategic objective is to use narrow width timber, which has lower economic cost, for the manufacture of glued timber such as finger-jointed lamellas. An industrial scanner (X-Scan, Luxscan), was used to analyze the boards in depth. By moving the boards longitudinally, the scanner provides detailed images of all four long faces, while capturing crucial data such as local density and fiber orientation. Fiber orientation data was obtained by detecting and processing laser points. Each face of the boards was subjected to a laser spot projected perpendicular to the surface, scattered into multiple laser spots via a diffractive optical element. The local orientation of the fibers is defined by the angle of the major axis of the ellipse, and these measurements over the entire surfaces (out of the front and end faces) of the boards were used to construct detailed maps. These maps were used for the visual representation of the data (Figure 2), and the MoE profile calculation along the board as described above.
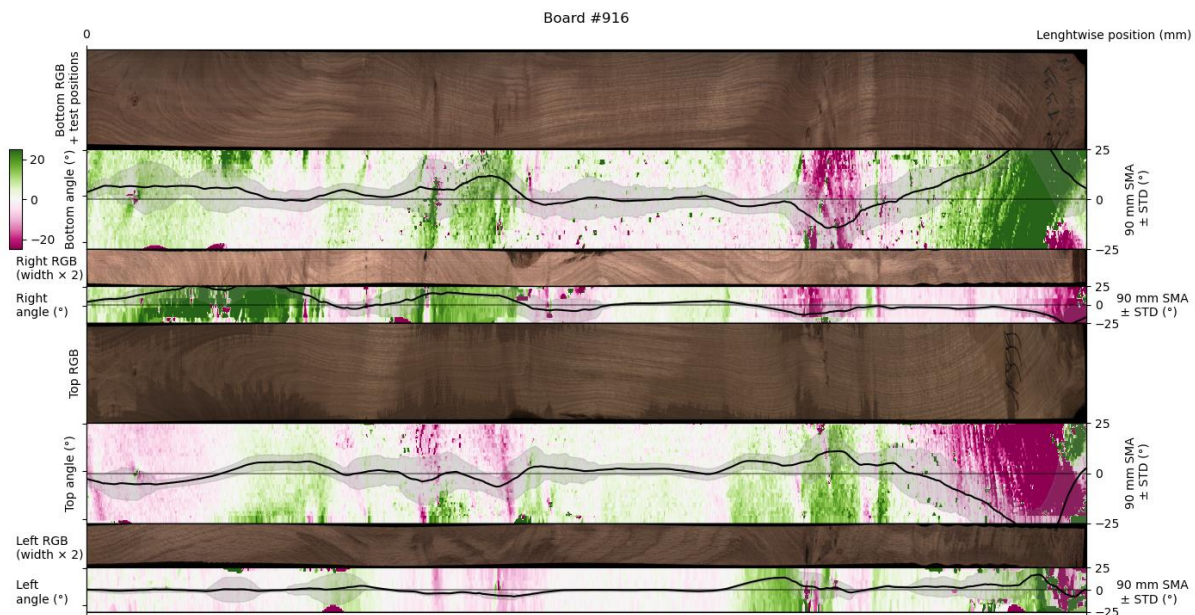
Figure 2: Visualisation of the distribution of angles on the 4 faces of a board. The profile shown is the average over 90 mm with an average standard deviation

Optimization of the boards cross-cutting for finger-jointing
Calculation of the tensile strength thresholds for lumber

This study focuses on developing a method ensuring the mechanical strength of finger-jointed lamellas corresponding to a single class. It was chosen to test the method for a tensile strength class T11 of (NF EN 338 2016) standard. This implies a strength of 11 MPa for clear wood and 16 MPa for the finger-

joints (NF EN 14080 2013). The IP thresholds corresponding to these requirements were defined as follows.

As explained in (Pot et al. 2024) for each of the 924 boards, the minimum value of $E_{a,app,90,BT}(x)$ along the profile was used as the IP representing the board tensile strength, which lead to the scatter plot of figure 3. For every possible IP threshold, the characteristic tensile strength of the boards whose IP values are higher than that threshold was calculated following (NF EN 14358 2016). The IP threshold value is the IP corresponding to the characteristic strength target (T11 class in this case). A similar analogy was made for finger-joints, following the strength condition recommended in the standard (NF EN 338 2016). The selected tensile class corresponds to thresholds of 6.55×10^3 MPa to ensure a wood tensile strength of 11 MPa (corresponding to the T11 class), and 9.23×10^3 MPa to ensure a finger-joint strength of 16 MPa (NF EN 14080 2013). They are shown in Figure 3.
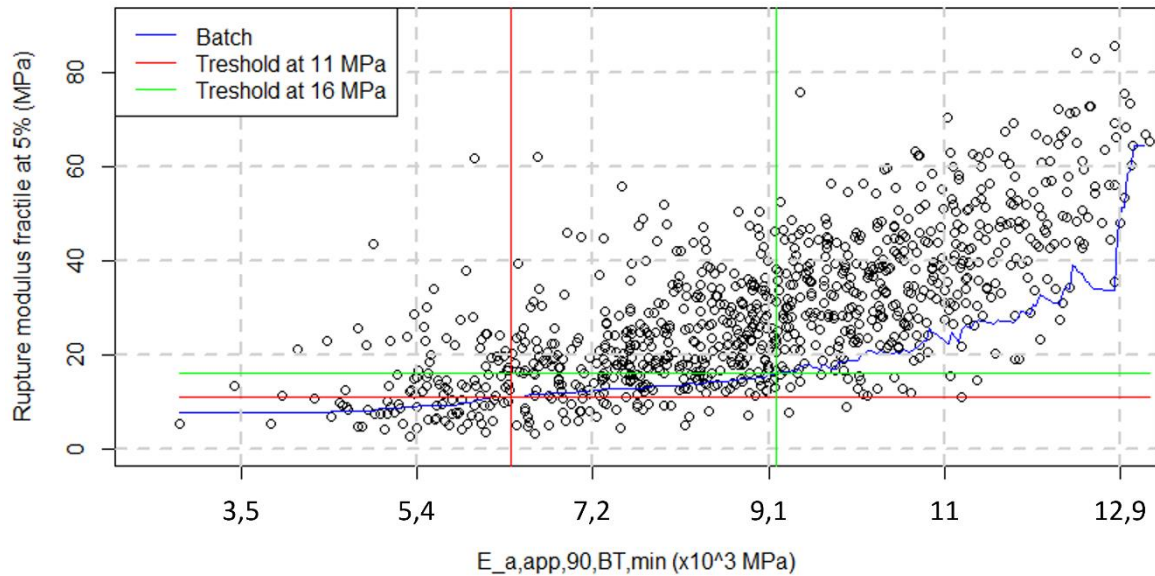

Figure 3: Tensile modulus of rupture thresholds determination

Digital twin for the cross cutting optimized localization

A numerical algorithm was developed to simulate the cross-cutting operation. The code is based on the stiffness profiles (Figure 4) to perform the cross-cutting in two distinct steps. The first step is to exclude areas of the board where the IP is below the threshold ensuring the wood strength of 11 MPa, while ensuring that the remaining pieces have a minimum IP at the ends ensuring the 16 MPa for finger-jointing.

The second step relates to the dimensions of the remaining pieces. The industrial finger-jointing line which was used imposes constraints on the length of the finger-jointed pieces, stipulating that they cannot be shorter than 250 mm or longer than 900 mm. So, the process consists of going through the profile in the sections to be kept. For each remaining piece longer than 900 mm, the cut is made at the 900 mm position, if the part at this position has a modulus at least equal to the finger-jointing threshold and that the rest of the piece is at least 250 mm long. If the remaining piece is less than 250 mm long, the 900 mm position is shifted backwards until the remaining wood is at least 250 mm long. In all cases, it is essential to ensure that the boards to be preserved are between 250 mm and 900 mm long, and that the cut-off positions have IP compatible with the required finger-joint strength. Figure 4 shows the cut-off positions as dotter red lines. In total, 236 cross cuts were performed from the 92 boards.

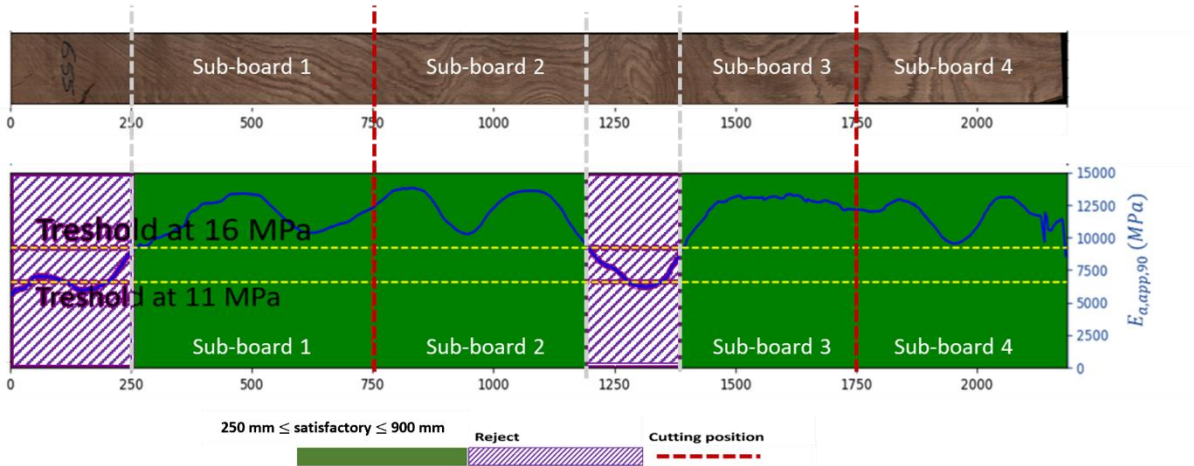|	Axial tensile strength (MPa)	Characteristic resistance (MPa)	Elastic modulus threshold (MPa)
Wood	$f_{t,0,k}$	11	6.55×10^3
Finger-joint	$f_{t,j,k}$	16	9.23×10^3

Figure 4: Example of the cross-cutting optimization algorithm application. In purple the removed parts, and in green the kept ones

A total of 79 finger-jointed lamellas of varying lengths, with a cross-section of 21×70 mm² were produced, cut into 183 small finger-jointed strips in order to test as many finger-joints as possible, while complying with the recommendations of the standard (NF EN 408+A1 2012). Figure 5 shows an example of a finger-jointed lamella made from the pieces of wood produced by cross-cutting. During finger-jointing, the ends of the boards are trimmed by 7 mm, and 10 mm long teeth are machined, with a pitch of 3.8 mm. These additional reduction were not anticipated during the cutting process, but the cut positions obtained ensure that the boards can be finger-jointed for at least 17 mm in the direction of reduction.
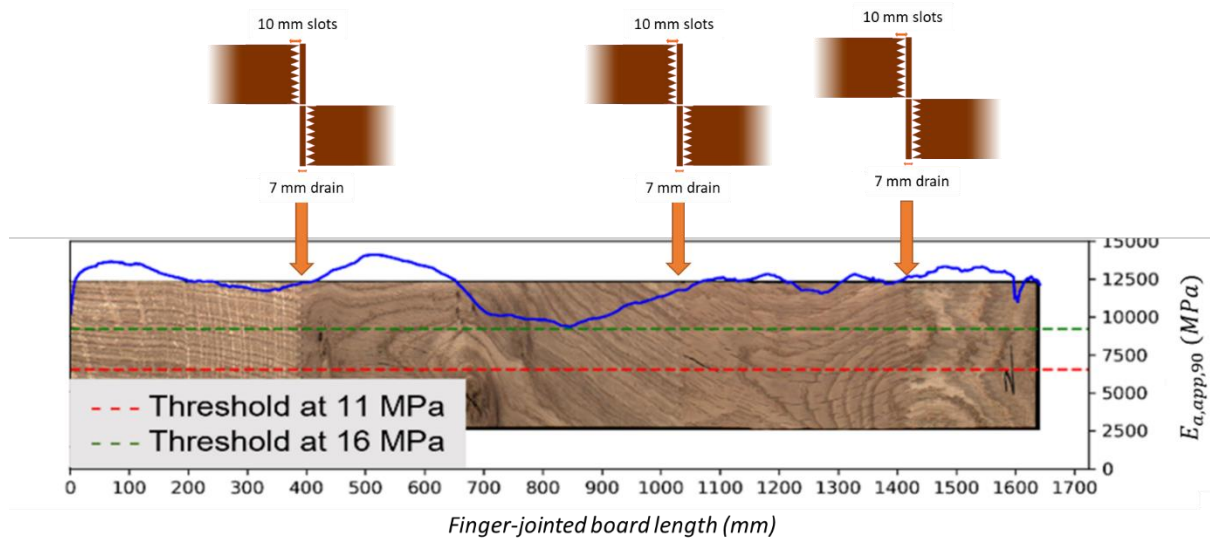
Figure 5: Example of a manufactured finger-jointed board glued with polyurethane (PU)

Tensile tests were carried out on the finger-jointed lamellas in accordance with (NF EN 408+A1 2012). Figure 6 shows the test conditions. Joint shall be located at the center span and the test length clear of machine grips is at least nine times the smallest cross-sectional dimension. The tensile strength ($f_{t,0}$) is given as function of the maximum load (F_{max}) and the cross-sectional area (A) by the following Eq. 7:

$$f_{t,0} = \frac{F_{max}}{A}$$ (7)
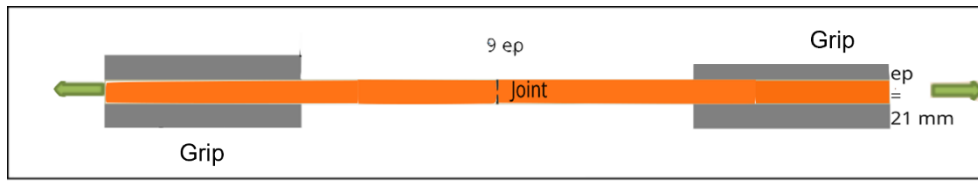
Figure 6: Tensile test

RESULTS AND DISCUSSIONS
Experimental strength of finger joints

Figure 7 shows the strength distribution obtained from finger-joints tensile tests. The average tensile strength for the full series is 28.69 MPa corresponding to a characteristic strength of 18.33 MPa.

However, two failure types can be distinguished. The test results were classified into two groups according to whether the lamella broke in the finger-joint or elsewhere in the wood other than in the finger-joint (see examples of failure types in Figure 7). The results are presented in Table 3. The failure rate of lamellae in finger-joints was 31%, whereas outside the finger-joints, it was 69 %. The corresponding characteristic strength were 20.41 MPa and 17.32 MPa, respectively. This behaviour was expected, because the full cross-cutting process was designed to ensure a wood tensile strength above $f_{t,0,k}$, which is 5 MPa lower than $f_{t,j,k}$. As a result, the chance of having a strength of the lamella within the 9 times h distance below $f_{t,j,k}$ is rather high, and finger-joints often exhibit a greater strength than the wood around it.
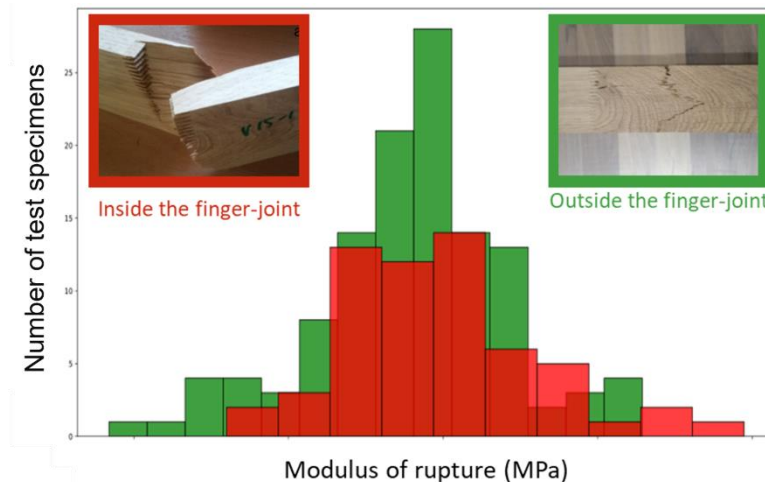
Figure 7: Histogram distribution of strength obtained from tensile tests: failure outside of the finger-joints (green); failure in the finger-joints (red) together with their post-failure figure

Table 3: Results of finger-joints tensile tests

Failure zone	Percentage	Characteristic strength
All	**100%**	**18.33 MPa**
Outside of the finger-joints	**69%**	**17.32 MPa**
In the finger-joints	**31%**	**20.41MPa**

The characteristic finger-joints tensile strength corresponds to the case when the failure occurs inside the finger-joints. The minimum value observed in this case is 15.99 MPa, which is sensibly equal to (even slightly higher than) the T11 class threshold. The absence of low-strength finger-joints could be due to the fact that the targeted class is low and thus the 16 MPa threshold is easy to reach. It is also important to remember that the profiles are averaged over a length of 90 mm centered, which can affect the precision of the cut positions and explain this behaviour.

Prediction of finger joint strength using image reconstruction and elastic modulus profiles

A Python code has been developed to reconstruct numerically the finger-joints. The code takes as input the positions and profiles of the finger-joints in the initial boards (boards before cutting), and assembles them exactly as it was done physically (Figure 8). The strength of the finger-joint is predicted as the minimum value between the average profile value in the left finger-joint (length of 10 mm) and the average profile value in the right finger-joint (length of 10 m) as finger-joints machining described in Figure 5.
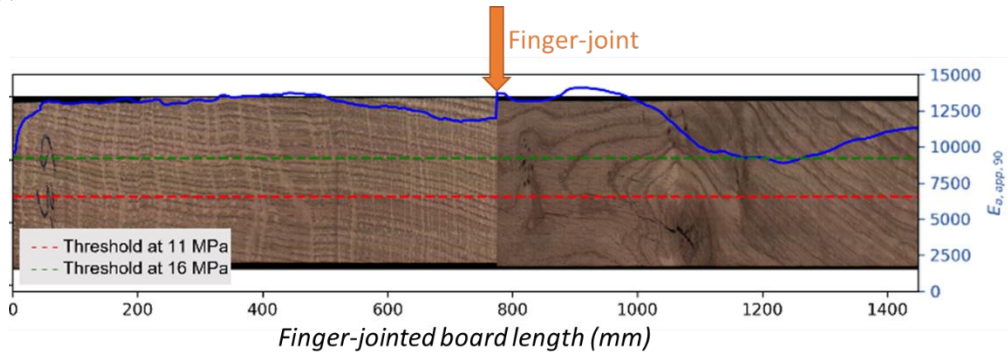
Figure 8: Example of a reconstructed finger-joint (in blue, $E_{a,app,90,BT}$)

The characteristic value of the finger-joint strengths predicted by image and profile reconstruction is 16.45 MPa, which satisfies the previously recommended joint strength condition.

Figure 9 illustrates the distribution between experimental and predicted strengths, along with the density in the finger-joints (averaged as above). The dispersion of points in the scatter plot could be attributed to the fact that the profile obtained by image reconstruction behaves as if the finger-joint assembly was perfect without discontinuity, while actually there is an effect of finger-joint and the strength of the adhesive used, which increases the strength within the finger-joints. Density may explain for some points that a predicted value may be low, for example (as the prediction is primarily based on fiber orientation), but high in reality due to its high density, and vice versa.

Figure 9: Correlation between tensile strengths (experimental and predicted) with their density

CONCLUSIONS

These findings represent another step forward, proposing an optimization method to cross-cut boards for finger-joints engineered wood products (CLT, GLT) based on surface fiber orientation scanning of the sawn boards. Since scans of the boards provide surface information, a very important phase is the interpolation within the volume and the mechanical global modelling of the board. The results show that the propose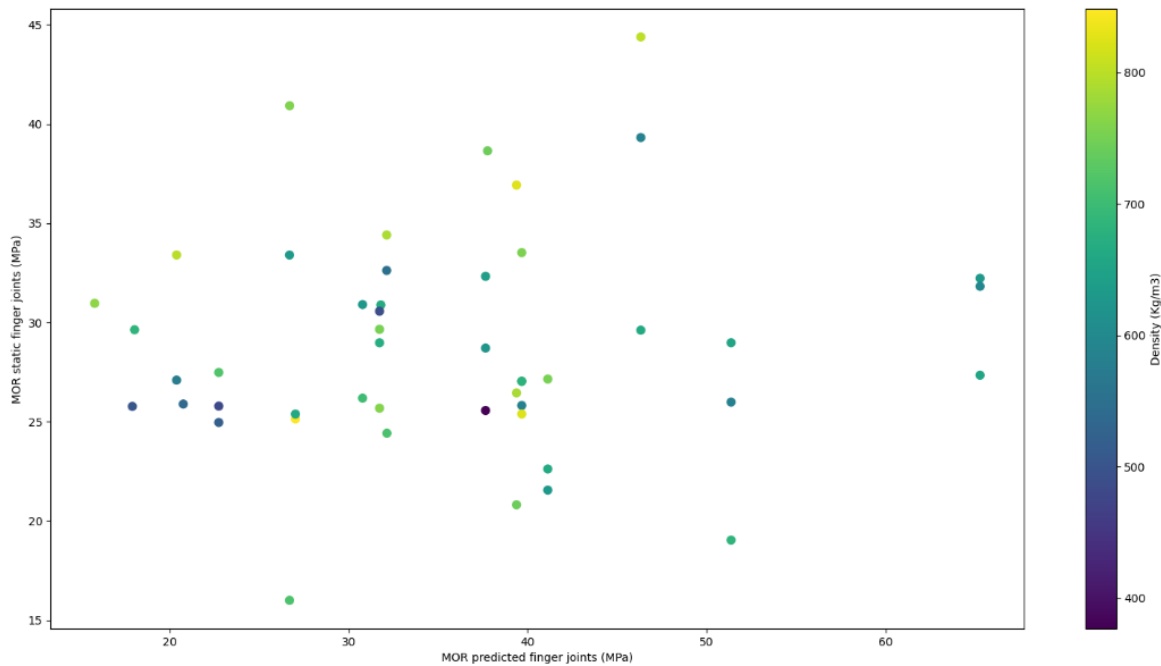d method effectively ensures lamellas of T11 class. However, the measured finger-joints characteristic tensile strength was higher than expected, suggesting that it could be improved to reduce material waste. A verification of the method could be made by applying it similarly for another class greater than T11 (T14 for example). Although the finger-joints strength prediction based on fiber orientation seems working, it's important to quantify the material yield because that's what will generate the added value in industrial context, thus, future works will focus on this matter.

ACKNOWLEDGEMENTS

REFERENCES

Besseau B (2021) Contribution au développement de procédés innovants pour une transformation plus efficiente du chêne. These de doctorat, HESAM

Daval V, Pot G, Belkacemi M, Meriaudeau F, Collet R (2015) Automatic measurement of wood fiber orientation and knot detection using an optical system based on heating conduction. Opt Express 23(26):33529–33539. https://doi.org/10.1364/OE.23.033529

EAD 130320-00-0304 (2018) Glued laminated timber made of solid hardwood

EN 14081-2+A1 (2022) Timber structures - Strength graded structural timber with rectangular cross section - Part 2: Machine grading; additional requirements for type testing

Kretschmann DE (2010) Wood handbook, chapter 05: mechanical properties of wood. For. Prod. Lab. Dep. Agric. For. Serv. Madison Wis. USA

NF EN 338 (2016) Structural timber - Strength classes

NF EN 408+A1 (2012) Timber structures - Structural timber and glued laminated timber - Determination of some physical and mechanical properties

NF EN 14080 (2013) Timber structures - Glued laminated timber and glued solid timber - Requirements. https://cobaz-afnor-org.rp1.ensam.eu/notice/norme/nf-en-14080/FA170492?rechercheID=2213043&searchIndex=1&activeTab=all#id_lang_1_descripteur Accessed 21 Jul 2021

NF EN 14358 (2016) Timber structures - Calculation and verification of characteristic values

Nyström J (2003) Automatic measurement of fiber orientation in softwoods by using the tracheid effect. Comput Electron Agric 41(1–3):91–99. https://doi.org/10.1016/S0168-1699(03)00045-0

Olsson A, Briggert A, Oscarsson J (2019) Increased yield of finger jointed structural timber by accounting for grain orientation utilizing the tracheid effect. Eur J Wood Wood Prod 77(6):1063–1077. https://doi.org/10.1007/s00107-019-01465-0

Pot G, Viguier J, Besseau B, Lanvin J-D, Reuling D (2024) Modelling tensile mechanical properties of oak timber from fibre orientation scanning for strength grading purpose. Sopron, Hungary

Purba CYC, Viguier J, Denaud L, Marcon B (2020) Contactless moisture content measurement on green veneer based on laser light scattering patterns. Wood Sci Technol 54:891–906. https://doi.org/10.1007/s00226-020-01187-0

Simonaho S-P, Palviainen J, Tolonen Y, Silvennoinen R (2002) Determination of wood grain direction from laser light scattering pattern. Opt Lasers Eng 41(1):95–103. https://doi.org/10.1016/S0143-8166(02)00144-6

Simonaho S-P, Silvennoinen R (2004) Light Diffraction from Wood Tissue. Opt Rev 11(5):308–311. https://doi.org/10.1007/s10043-004-0308-8

From Phenol-Lignin Blends towards birch plywood board production

Wilfried Sailer-Kronlachner [1,2], Peter Bliem [1,2*], Hendrikus van Herwijnen [1,2]

[1] Wood Kplus, Kompetenzzentrum Holz GmbH, Altenberger Strasse 69, 4040 Linz, Austria
[2] BOKU University of Natural Resources and Life Sciences Vienna, Institute of Wood Technology and Renewable Materials, Konrad Lorenz Strasse 24, 3430 Tulln, Austria

E-mail: w.sailer-kronlachner@wood-kplus.at; p.bliem@wood-kplus.at; e.herwijnen@wood-kplus.at

Keywords: lignin-phenol-formaldehyde (LPF) resin, phenol-lignin-blend (PLB), birch plywood, phenol substitution, lignin utilisation

ABSTRACT

One of the wood-based panel materials that is produced the most worldwide is plywood. Using the appropriate adhesive systems, veneer sheets from softwood or hardwood are pressed together to form the panel material. Especially in northern Europe, hardwood veneers are extensively used for plywood production. The adhesive systems commonly used within this industry are mostly fossil-based. Finding petroleum substitutes has become more important as concerns over the depletion of fossil fuels from an economic and socio-environmental standpoint have grown. The structural composition of the biopolymer lignin is similar to that of phenol-formaldehyde resins, which are often used in plywood production especially for exterior applications. Depending on the method, the pulp and paper industry produces large quantities of technical lignin as lignosulfonate or kraft lignin as a side-stream product. An obvious research strategy would be to replace the components of such resins with lignin. This opens up possibilities for partially bio-based adhesives in a variety of applications. The majority of technical lignins are available as lignin powder, which can cause issues during industrial use as powders are more difficult to handle than liquids. Problems or challenges include the powder's electrostatic behaviour, inadequate or very slow powder dissolution during synthesis of lignin-phenol-formaldehyde (LPF) resins, clump formation, valve clogging, and equipment contamination. In order to address these issues, Phenol-Lignin Blends (PLB), a mixture of lignin, phenol, and solvents, have been developed. One major benefit of using liquid blends instead of powdered lignin for LPF resin synthesis is their processability. The aim of this work is to demonstrate the potential of these Phenol-Lignin Blends in the efficient synthesis of LPF resins for use in plywood made out of birch hardwood.

INTRODUCTION

Veneer-based plywood panels have an odd number of veneers, with adjacent layers that are glued together and usually have fibre orientations perpendicular to one another. The worldwide production quantity of plywood and other commercially available wood-based panels are shown in Figure 16. Plywood is one of the most produced wood-based panel materials in the world.
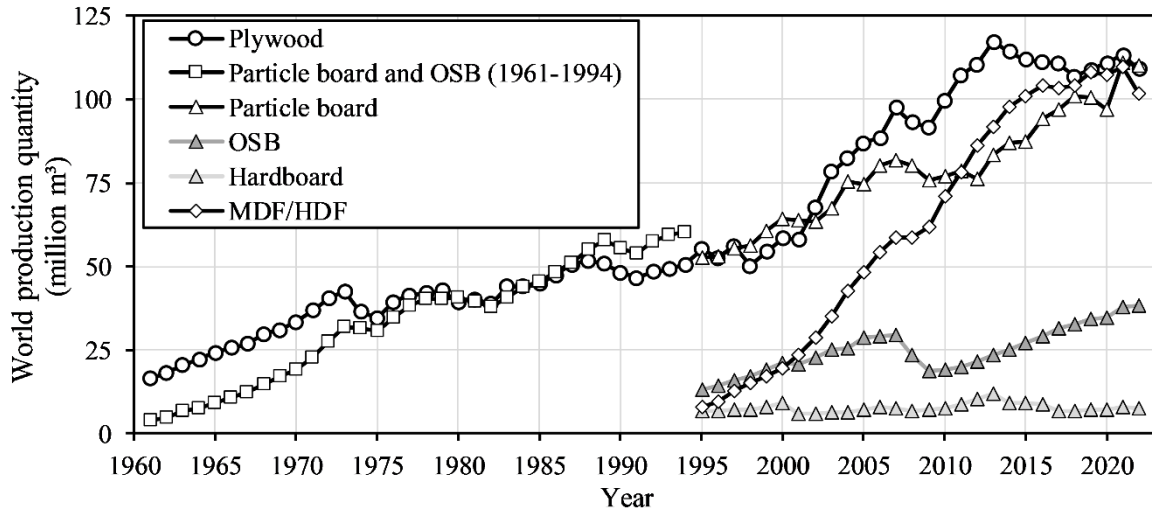

Figure 16: Worldwide production quantity of commercially available wood-based materials (1961-2021) (data from FAO stat accessed on 13th March 2024) (FAO STAT, 2024)

Due to the obvious anisotropic characteristics of wood, plywood panels consist of an odd number of glued veneer sheets to ensure symmetry. Wood veneers for plywood production can be sawed, sliced, or rotary peeled and can be made from both softwood and hardwood (Dunky & Niemz, 2002). The veneer-based products industry, especially in northern Europe, extensively uses birch wood for plywood production (Cakiroglu et al., 2019; Kallakas et al., 2020). The majority of Europe's hardwood plywood exports comes from birch plywood produced in Finland and the Baltic states (Abidov et al., 2018). Typical adhesive systems used in plywood production are urea- (UF), melamine- (MF) and phenol-formaldehyde (PF) resins depending on the use in interior or exterior applications (Curling & Kers, 2017; Ružiak et al., 2017). Formaldehyde and phenol, derived from fossil resources, are typically used in the synthesis of PF resins for plywood. Phenol is currently the primary raw material used in the synthesis of PF resins and it is the most expensive component used in this adhesive system (Xu & Ferdosian, 2017). An increasing number of socio-environmental and economic concerns regarding the depletion of fossil fuels have motivated the search for petroleum alternatives. The structural composition of lignin, which is a biopolymer composed of phenolic components, is comparable to that of synthetic phenol-formaldehyde resins (Sarika et al., 2020). Lignin derived from wood has gained significant interest in both science and industry in the last few decades. Various factors such as wood species, age, type of cell wall layer etc. influence the structure and concentration of lignin. Although lignin would have great potential, it is often not sufficiently utilized in terms of a cascading use. Lignin is frequently used to generate energy through combustion, particularly in the paper and pulp industry (Tribot et al., 2019). The substitution degree of the fossil-based phenol with sustainable lignin in adhesive applications is limited by the various requirements of the end products as well as processes. For instance, requirements for strength values have to be achieved in accordance with relevant product standards. The processability of the adhesives and sufficient reactivity must also be guaranteed. PF resins containing lignin as a phenol substitute are known as lignin-phenol-formaldehyde (LPF) resins. The use of Kraft lignin in phenol-formaldehyde resins has been investigated in several studies, but its industrial application remains limited (Karthäuser et al., 2021; Mansouri et al., 2007). Solt et al. (2019) observed significant variations in resin performance and reactivity when they replaced 50 wt.% of the phenol with pine kraft lignin. Ghorbani et al. (2018) investigated the performance of LPF resole resins for exterior-grade beech plywood prepared with commercial pine kraft lignin and a substitution rate of 40 wt.% of phenol by the lignin. They confirmed that the LPF resins used in their experiments fulfil standard threshold values. The possibility of replacing phenol with lignin in PF resin production for plywood

applications has been a topic of interest in the last decades (Danielson & Simonson, 1998; Karthäuser et al., 2024; Kouisni et al., 2011; Olivares et al., 1995). In most cases, the lignin is processed as a powder. Processing powdered lignin in the LPF resin synthesis encounters numerous difficulties and challenges. For instance, poor material flow due to clumping or bridging in storage silos could be one of these technical problems. Due to friction during transportation, lignin powder can become statically charged, which also makes handling more difficult. Pipes can also become clogged. Extended periods of lignin dissolution result in prolonged LPF resin synthesis times, which drastically lowers productivity and throughput. Liquid Phenol-Lignin Blends (PLB) are created out of lignin, phenol, and solvent (Carmona et al., 2021; Dunlop-Briere et al., 2023) in order to address these issues. The primary benefit is that, in contrast to the processing of powdered lignin, these blends can be processed as a pumpable liquid during the LPF resin production process, avoiding the previously discussed issues with powder handling. The purpose of this work is to show that these Phenol-Lignin Blends can be used to synthesise good LPF resins for plywood applications made out of birch hardwood.

MATERIALS AND METHODS
LPF resin syntheses and characterisation
This study focused on LPF resin syntheses using five PLBs (produced by Borealis, Austria). The Replacement Rate (RR = L / (L +P)) of phenol by kraft lignin was 50 wt.% in the blend. For the syntheses of the LPF resins, a round bottom flask was used to place the appropriate amount of liquid PLB. According to a defined LPF resin recipe, further reagents, such as 37% formaldehyde solution and 50% sodium hydroxide solution, were added to produce the LPF resins. The molar ratio of (F) formaldehyde to (P) phenol (F/P) was 2.5, while a ratio of 0.815 was used for (NaOH) sodium hydroxide to (P) phenol (NaOH/P). Sodium hydroxide was added in two stages, where 43 wt.% of the total amount was added in the first step and the remaining 57 wt.% in a second step. As a reference, two LPF resins were synthesised in accordance to the conventional method using powdered kraft lignin. For this, the corresponding quantities of pure phenol, deionised water, 37% formaldehyde solution, 50% sodium hydroxide solution as well as the powdered lignin were added in a round bottom flask according to a similar LPF recipe as before. The same molar ratios were used as in the experiments with the PLBs. In accordance to the LPF resin recipes, the calculated solid contents of the LPF resins to be produced was set to 60%. The condensation of the various LPF resins was conducted until a viscosity of 500 mPa*s was reached. Viscosity was measured with a rheometer (MCR 302, Anton Paar GmbH, Austria) equipped with a cone-plate measuring system (CP 50–1, Anton Paar GmbH, Austria) at a constant measuring temperature of 25°C and shear rate of 100 s^{-1}. The gap size between the cone and plate was set to 0.101 mm resulting in a LPF resin test volume of 0.57 ml. When reaching the desired end viscosity of 500 mPa*s, little amount of industrial grade urea (0.3 wt.%) was added to the LPF resins to reduce the free formaldehyde content. The post-addition of urea to a phenolic resin is, among other effects, a common method to decrease the content of free formaldehyde (Pizzi & Ibeh, 2014). Due to the high pH of phenolic resins, urea only reacts with the resin's free formaldehyde to form methylol groups, which then stop reacting further. The final LPF resins were then cooled down to room temperature in a cold-water bath.
The following properties of the LPF adhesives produced were investigated:
- solid content
- final viscosity
- pH
- free formaldehyde content
- bonding strength development

In case of the solid content, a double determination was conducted, referring to EN 3251 standard, where approx. 1 g of each LPF resin was weighed in an aluminium dish. The samples were then dried in a ventilated oven at 135°C for 1 hour until constant weight was reached. Using the previously mentioned test parameters for viscosity determination, the final viscosity of the LPF resins was measured. For measuring the pH, the final resins were diluted with deionised water in a weight ratio of 50:50 (EN ISO 8975). The pH was measured with a pH-meter equipped with a glass electrode. Conforming to EN ISO 11402, the free formaldehyde was determined employing the hydroxylamine hydrochloride method, however, due to the poor solubility of LPF resins, demineralised water was used instead of methanol or

a mixture of propan-2-ol and water as suggested in the standard. Therefore, five grams of the final resins were diluted with 50 ml of demineralised water. After dissolving the resins, the electrode of the pH-meter was introduced and the pH was adjusted to 3.5 using 1 mol/l hydrochloric acid. Then 25 ml of 10% hydroxylamine hydrochloride solution was pipetted to the mixture and stirred for 10 minutes. By titration with a 1 mol/l solution of sodium hydroxide, the pH was adjusted to 3.5 again using an auto-titrator. The amount of sodium hydroxide needed to bring the pH back to 3.5 was used for the free formaldehyde content calculation. The same procedure was repeated as a blank test, using the same reagents as before, but without the LPF resins. The free formaldehyde content was calculated according to the equation (Eq. 1):

$$\omega(CH_2O, free) = \frac{3c*(V_1 - V_0)}{m} \qquad (1)$$

where
c…is the actual concentration (mol/l) of the sodium hydroxide solution used
V_0…is the volume (ml) of the sodium hydroxide solution determined in the blank test
V_1…is the volume (ml) of the sodium hydroxide solution determined in the test with the LPF resin
m…is the mass (g) of the resin test portion

The bonding strength development of the produced LPF resins was analysed using Automated Bonding Evaluation System (ABES) in accordance to the standard ASTM D7998-15. The effect of press temperature and press time on the development of cohesive strength can be measured by applying a tensile load to a lap shear sample bonded with the adhesive of interest. Two sliced veneers out of beech wood with dimensions of 117×20×0.5 mm³ (length×width×thickness) were pressed together. The specific amount of applied LPF resin to the overlap area (5×20 mm² length×width) was 200 g/m². For the experiments, a constant pressing temperature of 120°C at different pressing times (i.e. 0.5, 1, 2, 3, 5, 10 and 20 minutes) and a specific pressure of 1.6 MPa was used. After applying pressure and heat, the adhesive joint was tested in the still hot/warm state of the bondline. Based on the recorded maximum tensile force for pulling apart the bonded samples and the actual measured overlapping area of the joint, the dry bond strength was calculated.

Birch plywood preparation and testing

Plywood panels were produced to further characterise the performance of the various LPF resins. In order to increase the viscosity of the resins, dry wheat flour and deionised water were added with a weight ratio of 100:10:10 (LPF adhesive:dry wheat flour:deionised water). To verify the effect of adding the additive, the viscosity was measured before the addition and after a waiting period of one hour after the addition using the same viscosity measuring method as described before. The addition of additives in industrial applications not only enhances the processing conditions (e.g. viscosity and flow behaviour) but also decreases the consumption of raw materials, thereby lowering the cost of the adhesive (Dunky & Niemz, 2002). Plywood panels out of 7 layers of rotary peeled birch veneers (1.6 mm thickness) with dimensions of 480 × 480 mm² (length × width) were pressed together using a hot press (LZT-OK 175L, Langzauner GmbH). The additive-modified LPF resins were applied on one side of each veneer with a specific resin application quantity of 155 g/m². The glued and stacked veneers were then hot-pressed at 135°C at a specific pressure of 1.6 MPa. On industrial scale phenol-formaldehyde (PF) bonded plywood panels are usually stacked in a pile as hot as possible in order to complete the thermal curing of the phenolic resins outside the press (Dunky & Niemz, 2002). In addition to the almost complete chemical curing of the adhesive, the final bonding strength and the hygroscopic properties could be improved and a reduced formaldehyde release could be achieved (Dunky & Niemz, 2002). For simulating these post-curing or stack maturation procedure, the prepared LPF-bonded plywood panels were stacked in the still hot/warm but switched off press (approx. 130°C) to cool down to room temperature. To record the temperature of the plywood stack over time, temperature sensors were placed at the centre of the stack as well as at the top and bottom of the plywood stack to the hot press. The plywood panels were then stored in a controlled environment (65% relative humidity and 20°C room temperature) for several days, before lap-joint specimens were cut in accordance to the plywood standard EN 314-1. The bonding quality of the plywood panels was tested by examining both the centre and outer layers. Two different

pre-treatments according to EN 314-1 of the lap-joint plywood specimens were carried out before testing, pre-treatment 5.1.2 (bonding class 2 – covered exterior applications) as well as pre-treatment 5.1.3 (bonding class 3 – non-covered exterior applications). The lap-joint specimens were then tested using a universal testing machine Z020 (Zwick GmbH & Co. KG, Ulm, Germany) equipped with a 20 kN load cell. The tensile force was applied constantly at a speed of 1 mm/min. The tensile shear strength (in N/mm²) was calculated by the maximum occurring tensile force (in N) related to the overlapping area measured before the pre-treatment (in mm²). In accordance to the standard, the wood failure content was determined visually. For each variant eight lap-joint plywood specimens were tested and analysed.

RESULTS AND DISCUSSION
LPF resin characteristic

The main resin characteristics (i.e. solid content, final viscosity, pH and free formaldehyde content) of the LPF resins produced with the Phenol-Lignin Blends as well as powdered lignin are listed in Table 4. The solid content reached values between 53.9% and 54.8% (LPF 1-5 prepared with PLB). Due to the releasing water during the condensation reaction, the measured solid content is slightly lower compared to the calculated value of 60% according to the LPF resin recipe. Both LPF resins which were produced by the conventional procedure using powdered lignin (LPF 6-7) showed slightly lower solids contents. One possible reason for this could be a residual amount of water in the powdered lignin. The final viscosity of the adhesives was between 535 mPa*s and 592 mPa*s, slightly higher than the desired 500 mPa*s, which indicates a minor further condensation during the cooling process of the LPF resins. These properties as well as the uniform pH of the resins (i.e. 10.2) and the measured free formaldehyde content between 0.2% and 0.3% show the high degree of reproducibility using the PLBs for LPF resin syntheses. Good reproducibility was also demonstrated by the LPF resins made using pulverised lignin (Table 4). One of the main advantages of using PLBs for LPF resin production is the significantly shorter total synthesis time. The syntheses of LPF resins using powdered lignin required on average 204 minutes, approximately 24% more time than resins prepared with PLBs, which required on average only 164 minutes. A possible industrial application of the Phenol-Lignin Blends would have a distinct advantage over the usual procedure, in which lignin is added in powder form during the production of the LPF resin.

Table 4: Main LPF resin properties

LPF resin	LPF 1[a]	LPF 2[a]	LPF 3[a]	LPF 4[a]	LPF 5[a]	LPF 6[b]	LPF 7[b]
Solid content [%]	54.8	54.3	53.9	54.8	54.2	52.8	53.3
Final viscosity [mPa*s]	553	580	582	584	535	592	584
pH	10.3	10.2	10.2	10.2	10.2	10.2	10.3
Free formaldehyde content [%]	0.2	0.3	0.2	0.2	0.2	0.2	0.2

[a]*LPF resins prepared with PLB;* [b]*LPF resins prepared with powdered lignin*

The investigation of the bonding strength development using ABES at different pressing times and a uniform pressing temperature of 120°C, reflects the clear reproducibility of the LPF resins prepared with the PLBs indicated by the small standard deviation in Figure 17. It displays the mean tensile shear strengths of the two LPF resin groups investigated (PLB vs. powdered lignin). However, no major differences in strength can be observed between the two groups of LPF resins.

In addition, the results demonstrate a significant decrease in the reactivity of the synthesized LPF resins compared to conventional PF resins, which is in line with the results of similar experiments conducted by Solt et al. (2019). Higher strength properties of the LPF resins can be expected if tested in the cooled state of the adhesive joint instead of performing the experiments in the still hot/warm state. This can be attributed to the thermoplastic behaviour of the lignin (Solt et al., 2019).
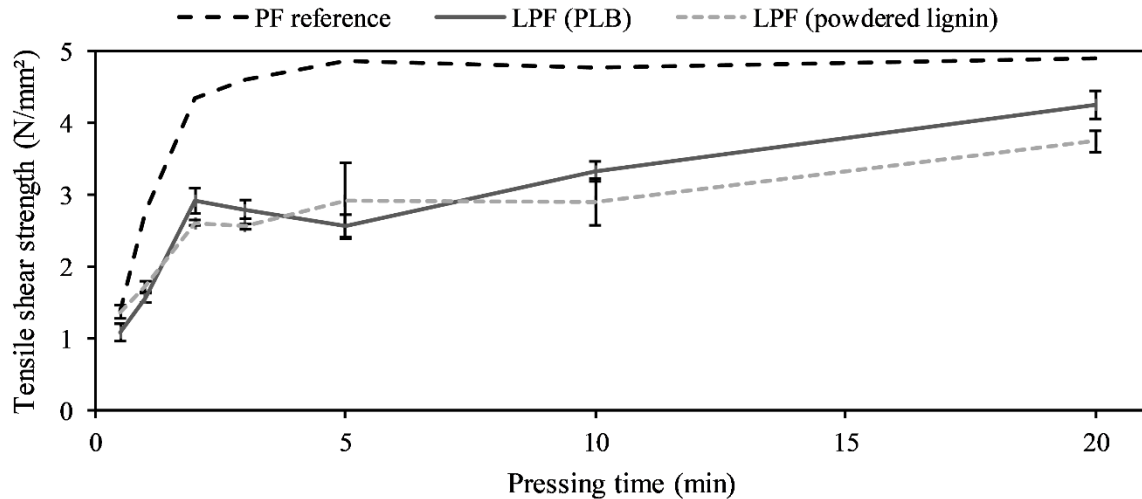
Figure 17: Average bonding strength development of the produced LPF resins using PLB and powdered lignin compared to a conventional PF resin at a pressing temperature of 120°C (error bars represent the standard deviation of each resin group)

Birch plywood performance

The viscosity of the various LPF resins synthesized with the PLBs (LPF 1-5) was increased by 61% on average after wheat flour and deionised water were added to the resins (52% in case of the powdered lignin-based LPF resins LPF 6-7). The detailed viscosity values are listed in Table 5. The production process in the plywood industry involves stacking boards while still hot, which results in additional curing, which was also simulated within this experiment.

Figure 18 illustrates the temperature curve of the stack maturation process in a plywood pile. The "Top and bottom side of the plywood pile" curve represents the mean temperatures between the surfaces between the first and the last plywood panel and the metal pressing surface. The starting temperature for the post-curing simulation was 130°C. The "Centre of the plywood pile" curve starts at approx. 40°C, which indicates that the surface temperature of each plywood panel had already cooled down beforehand. The entire plywood pile was heated up again by the still hot/warm metal pressing surface and the increased temperature in the core of each individual plywood panel. This resulted in an increase in temperature in the centre of the entire pile as indicated by the temperature curve "Centre of the plywood pile" in Figure 18 up to approx. 100°C in one hour. The temperature then slowly decreased, however still faster than data from industry published in literature (Dunky & Niemz, 2002). The post-curing or maturation simulation of the LPF resins is likely to improve the plywood panels bonding qualities, especially their increased water resistance.

Table 5: Viscosity of the LPF resins before and after the addition of deionised water and wheat flour and a waiting period of one hour

LPF resin	LPF 1[a]	LPF 2[a]	LPF 3[a]	LPF 4[a]	LPF 5[a]	LPF 6[b]	LPF 7[b]
Resin viscosity before the additive addition [mPa*s]	553	580	562	571	523	482	562
Resin viscosity after the additive addition and a waiting period of one hour [mPa*s]	901	938	928	913	817	708	882
Relative increase [%]	63	62	65	60	56	47	57

[a]*LPF resins prepared with Lignin-Phenol-Blend (PLB);* [b]*LPF resins prepared with powdered kraft lignin*
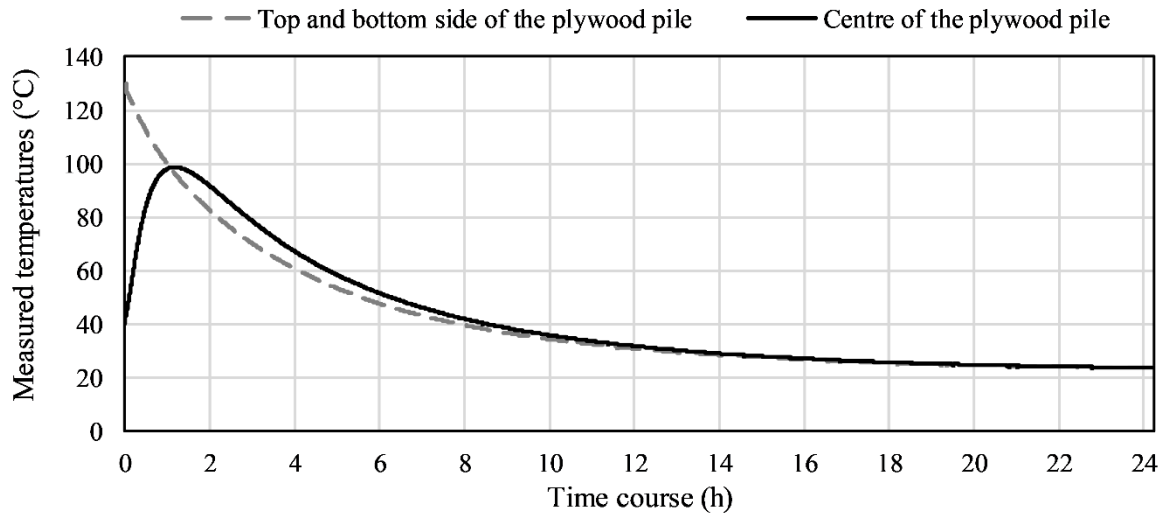
Figure 18: Measured temperatures on the top and bottom side of the plywood pile as well as in the centre for stack maturation/post-curing simulation of the plywood panels

The bonding quality of the plywood panels produced was tested for the middle and outer layers of each plywood (Figure 19). The testing was in accordance with the plywood standard EN 314-1. In case for the bonding class 2 (covered exterior applications) all LPF resins investigated fulfilled the minimum tensile shear strength requirement of 1 N/mm² according to the standard EN 314-2. For the PLB-produced LPF resins (LPF 1-5), the average tensile shear strength was slightly higher for the tested outer layer (1.64 N/mm²) than for the middle layer (1.57 N/mm²). For the powdered lignin-based LPF resins (LPF 6-7) the mean tensile shear strength of the outer layer was 1.49 N/mm², while the middle layer reached a slightly higher average strength value of 1.65 N/mm². Due to the obvious stricter pre-treatment, the test specimens of bonding class 3 (non-covered exterior applications) showed lower strength values than the specimens of bonding class 2. Nevertheless, for bonding class 3, the average tensile shear strength of the five LPF resins prepared with the PLBs (LPF 1-5) was 1.14 N/mm² for the middle layer and 1.32 N/mm² for the outer layer, while powdered lignin-based LPF resins (LPF 6-7) reached similar mean values (middle layer: 1.09 N/mm²; outer layer: 1.32 N/mm²). No distinct difference between the two groups, LPF resins prepared with PLBs vs. powdered lignin, could be observed. The corresponding wood failure for each test specimen that was examined was 0%.
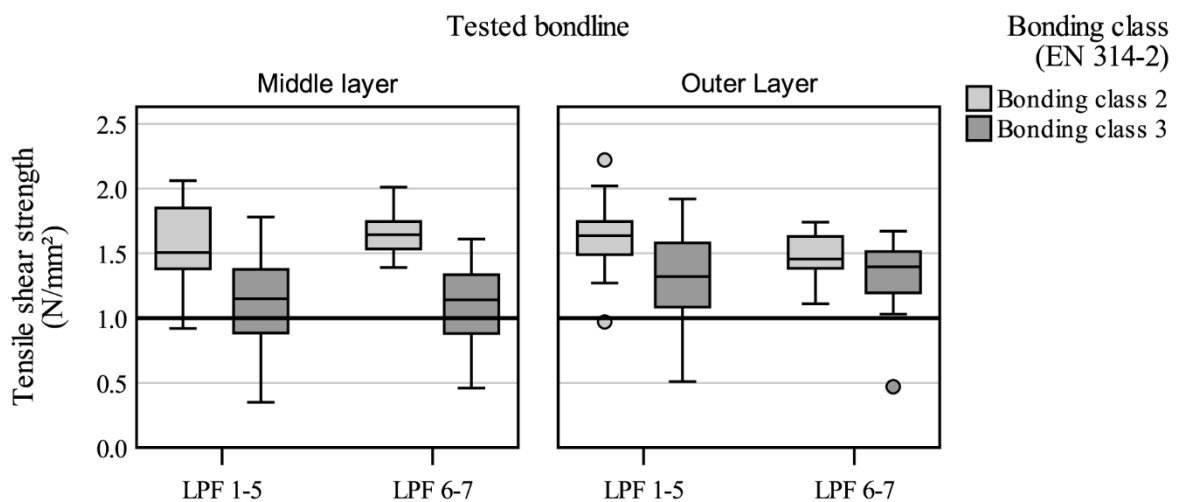

Figure 19: Combined results of tensile shear tests of plywood produced with the different LPF resins (LPF 1-5 synthesised using PLBs; LPF 6-7 synthesised using powdered lignin) for the middle and outer layer of the plywood as well as for the bonding classes 2 and 3. (Tested in accordance to EN 314-1; LPF 1-5 N=40 specimens/boxplot; LPF 6-7 N=16 specimens/boxplot)

CONCLUSIONS

The experiments show that lignin has the potential to replace the fossil-based raw material phenol in the production of plywood based on hardwood veneers. In this first experiment, 50% of the phenol could be substituted by the biopolymer lignin, while the minimum bonding strength requirement of 1 N/mm² could be still reached for the two bonding classes 2 and 3. In addition, important adhesive properties (solid content, pH, viscosity, free formaldehyde content) fulfil the requirements for processing the LPF resins in the plywood industry. The use of liquid PLB instead of powdered lignin in the synthesis of LPF resins offers enormous potential for increasing the utilisation of renewable resources. Not only can technical problems such as poor material flow, static charging, pipe clogging or long dissolving times of the powdered lignin be eliminated, but faster throughput times can also be achieved when PLBs are used in LPF resin syntheses. It can be assumed that the use of these PLBs would also be suitable in the production of laminated veneer lumber (LVL) due to the very similar processes compared to plywood.

ACKNOWLEDGEMENTS

REFERENCES

Abidov, O., Gaston, C., Novoselov, I., Abt, K., Glavonjić, B., Oliver, R., Aguilar, F., Koskinen, A., Pahkasalo, T., Akim, E., Kottwitz, K., Palacín, J., Alderman, D., Lombard, B., Sudekum, H., Dmitriev, V., Luppold, W., Taylor, R., Eastin, I., . . . Fernholz, K. (2018). *UNECE/FAO Forest Products Annual Market Review 2017-2018*. U. Nations.

Cakiroglu, E. O., Demir, A., & Aydin, I. (2019). Comparison of Birch and Beech Wood in Terms of Economic and Technological Properties for Plywood Manufacturing. *Drvna Industrija*, *70*(2), 169-174. https://doi.org/10.5552/drvind.2019.1828

Carmona, R. R., Dicke, R., Herwijnen, H. v., Zeppetzauer, F., Kamm, B., & Solt-Rindler, P. (2021). *Stable lignin-phenol blend for use in lignin modified phenol-formaldehyde resins*.

Curling, S. F., & Kers, J. (2017). Wood as bio-based building material. In D. Jones & C. Brischke (Eds.), *Performance of Bio-based Building Materials* (1 ed., pp. 21-96). Woodhead Publishing. https://doi.org/10.1016/B978-0-08-100982-6.00002-1

Danielson, B., & Simonson, R. (1998). Kraft lignin in phenol formaldehyde resin. Part 1. Partial replacement of phenol by kraft lignin in phenol formaldehyde adhesives for plywood. *Journal of Adhesion Science and Technology*, *12*(9), 923-939. https://doi.org/10.1163/156856198X00542

Dunky, M., & Niemz, P. (2002). *Holzwerkstoffe und Leime: Technologie und Einflussfaktoren*. Springer Berlin Heidelberg.

Dunlop-Briere, A., René, D., Carmona, R. R., Nerger, I. C., Krabác, L., Birgit, K., Franz, Z., Hendrikus, v. H., Pia, S.-R., & Bliem, P. (2023). *Method for preparing a stable lignin-phenol blend and a stable lignin-phenol blend obtained by said method*.

FAO STAT. (2024). Food and Agriculture Organization of the United Nations. Retrieved 13.03.2024 from https://www.fao.org/faostat/en/#home

Ghorbani, M., Liebner, F., van Herwijnen, H. W. G., Solt, P., & Konnerth, J. (2018). Ligneous resole adhesives for exterior-grade plywood. *European Journal of Wood and Wood Products*, *76*(1), 251-258. https://doi.org/10.1007/s00107-017-1249-9

Kallakas, H., Rohumaa, A., Vahermets, H., & Kers, J. (2020). Effect of Different Hardwood Species and Lay-Up Schemes on the Mechanical Properties of Plywood. *Forests*, *11*(6), 649. https://www.mdpi.com/1999-4907/11/6/649

Karthäuser, J., Biziks, V., Mai, C., & Militz, H. (2021). Lignin and Lignin-Derived Compounds for Wood Applications—A Review. *Molecules*, *26*(9), 2533. https://www.mdpi.com/1420-3049/26/9/2533

Karthäuser, J., Raskop, S., Slabohm, M., & Militz, H. (2024). Modification of plywood with phenol–formaldehyde resin: substitution of phenol by pyrolysis cleavage products of softwood kraft lignin. *European Journal of Wood and Wood Products*. https://doi.org/10.1007/s00107-023-02029-z

Kouisni, L., Fang, Y., Paleologou, M., Ahvazi, B., Hawari, J., Zhang, Y., & Wang, X.-M. (2011). Kraft lignin recovery and its use in the preparation of lignin-based phenol formaldehyde resins for plywood. *Cellulose Chemistry and Technology*, *45*, 515-520.

Mansouri, N.-E. E., Pizzi, A., & Salvado, J. (2007). Lignin-based polycondensation resins for wood adhesives. *Journal of Applied Polymer Science*, *103*(3), 1690-1699. https://doi.org/https://doi.org/10.1002/app.25098

Olivares, M., Aceituno, H., Neiman, G., Rivera, E., & Sellers, T., Jr. (1995). Lignin-modified phenolic adhesives for bonding radiata pine plywood. *Forest Products Journal*, *45*(1), 63. https://www.proquest.com/scholarly-journals/lignin-modified-phenolic-adhesives-bonding/docview/214635415/se-2?accountid=26468

Pizzi, A., & Ibeh, C. C. (2014). Phenol–Formaldehydes. In H. Dodiuk & S. H. Goodman (Eds.), *Handbook of Thermoset Plastics (Third Edition)* (pp. 13-44). William Andrew Publishing. https://doi.org/10.1016/B978-1-4557-3107-7.00002-6

Ružiak, I., Igaz, R., Kristak, L., Réh, R., Mitterpach, J., Očkajová, A., & Kučerka, M. (2017). Influence of Urea-formaldehyde Adhesive Modification with Beech Bark on Chosen Properties of Plywood. *Bioresources*, *12*, 3250-3264. https://doi.org/10.15376/biores.12.2.3250-3264

Sarika, P. R., Nancarrow, P., Khansaheb, A., & Ibrahim, T. (2020). Bio-Based Alternatives to Phenol and Formaldehyde for the Production of Resins. *Polymers*, *12*(10), 2237. https://www.mdpi.com/2073-4360/12/10/2237

Solt, P., van Herwijnen, H. W. G., & Konnerth, J. (2019). Thermoplastic and moisture-dependent behavior of lignin phenol formaldehyde resins. *Journal of Applied Polymer Science*, *136*(40), 48011. https://doi.org/https://doi.org/10.1002/app.48011

Tribot, A., Amer, G., Abdou Alio, M., de Baynast, H., Delattre, C., Pons, A., Mathias, J.-D., Callois, J.-M., Vial, C., Michaud, P., & Dussap, C.-G. (2019). Wood-lignin: Supply, extraction processes and use as bio-based material. *European Polymer Journal*, *112*, 228-240. https://doi.org/10.1016/j.eurpolymj.2019.01.007

Xu, C., & Ferdosian, F. (2017). Lignin-Based Phenol–Formaldehyde (LPF) Resins/Adhesives. In C. Xu & F. Ferdosian (Eds.), *Conversion of Lignin into Bio-Based Chemicals and Materials* (pp. 91-109). Springer Berlin Heidelberg. https://doi.org/10.1007/978-3-662-54959-9_6

Flatwise bending strength and stiffness of finger jointed beech lamellas (*Fagus sylvatica,* L.) using different adhesive systems and effect of finger joint gap size

Hannes Stolze[1*], Adefemi Adebisi Alade[1], Holger Militz[1]

[1] Georg-August-University Göttingen, Department of Wood Biology and Wood Products, Büsgenweg 4, 37077 Göttingen, Germany

E-mail: hannes.stolze@uni-goettingen.de; adefemi-adebisi.alade@forst.uni-goettingen.de; holger.militz@uni-goettingen.de

Keywords: Adhesion, beech (*Fagus sylvatica*), finger-jointing technology, hardwood, structural timber products

ABSTRACT

Currently, approvals for structural adhesive systems are largely limited to softwood bonding. With increasing interest in hardwood utilization for structural timber products, it is pertinent to identify suitable adhesive systems for approval and standardization of bonded hardwood-based materials. This study focused on evaluating the suitability and performance of polyurethane, melamine formaldehyde-based and emulsion polymer isocyanate adhesive systems for finger-jointing of beech (*Fagus sylvatica*, L.) wood. Finger-profiling and -jointing of the beech solid woods were performed using Weinig Grecon finger-jointing lines. Performance of the finger joints were evaluated in flatwise four-point bending test according to EN 408 standard. High mean bending strength up to 89.8 N mm^{-2} and mean bending stiffness up to 14025 N mm^{-2} were achieved. However, the bending properties of the finger-jointed beech lamellas vary with adhesive system. Nonetheless, the findings in this study established a high degree of suitability of the investigated adhesive systems for bonding beech solid wood finger joints. The study also established that the strength advantage of beech over softwoods are retained in finger-jointing, but the entire strength potential of the beech cannot be utilized. In addition to the adhesive systems, the influence of the finger joint gap size on the bending strength of the joint was investigated. It was found that the strength of the finger joint bending strength tends to decrease as the finger joint gap size increases.

INTRODUCTION

Hardwood potentials offer new possibilities for timber construction, which is largely dominated by softwood, in areas and forms of application that were previously not feasible. For instance, hardwoods such as beech (*Fagus sylvatica*, L.) can be used to produce components with a very high load-bearing capacity thus enabling smaller cross-sections compared to softwood such as spruce (*Picea abies*, L.) (Krackler et al., 2010; Informationsverein Holz, 2017). Similarly, with identical cross-sectional dimensions, larger spans can be achieved with hardwood than softwood. These hardwood potentials arouse the interest of structural engineers and can thus contribute to the realization of sophisticated architectural structures made of the natural raw material hardwood. In Europe, research and product development efforts have intensified toward utilization of the increasing hardwood resource, particularly beech wood. However, there is a pronounced difference in anatomical properties of hardwood compared to softwood which makes hardwood-based product development more challenging.

To produce acceptable load-bearing hardwood products, adaptation of production and process technology, particularly in jointing technology, is required for respective hardwood species. In engineered wood product manufacturing, finger-jointing is used to achieve desired longitudinal dimensions. Under optimal conditions in production and quality assurance, finger-jointed components can achieve comparable load-bearing capacity of single piece components (Collin, 1990b; Augustin, 2008; Neuhaus, 2017) giving rise to many finger-jointed laminated beams and glulam (Mönck and Rug, 2015; Purgstaller, 2010). Over the years, finger-jointing technology principles and strength grading has been standardized for softwood. Present day challenges include adaptation and standardization of the finger-jointing process parameters and strength properties for hardwood.

Most of the past research works on finger joint investigations focused on tensile strength assessment which is regarded as a more stringent quality control of the bonding quality than bending strength (Colling, 1990a; Aicher and Radovic, 1999; Serrano, 2000; Steiger et al., 2014; Gehri, 2015; Clerc et al., 2017). However, bending strength plays a key role in the current standards for research work and quality assurance during manufacturing process. One reason for this is that over 90% of glulam is subjected to bending loads during use (Ebner, 2016). This raises the need to better understand the behaviour of finger joints under flexural loading.

The important parameters for finger-jointing include wood milling process, finger profile, cross sections, finger joint orientation, and adhesive system to mention a few (Schusser, 2013). Emerging adhesive systems for hardwood bonding include polyurethane, melamine-based, resorcinol-based, and emulsion polymer isocyanate adhesives (Habenicht, 2006; Schmidt, 2013; Studiengemeinschaft Holzleimbau, 2018; Alade et al., 2022; Alade et al., 2023). Although, there are increasing studies focusing on finger-jointing solid beech lamellas (Krackler et al., 2010; Steiger et al., 2014; Volkmer et al., 2017), compatibility of adhesive systems still requires significant exploration towards approval and standardization for hardwood. Therefore, the goal of this study was to the investigate the bending strength and stiffness of beech lamellas finger-jointed using different adhesive systems and to investigate the effect of finger joint gap size as an important factor in the joint formation.

MATERIALS AND METHODS
Materials
Wood
Steamed and technical dried beech (*Fagus sylvatica*, L.) wood planks used in this study was obtained from Goettingen area in Germany. The planks were of high quality and contained rift and side boards.

Adhesive systems
Choice of adhesive systems used in this study was based on approval as structural adhesives for use in load-bearing timber construction by the German Institute for Building Technology (DIBt), weather-resistant and suitable for industrial production processes. Based on these requirements, two types of one-component polyurethane; PUR1 (Jowat SE, Jowapur 686.20) and PUR2 (Henkel & Cie. AG, Loctite, Purbond HB S109), a two-component melamine-formaldehyde; MF (Dynea AS, Prefere 4720/5020) and a two-component emulsion polymer isocyanate; EPI (Dynea AS, Prefere 6183/6683) adhesive from different manufacturers were used in this study. These adhesives are classified as type 1 according to EN 301. However, at the time of this study, approvals for these adhesives are limited to softwood. This study was therefore envisaged to contribute technical information on the suitability of these adhesive systems for use in hardwood bonding.

Specimen preparation and finger-jointing
270 mm long x 100 mm wide x 25 mm thick boards were cut from beech wood planks and planed. The planed boards were conditioned in standard climate (20 ± 2°C and 65 ± 5 % relative humidity) to 11 ± 1 % moisture content. The density of the beech boards was 0.67 ± 0.02 g/cm³. Finger-profiling and -jointing of the beech boards were performed using different finger-jointing lines from Weinig Grecon GmbH & Co. KG (Alfeld/Leine, Germany). Details of parameters related to the finger joint profile, adhesive application and bonding process are presented in Table 1.

Table 6: Parameters used in this study for finger-jointing beech lamellas

Parameter	Description
Wood cross-section	105 mm x 32 mm at finger-jointing and 100 mm x 25 mm at testing
Milling tool	Minifinger jointing cutter
Mill feed rate	24 m min^{-1}
Finger length	15.65 (±0.1) mm
Finger pitch	3.8 mm
Finger joint orientation	Vertical finger-jointing, visible on the broadside of the board
Adhesive application	One-sided, manually using a glue comb, profiles completely wetted with adhesive, processing according to manufacturer's recommendation, no primers
Press pressure and duration	19 N mm^{-2} and 15 s

To ensure that the pressing pressure is fully transferred to the finger joint flanks during the production of the finger joint, the standard EN 14080 specifies a slightly open finger joint base, the so-called finger joint gap, which is considered relative to finger length. The final length of the finger-jointed lamellas was 475 mm, and the finger joint was positioned in the centre of the board as shown in Figure 1.
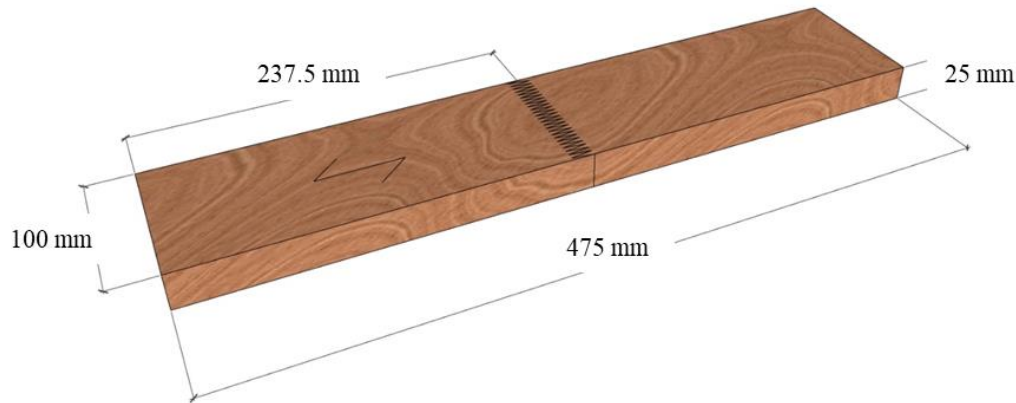

Figure 20: Dimensions of finger-jointed beech lamellas

Flatwise four-point bending test

Four-point bending test of the finger-jointed beech lamellas were carried out in accordance with EN 408 standard. Test span, position and distance of force loading clamps and supports are presented in Figure 2. The bending test was performed using a 100 kN capacity Zwick Roell GmbH & Co. KG (Ulm, Germany) universal testing machine equipped with a VideoXtense camera extensometer. The modulus of elasticity was determined between 1000-4000 N standard force. Bending test of finger-jointed lamellas from each of the investigated adhesives were performed in replicates n = 13 for PUR1, n = 16 for PUR2, n = 19 for MF and n = 22 for EPI. As a reference, n = 30 beech lamellas without finger joint (Reference) were tested.
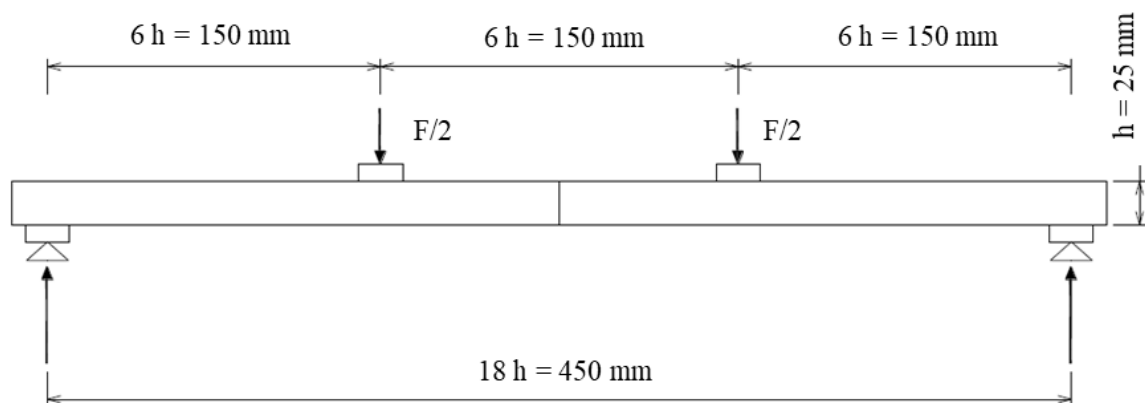
Figure 21: Set up of four-point bending test of finger-jointed beech lamellas adapted from EN 408

Determination of finger joint gap size

Before testing the bending strength, 28 finger joints of each specimen were digitised at 30x magnification using a VHX-5000 digital microscope (zoom lens VH-Z20R, Keyence, Osaka, Japan). These pictures in the state before testing were used to microscopically measure the area of the finger joint gaps. As the measuring required quite a lot of time, the gap size was not measured on all test specimens, instead on two test specimens from low, medium and high bending strength specimens for each adhesive system. Figure 3 shows an image section of the software-assisted measurement. The average area of finger joint gap was plotted against the bending strength.

(a) (b)

Figure 22: Section of the finger joint with finger gaps (a) and microscopic measurement of the area of finger joint gaps (b)

RESULTS AND DICSUSSION
Flatwise bending strength and modulus of elasticity

The test specimens bonded with MF achieved the highest average bending strength of 89.8 N mm^{-2} with the lowest standard deviation. A high proportion of wood failure was observed in the MF-bonded test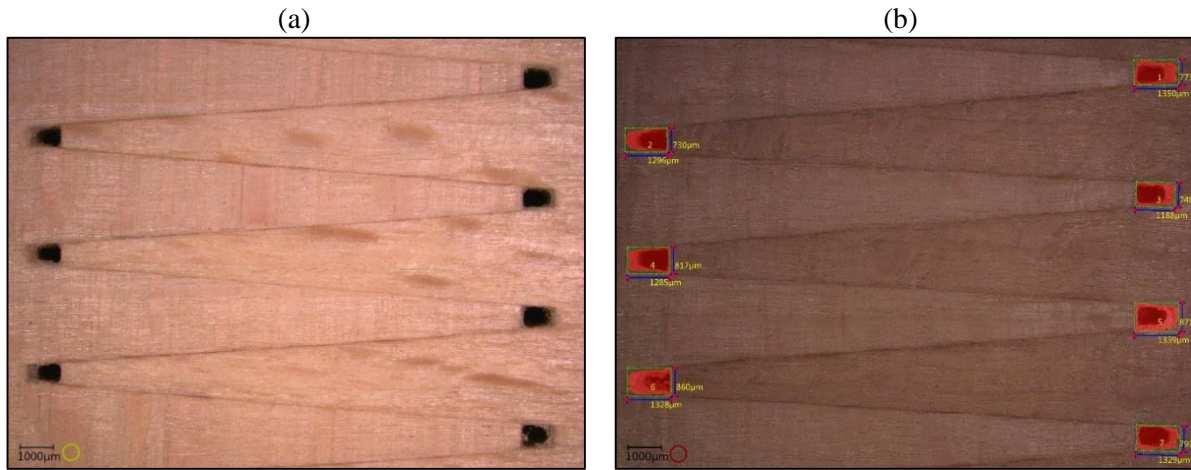 specimens and a higher level of adhesive failure in the test specimens bonded with PUR2. All adhesive systems achieved the characteristic finger-joint bending strength required to produce beech glulam of strength class GL 40. The test specimens bonded with PUR2 achieved the highest mean MOE of 14025 N mm^{-2}, which was above the mean value of the non-finger-jointed reference. The finger-jointed bending strengths achieved in this study were similar to the values achieved by Volkmer (2017), Schusser (2013), and Frese and Blaß (2006) with high-quality beech, and for MF-bonded specimens even slightly higher. The process parameters used in this study (pressing time, pressing pressure, adhesive application quantity) were above the industrial standard settings for softwoods. In addition, edge effects such as cracks, which can lead to a reduction in strength, were removed by planing the finger-jointed lamellas (105 x 32 mm²) to a smaller cross-section (100 x 25 mm²) before testing.

(a) (b)

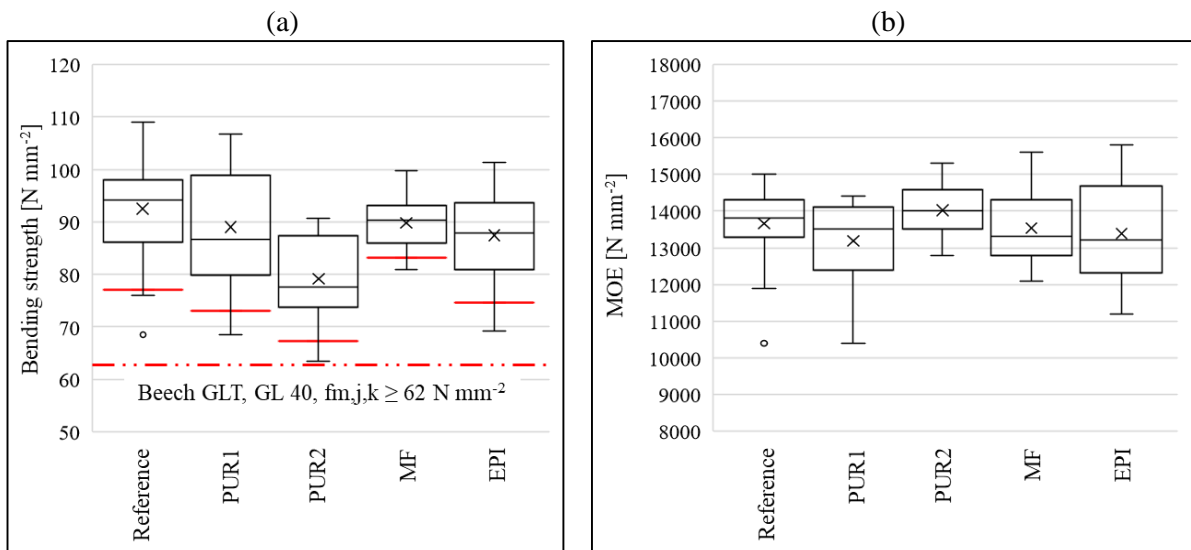***Figure 23: Bending strength of finger-jointed beech lamellas bonded with different adhesives and reference beech wood, red dotted line shows required characteristic finger joint bending strength of lamellas for GLT strength class GL 40 and red lines showing characteristic bending strength of the combinations (a); modulus of elasticity of finger-jointed beech lamellas bonded with different adhesives and reference beech wood (b)***

Bending strength and modulus of elasticity

A low coefficient of determination ($R^2 = 0.18$) for bending strength versus MOE was found for the finger-jointed lamellas, regardless of adhesive system, whereas R^2 of 0.61 was obtained for the non-finger-jointed reference. Thus, the MOE moderately accounts for the bending strength of the non-finger-jointed lamellas whereas the MOE is a weak predictor for the bending strength of the finger-jointed lamellas. Many strength-relevant factors are influenced during finger-jointing. Some of these are difficult to determine and result in finger-jointed material behaving differently to non- finger-jointed material (Wiegand, 2002 and Volkmer, 2017).
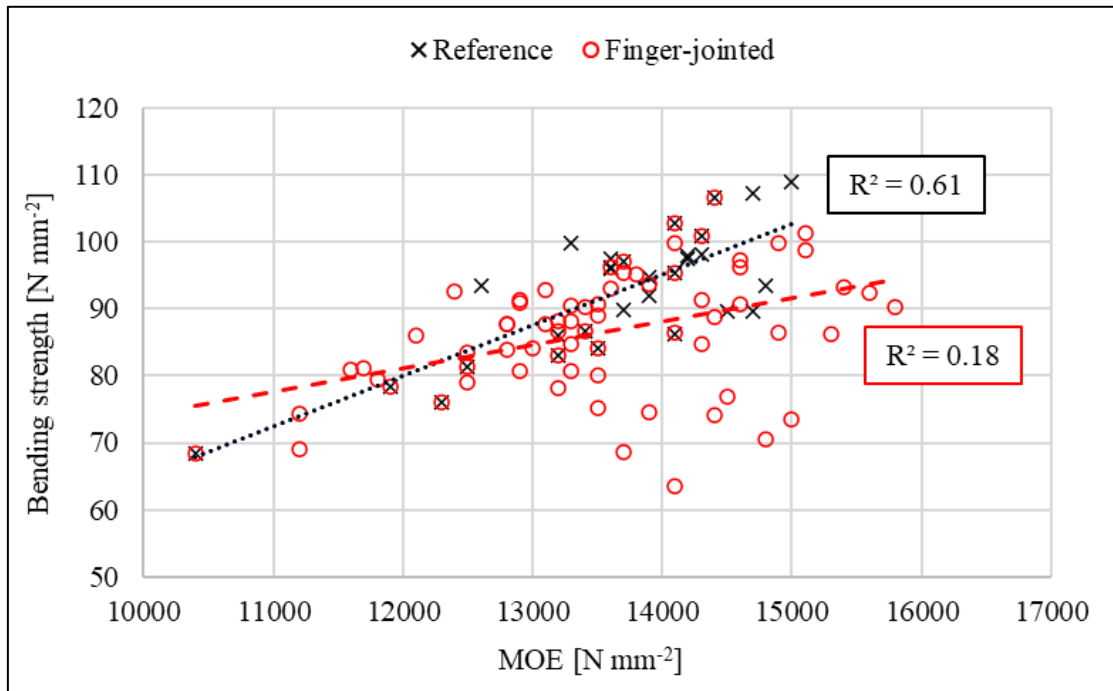

Figure 24: Relation between bending strength and modulus of elasticity for reference beech wood (n = 30) and finger-jointed beech lamellas (n = 70)

Bending strength and finger joint gap size

The small number of test specimens in this study have shown for all adhesive systems, that the bending strength tended to decrease with increasing area of the finger joint gap. The area of the finger joint gap varied the most with MF and the least with EPI. The coefficients of determination for bending strength versus finger joint gap size were more pronounced for MF ($R^2 = 0.71$) and EPI ($R^2 = 0.63$) than for the PUR1 ($R^2 = 0.04$) and PUR2 ($R^2 = 0.24$) finger-jointed lamellas. Thus, the finger joint gap size highly and moderately accounted for the bending strengths of MF and EPI finger-jointed lamellas, respectively. The finger joint gap size is a weak predictor for bending strength of PUR2 finger-jointed lamellas whereas the finger joint gap size in PUR1 finger-jointed lamellas had no predictor influence on its bending strength. Mostly, the decrease in bending strength is presumably due to the decrease in the effective bond area, a lower self-locking effect, and a weakening of the cross-section. Aicher (2014) made similar observations on universal finger joints. It was interesting to note that the PUR1, which was the only fibre-reinforced adhesive system, showed the largest average finger joint gap size and still achieved a high average bending strength which affirms that the gap size did not impact the bending strength. The fibres contained in the PUR1 may have contributed to the high strength and at the same time inhibited the joint closure during pressing due to additional friction. As the same pressing parameters were used for all finger-jointed lamellas, the wood and adhesive properties are expected to have an influence on the joint formation. In this context, it was also observed that more closed finger joints tended to crack and that the cracks occurred mainly at the edges of the joint. Bustos et al. (2011) carried out investigations on effects of end-pressure on softwood, and this would be interesting on hardwood as well, considering wood properties and pressing conditions differ.
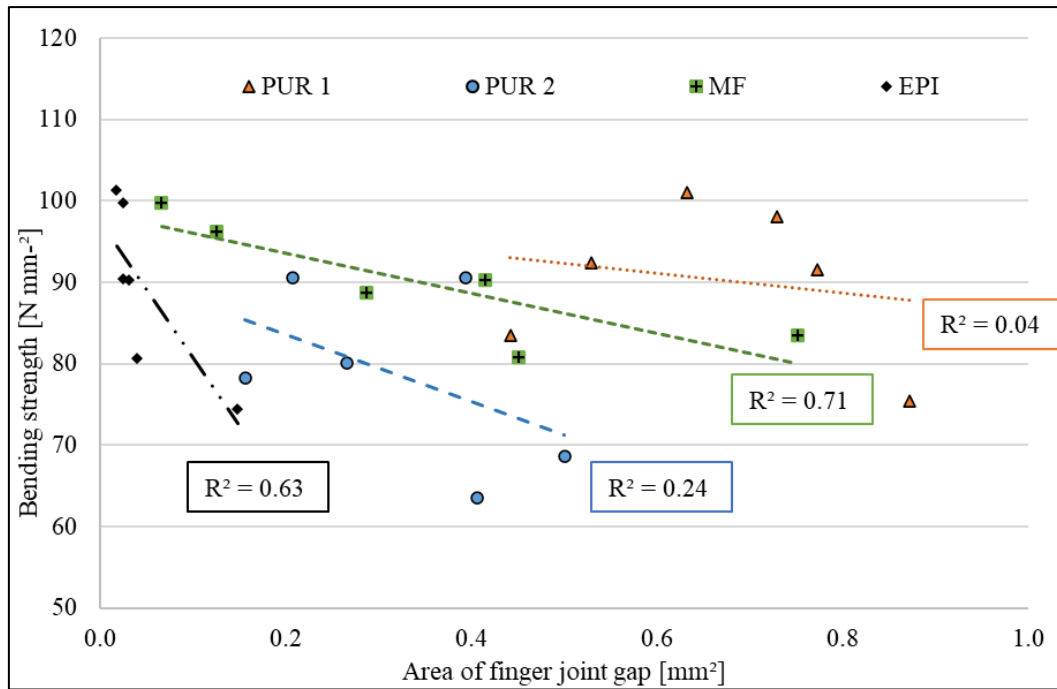
Figure 25: Bending strength of finger-jointed beech lamellas bonded with different adhesive systems in relation to their finger joint gap size

CONCLUSIONS

The findings in this study established that the investigated PUR-, EPI- and MF-based adhesive systems approved by the materials testing institute Stuttgart for softwood possess high degrees of suitability for bonding beech finger joints. The study also established that the strength advantage of beech over softwoods are retained in manufacturing finger-jointed wood products for structural applications. In addition, further findings on joint formation were obtained, which were to be tested on a larger number of specimens. Crack formation in hardwood finger joints caused by stress concentrations should be part of these further investigations.

ACKNOWLEDGMENTS

REFERENCES

Alade AA, Naghizadeh Z, Wessels CB, Stolze H, Militz H (2022): Compatibility of preservative with adhesive in Eucalyptus grandis laminates, International Wood Products Journal, 13:1, 57-69, DOI: 10.1080/20426445.2021.2018101

Alade AA, Wessels CB, Stolze H, Militz H (2022): Improved adhesive-bond performance in copper azole and disodium octaborate tetrahydrate-treated Eucalyptus grandis laminates, International Wood Products Journal, 13:3, 139-147, DOI: 10.1080/20426445.2022.2058277

Aicher, S. (2014): Geklebte Verbindungen in Holzbauprodukten und -Tragwerken; Holzverbindungen mit Klebstoffen für die Bauanwendung; S-WIN Swiss Innovation Network: Weinfelden, Schweiz, DOI: 10.13140/2.1.4101.6005

Aicher, S. and B. Radovic (1999): Investigations on the influence of finger joint geometry on the tensile strength of finger-jointed glulam lamellae. Wood as a raw material 57, 1-11

Augustin, M. (2008): Verification in the ultimate limit state - connections. In: Angst, V. and M. Augustin (eds.), Handbook 1: Timber structures. Teaching and learning materials for the design and construction of timber structures - TEMTIS, 142-166

Blaß, H.J.; Frese, M.; Glos, P.; Linsenmann, P.; Denzler, J. (2005): Biegefestigkeit von Brettschichtholz aus Buche; KIT Scientific Publishing, DOI: 10.5445/KSP/1000001371

Bustos, C.; Hernández, R.E.; Beauregard, R.; Mohammad, M. (2011): Effects of End-Pressure on the Finger-Joint Quality of Black Spruce Lumber: A Microscopic Analysis. Maderas, Cienc. tecnol., 13, 319–328, doi:10.4067/S0718-221X2011000300007.

Clerc, G., M. Lehmann and T. Volkmer (2017): Action Plan Wood: Glued laminated timber from hardwood - Technical basis for market implementation as a construction product in Switzerland. Report: Module 3, project no.: REF 1011-04200, beech glulam. Institute for materials and wood technology, Bern university of applied sciences, Switzerland

Colling, F. (1990a): Bending strength of glulam beams as a function of the strength-relevant influencing variables. Wood as a raw material 48, 269-273

Colling, F. (1990b): Load-bearing capacity of glued laminated timber beams as a function of the strength-relevant parameters. Dissertation. Faculty of Civil Engineering and Surveying, University Fridericiana zu Karlsruhe, Karlsruhe, Germany

EN 301:2018-01 Adhesives, Phenolic and Aminoplastic, for Load-Bearing Timber Structures - Classification and Performance Requirements; Beuth Verlag, Berlin, Germany

EN 408:2012-10: Timber structures- Structural timber and glued laminated timber- Determination of some physical and mechanical properties; Beuth Verlag, Berlin, Germany

EN 14080:2013-09, Timber Structures - Glued Laminated Timber and Glued Solid Timber - Requirements; Beuth Verlag GmbH, Berlin, Germany

Ebner, G. (17.2.2016): GL 24c - the new standard?: In Germany and Austria, low EN 14080 demand meets little supply. https://www.holzkurier.com/holzbau/2016/02/gl_24c_der_neue_standard.html

Frese, M. and H. J. Blaß (2006): The bending strength of finger joints made of planks of beech (Fagus silvatica L.). Wood as a raw material 64, 433-443

Gehri, E. (2015): Joining techniques for hardwood-based engineered timber - with special consideration of glulam and LVL made of beech: 21st International Timber Construction Forum IHF 2015

Habenicht, G. (2006): Bonding: Fundamentals, technologies, applications: with 37 tables. 5. Springer, Berlin, Germany

Informationsverein Holz E.V. (2017): Constructive building products made from European hardwoods: Informationsdienst Holz. spezial

Krackler, V., D. Keunecke and P. Niemz (2010): Processing and possible uses of hardwood: Decision-making basis for the promotion of hardwood processing and sales. Wood action plan. Zurich university of technology, institute for building materials.

Mönck, W. and W. Rug (2015): Holzbau: Bemessung und Konstruktion, Beuth Verlag

Neuhaus, H. (2017): Ingenieurholzbau: Grundlagen - Bemessung - Nachweise - Beispiele, Springer Fachmedien Wiesbaden

Purgstaller, T. (2010): The mechanical behavior of adhesive joints in timber construction. Master thesis. Institute of Timber Engineering and Wood Technology, Graz University of Technology, Graz, Austria

Schmidt, M. K. (2013): The bonding of beech wood for load-bearing timber components with special consideration of color bonding. Dissertation. Faculty Science Center Weihenstephan for Nutrition, Land Use and Environment, Technical University of Munich, Munich, Germany

Schusser, A. (2013): Investigation of finger-jointing for board lamellas in hardwood. Master thesis. Bern University of Applied Sciences, Biel, Switzerland

Serrano, E. (2000): Adhesive joints in timber engineering: Modeling and testing of fracture properties, Lund, Sweden

Steiger, R., S. Franke and A. Frangi (2014): Glued laminated timber made of beech and joints in beech glulam: Workshops to survey the current state of knowledge in Germany, Austria and Switzerland. Wood Action Plan - Project report

Studiengemeinschaft Holzleimbau e.v. (2018): Production and properties of glued solid wood products: Holzbau Handbuch-Informationsdienst Holz

Volkmer, T., M. Lehmann and G. Clerc (2017): Glued laminated timber made of beech: finger- jointing and surface bonding. 23rd International Timber Construction Forum IHF 2017. Berner Fachhochschule, Switzerland

Wiegand, T. (2003): Entwicklung eines Rechenverfahrens für keilgezinkte Rahmen-ecken und Biegeträger ohne oder mit Zwischenstück aus Brettschichtholz oder Holzwerkstoffplatten. Dissertation. Bauingenieurwesen, Bergische Universität Wuppertal, Wuppertal

Mode I fracture behaviour of bonded beech wood analysed with acoustic emission

Martin Capuder[1], Aleš Straže[2], Boris Azinović[1], Ana Brunčič[1]

[1] Slovenian National Building and Civil Engineering Institute, Dimičeva ulica 12, Ljubljana, Slovenia
[2] Biotechnical Faculty, University of Ljubljana, Jamnikarjeva 101, Ljubljana 1000, Slovenia.

E-mail: martin.capuder@zag.si; ales.straze@bf.uni-lj.si; boris.azinovic@zag.si; ana.bruncic@zag.si

Keywords: bonded beech wood, mode I fracture, acoustic emission, surface treatment, moisture, fibre orientation

ABSTRACT

In this study, acoustic emission (AE) technique was used to monitor changes in acoustic event properties of fracture propagation during double cantilever beam mechanical tests (DCB) of adhesive bonded joints in European beech wood. Polyurethane adhesive was used, and three variables monitored, namely moisture content, surface treatment, and orientation of fibres in lamellae. Fracture energy has proven to be highly dependent on all three studied variables. Increased moisture content of wood significantly degraded mechanical performance of bonded joint, using a primer before bonding was confirmed to result in higher fracture energy, and different orientation of the wood fibre in the cross-section of the two bonded lamellae, had negative effects on the mechanical properties of bonded joints. Furthermore, sanding of wood surface prior to adhesive application resulted in the highest fracture energy. AE activity during fracture formation indicated linear behaviour prior to fracture and non-linear behaviour after the occurrence of fracture, and enabled distinction between wood failure and adhesive bond failure, which was subsequently analyzed using reflected light microscopy.

INTRODUCTION

Timber construction relies heavily on bonding to overcome the inherent limitations of wood. It enables the realization of elements with the desired dimensions while minimizing anisotropy and other defects such as knots or discolored heartwood. However, joints are still potential weak points in timber constructions, so the principle that each joint must be stronger than the elements it joins must be respected, as required by EN 14080 European building standard. For over a century, Norway spruce (*Picea abies*) has been the most important wood species for timber construction in Europe, which has led to the development of testing standards that focus mainly on this wood species. However, transferring these standards to other wood species is a challenge due to the complexity of the material and the variability in structure and chemistry (Ammann 2015). The growing interest in the use of European beech (*Fagus sylvatica*) also for construction purposes is due to its increasing occurrence and superior mechanical performance (Gómez-Royuela et al. 2022). Latter has become an area of interest, especially in countries such as Slovenia, Austria, and Germany, where beech is the dominant deciduous species. Despite the increasing occurrence of these tree species, their share of sawn timber is negligible compared to coniferous tree species, especially spruce (Pramreiter and Grabner 2023). In Slovenia beech has overtaken spruce as the most common tree species (Zavod za gozdove Slovenije 2023). Its mechanical properties even exceed those of spruce wood when it is not exposed to outdoor conditions. However, the use of beech is likely to result in lower material yield in the production process, which underlines the need for further research and optimization of its use for construction purposes (Plos et al. 2022)

To effectively bond beech wood certain protocols must be followed. This includes observing a designated waiting period and, in the case of polyurethane (PUR) adhesives, applying a primer to the surface before bonding. This waiting period, open/closed assembly time (OAT/CAT), may extend up to an hour or more. These prerequisites not only escalate production costs but also hinder productivity, as achieving profitability often requires operating large-scale production facilities (Bamokina Moanda et al. 2022). In this study different surfacing methods were examined to see how they affect bonding in terms of fracture energy. There are recent studies by Bamokina Moanda et al. (2022), Hänsel et al.

(2023) and Sogutlu (2017) that explore different surface preparations and their relation to tensile shear strength according to the EN 302 standard for lap joints. But as mentioned in work of Veigel et al. (2012), the disadvantage of the lap joint test method is the fact that the shear stress within the joint line often exceeds the shear strength of the wood. In this case, the measured shear strength of the wood is tested. For this reason, the simpler Double Cantilever Beam test (DCB) could be more informative about the adhesive tested but could not be directly related to the results of the lap joint test also due to the application of different stresses on the joint.

As interest in the use of timber in construction increases and timber is more susceptible to decay than other commonly used materials, it is becoming increasingly important to develop non-destructive testing methods for structural health monitoring and quality control of timber structures. One of these is the acoustic emission (AE) method, which can indicate some defects in the construction based on the acoustic response (Nasir et al. 2022). For this reason, various methods have been used to show the different reaction to cracking in softwood and hardwood. One of these was carried out by Reiterer Reiterer et al. (2000) who concluded that softwoods are more ductile and therefore "produce" more acoustic events when microcracks are occurring. Recent work by Belalpour Dastjerdi and Landis (2023) show that with AE cell wall tearing, cell wall peeling, and fiber bridging were observed and based AE energy they could be distinguished. Not so many studies were made for adhesively bonded wood joints and AE. Clerc et al. (2019) successfully established corelation of AE events and different types of failure in bond during mode II fracture test. As concluded by Nasir et al. (2022) future research should prioritize developing data-driven monitoring models to enhance effectiveness, particularly in structural health monitoring applications and large-scale timber structures.

MATERIALS AND METHODS
Preparation of test specimens

Defect-free beech boards (*Fagus Sylvatica*) were collected and sawn into lamellas measuring 550 × 120 × 12 mm³. Most of the selected boards had a radial fibre, while some had a tangential fibre orientation. After sawing, some of the samples were stored in an air-conditioned room under normal conditions (T = 20 °C, RH = 65 %) to achieve a nominal equilibrium moisture content of 12 %. A smaller proportion of the lamellae were stored in a chamber with higher humidity (T = 20 °C, RH = 85%) to achieve a nominal equilibrium moisture content of 18 %.

Before bonding, the lamellae were planed on both sides to achieve a thickness of 10 mm. After planing, the test specimens were prepared as described in Table 7.

Table 7: Specimen nomenclature. Number 12 or 18 is indicating nominal MC (%) of wood

Specimen	Surface preparation	Lamellae orientation
R12	planed	R/R
P12	planed + primer	R/R
S12	planed + sanded	R/R
RT12	planed	R/T
R18	planed	R/R

Before bonding the P12 samples, the prescribed amount (20 g/m²) of Loctite PR 3105 primer solution was sprayed onto both lamellae. After the lamellae of the S12 samples had been planed, they were additionally sanded with an electric random orbital sander using P120 grit sandpaper. Four even passes were made with the sander for each lamella. The R12, R18 and RT samples were only planed and did not receive any additional surface treatment. The adhesive used for the experiment was a one-component polyurethane (1C-PUR) HB S309 from Purbond. The PUR was applied on one side with an application rate of 160 g /m². The pressing time for most samples was 75 minutes, except for the P12 samples where the time was doubled. The pressure applied to all samples was 1 MPa. After bonding, the lamellae were sawn into 20 mm wide and 200 mm long strips. For crack initiation, a 32 mm long end notch was made using a circular saw and a sharp knife. Two holes with a diameter of 4.5 mm were drilled 10 mm from the end of the specimen to clamp the specimens in the test fixtures. Finally, the samples were stored in an air-conditioned room and then wrapped in polyethylene film, which was removed before testing.

Mechanical testing

The fracture test of the DCB specimens was performed on an MTS tensile testing machine with a load cell of 25 kN. The specimens were fixed in test grips with 2 pins (4 mm diameter) pushed through the specimen. Two AE sensors were clamped 20 and 70 mm from the end of the notch and then attached around them with hot silicone adhesive. Introducing gel medium like grease or wax and clamping the sensors could provide a more reliable attachment, but would also effect the stiffness and loads of the specimen, therefore, it was not used. The amplitude threshold was set to 45 dB and low-voltage sensors operated at 55 kHz with 26 dB, connected to an integrated preamplifier and an SMA connector with a frequency range of 30 to 65 kHz. The number of hits was monitored.

The test speed was set to 1 mm/min until the maximum load was reached. After a load drop of 50 %, the test speed was increased to 10 mm/min to achieve complete separation of lamellae. The test parameters used in the experiment were the same as in the study by Veigel et al. (2012). The specific fracture energy (SFE) was calculated from the load-displacement curve, where the SFE is represented as the area under the curve divided by the bond area (168 × 20 mm). The SFE is therefore represented as the energy required to separate two parts of the DCB specimen. Selected joints were qualitatively analyzed at microlevel with the reflected light microscope Carl Zeiss Axio before and after mechanical testing.
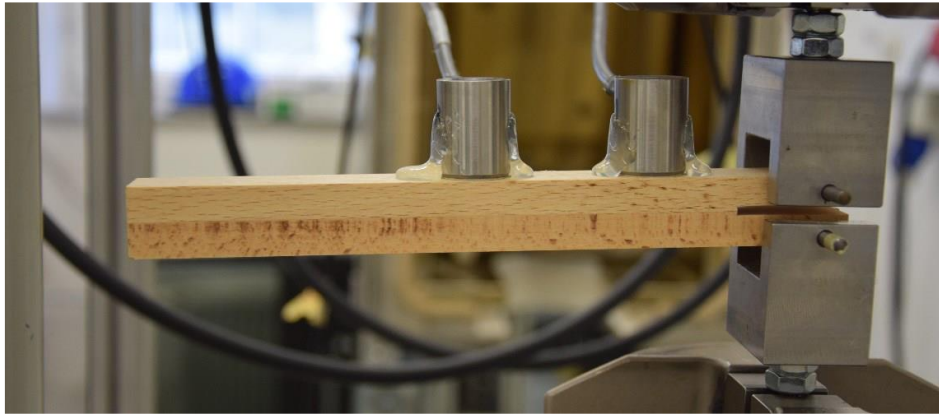
Figure 26: Mode I test

RESULTS AND DISCUSSION

Specific fracture energy evaluation

After acclimatisation of the specimens in an air-conditioned room, the final MC of the wood was 11.7 % ± 0,26 % for the specimens under normal conditions and 18.5 % ± 0.3 % for those in a room with higher relative humidity. The results of the Mode I fracture test are shown in Table 2 and Figure 1.

Table 8: Results of Mode I mechanical test

Specimen	No. of specimens evaluated	F max. [N]	St. dev. [N]	Displacement at F max.	St. dev	Specific fracture energy [J/m^2]	St. dev
R12	7	295.08	41.16	1.60	0.25	344.56	140.62
P12	10	284.85	67.69	1.40	0.35	386.20	195.79
S12	8	330.67	31.56	1.64	0.19	716.72	174.77
RT12	7	261.83	60.94	1.30	0.51	300.42	182.02
R18	9	215.91	57.49	0.89	0.40	210.53	141.57

Figure 27: Specific fracture energy for PUR bonded beech wood

The results of the SFE show that each type of surface treatment (sanding and application of a primer) leads to a higher SFE than for untreated surfaces. Some wood failure was observed when treated with primer, which contributed to a higher SFE. The results also show that a higher MC of the wood leads to a lower specific fracture energy. The results of the R12 samples (344 J/m^2) are directly comparable to the results found in the literature by different authors.
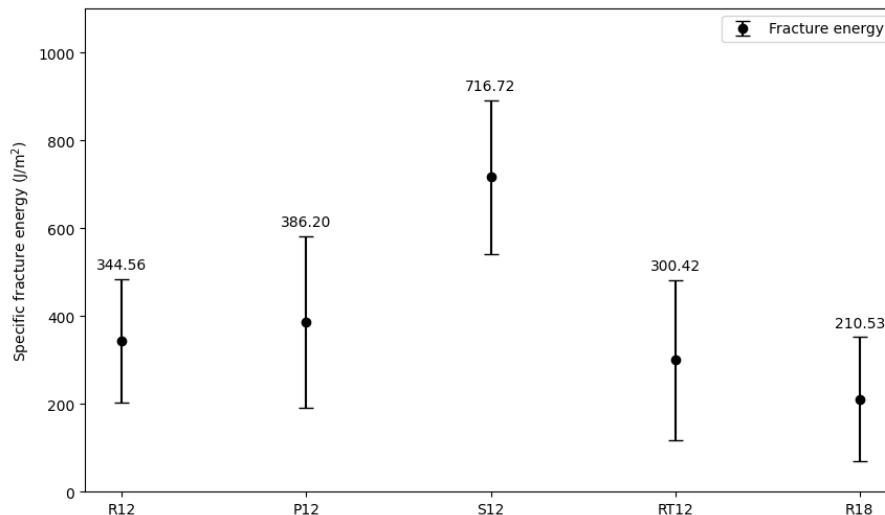
The results of Veigel (2012) for spruce wood using the same method to determine SFE, the same PUR adhesive and the same specimen dimensions gave an SFE of about 360 J/m^2, which is slightly higher than in this study. As suggested by Amman (2015), the Veigel et al. samples probably failed within the adhesive, so the percentage of wood failure in the joint leads to a higher SFE. In our case, the WFP was highest in the P12 specimens that were treated with a primer prior to bonding.

The results of Amman (2015) show a significantly lower specific fracture energy for glued beech wood samples than in the present study. An SFE of about 240 J/m^2 was calculated. Furthermore, no influence of a higher MC of the wood on the SFE was found in the literature. The results of Majano-Majano et al. (2022), who performed similar tests on eucalyptus wood (*Eucalyptus globulus*), showed an SFE of 730 J/m^2. The compliance-based beam method (CBBM) was used to evaluate the SFE. Calculated SFE is higher than the mean value obtained in this study, but the wood used in the experiments is also denser than the beech in our study.

The results of the S12 specimens are far above average. One reason for this could be the selected method of evaluating the SFE, where only the area under the curve is evaluated. The surface of these specimens was covered with visible adhesive residue after the test – a completely cohesive failure, while other specimens exhibit adhesive failure apart from the P12 specimens mentioned earlier, where adherend failure was observed. PUR adhesive is not as brittle as other structural adhesives such as MUF or PRF. Therefore, when cohesive failure occurs, the force/deformation curve is extended. A similar effect was observed by Ebewele et al. (1979) where the roughness of the surface was correlated with the fracture energy of a tapered double cantilever. Some more recent studies on surface preparation and its relationship to shear strength were conducted by Hänsel et al. (2023) who found that face milling gave the best results. The study by Bamokina Moanda et al. (2022) showed that sanding of surface in the dry state does not show a clear trend towards higher shear strength. In the wet phase, it was shown that the best results are achieved when sharp planing knives are used.

AE signal evaluation

The AE signal was evaluated for hits that exceeded the threshold. The AE signals from sensors were separated into channel 4 and channel 8. Channel 4 was the one near the crack tip. All signals from the AE sensors have a similar response with few hits when the first crack occurs at maximum force. As the crack propagates, the responses vary depending on whether the failure was cohesive or adhesive (Figure 28) and whether the wood was involved in the failure (Figure 29). The hits are shown as cumulative during crack propagation.
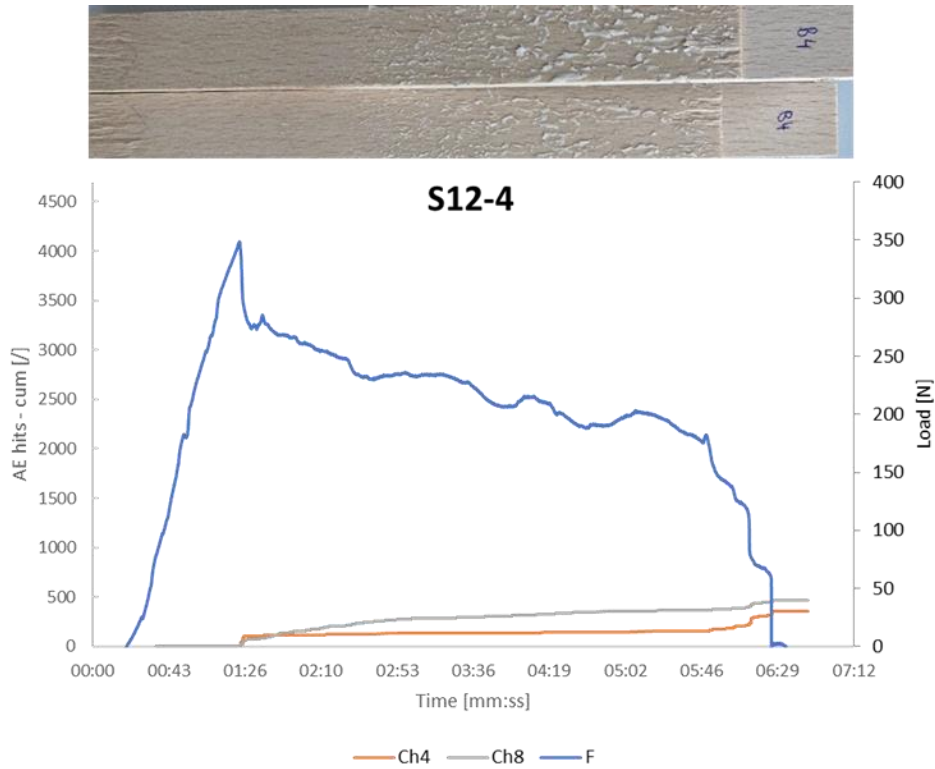
Figure 28: Characteristic AE response of adhesive failure
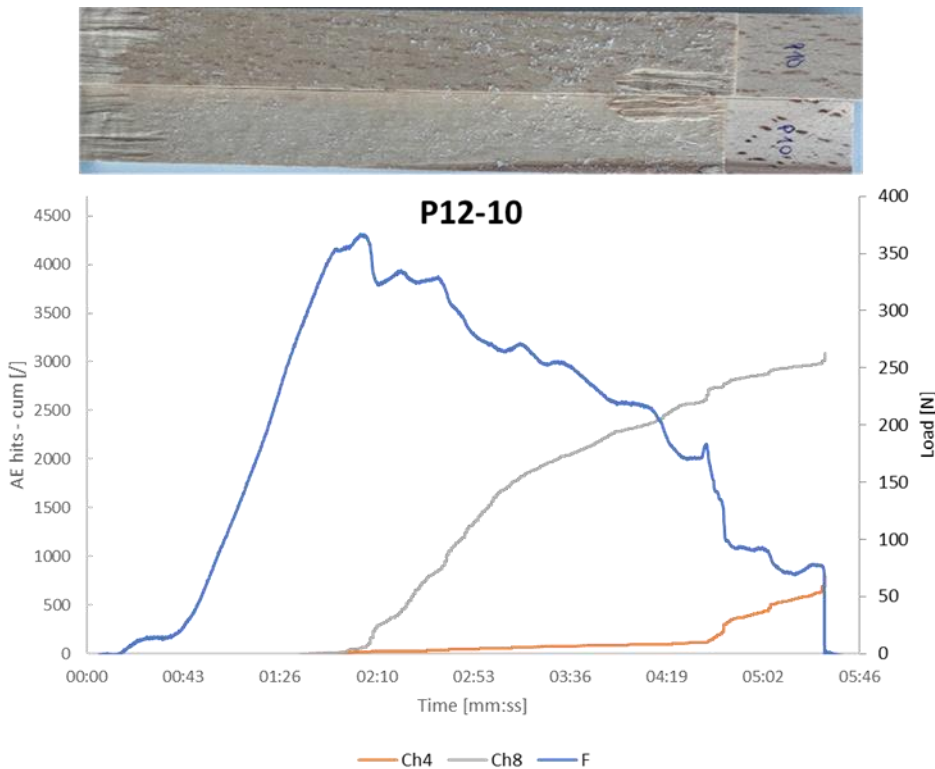
Figure 29: Characteristic AE response of adherend (wood) failure

The results suggest that the number of hits correlates with fracture of wood/adhesive: adhesive failure produces fewer acoustic hits even during plastic deformation (Fig. 3), while wood tearing causes more acoustic hits, detected at a certain distance from the fracture site (Fig. 4). A similar argument was made by Clerc et al. (2019), who correlated frequency clusters with wood- or adhesive failure when testing

end notch flexure specimens for Mode II fracture. A similar data processing technique was used by Baensch et al. (2015), who performed tensile tests on small spruce samples. They were able to indicate and separate slow crack growth associated with cell separation or transcellular cracks. The AE was used by Tu et al. (2021) to establish the relationship between the length of crack extension and the number of accumulated hits.

Microscopic images reveal certain level of looseness in adhesive joint (Fig. 5 right), which may be identified as places of weakening in the structure of glued pieces resulting in adhesive fracture with a quieter fracture process. Tearing of wood occurs in the softer wood area of P12 specimen (Fig. 6 left), and in case of adhesive failure of R18 specimen, the loosening of the structure in the area of the wood around the joint is also noticeable (Fig. 6 right).
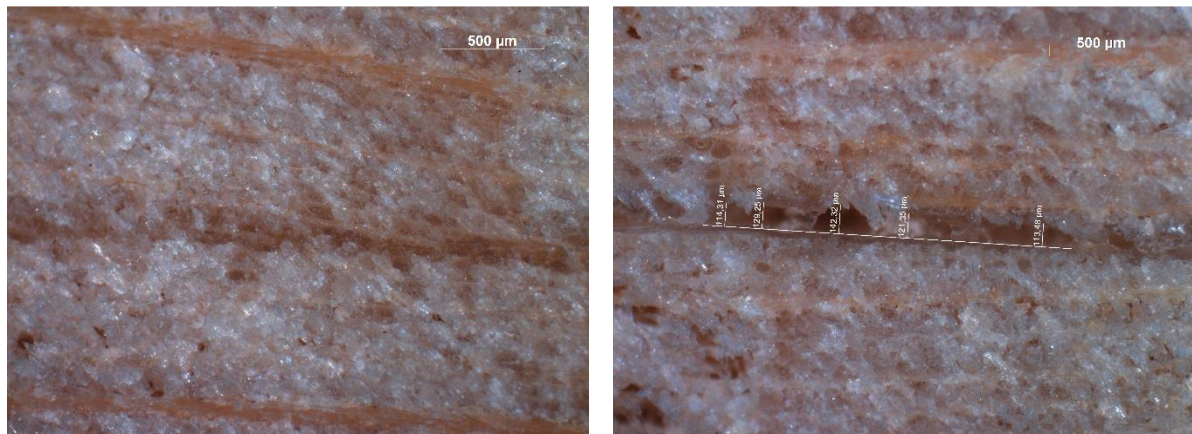
Figure 5: Microscopic image of an adhesive joint prior to mechanical testing: tight joint on the left, loose joint on the right
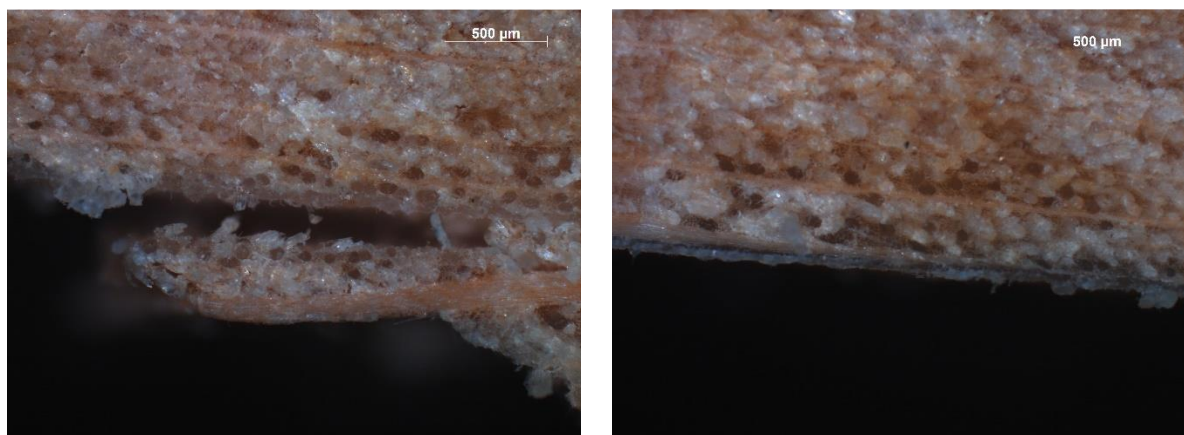
Figure 6: Microscopic image of an adhesive joint after mechanical testing: tearing of the wood fibre on the left, fracture of the adhesive on the right

CONCLUSIONS

The specific fracture energy (SFE) of adhesively bonded beech wood was determined using DCB tests. The area under the load/displacement curve was calculated to evaluate the SFE. The results showed that sanding of surface before bonding gave by far the highest SFE, followed by surface treatment with primer. In the case of primer, there was more wood failure than in other specimens. A different orientation of the lamellae and higher moisture content of the wood resulted in a lower SFE. Based on the acoustic response, the number of AE events was found to be higher in cohesive failure.

ACKNOWLEDGEMENTS

REFERENCES

Ammann SD (2015) Mechanical performance of glue joints in structural hardwood elements. ETH Zurich

Baensch F, Sause MGR, Brunner AJ, Niemz P (2015) Damage evolution in wood – pattern recognition based on acoustic emission (AE) frequency spectra. Holzforschung 69:357–365. https://doi.org/10.1515/hf-2014-0072

Bamokina Moanda D, Lehmann M, Niemz P (2022) Investigation of the Impact of Micro-Structuring on the Bonding Performance of Beechwood (Fagus Sylvatica L.). Forests 13:113. https://doi.org/10.3390/f13010113

Belalpour Dastjerdi P, Landis EN (2023) Cross-grain fracture characterization in softwood using artificial neural network analysis of acoustic emissions. Wood Sci Technol 57:1385–1400. https://doi.org/10.1007/s00226-023-01494-2

CEN European Committee for Standardization. EN 14080 - Timber structures – Glued laminated timber and glued solid timber – Requirements. 2013.

Clerc G, Sause MGR, Brunner AJ, et al (2019) Fractography combined with unsupervised pattern recognition of acoustic emission signals for a better understanding of crack propagation in adhesively bonded wood. Wood Sci Technol 53:1235–1253. https://doi.org/10.1007/s00226-019-01136-6

Ebewele RO, River BH, Koutsky JA Tapered Double Cantilever Beam Fracture Tests of Phenolic-wood Adhesive Joints Part II. Effects of Surface Roughness, the nature of surface roughness, and surface aging on joint fracture energy

Gómez-Royuela JL, Majano-Majano A, Lara-Bocanegra AJ, et al (2022) Evaluation of R -curves and cohesive law in mode I of European beech. Theor Appl Fract Mech 118:103220. https://doi.org/10.1016/j.tafmec.2021.103220

Hänsel A, Tröger J, Rößler M, et al (2023) Influence of surface treatment on the bonding quality of wood for load-bearing purposes. Wood Mater Sci Eng 18:2128–2139. https://doi.org/10.1080/17480272.2023.2269138

Majano-Majano A, Lara-Bocanegra AJ, Xavier J, et al (2022) Direct evaluation of mode I cohesive law of eucalyptus bonded joints. Procedia Struct Integr 37:492–499. https://doi.org/10.1016/j.prostr.2022.01.114

Nasir V, Ayanleye S, Kazemirad S, et al (2022) Acoustic emission monitoring of wood materials and timber structures: A critical review. Constr Build Mater 350:128877. https://doi.org/10.1016/j.conbuildmat.2022.128877

Plos M, Fortuna B, Šuligoj T, Turk G (2022) From Visual Grading and Dynamic Modulus of European Beech (Fagus sylvatica) Logs to Tensile Strength of Boards. Forests 13:77. https://doi.org/10.3390/f13010077

Pramreiter M, Grabner M (2023) The Utilization of European Beech Wood (Fagus sylvatica L.) in Europe. Forests 14:1419. https://doi.org/10.3390/f14071419

Reiterer A, Stanzl-Tschegg SE, Tschegg EK (2000) Mode I fracture and acoustic emission of softwood and hardwood. Wood Sci Technol 34:417–430. https://doi.org/10.1007/s002260000056

Sogutlu C (2017) Determination of the Effect of Surface Roughness on the Bonding Strength of Wooden Materials. BioResources 12:1417–1429. https://doi.org/10.15376/biores.12.1.1417-1429

Tu J, Zhao D, Zhao J, Zhao Q (2021) Experimental study on crack initiation and propagation of wood with LT-type crack using digital image correlation (DIC) technique and acoustic emission (AE). Wood Sci Technol 55:1577–1591. https://doi.org/10.1007/s00226-020-01252-8

Veigel S, Follrich J, Gindl-Altmutter W, Müller U (2012) Comparison of fracture energy testing by means of double cantilever beam-(DCB)-specimens and lap joint testing method for the characterization of adhesively bonded wood. Eur J Wood Wood Prod 70:3–10. https://doi.org/10.1007/s00107-010-0499-6

Zavod za gozdove Slovenije (2023) Poročilo Zavoda za gozdove Slovenije o gozdovih

Session IV
Hardwood structure and properties

Compression strength perpendicular to grain in hardwoods depending on test method

Marlene Cramer[1]

[1] Edinburgh Napier University

E-mail: m.cramer@napier.ac.uk

ABSTRACT

Compression strength perpendicular to grain is an important timber property that governs the bearing strength of beams and might influence connection design. According to modern standards, the design value for compression strength is determined according to EN 408, but historic values (including the ones given in EN 338 strength classes) might have been determined using different procedures. This study investigates how the compression strength perpendicular to grain is influenced by the test method. Small and full-size specimens of seven hardwood species were tested and results evaluated with methods described in three different standards. The compression strength perpendicular to grain varies between species but is also dependent on the test method. While individual values might vary significantly, results indicate that population values, such as mean and percentiles, can be readily translated between different procedures.

INTRODUCTION

Compression strength perpendicular to grain is an important timber property that governs the bearing strength of beams and might influence connection design. According to modern standards, compression strength as a design value for structural timber can be measured according to EN 408 (European Committee for Standardization & British Standards Institution, 2012), more commonly, however, it is not measured but calculated from characteristic density according to EN 384 (European Committee for Standardization & British Standards Institution, 2018). It is unsure how well the given equations work for temperate hardwoods. Several authors find no relationship between density and compression strength perpendicular to grain in various hardwood species and judge the given equations to be unsuitable for that reason (Kovryga et al., 2020; Schlotzhauer, 2016).

Existing data on the compression strength of temperate hardwoods is scarce and values given in literature might have been determined using small clear testing or procedures that differ in other ways from modern standards. It would be desirable to be able to use the limited existing data for assessing design values for compression strength perpendicular to grain in various hardwood species. To compare historic results with modern timber, or to use less material, one might want to use small-clear testing instead of full-sized testing also today, and it would be ideal if such studies could also yield design values for structural timber. The effects of using different test standards for measuring compression strength perpendicular to grain are therefore explored in this paper.

Some effect of size might influence the results when testing to different standards, even though the specimen size affects compression strength less than bending or tensile strength, but mostly compression strength parallel to grain has been studied (Schlotzhauer et al., 2017; Walley & Rogers, 2022). The different sizes used in this study are the EN 408 "full size" and a BS 373 "small clear" size (British Standards Institution, 1957). BS 373 uses 2-inch (51 mm) cubes for determining compression strength perpendicular to grain, and other national and international standards use different sizes, e.g. ISO 13061-5 proposes specimens of 20 to 50 mm height, length 1.5 to 3 times the height and width ≥0.5 times height. That means specimens tested according to the ISO could be close in size to the BS 373 2-inch standard, but could also be significantly smaller so that it would be interesting to test much smaller sizes too. This is planned for the future but not covered in the present study.

The American standard D 245 (ASTM International, 2002) uses a different test method in which a steel plate is applied only to part of the cross-section, which also influences results. This effect is not

investigated here, and it is assumed that it can be modelled as described by van der Put (Leijten et al., 2010; van der Put, 2008).

How the compression force is determined depends on which test standard is used, and this influences the result as well. For example, when testing small clear specimens, the British Standard BS 373 uses the force at a deformation limit of 0.1 inch (corresponding to 5% of the specimen height), while the American standard uses a deformation limit of 0.04 inch and the German standard DIN 52192 (Deutsches Institut für Normung e. V., 1979) uses a deformation limit of 2%, so that results between these methods will obviously differ. Other standards, e.g. EN 408 and ISO 13061-5 use a force value close to the proportional limit for calculating compression strength, but even these standards differ in the method they are using to determine this value. The effects of this are investigated.

MATERIALS AND METHODS

Material of seven hardwood species was sourced for testing. The species were chosen to cover a wide range of densities (and consequently mechanical properties (Table 2). Four-letter codes, normally according to EN 13556 (European Committee for Standardization & British Standards Institution, 2003), are used for referencing different species in graphs of this paper.

Table 9: Material used in this study

Common name	Scientific name	Four letter code	Origin
Ash	*Fraxinus excelsior*	FXEX	UK
Beech	*Fagus sylvatica*	FASY	
Sweet chestnut	*Castanea sativa*	CTST	
Oak	*Quercus robur* or *Q. petraea*	QCXE	
Sycamore	*Acer pseudoplatanus*	ACPS	
Poplar	*Populus* spp.	POXX	
Birch	*Betula pendula* or *B. pubescens*	BTXX	
Paulownia	*Paulownia* spp.	PWXX	Germany

Boards of the UK-grown hardwoods (besides birch) were sourced from a sawmill in Hereford, England. Specimens were also sourced from a batch of sycamore and birch battens that had been tested in 4-point bending as part of an earlier study (Price et al., n.d.). One imported log of paulownia was used to source additional specimens of a very low-density species.

Specimens of two different sizes were cut as shown in Figure 1. The small size was chosen to be closely aligned with recommendations of BS 373 for testing of small clear specimens, however, no attention was given to the orientation of the growth rings and specimens were not necessarily defect-free. The size also deviated slightly in some specimens: BS 373 suggests testing compression strength on 2-inch cubes, but some of the boards provided by the sawmill were less than two inches thick and specimens were nonetheless cut from these boards. The target size of the resulting specimens therefore ranges from $51 \times 51 \times 51$ mm^3 to $51 \times 51 \times 40$ mm^3. Since very limited material of the birch was available, no small specimens were produced for this species.

The large size conforms with EN 408 that is used for full-size testing. Specimens are cut from the undamaged ends of battens that had been tested in 4-point bending, in a random position along the batten length. Again, specimens are not necessarily defect-free. The specimens have target dimensions of $70 \times 45 \times 90$ mm^3 (l x b x h). Since the paulownia specimens had a much smaller cross section (38×63 mm^2), only small specimens were tested for this species.

All specimens were conditioned at 20°C and 65% relative humidity to a target moisture content of 12%. Their weight and dimensions were recorded, and note was made of any defects present. Specimens were then tested in compression perpendicular to grain using a Zwick Z50 universal testing machine. Different standards prescribe different test speeds and different end conditions for the test, and for the small specimens a slightly adapted method of BS 373 was used while the EN 408 method was used for full-size specimens.
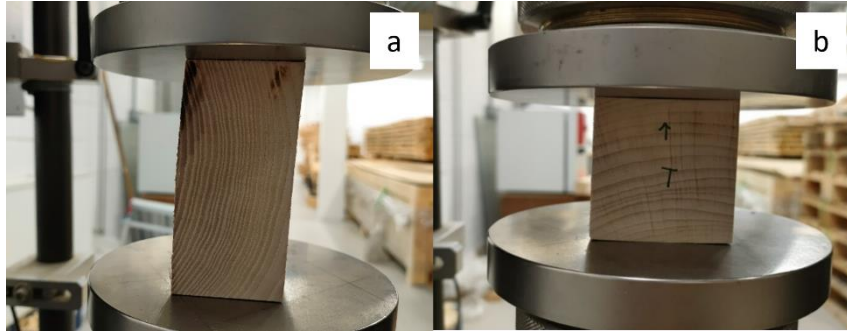
Figure 1: Different specimen sizes: full size specimens tested according to EN 408 (a) and small specimens tested according to BS 373 (b)

Conforming with BS 373, small specimens were tested at a speed of 0.025 inch/minute (0.635 mm/min). Note was made in which direction the load was applied, whether radial, tangential or in 45° growth ring orientation. It was attempted to test an equal number of specimens of each board and sampling height in radial and tangential direction. The load was applied until a deformation of at least 0.1 inch was reached. However, where the proportional limit had not clearly been exceeded at this time, the test was continued to allow the evaluation of the data according to other test standards.

Large specimens were tested according to EN 408 with the aim to reach the proportional limit force within 300 seconds. The test speed chosen to achieve this varied between 0.5 mm/min and 0.8 mm/min, depending on species. No attention was given to the orientation of the growth rings.

After testing the whole specimens were dried at 103°C until mass-consistency and their dry weight recorded. Moisture content at time of testing was calculated from mass at time of testing and oven-dry mass.

The results of both specimen sizes were evaluated with methods described in three standards: BS 373, EN 408 and ISO 13061-5 (which are in this paper simply called the BS, ISO and EN method respectively). Even though the specimen sizes and test speeds do not necessarily conform, all standards are used for the data evaluation of all specimens. This way the influence of specimen size and evaluation method can be assessed.

All the standards describe how to identify the force value which is used for calculating compression strength from the load-deformation curve. The BS uses the force at 0.1-inch deformation, while the other two standards use different methods to identify the proportional limit force.

According to the ISO, the linear part of the load deformation curve (with $R^2 \geq 0.99$) is first identified and its slope calculated. The proportional limit is then found by identifying the point in the curve where a tangent to the curve has an angle with the y-axis of 1.5 times the angle between the linear section and the y-axis (Figure 2a).

According to the EN, a force value at 1% plastic deformation is determined. First, the maximum compression force is estimated, and the linear part of the curve taken between 0.1 times and 0.4 times the estimated force. This line is moved in x-direction by 0.06 times h_0, where h_0 is 0.6 times the specimen height. The proportional limit force is taken as the value where the displaced line intersects with the curve (Figure 2b). If this value is not within 5% of the initially estimated force, the procedure is repeated. It is to be noted that the BS also allows to use proportional limit force for calculating compression strength, although it does not propose a procedure for identifying this force value. It is therefore valid to use either method for determining the proportional limit also on small specimens.

Regardless of specimen size, the methods of all three standards were used for evaluating the force-deformation curves of each specimen. All results were evaluated using R studio. The three force values identified for each specimen were used to calculate three different compression strengths using Eq. 2.

Figure 2: Determination of proportional limit force, according to the ISO (a) and according to the EN (b)
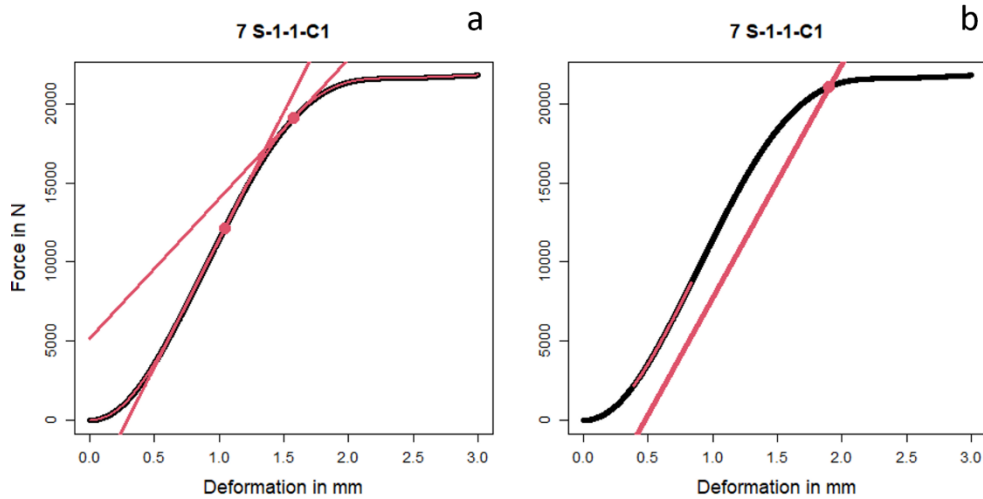
Figure 2: Determination of proportional limit force, according to the ISO (a) and according to the EN (b)

$$f_{c,i} = \frac{F_i}{A}$$ (2)

RESULTS AND DISCUSSION
Compression strength in different species
For most species the specimens are cut from only one tree, so that a comparison of the absolute results with literature has limited value. An overview of the results by species and specimen size can be seen in Figure 3, as well as Table 4 and Table 5 in the appendix. There is a clear tendency of higher-density hardwoods like oak, beech and ash to have higher compression strength than low-density species like sweet chestnut, poplar and paulownia.
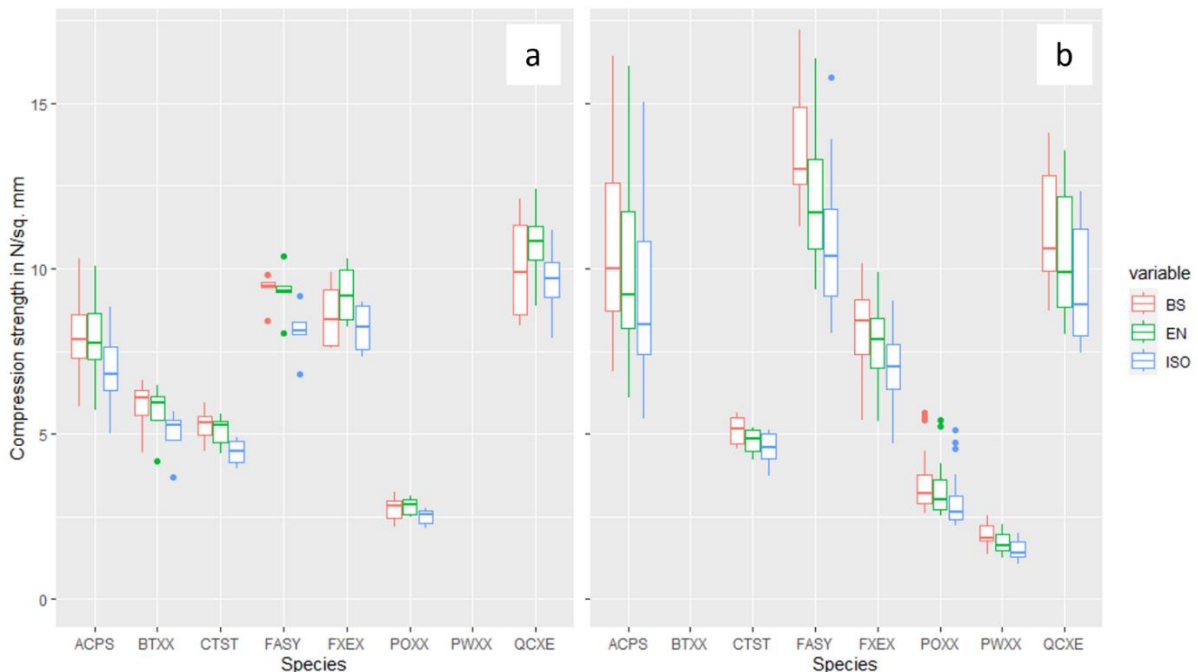
Figure 3: Compression strength in different species, measured in large specimens (a) and small specimens (b)

Variation of results by specimen size and influence of defects
The compression strength varied in the two different size groups, but there was no consistent trend in the different species groups, as some showed higher strength in larger specimens and others the opposite (Figure 3). The very low number of large specimens in some species groups can, however, mean this is a random observation and the following analysis was therefore applied only to the sycamore sample, where most data were available. For sycamore, compression strength of small specimens is significantly

higher than that of large specimens (p<0.01 for all methods). The lower compression strength in larger specimens could be a result of the higher frequency of defects in larger sizes, but defects were also present in small specimens and should have a larger influence in smaller cross sections. It is also common belief that the compression strength perpendicular to grain is not affected by the presence of knots (Senalik, 2021). In the present dataset more defects are present in the large specimens – 85% of small specimens and 44% of large specimens are free from potentially strength-reducing characteristics. This hypothesis seems doubtful, however, given that sycamore specimens with defects show a slightly higher compression strength than defect-free specimens, although not statistically significant.

The orientation of the growth rings might, on the other hand, influence the results in the two size groups differently. While the small specimens were sampled so that roughly equal numbers could be tested in radial and tangential direction, the growth ring orientation in large specimens was dictated by the ring orientation of the boards supplied by the sawmills. UK hardwood sawmills usually cut stems "through and through" which results in mostly boards with tangentially oriented growth rings. This is also reflected in the present dataset, and only two specimens (one of which sycamore) in the larger size group were tested with the load applied in radial direction. It can be demonstrated in the smaller size group of the sycamore sample that compression strength is higher when the load is applied to a tangential surface (i.e. in radial direction) than in when it is applied to a radial surface or in 45° to the growth rings (Figure 4). The same trend is well described in literature (Collins & Fink, 2022) and can be observed in all other species too, although the differences of the three directions are not always statistically significant (which might be influenced by the low specimen number). While this is likely to be a contributing factor to the different compression strengths in different size groups, there is still a significant difference (p<0.01) between the compression strengths of small and large specimens when the ones tested in radial direction are excluded from the analysis.
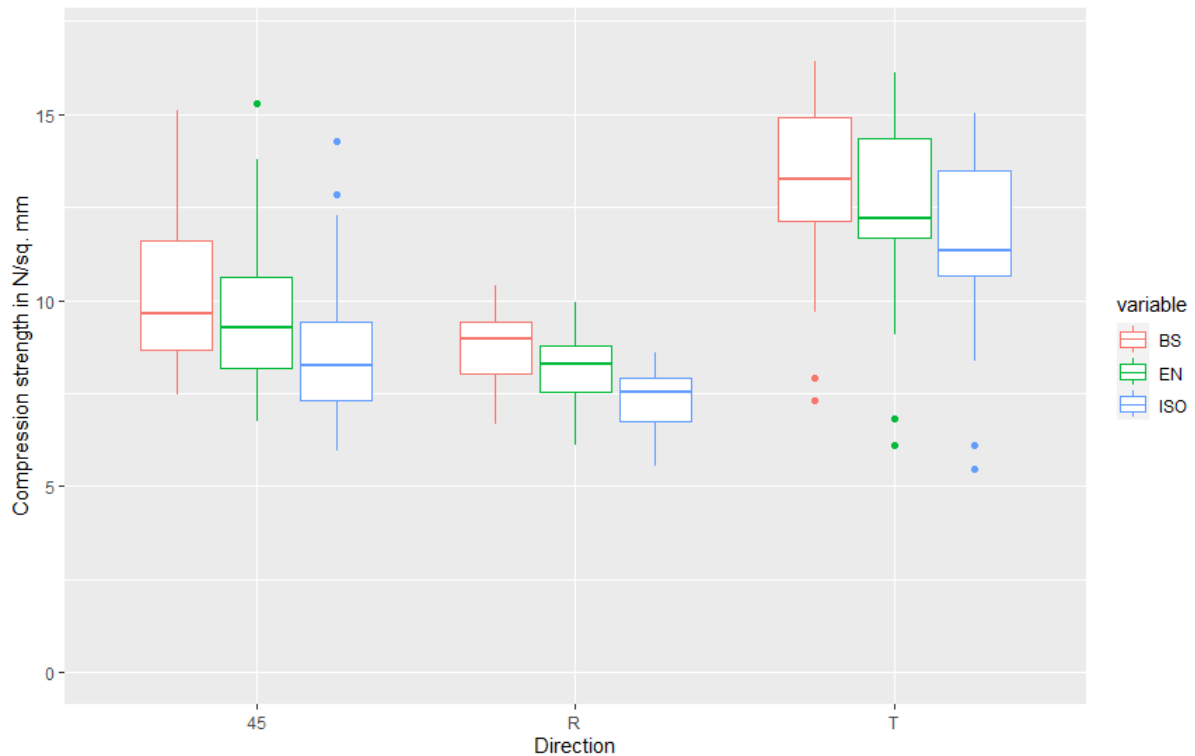
Figure 4: Directionality of compression strength in small sycamore specimens, R - load is applied to a radial surface, T - load is applied to a tangential surface, 45 - load is applied in 45° angle to the growth rings

The coefficient of variation in the compression strength of large sycamore specimens is only half of that in small sycamore specimens. This is largely explained by the absence of specimens tested in radial direction in the large specimen group, however, some of this effect is still apparent among specimens tested in tangential direction. There might be some homogenisation effect present in large specimens, somewhat neutralising the effect of macro and micro defects.

While it cannot be fully explained why small sycamore specimens tend to show higher strength, the results from small tests seem promising for predicting characteristic compression strength, which is a 5th percentile value (European Committee for Standardization & British Standards Institution, 2018). The lower tail of the distribution seems to align in both size groups (Figure 5). Especially the non-parametric 5th percentiles are closely aligned, and it is recommended to use the non-parametric determination, at least for small specimens where assuming normal distribution is not valid due to the effect of growth ring orientation. In the sycamore sample the non-parametric 5th percentile EN value between the small and large specimens differs by only 0.5 N/mm^2. If this can be confirmed in other species and with a larger sample, this would mean that characteristic (5th percentile) values for compression strength perpendicular to grain could be determined using non-parametric methods irrespective of specimen size. Two additional sizes will be studied in the future: 2-cm cubes (reflecting another commonly used size of BS 373) and specimens that comply with ISO 13061-5.
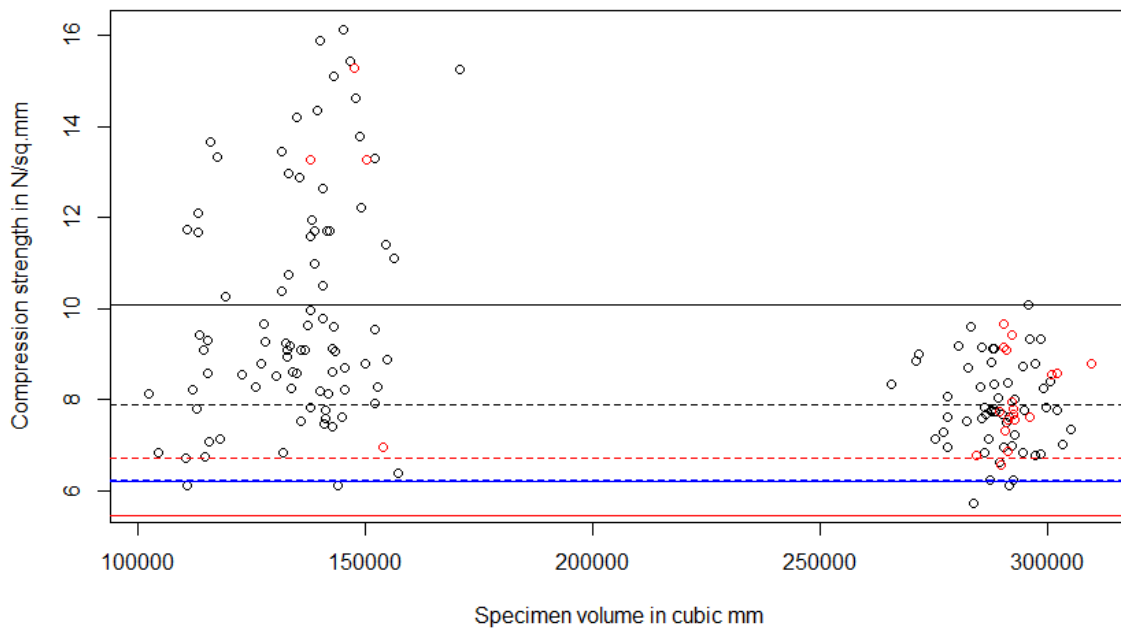
Figure 5: Compression strength (EN value) and specimen volume with mean in black, parametric 5th percentile in red and non-parametric 5th percentile in blue; small specimens – continuous line, large specimens – dashed line; specimens with defects are shown by red dots

Variation of results by evaluation method
The compression strengths determined with the three procedures are in good agreement overall. Comparing the results of each specimen determined with the ISO and BS or ISO and EN method yields high correlations with R^2=0.97 and R^2=0.99 respectively (Figure 6). However, individual specimen values can vary drastically, especially in small specimens where differences of up to 27% between ISO and EN values and up to 57% between ISO and BS values was found. Since it is not defined how to determine the proportional limit in 2-inch specimens according to BS 373, one could use the EN, the ISO or a different procedure, and the results suggest that this might lead to differences in species averages upwards of 10% (Figure 3). It would be preferable to specify the method that is used when determining the proportional limit for tests that are carried out according to BS 373 or other standards that don't specify a procedure.
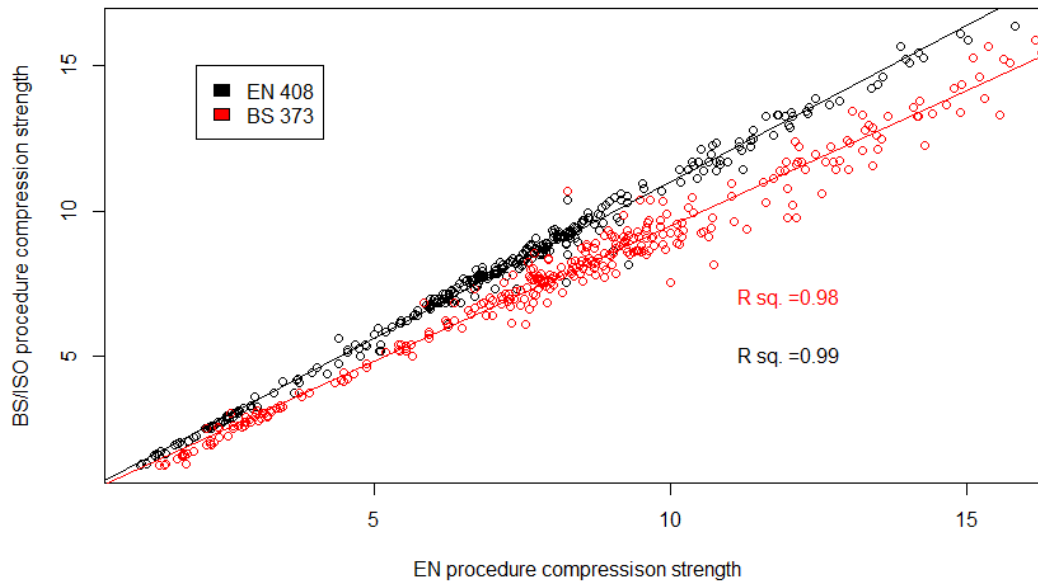
Figure 6: Relationship between compression strength perpendicular to grain of hardwoods determined with different procedures, data contains both small and full-size specimens

For the smaller size it is observed that the values determined with the BS procedure are consistently the highest, while the ones determined with the ISO procedure are the lowest. It can be easily seen from how the proportional limit is determined according to the different standards that the EN-values should be higher than the ISO-values, and in this study the EN-values were on average 11% higher than the ISO values. However, in two specimens where the force suddenly decreased after the curve started to flatten the EN value was actually lower than the ISO value. It seems that this might be associated with the crushing of the earlywood vessels, especially in ring-porous species, that leads to a rapid force reduction as was observed by Schlotzhauer in ash and Müller et al. in oak (Müller et al., 2003; Schlotzhauer, 2016). This means that the EN value in these specimens is lower than it should be, and it would perhaps be better to use the maximum force value before crushing occurs.

In small specimens the BS-values were higher than both EN- and ISO-values, as the proportional limit had usually been reached well before the 2.54 mm deformation limit BS 373 proposes – the average deformation at the proportional limit is the highest in sycamore with 1.6 and 1.9 mm for the ISO and EN procedure respectively. In large specimens, however, the deformations are larger as well so that the BS values are more in line with the forces determined by the other procedures. This means that the BS procedure is able to reliably determine a "maximum" force value well above the proportional limit in small specimens, while in large specimens it yields a value closer to the proportional limit force. But the BS procedure aims to estimate the maximum compression strength at an arbitrarily large deformation value, and to achieve a similar outcome for large specimens, the deformation limit could be interpreted as 5% of the specimen height, which corresponds to 4.5 mm in large specimens. This interpretation would again yield higher values than the other procedures. Even though tests were usually aborted before 4.5 mm deformation, the maximum force that was recorded can be used to approximate a compression strength value for the 5% deformation limit of the large specimens. However, even with this adjustment the relationships between ISO/EN and BS values remain different in the two size groups (p<0.01). The relationship between the EN and ISO values are also significantly different in both size groups (p<0.001). Still, the relationships established in one of the size groups can be used for predicting one value from another in the other size group with reasonable accuracy. For example, using the sycamore data for predicting BS (5% strain) values in large specimens from EN proportional limit force using the relationship established in small specimens leads to an average deviation of -3% from the real value. The average difference is even smaller when predicting EN values in small specimens from the relationship between EN and BS values in large specimens, although in this case the deviation of individual values is larger (-23 to +13%). The relationships in sycamore between the different compression strength values for different sizes are shown in Table 3. It remains to be seen whether similar relationships apply to other species as well.

Table 10: linear relationships between EN, ISO and BS values in the two size groups, f_{BS} means the compression strength at 5% strain rather than 0.1-inch total deformation

y	small	large
f_{EN}	y= -0.80 + 1.01 f_{BS} y= 0.48 +1.04 f_{ISO}	y= 0.36 + 0.89 f_{BS} y= 0.38 + 1.08 f_{ISO}
f_{BS}	y= 1.11 + 0.96 f_{EN} y= 1.42 + 1.01 f_{ISO}	y= -0.15 + 1.09 f_{EN} y= 0.37 + 1.16 f_{ISO}
f_{ISO}	y= -0.25 + 0.94 f_{EN} y= -1.17 + 0.97 f_{BS}	y= -0.23 + 0.91 f_{EN} y= 0.19 + 0.80 f_{BS}

The above relationships can be used to estimate proportional limit values from 5% deformation values or the other way around within the same size group. When comparing the results of different methods one might also want to translate between different sizes. One might have only results of small clear tests to hand (either proportional limit of 0.1-inch deformation values) and might want to estimate a mean or characteristic compression strength of full size specimens.

Over all species the relationship between proportional limit (ISO and EN) values of small specimens and EN values of large specimens is strong (R^2=0.79 and 0.78 respectively, see Figure 7). The BS value had a slightly lower predictive power with an R^2 of 0.76. The ISO proportional limit of small specimens might therefore be the best predictor for EN values on large specimens, but the 0.1-inch deformation value can also be used if a proportional limit force is not available. The linear models are shown in Eq. 3 and Eq. 4.
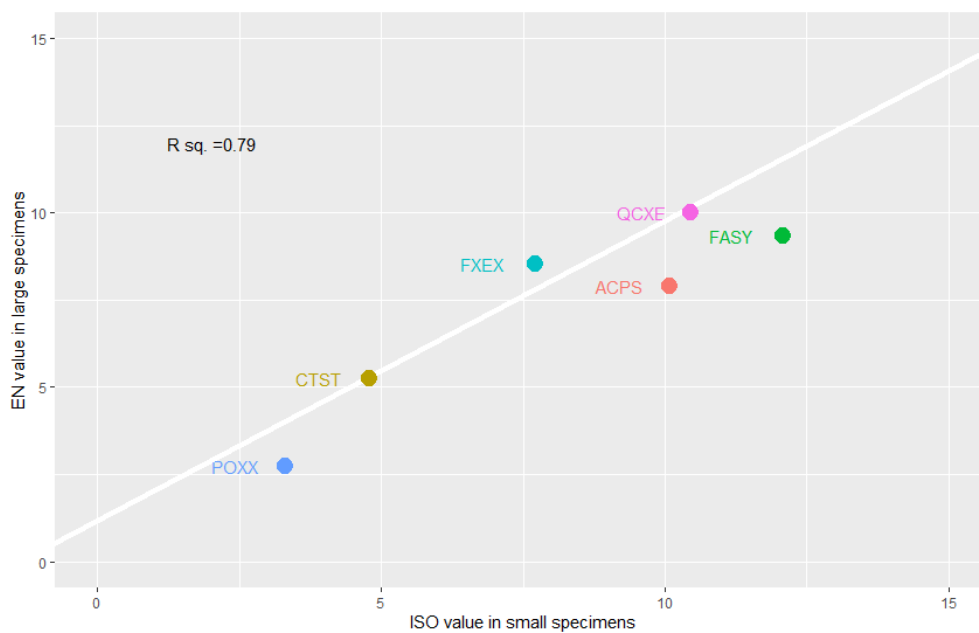
Figure 7: correlation of ISO compression strength of small specimens with EN compression strength of large specimens over all species

$$f_{EN,Large} = 1.21 + 0.86 f_{ISO,Small} \tag{3}$$

$$f_{EN,Large} = 1.63 + 0.67 f_{BS,Small} \tag{4}$$

For many species very few full-size specimens were tested to date, and the above relationship needs to be verified with further testing. It would be desirable to include paulownia as a very low density/ strength species to verify the lower tail of the curve.

For predicting the characteristic compression strength of full size specimens tested according to EN 408 (which would be the standard procedure if one wants to use test results as design values for structural timber) one could determine 5ᵗʰ percentile values of the compression strength in small specimens and convert these with Equation 3 or Equation 4. It is advisable to use non-parametric 5ᵗʰ percentiles where possible, as the assumption of normal distribution is unlikely to be valid (see above). When translating

literature values, however, one might have no choice but to use a parametric approach for calculating the 5th percentile. Both approaches were therefore tested on the sycamore data, with either ISO or BS 5th percentile values as input variable. Percentiles were calculated as the simple parametric percentile and ranked percentile without confidence adjustment according to EN 14358 (European Committee for Standardization & British Standards Institution, 2016). The results of the predictions as compared to the "real" 5th percentile of EN values in large specimens are shown in Table 4. Predictions are closely aligned with the values observed in reality. The parametric method is likely to yield conservative results in most cases, due to the large coefficient of variation in samples with specimens with radially- and tangentially-oriented growth rings.

Table 11: Characteristic compression strength (EN value) of large specimens, real and predicted values

In N/mm^2	parametric	non-parametric
Real	6.20	6.22
Predicted from small BS value	5.82	6.67
Predicted from small ISO value	5.34	6.39

CONCLUSION

Compression strength perpendicular to grain in hardwoods is influenced by different factors, such as the orientation of growth rings, which might be influenced by specimen size, and the test method used. Even though different test methods can yield very different results for individual specimens, population values seem to be closely aligned so that means and percentiles can potentially be translated between different sizes and test methods. Equations for doing this have been shown to give good results for UK sycamore, but more work is needed to determine if these are applicable to other temperate hardwoods.

ACKNOWLEDGEMENTS

REFERENCES

ASTM International. (2002). Designation: D 245 – 00. Standard Practice for Establishing Structural Grades and Related Allowable Properties for Visually Graded Lumber.

British Standards Institution. (1957). BS 373: Methods of testing small clear specimens of timber.

Collins, S., & Fink, G. (2022). Mechanical behaviour of sawn timber of silver birch under compression loading. Wood Material Science & Engineering, 17(2), 121–128. https://doi.org/10.1080/17480272.2020.1801836

Deutsches Institut für Normung e. V. (1979). DIN 52192:1979-05. Testing of wood; compression test perpendicular to grain.

European Committee for Standardization, & British Standards Institution. (2003). BS EN 13556:2003 Round and sawn timber. Nomenclature of timbers used in Europe.

European Committee for Standardization, & British Standards Institution. (2012). BS EN 408:2010+A1:2012 Timber structures: structural timber and glued laminated timber: determination of shear strength and mechanical properties perpendicular to the grain.

European Committee for Standardization, & British Standards Institution. (2016). BS EN 14358:2016 Timber structures-Calculation and verification of characteristic values BSI Standards Publication.

European Committee for Standardization, & British Standards Institution. (2018). BS EN 384:2016+A1:2018 Structural timber-Determination of characteristic values of mechanical properties and density.

Kovryga, A., Stapel, P., & van de Kuilen, J. W. G. (2020). Mechanical properties and their interrelationships for medium-density European hardwoods, focusing on ash and beech. Wood Material Science & Engineering, 15(5), 289–302. https://doi.org/10.1080/17480272.2019.1596158

Leijten, A. J. M., Larsen, H. J., & Van der Put, T. A. C. M. (2010). Structural design for compression strength perpendicular to the grain of timber beams. Construction and Building Materials, 24(3), 252–257. https://doi.org/10.1016/j.conbuildmat.2009.08.042

Müller, U., Gindl, W., & Teischinger, A. (2003). Effects of Cell Anatomy on the Plastic and Elastic Behaviour of Different Wood Species Loaded Perpendicular to Grain. IAWA Journal, 24(2), 117–128. https://doi.org/10.1163/22941932-90000325

Price, A., Ridley-Ellis, D., Adams, S., Lehneke, S., Ash, A., & Macdonald, E. (n.d.). Timber properties of species with potential for wider planting in Great Britain.

Schlotzhauer, P. (2016). Review of EN 338 characteristic (perpendicular to grain compression) strength and stiffness as well as density values for European beech, ash and maple wood (in German). 6. Doktorandenkolloquium „Holzbau Forschung Und Praxis",.

Schlotzhauer, P., Nelis, P. A., Bollmus, S., Gellerich, A., Militz, H., & Seim, W. (2017). Effect of size and geometry on strength values and MOE of selected hardwood species. Wood Material Science & Engineering, 12(3), 149–157. https://doi.org/10.1080/17480272.2015.1073175

Senalik, C. A. (2021). Mechanical Properties of Wood. In Wood Handbook Wood as an Engineering Material .

van der Put, T. A. C. M. (2008). Derivation of the bearing strength perpendicular to the grain of locally loaded timber blocks. Holz Als Roh- Und Werkstoff, 66(6), 409–417. https://doi.org/10.1007/s00107-008-0258-0

Walley, S. M., & Rogers, S. J. (2022). Is Wood a Material? Taking the Size Effect Seriously. Materials, 15(15), 5403. https://doi.org/10.3390/ma15155403

APPENDIX

Table 12: Compression strength measured on 2-inch specimens

Species	n	Density kg/m³	COV %	EN strength N/mm²	COV %	ISO strength N/mm²	COV %	BS strength N/mm²	COV %	MC %
ACPS	90	569	6.1	10.1	25.7	9.2	26.7	10.7	23.4	11.9
CTST	6	499	1.8	4.8	8.6	4.6	12.0	5.1	9.4	14.7
FASY	17	781	2.4	12.1	16.4	10.8	18.6	13.6	11.7	12.6
FXEX	30	646	6.9	7.7	12.6	7.0	14.2	8.3	13.9	12.7
POXX	26	394	5.6	3.3	25.3	2.9	26.8	3.5	24.9	12.8
QCXE	18	789	5.3	10.5	18.3	9.5	18.3	11.2	15.8	13.1
PWXX	18	253	5.8	1.7	19.4	1.5	20.9	1.9	17.4	12.1

Table 13: Compression strength measured on full-size specimens

Species	n	Density kg/m³	COV %	EN strength N/mm²	COV %	ISO strength N/mm²	COV %	BS strength N/mm²	COV %	MC %
ACPS	75	559	5.6	7.9	11.9	7.0	12.4	7.9	12.2	11.7
BTXX	4	586	6.9	5.6	17.8	5.0	17.6	5.8	16.4	11.0
CTST	6	545	3.4	5.1	9.4	4.5	8.8	5.2	9.8	13.4
FASY	5	761	2.0	9.3	9.0	8.1	10.4	9.4	5.8	12.4
FXEX	4	652	16.4	9.2	10.9	8.2	10.0	8.6	13.1	12.0
POXX	10	406	6.1	2.8	8.9	2.5	8.6	2.7	12.5	12.4
QCXE	4	741	9.0	10.7	13.4	9.6	13.9	10.0	18.3	12.7

Compensatory Anatomical Studies on *Robinia*, *Sclerocarya* and *Ulmus*

Fath Alrhman A. A. Younis[1,2]*, Róbert Németh*[1]*, Mátyás Báder*[1*]

[1] University of Sopron, Faculty of Wood Engineering and Creative Industries, Bajcsy-Zs. Str. 4, Sopron, Hungary, 9400
[2] University of Gezira, Faculty of Forest Sciences and Technology, Al Gezira, Wad Madani, Sudan.

E-mail: fath.alrhman.awad.younis@phd.uni-sopron.hu; nemeth.robert@uni-sopron.hu; bader.matyas@uni-sopron.hu

ABSTRACT
This study shows the differences in fibre characteristics of *Robinia pseudoacacia* growing in Hungary and *Sclerocarya birrea* growing in Sudan. Also, the analysis and comparison of the growing zone widths (the vessel lumina diameters in the earlywood and the wave amplitudes of the wavy vessel bands) for *Ulmus minor* were studied. The mean values of fibre length (mm), lumen diameter (µm), fibre diameter (µm), and cell wall thickness (µm) of *R. pseudoacacia* were 0.83, 13.18, 18.35, and 513, respectively. While they were 0.82, 26.37, 18.01, and 8.36 for *S. birrea*. The results also show that the fibre characteristics do not change gradually from pith to bark. The anatomical studies of *Ulmus minor* revealed significantly different results in the latewood widths, between 0.775 mm and 2.776 mm. Most vessels in the earlywood are below 0.721 mm diameter. The latewood vessel band amplitudes are mostly between 0.138 and 0.230 mm.

INTRODUCTION
The University of Sopron, Hungary deals extensively with the proper management of trees and wood from both scientific and practical perspectives. The Faculty of Forestry is the only place in Hungary to train, among others, forest engineers and nature conservation engineers, while the Faculty of Wood Engineering and Creative Industries trains, among others, engineers for the wood industry, specialists in the creative industry, and product designers. The former Institute of Wood Science, now part of the Institute of Basic Sciences, deals with the properties and modification possibilities of wood. Good examples are the following scientific publications: (Komán 2022; Fehér et al. 2014; Lublóy et al. 2023; Komán and Varga 2020; Kern et al. 2022; Bak 2012; Horváth and Fehér 2023; Fodor and Bak 2023). Our aim with this study is to present the activities and some of our important results we have carried out in the recent years, in order to present research in connection with the wood industry. We believe that the work we do is globally important. In this article, we mainly present some of our research and results on the anatomical properties of wood.

The comprehensive knowledge of the anatomical features of wood is crucial in the process of selecting the most suitable wood for a certain purpose. Anatomical traits can be classified into two broad categories: macro and micro. The measurement of fibre length in wood is a crucial factor that significantly impacts the overall quality and characteristics of pulp and paper products. Various methods can be employed to measure the fibre lengths of different wood species (Figure 1). Wood species exhibit great variations in their fibre lengths. In general, softwood fibres possess higher length and strength compared to hardwood fibres, hence contributing to the tensile strength of paper, as an example. Hardwood fibres are shorter and opaque, and they add smoothness and better printability to paper (Salminen et al. 2014). Environmental elements, including climate, soil conditions, and silviculture practices, can also exert an influence on the length of fibres in pulpwood (Desch and Dinwoodie 1996). Hence, the assessment of wood fibre length important in pulp and paper production. Several previous studies investigated the variation in wood anatomical properties (Adamopoulos and Voulgaridis 2002; Chowdhury et al. 2012; Nugroho et al. 2012; Salvo et al. 2017; Rungwattana and Hietz 2018; Liu et al. 2020). This article comprises a couple of parts, with the first part focusing on the investigation of radial variation in fibre characteristics of *Robinia pseudoacacia* and *Sclerocarya birrea* wood species.
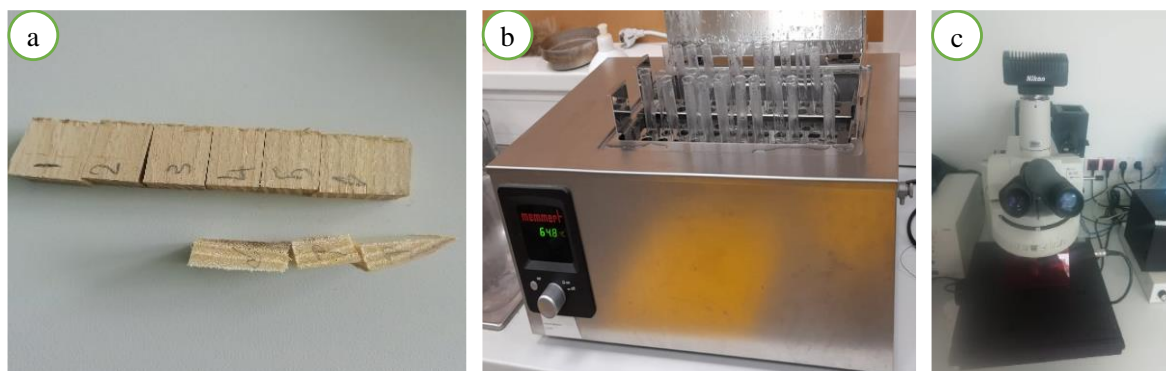
Figure 1: Three stages of measuring fibre characteristics: (a) R. pseudoacacia specimens marked from pith to bark, (b) specimens in water bath, (c) microscope with digital camera

Another topic was the examination of some anatomical properties of field elm (*Ulmus minor* Mill.). This wood species has a special vessel arrangement in the latewood region, called wavy vessel bands as it can be seen in Figure 2. The field elm can be classified as a ring-porous wood species, similarly to the *Robinia pseudoacacia*. Its vessels have an average diameter of 35 µm in the latewood and 150 µm in the earlywood. In the latewood, wavy vessel bands can be seen, which are interrupted in some places (Figure 2) (Molnár and Börcsök 2016). The aim of the second part of this article was the analysis and comparison of the growing zone widths; the vessel lumina diameters in the earlywood and the wave amplitudes of the wavy vessel bands.
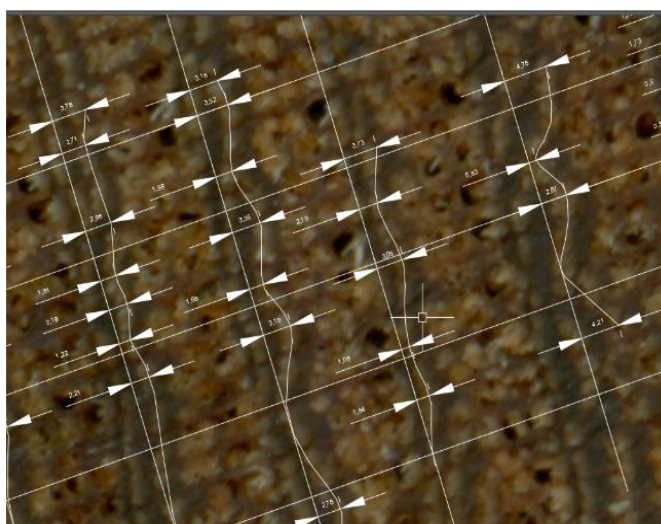
Figure 2: Wavy vessel band measurement in the latewood of field elm

MATERIALS AND METHODS
Fibre characteristics of Robinia pseudoacacia and Sclerocarya birrea

The wood samples of *S. birrea* were obtained from the Laboratory of Wood Science, Faculty of Forestry at the University of Khartoum, Khartoum, Sudan. The *R. pseudoacacia* wood samples were obtained from trees grown in Hungary and processed at the former Institute of Wood Science, University of Sopron, Sopron, Hungary. The radial strips were used to measure the fibre length (mm), fibre diameter (µm), lumen diameter (µm), and wall thickness (µm).

Continuous removal of small pieces, at intervals of 1 cm, was conducted from the pith to the bark for *R. pseudoacacia*. Similarly, for *S. birrea*, small pieces were continually removed, but at intervals of 2 cm. The wood samples underwent maceration using a Franklin solution, which is composed of glacial acetic acid and hydrogen peroxide in equal quantities. Subsequently, the samples were subjected to a temperature of 60°C for 24 hours (Kitin 1999). The fibre traits were assessed using a Nikon light microscope equipped with a digital camera (BR Nikon E80i) and an image-analysis software (NIS-Elements). A total of fifty wood fibres and twenty-five-lumen diameter and wall thicknesses were measured in each specimen.

Anatomical properties of Ulmus minor

The fresh-cut end grains of green *Ulmus minor* mature wood specimens were scanned on a HP Scanjet G4050 (Hewlett-Packard Development Company, USA). In AutoCAD software Autodesk, USA), with the help of a ruler scanned together with the specimens, we were able to scale the images to be able to measure accurate data.

We measured the width of the latewood and earlywood along a predetermined, radial straight line. Since the earlywood widths were almost the same, we later dealt only with the latewood.

In the earlywood vessel diameter examinations, we measured the diameters of the vessels in each annual ring within a 4 mm wide radial band of the test plots, and then calculated the averages and standard deviations.

In the third case, we examined the amplitudes of the vessel bands, that are the heights of the waves of the vessel bands. Along the predetermined 4 mm wide radial band, we marked in AutoCAD a vessel band in each latewood, which does not break in the examined area and well represents the properties of the other vessel bands. We measured the wave heights and calculated the averages and standard deviations.

RESULTS AND DISCUSSION

Table 1 presents the mean values, together with their corresponding standard deviations for fibre length, lumen diameter, fibre diameter, and double cell wall thickness in wood samples of *R. pseudoacacia* and *S. birrea*. The mean values of fibre length and fibre diameter of both species are similar. In comparison, the lumen diameter and cell wall thickness of *S. birrea* are larger than those of *R. pseudoacacia*.

Table 1: Some anatomical results of R. pseudoacacia and S. birrea wood species

	Fibre characteristics	MIN	MEAN	MAX	STD
R. pseudoacacia	Fibre length (mm)	0.71	0.83	0.99	0.09
	Lumen diameter (µm)	8.40	13.18	18.02	3.06
	Fibre diameter (µm)	14.05	18.35	22.58	2.75
	Wall thickness (µm)	4.56	5.13	5.74	0.38
S. birrea	Fibre length (mm)	0.73	0.82	0.90	0.05
	Lumen diameter (µm)	23.45	26.37	29.69	2.23
	Fibre diameter (µm)	14.81	18.01	21.26	2.18
	Wall thickness (µm)	7.51	8.36	9.48	0.57

The fibre length and cell wall thickness of *R. pseudoacacia* exhibit greater values close to the bark. Nevertheless, we observed that the lumen diameter and fibre diameter revealed a decrease near the bark, as shown in Figure 3. The fibres of *S. birrea* wood exhibited the smallest length near the bark. The length of the fibres revealed a rapid growth from the pith until specimen four, after which they exhibited instability towards the bark. Also, the lumen diameter, fibre diameter, and wall thickness decreased constantly after specimens 4–5 and then increased near the bark, as given in Figure 4.
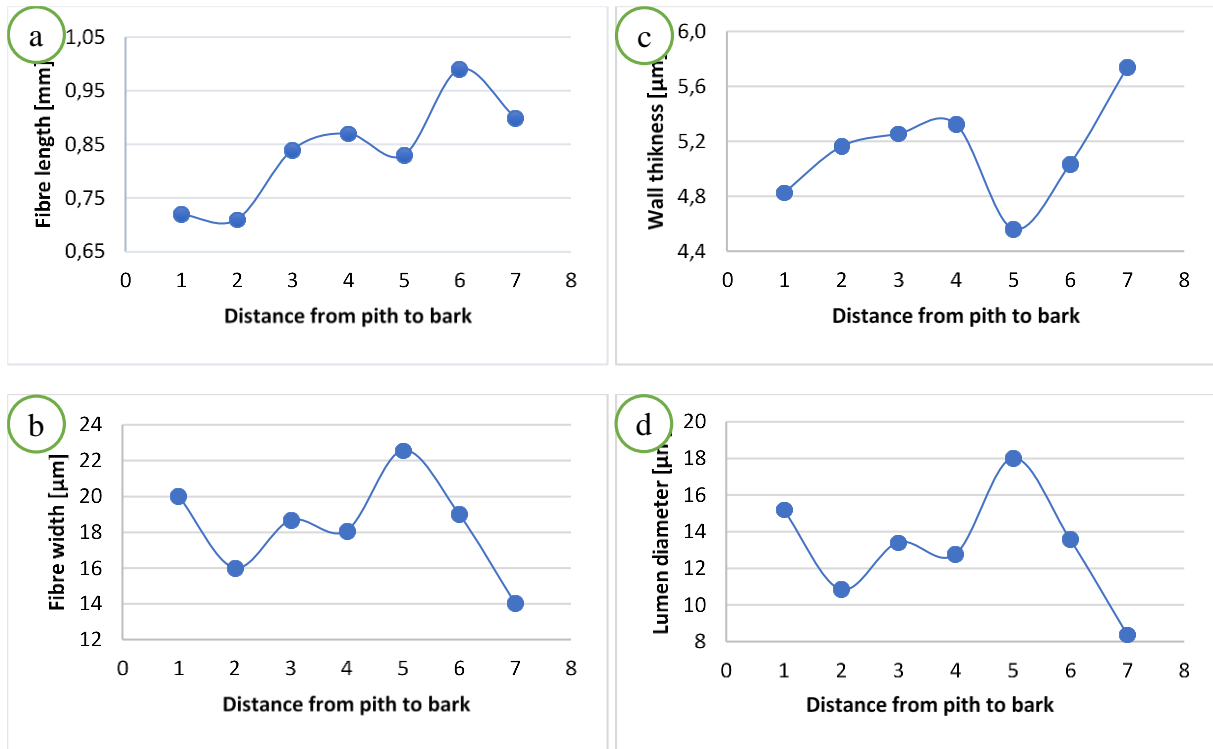
Figure 3: Fibre length (a; mm), fibre width (b; µm), cell wall thickness (c; µm), and lumen diameter (d; µm) of R. pseudoacacia from pith to bark
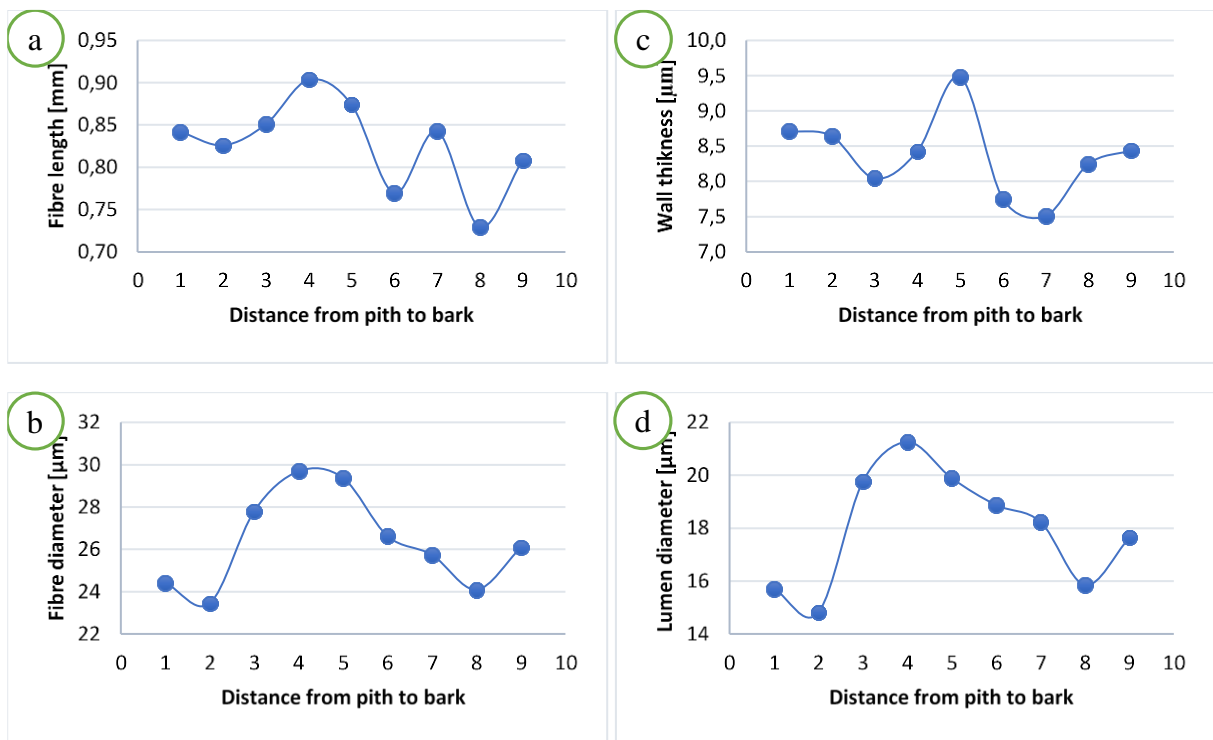
Figure 4: Fibre length (a; mm), fibre width (b; µm), cell wall thickness (c; µm), and lumen diameter (d; µm) of S. birrea from pith to bark

Figure 5 illustrates the significant difference in the mean of pair groups of samples for *R. pseudoacacia* (a) and *S. birrea* (b), as observed from the pith to the bark. Whenever, the interval between groups includes zero, it suggests that there is no statistically significant difference in the means of the groups.
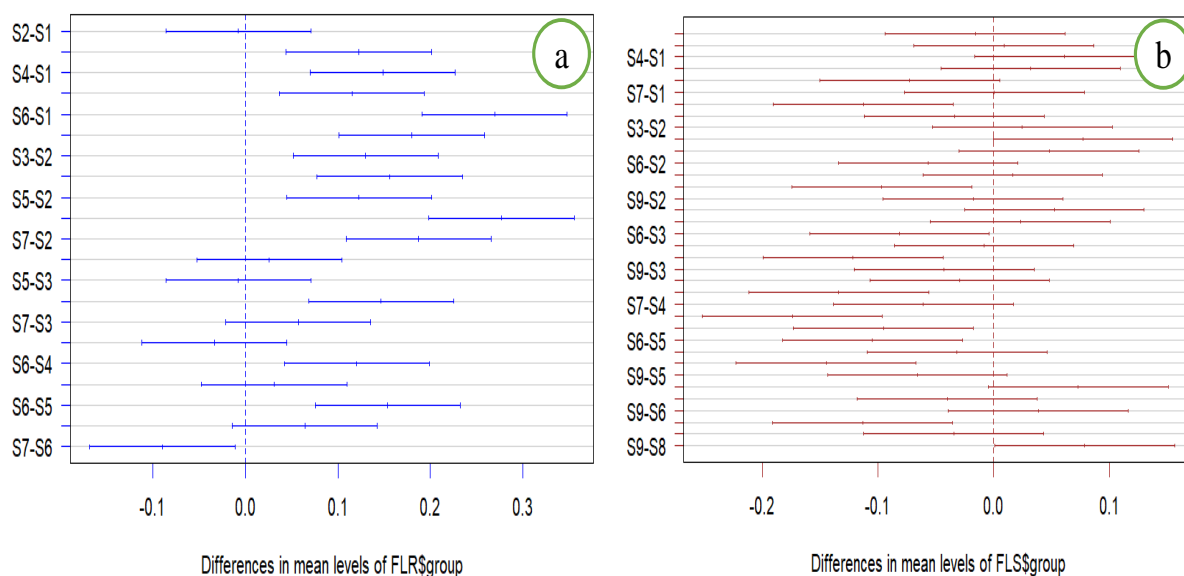
Figure 5: Graphic display of pair-wise comparisons from Tukey's HSD for R. pseudoacacia (a) and S. birrea (b). If the interval contains zero, that indicates the difference in group means is statistically not significant. Abbreviations: S1-S9: numbered specimens

The next results were obtained from the anatomical properties of the field elm. Comparing the earlywood and latewood widths, the standard deviation in the latewood was greater than in the earlywood, as we measured almost similar values in the earlywood. The average width of the earlywood was 1.018 mm, while that of the latewood was 1.537 mm with a relative standard deviation of 41.7%. That is, the significantly different ring widths of these specimens can be largely attributed to the variability of the latewoods, where very different results were obtained, between 0.765 mm and 2.776 mm. For almost half of the measurements there was an annual ring width of more than 2 mm.

The analysis of the vessel diameters of the earlywood was done taking into account the width of the earlywood. Almost identical vessel diameters are found regardless of the different widths of the earlywood. The mean diameter was 0.202 mm with a standard deviation of 0.045 mm. The relative standard deviation is 22.3%.

The amplitudes of the vessel bands in the latewood region range from very small to very large. Almost half of the results are between 0.138 and 0.230 mm. In some cases, very high results have also occurred, over 0.5 mm. The amplitude of vessel bands arranged in a nearly straight line was 0.104 mm on average, which is a value very close to zero if we take into account the circular shape of the annual ring section of these specimens. The smallest measured amplitude was 0.066 mm. In contrast, the amplitude of vessels clearly arranged in a wavy band was 0.336 mm on average. These waves can already be seen with the naked eye on the end-grain surface. It is worth noting that the length of some vessel bands is quite short, regardless of their amplitude.

CONCLUSIONS

Fibre lengths and fibre diameters of *R. pseudoacacia* and *S. birrea* have similar values. The lumen diameter and cell wall thickness of *S. birrea* are larger than those of *R. pseudoacacia*. The fibre length and cell wall thickness of *R. pseudoacacia* exhibit greater values close to the bark. Nevertheless, it was observed that the lumen diameter and fibre diameter revealed a decrease near the bark.

The earlywood widths were almost the same for the field elm (*Ulmus minor* Mill.). On the contrary, significantly different results were obtained for the latewood widths, from 0.775 mm to 2.776 mm. For vessel diameters in the earlywood, most results are below 0.721 mm. Amplitudes between 0.138 and 0.230 mm were mostly measured for vessels arranged in wavy lines in the latewood. In comparison to the average value, outstanding amplitudes occurred in few cases.

REFERENCES

Adamopoulos S, Voulgaridis E (2002) Within-tree variation in growth rate and cell dimensions in the wood of black locust (robinia pseudoacacia). IAWA J 23:191–199. https://doi.org/10.1163/22941932-90000297

Bak M (2012) The effect of oil-heat-treatment on some major properties of poplar wood (Növényi olajokban hőkezelt nyár faanyag tulajdonságainak vizsgálata). PhD Dissertation, University of West-Hungary

Chowdhury MQ, Ishiguri F, Hiraiwa T, et al (2012) Variation in anatomical properties and correlations with wood density and compressive strength in Casuarina equisetifolia growing in Bangladesh. Australian Forestry 75:95–99. https://doi.org/10.1080/00049158.2012.10676390

Desch HE, Dinwoodie JM (1996) Timber, structure, properties, conversion, and use, 7th edition. Macmillan Press Ltd, London

Fehér S, Komán S, Börcsök Z, Taschner R (2014) Modification of hardwood veneers by heat treatment for enhanced colors. BioResources 9:3456–3465

Fodor F, Bak M (2023) Studying the Wettability and Bonding Properties of Acetylated Hornbeam Wood Using PVAc and PUR Adhesives. Materials 16:2046. https://doi.org/10.3390/ma16052046

Horváth D, Fehér S (2023) Magas hozzáadott értékű termékek előállítási potenciálja termelésből kieső, alacsony minőségű tölgy alapanyagból: Előzetes eredmények. Gradus 10:. https://doi.org/10.47833/2023.1.ENG.001

Kern Z, Árvai M, Urdea P, et al (2022) First report on dendrochronological and radiocarbon studies of subfossil driftwood recovered across the Mureş/Maros Alluvial Fan. CEuGeol 65:40–48. https://doi.org/10.1556/24.2021.00120

Kitin P (1999) Variations in the Lengths of Fusiform Cambial Cells and Vessel Elements in Kalopanax pictus. Annals of Botany 84:621–632. https://doi.org/10.1006/anbo.1999.0957

Komán S (2022) Quality characteristics of the selected variant of Paulownia tomentosa (Robust4) wood cultivated in Hungary. Maderas, Cienc tecnol 25:. https://doi.org/10.4067/S0718-221X2023000100401

Komán S, Varga D (2020) Physical and mechanical properties of wood from invasive tree species. Maderas, Cienc tecnol 23:. https://doi.org/10.4067/S0718-221X2021000100411

Liu Y, Zhou L, Zhu Y, Liu S (2020) Anatomical Features and Its Radial Variations among Different Catalpa bungei Clones. Forests 11:824. https://doi.org/10.3390/f11080824

Lublóy É, Mészáros DT, Takács LG, et al (2023) Examination of the fire performance of wood materials treated with different precautions. J Therm Anal Calorim 148:4129–4140. https://doi.org/10.1007/s10973-023-12050-2

Molnár S, Börcsök Z (2016) Szil (szil fajok) - Ulmus spp. (Elm (elm species) - Ulmus spp). In: Molnár S, Farkas P, Böcsök Z, et al. (eds) Földünk ipari fái. Erfaret Nonprofit Kft, Sopron, Hungary, pp 112–114

Nugroho WD, Marsoem SN, Yasue K, et al (2012) Radial variations in the anatomical characteristics and density of the wood of Acacia mangium of five different provenances in Indonesia. J Wood Sci 58:185–194. https://doi.org/10.1007/s10086-011-1236-4

Rungwattana K, Hietz P (2018) Radial variation of wood functional traits reflect size-related adaptations of tree mechanics and hydraulics. Functional Ecology 32:260–272. https://doi.org/10.1111/1365-2435.12970

Salminen LI, Liukkonen S, Alava MJ (2014) Ground Wood Fiber Length Distributions. BioResources 9:1168–1178. https://doi.org/10.15376/biores.9.1.1168-1178

Salvo L, Leandro L, Contreras H, et al (2017) Radial variation of density and anatomical features of Eucalyptus nitens trees. Wood and Fiber Science 49:301–311

The influence of the type of varnish on the viscous-elastic properties of maple wood used for musical instruments

Roxana Gall[1*], Adriana Savin[1,2], Mariana Domnica Stanciu[1], Mihaela Campean[3], Vasile Ghiorghe Gliga[1,4]

[1*] Faculty of Mechanical Engineering, Transilvania University of Brașov, B-dul Eroilor 29, 500036, Brașov, Romania.
[2] Institute of Research and Development for Technical Physics, B-dul Mangeron 47, 700050, Iasi, Romania.
[3] Faculty of Furniture Design and Wood Engineering, Transilvania University of Brasov, B-dul Eroilor 29, 500036, Brasov, Romania.
[4] S.C. Gliga Musical Instruments S.A, Str. Pandurilor nr. 215, 545300, Reghin, Mures, Romania.

E-mail: roxana.gall@student.unitbv.ro, asavin@phys-iasi.ro, mariana.stanciu@unitbv.ro; campean@unitbv.ro, vasile@gliga.ro

Keywords: varnishing, maple wood, viscous-elastic properties, dynamic mechanical analysis (DMA).

ABSTRACT
In the dynamic behaviour of maple wood in the construction of stringed musical instruments, the viscous-elastic properties in terms of storage modulus, loss modulus and the ratio of these components in the complex domain provide information about the internal friction of the material known as damping. Studies have shown that finishing has a measurable influence on the final sound properties of violins through changes in mechanical properties. The most commonly reported impact is a decrease in specific stiffness in the longitudinal direction and an increase in the radial direction, as well as an increase in damping in both directions. Starting from these considerations, the objective of the paper is to highlight the effect of the type of varnish and the thickness of the film on the viscous-elastic behaviour of maple wood. The samples used for the determinations were extracted longitudinally from plates varnished with oil-based varnish, respectively alcoholic varnish, with different numbers of layers applied on a wooden support made of maple with different anatomical structures (wavy grain maple and straight grain maple). In case of samples varnished with alcohol varnish, all viscous-elastic parameters tend to increase with increasing exposure time compared to those finished with oil-based varnish. In the wavy grain maple samples, both the alcohol and the oil-based varnish produce an increase in the elastic component of the material as the number of layers, increases. In samples with the usual anatomical structure, the elastic behaviour is inversely proportional.

INTRODUCTION
Sycamore maple (*Acer pseudoplatanus L.*) is a wood species that is known for its wavy grain figure and its high-value utilization among luthiers for making musical instruments. The value of this wood species consists not only in the aesthetic aspect it gives to the musical instrument, but also in its elastic and acoustic properties, such as the dynamic elastic modulus, sound velocity in wood, damping (tan d), the quality factor Q (Alkadri et al. 2018, Spycher et al. 2008, Straže et al. 2020, Cretu et al. 2022). If the values of these elastic and acoustics properties have been determined for maple wood, through different testing methods as they were highlighted in the studies done by Kúdela & Kunštár (2011), Skrodzka et al. (2013), Sonderegger et al. (2013), the visco-elastic behavior of wood varnished with different types of varnish still arouses interest. Thus, based on the flexural vibration mode test, the values of the dynamic modulus E and of the damping were determined on samples painted with polyurethane varnish (Gunji et al. 2012), of alcohol varnish and oil varnish in correlation with temperature and frequency (Simonnet et al. 2002), or of the oriental lake urushi (Obataya 2001). In order to analyze the visco-elastic behavior of the varnish film, Laimmlein et al. (2020) studied three types of varnish films determining the modulus of elasticity in the tensile test, the dynamic modulus (storage and loss), damping (tan d) , and later simulated the dynamic behavior of some violin boards based on an inverse optimization problem. An in-depth study on the effect of the varnish film on the vibration capacity of

wood was carried out by Schelleng, (1968), a study that highlighted the influence of the thickness of the varnish film on the stiffness of spruce and maple boards, respectively on their acoustic impedance. Laimmlein et al. (2020) - Holz, analyzed the influence of different types of varnishes on rectangular boards made of maple wood and found that the new system wood-wood interface varnish and film varnish, leads to a decrease in the dynamic modulus of elasticity compared to unvarnished wood, and that important factors on the dynamic behavior, the longitudinal elasticity modulus, EL, radial, ER, and plane shear modulus, GRL, are studied. The evaluation of the propagation speeds of Lamb waves using ultrasound method, applied on thin maple wood plates varnished with alcohol varnish, respectively oil varnish, carried out by Faktorova et al. (2024), highlights that the increase in the number of varnish layers, regardless of the type of varnish , led to the decrease of the anisotropy ratio between the longitudinal and radial directions. Stanciu et al. (2024) studied the acoustic absorption of spruce wood samples varnished with alcohol varnish and maximum oil varnish, observing that the type of varnish changes the frequency at which the acoustic absorption is maximum. Thus, in the samples varnished with oil varnish, the acoustic absorption is not influenced by the varnish film, compared to the samples varnished with alcohol where the maximum coefficient of acoustic absorption occurs at different frequencies for the two parts of the samples: the unvarnished face absorbs the sounds with the maximum frequency in the 2-3 kHz range, and the varnished face absorbs sounds at frequencies higher than 4-5. kHz.

The objective of this paper is to highlight the effect of the type of varnish and the thickness of the film on the viscous-elastic behaviour of maple wood. Oil-based varnish, respectively alcoholic varnish, with 5, 10, 15 layers applied on a wooden support made of maple with different anatomical structures (wavy grain maple and straight grain maple) were compared to determine the difference in viscous-elastic parameters.

MATERIALS AND METHODS
Materials

The samples of maple wood (*Acer pseudoplatanus L*) with dimensions of 50x50x30 mm^3 as seen in Figure 1a), were extracted from plates varnished with oil-based varnish and alcohol varnish, with dimensions of 240 mm x 80 mm x4 mm. From the point of view of the anatomical structure of maple wood, the samples were grouped into two categories, wood with curly grain and wood with straight grain, classification based on the criteria presented in previous studies (width of annual rings, fiber undulation pitch, regularity of rings) (Dinulica 2023). From each anatomical category and type of varnish, samples with different thicknesses of the varnish layer (5, 10, 15 layers) were analysed (Figure 1b). All the samples investigated in this study were cut in the longitudinal direction, 3 samples from each category. Thus, varnished samples were prepared with oil varnish and alcohol varnish, according to the recipe of a musical instrument factory.
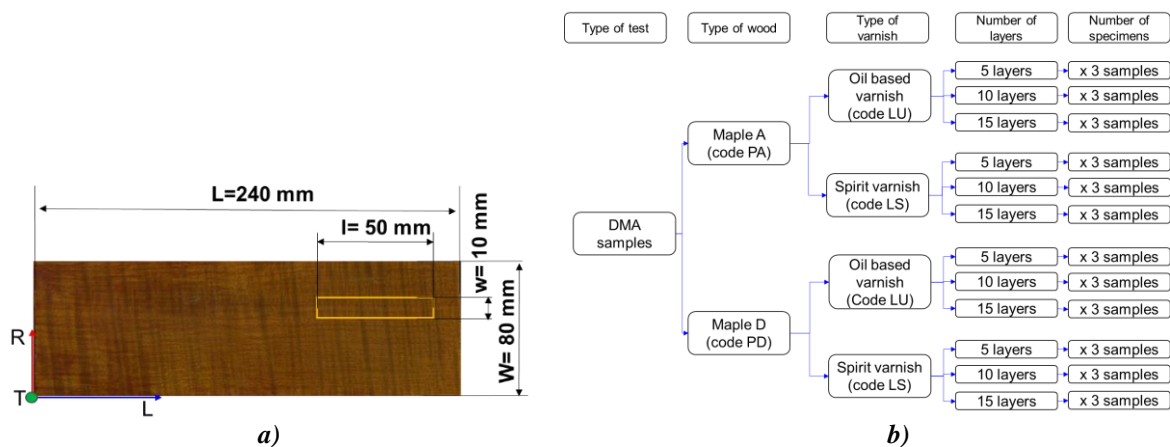

a)   *b)*

Figure 1: The maple wood samples for testing: a) sample preparation; b) types and codification of specimens

Methods
To determine the viscoelastic properties, the method of dynamic mechanical analysis (DMA 242C Netzsch equipment) was used, consisting in the application of an oscillating force at different frequencies (1 Hz, 3.33 Hz; 5 Hz; 10 Hz; 33.33 Hz; 50 Hz) with an intensity of force 6N, the samples being loaded to bend in 3 points, for a duration of 30 minutes. The low frequency data predicts varnished wood behaviour over longer timescales. The quantities determined were: the storage module E', the loss module E'', the damping, calculated as the ratio between E''/E'. For data processing, the time variation curves of the viscous-elastic properties were drawn, then the initial and final values of each quantity were extracted, for each frequency and sample, the results being averaged.

RESULTS AND DISCUSSION
The influence of the anatomical structure of the maple wood (curly grain versus straight grain)
Based on the response of the wooden sample, the viscous behaviour of the material can be determined in the form of the loss modulus, as well as the stiffness of the specimen in the form of the conservation modulus. These properties are often described as the ability to lose energy as heat (damping) and the ability to store energy to return to its original shape after deformation (elasticity). The anatomical structure of maple wood influences the viscous-elastic characteristics, especially the loss modulus and damping. At the time of initiation of the test, there are no notable differences in the storage modulus between the two anatomical quality classes of the wood, but the loss modulus and damping are higher in the case of samples with straight grain. But after 30 minutes of loading, an increase in the conservation modulus can be observed by approximately 20 - 35% compared to the initial moment, regardless of the grain type. With the increase of the stress frequency (50 Hz), the samples show a slight increase in the storage modulus by approximately 15% more than the initial moment. Overall, the storage modulus values are higher for samples with curly grain compared to straight grain (Figure 2).

a)

b)

c)

Figure 2: The influence of the anatomical structure of the maple wood on storage modulus: a) samples with 5 varnish layers; b) samples with 10 varnish layers; c) samples with 15 varnish layers

The deformation energy dissipation observed through the values of the loss modulus are influenced by both the anatomical structure and the type of varnish applied. Thus, in samples with oil-based varnish, the values are higher in samples with straight grain (Figures 3a and b). In the samples varnished with alcoholic varnish, the loss modulus registers a decrease in the values for wood with straight grain. It is

observed that the samples with 15 layers of alcoholic varnish register a stabilization of the conservation modulus values (Figure 3c). Taking into account the fact that the damping is calculated as the ratio between the loss module and the storage one, the trend is similar to those presented for the loss module (Figure 4).

a)

b)

c)

Figure 3: The influence of the anatomical structure of the maple wood on loss modulus: a) samples with 5 varnish layers; b) samples with 10 varnish layers; c) samples with 15 varnish layers

a)

b)

c)

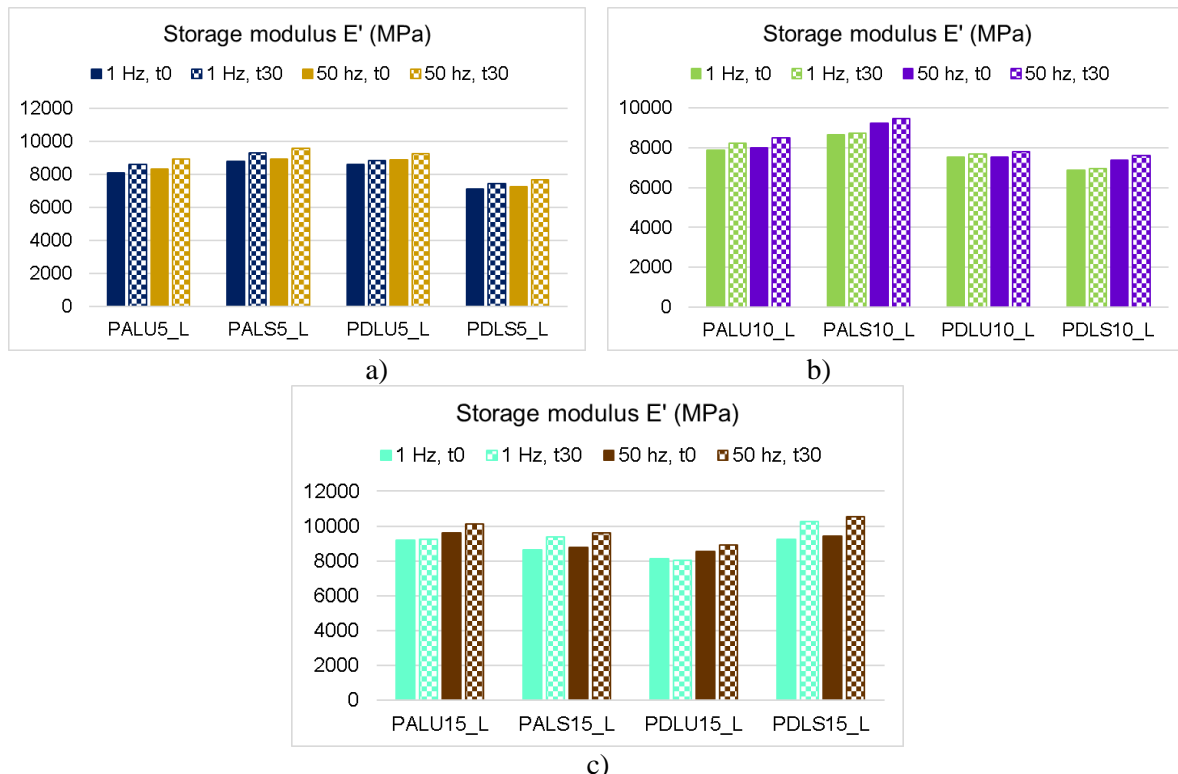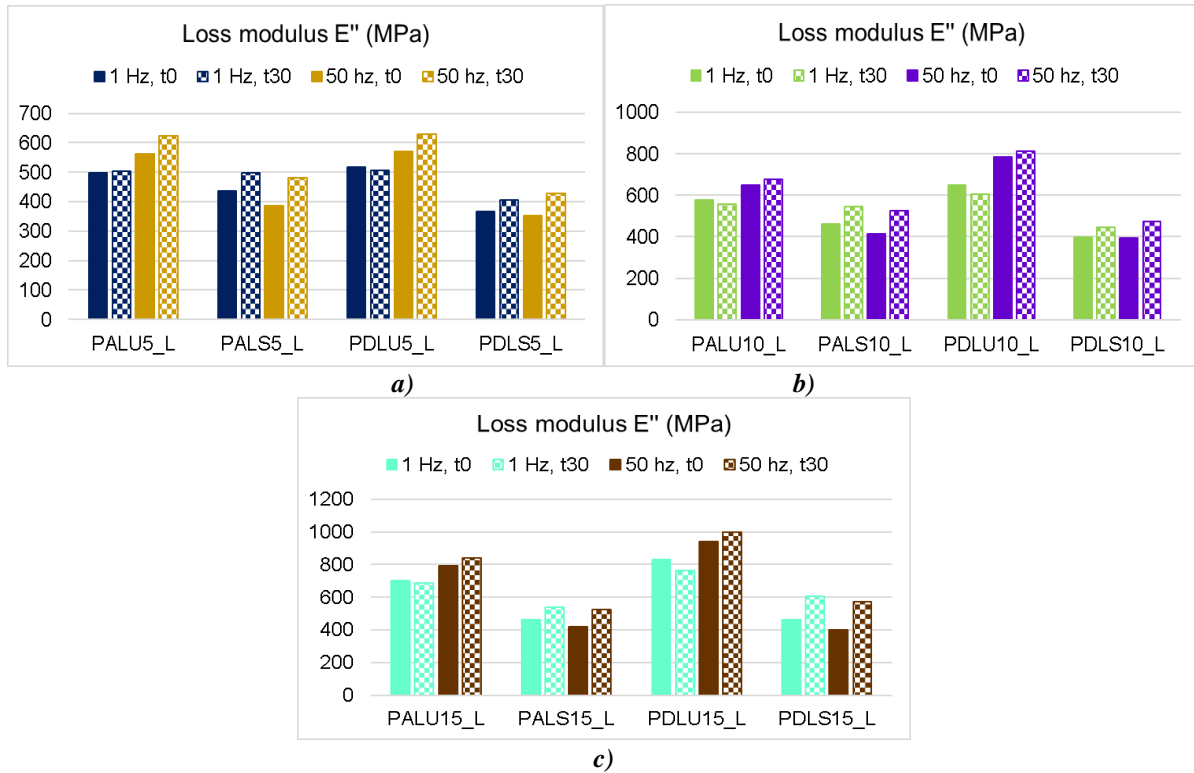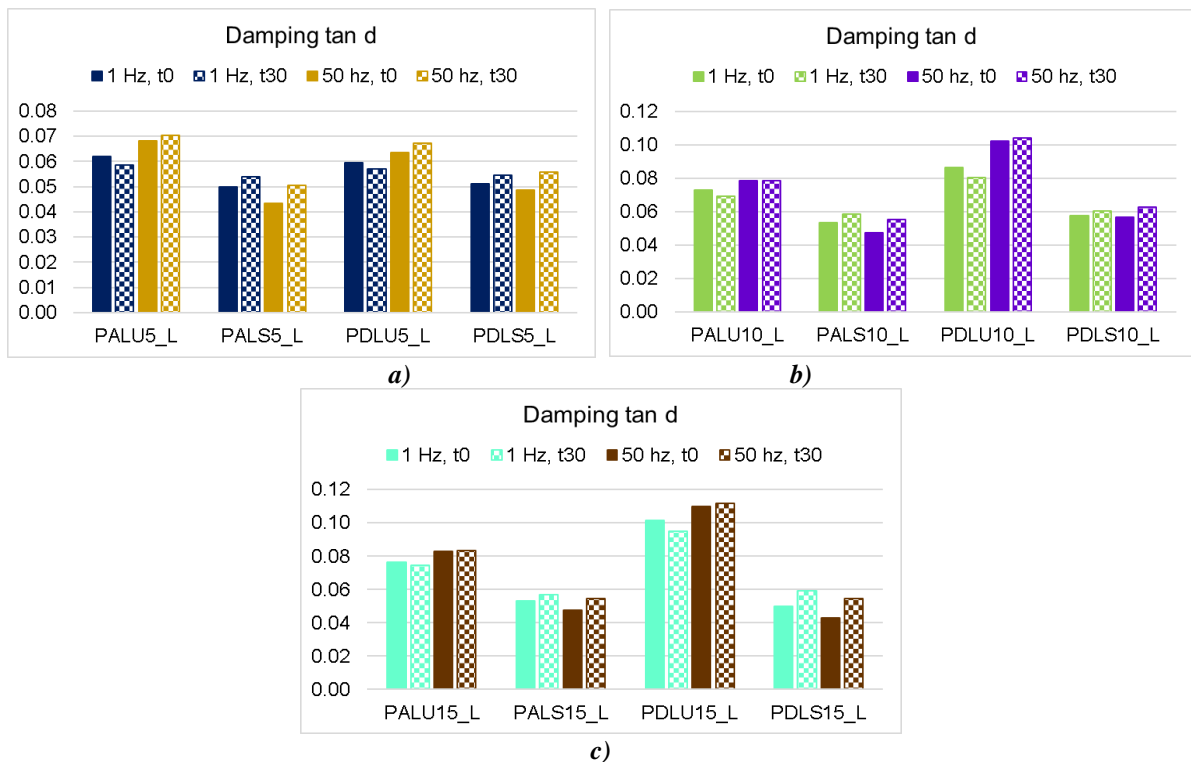**Figure 4: The influence of the anatomical structure of the maple wood on damping: a) samples with 5 varnish layers; b) samples with 10 varnish layers; c) samples with 15 varnish layers**

The influence of the type of varnish

According to Shelling (1968) the effects arising from the added stiffness of the lacquer can have negative effects on the vibrational capacity of the violin plates. The type of varnish influences the behaviour of the dynamic module. Thus, the curly grain samples covered with oil varnish, the stiffness increased with the increase of the varnish layer by approximately 13%, unlike the samples covered with spirit varnish where the differences given by the thickness of the varnish film are insignificant (Figure 5a and b). An interesting phenomenon is observed in wood with straight grain where the changes produced by the type of varnish are more significant for the alcohol varnish compared to the oil varnish, the variation between 5 and 15 layers being for the storage module of approx. 30% as can be seen in Figure 5c and d.

Figure 5: The influence of the varnish type on storage modulus: a) samples with curly grain varnished with oil varnish; b) samples with curly grain varnished with spirit varnish; c) samples with straight grain varnished with oil varnish; d) samples with straight grain varnished with spirit varnish (Legend: solid line represents the initial values of E'; dash line – final values of E' (after 30 minutes of stress))

With the increase in the loading frequency, damping increases both for samples varnished with oil varnish and for those with alcoholic varnish. But it is observed that at low frequencies (3.33, 5, 10 Hz), the samples with alcoholic varnish show a tendency to decrease the damping compared to the oil varnish (Figure 6). In general, the damping values are higher for samples varnished with oil varnish (tand=0.06 ÷ 0.11), compared to samples varnished with alcohol varnish (tand=0.042÷0.062). According to Schelleng, 1968, it can be considered that the oil varnish is a soft varnish, and the alcoholic varnish, a hard varnish. The obtained results confirm the fact that, although the oil varnish leads to a decrease in the quality factor for maple wood, this is compensated by the elastic properties along and across the grain and the higher density, which gives maple wood a higher rigidity compared to the alcoholic varnish that highlights an increase in the acoustic quality of the samples, but correlated with the stiffness of the material will lead to obtaining higher frequencies than spruce flat tops when building the violin body. Stanciu et al (2020), studied the effect of the anatomical structure of maple and spruce wood on the vibration modes of violin plates. Maple wood violin boards have been observed to exhibit nodal lines aligned with the anisotropic radial (R) direction of the wood and the direction of the medullary rays in the LR plane. The vibration of the curly grain maple plate produced the best resolution of the vibration mode pattern, with asymmetric modal shapes.

Knowing that the quality factor Q is 1/tand, the values of the quality factors were determined depending on the type of varnish, the thickness of the layers and the anatomical quality of the wood. Thus, Table 1 presents the centralized data for each loading frequency. It was found that, in general, the increase in

the thickness of the varnish film leads to a decrease in the quality factor, a more pronounced decrease in oil varnish. Increasing the loading frequency also leads to a decrease in the quality factor. In the samples covered with alcoholic varnish, an increase in the quality factor Q was observed with the increase in the loading frequency. Samples with straight grain show lower values of the quality factor compared to maple with curly grain.
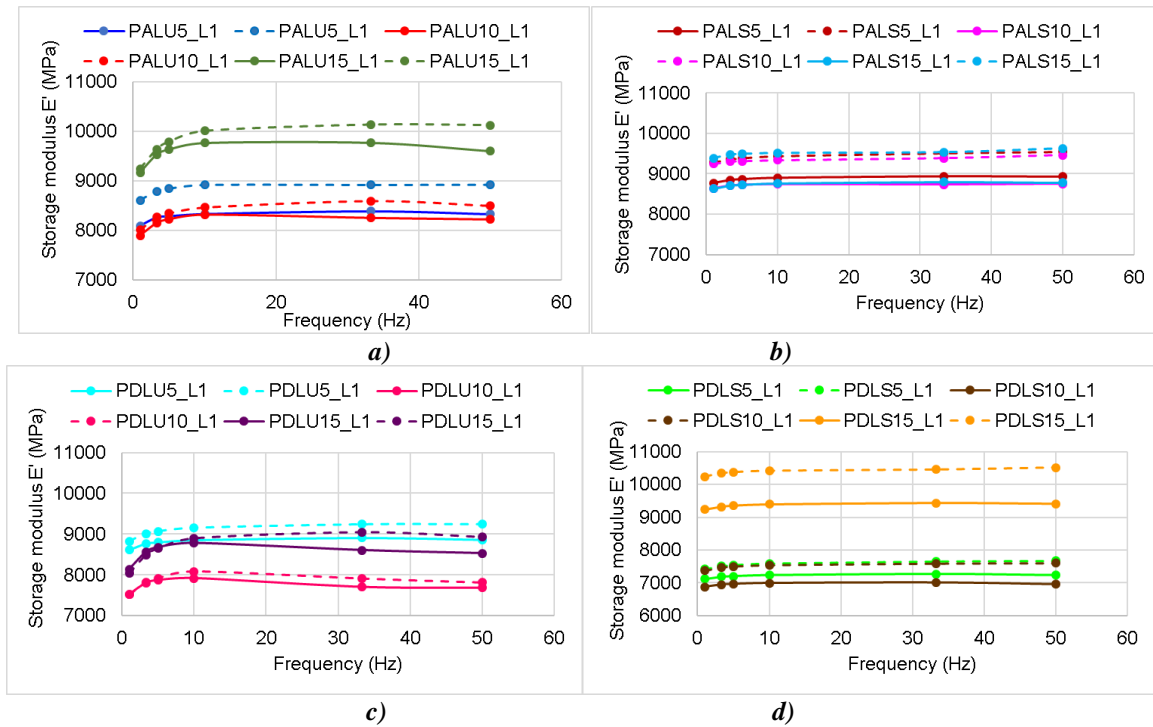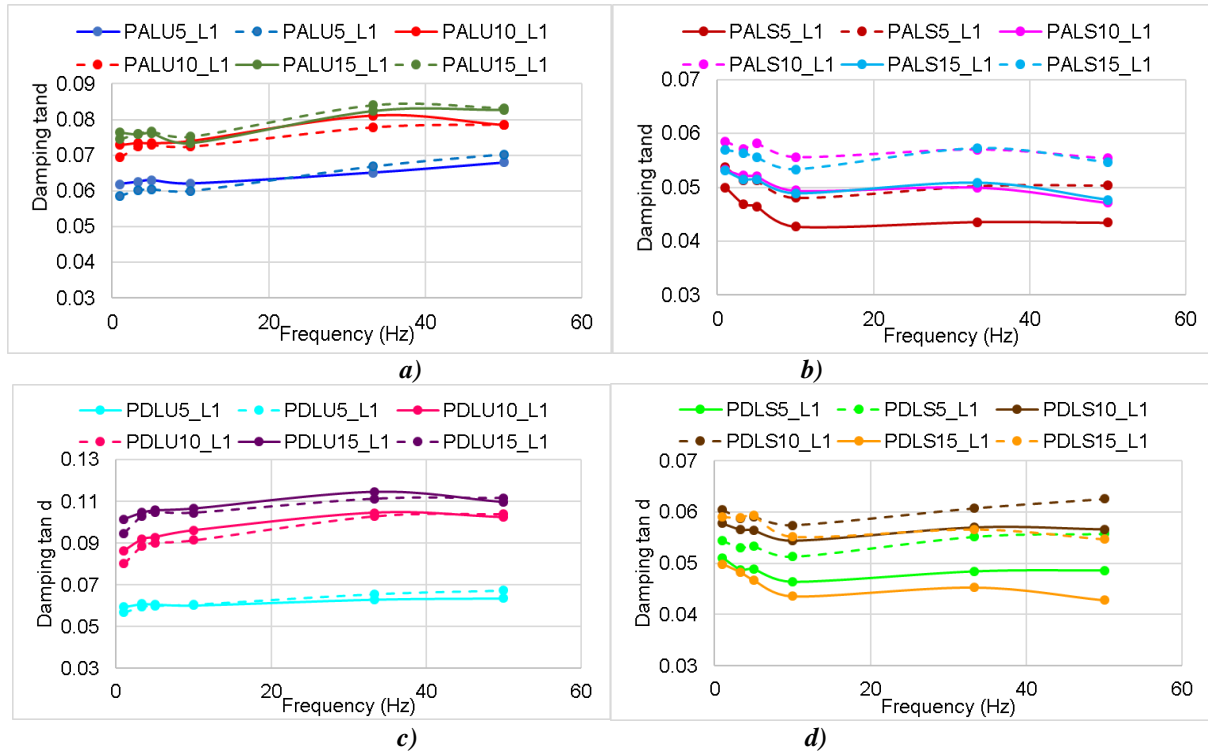

Figure 6: The influence of the varnish type on damping tand: a) samples with curly grain varnished with oil varnish; b) samples with curly grain varnished with spirit varnish; c) samples with straight grain varnished with oil varnish; d) samples with straight grain varnished with spirit varnish (Legend: solid line represents the initial values of E'; dash line – final values of E' (after 30 minutes of stress))

Table 1: The quality factor of studied specimens

Specimen	Loading frequency (Hz)					
	1	3.333	5	10	33.333	50
PALU5	17.05	16.63	16.54	16.68	14.96	14.23
PALU10	14.42	13.81	13.73	13.82	12.86	12.73
PALU15	13.43	13.15	13.05	13.30	11.91	12.02
PALS5	18.61	19.47	19.51	20.80	19.89	19.84
PALS10	17.09	17.50	17.20	17.97	17.53	18.05
PALS15	17.54	17.74	18.00	18.76	17.44	18.29
PDLU5	17.59	16.77	16.64	16.49	15.25	14.86
PDLU10	12.47	11.28	11.08	10.94	9.71	9.61
PDLU15	10.56	9.71	9.54	9.57	9.00	8.97
PDLS5	18.37	18.84	18.74	19.48	18.11	17.92
PDLS10	16.55	17.02	16.94	17.42	16.46	15.98
PDLS15	16.93	16.97	16.85	18.12	17.66	18.28

The influence of the number of varnish layers

In Figure 7, you can see the variation of the storage module in relation to the type of varnish and the number of layers. There is a trend for the dynamic modulus to increase with the increase in the number of layers, this being more pronounced for the oil varnish compared to the alcohol varnish. The same trend is observed in the case of the loss module, as shown in Figure 8. Being a result of the ratio between the loss modulus and the storage modulus, the damping follows the same increasing trend with the increase in the thickness of the oil varnish film, towards unlike the approximately constant behaviour in the case of alcohol varnish (Fig. 9).
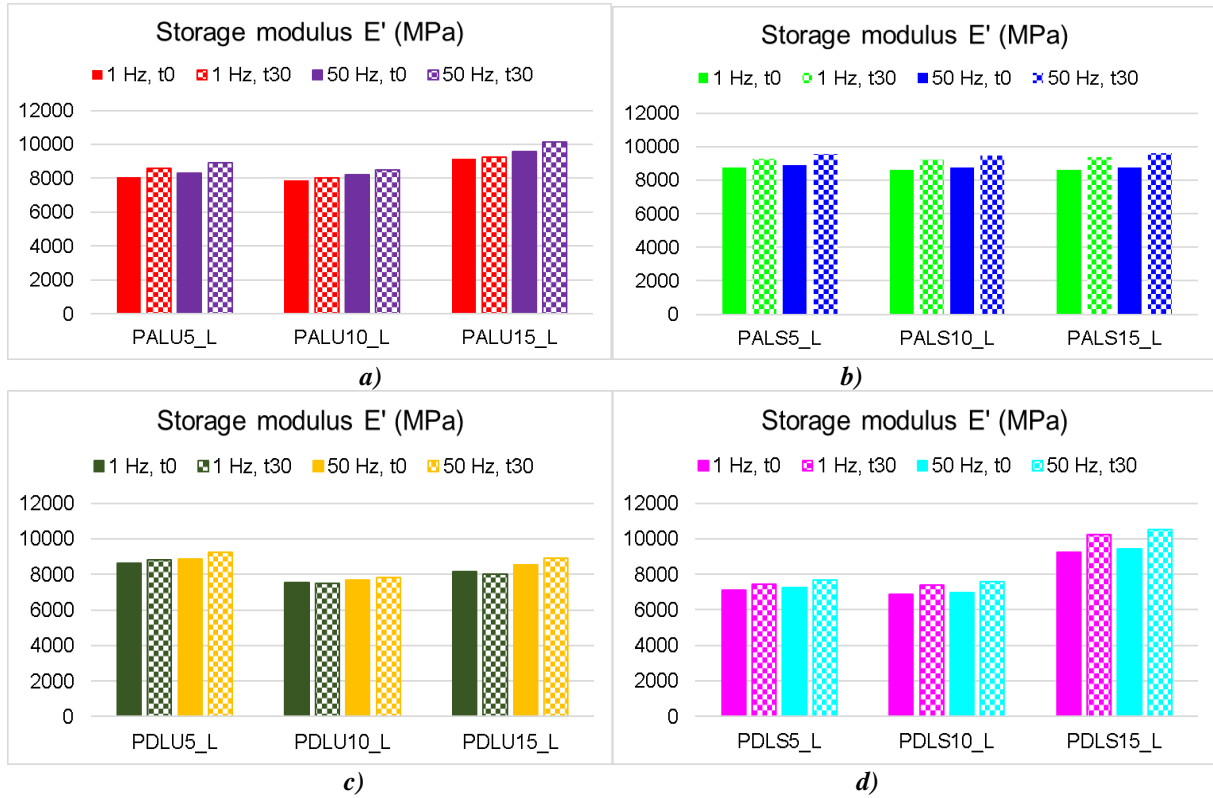
Figure 7: The storage modulus versus number of varnish layer: a) curly grain maple vanished with oil varnish; b) curly grain maple vanished with spirit varnish; c) straight grain maple vanished with oil varnish; d) straight grain maple vanished with alcohol varnish
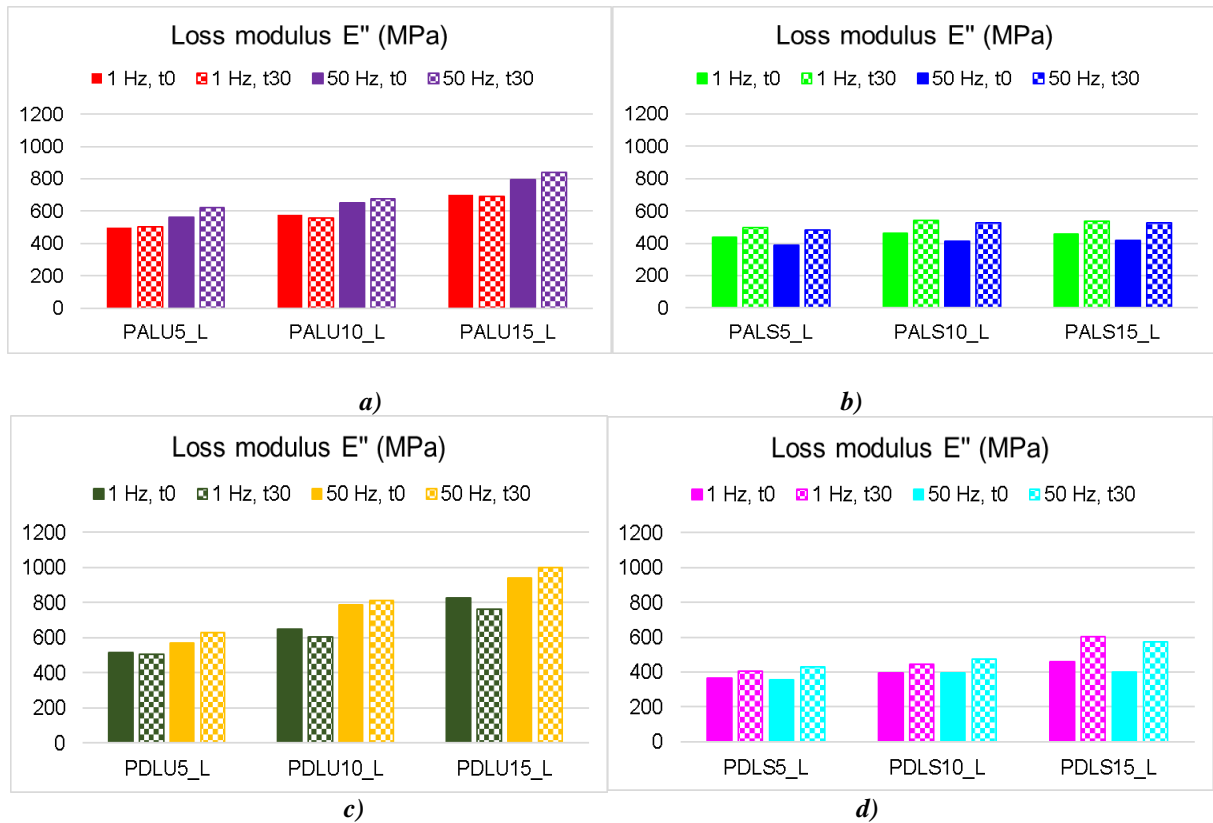
Figure 8: The loss modulus versus number of varnish layer: a) curly grain maple vanished with oil varnish; b) curly grain maple vanished with spirit varnish; c) straight grain maple vanished with oil varnish; d) straight grain maple vanished with alcohol varnish
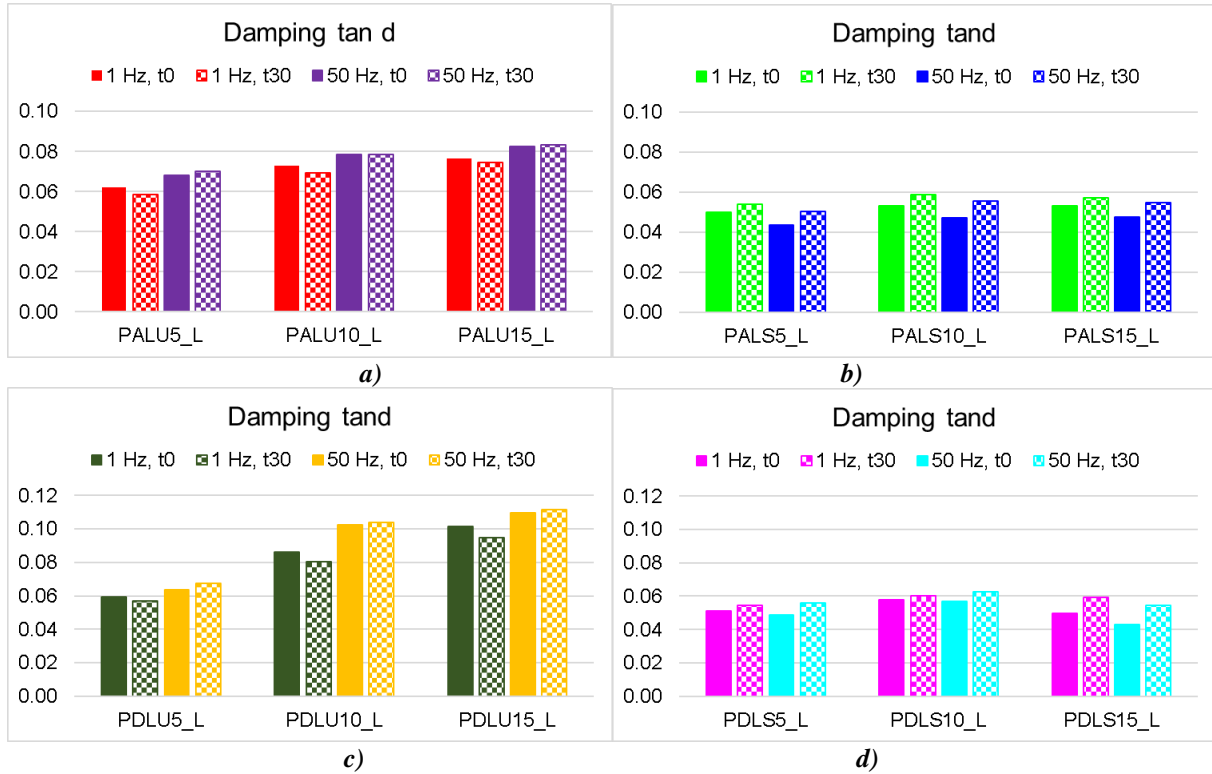
Figure 9: The damping versus number of varnish layer: a) curly grain maple vanished with oil varnish; b) curly grain maple vanished with spirit varnish; c) straight grain maple vanished with oil varnish; d) straight grain maple vanished with alcohol varnish

CONCLUSIONS

The purpose of the paper was to analyse the viscous-elastic behaviour of maple wood samples varnished with oil varnish and alcohol varnish, in different layer thicknesses, and the variation of the storage, loss and damping modulus was analysed in relation to different loading frequencies. applied for 30 minutes each. the results showed that the factors that influence the dynamic properties are the type of varnish, the thickness of the film and the anatomical characteristics of the wooden support. Future studies aim at the modal analysis of rectangular plates lacquered with the same types of lacquers and thicknesses, as well as the acoustic analysis of violins lacquered with the two categories of finishes presented in the current study.

ACKNOWLEDGMENTS

REFERENCES

Alkadri A, Carlier C, Wahyundi I, Grill J, Langbour P, Bremaud I (2018) Relationships between anatomical and vibrational properties of wavy sycamore maples . IAWA - Intern. Assoc. Wood Anatomists J. 39, 1: 63-86 Full-text: https://hal.archives-ouvertes.fr/hal-01667816

Crețu N, Roșca IC, Stanciu MD, Gliga VGh, Cerbu C (2022) Evaluation of wave velocity in orthotropic media based on intrinsic transfer matrix. Exp Mech, 62, 1595–1602, https://doi.org/10.1007/s11340-022-00889-9.

Dinulica F, Savin A, Stanciu MD (2023) Physical and Acoustical Properties of Wavy Grain Sycamore Maple (Acer pseudoplatanus L.) Used for Musical Instruments. Forests. 14, 197. https://doi.org/10.3390/f14020197.

Faktorová D, Stanciu MD, Krbata M; Savin A, Kohutiar, M, Chlada M, Năstac SM (2024) Analysis of the Anisotropy of Sound Propagation Velocity in Thin Wooden Plates Using Lamb Waves. Polymers, 16, 753. https://doi.org/10.3390/polym16060753

Gunji T, Obataya E, Aoyama K (2012) Vibrational properties of harp soundboard with respect to its multi-layered structure. Wood Sci. Technol. 58:322–326.

Kúdela J, Kunštár M (2011) Physical-acoustical characteristics of maple wood with wavy structure. Ann. Warsaw University of Life Sciences – SGGW, Forestry and Wood Technology, 75, 12–18.

Lämmlein S L, Van Damme B, Mannes D, Schwarze FWM, Burgert I (2020) Violin varnish induced changes in the vibro-mechanical properties of spruce and maple wood. Holzforschung, , 4(8), 765-776. https://doi.org/10.1515/hf-2019-0182.

Obataya E, Ohno Y, Norimoto M, Tomita B (2001) Effects of oriental lacquer (urushi) coating on the vibrational properties of wood used for the soundboards of musical instruments. Acoust Sci Tech 22:27–34.

Schelleng JC (1968) Acoustical Effects of Violin Varnish. The Journal of the Acoustical Society of America. Vol. 44 (5), 1175 – 1183.

Sedighi Gilani M, Pflaum J, Hartmann S et al. (2016) Relationship of vibro-mechanical properties and microstructure of wood and varnish interface in string instruments. Appl. Phys. A, 122, 260. https://doi.org/10.1007/s00339-016-9670-1

Simonnet C, Gibiat V & Halary J-L (2002) Physical and chemical properties of varnishes and their vibrational consequences. PACS Ref. 43, 75

Skrodzka EB, Linde BJB. Krupa A (2013) Modal Parameters of Two Violins with Different Varnish Layers and Subjective Evaluation of Their Sound Quality. Archives of Acoustics, , 38(1) 75-81.

Sonderegger W, Martienssen A, Nitsche C, Ozyhar T, Kaliske M, Niemz P (2013) Investigations on the physical and mechanical behavior of sycamore maple (Acer pseudoplatanus L.). Eur. J. Wood Prod. 71, 91–99. https://doi.org/10.1007/s00107-012-0641-8

Spycher M, Schwarze FWMR, Steiger R (2008) Assessment of resonance wood quality by comparing its physical and histological properties. Wood Sci. Technol. 42, 325–342, https://doi.org/10.1007/s00226-007-0170-5

Stanciu MD, Coșereanu C, Dinulică F, Bucur V (2020) Effect of wood species on vibration modes of violins plates. Eur. J. Wood Prod. 78, 785–799. https://doi.org/10.1007/s00107-020-01538-5

Stanciu MD, Cosnita M, Gliga GV, Gurau L, Timar C et al. (2024) Tunable Acoustic Properties Using Different Coating Sys-tems on Resonance Spruce Wood. Adv. Mat. Interfaces, , https://doi.org/10.1002/admi.202300781

Straže A, Jerman J, Brus R, Merela1 M, Gorišek Z, Krajnc L (2020) Selected structural, physical and acoustic properties of sycamore maple wood with fiddleback figure, 9th Hardwood Conference Proceedings PI. University of Sopron Press, Sopron, Hungary, pp 261–268.

XRF investigation of subfossil oak (*Quercus* spp) wood revealing colour - iron content correlation

Nedelcu Ruxandra[1*], Timar Maria Cristina[1*], Beldean Emanuela Carmen[1]

[1] Transilvania University of Brasov, B-dul Eroilor nr. 29, 500036 Brasov, Romania
E-mail: ruxandra.nedelcu@unitbv.ro; cristinatimar@unitbv.ro; ebeldean@unitbv.ro ;

Keywords: subfossil oak, XRF, elemental analysis, iron content, colour, CIELab, correlation

ABSTRACT
Subfossil oak wood is a precious and rare material, which was buried for hundreds to thousands of years in various humid anaerobic environments, such as riverbanks, bogs, water, swamps, conditions making possible an exchange of chemicals between the wood material and the environment. Water soluble extractives leach from wood while a variety of inorganic chemicals containing Ca, Si, Fe, Mg, Al, P, K, Cr, Mn, Cu, and others may penetrate into the wood structure. Iron is one of the most abundant chemical elements on earth and reactions of absorbed iron components of the sediments with tannins in oak wood result in a specific bluish grey to black colour. The main purpose of this research was investigation of subfossil oak by X-ray fluorescence (XRF) to have an image on the diversity of the main chemical elements contained, with a special focus on the iron content. Furthermore, it was intended to verify if a direct correlation could be found between the iron content in a certain point / small area and the CIELab colour parameters determined in the same location. Subfossil oak wood material from three buried trunks (S1, S2, S3) discovered accidentally in recent years in Romania was non-destructively investigated, employing a S1 Titan spectrometer from Nano Bruker (Germany). Measurements were carried out at 60s excitation time, in two phases (45/30 kV, 19.8/19.6 μA), with no filter and 8 mm collimator, on solid wood lamellae and sawdust samples, without any sample preparation. Several chemical elements such as: P, S, K, Ca, Cr, Mn, Fe and Cu were identified. The iron content determined by XRF was correlated with the CIELab colour parameters lightness (L*), redness (a*) and yellowness (b*), previously determined for the same samples and locations.

INTRODUCTION
Various analytical techniques, such as atomic absorption spectroscopy, X-ray fluorescence spectroscopy, and inductively coupled plasma mass spectroscopy may be employed for the precise determination and quantification of chemical elements in wood samples.
X-ray fluorescence (XRF) is recognised as a versatile, rapid, and cost-effective analytical method, allowing for quick and accurate elemental chemical characterisation across diverse types of materials and samples. XRF analysis is based on the principle of sample excitation, by a X- rays beam generated from a source, and subsequent emission of fluorescence X-ray photons by the sample components, enabling the recognition of specific elements contained. This method is particularly adequate and has been mostly employed for the investigation of inorganic materials, such as metal alloys, soil, rocks, glass, porcelain. Based on adequate analytical procedures, calibration chemical standards and data processing, both qualitative and quantitative elemental analysis is possible by XRF (Trojek and Trojkova 2023).
Different methods of qualitative and quantitative XRF investigation have been developed. They differ depending on various aspects, such as location of investigation (*in situ* or in the lab), principle of fluorescence X-rays detection and type of detector, their non-destructive or micro-destructive character in relation to the investigated artefact / material (directly on the object or on extracted samples), the size of the samples. Among the available methods, the followings were employed in the cited literature: energy dispersive (EDXRF) and portable (PXRF) X-ray fluorescence (Pereira Junior. et al. 2016, Ghavidel et al. 2020), total reflection X-ray fluorescence (TXRF) spectrometry (De La Calle et al., 2013, Wobrauschek 2007), Micro-XRF (μXRF) (Scharnweber et al. 2023).
Wood, as an organic, multi-polymeric composite material, with a complex chemical composition, containing only small amounts of inorganic compounds (often less than 1%), alongside its complex microscopic and macroscopic structural features, generating anisotropic properties and variability

among and within wood species, presents challenges for XRF investigations. Direct quantitative XRF measurements on wood, employing non-compatible calibration standards, such as those for soil or metal, is not really adequate, despite its widespread use (Zielenkiewicz 2012). It was also stated that while XRF analysis of wood should be typically limited to qualitative analysis if not further corroborated with another validation procedure. Procedures, enabling quantitative analysis would require species-specific calibrations due to variations in the matrix composition between species and sample forms (Zielenkiewicz et al. 2012 b).

Alternative analytical techniques, including Atomic Absorption Spectrometry/ Electrothermal atomization (AAS/ ETA-AAS) (Krutul et al. 2010, Kolar et al. 2014), Microfocus X-ray Absorption Spectroscopy (XAS) (Chadwick et al. 2016), Scanning Electron Microscopy with EDX (SEM/EDS), Electron Microprobe Analysis (EPMA) (Mustoe G.E 2023), and inductively coupled plasma optical emission spectrometry (ICP-OES) (Baar et al. 2019), recognised for their accuracy in determination and quantification of chemical elements in diverse samples, might be employed for validation.

Nevertheless, X-ray fluorescence spectroscopy maintains its efficacy as an effective method for elemental investigation of wood and subfossil wood (Pereira Junior. et al. 2016, Zielenkiewicz et al. 2012, Mustoe 2023, Gavrikov et al. 2022).

Subfossil wood refers to wood that has undergone partial fossilization but has not been yet fully mineralized to become a true fossil. This term is commonly used to describe wood that is relatively young geologically, ranging from thousands to tens of thousands of years old, as opposed to the millions of years typically associated with ancient fossils.(Mustoe 2018, Channing and Edwards 2013, Beldean and Timar 2021(citing Kolar 2012), Kolar et al. 2012 (citing Kaennel and Schweingruber 1995). Sub-fossilization and subsequent fossilization are very slow processes occurring in anaerobic wet conditions, in the ground or in water (Reinprecht 1992).

The subfossilisation process begins with the death of the tree, followed by quick burial underwater or in anaerobic sediments like swamps, bogs, or sedimentary deposits. Initially, microorganisms and fungi begin to decompose the organic components of wood. However, if the wood becomes buried in an environment with limited oxygen, decomposition and physical destruction are inhibited, allowing the wood to persist for longer periods without complete decay (https://aggie-horticulture.tamu.edu/earthkind/landscape/dont-bag-it/chapter-1-the-decomposition-process/, Simpson 2011, Viney 2020).Over time, mineral-rich groundwater can infiltrate into the buried wood. The minerals precipitate out of the water and fill in the spaces within the wood cellular structure. This infiltration process, known as permineralization, involves the gradual replacement of organic materials with minerals such as silica, calcite, or iron compounds. Permineralization helps preserve the wood's structure and can increase its hardness and durability (Saminpanya et al. 2024, Viney 2014, Mustoe 2018). Chemical changes occur as organic matter interacts with minerals, can alter the composition and appearance of wood, leading to colour change and physical transformations.

Certainly, the presence of reactive metals such as iron, copper, zinc, etc., can significantly impact the structural polymers in subfossil wood, especially when exposed to water during storage (Reinprecht 1992). The presence of these metals induces various chemical interactions with wood polymers, including corrosion and leaching, hydrolysis and oxidation, fungal and microbial growth as well as manifesting in distinct colour changes and staining, leaving a lasting imprint through long-term effects. The increased content of minerals and their diversity in terms of elemental chemical composition justify the interest of researchers in XRF analysis of subfossil wood, while also making it more suitable for such an approach compared to recent wood.

Oak wood contains tannins, organic polyphenolic compounds responsible for its characteristic properties, especially natural durability, and sensitivity to colourations. When iron ions are present in the environment, they can react with tannins present in the wood and produce colour changes or stains. In anaerobic condition, the chemical reactions between iron and tannins may proceed more rapidly. The formation of iron-tannin complexes results in significant colour changes in the wood, which turns to dark grey up to black. The iron-tannin complexes can contribute to the preservation of wood by imparting a degree of resistance to decay and microbial attack and can also make it challenging to assess the original appearance (Krutul et al. 2010, Sandoval-Torres et al. 2012, Kenrik-Klemens et al. 2022, Kolar et al. 2012, Baar et al. 2019, Ghavidel et al. 2020, Huang et al. 2020,). Iron is one of the most abundant chemical elements on earth (Frey and Reed 2012), so that the dark grey-black colour of subfossil oak is a featuring characteristic of this material.

These colour changes are significant markers in the study of subfossil oak wood, providing valuable information about the wood's preservation history, environmental conditions, and chemical interactions during the sub-fossilization process. Analysing the coloration patterns can offer insights into the presence of iron-rich minerals, the duration of sub-fossilization, and the depositional environment in which the wood was preserved (Baar. et al. 2019, Kolar 2014, Kolar et al. 2012). However, to the best of our knowledge, no attempt of directly correlate the colour changes with the iron content by a mathematical relation, was reported in the cited literature. Moreover, reported colour data on subfossil oak are rather limited.

The main purpose of this research was to explore the possibilities of direct, non-destructive XRF, actually EDXRF, investigation of subfossil oak, employing a Bruker S1 Titan equipment and no sample preparation. The analytical objectives were to highlight the diversity of the main chemical elements contained, with a special focus on the iron content, and to verify if a direct correlation could be found between the iron content, as locally determined by XRF, and the CIELab colour parameters determined in the same location. Subfossil oak wood material, originated from three buried trunks accidently discovered in different locations on Romanian territory, was comparatively analysed.

Accordingly, this study has potential to make a contribution to the available knowledge on the subfossil oak by correlating its colour with the iron content.

MATERIALS AND METHODS
Wood Material
Subfossil oak (*Quercus* spp) wood material originated from three buried trunks (S1, S2, S3) was comparatively analysed. The buried trunks were accidentally discovered at occasion of gravel excavations in quarries near riverbanks: S1 (excavated from 7 m depth, beneath groundwater level) and S2 (excavated from 2.5m depth above groundwater level) in two relatively close locations on Timis river (Timis County, western part of Romania), and S3 (excavated from 5 m depth) on river Iza (Maramures County, northern part of Romania). The material for investigations was provided as timber pieces (S1, S3) and two 100 mm thick log cross-sections (S2), one from the base of the trunk (S2a), and a second one cut from 6 m above (S2b). Accordingly, four different assortments of subfossil oak (SO) were investigated (S1, S2a, S2b, S3), as solid wood samples with various sections and fine sawdust samples (Figure.1). Recent (new) oak (*Quercus Robur*) wood material (NO) was also investigated as reference for comparison.
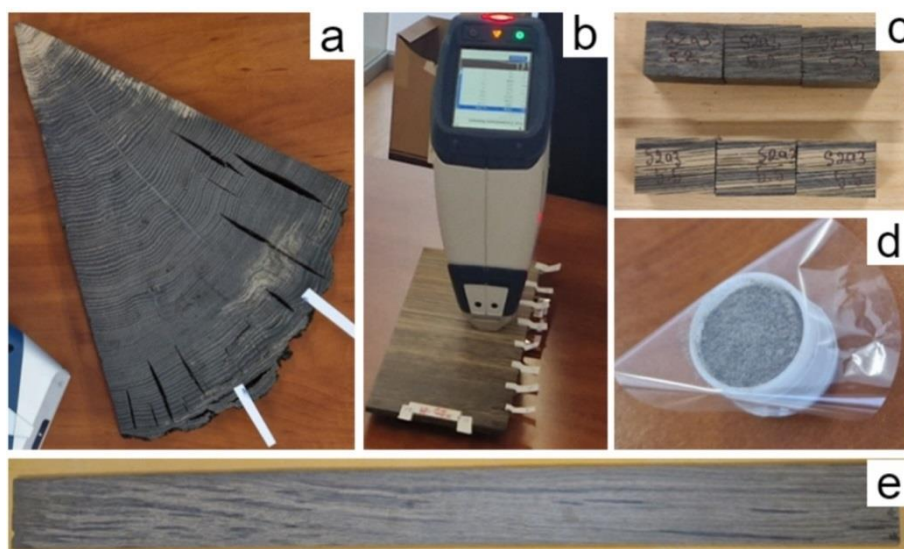
Figure 1: Types of SO samples investigated by XRF: sector of cross-cut trunk section (a); lamella with longitudinal radial face and measurements on radial direction (b); prismatic samples (c); sawdust in plastic cup covered with mylar film (d); lamella with longitudinal radial face for measurements on longitudinal direction

Solid wood test samples as prismatic pieces of 20×20×30 (mm×mm×mm) on the radial (Ra), tangential (Tg) and longitudinal (L) directions, respectively (Figure 1c), 8 mm thick lamellae with longitudinal–

radial faces (of 90-100 mm width and variable length) (Figure 1b, Figure 1e), were prepared by adequate mechanical processes from all assortments. Additionally, a sample with transversal crosscut face, representing a sector from a transversal slice through the trunk (Figure 1a) was prepared from assortment S2b.

XRF investigation

A Bruker S1 TITAN instrument (from Nano Bruker, Germany), which is a fully portable EDXRF (energy dispersive X-Ray Fluorescence) analyser, that can detect and quantify chemical elements from Magnesium (Z=12) to Uranium (Z=92), was employed. The instrument was used as hand-held or table-top equipment, depending on the type of samples and investigation needs (see Figure 1b, Figure 2). Soil contaminant standard was chosen for calibration before starting samples measurements. All samples were measured at 60s excitation time, with Rh X-rays radiation, in two phases (45/30 kV, 19.8/19.6 µA), with no filter and an 8 mm collimator. Results of measurements were saved to a PC and further processed. The report generator tool was employed to have a full record of analytical parameters and results. Experimental data were also saved as a Microsoft Excel file, for further data processing.

The investigation of solid wood lamellae (Figure. 1b, Figure 1e) and cross-section sector (Figure.1a) was done on several collinear measuring spots, 20-40 mm apart one of each other, on the longitudinal or radial directions of the wood material. A protective background plate was utilised under the sample to ensure the operator safety.

A desktop stand with protective covering lid was employed for the investigation of the small prismatic solid wood samples (Figure.2b) and for sawdust samples (Figure.2c). For the prismatic samples three measurements were made on each test piece, on the longitudinal, radial, and tangential directions. An average value of the three measurements was employed for comparisons among the investigated samples. Investigation of sawdust samples was carried out in special plastic cups covered with a thin (mylar) film (Figure. 2c).
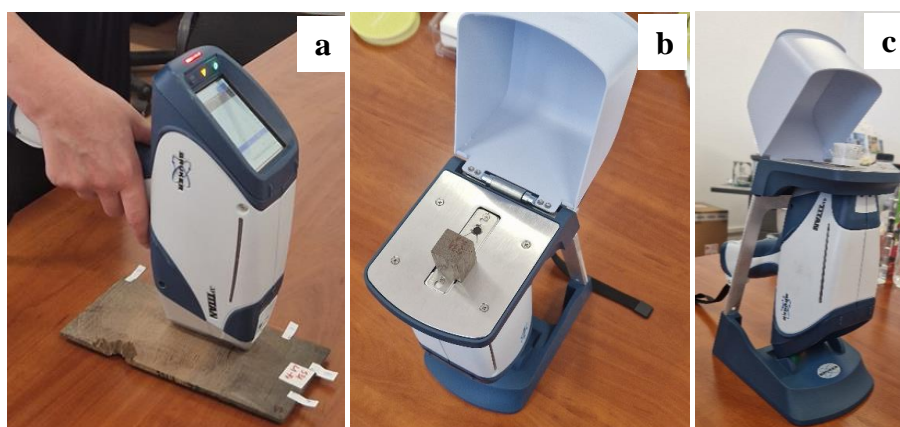
Figure 2: XRF -investigation of various subfossil oak samples with S1 Titan: solid wood lamella of SO (a); solid wood prismatic sample(b); sawdust sample (c); employment of S1 Titan as handheld equipment (a); configuration with desktop stand (b,c)

Colour measurements

Colour measurements in the CIELab system were previously performed (Nedelcu et al. 2023, Nedelcu et al. - in press), employing an AvaSpec USB2 spectrometer manufactured by Avantes, equipped with an 80 mm Ava Sphere diameter and a measuring aperture of 8 mm diameter. The CIELab colour parameters: L* - lightness (varying from 0 for black to 100 for white), a*- red-green coordinate (with positive and negative values, respectively), and b*- the yellow-blue coordinate (with positive and negative values, respectively) were determined in the same locations as XRF investigation.

RESULTS AND DISCUSSION
1. Elemental chemical analysis

The instrument was set up for the detection of 29 chemical elements, listed in the increasing order of their atomic number as follows: Mg, Al, Si, P, S, K, Ca, Ti, V, Cr, Mn, Fe, Co, Ni, Cu, Zn, As, Se, Rb,

Sr, Zr, Ag, Cd, Sn, Sb, Ba. Hg, Tl, Pb. Based on the XRF data recording sheet a total number of 22 chemical elements were detected: Mg, Al, Si, P, S, K, Ca, Cr, V, Mn, Fe, Ni, Cu, Zn, As, Se, Rb, Sr, Zr, Sb, Ba, and Pb, out of which 6 elements (V, As, Se, Zr, Sb, Pb) only in a few samples and very low amounts. In the further processing of quantitative data, Si, Al, and Mg were disregarded considering possible interferences. Accordingly, 13 elements were considered. Among the remaining 13 elements, certain elements (S, Ni, Zn, Rb,) were detected only seldomly, whereas other 9 elements were present in most of the samples. These are detailed in Table 1, alongside the percentage concentrations as directly determined by XRF. It can be observed that K content is lower in SO compared to NO, the content in P, Cr and Cu in SO and NO are quite similar, while the content in Ca, Mn, Fe and Sr is higher in SO compared to NO. The elements found in highest concentrations in SO were Ca (0.90-2.13%) and Fe (0.17-1.57%) compared to maximum 0.12% and 0.07%, respectively in NO.

Table 1: Main chemical elements detected and quantified by XRF in subfossil oak samples (SO) and recent oak (NO), as percentage concentrations determined on solid wood prismatic samples

Sort of material	Chemical element detected by XRF, %									Total, %
	P	**K**	**Ca**	**Cr**	**Mn**	**Fe**	**Cu**	**Sr**	**Ba**	
N2_A	0.0156	0.8784	0.1236	0.0165	0.0153	0.0560	0.0018	0.0006	< LOD	1.1078
N4_D	< LOD	0.8439	0.0565	0.0145	< LOD	0.0713	0.0023	0.0004	0.0061	0.9950
S1_A	0.0077	0.3047	0.9062	0.0174	0.0463	0.3789	0.0019	0.0011	< LOD	1.6642
S1_D	0.0059	0.3345	0.9968	0.0160	0.0566	0.4662	0.0023	0.0013	0.0052	1.8847
S2a_A	0.0102	0.3694	1.7875	0.0160	0.0322	1.2545	0.0019	0.0023	0.0121	3.4861
S2a_D	0.0090	0.4221	1.3720	0.0157	0.0692	0.4788	0.0023	0.0018	0.0060	2.3770
S2b_A	0.0124	0.3804	1.9990	0.0170	0.0221	1.5714	0.0025	0.0026	< LOD	4.0075
S2b_D	0.0104	0.3902	1.4282	0.0144	0.0348	0.5932	0.0030	0.0020	0.0117	2.4880
S3_A	0.0143	0.3843	2.1289	0.0157	0.0057	0.5301	0.0022	0.0014	< LOD	3.0825
S3_D	0.0079	0.4010	1.1525	0.0140	0.0036	0.1725	0.0024	0.0007	0.0132	1.7677

Note: A- wood from external part of the trunk corresponding to sapwood; **D** – from inner part of the trunk corresponding to heartwood; LOD - limit of detection

Considering the non-specific standard employed and no other validation method of these values, the relative concentrations reported to NO were also computed and are presented in Table 2. Values higher than 1 indicate increased concentrations compared to NO, while values lower than 1 indicate lower concentrations. Data in Table 1, Table 2 highlight variability of elemental chemical composition among the assortments of SO studied in this research and between sapwood and heartwood.

Table 2: Main chemical elements detected and quantified by XRF in subfossil oak samples (SO), as relative concentrations reported to recent oak (C_{SO}/C_{NO}), determined on solid wood prismatic samples

Sort of SO	Chemical element detected by XRF (relative concentration reported to recent oak)								
	P	**K**	**Ca**	**Cr**	**Mn**	**Fe**	**Cu**	**Sr**	**Ba**
S1_A	0.49	0.35	7.33	1.05	3.03	6.77	1.06	1.88	n.d.
S1_D	0.38	0.40	17.63	1.10	3.70	6.54	1.03	3.17	0.85
S2a_A	1.17	1.39	1.51	0.90	1.49	1.26	1.21	1.72	1.98
S2a_D	0.58	0.50	24.27	1.08	4.52	6.72	1.01	4.58	0.99
S2b_A	0.80	0.43	16.17	1.03	1.45	28.06	1.39	4.59	n.d.
S2b_D	0.67	0.46	25.26	1.00	2.28	8.32	1.31	4.92	1.92
S3_A	0.91	0.44	17.22	0.95	0.37	9.47	1.20	2.47	n.d.
S3_D	0.50	0.48	20.39	0.97	0.23	2.42	1.06	1.67	2.16

Note: A- wood from external part of the trunk corresponding to sapwood; **D** – from inner part of the trunk corresponding to heartwood; n.d.-not detected

In terms of variation of the elemental content in the external and inner parts (sapwood and heartwood) of the buried trunks, data in Table 1 indicated that calcium (Ca) and iron (Fe) generally exhibited a

decrease value from external to inner part for buried SO trunks, except one trunk, S1. Also, at phosphorus (P) appear a trend of decrease from sapwood to heartwood. Percentage concentration of potassium (K) increased from sapwood to heartwood.

Mankowski et al. (2013), with ED-XRF analysis, revealed a non-uniform distribution of iron in subfossil oak wood. Iron concentration was found to be higher in the heartwood, especially towards the outer region on the limit with sapwood, and towards the pith and decreased in the middle of the heartwood, the pith, and the sapwood. Another study indicated a general decrease in Silicon (Si) content from sapwood to heartwood, determined with ETA – AAS method (Kolar et al. 2014). Additionally, there was a decrease in Fe and Ca content, from the outer to inner part, with the middle zone exhibiting lower concentration, and a roughly increase of K, Mg, Zn content, determined with AAS method (Krutul et al. 2010).

Table 3: Main chemical elements detected and quantified by XRF in subfossil oak samples (SO), as relative concentrations reported to recent oak (C_{SO}/C_{NO}), determined on sawdust samples

Sort of SO	Chemical element detected by XRF (relative concentration reported to recent oak)						
	P	**K**	**Ca**	**Cr**	**Mn**	**Fe**	**Cu**
S1	1.03	0.50	8.71	1.01	6.24	9.05	0.33
S2a	1.06	0.64	14.22	1.01	7.64	17.76	0.94
S2b	1.05	0.75	10.92	0.96	4.68	10.38	0.23
S3	1.06	0.74	11.20	0.96	3.83	8.76	0.31

In Table 3 are presented, for comparison, the results obtained by XRF on wood sawdust samples, as relative concentrations. Sr and Ba are not included, as they were not detected in the sawdust sample of recent oak. It can be observed that for the sawdust samples higher relative concentrations of the detected elements were obtained. It must be specified that sawdust samples resulted from the mechanical processing of the raw material into prismatic samples and lamellae. It contained material from the external part and the inner part of the trunk (sapwood and heartwood). Also, the form of material and density (no compression) might have influenced the results (Zielenkiewicz et al. 2012 b).

The results obtained in this research are in line with previously reported literature data, though differences were observed in terms of the values reported.

For instance, the relative concentrations of calcium (Ca) determined for the 4 assortments of SO varied in the range 1.51-17.22 for sapwood and 17.63-25.26 for heartwood, indicate a much higher content of this element in SO compared to NO. Baar et al. (2019), determined Ca concentrations 7.67-8.58 times higher in SO compared to NO. In the study of Krutul et al. (2010), Ca concentration of subfossil oak was approximately 6-7 times higher than in recent oak, while Kolar et al. (2014) reported value 5 times higher in SO.

The relative concentration of iron (Fe) varied in the range 1.26-28.06 for sapwood and 2.42-8.32 for heartwood. However, much higher relative concentrations of Fe were reported by other researchers. A content of Fe 358-875 times higher in SO compared to recent oak (Baar et al. 2019), or 250 times higher (Krutul et al. 2010) were found.

Potassium (K) seems to have a lover concentration in subfossil oak than recent oak. In this research, the relative concentration of K varied in the range of 0.35-0.50 with one higher value of 1.39, while other researchers found values between 0.05-0.10 (Baar et al. 2019) or 0.04-0.15 (Krutul et al. 2010).

The variability of data among the assortments studied in this research, as well as the different values reported by other authors should be related with the great variability of subfossil oak as material. More research is needed, including validation of elemental chemical analysis by alternative methods, dating of the subfossil wood analysed and correlations with the nature and chemical composition of the burial sediments, if possible.

2. Correlation of Iron Content with Colour Parameters

The XRF data on iron percentage concentrations determined on solid wood lamellae, on successive measuring points on longitudinal or radial directions, were plotted in relation with the L*, a*, b* colour parameters, as (x-y) scatter graphs in excel. Colour parameters were plotted on y axis and iron concentration on x axis and the best fitting trendline, with maximum value of the coefficient of determination R^2, was considered. The plots for measurements on lamellae with longitudinal radial sections, for all the 4 assortments of SO, are presented in Figure 3.
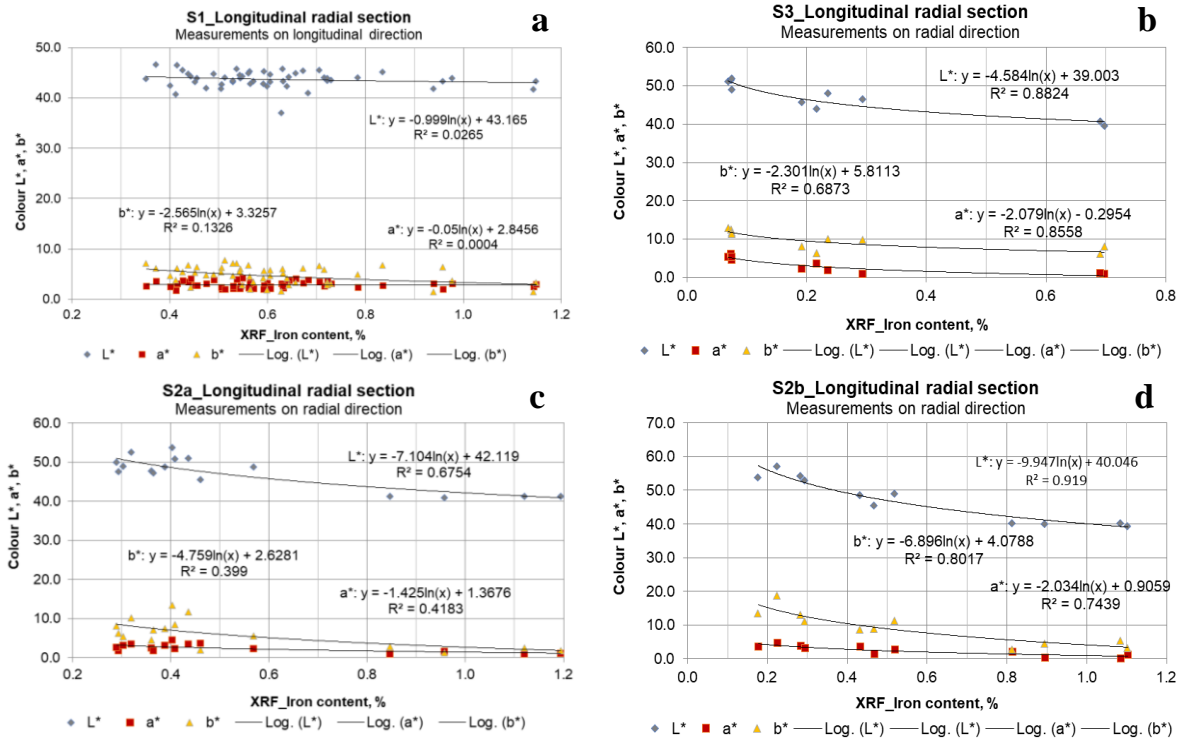
Figure 3: CIELab colour parameters – iron content correlation plots, with regression logarithmic functions and correlation parameters for the different assortments of subfossil oak: S1 (a);S3 (b); S2a (c) and S2b (d) – measurements on lamellae with longitudinal –radial section

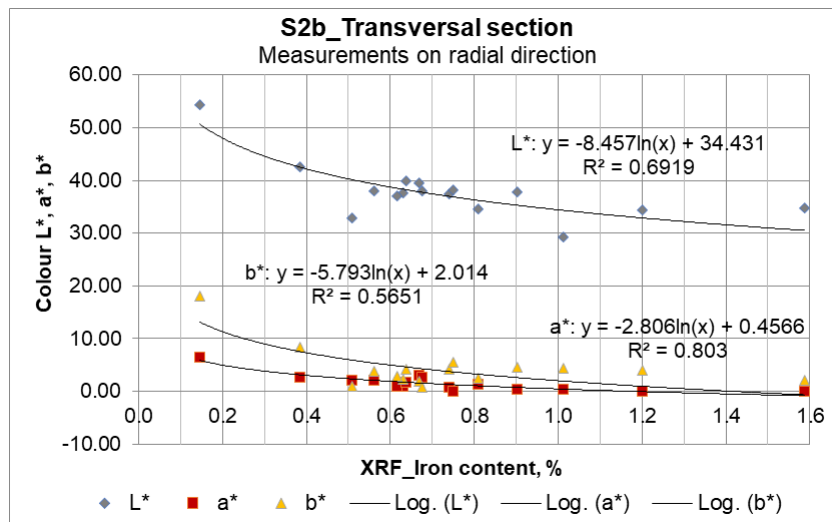*Figure 4: CIELab colour parameters – iron content correlation plots, with regression logarithmic functions and correlation parameters subfossil oak S2a – measurements on a cross-cut transversal section (depicted in Figure 1a)*

Analysing the plots in Figure 3 and Figure 4 it can be observed that generally all the CIELab colour parameters, namely lightness L*, redness* and yellowness b*, tend to decrease as the iron content

441

increases. Decrease of L*, a* and b* colour parameters means darkening and decrease of chromaticity, meaning turning progressively towards grey and black. As the characteristic bluish–grey up to black colour stains are due to the reaction of iron with tannins in oak, this trend is perfectly explainable. However, this trend did not fit a linear correlation. Reasonably good logarithmic correlations could be found instead between the colour parameters L*, a*, b* and the percentage iron content, as directly determined by XRF, for SO from 2 of the 3 buried logs (S2, S3). The regression curves are depicted in the plots, while the corresponding regression functions and characteristic parameters are summarised in Table 4.

Table 4: Summary of equation parameters for logarithmic correlation between CIELab colour parameters and the iron content determined by XRF

Sort of SO and measurement direction	Colour parameters	Log equation: y= -a×ln(x)+b		Coefficient of determination R^2
		a	b	
S1 Longitudinal direction	L*	0.999	43.165	0.0265
	a*	0.050	2.8456	0.0004
	b*	2.565	3.3257	0.1326
S3 Radial direction	L*	4.584	39.003	0.8824
	a*	2.079	0.2954	0.8558
	b*	2.301	5.8113	0.6873
S2a Radial direction	L*	7.104	42.119	0.6754
	a*	1.425	0.4183	0.4183
	b*	4.759	0.399	0.3990
S2b Radial direction	L*	9.947	40.046	0.9190
	a*	2.034	0.9059	0.7439
	b*	6.896	4.0788	0.8017
S2b Transversal section	L*	8.457	34.431	0.6919
	a*	2.806	0.4566	0.8030
	b*	5.793	2.014	0.5651

For the SO from the trunk S1 the R^2 correlation parameters for similar mathematical functions are extremely low for all colour parameters (0.0004-0.1326), indicating no reasonable correlation. This poor correlation results from the fact that even if for this type of SO material, the colour presented less variability compared to the other assortments (please see Figure 1e), a large variability of iron content was determined by XRF. More research and complementary investigation methods are needed to understand and explain this result. Also, the measurements on the S1 lamella followed the longitudinal direction of the trunk, while for the other lamellae measurements followed the radius direction from outer part inwards.

However, the fact that colour parameters for the other assortments could be correlated with the iron content, while also highlighting the variation of the iron content in subfossil oak from the outer part towards the inner part of the trunks, represent notable achievements of this research.

CONCLUSIONS

X-ray fluorescence (XRF) is a versatile and rapid analytical method for elemental chemical characterization, commonly used for inorganic materials. This method was found, however, as a very useful tool for rapid elemental characterisation of subfossil oak, mainly suitable for qualitative analysis. Due to the lack of specific standards, results of direct quantitative analysis should be validated by alternative methods or relative concentrations SO/NO should be considered.

Nine chemical elements P, K, Ca, Cr, Mn, Fe, Cu, Sr, Ba were found to be the most prevalent in the analysed samples. Among these, the highest relative concentration, when compared to recent oak (NO), was determined for Ca, followed by Fe. Additionally, it was noted that the K content was lower in subfossil oak (SO) compared to recent oak.

The presence of Fe in subfossil oak, and its reaction with tannins present in oak wood, leads to a colour change, resulting in shades ranging from grey to black, with occasional brown stains.

When considering the simultaneous measurement of colour and the presence of chemical elements, a strong logarithmic correlation was observed between the colour parameters L*, a*, b*, and iron (Fe)

content for all assortments of subfossil oak, except one (S1). More research is needed to explain this exception.

This study represents an original contribution to the available knowledge on subfossil oak by correlating its colour with the iron content.

ACKNOWLEDGEMENTS

REFERENCES

Aggie Horticulture, Earth-Kind Landscaping, Chapter 1, The Decomposition Process, Publication Revised February 2009, Member of the Texas A&M AgriLife University System https://aggie-horticulture.tamu.edu/earthkind/landscape/dont-bag-it/chapter-1-the-decomposition-process/ Accessed 11 Mar 2024

Baar J, Paschová Z, Hofmann T, Kolář T, Koch G, Saake B, Rademacher P (2019). Natural durability of subfossil oak: wood chemical composition changes through the ages. Holzforschung, 74(1),2020, 47-59. https://doi.org/10.1515/hf-2018-0309

Beldean E, Timar MC (2021). A new opportunity for research in Romania – subfossil wood. Bulletin of the Transilvania University of Braşov, 14(63)(1), 77–88. https://doi.org/10.31926/but.fwiafe.2021.14.63.1.7

Chadwick A V, Berko A, Schofield EJ, Smith AD., Mosselmans, JFW, Jones AM, Cibin G. (2016). The application of X-ray absorption spectroscopy in archaeological conservation: Example of an artefact from Henry VIII warship, the Mary Rose. Journal of Non-Crystalline Solids, 451, 49–55. https://doi.org/10.1016/j.jnoncrysol.2016.05.020

Channing A. and Edwards D. (2013), Wetland megabias: ecological and ecophysiological filtering dominates the fossil record of hot spring floras. Palaeontology, 56: 523-556. https://doi.org/10.1111/pala.12043

De La Calle I, Cabaleiro N, Romero V, Lavilla I, Bendicho C (2013). Sample pretreatment strategies for total reflection X-ray fluorescence analysis: A tutorial review. Spectrochimica Acta. Part B: Atomic Spectroscopy, 90, 23–54. https://doi.org/10.1016/j.sab.2013.10.001

Frey PA, Reed GH. (2012). The Ubiquity of Iron. ACS chemical biology. 7(9). 1477-81. https://doi.org/10.1021/cb300323q

Gavrikov V, Fertikov A, Sharafutdinov R, Vaganov E (2022). Elemental relationships in the wood of four Siberian conifers: Whether elements are an occasional mixture, Int. J. Plant Biol., vol. 13, no. 2, pp. 142–150. https://doi.org/10.3390/ijpb13020014

Ghavidel A, Hofmann T, Bak M, Sandu I, Vasilache V (2020) Comparative archaeometric characterization of recent and historical oak (Quercus spp.) wood. Wood Sci Technol 54, 1121–1137. https://doi.org/10.1007/s00226-020-01202-4

Henrik-Klemens Å, Bengtsson F, Björdal CG (2022). Raman spectroscopic investigation of iron-tannin precipitates in waterlogged archaeological oak. *Studies in Conservation*, *67*(4), 237–247. https://doi.org/10.1080/00393630.2020.1864895

Huang Y, Lin Q, Yu Y, Yu W. (2020). Functionalization of wood fibers based on immobilization of tannic acid and in situ complexation of Fe (II) ions. *Applied Surface Science*, *510*(145436), 145436. https://doi.org/10.1016/j.apsusc.2020.145436

IEC 62495 (2011), Nuclear instrumentation – Portable X-ray fluorescence analysis equipment utilizing a miniature X-ray tube was used as a guide.

Kolar T, Gryc V, Rybníček M, Vavrčík H (2012). Anatomical Analysis and Species Identification of Subfossil Oak Wood. Wood research. 57(2). 251-264.

Kolář T, Rybníček M, Střelcová M, Hedbávný J, Vit J (2014). The changes in chemical composition and properties of subfossil oak deposited in holocene sediments. Wood Research. 59(1). 149-166.

Krutul D, Radomski A, Janusz Zawadzki J, Zielenkiewicz T, Antczak A (2010). Comparison of the chemical composition of the fossil and recent oak wood. Wood research, 55(3), pp 113-120. ISSN:1336-4561

Mańkowski P, Kozakiewicz P, Zielenkiewicz T. Investigations of iron content in fossil oak from a medieval settlement in Płońsk. Ann. WULS - SGGW, For. and Wood Technol. 83, 2013

Mustoe GE. (2018). Non-Mineralized Fossil Wood. *Geosciences*. 2018; 8(6):223. https://doi.org/10.3390/geosciences8060223

Mustoe GE (2023). Silicification of Wood: An Overview. *Minerals*, 13(2):206. https://doi.org/10.3390/min13020206

Nedelcu R, Timar MC, Beldean EC (2023). Chromatic characterisation and colour variability of subfossil oak (*Quercus spp*) from three sources from Romania. In International Conference "Wood Science and Engineering in the Third Millennium" 13th edition, Book of abstracts, pp 36. ISSN 1843-2689

Nedelcu R, Timar MC, Beldean EC (2023). Chromatic characterisation and colour variability of subfossil oak (*Quercus spp*) from three sources from Romania.). BioRes - in press. ISSN 1930-2126

Pereira Junior SM, Maihara VA, Moreira EG, Salvador VLR, and Sato IM (2016), "Determination of Cu, Cr, and As in preserved wood (*Eucalyptus sp*.) using x-ray fluorescent spectrometry techniques, *J. Radioanal. Nucl. Chem.*, vol. 308, no. 1, pp. 7–12. https://doi.org/10.1007/s10967-015-4669-1

Reinprecht L. (1992). Strength of Deteriorated wood in relation to its structure. Vol 2 of Vedecké a pedagogické aktuality. Technická univerzita vo Zvolene. ISBN 802280195X, 9788022801959

Saminpanya S, Ratanasthien B, Jatusan W, Limthong R., Amsamarng T. (2024). Mineralogy, geochemistry, and petrogenesis of the world's longest petrified wood. *International Journal of Geoheritage and Parks*, *12*(1), 37–62. https://doi.org/10.1016/j.ijgeop.2023.11.003

Sandoval-Torres S, Jomaa W, Marc F, Puigalli J-R. (2012). Colour alteration and chemistry changes in oak wood (Quercus pedunculata Ehrh) during plain vacuum drying. Wood Sci Technol 46, 177–191. https://doi.org/10.1007/s00226-010-0381-z

Scharnweber T, Rocha E, González Arrojo A, Ahlgrimm S, Gunnarson BE, Holzkämper S, Wilmking M (2023). To extract or not to extract? Influence of chemical extraction treatment of wood samples on element concentrations in tree-rings measured by X-ray fluorescence. Frontiers in Environmental Science. Volume11-2023. https://doi.org/10.3389/fenvs.2023.1031770

Simpson P (2011). Studies on the Degradation of Horn, Antler and Ivory at Archaeological Sites, School of Biological Sciences, PhD Thesis

Trojek T, Trojková D (2023). Uncertainty of Quantitative X-ray Fluorescence Micro-Analysis of Metallic Artifacts Caused by Their Curved Shapes. *Materials* 16(3):1133. https://doi.org/10.3390/ma16031133

Viney M (2014). Petrified Wood : The Silicification of Wood by Permineralization. Geology

Viney M (2020). Fossils. Cosmology's Century, 114–183. https://doi.org/10.2307/J.CTVSS3ZT8.7

Wobrauschek P. (2007), Total reflection x-ray fluorescence analysis—a review, Xray Spectrom., vol. 36, no. 5, pp. 289–300. https://doi.org/10.1002/xrs.985

Zielenkiewicz T, Zawadzki J, Radomski A (2012a) XRF spectrometer calibration for copper determination in wood: Developing method of XRF spectrometer calibration, Xray Spectrom., vol. 41, no. 6, pp. 371–373. https://doi.org/10.1002/xrs.2416

Zielenkiewicz T, Radomski A, Zawadzki J (2012b). XRF examination of matrix uniqueness in chosen deciduous wood species. European Journal of Wood and Wood Products, 70(6), 845–849. https://doi.org/10.1007/s00107-012-0636-5

Investigating the Development of Heartwood in *Quercus robur* in Denmark

Andrea Ponzecchi[1*], Albin Lobo[1], Jill Katarina Olofsson[1], Jon Kehlet Hansen[1], Erik Dahl Kjær[1], Lisbeth Garbrecht Thygesen[1]

[1]University of Copenhagen, Department of Geosciences and Natural Resource Management, Rolighedsvej 23, DK-1958 Frederiksberg C, Denmark

E-mail: apo@ign.ku.dk; alo@ign.ku.dk; jko@ign.ku.dk; edk@ign.ku.dk; lgt@ign.ku.dk

Keywords: *Quercus robur*, heartwood formation, genotype, extractives, UV-VIS spectroscopy, ATR-FTIR spectroscopy

ABSTRACT

Quercus robur, commonly known as English oak, is renowned for its remarkable adaptability to various climates and its ability to produce high-quality wood. Its heartwood, prized for its exceptional strength and durability, is considered highly valuable in the forestry industry. Despite the high economic value, detailed insights into heartwood formation are still scarce. For this study, wood cores were extracted from 300 20-year-old *Q. robur* trees in Denmark, originating from 100 different maternal lineages (half-sib families), to explore the factors influencing both heartwood quantity and quality. The heartwood area (the cross-sectional area of the heartwood in the trunk at 50 cm above the ground) varied significantly among families reflecting that the heartwood area is partly heritable. Non-destructive assessments of the heartwood via UV-VIS reflectance and ATR-FTIR spectroscopy revealed their utility in assessing qualitative traits of heartwood, but they did not demonstrate similar simple inheritance. This study underscores the significance of investigating the genetics of heartwood formation in order to obtain information that will allow the integration of this parameter when selecting planting material for future afforestation efforts.

INTRODUCTION

Heartwood formation significantly influences timber durability and color. Despite the economic importance, studies on the possible genetic control of heartwood development and on its quality are scarce, presenting a gap in forestry science and wood product optimisation. Insights into the biochemical processes leading to heartwood formation (Celedon & Bohlmann, 2018), its economic implications, and variations across species (Miranda et al., 2009) underline the necessity for targeted research. This focus aligns with the EU 2030 forest strategy, aiming to enhance forest quality and sustainability (EU, 2022).

The genus *Quercus* is suitable for afforestation in many European countries and is already widely used for this purpose. Oaks are native to most of Europe, they have immense importance for biodiversity by hosting hundreds of fungi and invertebrate species, and their autecology as bare land colonisers make them suitable for the conversion of agricultural land to forests. It is also important that oaks have the potential to grow very old. As an oak tree matures and develops a substantial trunk, it accumulates significant amounts of carbon, thereby serving as a durable carbon sink. Even post-harvest, oak trees play a role in carbon storage through their utilization in wooden constructions and objects beyond the forest setting. Notably, it is the heartwood that holds significant value in this context.

Knowing of genetic influence on heartwood basal area in *Q. robur* by familial lineage, this study delves into the qualitative variations in heartwood across different genotypes. The primary objective is to identify and select superior *Q. robur* genotypes for afforestation endeavors, focusing on optimizing both the quantity and quality of heartwood content.

Wood durability develops in the living tree as a combined effect of the characteristics of the original sapwood formed (which determines ring width), and the later process of heartwood formation via deposition of extractives into existing xylem in the centre of the trunk and branches (Humar et al., 2008). In *Q. robur*, heartwood formation is characterised by creation and deposition of ellagitannins, especially the two isomorphs castalagin and vescalagin (Vivas, Laguerre, et al., 2004) (Figure 1a), with formation

assumingly taking place within ray parenchyma cells in the transition zone between sapwood and heartwood (Hillis, 1968). Extractives make up approximately 15-75 mg/g dry matter within the heartwood of *Q. robur* (Mosedale et al., 1996; Prida & Puech, 2006). When moving from the transition zone between sapwood and heartwood towards the centre of the heartwood, the overall content of extractable tannins decreases (Mosedale et al., 1996; Vivas, Nonier, et al., 2004), most likely due to polymerisation (Klumpers et al., 1994) (Figure 1b), which seems to take place via oxidation, and/or hydrolysis (Vivas, Nonier, et al., 2004).
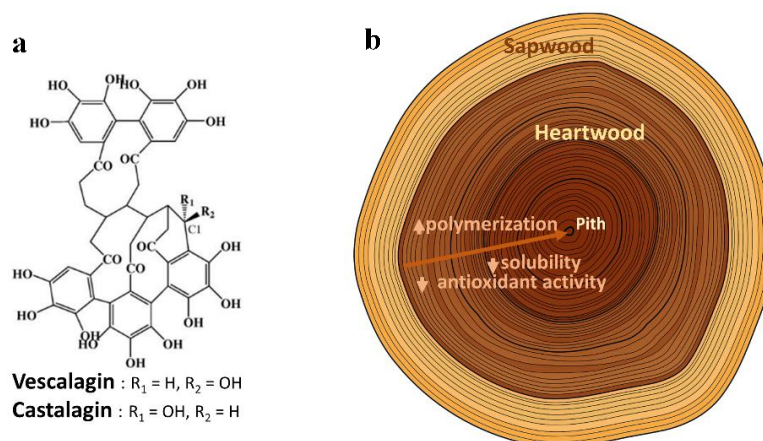

Figure 30: Molecular drawing of vescalagin and castalagin, from Vivas, Nonier, et al., (2004) (a) and schematic drawing of effect of aging to extractives in heartwood (b)

Polymerisation, i.e. heartwood aging, increases its reddish-brownish colouring (Klumpers & Janin, 1992), but seemingly decreases its durability (Klumpers et al., 1994). A previous study suggests a strong genetic element in heartwood ellagitannin content (Mosedale et al., 1996), while another study points to the importance of available soil water during spring for formation of the reddish-brownish colour (Klumpers et al., 1993), i.e., presumably the polymerisation of ellagitannins.

MATERIALS AND METHODS

To investigate the quantity of heartwood in oak trees, we analysed wood cores from 300 trees, originating from 100 open pollinated trees distributed across nine sites in Denmark. The wood cores were sampled from trees planted in a progeny trial in southern Jutland in Denmark in 2002, at a height of 50 cm above the ground level using a 5-mm increment borer.

Serving as indicators of heartwood quality, the physico-chemical properties of the heartwood sections were non-invasively examined using ultraviolet-visible (UV-VIS) spectrophotometry and attenuated total reflectance Fourier transform infrared (ATR-FTIR) spectroscopy across the core samples. (Bonifazi et al., 2015; Traoré et al., 2023).

After extraction, the cores were left to air-dry on core holders under ambient conditions. Initially, masking tape was employed to preserve their integrity and shape. Once dried, the cores were securely attached to the holders using a water-soluble wooden adhesive, to enable subsequent analysis. The cores were then sanded to ensure a smooth flat surface and the different phenotypic traits with respect to heartwood were measured using the Velmex Tree Ring Measuring System (Velmex Inc., USA).

Diameter of all the 300 trees were also measured from which the total length of each core (radius of tree) was calculated. The length of sapwood was measured precisely using Velmex. Heartwood length was estimated by subtracting the sapwood length from radius, and then used to calculate the heartwood basal area. This step was necessary because some of the sampled cores lacked the pith, resulting in imprecise measurements of heartwood length. Since all the trees were 21 years old when cored, the number of ring with heartwood could be calculate by 21 minus the number of sapwood rings. This

measure is an interesting biological parameter since it reflects trees to tree variation in how fast after formation that the most recent heartwood ring was modified from sapwood to heartwood.

In this study, after assessing the cores for anatomical characteristics, we analyzed these using non-destructive spectroscopic techniques, namely UV-VIS and ATR-FTIR, to evaluate heartwood quality (Figure 2). Overall, the analysis encompassed five traits, integrating both quantitative (anatomical) and qualitative (spectroscopic) dimensions. Preliminary findings suggest that among the anatomical and growth attributes—heartwood area, basal area, and the number of heartwood rings—family effects only showed to be significant in the case of heartwood area.

Therefore, this research aims to elucidate the relationship between heartwood area and the qualitative scores obtained from UV-VIS and ATR-FTIR spectroscopy. These scores were developed from a need to condensate relevant spectral information into numerical form in order to include these data in statistical evaluations.

These relationships were then analysed with Spearman correlation.

Non-destructive Spectroscopic Techniques
UV-VIS Spectrophotometry

UV-VIS spectrophotometry was utilized for the qualitative analysis of the heartwood in the sampled cores. Reflectance measurements were conducted on 207 samples using an Ocean View UV-VIS spectrophotometer, equipped with UV and visible lamps, and a reflection probe. For each core, two spectra were recorded: one near the pith (HW pith) and another close to the transition zone (HW transition) on the heartwood side (Figure 2a,c).

The collected UV-VIS data comprised spectra reflecting light from the wood, covering a wavelength range from approximately 200 nm to 800 nm. For practical reasons, reflectance spectra were transformed to absorbance data using Equation 1.

$$A = 2 - \log R \tag{1}$$

With A the absorbance and R the measured reflectance.
To make sure that all wood samples could be fairly compared, the spectra were normalized using the average value between 240 nm and 290 nm. This step removed inconsistencies caused by external factors like surface conditions or instrument differences, focusing purely on the wood's characteristics.

To discern differences in the spectral characteristics between the pith and transition wood, the analysis focused on the area under the curve for both the less energetic (440-820 nm) and more energetic (295-420) parts of the spectrum. Splitting the spectrum into two parts helped us look closely at how wood darkens, a process possibly tied to polymerization.

Drawing from the preliminary findings, the average area under the curve between 440-820 nm, calculated from the spectra obtained from both the pith and the heartwood zone, was utilized as the scoring metric for the UV-VIS analysis in subsequent correlation (Figure 2a).

ATR-FTIR Spectroscopy

ATR-FTIR spectroscopy was performed on 87 cores. The infrared measurements were conducted with a Nicolet 6700 FT-IR spectrometer (Thermo Scientific, Waltham, MA, USA) equipped with a Pike Technologies GladiATR diamond ATR. The spectra were obtained as the averages of 64 scans (128 for background) using a resolution of 4 cm−1 and a spectral range of 3800 − 400 cm−1.
The spectra were ideally obtained from 10 growth rings per core, encompassing rings 1-5 in the sapwood, counting outwards from the border to the bark, and rings 1-5 in the heartwood, counting inwards from the border to the pith (Figure 2b,c). This method allowed for the examination of the physicochemical composition of the core´s surface, providing insights into the molecular variations across the sapwood-heartwood boarder.

Our examination targeted the spectral region spanning from 3800 to 550 cm^{-1}. Our focus was particularly on the bands at 1230, 1325, 1590, and 1735 cm^{-1}, identified by Traoré et al., (2023) as critical for distinguishing between sapwood and heartwood. These bands correspond to key structural components: 1230 cm^{-1} to C–O stretching in lignin, 1735 cm^{-1} to C–O stretching in hemicelluloses, 1325 cm^{-1} to C–H bending in polysaccharides, and 1590 cm^{-1} to aromatic skeletal stretching in lignin. To enable comparison of peak intensities, the spectra were normalized over 1020 cm^{-1} peak intensity and lowest value of the spectra was set to 0. The absorption peaks within these regions varied in intensity between the sapwood and heartwood. By analyzing the intensity ratios of specific peaks (1735/1325, 1590/1735, 1590/1230, and 1230/1325), we were able to delve into these differences more deeply. A t-test was conducted on the means of intensity and ratios to determine the significance of the observed variances.

In our study, we focused on the heartwood zone to establish a consistent benchmark for evaluating ATR-FTIR data in subsequent correlation analyses. Specifically, we derived an average peak ratio of 1230/1325 by analyzing the spectra obtained from all five heartwood rings (Figure 2b,c). This approach was chosen to ensure a robust and uniform measure across the samples, exclusively utilizing data from the heartwood section.
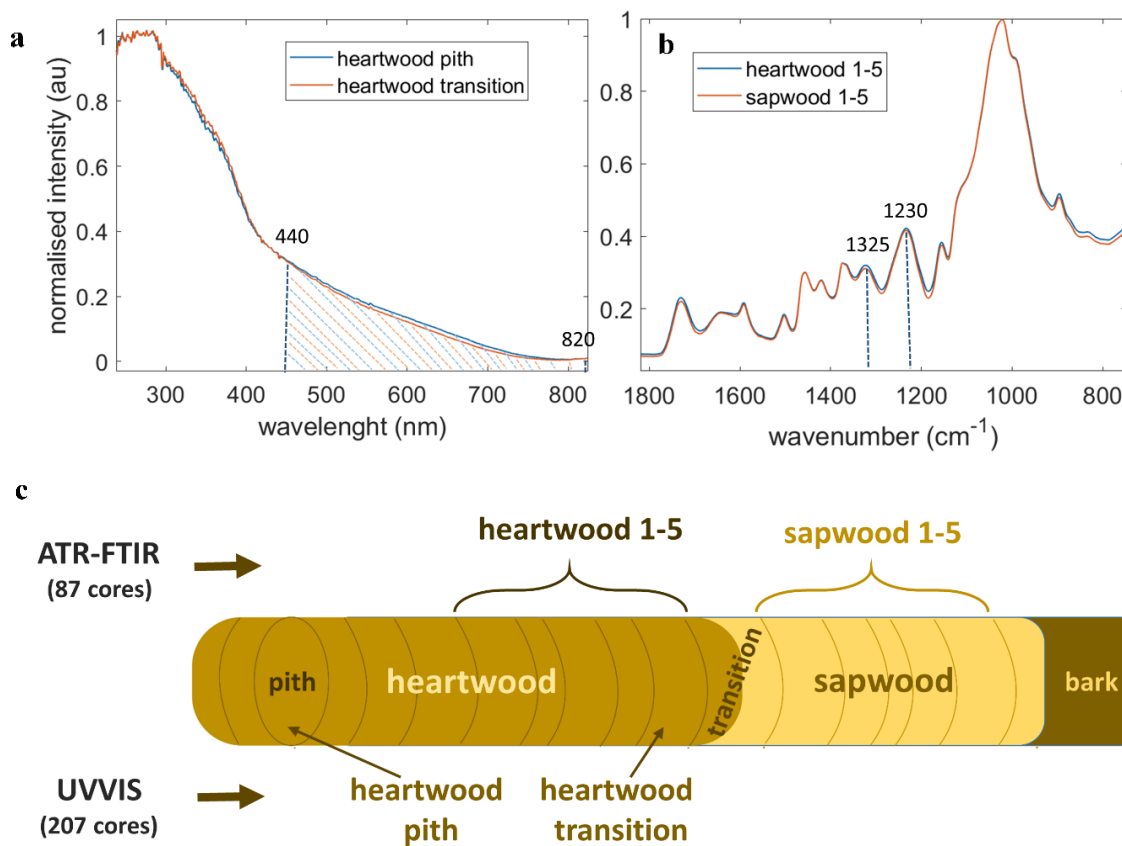
Figure 31: *(a) average UVVIS spectra measured at pith (heartwood pith) and at the first ring following the transition zone (heartwood transition). This figure also highlights the specific areas utilized for computing the UVVIS score. (b) ATR-FTIR spectra, averaged from five distinct rings within both the heartwood (heartwood rings 1-5) and sapwood (sapwood rings 1-5) for all analyzed cores. This part details the peak locations, marked by numbers and dotted lines, which are instrumental in deriving the ATR-FTIR score. (c) schematic diagram of a wood core with indications about the specific sections of the cores that were subjected to analysis using ATR-FTIR (above the core) and UVVIS spectroscopy (below the core)*

Statistical analysis

All statistical analyses, including the correlation matrix were conducted using MATLAB, version R2023b.

RESULTS AND DISCUSSION
Genetic control of heartwood quantity

Preliminary findings indicate a weak statistically significant (*p*-value of 0.05) family variance for heartwood area.

Populations and families did not show significant differences as regards the number of rings in the heartwood and total basal area. The phenotypic correlations of heartwood area with the basal area and the number of rings in the heartwood were as expected high with *r = 0.91* (*p < 0.005*) and *r =0.53* (*p < 0.005*), respectively.

Heartwood characteristics

UV-VIS spectral data obtained from the heartwood's pith exhibited higher reflectance ($p < 0.01$) in the longer wavelength region (440-820 nm) compared to those from the heartwood region close to the transition zone (Table 3). This spectral distinction underscores the potential for using UV-VIS spectroscopy as a non-destructive tool to differentiate between heartwood zones and to infer qualitative traits related to heartwood production and quality.

Table 14: Wilcoxon rank-sum test on two target regions of the UV-VIS spectra recorded close to the pith (HW pith) and close to the transition wood (HW transition)

Area range (nm)	Mean (±std) HW pith	Mean (±std) HW transition	*p*-value
295-420	228.2 (± 20.9)	232.8 (± 23.1)	0.10
440-820	133.4 (± 45.3)	123.4 (± 46.5)	*0.01*

The area under the lower energetic region of the UV-VIS spectra showed therefore more energy in the visible region of the spectra, and in a part of the heartwood (HW pith) where it is expected to see darkening probably due to polimerization of tannins. We used the average of the two values calculated for the HW pith and HW transition as a proxy for wood quality measured by UV-VIS spectroscopy.

For the ATR-FTIR analysis, differences in peak intensities between heartwood (HW) and sapwood (SW) were observed to align with the trends reported by Traoré et al., (2023) for three out of four peaks, excluding the peak at 1735 cm^{-1}. In terms of peak ratios, consistency with Traore's findings was noted in the peak ratio 1230/1325. The peak ratio of 1230/1325 in the heartwood was selected as the indicator for heartwood quality based on ATR-FTIR analysis. This choice was made due to its potential as a proxy for the presence and concentration of extractives in the heartwood, making it a critical factor for further correlation analyses.

Table 15: T-test on means of target peaks or peak ratios from ATR-FTIR spectra recorded for five HW rings and five SW rings around the transition zone

Peak (cm^{-1})	Mean (±std) HW	Mean (±std) SW	*p*-value
1230	0.42 (± 0.05)	0.42 (± 0.04)	0.077
1325	0.32 (± 0.05)	0.31 (± 0.04)	*0.008*
1590	0.20 (± 0.05)	0.20 (± 0.04)	0.069
1735	0.23 (± 0.05)	0.22 (± 0.04)	*0.001*
1590/1735	0.86 (± 0.08)	0.88 (± 0.09)	*0.001*
1590/1230	0.47 (± 0.06)	0.47 (± 0.06)	0.193
1230/1325	1.33 (± 0.09)	1.35 (± 0.09)	*0.005*
1735/1325	0.73 (± 0.06)	0.71 (± 0.06)	*0.002*

After establishing and computing the scores from the UV-VIS and ATR-FTIR analyses, we explored the relationships between the heartwood area and these spectroscopic measures. We aimed to determine if variations in heartwood size correlate with distinct qualitative characteristics, as indicated by the two types of spectroscopic analysis.

Spearman correlation analysis revealed that the only statistically significant correlation was observed between the heartwood area and UV-VIS absorbance, exhibiting a correlation coefficient of 0.16 (*p*-value = 0.02) (Table 5). This reflects a weak positive relationship, implying that with an increase in heartwood area, there's a marginal rise in UV-VIS absorbance. This finding could suggest that the processes of polymerization and wood darkening are, in some manner, associated with the size of the heartwood area, but not with the number of rings in the heartwood (not shown).

Table 5: Spearman correlation matrix of UV-VIS, ATR-FTIR derived scores and heartwood area in Quercus robur trees across Danish forests. Numbers in bold for p-value <0.05

	UV-VIS	ATR-FTIR	Heartwood area
UV-VIS	1.00	-	**0.16**
ATR-FTIR	-	1.00	-0.36
Heartwood area	**0.16**	-0.36	1.00

The correlation between ATR-FTIR peak ratio and heartwood area is negative but not significant, but the IR data refers to a smaller dataset than the UV-VIS.

The presence of negative values in ATR-FTIR analysis is attributable to the positioning of the reference score (peak at 1325 cm^{-1}) in the denominator of the calculated score (1230/1325 peak ratio). Our findings indicate a correlation where larger heartwood areas are associated with scores indicative of higher quality heartwood, characterized by an increased resemblance to heartwood rather than sapwood. This association may be attributed to either a greater concentration of extractives or a higher degree of polymerization within these extractives.
These outcomes are in line with prior research, which reported higher extractive contents in trees with broader ring widths (Prida et al., 2006).

Future steps will focus on using more detailed but destructive methods to better understand heartwood quality. A key focus will be on the extraction of tannins from selected groups of trees, specifically looking at their contribution to wood quality by quantifying phenolic content comprehensively. Concurrently, fluorescence spectroscopy will be employed to map the distribution of extractives within the cell walls. This dual approach promises to provide clearer insights into the roles and spatial distribution of these extractives, focusing on understanding the microstructural factors that influence heartwood quality.
Moving forward, another focus of the research will be into sequencing the full genomes of 300 trees to investigate the genetic markers, specifically Single Nucleotide Polymorphisms (SNPs), that relate to heartwood properties. This next step is pivotal in unravelling the genetic underpinnings of heartwood formation and characteristics, potentially paving the way for targeted breeding programs.

CONCLUSION
This study aimed to explore the connections between heartwood cross-sectional area and various factors, including genetic lineage (family), and wood quality, as inferred from UV-VIS and ATR-FTIR spectroscopic analyses.
Preliminary knowledge on which this paper was built upon is that a weak but statistically significant genetic variation in the heartwood cross-sectional area exists. This correlation persisted independently of the trees' growth rates, suggesting that genetic factors play a role in heartwood production that is not merely a function of the overall growth rate of the tree.
Our research demonstrates that non-destructive methods such as ATR-FTIR and UV-VIS spectroscopy, offer significant insights into the quality of heartwood. The results reveal a pattern where trees possessing smaller heartwood areas exhibit heartwood characteristics more closely resembling those of sapwood compared to trees with more extensive heartwood areas, as delineated by these analytical techniques.

It is important to underscore that the conclusions drawn from this study are based on a relatively small sample size. Additionally, while UV-VIS and ATR-FTIR spectroscopy provide valuable information on

wood characteristics, the direct correlation of these spectroscopic findings with overall quality of heartwood remains to be established.

ACKNOWLEDGMENTS

REFERENCES

Bonifazi, G., Calienno, L., Capobianco, G., Lo Monaco, A., Pelosi, C., Picchio, R., & Serranti, S. (2015). Modeling color and chemical changes on normal and red heart beech wood by reflectance spectrophotometry, Fourier Transform Infrared spectroscopy and hyperspectral imaging. Polymer Degradation and Stability, 113, 10–21. https://doi.org/10.1016/j.polymdegradstab.2015.01.001

Celedon, J. M., & Bohlmann, J. (2018). An extended model of heartwood secondary metabolism informed by functional genomics. Tree Physiology, 38(3), 311–319. https://doi.org/10.1093/treephys/tpx070

EU. (2022). The New Eu Forest Strategy for 2030. 45–66. https://environment.ec.europa.eu/strategy/forest-strategy_en

Hillis, W. E. (1968). Chemical aspects of heartwood formation. Wood Science and Technology, 2(4), 241–259. https://doi.org/10.1007/BF00350271

Humar, M., Fabčič, B., Zupančič, M., Pohleven, F., & Oven, P. (2008). Influence of xylem growth ring width and wood density on durability of oak heartwood. International Biodeterioration and Biodegradation, 62(4), 368–371. https://doi.org/10.1016/j.ibiod.2008.03.010

Klumpers, J., & Janin, G. (1992). Influence of age and annual ring width on the wood colour of oaks. Holz Als Roh- Und Werkstoff, 50(4), 167–171. https://doi.org/10.1007/BF02663260

Klumpers, J., Janin, G., Becker, M., & Lévy, G. (1993). The influences of age, extractive content and soil water on wood color in oak: the possible genetic determination of wood color. Annales Des Sciences Forestières, 50(Supplement), 403s-409s. https://doi.org/10.1051/forest:19930746

Klumpers, J., Scalbert, A., & Janin, G. (1994). Ellagitannins in European oak wood: Polymerization during wood ageing. Phytochemistry, 36(5), 1249–1252. https://doi.org/10.1016/S0031-9422(00)89646-6

Miranda, I., Gominho, J., & Pereira, H. (2009). Variation of heartwood and sapwood in 18-year-old Eucalyptus globulus trees grown with different spacings. Trees - Structure and Function, 23(2), 367–372. https://doi.org/10.1007/s00468-008-0285-9

Mosedale, J. R., Charrier, B., & Janin, G. (1996). Genetic control of wood colour, density and heartwood ellagitannin concentration in European oak (Quercus petraea and Q. robur). Forestry, 69(2), 111–124. https://doi.org/10.1093/forestry/69.2.111

Prida, A., Boulet, J. C., Ducousso, A., Nepveu, G., & Puech, J. L. (2006). Effect of species and ecological conditions on ellagitannin content in oak wood from an even-aged and mixed stand of Quercus robur L. and Quercus petraea Liebl. Annals of Forest Science, 63(4), 415–424. https://doi.org/10.1051/forest:2006021

Prida, A., & Puech, J. L. (2006). Influence of geographical origin and botanical species on the content of extractives in American, French, and East European oak woods. Journal of Agricultural and Food Chemistry, 54(21), 8115–8126. https://doi.org/10.1021/jf0616098

Traoré, M., Kaal, J., & Martínez Cortizas, A. (2023). Variation of wood color and chemical composition in the stem cross-section of oak (Quercus spp.) trees, with special attention to the sapwood-heartwood transition zone. Spectrochimica Acta - Part A: Molecular and Biomolecular Spectroscopy, 285(June 2022). https://doi.org/10.1016/j.saa.2022.121893

Vivas, N., Laguerre, M., De Boissel, I. P., De Gaulejac, N. V., & Nonier, M. F. (2004). Conformational Interpretation of Vescalagin and Castalagin Physicochemical Properties. Journal of Agricultural and Food Chemistry, 52(7), 2073–2078. https://doi.org/10.1021/jf030460m

Vivas, N., Nonier, M. F., de Gaulejac, N. V., & de Boissel, I. P. (2004). Occurrence and partial characterization of polymeric ellagitannins in Quercus petraea Liebl. and Q. robur L. wood. Comptes Rendus Chimie, 7(8–9), 945–954. https://doi.org/10.1016/j.crci.2004.06.004

Modelling tensile mechanical properties of oak timber from fibre orientation scanning for strength grading purpose

Guillaume Pot[1], Joffrey Viguier[1], Benoit Besseau[2], Jean-Denis Lanvin[3], Didier Reuling[3]

[1] Arts et Metiers Institute of Technology, LaboMaP, HESAM Université, F-71250 Cluny, France.
[2] Ducerf Groupe, Le Bourg, 71120 Vendenesse-lès-Charolles, France.
[3] FCBA, Allée de Boutaut BP227, 33028 Bordeaux, France.

E-mail: guillaume.pot@ensam.eu; joffrey.viguier@ensam.eu;benoit.besseau@ducerf.com; jean-denis.lanvin@fcba.fr; didier.reuling@fcba.fr

Keywords: strength grading machine, slope of grain, grain angle

ABSTRACT

Structural sawn timber must be graded to guarantee its mechanical characteristics in accordance with the European standards (EN 14081 parts 1-4). While these standards allow the strength grading of oak sawn timber, the technique typically used - visual grading by operators - is insufficient in producing viable material yields. As such, it remains a significant cause of material yield loss for oak timber. The objective of the present study is to assess the performance of a grading method based on fibre orientation scanning on a large sample of oak, fully representative of the French forest resource and the various cross-sections used in the industry. For this purpose, over 900 oak sawn timber boards were tested under tensile stress. A new method of interpolation of the measurement of fibre orientation on boards surface has been proposed and the mechanical model based on it allowed for predicting tensile strength with a coefficient of determination R²=0.49. This prediction level is sufficient to highly improve the grading yields compared to visual grading, and thus allow the usage of a strength grading machine for oak timber.

INTRODUCTION

In Europe, the timber construction market is dominated by softwoods, and this is also true in France, where production of softwood structural timber is well below demand. In terms of surface area, the French forest is made up of almost 75 % hardwoods, and oak in particular accounts for almost 25% of the surface area of the French forest. There is no problem finding outlets for the best quality oak, which is used in the cooperage and furniture industries. On the other hand, oak of secondary quality, with a high flexuosity, a small diameter and generally too many knots are only used as firewood. Consequently, the main objective of this work is to propose a means of grading that will enable this secondary-grade oak resource to be used for structural purposes.

To be used as structural member, sawn timber must be graded to guarantee its mechanical characteristics in accordance with the European standard EN 14081-1 (2016). While this standard allows the strength grading of oak sawn timber, the technique typically used - visual grading by operators - is insufficient in producing viable material yields (Lanvin and Reuling 2012). As such, it remains a significant cause of material yield loss for oak timber. In Europe, despite that the current standard EN 14081-2 (2018) permit it, no approved machine for grading oak exists yet.

Fibre orientation measurement is a technique included in many industrial scanning machines. It consists in lines of laser dots projected at each board surface frow which the fibre orientation is extracted thanks to the scattering of the light of the laser dot in fibres direction (phenomenon called the tracheid effect). Several publications have demonstrated the potential of using fibre orientation scanning in models to predict mechanical properties, in particular for softwoods (Olsson et al. 2013; Viguier et al. 2015; Viguier et al. 2017). Faydi (2017) and Olsson et al. (2018) dealt with the case of small cross-section sawn oak with good success, but on a reduced number of samples and under bending loading only. Rais et al. (2021) used the same measurement to predict the mechanical properties of beech in tension and Briggert et al. (2020) for Norway spruce.

The objective of this study is to propose and asses the performance of a method based on laser light scattering and mechanical modelling to predict the tensile mechanical properties of second quality oak sawn boards. It is aimed to enable to certify strength grading machines based in this principle.

MATERIALS AND METHODS

Sampling

Sampling was conducted following the guidelines of standard EN 14081-2 (2018). This standard requires obtaining the settings of a new grading machine from a sample of at least 900 boards, divided into four sub-samples. The sample must also include boards that are representative of the range of sizes, quality, and surface finish to be graded in actual production.

A total of 89 trees were selected for sampling from four different geographic regions: Bourgogne, Auvergne, Franche-Comté and Rhône-Alpes. All selected trees met either quality class C (approximately 45 %) or D (approximately 55 %) according to standard EN 1316-1 (2012), which can be described as secondary quality wood. A total of 924 oak boards were sampled, divided into eight different sections. The boards were planed in a factory to thicknesses varying from 21 to 35 mm and depth varying from 70 to 140 mm. The lengths were chosen according to the cross-section in order to be able to carry out the destructive tensile test according to EN 408+A1 (2012) and EN 384+A2 (2022) standards. In particular, the free test length should include the weakest assumed cross-section, *i.e.* the expected failure position, this is why the initial length of the boards was chosen to be greater than the required length to facilitate the positioning of the weakest section between the grips. Table 1 shows the distribution of the different boards by section and region of origin, the length between the grips used for different cross-sections and the initial length of the board.

Table 1: Number by region, length and distance between grips for each board cross-section

	70x21 [mm²]	85x21 [mm²]	105x21 [mm²]	140x21 [mm²]	105x28 [mm²]	105x35 [mm²]	140x28 [mm²]	140x35 [mm²]	Total
Bourgogne	31	40	53	19	33	17	25	18	236
Auvergne	0	33	118	75	32	0	19	5	282
Franche-Comté	69	50	30	17	0	0	5	0	171
Rhône-Alpes	17	48	10	27	38	48	20	27	235
Total	117	171	211	138	103	65	68	50	924
Average length [m]	2.2	2.7	3.1	3.7	3.3	3.2	3.7	3.7	
Distance between grips [m]	0.63	0.76	0.95	1.26	0.95	0.95	1.26	1.26	

Physical and mechanical properties measurements

Clear wood density of each board was, in accordance with EN 408+A1 (2012), determined using a specimen free of knots cut out as near as possible to the fracture zone. These specimens were also used to determine the moisture content in accordance with EN 13183-1 (2002), by oven-drying. The density, ρ was then, in accordance with EN 384+A2 (2022) adjusted regarding its moisture content following Eq. 1.

$$\rho_{12\%} = \rho \left(1 - 0.005 \left(u - u_{ref} \right) \right) \tag{1}$$

Where u is the moisture content of the board and u_{ref} taken equal to 12%.

The tensile strength and modulus of elasticity (MoE) of each board has been determined by a destructive tensile test. The tests were carried out to obtain a free test length of at least nine times the largest dimension of the cross-section, as required by EN 408+A1 standard (2012), with the weakest possible zone between the grips, as stated in EN 384+A2 (2022).

The tensile strength of each board $f_{t,0}$ was calculated using Eq. 2.

$$f_{t,0} = \frac{F_{max}}{b \times h} \tag{2}$$

where F_{max} is the maximum applied tensile force, and b and h are the smaller and the larger cross-section dimensions, respectively. Because of the size effects existing in wood material, the tensile strength was corrected from the effect of the depth h by using Eq. 3:

$$f_{t,0,h} = \frac{f_{t,0}}{k_h} \tag{3}$$

Where k_h is calculated according to Eq. 4:

$$k_h = \begin{cases} \min\left\{ \begin{matrix} \left(\frac{150}{h}\right)^{0.2} & if\ h < 150\ mm \\ 1.3 \end{matrix} \right. \\ 1\ if\ h \geq 150\ mm \end{cases} \tag{4}$$

Eq. 3 and Eq. 4 are proposed in EN 384+A2 (2022) standard, and apply if the characteristic density is lower than or equal to 700 kg/m³, which is the case in the present work, therefore these equations was applied to every board. As a result, the experimentally determined tensile strength was reduced for boards with a width smaller than 150 mm and not adjusted if larger than 150 mm.
The tensile MOE $E_{t,0}$ was calculated by using Eq. 5.

$$E_{t,0} = \frac{l_1\ (F_2 - F_1)}{b \times h\ (w_2 - w_1)} \tag{5}$$

Where $F_2 - F_1$ is an increment of load on the straight-line portion of the load deformation curve, and $w_2 - w_1$ the increment of deformation corresponding to this increment of load. The deformation are measured over a length of 5h (noted l_1 in Eq. 5) using an extensometer. Finally, $E_{t,0}$ is adjusted in accordance with EN 384+A2 (2022) using Eq. 6.

$$E_{t,0,12\%} = E_{t,0}\left(1 + 0.01(u - u_{ref})\right) \tag{6}$$

Non-destructive measurements
An industrial scanner was used to analyze the boards. By conveying the boards longitudinally, this scanner provides different images of the four long faces of the boards, as well as local density and local orientation of the fibers. The principle of board scanning is presented in Figure 1 and thoroughly described in a dataper dealing with Douglas-fir (Longuetaud et al. 2022).
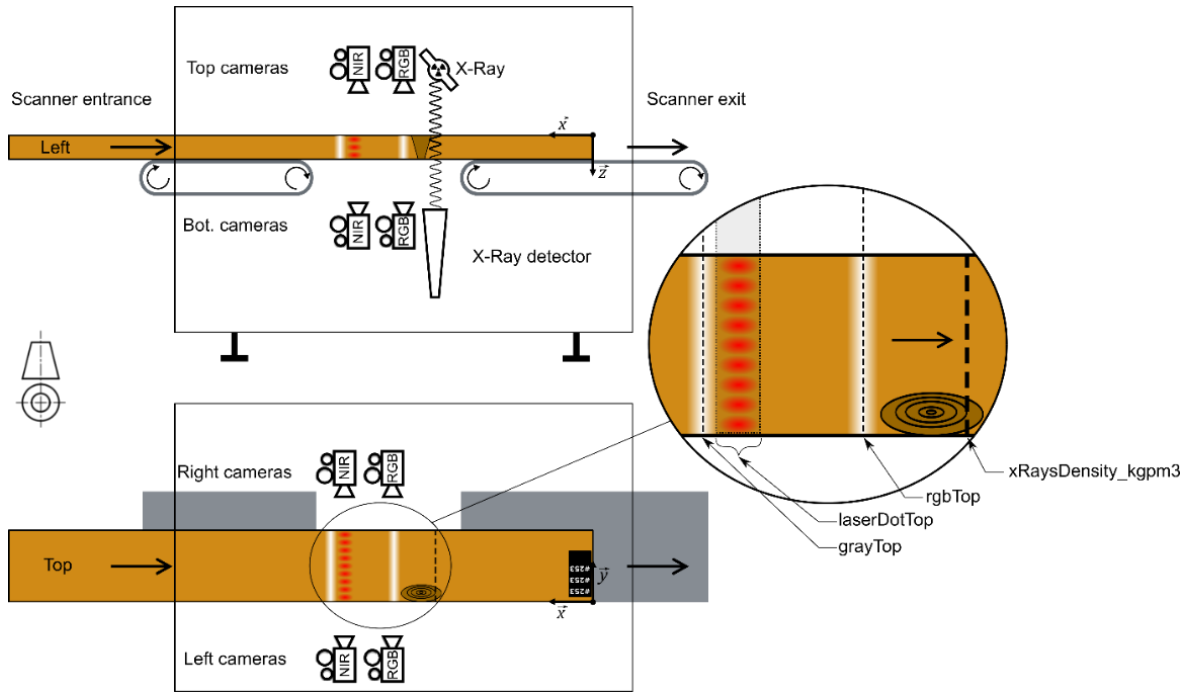
Figure 1: Illustration of board scanning with side view on the top of the figure, and top view on the bottom of the figure, corresponding to left hand top faces of the board, respectively. In the detail view, dashed lines represent a line of pixels which is recorded by the cameras while the board is conveyed longitudinally, and the greyed area with dotted line contour represents the region of interest used in the camera to treat ellipses information. From (Longuetaud et al. 2022)

In the present study, only the fibre orientation measurement has been used and will therefore be described more in detail. To determine the orientation of the fibres on the surface of the boards, the tracheid effect was utilised, as described by (Nyström 2003; Simonaho et al. 2004). This method takes advantage of the anisotropic light-scattering properties of wood. When a laser point is directed at the surface of the wood, the light observed resembles the shape of an ellipse. The ellipse's major axis aligns with the wood's fiber direction, specifically its projection onto the board's surface. Laser points diffracted from a single point are projected onto each face of the board, spaced approximately 4 mm apart. The image within the region of interest containing the elliptic pattern, as shown in detailed view in figure 1, is binarized to detect the contours of the ellipses. The contours of each binarized ellipse is then approximated using an ellipse equation, with parameters optimised in the least squares sense.

At this stage, the fibres orientation is only known in the plane of the face on which the elliptical laser scattering images were recorded. Recent work has proposed various models and estimates of fibre orientation within a sawn timber based on observable data on its external surfaces. In their grading models for mechanical strength, Olsson et al. (2013) and Olsson et al. (2018) assigned to discretized parts of board volume the fiber orientation values measured on the faces. To model the fiber orientation of a sawn timber, Lukacevic et al. (2019) used a scanner to determine the position and size of the knots to use them as input data for a model based on the Rankine-Foley model (Foley 2003). Therefore, they did not use fibre orientation measurements as a starting point. Rais et al. (2021) proceeded by interpolating the plane angles measured on the faces and edges and then calculating the angle in space using the product of the angles in each of the two planes.

In the present study, a different method is proposed, firstly described in (Besseau 2021). Figure 2 shows a wood volume element whose average fibre orientation is represented by the vector $\vec{u}_{Fiber}$. The projection of this vector in the plane $(\vec{x}, \vec{y})$ is denoted $\vec{u}_{xy}$ and that in the plane $(\vec{x}, \vec{z})$ is denoted $\vec{v}_{xz}$. The angles formed by these vectors and the board main direction $\vec{x}$ are denoted α_{xy} and β_{xz}, respectively. They correspond to the angles that can be measured at the surface of the boards by a scanner. The orientation in space of a fibre element is given by the angle γ_{xyz} between $\vec{u}_{Fiber}$ and the normal vector $\vec{n}$, here conflated with the direction $\vec{x}$.
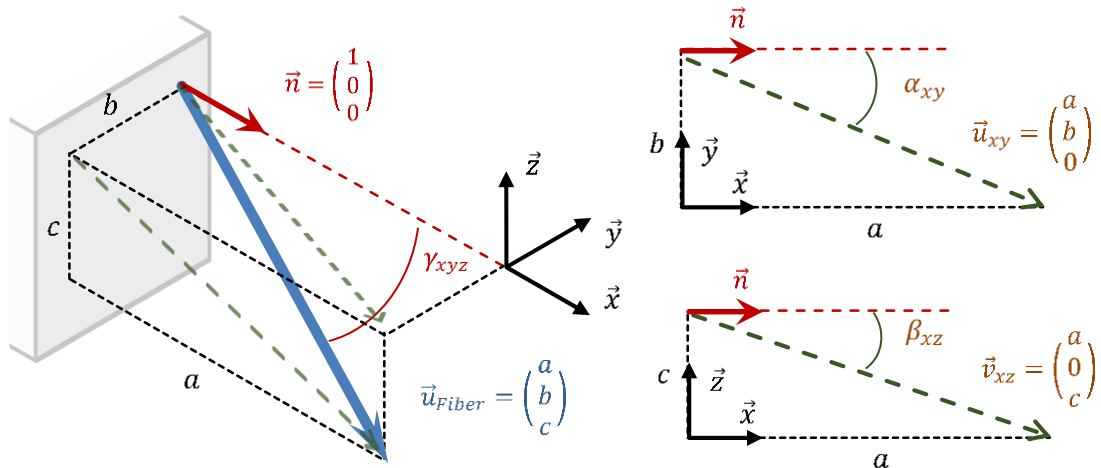

Figure 2: Definition of fibre orientation within a wood volume. From (Besseau 2021)

Following this representation, the lengths b and c can be expressed using Eq. 7 and Eq. 8:

$$b = a \times tan(\alpha_{xy}) \tag{7}$$

$$c = a \times \tan(\beta_{xz}) \tag{8}$$

and γ_{xyz} can be calculated using Eq. 9, Eq.10 and Eq. 11.

$$\vec{u}_{Fibre}.\vec{x} = \|\vec{u}_{Fibre}\|.\|\vec{x}\|.cos(\gamma_{xyz}) \tag{9}$$

$$cos(\gamma_{xyz}) = \frac{\vec{u}_{Fibre}.\vec{x}}{\|\vec{u}_{Fibre}\|.\|\vec{x}\|} = \frac{a}{\sqrt{a^2+b^2+c^2}} \tag{10}$$

$$\gamma_{xyz} = arccos\left(\frac{1}{\sqrt{1+tan^2(\alpha_{xy})+tan^2(\beta_{xz})}}\right) \tag{11}$$

Finally, the angle γ_{xyz} can be expressed only as a function of the angles α_{xy} and β_{xz}, which are plane angles. However, the measurements of α_{xy} on the faces of the boards and β_{xz} on the edges of the boards using tracheid effect described previously do not allow directly the calculation of γ_{xyz} in the wood volume. In order to obtain the missing values, it was decided to discretise the board into a 1x1x1 mm^3 cube and to perform a linear interpolation. Thus, α_{xy} is obtained by linear interpolation in the thickness of the boards from measurements taken on both sides of the boards and similarly β_{xz} is obtained by linear interpolation in the width of the boards.

Mechanical modelling and IPs calculation
Clear wood should be considered as an orthotropic material in a LTR-coordinate system where L is the longitudinal direction of the fibres, T the tangential direction, and R is the radial direction. In this study clear wood has been considered to have a transverse isotropic behaviour, in which tangential and radial properties are the same since no data were available to differentiate and locate T- and R- directions. As a result, the compliance matrix [S] of clear wood is presented in Eq 12.

$$[S] = \begin{bmatrix} \frac{1}{E_0} & -\frac{\nu_{TRL}}{E_{90}} & 0 \\ -\frac{\nu_{LTR}}{E_0} & \frac{1}{E_{90}} & 0 \\ 0 & 0 & \frac{1}{G_{LTR}} \end{bmatrix} \tag{12}$$

Young's modulus in the fiber direction (and corresponding to E_0 in Eq. 6) has been chosen equal to 14,620 MPa, in accordance with experimental tensile tests. E_{90}, the modulus of elasticity in the direction orthogonal to the local fibre direction in this transverse isotropic model was calculated as the average of the orthotropic ratios E_T/E_L and E_R/E_L from Kretschmann (2010). G_{LTR} the shear modulus in the transverse isotropic plane was similarly calculated as the average of the orthotropic ratios G_{LT}/E_L and G_{LR}/E_L from Kretschmann (2010) . Finally, ν_{LTR} the Poisson's ratio in the transverse isotropic model, was taken equal to the average of the orthotropic Poisson's ratios ν_{LT} and ν_{LR} from (Kretschmann 2010), which is 0.4. For each element of the grid of interpolated angles γ_{xyz}, the material compliance matrix [S] was rotated according to γ_{xyz} by application of Eq. 13 to obtain the local compliance matrix in the specimen system of axes $(\vec{x},\vec{y},\vec{z})$ [S'] for each (x, y, z) location.

$$[S'] = [T_\gamma^{-1}] [S] [T_\gamma] = \begin{bmatrix} S'_{11} & S'_{12} & S'_{16} \\ S'_{12} & S'_{22} & S'_{26} \\ S'_{16} & S'_{26} & S'_{66} \end{bmatrix} \tag{13}$$

with T_γ the transfer matrix, from the local fiber coordinate system to the global specimen coordinate system, dependent on the fiber orientation γ_{xyz} obtained locally (abbreviated γ in the following). E_x, the MoE in the main, lengthwise direction of the specimen $(\vec{x})$, is therefore calculated as the inverse of the first coefficient of the compliance matrix [S'] using Eq. 14.

$$E_x(x, y, z) = \frac{1}{S'_{11}} = \frac{1}{\frac{1}{E_{90}}\sin^4(\gamma)+\frac{1}{E_0}\cos^4(\gamma)+\left(\frac{1}{G_{LTR}}-2\frac{\nu_{LTR}}{E_0}\right)\sin^2(\gamma)\cos^2(\gamma)} \tag{14}$$

The average longitudinal boards stiffness can be calculated according to Beam Theory (BT) for each position x of the board by integrating over the surface of the cross-sectional area of the plank using Eq. 15.

$$E_{a,BT}(x) = \frac{\iint E_x \, dy \, dz}{b \times h}$$ (15)

The longitudinal displacement can be obtained using Eq. 16.

$$u_{x,l,BT}(x) = \int_0^x \frac{\sigma}{E_{a,BT}(\xi)} \, d\xi$$ (16)

The calculation was performed by numerical integration with $d\xi$ = 1 mm and σ the input axial stress has been set arbitrarily to 1 MPa.

Finally, an "apparent MoE" was computed from these displacements. It can be seen as the MoE that would be observed if a mechanical test could be done within a short portion of the beam, of length δ. Thus, this apparent axial MoE is calculated using Eq. 17. In this study this portion has been set to 90 mm as this length has been succesfully applied on numerous previous study dealing with calculation of IPs for strength grading purpose (Olsson and Oscarsson 2017; Olsson et al. 2018; Briggert et al. 2020).

$$E_{a,app,90,BT}(x) = \sigma \frac{90}{u_{x,l,BT}\left(x+\frac{90}{2}\right) - u_{x,l,BT}\left(x-\frac{90}{2}\right)}$$ (17)

Two different IPs were finally computed from this apparent MoE profile:
- the first one related to $f_{t,0,h}$ and noted $E_{a,app,90,BT,min}$ taken as the minimum of $E_{a,app,90,BT}(x)$ within the portion of the board which is between the grips in the tensile test. The assumption here is that the tensile strength is correlated to the minimum of the apparent MoE as suggested in several publications about strength grading of timber.
- the second one related to $E_{t,0,12\%}$ and noted $E_{a,l,BT}$ which is nothing more than a particular case of apparent MoE, calculated with computed displacement over the central area of the specimen over a distance of 5h. The calculation is described in Eq. 18.

$$E_{a,l,BT} = \sigma \frac{5h}{u_{x,l,BT}\left(x_{l,center} + 2.5h\right) - u_{x,l,BT}\left(x_{l,center} - 2.5h\right)}$$ (18)

RESULTS AND DISCUSSIONS
Physical and mechanical properties measurements

In Table 2, some descriptive statistics of corrected tensile strength ($f_{t,0,h}$), corrected tensile MoE ($E_{t,0,12\%}$), corrected clear wood density ($\rho_{12\%}$), and moisture content (u) are presented. The average moisture content of the tested boards was 9.5 %, with minimum and maximum values of 7.4 % and 12.2 % respectively. Only 21 boards had a moisture content of less than 8 %, the minimum limit to apply moisture content correction defined in EN 384+A2 (2022). Nevertheless, the same correction of density and MoE stated in EN 384+A2 (2022) was applied considering the fact that they were very close to this limit. The mechanical properties can be found rather low but it has to be kept in mind that the boards were produced from only second quality oak (grade C or D as stated in the sampling part). Nevertheless, a non-negligible proportion of boards meets the requirements for structural use.

Figure 3 shows the distribution and relationship between $\rho_{12\%}$, $E_{t,0,12\%}$ and $f_{t,0,h}$. It appears that there is no correlation between density and tensile strength (coefficient of determination $R^2 = 0$) and only a small correlation between density and tensile MoE ($R^2 = 0.02$). This result can be surprising since for coniferous species, such relationships exists. Indeed, (Briggert et al. 2020) reported R^2 of 0.23 between density and tensile strength and 0.53 between density and tensile MoE for Norway spruce. However, the results are in accordance with previous finding on European oak in bending (Olsson et al. 2018), and on beech in tension (Rais et al. 2021). The presence of singularities such as rather large knots and their associated strong grain angle variation for oak are of higher influence on the mechanical properties than the density. A R^2 of 0.42 is observed between $E_{t,0,12\%}$ and $f_{t,0,h}$ supporting the hypothesis that the

stiffness of boards can somehow be related to its strength. In (Olsson et al. 2018) a R^2 between MoE and bending strength was found equal to 0.53.

Table 2: Descriptive statistics for physical and mechanical properties measured

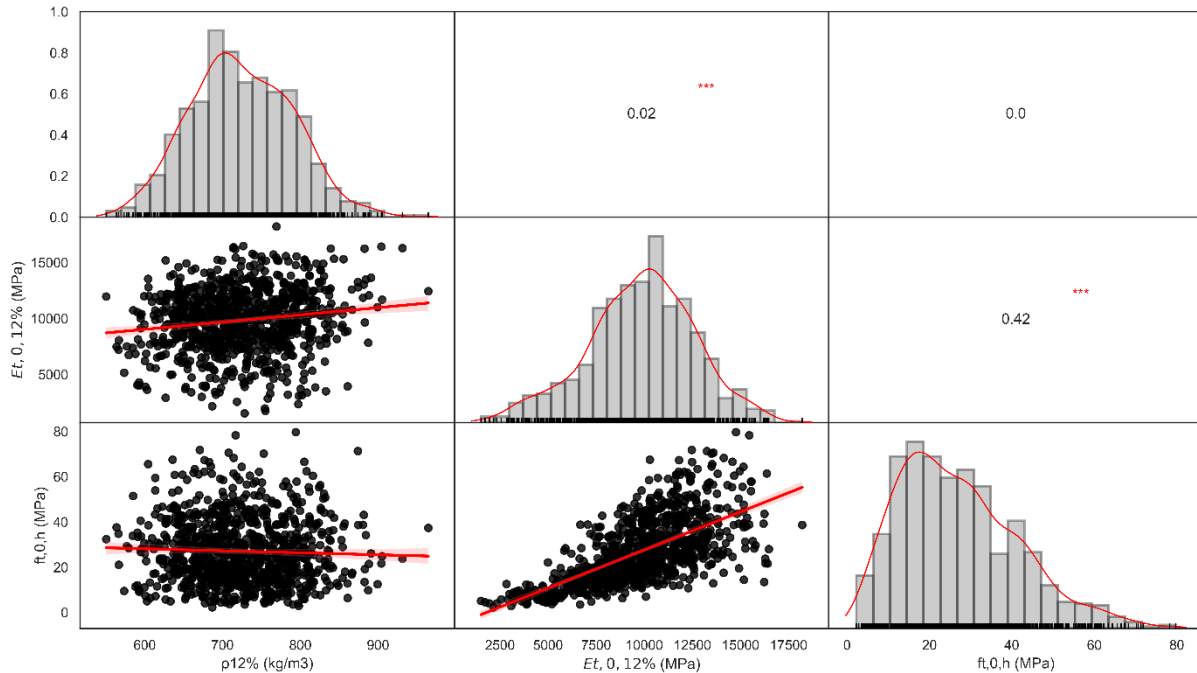|	u [%]	$\rho_{12\%}$ [kg/m3]	$E_{t,0,12\%}$ [MPa]	$f_{t,0,h}$ [MPa]
Mean	9.5	724.1	9.820	27.0
Std	0.7	65.4	2.780	14.4
Minimum	7.4	550.5	1.510	2.3
Maximum	12.2	964.5	18.210	79.7
5% percentile	8.2	621.0	4.720	7.3

Figure 3: Distribution and relationship between physical and mechanical properties measured

Mechanical behaviour prediction

Figure 4. shows the relationship between the computed IPs and their corresponding mechanical properties. The R^2 between $E_{a,l,BT}$ and $E_{t,0,12\%}$ is equal to 0.45 and the prediction gives slightly lower modulus of elasticity than the reality. The R^2 between the tensile strength $f_{t,0,h}$ and $E_{a,app,90,BT,min}$ appears to be higher, being equal to 0.49. Similar results were observed on Norway spruce by Briggert et al. (2020), with $R^2 = 0.51$ between $f_{t,0,h}$ and $E_{a,90,nom}$, an IP also obtained from fibre orientation data with a very similar modelling method (comparisons are made and discussed in (Pot et al. 2024)). Such level of R^2 is also consistent to what is obtained under bending loading, as a value of 0.56 was obtained in (Olsson et al. 2018) on a much smaller batch of boards comprising only one cross-section. The performance of the predictions can seem rather low compared to what can be obtained on coniferous species but would be sufficient for commercial grading of oak obtained from secondary quality logs.
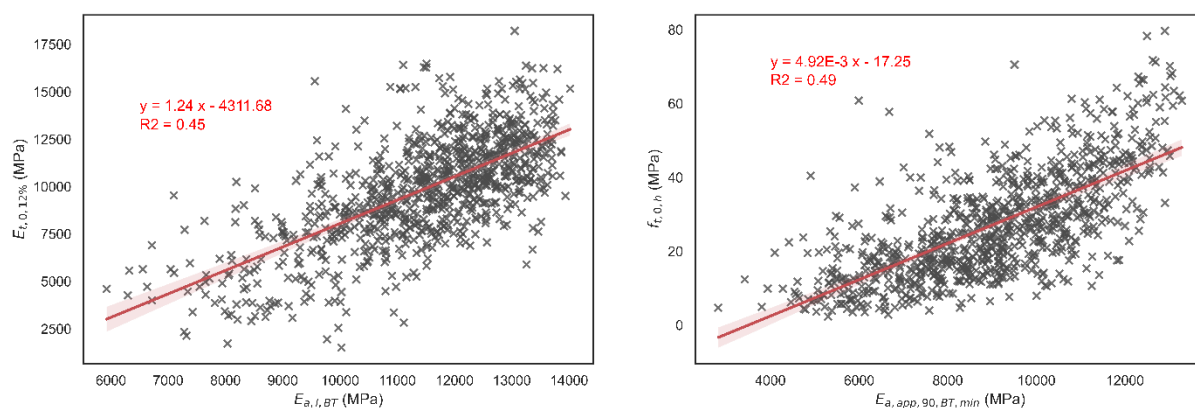
Figure 4: Linear relationship between computed IPs based on grain angle measurement and beam theory modelling and their corresponding mechanical properties in tension

CONCLUSIONS

The results confirm results that was observed in bending, global density is not correlated to the MoE and the tensile strength. This was explained by the fact that knots and fibre distortion around knots in oak boards often affect the entire cross section, resulting in very low local stiffness and low strength. This is not captured by a measure of a global density of a board.

A new method of interpolation of the measurement of fibre orientation on boards surface has been proposed and IPs based on these data alone gives a rather good prediction of tensile strength and MoE with a coefficient of determination equal to 0.49 and 0.45, respectively. This performance is good enough for commercial grading of oaks board and should lead to higher yield than using visual grading. Improvement are expected through a better interpolation of the fibre orientation within the volume of the board and/or by improving the way wood is modelled.

This work could also contribute to the development of engineered wood products made of oak (Glulam of CLT). Applying these methodologies to the production of finger-jointed lamellas is already an ongoing work and gives satisfactory results (Soh Mbou et al. 2024).

Finally, the results presented show that mechanical properties of a large proportion of oak boards obtained from second quality logs can be suitable for structural use. In particular the data presented in this work can also contribute to the development of hardwood tensile classes, which is needed since the tensile classes in (EN 338 2016) currently exist for softwoods only.

ACKNOWLEDGEMENTS

REFERENCES

Besseau B (2021) Contribution au développement de procédés innovants pour une transformation plus efficiente du chêne. These de doctorat, HESAM

Briggert A, Olsson A, Oscarsson J (2020) Prediction of tensile strength of sawn timber: definitions and performance of indicating properties based on surface laser scanning and dynamic excitation. Mater Struct 53(3):54. https://doi.org/10.1617/s11527-020-01460-5

EN 338 (2016) Structural timber — Strength classes

EN 384+A2 (2022) Structural timber — Determination of characteristic values of mechanical properties and density

EN 408+A1 (2012) Timber structures – Structural timber and glued laminated timber – Determination of some physical and mechanical properties

EN 1316-1 (2012) Hardwood round timber. Qualitative classification. Part 1: Oak and beech

EN 13183-1 (2002) Moisture content of a piece of sawn timber - Part 1: Determination by oven dry method

EN 14081-1 (2016) Timber structures - Strength graded structural timber with rectangular cross section - Part 1: General requirements.

EN 14081-2 (2018) Timber structures - Strength graded structural timber with rectangular cross section - Part 2: Machine grading; additional requirements for type testing

Faydi Y (2017) Classement pour la résistance mécanique du chêne par méthodes vibratoires et par mesure des orientations des fibres. Thèse de doctorat, Ecole doctorale n°432: Science des Métiers de l'Ingénieur

Foley C (2003) Modeling the effects of knots in structural timber. Thèse de doctorat, División of the Structural Engineering, Lund University

Kretschmann DE (2010) Wood handbook, chapter 05: mechanical properties of wood. Forest Products Laboratory, Department of Agriculture Forest Service, Madison, Wisconsin, USA

Lanvin J-D, Reuling D (2012) Caractérisation du Chêne sessile et pédonculé de France en vue de son utilisation en structure. Revue Forestière Française. https://doi.org/10.4267/2042/47474

Longuetaud F, Pot G, Mothe F, Barthelemy A, Decelle R, Delconte F, Ge X, Guillaume G, Mancini T, Ravoajanahary T, Butaud J-C, Collet R, Debled-Rennesson I, Marcon B, Ngo P, Roux B, Viguier J (2022) Traceability and quality assessment of Douglas fir (Pseudotsuga menziesii (Mirb.) Franco) logs: the TreeTrace_Douglas database. Annals of Forest Science 79(46). https://doi.org/10.1186/s13595-022-01163-7

Lukacevic M, Kandler G, Hu M, Olsson A, Füssl J (2019) A 3D model for knots and related fiber deviations in sawn timber for prediction of mechanical properties of boards. Materials and Design 166:107617. https://doi.org/10.1016/j.matdes.2019.107617

Nyström J (2003) Automatic measurement of fiber orientation in softwoods by using the tracheid effect. Computers and electronics in agriculture 41(1):91–99

Olsson A, Oscarsson J (2017) Strength grading on the basis of high resolution laser scanning and dynamic excitation: a full scale investigation of performance. European Journal of Wood and Wood Products 75(1):17–31. https://doi.org/doi.org/10.1007/s00107-016-1102-6

Olsson A, Oscarsson J, Serrano E, Källsner B, Johansson M, Enquist B (2013) Prediction of timber bending strength and in-member cross-sectional stiffness variation on the basis of local wood fibre orientation. European Journal of Wood and Wood Products 71(3):319–333. https://doi.org/10.1007/s00107-013-0684-5

Olsson A, Pot G, Viguier J, Faydi Y, Oscarsson J (2018) Performance of strength grading methods based on fibre orientation and axial resonance frequency applied to Norway spruce (Picea abies L.), Douglas fir (Pseudotsuga menziesii (Mirb.) Franco) and European oak (Quercus petraea (Matt.) Liebl./Quercus robur L.). Annals of Forest Science 75(4):102. https://doi.org/10.1007/s13595-018-0781-z

Pot G, Duriot R, Girardon S, Viguier J, Denaud L (2024) Comparison of classical beam theory and finite element modelling of timber from fibre orientation data according to knot position and loading type. Eur J Wood Prod. https://doi.org/10.1007/s00107-024-02055-5

Rais A, Bacher M, Khaloian-Sarnaghi A, Zeilhofer M, Kovryga A, Fontanini F, Hilmers T, Westermayr M, Jacobs M, Pretzsch H, van de Kuilen J-W (2021) Local 3D fibre orientation for tensile strength prediction of European beech timber. Construction and Building Materials 279:122527. https://doi.org/10.1016/j.conbuildmat.2021.122527

Simonaho S-P, Palviainen J, Tolonen Y, Silvennoinen R (2004) Determination of wood grain direction from laser light scattering pattern. Optics and Lasers in Engineering 41(1):95–103

Soh Mbou D, Besseau B, Pot guillaume, Viguier J, Marcon B, Milhe L, Lanvin J-D, Reuling D (2024) Oak timber cross-cutting based on fiber orientation scanning and mechanical modelling to ensure finger-joints strength. Sopron, Hungary

Viguier J, Bourreau D, Bocquet J-F, Pot G, Bléron L, Lanvin J-D (2017) Modelling mechanical properties of spruce and Douglas fir timber by means of X-ray and grain angle measurements for strength grading purpose. European Journal of Wood and Wood Products 75(4):527–541. https://doi.org/10.1007/s00107-016-1149-4

Viguier J, Jehl A, Collet R, Bleron L, Meriaudeau F (2015) Improving strength grading of timber by grain angle measurement and mechanical modeling. Wood Material Science & Engineering 10(1):145–156. https://doi.org/10.1080/17480272.2014.951071

Green oak building – small diameter logs for construction

Martin Huber[1*], Franka Brüchert[1], Nicolas Hofmann[1], Kay-Uwe Schober[2], Beate Hörnel-Metzger[2], Maximilian Müller[2], Udo H. Sauter[1]

[1] Forest Research Institute of Baden-Württemberg, Department of Forest Utilisation, Freiburg, Germany,
[2] Hochschule Mainz, Mainz University of Applied Sciences, Mainz, Germany.

E-mail: martin.huber@forst.bwl.de; franka.bruechert@forst.bwl.de; nicolas.hofmann@forst.bwl.de; kay-uwe.schober@hs-mainz.de; beate.hoernel-metzger@hs-mainz.de; maximilian.mueller@hs-mainz.de; udo.sauter@forst.bwl.de

Keywords: Oak, small-diameter logs, internal wood structure, strength prediction

ABSTRACT

In Germany, only half the annual increment is used in oak stands. Especially small-diameter oaks are currently either not used or only used as firewood. To achieve long-term carbon dioxide storage and higher added value, a finished research project aimed to make small-diameter oak logs available as structural timber members, e.g., for columns, frameworks, and agricultural buildings, such as barns. For sawn timber, strength grading classification is a pre-requisite for structural uses of wood. Machine strength grading in this context is based on statistical prediction models to relate internal and physical wood characteristics such as density and knot structure with mechanical properties from which strength grades are determined. We report on the results of stiffness and strength prediction for small-diameter oak logs applying similar approaches as known for sawn timber strength grading.

MATERIALS AND METHODS

66 oak (*Quercus petraea* (Matt.) Liebl.) logs from two sub-samples with a length of 5 m and an average mid-diameter of about 23 cm were included in the analysis. The experimental program included the characterisation of the test material by static bending tests (static MOE/MOR), dynamic MOE (Viscan), CT- and 3D-scanning for internal characteristics (wood density, knots, internal defects), as well as log geometry (curvature, taper), and external inspection in particular for branch position. Altogether, more than 60 variables were used for the statistical modelling based on GLM modelling approaches. However, several of the variables describe the same log features in slightly different ways. The external inspection was performed according to the "Rahmenvereinbarung für den Rohholzhandel in Deutschland" (RVR) (DFWR, DHWR 2020), while the geometric features were assessed using algorithms of the "Rahmenvereinbarung für die Werksvermessung von Stammholz" (RVWV) (DeSH, DFWR 2021). For the detection of knots in the CT images a conventional algorithm, which was developed for softwood, and a new machine learning approach were used. In order to take the knot position in the bending test into account the parameter "Sum of weighted knot positions" was defined. Each knot in the test area was assigned to the corresponding digit on a dial of a clock. Subsequently the position was weighted according to Figure 32, i.e. to a knot at 12:00 o'clock the value 0 was assigned and to a knot at 03:00 or 9:00 o'clock the value 3 for example. The weights of all knots in the test area were then summed up.
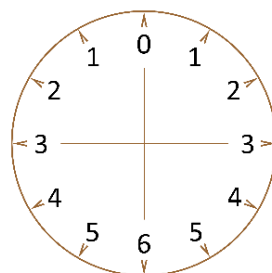

Figure 32: Weights of the knot positions for the definition of the parameter "Sum of weighted knot positions"

RESULTS AND DISCUSSION

In Table 1 the main characteristics of the logs are listed for the whole sample as well as separated by the two sub-samples.

Table 1: Characteristics of the test material. Mean plus-minus standard deviation

	All	sub-sample 1	sub-sample 2
Number of logs	66	44	22
Average diameter [cm]	23.4±3.4	22.6±3.3	25.0±2.9
Ovendry density [kg/m³]	696±56	678±47	730±58
Wood density CT [kg/m³]	869±40	858±37	892±36
Number of knot features RVR	25.6±19.0	23.2±16.7	30.5±22.6
Knot volume CT [%]	2.75±1.34	2.80±1.42	2.65±1.19
Curvature [cm/m]	1.81±0.76	1.60±0.65	2.22±0.82
Taper [cm/m]	0.66±0.24	0.66±0.23	0.66±0.26
Average width of growth rings [mm]	1.32±0.26	1.28±0.26	1.40±0.25
MOE_{dyn} [N/mm²]	12648.9±2155.6	11974.3±1866.5	13998.0±2095.0
MOE_{stat} [N/mm²]	11138.0±5455.9	9373.3±2527.7	14667.5±7712.2
MOR [N/mm²]	60.6±13.6	58.0±12.5	66.0±14.3

The mechanical characteristics are in line with the literature for other oak material (Nocetti et al. 2021). In
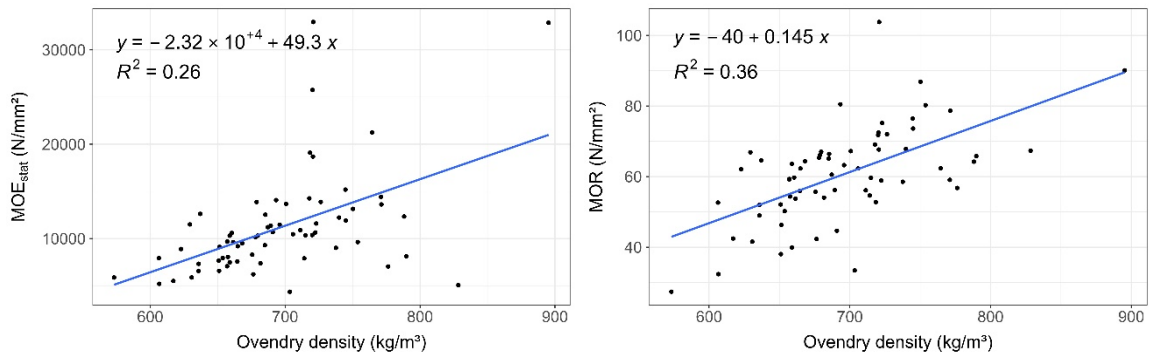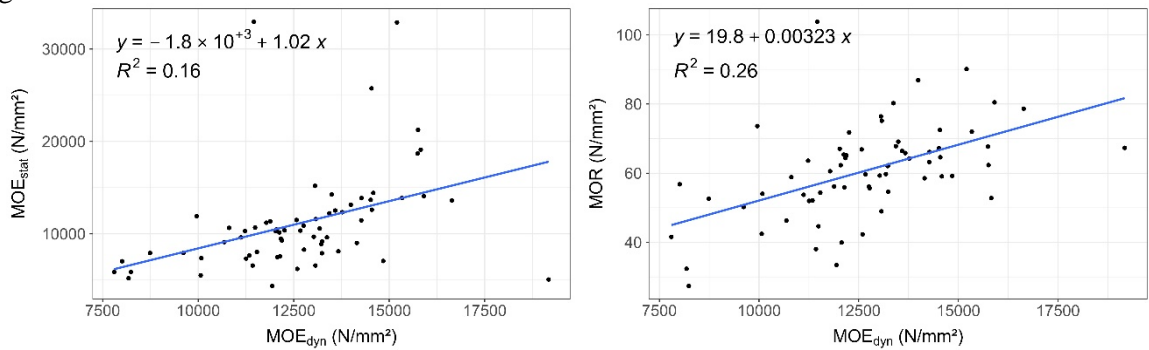
Figure 2 and

Figure 3 the variation of the two target variables MOE_{stat} and MOR over the log features ovendry density and MOE_{dyn} are illustrated.
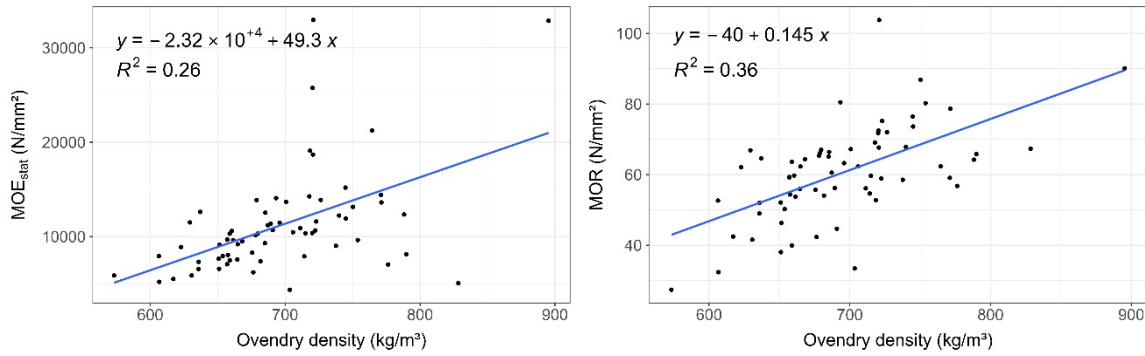
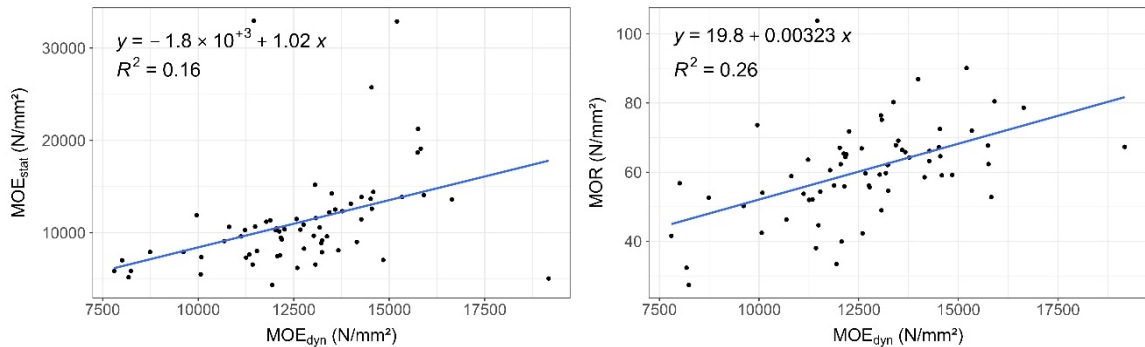**Figure 2: Variation of the MOE$_{stat}$ and MOR over the ovendry density**

Figure 3: Variation of the MOE$_{stat}$ and MOR over the MOE$_{dyn}$

Among the variables with the highest correlations to MOE$_{stat}$ and MOR were *ovendry density* and *moisture content*. As *ovendry density* and *MC* are difficult to measure with respect to an online grading process, both variables were excluded from the variable set and *green wood density* from CT was used as the proxy. The sub-samples also showed an effect on the variations of MOR and especially MOE$_{stat}$, since the average MOE$_{stat}$ for the sub-sample 2 was much higher and showed a far bigger variation (Table 1) than sub-sample 1. But as the final model should not depend on sub-samples, the sub-sample was not used as a predictor, either.

Without these three parameters, the R²$_{corr}$ of the models for MOE$_{stat}$ were low and varied between 0.32 to 0.34. The combination of the most expected predictors like *Green density*, *dynamic MOE* and some knot variables did not improve the model quality. Instead, *Green density* in combination with log geometry variables had a larger influence.

For MOR the R²$_{corr}$ varied between 0.41 to 0.52. *Green density*, *MOE$_{dyn}$*, *knot volume* and *sum of weighted knot positions* added to the simplest, meaningful model. In different combinations of predictors, also the variables *number of growth rings* and *stem taper* showed an acceptable relevance as predictors. However, due to the very small dataset and the variation in the target variables the number of predictors in the models needed to be restricted to avoid overfitting. The model including number of growth rings as well as its evaluation is presented in Table 2 and Table 3.

Table 2: Linear model for the MOR

Predictors	Estimate	Std. Error	t value	p value
Intercept	-18.52	37.53	-0.49	0.62
Green density CT	0.098	0.037	2.67	0.0097
(MOE$_{dyn}$)$^{1/2}$	0.041	0.14	2.82	0.0064
Number of growth rings	-0.49	0.17	-2.97	0.0043
Knot volume CT test area × Sum of weighted knot positions	-0.00016	5.95x10^{-5}	-2.85	0.0060

Table 3: Evaluation of the linear model for the MOR

Number of parameters	Degrees of freedom	Residual standard error	R-squared	Adjusted R-squared	F-statistic	p-value
4	61	9.93	0.5	0.46	15.05	1.3x10^{-8}

One of the main reasons for the difficulties in modelling the MOE_{stat} was the small sample size in combination with several outliers regarding the variation of the MOE_{stat} over *ovendry density* and *dynamic* *MOE* (

Figure 2 und
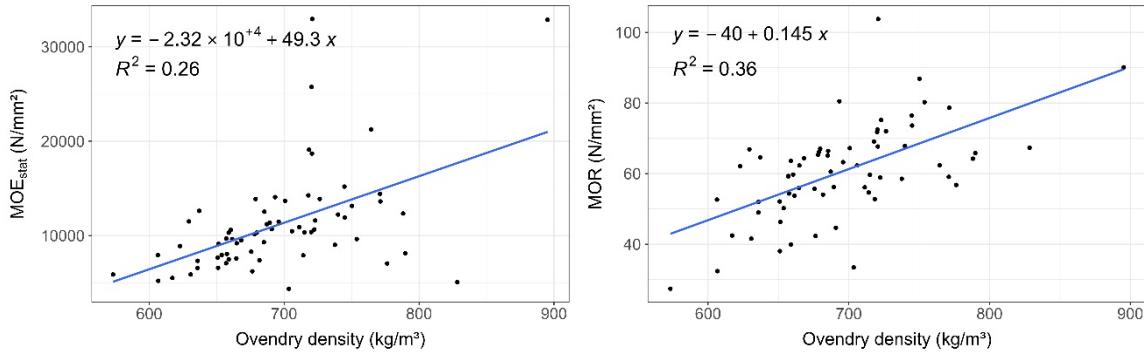
Figure 3). So far, no explanation for these extreme values could be found.

For the MOR the predictors, which were mostly used, describe features, which are the expected ones and are frequently discussed in literature. Several studies show a po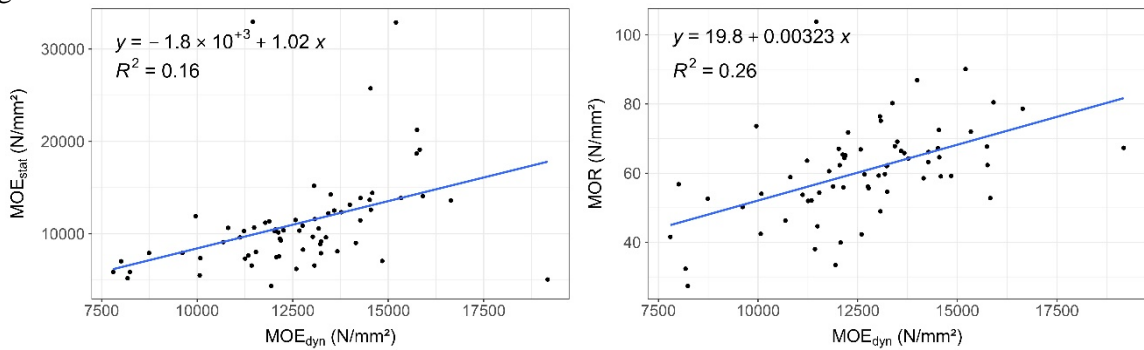sitive correlation between density as well as the dynamic MOE and strength of the logs. On the other hand, it is known, that knots have a negative impact on the strength.

The machine learning approach for the knot detection is still in development and while it already shows good results, there is still potential for improvement, which might lead to improved prediction models for MOE_{stat} and MOR. As especially the combination of *knot volume* and the *sum of weighted knot positions* was a good predictor in several models, it seems to be useful to develop a predictor, which combines the weighted knot position and volume of each individual knot. With the existing machine learning approach, this was not possible yet. Furthermore, the knot detection does not differentiate between different types of knot features but only considers their volume, although the different types most likely differ in their influence on the log strength.

CONCLUSIONS

In general a pre-classification of small-diameter oak logs seems promising. When regarding the results, the small sample size has always to be kept in mind. Because of the small sample size, the models could only include a limited number of predictors and quickly showed tendencies to overfit. The correlation of some further predictors with the target variables suggest, that including them would lead to further improvements. Therefore, the expansion of the sample would be an important next step. The expansion is also necessary, since all tested logs came from the same stock and therefore very likely do not represent the variation of wood features of oak logs that can be found in literature.

REFERENCES

Deutscher Forstwirtschaftsrat e.V. (DFWR), Deutscher Holzwirtschaftsrat e.V. (DHWR) (2020) Rahmenvereinbarung für den Rohholzhandel in Deutschland des Deutschen Forstwirtschaftsrates e.V. und des Deutschen Holzwirtschaftsrates e.V. (RVR). Berlin, Germany, Volume 3.

Deutsche Säge- und Holzindustrie Bundesverband e.V. (DeSH), Deutscher Forstwirtschaftsrat (DFWR) (2005) Rahmenvereinbarung für die Werksvermessung von Stammholz des Deutschen Forstwirtschaftsrates e.V. und des Verbandes der Deutschen Säge- und Holzindustrie e.V. (RVWV) [Version 2005-01-14]. Available online: http://www.werkeingangsvermessung.info/ (accessed on 25 June 2021).

Hofmann N., Brüchert F., Sauter U.H., Schober K.-U., Hörnel-Metzger B. (2023) Green oak building with high-tech methods, Part 1: Characterisation of the raw material. WCTE World Conference on Timber Engineering 2023; Timber for a Livable Future, Oslo, Norwegen, / [ed] Nyrud, A. Q. Malo, K. A.; Nore, K., World Conference on Timber Engineering 2023 (WCTE 2023), 2023, p. 711-716.

Nocetti, M., Aminti, G., Wessels, C. B., Brunetti, M. (2021) Applying Machine Strength Grading System to Round Timber Used in Hydraulic Engineering Works. Forests 2021, 12, 281. https://doi.org/10.3390/f12030281

Schober K.-U., Hörnel-Metzger B., Hofmann N., Brüchert F., Sauter U. H. (2023) Green oak building with high-tech methods, Part 2: Log bending tests for determination of strength and stiffness. WCTE World Conference on Timber Engineering 2023; Timber for a Livable Future, Oslo, Norwegen, / [ed] Nyrud, A. Q. Malo, K. A.; Nore, K., World Conference on Timber Engineering 2023 (WCTE 2023), 2023, p. 119-125.

An evaluative examination of oak wood defect detection employing deep learning (DL) software systems.

Branimir Jambreković[1], Filip Veselčić[2], Iva Ištok[1], Tomislav Sinković[1], Vjekoslav Živković[1], Tomislav Sedlar[1*]

[1] University of Zagreb, Faculty of Forestry and Wood Technology. Svetošimunska cesta 23, 10000 Zagreb, Croatia
[2] Bjelin Spačva d.o.o. Duga ulica 181, 32100 Vinkovci, Croatia.

E-mail: bjambreko@sumfak.unizg.hr; veselcic.filip@gmail.com; iistok@sumfak.unizg.hr; tsinkovic@sumfak.unizg.hr; vzivkovic@sumfak.unizg.hr; tsedlar@sumfak.unizg.hr

Keywords: defect detection, oak wood, convolutional neural network (CNN), deep learning (DL)

ABSTRACT

The increasing demand for wood products poses a significant challenge in light of the world's growing population. This requirement drives heightened production, leading to a focus on achieving high-quality and efficient utilization of basic materials. One of the inherent difficulties in working with a natural material like wood is the inevitability of defects in wood elements. Detecting these defects, even in modern times, involves visual scrutiny of the sawn surface and manual marking of identified defects.

To address this issue, industrial scanners equipped with software based on Convolutional Neural Networks (CNNs) have emerged as a solution for rapid defect detection. This technology holds the potential to enhance production efficiency and eliminate human subjectivity. This paper aims to compare the applicability of defect recognition software integrated into industrial scanners with software developed specifically for this purpose within the scope of a research project.

The research findings indicate that the software embedded in the industrial scanner proves more effective for analyzing knots (77.78% vs. 70.37%), sapwood (100% vs. 80%), and ambrosia wood (60% vs. 20%). Conversely, the software derived from the research project demonstrates greater effectiveness in analyzing cracks (70% vs. 65%), ingrown bark (42.86% vs. 28.57%), and wood rays (81.82% vs. 27.27%). These results underscore the nuanced strengths and weaknesses of the software approach, emphasizing the importance of considering specific wood defect types when selecting an appropriate detection system.

Comparison of surface roughness of milled surface of false heartwood, mature wood, and sapwood within beech wood

Lukáš Adamčík[1*], Richard Kminiak[1], Adrián Banski[1]

[1] Faculty of Wood Sciences and Technology, Technical University in Zvolen, T.G.Masaryka 24, 960 01 Zvolen, Slovakia

E-mail: xadamcikl@tuzvo.sk; richard.kminiak@tuzvo.sk; adrian.banski@tuzvo.sk

Keywords: beech wood, false heartwood, mature wood, sapwood, CNC milling, surface roughness, digital microscopy

ABSTRACT

Throughout history, beech wood (*Fagus sylvatica* L.) has gradually become one of the most widely used hardwoods in the furniture industry. However, when using it, often due to the yield, the presence of a false heartwood in the sawn timber cannot be avoided. This is found in wood to a high degree, while it is characterized by different physical and mechanical properties. Due to the modernization of production as well as the shape diversity of beech products, it is now common practice to use CNC milling technology for production. However, in order to achieve an acceptable quality of the created surface, the correct choice of technological parameters is crucial. Mainly due to the above-mentioned differences within beech wood, it is therefore necessary to deal with the changing surface roughness of wood from the false heartwood zone, mature wood and sapwood when milling parameters change. Therefore, the present paper deals with research into the influence of varying revolutions and feed speed of the tool on the resulting roughness of beech wood from three zones. The revolutions and feed speed of the shank cutter were chosen as the parameters most influencing the value of feed per tooth, which is considered an indicator of the size of waves after milling, affecting the overall unevenness of the wood surface. The most commonly used R-roughness parameters, namely Ra, Rz, Rv, Rp, Rsk and Rku, will be measured. All parameters will be measured using the Keyence VHX-7000 digital microscope. The examined roughness of three zones of beech wood after milling will be explained more comprehensively with the help of microscopy of the machined surface. The aim of the paper is to identify statistically significant differences between measured zones, which could be explained in the context of current knowledge about the effects on surface roughness.

INTRODUCTION

Wood milling using CNC machining centers is an increasingly modern method of machining. This technology is mainly used for milling or drilling of more complex workpiece profiles made of composite materials or native wood species. It was the versatility of CNC machining centers that predestined them to use a large number of cutting tools and the possibility of adjusting and optimizing machining parameters. At the same time, milling as a process is most often included before sanding. Despite the fact that sanding with higher grit sizes reduces surface irregularities (and therefore surface roughness), milling itself is equally important in terms of the quality of the created surface (Adamcik et al. 2023). By (Singer and Özşahin, 2022) the machining parameters with the greatest impact on surface quality are feed speed and revolutions. With an increase in feed speed, there is a deterioration in surface quality (Bendikiene and Keturakis, 2016; Çakiroğlu et al. 2019; Gochev, 2018). Roughness parameters, such as Ra, grow linearly with the increase in feed speed (Atanasov et al. 2023a; Smajic and Jovanovic, 2020; Yang et al. 2023). By (Pinkowski et al. 2018a) as the feed speed increases, so does the thickness of the chip, and more material is also cut off (Wei et al. 2021). With an increase in feed speed, the feed per tooth increases in direct proportion, which significantly worsens conditions below the cutting-edge zone and causes cracks. Thus, a higher feed per tooth also fundamentally affects the growth of parameters Ra and Rz (Pinkowski et al. 2018b). In addition, the fuzziness of the surface grows, and visible, larger "marks" are formed after the cycloid movement of the cutting edge. The higher feed speed loads the cutting edge, causing it to vibrate and therefore form roughness. Also, as the feed speed increases, the parameters Rz and Rk increase linearly (Smajic and Jovanovic, 2021). On the other hand, with a

decrease in feed speed, from a technological point of view, there is an increase in temperatures in the cutting zone, which negatively affects the tool life and increases its blunting (Igaz et al. 2019). The revolutions, as another important parameter of milling, also affects the quality of the surface created. With their increase, the feed per tooth decreases, and surface irregularities also decrease (Pelit et al. 2021). During milling, the amount of material that is milled at one time is reduced, reducing the load on the cutting edge. From the relationship (Ettelt and Gittel, 2004) it follows that if a higher speed leads to a decrease in feed per tooth, then the height of the marks created by the cutting edge is lower (with a constant diameter of the tool). This phenomenon can often be observed even with the naked eye.

For the above reasons, it is therefore essential to deal with the optimization of milling parameters with regard to the quality of the created surface (Atanasov et al. 2023b; Wei et al. 2021). In the presented experiment, the influence of basic milling parameters will be measured and evaluated on beech wood. Beech wood is a material commonly used for furniture production. By (Sedliačiková and Moresová, 2022) Slovak consumers prefer to buy solid furniture made of beech wood. That is why beech timber is a key raw material for the carpentry industry. However, in terms of optimizing CNC milling parameters, it is a complicated type of wood, due to different properties over the width of the sawn timber. The frequent presence of a false heartwood also affects the amount of surface roughness. The false heartwood is often unavoidable in production practice (in terms of blank yield). By (Michalec et al. 2022) the proportion of false heartwood in the cross-section may be up to 83 %. The average share values range from 30% to 4O%. By (Dzurenda et al. 2023) is a false heartwood chemically characterized by a higher content of lignin and hemicellulose compared to mature wood and sapwood. Of the physical properties, the false heartwood is characterized by a higher density compared to the zone of mature wood and sapwood (Dzurenda et al. 2023). On the contrary, the sapwood zone has the lowest density (Dzurenda et al. 2023). The above research shows that the density of beech wood decreases from the center of the trunk to the perimeter, which will also affect other properties, including surface irregularities after CNC milling. The same trend follows from (Dudiak, 2023). At the same time, the work shows that there is no statistically significant difference in density between mature wood and false heartwood. For sapwood, on the other hand, a significantly lower density was measured.

The aim of the present paper is to quantify the surface roughness after milling by a spiral shank cutter at a CNC 5 axis machining center. In the experiment, the values of the parameters Ra, Rz, Rv, Rp, Rsk and Rku measured in the zone of false heartwood, mature wood and sapwood within beech wood will be compared. In addition to the influence of these zones, it will be investigated how the changing values of feed speed and revolutions affect the final quality of the milled surface, which is defined by the roughness profile.

MATERIALS AND METHODS
Sample preparation
Beech wood (*Fagus sylvatica* L.) was used to produce 24 pieces of samples. Each sample was manipulated from the boards to include the false heartwood zone, the mature wood zone and sapwood zone. The selection of the false heartwood in the boards was carried out by visual assessment, since the false heartwood has a significantly darker colour (Dzurenda and Dudiak, 2023). The sapwood zone was cut out 1 centimeter behind the curves with bark (the perimeter of the trunk). The zone of mature wood was visually assessed on the boards in the wet state (Fig. 1). Partial colour differences between the mature wood and the sapwood zone were preserved even after the drying process. From boards of quality class I. samples measuring $20 \times 70 \times 400$ mm (thickness × width × length) were sawed and later milled. The width and length of the samples were determined depending on the design of the mechanical clamps and the design of the CNC machining center. The samples were dried to a moisture content of 8 to 10%, which corresponds to the moisture content of the wood achieved indoors (and thus the production conditions are dimensioned accordingly). All samples were subsequently machined on a planer and thickness milling machine to nominal thickness.

Figure 1: Sapwood, mature wood, and false heartwood zone in beech wood

CNC milling

For research of the influence of milling process on the quality of the created surface, the 5-axis CNC machining center SCM Tech Z5 was used. All samples were evenly clamped with two mechanical clamps. This clamping method ensured minimization of vibrations in the milling process. For milling, a finishing spiral shank cutter Klein T143 (Sistemi S.r.l., Pesaro, Italy) with a positive helix (up-cut spiral, positive) and monolithic tungsten carbide was used. The diameter of the cutter was 20 mm, and the total number of teeth was 3. The tool has been clamped in a GM 300 HSK 63F hydraulic chucks (Gühring KG, Albstadt, Germany) with high alignment, which can be used up to a maximum speed of 24,000 rpm. The type of milling was finishing, which is characterized by a low value of the thickness of the removed layer (in this case, ae = 1 mm). In the first step, the tool milled a layer 1 mm thick from the edge area, removing irregularities and dales (torn fibers) from the thickness milling process from the surface. In the second step, the tool again milled a layer 1 mm thick from the edge area, creating the final surface quality. It was then subjected to roughness measurements using a digital microscope. Milling was carried out at varying revolutions (12,000 rpm and 18,000 rpm) and at varying feed speeds (10 m·min⁻¹ and 14 m·min⁻¹). Higher values of revolutions and feed speed were set as optimal, recommended by the tool manufacture. The lower values were chosen as technologically minimum.

Surface roughness measurement

The Keyence VHX-7000 digital microscope (Keyence Corporation, Osaka, Japan) was used to measure surface roughness. In the first step, a digital image of the milled surface of beech wood was created. The milled edge of the samples was scanned in five, evenly spaced places. The purpose of evenly distributing scans (and therefore the measurement) was to capture the average value of surface roughness. Image scanning was performed at 100× magnification and using a VH-Z100R lens (Keyence Corporation, Osaka, Japan). The following conditions were chosen for the actual measurement of roughness parameters: S-filter (λs) = 8 μm, L-filter (λc) = 2.5 mm. The following parameters were subsequently evaluated from the filtered roughness profile: Ra, Rz, Rv, Rsk and Rku. The parameter Ra was chosen as a stable parameter, most commonly used in surface roughness measuring. However, its disadvantage is that several profiles with different shapes or heights of irregularities can have the same Ra value. Therefore, for a more detailed specification of the maximum heights in different zones of beech wood, the amplitude parameters Rz, Rp and Rv were also investigated. To find out the shape of the profile and the ratio of the profile hills and dales, the parameter Rsk and Rku was used.

Hardness measurement

Surface hardness was also considered to support the results of surface roughness measurements. The hardness was measured using a portable Leeb hardness tester ISH-SPHA (INSIZE Czech s.r.o., Brno, Czech Republic) with an external type D probe. Hardness results are reported in Brinell units (HB).

RESULTS AND DISCUSSION

The basic set of 238 measurements was statistically evaluated by the program STATISTICA 14 (TIBCO Software Inc., Palo Alto, California). In the first step, the outliers were removed from the set and the measurements were repeated. Subsequently, the set of measurements was evaluated with descriptive statistics.

Table 1: Values of individual measured parameters of roughness and hardness in the zone of sapwood, mature wood, and false heartwood. Values in parentheses represent standard deviation

Wood Zone	Ra [µm]	Rz [µm]	Rv [µm]	Rp [µm]	Rsk [µm]	Rku [µm]	Hardness [HB]
Sapwood	7,28	34,80	23,62	11,18	-1,29	3,20	56,40
	(1,14)	(6,24)	(4,63)	(2,53)	(0,19)	(0,59)	(9,74)
False Heartwood	6,25	27,65	18,46	9,19	-1,19	2,78	66,66
	(1,06)	(5,19)	(3,88)	(1,77)	(0,17)	(0,43)	(9,98)
Mature wood	6,05	28,20	19,17	9,04	-1,26	3,01	59,78
	(1,03)	(5,50)	(4,35)	(1,61)	(0,22)	(0,58)	(8,41)

Based on the data from Table 1, it can be argued that the highest roughness values after CNC milling were measured in the sapwood zone. This is confirmed by all amplitude parameters. The lowest surface roughness values (i.e. the highest quality after milling) were measured in the zone of mature wood and false heartwood. There is no statistically significant difference between the roughness in the zone of mature wood and false heartwood after milling. The measured values may have been due to the higher density of false heartwood and mature wood, between which there is also no statistically significant difference (Dudiak, 2023). Since there are no significant differences in anatomical structure between the three measured zones of beech wood, higher density may be the cause of a smoother surface after milling (Kang et al. 2023). In less dense types of wood, so-called protruded fibres (fuzziness of the surface) are often formed after machining (Landry et al. 2013). In this case, this may be the cause of a higher maximum height Rz in less dense sapwood. At the same time, the Rsk parameter shows that the sapwood zone is characterized mainly by dales of the profile, which is confirmed by the high Rv value. The sawood zone, as a less dense part of beech wood, thus shows the same tendencies (formation of fuzziness of the surface and dales after torn fibers) as wood species with lower density. The same surface property has been confirmed in the mature wood zone, with no statistically significant difference between the two zones in terms of Rsk. As part of the experiment, the hardness of wood was also measured according to Brinell, with a statistically significant difference between individual zones. At the same time, from the hardness values, it can be argued that they have the same approximately development as the parameter Rsk. The hardest zone of beech wood according to Table 1 is the false heartwood . The second hardest is the zone of mature wood. As the hardness decreases gradually, the Rsk parameter also decreases, which may indicate a greater tendency to torn fibers from the surface during milling. At the same time, the Rv parameter also increases, which again proves the presence of dales of the surface (this also results in an increase in the maximum height Rz). Thus, Table 1 shows that as the hardness increases, the roughness tends to decrease. On the other hand, with decreasing hardness, significant dales appear on the surface after torn fibers. However, for a more accurate determination of this dependence, it is necessary to measure the hardness and roughness on a larger number of samples. At the same time, hardness has a similar tendency to decrease towards the peripheral parts of wood, as well as density according to (Dzurenda et al. 2023).

The measured set was then evaluated using inductive statistics methods. Of these, the two-factor variance analysis ANOVA was chosen. In this method, the effect of changing tool revolutions and changing feed speed on roughness formation in sapwood and mature wood zone and false heartwood zone was verified. The ANOVA results showed that the change in revolutions does not cause statistically significant changes in individual zones for any of the measured roughness parameters. Conversely, the change in feed speed caused statistically significant differences in the mature wood zone and the false heartwood zone for the parameters Ra (p = 0.039), Rz (p = 0.002), Rp (p = 0.049) and Rv (p = 0.002). No statistically significant differences were found for the other roughness parameters measured.

Figure 2 shows that in the sapwood zone, the change in the value of the feed speed did not cause a statistically significant difference in roughness. However, in the false heartwood and mature wood, the

roughness values also increased with the increase in feed speed. There was an increase in the parameter Ra, as well as an increase in Rz parameter (due to the growth of Rp and Rv). This increase is consistent with the theory of the influence of feed speed on surface roughness. Subsequent microscopic analysis showed that at a feed speed of 14 m·min^{-1}, marks characteristic of rotary tools were formed on the surface. These were the reason why the roughness parameters increased. In the zone of the false heartwood , microscopic analysis showed the presence of torn fibers, as a result of which the roughness parameters increased again. At the same time, the graph shows that there is no statistically significant difference between the surface quality in the false heartwood zone and mature wood.
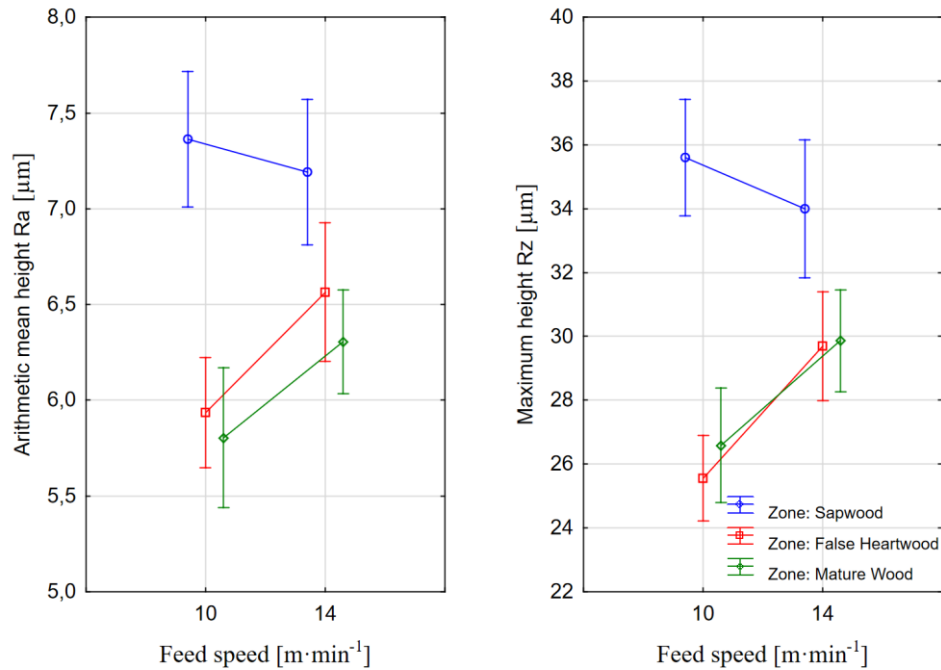

Figure 2: The effect of changing feed speed on roughness parameters Ra and Rz in three wood zones: sapwood, mature wood, false heartwood

CONCLUSION

The aim of the presented research was to quantify surface roughness after milling on a CNC 5-axis machining center in three zones of beech wood: sapwood, mature wood, and false heartwood. The effects of revolutions change and feed speed as the two main milling parameters on the resulting surface roughness were also evaluated. The methodology was also supplemented by the measurement of hardness in the zone of sapwood, mature wood, and false heartwood. The evaluated measurements show the following:

- The lowest surface quality after milling was created in the sapwood zone. From the results of research of other authors, it follows that this zone of beech wood has the lowest density (perimeter of the trunk). At the same time, hardness measurements showed that sapwood is the softest, which could significantly support the formation of not only fuzziness of the surface, but also torn fibres.
- The highest quality in terms of average values came out in the zone of mature wood. However, analysis of variances showed that there was no statistically significant difference between the false heartwood and mature wood zones. This statement correlates with the other authors' claim that there is no statistically significant difference in density between the two zones.
- The highest hardness was measured in the false heartwood zone. At the same time, there is a statistically significant difference in hardness between all three measured zones. Simultaneously, the highest hardness of the false heartwood caused that at this point the rate of formation of dales on the surface was the lowest (results from measurements of the parameter Rsk).
- Of the optimized parameters, only the change in feed speed had statistical significance in the three measured zones. The revolutions in the case of this experiment did not cause a significant change in roughness parameters.
- In a more detailed two-factor analysis, it was found that statistically significant roughness changes were caused by the feed speed in the zone of false heartwood and mature wood. With increasing feed speed, the surface roughness also increased significantly, which is consistent with the theory of woodworking. The increasing feed speed created larger marks on the surface, typical of rotary tools with cycloid movement of the cutting edge.

REFERENCES

Adamčík L, Kminiak R, Schmidtová J (2023) Measurement of the roughness of the sanded surface of beech wood with the profile measurement software of the keyence VHX-7000 microscope. In: Acta Facultatis Xylologiae Zvolen 65, pp 73–85. https://doi.org/10.17423/afx.2023.65.1.07

Atanasov V, Kovatchev G, Todorov T (2023a) Influence of Main Parameters of the Milling Process on the Roughness when Processing Solid Wood of meranti. In: Pro Ligno 19, pp 3–10.

Atanasov V, Kovatchev G, Todorov T (2023b) Study of the Influence of Basic Process Parameters on the Roughness of Surfaces During Milling of Scots Pine Wood. In: Acta Facultatis Xylologiae Zvolen 65, pp 89–98.

Bendikiene R, Keturakis G, (2016) The effect of tool wear and planning parameters on birch wood surface roughness. In: Wood research 61, pp 791–798.

Çakiroğlu E O, Demir A, Aydin İ (2019) Determination of the Optimum Feed Rate and Spindle Speed Depending on the Surface Roughness of Some Wood Species Processed with CNC Machine. In: Journal of Anatolian Environmental and Animal Sciences 4, pp 598–601. https://doi.org/10.35229/jaes.635310

Dudiak M (2023) Density of Beech (Fagus sylvatica L.) Wood through a Cross-section of the Trunk. In: Acta Facultatis Xylologiae Zvolen 65, pp 5–12.

Dzurenda L, Dudiak M (2023) Colourfulness of European beech wood with a round false heartwood in the color space CIE L*a*b*. In: Annals of WULS, Forestry and Wood Technology 122, pp 82–88. https://doi.org/10.5604/01.3001.0053.8671

Dzurenda L, Dudiak M, Kučerová V (2023) Differences in Some Physical and Chemical Properties of Beechwood with False Heartwood, Mature Wood and Sapwood. In: Forests 14, pp 1123. https://doi.org/10.3390/f14061123

Ettelt B, Gittel H.J (2004) Sägen, Fräsen, Hobeln, Bohren: Die Spanung von Holz und ihre Werkzeuge Die Spanung von Holz und ihre Werkzeuge, In: Sägen, Fräsen, Hobeln, Bohren: Die Spanung von Holz und ihre Werkzeuge Die Spanung von Holz und ihre Werkzeuge. DRW-Verlag.

Gochev Z (2018) Examination the Process of Longitudinal Solid Wood Profile milling. Part II: Influence of the Revolution Frequency and Feed Rate on the Roughness of the Treated Surfaces 1, pp 48–54.

Igaz R, Kminiak R, Krišťák Ľ, Němec M, Gergeľ T (2019) Methodology of Temperature Monitoring in the Process of CNC Machining of Solid Wood. In: Sustainability 11, pp 95. https://doi.org/10.3390/su11010095

Kang C W, Hashitsume K, Jang E, Kolya H (2023) Relationship Between Wood Anatomical Features and Surface Roughness Characteristics. In: Wood Research 68, pp 455–464. https://doi.org/10.37763/wr.1336-4561/68.3.455464

Landry V, Blanchet P, Cormier L M (2013) Water-Based and Solvent-Based Stains: Impact on the Grain Raising in Yellow Birch. In: BioResources 8, pp 1997–2009. https://doi.org/10.15376/biores.8.2.1997-2009

Michalec K, Wasik R, Gach M (2022) The occurrence and size of false heartwood in beech timber. Drewno. Prace Naukowe. Doniesienia. Komunikaty 65. https://doi.org/10.12841/wood.1644-3985.385.08

Pelit H, Korkmaz M, Budakçı M (2021) Surface roughness of thermally treated wood cut with different parameters in CNC router machine. In: BioResources 16, pp 5133–5147. https://doi.org/10.15376/biores.16.3.5133-5147

Pinkowski G, Szymański W, Krauss A, Stefanowski S (2018a) Effect of Sharpness Angle and Feeding Speed on the Surface Roughness during Milling of Various Wood Species. In BioResources 13, pp 6952–6962.

Pinkowski G, Szymański W, Krauss A, Stefanowski S (2018b) The effect of the feed speed and rotation speed of plane milling on the surface roughness of beech wood. In: Annals of Warsaw University of Life Sciences - SGGW 103, pp 5–12.

Sedliačiková M, Moresová M (2022) Are Consumers Interested in Colored Beech Wood and Furniture Products? In: Forests 13, pp 1470. https://doi.org/10.3390/f13091470

Singer H, Özşahin Ş (2022) Prioritization of factors affecting surface roughness of wood and wood-based materials in CNC machining: a fuzzy analytic hierarchy process model. In: Wood Material Science & Engineering 17, pp 63–71. https://doi.org/10.1080/17480272.2020.1778079

Smajic S, Jovanovic J (2021) Influence of Different Machining on the Roughness of Oak Wood. In: Bulletin of the Transilvania University of Brasov 14(63) No. 1-2021, pp 101–108. https://doi.org/10.31926/but.fwiafe.2021.14.63.1.9

Smajic S, Jovanovic J (2020) Study of the influence factors affecting surface roughness of oak and beech samples during machining with peripheral milling. https://doi.org/10.13140/RG.2.2.22050.66249

Wei W, Cong R, Xue T, Abraham A D, Yang C (2021) Surface roughness and chip morphology of wood-plastic composites manufactured via high-speed milling. In: BioResources 16, pp 5733–5745. https://doi.org/10.15376/biores.16.3.5733-5745

Yang C, Ma Y, Liu T, Ding Y, Qu W (2023) Experimental Study of Surface Roughness of Pine Wood by High-Speed Milling. In: Forests 14, pp 1275. https://doi.org/10.3390/f14061275

Session V
Hardwoods in composites and engineered materials

Developing Laminated Strand Lumber (LSL) based on underutilized Hungarian wood species

László Bejó[1], Tibor Alpár[1], Ahmed Altaher Omer Ahmed[1*]

[1] Institute of Wood Technology and Technical Sciences, University of Sopron, 9400 Sopron, Hungary

E-mail: bejo.laszlo@uni-sopron.hu; Altaher.Omer.Ahmed.Ahmed@phd.uni-sopron.hu

Keywords: Hungarian hardwood, the Carpathian Basin, raw materials, Laminated Strand Lumber

ABSTRACT

The demand for wood-based construction materials is increasing, and the current supply of softwood from Austria and Germany is likely to run out in the coming years. At the current rate of production, the supply of traditionally used softwood raw materials is unsustainable. In addition, the warming climate is making it more difficult to grow Softwood species such as pines, which are one of the most important raw materials for the wood industry. As a result, there is a need to find alternative tree species that can adapt to the changing climate, and whose technical properties are suitable for use in construction. One potential source of alternative wood is hardwood species from the Carpathian Basin. This study, which is the part of the ERDOLAB (Forest Lab) research project, aims to develop Laminated Strand Lumber (LSL) from underutilized Hungarian hardwood species for use in the construction industry. Several LSL panels were manufactured using poplar strands and MDI adhesive, with dimensions 340x340x35 mm, and 600 to 650 kg/m3 in density. Tests included bending and internal bond strength, as well as water absorption and thickness swelling.

Test results show that the experimental LSL meets most of the requirements of the standard for structural building materials, with the exception of tensile strength perpendicular to the plane, which is slightly lower than the required standard. However, all other properties of LSL meet or exceed the requirements of the standard. Therefore, LSL can be considered a suitable material for structural applications with the exception of applications where high tensile strength perpendicular to the plane is required.

INTRODUCTION

In recent years, there has been a growing interest in eco-friendly and long-lasting alternatives to conventional lumber, growing demand for large-section wood is straining traditional resources, and climate change threatens long-term viability. Traditionally, engineered wood products like LVL (Laminated Veneer Lumber) relied on softwoods like Scots pine Aro et al. (2017). However, there's increasing interest in exploring hardwoods for LVL production as well. Understanding the properties of different wood species is crucial to fully unlocking LSL's potential.

One such option is laminated strand lumber (LSL), a composite material made by bonding wood strands with adhesives. LSL's high strength-to-weight ratio and use of renewable resources make it a promising substitute.

Notably, a project at the University of Sopron in Hungary is currently investigating "The Role of Forest-Based Bioeconomy in Climate Change Mitigation through Carbon Storage and Material Substitution" European Commission (2021). This project aligns with the ongoing effort to discover innovative methods of reducing the greenhouse effect in the environment. LSL is a significant area of investigation within this project, as researchers explore ways to safeguard the environment by substituting conventional non-biodegradable structural materials with sustainable options.

LSL (Laminated Strand Lumber) is generally considered an advancement of OSB (Oriented Strand Board). However, LSL strands are differentiated by their length, measuring 12 inches (304.8 mm), which is significantly longer than those used in OSB production. Unlike OSB, LSL typically lacks distinct "hourglass" shapes or staining, making it a preferable choice for structural framing applications. When compared to PSL (Parallel Strand Lumber), glulam (glued laminated timber), and LVL (Laminated Veneer Lumber), LSL exhibits lower shear strength. This characteristic makes it more suitable for use in shorter framed structures SFS Group USA (2023).

Due to its exceptional strength, durability, and affordability, Laminated Strand Lumber (LSL) has emerged as a highly promising product, rapidly gaining popularity within the construction industry. LSL is manufactured by compressing thin strips of wood with a resin binder, resulting in the formation of a sturdy lumber with substantial thickness Liu, J., et al. (2008). This manufacturing process yields a consistently robust and uniform material, making it ideal for a wide range of building applications such as framing, beams, and columns Asdrubali, F., et al. (2017).

In Hungary, several hardwood species hold promise for laminated strand lumber (LSL) manufacture due to their desirable mechanical attributes. These species include Turkey oak, hornbeam, beech, and domestic poplars. Their advantages lie in high stiffness, strength, and dimensional stability in Hungary and other European countries Monlar Sandor (2002). This accessibility makes them a sustainable and cost-effective option for LSL production.

LSL offers several advantages over traditional hardwoods like Hungarian Turkey oak, hornbeam, beech, and even domestic poplars. Due to its consistent reliability, longevity, and performance, LSL emerges as a compelling choice for numerous construction applications.

Research has shown promising results for the mechanical, physical, thermal, and morphological properties of LSL derived from various hardwood species. This suggests that LSL has the potential to cater to the demands of diverse industries, including construction, furniture, and packaging.

Furthermore, manufacturing LSL from domestically available hardwoods could contribute to sustainable forest management practices and reduce reliance on imported wood. However, further research is necessary to fully understand the qualities of LSL made from these specific wood types and to optimize the manufacturing process.

Emphasizes LSL's potential as a sustainable and versatile resource for the timber sector and highlights the potential for economic and environmental benefits using locally sourced timber species. Hasan, KM Faridul, et al. (2023).

The study proposes a sustainable solution: Laminated Strand Lumber (LSL) made from domestic poplar trees in Hungary. While poplar itself isn't suitable for construction, LSL production can transform this abundant resource into a high-value composite lumber with properties comparable to conventional lumber. This research investigates the methodology for creating poplar-based LSL using various glue densities and assesses its potential as a sustainable alternative to traditional lumber sources.

MATERIALS AND METHODS

Materials and methods for fabricating and evaluating laminated strand lumber (LSL) panels using a combination of poplar and Scots pine strands. The primary objective is to optimize pressing parameters for LSL production using a laboratory press. This involves developing a process for creating LSL panels from pre-dried domestic wood strands with the goal of achieving optimal pressing parameters. The focus lies on establishing a method for LSL production that relies entirely on readily available domestic materials, promoting resource efficiency and potentially reducing reliance on imports.

Materials:
Strands: average dimension 120 x 30 mm, moisture content 4-5%, dominated by poplar with some Scots pine and PMDI resin and paraffin emulsion (obtained from Swiss-Krono, Vásárosnamény Hungary Kft.)**.**
Caul plates: Metal plates for even pressure distribution during pressing. Spacer rods: 30 mm thick metal rods to control panel thickness.

Process:
The process consisted of several key steps:
Strand Measurement and Mixing: Strands were measured for targeted density and then weighed.
Resin and paraffin emulsion were mixed in a lab blender while the strands were continuously agitated. To compensate for potential adhesive loss, slightly more resin (10% extra) was used.
Layup Formation: Resin-coated strands were spread in a 40x40 cm box, ensuring their long axis aligned in one direction. The forming box was then removed, a second caul plate placed on top, and the entire layup transferred to the preheated press (figure 1).
Hot Pressing: A three-stage pressing cycle (figure 2) with gradually decreasing pressure was applied to ensure uniform bonding throughout the panel.

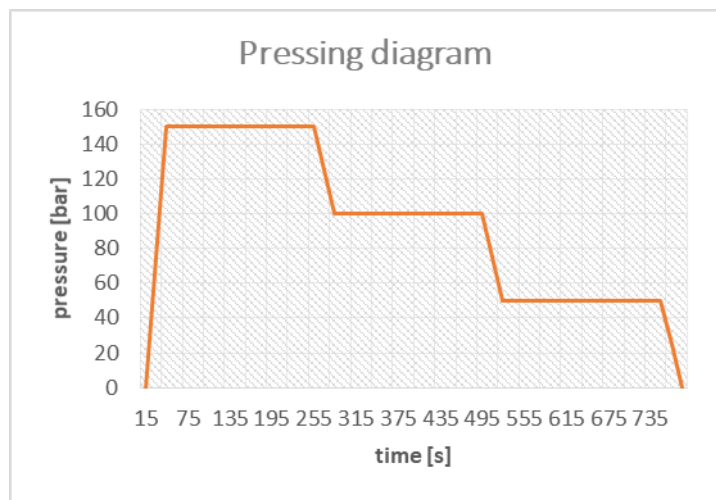*Figure 1: LSL panel formation and the produced panel*

Figure 2: Pressing diagram

After establishing the appropriate pressing time, first the resin content, then the panel density was optimised. This included creating six experimental panels, as shown in Table 1.

Table 1:

Pressing parameters	LSL Panels							
	A	B	C	D	E	F	R1	R2
Temperature (°C)	200	200	200	200	200	200	200	200
Resin content (%)	2.9	3.4	3.9	3.4	3.4	3.4	3.4	3.4
Paraffin content (%)	1.2	1.2	1.2	1.2	1.2	1.2	1.2	1.2
Tartget density (kg/m3)	600	600	600	500	550	650	600	600
Total pressing time (s)	750	750	750	750	750	750	900	900
t1 (s)	250	250	250	250	250	250	180	180
t2 (s)	250	250	250	250	250	250	180	180
t3 (s)	250	250	250	250	250	250	540	540

Cooling and Sample Preparation: After pressing, the panels cooled and trimmed to a standard size (340x340 mm) and machined into test specimens according to specific dimensions (Figure 3) for tensile strength, water absorption, and swelling tests (50x50 mm) and bending strength tests (320x15 mm). Evaluate Specimen Conditioning: The prepared samples were conditioned at 65% relative humidity and 20°C for 72 hours before testing.
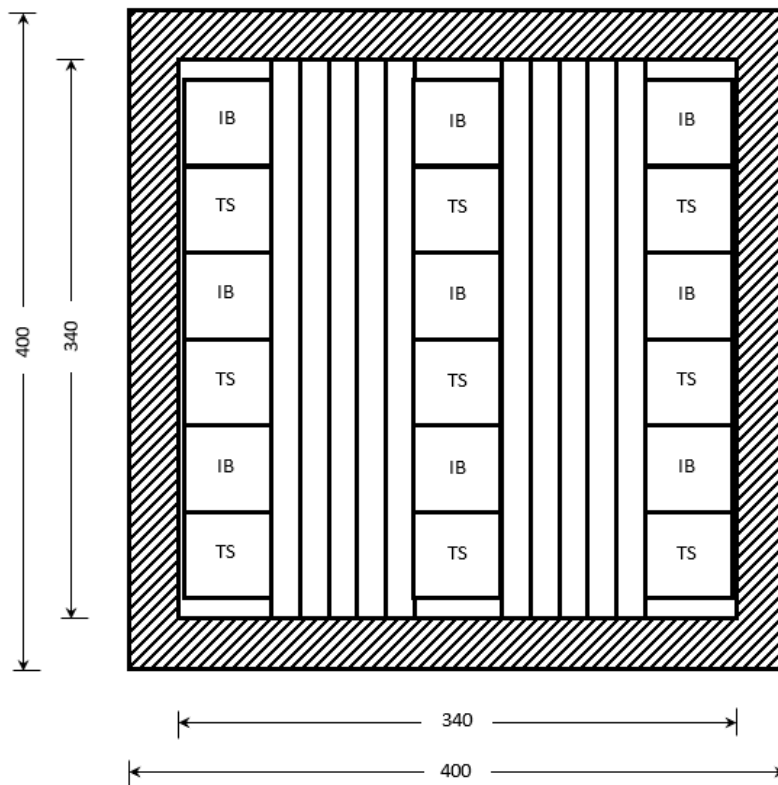
Testing Standards

Figure 3: Cutting pattern for the Bending (long vertical strips), Internal Bond (IB) and Thickness Swelling (TS) specimens produced from the 400 x 400 mm panels

Due to a lack of specific LSL standards, testing methods followed MSZ EN standards for load-bearing wood panels suitable for dry environments (MSZ EN 310, MSZ EN 317, MSZ EN 319). An INSTRON 5566 machine used for material testing according to MSZ EN 325 specifications for wood-based panel test specimen dimensions.

Panel evaluation included measuring the bending strength (MOR) according to MSZ EN 310, Internal Bond strength (IB) according the MSZ EN 319, and water absorption/thickness swelling according to MSZ EN 317 (see Figure 4). Density also measured using the bending specimens after failure, by measuring the weight and calculating the volume based on specimen size.
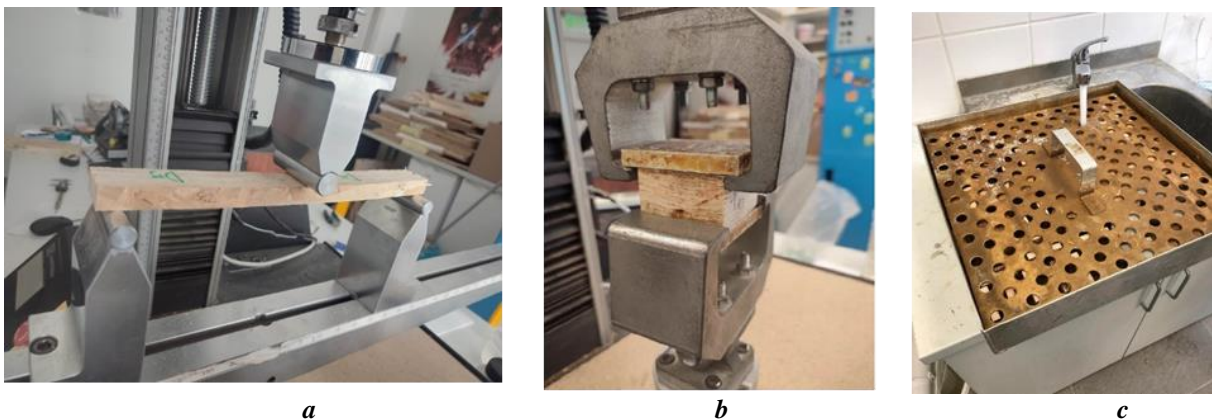

a   *b*   *c*

Figure 4: Bending (a), Internal Bond (b) and Thickness Swelling/Water absorption (c) tests

RESULTS AND DISCUSSION

Board Strength: A positive correlation observed between board strength and both adhesive content and density. The highest MOR values achieved with a target density of 600 kg/m³ and an adhesive content

of 3.4%. However, the internal bond (IB) strength remained relatively low at this level (0.16 N/mm² on average). Therefore, a target density of 650 kg/m³ was determined to be a safer option for further testing. Moisture Resistance: Thickness swelling decreased with increasing adhesive content and surprisingly, also with increasing density. Conversely, water absorption tended to increase with both higher adhesive content and density.

Replication Experiments: The results from the replicated experiments (panels R1 & R2) were generally consistent with those of the original panel (panel F). There were slight variations: MOR values were slightly lower, while IB strength was higher in the replicated panels. Thickness swelling and water absorption were also comparable, except for panel R2, which exhibited significantly lower thickness swelling compared to panels F and R1.

Pressing Time: The replicated panels utilized a longer pressing time compared to the original panel. There were no significant improvements in panel properties observed with the increased pressing time, suggesting that the original pressing time (750 seconds) is sufficient.
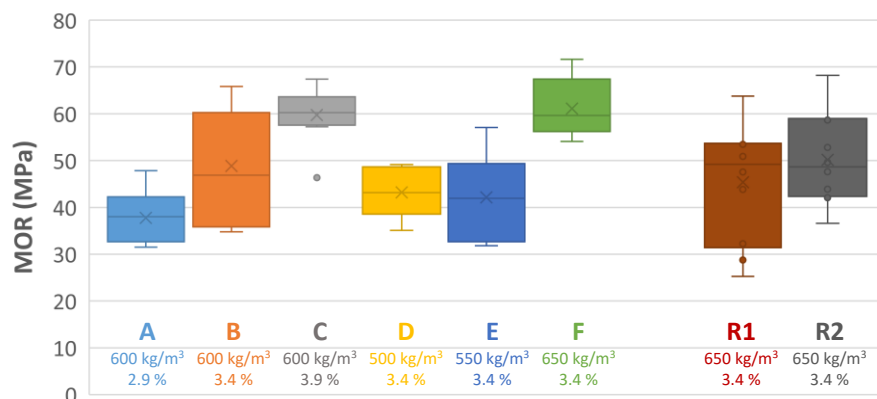

Figure 5: show the results of the MOR for all measured panels

Discussion

The target density of 650 kg/m³ (with actual densities ranging from 650 to 750 kg/m³ or higher) and an adhesive content of 3.4% identified as the most promising combination for further experimentation. However, achieving consistent density distribution throughout the panels proved challenging due to limitations of the small-scale laboratory layup process.

Industrial production methods expected to yield better results, potentially allowing for successful utilization of lower density panels.

The average Modulus of Rupture (MOR) of panels F, R1, and R2 (around 52 N/mm²) surpasses the minimum requirement for C24 solid wood structural lumber (the most common grade in Hungary). This indicates that the LSL material even at this early stage demonstrates promising qualities. Furthermore, LSL expected to outperform solid wood by an even greater margin, potentially reaching characteristic strength values as high as 40 N/mm².

The high standard deviation (11.7 N/mm²) observed in the MOR values is attributable to the challenges of maintaining consistent horizontal density distribution and strand orientation within the panels in a small-scale laboratory setting.

Industrial production anticipated to produce panels with similar average strength but with lower variation, leading to higher characteristic strength values.

CONCLUSIONS

The preliminary experiments demonstrate that panels manufactured with the established parameters for panel F (target density of 650 kg/m3 and total pressing time of 750 seconds, detailed in Table 1) exhibit very good average values for Modulus of Rupture (MOR), Internal Bond (IB) strength, Thickness Swelling, and Water Absorption. These results indicate the promising potential of poplar LSL for use in Hungary.

However, it is important to note that the laboratory experiments produced high variations in the results. This is likely due to limitations in controlling factors like density distribution and strand orientation within the smaller test panels.

REFERENCES

Aro MD, Wang X, McDonald DE, Begel M (2017) Tensile strength of thermally modifed laminated strand lumber and laminated veneer lumber. Wood Mat Sci Eng 12(4):228–235

Commission TE (2021) The role of the forest-based bioeconomy in mitigating climate change through carbon storage and material substitution. European Commission. Retrieved 17th May from https://publications.jrc.ec.europa.eu/repository/bitstream/JRC12   4374/brief_on_role_of_forest-based_bioeconomy_in_mitig ating_cc_online.pdf

SFS Group USA I (2023) Guide to Composite Lumber — OSB vs. LSL vs. LVL vs. PSL vs. Glulam. SFS Group. Retrieved 17th May from https://us.sfs.com/learn-more/composite-lumber-comparisons

Liu W, Yang H, Dong F, Jiang D (2008) Experimental study on f exural behavior of glulam and laminated veneer lumber beams. Modern Bamboo Structures. CRC Press, New York, pp 171–182

Asdrubali F, Ferracuti B, Lombardi L, Guattari C, Evangelisti L, Grazieschi G (2017) A review of structural, thermo-physical, acoustical, and environmental properties of wooden materials for building applications. Build Environ 114:307–332

Molnar Sandor BM (2002) Turkey Oak, Hornbeam, Beech, and Domestic Poplar. In K. Ildiko (Ed.), Wood species of Hungary. Szaktudas Kiado Haz Rt

Hasan, K. F., Bak, M., Ahmed, A. A. O., Garab, J., Horváth, P. G., Bejó, L., & Alpár, T. (2023). Laminated strand lumber (LSL) potential of Hungarian and Central European hardwoods: a review. European Journal of Wood and Wood Products, 1-20.

Feasibility study on manufacturing finger-jointed structural timber using *Eucalyptus grandis* wood

Adefemi Adebisi Alade[1*], Hannes Stolze[1], Coenraad Brand Wessels[2], Holger Militz[1]

[1] Georg-August-University Göttingen, Department of Wood Biology and Wood Products, Büsgenweg 4, Göttingen, Germany, 37077
[2] Stellenbosch University, Department of Forest and Wood Science, Private bag X1, Matieland, Stellenbosch, South Africa, 7602

E-mail: adefemi-adebisi.alade@forst.uni-goettingen.de; hannes.stolze@uni-goettingen.de; cbw@sun.ac.za; hmilitz@gwdg.de

Keywords: Eucalyptus, engineered wood product, finger jointing technology, hardwood, structural timber product, wood preservation

ABSTRACT

Hardwood utilization as alternative to declining softwood for structural timber products continues to attract global interest at exploiting the material potentials of hardwood for manufacturing engineered wood products. Recent attempts at refocusing utilization of eucalyptus wood have led to significant progress, mostly face-bonding of *Eucalyptus grandis* wood including natural and preservative-treated, to manufacture glued laminated and cross laminated timbers. Finger jointing technology enables the development of longer span board while utilizing shorter dimension woods. Thus, finger jointing could enhance emerging use of *E. grandis* wood for structural timber product but still requires more exploratory studies to establish this potential. Therefore, this study focused on demonstrating the feasibility of finger jointing *E. grandis* wood, including samples pre-impregnated with copper azole (CA) wood preservative. Phenol resorcinol formaldehyde (PRF) and polyurethane (PUR) adhesives were assessed in bonding the finger joints. Mechanical properties that include moduli of elasticity (MOE) and rupture (MOR) of the finger-jointed *E. grandis* boards were compared to those of its continuous solid wood (CSW), i.e., without finger jointing. The mechanical properties were determined via four-point bending test. Regardless of CA-impregnation and adhesive system, there were no significant differences ($p > 0.05$) between the mean MOEs of the *E. grandis* CSW (13243 MPa – 13975 MPa) and the finger-jointed laminates (13080 MPa – 14246 MPa). Likewise, CA-impregnation had no significant effect ($p > 0.05$) on the MORs of the *E. grandis* CSW (81 MPa – 84 MPa) and finger-jointed boards (60 MPa – 67 MPa). Finger jointing had a significant effect ($p < 0.05$) on the MOR. However, the finger-jointed *E. grandis* boards attained between 74% – 83% MOR of the CSW. The adhesive systems used had no significant effect ($p > 0.05$) on the MOE and MOR of the finger-jointed *E. grandis* boards. In conclusion, both CA-impregnated and untreated *E. grandis* wood showed promising stiffness and strength properties in comparison to the CSWs. Thus, adopting finger jointing technology has the prospect of enhancing *E. grandis* wood utilization in manufacturing engineered timber products for structural purposes.

INTRODUCTION

Hardwood utilization as alternative to declining softwood for structural timber products continues to attract global interest at exploiting the material potentials of hardwood for manufacturing engineered wood products. Eucalyptus is the most abundant plantation hardwood genus worldwide (Wessels et al., 2020). Due to its poor natural durability against biodegradation and been highly prone to defects during mechanical processing, eucalyptus wood has predominantly been converted into pulps for paper making or used to generate energy (Alade et al., 2022a; Bockel et al., 2020; Wessels et al., 2020). Recent attempts at refocusing utilization of eucalyptus wood have led to significant progress, mostly face-bonding of *E. grandis* wood, in manufacturing engineered wood product such as cross laminated timber (Dugmore, 2018). *E. grandis* wood pre-impregnated with wood preservatives has also been successfully face-laminated using different adhesive systems (Alade et al., 2022a, 2022b, 2022c).

Finger jointing technology involves bonding of predefined finger profiles at wood end-grains to form longer-span boards that are suitable for structural applications. Thus, finger jointing could further enhance emerging use of *E. grandis* wood for structural timber products but still requires more exploratory studies to establish this potential. The wood of *E. grandis* has high swelling and shrinkage values, and during drying it tends to crack and warp. Severe levels of twisting and checking were reported in *E. grandis* lamellas finger-jointed in green (wet) state before drying to an equilibrium moisture content of 13% (Crafford and Wessels, 2016; Wessels et al., 2020). Hence, the objectives of this study were to (1) demonstrate the practicality of manufacturing finger-jointed boards using dry *E. grandis* wood, including samples pre-impregnated with copper azole (CA) wood preservative; and (2) evaluate the mechanical properties of the finger-jointed *E. grandis* boards in comparison to the continuous solid wood (CSW), i.e., without finger jointing.

MATERIALS AND METHODS
Wood, preservative chemical, and adhesive systems
E. grandis wood was sourced from Merensky Eucalyptus plantation in Limpopo province of South Africa. CA wood preservative chemical – Tanalith® E was provided by Lonza Wood Protection (trading as) Arch Wood Protection (SA) (Pty) Ltd., South Africa. Two-component phenol resorcinol formaldehyde adhesive (PRF - Prefere 4040 resin + Prefere 5839 hardener) was provided by Dynea®, Norway while one-component polyurethane adhesive (PUR - HENKEL PURBOND® HB S309) was provided by Henkel AG & CO. KGaA, Germany.

Preservative impregnation
400 mm long x 100 mm wide x 19 mm thick boards were obtained from planed *E. grandis* planks. The planed boards were climatized at 20 ±2 °C and 65 ±5% relative humidity to 12 ±1% moisture content. The *E. grandis* wood contained sapwood and heartwood in random proportions with average density of 560 kg/m^3. Planed *E. grandis* boards randomly selected for preservative impregnation were pressure-impregnated with 8% CA solution at 640 kPa for 1 h to obtain a mean CA retention of 3.75 kg/m^3. The CA-impregnated boards were re-conditioned in standard climate to 12 ±1% moisture content. *E. grandis* boards without CA impregnation were maintained as untreated reference.

Finger profiling, adhesive application, and finger-jointing
Vertically oriented finger joints with 15.65 mm finger length and 3.8 mm finger pitch were profiled at both ends of each CA-impregnated and untreated *E. grandis* board (Figure 1). A finger jointing line (Weinig Grecon GmbH & Co. KG, Alfeld/Leine, Germany) equipped with a finger profile cutter was used to cut the finger profiles at a feed rate of 24 m/min. After finger profiling, each board was transversely halved to produce a pair of approximately 200 mm long by 100 mm wide and 19 mm thick boards for jointing of the finger profiles. Resin to hardener ratio of 100:20 (w/w) was used for the PRF adhesive system. One-sided adhesive application was carried out manually at spread rates of 380 g/m^2 for PRF and 160 g/m^2 for PUR. Each paired finger profiles were jointed in the hydraulic press of the finger jointing line at 11 MPa press pressure and 5 s press duration. CA-impregnated and untreated woods without finger profiling and jointing were maintained as CSW references.
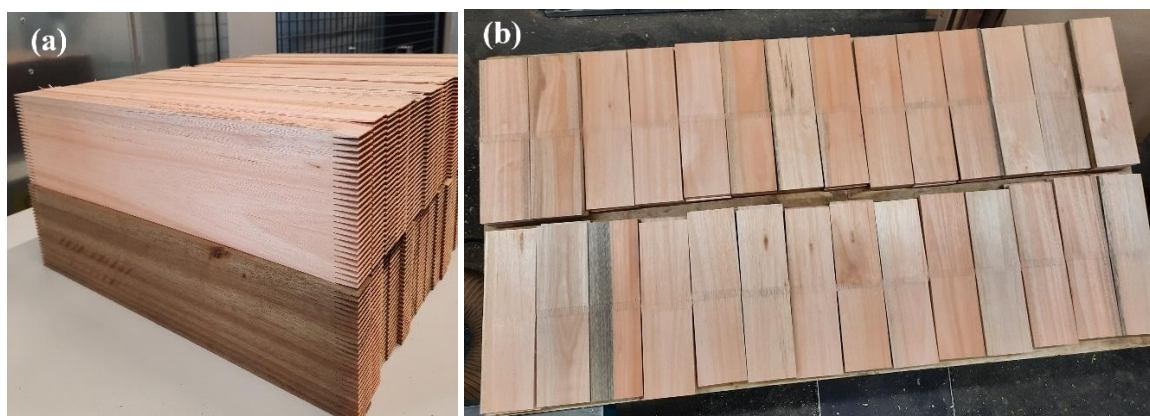

Figure 33: (a) Profiled finger joints at end grains of CA-impregnated (bottom) and untreated (top) E. grandis wood; (b) Samples of finger-jointed E. grandis boards

Four-point bending test

The bending moduli of elasticity and rupture was determined via four-point bending test at a test span of 18t (t= specimen thickness) and uniform loading rate of 5 mm/min. A universal testing machine, 100 kN capacity, equipped with VideoXtense extensometer (Zwick Roell GmbH & Co. KG, Ulm, Germany) was used to conduct the bending test. Four and nine replicates were tested for the untreated and CA-impregnated CSW, respectively. For each adhesive system, 15 to 17 replicates were tested for the finger-jointed CA-impregnated and untreated *E. grandis* boards.

RESULTS AND DISCUSSION

Bending modulus of elasticity

Bending modulus of elasticity (MOE) describes the stiffness of material within the linear-elastic range which is also known as the material's resistance to elastic deformation under applied bend stress. The results obtained showed that the stiffness of the finger-jointed *E. grandis* board is comparable to the stiffness of the CSW. Regardless of CA-impregnation and adhesive system, there were no significant differences between the mean MOEs of the *E. grandis* CSW (13243 MPa – 13975 MPa) and the finger-jointed boards (13080 MPa – 14246 MPa) (Figure 2). Statistically, the interaction and main effects of CA impregnation and finger jointing with either PRF or PUR adhesives on the modulus of elasticity of *E. grandis* wood were not significant (p > 0.05) (Table 1). In essence, both CA impregnation and finger jointing had no significant impacts on the bending stiffness property of *E. grandis* wood. Thus, both CA impregnated and untreated *E. grandis* woods are suitable for finger jointing to produce longer span boards without compromising the bending stiffness when compared to that of its CSW. The CA-impregnated and untreated *E. grandis* wood are potentially suitable for manufacturing finger joints in laminations for glued laminated timber beam lay-up.
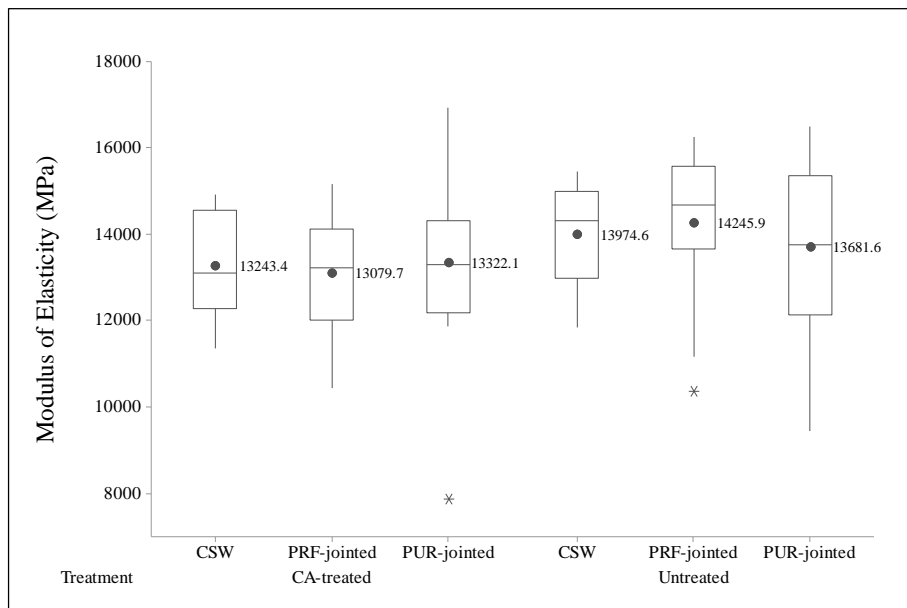

Figure 34: Boxplot of descriptive statistics for bending modulus of elasticity of E. grandis wood as influenced by CA impregnation and finger jointing

Table 16: ANOVA results for effects of CA impregnation and finger jointing on bending modulus of elasticity of E. grandis wood

Source of Variation	Df	Sum Sq	Mean Sq	F value	Pr(>F)
CA impregnation	1	11073958	11073958	3.5041	0.06534
Finger jointing	2	489850	244925	0.0775	0.92550
CA impregnation x Finger jointing	2	2600411	1300206	0.4114	0.66428
Residuals	71	224381416	3160302		

*Significance codes: 0 '***' 0.001 '**' 0.01 '*' 0.05 '.' 0.1 ' ' 1*

Modulus of rupture

The modulus of rupture (MOR) is the maximum bending stress at which the material failed under applied load. CA-impregnation had no substantial effect on the MORs of the *E. grandis* CSW (81 MPa – 84 MPa) and finger-jointed boards (60 MPa – 67 MPa) (Figure 3). Contrary, finger jointing had a significant impact on the MORs (Table 2). Statistically, the CA impregnation and finger jointing interaction effect, and the main effect of CA impregnation on the MORs were not significant ($p > 0.05$) (Table 2). On the other hand, the main effect of finger jointing on the MORs was significant ($p < 0.05$) (Table 2). Tukey post hoc analysis revealed that the differences between the MOR of *E. grandis* CSW and MORs of both PRF and PUR finger-jointed *E. grandis* boards were statistically significant ($p < 0.05$) (Table 2). The difference between the MORs for *E. grandis* boards finger-jointed with PRF versus PUR was not statistically significant ($p > 0.05$) (Table 2). These findings showed that the maximum bending stress that finger-jointed *E. grandis* boards can withstand before failure is significantly lower than that of the CSW. Notwithstanding, the finger-jointed *E. grandis* boards attained between 74% – 83% MOR of the CSW.
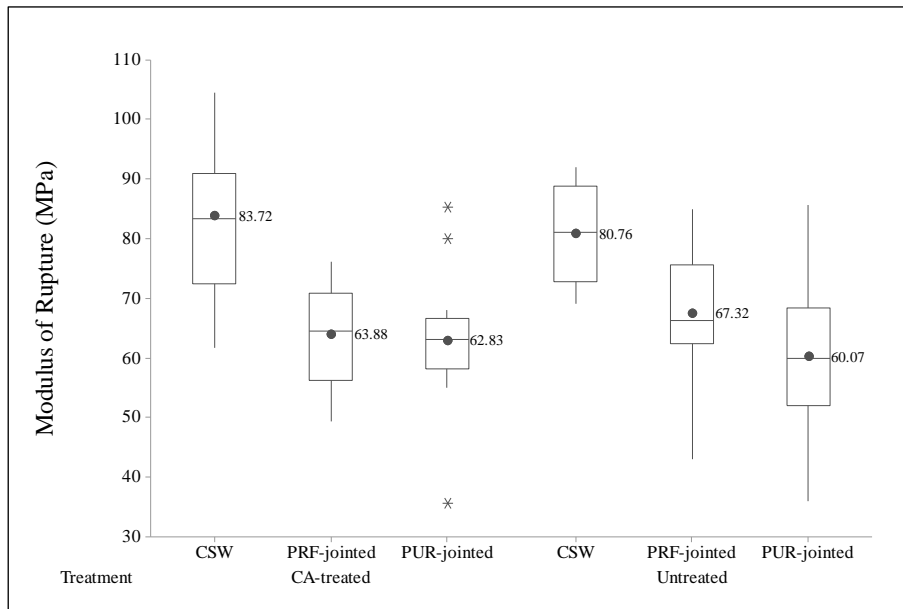

Figure 35: Boxplot of descriptive statistics for modulus of rupture of E. grandis wood as influenced by CA impregnation and finger jointing

Table 17: ANOVA and Tukey post hoc results for effects of CA impregnation and finger jointing on the modulus of rupture of E. grandis wood

ANOVA					
Source of Variation	**Df**	**Sum Sq**	**Mean Sq**	**F value**	**Pr(>F)**
CA impregnation	1	101.0	100.97	0.6914	0.4085
Finger jointing	2	4186.5	2093.24	14.3334	5.904e-06***
CA impregnation x Finger jointing	2	179.0	89.50	0.6129	0.5446
Residuals	71	10368.8	146.04		

Tukey post hoc analysis				
Pair comparison	**Difference**	**Lower**	**Upper**	**p adj**
PRF finger-jointed – CSW	-16.59	-26.11	-7.08	0.0002
PUR finger-jointed – CSW	-20.92	-30.44	-11.41	0.0000
PUR finger-jointed – PRF finger-jointed	-4.33	-11.56	2.90	0.3297

Significance codes: 0 '***' 0.001 '**' 0.01 '*' 0.05 '.' 0.1 ' ' 1

CONCLUSIONS

Based on findings from this study, finger jointing of CA-impregnated and untreated dry *E. grandis* wood is feasible for manufacturing longer span boards with promising stiffness and strength properties in comparison to the CSWs. Thus, adopting finger jointing technology has the prospect of enhancing *E. grandis* wood utilization in manufacturing engineered timber products for structural purposes.

ACKNOWLEDGEMENTS

REFERENCES

Alade, A.A., Naghizadeh, Z., Wessels, C.B., Stolze, H., Militz, H., 2022a. Adhesion performance of melamine-urea–formaldehyde joints of copper azole-treated Eucalyptus grandis at varied bonding process conditions. Construction and Building Materials 314, 125682. https://doi.org/10.1016/j.conbuildmat.2021.125682

Alade, A.A., Naghizadeh, Z., Wessels, C.B., Stolze, H., Militz, H., 2022b. Compatibility of preservative with adhesive in Eucalyptus grandis laminates. International Wood Products Journal 13, 57–69. https://doi.org/10.1080/20426445.2021.2018101

Alade, A.A., Wessels, C.B., Stolze, H., Militz, H., 2022c. Improved adhesive-bond performance in copper azole and disodium octaborate tetrahydrate-treated Eucalyptus grandis laminates. International Wood Products Journal 1–9. https://doi.org/10.1080/20426445.2022.2058277

Bockel, S., Harling, S., Grönquist, P., Niemz, P., Pichelin, F., Weiland, G., Konnerth, J., 2020. Characterization of wood-adhesive bonds in wet conditions by means of nanoindentation and tensile shear strength. European Journal of Wood and Wood Products 78, 449–459. https://doi.org/10.1007/s00107-020-01520-1

Crafford, P.L., Wessels, C.B., 2016. The potential of young, green finger-jointed Eucalyptus grandis lumber for roof truss manufacturing. Southern Forests: a Journal of Forest Science 78, 61–71. https://doi.org/10.2989/20702620.2015.1108618

Dugmore, M.K., 2018. Evaluation of the bonding quality of E. grandis cross-laminated timber made with a one-component polyurethane adhesive. Stellenbosch University, South Africa.

Wessels, C.B., Nocetti, M., Brunetti, M., Crafford, P.L., Pröller, M., Dugmore, M.K., Pagel, C., Lenner, R., Naghizadeh, Z., 2020. Green-glued engineered products from fast growing Eucalyptus trees: a review. European Journal of Wood and Wood Products 78, 933–940. https://doi.org/10.1007/s00107-020-01553-6

A novel approach for the design of flame-retardant plywood

Christian Hansmann[1,2][*], Georg Baumgartner [3], Christoph Preimesberger [1,2]

[1] Wood K plus - Competence Center for Wood Composites & Wood Chemistry, Kompetenzzentrum Holz GmbH, Altenberger Straße 69, A-4040 Linz
[2] University of Natural Resources and Life Sciences, Vienna, Department of Material Sciences and Process Engineering, Institute of Wood Technology and Renewable Materials, Konrad Lorenz-Straße 24, 3430 Tulln an der Donau, Austria
[3] Metadynea Austria GmbH, Hafenstraße 77, A-3500 Krems, Austria

E-mail: c.hansmann@wood-kplus.at, georg.baumgartner@metadynea.com, c.preimesberger@wood-kplus.at

Keywords: Birch, Plywood, Flame Retardants, Fire Behaviour, Mini-SBI, Cone Calorimeter

ABSTRACT

Plywood is a major building material in many countries around the globe. Already ongoing climate change and the thereby caused change in the natural forest structure from softwoods to more hardwoods, like beech or birch, could result in a rising production of plywood-based building materials in the future. But, engineered wood products (EWP) are still prone to fire incidents. To allow and promote the usage in high rise buildings, wood-based materials can be modified with flame retardants (FR) as an alternative way to reach fire safety by huge dimensions and long burn-through rates as a consequence. The production of flame-retardant plywood is nothing new, as veneers can be easily impregnated and drying is quite energy efficient.

But, to produce flame retardant plywood, either the whole cross section of the EWP is treated or just a surface finish is applied. As the typical fire burns from the surface into the panel, the layered structure of the plywood can be used to decrease costs and the amount of flame retardants used, by just treating the outer-most layers of the plywood. Thereby improving economic and ecological factors and combining it with an improved flame-retardant effect, as more FRs are stored in the wood compared to just a surface finish.

For this paper 9-layered birch plywood, glued with urea formaldehyde (UF) resin was produced with one, two and three layers of the surface veneers being switched for veneers impregnated with a commercial FR. The panels were tested on a self-built Mini-SBI experimental setup, additionally cone calorimetry was performed as a reference.

INTRODUCTION

Global demand for building materials based on renewable materials is rising, as it is seen as a major factor for carbon dioxide sequestration and has huge potential to reduce the carbon emissions from building industry (Hildebrandt et al. 2017). Already ongoing global warming leads to a change in the forest structure from coniferous dominated wood species towards more hardwoods. The wood industry needs to react to this change in supply material by identifying novel engineered wood products to meet the demand of the building industry (Pramreiter et al. 2023). But, at the same time the requirements for mechanical and especially fire protection properties are increasing and more important than ever (Brischke et al. 2017). Plywood, as an already established engineered wood product (EWP) could be one of the benefactors of this change. It has outstanding mechanical properties, it is primarily based on hardwood species like birch or poplar and the veneers can be economically modified or functionalised (Pramreiter et al. 2023).

Especially in buildings open to the public like sports halls or entrance halls plywood is already an established working material. Currently fire resistance demands are fulfilled by applying just a surface finish, treating the whole cross section (usually already finished plywood) of the panels with flame retardants or a combination of the two pathways. On the one hand coating of the surface is preferred as the flame retardants are then located where a fire usually starts and the application is quite easy, but on the other it might lead to undesired changes in aesthetics of the raw material. Furthermore, flame retardant coatings that have not only perfect fire retardant properties but also fulfil the demand for

natural looking wood can become quite expansive and degrees of loading are usually not too high. Treating the whole plywood cross section is possible and can fulfil all prerequisites, but in terms of a both economic and ecological usage of chemicals in building products, it might not be the preferred way to go (Rudzīte and Bukšāns 2021).

One option could lie in the impregnation of single layers of veneer with non-halogenated flame retardants and afterwards producing heterogeneous plywood panels. Therefore, increasing the degree of loading compared to just a surface finish and at the same time ensuring a natural look of the EWP.

Before committing to a possible way to go for the production of flame retardant plywood on a big scale and testing for the Euroclass classification system in accordance with EN 13501, fire behaviour analysis on a small to medium scale and a comparative study between treated and untreated samples can be performed to find the most promising combination of flame retardants (CEN 2018, S. Bourbigot et al.). The main test for classification in the European Union is the Single Burning Item Test according to EN 13823. For this standard test samples with dimensions of 1.5 x 1 m^2 and 1.5 x 0.5 m^2 are needed, which are joined along the long edge to form a corner (CEN 2020, Östman and Mikkola 2006). A small scale variant is described by Gossiaux et al. (2021) and was developed in an ongoing project at Wood K plus as well (not yet published). Globally, the go to method for comparative fire behaviour analysis is the cone calorimeter, where samples with a size of 100 x 100 mm^2 are heated up and ignited (ISO 2015).

For this study four variants of heterogeneous plywood with non, One Layer, Two Layers and Three Layers of flame-retardant impregnated veneers were produced and analysed for their reaction to fire in a self-built Mini-SBI experimental device, additionally the fire properties were characterised by cone calorimetry.

MATERIAL AND METHODS
Flame-retardant Plywood
Nine layered birch plywood was produced on a laboratory hot-press out of 1 mm thick veneers with the dimensions of 500x500 mm^2. Commercial urea formaldehyde (UF) resin was used with a glue spread of 130 g m^{-2} no additives or fillers were used in this study. The pressing program lasted for 17 minutes with a pressure of 1.5 MPa and a temperature of 120 °C.

Four variants with and without veneers impregnated with a commercial non-halogenated flame retardant were produced. The veneers were treated beforehand in a laboratory autoclave with a vacuum-pressure program (2 cycles: 10 min 0.25 bar and 20 min 6 bar). Afterwards the impregnated veneers were dried in a furnace with a maximum temperature of 60 °C. Before pressing all veneers were stored under standard climate (20 °C/ 65 % RH) for many weeks to equilibrate the moisture content.

Four symmetric variants of plywood were produced for this paper. For the heterogenous plywood samples the treated were always the outermost veneers.
1. Reference material without flame retardants
2. One Layer
3. Two Layers
4. Three Layers

For the Mini-SBI experiments 4 panels were pruned to dimensions of 470 x 470 mm^2. Each panel was then divided into two smaller pieces with widths of 300 mm and 160 mm and joined with screws on the edge of the longer part to form a corner.

Cone calorimetry samples with dimensions of 100 x 100 mm^2 were cut from different boards. From the reference, one layer and three layers variants four repetitions and for the two layers variant 3 repetitions were investigated by means of cone calorimetry.

All samples were stored in standard climate after production until the experiments happened.

Mini-SBI
The Mini-SBI experimental device is a downscaled version of the Single Burning Item Test described in EN 13823:2020 (downscaling factor approx. 1/3) (CEN 2020). A Line drawing of the device and a picture can be found in Figure 36 a and b. It consists of a burning chamber of approximate size of

580 x 580 x 760 mm^3 in which the triangular (isosceles triangle with 80 mm cathets and 115 mm hypothenuse) sand filled burner and the frame for fixing the corner sample in the right height are located. The burner is fuelled by propane gas. Emerging flue gases are extracted through a fume hood and the 1000 mm long measuring section with a diameter of 130 mm by a chimney fan. In the measuring section pressure difference is measured by a bi-directional probe and part of the flue gases are sucked out and analysed with a MRU VARIOluxx analyser for oxygen (O_2) and carbon dioxide (CO_2) content. On basis of this values calculations for heat release rate (HRR) are performed according to EN 13823 by oxygen consumption calorimetry (CEN 2020).

One measurement is performed as follows:
1. 0-120 s: Recording of ambient conditions (O_2, CO_2 and temperature) as baseline
2. 120-300 s: Ignition of burner and recording of variables with burning propane gas for HRR baseline
3. 300-1500 s: Burner is moved towards the sample, recording of variables of burning sample

All values are stored on the VARIOluxx analyser and afterwards calculations are performed according to EN 13823 (CEN 2020).
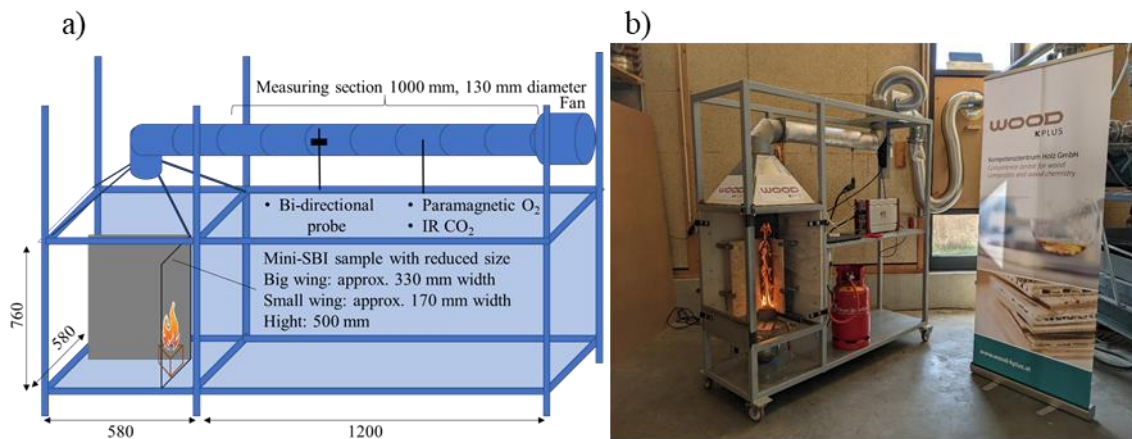

Figure 36: a) line drawing and b) picture of the Mini-SBI experimental device

Cone Calorimeter

Cone calorimeter experiments were conducted on a Netzsch TCC 918 in accordance with ISO 5660-1 (ISO 2015). The heat flux was set to 35 kW m^{-2} and a distance of 60 mm between the cone heater and the sample surface was used. In contrast to the Mini-SBI described briefly above, heat is introduced by an electrically powered cone shaped heater and the gases produced by pyrolysis of the material are ignited with an electrical spark when the enough flammable gases are present. During the experiment heat release (calculated by means of oxygen consumption), mass loss and smoke production are simultaneously recorded.
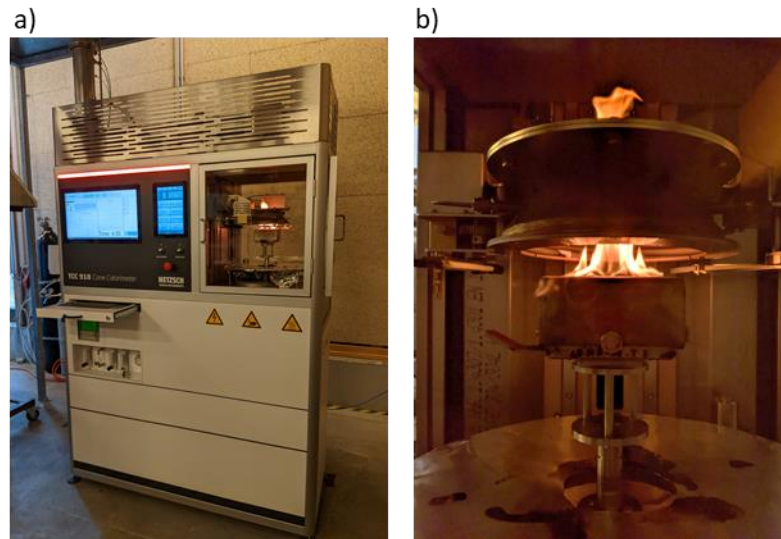
Figure 37: a) Netzsch TCC 918 Cone Calorimeter, b) burning sample under the cone heater

RESULTS AND DISCUSSION
Mini-SBI

Results from the Mini-SBI measurements are shown in Figure 38 and Figure 39. Clear differences between the panels with no, one, two and three layers of flame-retardant impregnated veneers can be seen. The main variables for classification according to EN 13823 (CEN 2020) are the total heat release during the first 600 s (THR600s) of the experiment and the fire growth rate (FIGRA). Due to the downscaling of the whole setup, the threshold values for the calculation of the FIGRA were also reduced to 0.02 MJ in accordance with a paper published by Gossiaux et al. (2021).

According to Babrauskas and Peacock (1992) the heat release rate (HRR) is one of the most important variables for the characterisation of the fire hazard by a burning material. Figure 38 shows the course of HRR of the different variants over the duration of the experiment. The mean and the standard deviation of 4 repetitions (shadowed area) is presented in Figure 38 a – d top row. For the reference sample a higher variation was measured, especially in the late stages of the experiment, where burn through of the sample can cause a severe rise in HRR. Already one layer of flame-retardant veneer decreases and shifts the first rise of HRR to later stages of the experiment. Substituting two or three veneers shifts the rise of the HRR even farther. For the panels with three veneers the deviation of the four repetitions was higher, as delamination of the treated veneers was an issue.

As shown in Figure 39 THR600s can be already reduced by 45 % by just adding one layer to the front of the panel. The FIGRA is reduced by 70 % compared to the reference material. Differences between two and three layers of impregnated veneer are small with approx. 80 % reduction in THR600s and 85 % in FIGRA compared to the reference sample. Especially the delay of the rise in heat release is an important factor, as the initial heat release of the fire is the phase that is particularly relevant in terms of safety.
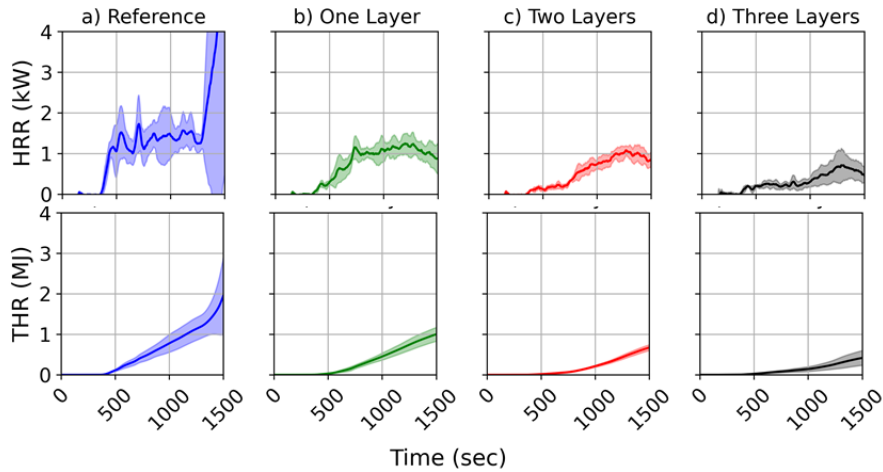
Figure 38: Heat release rate (HRR kW) and Total Heat Release (THR MJ) over time (sec). Full line is the mean value and shadowed area the standard deviation of 4 repetitions
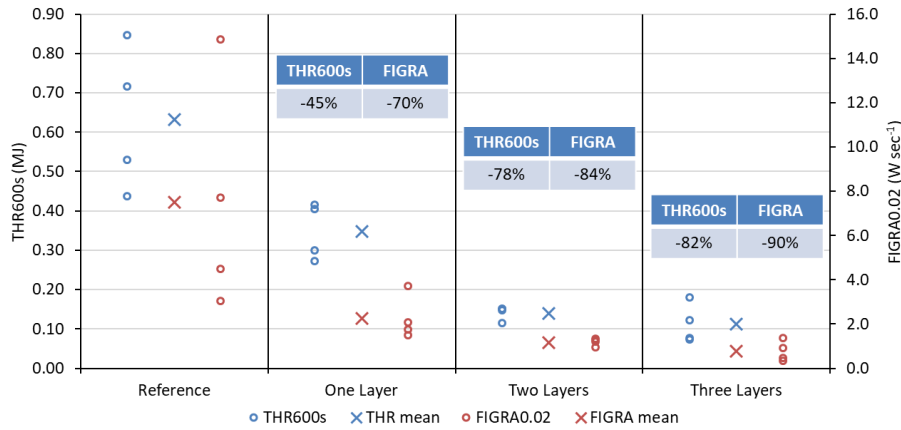

Figure 39: Main variables of the experiment Total Heat Release in the first 600 s (THR600s MJ) and the Fire Growth Rate with a threshold of 0.02 MJ (FIGRA0.02 W sec^{-1}). Indicated in the squares the reduction of the variables with regard to the reference

Cone Calorimetry

Cone calorimetry was used as a standardized method to investigate the fire behaviour of the produced plywood panels. In Figure 40 the main recorded variables are given as a mean (full line) and the standard deviation of 4 (Reference, One Layer and Three Layers) rsp. 3 samples (Two Layers) as the shadowed area. One layer of FR treated veneer leads to a visible retardation of the first rise in heat release and a reduction of the main peak. The Two and Three Layers variants show a similar yet a further delayed first heat release and reduced main peak compared to the One Layer panels (Figure 40 a). Similar effects can be seen in the total heat release (Figure 40 b THR). Mass loss of the samples (Figure 40 c and d) displays the reaction of the flame retardants, as already a loss in mass is happening, although almost no heat is released. This happens because the flame retardants react and are released from the material. Mass loss increases severely when the heat release increases, due to ignition of gases. Mean time to ignition and the single values can be found in Figure 41 a. Values for the Two and Three Layers variants scatter strongly, as in some cases the flame went out after the first ignition and the material reignited at a later stage. In accordance with ISO 5660-1 the time to ignition is defined as the time until sustained ignition happens (ISO 2015). Nevertheless, an increase in mean time to ignition is visible for samples with a rising amount of flame retardant treated veneers (One Layer 3 times, Two Layers 9 times, Three Layers 13 times higher compared to the reference). Figure 41 b shows a decrease in all heat release derived values. THR decreases by 20 % for One Layer variants and by 44 % for Two and Three Layers variants. The peak of the HRR curve is decreased by 44 %, 72 % and 80 % respectively for One, Two and Three Layers. By evaluating the MARHE value, the maximum average rate of heat emission, the heat emission during the whole experiment can be compared. For One Layer of treated veneer MARHE

is decreased by 33 % and for Two and Three Layers by 56 % and 59 % respectively. As seen in Figure 41 c the mass at sustained flaming decreases with rising number of treated veneers and the mass at the end of the experiment increases slightly. This is due to the fact, that there are also treated veneers on the bottom of the sample, as the panels are symmetric, which generally not burn completely resulting in more residual mass. In cone calorimetry the released amount of smoke can be evaluated by the attenuation of a laser beam. Smoke production rate (SPR) and total smoke production (TSP) are plotted in Figure 40 e and f. In Figure 41 d the calculated means and single values are shown. An increase in TSP for rising number of treated veneers is apparent. Especially during the non-flaming phase, the impregnated flame retardants increase the smoke production drastically from 29 m^2 m^{-2} for the reference sample to 67, 108 and 150 m^2 m^{-2} (One, Two and Three Layers). Smoke production during the flaming phase is decreased with rising number of treated veneers, as on the one hand the flaming time is reduced and on the other hand most smoke is already released during the non-flaming phase.
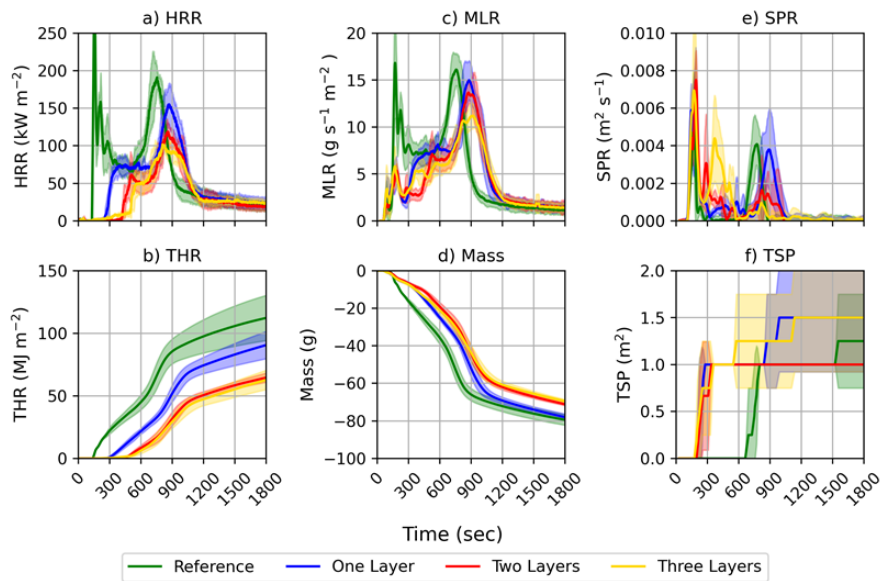
Figure 40: a) heat release rate (HRR), b) total heat release (THR), c) mass loss rate (MLR), d) total mass lost over time, e) smoke production rate (SPR) and total smoke production (TSP). Full line is the mean value and shadowed area the standard deviation of 4 repetitions, 3 repetitions in case of Two Layers variant
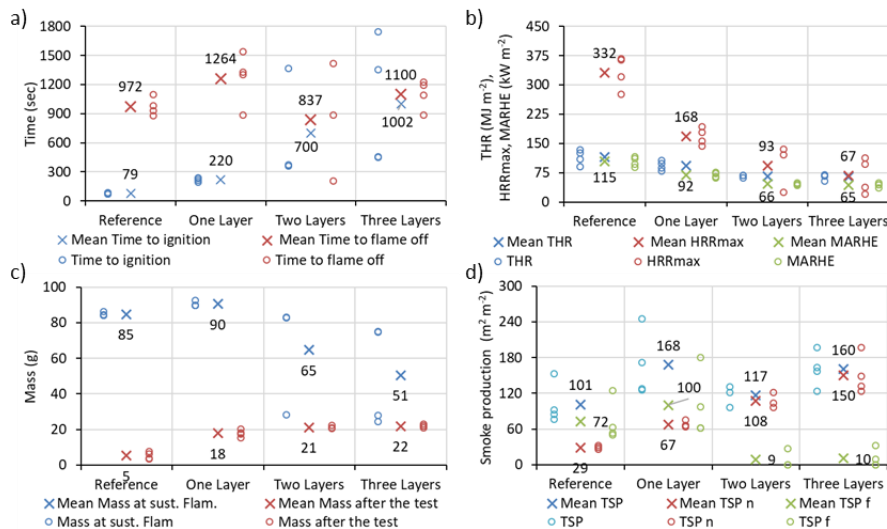
Figure 41: a) Time to ignition and time to flame off, b) total heat release (THR), maximum heat release rate (HRRmax) and maximum average rate of heat emission (MARHE), c) mass at sustained flaming and mass after test and d) total smoke production (TSP), total smoke production during non-flaming phase (TSP n) and total smoke production during flaming phase (TSP f). Values marked with (x) represent the mean and values marked with (o) the single values. Additionally, the values of the means are written besides the markings

CONCLUSION

For this study heterogenous, symmetrical plywood samples out of flame retardant impregnated and non-impregnated veneers were produced on a laboratory hot-press. Three different treated variants were produced with one, two and three layers of treated veneers as the top layer, additionally reference panels with no retardants were produced. Mini-SBI and cone calorimetry experiments were performed with the panels. By combining the results of these two experiments fire behaviour of the panels on a medium scale can be estimated. Reaction to fire in the Mini-SBI experimental device shows a reduction of total heat release (THR) by 45 % by adding one layer of treated veneer, the fire growth rate is reduced by 70 %. Two and Three Layers show similar results of reduction, THR approx. minus 80 % and FIGRA approx. minus 85 % for both variants. Cone calorimetry performed based in ISO 5660-1is a standard method used for the estimation of the fire behaviour on medium sized samples (100x100 mm^2). Multiple variables are evaluated at the same time and show a reduction in THR by 20 % (One Layer) and by 44 % for Two and Three Layers variants. The time to sustained flaming (time to ignition) is delayed 3-. 8- and 13-fold for One, Two and Three Layers respectively. In summary these results show, that the treatment of the outermost layers can have a positive influence on the ignition and fire behaviour of plywood, at the same time preserving the natural appearance of the material because no coating has to be applied.

REFERENCES

Babrauskas V, Peacock RD (1992) Heat release rate: The single most important variable in fire hazard. Fire Safety Journal 18(3):255–272. https://doi.org/10.1016/0379-7112(92)90019-9

Brischke C, Jones D, Jones D (eds) (2017) Performance of bio-based building materials. Woodhead publishing series in civil and structural engineering. WP - Woodhead Publishing an imprint of Elsevier, Duxford, Cambridge, MA, Kidlington

CEN (2018) Fire classification of construction products and building elements. Part 1: Classification using data from reaction to fire tests (EN 13501-1)

CEN (2020) Reaction to fire tests for building products. Building products excluding floorings exposed to the thermal attack by a single burning item (EN 13823)

Gossiaux A, Bachelet P, Bellayer S, Ortgies S, König A, Duquesne S (2021) Small-scale single burning item test for the study of the fire behavior of building materials. Fire Safety Journal 125:103429. https://doi.org/10.1016/j.firesaf.2021.103429

Hildebrandt J, Hagemann N, Thrän D (2017) The contribution of wood-based construction materials for leveraging a low carbon building sector in europe. Sustainable Cities and Society 34:405–418. https://doi.org/10.1016/j.scs.2017.06.013

ISO (2015) Reaction-to-fire tests — Heat release, smoke production and mass loss rate. Part 1: Heat release rate (cone calorimeter method) and smoke production rate (dynamic measurement) (ISO 5600-1)

Östman BA-L, Mikkola E (2006) European classes for the reaction to fire performance of wood products. Holz als Roh- und Werkstoff 64(4):327–337. https://doi.org/10.1007/s00107-006-0116-x

Pramreiter M, Nenning T, Huber C, Müller U, Kromoser B, Mayencourt P, Konnerth J (2023) A review of the resource efficiency and mechanical performance of commercial wood-based building materials. Sustainable Materials and Technologies 38:e00728. https://doi.org/10.1016/j.susmat.2023.e00728

Rudzīte S, Bukšāns E (2021) Impact of High-pressure Impregnation and Fire Protective Coatings on the Reaction to Fire Performance of Birch Plywood. Rural Sustainability Research 45(340):65–75. https://doi.org/10.2478/plua-2021-0008

S. Bourbigot, A Naik, P Bachelet, J Sarazin, P Tranchard, F. Samyn, M. Jimenez, S. Duquesne Latest developments in scale reduction for fire testing

The use of beech particles in the production of particleboards based on recycled wood

Ján Iždinský[1*], Emilia Adela Salca[2], Pavlo Bekhta[3]

[1] Technical University in Zvolen, Faculty of Wood Science and Technology, Department of Wood Technology. T. G. Masaryka 24, 960 01 Zvolen, Slovakia
[2] Transilvania University of Brasov, Faculty of Furniture Design and Wood Engineering. Universitatii 1, 500068 Brasov, Romania.
[3] Ukrainian National Forestry University, Department of Wood-Based Composites, Cellulose and Paper, 79057 Lviv, Ukraine
[3] Technical University in Zvolen, Faculty of Wood Sciences and Technology, Department of Furniture and Wood Products, 960 01 Zvolen, Slovakia
[3] Mendel University in Brno, Faculty of Forestry and Wood Technology, Department of Wood Science and Technology, 613 00 Brno, Czech Republic.

E-mail: jan.izdinsky@tuzvo.sk; emilia.salca@unitbv.ro; bekhta@nltu.edu.ua

Keywords: particleboards, recycled wood, beech wood, properties.

ABSTRACT
Some manufacturers of agglomerated materials also have sawmill processing within one plant, where waste (sawdust, cuttings, ...) is generated and can be used to manufacture agglomerated materials. Our goal in this article would be to point out the use of waste in manufacturing beech wood to produce particleboard. The properties of particleboard made of standard spruce particles with max. 20% addition of recycled wood and with 10, 20 and 30 % of beech wood particles were evaluated. In laboratory conditions, a three-layer particleboard was produced at a temperature of 240 °C, a maximum specific pressing pressure of 5.24 MPa, and a pressing factor of 8 s/mm. Selected physical (moisture, density, (density profile), thickness swelling (TS), and water absorption (WA), after 2 and 24 h) and mechanical properties (internal bond, modulus of rupture, modulus of elasticity in bending, surface soundness) of the manufactured particleboard were determined. The individual physical and mechanical properties of the manufactured particleboard were compared between individual variants with different proportions of beech particles and standard requirements. The presence of beech particles positively affected moisture properties (decrease in the range TS 24h of 25% or WA 24h of 32 % and some mechanical properties such as internal bond and surface soundness. The bending properties were negatively affected (decrease in the range of 11%), in which the bending strength did not reach the specific requirements of P2-type particleboard.

INTRODUCTION
Particleboard is made from wood particles from coniferous and soft hardwood. However, it can also be made from other locally available wood, lignocellulosic particles, and, nowadays, mainly recycled wood (Deppe and Ernst 2000, Maloney 1993, Müller et al. 2009) (if there is enough). According to Irle and Barbu (2010) approximately 95% of the ligno-cellulosic material used for particleboard production is wood. The rest consists mainly of seasonal crops such as flax, bagasse, and cereal straw. Large amounts of lignocellulosic residues suitable for composites production (about 2.4 billion tons) are produced every year after the end of the agricultural season of the various agricultural species (Barbu et al. 2014).
Woods with a lower density are used primarily. However, hardwoods such as beech can also be used due to the availability of timber in the given processing area, thus lowering transport costs. Hardwoods in particleboard increase particleboard density, or properties may decrease at a specific density. Medved and Resnik (2003) focused on determination of how beech particles of different sizes influence bending strength of the three-layer particleboard, when experimental board structure is altered in surface layer only. Beech wood has a long history of cultivation and processing in Slovakia. Even in the past, beech particles from sawmills were used to produce particleboard, but they have other properties far superior to the particleboard we know today.

MATERIALS AND METHODS
Material
The wood particles used in the experiment were made from European beech (*Fagus sylvatica* L.) and Norway spruce (*Picea abies* (L.) Karst.). Beech particles were produced in the laboratories of the Technical University from edges and cuttings by a two-stage process. Offcuts were firstly chipped using the 230H drum mower (Klöckner KG, Hirtscheid—Erbach, Westerwald, Germany) and subsequently milled to particles using the grinding SU1 impact cross mill (TMS, Pardubice, Czech Republic). The spruce particles were produced by Kronospan Zvolen and contained approximately 20% of the recycled wood mix. The particles were sorted into core and surface layers (Figure 1). Oversize (7 mm) and dust (below 0.125 mm) were removed from the particles.

Figure 1: Particles for particleboards: The beech particles (a) and spruce particles (b) used in surface layers (SL) and core layer (CL)

From Figure 2, we can see the results of the sieve analysis of the particles used in the surface and core layers.
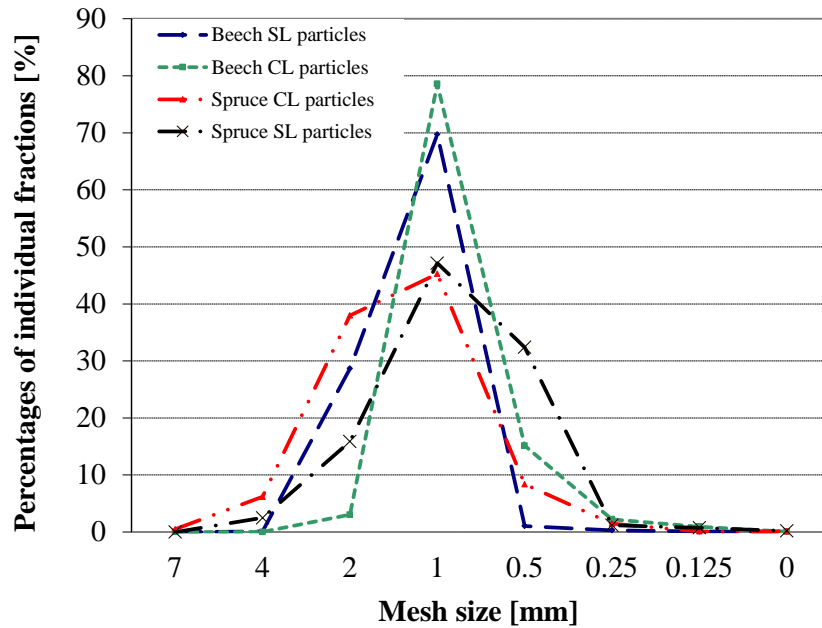
Figure 2: Size characteristics of the beech and spruce particles – percentage of individual fraction for surface layers (SL) and core layer (CL)

Urea-formaldehyde glue (UF) was used to glue the particles in an application of 11% on the particles for the surface layers (Kronores PBU 2140) and 7% on the particles for the core layer (Kronores PBU 1745). The detailed parameters of the glue are listed in Table 1. Other chemical auxiliaries used in the adhesive mixture were a hardener (57% ammonium hydroxide) in the amount of 2% for surface particles and 4% for core particles by weight of the applied glue and paraffin emulsion (35%), the application of which is 0.8% for surface particles and the same 0.8% is also for core particles.

Table 1: Properties of urea-formaldehyde (UF) resins

Quality Parameters	Unit	Method	KRONORES PBU 2140	KRONORES PBU 1745
Solid content	%	EN 827	64.6	67.73
Ford cup viscosity, 4mm/20 °C	s	EN ISO 2431	69	62
pH value		EN 1245	9.06	9.15
Gel time at 100 °C	s	Kronospan chloride test	93	51

Particleboard Preparation

The 3-layer particleboards (PBs) with the dimensions of 400 mm × 300 mm × 16 mm and with a density of 650 kg·m⁻³ ± 5 kg·m⁻³ were produced under laboratory conditions. The surface/core particle ratio was 37:63. The moisture content of the wood particles after applying the adhesive (in a laboratory rotary mixing device, TU Zvolen, Slovakia) was 9.4% to 9.9% (for the surface layers) and from 6.6% to 6.8% (for the core layer). The particle mats were layered manually in wooden forms. The particle mat was cold pre-pressed at a laboratory temperature, at a pressure of 1 MPa, and then it was pressed in the CBJ 100-11 laboratory press (TOS, Rakovník, Czech Republic) by the pressing diagram (Figure 3) at a maximum pressing pressure of 5.24 MPa. The maximum temperature of the pressing plates in the press was 240 °C, and the pressing factor was 8 s/mm. In total, 12 PBs were manufactured, i.e., 3 from each type (Table 2).
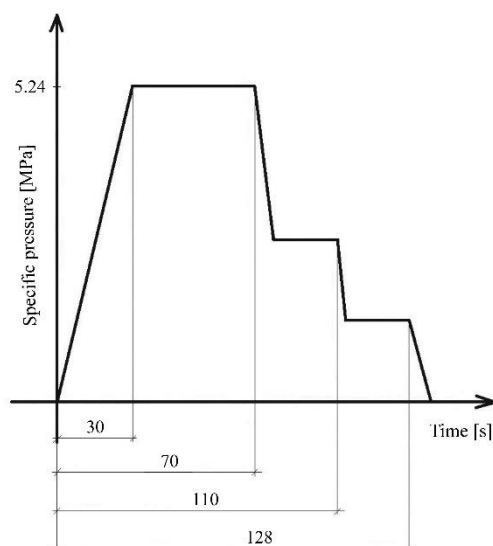
Figure 3: Standard three-stage pressing diagram for manufacturing the particleboards

Table 2: Individual types of manufactured particleboards

Variant	Amount of Beech Wood in PB, w/w (%)	Number of Produced Boards	Board Type
PB-C 80% particles of spruce wood with 20% mixture of recycled wood products	0	3	C
PB-B10 10% particles from beech wood combined with 90% particles of spruce wood with recycled wood	10	3	10 B
PB-B20 20% particles from beech wood combined with 80% particles of spruce wood with recycled wood	20	3	20 B
PB-B30 30% particles from beech wood combined with 70% particles of spruce wood with recycled wood	30	3	30 B

Properties of Particleboards

Selected physical and mechanical properties of PBs were determined according to the European (EN) standards and Slovak (STN) standards. Physical properties: the density by EN 323, the moisture content by EN 322, the thickness swelling (TS), and water absorption (WA) after 2 and 24h by EN 317 and STN 490164 were determined. Mechanical properties: the modulus of rupture (MOR) and modulus of elasticity (MOE) in bending by EN 310 and the internal bond (IB) by EN 319 were determined as well. Mechanical properties were determined with the universal machine TiraTest 2200 (VEB TIW, Rauenstein, Germany). The change in density over the thickness of the obtained samples was assessed with the X-ray density profile analyser – DPX300-LTE (IMAL, Modena, Italy). The density was measured at intervals of 0.05 mm. The classification of PBs was performed using the European standard EN 312, considering the requirements of the PB (type P2), with thickness ranging between 13 mm and 20 mm. The statistical software STATISTICA 12 (StatSoft, Inc., Tulsa, OK, USA) was used to analyse the gathered data.

RESULTS AND DISCUSSION

Physical and Mechanical Properties of Particleboards

Table 3 presents the meticulously measured physical and mechanical properties of particleboards manufactured in the esteemed laboratories of the TU in Zvolen. The average density of PBs, a key indicator of their quality, was found to be remarkably consistent, ranging between 645 kg·m^{-3} and 651 kg·m^{-3}, regardless of the amount of beech wood used. Similarly, the average moisture content of the manufactured boards was found to be a stable 5.9 to 6.0 percent (Table 1), further demonstrating the precision of our research.

The moisture properties of PBs, i.e., the thickness swelling (TS) and water absorption WA, significantly improved with a higher portion of beech particles. For example, TS-2h decreased from 27.3% for PB-C to 6.7% for PB-B30; TS-24h decreased from 35.1% for PB-C to 26.1% for PB-B30; WA-2h decreased from 81.3% for PB-C to 29.8% for PB-B30; and WA-24h decreased from 104.7% for PB-C to70.9% for PB-B30 (Table 3). The effect of the beech particles on the moisture properties of PBs was in all cases considered significant, as values of the coefficient of determination r^2 for the linear correlations "TS or WA = a + b × w/w" were high and ranged between 0.62–0.86, at which p was always 0.000 (Figures 4 and 5). The added beech particle had a more homogeneous character; the most significant percentage representation of individual fractions for surface and core layers was 1 mm (Figure 2).

Table 3: Physical and mechanical properties of control particleboard (PB-C) and of the particleboards (PBs) containing particles from beech wood (PB-B10, B20, B30)

Property of PB		Beech wood in PB *w/w* (%)			
		0	10	20	30
Density	[kg·m^{-3}]	649 (20.6)	646 (20.5)	651 (18.8)	645 (23.0)
Moisture content	[%]	5.9 (0.1)	5.9 (0.1)	6.00 (0.1)	5.9 (0.1)
Thickness swelling (TS) after 2 h	[%]	27.3 (2.0)	23.8 (1.5)	10.7 (5.7)	6.7 (1.6)
Thickness swelling (TS) after 24 h	[%]	35.1 (2.7)	32.6 (1.5)	26.7 (4.2)	26.1 (2.2)
Water absorption (WA) after 2 h	[%]	81.3 (5.8)	73.9 (5.2)	36.3 (7.8)	29.8 (3.1)
Water absorption (WA) after 24 h	[%]	104.7 (5.6)	100.3 (5.1)	77.5 (7.1)	70.9 (4.3)
Internal bond (IB)	[MPa]	0.33 (0.03)	0.34 (0.02)	0.40 (0.04)	0.38 (0.04)
Surface Soundness (SS)	[MPa]	0.56 (0.08)	0.70 (0.08)	0.69 (0.08)	0.72 (0.08)
Modulus of rupture (MOR)	[MPa]	9.7 (1.3)	9.6 (1.1)	9.1 (0.8)	8.6 (0.5)
Modulus of elasticity (MOE)	[MPa]	2257 (218)	2264 (163)	2137 (206)	2125 (193)

Notes: Mean values of density from 33 samples, Moisture content 15 samples, TS from 8 samples, WA from 8 samples, IB from 12 samples, Surface soundness from 12 samples, MOR and MOE from 9 samples. Standard deviations are in the parentheses.
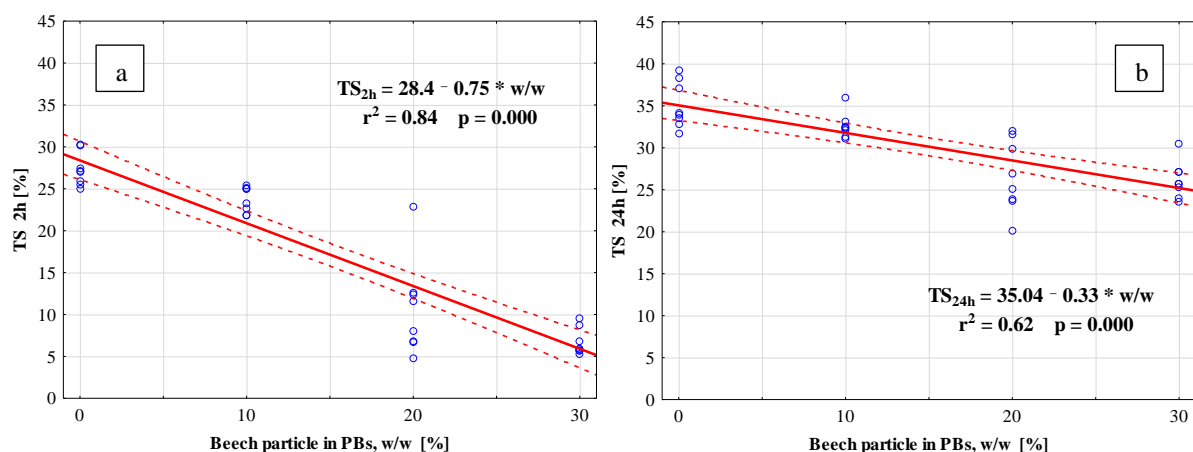

Figure 4: Thickness swelling (TS) after 2h (a) and 24h (b) of PBs containing different amount of particles from beech wood
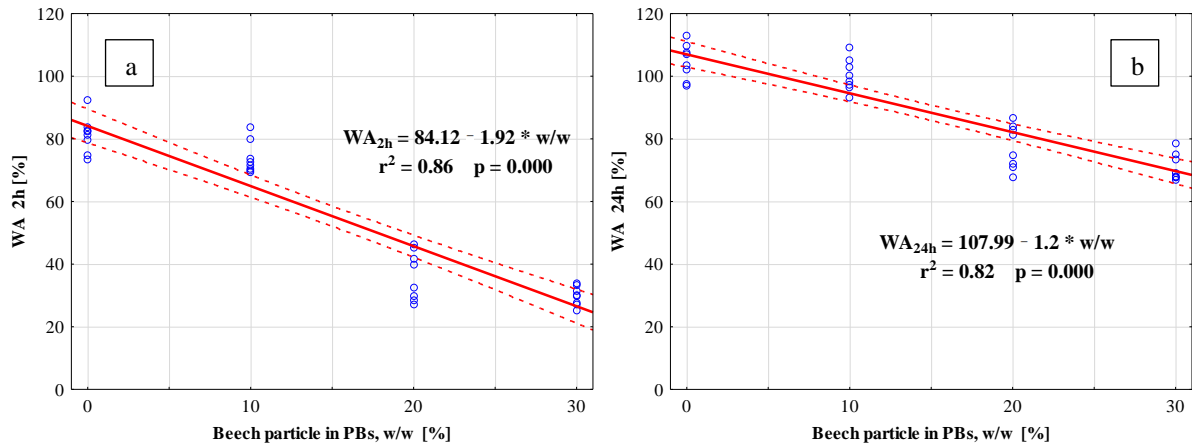
Figure 5: Water absorption (WA) after 2h (a) and 24h (b) of PBs containing different amount of particles from beech wood

The mechanical properties of the PBs in bending, i.e., the modulus of rupture (MOR) and the modulus of elasticity (MOE), were negatively influenced by beech wood (Table 3 and Figure 6a). The maximal decrease in the MOR, from 9.7 MPa of PB-C, was determined using the 30% amount of beech wood, i.e., by 11% to 8.6 MPa for PB-B30. The maximal decrease in the MOE, from the 2257 MPa of PB-C, was determined similarly when the highest 30% amount of beech wood was used, i.e., about 6% to 2125 MPa for PB-B30 (Tables 3 and Figure 6b).

A significantly negative effect of beech wood (especially at PB-B30) on the bending properties of PBs was confirmed by coefficients of determinations r^2 of linear correlations "MOR or MOE = a + b × w/w" from 0.19 for MOR to 0.09 for MOE (Figure 6).

From the mechanical properties (MOR and MOE) of PB based on beech wood, only the MOE property met the requirements of P2-type particleboard (according to EN 312: MOR 11 MPa; MOE 1600 MPa). The modulus of rupture (MOR) was lower compared to the requirements for the P2 board type by 12% for PB-C to 22% for PB-B30.
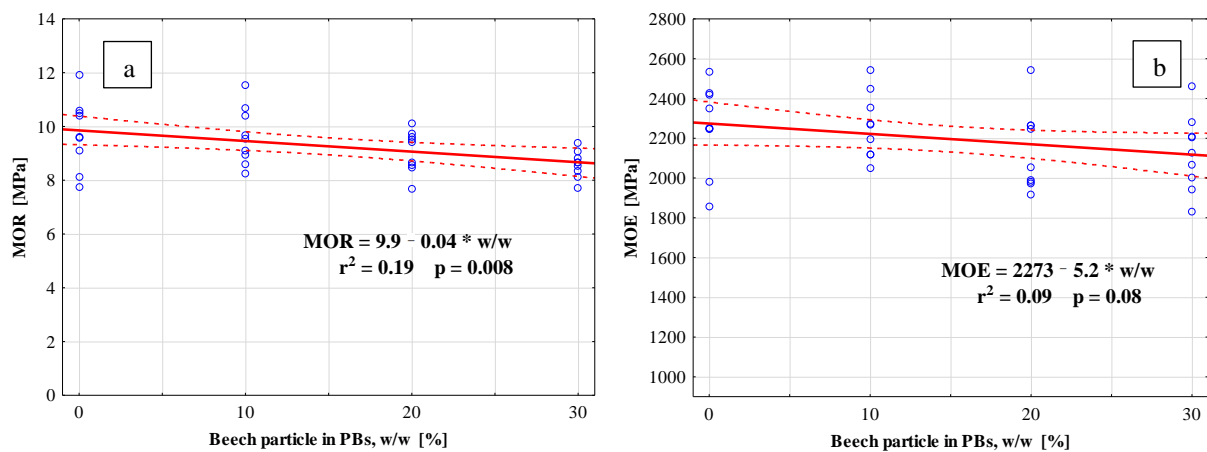
Figure 6: Modulus of rupture (MOR) (a) and modulus of elasticity (MOE) (b) of PBs containing different amount of particles from beech wood

The presence of beech particles in PB had a positive effect on their mechanical properties - significantly on the internal bond (IB) and surface soundness (SS) with r^2 equal to 0.31 and 0.31 for the linear correlations "IB or SS" = a + b × w/w (Table 3 and Figure 7).

When compared to the specific requirements of the EN 312 standard for type P2, the PB values based on beech wood in two cases for PB-B20 (0.40 MPa) and PB-B30 (0.38 MPa) reached the IB of 0.35 MPa, demonstrating the positive effect of beech particles on the internal bond (Table 3 and Figure 7a). Surface soundness did not reach the requirements of standard EN 312 for board type P2 (0.80 MPa) (Table 3 and Figure 7b).

The graphs show: (a) IB [MPa] vs Beech particle in PBs, w/w [%] with equation IB = 0.77 + 0.002 * w/w, $r^2 = 0.31$, $p = 0.000$; (b) Surface Soundness [MPa] vs Beech particle in PBs, w/w [%] with equation SS = 0.59 + 0.005 * w/w, $r^2 = 0.31$, $p = 0.000$
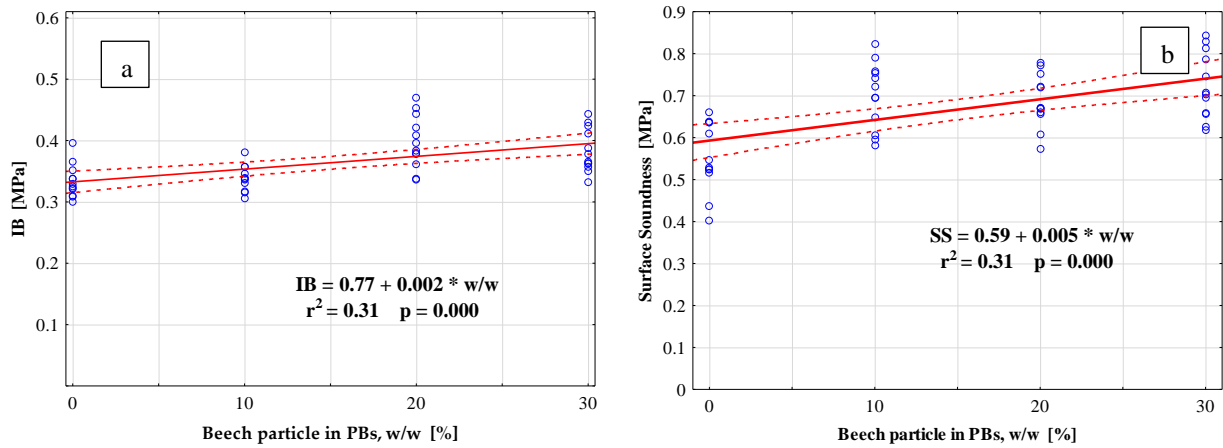
Figure 7: Internal bond (IB) (a) and surface soundness (SS) (b) of PBs containing different amount of particles from beech wood

In Figure 8, in all variants of PB can be observed the density profiles of particleboard made of spruce particles with a 20 % share of recycled wood mix (PB-C) and with different additions (10, 20, 30%) of beech particles that the point with the maximum density is shifted by up to 1 mm to the inside of the board. Thus, the surface soundness was negatively affected. Ideally, this point of highest density would be on the surface of the particleboard, which is achieved by sanding. Then, we could expect an improvement in the properties, especially the surface soundness.

Figure 8: Density profile PB-C (a), PB-B10 (b), PB-B20 (c), and PB-B30 (d) of PBs containing different amount of particles from beech wood

CONCLUSIONS

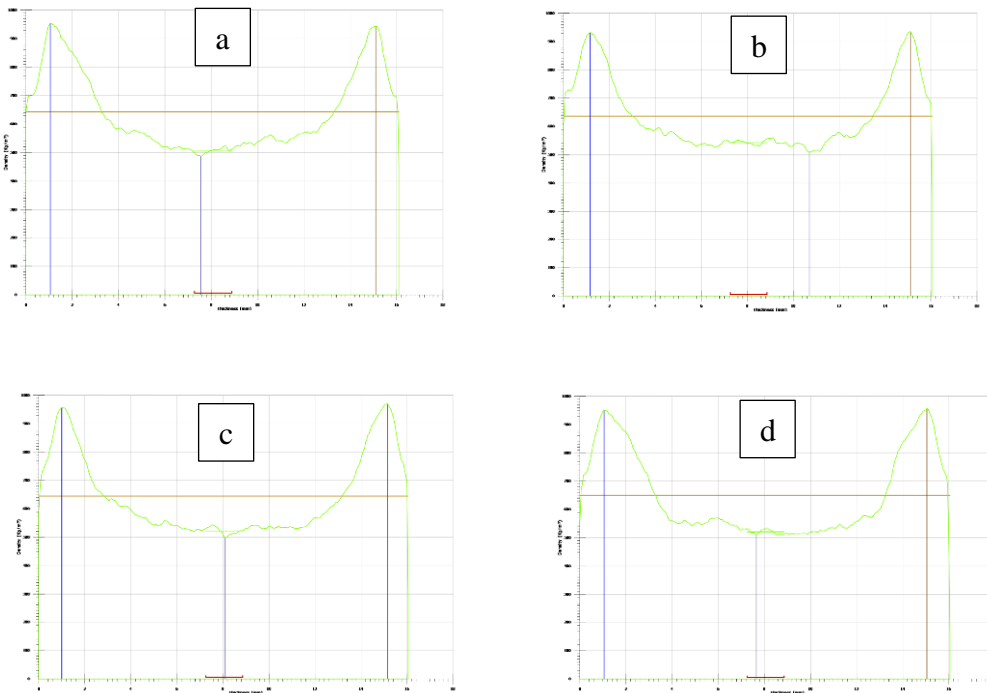The moisture properties of PBs based on spruce particles with 20% recycled wood mix were significantly improved with a higher amount of beech particles in their surface and core layers, e.g., after 24 hours the thickness swelling (TS) reduced from 35.1% up to 26.1% and the water absorption (WA) from 104.7% up to 70.9%.

Beech particles had a negative effect on the bending properties of PB, most notably on the modulus of rupture (MOR), which deteriorated from 9.7 MPa to 8.6 MPa. This meant that the modulus of rupture was lower compared to the requirements for the P2 board type by 12% at PB-C up to 22% at PB-B30. The modulus of elasticity (MOE) met the requirements for the P2 board type in all variants.

Beech particles positively affected the internal bond and surface soundness - with an internal bond with a proportion of beech particles of 20% and 30%, the particleboard met the requirements for board type P2. The requirements for the P2 board type for the mechanical property of surface soundness could not be met for all variants, which was also related to the displacement of the point with the highest density from the centre of the board, which we can divide by the density profile of the manufactured boards.

ACKNOWLEDGEMENTS

REFERENCES

Barbu MC, Réh R, Çavdar AD (2014) Non-wood lignocellulosic composites. In: Research Developments in Wood Engineering and Technology, 1st ed. Aguilera A, Davim JP (eds) IGI Global, Hershey PA, USA, pp 281–319

Deppe HJ, Ernst K (2000) Taschenbuch der Spanplattentechnik. 4th ed. DRW-Verlag, Leinfelden-Echterdingen, Germany, 552 p.

EN 310 (1993) Wood-based Panels-Determination of Modulus of Elasticity in Bending and of Bending Strength; European Committee for Standardization: Brussels, Belgium

EN 311 (2002) Wood-based Panels-Sourface Soundness-Test method; European Committee for Standardization: Brussels, Belgium

EN 317 (1993) Particleboards and Fibreboards-Determination of Swelling in Thickness after Immersion in Water; European Committee for Standardization: Brussels, Belgium

EN 319 (1993) Particleboards and Fibreboards-Determination of Tensile Strength Perpendicular to the Plane of the Board; European Committee for Standardization: Brussels, Belgium

EN 322 (1993) Wood-based Panels-Determination of Moisture Content; European Committee for Standardization: Brussels, Belgium

EN 323 (1993) Wood-based Panels-Determination of Density; European Committee for Standardization: Brussels, Belgium

Irle M, Barbu MC (2010) Wood-based panel technology. In: Wood-Based Panels - An Introduction for Specialists, 1nd ed.; Thoemen H, Irle M, Sernek M (eds), 1st ed. Brunel University Press, London, England, pp. 1–90

Maloney TM (1993) Modern particleboard and dry-process fiberboard manufacturing. 2nd ed. Miller Freeman, San Francisco, pp 626–669

Medved S, RESNIK J (2003) Influence of beech particle size used in surface layer on bending strength of three-layer particleboard. In: Zbornik gozdarstva in lesarstva (forest and wood science and technology). 72, pp 197–207

Müller G, Schöpper C, Vos H, Kharazipour A, Polle A (2009) FTIR-ATR spectroscopic analyses of changes in wood properties during particle- and fibreboard production of hard- and softwood trees. In: BioRes. 4(1), 49-71.

STN 490164 (1980) Particleboards-Determination of water absorption; Slovak Office of Standards, Metrology and Testing: Bratislava, Slovak Republic.

Thermal properties of highly porous wood-based insulation material

Kryštof Kubista[1], Přemysl Šedivka[1]

[1] Department of Wood processing and Biomaterials, Faculty of Forestry and Wood Sciences, Czech University of Life Sciences, Prague, Czechia

E-mail: kkubista@fld.czu.cz; sedivka@fld.czu.cz

Keywords: Agglomerated material, Foamed wood, Thermal insulation, Wood-based insulation, Wooden waste

ABSTRACT
This study is focuses on evaluating the thermal insulation properties of a new highly porous insulation material made from a foamed wood mixture. A key aspect is the use of wood fibres sourced from wood waste, aligning with the goal of promoting environmentally friendly materials. The main objective is to accurately determine important thermal parameters like the coefficient of thermal conductivity (λ) and thermal resistance coefficient, specific parameters characterizing thermal insulation properties of new material. Results are meticulously analysed and presented graphically for clarity. The research also emphasizes sustainability by incorporating wood waste into the material synthesis process, addressing environmental concerns and promoting resource efficiency. To assess the new material, it is compared with commercially available thermal insulation materials, providing insights into its performance compared to industry standards. By enhancing our understanding of its thermal performance and comparing it with existing options, this research contributes valuable insights to the discourse on sustainable and efficient insulation materials.

INTRODUCTION
Globally, the acceleration of climate change resulting from carbon dioxide emissions is directly impacting people's lives. The construction sector is responsible for nearly 40% of the world's annual carbon dioxide emissions, making it imperative to reduce emissions and reform the construction industry (Sovacool et al., 2021). Sustainable architecture trends offer solutions to mitigate the construction sector's carbon footprint, with a focus on building materials, particularly thermal insulation (Ali et al., 2020). Thermal insulation is crucial for maintaining comfortable temperatures in buildings and can significantly reduce energy consumption for heating and cooling, thus lowering greenhouse gas emissions. While traditional insulation materials are effective, they often require high energy and water consumption and pose challenges for recycling (Yildiz et al., 2021).

Due to the development of the prices of energy sources, increasingly strict requirements are placed on the overall energy balance of residential buildings (Wiprächtiger et al., 2020). With this, there are growing demands for the development of new types of building envelope compositions and new thermal insulation materials with optimal parameters in terms of mechanics, building physics, acoustics, fire resistance, durability, health safety, production costs and ecological degradability (Cabral et al., 2021). Despite the many advantages of natural insulation material, however, consumers and construction professionals are still facing many challenges, including technical limitations, lack of standards and regulations, and insufficient awareness of the potential of these materials. Consequently, continued research and development of these materials are necessary to overcome these obstacles (Hellová et al., 2020). The transition to natural insulation is not only a question of sustainability but also a question of future environmental protection (Ulutaş et al. 2023). This is the step we need to take in order to achieve goals such as reducing adverse effects on the climate and sustainable development (Pescari, 2022).

Foam wood has many advantages that make it an innovative and environmentally friendly material. Its light nature is due to the incorporation of air into its structure in the foaming process, giving it excellent insulation properties. This translates into improved energy efficiency in the construction sector and reduced heating and cooling costs. Moreover, foam wood has increased strength and durability and is sustainable, as it often comes from renewable sources. The capacity of sound absorption and fire resistance further enhances the attraction of this material, making it a versatile and promising material for a wide range of applications, especially in construction and manufacturing.

MATERIALS AND METHODS

Materials

A three types of test samples with dimensions of 500 mm x 500 mm and a thickness of 40 mm was made. The first type is based on wooden fibre (FW1), second sample is based on wooden flour (FW2) and third type of specimen is based on wooden flour with addition of brewer's spent grain (FW3). In the preparation of FW1 and FW2 an inorganic blowing agent was used. In preparation of FW3 was used an organic blowing agent. These input materials were chosen due to the recovery of production waste.

The test body of thermal insulation material based on foamed wood fibre is conditioned at 65 ± 5% relative humidity and 20 ± 2 °C air temperature for 168 hours. The moisture content of the thermal insulation material is determined by a moisture analyser type MB23 (OHAUS Europe GmbH) on samples taken from individual parts of the test material.

The percentage moisture content (u) was determined as the weight difference between the wet (m_w) and dry (m_0, dried at 105°C ± 2°C for 6 hours) sample according to the relationship:

$$u\ (\%) = \frac{m_w - m_0}{m_0} . 100 \tag{1}$$

where

u   moisture content (%)
m_w weight of the wet sample (kg)
m_0 weight of the dry sample (kg)

Measurement procedure

The tested material was inserted into the device to determine thermal insulation characteristics, enabling measurement of thermal insulation characteristics by the method of protected hot plates TAURUS TLP 900-GS (TAURUS Instruments GmbH, Germany). The principles of methodological procedure design, test equipment and the basic requirements that have to be meet for laboratory determination of thermal transfer properties of parts of buildings are derived from EN 12939. A sample of the plate with defined dimensions determined by the standard EN 12667 was placed between the hot and cold plates of the measuring device of the chamber with the temperature sensing sensors applied. Then the chamber was closed and started in measurement mode, the measurement took place for 30 hours until the temperature reached a stable state in the density profile of the measured sample. The required parameters for measuring the heat transfer coefficient were set in the device. The sensing probes were applied to the examined sample, and then the sample was isolated with polystyrene plates, allowing the examined material to be tested under the most accurate conditions.

Table 1: Device characteristics of calibrated box with an integrated hot plate TLP 900 (G)S

Characteristics	Technical data	
Measurement range	0,005-2,0 W.m^{-1}. K^{-1}	
Test size (mm)	500x500 – 800x800	
Sample thickness (mm)	10 – 240	
Temperature range	Cooling plate	-10 – +50°C
	Heating Plate	0 – +60°C
Voltage	110 – 230 V 50/60 Hz	

Thermal conductivity characterizes the ability of the tested material to conduct heat. It represents the rate at which heat flow spreads from one heated part to a cold part. The device measures thermal conductivity with an accuracy of ± 0.1%.
The calculation is given by the relation (EN 12667):

$$\lambda = \frac{\varphi\, d}{A\,(T_1 - T_2)} \tag{2}$$

where

λ	coefficient of thermal conductivity $(W.m^{-1}.K^{-1})$
T_1	average temperature on the warm side of the sample (K)
T_2	average temperature on the warm side of the sample (K)
d	thickness of the tested material (m)
A	specific area of the sample (m^2)
φ	average heat flow (W)

Calculation of thermal resistance R

Thermal resistance characterizes the amount of heat, how much heat passes through a structure with an area of 1 m^2 when the temperature difference of its surfaces is 1 K.
The calculation is given by the relationship (EN ISO 6946):

$$R = \frac{d}{\lambda} \qquad (3)$$

where

R	thermal resistance of the structure $(m^2.K.W^{-1})$
d	thickness of the tested material (m)
λ	coefficient of thermal conductivity $(W.m^{-1}.K^{-1})$

RESULTS AND DISCUSSION

The measurement results were compared with each other in table 2.

Table 2: Results of the measurement

Specimen	λ $[W.m^{-1}.K^{-1}]$	R $[m^2·K.W^{-1}]$	ρ $[kg.m^{-3}]$
FW1	0.041	0.97	97.8
FW2	0.044	0.90	265.7
FW3	0.051	0.97	228.3

The results were compared with each other. Thermal conductivity of FW1 and FW2 is similar, even though these are two quite different materials. FW1 has larger pore and much lower density. Longer wood fibres allow the material to create a more porous and lighter structure. FW2 and FW3 were made from wood flour which has fibre length about 0.2 mm, therefore, it produces a much denser material with much smaller pores. In a case of FW3 with addition of brewer's spent grain, the result of thermal conductivity is higher then other two materials. The structures of individual measured materials are shown in Figures 1, 2 and 3. The measured foamed wood base materials were magnified under a stereo microscope SMZ 1270 (Nikon, Japan) and photographed with DS-FI3 camera (Nikon, Japan).

The measured values of the three developed Foamed Wood materials were compared with selected commercially produced materials. Materials such as STEICO ISOVER (Wood fibre insulation) (Steico AG, Germany), ISOVER UNI (Mineral wool) (Saint-Gobain Construction Products CZ a.s., Czech Republic), KOBE ECO HEMP FLEX (Hemp fibre insulation)(KOBE-cz s.r.o., Czech Republic), EKOPANEL (straw insulation) (EKOPANELY CZ s.r.o., Czech Republic) were selected. The resulting values of the material parameters are shown in the following Table 3.

Table 3: Comparison of Foamed Wood (FW) with selected thermal insulations

Specimen	λ $[W.m^{-1}.K^{-1}]$	R $[m^2·K.W^{-1}]$	ρ $[kg.m^{-3}]$
FW1	0.041	0.97	97.8
FW2	0.044	0.91	265.7
FW3	0.051	0.97	228.3
STEICO ISOVER	0.040	1.00	160.0
ISOVER UNI	0.035	1.14	40.0
KOBE ECO HEMP FLEX	0.040	1.00	35.0
EKOPANEL	0.099	0.40	379.0

Figure 42: Structure of sample FW1, 12.7x6.3

Figure 43: Structure of sample FW2 12.7x6.3

Figure 44: Structure of sample FW3 12.7x6.3

The value of the coefficient of thermal conductivity was determined, for FW1 material $\lambda = 0.041$ (W.m^{-1}.K^{-1}), for FW2 $\lambda = 0.044$ (W.m^{-1}.K^{-1}) and for FW3 material $\lambda = 0.051$ (W.m^{-1}.K^{-1}). The results of FW1 and FW2 samples show that, compared to other commercially produced thermal insulation materials, it has comparable parameters as insulation materials based on wood or straw fibres, it shows worse parameters than insulation materials based on Mineral wool. In the case of FW3 the result is slightly worse in meaning of thermal conductivity. However, the FW3 material is made of 100% organic input material. At this point of view, we can compare it with straw-based insulation in the meaning of thermal conductivity.

The similar results are confirmed by the assessment of thermal resistance $R_{FW1} = 0.97$ (m^2·K.W^{-1}), $R_{FW2} = 0.91$ (m^2·K.W^{-1}), $R_{FW3} = 0.97$ (m^2·K.W^{-1}), where the results show that, compared to other commercially produced thermal insulation materials, it has comparable parameters as insulation materials based on wood or straw fibres, it shows worse parameters than insulation materials based on Mineral wool.

CONCLUSIONS

The purpose of this paper was to determine the basic thermal-insulating characteristics of the new thermal-insulating materials based on foamed wood for the potential of its application when it is implemented in the structure of the perimeter shell. The materials were made by using wooden fibres, wooden flour and brewer's spent grain. These input materials were chosen due to the recovery of production waste. The resulting parameters were compared to each other and with four other types of thermal insulation materials from commercial manufacturers.

The researched materials described in this post are some kind of prototypes of Insulating materials using the principle of inflating material based on wood fibres of various sizes. It is the ability to use even a small fraction of wood fibre in the form of wood flour that makes it possible to use even a smaller fraction of wood waste, or lower quality wood waste.

ACKNOWLEDGEMENTS

REFERENCES

Ahmed Ali, K., Ahmad, M. I., & Yusup, Y. (2020). Issues, impacts, and mitigations of carbon dioxide emissions in the building sector. Sustainability, 12(18), 7427.

Almusaed, A., Almssad, A., Alasadi, A., Yitmen, I., & Al-Samaraee, S. (2023). Assessing the Role and Efficiency of Thermal Insulation by the "BIO-GREEN PANEL" in Enhancing Sustainability in a Built Environment. Sustainability, 15(13), 10418.

Cabral, M. R., & Blanchet, P. (2021). A state of the art of the overall energy efficiency of wood buildings—An overview and future possibilities. Materials, 14(8), 1848.

EN 12267 Thermal performance of building materials and products - Determination of thermal resistance by means of guarded hot plate and heat flow meter methods - Products of high and medium thermal resistance, 2001. Praha: Český normalizační institut.

EN 12939 Thermal performance of building materials and products - Determination of thermal resistance by means of guarded hot plate and heat flow meter methods - Thick products of high and medium thermal resistance, 2001. Praha: Český normalizační institut.

EN ISO 6946 Building components and building elements - Thermal resistance and thermal transmittance - Calculation method, 2020. Praha: Český normalizační institut.

Fend, T., Hoffschmidt, B., Pitz-Paal, R., Reutter, O., & Rietbrock, P. (2004). Porous materials as open volumetric solar receivers: experimental determination of thermophysical and heat transfer properties. Energy, 29(5-6), 823-833.

Ferreira, E. S., Dobrzanski, E., Tiwary, P., Agrawal, P., Chen, R., & Cranston, E. D. (2023). Insulative wood materials templated by wet foams. Materials Advances, 4(2), 641-650.

Hellová, K. E., Unčík, S., & Cabanová, T. (2020). Sorption properties of thermal insulation composed of flax or hemp fibers. Slovak Journal of Civil Engineering, 28(3), 47-52.

Pescari, S., Merea, M., Pitroacă, A., & Vilceanu, C. B. (2022). A Particular Case of Urban Sustainability: Comparison Study of the Efficiency of Multiple Thermal Insulations for Buildings. Sustainability, 14(23), 16283.

Scrucca, F., & Palladino, D. (2023). Integration of energy simulations and life cycle assessment in building refurbishment: An affordability comparison of thermal insulation materials through a new sustainability index. Sustainability, 15(2), 1412.

Sovacool, B. K., Griffiths, S., Kim, J., & Bazilian, M. (2021). Climate change and industrial F-gases: A critical and systematic review of developments, sociotechnical systems and policy options for reducing synthetic greenhouse gas emissions. Renewable and Sustainable Energy Reviews, 141, 110759.

Ulutaş, A., Balo, F., & Topal, A. (2023). Identifying the Most Efficient Natural Fibre for Common Commercial Building Insulation Materials with an Integrated PSI, MEREC, LOPCOW and MCRAT Model. Polymers, 15(6), 1500.

Wiprächtiger, M., Haupt, M., Heeren, N., Waser, E., & Hellweg, S. (2020). A framework for sustainable and circular system design: Development and application on thermal insulation materials. Resources, Conservation and Recycling, 154, 104631.

Yildiza, G., Duraković, B., & Abd Almisrebb, A. (2021). Performances Study of Natural and Conventional Building Insulation Materials. International Journal on Advanced Science, Engineering and Information Technology, 11(4), 1395-1404.

Session VI
Modification & functionalization

Quantitative and qualitative aspects of industrial drying of Turkey oak lumber

Iulia Deaconu[1], Bogdan Bedelean[1], Sergiu Georgescu[1], Octavia Zeleniuc[1], Mihaela Campean[1*]

[1] Transilvania University of Brasov, Faculty of Furniture Design and Wood Engineering. Str. Universitatii nr. 1, 500036 Brasov, Romania

E-mail: iulia.deaconu@unitbv.ro; bedelean@unitbvro; sergiu.georgescu@unitbv.ro; zoctavia@unitbv.ro; campean@unitbv.ro

ABSTRACT

The main objective of this research was to evaluate the drying time and drying quality of Turkey oak lumber (*Quercus cerris* L.) compared to European oak lumber (*Quercus robur* L.). For both species, 50mm thick lumber boards were cut from freshly harvested logs, and then dried within the same batch, in a conventional kiln. The drying rate, the uniformity of the final moisture content, the casehardening degree, and the number and gravity of cracks were assessed for both species. The research showed that Turkey oak wood requires a longer time to eliminate the bound water than European oak when exposed to the same drying conditions. The final moisture content is more scattered, the casehardening degree is higher. Surface cracks and end cracks prevailed in the European oak boards. Internal cracks occurred only in Turkey oak boards, but in a very low amount.

INTRODUCTION

Turkey oak (*Quercus cerris* L.) is a fast-growing deciduous tree species which naturally grows in the southern Europe and Asia Minor (De Rigo *et al.* 2016). Its distribution area, in mixed hardwood forests, also includes France, Italy, England, Balkan Peninsula, Albania and Lebanon (Stafasani and Toromani 2015; Najib *et al.* 2021). In Romania, Turkey oak (*Quercus cerris*) is widespread in the plains, in the forest-steppe area and in the forest area of Muntenia and Oltenia, from where it rises to the hills, so that it frequently can be found in the western part of Transylvania and in the Banat. It also appears isolated, in the Apuseni Mountains and in the south of Dobrogea (Vlasin and Vlasin 2015) (Figure 1).
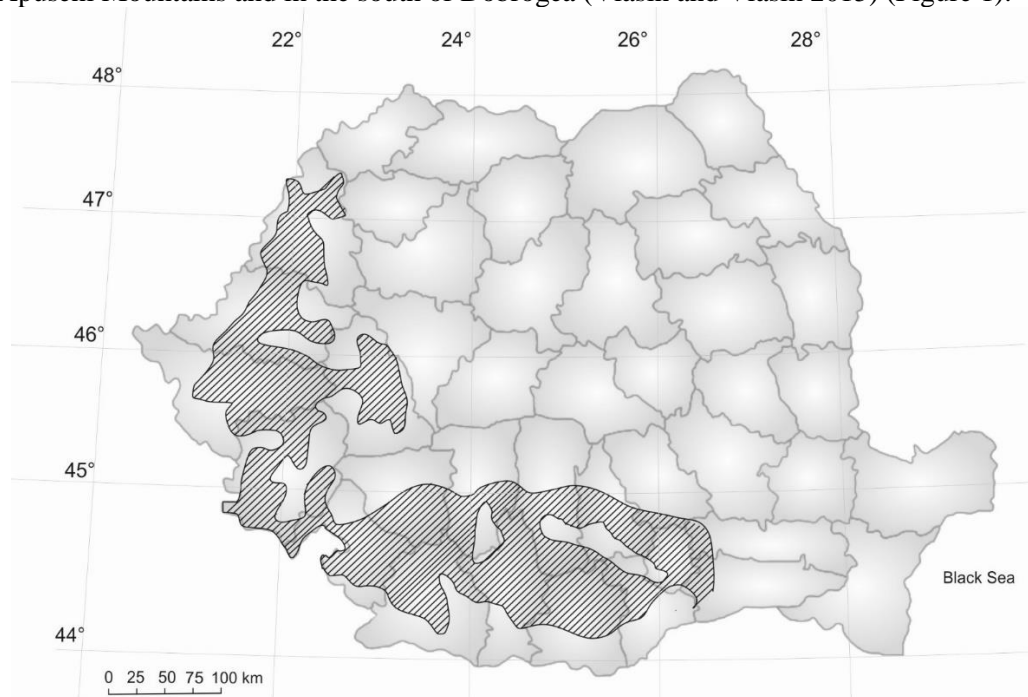

Figure 1: Areal of natural Turkey oak forests in Romania (after Stanescu 1979)

The surface covered by oak forests represents 17.3% from the total forest area in Romania. The sessile oak represents the most spread oak species with 10.8% of the total forest area in Romania, followed by Turkey oak (2.9%), and European oak (2.2%). Out of this volume, about 2.2 million m^3 are harvested annually (https://insse.ro).

The Turkey oak tree is considered tolerant to air pollution (De Rigo *et al*. 2016) and it is known for its role in the soil conservation and erosion control. The wood is used for lumber production (Praciak, et al 2013), railway sleepers, but most frequently as firewood (Clinovschi 2005).

Considering its high tendency to crack or warp during drying (Ferrari *et al.* 2013), Turkey oak is known as one of the most difficult to dry European species.

Turkey oak has an inhomogeneous annual ring structure, and higher density (720-810 kg/m^3) than other species of oak (Fodor and Hofmann 2024; Deaconu et al. 2023b). Therefore, choosing a proper drying method becomes difficult and challenging. The drying methods which are most frequently used in lumber industry (Avramidis *et al*. 2023) are synthetised in Table 1.

Table 1: Drying methods

A. Convective drying		B. Vacuum drying		
A1.Conventional drying with low/high air temperature	**A2**.Dehumidification drying	**B1**.Conductive drying	**B2**.Superheated steam drying	**B3**.Dielectric drying
-industrial kilns the most used; different kiln types depending on the manufacturers	-electrical dryers; longer drying time and no conditioning capacity; lower cost	-with hot plates as heating elements	-convective drying in vacuum, with lower drying rates	-heating by electromagnetic waves at various frequencies -1-40MHz radio frequency vacuum
At atmospheric pressure		The atmospheric air pressure of about 1000 mbar		

Generally, each of these drying methods could be employed for the drying of any wood species, but in order to obtain a quality drying (as required by furniture industry), it is necessary to acknowledge their advantages and limitations (Table 2).

According to the data presented in Table 1 and Table 2, the most economic and qualitative drying method for Turkey oak is by vacuum drying with superheated steam, especially for lumber with lower moisture content. Conventional drying can also be applied, following a customized drying schedule taking into account that Turkey oak is sensitive to temperature, has a lower saturation point and the wood has growth defects (Deaconu *et al.* 2023a). On the other side, the drying temperature should be low enough to avoid the undesirable discolorations that could appear during drying due to the large amount of sapwood extractives (Deaconu et al. 2023b). The improper drying could lead to devaluation of the lumber due to defects occurring during drying such as cracks, casehardening, discoloration, deformation, causing losses for the factory.

Literature data concerning the proper drying of Turkey oak wood are scarce. Ferrari *et al*. (2013) applied with good results a combined steaming air-drying-thermo-vacuum treatment on the air-seasoned Turkey oak boards. The steaming was performed at temperatures around 100-110°C, and 160°C for the vacuum treatment. The applied treatment led to an increase of the dimensional stability and colour homogeneity. Other authors have studied wood modification processes (heat and steam treatments) to improve the Turkey oak wood properties and also the uniformization of the surface colour (Todaro *et al.* 2012, Todaro *et al*. 2013). The dry thermal treatment (with temperatures ranging between 180-200°C) was applied to enhance the fungal decay resistance of both sapwood and heartwood of Turkey oak (Horváth and Csupor 2012). There are no data in the literature about drying schedules or defects that could appear in the conventional drying.

Though vacuum drying in superheated steam seems to be the the best choice for Turkey oak wood, this is a very low spread drying method in Romania. Most companies use conventional drying for all species. Thus, the need for investigating the drying behaviour of Turkey oak wood under different drying conditions was emphasised, in order to establish an industrially applicable drying schedules, for the qualitative conventional drying of Turkey oak lumber.

Table 2: The advantages and disadvantages of the drying methods

Drying methods				
• A1	• A2	• B1	• B2	• B3
Advantages				
A1.1.Temperatures <100⁰C • suitable for all species, especially for softwoods and hardwoods with different thickness; • good quality according to the market requirements **A1.2.Temperatures >100⁰C** • short drying time; • freshly cut material can be dried; • the wood keeps its natural colour	• suitable for high thicknesses, especially for hardwood species; • lower energy consumption	• suitable for high or medium permeability species (e.g. beech)	• suitable for softwood and hardwoods beams; • recommended for hardwoods with typically ring-arranged pores (e.g. oak; • good quality without discoloration	• suitable for thick boards; • very short drying time; • excellent quality of dried products • for species prone to collapse that cannot be dried qualitatively by any other process.
Disadvantages				
A1.1.Temperatures <100⁰C • maintenance of the wetting pipes; • low thermal efficiency at removing air from the installation and high thermal energy consumption (560-700 kWh/m³); • long drying time. **A1.2.Temperatures >100⁰C** • the temperature exceeds 100°C, which determines the application of this procedure only to the softwoods; • the internal tensions could develop; • inadequate quality of lumber; • the highest cost	• the maximum temperature used is 60°C; • the drying time is increased in the case of softwoods • high electricity consumption (120-380 kWh/m³)	• steam under vacuum has lower heat capacity; • lower drying rates; • not suitable for timber with higher moisture content • maintenance is costly; • high energy consumption		• very high initial investment; • small capacity; • higher drying cost

After carrying out a series of preliminary studies (Deaconu et al. 2023a; Deaconu et al. 2022), the authors pursued to the next level, and implemented the gained knowledge for building-up a drying schedule for the industrial-scale drying of Turkey oak lumber by the conventional method. The objective of the present research was to evaluate comparatively the effects of this drying schedule upon the drying time and drying quality of 50mm thick Turkey oak lumber (*Quercus cerris* L.) and European oak lumber (*Quercus robur* L.), dried within the same batch, in an industrial dryer.

MATERIALS AND METHODS
The wooden material used within this research consisted of 2-3.5m long, 10-30cm wide, and 50mm thick lumber boards, cut from freshly harvested Turkey oak and European oak logs, originating from the Southern Sub-Carpathians area (Valcea county, Romania).
Eight stacks of Turkey oak and twenty-four stacks of European oak lumber boards were dried within the same batch, in a 100m³ conventional industrial dryer by SECAL (Italy). The average initial moisture content, measured on 20 of the wettest boards from each species by means of a LG9NG moisture-meter from Holzmeister (Italy) was 66.2±7% for the Turkey oak lumber, and 66.9±2% for the European oak lumber.
The applied drying schedule is presented in Table 3. This is a very mild drying schedule, usually applied for the industrial drying of thick oak lumber in the company where the experimental batch was dried.

Table 3: Drying schedule applied for the kiln-drying of 50mm thick lumber

Phase	Wood moisture content [%]	Air temperature [°C]	Equilibrium moisture content [%]	Drying gradient
Initial heating	Initial MC	32	18	-
Actual drying	Initial MC…30	35	18	-
	30…24	38	15.8	2.2
	24…16	44	10.9	2.3
	16…8	48	7	2.5
Conditioning	8	44	8	-
Cooling	8	30	-	-

The moisture content inside wood ($\omega_{1/3}$) was measured by means of eight resistive sensors, half being placed in Turkey oak, and half in European oak lumber boards. The temperature was measured by means of a resistive sensor, and the equilibrium moisture content (EMC) by means of a cellulosic-plate sensor. The process was continuously monitored by means of an automatic kiln control system endowed with EPL SuperVisor software. Also, a kiln record sheet was manually kept throughout the whole process, with daily recordings of the main drying parameters, in order to enable the calculation of the drying rate (w) (Eq. 1) in each stage of the moisture decrease interval.

$$w = \frac{\Delta \omega}{24h} \ [\%/day] \tag{1}$$

At the end of the process, the drying diagram was saved. The kiln record sheet and the drying diagram were used as main tools for the assessment of the drying time and drying rate. They were also a facile way to compare the two species in terms of their drying dynamics under the same drying schedule.

According to EN 14298:2004, the drying quality is expressed by the uniformity of the final moisture content within a batch. Optionally (for lumber thicker than 40mm), the quality control may also be completed by assessing the casehardening degree as well (ENV 14464:2002).

According to the batch size, EN 12169:2000 establishes how many stacks must be randomly selected and opened (*e.g.* for a batch with 12+ stacks, 4 stacks must be opened). In the present research, 2 stacks for each species were selected. Furthermore, the standard also specifies how many lumber pieces should be measured, depending on the sampling procedure and the batch size. In the present research, when opting for the simple sampling procedure, AQL 6.5, for a batch comprising 1201-3200 lumber pieces, the standard states that 125 should be measured. A number of 126 pieces was adopted, 63 for each species.

The final moisture content was measured in three positions (at 40cm distance from the board ends and at mid-length) on the 63 selected boards of each species, by means of a HM9 moisture-meter by Merlin, Austria (non-destructive capacitive measurement). The average value was calculated for each board, then for the whole batch (for each species, separately).

In order for the lumber batch to be compliant, two criteria must be met:
- the average moisture content of the 63 values compared to should be within $\omega_{tar} \pm 1,5\%$ (when $\omega_{tar}=10…12\%$), and $\omega_{tar} \pm 1\%$ (when $\omega_{tar}=7…9\%$), where ω_{tar} is the targeted moisture content (in the present research, we considered: $\omega_{tar}=10\%$ for Turkey oak and $\omega_{tar}=8\%$ for European oak);
- 93.5% of the pieces must have an individual moisture content between $0.7\omega_{tar}$ and $1.3\omega_{tar}$.

If either one of these requirements is not fulfilled, then the batch cannot be considered compliant with regard to the moisture content uniformity.

Having in view the thickness of the lumber dried within this research (50mm), a casehardening test was also considered necessary. The testing method, by measuring the gap opening between the two halves of the samples after conditioning in a climate chamber (ENV 14464:2002), is schematically presented in Figure 2. According to reference literature (Welling 1994), a casehardening degree below 3mm is considered allowable, while 3mm already indicates severe casehardening, which means a high level of internal stresses, and thus, high risk for cracks. The test was performed on 16 boards from each species. One-Way ANOVA was applied to determine if there is a significant difference between the

casehardening degree of the samples obtained from Turkey oak wood and European oak wood. An alpha significance level of 5% ($\alpha = 0.05$) was used in the analysis. The statistical test was performed in the Microsoft Excel program using the Data Analysis Toolpack (Oleksik and Rosca 2023, Gravetter and Wallnau 2011).

A visual analysis of all 63 selected boards from each species was also performed after drying. in order to assess the number and gravity of cracks.
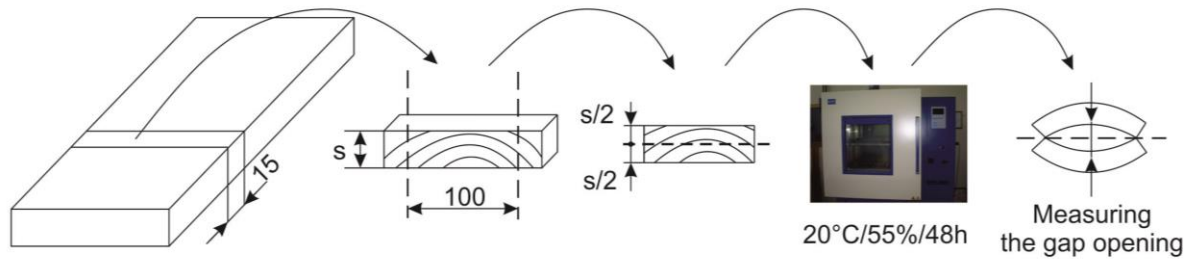

Figure 2: Test for the determination of the casehardening degree of lumber after drying

RESULTS AND DISCUSSION

Drying Time and Drying Rate

The drying diagram is presented in Figure 3. As can be noticed, the process began with an initial heating phase where the temperature reached 32°C and the EMC was increased up to 18.2%. During this phase, the moisture content of Turkey oak wood increased by 3.5 %, and that of European oak wood by 1.8%. The initial heating was performed within 24 hours. Afterwards, the EMC was lowered to 17.1% in order to begin the actual drying. The temperature was maintained fairly constant at 35.2°C, and the EMC gradually decreased from 17.1% to 14.8% within the 51 days of actual drying until the average moisture content measured by all 8 MC-sensors reached 30%. At this point the gradual increase of the temperature began, at a rate of around 0.3°C/day, up to a maximum value of 52°C towards the end of the process. Simultaneously, the EMC was continuously lowered from 14.8% to 3.9%. The actual drying period lasted 2664 hours. During this time, the Turkey oak boards reduced their moisture content from 66.2% to 10.8%, while the European oak boards dried from 66.9% to 8%, which equivalates to a drying rate of 0.5%/day for Turkey oak, and 0.53%/day for European oak. Finally, the heating and spraying were stopped, and the air vents were opened in order to perform cooling for 24 hours. The total time of the process was 2712 hours (3.7 months).
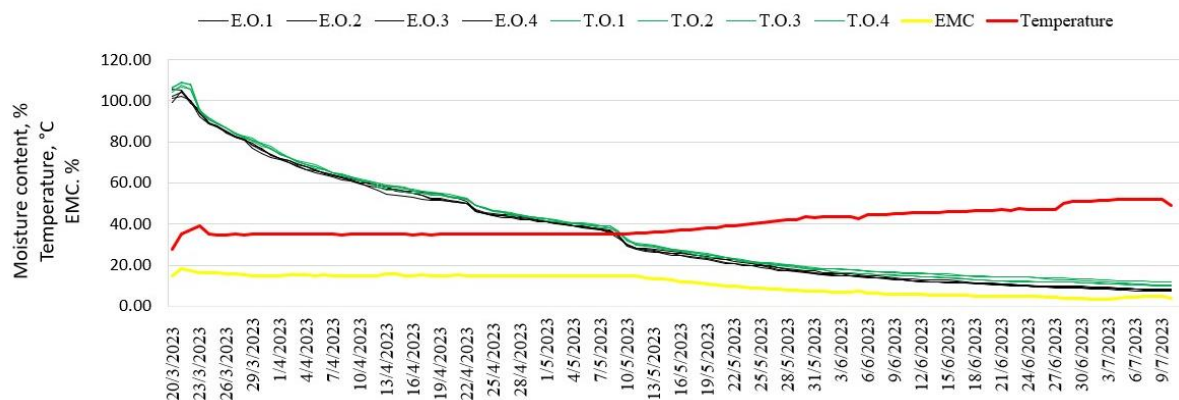
Figure 3: Drying diagram for Turkey oak and European oak boards dried in an industrial kiln
E=European oak; T=Turkey oak

When comparing the industrially applied drying schedule with the one used by the authors within a laboratory-scale drying test of Turkey oak lumber (Deaconu et al. 2023a), it can be observed that they are similar, yet some differences can be noticed:

- the industrial schedule foresees a slightly higher temperature (35°C instead of 30°C) for the actual drying above the fibre-saturation moisture content, and a much lower temperature (48°C

- compared to 60°C in the laboratory-scale trial) for the actual drying below the fibre-saturation point;
- the moisture content chosen for the raise of temperature was slightly higher (30% instead of 24% adopted within the laboratory-scale drying);
- the industrial schedule did not foresee a conditioning period.

In order to assess more accurately the differences regarding the drying dynamics of the two species, the drying rate was calculated over several moisture decrease intervals. The results are given in Table 4.

Table 4: Drying rate of 50mm thick Turkey oak and European oak lumber in an industrial kiln

Moisture decrease interval	Drying rate [%/day]	
	Turkey oak	European oak
60 … 30	1.4…1.0…0.6	1.4…1.0…0.6
30 … 20	0.9…0.6…0.3	0.8…0.6…0.4
20 … 15	0.3	0.5
15 … 10	0.2	0.3
10 … 8	-	0.1

The values in Table 4 show that the free water removal takes place with similar speed in both species, with a maximum rate of 1.4%/day. The value is slightly higher than in the laboratory-scale test (1.3%/day), which was expected due to the higher temperature applied in the industrial kiln in the initial stage of actual drying.

As far as the bound water removal is concerned, Table 4 clearly shows that the drying of European oak is faster in this stage than that of Turkey oak. This is the reason why within the given time, European oak reached a lower final moisture content (8%) than Turkey oak (10.8%). The values obtained within the industrial test are much lower than in the laboratory-scale test (0.8%/day), which must be due to the lower temperature applied in the industrial dryer.

Trying to compare the obtained values with results obtained by other researchers, no data were found in reference literature for the drying rate of Turkey oak. For 50mm thick European oak, Sergovski (1968) indicates an average drying rate of 0.1%/h, meaning 2.4%/day from 60% to 12% moisture content, and Unsal (2002) indicates an average drying rate of 0.04%/h, meaning 0.96%/day from 60% to 9.7% moisture content. The higher drying temperatures used in the the two cited references, and the fact that no differentiation between the free water and bound water removal was made, may explain why their reported values were higher.

Drying Quality

## Uniformity of Final Moisture Content

As far as the quality control is concerned, first the final moisture content was measured, on 63 boards, randomly selected from 2 stacks of each species, which were also randomly selected.from the 32-stacks batch. The results are presented in Figure 4.

It can be noticed that for both species, the average value is situated within the admittance interval given as function of the targeted moisture content:

- for European oak $\omega_{final, average} = 8.06 \in [\omega_{tar}\pm1\%]$, meaning 7…9%;
- for Turkey oak: $\omega_{final, average} = 10.17 \in [\omega_{tar}\pm1.5\%]$, meaning 8.5…11.5%.

Thus, the first compliance criterion required by EN 14298:2004 is fulfilled for both species. However, the values are more scattered in the case of Turkey oak, as indicated by the higher standard deviation. This was an expected result considering the higher inhomogeneity of this species.

By counting the boards which had a final moisture content within the interval $[0.7\omega_{tar} …1.3\omega_{tar}]$ it was revealed that 59 boards (93.5%) in case of Turkey oak, and 62 boards (98.41%) in case of the European oak boards fulfilled this criterion. This means that, according to EN 14298:2004, the Turkey oak boards barely fulfilled this second criterion of compliance, while with the European oak clearly fulfilled it.
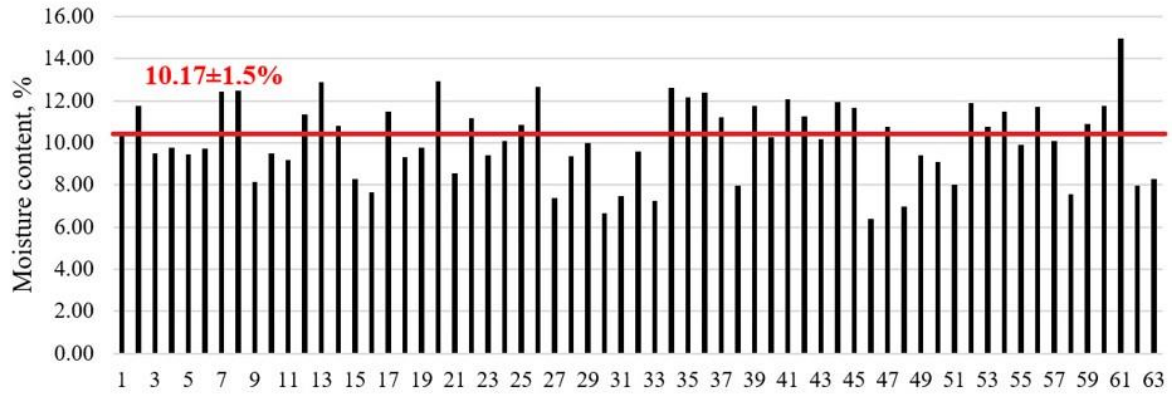
a.
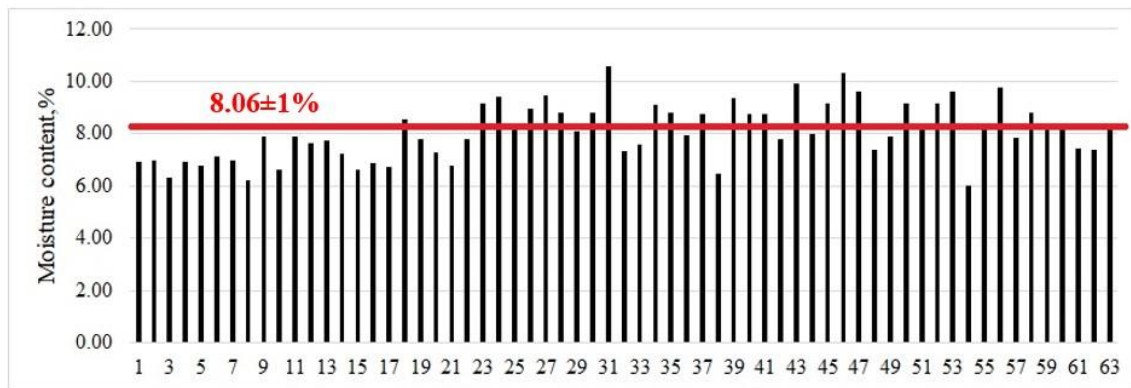
b.

Figure 4: Final moisture content of Turkey oak (a) and European oak (b) lumber dried in an industrial kiln by conventional drying

Casehardening

A number of 16 samples from each species were tested and their casehardening degree was assessed by measuring the gap opening after conditioning in a climate chamber (Figure 5). The measured gap opening values are presented in Figure 6. From both Figure 5 and 6 it can be noticed that the Turkey oak boards displayed a higher casehardening value. The One-Way ANOVA test performed with the 16 samples demonstrated that there is a significant difference between the two species regarding the casehardening degree after drying (p-value < 0.05, according to Table 5).

a.   *b.*

Figure 5: Casehardening samples: a – Turkey oak; b – European oak

a.

b.
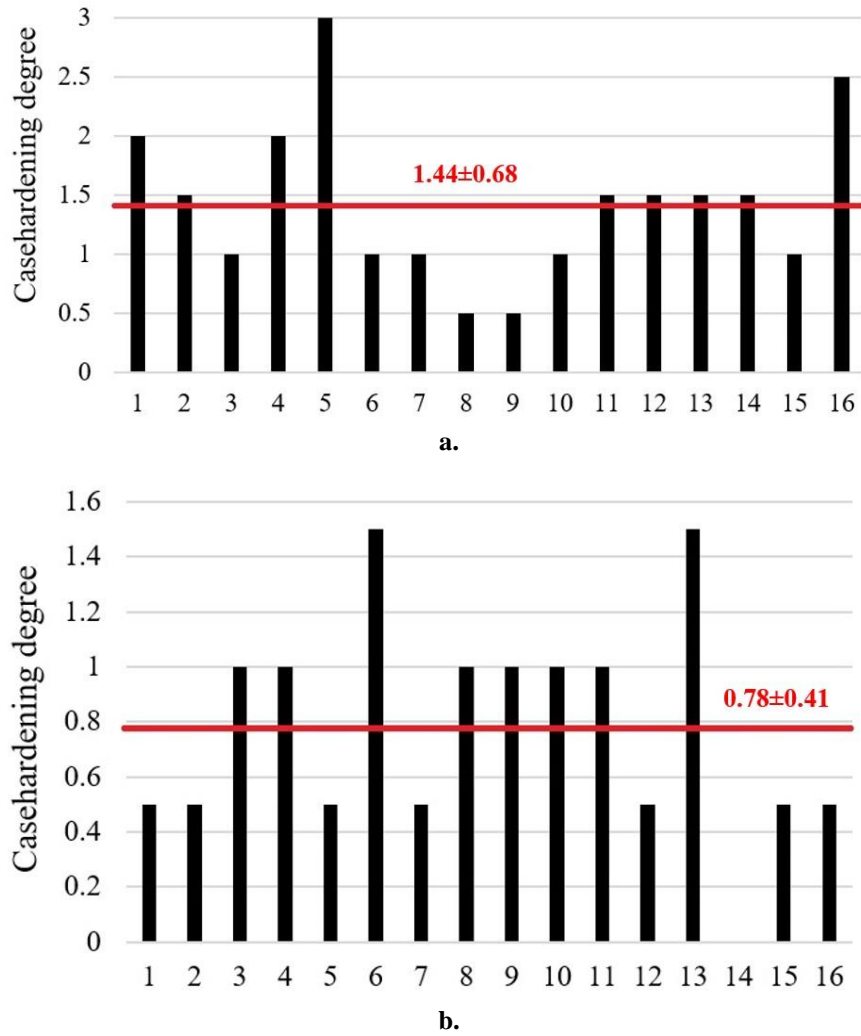
***Figure 6: Casehardening degree** of Turkey oak (a) and European oak (b) lumber dried in an industrial kiln by conventional drying*

Table 5: ANOVA results concerning the casehardening degree of Turkey oak wood vs. European oak wood

Groups	Count	Sum	Average	Variance	Standard deviation
Turkey oak	16	23	1.4375	0.4625	0.680074
European oak	16	12.5	0.78125	0.165625	0.406971

Source of Variation	SS	df	MS	F	P-value	F crit
Between Groups	3.445313	1	3.445313	10.97015	0.002422	4.170877
Within Groups	9.421875	30	0.314063			
Total	12.86719	31				

Compared to the gap opening values obtained after the laboratory-scale drying (2.5±0.5mm for 50mm thick Turkey oak lumber) (Deaconu et al. 2023a), it could be noticed that the industrial schedule lead to lower casehardening of Turkey oak wood. The lower temperature throughout the process enhanced this better result, which was also sustained by a quite good result concerning the cracks occurrence.

Cracks

The visual examination of the boards revealed that:

- in case of Turkey oak: 6 (9.5%) of the analysed boards presented severe surface cracks, and 14 (22.22%) presented end cracks in spite the end protection with paraffin-based sealer. Only 2 boards of the inspected ones (3.17%) presented internal cracks as well;
- in case of European oak: 37 (58.7%) of the analysed boards presented severe surface cracks, and 55 (87.3%) presented end cracks. 35 boards (55.55%) presented surface and end cracks, but no board displayed internal cracks.

The better result for Turkey oak wood than for European oak is related to the fact that the latter consisted in wider lumber pieces, including the wood heart (which is removed after drying).

CONCLUSIONS

The performed research allowed formulating the following conclusions:

- The initial moisture content of Turkey oak is quite similar to that of European oak.
- The free water removal occurs with similar speed, with an average of 1%/day. So basically, the actual drying down to the fibre saturation moisture content usually lasts about 1-1.5 months at a temperature of 35°C and an EMC gradually decreasing from 18% to 14.8%.
- The bound water removal is slower in Turkey oak than in European oak wood. The average drying rate is 0.6%/day for a moisture decrease from 30% to 20%; 0.3%/day for 20%...15%, and 0.2%/day for 15…10%. This is the reason why when drying both species within the same batch, a difference of 2-3% between the final moisture contents will occur (e.g. 10-11% for Turkey oak wood, while European oak reaches 8%).
- The European oak lumber dries more evenly than the Turkey oak lumber. The final moisture content is less scattered than in the case of Turkey oak. However, with a mild drying schedule as applied in this industrial test, the compliance requirements can be reached for the Turkey oak lumber as well.
- The Turkey oak lumber develops higher stresses during drying. The gap opening values obtained were significantly higher than the ones obtained with the European oak samples dried under the same conditions. However, due to the mild drying schedule applied, no severe casehardening (>3mm) was recorded.
- Both species developed an important percentage of cracks. Surface cracks and end cracks affected more the European oak lumber. More than half of the tested pieces displayed cracks. This was mainly due to the fact that the heart has not been cut out of the boards prior to drying. Internal cracks were present only in the case of Turkey oak lumber, but in a very low proportion.

REFERENCES

Avramidis S, Lazarescu C, Rahimi S (2023) Basics of wood drying. In: Springer Handbook of Wood Science and Technology, Springer Nature Switzerland AG, pp. 679-704 https://doi.org/10.1007/978-3-030-81315-4_13

Clinovschi F (2005) Dendrology (in Romanian language), Publishing House of Suceava University

De Rigo D, Enescu CM, Caudullo, G (2016) Quercus cerris in Europe: distribution, habitat, usage and threats. Chapter in book: European Atlas of Forest Tree Species Publisher: Publication Office of the European Union, Luxembourg, pp 148-149

Deaconu IT, Georgescu SV, Campean M (2023a) Drying behaviour of 50 mm thick Turkey oak lumber. Appl. Sci. 13(19): 10676. https://doi.org/10.3390/app131910676

Deaconu IT, Porojan M, Timar MC, Bedelean B, Campean M (2023b) Comparative research on the structure, chemistry, and physical properties of Turkey oak and sessile oak wood. BioResources 18(3): 5724-5749.

Deaconu IT, Georgescu SV, Campean M (2022) Evaluating a drying schedule for oak lumber through drying rate calculation and quality assessment. PRO LIGNO 18(2): 42-47.

EN 12169:2000 Criteria for the assessment of conformity of a lot of sawn timber. https://standards.iteh.ai/catalog/standards/cen/ff8f923d-1bba-4d0b-ad08-3c28c1b6c2fc/env-12169-2000

EN 14298:2004 Sawn timber- Assessment of drying quality. https://standards.iteh.ai/catalog/standards/cen/aa69f719-6a33-442c-95a0-bbd7dd3c679f/en-14298-2004

ENV 14464:2002 Sawnt timber- Method for assessment of case-hardening. https://standards.iteh.ai/catalog/standards/cen/016624f6-9158-4a8e-83bb-3ca54dc4659d/env-14464-2002

Ferrari S, Allegretti O, Cuccui I, Moretti N, Marra M, Todaro L (2013) A revaluation of Turkey oak wood (Quercus cerris L.) through combined steaming and thermo-vacuum treatments. BioResources 8(4): 5051-5166. https://doi.org/10.15376 biores.8.4.5051-5066

Fodor F, Hofmann T (2024) Chemical Composition and FTIR Analysis of Acetylated Turkey Oak and Pannonia Poplar Wood. Forests, 15(1): 207. https://doi.org/10.3390/f15010207

https://insse.ro/cms/sites/default/files/field/publicatii/statistica_activitatilor_din_silvicultura_in_anul_2022.pdf. Accessed: February 2024

Gravetter FJ, Wallnau LB (2011) Essentials of statistics for the behavioral Sciences, Seventh Edition,Wadsworth, Cengage Learning, Belmont, CA, USA

Horváth N and Csupor K (2012) The protective effectiveness of dry heat treatment on Turkey oak against fugal decay. In the Proceedings of the 5th Conference on Hardwood Research and Utilisation in Europe - Hardwood Science and Technology (Sopron, Hungary) pp. 361-369

Najib R, Houri T, Khairallah Y, Khalil M (2021) Quercus cerris L.: An Overview. – Forestry Studies | Metsanduslikud Uurimused 74: 1–9. https://doi.org/10.2478/fsmu-2021-0001

National Institute of Statistics (INS) (2022) Statistica activitatilor din silvicultura https://insse.ro/cms/sites/default/files/field/publicatii/statistica_activitatilor_din_silvicultura_in_anul_2022.pdf. Accessed 2 March 2024

Oleksik M, Rosca L (2023) Data analysis with Microsoft Excel (in Romanian). Pro Universitaria Publishing House, Bucharest, Romania.

Praciak A (2013) The CABI encyclopedia of forest trees (CABI, Oxfordshire, UK). https://doi.org/10.1079/9781780642369.0000

Sergovski PS (1968) Heat treatment and preservation of wood. Publishing House "Lesnaia promAslennoti", Moskow, Rusia

Stafasani M, Toromani E (2015) Growth-Climate Response of Young Turkey Oak (Quercus cerris L.) Coppice Forest Stands along Longitudinal Gradient in Albania. SEFOR South-East Eur Forestry 6 (1): 25-38. http://dx.doi.org/10.15177/seefor.15-05

Stanescu V. (1979) Dendrologie. Didactica si Pedagocica Publishing, Bucharest

Unsal, Ö (2002) Effect of kiln dimensions and air speed on drying quality and duration in technical drying (in Turkish language). Journal of İstanbul University 52(1): 101-109

Vlasin VA, Vlasin HD (2015) Species with restrained areal: Quercus cerris, Quercus frainetto and Larix decidua (in Romanian language). Caietele Sextil Puşcariu, II, Cluj-Napoca, pp. 498–519. Online at: http://inst-puscariu.ro/SextilPuscariu/SPII/pagini/CSP%20II%20[Pages%20498%20-%20519].pdf. Accessed 2 March 2024

Todaro L, Zanuttini R, Scopa A, Moretti N (2012) Influence of combined hydrothermal treatments on selected properties of Turkey oak (Quercus cerris L.) wood. Wood Science and Technology 46 (1-3): 563-578

Todaro L, Dichicco P, Moretti N, D'auria M (2013) Effect of combined steam and heat treatments on extractives and lignin in sapwood and heartwood of turkey oak (Quercus cerris L.) wood. BioResources 8(2): 1718-1730.

Welling, J (1994) EDG Recommendation. Assessment of drying quality of timber. Pilot edition.

Changes in properties of maple by hygrothermally treatment for accelerated ageing at 135-142°C

Tobias Dietrich[1*], Herwig Hackenberg[1], Mario Zauer[1], Holger Schiema[2], André Wagenführ[1]

[1] TUD Dresden University of Technology, Institute of Natural Material Technology, 01062 Dresden
[2] Institute für Musikinstrumentenbau IfM e.V., 08267 Zwota

E-mail: tobias.dietrich@tu-dresden.de; herwig.hackenberg@tu-dresden.de;
mario.zauer@tu-dresden.de; andre.wagenfuehr@tu-dresden.de

Keywords: Maple, hygrothermal treatment, accelerated ageing

ABSTRACT
The subject of the investigations carried out was the artificial ageing of European maple (*Acer* L.), which is used for the production of bodies in violins. Typically, instrument makers air drying their planks for several years in different conditions before the use as tone wood in violins. The investigated process could shorten this storage time and the achieved colour change make an artificial colouring in the process chain obsolete. Additionally, acoustic properties and moisture behaviour can be improved. European maple was used for the treatment process in a closed chamber. After air conditioning at 35% relative humidity (R.H.) at 20°C, maple planks where thermally modified (hygrothermal treatment) in a closed system at elevated pressure levels. The humidity inside the autoclave adjusted at 35% R.H. by calculation. The treatment temperature was set at 135°C and 142°C for twelve hours. Physically properties such as MOE, MOR, hardness, impact bending strength and vibrational behaviour were carried out. Water storage and sorption tests were also performed. Three reference and 3 modified violins where build and acoustic tests were performed.
Due to the moist atmosphere during treatment, there are some significant changes, even at these "low" treating temperatures. Acoustic properties such as resonance quality and damping could be improved slightly, while impact bending was decreased with increasing treatment temperature. EMC and swelling properties could be improved as well even at 135°C. Instruments build of these materials at this temperature showed a slightly better acoustic.
The investigated process could be interesting in the construction of musical instruments, as natural aging processes can be accelerated with less primary energy compared to a classical thermowood processes and the swelling and shrinkage behaviour is improved.

INTRODUCTION
For the production of high quality violins, only superior maple qualities are used for the back plate and the sides of the body. Typically, the instrument makers are searching for specific trees to cut down and after trimming these to planks a long naturally drying process is done. Therefore, the end grain is sealed with paraffin and these planks are air dried outdoors under roof. Once the equilibrium moisture content (EMC) has been reached, these planks are dried further indoors. Many instrument makers say that the longer these processes take, the better the tonewood. Storage periods of 5 to 10 years are not uncommon. Technical drying of tonewood is also practiced, but this wood is rarely used for high-quality instruments due to its susceptibility for cracking. A survey study by Kránitz et al. shows that the properties of naturally aged wood are partially altered by long storage times (Kránitz et al. 2016). This strongly depends on the type of wood and different studies come to partly contradictory results. For example, the swelling does not change, but the EMC is slightly reduced. The impact bending strength is also lower. This is generally attributed to the reduced hemicellulose content that occurs during natural wood ageing. The colour also changes to a light brown tone. The statements on bending strength and modulus of elasticity are contradictory. Most of the summarized tests were carried out on spruce, pine and Asian softwoods, there is hardly any data on naturally aged maple. The assortments examined were 60-1600 years old.
It has to be stated, that these changes may not be stable. If the naturally aged wood is exposed to humidity levels above 95%, these changes in properties are reversed (Obataya et al. 2017). Kránitz et al. notes

that the changes are similar to those that occur during artificial wood ageing at temperatures of up to 150°C. Zauer for example examined beech wood (*Fagus sylvatica* L.) that was modified at 140°C and 160°C in a latex bag (self-atmosphere). Slight improvements in damping behaviour, resonance quality and hygric properties were observed (Zauer et al. 2016).

The behavior of wood after hygrothermal treatment at low temperatures has been little studied except for a few studies (Endo et al. 2016, Zeniya et al. 2019). These studies show, that the effects of long-term ageing can be qualitatively reproduced by hygrothermal treatment. Thereby, the thermal modification is taking place under presence of humidity or water in a pressurised atmosphere.

Endo et al. discovered a reduction of tan δ and an improved relationship of E/ρ after hygrothermal treatment of sitka spruce (*Picea sitchensisat* BONG) 120°C and 65% R.H. between 1 and 7 days. He also mentioned, that these changes are reversible after treating such treated wood at high humidity's over 95% (Endo et al. 2016). Zeniya measured a reduced EMC with deceasing humidity in dependency of the mass loss. At 35% R.H. during the treatment, the EMC was lowest. The weight loss was highest at 92 % R.H. and 120°C (Zeniya et al. 2019, Endo et al. 2016). Damping (tan δ) and the specific dynamic Young's modulus where improved under 62% R.H. and worsened at 92% R.H.. Some of these improvements were completely lost if the wood was subsequently treated with high humidity (Endo et al. 2016). Wentzel, on the other hand, was able to determine that eucalyptus wood (*Eucalyptus nitens* MAIDEN) stored in a closed reactor at 35% R.H. at 160°C did not lose its altered properties until it was subsequently stored in water. Storage alone at 95% R.H. was not sufficient for this (Wentzel 2018).

Also, most studies on artificial wood ageing have been carried out on spruce, pine and Asian softwoods. There is hardly any data on artificially aged maple.

For instrument making, it makes sense to investigate the process of artificial wood ageing further. The effects of natural wood ageing can be achieved through much faster artificial wood ageing. For example, effects could be recreated that only occur in very old instruments due to the long natural ageing process. The aforementioned effects of reduced EMC and slightly darker colours should be viewed positively. Since a reduced EMC will have an influence on the tonal properties due to the lower internal friction, artificial ageing can also be expected to have tonal advantages. Furthermore, the reduced swelling leads to less loading stress in the instrument. In large instruments such as the double bass, the top and back can be destroyed by cracks. These cracks occur in certain places and are caused by the large swelling shrinkage movement of the sides. The construction causes localized stress peaks that lead to cracks. In this study, therefore, in addition to examining THM maple, instruments made of this wood were also built and acoustically examined.

EXPERIMENTAL
Wood selection

European maple (*Acer* L.) retrieved from a violin maker as one plank was cut down to 9 pieces of 390x7,5x62mm³ (LxTxR), three for each set. These pieces were conditioned at 20°C/35% R.H. After modification these pieces where cut down to samples with a size of 190x6,5x28 mm³ (LxTxR) and conditioned at 20°C/50% R.H. as these climate is typically for the storage of musical instruments. Acoustic and mechanical tests were carried out on this sample size and this climate.

Hydrothermal Modification

Modification took place in a closed stainless steel autoclave. The humidity inside the autoclave at elevated pressures was set to 35 % R.H. and the needed moisture was calculated. For this calculation, the amount of water from the wood and the atmosphere was calculated and the needed moisture to achieve the atmosphere was calculated. If there was a difference, a petridish with the exact amount of water was added inside the autoclave. Thereby temperature and pressure could be measured during the treatment. With these values, it could be checked, if the calculated pressure was reached and therefore if the moisture of 35 % inside the autoclave was reached during the process.

The autoclave was placed in an oven and the heating ramp, temperature and time was set.

Treatment took place at 135 °C and 142 °C, the heating and cooling ramp was set to 20 K h^{-1} and the treatment time was set to 12 hours. The process took 23,5 h at 135 °C and 24,2 h at 142°C. These parameters were chosen because of the study of Zeniya et al. and Endo et al. , which showed the best improvement of tan δ, E/ρ and EMC. An uncorrected mass loss was calculated with the dry mass before and after the treatment.

Violin making

Three reference violins and three violins with modified maple back and sides at 135°C where build by a professional violin maker. To reduce scattering, the wood for the violins was taken from the same piece of trunk. Afterwards all violins where stored at 20°C/50% R.H..

Acoustic properties

Experimental modal analysis (EMA) was conducted after conditioning the samples in 20 °C/50 % R.H.. Measurement was done described by Sproßmann et al. (Sproßmann 2017). Dynamic MOE and damping were also calculated according to the study mentioned.

With calculating the density, the sound radiation coefficient R was calculated (1) with the dynamic modulus of elasticity E` and the density ρ.

$$R = \sqrt{\frac{E`}{\rho^3}} \tag{1}$$

To determine the sound characteristics of violins, frequency curves were recorded in an anechoic chamber, with the instruments being fixed in an appropriate device and excited with an impulse hammer pendulum on the bridge. The pendulum is deflected manually by an operator who simultaneously damps the strings by holding the instrument by the neck. The knocking sound resulting from the impulse hammer strike is recorded with three microphones distributed around the room. The excitation at the bridge takes place at two points: in the middle of the bridge, perpendicular to the soundboard, and at the upper corner on the outer edge of the bridge on the bass bar side parallel to the soundboard. There are 10 taps per excitation point. Three frequency responses are calculated in the analyser from the three tapping tone spectra and the impulse hammer spectrum also recorded, as an average over the 10 tapping points. The result of the measurement is six frequency response curves.

Mechanical properties

Three-point bending was done according to DIN 52186 for measuring the MOE and MOR. Impact bending tests were done with an Instron CEAST 9050 according to DIN EN ISO 179-1 but with samples of 6,5x6,5x80 mm (RxTxL) loaded in tangential direction to measure the impact bending strength (IBS).

Moisture related properties

Equilibrium moisture content was measured at 33%, 50% and 85% R.H. to calculate the swelling coefficient h in accordance with DIN 52184. The moisture levels were adjusted in a climate chamber at 20°C. Samples were cut down to 30x6,5x28 (LxTxR). Swelling was also measured by putting these samples is distilled water and applying a vacuum of 0,005 MPa. After full moisture uptake, the dimensions were measured.

RESULTS AND DISCUSSION

A mass loss can be observed as a result of hygrothermal treatment, which increases with increasing treatment temperature (Table 1). Compared to classic unpressurized thermal processes at comparable temperatures (140°C), the mass loss measured here is higher (Cermàk et al. 2021). Studies on spruce (*Picea abies* L.) treated hygrothermally at 130°C for 7 days showed a similar mass loss of 1.35 % (Karami et al. 2020). It can therefore be concluded that the degradation of hemicellulose by this hygrothermal treatment at these low treatment temperatures is greater than with open thermal processes due to the humid pressurized atmosphere. An accumulation of carboxylic acids within the wood in closed systems has been suggested as cause (Altgen et al. 2016).

The density does not change significantly as a result of treatment at 135°C; only at a temperature of 142°C can a slight significant reduction in density can be observed. The influence of this change in density on the sound properties is discussed below.

Table 1: Mass loss (ML) and density (ρ) and MOE after hygrothermal treatment

Temperature [°C]	ref	135	142
ML Mean [%]	-	0,92	1,26
ML SD [%]	-	0,09	0,12
ρ Mean [kg/m³]	769	761	748
ρ SD [kg/m³]	18	23	16
MOE Mean [MPa]	19365	19733	18628
MOE SD [MPa]	1571	1213	1796

The resonance quality can be increased significantly but only slightly at 135°C (Fig. 1). A further increase in temperature brings no further improvement. This is solely due to the increased modulus of elasticity and the relatively constant densities of the treated material. Zauer was also able to determine an increase in the resonance quality of beech wood at 140°C and 12 hours of treatment in vacuumised sealed bags (Zauer 2016). The damping behavior, on the other hand, is only significantly improved from a temperature of 142°C and reaches values that correspond to the established sound wood rosewood (*Dalbergia latifolia* ROXB.).
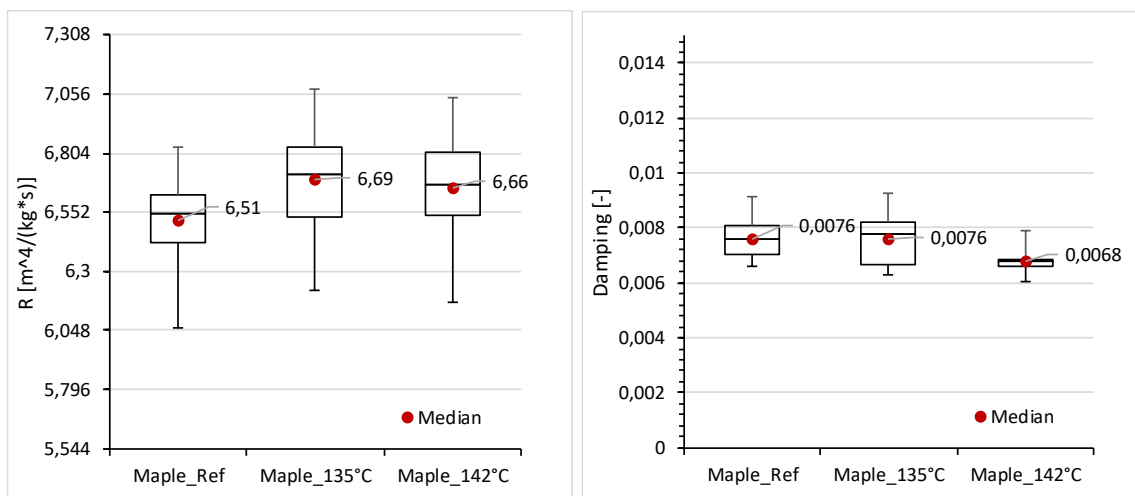

Figure 1: Left: Resonance quality; right: damping of unmodified and hygrothermal modified maple at 135°C and 142°C

The frequency curve measurements on the instruments show hardly any change in the Helmholtz resonance (f1) and the 1st top plate resonance (f2) (Fig. 2). But the clarity, sharpness and loudness improves. To summarize, it can be stated that the violins made from the modified material do not sound worse, but also no serious improvements in sound can be observed either compared to the reference instruments. In order to analyse the effects even more precisely and statistically reliably, many more violins would be needed, which is not possible given the price per violin.
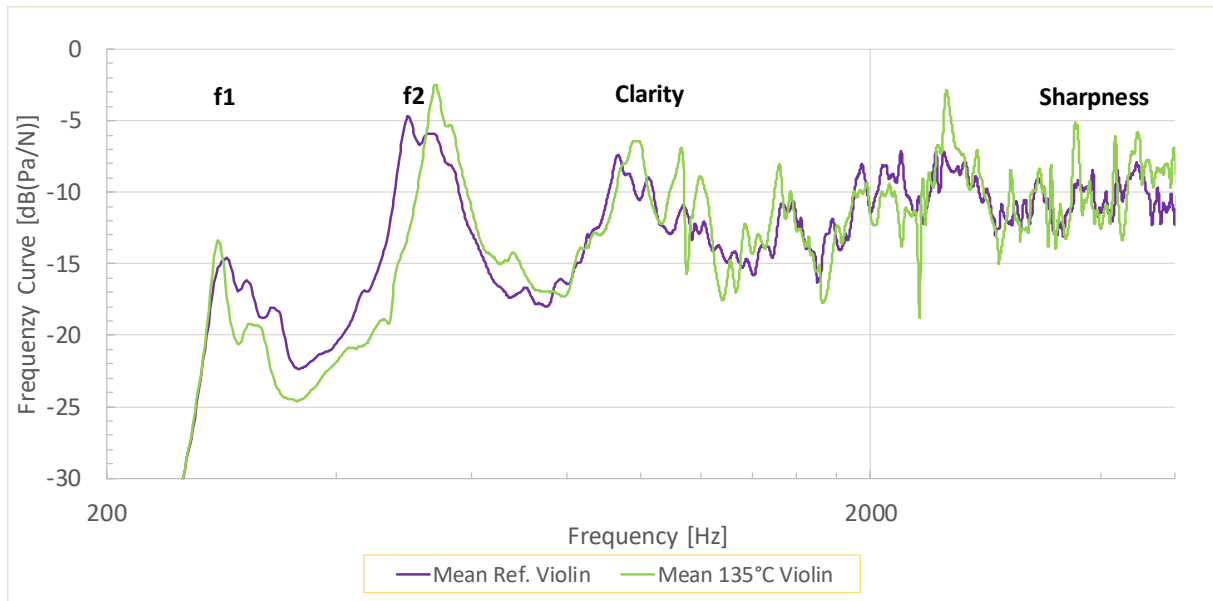
Figure 2: Frequency curves (mean) of reference and modified violins

While the bending strength does not drop significantly until a temperature of 142°C, the impact bending strength already drops significantly at 135°C and is halved at 142°C compared to native maple (Fig 3.). This clearly shows that despite the relatively low mass losses and the low treatment temperatures, the degradation of the hemicelluloses due to the moist pressurized atmosphere is high even at low temperatures leading to this brittleness. This must be taken into account with regard to the processing and use of such wood in instruments. During use and transportation, such instruments are exposed to mechanical stress, which can lead to damage if the material becomes brittle. A maximum treatment temperature of 135°C is therefore preferable.
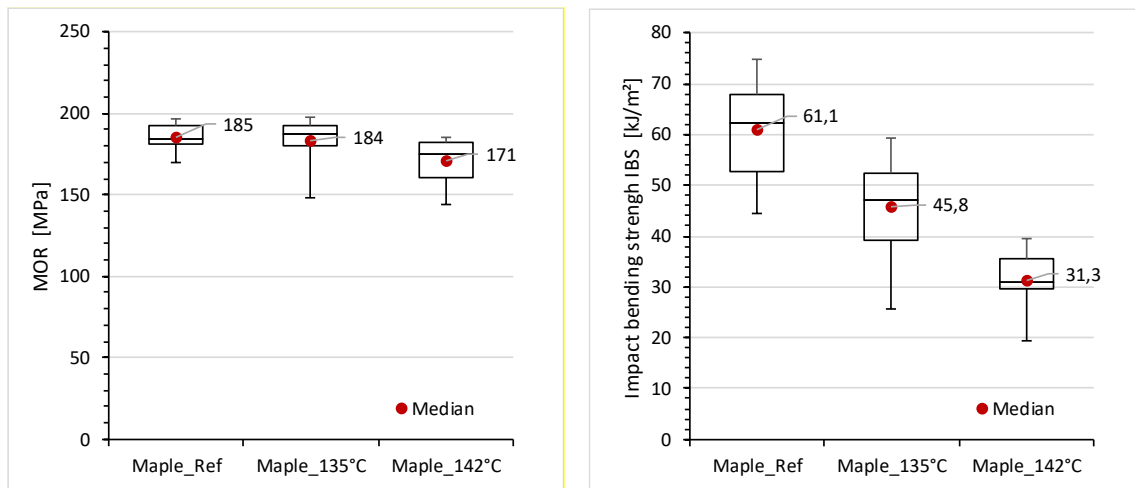
Figure 3: Left: Bending MOR; right: IBS of unmodified and hygrothermal modified maple at 135°C and 142°C

The equilibrium moisture content at 85% R.H. is already reduced by 17% at 135°C as a result of the treatment; increasing the temperature to 142°C reduces the equilibrium moisture content by 25% compared to untreated wood (Table 2). These reductions are also present at 50% R.H, but to a lesser extent. This known effect can be explained by the degradation of the hemicelluloses and the reduction of very small cell wall pores (Zauer et al. 2014), which is already pronounced at 135°C in the moist pressurized atmosphere.

Table 2: EMC at 85% R.H.

Temperature [°C]	ref	135	142
EMC$_{85}$ Mean [%]	14,9	12,3	11,3
EMC$_{85}$ SD [%]	0,2	0,2	0,4

The greatest changes can therefore also be observed in the swelling in liquid water and in the swelling coefficient (35% R.H. - 85% R.H.). Due to the hygrothermal treatment, both parameters decrease with increasing temperature (Fig 4.). Even at 135°C, the tangential swelling decreases by 12% and the swelling coefficient is reduced by 20%. This has advantages for use in the instrument, as the back and sides of the instruments swell and shrink less with changing humidity, thus reducing the load on the instrument. This is positive with regard to typical cracking of the soundboard in changing humidities.
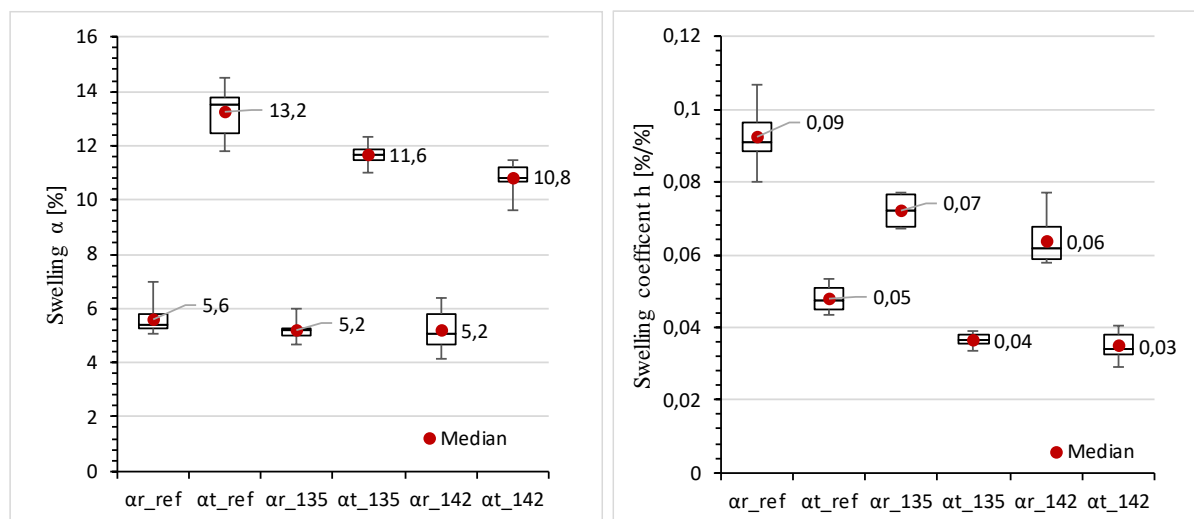

Figure 4: Left: Radial and tangential swelling of unmodified and hygrothermal modified maple; right: Radial and tangential swelling coefficient of unmodified and hygrothermal modified maple

CONCLUSION

The hygrothermal treatment of maple at 135°C and 142°C leads to changes in the mechanical, sorptive and acoustic properties. The sound-relevant properties of resonance quality and damping change only insignificantly. Instruments made of modified maple at 135°C showed also only slight improvements.

A temperature of 135°C was chosen for the production of the instruments. On the one hand, there is no serious deterioration in the bending strength and the deterioration of impact bending strength is acceptable at this temperature, but on the other hand the moisture-relevant properties are already improving. This means that fewer stress peaks occur in the instrument due to the reduced swelling shrinkage movement. As a result, there will be fewer cracks in the top plate.

Compared with the studies by Obataya, Zeniya and Endo, similar effects of hygrothermal treatment on maple could thus be demonstrated. Whether these changes are reversible is still being investigated.

REFERENCES

Altgen, M., Willems, W., Militz, H. (2016). Wood degradation affected by process conditions during thermal modification of European beech in a high-pressure reactor system. Eur. J. Wood Prod. 74, 653–662. https://doi.org/10.1007/s00107-016-1045-y

Čermák, P., Hess, D. Suchomelová, P. (2021). Mass loss kinetics of thermally modified wood species as a time–temperature function. Eur J Wood Prod 79:547–555. https://doi.org/10.1007/s00107-020-01634-6

DIN EN ISO 179-1:2010-11. Kunststoffe_- Bestimmung der Charpy-Schlageigenschaften - Teil_1: Nicht instrumentierte Schlagzähigkeitsprüfung (ISO_179-1:2010); Deutsche Fassung EN_ISO_179-1:2010, n.d. . Beuth Verlag GmbH. https://doi.org/10.31030/1625765

DIN 52186:1978-06. Prüfung von Holz; Biegeversuch, n.d. . Beuth Verlag GmbH. https://doi.org/10.31030/1260171

DIN 52184:1979-05. Prüfung von Holz; Bestimmung der Quellung und Schwindung, n.d. . Beuth Verlag GmbH. https://doi.org/10.31030/1260153

Endo, K., Obataya, E., Zeniya, N., Matsuo, M. (2016). Effects of heating humidity on the physical properties of hydrothermally treated spruce wood. Wood Sci Technol 50, 1161–1179. https://doi.org/10.1007/s00226-016-0822-4

Karami, E., Bardet, S., Matsuo, M., Bremaud, I., Gaff, M., Gril, J. (2020). Effects of mild hygrothermal treatment on the physical and vibrational properties of spruce wood. Composite Structures 253, 112736. https://doi.org/10.1016/j.compstruct.2020.112736

Kránitz, K., Sonderegger, W., Bues, C.-T., Niemz, P. (2016). Effects of aging on wood: a literature review. Wood Sci Technol 50, 7–22. https://doi.org/10.1007/s00226-015-0766-0

Obataya, E. (2017). Effects of natural and artificial ageing on the physical and acoustic properties of wood in musical instruments. Journal of Cultural Heritage 27, s. 63–69. https://doi.org/10.1016/j.culher.2016.02.011

Sproßmann, R., Zauer, M., Wagenführ, A. (2017). Characterization of acoustic and mechanical properties of common tropical woods used in classical guitars. Results in Physics 7, 1737–1742. https://doi.org/10.1016/j.rinp.2017.05.006

Wentzel, M., Altgen, M., Militz, H. (2018). Analyzing reversible changes in hygroscopicity of thermally modified eucalypt wood from open and closed reactor systems. Wood Sci Technol 52, 889–907. https://doi.org/10.1007/s00226-018-1012-3

Zauer, M., Kowalewski, A., Sproßmann, R., Stonjek, H., Wagenführ, A. (2016). Thermal modification of European beech at relatively mild temperatures for the use in electric bass guitars. Eur. J. Wood Prod. 74, 43–48. https://doi.org/10.1007/s00107-015-0973-2

Zauer, M., Hempel, S., Pfriem, A., Mechtcherine, V., Wagenführ, A. (2014). Investigations of the pore-size distribution of wood in the dry and wet state by means of mercury intrusion porosimetry. Wood Sci Technol 48, 1229–1240. https://doi.org/10.1007/s00226-014-0671-y

Zeniya, N., Obataya, E., Endo-Ujiie, K., Matsuo-Ueda, M. (2019). Changes in vibrational properties and colour of spruce wood by hygrothermally accelerated ageing at 95–140 °C and different relative humidity levels. SN Appl. Sci. 1, 7. https://doi.org/10.1007/s42452-018-0004-0

Change of chemical composition and FTIR spectra of Turkey oak and Pannonia poplar wood after acetylation

Fanni Fodor[1*], Tamás Hofmann[2]

[1] University of Sopron, Institute of Wood Technology and Technical Sciences. Bajcsy-Zs. Str. 4, Sopron, Hungary, 9400.
[1] University of Sopron, Institute of Environmental Protection and Natural Conservation. Bajcsy-Zs. Str. 4, Sopron, Hungary, 9400.

E-mail: fodor.fanni@uni-sopron.hu; hofmann.tamas@uni-sopron.hu

Keywords: acetylation, wood modification, Turkey oak, Pannonia poplar, FTIR, wood chemistry

ABSTRACT

In this research, acetylation was applied under industrial conditions to improve the properties of Turkey oak and Pannonia poplar wood. Both species are potential "climate winners" in Hungary, yet they are currently underused due their low durability and poor dimensional stability. Acetylation modification process may be a suitable method to improve their properties. In order to verify the effectiveness of the process, comparative chemical analyses (cellulose, hemicelluloses, lignin, extractives, and ash, buffering capacity and pH) of the untreated and acetylated heartwood and sapwood was carried out for both species for the first time. Diffuse reflectance infrared Fourier-transform (DRIFT) spectroscopy was also used to support the evaluation of the chemical analyses. The Weight Percent Gain was 11.54% for poplar and 0.94% for Turkey oak, indicating poor treatment efficiency for the latter. The cellulose, hemicellulose and lignin content changed significantly in poplar, having the highest change (+81%) by acetylating the hemicelluloses. Only the alpha-cellulose content decreased significantly in Turkey oak, presumably due to the degradation of the non-crystalline part of cellulose. Acetylation may improve the resistance of Pannonia poplar against moisture, weather, decay and wood-boring insects, but the process parameters need to be optimized in order to prevent degradation and discoloration in poplar. Turkey oak was found to be less suitable for acetylation due to its low permeability and tendency to crack.

INTRODUCTION

A significant part of Hungary's wood production is made up of Pannonia poplar (*Populus × euramericana* cv. Pannónia) (1,306,000 m^3) and Turkey oak (*Quercus cerris* L.) (801,000 m^3) (HCSO 2021). However, due to their unfavorable properties (e.g. low natural durability, poor dimensional stability) they are mainly used as firewood and in the wood-based panel production and packaging industry. One possible way of improving wood quality is the application of modification methods, which have proven their efficiency and potential in the last decades (Mai and Militz 2023).

Poplar species, specifically Pannonia poplar, are hard to dry and modify because the freshly-cut heartwood (ripewood) has higher moisture content than its sapwood. Also, more tyloses and extractive substances form in older trees which enable false heartwood formation and discoloration, which impairs their quality and value (Komán 2012). Because of this phenomenon, hybrid poplar species such as Pannonia poplar are mainly felled at about 15 years, especially those that are intended for veneer production. Usually its sapwood, heartwood and juvenile wood are hard to differentiate, especially after drying (Németh et al. 2013). In Pannonia poplar, the borderline of sapwood and heartwood is faintly visible (Horváth and Schantl 2017). The difference between the physical properties of sapwood and heartwood is not significant (Molnár et al. 2002). There is no visible distinction between earlywood and latewood within the annual rings. The annual ring width varies between 2-30 mm (Molnár and Bariska 2002). Pannonia poplar has higher density than most poplar species (> 401 kg/m^3), which makes it suitable for structural applications and the furniture industry (Mirzaei et al. 2017).

The color of Pannonia poplar was successfully modified to a darker tone by steaming (Banadics and Tolvaj 2019; Banadics et al. 2022), thermal modification (Molnár et al. 2006) and heat-treatment in different oils (Bak and Németh 2012; Bak et al. 2012). Heat treating it at 180°C and 200°C improved its durability, dimensional stability, and compression strength (Molnár et al. 2006; Horváth 2008).

Similar results were found for oil-heat-treated Pannonia poplar (Bak and Németh 2012; Bak et al. 2012). On the other hand, its color was not stable against weathering (Bak et al. 2012). Promising results were found with the thermo-mechanical densification of Pannonia poplar with increased mechanical properties (Ábrahám et al. 2010).

There are several publications regarding the chemical modification and impregnation modification of poplar species – these processes could be applied to Pannonia hybrid as well, in order to improve its physical and mechanical properties, and to modify its color.

Turkey oak logs grown in optimal sites can have a diameter of 30 – 50 cm and length of 12 – 15 m, usually smaller than sessile or pedunculate oak species. This is due to their short lifespan: they are attacked by diseases and grow slowly after an age of 60 – 80 years. They are usually harvested at this age. If they grow in closed stands, they usually develop straight, cylindrical trunks, which is more favorable for industry. They have wide, light-grey sapwood and dark, reddish-brownish heartwood, often having a false heart. The wood is prone to have frost ribs or cracks, ring shakes, crooks or springs, tapered trunk, warping, splitting, and knots. Due to its inhomogeneous annual ring structure and density, its high shrinkage anisotropy, the stress results in ring shakes and cracks; their wood is less suitable for sawlog production (Molnár and Bariska 2002). Its usage is also hindered by having low durability against fungi species and wood-boring insects (Bajraktari et al. 2018). Due to its disadvantages and high calorific value (11,592 MJ/m^3 for air-dry wood), it is mainly used as firewood. Turkey oak has somewhat higher density than that of other oaks (720-810 kg/m^3) so it can be used for similar purposes, except for the production of barrels and outdoor, durable wood products. Its low extractive content, and low amount of polyphenols are connected to its low durability (Lavisci et al. 1991; Molnár and Bariska 2002; Bajraktari et al. 2018).

The modification of Turkey oak was less studied in scientific literature. Hydrothermal (steaming) and thermal treatments have been carried out with promising results, like reduced equilibrium moisture content, anti-swelling efficiency and homogenized color (Tolvaj and Molnár 2006; Todaro et al. 2013, 2018; Cetera et al. 2016, 2019). Steaming enables the homogenization and darkening of wood color, but compared to thermal modification it is less suitable for durability enhancement. There was no report found on the acetylation of Turkey oak. If high dimensional stability and durability are achieved, it could be used for glulam production (Uzelac Glavinić et al. 2023). The gluing difficulties of Turkey oak are the same as of other oaks: too high variation in density and permeability between earlywood and latewood, which hinders an adequate adhesive bond (Lavisci et al. 1991). Chemical surface modification could enable better interaction between the surface of oakwood and polyurethane (PUR) adhesives (Sahula et al. 2023).

In the present work the acetylation modification of Pannonia poplar and Turkey oak has been carried out for the first time using a semi-industrial process by investigating both sapwood and heartwood. The main chemical constituents (cellulose, hemicelluloses, and lignin) as well as extractive content, ash content, buffering capacity and pH were measured and compared in untreated and acetylated wood. Diffuse reflectance infrared Fourier-transform (DRIFT) spectroscopy supported the evaluation of the chemical analysis. The results contribute to the understanding of the chemical changes taking place during the acetylation of Pannonia poplar and Turkey oak and provide data for the elaboration of techniques for the acetylation and better utilization of these currently underused wood species.

MATERIALS AND METHODS
Wood material

One Pannonia poplar log was obtained from Újrónafő 11/G and one from Győr 540/B (Hungary), with breast height diameter of 21.3 cm and 39.5 cm, from 22 and 24 year-old trees, respectively. The logs were about 150 cm long. The density of the sapwood was 444 and 427 kg/m^3 for the poplar from Győr and Újrónafő, respectively (Horváth and Csiha 2022). The heartwood density was 470 and 413 kg/m^3 for the poplar from Győr and Újrónafő, respectively.

One Turkey oak log was from the mountains of Sopron forestry (Hungary), with breast height diameter of 30 cm and length of about 150 cm.

Acetylation

The logs were sawn into 30 and 50 cm thick boards. There were 10 pcs of thinner and 4 pcs of thicker Pannonia poplar boards, and 7 pcs of thinner and 6 pcs of thicker Turkey oak boards. Half of them were acetylated at Accsys Technologies (Arnhem, the Netherlands) under semi-industrial conditions (Girotra 2013). The process was carried out with batches of Radiata pine with corresponding thickness and process parameters. The WPG was determined at Accsys Technologies, where it was calculated by dividing the density change after acetylation by the initial oven-dry density of the boards.

Preparation of particles for chemical analysis

Samples (about 100-200 g) were ground in a hammer mill and sieved. The 0.2-0.63 mm sieve fraction was taken for chemical analyses. All measurements were run in triplicates and the results were given based on dry wood mass. The particles were stored at 20°C 65% relative humidity until reaching constant mass.

Measurement of wood polymers, total extractive and ash content

For determining the holocellulose content, 2.5 g of wood particles were transferred into an Erlenmeyer flask. Subsequently, 80 mL of hot distilled water, 0.5 mL of acetic acid (96%), and 1 g of sodium chlorite were added. The mixture was heated in a water bath at 70 °C for 1 h. After each succeeding hour, portions of 0.5 mL acetic acid and 1 g sodium chlorite were added by shaking. This process was repeated 7 times. After six cycles, the samples were left in the water bath overnight. At the end of 24 h of reaction, samples were cooled and filtered on a G2 glass funnel filter and the holocellulose was washed with 10 mL acetone and water until the yellow color was removed (Rowell 2012). The prepared holocellulose was dried at 105 °C and then weighed.

Then the alpha-cellulose content was determined by transferring the previously prepared holocellulose into a 250-mL glass beaker, and adding 10 mL of 17.5% NaOH solution. At 5-min intervals, portions of 5 mL NaOH solution were added until the holocellulose was fully covered with solution. The reaction time was 1 h. The α-cellulose was filtered on a G2 porosity glass funnel filter and washed with 5% NaOH, acetic acid, and water. This washing cycle was repeated twice. The prepared α-cellulose was dried at 105 °C and then weighed (Rowell 2012). Similar methods were used in recent articles (Ghavidel et al. 2020b, a; Amato et al. 2021).

The hemicellulose content was calculated by the subtraction of the alpha-cellulose content from the holocellulose content.

The acid-insoluble lignin content was determined using Klason's method (TAPPI standard T 222).

Two solvent-systems were used to assess its extractive content: cyclohexane:ethanol 50:50 (v/v) and methanol:water 50:50 (v/v). 0.4 g sample was mixed with 40 ml solvent in a 100 ml glass beaker. The beaker was covered with aluminium foil to avoid evaporation. Samples were placed in an ultrasonic bath (Elma Transsonic T570, Elma Schmidbauer GmbH, Singen, Germany) and extracted for 60 min. Extract solutions were filtered through filter paper and 10 ml of the clean solutions were evaporated to dryness at room temperature; then the remaining solids were weighed. Results for the total extractive content are given as the sum of the values obtained by the two solvent systems.

Determination of pH and buffering capacity

In order to measure the pH and buffering capacity, extraction was carried out as follows: 2.5 g of wood was extracted with 50 ml water for 24 h in a closed beaker. The solutions were filtered and the particles were washed with water into a conical flask to a final volume of 100 ml.

The pH of the remaining part of the aqueous extract solution was determined by a Hanna HI 2550 pH meter, which corresponded to the pH of the wood. The buffering capacity of the solution was measured by titration using 0.02 M NaOH to pH=7.00.

Equillibrium moisture content

An Ohaus MB 23 moisture analyzer (Ohaus Corporation, Parsippany, Unites States) was used to determine the equilibrium moisture content of the samples.

FTIR analysis

The tangential surface was analyzed and samples of 5 mm thickness × 10 mm width × 30 mm length (t × w × l) were used for diffuse reflectance infrared Fourier-transform (DRIFT) spectroscopy with a JASCO FT/IR-6300 spectrophotometer and Spectra Manager program. First, the background spectrum was obtained against an aluminum plate in order to see the contribution of the instrument and environment to the spectrum.

These effects were removed from the samples' spectrum by making a ratio of the sample single beam spectrum to the background spectrum. Secondly, the spectrometer did 50 scans of each sample. There were 8 untreated and 48 acetylated Pannonia poplar samples, and 10 untreated and 44 acetylated Turkey oak samples. After measurement, the spectra were smoothed with 15 points convolution. A two-point base line correction was made by setting the lowest point between 3800 cm^{-1} and 1900 cm^{-1} to a zero absorbance. The intensity of the infrared peaks was converted to Kubelka-Munk (K-M) units for quantitative analysis. The chemical changes in wood were evaluated observing the difference of the spectra of untreated samples subtracted from the spectra of acetylated samples. Here, the absorption increase was represented by positive band while an absorption decrease was represented by a negative band. The band assignments were made using the difference of the two spectra.

Statistical analysis

All wet-chemical analyses have been conducted in duplicates. Statistical analysis was performed using the Dell Statistica software (version 13, Dell Inc., Round Rock, TX, USA). Factorial analyses of variances (ANOVA) combined with the Tukey's HSD test and Levene's test for homogeneity of variances were conducted, and the differences were considered significant at $p < 0.05$.

RESULTS AND DISCUSSION

Although the sapwood of Pannonia poplar seemed to be successfully acetylated, degradation and discoloration was visible in the sapwood-heartwood transition zone. The density of Pannonia poplar increased from 453 to 486 kg/m^3 (Újrónafő), and from 476 to 489 kg/m^3 (Győr). The (indicative) WPG was 11.72 % and 11.36 % for poplar from Újrónafő and Győr, respectively.

After acetylation, the quality of Turkey oak wood was impaired by a significant amount of cracks. The density of Turkey oak decreased from 796 to 757 kg/m^3. The (indicative) WPG was low, only 0.94 %.

Table 1 and Table 2 lists the chemical composition, pH and buffering capacity of Pannonia poplar and Turkey oak, respectively. Table 3 lists the most important wavenumbers for both species after acetylation which are assigned in their difference spectra in Figure 1. The band numbers are referred in brackets in the text. Structural changes in the wood were evaluated according to these results and compared to the relevant literature.

The moisture content of Pannonia poplar and Turkey oak decreased significantly by 20-58 % due to the incorporation of acetyl groups in their cell walls. Positive and negative peaks were observed between 3200-3600cm^{-1} (1) on the spectra of both species, which are the signs of OH group rearrangement in the wood structure. Their lower moisture content indicates that the wood of Pannonia poplar and Turkey oak absorbs less moisture after acetylation, and thus the material swells less in humid or wet conditions, and its dimensional stability is higher when exposed to changing climatic conditions. The degraded part of acetylated poplar had a little higher moisture content than its sapwood and heartwood, which may indicate lower acetyl content. Acetylation reduced the moisture content of Turkey oak less than Pannonia poplar, probably due to its lower permeability and higher density. The difference between the moisture content of sapwood and heartwood evened after acetylation.

The holocellulose content is made up of the cellulose and hemicellulose content of the wood material. In Pannonia poplar, the hemicellulose content increased significantly after acetylation from 33.52 % to 60.68 % for sapwood, and from 33.81 to 58.08 % for heartwood. For Turkey oak, where the hemicellulose content increased from 29.66 % to 44.95 % for sapwood, and from 31.73 % to 38.85 % for heartwood. The increase was higher in sapwood than heartwood, for both wood species.

During acetylation, some of the hydroxyl groups are substituted by acetyl groups, which increase the weight of the polymer. As the hemicellulose fraction has proportionally the most hydroxyl groups, its weight increased after acetylation. Higher absorption of carbonyl groups in xylan (2), symmetric C-H deformation in hemicelluloses (3), and absorption of C-O stretching in xylan (4) confirm this finding on the differential spectrum. The increment at these wavenumbers after acetylation was found by other

researchers as well (Stefke et al. 2008), e.g. for spruce (Schwanninger et al. 2011), for Scots pine and beech (Mohebby 2008), and for European hornbeam (Fodor et al. 2018; Bari et al. 2019).

Table 1: Chemical composition, pH and buffering capacity of untreated and acetylated Pannonia poplar, showing results for sapwood (S), heartwood (H) and degraded part separately. Average values are presented with standard deviation in brackets. Different superscript letters in a row denote significant difference at p<0.05 level

Chemical composition	Untreated		Acetylated		Difference (pp)		Percent change (%)		Acetylated
	S	H	S	H	S	H	S	H	Degraded
Moisture content [%]	5.9	5.9	2.5	2.5	- 3.40	- 3.40	- 58	- 58	2.8
Holocellulose content [%]	77.59[a] (2.65)	78.47[a] (0.34)	91.55[b] (1.03)	90.26[b] (4.26)	+ 13.96	+ 11.79	+ 18	+ 15	84.36[ab] (2.60)
Hemicellulose content [%]	33.52[a] (3.64)	33.81[a] (1.45)	60.68[b] (0.19)	58.08[b] (0.59)	+ 27.16	+ 24.27	+ 81	+ 72	54.44[b] (2.99)
Alpha-Cellulose content [%]	44.07[bc] (0.98)	44.66[c] (1.11)	30.87[a] (0.84)	32.19[ab] (3.67)	- 13.20	- 12.47	- 30	- 28	29.92[a] (5.59)
Klason lignin content [%]	17.10[b] (0.43)	19.11[b] (1.95)	6.47[a] (0.47)	8.14[a] (1.98)	- 10.63	- 10.97	- 62	- 57	7.17[a] (0.23)
Extractive content [%]	4.41[c] (0.03)	3.38[b] (0.14)	2.72[a] (0.15)	2.41[a] (0.01)	- 1.69	- 0.97	- 38	- 29	3.79[b] (0.13)
Ash content [%]	0.90[b] (0.06)	1.11[b] (0.10)	0.22[a] (0.08)	0.88[b] (0.19)	- 0.68	- 0.23	- 75	- 20	0.83[b] (0.03)
pH	5.79[a] (0.01)	6.59[b] (0.12)	5.35[a] (0.21)	6.52[b] (0.10)	-	-	-	-	5.70[a] (0.07)
Buffering capacity [mg/g]	0.36[b] (0.03)	0.11[a] (0.03)	0.35[b] (0.08)	0.13[a] (0.05)	- 0.01	+ 0.02	- 3	+ 18	0.56[c] (0.00)

Table 2: Chemical composition, pH and buffering capacity of untreated and acetylated Turkey oak, showing results for sapwood (S) and heartwood (H) separately. Average values are presented with standard deviation in brackets. Different superscript letters in a row denote significant difference at p<0.05 level

Chemical composition	Untreated		Acetylated		Difference (pp)		Percent change (%)	
	S	H	S	H	S	H	S	H
Moisture content (%)	5.4	4.1	3.3	3.3	- 2.10	- 0.80	- 39	- 20
Holocellulose content (%)	77.87[a] (0.08)	75.96[a] (1.91)	79.27[a] (2.77)	76.26[a] (5.23)	+ 1.40	+ 0.30	+ 2	+ 0
Hemicellulose content (%)	29.66[a] (0.95)	31.73[a] (4.65)	44.95[a] (0.29)	38.85[a] (7.51)	+ 15.29	+ 7.12	+ 52	+ 22
Alpha-Cellulose content (%)	48.21[c] (0.87)	44.23[bc] (2.74)	34.32[a] (2.47)	37.41[ab] (2.28)	- 13.89	- 6.82	- 29	- 15
Klason lignin content (%)	16.27[a] (0.23)	16.20[a] (1.60)	13.25[a] (1.07)	17.27[a] (2.16)	- 3.02	+ 1.07	- 19	+ 7
Extractive content (%)	4.89[a] (0.09)	5.09[a] (0.11)	4.70[a] (0.23)	5.64[b] (0.04)	- 0.19	+ 0.55	- 4	+ 11
Ash content (%)	1.13[a] (0.22)	1.16[a] (0.27)	0.60[a] (0.10)	0.61[a] (0.08)	- 0.53	- 0.55	- 47	- 47
pH	5.58[a] (0.04)	5.39[a] (0.04)	5.86[a] (0.47)	5.13[a] (0.24)	-	-	-	-
Buffering capacity (mg/g)	0.45[b] (0.01)	0.48[b] (0.00)	0.27[a] (0.04)	1.02[c] (0.03)	- 0.18	+ 0.54	- 40	+ 113

In the transition zone of acetylated Pannonia poplar, the hemicellulose content was only 54.44 %, lower than that of sapwood and heartwood. This may indicate a lower rate of acetylation and WPG. On the other hand, there was no remarkable difference between the FTIR spectrum of acetylated Pannonia poplar sapwood, heartwood or the degraded part.

In a study where *Populus ussuriensis* was acetylated under laboratory conditions at 100 °C, 120 °C and 140 °C, a WPG of 12.6 %, 19.7 % and 21.3 % were achieved, respectively (Chai et al. 2016). According to their report, the intensities at peaks 1740, 1370, and 1230 cm^{-1} increased with increasing WPG, which correspond to our results.

Table 3: Wavenumber characterization (Mohebby 2008; Tolvaj 2013) of the infrared spectra of untreated and acetylated Pannonia poplar and Turkey oak. (Band number): numbers assigned to the bands in Figure 1

| Band number	Wavenumber (cm⁻¹) Pannonia poplar	Wavenumber (cm⁻¹) Turkey oak	Functional group	Assignment
1	3534 3351 3201	3567 3348 3135	OH stretching (bonded)	
2	1761	1765	C=O (carbonyl) stretching in unconjugated acetyl groups	Xylan (hemicellulose)
3	1378	1382	Symmetric C-H deformation in CH3	Cellulose and hemicelluloses
4	1260	1267	Syringyl ring and C-O stretching in the ester bond	Lignin and xylan (hemicellulose)
5	1174	1177	Asymmetric C-O-C stretching	Cellulose and hemicelluloses
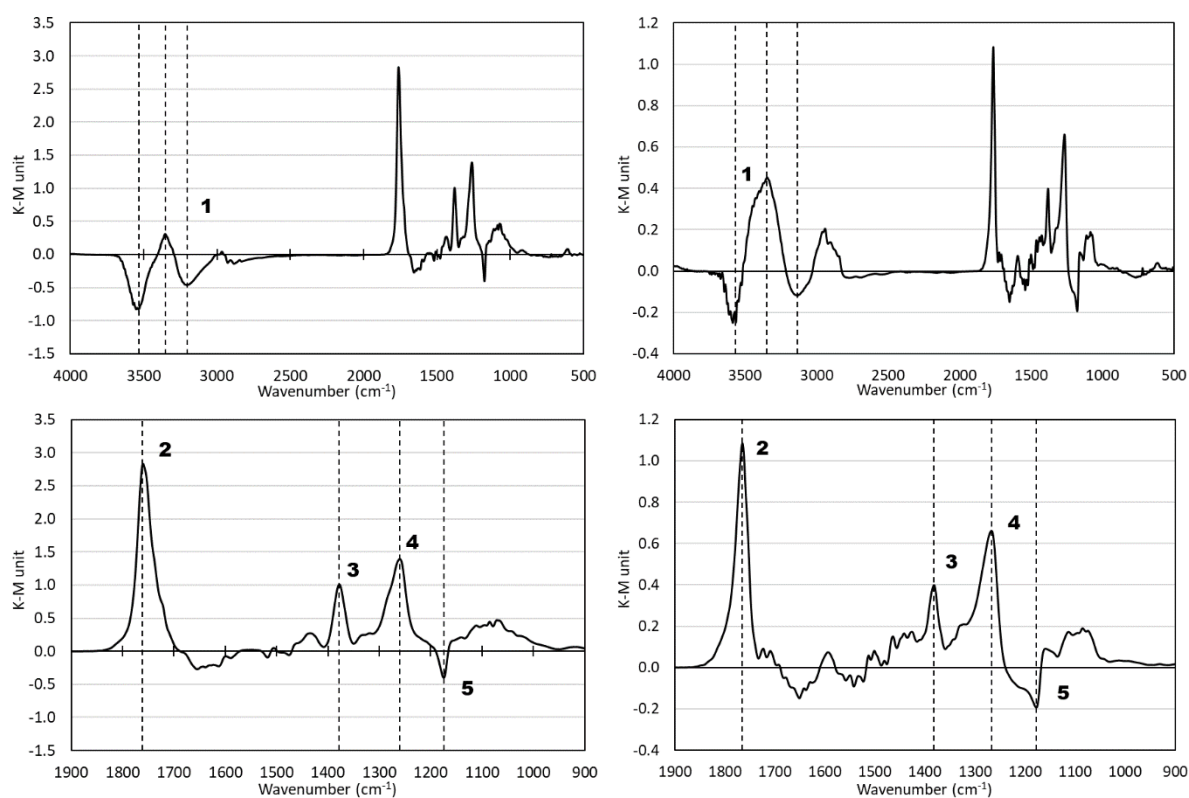
Figure 1: FTIR difference spectrum of Pannonia poplar sapwood (left) and Turkey oak sapwood (right). The spectra above are shown between wavenumbers 4000 – 500 cm⁻¹, and the fingerprint regions are highlighted from it in the bottom between wavenumbers 1900 – 900 cm⁻¹. The differential spectrum was calculated by subtracting the spectrum of untreated wood from that of acetylated wood. Description and assignments of band numbers are listed in Table 3

The alpha-cellulose content of both wood species decreased significantly by 15-30 % after acetylation. There was a negative peak of C-O-C stretching in cellulose (5) on the FTIR differential spectra. As the cellulose, hemicellulose and lignin fractions were not analyzed separately by FTIR, only assumptions can be drawn. The increase of hemicellulose content and the reduction of cellulose content can be explained by the difference in reactivity. Acetylation mainly affects the hemicelluloses and lignin as they are more reactive than cellulose (Ohkoshi and Kato 1997; Cetin and Ozmen 2011; Schwanninger et al. 2011). This leads to their increased share in chemical composition. As only the cellulose changed significantly in Turkey oak, here the amorph parts of the cellulose chains were degraded in the acidic medium, reducing its crystallinity. Fodor and colleagues examined acetylated hornbeam, and reported

no remarkable elevation of the soluble carbohydrate content or the levunilic acid concentration, which are the main breakdown products of cellulose (Fodor et al. 2018). Comparing the results of these species, Pannonia poplar had higher WPG then Turkey oak, which corresponds to the higher increment of hemicellulose content. On the other hand, the reduction of cellulose content was comparable, leading to the assumption that cellulose did degrade during acetylation.

The lignin content of Pannonia poplar decreased significantly by more than half after acetylation, while the lignin of Turkey oak changed at a lower rate. The initial values were not remarkably different between its sapwood and heartwood, similar to literature (Todaro et al. 2013). The higher the rate of acetylation is, the more lignin is degraded or dissolved in the acidic medium (Rowell 2012). Here, Klason (acid-insoluble) lignin content decreases by acetylation because some parts of lignin (e.g. ester bonds) hydrolyze during reaction with acetic anhydride and dissolve (Ying et al. 2022). In a study on acetylated hornbeam, only internal structural changes took place in the lignin matrix without any significant change in the lignin content (Fodor et al. 2018). The color darkening was also attributed to the change in lignin and extractive content.

The extractive content was exceptionally higher for sapwood than heartwood in Pannonia poplar, and decreased after acetylation. As the tested material was felled after its "optimal" age (after 15 years), it also had higher extractive content than the corresponding literature data. After acetylation, the difference between the extractive content of sapwood and heartwood is less remarkable. It can be hypothesized that there is no actual difference between the extractive content in sapwood and in heartwood, as Pannonia poplar has no colored heartwood which would indicate that. The sapwood contains more sugars and starch, which may explain its higher water-soluble extractive content. Related scientific articles report an average extractive content of poplar species below 3 % (Osman et al. 2013; Szadkowska et al. 2021).

Turkey oak has low extractive content corresponding to its low durability. Compared to pedunculate oak, it has similar content of proanthocyanidins (condensed tannin). However, it cannot accumulate ellagitannins as much as pedunculate oak which reduces its biological resistance (Lavisci et al. 1991). In general, heartwood has higher durability due to its higher extractive content, which was true in the case of Turkey oak. Similar results were found for Turkey oak (Todaro et al. 2013). The extractive content did not change remarkably after acetylation, indicating low rate of acetylation.

It is known that the anatomy and components of sapwood and heartwood are the same, except for extractives (Rowell 2012). These impregnate the individual cells after they die to form heartwood. The heartwood of Pannonia poplar and Turkey oak can develop tyloses which inhibit the rate of acetylation. The ash content seemingly decreased for both wood species, but it was probably not affected by acetylation.

As the acetylation process takes place in an acidic medium, and acetic acid forms as a byproduct, the acetylated material becomes more acidic, having a lower pH and a higher buffering capacity (Bongers et al. 2016). In Pannonia poplar and the heartwood of Turkey oak, the pH decreased accordingly. The buffering capacity results did not show a clear trend or a great difference. The compatibility of the wood material with adhesives and coatings is influenced by its pH and the buffering capacity, and thus it is an important factor of the finished product. If it is too acidic, base needs to be added for better bonding strength or coating stability. Turkey oak fundamentally has problems with bonding and surface finishing (stains) (Lavisci et al. 1991).

Based on the work of Beckers et al., the degree of acetylation or HPLC acetyl content can be determined approximately by correlating the peak of 1740 to 1510 cm^{-1} (Beckers et al. 2003). Here, the HPLC acetyl content is only an indicated value. It was determined 24% or more for acetylated Pannonia poplar, and 15% and 8% for acetylated Turkey oak sapwood and heartwood, respectively. The values for Pannonia poplar and Turkey oak were read from the correlation diagram for acetylated poplar and beech, respectively. The results are higher than the WPG calculated from weight, which was also shown in the acetylated hornbeam (Fodor et al. 2018).

As diverse as they are, wood species react to the same acetylation process diversely and show different properties, which have been studied well in literature (Sandberg et al. 2021).

The degraded part of Pannonia poplar was found on the borderline of sapwood and heartwood, in the transition zone. This part may have been a wet pocket in the original material. The initially higher moisture content in these parts can account for their lower acetyl content. Poplars are well-known for having wet pockets, water pockets or wetwood which complicate the drying process and cause the

formation of wood defects like warping, splitting, checks and collapses (Boever et al. 2011). These are associated with a bacterial infection of the living tree, where the moisture content grows as the bacteria grows while a bacterial slime prevents the moisture from leaving the wetwood zone thus it will have an exceedingly (at least +5 %) higher moisture content compared to the rest of the wood (Ward and Pong 1980).

Turkey oak was not successfully acetylated under industrial conditions, which was confirmed by its low WPG and slight changes in its chemical properties and FTIR differential spectrum.

CONCLUSIONS

In this research, semi-industrial acetylation was carried out on Pannonia poplar and Turkey oak. These wood species are less utilized and have not been subjected to acetylation before. The moisture content of both Pannonia poplar and Turkey oak decreased significantly by 20-58 % after acetylation. The ratio of alpha-cellulose decreased significantly by 15-30 % for both wood species. A higher hemicellulose content was experienced after acetylation for both wood species, by 22-81%. The increase was higher in sapwood than in heartwood, in Pannonia poplar than in Turkey oak. The lignin content decreased for both wood species, indicating that a part of the lignin degraded or dissolved in the acidic medium during acetylation. The extractive and ash content was not affected by acetylation for neither tested wood species. The wood material became more acidic as the pH decreased after acetylation. After acetylation, the changes were less significant in the degraded part than in the rest of Pannonia poplar, which indicates a lower WPG, lower acetyl content. Sapwood is more suitable for acetylation than heartwood, having a higher WPG. Based on these results, acetylation may improve the resistance of Pannonia poplar against moisture, weather, decay and wood-boring insects, but the process parameters need to be optimized in order to exclude the probability of degradation in poplar. Turkey oak was found to be less suitable for acetylation due to its low permeability and tendency to form cracks.

ACKNOWLEDGEMENTS

REFERENCES

Ábrahám J, Németh R, Molnár S (2010) Thermo-mechanical densification of Pannonia poplar. In: Proceedings of the final conference of COST Action E53: 'Quality control for wood & wood products.' Edinburgh, pp 282–292

Amato D, Squillaci G, Giudicianni P, et al (2021) Valorization of Agroindustrial Waste from Chestnut Production. Chemical Engineering Transactions 87:445–450. https://doi.org/10.3303/CET2187075

Bajraktari A, Nunes L, Knapic S, et al (2018) Chemical characterization, hardness and termite resistance of Quercus cerris heartwood from Kosovo. Maderas Ciencia y tecnología 20:305–314. http://dx.doi.org/10.4067/S0718-221X2018005003101

Bak M, Németh R (2012) Changes in swelling properties and moisture uptake rate of oil-heat-treated poplar (Populus x euramericana cv. Pannónia) wood. Bioresources 7:5128–5137. https://doi.org/10.15376/biores.7.4.5128-5137

Bak M, Németh R, Tolvaj L (2012) The Colour Change of Oil-Heat-Treated Timber During Weathering. Óbuda University e-Bulletin 3:339–345

Banadics EA, Tolvaj L (2019) Colour modification of poplar wood by steaming for brown colour. Eur J Wood Prod 77:717–719. https://doi.org/10.1007/s00107-019-01397-9

Banadics EA, Tolvaj L, Varga D (2022) Steaming of poplar, black locust and beech timbers simultaneously to investigate colour modification effect of extractive transport. Drewno : prace naukowe, doniesienia, komunikaty 65:. https://doi.org/10.12841/wood.1644-3985.368.04

Bari E, Jamali A, Nazarnezhad N, et al (2019) An innovative method for the chemical modification of Carpinus betulus wood: a methodology and approach study. Holzforschung 73:839–846. https://doi.org/10.1515/hf-2018-0242

Beckers EPJ, Bongers F, van der Zee ME, Sander C (2003) Acetyl content determination using different analytical techniques. In: Proceedings of the first European conference on wood modification. Ghent university, Ghent, pp 83–103

Boever LD, Vansteenkiste D, Stevens M, Acker JV (2011) Kiln Drying of Poplar Wood at Low Temperature: Beam Distortions in Relation to Wood Density, Tension Wood Occurence and Moisture Distribution. Wood Research 56:245–256

Bongers F, Meijerink T, Lütkemeier B, et al (2016) Bonding of acetylated wood. International Wood Products Journal 7:102–106. https://doi.org/10.1080/20426445.2016.1161944

Cetera P, Russo D, Milella L, Todaro L (2019) Thermo-treatment affects Quercus cerris L. wood properties and the antioxidant activity and chemical composition of its by-product extracts. Industrial Crops and Products 130:380–388. https://doi.org/10.1016/j.indcrop.2018.12.099

Cetera P, Todaro L, Lovaglio T, et al (2016) Steaming Treatment Decreases MOE and Compression Strength of Turkey Oak Wood. Wood Research 61:255–265

Cetin NS, Ozmen N (2011) Acetylation of wood components and fourier transform infra-red spectroscopy studies. AJB 10:3091–3096. https://doi.org/10.5897/AJB10.2630

Chai Y, Liu J, Wang Z, Zhao Y (2016) Dimensional Stability and Mechanical Properties of Plantation Poplar Wood Esterified Using Acetic Anhydride. BioResources 12:912–922. https://doi.org/10.15376/biores.12.1.912-922

Fodor F, Németh R, Lankveld C, Hofmann T (2018) Effect of acetylation on the chemical composition of hornbeam (Carpinus betulus L.) in relation with the physical and mechanical properties. Wood Material Science & Engineering 13:271–278. https://doi.org/10.1080/17480272.2017.1316773

Ghavidel A, Gelbrich J, Kuqo A, et al (2020a) Investigation of Archaeological European White Elm (Ulmus laevis) for Identifying and Characterizing the Kind of Biological Degradation. Heritage 3:1083–1093. https://doi.org/10.3390/heritage3040060

Ghavidel A, Hofmann T, Bak M, et al (2020b) Comparative archaeometric characterization of recent and historical oak (Quercus spp.) wood. Wood Sci Technol 54:1121–1137. https://doi.org/10.1007/s00226-020-01202-4

Girotra K (2013) Process for wood acetylation and product thereof

HCSO (2021) Fakitermelés az erdőgazdálkodási célú erdőterületeken fafajcsoportok szerint [ezer m3]

Horváth N (2008) A termikus kezelés hatása a faanyag tulajdonságaira, különös tekintettel a gombaállóságra. Doctoral thesis, University of West Hungary

Horváth N, Csiha C (2022) Measurements of the Load-bearing Structural Aspects of Pannónia Poplar from Sites in Western Transdanubia, Hungary. Acta Silvatica et Lignaria Hungarica 18:119–127. https://doi.org/10.37045/aslh-2022-0008

Horváth N, Schantl I (2017) Hazai ültetvényes Pannonia nyár fatestének anyagtudományi vizsgálata. In: Alföldi Erdőkért Egyesület Kutatói Nap: Tudományos Eredmények a Gyakorlatban. Alföldi Erdőkért Egyesület, Kecskemét, Hungary, pp 149–154

Komán S (2012) Nemesnyár-fajták korszerű ipari és energetikai hasznosítását befolyásoló faanatómiai és fizikai jellemzők. Doctoral thesis, University of West Hungary

Lavisci P, Masson D, Deglise X (1991) Quality of Turkey Oak (Quercus cerris L.) Wood. II. Analysis of some Physico-Chemical Parameters Related to its Gluability. Holzforschung 45:415–418. https://doi.org/10.1515/hfsg.1991.45.6.415

Mai C, Militz H (2023) Wood Modification. In: Niemz P, Teischinger A, Sandberg D (eds) Springer Handbook of Wood Science and Technology. Springer International Publishing, Cham, pp 873–910

Mirzaei G, Mohebby B, Ebrahimi G (2017) Glulam beam made from hydrothermally treated poplar wood with reduced moisture induced stresses. Construction and Building Materials 135:386–393. https://doi.org/10.1016/j.conbuildmat.2016.12.178

Mohebby B (2008) Application of ATR Infrared Spectroscopy in Wood Acetylation. Journal of Agricultural Science and Technology 10:253–259

Molnár S, Bariska M (2002) Magyarország ipari fái. Szaktudás Kiadó Ház Zrt, Budapest

Molnár S, Csupor K, Horváth N (2006) The effect of thermal modification on the durability of wood against fungal decay. In: Proceedings of the 5th International Symposium Wood Structure and Properties '06. Technical University in Zvolen, Zvolen, Slovakia, p 517

Molnár S, Németh R, Paukó A, Göbölös P (2002) A fehérnyár hibridek faanyagminőségének javítási lehetőségei. Faipar 50:24–26

Németh R, Ott Á, Takáts P, Bak M (2013) The Effect of Moisture Content and Drying Temperature on the Colour of Two Poplars and Robinia Wood. BioResources 8:2074–2083. https://doi.org/10.15376/biores.8.2.2074-2083

Ohkoshi M, Kato A (1997) 13C-NMR analysis of acetyl groups in acetylated wood II. Acetyl groups in lignin. Mokuzai Gakkaishi 43:364–369

Osman NB, McDonald AG, Laborie M-PG (2013) Characterization of water-soluble extracts from hot-pressed poplar. European Journal of Wood and Wood Products 71:343–351. https://doi.org/10.1007/s00107-013-0686-3

Rowell R (2012) Handbook Of Wood Chemistry And Wood Composites. CRC Press, Boca Raton

Sahula L, Šedivka P, Zachara T, Borůvka V (2023) The effect of chemical modification of the surface of the glued surface on the strength of the structural joint of oak wood. Central European Forestry Journal 69:120–125. https://doi.org/10.2478/forj-2023-0009

Sandberg D, Kutnar A, Karlsson O, Jones D (2021) Wood Modification Technologies - Principles, Sustainability, and the Need for Innovation. CRC Press, Boca Raton

Schwanninger M, Stefke B, Hinterstoisser B (2011) Qualitative Assessment of Acetylated Wood with Infrared Spectroscopic Methods. Journal of Near Infrared Spectroscopy 19:349–357. https://doi.org/10.1255/jnirs.942

Stefke B, Windeisen E, Schwanninger M, Hinterstoisser B (2008) Determination of the Weight Percentage Gain and of the Acetyl Group Content of Acetylated Wood by Means of Different Infrared Spectroscopic Methods. Analytical Chemistry 80:1272–1279. https://doi.org/10.1021/ac7020823

Szadkowska D, Zawadzki J, Kozakiewicz P, Radomski A (2021) Identification of Extractives from Various Poplar Species. Forests 12:647. https://doi.org/10.3390/f12050647

Todaro L, Dichicco P, Moretti N, D'Auria M (2013) Effect of Combined Steam and Heat Treatments on Extractives and Lignin in Sapwood and Heartwood of Turkey Oak (Quercus cerris L.) Wood. BioResources 8:1718–1730. https://doi.org/10.15376/biores.8.2.1718-1730

Todaro L, Rita A, Pucciariello R, et al (2018) Influence of thermo-vacuum treatment on thermal degradation of various wood species. European Journal of Wood and Wood Products 76:541–547. https://doi.org/10.1007/s00107-017-1230-7

Tolvaj L (2013) A faanyag optikai tulajdonságai. University of West Hungary, Sopron

Tolvaj L, Molnár S (2006) Colour homogenisation of hardwood species by steaming. Acta Silvatica et Lignaria Hungarica 2:105–112

Uzelac Glavinić I, Boko I, Lovrić Vranković J, et al (2023) An Experimental Investigation of Hardwoods Harvested in Croatian Forests for the Production of Glued Laminated Timber. Materials 16:1843. https://doi.org/10.3390/ma16051843

Ward JC, Pong WY (1980) Wetwood in trees: A timber resource problem. U.S. Department of Agriculture, Forest Service, Pacific Northwest Forestry and Range Experiment Station

Ying W, Ouyang J, Lian Z, et al (2022) Lignin removal improves xylooligosaccharides production from poplar by acetic acid hydrolysis. Bioresource Technology 354:127190. https://doi.org/10.1016/j.biortech.2022.127190

Change of cellulose crystal structure in beech wood (*Fagus sylvatica* L.) due to gaseous ammonia treatment

Herwig Hackenberg[1*], Tobias Dietrich[1], Mario Zauer[1], Martina Bremer[2], Steffen Fischer[2], André Wagenführ[1]

[1] TUD Dresden University of Technology, Institute of Natural Material Technology, 01062 Dresden
[2] TUD Dresden University of Technology, Institute of Plant and Wood Chemistry, 01737 Tharandt

E-mail: herwig.hackenberg@tu-dresden.de; tobias.dietrich@tu-dresden.de; mario.zauer@tu-dresden.de; martina.bremer@tu-dresden.de; steffen.fischer@tu-dresden.de; andre.wagenfuehr@tu-dresden.de

Keywords: beech wood, ammonia, cellulose, density, self-densification

ABSTRACT

The subject of this study was the change of the crystal structure of cellulose in beech wood (*Fagus sylvatica* L.) specimens due to the treatment with gaseous ammonia. The density of the samples was then analysed and compared with the previous results.

The treatment with gaseous ammonia was done in an autoclave at isothermal conditions (20 °C) for 24 hours. The ammonia gas pressure is given in a relative pressure ratio and was divided in 9 pressure levels, ranging from 0.1 to 0.9 (p_i/ p_s, partial pressure/ saturated steam pressure) in 0.1 pressure steps.

The subsequent investigations focused on the change in the crystal structure of the cellulose, which was investigated with the help of Raman spectroscopy. Furthermore, these chemical investigations were related to changes in the density of the specimens after the treatment.

INTRODUCTION

Wood is a versatile, renewable and in cascades usable material. In order to extend the possible field of application for wood, it is important to customise the properties of the wood specifically to the needs of the products. Against the background of a technological application, a material with a high mechanical strength is generally required. With regard to wood, strength is usually associated with high density. In addition to selecting wood that already has a high density, it is also possible to increase the density by means of a modification process. Possible modifications are the Staypak treatment (Seborg et al., 1956) or the thermo-hydro-mechanical densification process (Navi & Heger, 2004). A special modification process, that also leads to an increase in density of the wood, is the treatment with ammonia. Ammonia treatment can be conducted by the use of amines, an aqueous solution, liquid ammonia or gaseous ammonia. Gaseous ammonia treatment has two main advantageous, as the wood can be impregnated very easily and the treatment intensity can be controlled by varying the gas pressure.

The phenomenon of densifying wood with ammonia lies in the fact, that ammonia leads to a so called self-densification without the need of additional mechanical forces. This behaviour is already known and has been described in literature (Bariska, 1975; Hackenberg, 2018; Hackenberg et al., 2021; Pollisco et al., 1971). However, the relationship between self-densification and the applied process intensity remains open. When considering the treatment of wood with ammonia, the behaviour of the cellulose is of great importance: Water and ammonia are both molecules of similar size and both are strong dipoles. They interact with the cellulose by forming hydrogen bonds. But unlike water, ammonia and ammonia derivatives are able to swell the crystalline regions of cellulose and cause a change in the crystal structure (Yamashita et al., 2018).
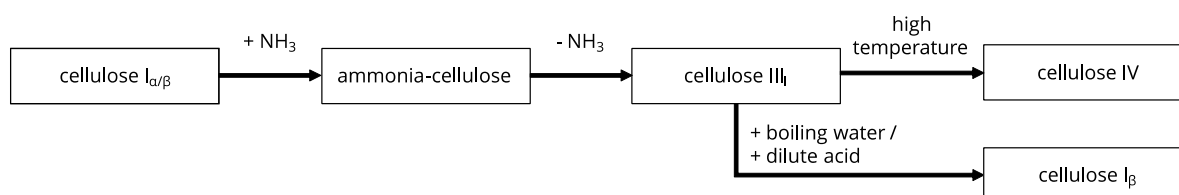

Figure 45: Change of crystal structure due to ammonia treatment and its reconversion (Schuerch, 1964)

A simplified overview of the conversion of cellulose is given in Fig. 1. Native cellulose is converted by ammonia to amorphous ammonia cellulose. After the ammonia is removed, the cellulose recrystallizes into a modified crystal structure, cellulose III (Wada et al., 2004). Depending on the starting material (cellulose I or II), the product is named cellulose III_I or III_{II} (Sarko et al., 1976). As only untreated wood is used as a starting material in this investigation (cellulose I), cellulose III_I will be referred to as cellulose III. Since the conversion of cellulose I to III in the wood is a profound change in the wood and cellulose makes up the largest proportion of the mass, it is assumed that the cellulose conversion is related to the change in the density of the wood (self-densification).

Against this background, the aim of this paper is to investigate the effect of gaseous ammonia on wood and to find out whether a transformation of the crystalline structure of cellulose occurs. Further, the gas pressure at which this transformation takes place and the influence of the moisture of the initial material before the treatment are to be investigated. The change in the density of the wood should be related to the changes in the crystalline structure.

EXPERIMENTAL
Starting material Raman spectroscopy
A beech wood (*Fagus sylvatica* L.) board was cut in 20 specimens (2 rows with 10 pieces) to a dimension of 50 x 50 x 50 mm³ (L x T x R) and then dried at 103 °C. The specimen set was then divided into two series of which one half of the set (1 row/ 10 pieces) has been stored dry (silica gel) and the other half was conditioned at 20 °C/ 65 % relative humidity.

Starting material density investigation
9 series (20 x 20 x 20 mm³ L x T x R) were made out of flawless beech wood (*Fagus sylvatica* L.). In order to achieve the greatest possible comparability between the series, 9 bars of wood were cut into 10 specimens each. The samples of the individual bars were each assigned to the 9 series in the same order. Thus, the number of samples per series was 10 specimens and 90 specimens in total. All specimens were dried at 103 °C to obtain the dry dimension (after cooling). Afterwards one half of the series has been stored dry (silica gel) and the other half of the series was conditioned at 20 °C/ 65 % relative humidity.

Gaseous ammonia treatment
The gaseous ammonia treatment was carried out in a stainless steel autoclave whose shell was temperature-controlled to 20 °C. The treatment was carried out for 24 hours and at 9 different pressure levels. The gas pressure was kept constant with an automatically controlled valve with a hysteresis of ±3 kPa relative to the set target pressure. The pressure levels are listed in Table 1. They are given as a ratio of partial pressure to saturated steam pressure.

Table 1: pressure levels

ratio p_i/p_s[a]	0.1	0.2	0.3	0.4	0.5	0.6	0.7	0.7	0.9
pressure, absolute [kPa]	106	171	257	343	429	514	600	686	771

[a] p_i: partial pressure, p_s: saturated steam pressure (at 20 °C: 857 kPa)

Due to the relative measuring sensor of the automatic pressure control, the lowest pressure level was slightly above ambient pressure. The highest pressure level was close to saturated steam pressure to avoid condensation effects.

Gaseous ammonia treatment begins with the positioning of a specimen inside of the autoclave and closing it. The autoclave was then evacuated to a final pressure of 5 kPa for 5 minutes. The ammonia gas was then fed from a gas cylinder (99.98 % purity) into the autoclave up to the defined pressure and kept constant. After 24 hours the ammonia gas was drained and the specimen was removed for ventilated storage in a laboratory fume hood.

Raman spectroscopy
The Raman spectrometer used was a BRUKER MultiRAM (1064 nm Nd:YAG laser). The measurement parameters were 300 mW, 200 scans and a resolution of 1/cm⁻¹. A sample piece measuring 10 mm x 10 mm x 2 mm (L x R x T) was cut out of the centre of each 5 cm x 5 cm x 5 cm specimen. The measurement was carried out on the radial surface.

Analysis was performed using the software OPUS 7.5 (Bruker). All Raman spectra were baseline corrected. The band at a wavelength of 1096 cm^{-1} was used as a normalisation since it remains unchanged for cellulose I and III (Agarwal, 2014). For this purpose, a min-max normalisation was performed in the range between 900 – 1100 cm^{-1}.

Investigation of density
After evaporation of the ammonia, the density specimens were dried (103°C) and cooled over dry silica gel. The reference sample was also dried accordingly.

RESULTS AND DISCUSSION
The results of the Raman spectroscopy are shown in Figure 2. A selected wave number range has been chosen in which the change in cellulose can be detected. Cellulose I shows a strong band at 380 cm^{-1} (Agarwal, 2014). This can be seen in native beech wood that was oven dry before treatment (Fig. 2, left). Treatment with ammonia gas does not change this band up to a pressure level of $p_i/p_s = 0.5$. Only from a higher pressure level ($p_i/p_s = 0.6$) does the spectrogram change in that the band at 380 cm^{-1} becomes weaker and shifts to a band at 375 cm^{-1}. In addition, a new band at 355 cm^{-1} appears distinctly. This shifts are characteristic features of the formation of cellulose III (Agarwal, 2014). With higher treatment pressure and therefore process intensity, the band at 355 cm^{-1} becomes even stronger and it can be assumed that the cellulose is only present as polymorph III.
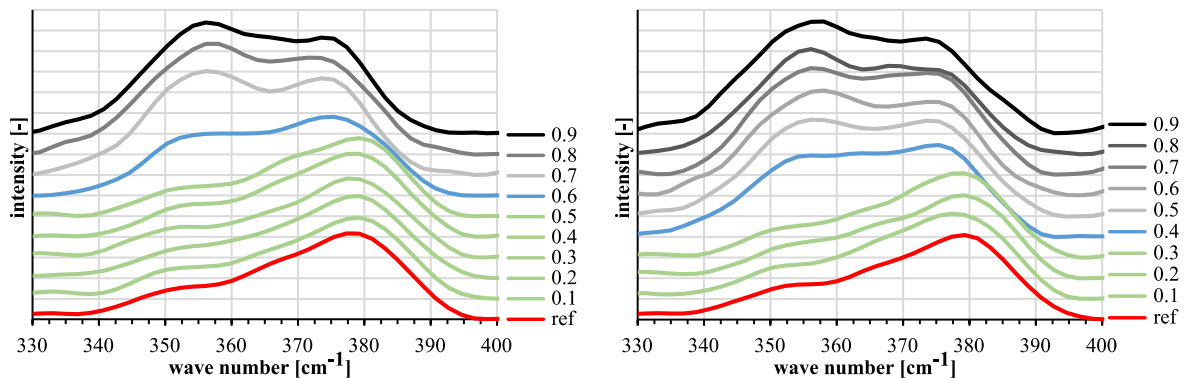

Figure 2: Raman spectra of untreated and ammonia treated beech wood, left: oven-dry (103 °C) prior to treatment, right: humid prior to treatment, intensity of ammonia treatment is indicated in vapour pressure ratio p_i/p_s

In the case of the wood, that was prior to treatment in humid condition, an almost identical behaviour can be seen (Fig. 2, right). The only difference is that the initial pressure level of the first constitution of cellulose III is lowered to $p_i/p_s = 0.4$. Water acts in this case as a catalyst, as a lower process intensity is needed to swell the crystal structure of the cellulose in the wood.

Based on the results of the Raman spectroscopy, the test plan for the density investigation could be adapted accordingly. Only the lowest pressure level ($p_i/p_s = 0.1$), the highest pressure level ($p_i/p_s = 0.9$) and the pressure levels before and after the complete conversion of the cellulose were analysed. For the oven-dry samples these were $p_i/p_s = 0.5$ and 0.7 and for the humid samples $p_i/p_s = 0.3$ and 0.5.
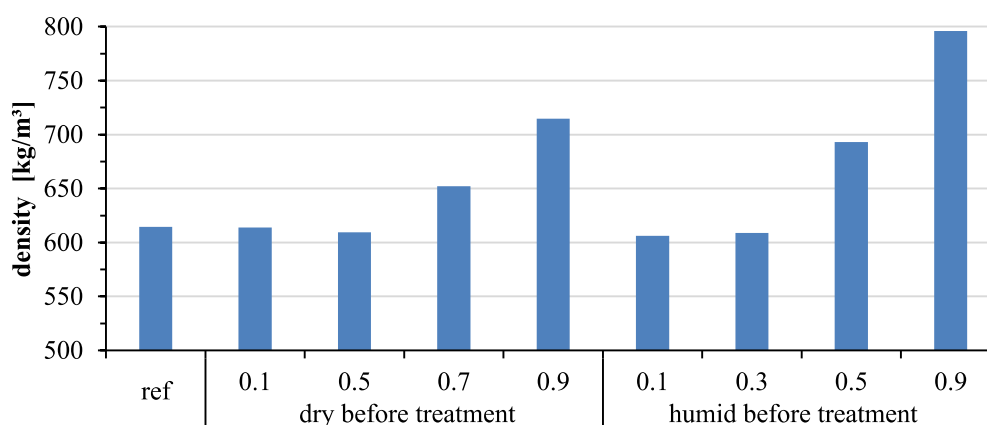
Figure 3: density of untreated and ammonia treated beech wood, oven-dry (103 °C) and humid prior to treatment, intensity of ammonia treatment is indicated in vapour pressure ratio p_i/p_s

The results of the density analysis are shown in Figure 3. Based on the density of the reference samples, it can be seen in both the previously oven-dry and humid samples that no changes in density occurred in 2 test series and that an increase in density was caused in the other 2 series. This increase in density is consistent with the conversion of cellulose from cellulose I to III. The self-densification described in the literature can be determined here on the basis of the increase in density and correlated with the cellulose conversion. It is important to mention that there is a correlation here, but not necessarily a causality. The mechanism behind the increase in density is not yet known.

CONCLUSION

It was found that, above a certain process intensity of the ammonia treatment, the cellulose in the wood is converted from cellulose I to cellulose III. This conversion correlates with an increase in the density of the wood. This correlation is not necessarily based on causality. The exact background to this phenomenon still needs to be investigated further.

REFERENCES

Agarwal, U. P. (2014). 1064 nm FT-Raman spectroscopy for investigations of plant cell walls and other biomass materials. Frontiers in Plant Science, 5. Frontiers. https://doi:10.3389/fpls.2014.00490

Bariska, M. (1975). Collapse phenomena in beechwood during and after NH3-impregnation. Wood Science and Technology, 9 (4), 293–306. https://doi:10.1007/BF00353479

Hackenberg, H. (2018). Alteration of mechanical properties of ammonia treated and densified beech (Fagus sylvatica L.). Hardwood Conference Procedings Vol. 8 (S. 101–102). Sopron.

Hackenberg, H., Zauer, M., Dietrich, T., Hackenberg, K. A. M. & Wagenführ, A. (2021). Alteration of Bending Properties of Wood Due to Ammonia Treatment and Additional Densification. Forests, 12 (8), 1110. https://doi:10.3390/f12081110

Navi, P. & Heger, F. (2004). Combined Densification and Thermo-Hydro-Mechanical Processing of Wood. MRS Bulletin, 29 (5), 332–336. https://doi:10.1557/mrs2004.100

Pollisco, F. S., Skaar, C. & Davidson, R. W. (1971). Some physical properties of maple treated with ammonia vapor. Wood Science, 4 (2), 65–70.

Sarko, A., Southwick, J. & Hayashi, J. (1976). Packing Analysis of Carbohydrates and Polysaccharides. 7. Crystal Structure of Cellulose III and Its Relationship to Other Cellulose Polymorphs. Macromolecules, 9 (5), 857–863. https://doi:10.1021/ma60053a028

Schuerch, C. (1964). Wood Plasticization. Forest Products Journal, 14 (9), 377–381.

Seborg, R. M., Millett, M. A. & Stamm, A. J. (1956). Heat-stabilized Compressed Wood (Staypak). Forest Products Laboratory Report, 1580.

Wada, M., Chanzy, H., Nishiyama, Y. & Langan, P. (2004). Cellulose III Crystal Structure and Hydrogen Bonding by Synchrotron X-ray and Neutron Fiber Diffraction. Macromolecules, 37 (23), 8548–8555. American Chemical Society. https://doi:10.1021/ma0485585

Yamashita, D., Kimura, S., Wada, M., Samejima, M. & Takabe, K. (2018). Effect of ammonia treatment on white birch wood. Holzforschung, 72 (1), 31–36. https://doi:10.1515/hf-2016-0200

Evaluation of weathering performance of acetylated hardwood species

Rene Herrera Diaz[1,2*], Jakub Sandak[1,2], Oihana Gordobil[3], Faksawat Poohphajai[1,2,4], Anna Sandak[1,2]

[1] InnoRenew CoE, Livade 6a, 6310 Izola, Slovenia;
[2] University of Primorska, Glagoljaška 8, 6000 Koper, Slovenia;
[3] University of the Basque Country (UPV/EHU), Plaza Europa 1, 20018, Donostia-San Sebastián, Spain
[3] Aalto University, School of Chemical Engineering, P.O. Box 16300, 00076 Aalto, Finland.

E-mail: rene.herdiaz@innorenew.eu; jakub.sandak@innorenew.eu; oihana.gordobil@ehu.eus; faksawat.poohphajai@innorenew.eu; anna.sandak@innorenew.eu

Keywords: natural weathering, acetylation, wood modification, beech, alder, performance evaluation.

ABSTRACT

Wood is a versatile, natural, and environmentally friendly resource that has attracted attention as a material for sustainable building for many years. In order to enlarge application fields of wood several properties, such as dimensional stability, thermal steadiness, fire resistance, biotic and abiotic degradation resistance or mechanical properties need to be improved. Acetylation is the most well-established treatment when acetic anhydride reacts with hydroxyl groups of cell wall polymers by forming ester bonds. Acetylation improves UV resistance and reduces surface erosion what is important while using wood as façade material. The mechanical strength properties of acetylated wood are not considerably different than not-treated wood, however, its durability is substantially improved. Softwood, mainly Radiata pine, is most used species for commercial acetylation process, nevertheless use of alternative hardwood species is of hight interest. The goal of this research was to comprehensively evaluate the effect of wood acetylation on performance on two hardwood species when exposed to natural weathering. Acetylated wooden boards having a 20% acetyl weight gain on average manufactured from two hardwood: black alder (*Alnus glutinosa* L.), European beech (*Fagus sylvatica* L.), were used for the preparation of experimental samples. The wood modification was performed within the commercial production facilities of Accsys Technologies in the Netherlands. Natural weathering tests were performed for 15 months in San Michele, Italy. Samples were exposed on vertical stands representing a building façade. The stand was oriented to face the southern direction. Differences observed between both species related to surface appearance, erosion, wettability behaviour and changes in chemical composition are important for understanding species-dependent drawbacks of the acetylation process and its further improvement.

INTRODUCTION

All building components that are exposed to environmental elements, including fluctuations in humidity and temperature, rainfall, or ultraviolet radiation, undergo alterations in both appearance and structural integrity (Arpaci et al. 2021; Reinprecht et al. 2017). One major limitation of using unprotected wood on building façades is its aesthetic variation, notably the shift toward a grey tonality due to dark mold growth and UV-induced bleaching (Cogulet et al. 2016; Hill 2006; Pandey 2005). Additionally, the intrinsic variability of wood leads to a non-uniform appearance, and weathering is typically an uneven process resulting in different deterioration rates across various zones of a building (Sandak et al. 2019). Wood may also crack, split, or distort, particularly if the façade is poorly designed or if wooden boards are incorrectly installed (Rüther and Time 2015). Due to their natural composition and intrinsic properties, bio-based materials like wood undergo rapid transformation, prompting the use of various modification methods to minimize degradation from fungal decay and dimensional changes (Williams 2005).

Modification processes enhance specific wood properties using chemical, biological, or physical agents. Chemical modification, such as anhydride treatment, functionalizes the molecular structure of wood polymer constituents, reducing hygroscopicity and enhancing hydrophobicity and dimensional stability (Hill 2000, 2006).

Acetylation, a well-established chemical treatment, involves forming ester bonds with the hydroxy groups of cell wall polymers, significantly improving UV resistance and reducing surface erosion critical for façade materials (Qin et al. 2014; Rüther and Time 2015). The global commercial production of acetylated wood reaches 120,000 m³/year (Jones and Sandberg 2020). Although acetylated wood's mechanical strength properties are comparable to untreated wood, its durability and dimensional stability are greatly enhanced. Despite its initial stability against UV radiation, acetylated wood eventually fades and greys, similar to other woods. As weathering progresses, deacetylation and the effects of dilute acids may increase degradation (Evans 2009). Moreover, acetylated wood remains vulnerable to mold and blue stain fungi since no toxic chemicals are added. However, its improved dimensional stability and resistance to fungal decay enhance the performance of coatings. This research aims to comprehensively evaluate the effect of wood acetylation on two hardwood species exposed to natural weathering, contributing to understanding the drawbacks of the process and suggesting improvements.

MATERIALS AND METHODS
Experimental samples
Acetylated wooden boards with a 20% acetyl weight gain on average, manufactured from the hardwood's black alder (*Alnus glutinosa* L.) and European beech (*Fagus sylvatica* L.) were used for the preparation of experimental samples. Fifty-four small blocks (150 L × 75 W × 20 T mm3, respectively) were cut out from each of the 3 sample types, for 6 natural weathering scenarios and 3 replicas for each test scenario. The wood modification was performed at the commercial production facilities of Accsys Technologies in the Netherlands.

Weathering tests
Natural weathering tests were conducted in San Michele, Italy (46°11'15''N, 11°08'00''E). The purpose of these tests was to gather a reference dataset on material performance over varying exposure durations. Samples were mounted on vertical stands designed to simulate a building façade, facing south. The experiment spanned a total of 15 months. Every three months, three replicas were removed from the stand to halt further deterioration, resulting in a collection of samples exposed for 0, 3, 6, 9, 12, and 15 months. Three replicated samples were measured at each interval representing a distinct experimental scenario. Prior to subsequent measurements, all samples were stored in a climatic chamber maintained at 20°C and 65% RH to ensure stable conditions.

Characterisation methods
Digitalisation
After conditioning samples were scanned with an office scanner HP Scanjet 2710 (300 dpi, 24 bit) and saved as TIF files.
Colour measurement
Colour changes were assessed with a spectrometer following the CIE Lab system, where colour is expressed with three parameters: L* (lightness), a* (red-green tone) and b* (yellow-blue tone). CIE L*a*b* colours were measured using a MicroFlash 200D spectrophotometer (DataColor Int, Lawrenceville, USA). The selected illuminant was D65 and the viewer angle was 10°. Specimens were measured on five randomly selected spots over the weathered surface. The mean values were considered as a representative colour, even if the maximum and minimum readings were preserved to assess the natural variation of the colour distribution.
Microscopic observation and 3D roughness measurement
Keyence VHX-6000 digital microscope (Keyence, Osaka, Japan) was used for microscopic observation, high magnification image acquisition, and 3D surface topography scanning. Colour images were collected with an optical configuration corresponding to ×30 and ×200 magnifications. The light direction and intensity were adjusted to assure a wide dynamic range of the image and avoid generation of saturated pixels. Part of the high magnification images were acquired in the real-time 3D depth reconstruction mode. Data was used to determine surface profile as well as surface roughness indicators.
Contact angle and surface free energy
Dynamic contact angle measurements were performed using the optical tensiometer Attention Theta Flex Auto 4 (Biolin Scientific, Sweden). Five replicates of a sequence with distilled water and

formamide were run on each sample using the sessile drop method. The measurement of each drop started at initial contact of the drop with the sample surface and lasted for 20 seconds. The series of images collected were post-processed with the software of the tensiometer. The surface free energy was computed following OWRK/Fowkes method.

RESULTS AND DISCUSSION

The appearance changes in the studied samples after natural weathering at various exposure times are shown in Figure 1. Initially, acetylated samples showed a lightening in color after three months, which then stabilized for the next three months. Photo bleaching of acetylated wood, primarily caused by visible light, progressed, turning in acetylated wood to a grey tonality by the end of the 15-month weathering test.

Biotic attacks often cause spots on the surface, a phenomenon that could be used a rapid homogenization strategy. However, such visual changes are in general viewed negatively on wooden façade claddings. Concurrently with these color changes, all samples also displayed minor surface disintegration, including raised fibers and small cracks (Žlahtič 2016).

Figure 1: Coloured scanning electron micrograph of ash cross-section (a) and the centre of the same cross-section enlarged and rotated by 180• (b). #1 black alder, #2 European beech

Figure 2 presents colourimetry changes of acetylated wood samples exposed to natural weathering. The apparent lightness (CIE L*) was relatively stable, with only a slight and steady rise at the initial phase of the weathering test. CIE a* gradually decreased for both samples, reaching more stable values from the 6th month of exposure. Values of CIE b* progressively dropped after a slight gradual increase at the beginning of the weathering test.
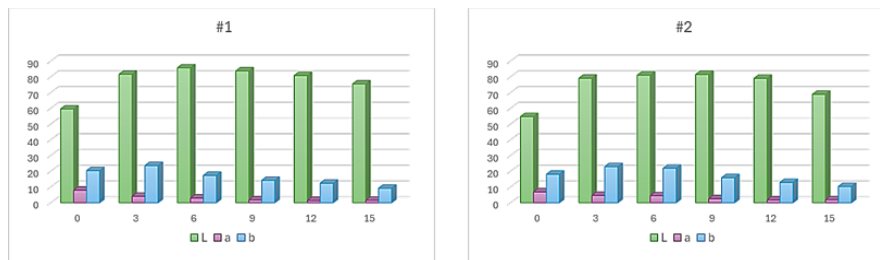
Figure 2: CIE L*a*b* coordinates of acetylated samples exposed to natural weathering. #1 black alder, #2 European beech

Furthermore, a noticeable increase in surface roughness was observed in all acetylated samples. For instance, the surface topography analysis of sample #2 is shown in Figure 3. The 3D topography map, combined with the color image, reveals that hardwood vessels are a primary cause of surface irregularities. Nonetheless, the surface profile outline clearly shows ongoing surface erosion, confirmed by the continuous increase in surface roughness parameters. Three-dimensional (3D) area surface texture assessment is advantageous for characterizing surfaces of heterogeneous and anisotropic materials like wood. The roughness profile (Ra), typically determined from two-dimensional roughness profiles, shows that values of Arithmetical mean surface height (Sa) steadily increased for acetylated alder #1 and beech #2. A steady reduction in skewness (Ssk) suggests a normalization of the top material ratio, indicative of fiber loss and general erosion of the uncoated wood surface. Overall, an increase in

surface roughness during weathering corresponds to the removal of individual fibers, leaching of photodegraded components, and overall erosion of the wood surface. Despite the acetylation process generally enhancing mould resistance in wood, acetylated beech (#2) was the most affected by mould growth.
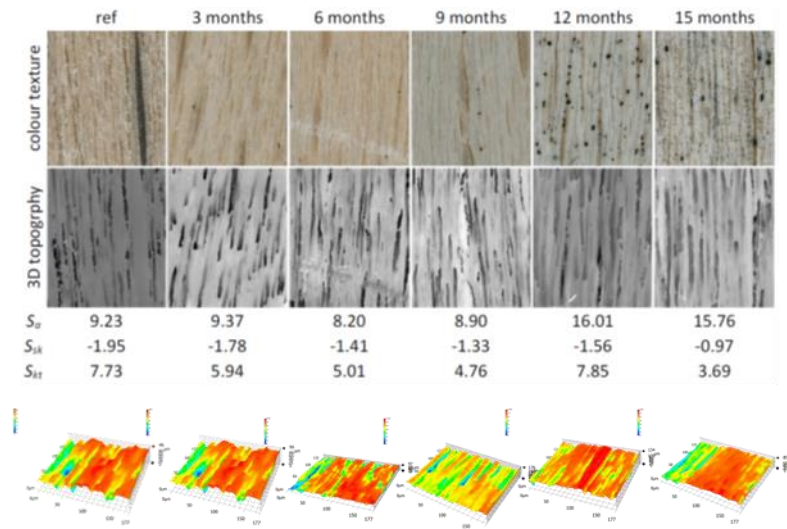

Figure 3: 3D surface topography map, surface profiles, and images of the acetylated beech (#2) exposed 15 months to natural weathering

Regarding the measurement of the dynamic contact angle, a low initial contact angle (θ) was observed in all cases after the weathering process. A drop in θ value occurred after three months, followed by relatively stable values from month 3 to month 15. The estimates of the surface free energy (SFE) are presented in Figure 4, which includes the total surface free energy (γtot) along with its polar (γp) and disperse (γd) components. The values of the SFE for the acetylated species generally fluctuated around 70 mJ·m^{-2}. The values of γp remained fairly constant, while γd showed a drop after the initial 3 months, subsequently oscillating around 15 mJ·m^{-2}. Generally, the weathering process in unprotected wood increases wettability.
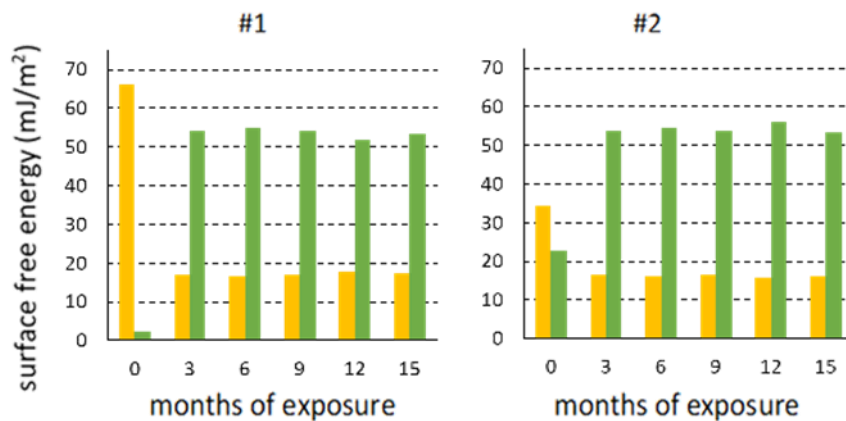

Figure 4: Surface free energy (γtot) including polar (γp) (yellow) and disperse (γd) (green) components. #1 black alder, #2 European beech

CONCLUSIONS

The performance of acetylated wood samples was evaluated using several methods that assess materials at different levels. Although the outward appearance varied, all samples maintained their functionality as cladding material, protecting the building envelope. The grey color and uniform mould growth provided an aesthetic appeal that may be desired by customers. An increase in surface roughness during the weathering process was observed for both hardwoods, associated with the removal of single fibers, leaching of photodegradation components, and general erosion of the wood surface. For both hardwood

species, a significant drop in contact angle was observed after three months, followed by relatively stable values from month 3 to month 15. Differences in surface appearance, erosion, wettability behavior, and changes in chemical composition are crucial for understanding species-dependent drawbacks of the acetylation process and its potential for further improvement.

ACKNOWLEDGEMENTS

REFERENCES

Arpaci, S. S., Tomak, E. D., Ermeydan, M. A., & Yildirim, I. (2021). Natural weathering of sixteen wood species: Changes on surface properties. *Polym Degrad Stability* 183, 109415. https://doi.org/10.1016/j.polymdegradstab.2020.109415

Cogulet, A., Blanchet, P., & Landry, V. (2016). Wood degradation under UV irradiation: A lignin characterization. *J Photochem Photobiology B: Biology*, 158, 184–191. https://doi.org/10.1016/j.jphotobiol.2016.02.030

Evans, P. D. (2009). Review of the weathering and photostability of modified wood. *Wood Mater Sci Eng*, 4(1–2), 2–13. https://doi.org/10.1080/17480270903249391

Hill, C. A. S. (2006). Wood Modification Chemical, Thermal and Other processes. John Willey & Sons Ltd., Chichester, England. https://doi.org/10.1002/0470021748

Hill, C. A. S., Cetin, N. S., & Ozmen, N. (2000). Potential Catalysts for the Acetylation of Wood. *Holzforschung*, 54(3), 269–272. https://doi.org/10.1515/hf.2000.045

Jones, D.; Sandberg, D. A . (2020). Review of Wood Modification Globally – Updated Findings from COST FP1407. Interdisciplinary Perspectives on the Built Environment, 1, 33pp. https://doi.org/10.37947/ipbe.2020.vol1.1

Pandey, K. K. (2005). A note on the influence of extractives on the photo-discoloration and photo-degradation of wood. *Polymer Degradation Stability,* 87(2), 375–379. https://doi.org/10.1016/j.polymdegradstab.2004.09.007

Qin, Z., Gao, Q., Zhang, S., & Li, J. (2014). Surface Free Energy and Dynamic Wettability of Differently Machined Poplar Woods. BioResources, 9(2). https://doi.org/10.15376/biores.9.2.3088-3103

Reinprecht, L., Mamoňová, M., Pánek, M., & Kačík, F. (2017). The impact of natural and artificial weathering on the visual, colour and structural changes of seven tropical woods. *European J Wood Wood Prod,* 76(1), 175–190. https://doi.org/10.1007/s00107-017-1228-1

Rüther, P., & Time, B. (2015). External wood claddings – performance criteria, driving rain and large-scale water penetration methods. *Wood Mater Sci Eng*, 10(3), 287–299. https://doi.org/10.1080/17480272.2015.1063688

Sandak, A., Sandak, J., Brzezicki, M., & Kutnar, A. (2019). Bio-based Building Skin. In Environmental Footprints and Eco-design of Products and Processes. Springer Singapore. https://doi.org/10.1007/978-981-13-3747-5

Williams, R.R. 2005. Weathering of wood. In Handbook of Wood Chemistry and Wood Composites 1st ed.; Rowell R.M. ed.; CRC Press: Boca Raton, US, 2005; pp. 139-185. https://doi.org/10.1201/9780203492437-11

Žlahtič, M., & Humar, M. (2016). Influence of Artificial and Natural Weathering on the Hydrophobicity and Surface Properties of Wood. BioResources, 11(2). https://doi.org/10.15376/biores.11.2.4964-4989

Unlocking a Potential Deacetylation of Acetylated Beech (*Fagus sylvatica* L.) LVL

Maik Slabohm[1], Holger Militz[1*]

[1] Wood Biology and Wood Products, Burckhardt Institute, Georg-August University of Göttingen, Büsgenweg 4, 37077 Göttingen, Germany

E-mail: maik.slabohm@uni-goettingen.de; hmilitz@gwdg.de

Keywords: Wood modification, Laminated veneer lumber (LVL), Beech, Acetylation

ABSTRACT
Acetylation with acetic anhydride is well-known to reduce the wood-moisture interaction at the cell wall level. However, it is unknown if high temperature, which is needed during manufacturing of veneer-based products to cure the adhesive, cleaves off added acetyl groups (deacetylation). In this study, acetylated veneer was heat-treated at 150°C. Furthermore, acetylated veneers were bonded to LVL by using one-component polyurethane (PUR) and phenol-resorcinol-formaldehyde (PRF) adhesive at room temperature (20°C) and at 150°C. The material was stored in climatized boxes with selected relative humidity's (RH) using various salt solutions. The data showed that the heat-treatment had no effect on the wood-moisture interaction of the acetylated wood.

INTRODUCTION
Acetylation is well-known to reduce the wood-moisture interaction at the cell wall level. After acetylation improved durability against fungi and insects and less shrinking and swelling are regularly found (Beck et al., 2018; Digaitis et al., 2021; Militz, 1991; Ohkoshi et al., 1999). The acetylation process has been industrialized, known as ACCOYA® for solid wood and TRICOYA® for wood fibers. Currently acetylated veneer based products are under development (Joeressen et al., 2022; Slabohm et al., 2023b, 2023a, 2022; T. Wang et al., 2022; Wang et al., 2021; Y. Wang et al., 2022). Basically, wood hydroxyl groups (–OH) esterify with acetic anhydride ($C_4H_6O_3$) to acetylated wood (wood–$C_2H_3O_2$) and acetic acid ($C_2H_4O_2$) as by-product (Hill, 2006).

To manufacture thicker dimension veneer-based products usually two bonding processes are applied: 1) primary hot-bonding with phenol-formaldehyde adhesive and 2) secondary bonding at room temperature using cold-curing adhesives, such as one-component polyurethane (PUR) and phenol-resorcinol-formaldehyde (PRF).

It is unknown if high temperatures (up to 150°C) during the primary bonding effect acetylated veneer negatively under the presence of adhesive and remaining acetic acid. The added acetyl groups due to acetylation with acetic anhydride might cleave off (deacetylate) and hydroxyl groups might become available again. As a result, the wood-moisture interaction would increase again. This investigation was done to look into a possible deacetylation.

MATERIALS AND METHODS
Rotary-cut beech (*Fagus sylvatica* L.) veneers (2200 mm x 600 mm x 2.4 mm, longitudinal x tangential x radial) were acetylated with acetic anhydride using the industrial production plant of Accsys Technologies S.A., in Arnhem, the Netherlands. Half of the veneers were kept as untreated references. Veneers were separated in veneers with and without visible red-heart parts. On 110 beech veneers (500 x 500 x 2.4 mm³) without visible red-heart parts was the weight percent gain (WPG, see Equation 1) determined as well as on 51 with discolored red-heart parts.

$$WPG = \frac{M_{ace} - M_{od}}{M_{od}} \; x \; 100 \; [\%] \tag{1}$$

The oven-dry weight was determined by drying the veneers at 103±2°C for 24 hours and storing them in a self-made exicator (sealed plastic box filled with silica gel). Although the exposure of the veneers to up to 105°C was not ideal, it might not have much of an impact on the acetylated veneer.

In total, 24 (250 mm x 250 mm) four-layered LVL boards were bonded using different manufacturing combinations (Table 18). A hand roller was used to apply 180 g/m^2 of the adhesive (PRF or PUR) one-sided on three of the four veneers (with and without sections of discolored red-heart) per board. The boards were manufacturing using a hydraulic press (HPS 250, Gottfried Joos Maschinenfabrik GmbH & Co. KG) at a pressure of 1 N/mm^2.

Deutsche Holzveredelung Schmeing GmbH in Kirchhundem, Germany, produced acetylated and untreated beech LVL (2200 mm x 600 mm) in a press with 12 platforms at 150°C. Since acetylated veneers do not densify considerably, 17 acetylated veneers and 19 untreated veneers (≈ 1.3 mm) were utilized to create a 20 mm thick board. On both sides of the veneers, 200 g/m² of phenol-formaldehyde (PF) was applied and pre-dried at roughly 90°C. A pressure of 3.5 N/mm² was chosen. For greater comparability, the LVL was planed one-sided to the same thickness as the lab-scale specimen.

In addition, three veneers of each material (acetylated and untreated) were cut to 250 mm squares and treated according to Table 1. Of each veneer one square was kept as reference but pressed at room temperature, one square was hot-pressed at 150°C for 20 minutes and on a third square ≈10 g water was sprayed shortly before hot-pressing, to facilitate potential chemical reactions (deacetylation) during hot-pressing.

Table 18: Manufacturing combinations to produce LVL

Combination	Material	Adhesive	Pressing time [min]	Pressing Temperature
1	acetylated LVL	PUR	180	room temperature
2	untreated LVL			
3	acetylated LVL	PUR	20	150°C
4	untreated LVL			
5	acetylated LVL	PRF	180	room temperature
6	untreated LVL			
7	acetylated LVL	PRF	20	150°C
8	untreated LVL			
9	acetylated LVL	PF	30	150°C
10	untreated LVL	PF	30	150°C
11	acetylated veneer	-	20	room temperature
12	untreated veneer	-	20	room temperature
13	acetylated veneer	-	20	150°C
14	untreated veneer	-	20	150°C

The material was subjected to perforated stainless-steel panels over saturated, aqueous over-saturated salt solutions (Broudy, 1933; Emmerich et al., 2020; Greenspan, 1977; Kurkowiak et al., 2021; Papadopoulos and Hill, 2003) in one sealed plastic box per solution. Specimens were not leached as in other studies (Kurkowiak et al., 2021), as it is known that acetylated wood has minimal mass loss during leaching (Slabohm et al., 2023a). After storing, was the mass determined (±0,001g). The specimens were dried at 103°C and the mass measured was again. The MC as well as MC ratios were calculated as described in the section above.

Table 19: Chemical solutions used for specimen climatization at 20°C

Number	Symbol	Name	Aimed rel. HD [%]	Aimed MC untreated wood (%)
1	CH_3CO_2K	potassium acetate	20	5
2	NaCl	sodium chloride	75	14
3	KCl	potassium chloride	85	17
4	K_2SO_4	potassium sulphate	97	26
5	diH_2O	deionized water	100	30

RESULTS AND DISCUSSION
Weight-percent-gain

Veneers of 2.4mm thickness without visible red-heart parts had a WPG of 22.7 % (SD 0.7; n = 110) after acetylation and the ones with visible red-heart 23.6 (SD 0.6; n=51). This shows that even difficult to treat parts of beech were successfully acetylated at an industrial scale. The WPG might be even higher, because extractives and other water-soluble parts were washed out during the acetylation process, which lowers the dry weight and therefore the WPG. Leaching the veneers before determining the WPG could help to minimize this problem, but was not applied because it would be less practically. However, a WPG of around 20% is needed to protect the modified hardwood from brown and white rot (Hill, 2006) and 18-19% for protection in-ground contact (Larsson-Brelid and Westin, 2010).

Long-term conditioning over salt solutions

The data of the ad- and desorption isotherms of the modified wood indicates, that post-heat-treatment at 150°C (typical during LVL and plywood manufacturing) after acetylation does not affect the wood-moisture interaction (Figure 1). It is evident from the plots that the MC of all acetylated materials is clearly decreased compared to the unmodified references and no great differences between the acetylated materials was found.

The reduced wood-moisture interaction after acetylation corresponds to earlier studies on acetylated beech wood and other acetylated wood species (Beck et al., 2017; Čermák et al., 2022; Digaitis et al., 2021; Forsman et al., 2020; Hill et al., 2005; Himmel and Mai, 2015; Militz, 1991; Popescu et al., 2014, 2014; Thybring et al., 2020; Thygesen et al., 2010; Yang et al., 2023). During acetylation woods accessible hydroxyl groups react with acetic anhydride to form ester groups with the wood and acetic acid as by-product (Hill, 2006). As a result, the wood-water interaction is reduced at the cell wall level, which is most likely due to due to steric hindrance by added acetyl groups (Beck et al., 2017; Hill et al., 2005; Papadopoulos, 2010; Popescu et al., 2014). It should be noted that in climates 4 and 5, condensation of water on the specimen may have increased the MC. That the added acetyl groups cleaved of after post-heat-treatment and remained inside the cell wall (bulking effect remained) and that this is the reason that the acetylated wood still shows reduced wood-moisture interaction is much unlikely, but will be investigated in another study.
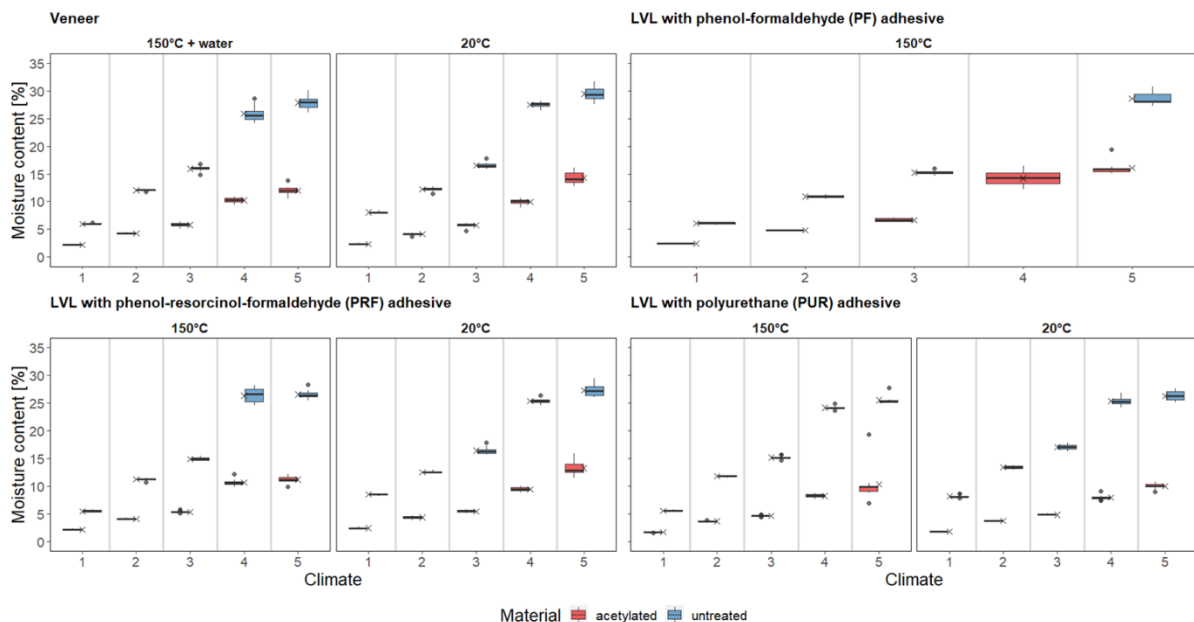

Figure 46: Long-term conditioning over salt solutions of acetylated veneer, LVL and untreated references

CONCLUSIONS

Additional heat-treatment at 150°C, which is typically needed to manufacture veneer-based products, had no impact on wood-moisture interaction of acetylated veneer and LVL. When compared to untreated controls, the acetylated wood had a significantly lower MC.

Aside from that, veneers with discolored red-heart parts exhibited similar WPG to those without discolored red-heart parts. This indicates that even difficult-to-treat parts were successfully modified. Further research will be done on the chemical composition of acetylated veneer after a similar heat-treatment.

ACKNOWLEDGEMENTS

REFERENCES

Beck, G., Strohbusch, S., Larnøy, E., Militz, H., Hill, C., 2017. Accessibility of hydroxyl groups in anhydride modified wood as measured by deuterium exchange and saponification. Holzforschung 72, 17–23. https://doi.org/10.1515/hf-2017-0059

Beck, G., Thybring, E.E., Thygesen, L.G., 2018. Brown-rot fungal degradation and de-acetylation of acetylated wood. International Biodeterioration & Biodegradation 135, 62–70. https://doi.org/10.1016/j.ibiod.2018.09.009

Broudy, H., 1933. An attempt to find salts which in saturated solution yield relative humidities not yet obtainable for use in biological research. Master thesis, University of Massachusetts, Amherst.

Čermák, P., Baar, J., Dömény, J., Výbohová, E., Rousek, R., Pařil, P., Oberle, A., Čabalová, I., Hess, D., Vodák, M., Brabec, M., 2022. Wood-water interactions of thermally modified, acetylated and melamine formaldehyde resin impregnated beech wood. Holzforschung 76, 437–450. https://doi.org/10.1515/hf-2021-0164

Digaitis, R., Thybring, E.E., Thygesen, L.G., Fredriksson, M., 2021. Targeted acetylation of wood: a tool for tuning wood-water interactions. Cellulose 28, 8009–8025. https://doi.org/10.1007/s10570-021-04033-z

Emmerich, L., Altgen, M., Rautkari, L., Militz, H., 2020. Sorption behavior and hydroxyl accessibility of wood treated with different cyclic N-methylol compounds. J Mater Sci 55, 16561–16575. https://doi.org/10.1007/s10853-020-05224-y

Forsman, K., Serrano, E., Danielsson, H., Engqvist, J., 2020. Fracture characteristics of acetylated young Scots pine. Eur. J. Wood Prod. 78, 693–703. https://doi.org/10.1007/s00107-020-01548-3

Greenspan, L., 1977. Humidity fixed points of binary saturated aqueous solutions. J. RES. NATL. BUR. STAN. SECT. A. 81A, 89–96. https://doi.org/10.6028/jres.081A.011

Hill, C.A.S., 2006. Wood modification: chemical, thermal and other processes, Wiley series in renewable resources. John Wiley & Sons, Chichester, England ; Hoboken, NJ.

Hill, C.A.S., Forster, S.C., Farahani, M.R.M., Hale, M.D.C., Ormondroyd, G.A., Williams, G.R., 2005. An investigation of cell wall micropore blocking as a possible mechanism for the decay resistance of anhydride modified wood. International Biodeterioration & Biodegradation 55, 69–76. https://doi.org/10.1016/j.ibiod.2004.07.003

Himmel, S., Mai, C., 2015. Effects of acetylation and formalization on the dynamic water vapor sorption behavior of wood. Holzforschung 69, 633–643. https://doi.org/10.1515/hf-2014-0161

Joeressen, J., Baumann, G., Spirk, S., Krenke, T., Schönauer, T., Feist, F., 2022. Chemical resistance of acetylated radiata pine sliced veneers. Wood Material Science & Engineering 1–11. https://doi.org/10.1080/17480272.2022.2155565

Kurkowiak, K., Emmerich, L., Militz, H., 2021. Sorption behavior and swelling of citric acid and sorbitol (SorCA) treated wood. Holzforschung 75, 1136–1149. https://doi.org/10.1515/hf-2021-0068

Larsson-Brelid, P., Westin, M., 2010. Biological degradation of acetylated wood after 18 years in ground contact and 10 years in marine water, in: The Proceedings IRG Annual Meeting. Presented at the International Research Group on Wood Protection IRG/WP 10-40522, Biarritz, France.

Militz, H., 1991. The improvement of dimensional stability and durability of wood through treatment with non-catalysed acetic-acid anhydrid. Holz als Roh-und Werkstoff 49, 147–152. https://doi.org/10.1007/BF02607895

Ohkoshi, M., Kato, A., Suzuki, K., Hayashi, N., Ishihara, M., 1999. Characterization of acetylated wood decayed by brown-rot and white-rot fungi. J Wood Sci 45, 69–75. https://doi.org/10.1007/BF00579526

Papadopoulos, A., 2010. Chemical modification of solid wood and wood raw material for composites production with linear chain carboxylic acid anhydrides: A brief review. BioResources 5.

Papadopoulos, A.N., Hill, C.A.S., 2003. The sorption of water vapour by anhydride modified softwood. Wood Science and Technology 37, 221–231. https://doi.org/10.1007/s00226-003-0192-6

Popescu, C.-M., Hill, C.A.S., Curling, S., Ormondroyd, G., Xie, Y., 2014. The water vapour sorption behaviour of acetylated birch wood: how acetylation affects the sorption isotherm and accessible hydroxyl content. J Mater Sci 49, 2362–2371. https://doi.org/10.1007/s10853-013-7937-x

Slabohm, M., Brischke, C., Militz, H., 2023a. The durability of acetylated beech (Fagus sylvatica L.) laminated veneer lumber (LVL) against wood-destroying basidiomycetes. Eur. J. Wood Prod. https://doi.org/10.1007/s00107-023-01962-3

Slabohm, M., Mayer, A.K., Militz, H., 2022. Compression of Acetylated Beech (Fagus sylvatica L.) Laminated Veneer Lumber (LVL). Forests 13, 1122. https://doi.org/10.3390/f13071122

Slabohm, M., Stolze, H., Militz, H., 2023b. Evaluation of wet tensile shear strength and surface properties of finger-jointed acetylated beech (Fagus sylvatica L.) laminated veneer lumber. Eur. J. Wood Prod. https://doi.org/10.1007/s00107-023-01970-3

Thybring, E.E., Piqueras, S., Tarmian, A., Burgert, I., 2020. Water accessibility to hydroxyls confined in solid wood cell walls. Cellulose 27, 5617–5627. https://doi.org/10.1007/s10570-020-03182-x

Thygesen, L.G., Tang Engelund, E., Hoffmeyer, P., 2010. Water sorption in wood and modified wood at high values of relative humidity. Part I: Results for untreated, acetylated, and furfurylated Norway spruce. Holzforschung 64. https://doi.org/10.1515/hf.2010.044

Wang, T., Wang, Y., Crocetti, R., Wålinder, M., 2022. The Embedment Behavior of Acetylated and Unmodified Birch Plywood. Presented at the 10th European Conference on Wood Modification, Nancy, France, pp. 400–406.

Wang, Y., Wang, T., Crocetti, R., Wålinder, M., 2022. Experimental investigation on mechanical properties of acetylated birch plywood and its angle-dependence. Construction and Building Materials 344, 128277. https://doi.org/10.1016/j.conbuildmat.2022.128277

Wang, Y., Wang, T., Crocetti, R., Wålinder, M., 2021. Mechanical properties of acetylated birch plywood loaded parallel to the face grain. Presented at the 16th World Conference on Timber Engineering, Santiago, Chile.

Yang, T., Mei, C., Ma, E., Cao, J., 2023. Effects of acetylation on moisture sorption of wood under cyclically changing conditions of relative humidity. Eur. J. Wood Prod. 81, 723–731. https://doi.org/10.1007/s00107-022-01903-6

Fork and flying wood tests to improve prediction of board stress development during drying

Antoine Stéphan[1*], Patrick Perré[2,3], Clément L'Hostis[4], Romain Rémond[1]

[1] Université de Lorraine, INRAE, LERMAB, 88000 Épinal, France
[2] Université Paris-Saclay, CentraleSupélec, LGPM, 91190 Gif-sur-Yvette, France
[3] Université Paris-Saclay, CentraleSupélec, LGPM SFR Condorcet FR CNRS 3417, Centre Européen de Biotechnologie et de Bioéconomie (CEBB), 51110 Pomacle, France
[4] FCBA – Institut Technologique Forêt Cellulose Bois-construction Ameublement, 77420 Champs-sur-Marne, France

E-mail: antoine.stephan@univ-lorraine.fr; patrick.perre@centralesupelec.fr; clement.lhostis@fcba.fr; romain.remond@univ-lorraine.fr

Keywords: drying quality, drying modelling, mechanical model, mechanosorptive strain

ABSTRACT

Drying of hardwoods is essential to bring the wood products to an equilibrium moisture content appropriate for their use. During drying, some checks, cracks and significant residual drying stresses can occur, which can considerably reduce the final quality of the product. Therefore, in order to optimize the drying schedule, it is important to be able to compute the drying stress and deformation during the process. The mechanical behavior is a combination of different contributions such as elasticity, plasticity, viscoelasticity and mechanosorption. The memory strain (i.e. viscoelastic and mechanosorptive creeps) is perhaps the largest source of prediction uncertainty. In this work, two experimental tools, the fork and the flying wood tests, were used together to test the predictive ability of a mechanosorptive model. A first example is given here by comparing the prediction of the mechanical model used by (Salem 2016) with the memory strain measured by the fork test on beech wood samples. This mechanical model is then implemented in a multiphysics model to simulate asymmetrical drying of a wood plank. The predicted curvature is compared with measurements from the flying wood test. The results show that the mechanosorptive model of (Fortino et al. 2009) has a fairly good predictive potential for memory strain and stress development during drying, but improvements in the formulation and choice of parameter values seem necessary.

INTRODUCTION

Quality of dried wood is taken into account in industry as it assets the performances of the final product and ensure the future use of the material. During drying, the internal mass transfer resistance of wood causes the board to present a moisture gradient according to its thickness, inducing inhomogeneous shrinkage and creating a stress field in the board. The quality considered in this work is the reduction of the drying stresses in order to avoid the cracks that are internal or on the surface of the board. They result from significant stresses that exceed the strength of the wood, due to inappropriate drying schedule or accidental misdirection.

In industry, the mechanical drying stress within the board is sometimes quantified in order to better assess the quality of the drying process and to improve the drying schedule. Some of them are destructive and performed a posteriori, such as the prong test and the slicing test (McMillen 1958), and rare are those used to monitor the stress along the process (Allegretti and Ferrari 2008).

The prediction of the drying stresses is another solution that has been widely studied for decades. Therefore, a rheological model of the material is sought to reproduce the observed behavior of the material and to be implemented in a computational model for heat and mass transfer. The mechanical state of wood is difficult to simulate as expected, since it has instantaneous and delayed linear behavior, but also non-linear behavior, in particular when it is subjected to moisture variations (Ugolev 1976). The mechanosorption of wood, which is affected by the history of moisture content and load of the material, requires an advanced modeling as it has a non-linear response to moisture variations and material stresses. From the primary works (Leicester 1971) on the fitting of a model to more recent

works (Yu et al. 2022), important progress has been made, particularly on the prediction of recoverable and unrecoverable strains. The complexity of some means that many parameters need to be identified through experimental campaigns.

The flying wood test (Brandao and Perré 1996) is an asymmetrical drying of a wood plank. It is a way of expressing the evolution of stress during drying through the evolution of the global curvature of the plank. The stress reversal due to memory strain is clearly shown by the reversal of the plank curvature. Such a test is on the right scale for quality assessment. However, it is difficult to assess the relevance of the assumed memory strain model on the basis of the flying wood test experience alone. In fact, the development of curvature results from the development of moisture and stress fields within the board. The fork test (Stéphan et al. 2024) can complement this initial test by characterizing the memory strain without a moisture gradient within the sample. It is then possible to test the relevance of the mechanical formulation alone.

In the first part of this work, a comparison was made between the simulation of a simple mechanical model and a fork test on a beech sample. Finally, the prediction of stresses during drying requires the evolution of the moisture gradient in the material during drying to be taken into account. For this purpose, the flying wood tests performed on the same hardwood species are presented and compared with the model.

MATERIALS AND METHODS
Memory strain measure
Wood sampling and drying conditions

The samples used in this work are of beech (*Fagus sylvatica*). These hardwood samples were taken from two different trees in the Vosges area. For each test, all the samples were twins, i.e. were taken from a plank sawn in the grain direction and therefore have the same annual growth rings. For the fork test, three twins samples have been used with dimensions of 3 mm in the grain direction, 75 mm in the radial direction and 10 mm in the tangential direction.

The samples have been cut in the green state, in the heartwood part, with a precision cutting machine and installed on the different devices (one for the measurement of constrained strain, one for the measurement of free shrinkage and swelling on a dedicated rig and one kept for the measurements of young modulus), but in the same climatic chamber, and under the temperature and relative humidity presented in Figure 1. The drying schedule was composed of drying steps followed by several cyclic drying and wetting phases. For these cycles, the period was set at 12 hours to allow the wood samples to reach the equilibrium moisture content at each step.
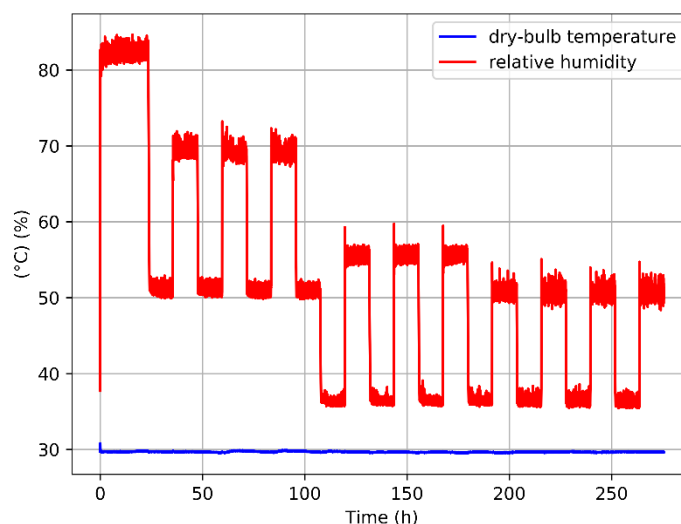

Figure 1: Temperature of dry air (blue) and relative humidity (red) during the fork test in the climatic chamber

The fork test

The data used to test the mechanical model alone come from experimental measurements on a "fork" test. It was performed on the prototype of a new experiment currently under review (Stéphan et al. 2024). It consists of measuring the memory strain of a loaded sample of wood, under varying moisture content. This deformation is estimated from the total deformation measured on the loaded sample, from which we subtract the elastic deformation, estimated by Hook's law, and the free shrinkage/swelling deformation which is measured on a twin sample (Fig. 2). The thickness of the sample in the grain direction (3 mm) benefits the moisture content equilibrium, so that no gradient of moisture content in the radial and tangential directions is considered. The same device measures the force applied to the sample by the fork device in one material direction (radial in this work).

Such constrained shrinkage and swelling shows the contribution of the viscoelasticity and mechanosorption to the sample strain.

The memory strain measured by the fork test was compared with those simulated by the mechanical model.

Flying wood test

The results of the Flying wood tests are those obtained in a previous work by (Salem et al. 2017) with an apparatus described by (Brandao and Perré 1996) and presented in Figure 3. The samples for flying wood were cut with the dimensions 150x100x5 mm in longitudinal, tangential and radial direction respectively. The sag of the sample curvature has been measured with a linear variable differential transformer during the drying at constant dry-bulb temperature (31 °C) and equilibrium moisture content (8 %).
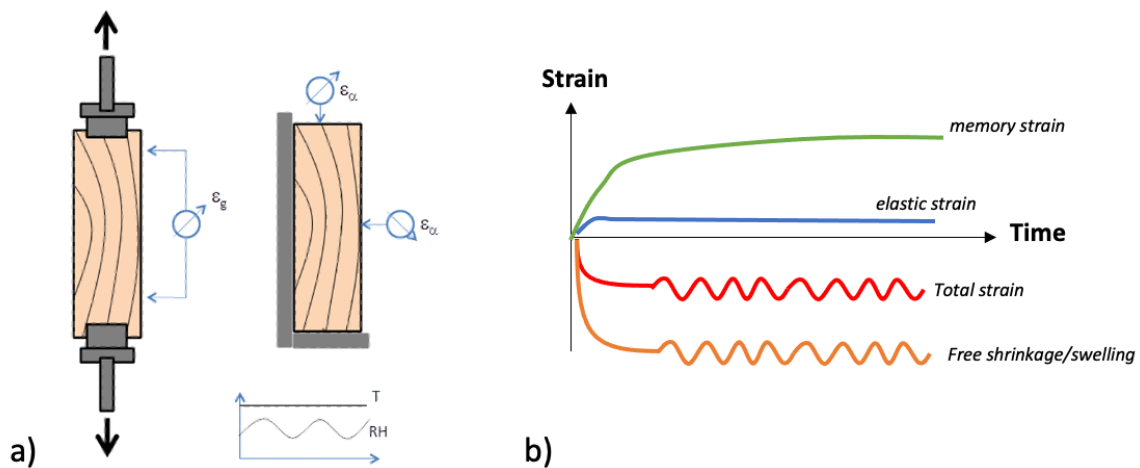

Figure 2: Schematic diagrams of measuring principle of the "fork" experiment (a) and results (b)
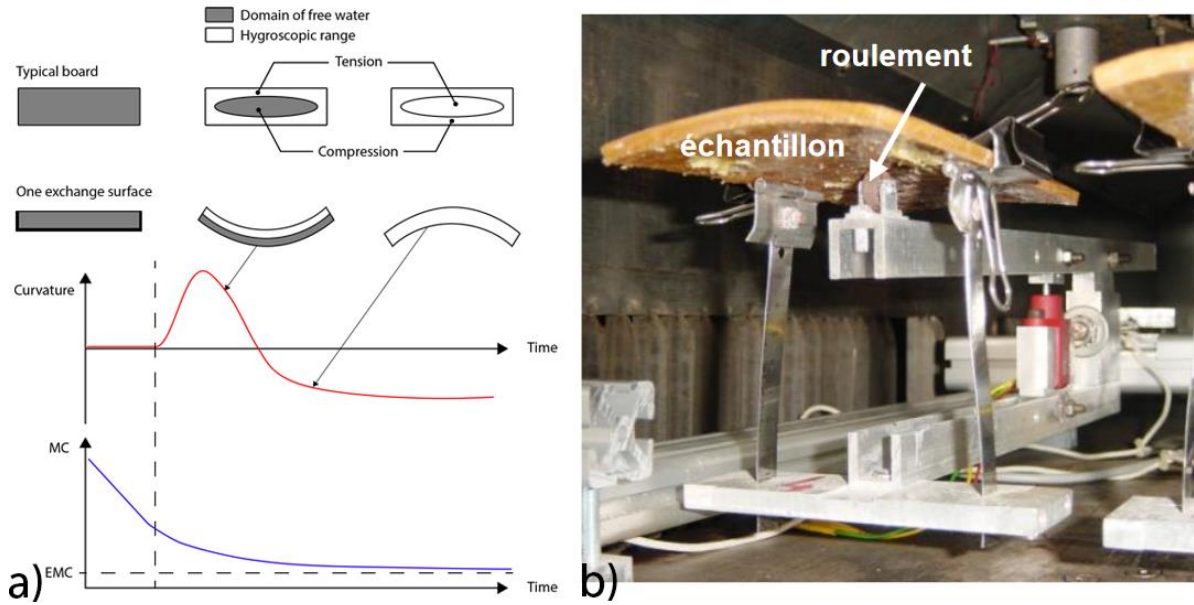
Figure 3: Principle (a) and picture (b) of the Flying Wood test, adapted from (Perré 2007) and (Salem 2016)

The results of the flying wood tests were compared with the simulation from the code *TransPore* coupled with a mechanical model. The measured sample curvature and the average moisture content of samples were compared with the predictions.

Computational model
Mechanical model

A one-dimensional mechanical formulation was adopted (Rémond et al. 2007).

In the constitutive equation the mechanical strain is divided into an elastic strain, related to the stresses via Hooke's law, shrinkage, and a memory strain related to the viscoelasticity and the mechanosorption of the wood (Eq. 1). The plasticity strain is not considered in this work. Since the experiment was carried out at low temperature (35 °C), the contribution of the viscoelasticity to the memory strain could be neglected. The shrinkage strain was assumed to be proportional to the change in bound water.

The mechanosorptive model of (Svensson and Toratti 2002) was used in this work, with the parameters proposed by (Fortino et al. 2009) and reused in (Salem 2016) for beech. The mechanosorptive strain in this model is calculated with Eq.2. The following equations are from (Fortino et al. 2009).

$$\epsilon = \epsilon_e + \epsilon_\alpha + \epsilon_{ve} + \epsilon_{ms} \tag{1}$$

$$\dot{\epsilon}_{ms} = \dot{\epsilon}_{ms,v} + \dot{\epsilon}_{ms,r} \tag{2}$$

$$\dot{\epsilon}_{ms,v} = m_v \sigma |\dot{U}| \tag{3}$$

$$\dot{\epsilon}_{ms,r} = \sum_{i=1}^{3} \frac{J_i \sigma - \epsilon_{ms,ri}}{\tau_i} |\dot{u}| \tag{4}$$

where m_v, J_i and τ_i are material parameters, $\dot{u}$ the moisture rate and σ the stress. U indicates a moisture level that has not been reached during the previous load history.

The parameters of the three Kelvin elements are from (Fortino et al. 2009) and the coefficient m_v for irrecoverable strain $\varepsilon_{ms,v}$, defined in Eq. 3, is from (Salem 2016). They are listed in Table 1. The elastic ratio used to fit the coefficients in the tangential direction to the radial direction has been obtained from modulus measurements of fork test samples.

Table 1: Parameters of the mechanosorptive model in radial direction

I	τ [-]	m_j [MPa^{-1}]	m_v [MPa^{-1}]
1	0.01	0.0006	
2	0.1	0.0006	55.10^{-9}
3	1	0.005	

Coupling with the heat and mass transfer model

In order to simulate the flying wood test, the one-dimensional mechanical formulation was embedded in the computational code of heat and mass transfer *TransPore* (Perré and Turner 1999). *TransPore* solves the coupled heat and mass transfer equations within the board. It calculates the one-dimensional moisture content and temperature profiles within the board thickness during its non-symmetric drying. At the surface exchange of the board, the measured climatic conditions were input into the model as boundary conditions. From the moisture content and temperature profiles, the one-dimensional mechanical model calculated the stress and strain evolution within the board due to shrinkage and the resulting global curvature of the board.

Noted that in the fork test, the sample was very thin in the longitudinal direction of the material, less than 3 mm thick. As moisture transport is much easier in the fibre directions, a fairly homogeneous moisture content can be assumed across the thickness of the sample. Therefore, the moisture content distribution was not calculated by *TransPore* for this test.

RESULTS AND DISCUSSION

The fork test results

The fork experiment was performed for 250 hours up to a radial stress of 1.8 MPa, as shown in Figure 4. The stress occurs according to the drying or wetting of the sample: starting from the green state, the wood sample dries at each lower level of relative humidity, corresponding to a lower equilibrium moisture content. The material shrink as its moisture content decreases, generating a tensile stress at its constrained ends. As the relative humidity increases, the sample moistens and swell, reducing the tensile stress. It should be noted that a slight decrease in tensile stress can be observed with successive moisture cycles, in particular between 35 and 107 hours. This behavior may be due to both the hysteresis of the sorption isotherm of wood and the mechanosorptive creep of the sample.
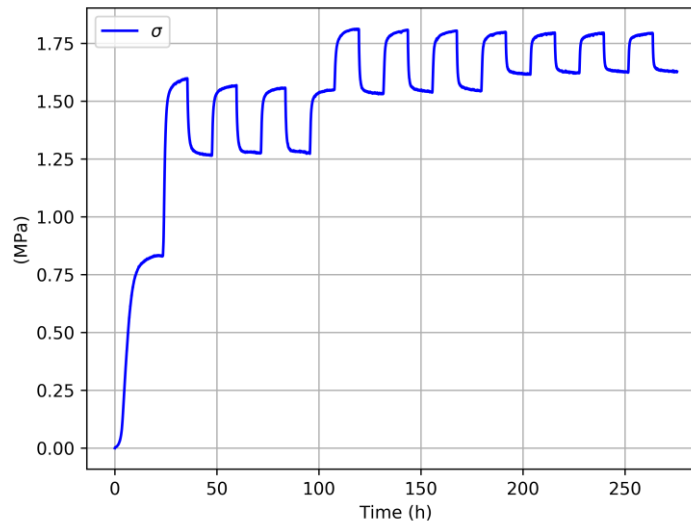

Figure 4: Evolution of the sample stress in the "fork" experiment

The memory strain measured is shown in Figure 5 and is expressed as a function of the cumulative variation of the absolute value of the moisture content of the sample. The memory strain increases as the moisture cycles accumulate. Memory creep tends towards a limit cycle by cycle. The well-known mechanosorptive limit is highlighted in this curve.
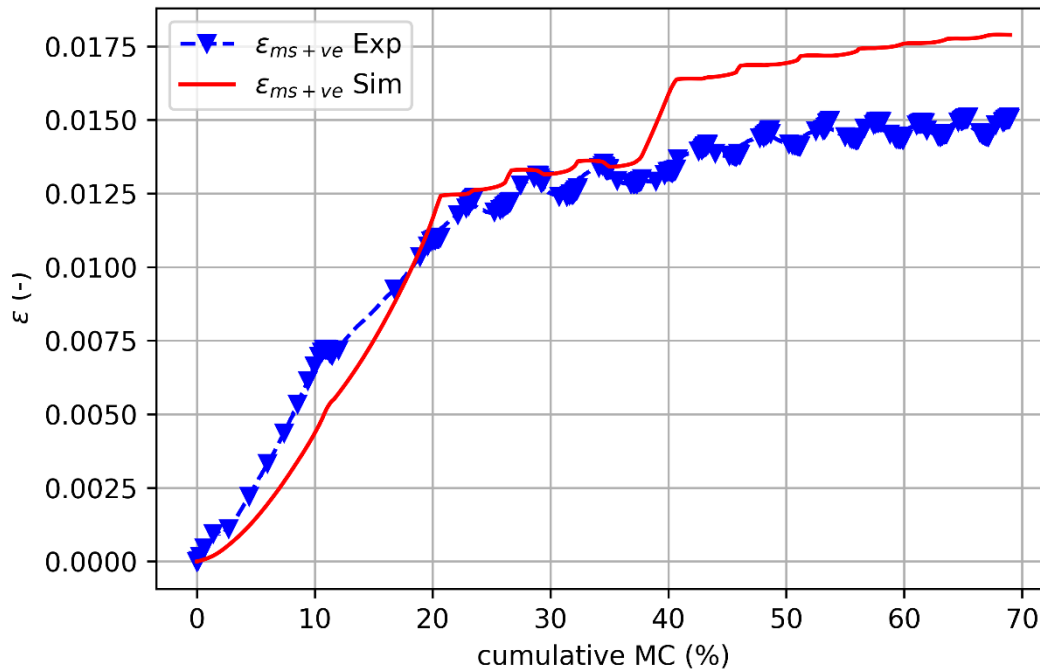
Figure 5: Results from the "fork" test: memory strain measured and simulated with the mechanical model, as function of accumulation of MC variations

Simulation using the model with parameters selected in (Fortino et al. 2009) is close to the experimental measure for the first moisture variations and cycles.

Because the sample was in the green state at the beginning of the test, it tends to reach unprecedented moisture contents several times during the test, typically for cumulative MC = 0 %, cumulative MC = 10 % and cumulative MC = 37 %, (that correspond to t = 0 h, t = 23 h and t = 99 h respectively). When such a moisture content is reached for the first time, the memory strain predicted by the model of (Fortino et al. 2009) shows a significant increase. This behavior was expected at t = 107 h, but didn't happen experimentally.

The Flying Wood test results

The drying kinetics of the Flying Wood tests are shown in Figure 6 for quarter sawn and flat sawn boards. The drying conditions measured during each test and the characteristics of our samples (geometric dimensions, initial moisture content) are entered into the *TransPore* code. The average physical properties of beech are used, except for the diffusion coefficient, for which the value has been adjusted so that the changes in the experimental and simulated average moisture content are close.

At the end of the drying process, the simulated kinetics tend towards a lower equilibrium moisture content than that observed experimentally.

In terms of mechanics (Figure 7), the code correctly predicts the trends observed experimentally: the different phases of curvature evolution and the moment of curvature inversion.

However, the intensity of the positive curvature is always underestimated by the code compared to the measured value.

This positive curvature, concave shape for the exchange surface, should occur as when the surface of the material enters its hygroscopic range. The peak in curvature corresponds to the maximum tensile stress on the surface. Because the simulation underestimates this curvature peak by a factor of two, the tensile stress at the beginning of the drying may be underestimated. In this case, the risk of cracking is misjudged and further work is required to assess the drying quality of boards.

These two experiments, the fork and the flying wood, are complementary here. The fork test allows to isolate and characterize the memory strain of wood during drying, and the flying wood allows to follow

the consequences of the evolving memory strain on stress development. Testing the material at low temperature limits the viscoelasticity and focuses on the mechanosorptive behavior of wood.
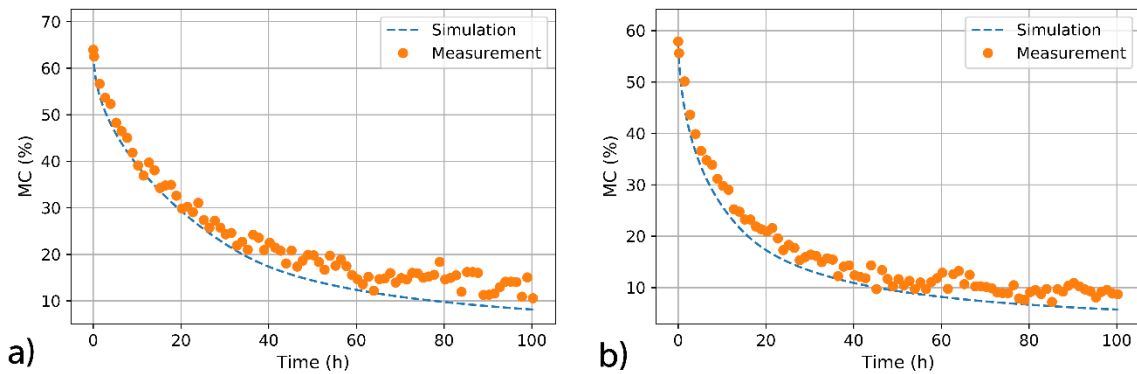

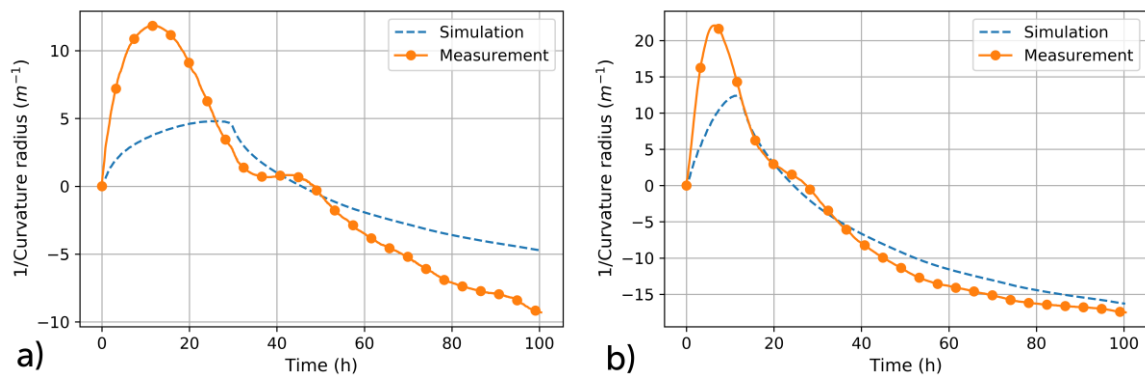*Figure 6: Drying kinetic of quarter (a) and flat (b) sawn flying wood test*

Figure 7: Sags of Flying wood tests

CONCLUSIONS AND PERSPECTIVES

A simple mechanical model for wood drying has been compared with a fork experiment. The memory strain simulated is of the same magnitude as measured experimentally, and tends also to a mechanosorptive limit as cumulative MC variations occur. The increment of memory strain predicted by the model at each new level of moisture content not yet reached during the previous strain history, was not observed on the fork test. Further investigation is required on the irrecoverable mechanosorption if the load on the sample is variable. Benefiting of parameters defined in a previous work, the simulation of the drying using this mechanistic model and the code *TransPore* for heat and mass transfer through porous media predicts quite successfully the mechanosorptive behavior observed in the flying wood test. This combination of computational tools and experiments shows its potential for quantifying stresses during wood drying and could be useful for quality control and prediction during the process. This approach will be repeated with varying drying conditions and material cutting plans to find the most adequate parameters of the model and to make it implementable in an intelligent controller for wood drying with intermittent energy sources.

ACKNOWLEDGMENTS

REFERENCES

Allegretti O, Ferrari S (2008) A Sensor for Direct Measurement of Internal Stress in Wood During Drying: Experimental Tests Toward Industrial Application. Drying Technology 26:1150–1154. https://doi.org/10.1080/07373930802266256

Brandao A, Perré P (1996) The Flying Wood - A quick test to characterize the drying behaviour of tropical woods. Québec, pp 315–324

Fortino S, Mirianon F, Toratti T (2009) A 3D moisture-stress FEM analysis for time dependent problems in timber structures. Mech Time-Depend Mater 13:333. https://doi.org/10.1007/s11043-009-9103-z

Leicester RH (1971) A rheological model for mechano-sorptive deflections of beams. Wood Science and Technology 5:211–220. https://doi.org/10.1007/BF00353683

McMillen JM (1958) Stresses in wood during drying. Forest Product Laboratory, United States Department of Agriculture, Madison 5, Wisconsin

Perré P (2007) Fundamentals of wood drying. Nancy

Perré P, Turner IW (1999) TransPore: a generic heat and mass transfer computational model for understanding and visualising the drying of porous media. Drying Technology 17:1273–1289. https://doi.org/10.1080/07373939908917614

Rémond R, Passard J, Perré P (2007) The effect of temperature and moisture content on the mechanical behaviour of wood: a comprehensive model applied to drying and bending. European Journal of Mechanics - A/Solids 26:558–572. https://doi.org/10.1016/j.euromechsol.2006.09.008

Salem T (2016) Séchage intermittent du bois d'oeuvre : étude expérimentale et numérique

Salem T, Perré P, Bouali A, et al (2017) Experimental and numerical investigation of intermittent drying of timber. Drying Technology 35:593–605. https://doi.org/10.1080/07373937.2016.1195842

Stéphan A, Perré P, L'Hostis C, Rémond R (2024) Mechanistic-based probabilistic optimization of industrial wood drying considering energy consumption, process duration, quality and cost. Drying Technology 0:1–10. https://doi.org/10.1080/07373937.2024.2323095

Svensson S, Toratti T (2002) Mechanical response of wood perpendicular to grain when subjected to changes of humidity. Wood Science and Technology 36:145–156. https://doi.org/10.1007/s00226-001-0130-4

Ugolev BN (1976) General laws of wood deformation and rheological propertions of hardwood. Wood Science and Technology 10:169–181. https://doi.org/10.1007/BF00355738

Yu T, Khaloian A, van de Kuilen J-W (2022) An improved model for the time-dependent material response of wood under mechanical loading and varying humidity conditions. Engineering Structures 259:114116. https://doi.org/10.1016/j.engstruct.2022.114116

Modification of different European hardwood species with a bio-based thermosetting resin on a semi-industrial scale

Christoph Hötte[1], Holger Militz[2]

[1,2]Georg-August-Universität Göttingen, Holzbiologie und Holzprodukte, Büsgenweg 4, D-37077 Göttingen, Deutschland

E-Mail: christoph.hoette@uni-goettingen.de; holger.militz@uni-goettingen.de

Keywords: curing, drying quality, modification quality, up-scaling

ABSTRACT

Recently, wood modification processes based on formaldehyde-free, bio-based chemicals have been gaining in importance. One of these processes, modification with sorbitol and citric acid (SorCA), is now well developed on laboratory scale and shows promising results, especially for pine sapwood (*Pinus sylvestris* L.), in terms of improved durability and dimensional stability (KURKOWIAK et al. 2021a, 2023). In this study, the suitability of three European hardwood species for modification with SorCA on a semi-industrial scale was investigated. For this purpose, boards of beech (*Fagus sylvatica* L.), birch (*Betula pendula* ROTH) and poplar (*Populus spec.*) measuring 85 x 35 x 2000 (ax.) mm were impregnated with a 1:3 mixture of sorbitol and citric acid (ω: 30%) in a vacuum-pressure process. The boards were then cured at 140 °C in a high-temperature kiln. As a softwood reference material, additional pine sapwood boards were also modified using the same process. With the exception of minor non-impregnated areas in the case of poplar, all wood species were completely penetrated with the impregnation solution and showed solution uptakes between 100 % and 140 % (figure 1). The highest Weight Percent Gain (WPG) was found for pine, followed by poplar. The WPGs of beech and birch were significantly lower. While the process had no negative effects on the drying quality in the case of pine and the beech also showed only minor drying damage, the quality of the modified poplar suffered from significant deformation (warping, bowing etc.) and that of the birch from severe cell collapse.

INTRODUCTION

Current approaches to wood modification are investigating the formaldehyde-free improvement of material-specific properties using polycarboxylic acids and sugar alcohols. Among these, modification with citric acid and sorbitol (SorCA) in particular has shown promising results with regard to an increase in the biological durability and dimensional stability of the modified wood (LARNOY 2018; MUBAROK et al. 2020; KURKOWIAK et al. 2021a). The reaction mechanism is based on esterification of the hydroxyl groups of the cell wall polymers by the carboxyl groups of the citric acid on the one hand, and on copolymerisation between the citric acid and sorbitol on the other (DOLL et al. 2006). In addition to the reaction of the chemicals with the hydroxyl groups of the cell wall polymers, a combination of the polymerisation of the modifying chemicals in the cell wall (bulking effect) and the cross-linking of the cell walls is assumed to be the mode of action for the modification with SorCA (KURKOWIAK et al. 2021b). The process has been well researched and developed on a laboratory scale. There are currently attempts to launch the process on the market in Germany (SorCA) and Norway (CIOL®).

Modification with sorbitol and citric acid consists of two process steps. Firstly, the wood is impregnated with the chemicals dissolved in water. This is followed by curing at a temperature of approx. 140 °C, which serves to fix the chemicals in the cell wall. During this phase, the chemical modification of the cell wall and the polymerisation of the chemicals take place. At the same time, the solvent is removed: the wood is dried. While good modification results could be achieved in this way for specimens on a laboratory scale (high WPG, good fixation), the chemical distribution within the specimens becomes increasingly important for the performance of the modified wood with increasing specimen size as part of the upscaling of the process. After curing in a drying oven, a pronounced accumulation of chemicals in the edge zones of the specimens and thus a highly inhomogeneous chemical distribution on the material cross-section was observed for scots pine sapwood (KURKOWIAK et al. 2022). In addition to

the modification quality, the drying quality becomes more important for the subsequent product properties as the dimensions of the raw material increase. Here, a conflict of objectives develops between curing and drying: if high temperatures and rapid heating of the wood have a positive effect on the WPG and the fixation of the chemicals, they simultaneously lead to a deterioration in the drying quality.

As a result of its impregnability and availability, modification with SorCA on a laboratory scale as well as initial trials to upscale the technology were largely carried out with scots pine sapwood. A study by MUBAROK et al. (2020) shows that under laboratory conditions, the modification of beech wood also shows promising results in terms of increasing durability and dimensional stability. In this study, the suitability of three hardwood species - beech, birch and poplar - as a raw material for modification with SorCA was tested. For comparison, scots pine sapwood was modified with SorCA. The modification was carried out on boards on a semi-industrial scale in order to obtain an impression of the modification and drying quality of the different wood species that was as close to practice as possible. The study focussed on the question of whether the curing process established for pine sapwood can be transferred to the modification of hardwoods or whether a process adaptation is necessary for hardwood modification.

MATERIAL AND METHODS

Boards of pine sapwood (*Pinus sylvestris* L.), Beech (*Fagus sylvatica* L.), Poplar (*Populus spec.*) and birch (*Betula pendula* ROTH) measuring 35 mm x 85 mm x 2000 mm (ax.) were impregnated with a 30 % SorCA solution (molar ratio 1:3) in a vacuum-pressure process. The boards were pre-dried for a week in a room climate and then cured in a pilot high-temperature kiln under dry conditions (dry curing) using an industry-oriented process. The maximum temperature during the process was 140 °C. The solution uptake was determined gravimetrically as the ratio of the masses before and after impregnation. The modification quality was determined on the basis of the weight percent gain (WPG, Formula 1) and the fixation of the chemicals was measured as the mass loss after two weeks of cold water leaching in accordance with DIN EN 84 (2020) on 50 mm x 35 mm x 50 mm (ax.) specimens, which were taken 20 cm from the ends of the boards to exclude any effects of longitudinal chemical migration (Formula 2). Following the EN84 procedure, the fixation of the chemicals was tested under long-term exposure to moisture. For this purpose, the same specimens were stored submerged in cold water for a further 12 weeks with weekly water changes. The percentage mass loss after the extended leaching was calculated according to Formula 3.

$$WPG = (m_1 - m_0) / m_0 \times 100 \tag{1}$$

$$WPG_{theoretical} = (m_0 + (m_1 - m_0) \times \omega - m_0)/m_0 \times 100 \tag{2}$$

$$Mass\ loss_{EN\ 84}\ (\%) = (m_2 - m_3) / m_2 \times 100 \tag{3}$$

$$Mass\ loss_{long\text{-}term} = (m_3 - m_4) / m_3 \times 100 \tag{4}$$

where
m_0 = mass untreated, oven-dried [g]
m_1 = mass after impregnation [g]
m_2 = mass after curing, oven-dried [g]
m_3 = mass after leaching (EN84), oven-dried [g]
m_4 = mass after long-term leaching, oven-dried [g]
ω = solution concentration [%]

The chemical distribution was assessed using an X-ray based density profile measuring device (GreCon, Germany) on the basis of specimens measuring 50 mm x 50 mm x 35 mm. Before measuring the density profiles, the specimens were oven-dried so that the average density of the cross-section corresponded to the oven-dry density of the specimens.

The parameters analysed for drying quality were deformations (bowing, twisting, cupping), crack formation and the occurrence of cell collapse. Deformations and cracking were categorized according to the following scale:

0   No or only minor occurrence of the characteristic
1   Sporadic occurrence of the characteristic with moderate manifestation. Utilisation possibly restricted or quality reduced
2   Characteristic is so pronounced that further utilization is impossible

As cell collapse represents a significant drying defect in any case, it was only categorized according to occurrence or non-occurrence.

RESULTS AND DISCUSSION
Modification quality
All of the analysed materials are wood species with high permeability. The solution uptake was therefore over 100 % for all four investigated species (table 1). When the boards were later cut for specimen preparation, small, non-impregnated areas were only found in the poplar. This is a peculiarity of poplar wood, the cause of which has not yet been precisely clarified (BUSCHALSKY et al. 2022).

The highest WPG (20 %) was determined on the softwood reference (scots pine). In contrast to values determined on a laboratory scale, which are usually over 30 % with the same chemical concentration, this WPG is low (LARNOY et al. 2018, BECK 2020, KURKOWIAK et al. 2021a). However, the WPG decreases in the context of up-scaling (larger specimen dimensions, larger quantities of wood, semi-industrial equipment) compared to the WPG achievable under laboratory conditions (HÖTTE 2022). The WPG varied significantly between the three hardwood species. The highest value was found for poplar. Despite also high solution uptake, the WPG of beech and birch was significantly lower than that of poplar and the scots pine. This contradicts the descriptions of MUBAROK et al. (2020) who modified small specimens (25 x 25 x 10 ax. mm) made of beech wood under laboratory conditions and measured a WPG of over 30 %. Here too, the scaling of the modification probably plays a significant role in the discrepancy of the results.

Table 20: Solution uptake [%] after impregnation and Weight Percent Gain [%] after modification

	solution uptake [%]	WPG [%]	WPG$_{theoretical}$ [%]	ratio WPG/WPG$_{theoretical}$ [%]
Scots Pine	133.7 ± 20.1	20.0 ± 18.0	44.3 ± 6.6	43.6 ± 8.4
Beech	104.4 ± 7.3	5.1 ± 1.5	34.2 ± 2.3	8.2 ± 4.5
Birch	109.9 ± 16.0	10.8 ± 3.2	36.3 ± 5.3	22.6 ± 5.2
Poplar	138.5 ± 11.5	17.5 ± 2.8	45.6 ± 3.7	33.2 ± 3.2

The theoretical WPG provides information on how high the WPG would be without any loss of chemicals or loss due to wood degradation. Differences in the theoretical WPG of the individual wood species result from the different solution uptake rates. The ratio of actual WPG to theoretical WPG, sometimes referred to as retention, indicates how effectively the chemicals used are converted during modification. The ratio of WPG to theoretical WPG makes evident that high losses of either chemicals and/or wood mass must have occurred, particularly in the case of birch and beech.

In beech and birch in particular, both wood species with very low WPG, the modification was accompanied by an intensive change in wood colour and darkening (Figure 1). Both wood species were discoloured deep brown to black, while poplar and beech took on more of a lighter brown colour.

Figure 47: appearance of the modified wood (from left to right: scots pine, beech, birch, poplar). Surfaces planed

When wood is heated, chromophoric degradation products are formed, which cause a decrease in brightness and an increasing brown colouration (Sikora et al. 2018). The dark discolouration of the wood is an indication of an increased concentration of degradation products due to the effect of heat or acid hydrolysis. It can therefore be assumed that the darker colour of beech and birch is due to a greater degradation of wood constituents. Compared to the softwood reference, the low WPG may therefore be due to the higher hemicellulose content of the hardwoods, which are susceptible to acid hydrolysis (Fengel and Wegener 2003). Nevertheless, this hypothesis cannot explain the difference between the WPGs of the hardwoods.

Chemical fixation
The fixation of the chemicals after modification was quantified on the basis of the mass losses due to water leaching based on EN 84 and a subsequent long-term water leaching. The results are shown in Figure 2. After the first leaching procedure, the highest leaching losses were found for birch. However, the losses were generally low at a maximum of 3 % for birch and were in line with the results of Beck (2020) for pine and Mubarok et al. (2020) for beech. The results of the subsequent long-term leaching clearly show that although the mass losses decrease with increasing storage time in cold water, one EN84 cycle is probably not sufficient to determine the leaching behavior of the modified material and thus to estimate the performance of the modification under moisture exposure.
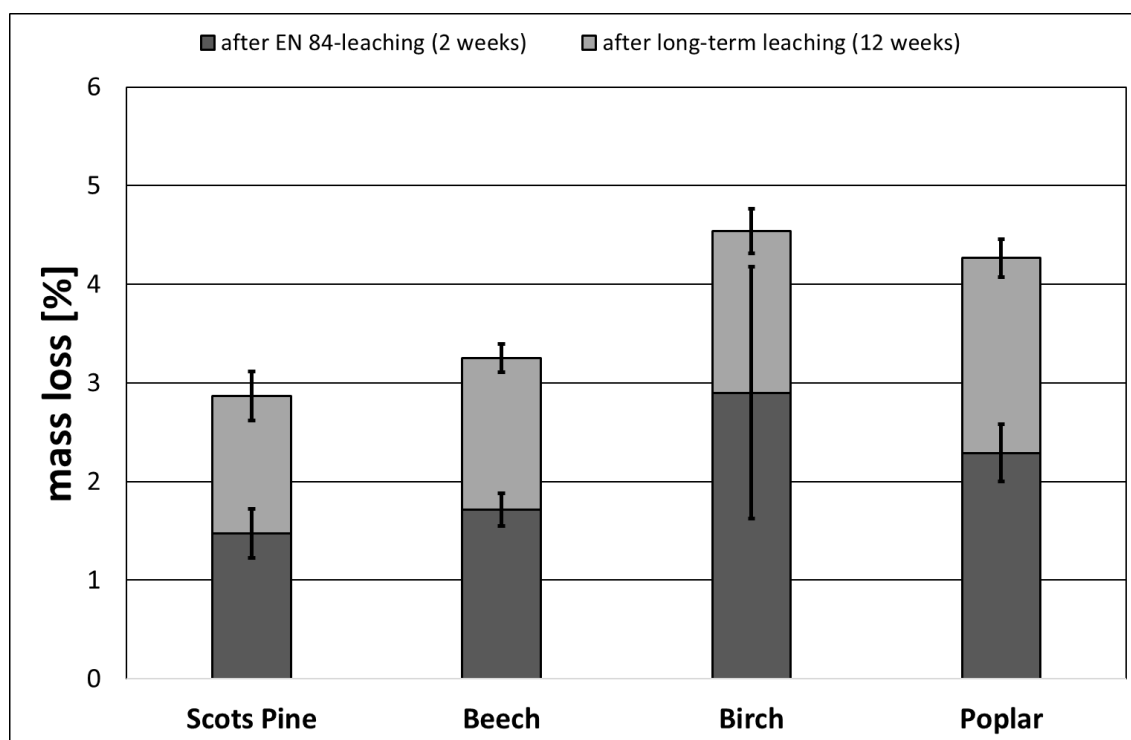
Figure 2: Mass losses [%] after EN 84-leaching and long-term leaching

Both the leaching of non-fixed chemicals and the leaching of hydrolysis products are possible causes of the mass losses. It is noteworthy that despite the significant differences between the WPGs, only slight differences were found between the mass losses caused by leaching. This indicates good fixation of the SorCA polyester regardless of the increase in mass caused by the modification.

Chemical distribution

Differences in the distribution of chemicals across the board cross-section were found between the wood species. Figure 3 shows the density profiles of the modified wood from the surface to the centre of the board. After modifying scots pine sapwood with SorCA and subsequent curing under laboratory conditions, KURKOWIAK et al. (2022) described an intensive uneven distribution of the modification chemicals across the cross-section of the specimens. The reason for this is convective lateral chemical transport with the capillary flow that occurs during drying (KLÜPPEL and MAI 2013). The uneven distribution observed in this study on scots pine sapwood is much less pronounced. It can be assumed that the comparatively low WPG of the specimens may also be the cause here. The almost homogeneous density profile of the beech can also be explained by the extremely low WPG, but not by a process-related prevention of chemical migration. In contrast, the most pronounced uneven distribution, i.e. the greatest difference in density between the centre of the board and the edge zone, was measured for scots pine, which also had the highest WPG of the wood species tested. An exception is poplar, which despite relatively high WPGs shows a very even distribution of chemicals and only a weak accumulation of chemicals in the edge zone.

A highly inhomogeneous distribution of chemicals poses a high risk of cracks between the edge and core zones of the modified product (ASHAARI et al. 1990). This is due to a build-up of stress between the two zones, as the better modified edge zone has a significantly higher dimensional stability than the core zone. Inhomogeneous chemical distributions across the wood cross-section are also disadvantageous for subsequent processing of the modified wood. On the one hand, the chemical-rich edge zones can be removed during surface processing, while on the other hand, the less modified core zone is exposed when the product is cut in the centre, which increases the risk of infestation by wood-destroying organisms.
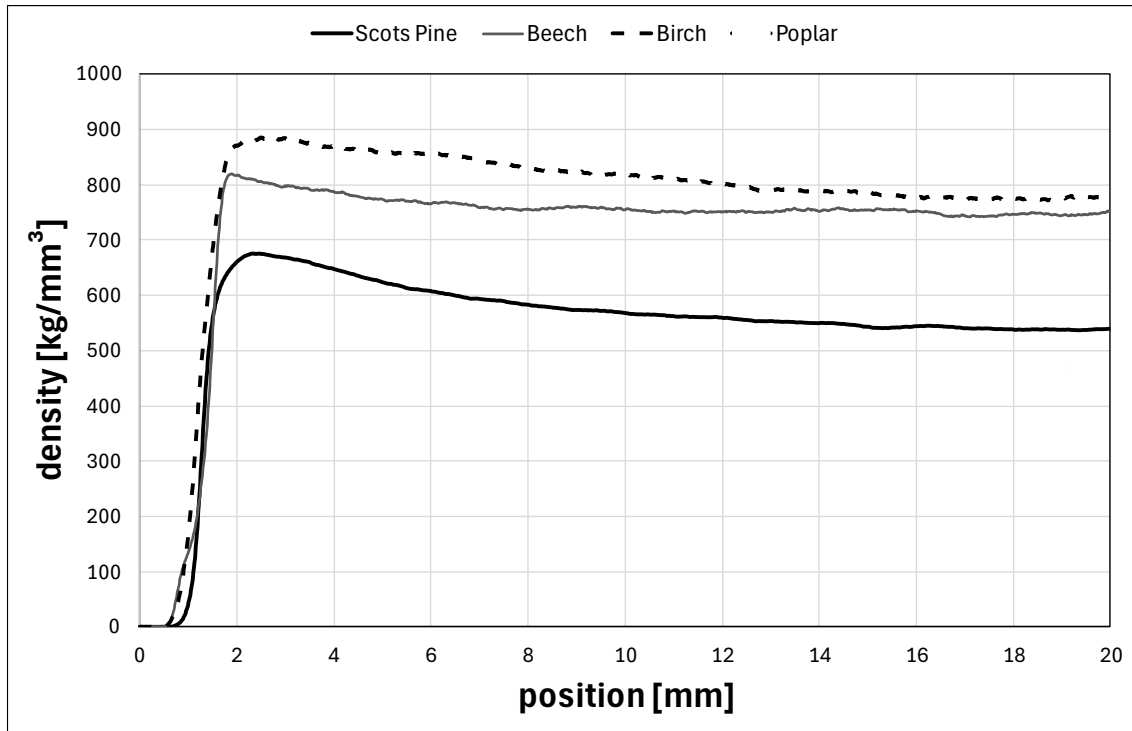
Figure 3: Density profiles of specimens from different wood species after modification (oven-dried). Each curve corresponds to the mean value of n = 10 specimens)

Drying quality

The drying quality varied depending on the wood species (table 2). Only slight losses in quality were observed for scots pine and beech. In the case of scots pine, these manifested themselves as slight crack formation, particularly at the axial ends of the boards. In beech, deformation of the cross-section (diamond shaped cross-section after drying) occurred, but only slight deformation in the longitudinal direction. However, these were very pronounced in the poplar and manifested themselves as twisting and bending. The drying quality of the birch was primarily determined by intensive cell collapse.

Table 21: Median of various drying quality parameters and occurrence of cell collapse

	Board deformation	Crack formation	Cell collapse
Scots Pine	0	1	-
Beech	1	0	-
Birch	1	0	yes
Poplar	2	1	-

0 = no/ minor occurrence; 1 = sporadic occurrence/ moderate level 2 = frequent occurrence/ severe level

It should be noted that the drying damage is not primarily caused by the chemical modification and is largely due to wood characteristics, but can be intensified by chemical wood degradation and exposure to high temperatures. The process control required for the modification, in particular the high process temperature of 140 °C, means that the different types of wood cannot be optimally and gently re-dried. Dense hardwood species in particular, such as birch and beech, require slow and gentle drying in order to maintain a high drying quality.

CONCLUSIONS

Three Central European hardwoods, beech, birch and poplar, were tested for their suitability for modification with SorCA. Scots pine sapwood was treated as a softwood reference. The process was carried out on a semi-industrial scale. The modification quality of all hardwoods was worse than that of the softwood reference. The WPG of birch and beech in particular was so low that a permanent improvement in the material properties cannot be assumed. Chemical fixation, measured as mass loss due to cold water leaching, was high for all wood species and showed no correlation to the WPG. Gradients of chemical distribution were found between the centre and the edge zones of the specimens.

However, these were moderate in their severity - presumably a result of the rather low WPG. The drying quality of birch and poplar in particular suffered greatly from the modification process. Planned investigations will concentrate on modification process development and adaptation for the individual hardwood species. The effect of scaling up from laboratory scale to semi-industrial scale on the properties of the modified material will also be analysed in more detail.

REFERENCES

Ashaari, Z., Barnes, H. M., Vasishth, R. C., Nicholas, D. D. and Lyon, D. E. (1990) Effect of aqueous polymer treatments on wood properties. Part I: Treatability and dimension stability. The International Research Group on Wood Preservation, IRG/WP/90–3610

Beck G (2020) Leachability and decay resistance of wood polyesterified with sorbitol and citric Acid. Forests 11(6):650

Buschalsky A, Löning S, Militz H, Koddenberg T Structural characterisation of the variable impregnation of poplar wood. In Hardwood Conference Proceedings, 28–36, Sopron, Hungary, 2022. University of Sopron Press

DIN EN 84 (2020) Durability of wood and wood-based products - Accelerated ageing of treated wood prior to biological testing - Leaching procedure, German Version. Beuth, Berlin

Doll M, Shogren R L, Willett J L, Swift G (2006) Solvent-free polymerization of citric acid and D-sorbitol. Journal of Polymer Science 44(14):4259–4267

Fengel D, Wegener G (2003) Wood - Chemistry, ultrastructure, reactions. Kessel Verlag, Kassel

Hötte C (2022). Holzmodifizierung mit Zitronensäure und Zuckeralkoholen – Optimierung des Trocknungs- und Aushärtungsprozesses. Faculty of Forestry and Forest Ecology, Georg-August-Universität Göttingen. Unpublished Master's Thesis

Kurkowiak K, Emmerich L, Militz H (2021a) Wood chemical modification based on bio-based polycarboxylic acid and polyols – status quo and further perspectives. Wood Material Science & Engineering 1–15

Kurkowiak K, Emmerich L, Militz H (2021b) Sorption behavior and swelling of citric acid and sorbitol (SorCA) treated wood. Holzforschung 75(12)

Kurkowiak K, Mayer A K, Emmerich L, Militz H (2022) Investigations of the chemical distribution in sorbitol and citric Acid (SorCA) treated wood—Development of a quality control method on the basis of electromagnetic radiation. Forests 13:151

Kurkowiak, K., Emmerich, L., Militz, H. (2023) Biological durability and wood–water interactions of sorbitol and citric acid (SorCA) modified wood. Journal of Wood Science 69 (1):34

Larnøy E, Karaca A, Gobakken LR, Hill C A S (2018) Polyesterification of wood using sorbitol and citric acid under aqueous conditions. International Wood Products Journal 9(2):66–73.

Mubarok M, Militz H, Dumarçay S, Gérardin P (2020) Beech wood modification based on in situ esterification with sorbitol and citric acid. Wood Sci Technol 54(3):479–502

Sikora A, Kačík F, Gaff M, Vondrová V, Bubeníková T, Kubovský I (2018) Impact of thermal modification on color and chemical changes of spruce and oak wood. Journal of Wood Science 64:406–416

11th Hardwood Conference

30-31 May 2024
Sopron

WOOD KPLUS

FATE
FAIPARI TUDOMÁNYOS EGYESÜLET

UNIVERSITY of SOPRON